CAADRIA 2021 - Hong Kong

'PROJECTIONS'

Proceedings of the 26th International Conference of the Association for Computer-Aided Architectural Design Research in Asia

Edited by:
Anastasia Globa
Jeroen van Ameijde
Adam Fingrut
Nayeon Kim
Tian Tian Sky Lo

VOLUME 1

PROJECTIONS

Proceedings of the 26th International Conference on Computer-Aided Architectural Design Research in Asia (CAADRIA 2021)

Volume 1

Edited by

Anastasia Globa
University of Sydney

Jeroen van Ameijde
The Chinese University of Hong Kong

Adam Fingrut
The Chinese University of Hong Kong

Nayeon Kim
Yonsei University

Sky Lo Tian Tian
Harbin Institute of Technology (Shenzhen)

Projections
26th International Conference on Computer-Aided Architectural Design Research in Asia (CAADRIA 2021)

29 March – 1 April 2021
School of Architecture
The Chinese University of Hong Kong

ISBN: 978-988-78917-5-8
ISSN: 2710-4257 (print)
2710-4265 (online)

Printed in Hong Kong

Foreword

The annual CAADRIA (Association for Computer-Aided Architectural Design Research in Asia) conference provides an international community of researchers and practitioners with a venue to exchange, to discuss and to publish their latest ideas and accomplishments. The proceedings have two volumes containing the research papers that were accepted for presentation at the Projections – 26th International CAADRIA Conference, hosted and organised by the Faculty of Architecture at Chinese University of Hong Kong. The papers are also available online at the open access cumulative database CumInCAD {http://papers.cumincad.org}. The proceedings are the outcome of an extensive collaborative effort of a team of volunteers and CAADRIA's international Academic Review Committee.

Within the context of continued challenges and restrictions imposed by the ongoing world-wide pandemic, our CAADRIA community have shown its resilience and strength. Initial calls for papers in July 2020 resulted in a round number of 400 abstract submissions. These abstracts were assessed by the Paper Selection Committee and were a subject to a double-blind peer review performed by a team of 151 international reviewers. 250 papers were invited to proceed to the next stage - the full-length paper submission. Those manuscripts went through another series of double-blind reviews, with two-to-four for each paper. As a result, 152 submissions were accepted and 149 of these were ultimately published in the CAADRIA 2021 proceedings. We congratulate the authors for their accomplishment.

Next to the authors, the reviewers, who volunteered their valuable time and effort, deserve our sincere thanks and acknowledgements. We thank the Organising Team at The Chinese University of Hong Kong for hosting the 26th International CAADRIA Conference online.

We extend our special thanks to the ProceeDings team, and in particular Gabriel Wurzer, for his support with customizing the submission and review system to the needs of CAADRIA from the full-paper submission to the production stage. On the following pages, we acknowledge and thank those who contributed to the production of this volume. In closing, we sincerely thank the CAADRIA community for offering us the honour to serve as members of the paper selection committee for *Projections, the 26th International CAADRIA Conference 2021.*

Anastasia Globa	*University of Sydney (Chair)*
Jeroen van Ameijde	*The Chinese University of Hong Kong*
Adam Fingrut	*The Chinese University of Hong Kong*
Nayeon Kim	*Yonsei University*
Sky Lo Tian Tian	*Harbin Institute of Technology (Shenzhen)*

CAADRIA 2021

Theme: ***'Projections'***

In a time of unprecedented global challenges, the need for researchers and designers to reflect on our changing society has rarely been more obvious. As the pandemic highlights the precariousness of our fragile climate, limited resources and unequitable urban areas, there is a new mandate for research and innovation, searching for new technology-enabled processes that positively impact our profession, communities, and planet.

The advancement and adoption of new technologies in all aspects of our society have started to profoundly change the nature of architectural design and materialisation processes, bridging between the digital and the physical worlds. Fluid communication allows for unprecedented new levels of complexity, control and feedback between design and the built environment. Large quantities of information allow us to forecast how architectural and urban structures perform over time, against a detailed understanding of their contexts.

'Projections' focuses on the implementation of our work, asking us to reflect upon the different ways innovation will impact the future of our industry. We will invite conversations and debate around the status of computational research and design, reflecting on recent challenges and opportunities, and how these translate into futures that are different from what was previously predicted. As we assess our projects within the context of our shared realities, we position our work as prototypes for alternative futures in our collective field.

The 2021 annual conference for Computer-Aided Architectural Design Research in Asia (CAADRIA), will bring together academics, researchers and practitioners involved in innovating, disrupting or revolutionising processes for the conceptualisation, evaluation and materialisation of the built environment. By inviting participants from universities and practices throughout Asia, we aim to create a platform for shared moments of inspiration, reflection, and projection.

Conference Organisers & Hosts,

Kristof Crolla *The University of Hong Kong*
Adam Fingrut *The Chinese University of Hong Kong*
Jeroen van Ameijde *The Chinese University of Hong Kong*

{https://caadria2021.org}

About CAADRIA

The *Association for Computer-Aided Architectural Design Research in Asia* (CAADRIA) promotes teaching and research in CAAD in the larger Austral-Asian and Pacific region supported by a global membership.

CAADRIA was founded in 1996 with the following objectives:

- To facilitate the dissemination of information about CAAD among Asian schools of architecture, planning, engineering, and building sciences.
- To encourage the exchange of staff, students, experience, courseware, and software among schools.
- To identify research and develop needs in CAAD education and to initiate collaboration to satisfy them.
- To promote research and teaching in CAAD that enhances creativity rather than production.

CAADRIA organizes among others an annual conference, the first of which was held in 1996 in Hong Kong. Since then, 25 conferences have been held in Australia, China, Hong Kong, India, Japan, Korea, Malaysia, New Zealand, Singapore, Taiwan, and Thailand. The annual CAADRIA conferences provide an opportunity to meet, to learn about the latest research, and to continue the discourse in the field. The 26th conference, in 2021, is held at The Chinese University of Hong Kong. CAADRIA 2021 is held as a virtual conference for the second time in the history of the Association to bring together researchers, practitioners and schools of the pacific region even at a time of continued global Covid-19 related travel restrictions.

CAADRIA is one of the four founding organizations of the *International Journal of Architectural Computing* (IJAC), and typically co-edits one issue each year. IJAC is published by SAGE in both paper and electronic versions.

Christiane M. Herr
President, CAADRIA

CAADRIA Officers

President: Christiane M. Herr
Xi'an Jiaotong-Liverpool University, China

Secretary: Urvi Sheth
CEPT University, India

Treasurer: Hyoung-June Park
University of Hawaii, USA

Membership Officer: Immanuel Koh
Singapore University of Technology and Design, Singapore

Web Master: Kyung Hoon Hyun
Hanyang University, Korea

Administrative Officer: Marc Aurel Schnabel
Victoria University of Wellington, New Zealand

CAADRIA 2021 Conference Committees

Hosting Institution:
The Chinese University of Hong Kong

Organising Committee:

Kristof Crolla *The University of Hong Kong*	*Conference Co-Chair*
Adam Fingrut *The Chinese University of Hong Kong*	*Conference Co-Chair*
Jeroen van Ameijde *The Chinese University of Hong Kong*	*Conference Co-Chair*
Donn Holohan *The University of Hong Kong*	*Workshop Coordinator*
Hoi Lam Melody *The Chinese University of Hong Kong*	*Tour Coordinator*
Garvin Goepel *The Chinese University of Hong Kong*	*Technical Coordinator*
Lidia Ratoi *The University of Hong Kong*	*Exhibition Coordinator*

Paper Selection Committee:

Anastasia Globa
University of Sydney — *Chair*

Jeroen van Ameijde
The Chinese University of Hong Kong

Adam Fingrut
The Chinese University of Hong Kong

Nayeon Kim
Yonsei University

Sky Lo Tian Tian
Harbin Institute of Technology (Shenzhen)

Post Graduate Students Consortium:

Dagmar Reinhardt — *Co-Chair*

Sky Lo Tian Tian — *Co-Chair*

Christiane M. Herr

Sasada Prize Committee:

Tom Kvan — *Chair*

Christiane M. Herr

Atsuko Karga

Young CAADRIA Award Committee:

Sky Lo Tian Tian — *Chair*

Christiane M. Herr

Rudi Stouffs

Jeroen van Ameijde

International Review Committee

Wael Abdelhameed
Applied Science University
Henri Achten
Czech Technical University, Prague
Ayşegül Akçay Kavakoğlu
Istanbul Technical University
Mostafa Alani
Aliraqia University
Miktha Farid Alkadri
TU Delft
Jeroen van Ameijde
The Chinese University of Hong Kong
Nan Bai
TU Delft
Ardavan Bidgoli
Carnegie Mellon University
Luis Borunda
Virginia Tech
Kristina Boychenko
The University of Queensland
Johannes Braumann
Creative Robotics
Robots in Architecture
Michael Budig
SUTD
Inês Caetano
INESC-ID/IST, University of Lisbon
Jason Carlow
American University of Sharjah
Renata Castelo-Branco
INESC-ID/IST, University of Lisbon
Mohammed Aqil Cheddadi
Keio University
Jia-Yih Chen
CS CHENG & JY CHEN
Zi-Ru Chen
STUST
Feihao Chen
The Chinese University of Hong Kong
Angelos Chronis
Austrian Institute of Technology
I-Ting Chuang
SUTD
Verina Cristie
SUTD
Kristof Crolla
The University of Hong Kong
Tatjana Crossley
The Chinese University of Hong Kong
Weiwen Cui
Tsinghua University
Pierre Cutellic
ETH Zurich
Mohammad Reza Dastmalchi
University of Missouri
Marie Davidova
Welsh School of Architecture Collaborative Collective
Aurélie de Boissieu
The University of Liège
Danilo Di Mascio
The University of Huddersfield
Wowo Ding
Nanjing University
Thomas Dissaux
The University of Liège
Theodoros Dounas
Robert Gordon University
Halil Erhan
Simon Fraser University
Alberto T. Estevez
iBAG-UIC Barcelona
Mohammed Ezzat
ME Architects
Paolo Fiamma
University of Pisa
Adam Fingrut
The Chinese University of Hong Kong
Antonio Fioravanti
Sapienza University of Rome
Haruyuki Fujii
Tokyo Institute of Technology
Tomohiro Fukuda
Osaka University
Song Gao
Independent Researcher
Fernando García Amen
UdelaR
Nadja Gaudilliere
TU Darmstadt

Andrew Wit
Temple University
Thomas Wortmann
University of Stuttgart
Yen-Liang Wu
NTCUST
Xinchang Xiong
Tsinghua University
Chao Yan
Tongji University
Lijing Yang
Tsinghua University
Jiawei Yao
Tongji University
Hatzav Yoffe
Technion-Israel Institute of Technology
Jungwon Yoon
University of Seoul
Rongrong Yu
Griffith University
Hao Zheng
University of Pennsylvania
Jianjia Zhou
Tongji University
Guanqi Zhu
The University of Queensland

Keynote Lectures

Worlds Less Travelled

Liam Young
Coordinator, MA in Fiction and Entertainment, SCI-Arc
Founder, Tomorrows Thoughts Today
Co-director, Unknown Fields Division

Our perception of the world is largely shaped through the mediums of fiction. Through film we have always imagined alternative worlds as a way of understanding our own world in new ways. A critical role of Science Fiction is to provide a counterbalance to the prevailing media narratives around emerging urban technologies. Typically, our imagined futures are based on a solutionist view of technology and are marketed to us as simplified worlds of better and brighter often ignoring the complexities, subcultures and unintended consequences that result when technologies are democratized and rolled out at scale. In this talk, Liam Young will narrate a series of stories from these worlds less travelled, just small glimpses, fragments, vignettes and snapshots from a series of his films that will come together to create a portrait of an alternative future of technology, urbanisation and automation.

BIOGRAPHY

Liam Young is a speculative architect and director who operates in the spaces between design, fiction and futures. He is cofounder of Tomorrows Thoughts Today, an urban futures think tank, exploring the local and global implications of new technologies and Unknown Fields, a nomadic research studio that travels on expeditions to chronicle these emerging conditions as they occur on the ground.

Described by the BBC as ‘the man designing our futures’, his visionary films and speculative worlds are both extraordinary images of tomorrow and urgent examinations of the environmental questions facing us today. As a concept designer he visualizes the cities, spaces and props of our imaginary futures including work on the forthcoming features Swan Song, starring Mahershala Ali and Awkwafina for Apple TV and Folding City for Chinese Production company Wanda in addition to production designing an unannounced new sci fi series for eOne. With his own films he is a BAFTA nominated producer and has premiered with platforms ranging from Channel 4, SxSW, the New York Metropolitan Museum, The Royal Academy, the BBC and the Guardian.

His fictional work is informed by his academic research and he has held guest professorships at Princeton University, MIT, and Cambridge and now runs the ground-breaking Masters in Fiction and Entertainment at SCI Arc in Los Angeles. He has published several books including the recent Machine Landscapes: Architectures of the Post Anthropocene and Planet City, a story of a fictional city for the entire population of the earth.

Leveling-up our Design Methodologies

Ben van Berkel
Professor, AA Dipl. (Hons), (F)RIBA, Hon. FAIA
Founder / Principal Architect, UNStudio
Founder, UNSense

In light of the challenges society is facing, UNStudio's founder Ben van Berkel will present on the integral and human centric approach to health, flexibility and technology in their work. Leveling-up our built environment requires thinking about the relation between different scales. UNStudio has produced a wide range of work, from public buildings to infrastructure, offices to residential as well as interiors and products to urban master plans. With their focus distinctly placed on the future, in 2018 the practice founded a sister company, UNSense, an arch tech company that aims to create impact by developing technology and innovative solutions that improve quality of life for individuals, communities and the planet.

BIOGRAPHY

Ben van Berkel studied architecture at the Rietveld Academy in Amsterdam and at the Architectural Association in London, receiving the AA Diploma with Honours in 1987. In 1988 he and Caroline Bos set up UNStudio, an architectural practice in Amsterdam. Current projects include the Southbank mixed-use development in Melbourne, 'Four' a large-scale mixed-use project in Frankfurt and the Wasl Tower in Dubai.

With UNStudio, he realised amongst others the Mercedes-Benz Museum in Stuttgart, Arnhem central Station in the Netherlands, the Raffles City mixed-use development in Hangzhou, the Canaletto Tower in London, a private villa upstate New York and the Singapore University of Technology and Design. In 2018 Ben van Berkel founded UNSense, an Arch Tech company that designs and integrates human-centric tech solutions for the built environment.

Ben van Berkel has lectured and taught at many architectural schools around the world. From 2011 to 2018 he held the Kenzo Tange Visiting Professor's Chair at Harvard University Graduate School of Design, where he led a studio on health and architecture. In 2017, Ben van Berkel also gave a TEDx presentation about health and architecture. In addition, he is a member of the Taskforce Team / Advisory Board Construction Industry for the Dutch Ministry of Economic Affairs.

Planetary Reticulum: Considerations for Global Multi-Modal Connectivity in the Post-COVID Era

Cristiano Ceccato
FRAeS FRSA
Director, Zaha Hadid Architects, London

In today's globalised economy, multi-transport nodes bind cities together as part of an ever-growing, singular planetary network of complex urban environments. In the post-COVID world, we are confronted with the question of how to fill the intangible space between them and create a new balance across cultural boundaries, geographical barriers and growing political divides. This 'infrastructural glue', combined with new forms of travel, communication and decentralised collaborative work environments, is rapidly becoming the major catalyst for societal transformation in a 21st century tempered by pandemic and its politics.

Touching on examples from ZHA, this presentation will reflect on how multimodal infrastructure projects of increasing complexity are designed and constructed to provide the innervation for cities around the world – the connective tissue for a truly global meta-urban condition. These excursions into transport design provide a thematic and functional counterpoints of nodes and connectors, and speculates on an architectural vision of inter-urban development on a worldwide scale.

BIOGRAPHY

Cristiano Ceccato is a Director at Zaha Hadid Architects (ZHA) in London, having previously worked for Frank O. Gehry Partners in Los Angeles. Trained as an architect and computer scientist, he engages across all levels of design and technical development, with worldwide project delivery experience on a wide range of typologies. Cristiano is also an accomplished software developer, having previously co-founded the BIM company Gehry Technologies in California.

Cristiano has spearheaded ZHA's entrance into the aviation market since 2010. He is the Project Director for the Beijing Daxing Airport in China completed 2019; the Navi Mumbai International Airport in India; and the Western Sydney Airport under construction in Australia. Cristiano is a graduate of the Architectural Association and Imperial College in London. He is a Fellow of the Royal Society of Arts and a Fellow of the Royal Aeronautical Society, where he sits on the Air Transport Specialist Group board.

Senseable Cities

Carlo Ratti
Director, MIT Senseable City Lab
Founding Partner, Carlo Ratti Associati

The way we live, work, and play is very different today than it was just a few decades ago, thanks in large part to a network of connectivity that now encompasses most people on the planet. In a similar way, today we are at the beginning of a new technological revolution: the Internet is entering the physical space – the traditional domain of architecture and design – becoming an "Internet of Things" or IoT. As such, it is opening the door to a variety of applications that – in a similar way to what happened with the first wave of the Internet – can encompass many domains: from energy to mobility, from production to citizen participation. The contribution from Prof. Carlo Ratti will address these issues from a critical point of view through projects by the Senseable City Laboratory, a research initiative at the Massachusetts Institute of Technology, and the design office Carlo Ratti Associati.

BIOGRAPHY

An architect and engineer by training, Professor Carlo Ratti teaches at the Massachusetts Institute of Technology (MIT), where he directs the MIT Senseable City Lab, and is a founding partner of the international design and innovation office Carlo Ratti Associati. He graduated from the Politecnico di Torino and the École Nationale des Ponts et Chaussées in Paris, and later earned his MPhil and PhD at the University of Cambridge, UK.

A leading voice in the debate on new technologies' impact on urban life and design, Carlo has co-authored over 500 publications, including "The City of Tomorrow" (Yale University Press, with Matthew Claudel), and holds several technical patents. His articles and interviews have appeared on international media including The New York Times, The Wall Street Journal, The Washington Post, Financial Times, Scientific American, BBC, Project Syndicate, Corriere della Sera, Il Sole 24 Ore, Domus. His work has been exhibited worldwide at venues such as the Venice Biennale, the Design Museum Barcelona, the Science Museum in London, MAXXI in Rome, and MoMA in New York City.

Carlo has been a presenter at TED (in 2011 and 2015), program director at the Strelka Institute for Media, Architecture and Design in Moscow, curator of the BMW Guggenheim Pavilion in Berlin, and was named Inaugural Innovator in Residence by the Queensland Government. He was the curator of the Future Food District pavilion for the 2015 World Expo in Milan and chief curator of the "Eyes of the City" section at the 2019 UABB Biennale of Architecture and Urbanism of Shenzhen. He is currently serving as co-chair of the World Economic Forum's Global Future Council on Cities and Urbanization.

Roundtable Conversations

Projections on Automation and Architecture
Gilles Retsin (convenor)
Marina Otero Verzier
Deborah Lopez & Hadin Charbel
Jelle Feringa

Innovation Re-Origination
David Erdman (convenor)
Debora Mesa Molina
Elora Hardy
Philip Yuan
Jing Liu

Future Practice: Challenges and Opportunities of Technology Integration in Building Engineering
Ramon van der Heijden (convenor)
Emidio Piermarini
Susanne Knorr
Man Kit Thomson Lai
Nick Williams

From Lab to Site: Promises of Disruptive Technology Implementations in AEC
Diego Pinochet (convenor)
Stefana Parascho
Skylar Tibits
Kevin Saey
Victor Leung

Encoding and Decoding Patterns of Planetary Urbanization
Enriqueta Llabres-Valls (convenor)
Michael Weinstock
Ying Jin
Rosalea Monacella

Projections on Automation and Architecture

Recent tendencies in architecture have moved on from an obsession with continuous form to develop a more critical understanding of the disciplines' relation to "the Digital". Part of this shift is a variegated group of practitioners and theorists that interrogate the notion of automation as an alternative angle to understand the relation between architecture and digital technologies.

Framing architecture's engagement with digital technologies as a form of automation opens up a vast territory of investigation, ranging from robotics and fabrication, to platform economics, the politics of the digital, and planetary issues such as climate change. While this is a welcome departure from the often-isolated viewpoint of the early digital experiments in architecture, the question arises how this reflects back on core issues architecture itself – space, form and experience. Returning from these vast territories of automation, have we lost the desire to formulate a position on space and form?

This panel of experts will debate how automation has impacted our understanding of design and architecture itself. Covering the politics of automation and its repercussions on architecture, the discussion will project possible architectural attitudes, ideas and positions.

Gilles Retsin (convenor)
Programme Director, M.Arch Architectural Design, the Bartlett School of Architecture, UCL
Co-founder, UCL AUAR Labs (Automated Architecture Labs)
Co-founder, AUAR ltd (Automated Architecture)

Originally from Belgium, Gilles Retsin is an architect and designer living in London. He studied architecture in Belgium, Chile and the UK, where he graduated from the Architectural Association. His design work and critical discourse has been internationally recognised through awards, lectures and exhibitions at major cultural institutions such as the Museum of Art and Design in New York, the Royal Academy in London and the Centre Pompidou in Paris. He recently edited an issue of Architectural Design (AD) on the Discrete and has co-edited Robotic Building: Architecture in the Age of Automation, with Detail Verlag.

Gilles Retsin is Programme Director of the M.Arch Architectural Design at UCL, the Bartlett School of Architecture. He is also co-founder of the UCL Design Computation Lab, which does high profile research into new design and fabrication technologies. He is also co-founder of AUAR ltd (Automated Architecture), a start-up working towards an automated platform for affordable housing.

Marina Otero Verzier
Head of the Social Design MA, Design Academy Eindhoven

Marina Otero Verzier is an architect based in Rotterdam. She is Director of Research at Het Nieuwe Instituut (HNI) and head of the Social Design MA at Design Academy Eindhoven. At HNI, Otero works to give visibility to research projects, practices, and initiatives that depart from established modes of thinking. Examples include Automated Landscapes (focusing on emerging architectures of automated labour) and BURN-OUT. Exhaustion on a planetary scale (instigating other forms of coexistence and care for multispecies, collective bodies). She was previously Director of Global Network Programming at Studio-X in New York. Otero was a member of the Artistic Team for Manifesta 13, and Curator of WORK, BODY, LEISURE, the Dutch Pavilion at the 16th Venice International Architecture Biennale in 2018. With the After Belonging Agency, she was Chief Curator of the Oslo Architecture Triennale 2016. Currently, she is one of the curators of the 13th Shanghai Art Biennial. Otero studied at TU Delft and ETSA Madrid and Columbia University GSAPP. In 2016, she received her PhD at ETSA Madrid.

Deborah Lopez & Hadin Charbel
Lecturers, the Bartlett School of Architecture, UCL
Co-founders, Pareid Office

Deborah Lopez and Hadin Charbel are architects and founders of Pareid; an interdisciplinary design and research studio currently located in London. Their works adopt approaches from various fields and contexts, addressing topics related to climate, ecology, human perception, machine sentience, and their capacity for altering current modes of existence through iminent fictions (if) believing that disruptions to existing norms can be useful in generating alternate versions of future realities. They have been recently awarded with the Arquia Innova Award in the VII Arquia Próxima Awards by Fundación Arquia and their work has been presented in different international institutions and exhibitions such as Royal Academy of Arts, Centre Pompidou, Seoul Biennale or Venice Biennale.

They are both Lecturers (Teaching) at The Bartlett School of Architecture UCL in the B-Pro program where they run the cross-Research Cluster (1+20) in Architectural Design and Urban Design entitled “Monumental Wastelands”, By using climate fiction as a vehicle, speculations are put forward that engage various ecologies via sentient machines and automated landscapes, through which current economically profitable models are challenged.

Jelle Feringa
Chief Technology Officer, Aectual

Jelle Feringa is an architecture and robotics specialist and as CTO of Aectual responsible for the development and production of tailor-made building products at scale. While developing his PhD thesis at TU Delft, Jelle established a full robotics lab in the docks of Rotterdam. Here he developed the technical underpinnings for Odico formwork robotics, the first publicly traded architectural robotics company which he co-founded in 2012. Technologies that Jelle developed, include hotwire, hotblade, diamond wire cutting and large scale 3d printing and are applied in high-profile construction projects.

Jelle has taught & lectured internationally at the Bartlett, Architectural Association, Paris-Malaquias, IAAC, ETH Zürich, TU Delft and Aarhus School of Architecture. He is a founding partner of EZCT Architecture & Design Research. The work of the office is widely exhibited, exhibitions include the Mori Art Museum, Tokyo, Archilab, Orléans, Barbican Gallery Design Miami/Basel. Projects by the office are part of Pompidou Center permanent collection and the FRAC Centre Orléans. Jelle is a long-term contributor of the PythonOCC project, and some of his fascinations include levelsets, stereotomy and powertools.

Innovation Re-Origination

This panel will be discussing how the displacement of the origins of existing contexts can constitute new, future origins. Innovation is not always what's new and what is next; it may be directly in front of us. This is an increasingly important consideration for architectural education and the profession; one which foregrounds the reuse of buildings, building systems, materials, infrastructures, trades, craftsmanship, and landscapes as a viable arena for scholarly research, design development and technical innovation. Within the context of CAADRIA, the importance of this subject lies in the numerous technological promises that come with the hybrid, mixed systems and which contradict and complicate the clean, singularity of 20th century, holistic, ground-up construction. In focusing on this area of research, the smooth streamlined mythology of BIM software might be reconsidered and expose latent technical horizons.

The scope of research on "re-origination" and its requisite praxes locates itself on the fringes of architecture discourse. Existing research on this subject has been limited due to the fact that the majority of architecture schools and practices largely see solutions to sustainability as tethered to the continued necessity for new, novel construction systems, materials and tradecrafts. This panel will explore ways in which research in this area emphasises and explores the robust space between social and environmental justice afforded by the primary lens of "alteration." Through this framework, small-scale, highly attenuated, design moves that draw concisely from their context, minimize displacement, limit resources, and capitalize on obsolete square footage and/or practices will be discussed as having the capacity to innovate and re-originate.

David Erdman (convenor)
Chairperson, Graduate Architecture and Urban Design, Pratt Institute's School of Architecture

David Erdman is the chairperson of Graduate Architecture and Urban Design at Pratt Institute's School of Architecture in Brooklyn, NY. He was a co-founding partner of the design collaborative servo where he designed and completed numerous projects exhibited in museums in North America and Europe. Erdman co-founded davidclovers (now plusClover) with former partner Clover Lee where from 2006-2016 he designed and completed over twenty built projects in Hong Kong, China and North America. In addition to the receipt of numerous awards and having work from both firms exhibited and collected in museums, Erdman was awarded the prestigious Rome Prize in 2008-2009.

In addition to Pratt, Erdman has taught at UCLA and HKU and held visiting positions at various universities including Yale, UC Berkeley and Rice University. He is the author of Introducing (AR+D 2021), Pratt Sessions Volumes 1 and

2 (ORO 2018, 2020) and co-author of Future Real (Yale SoA 2018). He has lectured throughout Asia, North America and Europe. Erdman is currently working on several books and a series of collaborative design research projects with government organizations in New York City and Hong Kong.

Debora Mesa Molina
Principal, Ensamble Studio
Ventulett Chair, Georgia Tech

Débora Mesa Molina, (Madrid, 1981) is European Licensed Architect and principal of Ensamble Studio, a cross-functional team she leads with her partner Antón García-Abril, based in Madrid and Boston. Balancing imagination and reality, art and science, their work innovates typologies, technologies and methodologies. From their early works – Hemeroscopium House or The Truffle- to their most recent – Ca'n Terra and Ensamble Fabrica -, every project makes space for experimentation aiming to advance their field. Currently, through their startup WoHo, they are developing ways to increase quality and affordability in architecture through the integration of offsite technologies.

Debora is committed to sharing ideas and cultivating synergies between professional and academic worlds through teaching, lecturing and researching: she is Ventulett Chair in Architectural Design at Georgia Tech since 2018 and previously served as research scientist at MIT where she co-founded the POPlab – Prototypes of Prefabrication – in 2012. Above all, she is a doer, committed to making poetic ideas happen.

Elora Hardy
Founder, IBUKU

Elora is the Founder and Creative Director of IBUKU. The team of designers, architects and engineers that is exploring ground-breaking ways of using bamboo to build homes, hotels, schools, and event spaces in Bali, Indonesia. Creating a new design vocabulary based on this one material and exploring the way sustainable architecture and design can redefine luxury. The traditional skills of Balinese craftsmen, combined with their design ideas and modern engineering enable them to create original bamboo structures that meet the needs of a diverse clientele. "IBUKU's goal is to provide spaces in which people can live in an authentic relationship with nature. IBUKU is creating spaces where living in nature is living in style. IBUKU has built over 72 bamboo structures in Bali, Indonesia, and 5 internationally. Completed key projects include the Green School, Green Village, Sharma Springs, and Bambu Indah Eco Resort, which have appeared in international publications like Architectural Digest, Elle Decor, Vogue and the Huffington Post.

Philip Yuan
Associate Dean and Professor, College of Architecture and Urban Planning (CAUP), Tongji University

Philip F. Yuan Associate Dean, tenured professor of the College of Architecture and Urban Planning (CAUP) at Tongji University, Council Member of Architects Sector, Virtual and Automated Construction Sector as well as Academic Committee of Computational Design Sector at Architectural Society of China; Director of Academic Committee of Shanghai Digital Fabrication Engineering Technology Center; Co-Chair of DigitalFUTURES Association. He founded Shanghai based firms: Archi-Union Architects and Fab-Union Technology. Yuan is also a member in the Scientific Committee of The International Association on Spatial Structures (IASS) and the International Conference on 3D Printing and Transportation3D Printing and Transportation (3DTRB).

His research mainly focuses on the field of performance-based architectural tectonics, the application of robotic fabrication equipment as weak as developments of robotic fabrication technologies and is able to realize many of his research theories in architectural practices.

Jing Liu
Co-Founding Principal, SO-IL
Visiting Professor, Pratt Institute

Jing Liu has been practicing for more than 15 years working on a wide range of projects both in the US and abroad. Through building practice and interdisciplinary research projects, Liu has led SO–IL in the engagement with the socio-political issues of contemporary cities — in projects like the Artists Loft North Omaha and the Martin Luther King, Jr. Library in Cleveland. Her projects range from artistic collaborations with contemporary choreographers and visual artists to master plan and major public realm design in cities like Melbourne and Indianapolis.

Liu brings an intellectually open, globally aware, and locally sensitive perspective to architecture. Her intellectual curiosity and artistic imagination allow her to bring a more nuanced cultural perspective to the table. Her keen skills in combining digital technology with traditional craft and firm belief in design's ability to re-engage people with the physical world around them allow the buildings she designs to become places of exchange that welcome interpretation and transformation.

FUTURE PRACTICE: Challenges and Opportunities of Technology Integration in Building Engineering

Moore's law predicts the number of transistors in a dense integrated circuit to double approximately every two years. This means that every 24 months, computational devices can perform their tasks twice as fast. For over 50 years, this theory has held up. In the meantime, while our industry still considers decade-old BIM technology to be "new", Automation, Machine Learning, and Artificial intelligence are increasingly taking over the laborious and repetitive tasks that are part of our design and engineering work.

Designers will in the future interface with machines through AI assistants and use human qualities, such as creativity, emotion, inter-human relationships, experience, and common sense to make decisions. At Arup Group we are currently developing a design automation platform called "Total Design Automation" (TDA) which will make it easy to both develop automated workflows and use them across projects around the world. Through cloud technologies, automated design tasks are linked together by the data they produce and subsequently consume, orchestrating entire design workflows from start to end. In doing so, a gap has been exposed between what is theoretically possible and what is needed now. The biggest industry challenge is hardly ever the design and delivery of complex, iconic architecture, but to provide sufficient housing and places to work for the exponentially growing world population.

By touching on issues related to standardisation, industry skills, business strategies, and future design and delivery methodologies, this roundtable panel of experts in computational design engineering and construction will discuss how our industry can (prepare itself to) utilise future computation and automation to improve the quality of our built environment.

Ramon van der Heijden (convenor)
Digital Design Leader, Arup East Asia

Ramon is Digital Design Leader at Arup East Asia. His work in Research and development, Building Information Modeling and Building Data Management has allowed him to develop a deep understanding of the technology that drives innovation in construction data management and design. Specializing in the generation of large, data rich building models has enabled him to create the Elefront add-in for Grasshopper. He is currently the Programme Director of the development of a cloud-based design automation platform that allows anyone to develop and use automated design solutions through the web.

Ramon has taught computational design at Eindhoven University of Technology, and Construction Communication and Architectural Design at The University of Hong Kong. He has hosted seminars on Elefront at The Chinese University

Hong Kong, The University of Hong Kong and for the AA Visiting School, Hong Kong. Leading the Digital Design Team, his work focuses on optimizing and digitizing existing design and engineering processes as well as exploring new business opportunities using digital design technologies.

Emidio Piermarini
Associate, Buro Happold Asia

Emidio is an Associate with Buro Happold Asia, where he is the lead for their new Computational Consulting offering. He works with clients in all stages of the real estate life cycle to help clients realize solutions to their most complex problems using big data and analytics. He is an early contributor to the open-source Buildings and Urban Habitat Object Model (BHoM) and believes the open-source era of AEC represents the future of our industry–design professionals who can communicate and design using code.

Susanne Knorr
Global Client Development Lead Data & Analytics, Arcadis

Susanne is managing the Global Client Development of Arcadis' Data Analytics services, with a focus on driving sustainability. She is responsible for identifying opportunities to apply advanced statistical methods and solutions for key-clients, helping them to address their challenges and enhance the performance. Therefor Susanne and her team partner with the technical engineering team, focusing on analytics key methods like Data Management & Engineering, Data Visualization, Data Science & Machine Learning, NLP, Computer Vision and IoT, and the client development community across all sectors and solutions.

In 2017 Susanne was selected as an Arcadis Global Shaper, in 2018 she was awarded the Start- up Digital Award. She is a mentor of Techstars X Arcadis City Accelerator 2019. In 2020 Susanne was selected for the W50 Emerging Leaders Programme by the London School of Economics and Political Science supported by the Becas Santander Scholarship.

Lai, Man Kit Thomson
Executive Director of Innovative Solutions,
Digital Transformation Lead, Greater China, AECOM

Thomson Lai is a technology veteran with over 20 years of experience in the geospatial industry and is an expert in a wide variety of digital technology. He is a chartered surveyor, CIC Certified BIM Manager, and a Project Management Pro-

fessional (PMP) certified project manager. Thomson's involvement has been integral to many large- scale civil infrastructure projects, and he's responsible for many digital solutions, including BIM processes and workflows. His recent projects include the Hong Kong International Airport Three-runway System, pilot study on underground space development for the HKSAR Civil Engineering and Development Department, study on integration of BIM & 3D spatial data for the HKSAR Lands Department, and APAC datacenter BIM managed service for multinational technology company.

As an experienced technology practitioner, Thomson is a pioneer who integrates technologies — including BIM, GIS, photogrammetry, IoT, and immersive technology — for civil and infrastructure projects. He is also the Asia Digital leader of AECOM and is currently leading the digital business in Asia, pushing the adoption of digital technology across the region.

Nick Williams
Principal, Computational Design & Automation Leader, Aurecon

Nick Williams is a Principal at Aurecon and leads digital modelling, computational design and automation across the firm. In this role Nick has created both a distributed network of practitioners across regional teams, and a central software and business transition team. These two streams enable both a nimble response to specific project needs, and the creation of standards and tools to reshape engineering and design services at scale.

Prior to joining Aurecon, Nick trained as an architect and practiced in Australia and Europe. He has a Master's degree from The Architectural Association, London, and a PhD from RMIT University, Melbourne. In academic roles, Nick has led various applied research around digital design and construction, prototyping data-driven approaches across multiple scales, materials and types of performance. He has also authored over 20 peer-reviewed journal and conference papers and remains a regular contributor to several academic forums.

FROM LAB TO SITE: Promises of Disruptive Technology Implementations in AEC

Having overcome the debate of the transition between the digital and the physical, architectural design faces a challenge about applying lab research into real-life scenarios to produce a true impact in our society. Whereas technology keeps driving definitive changes in architecture education and research, the demand for disruptive technological solutions addressing humanity's future challenges, behest a clear position on how to move beyond 'the lab' in the short, mid, and long term.

From the development of discrete 'chunky' architectures based on the mass production of building components, to the proposition of smart architectures from a material perspective that can self-assemble into complex objects and spaces, to the final realization of a digital continuum from the 3d model to the physical environment using robots collaborating in a coordinated dance, lab research is under scrutiny. The proposition of building systems and narrow applications representing the state-of-the-art research faces questions about their real impact in our society in the short, mid, and long term. Can architecture – through computational design – drive the necessary changes in the light of the challenges humanity will face in the next 30 to 50 years? Furthermore, what are the necessary steps that could lead to a disruptive implementation of the promising research that lays in lab setups' boundaries?

Diego Pinochet (convenor)
Professor, School of Design, UAI Chile
PhD Researcher, MIT

Diego Pinochet is a PhD student at the Design and Computation group at MIT, researcher at the Encoded elements lab in the International Design Center at MIT, a visiting Ph.D. Student at the Human-computer interaction group at MIT CSAIL, and a Professor at the School of Design at UAI Chile. Diego Pinochet holds a B.Arch and a M.Arch in the Pontifical Catholic University of Chile (PUC) and a Master of Science in Architectural Studies (SMArchS) from MIT.

His research is focused on computational design and interactive fabrication methodologies, Artificial Intelligence, Robotic Fabrication, Building Information Modelling BIM, and Interactive Applications for creative purposes. His research is focused on advanced computational design and interactive fabrication methodologies using Artificial Intelligence. He is pursuing his PhD degree in Design and Computation at MIT with a major in Human-Computer Interaction and a minor in Machine Learning. He seeks to bridge robotic fabrication with design methodologies to push innovation in architecture and construction through his research.

Stefana Parascho
Assistant Professor, Director creAte Laboratory, Princeton University

Stefana Parascho is a researcher, architect, and educator whose work lies at the intersection of architecture, digital fabrication and computational design. She is currently an Assistant Professor at Princeton University where she founded the CREATE Laboratory Princeton and is co-leading the PhD program in Technology of Princeton's School of Architecture. Through her research, she has explored multi-robotic fabrication methods and their relationship to architectural design. Stefana investigated computational design techniques ranging from agent-based systems to sequential design and optimisation methods. Her goal is to strengthen the connection between design, structure, and fabrication, and boost the interdisciplinary nature of architecture through the development of accessible computational tools and robotic fabrication methods.

Stefana completed her doctorate in 2019 at ETH Zurich, Gramazio Kohler Research. Previously, she received her Diploma in Architectural Engineering in 2012 from the University of Stuttgart and worked with DesignToProduction Stuttgart and Knippers Helbig Advanced Engineering.

Skylar Tibits
Associate Professor of Design Research, MIT
Co-director and Founder, MIT Self-Assembly Lab

Skylar Tibbits is a designer and computer scientist whose research focuses on developing self-assembly and programmable materials within the built environment. Tibbits is the founder and co-director of the Self-Assembly Lab at MIT, and Associate Professor of Design Research in the Department of Architecture.

He is the author of the book Self-Assembly Lab: Experiments in Programming Matter (Routledge, 2016), Active Matter (MIT Press, 2017), co-editor of Being Material (MIT Press 2019) and the Editor-In-Chief of the journal 3D Printing and Additive Manufacturing. He has exhibited installations in galleries around the world, including the Centre Pompidou, Philadelphia Museum of Art, Cooper Hewitt Smithsonian Design Museum, Victoria and Albert Museum and various others.

Awards include LinkedIn's Next Wave Award for Top Professionals under 35 (2016), R&D Innovator of the Year (2015), National Geographic Emerging Explorer (2015), an Inaugural WIRED Fellowship (2014), the Architectural League Prize (2013), Ars Electronica Next Idea Award (2013), TED Senior Fellow (2012) and 2008 he was named a Revolutionary Mind by SEED magazine.

Kevin Saey
Tutor, The Bartlett School of Architecture, UCL
Architect and Researcher, Automated Architecture (AUAR) Ltd.

Kevin Saey is a London based architect and researcher at design and technology consultancy Automated Architecture (AUAR) and Automated Architecture Labs at The Bartlett. He is invested in automation, digital fabrication and computational design. With his background in both architecture, game design and digital arts, he combines various interdisciplinary techniques to develop new and innovative systems, with a focus on innovative timber construction. Currently, he is an architectural design tutor in the B-Pro Program at the Bartlett.

He studied Digital Arts and Entertainment and Architecture in Belgium and obtained a post-professional masters from UCL The Bartlett, where he was awarded the Gold Price for his final project. His collaborative work with Gilles Retsin Architecture has been exhibited at the Tallinn Architecture Biennial in Estonia, the Royal Academy of Arts in London and Digital Futures in Shanghai.

Victor Leung
PhD Candidate, Gramazio Kohler Research, ETH Zurich

Victor Leung received his Bachelor of Arts in Architectural Studies from HKU in 2011 and Master of Science in Architectural Studies (Design and Computation) from MIT in 2016. Victor is currently a PhD candidate in ETH Zurich, working on robotic assembly methods of timber structures with integral timber joints. Victor is obsessed with designing and making custom robots/machines/end effectors for various types of fabrication. He is the technical co-founder of AWAWA timber research, which focuses on the design-to-production cycle of freeform timber joinery. From 2016 to 2018, Victor worked as a technical consultant for digital artist and architects in the realization of kinetic installation and digitally fabricated bespoke components. He has taught digital fabrication and computational design courses in MIT (Boston), ETH (Zurich), HKU (Hong Kong), SUTD (Singapore) and AA Visiting School (Hong Kong).

Encoding and Decoding Patterns of Planetary Urbanization

In 1986 the Earth System Sciences Committee from NASA Advisory Council raised the importance of an understanding of Earth Systems, and how the complex interactions among Earth's components affect its history and evolution. It emphasized humanity's new role as an active participant in the Earth's evolution and, therefore, the need to understand the consequences of human economic and technological activity on the Earth's biochemical cycles. This planetary perspective is rising among the academic community, bringing back epistemological questions that challenge a city-centric approach to the urban phenomenon. The alternative is the concept of "Planetary Urbanization" to describe the extensive, uneven urban fabric shaped in a neoliberal global context.

35 years after NASA's report, the Covid-19 Pandemic demonstrates how unsuccessful humanity is in facing global challenges. Similarly, the disciplines of the built environment seem to be poorly equipped to engage with this Planetary condition. This panel will discuss the positions and approaches that urban designers can adopt to take advantage of the advances in global observations, information systems, and computational methods for the analysis and planning of landscapes, urban and infrastructural systems in the context of Planetary Urbanization. How can we challenge the negative externalities and consequences of a capital-driven Earth System in which a large variety of agents interact in a non-linear way, returning different levels of organization and hierarchies, each of them ruled by their own laws?

This roundtable will bring together researchers with different areas of expertise around the analysis and modelling of natural and urban environments as complex adaptive systems, enquiring how global indicators and changes occurring at the Planetary scale require the incorporation of emerging disciplines. It will explore how the incorporation of decision-making and behaviour might help to inform design scenarios, in the context of a non-linear Planetary Urbanization.

Enriqueta Llabres-Valls (convenor)
Lecturer, the Bartlett School of Architecture, UCL
Mittelsten Scheid Guest Professor, Wuppertal University

Enriqueta Llabres-Valls is a Lecturer in Architecture and Urbanism at the Bartlett School of Architecture, University College London, and Mittelsten Scheid Guest Professor in the Faculty of Architecture and Engineering at Wuppertal University. She holds a degree in Architecture from UPC, Barcelona, and Local Economic Development from the London School of Economics. Her research interest expands from the studies of the built environment to local development concepts such as environmental policy and regulation, globalization, and inequalities.

In her career, she has focused on integrating the concept of Relational Capital in the design process. She leads with Zach Fluker Research Cluster 18 in the MArch Urban Design BPro at the Bartlett. Her career in the practice has been awarded on numerous occasions since she co-founded Relational Urbanism in 2009. In 2017 she co-founded LlabresTabony Architects; Relational Urbanism continues its mission as Relational Urbanism Lab under the umbrella of LlabresTabony Architects.

Michael Weinstock
Chair of Academic Committee,
Founding Director, Emergent Technologies and Design Programme, The Architectural Association School of Architecture

Dr Michael Weinstock is an Architect and a Fellow of the Royal Society of Arts. He is the Founder and Director of the Emergent Technologies and Design program and Director of Research and Development at the Architectural Association. Whilst his principal research and teaching have been conducted at the Architectural Association, he has published and lectured widely at many other schools of architecture worldwide.

His long-term interdisciplinary research agenda, *The Evolution of Sentient Cities*, focuses on the development of 'metabolic' and intelligent urban infrastructures that interconnect buildings, cities and conurbations with a special focus on the evolution of adaptive and responsive systems of existing cities and on developing new paradigms for sentient cities in extreme climates and ecological contexts. His upcoming book is titled "The Architecture of Intelligence: The Evolution of Sentience and the City" (Wiley Academy).

Ying Jin
Reader in Architecture and Urbanism,
Director, Martin Centre for Architectural and Urban Studies, University of Cambridge

Dr Ying Jin lectures on city planning, urban design, and urban modelling. He is particularly interested in understanding how technology, policy and human behaviour affect the development of cities and their infrastructure, and in using this knowledge to create new design solutions. At the Department of Architecture, he leads the Cities and Transport Research Group, which is one of the world's leading centres in the creation and use of conceptual and practical models for cities and city-regions. Among a wide range of research projects, Dr Jin leads the city-scale data science and urban modelling applications at the EPSRC Centre for Smart Infrastructure and Construction.

Dr Jin is the current Director of the Martin Centre for Architectural and Urban Studies, and is the lead convenor of the international symposia on Applied Urban Modelling. He currently leads the COVID-19 related modelling efforts in Cambridge within the Royal Society's Rapid Assistance in Modelling the Pandemic (RAMP) programme.

Rosalea Monacella
Design Critic in Landscape Architecture, Harvard GSD
Co-founder, OUTR Research Lab, RMIT

Rosalea Monacella is a registered Landscape Architect and has undertaken research on a number of cities around the world, and generated urban masterplans that explore design at the nexus of the urban and natural environments. She has been the recipient of a number of national and international awards and grants related to her practice-based research as co-founder of the OUTR Research Lab at RMIT University Melbourne, Australia.

Rosalea's expertise is in the transitioning of the urban environment through a careful indexing and shifting of dynamic resource flows that inform the landscape of contemporary cities. As Chief Editor for 10 years, she has led the development of Kerb Journal to become a significant publication in the discipline that engages and challenges the discourse of landscape architecture. She holds a PhD from RMIT University, a Master's in Landscape Urbanism from the AA School London, UK, and a Bachelor of Architecture from RMIT University.

TABLE OF CONTENTS

AI, Machine Learning and Generative Design

AUTOMATIC GENERATION OF SIGNBOARDS IN LARGE-SCALE TRANSPORTATION BUILDING DRIVEN BY PASSENGERS' PATHS

CHENGYU SUN[1], YINSHAN LIN[2] and SHUYANG LI[3]
[1,2,3] *Tongji University*
[1] *ibund@126.com* [2] *lilianlin003@163.com*
[3] *lishuyang1995@gmail.com*

Abstract. The signage design of any large-scale transportation building is vital to its passengers' wayfinding experiences. Firstly, a set of passengers' paths should be re-designed by signage designers according to the latest requirements, which always deviates from the initial ones in large-scale projects or inevitably updates during a long-term running. Afterwards, the path design has to be transformed into the layout and content of signboards manually. It is a time-consuming and error-prone process. This study introduces a human-computer hybrid workflow keeping the flexible path design in the hands of designers and leaving the following procedures to an algorithm, which automatically generates signboard contents ready for construction. It is proved efficient with more than 3000 signboards in the project of PVG Airport, Shanghai. Furthermore, the designer got an opportunity to optimize his path design through various alternatives, which impossible traditionally.

Keywords. Design Automation; Human-Computer Hybrid; Signboard; Passenger Path; Transportation Building.

1. Introduction

Signage system design is an important part of the public buildings. Especially in large-scale transportation buildings, the design quality will significantly affect the user's wayfinding efficiency (Berger, C, 2005). The traditional signage system design method is time-consuming and laborious, and the accuracy of the design is difficult to measure. Essentially, the signage system design is a generation process based on established rules, which can be described as a programming language. Therefore, the computer-aided design method can be adopted to intervene in the designer's familiar workflow to achieve a human-computer process.

1.1. TRADITIONAL DESIGN PROCESS OF SIGNAGE SYSTEM

The traditional signage design work is a sequential process. First, obtain and analyze the expected setting of passengers' paths based on the architecture design, and draw them on the building plan (see Figure 1). Secondly, according to the relevant design specifications and design experience, decide on the locations to set signboards where needed from all potential wayfinding decision points (Han, Y, 2010), that is, to complete the layout design of the signboards. Then, think

PROJECTIONS, Proceedings of the 26th International Conference of the Association for Computer-Aided Architectural Design Research in Asia (CAADRIA) 2021, Volume 1, 11-20.

over passengers' paths around the location of each signboard, installation form, and specifications of font and color to design the content of the signboards (Han, Y, 2010). Finally, the construction documents are compiled to guide where to be installed.

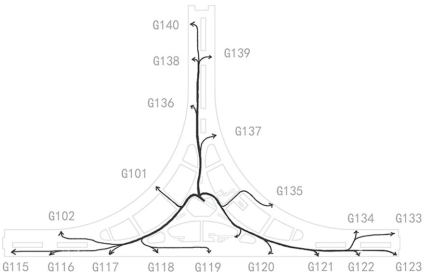

Figure 1. Passengers' paths drawn by designer.

The sequential design process means that once a modification occurs, the designer must restart the entire design, which restricts the design, update, and iteration of the signage system. In the large-scale transportation building, it contains complex passengers' paths. On the one hand, the design of the content on signboards is a tremendous workload, and it is fallible. On the other hand, although the initial passengers' paths are the most concise, they are the foundation of the whole design process, any changes to the paths will bring a series of follow-up revisions. The resulting content design and construction documents are highly repetitive and arduous.

1.2. COMPUTER AIDED DESIGN AUTOMATION

In the field of computer-aided architecture design, a direction called design automation develops rapidly in recent years. It mainly uses various algorithms to automatically complete the tasks with computable rules in the human's design process to improve design efficiency (Sun, C and Ke, X, 2016).

To aid the signage design, automation algorithms and tools are developed. Dubey, RK et al (2020) developed a tool named AUTOSIGN that automatically optimize the signboard layout with multi-criteria in office buildings. Fu, M and Liu, R (2019) found the coherence between interior main paths and the straight skeleton of its plan, with which their algorithm can generate paths from BIM models for the following automatic signage layout. Huang, H et al. (2017) proposed an automatic approach to generate a highly optimized signage layout and contents from a building plan. The idea is to involve the designer's evaluation and to adopt simulation agents to find out the design error.

Evidently, none of these algorithms or tools takes the signage designer's subjective intention on paths as a key input, which makes the automatic process a solo of computer. The requirements of a path design always deviates from the initial ones in large-scale projects or inevitably updates during a long-term running in the whole building life-time. Thus, how to involve the signage designer's key

input in an automation process becomes the main question for this study.

In the following, a human-computer hybrid workflow is introduced firstly. It keeps the flexible path design in the hands of designers and leaves the following procedures to an algorithm, which automatically generates signboard contents ready for construction. It takes the satellite terminal of Shanghai Pudong International Airport (Hereinafter PVG Airport) as an example to demonstrate the whole process. In the Grasshoppers' programming environment (including GH Python), the designer inputs the passenger paths and the signboards' layout designed by himself/herself; the content of the signboard and the construction documents are automatically generated according to the relevant design specifications and standards. The automation method can be embedded into the traditional design process, saving time for designers from repetitive work. Therefore, designers can focus on the optimization design of passengers' paths and layout of signboards, and continuously improve design quality.

2. Automatic Generation Method for the Signage Driven by Passengers' Paths

2.1. HUMAN-COMPUTER HYBRID AUTOMATION DESIGN PROCESS

A design process of signboards' content with human-computer hybrid is proposed, incorporating existing automation design algorithmic efficiency and passengers' paths drawn by the designer (see Figure 2). The basic steps are consistent with the traditional method. Only the following two steps are different: the computer 'automatic generation of signboards content', and finally the computer 'automatic storage construction document'. In this way, on the premise of retaining the designer's initiative to design the passengers' paths, the efficiency of computers can be fully utilized, and the design iteration period can be greatly shortened.

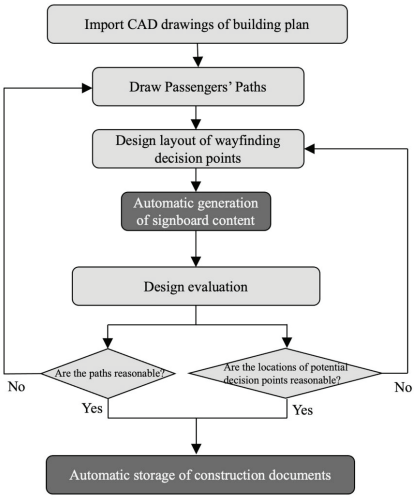

Figure 2. Human-computer hybrid workflow of signage system design (Note: dark grey - algorithm's operation, light grey - designer's operation) .

Hereafter, we take the optimization design of the signage system of the satellite terminal of PVG airport as an example to verify the feasibility and efficiency of this human-computer hybrid design process in the Grasshopper programming environment (including GH Python) of Rhino 3D.

2.2. IMPORT CAD DRAWINGS OF BUILDING PLAN

The designer imported the CAD drawings of the building plan into Rhino 3D. The Grasshopper programming identifies wall line, boarding gate names and locations, elevators, walkable area boundary and planar contour which are the corresponding geometric information in the two-dimensional building plan drawings.

2.3. DRAWING PASSENGERS' PATHS

Passengers' paths can be divided into one-direction and two-direction. Judging whether or not paths cross different floors we can classify them into vertical paths and horizontal paths. Vertical paths are usually organized by stairs, elevators, and escalators. Horizontal paths are divided into line, bifurcated line, ring, and grid type (see Figure 3). Among them, grid-type paths rarely appear in PVG airport, therefore, this research doesn't take grid-type paths into account.

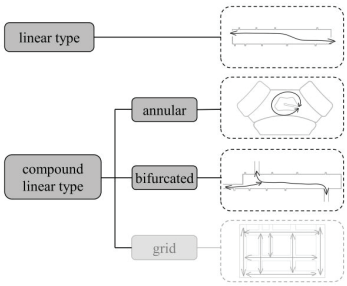

Figure 3. Classification of passenger paths.

The above several paths are combined to form the prototype of the passengers' paths in the building. The passengers' paths are the foundation of signage system design, and it is also the part that most reflects the designer's design thinking and intention. The designer uses the curve tools to draw various passengers' paths in the Rhino 3D (see Figure 1), which are read by the programming.

2.4. DESIGN LAYOUT OF WAYFINDING DECISION POINTS

After analyzing the two-dimensional building plan, designers can obtain the locations of the three types of wayfinding decision points. The target points (the black solid dot in Figure 4) are the boarding gate. The directional decision points (the gray solid dot in Figure 4) are located at the intersection of multiple paths or in a long corridor. The end decision points (the black hollow dot in Figure 4) are distributed evenly in a small corridor and look evenly distributed everywhere. On the building plan, the designer marks the wayfinding decision

points location where the signboard can be installed in the future. This is equivalent to a preliminary signboards' layout design, which is generally carried out following the relevant design specification 'Guidance System for Public Information-Setting Principles and Requirements (GB/T15566.1-2007)' in China. For example, along the passengers' paths, directional decision points should be arranged at all locations where passengers may choose from which direction to go. Besides, when the distance between two wayfinding decision points on the passenger's paths is too far, the directional decision points should also be added at a visible distance for the passenger.

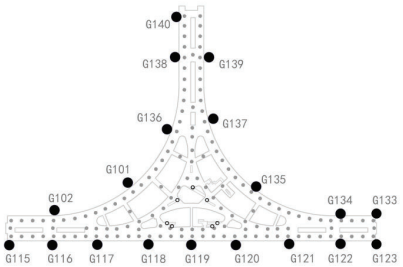

Figure 4. Decision points in international departure of satellite terminal 1 of PVG Airport (Note: black solid dots as target points; gray solid dot as directional decision points; black hollow dots as end decision points).

The algorithm contains a preset distance, when the distance between each wayfinding decision points and the passengers' paths is less than the preset distance, it is considered that the passengers' path through the wayfinding decision points. It gives designers more freedom to drawing the passengers' path in the building plan.

2.5. AUTOMATIC GENERATION OF SIGNBOARD CONTENT

Following the design specification of the signage system, the algorithm automatically generates the content of signboards according to the direction of the passengers' paths, the position of targets, and the direction of signboards.

Some signboards are fixed in their directions before the generation, such as boards under beams. In this case, the algorithm only generates their contents. While other signboards are free in direction of installation, which means the algorithm should generate not only the contents but also the directions according to visual accessibility of passengers along the paths. One signboard can show panels in two directions, and the contents in each direction are different. Therefore, a single signboard in reality is programmed as two pieces in computer programming. When the passengers' path is determined, two different algorithm situations are possible depending on whether the direction of the signboard is determined or not. The specific algorithm diagram is shown in Figure 5.

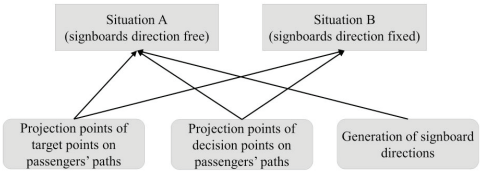

Figure 5. The algorithm of signboard generation.

2.5.1. PROJECTING THE TARGET POINTS TO THE PASSENGERS' PATHS

Due to the different attributes of the target points, their radiation range varies as well. In general, the service range of the restroom is larger than range of the boarding gate, so the radius of the restroom as a target point is larger than the latter. If there are obstacles (columns, wall, and other objects that hinder the sight) in the space, the service range of the target point will be fan-shaped. When the passenger path is within the range of the target point, the target point will be projected on his/her path (see Figure 6). When the path is bi-directional for the passengers, the both directions labeled as 'left-to-right' and 'right-to-left' in the figure should be calculated separately. According to the different directions of the passengers' path, two types of projections are created, either from right to left or from left to right. Taking G013 as an example, in the case of 'left-to-right' the algorithm will read the information of G013 before the toilet. When a signboard is located in the projection point of toilet, the content of this signboard will not contain the information of G013.

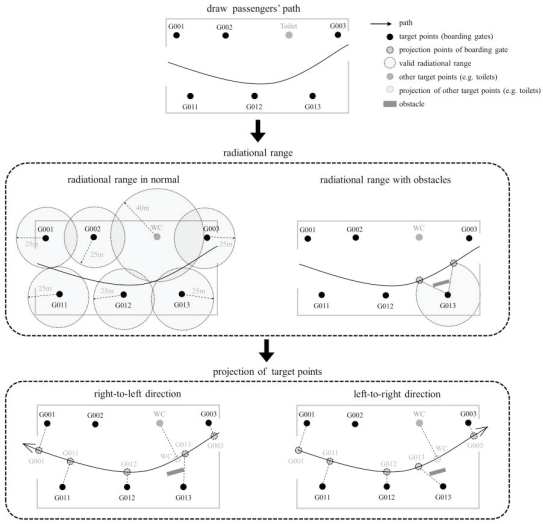

Figure 6. Projection of target points on the passengers' path.

2.5.2. PROJECTING THE DECISION POINTS TO THE PASSENGERS' PATHS

The projection of decision points has two possibilities: in situation A, the signboards' location is fixed but the direction free (see left part of Figure 7); in situation B, the signboards' location and direction are both fixed (see right part of Figure 7). Due to the variable of direction, the location of the projection of decision points will be changed accordingly.

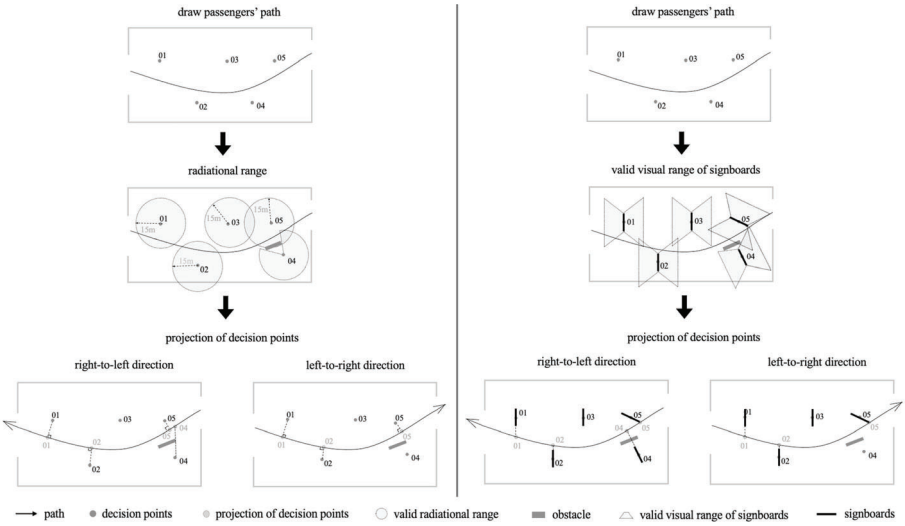

Figure 7. Projection of decision points on the passengers' path.

2.5.3. THE CONTENT OF SIGNBOARD BASED ON PASSENGER PATH AND SIGNBOARDS' DIRECTION

If the path is two-way, the front and back sides of the signboard need to be generated respectively. Based on the above generation principle, the contents of the signboard at the same decision point will alter in different directions of the signboard, namely, four results. In this section, one of the four is illustrated in Figure 8. Taking decision point 05 as an example, the direction of passengers' path is from right to the left, with the fixed signboard direction facing right. Thus, the content of signboard displays the information of the target points' projection that can be read on the path starting from point 05.

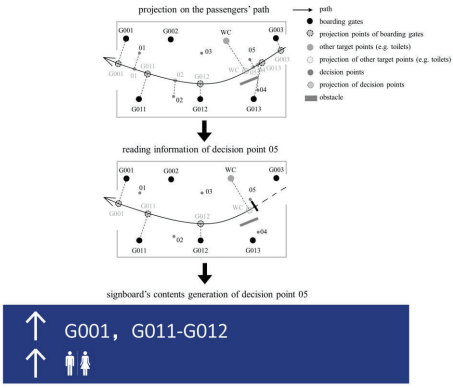

Figure 8. Decision point 05's signboard contents when signboard's direction is fixed.

2.5.4. PARAMETER OF SIGNBOARD CONTENT

The size of the font, font type, color, symbols, and format are formulated by parameters according to the local specifications. Therefore, the parameters can also be modified in accordance with the relevant specifications of various countries and regions.

2.5.5. SELECTION OF SIGNBOARDS SIZE

According to the contents generated by the algorithm, the minimum size of the signboard is estimated, and the choice is made among the common size according to the construction modules.

2.5.6. AUTOMATIC GENERATION OF SIGNBOARDS

Upon the above design and algorithm operation, the 3D signboard models are generated and can be previewed in the viewport of Rhino (see Figure 9).

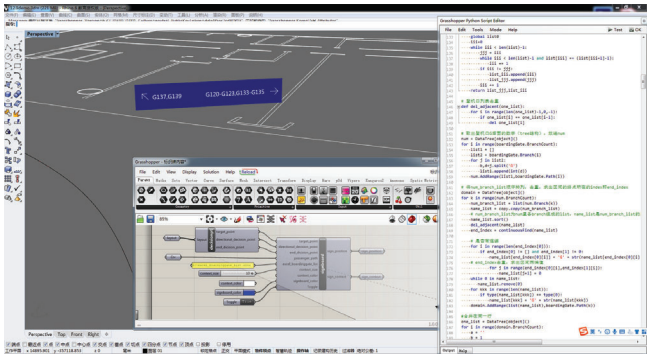

Figure 9. The algorithm and preview of automatically generated suspended signboard.

2.6. RAPID UPDATE OF PATH ADJUSTMENT

The process of path adjustment reflects the advantages of human-computer hybrid workflow. If the designer wants to adjust the passengers' paths, the contents of the signboards will also need to be modified. Meanwhile, the location of the wayfinding decision points can also be moved by the designer's intention.

For example: if the passengers' paths are changed due to the cancellation of gate G120, the designer only has to delete the path which leads to G120 (the bold black curve in Figure 10), then the content of the signboard located in the black dot position (see Figure 10) will change immediately (see Figure 11).

Figure 10. Passenger's path changed by the designer.

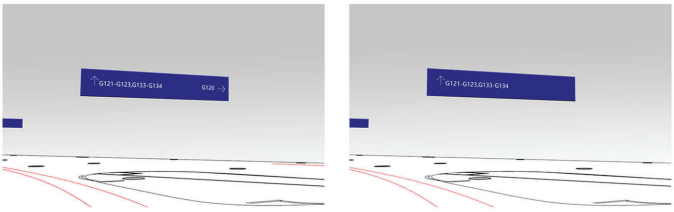

Figure 11. Content of signboard before (left) and after (right) passenger path change.

2.7. AUTOMATIC STORAGE OF CONSTRUCTION DOCUMENTS

Storage of construction documents is also automatically completed by the computer, which considerably improves the efficiency of compiling such documents, and eliminates the mistakes and omissions caused by the human operation. After the designer specifies a path to store the construction document, all signboards will be stored as the format of .bmp in the archive path. The file name is 'size + wayfinding decision points number'. For example, '3600_ 600_ 23.bmp' (see Figure 12) refers to the signboard with 3600mm in length and 600mm in height at the 23rd wayfinding decision points.

In this way, designers can quickly know the number of signboards and each signboards' size, which is convenient for designers to manage the signage system. Finally, it can also be directly delivered to people who produce and install signboards.

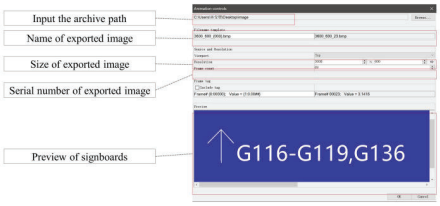

Figure 12. The export Interface of construction document.

3. Conclusion

This study provides a human-computer hybrid workflow supported by an automatic generation algorithm transforming passenger's paths into well-documented signboard contents in seconds. It reduces the labor cost significantly in large-scale projects and provides signage designers an opportunity to test various alternatives in the path design stage, which makes a quicker and better design possible.

Future research will focus on how the algorithm can automatically generate wayfinding decision points in a complex building plan through existing rules. At the same time, research will also focus on how designers can achieve an integrated human-computer hybrid workflow by adding, reducing, or moving computer-generated wayfinding decision points.

Acknowledgments

The research was supported by a project of Natural Science Foundation of China titled "An internet-plus-based approach of crowd simulation for public buildings" (no. 51778417), and the Shanghai Science and Technology Committee's project titled "Study and application of 3D modeling technologies in urban renewal regions" (no. 19DZ1202300).

References

Berger, C.: 2005, *Wayfinding: designing and implementing graphic navigational systems*, Page One Pub.

Dubey, R.K., Khoo, W., Moard, M.G., Holscher, C. and Kapadia, M.: 2020, Autosign: a multi-criteria optimization approach to computer aided design of signage layouts in complex buildings, *Computers & Graphics*, **88**, 13-23.

Fu, M. and Liu, R.: 2019, Automatic Generation of Path Networks for Evacuation Using Building Information Modeling, *Proceedings of Computing in Civil Engineering 2019*, 320-327.

Han, Y.: 2010, *Optimization Method Research of Sign-oriented Identification System in Large Passenger Station*, Master's Thesis, Beijing Jiaotong University.

Huang, H., Lin, N., Lorenzo, B., Darian, S., Wang, H., Pomplun, M. and Yu, L.: 2018, Way to Go! Automatic Optimization of Wayfinding Design, *IEEE Transactions on Visualization and Computer Graphics*, **24**(9), 2516-2530.

Sun, C. and Ke, X.: 2016, Method of Automatic Design Code Checking for BIM Models, *Building Science*, **32**(4), 140-145.

AUTOMATICALLY GENERATING LAYOUTS OF LARGE-SCALE OFFICE PARK USING POSITION-BASED DYNAMICS

SHUQI CAO[1] and GUOHUA JI[2]
[1,2]*School of Architecture and Urban Planning, Nanjing University, China*
[1]*dg20360001@smail.nju.edu.cn* [2]*jgh@nju.edu.cn*

Abstract. In this paper we propose an automatic layout algorithm using PBD (Position-Based Dynamic) for large-scale office park planning. Typically, the organization of buildings into a layout is a labor-intensive problem, and takes up most of designers' working time. Unlike Evolutionary Algorithms who has high computational cost, and GAN (Generative Adversarial Networks) whose constraints are not explicit, PBD can handle complex geometric constraints fast enough to be used in interactive environments. The high efficiency will not only accelerate the design iteration from draft to drawings, but also provide precious feasible sample for performance optimization. Furthermore, PBD is intuitive and flexible to be implemented which makes it a potential technique to be used in real design workflow.

Keywords. Generative Design; Automated Layout Generation; Position-Based Dynamics; Real-time Design Tool; Exploratory Design.

1. Introduction

Planning an office park, like all architectural layout tasks, is a labor-intensive problem. Besides satisfying complex topological and geometric constraints, designers also need to adjust their layouts constantly to pursuit perfect user experience and optimal environment performance. Obviously, arranging buildings with architectural criteria into a certain site is an iterative and complex task, which becomes ever less impossible as a manual process as the scale increases.

Automated computational techniques are considered to be feasible and necessary to address this dilemma. Multiple algorithms have been successfully developed to automate generation of floorplans, from more conventional ones such as exhaustive search, shape grammar and rule-based methods, to more recent ones such as heuristic search (performance-driven) and machine learning methods (data-driven). However, the existing algorithms, which are either small-in-scale, or time-costing, or loose-constrained, can't work well with the task of organizing a group of buildings on one site, as this task usually has less definite adjacency constraints and more strict geometric constraints (e.g., keeping minimum distance and assuring natural illumination). Additionally, we learned that designers are interested in computer's rapid feedback on whether their concept was feasible or

PROJECTIONS, Proceedings of the 26th International Conference of the Association for Computer-Aided Architectural Design Research in Asia (CAADRIA) 2021, Volume 1, 21-30.

not, and which feasible layouts their concept could be. The requirement places greater demands on the speed of layout algorithms.

This paper proposes a fast and controllable algorithm using Position-Based Dynamic (PBD) (Müller et al. 2007) to layout large-scale office park automatically. This strategy, which formulates layout problem as to position and orient a set of rigid bodies, has several early precedents applied to floorplan layout (Harada et al. 1995). The process of satisfying complex geometric constraints has been accelerated based on laws of dynamics. Then, PBD, one of the most state-of-the-art and universal techniques using computer animation, has further significantly accelerated the process. Meanwhile, the scalability and interactivity of this algorithm also contributes to its application of buildings layout design. Weiss et al. (2018) have applied PBD to indoor scene synthesis, and demonstrated that it can achieve results similar to conventional layout synthesis faster.

We implemented the algorithm in C# as a Grasshopper (GH) component library, and carried out a number of office park layout experiments. The present results show that the method can achieve multiple feasible solutions faster than universal optimization solvers commonly used on GH platform even if the scale is large and the constraints are relatively complex. In brief, the algorithm can be regarded as a potential technique to be implemented and promoted in the real design workflow.

2. Related work

There are years of research and diversity of approaches to various architectural layout problems. Our discussion mainly focuses on design tasks similar to office park planning. They are NP-complete problems, and early studies have shown that exhaustively enumerating cannot handle the exponential growth of possible arrangements as the size of the problem increases (Kalay 2004, p.241). Some procedural methods (Yang 2013) can model visually plausible urban scene, but they scarcely could satisfy architectrual criteria. Researchers have realized that the main challenge of this problem stems from the great number of geometric variables and complex constraints, which can only be solved using AI technology such as intelligent optimization algorithm and machine learning.

Genetic algorithms (GA), Evolutionary Strategy(ES), and other Evolutionary Algorithms (EAs), are regarded as a powerful tool for design explorations of performance-driven geometry in architectural design (Turrin 2011). As we know, most early applications such as Kämpf et al. (2010) have been limited to highly codified and regular basic templates. Yi and Kim (2015) successfully used GA to optimize the solar right of tall apartments with complex shape at the expense of tackling only 5 buildings. Compare with single-objective, multi-objective optimization has been valued more practical worth for synthetical consideration in design (Kim and Yi 2019). However, countless Pareto optimals just lead more inoperability to this task, and researchers in this field have to figure out how to interact with their user to select the “optimal” (Vierlinge 2018).

EAs can also be used to solve the numerous geometric constraints, and have proved their innovative abilities in part through their application to the generation

of floor plans (Rodrigues et al. 2017). Simulated Annealing (Merrell et al. 2010), Markov Chain Monte Carlo (Yeh et al. 2012) and Multi-Agent System (MAS) (Guo and Li 2017) are widely-used methods too. Nevertheless, all of these non-gradient stochastic optimization algorithms are extremely tedious to be implemented and expensive to be calculated. Therefore, few architects apply these methods to indeed support their design and creation process.

Making computational design process comes alive, interactive and exploratory might play a more utilitarian role for designers' creative work. As early as 1999, Arvin and House (1999) had introduced the concept of responsive design, and applying physically based modeling techniques to space layout planning. MAS is considered to be potential for interactivity with the same reason. But when it comes to real time response and knowing what designers want to do, existing instances are not persuasive enough up to now.

With the tide of Deep Learning in recent years, Data-driven generative design has back into view. The cases provided by Autodesk (Davis 2019), Spacemaker.ai (Chaillou 2019), and XKool Group has shown the surprising abilities of GAN (Generative Adversarial Networks). Although they can instantaneously convert a very simple draft to a complete drawing, the inherent weakness of these approaches cannot be denied–they are precedent dependent, i.e., we can't assure the accuracy of GAN when we just change a simple constraint different from its examples.

But the power of Machine learning is still inspiring. Accordingly, we believe that some state-of-the-art technologies in other fields can reinvigorate aged method. PBD is one of the most popular methods of nowadays interactive computer graphics community, and its superiority in layout synthesis has been proved. We propose the technique can play a more pragmatic role in computational design process.

3. Position-Based Layout

3.1. PROBLEM DEFINITIONS

An office park layout problem can be modeled as to position and orient a given number of buildings with different dimensions onto a given site while strictly satisfies the code, and then to find the arrangement which satisfies functional and aesthetic criteria given by the designer as much as possible. Thus, we express the buildings we need to arrange as a set of n buildings $B = \{b_1, b_2, \ldots, b_n\}$. Each $b_i \in B(i = 1, 2, \ldots, n)$ has (1) a position p_i, (2) an orientation θ_i, (3) an associated building shape mesh, (4) a set of associated agent model, and (5) an inverse mass w_i. The w_i is the reciprocal of the building's mass m_i, and the m_i is determined by the volume of the building shape mesh. $w_i = 0$ means that the building is immovable with infinite mass.

We express building code, and other design criteria as a set of m constraints $D = \{d_1, d_2, \ldots, d_m\}$. Each $d_j \in D(j = 1, 2, \ldots, m)$ consists of

- the set of nj indices $\{i_1, i_2, \ldots, i_n j\}, i_k \in [1, 2, \ldots, n]$ to find the buildings the constraint works with,
- a stiffness $k_j, 0 \leq k_j \leq 1$, and

- a function $C_j\left(p_{i1}, p_{i2}, \ldots, p_{i(nj)}\right)$ with the type of either equality or inequality.

If we measure the quality of a layout by how much the constraints are satisfied, we can introduce the conception of elastic potential energy. By loosely applying Hook's law, the potential energy may be considered as proportional to the square of embed-ding depths, so we employ the energy function $E = \sum_{j=1}^{m} \gamma_j C_j^2$,where γ_i is the respective weight of the constraints.

Obviously, it's a non-convex optimization problem, while the compulsory constraints make it thornier. From the review in previous section, we learn that designers hate EAs' inefficient and heavy-to-implement. For real-time interaction, we seek help from the most popular technique in interactive computer graphic, and is inspired by the lowest energy principle of the rigid bodies dynamics system (the potential energy will decline to the local lowest as the system convergences to its steady state). We find that the process of organizing buildings inside a boundary to satisfy multiple constraints is similar to the process of putting rigid bodies in a container to equilibrate various force. Hence, we propose that animation physics tech might help.

We first realized a simple prototype using Kangaroo, a live physics engine on GH, before we turned to PBD. For the same case (see Site1 in Section 4) , Kangaroo produced satisfactory results faster than Galapagos (based on ES and SA) (see top in figure 1). However, when we tested the more complex cases, we observed obvious drawback of Kangaroo in solving layout problem. First, in the Kangaroo's simulation process, some potential energy converts to velocity, which is redundancy. Second, owing to the collision constraints, one object can hardly across another to reach its more ideal position, which means the local optima. Third, it's difficult to represent some design criteria by directly using Kangaroo's existing constraints.

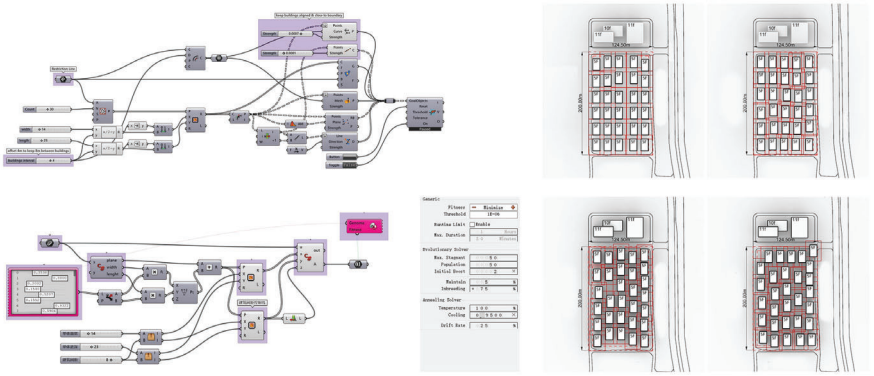

Figure 1. Top:settings and results using Kangaroo. Bottom:settings and results using Galapagos.

PBD, which is proposed by Muller, contributes to overcoming these faults. PBD omits the velocity layer from the traditional acceleration-velocity-displacement time integration, and immediately correct the position based on the solution of a quasi-static problem. Despite not as accurate as force-based methods, position-based approaches are fast, stable and controllable, which make them well-suited for use in interactive environment (Bender 2016). As we only care for the system's steady state, we can further ignore all the velocities, and directly work on the positions.

3.2. ALGORITHM OVERVIEW

In this Section we will overview the algorithm , and only explain the issues what is important or different from original PBD. Our algorithm is as follows:

```
(1) forall Buildings b_i do Randomly Initialize p_i, theta_i
(2) for SolverIteration=0 to Max do:
(3)    UpdateStiffnesses(C_1,...,C_m)
(4)    UpdateAgentModel(AM_1,...,AM_n)
(5)    GenerateCollisionConstraints(b_1,...,b_n)
(6)    if no collision constraints generated then return
(7)    ProjectConstraints(C_1,...,C_m)
```

Lines (1) just randomly initialize the position and orientation of buildings, for generating various and novel solutions. **Lines (2)-(7)** is an iterative solver which tried to adjust the positions of buildings or other points associated to the buildings to satisfy all the constraints. PBD applies the idea of Gauss-Seidel-type iteration (GS) to solve each constraints using the Project Constraints Function (**Line(7)**) independently one after the other, i.e., positions change immediately get visible to the process. Muller demonstrated the mechanism why GS can significantly speed up convergence in his paper, and suggested to solve the constraints in a random order to avoid oscillations.

In **Line(7)**, the Project Constraints Function finds the correction $\Delta\mathbf{p}$ to make $C(\mathbf{p}+\Delta\mathbf{p}) = \mathbf{0}$ in the fastest speed. The $\mathbf{p}$ is a set of positions of not only the buildings but the points associated to the buildings. Because only positions will change the value of constraints $C(\mathbf{p})$, we directly correct p instead of the orientation in the function. The gradient $\nabla_{\mathbf{p}}C(\mathbf{p})$ is the direction of maximal change, A first-order Taylor approximation $C(\mathbf{p}+\Delta\mathbf{p}) \approx C(\mathbf{p})+\nabla_{\mathbf{p}}C(\mathbf{p})\cdot\Delta\mathbf{p} = \mathbf{0}$ is used to linearize the constraint. The final displacement vector is determined by $\Delta\mathbf{p}_i = -s\nabla_{\mathbf{p}}C(\mathbf{p})$, where $s = \dfrac{w_i C(\mathbf{p})}{\sum_{i=1}^{n} w_i ||\nabla_{\mathbf{p}}C(\mathbf{p})||^2}$. Here, we also need a stiffness k obtained in **line (3)** to control the priority of different constraints. The process is analogous to finding local optimal solution using gradient descent, but the random initialization has provided a global view. In the following modifying, either with user or not, the drastic change of layout is not expected.

In **Line (3)**, we accepted Weiss's proposal to use dynamic stiffness. Starting from a random initial layout, stiffness of the collision constraints increases over time, and others decrease.

Line (4) updates the agent model of each building according to its real time position. In real planning task, besides the building entities, some virtual volumes, which be called agent models, also should be no overlap and fit other rules. A building might have several corresponding agent models which will change as the building moves, such as volume agent model, distance agent model, view field agent model, shadow agent model, and so on (see in figure 2). At present, all of our constraints are collision constraints between different agent models.

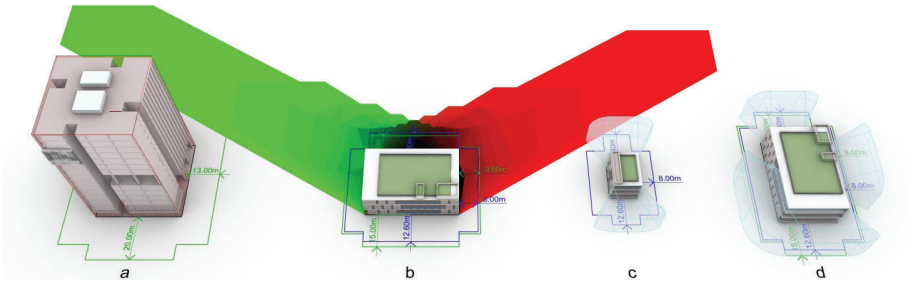

Figure 2. The greean and bule cruves are the outlines of distacne agent models which will be updated in different stations, and each building is showing its a:volume agent model. b: shadow agent model with time information represented by colour. c,d:view field agent model.

Line (5) generates collision constraints. Solving collision constraints is not different from solving general constraints, but there are many sophisticated collision detection approaches in the field of computer graphic. Generating collision constraints independently can accelerate the computation and reduce the number of constraints in **Line (7)**.

Line (6) checks whether all the compulsory constraints are satisfied, and terminates the iteration if true. We cannot assure a solution to an over-constrained situation, but our tests yet, even whose floor area rates and building densities are slightly over the limitation, can all be successfully solved in an acceptable time.

4. Case Studies

We selected two sites to test the ability of PBD method to deal with the layout tasks with regular boundary, small scale but compact constraints, and the layout tasks with irregular, large-scale and relatively compact constraints.

Site 1 is a completed office park in Dongguan City, Guangdong Province, China. Its boundary is almost a perfect rectangle, 124.5m wide, 200m long, with a total area of $2.49hm^2$. Its east side is adjacent to a road, and the location of its entrances are determined (see in figure 3a-3c). The local code limits the buildings setback line and the intervals between various types of products. We take the existing design as the baseline (see in figure 3d, 3e), and 3 types of products should be arranged. **15 Office Houses** with a floor area between $240 - 500m^2$, 4 floors, a height of 19m and a building area of no more than $1,600m^2$; **2 Semi-detached Office Houses** with a plane size of $30m \cdot 20m$, 4 floors and a height of 19m; **3 Multi-layer Office Buildings** with a plane size of $21m \cdot 52m$, 6 floors and a height

of 28m. Then, the plan has a total floor area of $9,476m^2$, a total buildings area of $44,456m^2$, a building density(BD) is 38%, and a Floor Area Ratio (FAR) of 1.78.

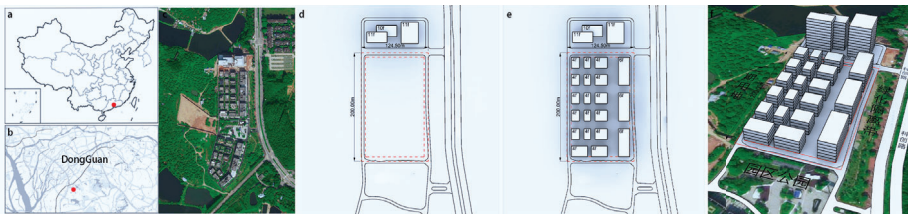

Figure 3. Information of Site 1.

Each product in our experiment is slightly smaller than the baseline, with BD of 35.9% and FAR 1.68. Using the smaller dimensions is a strategy for producing diverse results, and the results can easily exceed the baseline by further detail optimization. In a set of 800 tests, the average time per test was 11.18s, of which 798 were feasible results. Some of the results are shown in figure 4.

Figure 4. Some results of Case 1.

Site 2 is an undeveloped site in Danyang City, Jiangsu Province, China. Its boundary is very irregular, with an area of $12.6hm^2$. Its south side and west side are adjacent to the road, a residential area is on its north side, and its completed Phase I project is on its west side across a landscape lake. In addition to more complex boundary and interval limitation, this site requires a ceremonial entrance landscape in the southwest corner, two motor vehicle entrances settled autonomously, and an arrangement coordinated and connected with the phase I project. We manually draw control lines for these requirements (see in figure 5).

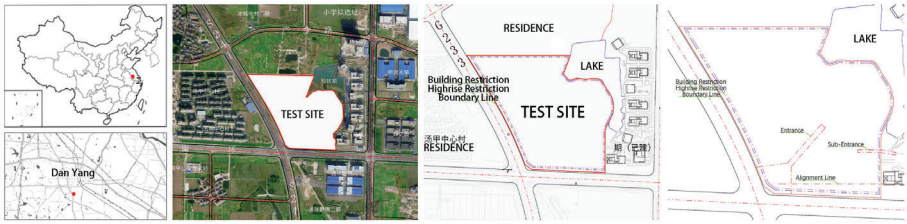

Figure 5. Information of Site 2.

A total of 92 products of 8 different types need to be arranged in the plot with the total building area of $107572m^2$, the total floor area of $28193m^2$, the FAR is 0.86, and the BD of 22.6% (see in figure 6).

PRODUCT TYPES	Office House1	Office House2	Semi-detached Office1	Semi-detached Office2	Semi-detached Office1	Multi - Layer Office	Highrise Office	Highrise Apartment
Building Massing								
Dimensions	11m*12m	18m*10m	24m*12m	30m*12m	30m*14m	40m*24m	35m*35m	32m*32m
Height	12.6m	12.6m	12.6m	12.6m	12.6m	20.7m	51.3	38.7m
Building Area	132 m^2	180 m^2	288 m^2	360 m^2	420 m^2	960 m^2	1225 m^2	1024 m^2
Floor Area	396 m^2	540 m^2	864 m^2	1080 m^2	1260 m^2	3840 m^2	14700 m^2	10240 m^2

Figure 6. Types, dimensions and quantities of the buildings should be arranged in Case 2.

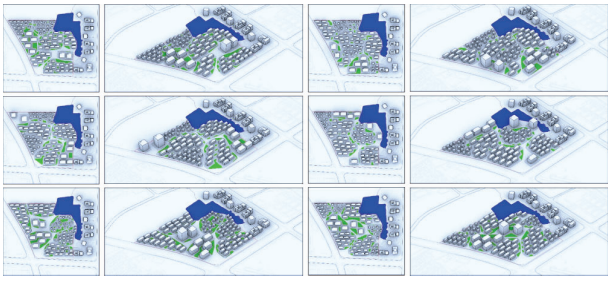

Figure 7. Some results of Case 2.

We added additional constraints to regularize the cluster boundary, and finally screened out the part of the automatically adjusted results (see in Figure 7), which

showing an overall diversity. Although the results still cannot be directly used as design, through the analysis and comparison of these possibilities provided by the computer, designers can draw many valuable preliminary design judgments.

5. Discussion

Our experiments have preliminary shown the advantage of Position-Based Methods using in Large-scale Layout. At present, it can organize a big number of buildings on a continuous planar space at low computational cost. Architectural design is a repetitive and iterative work. The high efficiency of converting from draft to drawings will accelerate the design iteration, and then contribute to the whole design process. At the same time, from random initial states, PBD can generate abundant solutions for comparison to achieve the layout with higher quality.

In our tests on the GH platform, PBD is faster than Galapagos by at least an order of magnitude with more satisfactory solutions, for the reason that it uses the gradient information what stochastic optimization solvers do not use. Compared with the faddish methods based on GAN, PBD provides more exact, multiple and scalable constraints, which makes the solutions provide more valuable information for design.

Another significant superiority of PBD is its flexible interaction mode. Working in akin way as Kangaroo (see in figure 8), our components can be smoothly understood and implemented by the designers who are familiar to GH, and the developer can easily promote or expand some functions of components separately. Furthermore, it is intuitive and flexible to define the buildings or constraints using our components. The conception should be simple from the user's point of view that moving buildings based on design intentions just like moving physical objects. The mechanism of PBD also supports to add, subtract or modify both buildings and constraints during the generation process. All of these make PBD more suitable in practical design environment.

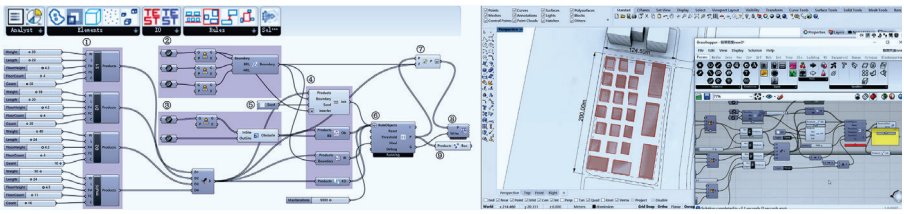

Figure 8. User Interface.

However, we cannot deny the inherent limitations of PBD that not all the design conceptions can be easily converted to position-related constraints. In the present study, we encoded some basic constraints relevant to layout design, and we will deal with layout constraints as broader as possible in our future work. Moreover, PBD could not optimize environmental performance, but it could help the search of precious feasible sample for stochastic optimization.

In our future work, more types of elements such as terrain, roads and

comprehensive buildings also should be introduced to our system. To optimize the user interface of inputting and manipulating design elements is also an interesting issue. From technical perspective, incorporating GPU parallelization or applying hierarchical approaches can further speed up the procedure, and how to update the stiffness in solution iteration is still an immature and ambiguous problem need to be explored.

References

Arvin, S.A. and House, D.H.: 1999, Making Designs Come Alive: Using Physically Based Modeling Techniques in Space Layout Planning, *Computers in Building: Proceedings of the CAADfutures'99*, Georgia Institute of Technology, Atlanta, Georgia, USA, 245-262.

Bender, J.: 2016, "PositionBasedDynamics" . Available from <https://github.com/InteractiveComputerGraphics/PositionBasedDynamics> (accessed 2rd December 2020).

Chaillou, S.: 2019, "ArchiGAN: a Generative Stack for Apartment Building Design" . Available from <https://developer.nvidia.com/blog/?p=15310> (accessed 2rd December 2020).

Davis, M.: 2019, "Could Machine Learning Improve Work-Life Balance in the Future of Architecture?" . Available from <https://redshift.autodesk.com/future-of-architecture/> (accessed 2rd December 2020).

Guo, Z. and Li, B.: 2017, Evolutionary approach for spatial architecture layout design enhanced by an agent-based topology finding system, *Frontiers of Architectural Research*, **6**(1), 53-62.

Harada, M., Witkin, A. and Baraff, D.: 1995, Interactive Physically-Based Manipulation of Discrete/Continuous Models, *SIGGRAPH '95*, New York, NY, United States.

Kalay, Y.E.: 2004, *Architecture*, MIT Press, Cambridge, MA, the United States.

Kim, H. and Yi, Y.K.: 2019, QuVue implementation for decisions related to high-rise residential building layouts, *Building and Environment*, **148**, 116-127.

Kämpf, J.H., Montavon, M., Bunyesc, J., Bolliger, R. and Robinson, D.: 2010, Optimisation of buildings' solar irradiation availability, *Solar Energy*, **84**(4), 596-603.

Merrell, P., Schkufza, E. and Koltun, V.: 2010, Computer-generated residential building layouts, *ACM SIGGRAPH Asia 2010*, Seoul, South Korea, Association for Computing Machinery: Article 181..

Müller, M., Heidelberger, B., Hennix, M. and Ratcliff, J.: 2007, Position based dynamics, *Journal of Visual Communication and Image Representation*, **18**(2), 109-118.

Rodrigues, E., Sousa-Rodrigues, D., Teixeira de Sampayo, M., Gaspar, A.R., Gomes, A. and Henggeler Antunes, C.: 2017, Clustering of architectural floor plans: A comparison of shape representations, *Automation in Construction*, **80**, 48-65.

Turrin, M., Buelow, P.v. and Stouffs, R.: 2011, Design explorations of performance driven geometry in architectural design using parametric modeling and genetic algorithms, *Adv. Eng. Inform.*, **25**(4), 656-675.

Vierlinge, R.: 2018, "Octopus | Food4Rhino" . Available from <https://www.food4rhino.com/app/octopus> (accessed 2rd December 2020).

Weiss, T., Litteneker, A., Duncan, N., Nakada, M., Jiang, C., Yu, L. and Terzopoulos, D.: 2019, Fast and Scalable Position-Based Layout Synthesis, *IEEE Transactions on Visualization and Computer Graphics*, **25**(12), 3231-3243.

Yang, Y.L., Wang, J., Vouga, E. and Wonka, P.: 2013, Urban pattern: layout design by hierarchical domain splitting, *ACM Trans. Graph.*, **32**(6), Article 181.

Yeh, Y.T., Yang, L., Watson, M., Goodman, N.D. and Hanrahan, P.: 2012, Synthesizing open worlds with constraints using locally annealed reversible jump MCMC, *ACM Trans. Graph.*, **31**(4), Article 56.

Yi, Y.K. and Kim, H.: 2015, Agent-based geometry optimization with Genetic Algorithm (GA) for tall apartment's solar right, *Solar Energy*, **113**, 236-250.

GENERATIVE DESIGN OF URBAN FABRICS USING DEEP LEARNING

JINMO RHEE[1] and PEDRO VELOSO[2]
[1,2]*Computational Design Laboratory, CRAIDL, Carnegie Mellon University*
[1,2]*{jinmor|pveloso}@andrew.cmu.edu*

Abstract. This paper describes the Urban Structure Synthesizer (USS), a research prototype based on deep learning that generates diagrams of morphologically consistent urban fabrics from context-rich urban datasets. This work is part of a larger research on computational analysis of the relationship between urban context and morphology. USS relies on a data collection method that extracts GIS data and converts it to diagrams with context information (Rhee et al., 2019). The resulting dataset with context-rich diagrams is used to train a Wasserstein GAN (WGAN) model, which learns how to synthesize novel urban fabric diagrams with the morphological and contextual qualities present in the dataset. The model is also trained with a random vector in the input, which is later used to enable parametric control and variation for the urban fabric diagram. Finally, the resulting diagrams are translated to 3D geometric entities using computer vision techniques and geometric modeling. The diagrams generated by USS suggest that a learning-based method can be an alternative to methods that rely on experts to build rule sets or parametric models to grasp the morphological qualities of the urban fabric.

Keywords. Deep Learning; Urban Fabric; Generative Design; Artificial Intelligence; Urban Morphology.

1. Introduction

Urban fabric is a key concept in urban design that consists of the configuration of streets, parcels, lots, and buildings (Oliveira, 2016, p. 8). It operates in the intersection of urban and architectural scale and can reflect important aspects of social phenomena and cultural practices. Given the importance of the configuration of the urban fabric in its inhabitants' lives, understanding, categorizing, and designing them has been a long-lasting challenge for design researchers.

In the past decades, there have been several studies on the computational synthesis of urban fabrics using different computational methods, such as multi-agent system (Biao et al., 2008), diffusion-limited aggregation (Koenig, 2011), rule-based system (Pellitteri et al., 2010), L-systems (Parish & Müller, n.d.), etc. While these computational methods can generate good results, they

PROJECTIONS, Proceedings of the 26th International Conference of the Association for Computer-Aided Architectural Design Research in Asia (CAADRIA) 2021, Volume 1, 31-40.

are limited to (1) modes of operation of existing generative models and (2) the designers' capacity to understand and encode the desired morphological qualities and contextual adaptations in principles, rules, and parameter calibration of the models.

In this research, we present Urban Structure Synthesizer (USS), a learning-based model to synthesize urban fabric diagrams that alleviate the reliance on knowledge explicitly embedded in generative models. Unlike rule-based or agent-based system, which depends on experts to create rules for generation, USS learns the morphological features of urban fabrics from data.

Firstly, we use a method to convert site data from GIS into diagrammatic images with contextual information introduced in the previous research (Rhee et al., 2019). After curating the site data with the desired patterns of urban forms and features, we use the resulting context-rich dataset to:

- train an analytical model that organizes the data into clusters with similar morphological types (Rhee et al., 2019).
- train a WGAN model to synthesize site-responsive diagrams of urban fabric based on the morphological qualities of the sites in the dataset (Figure 1).

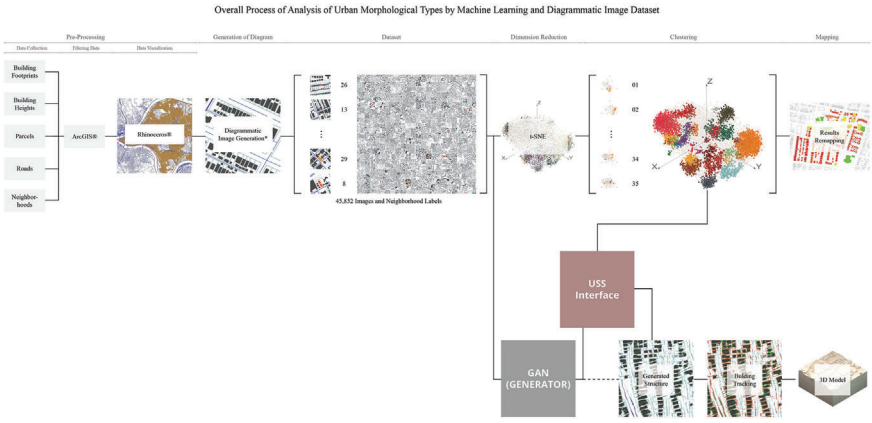

Figure 1. Two different processes: analysis (top) and generation (bottom) of urban fabrics using different machine learning models. USS interface connects the analytical and generative model.

2. Learning

2.1. DATA

USS employs a diagrammatic image dataset (DID), a data synthesis technique for raster images with a diagrammatic representation of two-dimensional building form and its neighboring urban contexts. Diagrammatic image representation in the dataset "offers two advantages in machine learning: low level of image noise

and support for custom selection of morphological information".(Rhee et al., 2019, p. 345).

Currently, the most popular way to create images of urban information is by using satellite and map images. Both methods can add unnecessary information or noise to the images. Therefore, a method such as image segmentation is typically employed to remove the noise of the representation for datasets based on satellite images. In contrast, diagrammatic image representation is synthesized from GIS information selected by the user, which preemptively removes or even excludes image noise from the dataset.

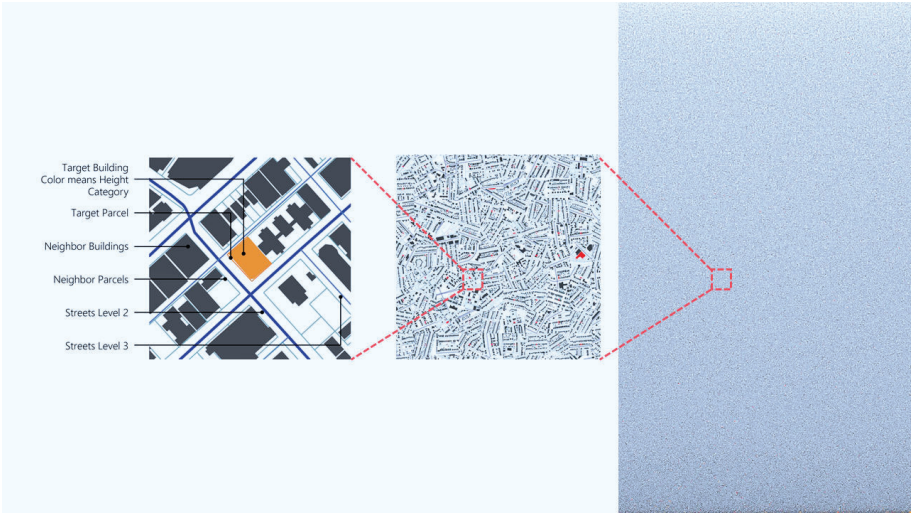

Figure 2. Composition of DID-PGH dataset in three different level.

Taking advantage of these qualities, we use DID to create a dataset of Pittsburgh, USA, which we will referreferred to as DID-PGH. DID-PGH comprises images with a target building placed on the center, and their neighboring building footprints, street network, and the parcel shapes around. The height of center building is represented through the color of the solid inside the polygon of the footprint. The more reddish color indicates that the building is lower, while the more yellowish color indicates that the building is higher. Each image is 512 x 512 pixels, and the dataset has a total of 45,852 images (see previous research for more information, Rhee et al., 2019).

2.2. GENERATIVE MODEL AND TRAIN

The selection of the generator for USS was based on an initial test of three different generative deep learning models for urban fabric synthesis: Variation Autoencoder (VAE), Generative Adversarial Networks (GAN), and Wasserstein Generative Adversarial Networks (WGAN). We compared the resulted images from each model after training all models with the context-rich dataset in the same training epochs. VAE resulted in the blurriest images. The images from GAN was

sharper than VAE's one, but it hardly captures the morphological features form the context-rich dataset. With more stable training, the images created by WGAN tend to be sharper than the images generated by the simple GAN.

USS specifically uses Wasserstein Generative Adversarial Networks - Gradient Penalty (WGAN-GP) (Gulrajani et al., 2017) as the model to generate new urban fabric diagrams based on the captured patterns of contextual and morphological features of the dataset. The overall structure of this model is similar to other Generative Adversarial Networks (GAN) model, except for some changes in the components of the optimization, such as the error function and the gradient penalty term. It has two networks: a generator and a critic. During training, the generator creates images conditioned on random input vectors, and the critic provides a value signal indicating how real each input image is. In the initial step of training, the generator synthesizes random images, and the critic provides random signals. The key to GAN lies in how we alternate the training of the two networks so that the generator becomes more adept at fooling the critic and the critic at identifying which observations are fake (Foster & Safari, 2019, p. 100).

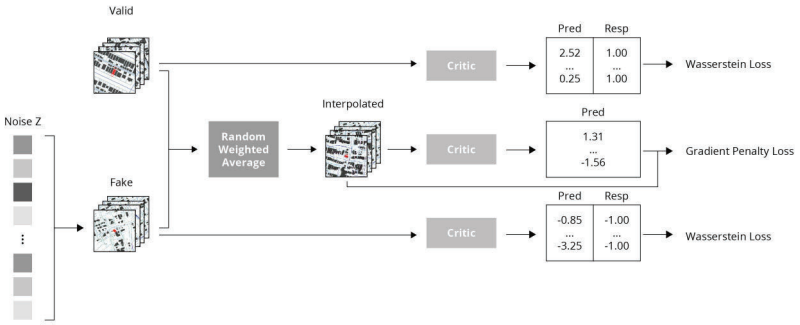

Figure 3. The structure of WGAN-GP model for training DID-PGH dataset.

In this research, the model generates a new urban fabric by learning patterns of contextual features of a given building. The generator of WGAN-GP creates an urban fabric image using a noise vector of size 100 as the input parameters.

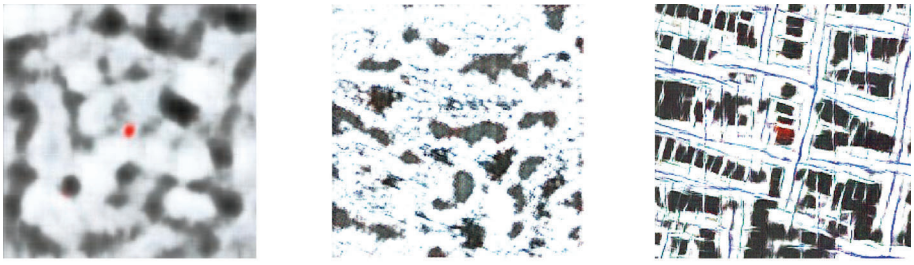

VAE GAN WGAN

Figure 4. Comparison of images generated by different deep learning models.

We trained this model for about 10000 batches (15 epochs) with 64 for batch size. The model's optimizer is 'Adam' (Kingma & Ba, 2017), and the learning rate is 2.0E-4. The model has no dropout layers, and both discriminator and generator use Leaky Rectified Linear Unit (Leaky ReLU) as the activation function. This model was trained on a computer with the following specifications: 'Intel(R) Core (TM) i7-8700k @ 3.70GHz', 64GB memory, and two GTX-1080ti graphic cards. It took almost 37 hours to train the model. The losses reduced significantly until 3000 batches, , and after that, the changes were subtle.

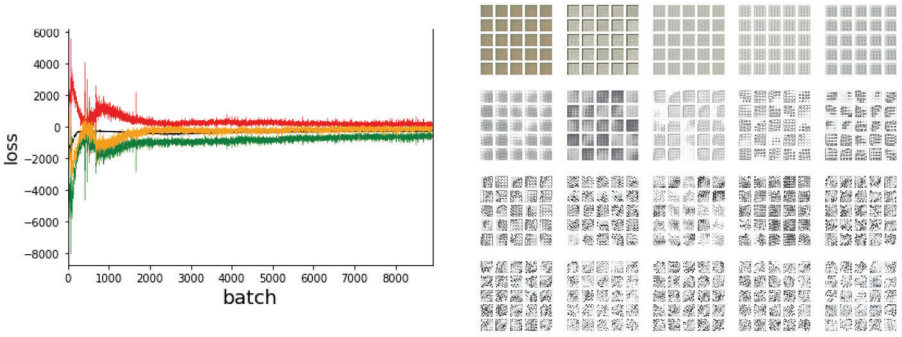

Figure 5. Changes of loss and image quality during the training process.

3. Design Implementation

3.1. USER INTERFACE

To generate urban fabric configurations, USS has an interface that relies on three steps: loading the trained model in the back-end, communication between front-end and back-end, and object tracking system.

When the USS is launched, the trained model is loaded in the back-end of the interface. Users can see an image of the urban fabric, sampled sliders, and buttons in the front-end fo the interface. The sliders represent the values of the noise Z vector for image synthesis. After training, each value of the vector can capture a design variation consistent with the design space of the original dataset. From the users' perspective, these sliders can be used to control morphological variations of the synthetic urban fabric in real-time. Although the original size of the vector is 100, we sampled 31 values that are represented as sliders in the interface. After manually changing the values of the sliders, the users can click on the 'GENERATE' button to pass the updated noise vector to the generator, which returns an updated synthetic image.

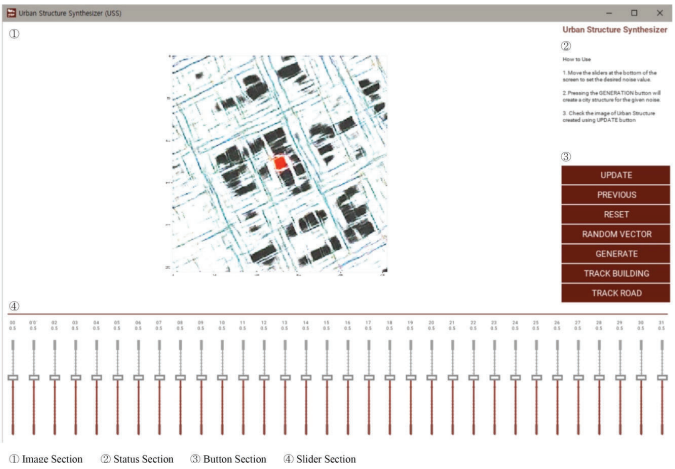

Figure 6. Interface of USS.

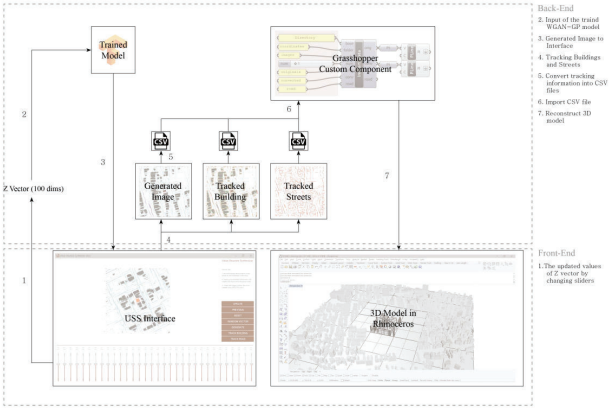

Figure 7. USS user interface system configuration.

To store the results, USS extracts the polylines of buildings and using OpenCV - a library for real-time computer vision. Each detected and tracked 2D information is reconstructed into 3D information using Rhinoceros®, the popular modeling tool in architectural design, and Grasshopper, a graphical algorithm editor tightly integrated with Rhinoceros.

Through custom components in Grasshopper, USS can communicate with Grasshopper in real-time and users can import the tracked object's outlines and its bounding boxes. After importing, users can see automatically reconstructed a 3D urban fabric based on the synthesized image from USS. USS tracks the color of the center building,converts the color value into height value according to the preset of color range, and saves this value so that users can import this height

information in Grasshopper to build a 3D model.

3.2. A DESIGN EXPERIMENT WITH USS

In order to test USS, we propose a speculative design exercise in Pittsburgh. The design uses USS to insert urban elements based on the morphological qualities of downtown Pittsburgh into the typical low-rise residential area of Shadyside. This exercise delves into the potential of how USS can be used for speculating about conflicts of scale and morphology.

Figure 8. The changes in urban fabric images according to the 25th and 11th feature slider values.

Firstly, a urban fabric grid is applied to the site. The tiles of the grid have the same range and size as the image to be synthesized by USS. Then, part of the existing urban fabric is removed from several grid tiles to secure the place for new tiles.

Figure 9. Urban fabric design process using USS.

Secondly, the downtown fabric tiles are customized, produced, and displayed in real-time based on slider values of the interface. Each slider captures different functional features. For example, the 11th slider influences the orthogonal arrangement of buildings and streets. The 25th slider controls the merging of buildings in the bottom center of the tile.

Designing an urban tile with sliders in USS consists of two main steps: global and local setting. The global setting loads a synthesized image of the desired urban

fabric through presets. The slider values will be changed according to the presets. The local setting contains adjusting the preset sliders for fine-tuning the global setting.

While the user changes sliders, USS uses the analytical model to show the types of urban fabrics that the currently generated image is most similar to. The analytical model becomes a visual guide that indicates how users can modify the global and local settings to design the intended fabric. When users finished modifying the sliders and press to confirm button, USS places the reconstructed 3D model of the fabric on the site. Repeating these adjusting and confirming process eight times, we have generated eight downtown-like urban fabric tiles.

USS is used to transplant the synthesized downtown urban fabric to the residential area of Shadyside. The downtown tiles are placed without rigid borders between the existing and newly proposed fabrics. Therefore, the existing residential grid was replaced by the downtown business grid, which meant that the proposed fabrics had to be re-aligned with the residential fabrics. Through this design process, a downtown-like organization was created in the given area.

3.3. DESIGN EVALUATION

The speculative design presented in the previous section resulted in a heterogeneous fabric at the center of the urban residential site in terms of building sizes, shapes, and the axis of the grid with the gradual changes at the periphery. The buildings in the proposed urban fabric are larger and higher than the buildings in the previous fabric. The grid axes of the previous fabric are almost orthogonal and form rectangular grid patterns. On the other hand, the proposed fabric has diagonal axes that form triangular grid patterns. This resulting urban collage exposes the contrast between the different morphologies with an intricate geometric model generated in real-time.

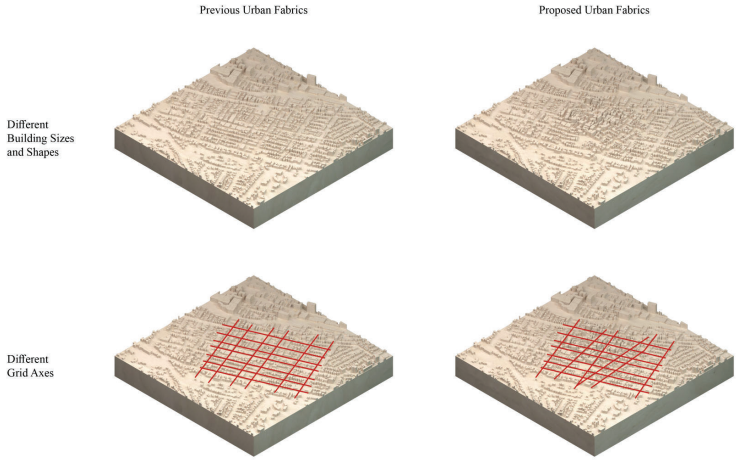

Figure 10. Comparison of the previous and proposed urban fabrics.

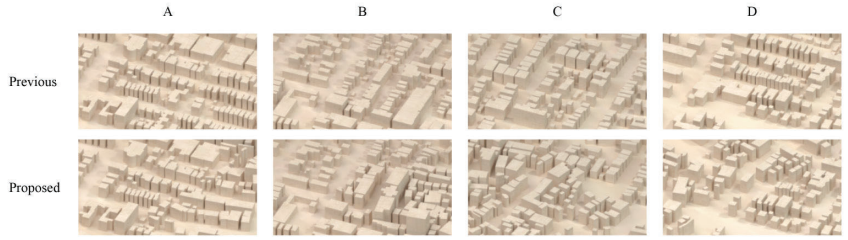

Figure 11. Different form of urban space in the previous and proposed urban fabrics.

Figure 11 shows the difference between the previous residential urban fabrics and the proposed business urban fabrics in detail. In cases A and B, the proposed fabric designed through USS has different size of buildings, clusters, and blocks, but keeps the existing street system and its axes. Cases C and D show that the streets in a new direction were created by utilizing characteristics of the existing fabrics. In the areas where different fabrics conflict, the periphery of the fabrics became indistinct by gradually changing the size of the buildings and directions of streets.

Our experiment shows the potential of USS to support a new urban design approach based on the investigation of urban fabric designs that are morphologically consistent. For example, like the experiment above, designers could create another downtown variation with multi-core structure (instead of uni-core) by preserving a the global downtown setting and exploring local solutions with the slides. Instead of explicitly modeling streets, building blocks, urban amenities, and public space, urban designers or planners can interact with real-time variations of fabric morphology on the site for design ideation.

4. Conclusion

USS illustrates the potential of using deep learning model in the generation of urban fabric, which enables designers not only to get access to the statistical features of datasets but also to produce novel designs from these features.

Through deep learning, it was possible to design a new urban fabric by extracting complex patterns from the existing fabrics and synthesizing the patterns according to a dataset curated by the designer. The deep learning-based design system is an alternative to generative systems that require human expertise to access and set generative rules and parameters. Learning-based systems can handle larger amounts of and more complex features than hand-craft rule-based and parametric systems. For example, in the design example of this study, the user did not define the rules of how to generate and position the new urban fabric. The deep learning model synthesized a new fabric by learning the pattern of the numerous existing fabrics. The learned function contains transformations that are potentially more complex and adaptive than rules explicitly defined by experts. Models based on more intricate rules can reveal design patterns and knowledge embedded in the built environment and, therefore, can support designers to devise

new design realms.

One of the main limitations of USS is the lack of control over the results. By relying on a random vector, the control of the variations of the result is not easy to grasp by the users. In order to extend USS to real-design applications, it is necessary to explore useful and reliable human-computer interactions and control mechanisms. There are some interesting alternatives from the generative modeling perspective, such as using paired datasets for a conditional generation. Considering that the dataset used in USS is already pre-processed, it is straightforward to derive custom diagrammatic controls such as the axes, masses (Zheng, 2018), connections in the border, etc. From the human-computer interaction, it is necessary to establish systematic studies with the users to identify adequate interaction modes with design variations.

References

Biao, L., Rong, L., Kai, X., Chang, L. and Qin, G.: 2008, A GENERATIVE TOOL BASE ON MULTI-AGENT SYSTEM, *Proceedings of the CAADRIA 2008*.

Foster, D.: 2019, *Generative Deep Learning : Teaching Machines to Paint, Write, Compose, and Play*, O'Reilly Media.

Gulrajani, I., Ahmed, F., Arjovsky, M., Dumoulin, V. and Courville, A.C.: 2017, Improved Training of Wasserstein GANs, *Advances in Neural Information Processing Systems 30*, 5767–5777.

Kingma, D.P. and Ba, J.: 2017, Adam: A Method for Stochastic Optimization, *ArXiv:1412.6980*.

Koenig, R.: 2011, Generating urban structures: A method for urban planning supported by multi-agent systems and cellular automata, *Przestrzeń i Forma (space & FORM)*, **16**, 353-376.

Oliveira, V.: 2016, *Urban Morphology: An Introduction to the Study of the Physical Form of Cities*, Springer International Publishing.

Parish, Y.I.H. and Müller, P.: 2001, Procedural Modeling of Cities, *Proceedings of the 28th Annual Conference on Computer Graphics and Interactive Techniques*, New York, 301–308.

Pellitteri, G., Lattuca, R. and Conti, G.: 2010, A Generative Design System to Interactively Explore Different Urban Scenarios, *Proceedings of the eCAADe2010*.

Rhee, J., Cardoso Llach, D. and Krishnamurti, R.: 2019, Context-rich Urban Analysis Using Machine Learning: A case study in Pittsburgh, PA, *Proceedings of the 37th eCAADe and 23rd SIGraDi*.

Zheng, H.: 2018, Drawing with Bots: Human-computer Collaborative Drawing Experiments, *Proceedings of CAADRIA 2018*.

PARAMTR V2

Human-Generative Design tools for prefabricating large-scale residential developments.

JOSHUA JOE[1] and ANTONY PELOSI[2]
[1,2]*Victoria University of Wellington*
[1]*joejosh@myvuw.ac.nz* [2]*antony.pelosi@vuw.ac.nz*

Abstract. Designers are encountering more issues with complexity, scale and performance requirements increase in residential projects. Prefabrication and generative design tools have the potential to significantly reduce construction time, cost, and material waste at scale. Building upon existing research, this paper further investigates how human-generative design tools can improve building performance and feasibility of prefabrication at scale whilst encouraging design variance. In this context, human-generative design tools refer to a partially algorithmic design tool that facilitates an open-box, collaborative approach to design. Following initial research-based design, a new human-generative tool was created (PARAMTR) to address the aforementioned issues using a design-based research methodology. Based on the research performed during the literature review and from initial design results, PARAMTR shows the potential to halve construction time on residential projects in combination with increased manufacturing efficiency. Design outputs share no design commonality, yet use almost 10 times less unique components across four houses when compared to existing residential projects. In combination with the overall benefits discussed and associated with prefabrication, material waste, cost, design time and complexity are expected to be reduced. The paper will discuss further progress towards designing and building smarter homes at scale.

Keywords. Generative design; generative prefabrication; parametric; residential; prefabrication.

1. INTRODUCTION

As the world's population continues to rapidly accelerate, cities and countries are now facing some of the largest housing shortages in history - a problem that New Zealand is not excluded from. Despite the explosive demand for more residential projects, existing design and construction practices have failed to adapt as quickly, resulting in additional cost, time and construction limitations when working at an ever-increasing scale.

PROJECTIONS, Proceedings of the 26th International Conference of the Association for Computer-Aided Architectural Design Research in Asia (CAADRIA) 2021, Volume 1, 41-50.

Residential subdivisions of near-identical design are painstakingly constructed by hand, traditionally and on-site, at the risk of weather, quality defects and construction delays (Shahzad et al., 2015). Additionally, houses designed at present are not well-optimised for climate performance, with over 40% of New Zealand's housing stock damp or mouldy (NZGBC, 2020), including new builds.

Such problems can be largely addressed with the manufacturing and technological advancements of recent years. BIM, generative tools and fabrication have evolved to the point where a synergy of manufacturing efficiency, variety, quality and data-driven performance can be achieved at scale, and this is what the research paper focuses on. The objective of this research was to create, implement and investigate generative tools and prefabrication to enhance, accelerate and optimise the design and construction workflow of residential projects at scale.

2. Literature review - overall prefabrication concepts

Instead of relying on a singular proprietary prefabrication system that may become obsolete, superseded or inferior in time, the authors created a generative system that works with the fundamental concepts of prefabrication consistent across most systems, methods and types. Understanding this underlying "logic" was particularly important when creating PARAMTR. From research performed during the literature review, it was found that prefabrication methodologies typically benefit from having standardized components with less variation (J. Betz, personal communication, June 11, 2020). However, when working on large-scale projects, variation is inevitable and often required (Jaillon & Poon, 2010). Successfully maintaining distinct levels of modularity and variability allows the designer and/or end-user enough choices without compromising the economic and manufacturing benefits of production at scale and in volume (Gravina da Rocha et al., 2019).

3. Literature review - the construction industry & prefabrication

The benefits of prefabrication have been widely documented, particularly at scale and in comparison, to other methodologies. A New Zealand-based study found that up to 50% time reduction could be achieved in residential projects with standardised designs at scale (Shahzad et al., 2015) when compared to traditional construction. Two primary issues were identified as stopping the widespread adoption of prefabrication at scale. Designers have often struggled to balance variability and consistency of parts, not only on singular but also multiple projects and in a variety of site conditions (Jaillon & Poon, 2010). Any changes would require reconsideration of either existing prefabrication or design, often restricting and limiting design ability. Secondly, lack of awareness, increased risk, capital cost and stigmatism around prefabrication has led to banks, developers and companies being hesitant to procure projects not using a "tried and true" construction approach (Kulla, 2019). In addition, one of the authors currently works for a company that is producing houses at scale, at high volume. Such companies have enormous buying power and with the constant vertical integration of design, consultants and construction services, could easily incorporate manufacturing allowing for end-to-end control and cost benefits at

scale.

4. Literature review - existing generative tools & software

As part of the literature review, the authors investigated several existing tools that fall within the research topics of this paper. The intention was to evaluate how a tool such as PARAMTR may contribute to existing work and research. A common limitation found amongst existing tools and research was that they often did not address or consider construction methodology. Tools such as Finch3D are "...a tool for Architects to leverage their designs in the early phases of a project" (FINCH, 2019) and are designed to accelerate the conceptual design process. Secondly, it was found that most tools do not actively take site conditions or climate performance into account. Whilst there are tools such as Ladybug Tools that provide accurate climate simulation, they mainly act as aids to an existing design, rather than actively creating, altering and developing design elements (Mackey & Roudsari, 2013). In addition, existing research highlighted the predominance of the "closed-box" computing approach, which has disadvantages when compared to an "open-box" approach (refer fig. 1). An open-box approach to generative tools allows for flexibility and adaptability, whilst avoiding the common weaknesses and limitations in both human and generative designers (Welch & Moleta, 2014). Prioritising the strengths and weaknesses of human and generative tools is particularly important when using these tools in an architecture and design context. Generative tools typically struggle to computationally "improve" design (Kalay, 1992), whereas humans struggle with vast amounts of data, numbers and complex problems with multiple variables (Peters & De Kestelier, 2013).

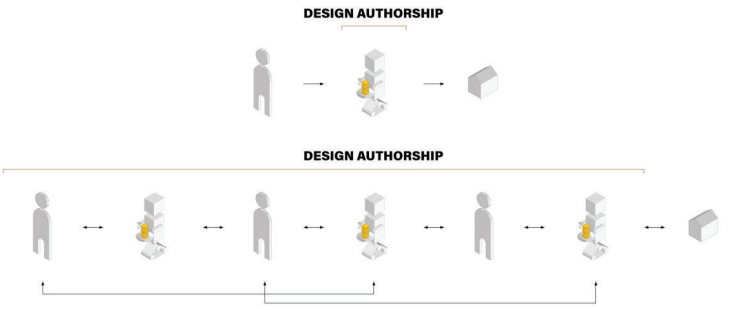

Figure 1. Whereas existing tools retain a 'closed-box' approach, PARAMTR was designed with an 'open-box' approach. Benefits of this approach include better collaboration between human and generative designer.

5. RESEARCH GOALS

PARAMTR aims to improve on existing prefabrication design strategies by enhancing designers with generative tools to reduce component complexity and variety. The tool also aims to balance standardization with flexibility, allowing for dynamic changes in both design and component variance on the fly. Finally, PARAMTR v2 should take into consideration climate performance and prefabrication logic, to ensure that any designs generated can be easily adapted to multiple systems and sites using the tool.

6. RESEARCH METHODS

6.1. RESEARCH FOR DESIGN

Research for design was performed at the start of the research with an in-depth literature review. The authors chose to perform a literature review to identify common weaknesses and strengths in existing research and software tools before producing PARAMTR. Relevant material was sourced from conference papers, peer-reviewed theses, books and digital tools used for investigation. Additionally, research for design was also performed throughout the design-based research phase. Although this method of research does not address personal opinion or theory, it ultimately resulted in more focused, efficient and relevant information gained before and during the design-based research phase. Identifying the existing context of the research was insightful and prevented the authors from 'doubling up' on existing work, whilst improving on and contributing to new areas of research.

6.2. DESIGN-BASED RESEARCH

As the research is evaluating the development and implementation of an enhanced generative system, design-based research was critical. Continual, rapid design-based research was critical for the authors to develop the generative tool in an agile, effective manner in response to both findings and additional research performed throughout the research period. The authors utilised a versioning number system with continuous evaluation before the development of the next version. Evaluations performed by the authors assessed computational, logical and practical constraints, with the next version addressing or eliminating any issues identified.

Based on the research performed in section 2.3, a combination of Rhino 7 and Grasshopper was chosen for the software platform of which this research uses. Grasshopper is a visual scripting generative program that interfaces with the popular BIM/CAD tool Rhinoceros 7. In addition to easily supporting workflows to Revit (a BIM program common in the architecture industry) (McNeel & Associates, 2019), the authors were familiar with both programs, which allowed for more time spent on the research rather than learning. Design-based research as a methodology was highly effective for this research due to the constant loop of investigation, design, evaluation and refinement. The authors could rapidly develop PARAMTR using software tools that enable agile, flexible and rapid research. Without design-based research, PARAMTR would not have been as rapidly developed or have fewer substantial findings.

7. PARAMTR v2 - how does an enhanced generative tool accelerate prefabrication at scale?

Whilst previous research documenting PARAMTR v1 focuses on the implementation of shared authorship and generative design strategies in residential design, this paper documenting PARAMTR v2 focuses on the feasible implementation of generative prefabrication tools particular focus on the produced outputs and prefabrication benefits (Joe & Pelosi, 2020). Although the tool itself is complete, the research is still in progress and thus any evaluation or conclusions reached are subject to change.

8. PARAMTR v2 - strategy, logic & methodology

A strategy was formed to implement efficiency and dynamic prefabrication using generative tools. Based on the research performed in sections 1.1-1.3, the underlying concept of prefabrication to be used in PARAMTR was clear - reduce the number of unique components, whilst balancing design variability and flexibility. A balance between human and generative tool was achieved by delegating all design aspects to the human, with all complex number and data-based problems handled by PARAMTR. As per the research in section 1.3, this ensured that each was performing tasks in their best strengths and with reduced weaknesses. This strategy begins from the initial conceptual design phase, where rooms and overall dimensions are standardised to identical dimensional tolerances (such as to the nearest 1000mm, 600mm etc). These tolerances mean the conceptual designs produced are practically constructible and adjustable to suit, with timber lengths to the nearest metre and plasterboard sheets typically in 600mm widths. Additionally, from the authors' industry experience overall dimensions are rounded regardless, with overall dimensions having little effect or limitation on the overall design. The initial floorplan is generated by PARAMTR, with additional design tweaks and circulation performed by the designer. This was found to be far more efficient compared to letting the generative system handle all design, which added 1-2 hours as opposed to the 4-5 minutes for a single author to make similar adjustments.

PARAMTR takes a "process of elimination" approach to prefabrication, with wall elements then gradually separated into smaller subsets depending on their function and requirements. Regardless of construction system, exterior and interior walls will differ in terms of both structural and environmental requirements. For this reason, walls are divided based on if they are exterior or interior. Exterior walls are then created with generatively informed windows (see section 3.5) that balance climate performance across all designs in all instances of each wall. Interior walls are then separated into those that do or do not require doorways (which will change construction requirements when compared to a uniform wall). The generative system then dynamically standardises components until there are a few unique parts as possible across all designs and all wall instances, exterior or interior (refer fig. 2). The result of this approach to generative prefabrication is a near-real-time system that can dynamically adapt to design changes, whilst maintaining manufacturing efficiency and climate

performance at scale. Section 3.5 will further discuss the results.

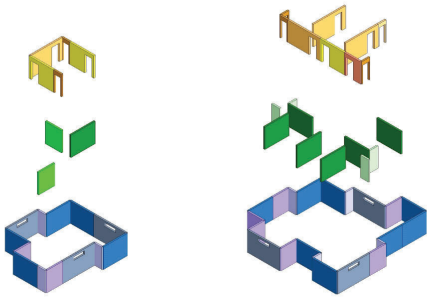

Figure 2. Wall components were optimised to as little variance within three categories - exterior, interior, and interior with door openings. .

9. PARAMTR v2 - results

As part of the ongoing research, initial design concepts were produced earlier this year based on an earlier version of PARAMTR (v1). 4 designs were produced generatively using PARAMTR v1 that shared no design commonalities in terms of layout, floorplan or type with unique program requirements, unique site conditions and priorities. These were then run through PARAMTR v2's new prefabrication logic to optimise the designs for standardised parts. Despite containing 127 total wall elements, only 16 elements were unique (refer fig. 3). By comparison, a single residential project with 42 total wall elements contained 33 unique elements. PARAMTR v2 represents a massive improvement in potential manufacturing and design time efficiency, with a single author able to produce all 4 designs in 90 minutes. When considering prefabrication, climate considerations and the sheer number of contributing factors dedicated to making design decisions with this logic, it would take a human designer far more time to reach the same level of complexity and efficiency at scale.

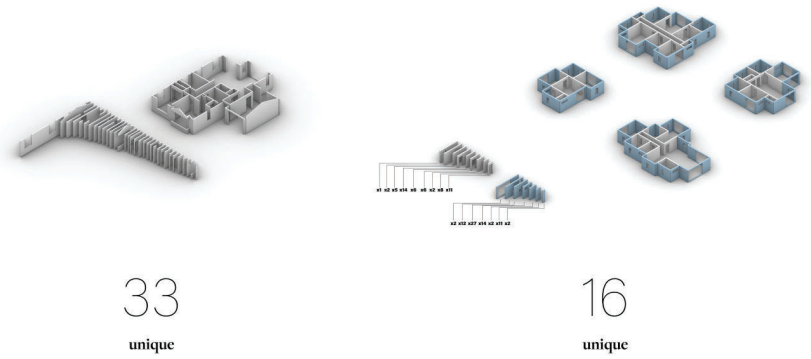

Figure 3. Four designs produced using PARAMTR v2 share 16 unique elements, whereas a single standard residential design has 33. Reduced variance in parts means increased manufacturing efficiency at scale.

PARAMTR v2 includes improvements designed to further reduce time spent and improve the overall practicality and quality of designs produced. Version 2 of PARAMTR includes a user interface (refer fig. 4) for faster workflow (which hampered time efficiency in v1), the ability to optimise up to 8 unique designs for prefabrication and also automatically size windows based on sunlighting performance per design, per wall instance, per location across all designs. It is also worth pointing out that the number of designs that could be optimised at once is arbitrary. Due to a limitation in Grasshopper, the authors have to manually add additional code repeaters for each additional design to be optimised - in theory, PARAMTR could evaluate and optimise 8 or more designs with a similar or greater level of efficiency.

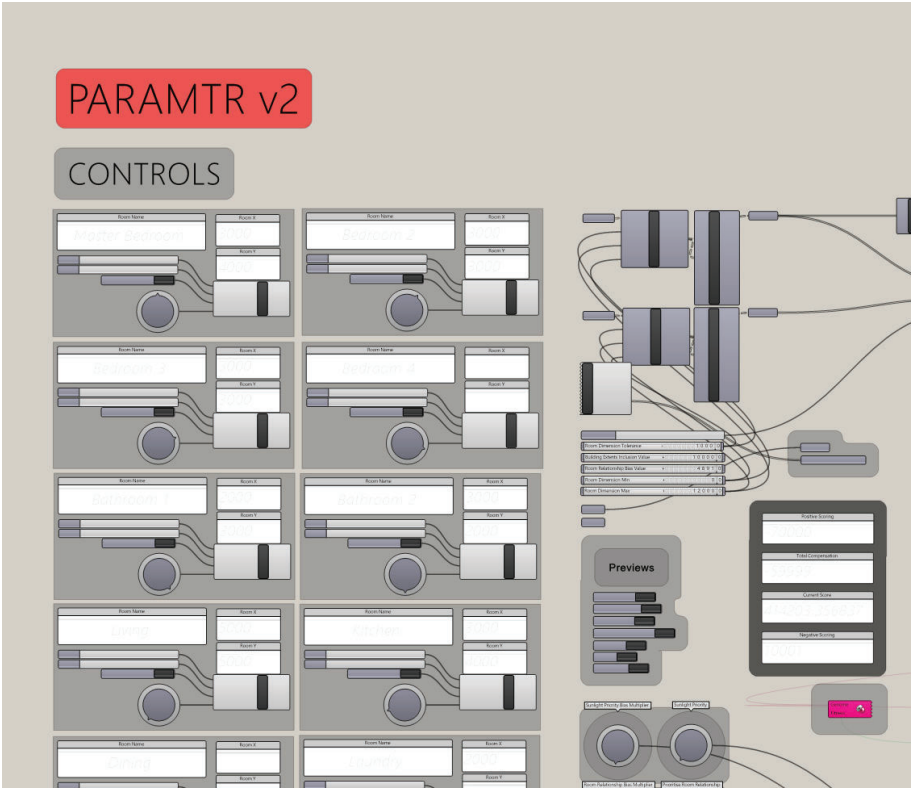

Figure 4. Amongst PARAMTR v2's improvements, a UI was developed which drastically reduced error rates and increased time efficiency when compared to v1.

Research to date in sections 1.1-1.3 indicates a construction time reduction of up to 50% (Shahzad et al., 2015), with significant economic gains and quality increases due to the benefits of manufacturing using economies of scale (Orlowski, 2020). Future research will address and evaluate tangible observations at a greater level of detail.

10. Critical reflection

Based on current research, the potential for a system such as PARAMTR to radically improve residential projects at scale is clear. Alongside massively reducing the overall design complexity and time associated with prefabricated residential projects, the benefits of prefabrication bring reduced material waste, construction time and cost. These benefits are particularly important at scale, where the rate of improvement is exponentially increased across multiple, large-scale projects. In addition, PARAMTR encourages design variance, with better performing, unique designs and with designers focusing more on the design rather than the numbers, data and calculations. This falls in line with the authors' goal of producing more houses at scale, better, faster and more cost-effectively.

However, the downside of PARAMTR's agnostic approach to prefabrication means that no specified prefabrication system or connections have been considered. In response, the authors will address this in future with the evaluation of existing prefabrication systems to demonstrate the feasibility of integrating PARAMTR. Additionally, the approach of production at scale requires extensive manufacturing facilities, of which there are few in New Zealand. These downsides should be considered when implementing a system such as PARAMTR, which may require tailoring to meet specific system and regional requirements.

In terms of limitations, this approach has only been applied to wall framing, with the current system designed for "green-field developments" - single-storey developments on relatively flat terrain. Whilst this is a limitation, the authors recognise that subdivisions are commonly built on mostly flat terrain in New Zealand, with most residential projects utilising a slab on grade for their flooring system. A similar approach could easily be taken to optimise the roof and flooring systems of houses at scale, based on existing research, systems and findings to date.

11. Conclusion

Research on PARAMTR proves that there are superior ways of designing and building residential projects at scale. Lack of innovation has cost the industry in time, cost and complexity. With generative tools and prefabrication advancing at a rapid pace, it is now possible to use these tools at scale to improve design and construction processes when working at scale. PARAMTR proves that combining a human-generative approach with prefabrication has the potential to reduce construction time by up to 50%, enable designers to produce 4 optimised, unique designs in under 2 hours and in turn increase productivity and quality for the masses. The authors imagine PARAMTR integrating into large-scale BIM developments, accelerating design processes whilst reducing construction cost and time. A tool like PARAMTR facilitates the ability to create greater design variety at scale, whilst substantially improving cost and time efficiency.

The research will continue to assess and evaluate the design outputs produced by PARAMTR, with tangible evaluations on aspects such as cost, time and quality benefits performed. The authors have chosen to not consider specific systems of prefabrication in the interests of keeping PARAMTR v2 agnostic to any prefabrication methodology. Future research could investigate creating a prefabrication system suitable for generative prefabrication, or investigate ways of designing with an existing, generated range of wall components.

The future in human-generative tools brings many benefits to an industry constantly struggling with an bespoke approach to construction and design. Research and implementation of forward-thinking technologies will enable our ability to build faster, at greater scales and more cost-effectively to rectify the global housing shortage.

Acknowledgements

This research was made possible by the BRANZ and Building Research Levy.

References

McNeel \, R.: 2019, “Rhino 7 Features” . Available from <https://discourse.mcneel.com/t/rhino-7-features/80163>.

Harness, C.H.: 2020, “TestFit Home” . Available from Library Catalog: blog.testfit.io<https://blog.testfit.io>.

Jaillon, L. and Poon, C.S.: 2010, Design issues of using prefabrication in Hong Kong building construction, *Construction Management and Economics*, **28**(10), 1025-1042.

Kalay, Y.E.: 1992, *Evaluating and predicting design performance*, Wiley, New York, N.Y.

Mackey, C. and Roudsari, M.: 2013, “Ladybug Tools” . Available from <https://www.ladybug.tools/ladybug.html>.

NZGBC, N.: 2020, “Budget boost for warmer homes will bring healthy, safe places for New Zealanders but leaves thousands in the cold.” . Available from <https://www.nzgbc.org.nz/KNOWLEDGEHUB/Story?Action=View&Story_id=563>.

Orlowski, K.: 2020, *Automated manufacturing for timber-based panelised wall systems*, Ph.D. Thesis, University of Melbourne.

Peters, B. and De Kestelier, X.: 2013, *Computation works: the building of algorithmic thought*, John Wiley \& Sons, Chichester.

Gravina da Rocha, C., El Ghoz, H.B. and Jr Guadanhim, S.: 2019, A model for implementing product modularity in buildings design, *Engineering, Construction and Architectural Management*, **27**(3), 680-699.

Shahzad, W., Mbachu, J. and Domingo, N.: 2015, Marginal Productivity Gained Through Prefabrication: Case Studies of Building Projects in Auckland, *Buildings; Basel*, **5**(1), 196-208.

Wallgren, J.W.: 2019, “FINCH” . Available from Library Catalog: finch3d.com<https://finch3d.com/>.

Welch, C. and Moleta, T.J.: 2014, Selective Interference: Emergent Complexity Informed by Programmatic, Social and Performative Criteria, *ACADIA 2014*, **34**, 719-726.

OPTIMIZING CONTAINER HOUSING UNITS FOR INFORMAL SETTLEMENTS

A parametric simulation & visualization workflow for architectural resilience

JAYEDI AMAN[1], NUSRAT TABASSUM[2],
JAMES HOPFENBLATT[3], JONG BUM KIM[4] and
MD OBIDUL HAQUE[5]
[1,3,4]*University of Missouri Columbia*
[1,3]*{jayediaman|jphf39}@mail.missouri.edu* [4]*kimjongb@missouri.edu*
[2]*Institute for Advanced Architecture of Catalonia*
[2]*smita.aust@yahoo.com*
[5]*Premier University*
[5]*obidul.line@gmail.com*

Abstract. In rapidly growing cities like Dhaka, Bangladesh, sustainable housing in urban wetlands and slums present a challenge to more affordable and livable cities. The Container Housing System (CHS) is among the latest methods of affordable, modular housing quickly gaining acceptance among local stakeholders in Bangladesh. Even though container houses made of heat-conducting materials significantly impact overall energy consumption, there is little research on the overall environmental impact of CHS. Therefore, this study aims to investigate the performance of CHS in the climatic context of the Korail slum in Dhaka. The paper proposes a building envelope optimization and visualization workflow utilizing parametric cluster simulation modeling, multi-objective optimization (MOO) algorithms, and virtual reality (VR) as an immersive visualization technique. First, local housing and courtyard patterns were used to develop hypothetical housing clusters. Next, the CHS design variables were chosen to conduct the MOO analysis to measure Useful Daylight Illuminance and Energy Use Intensity. Finally, the prototype was integrated into a parametric VR environment to enable local stakeholders to walk through the clusters with the goal of generating feedback. This study shows that the proposed method can be implemented by architects and planners in the early design process to help improve the stakeholder's understanding of CHS and its impact on the environment. It further elaborates on the implementation results, challenges, limitations of the parametric framework, and future work needed.

Keywords. Multi-objective Optimization; Building Energy Use; CHS; Informal Settlements; Parametric VR.

PROJECTIONS, Proceedings of the 26th International Conference of the Association for Computer-Aided Architectural Design Research in Asia (CAADRIA) 2021, Volume 1, 51-60.

1. Introduction:

Making cities and settlements sustainable, inclusive, and resilient is one of the UN's seventeen goals for sustainable development. Additionally, ensuring universal access to affordable, appropriate, and safe accommodations for slums is its primary goal (UN, 2015). However, in rapidly growing cities like Dhaka, Bangladesh, sustainable housing has become an increasingly significant problem and does not reflect the concept of an affordable, livable, and equitable city to all its residents (RAJUK, 2015). Within the metropolitan area of just ˜300 square kilometers, Dhaka houses well over 12 million people (BBS, 2009), which is projected to grow to 26 million by 2035 (RAJUK, 2015). Currently, most low-income communities already reside in sub-standard unsustainable conditions in urban wetlands scattered within Dhaka, requiring immediate critical intervention, as the expected population growth is expected to worsen the issue. Worldwide, slums accommodate nearly 1 billion people, representing one-third of the global urban population. Dhaka accommodates a total of 3.5 million slum occupants (Fan et al., 2017), and current materials used for constructing the houses in informal settlements are prone to fire and natural calamities.

Module-based housing out of recycled containers is a construction practice that is currently gaining acceptance in the building industry. Due to the globalization of supply chains, over 17 million used shipping containers exist globally (Steve, 2019). This surplus has initiated a trend towards the usage of these as construction units in architecture. Bangladesh has seaports and riverports, which prompted container housing units to become popular among local urban wetland dwellings. In general, the containers can cut construction times, costs, and waste due to their stackable nature and modular construction (Steve, 2019). However, the container envelope design is critical due to its nature of heat and cold conducting properties. Several previous papers focused on CHS as a sustainable solution to meet the housing demand in slums, but these research projects did not provide an in-depth assessment of container envelope design optimization to achieve high-level building energy performance.

This study proposes a parametric envelope optimization and immersive visualization framework applicable to sustainable informal settlement development. The envelope optimization process was tackled through multi-objective optimization algorithms. On the other hand, the immersive visualization process addressed socio-cultural values via stakeholder feedback. The simulation workflow was implemented in the Korail slum, which houses over 20,000 families adjacent to a lake as one of the largest and densest slums in Dhaka. The living situations in Korail are mostly deplorable due to untenable housing conditions. Korail's residents construct houses using either locally sourced materials or recycled containers, and place their dwellings in unplanned arrangements without considering the impact on the surrounding environment or ecology. Therefore, restructuring the housing provision through different sustainable approaches is a much-needed change to improve these housing conditions. This research assumes that the proposed framework in this study can be employed by architects and planners in the early design stage to help improve the local dweller's understanding of the container housing system.

2. CHS optimization and immersive visualization framework:

2.1. METHODOLOGY

The design optimization and visualization framework to investigate the performance of CHS in this paper (Figure 1) is structured as follows: First, the container cluster pattern was selected through local housing cluster typologies observation in Step 01. Step 02 was comprised of hypothetical container cluster formations and the selection of the design variables. In Step 03, the MOO results were derived from the daylight and energy simulation process. The optimization progression continued until termination, and the optimized design options were integrated with parametric virtual reality (VR) in Step 04.

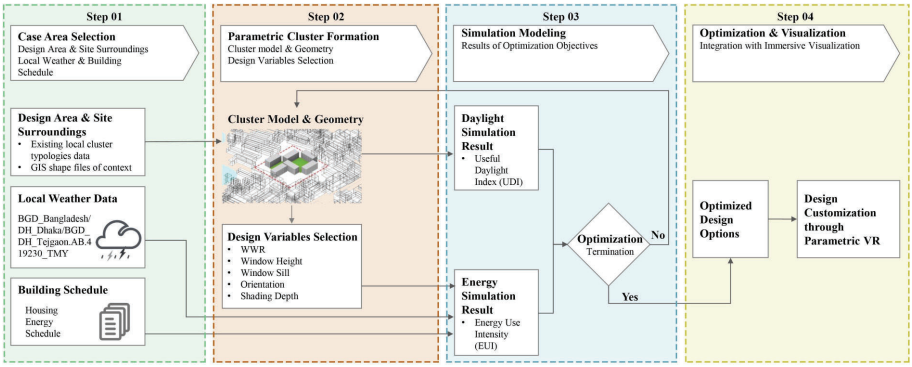

Figure 1. CHS optimization and visualization framework.

2.2. PROTOTYPE DEVELOPMENT

Figure 2 shows the software prototype for simulation and immersive visualization. First, the building footprints were applied as inputs in ArcGIS pro. Then the outputs were taken to the Rhinoceros-Grasshopper platform. Here, parametric simulation modeling and simulations were operated by using Ladybug tools, Octopus, OpenStudio, Radiance, and Daysim cross-platforms. Finally, immersive visualization is an ongoing development using the Unity game engine.

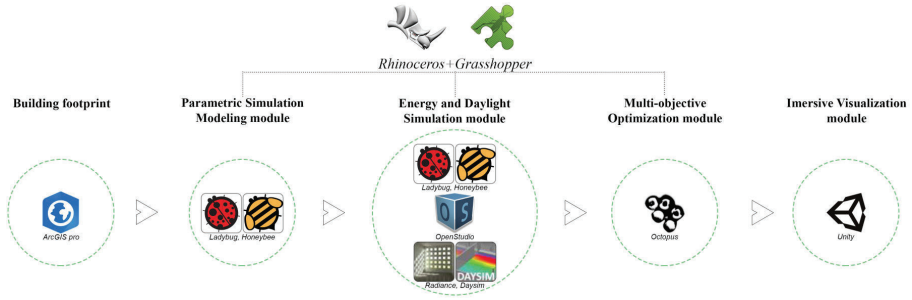

Figure 2. Software prototype for simulation and visualization.

3. Implementation:

3.1. CLUSTER PATTERN SELECTION

Generally, three groups of typological approaches for hypothetical cluster formation can be identified: (a) generic targets with unvarying contexts; (b) existing built urban arrangements; and (c) hybrid targets with unvarying contexts (Natanian et al., 2019), which was applied in this research.

The generic method is guided by vernacular building/block typologies. That type is generated from the traditional courtyard (Figure 3), which family members use for home-based activities, such as work or leisure (Zahir & Aman, 2017). The generic pattern may cause unnecessary experiments due to oversimplifying complex building geometries, and it does not respect traditional settlements. Yet, the existing built urban arrangements require an unnecessary level of details and limit the transferability for site variations. The hybrid approach allows keeping existing constructed municipal arrangements as it impacts the energy performances and confirms the transferability and computational efficiency. Hence, the hybrid method was considered to model the hypothetical CHS clusters for this research.

There are two ways to collect footprint data of the dense areas of the Korail slum. Firstly, from different online sources like Open Street Maps or Grasshopper plugins such as Urbano, Elk, Gismo, and Heron. However, these online sources have two drawbacks: a lack of up-to-date footprint information, and no consideration of the fluid nature of slum architecture. For this study, the second option of collecting dwelling footprint data from the local Bangladeshi government survey institute (BBS) in .shp and .csv formats was used to import data in ArcGIS pro for processing. Hourly weather data 'BGD_Bangladesh/DH_Dhaka/BGD_DH_Tejgaon.TMY', originated from the US Department of Energy was used for the simulation analysis.

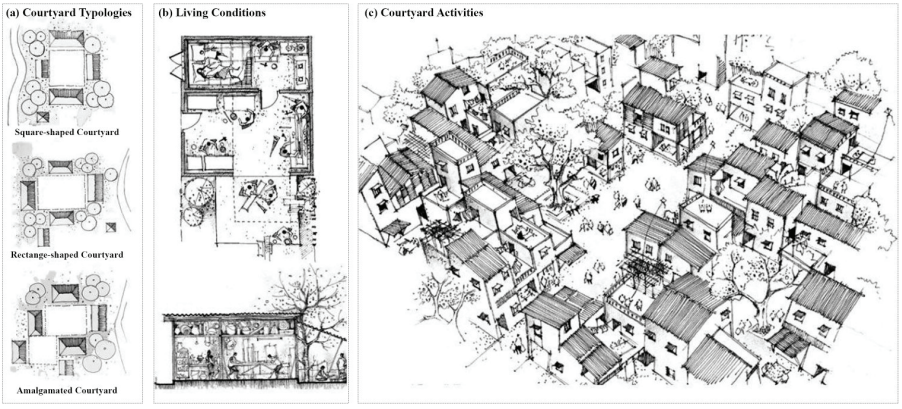

Figure 3. Vernacular housing cluster and courtyard patterns in Bangladesh; (a) courtyard typologies, (b) living conditions, and (c) courtyard activities (Source: Zahir, 2017).

3.2. PARAMETRIC CLUSTER FORMATION

The standard container dimensions were obtained from industry literature and verified on locally available shipping containers in Bangladesh. The number of container houses per cluster was considered following local regulations for standard living measures in affordable housing. A physical survey of 350 families showed that an average family consists of 4-6 persons, and about 200 people live in one cluster in the case area. To model the cluster, one of the three common types of courtyards in Bangladesh, which is the 'Amalgamated courtyard' (Figure 3) was considered. In this research, the typologies for the cluster are the single tier to give every family access to the courtyard.

Figure 4. (a) Urban layers, (b) site context, and (c) hybrid typology placed in the existing site.

The hybrid parametric model was developed in the Rhino-Grasshopper platform considering the design variables, which were measured in the multi-objective optimization process. The design variables were: window-to-wall ratio (WWR_North/South/East/West), window height, windowsill, orientation, and shading depth. The range of these design variables was determined through locality survey in the urban wetland areas and location regulations (Table 1). The median value of each variable's range was considered for the base proposal geometry to compare with the most optimal options.

Table 1. Initial value for the base model and design variables ranges.

	Variables	Initial Value	Range	
			Minimum	Maximum
V1	Shading depth (m)	0.375	0.25	0.5
V2	WWW_North (m)	0.4	0.1	0.7
V3	WWR_West (m)	0.4	0.1	0.7
V4	WWR_South (m)	0.4	0.1	0.7
V5	WWR_East (m)	0.4	0.1	0.7
V6	Window height (m)	1.35	0.7	2
V7	Window sill (m)	0.75	0.5	1
V8	Orientation (degree)	90	0	180

3.3. MULTI-OBJECTIVE OPTIMIZATION PROCESS

A Pareto-front algorithm was considered in this study for the MOO process, which determines the bargain within multiple outcome objectives (Evins, 2013). In this study, multiple outcome objectives - Useful Daylight Illuminance (UDI) and Energy Use Intensity (EUI) - were considered to be optimized for acquiring the insights regarding the best possible options and determining the impact of design variables on the solutions. UDI is measured through the proportion of the number of useful hours to the total yearly occupied hours. EUI is the sum of annual heating, cooling, equipment, and illumination loads. Therefore, a lower EUI value is ideal as it designates a lower energy requirement; and a greater UDI value is wanted as it points to an increased usage of available sunlight. Along with these two outcome indices, the envelope construction cost is another crucial element that stakeholders need to consider. To properly calculate and identify the optimal results, the total cost was analyzed for each iteration using the following formula:

$$\sum C_{\cos t} = C_{wall} + C_{r\infty f} + C_{flr} + C_{glz} \tag{1}$$

For CHS, material properties play a critical role in the optimization process. As an uncommon material for the context, steel is more sensitive to microclimatic impacts of high-density urban wetlands. Therefore, customized CHS material properties were fed into the simulation process to generate more accurate predictions. An average insulation thickness of 12.5 cm was used and kept constant for the entire series of iterations. For the MOO process, the initial cohort's populace extent was 50, meaning 100 design resolutions are arbitrarily nominated from all choices. The termination criterion was considered for this research, which denotes the maximum number of the generation. The limit generation was specified as generation 8. The algorithm randomly selected about 775 solutions from the present population.

3.4. VISUALIZATION

Co-design via immersive media can transform how architects and stakeholders design future places, mainly where vernacular architecture and socio-cultural factors are important (Vosinakis et al., 2018). Tools such as Mindesk and Enscape allow experts to navigate, manipulate, and design in VR with a high level of immersion and enable designers to interact with and modify 3D models of buildings. Few tools exist which empower underprivileged users with technologies to facilitate their design input for prospective eco-friendly dwellings (Chowdhury & Schnabel, 2020).

This paper proposes a parametric VR structure, which caters to future dwellers of these container units. The occupants have unique personal insights and contextual knowledge about their spatial preferences. However, they do not have the technical or design background to use complex computational tools like Grasshopper and Revit. Therefore, the system uses the optimized 3D models that resulted from the MOO simulations as input and moves the model to an immersive customization phase in a VR environment. Here, the user interacts with the container unit where variables that modify its spatial qualities have been

pre-determined. The opportunities for design were split into three major categories of variables: interior, exterior, and communal.

Interior variables enable the user to partition spaces, select finishing materials, add and move built-in furniture, and modify lighting options. Exterior variables permit the user to choose paint colors and local cladding materials and manipulate vegetation parameters. Last but not least, the communal assets include the ability to add and modify the placement of gathering areas, leisure spaces, and other shared assets (Figure 5).

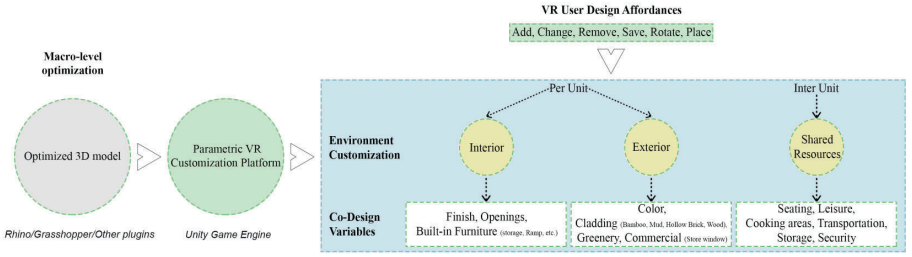

Figure 5. Parametric VR workflow.

This tool aims to address socio-cultural values as an essential aspect of sustainability. If users maximize the functionality of individual units, then this portion of the framework can enhance the efficiency of the units. This is achieved by incorporating the occupants' needs and knowledge into the proposed unit design. The opportunities that VR brings with increased immersion and presence to the participatory design arena is supported by this application (Figure 6).

Figure 6. VR immersion and participatory design.

4. Results & Discussion:

A Pareto optimization aims to find the trade-off front (Pareto-front) between multiple outcome objectives. The Octopus plugin handled the MOO process using Pareto-front algorithms. A scatterplot was generated grounded on the optimization data composed by the iterations in Octopus (Figure 7), in which one individual data point denotes one design option. Due to the eight used predictor variables introduced above, the results are more complicated, and it may be difficult to interpret by measuring scatterplots only. Therefore, parallel coordinates coupled with scatterplots were plotted to analyze the data exported through the TT Toolbox plugin for Grasshopper.

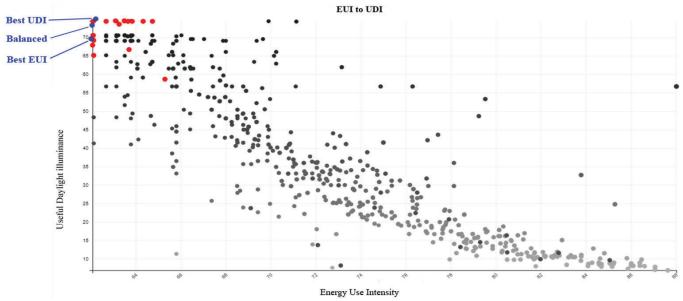

Figure 7. Pareto-front plot for multi-objective optimization.

The data points marked in red are the non-dominant results, which show the optimized products combining UDI and EUI simultaneously. Among several non-dominant optimized options, two optimal options based on EUI, UDI, and one balanced Pareto-front model were bunched in the information plot. Hence, their conduct and shapes demonstrate significant resemblances.

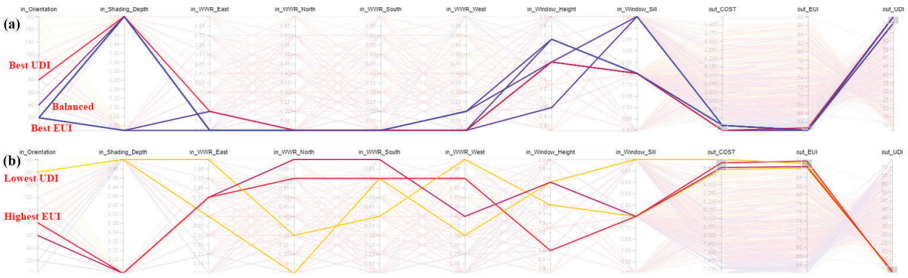

Figure 8. (a) Parallel coordinate plot to show the relationship between optimal solutions, (b) lowest UDI-Height EUI plot.

The low glazing ratios at the South and West walls are the main reason why EUI is reduced. Yet, the highest EUI and lowest UDI are seen by the higher WWR_South and WWR_West. It is worth noting that the iterations with the least energy use have a much lower WWR at the South without reducing useful daylighting. This is caused primarily by orientation, shading depth, and window

height. However, the arbitrary distribution on the plot shows it has no impact on EUI. One assumption was that greater window height would be desired for the container's metal envelope to achieve lesser EUI, which was not observed as this results in greater EUI - a surprising finding for a CHS. The results further show that a window height range of 0.75-1.5 meters is satisfactory, and a windowsill at 1 meter provides a more optimal solution than a windowsill at 0.5 meters.

Even though a balanced model balances daylight use and energy consumption, this option is more expensive than the other non-dominant optimized option. This means cost should be another outcome objective in this process to find a better-balanced model. For the base model comparison with the optimized model, the initial values were calculated as one of the optimized Pareto-front models. After inputting the achieved values, greater UDI by about 29%, lesser EUI by about 17%, and lesser costs were achieved, as seen in Figure 9.

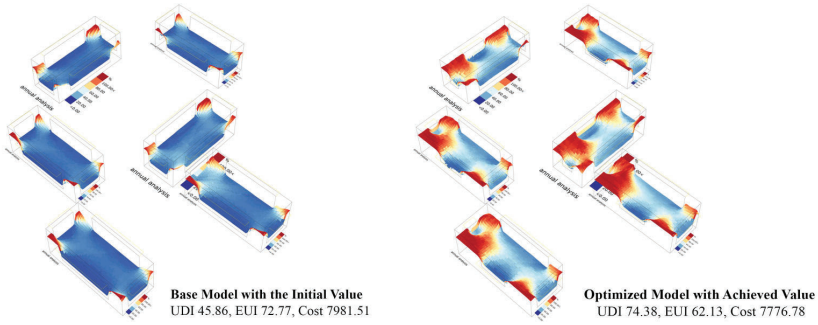

Figure 9. Comparison model of the base model and the optimized model.

Ongoing research and testing are focused on transferring the optimized clusters onto the VR design parametric environment. Special consideration is placed upon creating parametric materials and spatial labeling tools. By maximizing iterative design alternatives and keeping stakeholders engaged in the design process, the virtual environment takes advantage of prior research in this area and VR as a medium for design. (Hopfenblatt & Balakrishnan, 2018).

5. Conclusion:

The purpose of this research was to propose a computer-aided parametric envelope optimization and immersive visualization framework that can measure the most appropriate container cluster options considering sustainable measures. The envelope optimization method was implemented through multi-objective optimization algorithms. Moreover, the immersive visualization process focused on feedback-based customization of the optimized options keeping the stakeholders in the loop. This paper applied the framework to the Korail slum in Dhaka, Bangladesh as a case study.

During this application, several drawbacks of the framework were identified. For instance, more design variables such as insulation thickness and glazing type require consideration. Additionally, outcome objectives such as thermal comfort,

airflow, and outdoor courtyard comfort can further enhance the design. Lastly, computing time is another major limitation that can be solved if other intelligent algorithms like Artificial Neural Network (ANN) could be incorporated for more accurate sampling prediction with a higher number of predictive iterations. The use of multiple simulation platforms and plugins adds to the overall processing time. Other limitations include the time required to develop customized VR design tools. Furthermore, a generalized system that is implementable into any project would be appropriate. This approach is more adaptable as such a device can address multiple projects involving multiple cultures, building typologies, and incorporate other problem areas if required. Additionally, advanced technologies such as Mixed or Augmented Reality may provide an improved platform for participatory design since they offer real-world interaction in addition to rich digital content.

The novelty of this research lies in its approach towards the parametric simulation considering the environment and economy for a CHS. Also, feedback-based design through immersive visualization to achieve socio-cultural aspects in the selected context has not been undertaken before. The future scope of this research indicates a more resilient living condition in informal settlements in the urban wetlands.

References

Chowdhury, S. and Schnabel, M.: 2020, Virtual environments as medium for laypeople to communicate and collaborate in urban design, *Architectural Science Review*, **63**(5), 451-464.

Evins, R.: 2013, A review of computational optimisation methods applied to sustainable building design, *Renewable and Sustainable Energy Reviews*, **22**, 230-245.

Fan, Q., Rama, M. and Qian, J.: 2017, "Seize the Opportunity to make Dhaka a great, vibrant City" . Available from <https://blogs.worldbank.org/endpovertyinsouthasia/seize-opportunity-make-dhaka-great-vibrant-city>.

Hopfenblatt, J. and Balakrishnan, B.: 2018, The" Nine-Square Grid" Revisited: 9-Cube VR-An Exploratory Virtual Reality Instruction Tool for Foundation Studios, *CAADRIA 2018*, Beijing, China.

Kendra, D.S.: 2012, "Moving backwards: Korail slum eviction" . Available from <http://r4d.dfid.gov.uk/PDF/Outputs/EEP/Korail-Eviction-Report.pdf>.

Natanian, J., Aleksandrowicz, O. and Auer, T.: 2019, A parametric approach to optimizing urban form, energy balance and environmental quality: The case of Mediterranean districts, *Applied Energy*, **254**, 113637.

RAJUK, B.: 2015, *Draft Dhaka Structure Plan 2016—2035 (pp. Chapter 6 (117-132). Dhaka: The Rajdhani Unnayan Kartripakkha (RAJUK)*, Ministry of Housing and Public Works, the Government of Bangladesh (GoB).

UN, H.: 2015, "A Practical Guide to Designing, Planning, and Executing Citywide Slum Upgrading Programmes. Nairobi: UN Human Settlements Programme" . Available from < http://unhabitat.org/>.

Vijayalaxmi, J.: 2010, Towards sustainable architecture – a case with Greentainer, *Local Environment*, **15**(3), 245-259.

Vosinakis, S., Koutsabasis, P., Stavrakis, M., Viorres, N. and Darzentas, J.: 2008, Virtual environments for collaborative design: requirements and guidelines from a social action perspective, *Co-Design*, **4**(3), 133-150.

Zahir, S. and Aman, J.: 2017, Evolution of Home-Based Work, *International Journal of Civil Engineering (IJCE)*, **6**, 1-8.

GENERATIVE DESIGN METHOD OF BUILDING GROUP

Based on generative adversarial network and genetic algorithm

JIAWEI YAO[1], CHENYU HUANG[2], XI PENG[3] and
PHILIP F. YUAN[4]
[1,4]*College of Architecture and Urban Planning, Tongji University*
[1,4]*{jiawei.yao|philipyuan007}@tongji.edu.cn*
[2]*School of Architecture and Art, North China University of Technology*
[2]*huangchenyu303@163.com*
[3]*Department of Architecture, Tamkang University*
[3]*mavispengxi@gmail.com*

Abstract. From parametric shape finding to digital shape generation, the discussion of generative design has never stopped in recent years. As an important watershed of building intelligence, generative design method has dual significance of scheme selection and building performance optimization in digital architectural design workflow. In this paper, the generative design method for the layout of residential buildings is studied. The pix2pix network, a kind of generative adversarial network, is used to learn the layout method of residential buildings in Shanghai. The generated layout uses Octopus, a genetic algorithm tool of Grasshopper, to generate the volume and optimize the sunshine hours and other performance parameters. In the generation process, different training sample sets and Pareto genetic algorithm optimization are used to realize the control of building density, plot ratio and height limit. This method can meet the real application scenarios in the early stage of architectural design to a certain extent, and has more expansibility, providing ideas for the generative design method of building group.

Keywords. Generative design method; generative adversarial network; genetic algorithm; sunshine optimization.

1. Introduction

As early as 1975, William Mitchell predicted the role and ability of computer in design in his book *Computer-Aided Architectural Design*(Mitchell, 1975). Nowadays, the development of computer technology and artificial intelligence has led to more expectations for computer aided architectural design (CAAD) in the field of architecture. From CAAD to the cyborg futures of man-machine symbiosis, such architectural design works are growing at a visible speed. It not only depends on the improvement of computer computing power and excellent performance and more intelligent algorithms, but also needs the transformation

PROJECTIONS, Proceedings of the 26th International Conference of the Association for Computer-Aided Architectural Design Research in Asia (CAADRIA) 2021, Volume 1, 61-70.

of architects' thinking paradigm. Generative design has been discussed for a long time. This design method combined with computer operation and algorithm optimization has great advantages in the diversity of generated schemes and the accuracy of building performance, which makes it gradually become a necessary step in architectural design, and gradually increases its proportion with the improvement of algorithm.

In 2014, the design work "Assignment of Ji Village" completed by students of School of Architecture in Southeast University, China, has applied multi-agent evolutionary model, which is an important exploration of generative design method(LI, GUO, & JI, 2015). On the basis of "quasi rectangular base dissection", the application of digital technology takes into account the deduction process of the scheme and the algorithm construction of objective constraints, and finally obtains the optimal combination of complex problems. SUN Chengyu of Tongji University applies a hierarchical parameter optimization system in the district planning of Beihai city in China(SUN, LUO, SONG, XIE, & RAO, 2017). By establishing the mathematical model of each control index and searching the multi solution space, the automatic generation of design scheme is realized. At the same time, the ventilation corridor evaluation is introduced to optimize the building layout repeatedly, which provides us with a generation idea of index constraint and performance optimization system. Liu Huijie uses multi-agent to study the sunshine constraint in the layout of residential buildings(LUI & JI, 2009). Through the establishment of mathematical model, the accumulated sunshine hours of buildings are optimized. As the pioneer of intelligent design under the background of big data and artificial intelligence, XKool tech explores the use of big data technology to quantitatively study(HE & YANG, 2018). The site value is quantified, and an algorithm model is designed to meet the architectural functional requirements. The convolutional neural network (CNN) is used to generate the optimal solution beyond the architect's ability. So far, there have been mature solutions to the technical problems of residential layout. Compared with the automatic generation method of building group layout, the method of single building form generation is difficult to quantify due to its morphological diversity. YUAN and LIN (2019) create a variety of mechanical torsion deformation building prototype. Combined with a small wind tunnel, the environmental performance-oriented form generation of single building is realized. Genetic algorithm and neural network are used in the optimization of architectural form, which is very enlightening.

Genetic algorithm (GA) is a complete set of theoretical methods proposed by Professor John Holland and his colleagues in the study of cellular automata in 1975(Holland, 1992). GA is a computational model to simulate the natural selection and genetic mechanism of Darwinian biological theory. It is a method to search the optimal solution by simulating the natural evolution process. As the most popular tool of generative design, GA has produced mature plug-ins or software tools for generative design in the past few years. Galapagos and Octopus of Rhino platform are both mainstream GA tools. Designers' use of this tools for scheme selection was once considered as the "standard answer" of generative design method. Many applications are focused on building layout

automatic generation, building lighting, ventilation, and other fields.

GA and other traditional optimization algorithms such as Simulated Annealing algorithm, Particle Swarm Optimization algorithm and Pareto Front Optimization algorithm are mainly characterized by finding local optimal solution in limited solution space. The advantage of these methods is the high efficiency in a limited range, and the quality of the optimal solution will be guaranteed due to the controlled solution space, while its disadvantage is the lack of diversity of solutions. With the development of artificial intelligence technology, including machine learning and deep learning algorithm, some scholars turn to a generation algorithm which can create unknown form through a lot of known experience: Generative Adversarial Networks (GAN). Huang and Zheng (2018) use GAN to find the relationship between manually marked apartment plans and real drawings, and can output fuzzy floor plans after training. Mohammad (2019) uses GAN to generate building facade, which proves the possibility of the application of GAN in architectural design. Mokhtar et al. (2020) use GAN to learn the wind speed map, hoping to replace the traditional simulation software and realize the faster performance-based iterative generation method. Duering et al.(2020) propose an environment driven building group generation method combining GAN and GA. Ladybugs tools of Grasshopper are used to calculate the wind speed map(Duering, Chronis, & Koenig, 2020). It is clear that, GAN is used to guide GA to find the optimal solution of building group layout which provides a lot of inspiration for this paper.

2. Method

This study mainly relies on pix2pix GAN and octopus genetic algorithm tools to realize the volume generation of building under certain controllable indicators and environmental constraints. Firstly, the land and building data of Shanghai is collected, and then the data is cut by using the Geopandas package of Python, and two kinds of data sets for GAN training are constructed. The trained GAN model is used to predict the layout of a certain plot, and the prediction result is input into rhino platform, and the Octopus tool is used to generate the volume. The generated control indicators include height limit and plot ratio, and environmental constraints include the maximum sunshine hours calculated by Ladybug tools. The research workflow is shown in Fig.1.

2.1. DATA PREPARATION

The acquisition of data set is very important for the training of network. The quality of data set largely determines the accuracy and diversity of network prediction results. Before this research, the author has already had rich experience in the application of GAN and has been actively looking for network models suitable for architectural form generation among about 100 kinds of GANs, the collection of which is called as GAN Zoo. Conditional GAN seems to have great potential in the field of architecture, but the algorithm itself still does not support images and quantitative constraints both as the training conditions of the network.

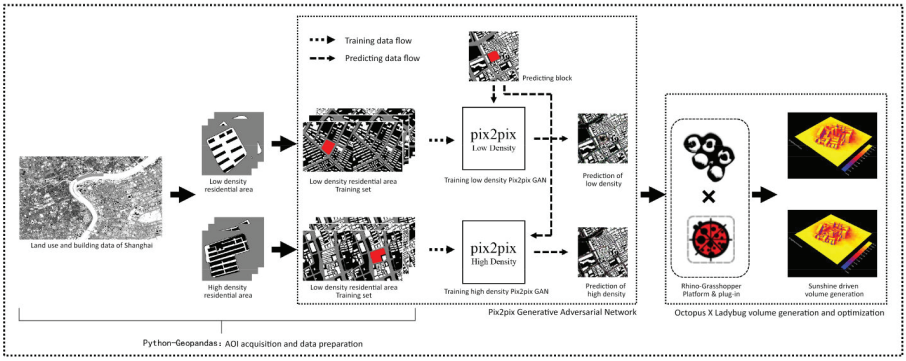

Figure 1. The research workflow.

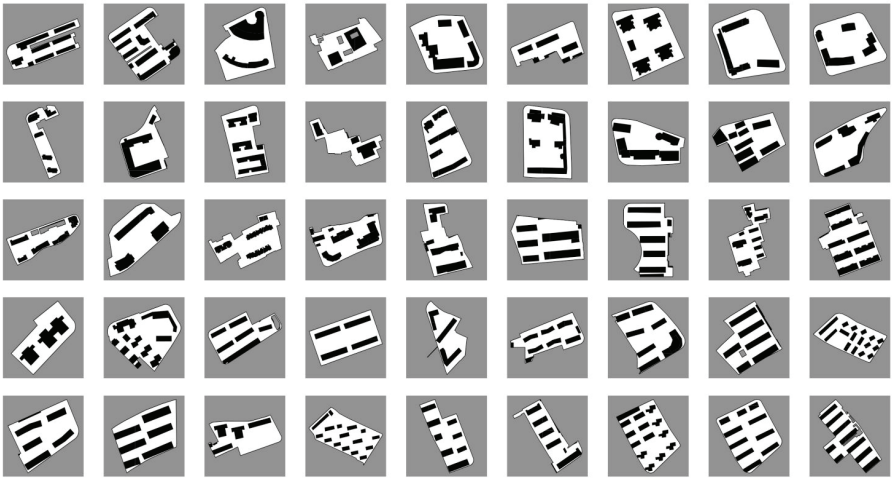

Figure 2. Low density residential layout dataset.

Facing the basic problem of building group generation, that is, the control of building density, plot ratio and other morphological indicators, we design two generation steps. In the GAN model, the network is trained by sorting out the data sets of buildings with different building densities, which can generate the layout of buildings with specified range of building density, while in the volume generation by using GA, the control of plot ratio is considered.

In this study, the building density of the building complex data set is mainly divided into two categories: low density (0.2-0.5) and high density (0.5-0.8) shown in Fig.2 & Fig.3. The Python development package Geopandas is used to cut the building and land use data in Shanghai, the area of interest (AOI) data of residential land is extracted and its building density is calculated and then classified.

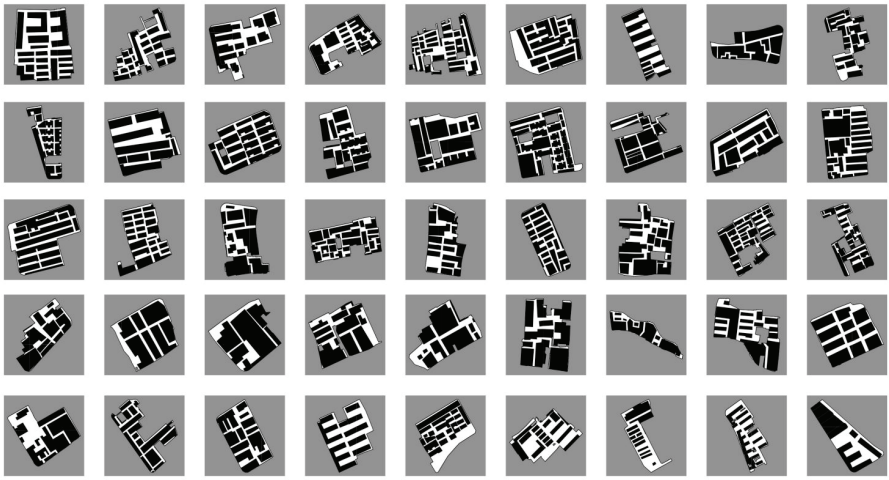

Figure 3. High density residential layout dataset.

The training set shown in Figure 1 is constructed for the two types of datasets. In the training set, each sample is composed of a labeled image (left) and an original image (right). The size of the image is 256 * 256, so as to meet the needs of GAN.

2.2. TRAINING PIX2PIX GAN

GAN involves a kind of unsupervised architecture as shown in Fig.4. It consists of two sets of independent networks, which are the targets of mutual confrontation. The first network is the classifier we need to train (D in the Fig.4) to distinguish whether it is real data or false data; The second networks is a generator (G in the Fig.4), which generates fake samples similar to real samples. The goal of generator G is to draw a fake image that is very close to the real image to cheat D. the method is to select the elements in the potential space of training data and add random noise. In the training process, D will receive the true data and the false data generated by G. its task is to determine whether the image belongs to the true data or the false data. In order to train a good generator, we need to tune the parameters of both sides at the same time. If D is correct, the parameter of G should be adjusted to make the false data more realistic; while if D is wrong, it is necessary to adjust the parameters of D to avoid the next similar judgment error. Training will continue until the two enter a state of balance. Through continuous training of classifier D and generator G, the generated images gradually highly resemble real images.

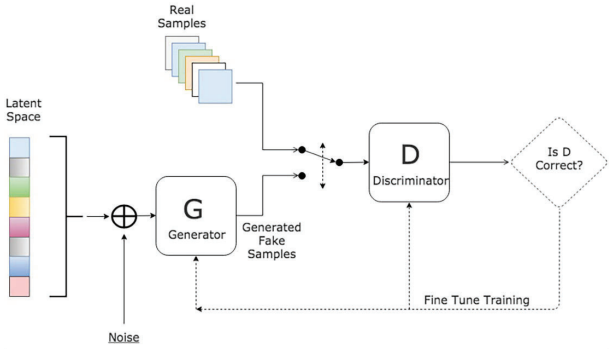

Figure 4. Algorithm principle of GAN.

Pix2pix, as a conditional GAN, can learn a conditional generation model, that is, the corresponding relationship between input image and output image(Isola, Zhu, Zhou, & Efros, 2017). In this paper, the input image is the label image whose target area is erased by red color block, and the output image is the generated building layout.

2.3. OPTIMIZATION BY OCTOPUS GA TOOLS

Different from Galapagos, octopus is a multi-objective optimization algorithm based on grasshopper platform. It is developed by Vienna University of Applied Arts in Austria and Bollinger + Grohmann engineering firm in Germany. It combines Pareto optimal principle and GA. For multi-objective optimization problems, the software provides user-defined optimization parameter options. At the same time, octopus provides rich interactive operation methods and convenient data storage and transmission functions. Compared with Galapagos, octopus not only can deal with multi-objective optimization calculation, but also has a higher degree of visualization. The solution process and many optimization feasible solutions are presented in 3D interface, in which designers can screen the results. In short, octopus provides architects with a simple and easy to learn multi-objective optimization tool and brings many possibilities for design work.

In this study, a series of constraints are set for the volume generation using the building layout generated by GAN including height limit, plot ratio and maximum sunshine hours. The maximum height of the building group is less than the height of the surrounding highest building after adding or reducing three floors, so as to ensure the transition of urban facade, as well as the generated results are as reasonable as possible when the specific height limit value is unknown. The three plot ratio ranges are 0.8-1.2; 1.5-2.0; 2.0-2.5. It is hoped to generate as rich and controlled volume as possible under the same building layout by setting different plot ratios. Maximum sunshine hours is calculated by Ladybug sunshine calculator shown in the Fig.5, Fig.6 shows more details of the link of the battery.

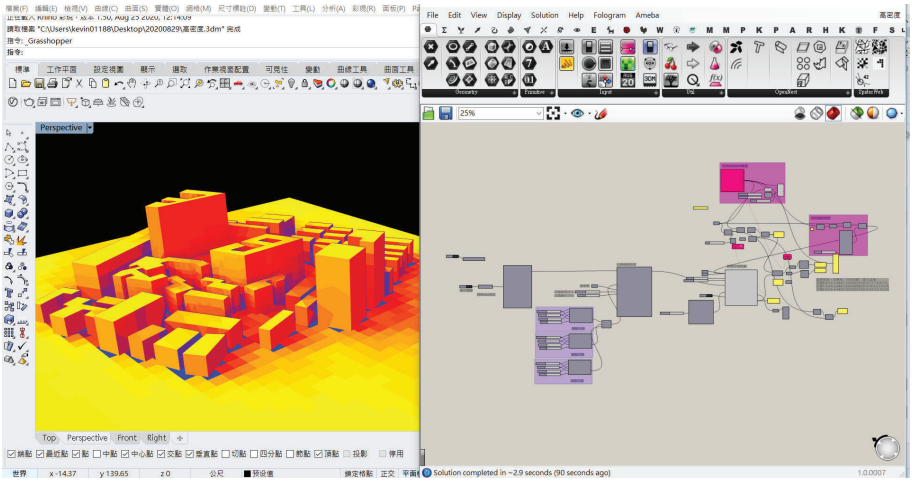

Figure 5. Ladybug sunshine calculator visual interface.

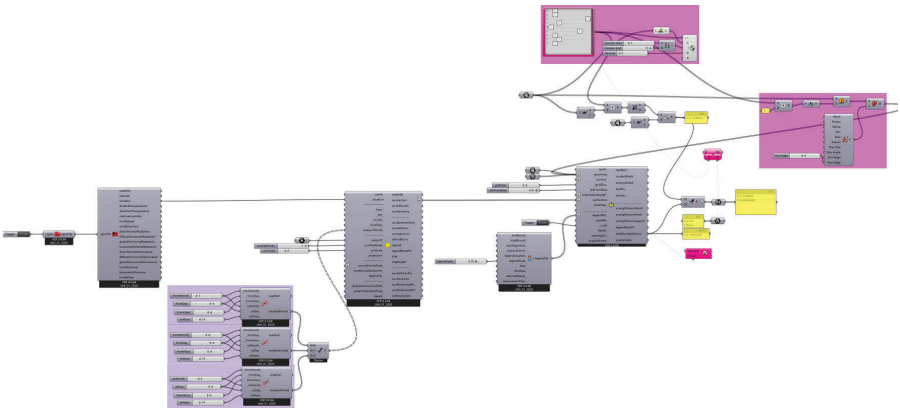

Figure 6. Details of the link of the battery.

3. Results and Discussion

3.1. GENERATION RESULTS OF PIX2PIX GAN

The results of pix2pix generation are shown in Fig.7. It can be seen that the generation results of label images in low density and high density models show certain regularity. In the result of low density generation, the buildings respond effectively to the boundary of the site and leave public space in the center. It reflects the advanced nature of the network algorithm, not only learning the layout of the building group, but also learning the relationship between the building group and the site. The building density of the result is 0.377, which meets the requirement of low density generation.

In the high density generation results, it shows that the consideration of the network for high density layout is not only in line with the local texture, but also learns the surrounding E-shaped and C-shaped architectural forms and integrates them into the generation scheme, which makes the scheme more specific with local characteristics. The building density of the result is 0.684, which meets the requirement of high density. Considering that GAN is an algorithm to generate bitmap, so the computer can not understand the content of the image, and can only generate the required pixel distribution, which makes the generated results have a certain degree of ambiguity, and add more image noise. But even so, the above generated results can provide architects with the analysis and inspiration of the preliminary general plan of the scheme and will further enter the Octopus tool for volume generation.

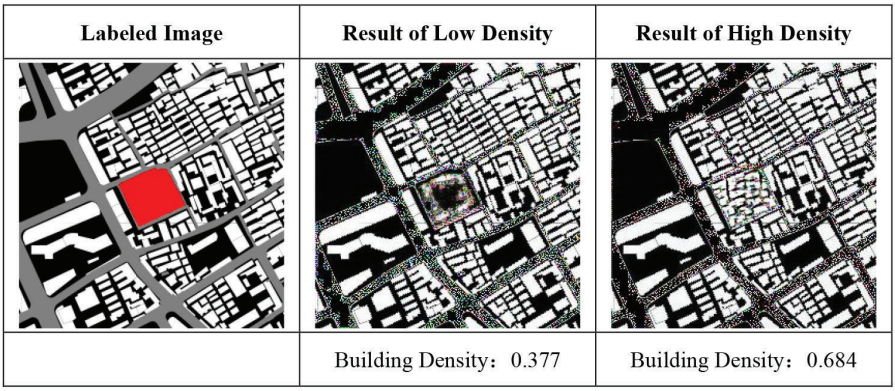

Figure 7. The generation results of pix2pix .

3.2. GENERATION RESULTS OF OCTOPUS

The generation results of Octopus are shown in Fig.8. The result is very interesting, and it is very close to the design of a real designer. We have generated the volume of low density and high density layout, and listed the scheme with the largest sunshine hours in the range of three plot ratios. Apparently, the height of the generated building is relatively uniform, which is due to the height constraint of the generation process. Because Octopus directly operates the Rhino model, the generated results can be directly connected to the architect's design workflow, so it has strong practicability.

Volume Generation Result of low Density	Volume Generation Result of High Density
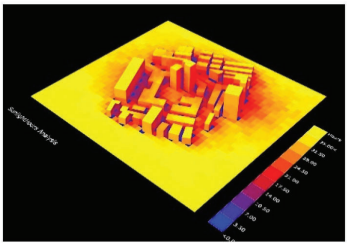	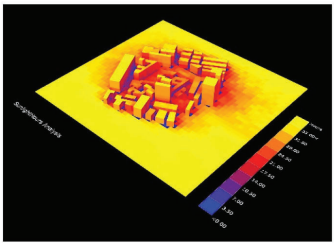
Plot Ratio：1.10	Plot Ratio：1.12
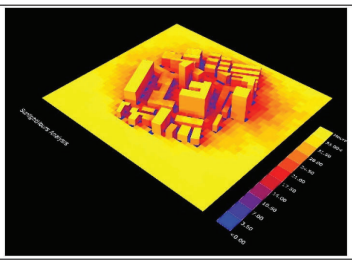	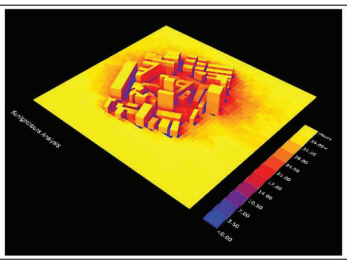
Plot Ratio：1.84	Plot Ratio：1.83
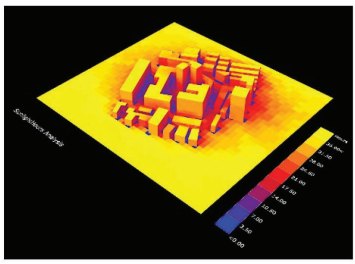	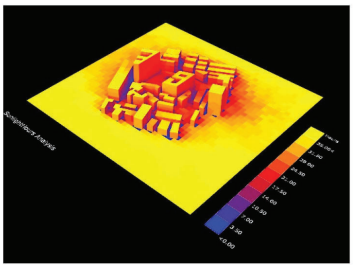
Plot Ratio：2.36	Plot Ratio：2.30

Figure 8. The Generation Results of Octopus.

4. Conclusions

The combination of Generative Adversarial Network and Genetic Algorithm of traditional generative design algorithm not only expands the diversity of genetic algorithm, but also makes up for the instability of the generation form of GAN. This exploration is of great significance to the development of generative design method. The consideration of performance optimization in this study is feasible. At present, the generation of GAN needs to be further optimized. For example, in the high density layout generation, it is obvious that the generated results are against the architect's rationality, which is the plan is too complex. The future effort should be put in the preparation process of the dataset. More quality plans need to be prepared for network training. Meanwhile, in the future, more

environmental parameters could be added to Octopus multi-objective optimization to control the generation of building form including wind environment, light environment, energy consumption, carbon emissions, etc., to truly achieve performance-oriented form generation.

Acknowledgments: This research was financially supported by the National Natural Science Foundation of China (grant number 51908410) and Shanghai Sail Program (grant number 19YF1451000).

References

Duering, S., Chronis, A. and Koenig, R.: 2020, Optimizing Urban Systems: Integrated Optimization of Spatial Configurations, *Proceedings of SimAUD 2020*.

HE, W.Y. and YANG, X.D.: 2018, Artifictial Intelligence Design, from Research to Practice, *Time+Architecture*, **01**, 38-43.

Holland, J.H.: 1992, *Adaptation in natural and artificial systems: an introductory analysis with applications to biology, control, and artificial intelligence*, MIT Press.

HUANG, W.X. and ZHENG, H.: 2018, Architectural drawings recognition and generation through machine learning, *Proceedings of the 38th Annual Conference of the Association for Computer Aided Design in Architecture*, Mexico City, Mexico.

Isola, P., ZHU, J.Y., ZHOU, T.H. and Efros, A.A.: 2017, Image-to-image translation with conditional adversarial networks, *Proceedings of the IEEE conference on computer vision and pattern recognition*.

LI, B., GUO, Z.F. and JI, Y.Z.: 2015, Modeling and Realizing Generative Design–A Case Study of the Assignment of Ji Village, *Architectural Journal*, **05**, 94-98.

LUI, H.J. and JI, G.H.: 2009, Automatic Planning of Residential Quarter Under Isolation Condition Based on Multi-agent Simulation, *Architectural Journal*, **1**, 12-16.

Mohammad, A.S.: 2019, *Hybrid Elevations Using GAN Networks*, Ph.D. Thesis, The University of North Carolina at Charlotte.

Mokhtar, S., Sojka, A. and Davila, C.C.: 2020, Conditional generative adversarial networks for pedestrian wind flow approximation, *Proceedings of SimAUD 2020*.

SUN, C.Y., LUO, Q.M., XIE, J.M. and RAO, J.: 2017, A Practical Approach to Generating 3D City Models–A Case Study of the Density Zoning Project in Beihai, *Architectural Journal*, **08**, 77-81.

YUAN, F. and LIN, Y.Q.: 2019, Research on High-Rise Building Group Morphology Generative Design Method Based on Physical Wind Tunnel and Neural Network Algorithm, *Journal of Human Settlements in West China*, **01**, 22-30.

EXPLORING THE KEY ATTRIBUTES OF LIFESTYLE HOTELS: A CONTENT ANALYSIS OF USER-CREATED CONTENT ON INSTAGRAM

YOOJIN HAN[1] and HYUNSOO LEE[2]
[1,2]*Yonsei University, Seoul, Republic of Korea*
[1,2]*{yoojin79|hyunsl}@yonsei.ac.kr*

Abstract. This study aims to investigate the key attributes of lifestyle hotels by analyzing user-created content on Instagram, an image-based social network service. In an era of uncertainty in the tourism and hospitality industry, it is inevitable that hotels must create a competitive identity. However, even with the significant growth of the lifestyle hotel segment, the concept of a lifestyle hotel is still vague. Therefore, to explore how to define, perceive, and interpret lifestyle hotels and to suggest their crucial attributes, this paper examines user-created content on Instagram. The data from 20,886 Instagram posts related to lifestyle hotels, including 2,209 locations, 43,586 hashtags, and 20,866 images, were analyzed using Vision AI, a social network analysis method and computer vision technology. The results of this study demonstrated that lifestyle hotels are perceived as design-focused branded hotels that represent the urban lifestyle and share both vacation and urban activities. Furthermore, the results reflected one of the latest hospitality trends-a holiday in an urban setting in addition to the primary purpose of traveling. Finally, this research suggests broader uses of big data and deep learning for analyzing how a place is consumed in a geospatial context.

Keywords. Lifestyle Hotel; Hospitality Experiences; User-Created Content; Social Network Analysis; Vision AI.

1. Introduction

With the rising uncertainty in tourism and fiercer competition in the hospitality industry, global hotels face many challenges, and the lifestyle hotel concept has been highlighted as a differentiator. Numerous global players have developed lifestyle brands and attached enriched experiences to their spaces. Particularly, the lifestyle hospitality experience has been shaped to capture the interests of millennials, who can be difficult to attract. Lifestyle hospitality has unique design features, providing more personalized services and local ambiance. Lifestyle hotels have transformed their hotels into places where customers want to visit, not just stay, adding new value. Lifestyle hotels are like an oasis among standardized brand hotels. However, lifestyle hotels have had difficulty maintaining their uniqueness and gaining a competitive edge within the industry. With the

PROJECTIONS, Proceedings of the 26th International Conference of the Association for Computer-Aided Architectural Design Research in Asia (CAADRIA) 2021, Volume 1, 71-80.

rapid growth of the lifestyle market, it is inevitable that lifestyle hotels would begin to standardize like branded hotels (Pizam, 2015), making it impossible to provide personalized services tailored to every individual lifestyle and preference. Therefore, it has become difficult for lifestyle hotels to differentiate themselves from other segments, such as boutique or design hotels. Since a strong identity is crucial for sustainable growth in the hospitality industry (Jones, Day, and Quadri-Felitti, 2013), the lifestyle hotel segment should rebuild and strengthen its identity to provide a clear distinction for customers. Hotel guests must be able to match the hotel's identity with its perceived image. Therefore, by focusing on user-created content on Instagram, an image-based social network service, this paper examines how guests perceive, interpret, and define lifestyle hotels. This research redefines the lifestyle hotel segment and suggests crucial attributes for future lifestyle hotels.

2. Related Works

2.1. LIFESTYLE HOTEL

Since the mid-20th century, lifestyle hotels have differentiated themselves from traditional hotels. Global hotel groups have used the term lifestyle hotel brand to describe a new type of hotel that represents individual lifestyles and captures customers' preferences. Lifestyle hotel brands have mainly targeted the Millennial generation, also known as Generation Y. Millennials tend to have spending power in tourism, as they value leisure time, want more personalized services, and are curious about new experiences (Liu et al., 2018). Also, millennials visit hotels for more diverse activities than previous generations, such as having fun, unplugging or escaping, celebrating a special arrangement, being inspired, and attending an event (Gail, 2018). Thus, to appeal to these millennials, lifestyle hotels offer unique designs, differentiated facilities, customized services, and a unique experience that is different from the traditional cookie-cutter branded hotels (Jones, Day, and Quadri-Felitti, 2013).

Nevertheless, the concept of lifestyle hotels has not been defined clearly and is often confused with that of boutique hotels or design hotels. Thus, previous studies have tried to distinguish lifestyle hotels by defining their intangible and tangible characteristics as follows: (1) small-sized properties with unique architecture and interior design, (2) smart hotel rooms offering high-tech amenities, (3) a unique and modern atmosphere, and (4) personalized services providing a sense of belonging (Freund de Klumbis, 2002; Milburn, Stotts, and Hall, 2006). Furthermore, many studies have emphasized lifestyle hotels‘ experiential aspects and physical characteristics, such as featuring innovative, functional, and stylish environments that evoke diverse and unique experiences for their guests (BLLA, n.d.; Jones, Day, and Quadri-Felitti, 2013; Kosar, 2014). Among their many characteristics, lifestyle hotels provide highly personalized services that appeal to individual lifestyles (Pizam, 2015). However, since lifestyle hotels adopt global franchising (Jones, Day, and Quadri-Felitti, 2013; Ricca, 2015), unlike independent small-sized boutique hotels, it is impossible for them to meet all customers' needs and desires (Pizam, 2015). Lifestyle hotels have also become

standardized (Schmidt, 2017), losing their primary essential feature of uniqueness.

2.2. INSTAGRAM AND USER-CREATED CONTENTS

Instagram is one of the most popular photo-sharing social network services (SNS), along with Facebook and Twitter (ZDnet, 2018). Instagram provides users with a variety of information and image-based experiences (Rainie, Brenner, and Purcell, 2012). An Instagram post includes creator-related features (ID, profile), contextual features (date/time, location) and content features (image, hashtag, caption, comment). Instagram data shows traces of users' experiences and activities in the place, as it can tag the location information for a particular place. The collected data reflect individual actions, perceptions, and interactions, representing urban social behavior (Guerrero et al., 2016). Likewise, Instagram data helps in understanding user behaviors from a social, cultural, and environmental perspective (Hu, Manikonda, and Kambhampati, 2014).

Photos that users post on image-based social media represent the individual's collected interests at a given moment, reflecting their activities, perceptions, and interactions (Silva et al., 2013). Furthermore, user-created content on Instagram not only indicates users' perceptions of a place but also affects other users' future behaviors (Bahtar, 2016). Since images may convey more than a thousand words, analyzing many images can be difficult. However, deep learning-based computer vision technology provides an opportunity to identify image content automatically. With the help of this technology, Hu (2014) analyzed a large number of Instagram images for the first time and classified them into eight categories: Friends, Food, Gadget, Captured Photo, Pet, Activity, and Selfie & Fashion. Jaakonmäki (2017) also analyzed the visual features of Instagram images by utilizing machine learning-based Clarifai's API. Thus, this study adopted a deep-learning approach for analyzing Instagram image content.

3. Materials and methods

To explore users' perceptions of the latest lifestyle hotels, this research was based on a quantitative approach adopting mixed methods. Focusing on user-created content related to lifestyle hotels on Instagram, this research analyzed both content and contextual features. The proposed methods are illustrated in Figure 1.

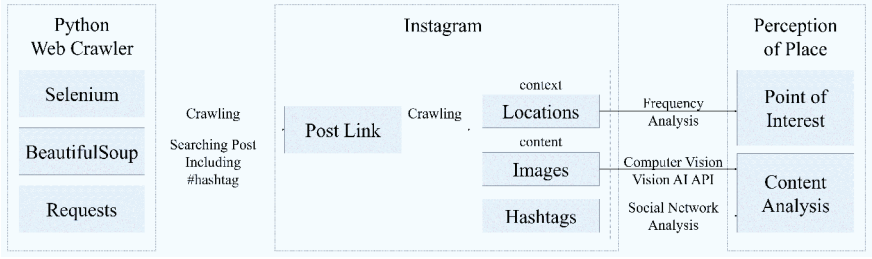

Figure 1. Research methods.

3.1. DATA COLLECTION AND INCLUSION CRITERIA

This research investigates the utilization of user-created content on Instagram for understanding the perceived image of lifestyle hotels and extracting key attributes. Instagram posts that included the lifestyle hotel hashtag were collected since hashtags created by the image creator represent an important description for audiences (Giannoulakis and Tsapatsoulis, 2016). Specifically, this research developed a web crawler with Python that used Selenium, BeautifulSoup, and Requests libraries. As illustrated in Figure 2, a post consists of user ID, location, images (or videos), captions (including hashtags), comments, and date of creation. Instagram posts can be searched with a specific hashtag (#), location, or user ID, showing the most recent results first. The geographical scope of this study is the city of Seoul, where many lifestyle hotels are currently in development but still have ambiguous identities. Thus, all Instagram posts available at the time of the search that contained lifestyle hotel hashtags (both in English and Korean) were included in the dataset. The Python web crawler collected Instagram post links first. The collected data were preprocessed by eliminating redundant post links. Then, from the post links, four types of data were gathered: date, location, image, and hashtag. Among the extracted hashtags, keywords that solely meant the word hotel, for example 'hotels,' were excluded. The data collection took place twice during October 2020.

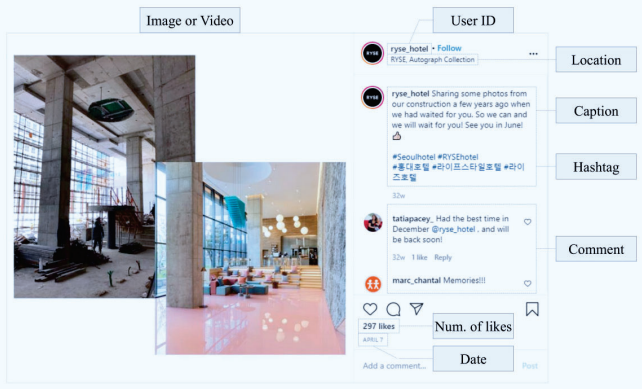

Figure 2. Structure of an Instagram post.

3.2. DATA ANALYSIS

To analyze the data's contextual features, this study conducted a frequency analysis on location. Specific locations and points of interest (POI) were mapped, indicating where people perceived and visited a lifestyle hotel. Spatial analysis was conducted based on Seoul's urban planning system (The Seoul Institute, 2017). Then, the content features-images-were analyzed using computer vision technology. To deal with huge images, this study adopted Google Vision AI, an optimized computer vision API for analyzing image content. The deep learning-based image recognition technology enabled understanding what images

were without the help of many additional researchers. The technology recognized objects expressed in images and classified them automatically, assigning several labels, the keyword that illustrates the image content, and probabilistic scores for each image. After analyzing image data with Vision AI, the research examined crucial labels based on the total count of each label multiplied by the predicted scores. After that, the labels were classified based on five categories defined by previous research on photograph-based hospitality (Pullman and Robson, 2007) and atmospheric dimensions (Baker,1986; Baker, Grewal, and Parasuraman, 1994; Berman and Evans, 1995; Turley and Milliman, 2000). Furthermore, as studies on social networks help understand the diverse relationships between societies (Scott, 2000), this study conducted social network analysis (SNA) on hashtags. The top 100 frequent hashtags were analyzed based on statistics and the SNA metrics framework provided by Gephi, a network analysis and visualization tool. Focusing on eigenvector centrality, which indicates the level of importance of a node within a network, this study explored the crucial keywords and visualized the results (Grandjean, 2015). Finally, based on the obtained results, a semantic analysis was conducted on how Instagram users perceive lifestyle hotels. This study redefines the concept of lifestyle hotels by comparing the traditional definition with reality and suggesting key attributes for lifestyle hotels.

4. Findings and Discussion

4.1. BASIC STATISTICS OF DATASET

In total, this research collected 20,886 posts. The posts were created during the period between February 2015 and October 2020. Table 1 shows the basic statistics of the dataset.

Table 1. Statistical summary of Instagram dataset.

Data	N
Locations (Total)	2,209
Images (Total)	20,866
Hashtags (Total)	43,586
Hashtags per post (Mean)	18

4.2. LOCATION ANALYSIS

This study specified highly ranked locations as POI through a frequency analysis that examined 20,886 lifestyle hotel posts. A total of 2,209 locations were retrieved from the dataset (i.e., among a total of 20,886 posts, 13,587 posts tagged location). As a result of analyzing the location data, the most popular locations in Seoul are shown in Table 2. The most visited locations tagged with ‘lifestyle hotel’ in Seoul were mostly branded hotels (Hotel Cappuccino, L7, RYSE, PATIO7, and GLAD). Among the five cases, four hotels were in the city’s center. Therefore, most lifestyle hotel posts were created in a certain branded hotel within downtown Seoul. This result supports the perspectives of previous studies that defined

lifestyle hotels as franchised branded hotels. Additionally, the findings showed that many people perceived hotels located in the city center as lifestyle hotels, not hotels in tourist attractions or destinations far from the city.

Table 2. Frequency analysis of location.

No.	Location Name	Regions	Type	Freq.	%*
1	Hotel Cappuccino	City Centers	Branded	1,816	82.2
2	L7 Hotel	City Centers	Branded	181	8.2
3	RYSE, Autograph Collection	Metropolitan Centers	Branded	62	2.8
4	PATIO7 Hotel	City Centers	Independent	37	1.7
5	GLAD Hotel	City Centers	Branded	26	1.2

* Total number of locations = 2,209. Percentage = frequency of location divided by total number of locations.

4.3. IMAGE ANALYSIS

Table 3 shows the results of a content analysis of the 20,886 lifestyle hotel-related post images. On average, nine labels were assigned to one image. The results show that the key attributes of lifestyle hotel images created by their guests were architecture and interior design. The most prominent labels were *Room* (29.52%) and *Interior Design* (23.77%), reflecting the core experience of a hotel-staying inside the room. Additionally, general interior features appeared frequently (e.g., *Wall*, *Floor*, *Ceiling*), composing almost 67% of images. FF&E in indoor spaces, including *Furniture* (22.2%), *Table* (9.98%), *Bed* (6.16%), and *Lighting* (5.22%), was crucial in lifestyle hotel images. Furthermore, labels related to architecture, such as *Building* (18.92%), *Architecture* (16.82%), and *Property* (16.25%), were also shown in many cases.

Following this, nature (e.g., *Sky*, *Tree*, *Plant*, *Water*) and food (e.g., *Cuisine*, *Dish*, *Ingredient*) emerged frequently. Furthermore, lifestyle hotel images contained *City* (4.28%) and *Urban Area* (3.55%), as well as *Vacation* (4.49%) and *Leisure* (3.90%). This result represents the emerging trend in the travel and tourism industry of people spending their vacation in an urban hotel (i.e., hocance: hotel+vacance). Additionally, certain colors (particularly yellow and blue) appeared frequently, which can be due to the brand identity colors of lifestyle hotel brands, such as the yellow of L7 and the blue of the Hotel Cappuccino.

In summary, regarding lifestyle hotels, people posted an overwhelming number of spatial images showing the general interior, FF&E, and architecture design, particularly for the guests' rooms. Aligning with previous studies that highlighted unique architecture and interior design, this research found that architecture and interior attributes represented a large portion of lifestyle hotel images. Furthermore, vacation activities related to nature, food, and the urban landscape also seem to be crucial visual attributes in lifestyle hotels. However, in-room high-tech was not seen in this research, although it had been one of the main characteristics of lifestyle hotels in previous studies.

Table 3. Top 40 labels of Instagram images.

Category	Attributes	Labels	Rank	%*
Design	Facilities	Room	1	29.52
		Living room	26	5.02
		Bedroom	19	6.13
	General Interior	Interior design	2	23.77
		House	8	10.55
		Wall	10	8.89
		Floor	14	6.76
		Ceiling	17	6.48
		Home	20	5.40
		Design	28	4.62
	FF&E	Furniture	3	22.22
		Table	9	9.98
		Bed	18	6.16
		Lighting	22	5.22
		Bed sheet	38	3.54
	Architecture	Building	4	18.92
		Architecture	5	16.82
		Property	6	16.25
		Real estate	24	5.18
Setting	Activities	Vacation	30	4.49
		Leisure	35	3.90
	Landscape	City	32	4.28
		Urban area	37	3.55
	Nature	Sky	7	11.99
		Tree	12	7.28
		Plant	21	5.28
		Water	31	4.28
Service	Food/Drink	Food	11	8.49
		Cuisine	15	6.71
		Dish	16	6.60
		Ingredient	27	4.97
		Drink	33	4.15
		Meal	36	3.75
		Brunch	40	3.13
Others	Captioned Photo	Font	13	7.23
		Text	23	5.19
	Etc.	Photography	25	5.02
		Yellow	29	4.53
		Blue	34	4.08
		White	39	3.53

* Percentage was calculated by dividing frequency of label total rumber of images

4.4. HASHTAG ANALYSIS

A total of 43,586 hashtags were collected along with the lifestyle hotel posts. Based on social network analysis, the average clustering coefficient was 0.81, indicating a densely connected network (Latapy, 2008). The following categories were found: hotel concepts, architecture & interior design, vacation & travel, facilities, hospitality & lifestyle trends, and hotel brands & regions. Through measuring eigenvector centrality, key hashtags were investigated (Figure 3).

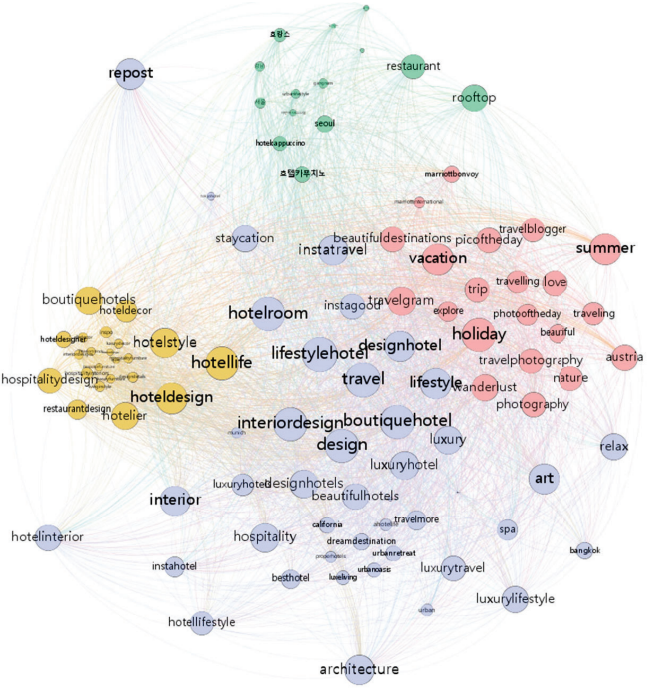

Figure 3. Visualization of hashtag analysis.

In terms of hotel concept, *boutique hotel* and *design hotel* had a higher eigenvector centrality, measuring 0.981 and 0.900, respectively. People perceive lifestyle hotels as similar to boutique hotels and design hotels. Following this, some of the most outstanding hashtags involved hospitality interior and architecture, such as *design* (0.970), *interior design* (0.966), *hotel design* (0.919), *interior* (0.896), and *architecture* (0.874). Thus, the guests highlighted the hotels' architecture and interior design the most. Additionally, general travel and vacation keywords also seemed to be important, for example *travel* (1), *holiday* (0.972), *vacation* (0.921), *instatravel* (0.882), and *travelgram* (0857). For facilities, *hotel room* (0.981), *rooftop* (0.811), and *restaurant* (0.756) emerged.

Unlike conventional travel keywords, lifestyle hotel posts have hashtags describing urban experiences, such as *urban retreat* (0.568), *urban oasis* (0.535), and *urban lifestyle* (0.410). Some hashtags reflect the new hospitality trend of spending vacations in a hotel, such as *hotel life* (0.954), *staycation* (0.812), and *hotel lifestyle* (0.743). In addition, even showing relatively weak centrality, the city of *Seoul* (0.589) and the specific hotel brand *Hotel Cappuccino* (0.536) emerged. Thus, the hashtags collected from lifestyle hotel posts reflect not only general hospitality and tourism-related attributes but also new trends in the hospitality industry, such as spending vacation time in an urban area or enjoying leisure activities nearby. This result supports previous studies that argued that lifestyle hotels appeal to specific lifestyles reflecting the latest trends.

5. Conclusion

In an era of significant change, this study investigated customers' perceptions of lifestyle hotels and extracted key attributes by analyzing up-to-date user-created content on social media. Within this research, it is evident that there were similarities and differences between the perception of lifestyle hotels by their guests and the concept of lifestyle hotels organized through the hospitality literature. The findings indicated that people perceive lifestyle hotels as downtown branded hotels with unique architecture and interior design features that provide urban experiences. This result supports the previously defined concept of lifestyle hotels as featuring unique and modern characteristics and design-centric interior architecture with stylish FF&E. However, previous literature highlighted personalized services and high-tech touches in guestrooms, yet those kinds of attributes did not show noticeably in this research. Instead, the findings demonstrated that guests perceive lifestyle hotels as places to enjoy urban and trendy experiences. Therefore, for the sustainable growth of the lifestyle segment, lifestyle hotels should rebuild their identity as hotels with distinctive architecture and design where urban experiences and the latest hospitality trends are situated.

Lifestyle hotel brands must continuously ask how and in what ways their environments and experiences should be designed. Therefore, while hospitality experiences and perceptions of a place have been studied qualitatively, this study finally utilized a big data approach to understand the perceptions of places. However, much deeper validation is still needed because the studied images were analyzed only to determine their contents without considering stylistic issues. In the face of rapid market changes, this approach with deep learning can provide an opportunity for hospitality brands to rebuild their competitive and sustainable identities in spatial contexts.

Acknowledgements

This work was supported by the BK21 funded by the Ministry of Education of Korea.

References

Bahtar, A. Z. and Muda, M.: 2016, The impact of User–Generated Content (UGC) on product reviews towards online purchasing–A conceptual framework, *Procedia Economics and Finance*, **37**(16), 337-342.

Baker, J.: 1986, The role of the environment in marketing services: The consumer perspective, *The services challenge: Integrating for competitive advantage*, **1**(1), 79-84.

Baker, J., Grewal, D. and Parasuraman, A.: 1994, The influence of store environment on quality inferences and store image, *Journal of the academy of marketing science*, **22**(4), 328-339.

Evans, J. R. and Berman, B.: 1995, *Principles of marketing*, Prentice Hall.

GAIL, M.: 2018, "THE GENSLER EXPERIENCE INDEX: HOSPITALITY" . Available from <https://www.gensler.com/research-insight/publications/dialogue/32/the-gensler-experience-index-hospitality> (accessed 1st December 2020).

Giannoulakis, S. and Tsapatsoulis, N.: 2016, Evaluating the descriptive power of Instagram hashtags, *Journal of Innovation in Digital Ecosystems*, **3**(2), 114-129.

Grandjean, M.: 2015, "GEPHI: Introduction to Network Analysis and Visualisation" . Available from <http://www.martingrandjean.ch/gephi-introduction> (accessed 1st December 2020).

Guerrero, P., Møller, M. S., Olafsson, A. S. and Snizek, B.: 2016, Revealing cultural ecosystem services through Instagram images: The potential of so-cial media volunteered geographic information for urban green infrastructure planning and governance, *Urban Planning*, **1**(2), 1-17.

Hu, Y., Manikonda, L. and Kambhampati, S.: 2014, What we instagram: A first analysis of instagram photo content and user types, *Proceedings of AAAI International Conference on Web and Social Media*.

Jaakonmäki, R., Müller, O. and Vom Brocke, J.: 2017, The impact of content, context, and creator on user engagement in social media mar-keting, *Proceedings of the 50th Hawaii international conference on system sciences*.

Jones, D. L., Day, J. and Quadri-Felitti, D.: 2013, Emerging definitions of boutique and lifestyle hotels: A Delphi study, *Journal of Travel & Tourism Marketing*, **30**(7), 715-731.

Kim, S.W.: 2017, "The Seoul Institute: Urban Planning System of Seoul" . Available from <https://www.seoulsolution.kr/en/node/6310> (accessed 1st December 2020).

Freund de Klumbis, D.: 2003, Seeking the "ultimate hotel experience", *XII International Tourism & Leisure Symposium 2003*, Barcelona (Spain), 1-13.

Kosar, L.: 2014, Lifestyle hotels: New paradigm of modern hotel industry, *Turističko poslovanje*, **14**, 39-50.

Latapy, M.: 2008, Main-memory Triangle Computations for Very Large (Sparse (Power-Law)) Graphs, *Theoretical Computer Science (TCS)*, **407**(1-3), 458-473.

Lee, J. H.: 2018, "ZDnet: Instagram Has Over 1 Billion Monthly Users" . Available from <https://zdnet.co.kr/view/?no=20180621085334> (accessed 1st December 2020).

Liu, C. R., Wang, Y. C., Chiu, T. H. and Chen, S. P.: 2018, Antecedents and outcomes of lifestyle hotel brand attachment and love: The case of Gen Y, *Journal of Hospitality Marketing & Management*, **27**(3), 281-298.

Milburn, R., Stotts, S. and Hall, L.: 2006, "Standing out in a crowd: PricewaterhouseCoopers" . Available from <https://www.hospitalitynet.org/file/152002774.pdf> (accessed 1st December 2020).

Olahut, M. R., El-Murad, J. and Plaias, I.: 2012, Store atmosphere: Conceptual Issues and It's Impact on Shopping Behavior, *Proceedings of the International Conference" Marketing-from Information to Decision"*, Babes Bolyai University, 317.

Pizam, A.: 2015, Lifestyle Hotels: Consistency and Uniformity vs. Individuality and Personalization, *International Journal of Hospitality Management*, **46**, 213-214.

Pullman, M. E. and Robson, S. K.: 2007, Visual methods: Using photographs to capture customers' experience with design, *Cornell Hotel and Restaurant Administration Quarterly*, **48**(2), 121-144.

Rainie, L., Brenner, J. and Purcell, K.: 2012, "Photos and videos as social currency online: Pew Internet & American Life Project" . Available from <https://www.pewresearch.org/internet/2012/09/13/photos-and-videos-as-social-currency-online>.

Ricca, S.: 2015, "Report defines boutique, lifestyle, soft brand" . Available from <http://www.hotelnewsnow.com/articles/25561/Report-defines-boutique-lifestyle-softbrand> (accessed 1st December 2020).

Schmidt, P.: 2017, "The Proliferation of Lifestyle Brands: Differentiate or Die" . Available from <https://www.luxury-branding.com/library/lifestyle-hotel-brands-differentiate-die> (accessed 1st December 2020).

Silva, T. H., De Melo, P. O. V., Almeida, J. M., Salles, J. and Loureiro, A. A.: 2013, A picture of Instagram is worth more than a thousand words: Workload characteriza-tion and application, *2013 IEEE International Conference on Distributed Computing in Sensor Systems*, 123-132.

Turley, L. W. and Milliman, R. E.: 2000, Atmospheric effects on shopping behavior: a review of the experimental evidence, *Journal of business research*, **49**(2), 193-211.

CUBIGRAPH5K

Organizational Graph Generation for Structured Architectural Floor Plan Dataset

YUEHENG LU[1], RUNJIA TIAN[2], AO LI[3], XIAOSHI WANG[4] and GARCIA DEL CASTILLO LOPEZ JOSE LUIS[5]
[1,2,3,4,5]*Harvard Graduate School of Design*
[1,2,3,4,5]*{lu|runjia_tian|aoli|xwang4|jgarciadelcasti}@gsd.harvard.edu*

Abstract. In this paper, a novel synthetic workflow is presented for procedural generation of room relation graphs of floor plans from structured architectural datasets. Different from classical floor plan generation models, which are based on strong heuristics or low-level pixel operations, our method relies on parsing vectorized floor plans to generate their intended organizational graph for further graph-based deep learning. This research work presents the schema for the organizational graphs, describes the generation algorithms, and analyzes its time/space complexity. As a demonstration, a new dataset called CubiGraph5K is presented. This dataset is a collection of graph representations generated by the proposed algorithms, using the floor plans in the popular CubiCasa5K dataset as inputs. The aim of this contribution is to provide a matching dataset that could be used to train neural networks on enhanced floor plan parsing, analysis and generation in future research.

Keywords. Graph Theory; Algorithm; Architecture Design Dataset; Organizational Graph.

1. Introduction

Graph theory plays a significant role in the design and analysis of building layouts. Architects have been used bubble diagrams-a schematic diagram of organizational graph-to represent the spatial relationship of architectural spaces as early as 1938 (Emmons & Paul 2017), and various definitions have been proposed by researchers for such organizational structures (Baglivo & Graver, 1983; Roth & Hashimshony, 1988).

A major part of the creative work for an architect is to translate a high-level organizational graph into a concrete dimensioned architectural floor plan. The automation of this translation process has been studied intensively, but traditional approaches mainly rely on rasterized architectural drawing datasets, i.e. bitmaps of floor plans. This research creates a cornerstone for future studies by developing algorithms to generate a dataset of the graph representations of architectural

PROJECTIONS, Proceedings of the 26th International Conference of the Association for Computer-Aided Architectural Design Research in Asia (CAADRIA) 2021, Volume 1, 81-90.

layouts based on existing drawing documents. The proposed algorithms can be further applied to three-dimensional Building Information Model (BIM) datasets by adding vertical relations to the edge mapping.

Our algorithms are successfully implemented on CubiCasa5K, a large-scale architectural floor plan dataset containing 5000 samples, which are also manually annotated into over 80 architectural element categories (Kalervo et al. 2019). For each floor plan, both raster images and a vectorized model are stored. Annotations are also included as metadata on the vector group objects. As a result, we present CubiGraph5K, a dataset of graph representations of structured floor plans, published open-source as part of this work.

In this paper, we describe the structure of the proposed organizational graphs, present the graph-generation algorithms, explain its application to the proposed floor plan dataset, and discuss the results obtained in the process.

2. Previous Work

The CubiCasa5K dataset was first used by its authors to analyze floor plans of residential buildings: the dataset was first explained, and a multi-task model was then introduced and applied on the dataset to predict the labels of architectural elements for a given floor plan image. The authors conclude that the performance of any machine learning model is dependent on the design of the dataset it is trained on, suggesting that future floor plan generation related machine learning research could benefit from the contributions of their work.

The traditional methods used to automate floor plan generation include rule-based (Levin, 1964) or optimizations algorithms (Roth & Hashimshony, 1988). More recently, organizational graphs have been used to train neural networks (Scarselli et al., 2009). CNNs and convolutional autoencoders have also been used to predict the location of rooms and walls inside of a floor plan boundary (Wu et al. 2019). Graph Convolutional Networks (GCN) have also shown potential in handling 2D images whose components are related to each other as a graph. Research work has been performed by using GCN along with other types of networks to generate images from a given scene graph which illustrates the spatial relation among different objects in the scene (Johnson et al., 2018).

A more recent example of graph-related research is the floor plan generating GAN model “House-GAN” (Nauata et al., 2020). This work shows that bubble diagrams, as a graph embodying organizational information, can be used as inputs of GAN models, facilitating the generation of floor plans. Similar work has been proposed in this direction (Ruizhen et al., 2020). One shortcoming of House-GAN is that the organizational graphs for training had to be manually generated by human annotators, which is a rather labor-intensive operation difficult to scale for larger datasets. In this research, we focus on the automatic generation of such graphs.

3. Method

3.1. GRAPH EXTRACTING ALGORITHM

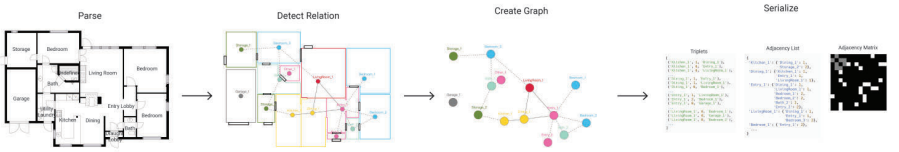

Figure 1. Synthetic Workflow.

Our goal is to extract geometric information from structured floor plan data, and generate a graph representation that describes the room relations in such a floor plan. The graph-generating algorithm consists of two steps: 1) machine-parsing the structured floor plan data, to retrieve geometric information of related elements (i.e. rooms, doors); 2) discriminating the relationships between rooms pairwisely to construct the graph. We first present the format of the input data followed by the relationship definition between two rooms, then explain the algorithm in detail followed by the possible output formats, and finally discuss the resulting algorithm complexity.

3.1.1. Input: Structured Floor Plan Data

The input of the graph-generating algorithm is structured floor plan data represented in vector format, like for example Scalable Vector Graphics (SVG), Drawing Exchange Format (DXF), etc. As a minimal requirement, each floor plan should include tags for different types of architectural elements and each element should include precise euclidean coordinates of their inner boundary.

3.1.2. Room Relations

In architectural practice, designers use bubble diagrams to study the relationship of rooms. Many kinds of relationships can be illustrated using these diagrams, such as program proximity, spatial connectivity, flow of humans, etc. In this paper, since our study focuses on residential floor plans, we present three possible relations between each room pair to describe connectivity: adjacent, door-connect and not-connect.

Adjacent. When no physical partition between two rooms is present, these two rooms are considered adjacent. Geometrically, the two polygons representing adjacent rooms should touch each other by more than a single point.

Door-connect. When two rooms can be and can only be traversed through a door, they are considered as door-connect. Geometrically, the two polygons representing the two door-connect rooms should touch the same door polygon by more than a single point. If two rooms are both adjacent and door-connect, they are considered adjacent, since direct connectivity is prioritized here. Door-connect relation does not have transitivity.

Not-connect. Rooms that are not adjacent or door-connect are considered

not-connect. In another word, people cannot go from one room to the other without entering a third room or a space that is not visible in the floor plan.

Figure 2. Adjacent Relationship and Door-connect Relationship.

3.1.3. Algorithm for Single Floor Plan

Our proposed graph-generation algorithm features two steps: 1) parsing the floor plan data to obtain the geometry of rooms and doors, and 2) calculating the geometric relationships for each room pair to generate the graph.

Parsing. As discussed previously, this algorithm relies on the floor plan data to contain annotated and classified room and door boundaries. Our implementation has been tested with input SVG files, an extended form of Extensible Markup Language (XML), where each room and the door between them is explicitly labelled and includes Euclidean coordinates of the curves of their inner boundaries.

Algorithm 1: Room Relation Calculation

Given P_{room}, P_{door}
$A_{door} \leftarrow$ empty list to store adjacent doors of each room.
while $r, d \leftarrow$ *each pair of room and door* **do**
  if r *intersect with* d **then**
    Record d as r's adjacent door in A_{door}.
  end
end
$R \leftarrow$ empty list to store pairwise relationship of rooms as adjacency list.
while $r_1, r_2 \leftarrow$ *each pair of rooms* **do**
  if r_1 *intersect with* r_2 **then**
    Record r_1 and r_2 in each other's adjacent rooms with relationship **ADJACENT**.
  else
    if r_1 *and* r_2 *share same adjacent door according to* A_{door} **then**
      Record r_1 and r_2 in each other's adjacent rooms with relationship **DOOR_CONNECT**.
    end
  end
end
Return R.

Algorithm 2: Dataset Iteration

input : A sequence of floor plans D such that for all $P \in D$, P represents a XML file that represents one floor plan data structure
output: A sequence of graph data structure of the same size as D
initialize G arbitarily;
for $i \leftarrow 0$ **to** $|D|$ **do**
  $P \leftarrow D[i]$;
  $(P_{ROOM}, P_{DOOR}) \leftarrow PARSE(P)$;
  $G_{j,k} \leftarrow ROOMRELATION(P_{ROOM}, P_{DOOR})$;
end
return G;

Figure 3. Pseudo Code for Room Relation Calculation and Dataset Iteration Algorithm.

Calculating Room Relation. We iterate the dataset and calculate pairwise room-room and room-door relationships in each floor plan to generate the graph. For disambiguation, we prioritize room-room relationship over room-door relationship. After the two rounds of iteration, the relation between all pairs of rooms in the floor plan is recorded to construct the graph representation. Pseudo code for room relation calculation is detailed in Figure 3.

We implement a robust algorithm for relationship calculation by dilating the polygons by a small distance D and calculating the intersection of the two targeting

polygons, and set a threshold T for detecting adjacency. Some examples of inaccurate data labeling that can be accommodated by our algorithm will be discussed in Section 3.3.3.

3.1.4. Output: Data Structure for Room Relation Graph

We propose three types of representations for the output graph: triplets, adjacent list and adjacency matrix (Figure 4). The time complexity and space complexity of all methods are similar, but they can be applied to various use cases, and the advantage of each representation will depend on the network structure that is applied for performing geometric deep learning on the relational graph dataset.

Figure 4. Plan 41: Graph, Triplet, Adjacency List and Adjacency Matrix as Rasterized Image.

Triplet. This is a common representation used in Message Passing Networks (MPN) (Gilmer, J, et al., 2017). It is a generic representation for all types of weighted graphs. It uses a triplet (i, w, j) to represent an edge with weight w between node i and j.

Adjacency List. This representation features a structured room-adjacencies set of relations, where each room is associated with an object composed of all the room labels that it is connected to, and their connectivity type.

Adjacency Matrix. The output of this representation features a pixelated square image, where the value of each pixel $w_{ij} = w_{ji} = w(i, j)$ represents the category of connection between two connected rooms. This representation is mainly used for graphs that are very dense.

3.1.5. Workflow for a Dataset

In this work, we propose an algorithm to generate the floor plan graph representation for a given architectural dataset in pseudo polynomial time, defining the following mathematical formulation of an architectural floor plan dataset:

Room: We represent R_j as a polygon composed of a array of two-dimensional points: $R_j = \{p_k | k = 0, \dots c_j\}$, where c_j is the total number of points in the geometry layout of room .

Floor Plan $P_i = \{R_j | j = 0, 1, \dots, n_i\}$ where ni represents the number of Rooms in each floor plan and max $(n_0, \dots n_i) = n$. Therefore Floorplan P_i is composed of at most n Rooms.

Annotated Floor Plan Dataset $D = \{P = D_i | f \quad \text{or} \quad i = 0, 1, \dots, m\}$, where P is an element in the Dataset and m is the total number of Floorplans in the Dataset.

Graph Dataset $G = \{G_i | f \quad \text{or} \quad i = 0, 1, \ldots, m\}$ where G_i represents the Graph in Floor Plan D_i.

Our dataset-iteration algorithm is detailed in Fig 3. The parsing function for each floor plan is trivial. The ROOMRELATION function calls the room relation calculation algorithm defined in Section 3.1.3.

3.1.6. Algorithm Complexity Analysis

We formulate the graph parsing into the following mathematical problem: from Section 3.1.5, we assume there are m rooms in the data set in total, and maximum n rooms and d doors in the floor plan, each represented by the a set of two-dimensional points $R_i = \{p_j\}$, and the point set has maximum cardinal c, where $|R_i| \leq c$, for $i = 0, 1, \ldots, n$. Then the time complexity for computing the relational graph for each plan will be $O\left(m\left(nd + \frac{n^2}{2}\right)c^2\right)$. It is noticeable that in most architecture design dataset, n will not be arbitrarily large, as the smallest using units in architecture that counts as a room should not be arbitrarily small. Therefore in most cases, it does not contribute to the overall time complexity, thus the time complexity would be reduced to $O(mdc^2)$. Our algorithm runs in a pseudo-polynomial time of total number of floor plans. Note that normally the number of doors and rooms are on the same scale, since rooms in a floor plan usually form a tree-like structure. As a result the complexity can be further simplified as an expression of m and c: $O(mc^2)$.

3.2. CASE STUDY

In order to prove the validity of the algorithm, we applied it to all floor plans in the CubiCasa5K dataset (Kalervo et al. 2019), a collection of annotated architectural floor plans in both raster and vector format. As a result, we present CubiGraph5K, a dataset of graph representations of architectural floor plans that mirrors the structure of CubiCasa5K, and which could be used as stand-alone or in tandem with the original for machine learning applications.

3.2.1. Single Floor Plan

To generate the CubiGraph5K dataset, an object model was implemented representing the key classes for elements available in the source dataset: Plan, Room and Door. These classes represent concretions of the high-level graph, node and edge elements they represent in the graph structure, and feature properties and methods that allow them to be queried as part of the proposed algorithms.

For simplicity, all Room types found in the original dataset were mapped into a set of basic types: LivingRoom, Bedroom, Kitchen, Dining, Bath, Storage, Entry, Garage, Outdoor and Other. If multiple instantiations of the same Room type are present in a Plan, correlative 1-based indices are assigned as ID.

We use Plan 41 in the dataset as an example to show case the creation of single floor plan.

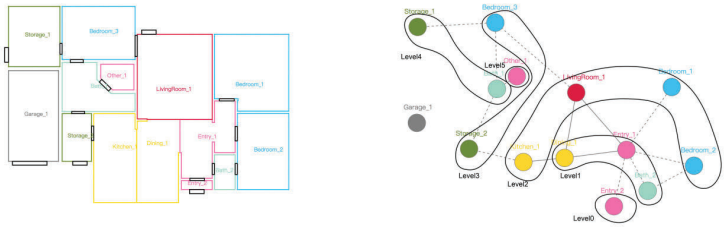

Figure 5. Plan 41 and Diameter of Plan 41.

Rooms. Calling plan.room_names would return a list of all room labels, with unique correlative IDs concatenated.

Number of Instances for Each Room Type. The attribute plan.room_type_count will return a dictionary with key, value pairs representing room types and their corresponding number of occurrences in the plan.

Diameter of a Floor Plan. As the space gets larger, one may be interested in the complexity of a floor plan. We define the 'diameter' of a floor plan as the number of edges passed between two farthest rooms. Figure 5 illustrates the definition of plan diameter using Plan 41 as an example (in this case, $diameter = 5$). The metric of diameter finds its meaning in design as well, it can reflect the spatial progression in the floor plan, indicating the layering of the space, which can, to some extent, impact the design of circulation, acoustics or even energy flow.

Shortest Path. Since the floor plan is represented as a graph, graph search algorithms such as Breadth First Search can be easily applied to get the shortest path(s) between two rooms. One thing worth mentioning is that both adjacent and door-connect are treated the same as opposed to not-connect in the calculation. With our tool, user can get all possible shortest path(s) between two rooms.

3.2.2. Multiple Floor Plans

The single plan methods and attributes provide flexible subroutines to iterate over the multiple plans and the entire dataset, so that users can explore its statistics and filter plans with specific characters. The diameters of floor plans in CubiGraph5K concentrate around 3, 4, 5 and the most common room types are Studio, 1B1B, 2B1B and 3B2B (See Figure 6). Occasionally, rooms in the floor plan are not connected to any other rooms, which makes up 2.1% of the total rooms. As one may expect, 54.6% of the "islands" are Garage and Storage (outdoor).

To maximize the convenience for the users, we also provide utility functions on the whole dataset, which are also documented in the repository. The open-source nature of the project also gives users the flexibility to extend the existing functions library. Using these attributes and methods as subroutines, users can further develop their own functions or classes to achieve specific goals with the dataset.

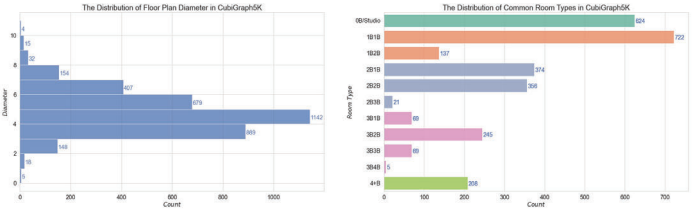

Figure 6. Dataset Statistics: Diameter Distribution (left), Room Type Distribution (right).

3.3. EVALUATION

To estimate the validity of the algorithm and its implementation, an initial exploratory analysis of the CubiGraph5K dataset was conducted. First, the contributed graph dataset was compared to the original CubiCasa5K dataset in terms of number of rooms per each room type. Second, the resulting graph representation of floor plans was examined by human experts in order to verify its correctness. To better facilitate this process, a visualization tool was developed.

3.3.1. Dataset Verification

In Table 1, The statistics of each room type in both datasets show that the proposed algorithm captures most of the major room types in the CubiCasa5K dataset. The statistics of the original dataset are estimated from Fig.3. in the original paper. The minor differences between CubiCasa5K and results generated by our parsing algorithm appear to be caused by different definitions of room types when grouping all original 62 types into the 10 major types in our CubiGraph5K implementation. Since the graph generation algorithm only works for single-story floor plans, the total number of rooms in CubiGraph5K shrinks by 42.8%.

Table 1. Statistics Comparison between CubiCasa5K and CubiGraph5K.

Room Type	# of Room in CubiCasa5k	# of Room Parsed	# of Room in CubiGraph5K
LivingRoom	11347	4611	3001
Bedroom	7353	8274	4853
Kitchen	4109	4525	3125
Dining	941	949	502
Bath	6475	7241	4252
Storage	6214	6347	3303
Entry	5393	5843	3524
Garage	729	687	326
Outdoor	6976	7805	4272
Other	12750	14732	7731
All	62287	61014	34889

3.3.2. Graph Visualization and Verification

In order to easily visualize and verify the generated graph results, a tool for visually overlaying the nodes and weights of a graph on its associated floor plan was developed. To manually verify the correctness of a room relation graph, the output as adjacency list and the visualized graph will be generated and laid out side-by-side with the original floor plan.

A random sample of 50 floor plans were evaluated by the authors, following the above procedure. 68.0% of the graph results correctly reflected the original floor

plans. It is worth mention that 93.8% of the incorrect cases were caused by data labelling mistake from CubiCasa5K, which proved the correctness and robustness of the proposed algorithms.

3.3.3. Improvements

The original algorithm relied heavily on the correct overlapping of polygon boundaries and the low-tolerance matching of their vertices. As discussed in Section 1.3, many architectural plans are not drawn so precisely, including many of the CubiCasa5K dataset, resulting in incorrect graph topographies. In our improved room relation calculation algorithm, geometric operations (i.e. dilation and intersection calculation) are performed to decide if two polygons are adjacent. Instead of simply deciding if the boundaries of the two polygons share more than a single point, two thresholds are set for the minimum intersection between two rooms and between a room and a door. We demonstrate the necessity of such operations by comparing the graph results generated by two earlier versions of our algorithm.

No Threshold between Two Rooms. When room polygons are not accurately drawn, meaning that they don't share boundaries when they should (see Figure 7), adjacent rooms would not be detected by the algorithm.

No Threshold between Door and Room. When a door polygon fails to touch its intended adjacent room or accidentally touches a room other than its intended neighbor, the algorithm is not able to decide the correct door-connect relation. (See Figure 7).

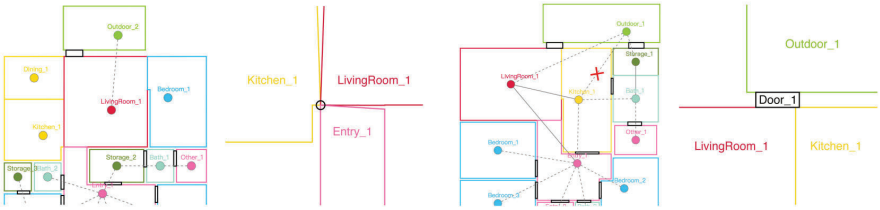

Figure 7. Visualized Graph and Diagram: Plan 353 (left), Plan 283 (right).

Other limitations of CubiCasa5K dataset, such as incorrectly labelled rooms or elements with invalid polygons, cannot be handled at this time by our proposed algorithm. A complete list of floor plans with invalid features is available in the repository's documentation. We leave the handling of those edge conditions to future work.

4. Contribution

CubiGraph5K, the matching graph dataset of CubiCasa5K, is created by our proposed algorithms. It is published along with our implementation of the algorithms and additional graph query functions library at https://github.com/luyueheng/CubiGraph5K".

5. Discussion and Conclusion

In this paper, we proposed a novel algorithm to systematically parse structured floor plans, generate graph representations and serialize the results in portable format. Our approach was tested on CubiCasa5K, generating the corresponding CubiGraph5K and providing accessibility to future researchers in the realm of architecture design computation.

There are mainly two limitations of the proposed workflow. First, it highly relies on the consistency of the vectorized floor plans thus it was only tested on CubiCasa5K with properly labelled SVG files. Second, our definition of room relations didn't take cross-level connections into account thus it only works for single-level floor plans. Despite the limitations, our approach has the potentials to be integrated in graph-based floor plan generation network, i.e. Graph Convolution Network. By defining more targeting room relations, the generated graph could depict more complex floor plan layouts. Especially, similar workflows could be applied on structured three-dimensional BIM datasets.

We hope the proposed approach and dataset contributed with this research will be beneficial for further studies dealing with topological representations of architectural drawings.

References

Baglivo, J.A. and Graver, J.E.: 1983, *Incidence and Symmetry in Design and Architecture*, Cambridge University Press Cambridge.

Emmons, P.: 2017, Embodying Networks: Bubble Diagrams and the Image of Modern Organicism, *The Journal of Architecture*, **22**(5), 854–874.

Gilmer, J., Schoenholz, S.S., Riley, P.F., Vinyals, O. and Dahl, G.E.: 2017, Neural Message Passing for Quantum Chemistry, *Proceedings of the 34th International Conference on Machine Learning*, 1263–1272.

Hu, R., Huang, Z., Tang, Y., van Kaick, O., Zhang, H. and Huang, H.: 2020, Graph2Plan: Learning Floorplan Generation from Layout Graphs, *ACM Transactions on Graphics*, **39**(4).

Isola, P., Zhu, J.Y., Zhou, T. and Efros, A.A.: 2017, Image-to-Image Translation with Conditional Adversarial Networks, *Proceedings of the IEEE Conference on Computer Vision and Pattern Recognition*, 1125-1134.

Johnson, J., Gupta, A. and Fei-Fei, L.: 2018, Image Generation from Scene Graphs, *Proceedings of the IEEE Conference on Computer Vision and Pattern Recognition*, 1219-1228.

Kalervo, A., Ylioinas, J., Häikiö, M., Karhu, A. and Kannala, J.: 2019, CubiCasa5k: A Dataset and an Improved Multi-task Model for Floorplan Image Analysis, *Scandinavian Conference on Image Analysis*, 28-40.

Levin, P.H.: 1964, *Use of Graphs to Decide the Optimum Layout of Buildings*, Building Research Station, Garston.

Nauata, N., Chang, K.H., Cheng, C.Y., Mori, G. and Furukawa, Y.: 2020, House-GAN: Relational Generative Adversarial Networks for Graph-constrained House Layout Generation, *Computer Vision – ECCV 2020 Lecture Notes in Computer Science*, 162–177.

Roth, J. and Hashimshony, R.: 1988, Algorithms in Graph Theory and Their Use for Solving Problems in architectural design, *Computer-Aided Design*, **20**(7), 373-381.

Scarselli, F., Gori, M., Tsoi, A.C., Hagenbuchner, M. and Monfardini, G.: 2008, The Graph Neural Network Model, *IEEE Transactions on Neural Networks*, **20**(1), 61-80.

GENSCAN: A GENERATIVE METHOD FOR POPULATING PARAMETRIC 3D SCAN DATASETS

MOHAMMAD KESHAVARZI[1], OLADAPO AFOLABI[2],
LUISA CALDAS[3], ALLEN Y. YANG[4] and AVIDEH ZAKHOR[5]
[1,2,3,4,5] *University of California, Berkeley*
[1,2,3,4,5] *{mkeshavarzi|oafolabi|lcaldas|allenyang|avz}@berkeley.edu*

Abstract. The availability of rich 3D datasets corresponding to the geometrical complexity of the built environments is considered an ongoing challenge for 3D deep learning methodologies. To address this challenge, we introduce GenScan, a generative system that populates synthetic 3D scan datasets in a parametric fashion. The system takes an existing captured 3D scan as an input and outputs alternative variations of the building layout including walls, doors, and furniture with corresponding textures. GenScan is fully automated system that can also be manually controlled by a user through an assigned user interface. Our proposed system utilizes a combination of a hybrid deep neural network and a parametrizer module to extract and transform elements of a given 3D scan. GenScan takes advantage of style transfer techniques to generate new textures for the generated scenes. We believe our system would facilitate data augmentation to expand the currently limited 3D geometry datasets commonly used in 3D computer vision, generative design and general 3D deep learning tasks.

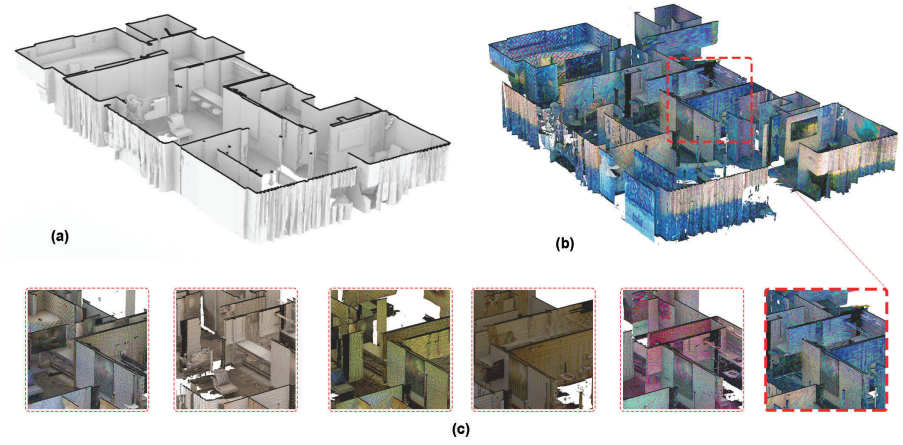

Figure 1. GenScan takes an existing captured 3D scan (a) as an input and outputs alternative parametric variations of the building layout (b) including walls, doors, and furniture with (c) new generated textures.

PROJECTIONS, Proceedings of the 26th International Conference of the Association for Computer-Aided Architectural Design Research in Asia (CAADRIA) 2021, Volume 1, 91-100.

Keywords. Computational Geometry; Generative Modeling; 3D Manipulation; Texture Synthesis.

1. Introduction

The utilization of 3D deep learning techniques has been widely explored in cross-disciplinary fields of architecture, computer graphics, and computer vision. For tasks such as synthesizing new environments, semantic segmentation (Armeni, Sener, et al. 2016; McCormac et al. 2017), object recognition (Qi et al. 2016), and 3D reconstruction (Guo, Zou, and Hoiem 2015; Song, F. Yu, et al. 2017), integrating 3D deep learning methodologies have brought a promising direction in the state-of-the-art research. However, like many other learning approaches, the success of this approach is highly dependent on the availability of the appropriate datasets. In contrast to 2D image recognition tasks, where training labeled datasets are available in large quantities, 3D indoor datasets are limited to only a small number of open-source datasets. Capturing 3D geometry is seen to be much more expensive than capturing 2D data in terms of both hardware and human resources.

3D data for training resources for computer vision tasks can be found in two general categories (a) real-world captured data and (b) synthetic data. The first approach involves scanning RGB-D data using high end capturing systems or commodity-based sensors. To this extent, a number of open-source datasets are available with various scales and capture qualities. The ETH3D dataset contains a limited number of indoor scans (Schops et al. 2017), and its purpose is for multi-view stereo rather than 3D point-cloud processing. The ScanNet dataset (Dai et al. 2017) and the SUN RGB-D (Song, Lichtenberg, and Xiao 2015) dataset capture a variety of indoor scenes with added semantic layers. However, most of their scans contain only one or two rooms, not suitable for larger scale layout reconstruction problem. Matterport3D (Chang et al. 2018) provides high-quality panorama RGB-D image sets for 90 luxurious houses captures by the Matterport camera.

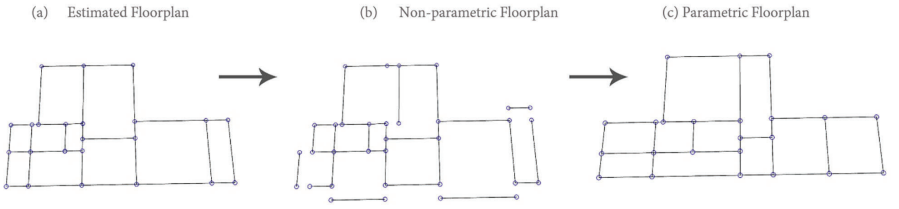

Figure 2. Applying individual transformations to wall segments results in inconsistency of the output layout (b). Using the Parametrizer module we avoid unwanted voids and opening in the building's walls.

The second approach is to utilize synthetic 3D data of building layouts and indoor scenes, which has also been recently produced in mass numbers to fill the void of rich semantic 3D data. SUNCG (Song, F. Yu, et al. 2017) offers a variety of indoor scenes with CAD-quality geometry and annotations. However, the level of detail and complexity of the different building elements

in such crowd-sourced synthetic approaches is extremely limited when compared to 3D scanned alternatives. Synthetic datasets lack natural transformation and topological properties of objects in real-world settings. Furthermore, there is a broad body of literature focused on synthesizing indoor scenes by learning from prior data (Zhang et al. 2019). While such approaches are mainly focused on predicting furniture placements and arrangement in an empty (Li et al. 2019; Fisher et al. 2012) or partially populated scene (Kermani et al. 2016; Keshavarzi, Parikh, et al. 2020), they are also dependent on the quality and diversity of the input data in their training stage. Procedural models have also been widely used in generating full buildings (Mu¨ller et al. 2006; Saldana and Johanson 2013), furniture layout (Merrell et al. 2011; Germer and Schwarz 2009) and manipulating indoor scenes (L.F. Yu et al. 2011; Keshavarzi, Yang, et al. 2020). Yet again, the output of such methods lack the complexity of real-world captured data, falling short of being effectively utilized in common computer vision tasks.

Therefore, augmenting large-scale datasets of 3D geometry that correspond to the complexity of the built environments is still an open challenge. Motivated by this challenge, we introduce GenScan, a generative system that populates synthetic 3D scan datasets. GenScan generates new semantic scanning datasets by transforming and re-texturing the existing 3D scanning data in a parametric fashion. The system takes an existing captured 3D scan as an input and outputs alternative variations of the building and furniture layout with manipulated texture maps. The process is fully automated and can also be manually controlled with a user in the loop. Such an approach results in the production of multiple data points from a single scan for 3D deep learning applications.

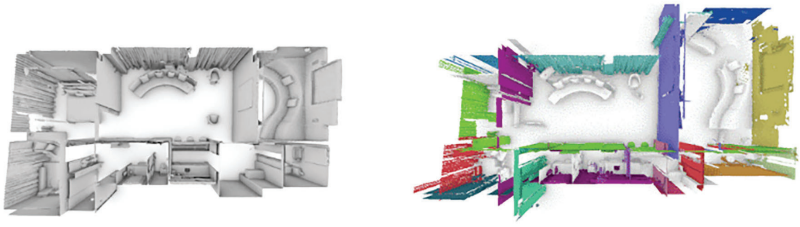

Figure 3. Results of the parametric modification (right) of an input scan (left).

2. Methodology

The general workflow of the system consists of four main components. First, we predict the floorplan of the input 3D scan using a hybrid deep neural network (DNN). We classify what type of building the input model is and estimate what common finishing wall to wall distance the input model holds. Second, to avoid inconsistencies in the manipulated walls, we parameterize all generated vectors to prepare for element transformation. Third, we classify wall elements of the 3D scan using the predicted floorplan and automated thresholds and apply parametric transformations to all wall and non-wall elements separately. Finally, we apply a style transfer algorithm using a combination of a pre-trained VGG network and

gradient descent module to current texture maps to generate new textures for the generate scenes.

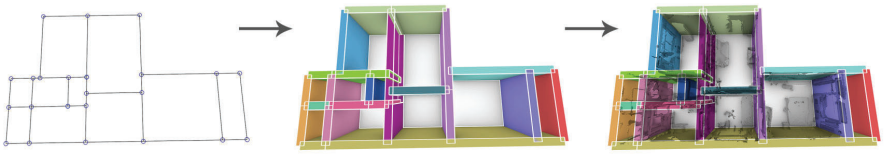

Figure 4. Wall extraction module. We use the estimated floorplan layout and door sizes to construct threshold bounding boxes centered on each parametric line. With this method, we classify wall elements (colored) and non-wall elements (white) in the scene.

2.1. PARAMETERIZATION

As shown in Figure 2.b, moving an individual wall or a group wall with a certain transformation matrix produces inconsistency in the generated output layout, with unwanted gaps and voids emerging between corner points of the floorplan. We instead assign transformations to the corresponding nodes of the corner coordinates of the target wall elements. We utilize a modified implementation of (Keshavarzi, Hutson, et al. 2020) to parametrize the extracted floorplan. This would manipulate all lines connected to the transformed node. However, to avoid distortion of the orthogonal nature of the building floorplans, we merge co-linear paths that connect to each other with a mutual node and share the same direction vector. Next, we identify the array of nodes that are located on the co-linear lines. After applying transformations to the connected line node array, we construct new polylines from each node array. This would result in fully automated parametric model that takes transformation vectors and connected line indices as an input and outputs a new floorplan layout without producing undesired gaps and floorplan voids

2.2. WALL EXTRACTION

To classify the walls and movable edges of the input 3D scan, we use the original parametric model to extrude threshold bounding boxes centered on each of co-linear parametric lines generated in the previous step. We then construct a bounding box for each available mesh in the 3D scan input, and test if inscribes within any of the connected line bounding boxes. With this method, we estimate whether a mesh is part of the building wall system or not, and if so, we can find out which connected wall it is subscribed to.

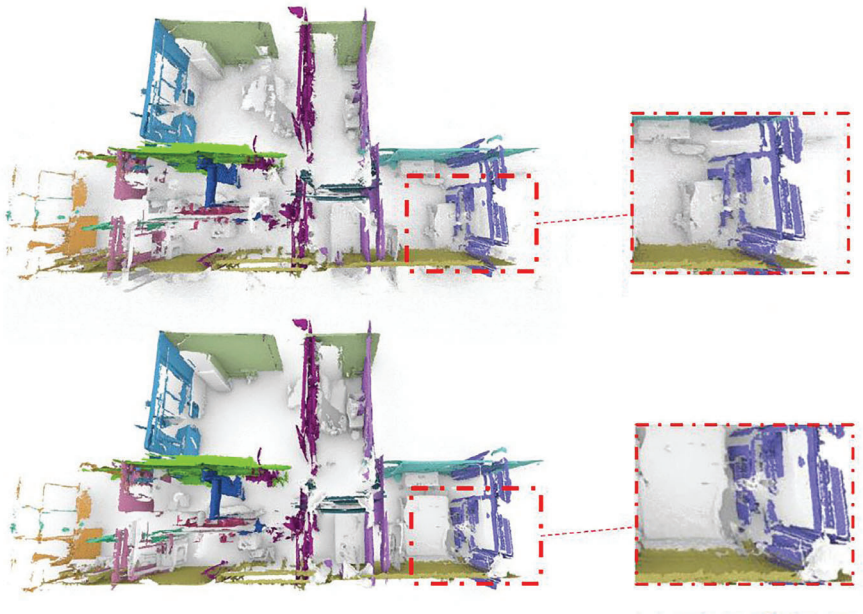

Figure 5. Transformation on wall elements only (top). Transformations on wall elements and closest furniture correspondingly.

To define the width and threshold of the connected line bounding box, we take advantage of the extracted door sizes provided by the hybrid DNN module introduced in Liu et al method (Liu, Wu, and Furukawa 2018). Based on the door sizes, we can heuristically classify the building type of the input model and estimate what common finishing wall to wall distance the input model holds. This distance can later be verified by measuring whether a significant peak in the average height takes place within the calculated range. However, both heuristics are is not always precise, as elements such as tall bookshelves and cabinets may interfere with thickness estimation of the walls.

2.3. MODEL TRANSFORMATION

Given a connected line index and an offset value, all nodes corresponding to the target line would be transformed in the direction perpendicular to the connected line. In many cases, this would not only affect the target line itself, but also change the size of neighboring connected lines (Figure 2.c). After all transformations are applied to the nodes of the graph, we calculate the difference between the transformation matrix of the initial geometry and the final geometry. This includes a two-dimensional translation vector defining the variance in the position and also a scale factor computed from the center of each line. Next, we apply the transformation vector of each connected line to all input meshes included in the corresponding bounding box. This would result in the parametric movement of the estimated walls, while maintaining the overall node graph constructed between

all wall elements. By applying the scale transformation specifically to the x and y directions, we stretch and shrink the walls to avoid unwanted architectural inconsistencies and prevent the transformed output from containing irrelevant void and structural gaps.

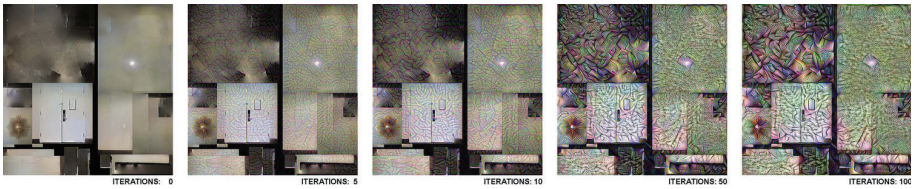

Figure 6. Iterations of the style transfer gradient descent algorithm.

However, as shown in Figure 4, in many cases the modification made to the walls can overlap with non-wall elements or the building furniture. This can result in conflicting mesh artifacts in certain clusters. To address this problem, we calculate the center coordinates of each bounding box assigned to non-wall meshes and perform a closest point search with the parametric line system to find the closest wall. We then transform each mesh with the two-dimensional position translation vector of the corresponding closest wall, with a non-linear factor of its distance to the wall. Therefore, a non-wall mesh element closer to the wall would have a much similar transformation function to the wall itself, than a non-wall mesh element located in the middle of the room. This would allow furniture to move close and far in relation to each other, instead of moving in a similar direction altogether.

2.4. MODEL GENERATION

The parametric model can be modified to alternate layouts using two main approaches. First, by manually inputting the system a list of parametric line indices and a corresponding offset value, which requires a user in the loop. The second approach is by providing a random range of offsets values to be assigned to random parametric lines of the model. Such method allows mass generations of synthetic 3D scans which can be later filtered and sorted by implementing evaluation functions. Figure 5 illustrates a random floorplan generation of 3D scan using this method.

3. Texture Generation

After applying parameterized geometry transformations to the scanned data, we aim to change the overall visual appearance of the newly generated mesh by editing the associated texture maps. Within our texture modification pipeline, we follow two steps to modify the texture maps of the original mesh provided by the the input scan data. First, we take all the texture maps associated within one scan and apply a simple style transfer to each of the textures. Next, we take the generated texture map and apply corrections to its image characteristics such as hue, saturation, and tint, etc. Finally by updating the texture coordinates of the vertices in the

newly generated geometry, we are able to match the style transferred texture maps accordingly.

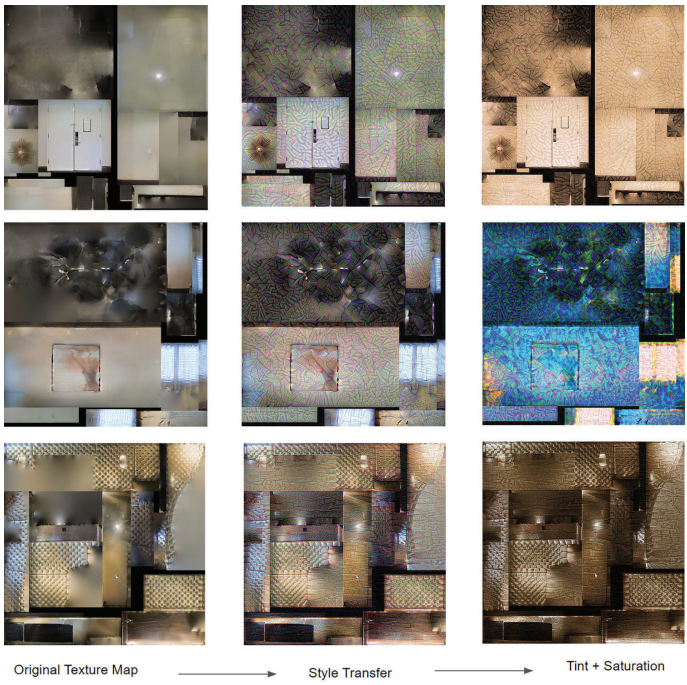

Figure 7. Different texture maps modified through style transfer and color modification. Permutations of matching style transfer with modified tints, hues, and saturation can be applied to generate diverse texture maps.

We implement the style transfer method introduced by Gatys et al. (Gatys, Ecker, and Bethge 2015). We incorporate a pre-trained VGG network to output a style transferred texture map. We calculate the content loss and style loss of our generated image at each iteration of the algorithm and run a gradient descent module until we reach an iteration that looks visually convincing. In figure 6, we illustrate how the output image converges to the style image while the content loss and image loss are being minimized. The higher the number of iterations the more distinct the style is on the texture map, therefore, for a more subtle effect we choose a lower number of iterations for its realism. We apply the transfer technique to modify the texture maps included with the Matterport scans. Style transfer would allow diverse modifications of the input textures, an easy and efficient way to blend a generate variations within a single content texture. The style transfer implemented can be the same for each texture or unique. For example, each room or part of the mesh can have its own different texture modification. Our application of style transfer is to change our existing texture maps to look like new textures using this established technique. By using different style images we create rooms

that look like they are made from brick, wood, or even a wallpaper laid on them. This versatility of style transfer allows the subset of data regeneration limitless and provides a unique enough new mesh that can be used for our original motivation.

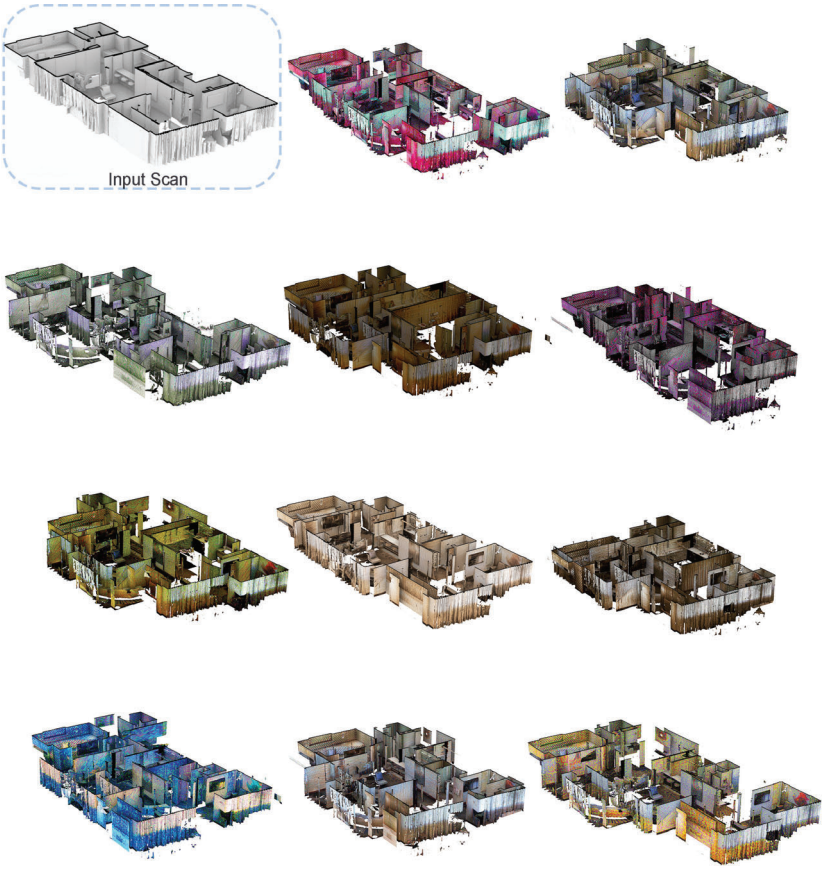

Figure 8. Examples of 3D mesh population from an input scan (top left) with modified floor geometries, texture elements, and colors.

Finally to allow for more texture variation and realism, we apply a postprocessing module of hue, saturation, and tint adjustment to the texture maps. In figure 7, we illustrate variety of textures we can generate with control over these parameters. At the end of our pipeline we use the original texture to adjust these parameters of the texture map image. We achieve this by converting the image into an RGBA array that we can shift and scale dictated by the desired effect. Overall, through just the texture modification process, we have control and access to infinite choices in style image and parameterization of image characteristics mentioned above. Figure 8 displays just a few of the possible final floor layouts created with GenScan.

4. Discussions and Conclusion

GenScan applies automated parameterization and texture modification of 3D scanned geometrical data to produce bootstrapped samples of 3D scanned data. Given data for just a single scan, GenScan actively produces valid synthetic geometric and textured data of multiple potential layouts resulting in floor plans with modified floor geometries, texture elements, and colors. We believe our system would allow for mass parametric augmentation to expand the currently limited 3D geometry datasets commonly used in 3D computer vision and deep learning tasks. Such an approach results in the production of multiple data points from a single scan for 3D deep learning methodologies. This methodology can facilitate applications across multiple disciplines including design optimization, computer vision, virtual and augmented reality, and construction applications.

While the current GenScan system has the ability to parameterize walls and major building elements extracted from the floorplan layout, it does not cover parameterizing smaller room elements such as chairs, beds, tables, desk, etc. Such objects not only need to be identified using semantic segmentation methods, a parametric relationship would also need to be established to allow relevant layout modifications. Furthermore, generating non-orthogonal layouts and extend parameterization to distorted and curved layouts can be also considered as next steps to this study. Another limitation of our system lies in the inability to modify the textures of specific walls and non-wall objects of our choosing. Identifying specific areas of the texture maps to regenerate and filling in gaps produced by expanding layout would result in a cleaner 3D model. Moreover, applying unique changes to specific parts of the texture maps instead of the whole map would allow for even greater customization, variability, and realism of the data. Finally, streamlining our implementation of the texture modification process in our pipeline will achieve higher texture resolution quality in an efficient time period.

Acknowledgments

We acknowledge the generous support from the following research grants: the FHL Vive Center for Enhanced Reality Seed Grant, and the Siemens Berkeley Industrial Partnership Grant, ONR N00014-19-1-2066. Furthermore, we would like to thank Woojin Ko and Avinash Nandakumar for their assistance in generating synthetic texture maps, and Chen Liu and Tommy Wei for their help in integrating and troubleshooting the FloorNet module within our system.

References

Armeni, I., Sener, O., Zamir, A.R., Jiang, H., Brilakis, I., Fischer, M. and Savarese, S.: 2016, 3d semantic parsing of large-scale indoor spaces, *Proceedings of the IEEE Conference on Computer Vision and Pattern Recognition*, 1534-1543.

Chang, A., Dai, A., Funkhouser, T., Halber, M., Niessner, M., Savva, M., Song, S., Zeng, A. and Zhang, Y.: 2017, Matterport3d: Learning from rgb-d data in indoor environments, *arXiv preprint arXiv:1709.06158*.

Dai, A., Chang, A.X., Savva, M., Halber, M., Funkhouser, T. and Niessner, M.: 2017, Scannet: Richly-annotated 3d reconstructions of indoor scenes, *Proceedings of the IEEE Conference on Computer Vision and Pattern Recognition*, 5828-5839.

Fisher, M., Ritchie, D., Savva, M., Funkhouser, T. and Hanrahan, P.: 2012, Example-based synthesis of 3D object arrangements, *ACM Transactions on Graphics (TOG)*, **31**(6), 1-11.

Gatys, L.A., Ecker, A.S. and Bethge, M.: 2015, A neural algorithm of artistic style, *arXiv preprint arXiv:1508.06576*.

Germer, T. and Schwarz, M.: 2009, Procedural Arrangement of Furniture for Real-Time Walkthroughs, *Computer Graphics Forum*, 2068-2078.

Guo, R., Zou, C. and Hoiem, D.: 2015, Predicting complete 3d models of indoor scenes, *arXiv preprint arXiv:1504.02437*.

Kermani, Z.S., Liao, Z., Tan, P. and Zhang, H.: 2016, Learning 3D Scene Synthesis from Annotated RGB-D Images, *Computer Graphics Forum*, 197-206.

Keshavarzi, M., Hutson, C., Cheng, C.Y., Nourbakhsh, M., Bergin, M. and Asl, M.R.: 2020, SketchOpt: Sketch-based Parametric Model Retrieval for Generative Design, *arXiv preprint arXiv:2009.00261*.

Keshavarzi, M., Parikh, A., Zhai, X., Mao, M., Caldas, L. and Yang, A.Y.: 2020, SceneGen: Generative Contextual Scene Augmentation using Scene Graph Priors, *arXiv preprint arXiv:2009.12395*.

Keshavarzi, M., Yang, A.Y., Ko, W. and Caldas, L.: 2020, Optimization and Manipulation of Contextual Mutual Spaces for Multi-User Virtual and Augmented Reality Interaction, *2020 IEEE Conference on Virtual Reality and 3D User Interfaces (VR)*, 353-362.

Li, M., Patil, A.G., Xu, K., Chaudhuri, S., Khan, O., Shamir, A., Tu, C., Chen, B., Cohen-Or, D. and Zhang, H.: 2019, Grains: Generative recursive autoencoders for indoor scenes, *ACM Transactions on Graphics (TOG)*, **38**(2), 1-16.

Liu, C., Wu, J. and Furukawa, Y.: 2018, Floornet: A unified framework for floorplan reconstruction from 3d scans, *Proceedings of the European Conference on Computer Vision (ECCV)*, 201-217.

McCormac, J., Handa, A., Davison, A. and Leutenegger, S.: 2017, Semanticfusion: Dense 3d semantic mapping with convolutional neural networks, *2017 IEEE International Conference on Robotics and automation (ICRA)*, 4628-4635.

Merrell, P., Schkufza, E., Li, Z., Agrawala, M. and Koltun, V.: 2011, Interactive furniture layout using interior design guidelines, *ACM transactions on graphics (TOG)*, **30**(4), 1-10.

Muller, P., Wonka, P., Haegler, S., Ulmer, A. and Van Gool, L. 2006, Procedural modeling of buildings, *in* initials missing surname missing (ed.), *ACM SIGGRAPH 2006 Papers*, 614-623.

Saldana, M. and Johanson, C.: 2013, Procedural modeling for rapid-prototyping of multiple building phases, *International Archives of the Photogrammetry, Remote Sensing and Spatial Information Sciences*, **5**, W1.

Schops, T., Schonberger, J.L., Galliani, S., Sattler, T., Schindler, K., Pollefeys, M. and Geiger, A.: 2017, A multi-view stereo benchmark with high-resolution images and multi-camera videos, *Proceedings of the IEEE Conference on Computer Vision and Pattern Recognition*, 3260-3269.

Song, S., Lichtenberg, S.P. and Xiao, J.: 2015, Sun rgb-d: A rgb-d scene understanding benchmark suite, *Proceedings of the IEEE conference on computer vision and pattern recognition*, 567-576.

Song, S., Yu, F., Zeng, A., Chang, A.X., Savva, M. and Funkhouser, T.: 2017, Semantic scene completion from a single depth image, *Proceedings of the IEEE Conference on Computer Vision and Pattern Recognition*, 1746-1754.

Yu, L.F., Yeung, S.K., Tang, C.K., Terzopoulos, D., Chan, T.F. and Osher, S.J.: 2011, Make it home: automatic optimization of furniture arrangement, *ACM Transactions on Graphics (TOG)-Proceedings of ACM SIGGRAPH 2011, v. 30,(4), July 2011, article no. 86*, **30**(4).

Zhang, S.H., Zhang, S.K., Liang, Y. and Hall, P.: 2019, A survey of 3D indoor scene synthesis, *Journal of Computer Science and Technology*, **34**(3), 594-608.

INTUITIVE BEHAVIOR

The Operation of Reinforcement Learning in Generative Design Processes

DASONG WANG[1] and ROLAND SNOOKS[2]
[1,2]*RMIT Architecture | Tectonic Formation Lab*
[1,2]*{dasong.wang|roland.snooks}@rmit.edu.au*

Abstract. The paper posits a novel approach for augmenting existing generative design processes to embed a greater level of design intention and create more sophisticated generative methodologies. The research presented in the paper is part of a speculative research project, Artificial Agency, that explores the operation of Machine Learning (ML) in generative design and robotic fabrication processes. By framing the inherent limitation of contemporary generative design approaches, the paper speculates on a heuristic approach that hybridizes a Reinforcement Learning based top-down evolutionary approach with bottom-up emergent generative processes. This approach is developed through a design experiment that establishes a topological field with intuitive global awareness of pavilion-scale design criteria. Theoretical strategies and technical details are demonstrated in the design experiment in regard to the translation of ML definitions within a generative design context as well as the encoding of design intentions. Critical reflections are offered in regard to the impacts, characteristics, and challenges towards the further development of the approach. The paper attempts to broaden the range and impact of Artificial Intelligence applications in the architectural discipline.

Keywords. Machine Learning; Generative Design Process; Multi-Agent Systems; Reinforcement Learning.

1. Introduction

The discipline of architecture is rapidly absorbing machine learning methodologies and searching for meaningful applications of these algorithms to design. This paper proposes an approach that augments known generative design strategies through a heuristic strategy that hybridizes a Reinforcement Learning (RL) based evolutionary approach with self-organizing generative processes. In contrast to the popular appropriation of image-based Generative Adversarial Networks that operate on the surface effects of architecture, this approach seeks to heuristically train generative algorithms that deeply embed architectural design intention within the algorithmic generative process.

Self-organizing algorithms that underlie complex systems have emerged over the past two decades as the basis for highly creative and volatile design strategies

PROJECTIONS, Proceedings of the 26th International Conference of the Association for Computer-Aided Architectural Design Research in Asia (CAADRIA) 2021, Volume 1, 101-110.

that privilege bottom-up generative logic. Methodologies such as Behavioral Formation (Snooks, 2014), that engage multi-agent algorithms enable design intention to be embedded within the bottom-up rules of generative systems. However, these are often limited by their logic of local interaction that resists encoding systemic top-down design intention (Snooks, 2014).

This paper posits an approach in which the self-organizing behavioral logic of multi-agent algorithms is hybridized with the top-down evolutionary reward logic of Reinforcement Learning algorithms to enable the interaction of top-down and bottom-up design intention within a systemic design methodology. This augmented approach enables the hybridization of ideologically opposed, albeit complementary, algorithmic strategies to effectively compensate, or respond, to each algorithm's limitations.

The structure of the paper includes a background section covering the existing multi-agent and reinforcement learning algorithmic approaches, a methodology section that describes the hybridization of these approaches, and a discussion section that outlines the efficacy and implications of this hybridization. The posited approach is explored through a prototypical algorithmic framework that utilizes a mesh-based RL agent to evolve proto-architectural surface topology. While directly exploring the hybridization of multi-agent algorithms and reinforcement learning, this paper offers a generalizable approach to augmenting generative design.

2. Background

2.1. BEHAVIORAL FORMATION

Behavioral Formation is a generative design methodology that draws on the logic of swarm intelligence within a self-organized emergent process, which operates through Multi-Agent algorithms. This approach privileges encoded local interactions of autonomous computational agents, achieving intensive, intricate, heterogeneous phenomena in generative processes (Snooks, 2014). The exploration and development of this behavioral approach over the past two decades has expanded the realm of generative design paradigms (Leach, 2017).

Multi-Agent Systems (MAS), which trace their logic back to the Cellular Automata, are the key technical foundation of Behavioral Formation. The Multi-Agent algorithmic approach discussed here is an extension of the 'Boids' algorithm (Craig, 1987) which has been expanded and developed into various generative strategies including: 'Manifold Swarm' (Snooks, 2014), and 'Cellular Forms' (Lomas, 2014). Multi-Agent Systems depend on local interactions to generate self-organized emergence. However, this localized operation prohibits a more macro awareness and leads to an inherent limitation of global ignorance (Snooks, 2014). In practical design scenarios, this is regarded as a significant problem as a certain number of design intentions/constraints can only be defined from a global scale. For instance, the overall topology and structural performance of a form is a global issue. In order to augment the behavioral generative process, this paper purposes an approach that is based on the application of a complementary algorithm: Reinforcement Learning and Multi-Agent Systems.

2.2. ARTIFICIAL INTUITIONS

Artificial Intuitions speculate on a design process driven by Machine Learning (ML), with the capacity to develop typical and specific generative 'intuitions' towards quantitative subjective intentions and objective constraints of design (Wang, 2020). In regard to the scenario of Behavioral Formation, artificial intuitions are global awareness of encoded design intentions to be hybridized with the local interactions. The approach operates with the implementation of a Reinforcement Learning algorithm.

Reinforcement Learning algorithm is a long-standing Machine Learning framework with close association of optimal control. The mechanism of RL can be summarized as an agent seeks an optimal policy by interacting with its environment through feedback between observation states and quantified rewards, which can be traced back to a Markov Decision Process (Sutton, 1998). Different from other existing ML frameworks, RL is a heuristic approach that cultivates machine intelligence through training based on the accumulation of self-experiences instead of known human knowledge. The definition of RL is structured with several algorithmic elements: Agent, Observation States, Actions, Rewards and Policy (Henderson, 2018). Based on previous research (Wang, 2020), the paper demonstrates these elements through their application within a generative design context, as shown in Figure 1.

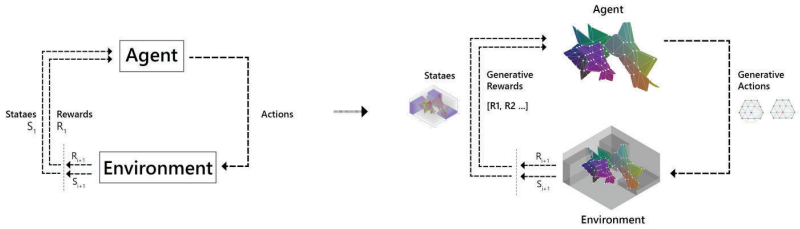

Figure 1. Translation of RL Algorithm within Generative Design Context.

- Agent: represents the entirety of the generative system itself (distinguished from each single agent in MAS). The Agent is capable of making decisions to undertake certain actions to achieve optimal generative outcomes.
- Action: demonstrates how the agent evolves and interacts with its environment through each step.
- Observation State: is a fixed-dimension matrix of information that summarizes the current status of the generative system and environment.
- Reward: assesses the performance of generative action with encoded quantitative criteria of design intention or constraints.
- Generative Policy: is the outcome of the training approach which can be regarded as the artificial intuition of agent. It maps states to actions, supervising the agent to take optimal decisions at each step to generate reward-oriented results.

2.3. COMPUTATIONAL FIELD

The term computational field within the paper refers to a strategy to represent three-dimensional topological information through a vector field. The mechanism of a computational field is to generate a 3D grid with a collection of vectors mapping to a series of information: position, direction, topological condition, etc. The strategy is implemented in the design process for two purposes: converting the agent's condition to a matrix data type for observation states, as well as bridging the generative outcome from training to behavioral formation process. This has been further discussed in Chapter 3.1 and 3.4.

3. Methodology

The design methodology of 'Intuitive Behavior' is demonstrated with a speculative design experiment aiming to explore and test the impact of the proposed RL approach by training a topological field with intuitive global awareness of pavilion-scale design criteria.

3.1. OVERALL METHOD

As shown in Figure 2, the overall design method is structured with three major steps:

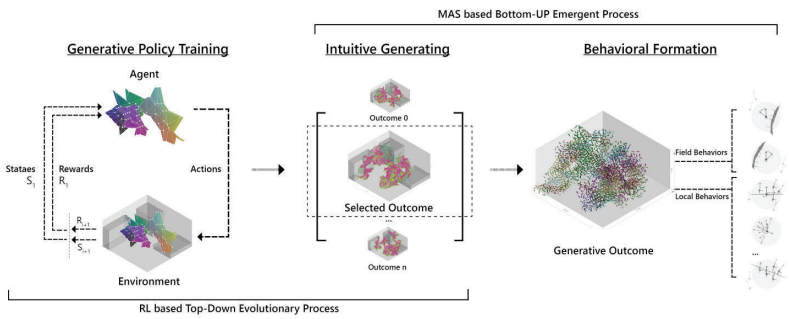

Figure 2. Overall Method of Structuring the RL based Intuitive Generative Approach.

- Generative-Policy Training: forms the main step added prior to the existing generative design procedure, which aims to train a generative system to achieve encoded global design intentions. The training process is inspired by and based on an evolutionary deep RL algorithm which is demonstrated in the following sub-chapters from 3.2 to 3.6 with particular emphasis.
- Intuitive Generating: is a process that a specific design context that will be inputted to generate potential design outcomes. An eventual generative outcome will be selected based on top-down unprogrammable criteria and forward to the next step.
- Behavioral Formation: The selected outcome will be used as a global topology for the Behavioral Formation process aiming to increase design resolution and

intricacy. The behaviors in the process will be encoded both in regard to local interactions and global response to the generated global topology.

3.2. RL AGENT AND ENVIRONMENT

Within the Generative-Policy Training process, the RL Agent is defined as a mesh graph that consists of certain vertices and predefined topology. As initialization of each training episode, the position and orientation of the mesh-Agent will be randomly generated as well as individual vertices (Figure.3). The purpose of using a mesh graph as RL Agent is due to its characteristic of efficiency, controllability, and flexibility in terms of representing a three-dimensional geometry. While the random initialization operation aims to expand the optimal solution pool with as much as potential possibilities.

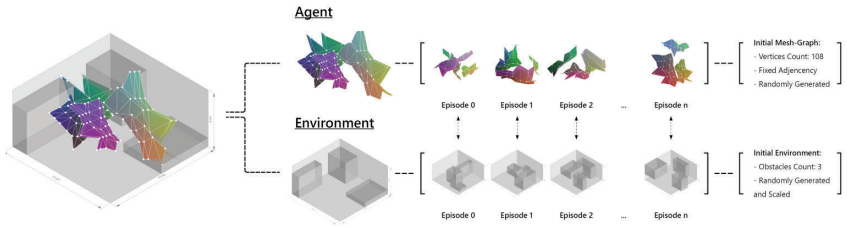

Figure 3. Strategies of Initializing RL Agent and Environment.

The environment is defined as a cuboid space with a scale of 10*10*5 meters, (Figure.3), in which several obstacles will be randomly generated as site conditions and constraints in order to train the adaptability of the generative policy with the capability of unpredictable initial conditions.

3.3. RL ACTIONS: STOCHASTIC + GENERATIVE BEHAVIORS

In the experiment, the agent action is encoded as a combination of stochastic RL actions and topological generative behaviors. Stochastic action is a typical strategy used in the RL algorithm that each vertex makes a random decision to move towards the six-axis. The stochastic actions will later be supervised by the algorithmic training process. Simultaneously, the vertices will also undertake topological behaviors: spatial separation and tension cohesion (Figure 4) which is encoded with the intention to maintain the topological condition of the geometry from unexpected intersections. The strategy of integrating stochastic RL actions with generative behaviors is inspired by the description of intelligent agency in 'Complex Adaptive Systems' (Holland, 1992), that each Agent is expected to make individual decisions but also subjects to interactive behaviors to form an emergent complex system.

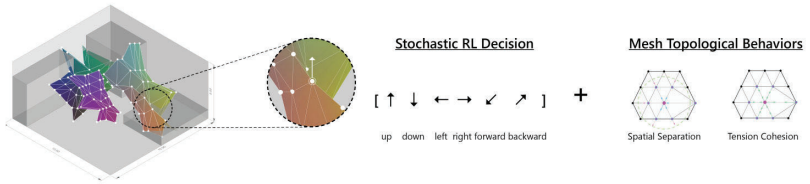

Figure 4. Strategies of Encoding RL Actions: Stochastic RL Decisions + Mesh Topological Behaviors.

3.4. RL OBSERVATIONS: COMPUTATIONAL FIELD

In response to the technical character of RL observation states, the RL Agent and Environment will be converted into a computational field with a three-dimensional voxel grid. Each voxel within the field contains informative states of the Agent and Environment (Figure 5). The states will then be calculated into a weighted value in order to structure a three-dimensional matrix for the Artificial Neural Network to proceed.

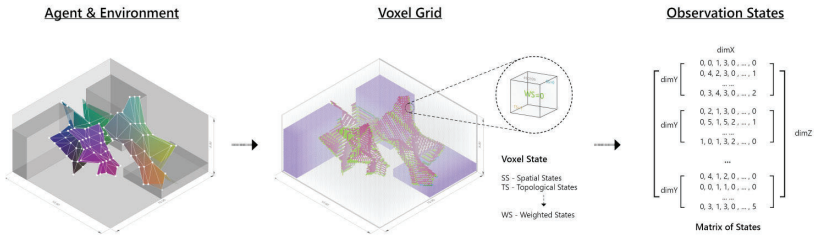

Figure 5. Strategies of Encoding Observation States.

3.5. RL REWARDS: GLOBAL DESIGN INTENTIONS

As the most critical element of the training process, the reward is defined towards global/macroscopical design intention that is not capable of a local behavioral system to achieve.

- Spatial Coverage (R1): is a criterion quantified based on a design intention of forming a mushroom-like topology. The design outcome is expected to generate spatial coverage above a certain height but remaining a minimum amount of coverage as a foundation (Figure 6).

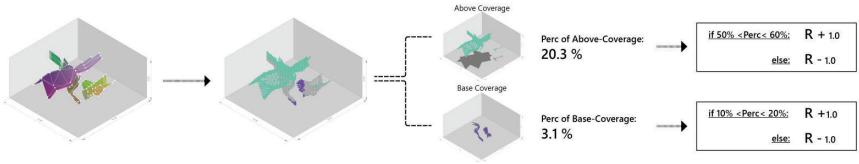

Figure 6. RL Reward 01 - Spatial Coverage.

- Topological Performance (R2): is defined based on the design intention of optimal structure-oriented topology. In the experiment, to avoid heavy calculation, a customized structure analysis algorithm is developed which calculates the topological states of each voxel based on the adjacent voxels below it (Figure 7).

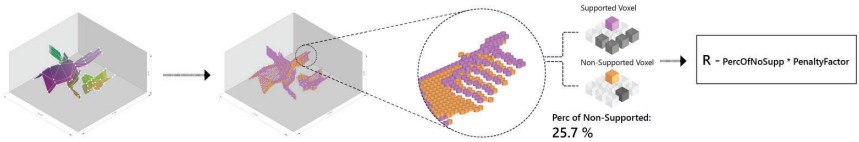

Figure 7. RL Reward 02 - Topological Performance.

- Site/Environmental Response (R3): is quantified from objective design constraints of collision avoidance with an unpredictable environment. As shown in Figure 8, the overlapping percentage of the form will be calculated each step and converted into a negative figure as a reward signal.

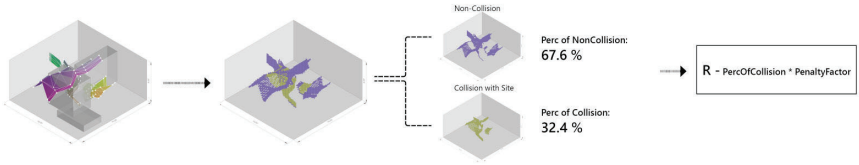

Figure 8. RL Reward 03 - Site/Environmental Response.

- Hierarchical Reward (HR): is defined to encourage the generative system (Agent) to achieve all the encoded rewards simultaneously. An additional reward signal will be added since the agent achieve more than any two rewards defined above, which increases exponentially according to the count of satisfied reward task.

3.6. TECHNICAL SETTINGS

The generative training process is based on a Deep Reinforcement Learning algorithmic framework, Proximal Policy Optimization (PPO), implemented on

the Unity platform with ML-Agent toolkit (Brockman, 2018). The technical settings and parameters of the experiment are listed in Table 1, with regard to the instructions from ML-Agent documentations.

Table 1. Parameters and Settings of Deep Reinforcement Learning Algorithm.

RL Hyper-Parameters	Network-Settings	Reward-Signals
batch_size: 128 buffer_size: 2480 learning_rage: 0.0003 beta: 0.005 epsilon: 0.2 lambd: 0.95	normalize: true hidden_units: 512 num_layers: 3 vis_encode_type: simple	extrinsic: gamma: 0.995 strength: 1.0

3.7. INTERACTIONS WITH BEHAVIORAL FORMATION PROCESS

As demonstrated in sub-chapter 3.1, an intuitively generative outcome will be selected and proceed as a global field for secondary behavioral formation processes. The paper speculates on several design strategies to demonstrate how two approaches being hybridized. Firstly, multiple agents are populated within the global field as initial states, which undertake both local behaviors and global interactive behaviors with the field to balance the local intricacy and global awareness. In Figure 9, a typical 'Manifold Swarm' (Snooks, 2014) generative strategy is implemented to continuously conduct the generative process.

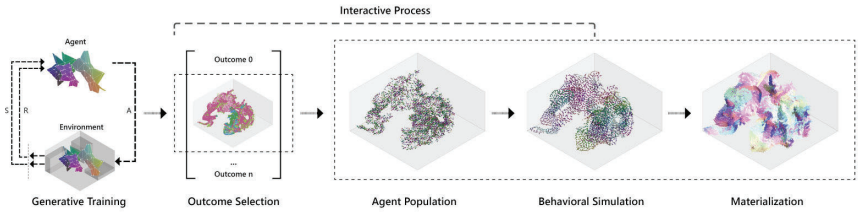

Figure 9. Interactions between RL Training Outcome and Behavioral Formation Process.

4. Discussions

4.1. GENERATIVE TRAINING OUTCOMES

The demonstrated RL-based generative training experiment has been conducted with a total episode of 20,000 (500 steps each). The generative training outcomes are recorded every 200 episodes, as well as the mean-reward recorded every 500/2000 episodes. As shown in Figure 10, the procedural generative outcomes present an obvious tendency of evolving from poor (blue) to optimal (red). This can be also observed from the mean reward chart that the performance of the

generative system increases rapidly in the first 5,000 episodes and gradually improves in the following with minor fluctuations. Based on the performative data, the paper speculates that the result can be more robust with additional training episodes in response to the complexity of the training scenario. Two procedural outcomes are highlighted to illustrate the intuitively evolving effect in response to the three predefined global rewards of spatial coverage, topological performance, and site/env response.

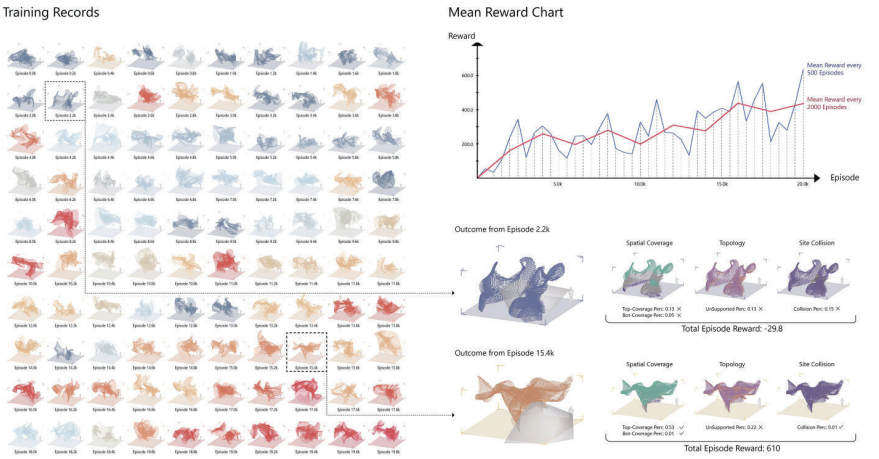

Figure 10. RL Training Processes and Outcomes.

4.2. REFLECTIONS ON THE APPROACH

Based on the training experiment, several reflections are summarized in regard to its characteristics, potential impacts, and challenges. Within the designing/training experiment, the generated global fields have evolved from a primordially stochastic status to be more intelligent and adaptive, forming an autonomous self-optimal process to potentially overcome the global ignorance of behavioral processes of formation. The Deep Reinforcement Learning approach demonstrates a heuristic procedure to computationally evolve generative policies for particular design criteria independent of direct human knowledge. This heuristic strategy enables the generative process to produce large quantities of outcomes that resist habitual aesthetics and formal tropes but still satisfy the predefined design intentions. Besides the application to behavioral processes of formation, the approach also shows significant potential to be applied in other generative processes, as its several key algorithmic components (Agent, Actions, Reward, etc.) can be fully customized in regard to various generative algorithms.

The experimental case described here hybridizes two independent approaches of intuitive training and behavioral formation, instead of directly training each single agent with global generative intentions. This is subject to the fact that

the RL algorithm is under development dealing with Multi-Agent circumstances. Emerging techniques have been proposed to tackle the problem, such as MADDPG (Multi-Agent Deep Deterministic Policy Gradient) algorithm (Lowe, 2020), which presents a promising methodology to train multi-agent algorithms with respect to global rewards. A series of technical challenges exist in terms of applying the proposed approach in a wider range. Firstly, the RL algorithm is an extremely computationally expensive process, fundamentally due to its heuristic character. In this case, the design intentions (rewards) are expected to be general rather than specific, which enables the training outcome to be adaptable in various analogous circumstances. Besides, the balance of precision and efficiency of the RL reward definition is also a challenge to achieve a reasonable result. As shown in the Intuitive Field experiment, the rewards definition is relatively lightweight instead of implementing a professional analysis algorithm (FEM structural assessment, for instance), which involves heavy calculations of million-magnitude iterations.

5. Conclusion

By hybridizing the intuitive field and behavioral formation processes, the RL based approach shows a meaningful impact on augmenting generative design with intuitive capacity and sophisticated control. Through the design experiment, the research presents a series of theoretical strategies and technical definitions for structuring a generative training process and evolving it through encoded design intentions. An augmented approach to the application of Machine Learning techniques has been proposed with the intention to broaden the range and impact of AI applications in the architectural discipline. The subsequent reflections in the paper also anticipate an interactive correlation between designers and computational intelligence.

References

Brockman, G., Cheung, V., Pettersson, L., Schulman, J., Tang, J. and Zaremba, W.: 2016, "OpenAI Gym" . Available from <arXiv:1606.01540> (accessed 12th December 2020).

Craig, R.: 1987, Flocks, herds and schools: A distributed behavioral model, *Proceedings of the 14th Annual Conference on Computer Graphics and Interactive Techniques*.

Henderson, P., Bachman, R., Precup, J. and Meger, D.: 2018, Deep Reinforcement Learning that Matters, *The Thirty-Second AAAI Conference on Artificial Intelligence(AAAI-18)*.

Holland, J.: 1992, *Complex Adaptive Systems*, The MIT Press.

N. Leach and R. Snooks (eds.): 2017, *Swarm Intelligence: Architectures of Multi-Agent Systems*, Tongji University Press, Shanghai.

Lomas, A.: 2014, Cellular Forms: an Artistic Exploration of Morphogenesis, *AISB-50*.

Lowe, R., Wu, Y., Tamar, A., Harb, J., Abbeel, P. and Mordatch, I.: 2020, "Multi-Agent Actor-Critic for Mixed Cooperative-Competitive Environments" . Available from <arXiv:1706.02275> (accessed 12th December 2020).

Snooks, R.: 2014, *Behavioral Formation: Multi-Agent Algorithmic Design Strategies*, Ph.D. Thesis, RMIT.

Sutton, R. and Barto, A.: 1998, *Reinforcement Learning: An Introduction*, The MIT Press.

Wang, D. and Snooks, R.: 2020, Artificial Intuitions of Generative Design: An Approach based on Reinforcement Learning, *Proceedings of CDRF 2020*.

SEARCHING FOR DESIGNS IN-BETWEEN

Exploration of design space using a 3D printing-inspired evolutionary system.

CAMILO CRUZ GAMBARDELLA[1] and JON MCCORMACK[2]
[1,2]*SensiLab, Monash University*
[1,2]*{camilo.cruzgambardella|jon.mccormack}@monash.edu*

Abstract. The use of evolutionary methods in design and art is increasing in diversity and popularity. Approaches to using these methods for creative production typically focus either on optimisation or exploration. In this paper we introduce an evolutionary system for design that combines these two approaches, enabling users to explore landscapes of design alternatives using design-oriented measures of fitness, along with their own aesthetic preferences. We test our methods using a biologically-inspired generative system capable of producing 3D objects that can be exported directly as 3D printing toolpath instructions. For the search stage of our system we combine the use of the CMA-ES algorithm for optimisation and linear interpolation between generated objects for feature exploration. We investigate the system's capabilities by evolving highly fit artefacts and then combining them with aesthetically interesting ones.

Keywords. Generative Design; Evolutionary Design; 3D Printing.

1. Introduction

Evolutionary Computing (EC) methods have been used to address a wide variety of formal and functional problems in creative practice since the mid 1980s (see Frazer 1995 for an introduction). The most common applications of these techniques are the optimisation of performance-oriented attributes of artefacts, and the exploration of novel design alternatives. For instance, in architecture, evolutionary methods, among other metaheuristics (Wortmann and Nannicini 2016), are used in conjunction with parametric models (Woodbury 2010) to search for efficient design alternatives, where efficiency is clearly defined through formal fitness measures. In contrast, visual artists and researchers in creative fields commonly use search methods that incorporate aesthetic selection mechanisms along with stochastic generative systems, to explore vast landscapes of alternatives looking for 'interesting' and novel phenotypes (McCormack 2005).

Typical design problems addressed with these techniques in architecture and engineering are the optimisation of structural elements (Goldberg and Samtani 1986, Jenkins 1991), the design of efficient building layouts (Jo and Gero 1998, Wong and Chan 2009), sunlight and energy performance of buildings (Caldas

PROJECTIONS, Proceedings of the 26th International Conference of the Association for Computer-Aided Architectural Design Research in Asia (CAADRIA) 2021, Volume 1, 111-120.

2001) and acoustic optimisation of concrete shells (Mendez et al. 2013), to mention a few. All of these examples use EC methods to drive mostly deterministic parametric models, which generate alternative phenotypes. In other words, it is via the combination of these computational methods that the designed artefacts they produce acquire their characteristics.

Creative exploration using EC differs from optimisation-oriented approaches in that the main objective is not efficiency, but finding novel alternatives. In many cases artists substitute formal fitness functions with their own aesthetic judgement, putting a "human in the loop" of the evolutionary algorithm (Dawkins 1986). Seminal examples in this field can be found in the work of William Latham and Karl Sims, who in the late 1980s began using evolutionary techniques, like selection and mutation, to generate complex forms and imagery (Sims 1991, Todd and Latham 1992), as well as to evolve Virtual Creatures (Sims 1994). Another example is the work on aesthetic fitness and evolution by Dorin (2001), who explores the aesthetic capabilities of human-guided computational evolution via the generation of digital images. More recently, Dutch artists Erwin Driessens and Maria Verstappen's *Accretor* (Whitelaw 2015) used evolutionary techniques to produce 3D shapes by evolving sets of rules for a cellular automaton. In this case the artists' process involves monitoring the state of the evolving objects, in search of abrupt changes along their evolutionary trajectory. Then, the process is interrupted and the objects are fine-tuned manually. Another example is the work of artist Andy Lomas (2013), who combines the use of a cellular division-inspired generative system with *interactive genetic algorithms* to generate aesthetically complex digital 3D objects, which he then categorises and evaluates aesthetically based on his own preference. Lomas' latest work builds on his generate and evolve process, focusing on the exploration of the areas of the fitness landscape of his system located in-between categories by interpolating between objects, and looking for sudden/unexpected changes as the objects transition between states.

In this paper we introduce a prototype EC system for the creation of physical artefacts that combines evolutionary strategies (ES) with a novel, bio-inspired, agent-based generative system. By coupling a stochastic generative method capable of producing a wide range of diverse alternatives with a flexible ES driven by fitness functions that respond to holistic design objectives, our system integrates elements of creative exploration with design optimisation, enabling users to purposefully and holistically explore complex design spaces.

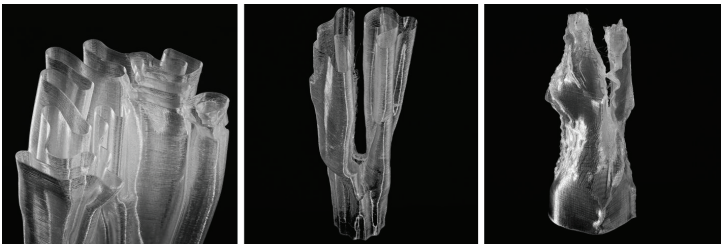

Figure 1. Examples of 3D printed forms grown using our generative system.

2. Generative System

The guiding principle behind the implementation of our generative system was the generation of interesting 3D forms that could be directly translated into digital fabrication instructions. For this purpose we defined a model that generates 2D shapes and transforms them over time. By capturing the state of these shapes at discrete time intervals as they develop, we obtain geometric information analogue to the representation used by slicing software to prepare 3D models for fused deposition modelling 3D printing (FDM): a series of stacked contours (Figure 1).

To drive the dynamics of the 2D shapes and produce complex geometry we borrowed concepts from natural differential growth processes (Barlow 1989), as seen in the work of Anders Hoff (2015). We use the metaphor of "organisms": sequences of artificial cells connected to their neighbours to form closed loops. Cellular processes - a rich source of complexity and diversity (Ball 1999) - serve as inspiration for our system, directing the behaviours of our synthetic organisms. However, it is important to emphasise that the focus of our model is form-generation for creative purposes, and not the accurate reproduction of physical or biological phenomena.

2.1. BUILDING BLOCKS

Our generative system operates on the metaphor of *colonies of organisms*, that develop over time in discrete timesteps. Each organism in a colony is defined as an array of cells $(C_1, C_2 \dots C_n)$ connected by edges $(e_1, e_2 \dots e_n)$, where $e_i = (C_i, C_{i+1})$ and $e_n = (C_n, C_1)$, forming closed loops.

Colonies develop in a synthetic environment - a simulated viscous medium of uniform density. Sources of *nutrients* are randomly distributed across the environment. Each source has a limited amount of nutrition units, which are released, one at the time, every timestep, and diffused over their neighbouring area. Once nutrients have been released they progressively loose nutritional value over time. Once the source of nutrients is fully depleted, it disappears, giving rise to a new source randomly positioned within the development environment.

The dynamics of a colony are determined by how its components interact with each other and with the environment. The behaviours of cells and edges - acquiring nutrients, attracting/repelling neighbouring cells (Figure 2a), and reproducing (Figure 2b) - determine the shape of organisms as they develop. As a consequence organisms expand, contract, move, change shape and split into multiple organisms, forming a larger colony (Figure 3). The characteristics of these behaviours are defined by the genetic composition of the colony, detailed in Section 2.2.

2.2. GENETIC PARAMETERS

The genetic information (*genome*) of a colony consists of the following five alleles:

- **Metabolic rate** (η), determines how efficient the cells in a colony are at transforming nutrients into energy. A more efficient metabolism comes at the cost of a higher energy consumption.

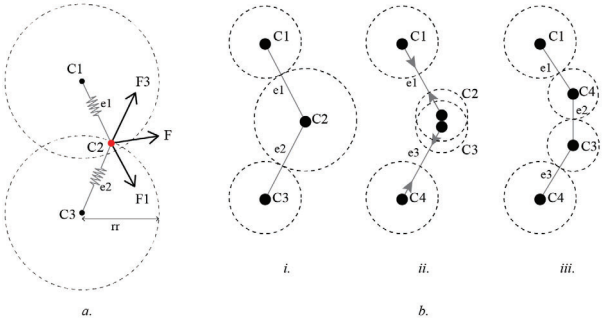

Figure 2. Behaviours of cells (C) and edges (e). a) Forces acting on C2. F1 is the sum of forces exerted by C1 and e1, F3 is the sum of forces exerted by C3 and e2, and F is the sum of repulsion forces exerted by all the other cells in the system within repulsion radius (rr) distance to C2. b) Cellular division: (i) C2 has reached εmax (see Sec. 2.2). (ii) C2 splits into new cells, C2 and C3. (iii) C2 and C3 reach equilibrium. Dotted circles show each cell's energy.

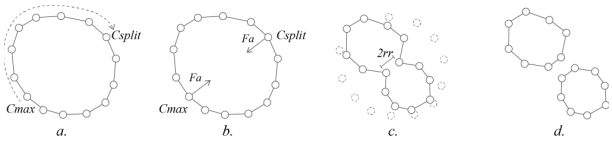

Figure 3. Stages of organism splitting. a) The cell with highest amount of energy Cmax and Csplit are defined. b) Attraction forces Fa between Cmax and Csplit are applied. c) Distance between Cmax and Csplit reaches splitting threshold (2rr). d) Organism splits, producing two separate and independent organisms.

- **Cell drag coefficient** (ν) represents the surface drag per unit area of cells. Cells with low drag move quickly, making stable configurations more unlikely.
- **Energy Capacity** ($\epsilon_{\max}$) represents the maximum amount of energy a cell can store. As capacity increases, so does the mass of the cells, along with the amount of energy required for movement and metabolism.
- **Edge spring coefficient** (k) determines the stiffness of the edges connecting adjacent cells. High k results in rigid organisms. On the contrary, low k results in organisms that move with fluidity, which leads to stretched edges making the transmission of energy between cells less efficient.
- **Energy ratio** (ρ) determines the relative size of new organisms after one of them splits into two.

3. Form-finding

To purposefully explore the diverse landscape of design alternatives that our generative system is capable of producing, we developed a set of quantitative representations of design objectives, which are used as fitness functions to drive two evolution-based strategies.

3.1. FITNESS FUNCTIONS

We developed three proof of concept fitness functions, each of which attempts to address a different type of design objective: technical, spatial and aesthetic.

3.1.1. Printability

We base our printability measure on the principles of FDM. The goal is to generate objects that can be printed using a single strand of plastic filament with no additional supports, thus minimising the use of material and eliminating the removal of supporting structures. For this to be feasible two conditions must be met: (i) the smallest diameter of the convex hull of all organisms cannot be smaller than $5mm$ (determined empirically for our specific 3D printer) and (ii) each layer of material has to be supported by the layer below it.

At every timestep during the generation process, the system calculates the minimum diameter of the convex hull of all organisms in a colony, as well as the ratio $P = P_s/P_t$ where P_s is the perimeter of an organism that is in contact with the layer immediately below, and P_t is the total perimeter of the organism.

3.1.2. Relative Coverage

This metric determines the area of the largest canopy that can be supported by a given 3D object as a ratio of the area of the environment. We use a 2D iso-surface approach, as it provides a reasonable approximation. The size of the canopy is calculated by subdividing the environment into equal area square tiles, which are then assigned a support score $m = \sum_{i=1}^{n}(r_i)/(d_i)$, where n is the total number of organisms in the top layer of a 3D shape, d_i is the distance between the centroid of the tile t_c and the centroid of the i^{th} organism and r_i is the distance between the centroid of the i^{th} organism and the point where the line connecting it to t_c intersects the organism's perimeter. If $m \geq 0.85$ for a tile, it is considered supported. It is important to emphasise that this is an approximation, and that further structural analysis would be required for the development an accurate metric to calculate the load-bearing capabilities of generated objects.

Relative coverage is then calculated as $R_c = R - A$ where A is the ratio of the area of the environment covered by the organisms in the first layer, and R is the ratio of supported tiles ($m \geq 0.85$) over the total number of tiles.

3.1.3. Formal Complexity

This metric attempts to determine if a generated object has physical features that we considered desirable: surface diversity (smooth/rugged), and "branching".

To measure surface diversity we consider the convexity of every organism in a colony at every timestep, as well as the quartile coefficient of dispersion of the angles between consecutive edges.

Convexity is calculated as $c = p_h/p$, where p_h is the perimeter of the convex hull of an organism and p is its total perimeter. A highly convex object, such as a

circle, should be smooth.

Quartile coefficient is calculated as $Q = (q_3 - q_1)/(q_3 + q_1)$ where q_1 and q_3 are the first and third quartiles of the array of all angles between consecutive edges (e_n, e_{n+1}) sorted by size.

"Branching" measures the number of times organism splits occur as a colony develops (see Figure 3 for reference). We then calculate a splitting score $S = d^{1/(1+n_s)}$ where d is a constant and n_s is the total number of splits.

The overall complexity of a generated object is calculated as the equal-weighted sum of the three metrics described above: $C = (c + Q + S)/3$.

3.2. EXPLORATION STRATEGIES

The general aim of this research was to develop a system that enables designers to explore diverse landscapes of designs using a combination of domain knowledge and intuition, in search of functional alternatives with novel/unexpected features.

We approximate the desired characteristics with our fitness functions (see Section 2.2). However, due to the uncertain nature of some design goals - especially those related to perceptual attributes, like aesthetic complexity - we regard optimisation processes as instrumental for exploration, rather than tools for the efficiently searching for the best alternative. This is why we used a hybrid, two-stage exploration strategy that combines a powerful optimisation algorithm with a method that introduces some intuitive aspects of creative exploration.

3.2.1. Evolution Strategy

Firstly we leverage the optimisation capabilities of the *Covariance Matrix Adaptation Evolution Strategy* (CMA-ES) (Hansen and Ostermeier 2001), a state of the art population-based optimisation algorithm that works by randomly sampling alternatives in the area of the fitness landscape close to other successful alternatives, using a distribution that is updated every generation based on the previous generation's most successful individuals. Despite the fact that the efficiency of evolutionary algorithms for design optimisation has been contested (Wortmann et al. 2017), we selected CMA-ES for two specific reasons: (i) its adaptive capabilities make it suitable for the exploration of multimodal fitness landscapes, a characteristic that our generative system displayed during preliminary testing, and (ii) it works well with low-dimensional floating point vectors as genomes, as it does not rely on crossover to generate new genotypes.

An argument could be made against the suitability of CMA-ES to address a multi-objective problem. We believe that, given the imprecise nature of some of the design objectives being pursued, it is beneficial to address them individually, and then allow the user to fill-in the shortcomings of the formal implementation of said objectives via a procedure that enables intuitive selection.

3.2.2. Linear Interpolation Search

For the second stage of our method we produce a series of new genotypes by interpolating between the genotypes of two user-selected CMA-ES evolved

objects. To do this we calculate the Euclidean distance between them, and then divide it by the number of desired "in-between" objects. These genotypes generate new objects that can be examined by the user, both visually and by evaluating their properties using the measures described in Section 3.1. This allows the user to optimise to taste, while preserving measurable fitness, fine-tuning the details that formal fitness measures are unable to capture sufficiently.

We believe that this method, coupled with the more traditional use of CMA-ES, has the potential to expand the creative capabilities of designers, as it enables the user of the system to introduce their own aesthetic preference as part of a process that is also capable of maintaining performance standards.

4. Experiments

4.1. EXPERIMENTAL SETUP

The first stage of our experiments involved the progressive transformation of the genome vector $(\eta, \nu, \epsilon_{\max}, k, \rho)$ using CMA-ES. We did 5 evolutionary runs of 150 generations each, using a population of $\lambda = 40$ individuals at each generation. From each population, a set of 2 *parents* was selected to define the distribution for the sampling of the new population. For the generation of individual objects we set the environment size to (600×600) units. Each object was initialised as a colony of 4 organisms, located on the midpoints of the diagonal lines connecting the centre of the environment and its vertices. Colonies were developed for 200 timesteps (with 100 timesteps of warmup), resulting in objects 200 layers high. For each evolutionary run the environment was initialised with a different random seed, in order to obtain variation in form via the random distribution of nutrient sources. For the second stage of the experiments two individuals generated on identical environments were selected based on their aesthetic characteristics and fitness. These individuals were used to run a linear interpolation between genome vectors, generating 99 in-between new individuals which were then evaluated for fitness, as well as by visual inspection.

4.2. RESULTS

The first stage of experiments tested the ability of the CMA-ES algorithm to find designs with specific characteristics. Figure 4 shows the results when optimising for overall fitness (averaging printability, complexity and relative coverage) (a), and when optimising for relative coverage (b). Even though both graphs show similar results, it is possible to make interesting observations. For instance, in (a) printability (blue) quickly reaches its optimum value and exhibits little variance, whereas complexity (light grey) and relative coverage (dark grey) exhibit a fairly dramatic relative increase and follow remarkably similar trajectories, but do not reach high values. This suggests that once the system finds a highly printable alternative, it becomes difficult for it to find objects that perform well in other metrics. However, an assessment of graph (b) indicates that the system struggles to reach high scores for relative coverage in general.

To further understand the characteristics of the objects that the system can generate, we digitally render the highest performing individual for each generation.

We then manually select the ones that exhibit interesting characteristics or are highly fit. Figure 5 shows an example obtained from one of the runs in which we optimised for relative coverage. The pavilion-like shape of the object exhibits a set of complex structures capable of supporting a canopy that covers about 60% of the environment. However, a printability $P < 1.0$ renders the object unprintable.

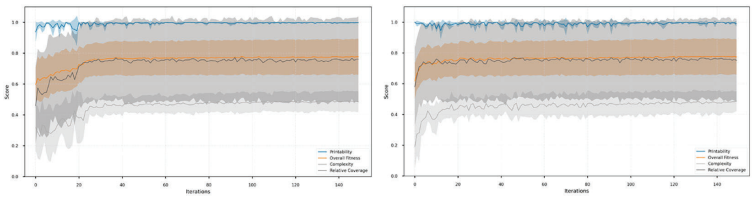

a. *b.*

Figure 4. Plots of evolutionary runs showing mean scores for the best individual at every generation averaged over 5 runs. Shaded areas illustrate the variance. In a) we optimise for full fitness, and in b) we optimise for relative coverage.

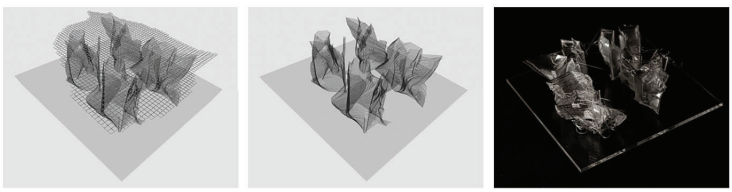

a. *b.* *c.*

Figure 5. Object obtained by optimising coverage. a) Contour 3D rendering (with projected canopy), b) Contour 3D rendering (no canopy) and c) 3D printed version.

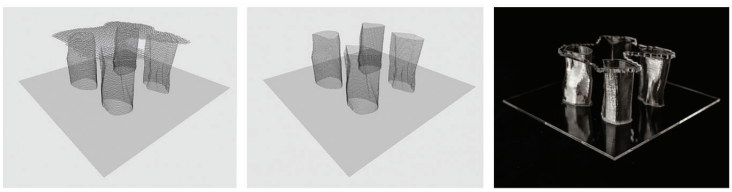

a. *b.* *c.*

Figure 6. Object obtained by optimising for full fitness. a) Contour 3D rendering (with projected canopy), b) Contour 3D rendering (no canopy) and c) 3D printed version.

The object shown in Figure 6, in contrast, exhibits simple geometry, low relative coverage and high printability, allowing for a successful 3D print (to which we added a laser-cut canopy for reference). The lack of formal complexity is not necessarily negative, as from an aesthetic point of view the object appears structurally robust and its components are easily discernible. This is why we selected it as the second end point for the interpolation procedure.

Figure 7 shows the outcomes of the exploration stage. In the graph (a) it is possible to observe unexpected behaviours of the fitness values for complexity and relative coverage as we interpolate between objects. The overall trend shows complexity increasing as coverage decreases. However the random value spikes and drops between steps 40 and 50 suggest that the fitness landscape is not smooth, making it harder for the optimisation algorithm to find the overall best solutions. Nevertheless, this can be fertile ground for creative opportunities, as the user of our system may encounter unexpected attributes in objects found in those areas of the landscape. For instance, the object depicted in (b) and (c) - iteration 78 - exhibits similar characteristics to the object in Figure 5, yet, on closer inspection, it is also possible to see that its contours are smoother, which indicates that some features of the object in Figure 6 have been captured to produce an object *in-between*.

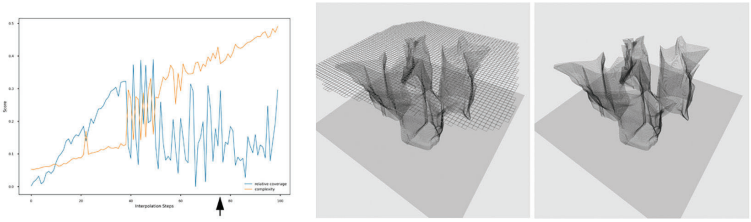

a. *b.* *c.*

Figure 7. Interpolation results. a) Relative coverage (blue) and complexity (orange) scores through interpolation. b) Selected 3D object (with projected canopy). c) Selected 3D object.

5. Discussion and conclusion

This paper introduced a novel generate/explore digital design system inspired by natural and digital-fabrication processes. The method enables users to produce and purposefully search through a vast landscape of design alternatives. Our goal was to examine the capability of our novel stochastic agent-based generative system to produce a diverse landscape of design alternatives, as well as how the integration of automated and "manual" selection mechanisms can widen the range of creative opportunities for designers.

Via the implementation of a two-stage approach that considers optimisation and guided exploration through interpolation – searching in-between designs – we took initial steps toward the development of a system that enables users to uncover areas of the design landscape that hold unexpected design solutions. Our results indicate that these systems have the potential to expand the creative capabilities of the designers who use them.

The strength of our system lies on its capability to combine the optimisation power of the CMA-ES algorithm with human creative judgment. This opens up areas of the design landscape that are extremely difficult to discover by either approach if used separately. We foresee many opportunities to continue this work, beyond the further development of the system's components. This includes the exploration of new methods for generation and optimisation, and

the implementation of a user interface. Another avenue for investigation is the development of fitness functions informed by human perception, to evaluate hard-to-measure features, like "spatial continuity" or "openness". This could be achieved by, e.g., generating a large database of categorised objects to train a classifier model for the recognition of features in newly generated objects.

References

Ball, P.: 1999, *The self-made tapestry: pattern formation in nature*, Oxford University Press.

Barlow, P., Brain, P. and Adam, J. 1989, Differential growth and plant tropisms: a study assisted by computer simulation, *in* P. Barlow (ed.), *Differential Growth in Plants*, Elsevier, 71-83.

Caldas, M.: 2001, *An evolution-based generative design system: using adaptation to shape architectural form*, Ph.D. Thesis, Massachusetts Institute of Technology.

Dawkins, R.: 1986, *The Blind Watchmaker*, Longman Scientific & Technical, Essex, UK.

Dorin, A.: 2001, Aesthetic fitness and artificial evolution for the selection of imagery from the mythical infinite library, *European Conference on Artificial Life*, 659-668.

Frazer, J.: 1995, *An evolutionary architecture*, Architectural Association, London.

Goldberg, D.E. and Samtani, M.P.: 1986, Engineering optimization via genetic algorithm, *Electronic computation*, 471-482.

Hansen, N. and Ostermeier, A.: 2001, Completely derandomized self-adaptation in evolution strategies, *Evolutionary computation*, **9**(2), 159-195.

Hoff, A.: 2015, "Differential Line" . Available from <https://inconvergent.net/generative/differential-line/>.

Jenkins, W.: 1991, Towards structural optimization via the genetic algorithm, *Computers & Structures*, **40**(5), 1321-1327.

Jo, J.H. and Gero, J.S.: 1998, Space layout planning using an evolutionary approach, *Artificial intelligence in Engineering*, **12**(3), 149-162.

Lomas, A.: 2020, "Cellular Forms" . Available from <https://andylomas.com/cellularForms.html>.

McCormack, J.: 2005, Open problems in evolutionary music and art, *Workshops on Applications of Evolutionary Computation*, 428-436.

Mendez, T., Pugnale, A. and Sassone, M.: 2013, Multi-objectiveoptimization of concrete shells, *2nd International Conference on Structures and Architecture, ICSA 2013*.

Sims, K.: 1991, Artificial evolution for computer graphics, *Proceedings of the 18th annual conference on Computer graphics and interactive techniques*, 319-328.

Sims, K.: 1994, Evolving virtual creatures, *Proceedings of the 21st annual conference on Computer graphics and interactive techniques*, 15-22.

Todd, S. and Latham, W.: 1992, *Evolutionary Art and Computers*, Academic Press, London.

Whitelaw, M.: 2015, Accretor: Generative materiality in the work of Driessens and Verstappen, *Artificial life*, **21**(3), 307-312.

Wong, S.S. and Chan, K.C.: 2009, EvoArch: An evolutionary algorithm for architectural layout design, *Computer-Aided Design*, **41**(9), 649-667.

Woodbury, R.: 2010, *Elements of parametric design*, Taylor & Francis Group.

Wortmann, T. and Nannicini, G.: 2016, Black-box optimization for architectural design: An overview and quantitative comparison of metaheuristic, direct search, and model-based optimization methods, *Proceedings of the 21th CAADRIA conference*, 177-186.

Wortmann, T., Waibel, C., Nannicini, G., Evins, R., Schroepfer, T. and Carmeliet, J.: 2017, Are genetic algorithms really the best choice for building energy optimization?, *Proceedings of the Symposium on Simulation for Architecture and Urban Design*, 1-8.

PARAMETRIC DESIGN FOR INDUSTRIAL PRODUCTS

Taking Ergonomic Seat Design as an Example

SHAOTING ZENG[1] and SONG QIU[2]
[1,2]*Tsinghua University*
[1]*sjmjzst@gmail.com* [2]*qiusongtty@sina.com*

Abstract. The main contents of this paper are the parametric design and its applications in industrial design, taking the ergonomic chair as the main design research carrier, conducting the experimental study, and explored the parametric industrial product design procedures and methods based on personalized design notion of "Form follows behaviors". The research map focused on two fundamental parts of parametric design definition: the construction of the parameter relationship and the acquisition of parameters. The first part, through design space exploration (DSE), to translate the design problem into parameters relationship and variable ranges. The second part, using various software and hardware tools (Grasshopper, Arduino with pressure sensors, Kinect, etc.) to facilitate parameter acquisition and its application in the 10-person customer-driven experiments to the resulting design models and user datasets. Finally, through the formulation of quantitative evaluation for 110 sets of user data and models, selecting the best design solution for the 3D printed prototype, and conducting the user test.

Keywords. Parametric industrial design; Ergonomic seat; Customer-driven design experiment; Posture sensing; Form follows behaviors.

1. INTRODUCTION

Parametric design and digital technologies have been becoming increasingly essential for industrial design in recent years (Connors et al. 2019). The progress of sensors and smart hardware also enables more ergonomics and anthropometry to permeate into design studies (Baek and Lee, 2012). We take the ergonomic chair as the research carrier, conducting 10-person customer-driven design experiments with multi-sensors, exploring the construction of the parameter relationship in algorithmic industrial product design.

There have been various design studies on ergonomic seats based on parametric platforms and different sensory devices. Digital artist Zhoujie Zhang equipped the Sensor Chair with a tactile-sensitive sensor system and visualizing the self-generating chair designs as they were in the formation via user interaction

PROJECTIONS, Proceedings of the 26th International Conference of the Association for Computer-Aided Architectural Design Research in Asia (CAADRIA) 2021, Volume 1, 121-130.

(Zhang and Yan, 2020). Li et al. (2020) installed pressure and ultrasonic sensors with Arduino on a seat for sitting posture correction based on ergonomics. In addition to sensors fixed on chairs, wearable devices with sensors have been widely used in ergonomic design (Salvado, 2016). In our study, we adopted the wearable pressure sensing device that can provide participants more choices, such as shifting chairs and sitting positions by favor, or even sitting on the ground, in order to generate more innovative seat shapes from their natural postures.

The Microsoft Kinect has been applied in ergonomic design researches. ActiveErgo system used the Kinect sensor for monitoring to determine the ideal personalized furniture positions for different users (Wu,2018). The Kinect v2 has standing and sitting modes, which can accurately measure the sitting posture details of participants for our experiment.

The statistical and mathematical methods for ergonomic evaluation are also significant for the study (Burkov, 2019). We formulated a criterion of ergonomics evaluation for the 110 sets of personal data we detected during the experiments and selected the optimal seat surface shape for the 3D printed prototype.

2. RESEARCH DESIGN

2.1. DESIGN SPACE EXPLORATION

Design Space Exploration (DSE) refers to the activity of exploring design alternatives prior to implementation. DSE allows designers to translate design problems into different variables in the design space, by adjusting variables to optimize and get ideal designs. The parametric design platform is ideal for DSE, there are two fundamental parts in the parametric design process: the construction of parameter relations and the parameters acquisition. In our study, we used Microsoft Kinect v2 camera to capture 25 points of spatial position parameters of human body skeletal tracks, and Force Sensing Resistor (FSR) pressure sensors based on Arduino Uno to get six pressure value parameters. We input the parameters above through the plugin Firefly into the Grasshopper. In the Grasshopper, the base seating surface was generated by connecting adjacent every 3 points of the 16 skeletal tracking points of Kinect, the purpose of 3 points connection is in order to get the flat unit triangle surfaces. The 16 points of Kinect's skeletal tracks can perfectly represent the sitting posture of a human body, the point joint types and the IDs are respectively following: Spine Base 0, Spine Mid 1, Neck 2, Shoulder Left 4, Elbow Left 5, Wrist Left 6, Shoulder Right 8, Elbow Right 9, Wrist Right 10, Hip Left 12, Knee Left 13, Ankle Left 14, Hip Right 16, Knee Right 17, Ankle Right 18, Spine Shoulder 20 (see Figure 1).

The base seating surface above generated by Kinect points can only represent the sitting posture instead of the person's physical characteristics. Accordingly, we applied the Arduino FSR pressure sensors to detect the pressure values between the human body and chair and then manipulated the data to the iterative design of the seating surface. In the Grasshopper, we could get 6 pressure parameters (A0 - A5) based on the Firefly Arduino Uno component. We applied the 6 parameters to manipulate local shapes of seat-hip-contact panels.

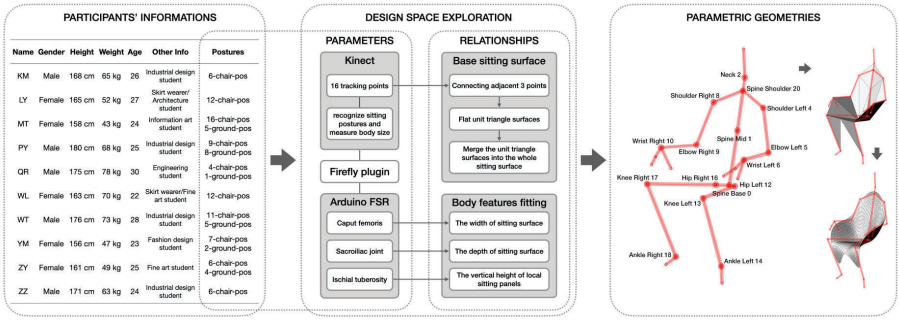

Figure 1. Experiment participants' information and design space exploration process.

2.2. EXPERIMENT SYSTEM DESIGN

After finishing the DSE, we have got the Grasshopper definition and the construction of parameter relations, and the next step is the acquisition of parameters from the real world. Firstly, we considered how to use the Arduino toolkits and 6 pressure sensors in an appropriate way. From the related work reviews above, researchers usually put the pressure sensors on the chair and fixed them on the seating surface. In our study, we hope experiment participants have several different options rather than just sitting in one seat to take the test. In our scheme, we expect that participants not only have more chair choices but also can sit on any place, such as the ground, thus, to get more creative sitting postures. In addition, the FSR thin-film pressure sensor is suitable for sticking on the body because of its lightweight. Therefore, we designed a wearable pressure detection device, as shown in Figure 2, which was modified from a hip protector. We attached the 6 pressure sensors to the 3 pairs of symmetric areas according to the hip skeletal structure associated with sitting posture, which includes caput femoris (A0, A1), sacroiliac joint (A2, A3), ischial tuberosity (A4, A5). The pressure values of these three areas are important references for ergonomic chair design, many illnesses related to sitting are caused by the improper usages of these joints, such as sciatica, sacroiliitis, coxalgia, ONFH (osteonecrosis of the femoral head), etc. Meanwhile, those three joints are also important design nodes in a human sitting. We defined three types of transformations of base sitting panels corresponding with these three groups parameters: First, caput femoris pressure parameters (A0 and A1) control the width of the sitting surface, because caput femoris locate on both sides of the human body, in addition, the forces at these two points are also located on the edge of the hip forces distribution. Second, the depth of the chair is manipulated by the pressure parameters of sacroiliac joints (A2 and A3) in that they are important junctions between the spine and femur and mainly affect the front and back movements of the human body on the seat. Thirdly, the pressure parameters of ischial tuberosity control the vertical height of local sitting panels, which are the two triangle panels contacting the hip. These 6 pressure parameters add thickness to the human body of contact surface with the chair on the basis of the Kinect skeletal tracking body. We applied the Arduino

Uno and the plugin Firefly gathering and acquiring these pressure parameters in Grasshopper, as shown in Figure 1. The latticework on the hip pad helps us find these symmetrical positions easily, and we used Velcro with 3M glue to fix the FSR pressure sensors on the hip pad. We had M and XL two sizes hip pads to fit people of different heights and weights. Moreover, we could adjust the positions of pressure sensors by adhering to more Velcro in order to fit different persons' body shapes (Figure 2:A, B, C).

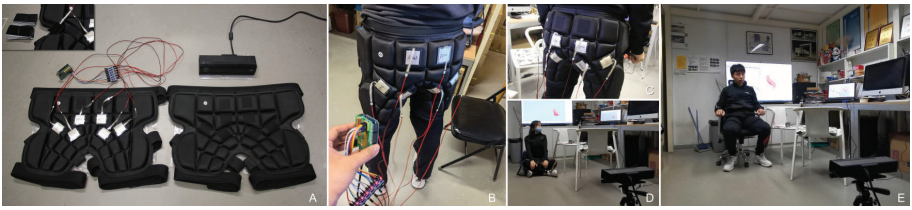

Figure 2. The wearable sensors devices and the experimental space.

After getting the pressure sensing wearables, the next step is to layout the experimental space. As shown in Figure 2E, we had a 3 by 3 square meters of space, and we placed a Kinect v2 camera at the front of the space. We marked a 0.6 by 0.6 square meter area 2 meters in front of the Kinect camera for the seat to be tested. We placed different types of chairs around the test area, including an ergonomics office chair, a Chinese style round-backed armchair, a plastic chair with arms, a non-folding chair without arms, and a foldable chair without arms. We asked participants to put on pressure testing wearables, choose the chair that they thought comfortable and put in the test square, sitting facing Kinect camera, and could change the chair during the experiment. According to our pre-test, when the human body is sitting facing the Kinect camera, the test data is the most stable. Meanwhile, we provided participants with some soft cushions and pillows, which they could use to sit on the chair more comfortably. Furthermore, they were also given the option of abandoning the chair and placing the cushion on the ground, thus sitting on the floor (Figure 2D). Our experiment scheme was to capture at least 5 of the most comfortable sitting postures of an experimental participant while sitting in the testing area and to generate a real-time seat surface model corresponding to that sitting position in the Grasshopper and record relevant parameters in the Excel table.

3. IMPLEMENTATION

We recruited 10 participants for our experiment, including 5 males and 5 females (see Figure 1). According to the experiment scheme above, we conducted the ergonomic seating design experiment and recorded the whole procedures by video. After confirming the positions of the testing square area and the Kinect camera, we helped the participants wear the pressure sensing wearables according to their sizes and asked them to choose the favorite chair they thought comfortable. Among the participants, there were two female participants wearing skirts, which we thought was a good opportunity to test the most comfortable sitting position data

of skirt wearers and generating corresponding seating surfaces for them. Our hip protectors have three sets of buckles that of the waist, groin, and near the knees. When wearing the pad for skirt wearers, we only squeeze the buckles on the waist and near the knees, which had no effect on the data collection, as the skirt wearer's movements were already restricted.

When the experiment started, we asked participants to sit in the most comfortable way and changed different favorite positions or chairs. During the experiment, participants usually chose two or three different chairs to sit, and 6 participants provide us ground sitting postures. All the real-time information, including the generated seat surfaces, Kinect skeletal bodies, and the 6 pressure values, were shown in the Grasshopper. We chatted with participants and asked them whether they were currently sitting comfortably. Once a comfortable sitting position was confirmed, we exported geometries of the Kinect skeletal body and the seating surface to Rhino and recorded the parameters in Excel by the plugin Lunchbox Excel writer component. The Excel data would be used in the subsequent evaluation procedure, including the pressures value A0 to A5 and their expectations, standard deviations, and tolerances, which will be explained specifically in the following evaluation part.

4. EVALUATION

The qualitative visual observation cannot help us decide which seat surface is the most comfortable and ergonomic. Therefore, we designed a quantitative evaluation method, in which we mainly conduct further statistical analysis of six Arduino pressure values. The function of 6 pressure sensing values is not only to control the six triangular panels corresponding with body joints but an important reference for ergonomic chair design. A prominent ergonomic chair, when the user sits on it, the pressure distribution should be average, just like a bed that can smoothly offset the user's weight and physical pressure. It certainly makes the user feel uncomfortable if the force on a local part of the body is much greater than in the other 5 areas. Accordingly, the first evaluation target is the degree of dispersion of the six pressures data, which is the variance in mathematics. In order to simplify the calculation, we used the standard deviation (SD) in our study, which is the square root of the variance (see Formula 1, 2).

$$\overline{x} = \frac{x_1 + x_2 + \ldots + x_n}{n} = \frac{\sum_{i=1}^{n} x_i}{n} \tag{1}$$

$$SD = \sqrt{\frac{\sum_{i=1}^{n} (x_i - \overline{x})^2}{n}} \tag{2}$$

Standard deviation is used to describe the degree of dispersion of 6 random variables, in other words, it is for knowing whether the forces of the 6 pressure sensors are even. On the other hand, in the experiment, it might happen that one of the three sets of data is much higher than the mean of the other two sets, however, each group has balanced paired 2 values. For instance, the participant leaned forward or did not lean heavily against the back of the chair, which might put much more pressure on the ischial joints than the other two joints. In order to

know whether the 2 pressure values of the paired symmetric sensors are average, we also introduced the reference parameter of the Tolerance, which is the sum of the absolute value of the difference between two paired pressure values of three groups. Tolerance (T) is used to assess whether the joint positions on both sides of the participant's body are balanced, as well as to judge whether the participant's sitting posture is correct and healthy (see Formula 3).

$$T = |A_0 - A_1| + |A_2 - A_3| + |A_4 - A_5| \tag{3}$$

During the experiment, we recorded in total 110 sets of data that as shown in Figure 3 left, which includes the 6 pressure values as well as the expectation (average value), the standard deviation, and the tolerance. We could make a longitudinal comparison of each person based on these data but cannot conduct horizontal comparison among different people.

As shown in Figure 3 left, different people with different weight has different pressure forces to the sensor which were ranged from dozens to hundreds. For instance, in our experiment, female participant LY's weight is much smaller than male participant KM, the pressure values of A0-A5 measured from former's posture LY02 are 39, 34, 29, 22, 30, 27, and the latter's data of posture KM03 are 235, 179, 129, 161, 135, 125. The expectation of the two sets respectively are ELY02 = 30 and EKM03 = 160, the YL02_A2 = 29, and has difference between the ELY02 is 30-29=1; the KM03_A3 = 161, and has difference between the EKM03 is 161-160=1 identically. The 2 data have the same difference from the expectation, but we cannot say they have the same deviation, because they have different expectations, in other words, different weights and measures.

Accordingly, before the horizontal comparison, we should unify the metrics. We applied the mathematical concepts of the Relative Standard Deviation (RSD) and the Relative Mean Deviation (RMD) to unify metrics of the SD and the Tolerance respectively. RSD is used to describe several sets with different expectation, which is the quotient of the SD divided by the expectation thus eliminating the effects of different expectation of each set, as the following Formula 4:

$$RSD = \frac{SD}{\overline{x}} = \frac{\sqrt{\frac{1}{n}\sum_{i=1}^{n}(x_i - \overline{x})^2}}{\overline{x}} \tag{4}$$

The RMD is the value that eliminates the influence of the mean difference between each pair of data based on the Tolerance. After derivation, Formula 5, 6 are as follows:

$$\overline{A} = \frac{A_i + A_{i+1}}{2}, (i = 0, 2, 4; A_i > 0) \tag{5}$$

$$RMD = \frac{A_i - \overline{A}}{\overline{A}} = \frac{|A_i - A_{i+1}|}{A_i + A_{i+1}} \tag{6}$$

Finally, we added the values of the RSD and RMD, thus sorted their sums from small to large to get the evaluation results of 110 sets of data, as shown in Figure 3 right. Table 1 left shows the top 7 data of the Excel table. At the same time, we extracted the extreme values and quartiles from the overall ranking table, as

is shown in Table 1 right. The quartiles divided the data into 4 sublists with the range respectively of List 1: Min to Q1, List 2: Q1 to Q2, List 3: Q2 to Q3, List 4: Q3 to Max.

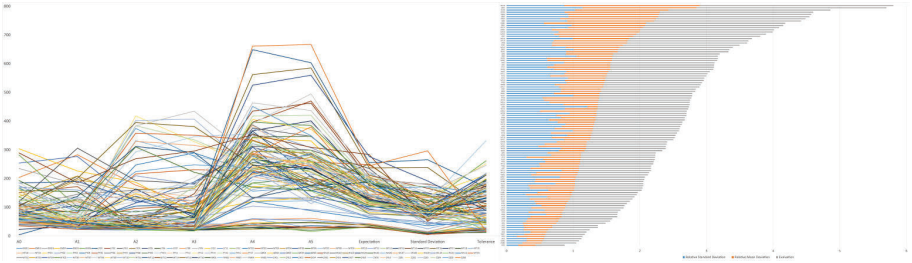

Figure 3. The visualization of all 110 personal data.

Table 1. Top 7s in design evaluation (left) and quartiles of the overall rank (right).

Name	A0	A1	A2	A3	A4	A5	Expectation	SD	RSD	RMD	Evaluation
LY02	39	34	29	22	30	27	30.17	5.33	0.18	0.26	0.44
KM03	235	179	129	161	135	125	160.67	38.29	0.24	0.28	0.52
KM05	254	277	116	137	226	178	198.00	59.17	0.30	0.26	0.54
LY11	42	45	31	22	60	54	42.33	12.90	0.30	0.26	0.56
ZY04	35	23	26	34	36	31	30.83	4.81	0.16	0.41	0.57
YM01	48	43	30	20	42	48	38.50	10.23	0.27	0.32	0.59
LY06	48	49	26	23	28	20	32.33	11.70	0.36	0.24	0.60

	Name	A0	A1	A2	A3	A4	A5	Expectation	SD	RSD	RMD	Evaluation
Minima	LY02	39	34	29	22	30	27	30.17	5.33	0.18	0.26	0.44
Q1	PY12	70	79	121	203	341	395	201.50	126.28	0.62	0.38	1.01
Q2	WT06	51	66	60	114	322	246	143.17	103.90	0.73	0.57	1.30
Q3	WL03	86	125	50	19	284	187	125.17	88.98	0.71	0.84	1.55
Maxima	WT16	423	34	164	65	246	35	161.17	139.70	0.87	2.03	2.90

5. RESULTS

After getting the ranking list of all the data and the quartiles lists, we conducted the qualitative and quantitative analysis. Firstly, we wanted to confirm whether the top 7 ranking list is the best options for the design, and secondly, we also wanted to know what are the characteristics of the 4 quartiles lists and whether the sitting postures and seat shape corresponding to each list have any commonalities or regularities? We imported the video screenshots of each set of data recorded during the experiment into Adobe Animate according to the sequence of evaluation results and adjusted the frame rate to 1 second per frame to produce video animation in SWF format. By repeatedly watching the animation to search patterns and characteristics of each list, we found that each list has its own typical seat shape and sitting postures, which appeared more times saliently than other types, as shown in Figure 4. First, the typical seat surfaces of list 1 look like “Patrick Star”, they have clear limb shapes and a straight belly. The characteristics of corresponding sitting postures are that the limbs are extended relative to each other, and the femur presents a downward sloping angle to the seat surface, the participants‘ hips usually sit in the front of the seat, with the back leaning against the chair back. At this time, participants’ pelvis tilted forward, which is healthy to the human body’s spine and similar to the sitting position of the saddle chair (Wallace,2010).

Secondly, we observed that there was more ground sitting positions in list 2, which suggested that the ergonomic performance of sitting on the floor ranked at the upper-middle level. This sitting posture is inherent to primates and is the result of long-term evolution, so it was not surprising that it ranked as a relatively

higher level. Thirdly, slopping back or sitting to relaxed are the typical postures in list 3, in which the body leaned back hard while sitting with flat thighs on the chair. At this time, the body presented a large elevation angle and was in a state of tension against the chair back. However, from the pressure test results, this seemingly comfortable posture increased pressure on the hips rather than reduced it. Fourthly, in list 4 with a lower score, there were more unhealthy sitting postures such as lifting a leg and reclining sitting, etc. in these situations, the posture of the body showed an asymmetry, so it had the lowest score.

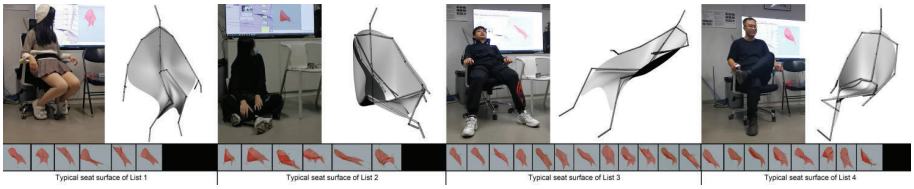

Figure 4. 4 quartiles lists typical seat shapes.

Through the analysis of the interquartile ranges above, we can conclude that our evaluation system and the ranking list work. With auxiliary means of the ranking table and visual observations, we finally chose the KM03 chair that ranked second in the ranking table and with a decent seat surface shape as the final design proposal for 3D printing.

By watching the screenshots recorded during the experiment, we noticed that KM03 and KM05 as well as the KM04, which were recorded in a short time where the participant was sitting on the ergonomic chair in a relaxed sitting position and rotating the chair, see Figure 5 left part. We assumed that the rotation of the seat might create a centripetal force that pushed the participant's body toward the seat surface, so that all parts of the body were evenly stressed, which was also reflected in the pressure value panels. Therefore, the corresponding seat surface generated in the Grasshopper at that moment could be the best option for an ergonomic chair seat surface.

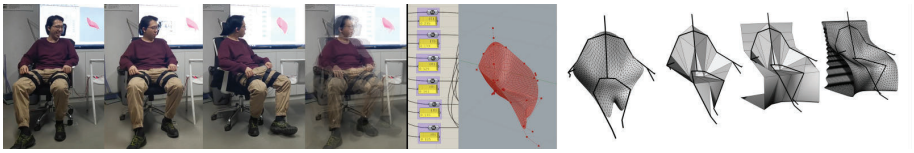

Figure 5. The formation process of KM03 chair.

Next, we used Rhino the SubD component, and plugin weaverbird to modify and refine the basic seat panels generated in Grasshopper to ensure the structural stability and implementation for 3D printing, see Figure 5 right part. We applied the robotic arm 3D printer fabricating the tangible chair, the whole production process cost just 6 hours. In addition to rapid prototyping, the chair surface produced by 3D printing is exquisite, and the modeling details of the digital model were highly restored.

Finally, we got the 3D printed chair as shown in Figure 6, we conducted the using evaluation with the participant who created the KM03 chair with sitting posture. We used the Velcro with glue to arrange the pressure sensors on the surface of the chair. And we asked the participant sit in the chair, recording the pressures value at the same time, the pressure values were evenly distributed. The comfort of the chair was also proved by the interview with the participant.

Figure 6. The pictures of 3D printed chair and users test.

6. CONCLUSION

6.1. PERSONALIZED PARAMETRIC CHAIR DESIGN PROCEDURES AND METHODS

The procedures of our study can be divided into two parts which are also the two fundamental parts of the parametric design definition: the construction of the parameter relationship and the acquisition of parameters. In the first part, we used DSE to translate the design problem and then defined the range of design parameters to get the corresponding parametric geometries with the variation of the range. In the second part, we used the Kinect smart camera, and the wearables with Arduino FSR pressure sensors to acquire parameters from the participants in the ergonomic design experiment.

6.2. FORM FOLLOWS BEHAVIORS

The acquisition of personalized data provided the probability for the customized design. In our case, we used Kinect to capture the subtle postures and behaviors of participants, and we applied the wearables with pressure sensors to detect the pressure value of six parts of hips, we aimed to conduct a design pattern of not only data-driven design but also a “form follows postures or behaviors” paradigm. In particular, the use of the pressure wearable device enables the experiment participants to move more freely, which not only provides participants with a variety of seat options but also enables participants to creatively make more sitting postures, such as sitting on the ground.

6.3. EVALUATION WITH THE QUANTITATIVE METHODS

In our study, we got 110 sets of data based on the experimental sensor detections. We applied mathematics quantitative methods searching the regulations of the data firstly and conducted the evaluations to choose the best option. We utilized the statistic concepts SD, RSD, and RMD, etc. to investigate the data and used the quartiles to analyze the data list. Finally, we combined the quantitative analysis

methods and qualitative research strategy to make the choice of the final design proposal.

7. DISCUSSION and FUTURE WORK

Through experiments, we found that the sitting postures of male and female participants and the corresponding generated seat surfaces were distinct. All the female participants were presented with the same female-specific sitting posture that resulted in a distinctively rounded top and pointed bottom with a unique inverted droplet shape or ginkgo biloba shape surface, as shown in Figure 7. At this time, female participants sat with their thighs opened at a small angle and their legs in a parallel position or crossed. This sitting posture and seat surface shape never appeared in the experiment with male participants. On the other hand, the male participants were more likely to sit with their legs open at a wide-angle, but this posture was not unique to men. This small accidental discovery once again confirmed the notion of the study: Form follows postures/behaviors. This paper provided a general method to conduct parametric design based on the users' postures and physical data, the future work would be more specific, for instance, we can design products aimed at users of a certain gender, such as the feminine chair, etc.

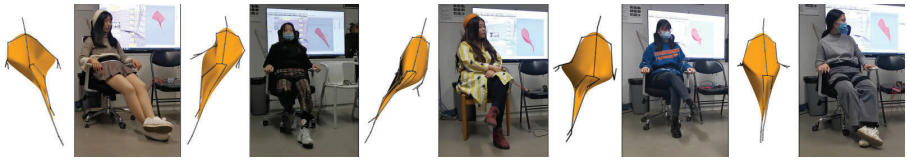

Figure 7. The 5 generative female-specific seat shapes.

References

Baek, S.Y. and Lee, K.: 2012, Parametric human body shape modeling framework for human-centered product design, *Computer-Aided Design*, **44**, 56-67.

Burkov, A.F., Zaychenko, I.V. and Goncharova, S.A.: 2019, Development of a Comprehensive Criterion for Evaluating the Ergonomics Configuration of the Seat, *2019 International Science and Technology Conference "EastConf",IEEE*.

Connors, M. and Li, L.: 2019, Bioinspired design of flexible armor based on chiton scales, *Nature Communications*, **5413(2019)**, 1-13.

Li, X., Xiao, Z. and Yang, K.: 2020, The Design of Seat for Sitting Posture Correction Based on Ergonomics, *2020 International Conference on Computer Engineering and Application (ICCEA)*, 703-706.

Salvado, L.M. and Arsenio, A.: 2016, Sleeve Sensing Technologies and Haptic Feedback Patterns for Posture Sensing and Correction, *IUI '16 Companion*, 74-78.

Wallace, J.S.: 2010, "Ergonomic saddle chair patent" . Available from <https://patents.google.com/patent/US8317267B2/en>.

Wu, Y.C. and Chen, M.Y.: 2018, ActiveErgo: Automatic and Personalized Ergonomics using Self-actuating Furniture, *CHI '18: Proceedings of the 2018 CHI Conference on Human Factors in Computing Systems*, 1-8.

Zhang, Z. and Yan, C.: 2020, *Digital nature decoding zhang zhoujie digital lab*, Tongji University Press, Shanghai.

FROM EXPLORATION TO INTERPRETATION

Adopting Deep Representation Learning Models to Latent Space Interpretation of Architectural Design Alternatives

JIELIN CHEN[1] and RUDI STOUFFS[2]
[1,2]*Department of Architecture, National University of Singapore*
[1]*chen.jielin@u.nus.edu* [2]*stouffs@nus.edu.sg*

Abstract. An informative interpretation of the hyper-dimensional design solution space can potentially enhance the cognitive capacity of designers with respect to both conventional design practice and the research domain of computational-aided generative design. However, the hitherto research of design space exploration has had limited focus on the interpretation of the hyper solution space per se due to the knowledge gap pertaining to representation and generation. Representation learning techniques, as a core paradigm in the statistically empowered domain of machine learning, possess the capability of extracting a convoluted probabilistic distribution of hyperspace with latent features from unorganized data sources in a generalized manner, which can be an intuitive modus operandi for a structural interpretation of the intricate latent design solution space and benefit the challenging task of architectural design exploration. We examine and demonstrate the potential capabilities of representation learning techniques for the interpretation of latent architectural design solution space with consideration of disentanglement and diversity.

Keywords. Design space exploration; latent space interpretation; representation learning; deep generative modelling; generative architectural design.

1. Introduction

The exploration of design alternatives is a routine practice for designers, the workflow of which can be perceived as an iterative framing process of design alternatives given explicit and implicit sets of contextual constraints, which are typically tricky to exhaustively codify. The nature of architectural design is discrepant from most problem-solving tasks in that the latent problems in architectural design are often ill-structured; defining the problem space is an intricate part of the design task (Eastman 2001). Hence, the process of design exploration can be depicted as mapping a series of latent design solution spaces and searching for optimal solutions within them. As the scope of manual design exploration is limited by the cognitive capacity of human designers, it grants chances for computational support and assistance (Woodbury & Burrow 2006).

PROJECTIONS, Proceedings of the 26th International Conference of the Association for Computer-Aided Architectural Design Research in Asia (CAADRIA) 2021, Volume 1, 131-140.

Generative design has been developed as a powerful assistant for designers in the field of architecture and engineering. Two successive generations of generative design epistemology so far have leveraged the design exploration capability of generative systems. The first generation of generative design frameworks involves rule-based or performance-driven algorithms to transform a set of design objectives into a solid design product with certain criteria constraints. To satisfy such constraints, a series of objective functions need to be predefined with a set of design attributes (Sönmez 2015). In general, the first generation of generative design exploration regards design practice as a pathfinding task within a latent solution space at a local level using predefined navigation mechanisms, which has intrinsically hindered its potential generalization in practical applications. Such generative design systems can lead to a potential cognitive overload of its users, due to the large number of generated alternatives which need further clustering and grouping (Erhan et al. 2017).

In fact, without a global cognition of the hyper-dimensional latent design solution space, the scope of design exploration is doomed to be limited. Hence, it is necessary to advocate an epistemic shift and focus on the interpretation of the hyper solution space with a possibly global perspective. However, research in design space exploration has had limited focus on the interpretation of the design space per se ascribed to the knowledge gap pertaining to representation and generation (Woodbury & Burrow 2006). The emerging second generation of generative design schemes, benefitting from the boost of deep generative modelling in the field of machine learning, shows signs of being embedded with an intrinsic epistemology pertaining to the interpretation of the hyper solution space. The notion of deep generative modelling refers to a statistical modelling technique, which is capable of learning the latent feature distribution space from raw data in any format, and generating previously non-existing data samples from the estimated feature distribution space (Bengio et al. 2013; Gui et al. 2020).

Representation learning techniques, as a core machine learning paradigm playing a pivotal role in deep generative modelling, possess the capability of extracting convoluted probabilistic distributions of hyperspace with latent features from unorganized data in a generalized manner and map any feature vector from a random distribution to a semantically organized one (Bengio et al. 2013). This can be an intuitive modus operandi for structural interpretation of the intricate hyper design solution space and benefitting the challenging task of architectural design exploration. As deep representation learning can be used to leverage the abstraction of significant design features as decodable factors (Bengio et al. 2013; Han et al. 2019), the learned hyper-dimensional feature space can possibly represent the architectural design solution space with latent features reflecting any physically expressible design codes.

2. Research methodology

The rationale behind both deep generative modelling and representation learning is to learn a non-linear mapping between a latent feature distribution space and the real data space (Goodfellow et al. 2014; Xiao et al. 2019). A qualified deep representation learning model is required to automatically learn a disentangled

representation from the input data and minimize the distance between real and learned feature distribution (Tsai et al. 2019). A series of works have been done to address the automatic variation disentanglement task in the machine learning domain. Bau et al. (2020) have identified that some neural units of intermediate layers of a trained deep generative model are specialized to synthesize specific visual concepts. Meanwhile, Yang et al. (2020) found that a highly-structured semantic feature hierarchy can spontaneously emerge without any supervision from the learned representations of deep generative models adopting layer-wise stochasticity, such as BigGAN (Brock et al. 2019) and StyleGAN (Karras et al. 2019). The mechanism of layer-wise stochasticity indicates that the input latent codes for data synthesis are fed into all network layers of a deep neural net instead of only fed into the first layer, which enables better interpolation and disentanglement of the learned semantic features. Thus, we identify deep generative models with layer-wise stochasticity as our experimental backbones.

Meanwhile, both BigGAN and StyleGAN have the capability to synthesize diverse and high-quality image data. The difference between them is that the former is a conditional deep generative model while the latter is unconditional. BigGAN concatenates the latent code with a class-embedded code before feeding it to the generator (Brock et al. 2019). StyleGAN first maps a randomly sampled latent code from an initial latent space Z to an intermediate high dimensional space W using an auxiliary multilayer perceptron network before feeding it into the generator. The intermediate space W possesses a stronger disentanglement property than the initial space Z (Karras et al. 2019). Such property offers better interpolation and disentanglement of the learned latent semantic features, and further allows for scale-specific control of the data synthesis. The recently proposed StyleGAN2 model (Karras et al. 2020) further advances StyleGAN with better conditioning for the mapping from latent space to real data space.

As extensive coverage of the real data space ensures closer approximation to the right scope of data that a human architect would experience, access to large-scale datasets with quasi-exhaustive coverage and diversity of the real data space can be essential. Hence, we adopted a customized dataset of outdoor architectural imagery (roughly 37K images) retrieved from ArchDaily® and Dezeen® (online repositories of architectural projects worldwide) to train the selected models with desired properties, namely BigGAN, StyleGAN and StyleGAN2. We use image data as they are comparatively easier to acquire in bulk. All training was performed on Nvidia Tesla V100 16GB GPU or Nvidia Tesla V100 32GB GPU. StyleGAN2 outperforms the other two models evaluated using Frechet inception distances (Heusel et al. 2017; BigGAN: 175.5853; StyleGAN: 10.1867; StyleGAN2: 8.7180; lower is better). All subsequent experiments here described were performed with StyleGAN2 (Figure 1).

3. Interpretation of hyper-dimensional latent architectural design space learned by deep generative models

StyleGAN (and StyleGAN2) can automatically learn an unsupervised separation of high-level factors and stochastic variation in the data space which control the appearance of synthesized data (Karras et al. 2019). We leverage the ability of

StyleGAN2 to achieve semantic architectural design exploration by providing a rigorous interpretation of the semantic features emerging in the learned latent space of the well-trained deep generative model and manipulating the semantics in the learned latent space for architectural design attribute exploration.

Figure 1. Generated architectural image samples using well-trained StyleGAN2.

The generator of a trained deep generative model can be formulated as a deterministic function $g : Z \rightarrow X$, where $Z \subseteq R^d$ denotes the d-dimensional latent space and X the synthesized data space, with each synthesized sample x possessing certain sets of semantic information (Shen et al. 2020). A semantic scoring function $f_S : X \rightarrow S$ with $S \subseteq R^m$ representing the semantic latent space with m semantics can be introduced to link the latent space Z and the latent semantic space S with

$$s = f_S(g(z)), \tag{1}$$

where s denotes the semantic scores and z the sampled latent code. The linear interpolation between two latent codes z_1 and z_2 forms a linear direction in the latent space which can be regarded as the normal vector of a separation boundary, namely a hyperplane separating the corresponding semantic features. The distance between a sample latent code z and a hyperplane can be defined as

$$d(n, z) = n^T z, \tag{2}$$

where $n \in R^d$ is a unit normal vector and $d(\cdot, \cdot)$ can be both positive or negative; the semantic attribute will be reversed when z moves across the hyperplane. $f_S(g(z))$ and $d(n, z)$ are expected to be dependent upon each other, having

$$f_S(g(z)) = \lambda d(n, z), \tag{3}$$

where the scalar $\lambda > 0$ measures the unit magnitude of the latent semantic variation concomitant with the changing distance between the latent code z and the corresponding hyperplane. To disentangle multiple semantics, the latent semantic space needs to be further extended as

$$\mathbf{s} \equiv f_S(g(\mathbf{z})) = \mathbf{\Lambda} \mathbf{N}^T \mathbf{z}, \tag{4}$$

where $\mathbf{s} = [s_1, \ldots, s_m]^T$ indicates multiple semantic scores, and $\mathbf{N} = [n_1, \ldots, n_m]$ contains the unit normal vectors of the corresponding separation boundaries of semantic features, while $\mathbf{\Lambda} = diag(\lambda_1, \ldots, \lambda_m)$ denotes the diagonal matrix containing the coefficients between the variation of semantic score and corresponding distance to the boundary. Assuming that the distribution of latent code samples $\mathbf{z}$ can be approximated as Gaussian distribution $N(\mathbf{0}, \mathbf{I}_d)$, then $\mathbf{s} \approx N(\mathbf{0}, \mathbf{\Sigma s})$ is a multivariate normal distribution. Consequently, the manipulation of any semantic attribute of the synthesized data can be done by moving the latent code z along the unit normal vector of the hyperplane of the

corresponding semantic feature (Figure 2) with

$$\check{\mathbf{z}} = \mathbf{z} + \alpha\mathbf{n}. \quad (5)$$

To extract architectural semantic attributes from the learned latent space of the well-trained deep generative model, we further employ an auxiliary wide-resnet-based attribute prediction model trained with the SUN attribute database, which is manually labelled with 102 pre-defined scene attributes (Patterson et al. 2014; Zagoruyko & Komodakis 2017). The attribute prediction model was trained with multi-label losses to predict multiple attributes synchronously, and all attributes of the pre-trained prediction model were learned as bi-classification tasks. We use the adopted attribute prediction model to assign semantic attribute scores to the synthesized images and use the obtained attribute scores to further retrieve latent semantic boundaries inside the learned hyper architectural design space.

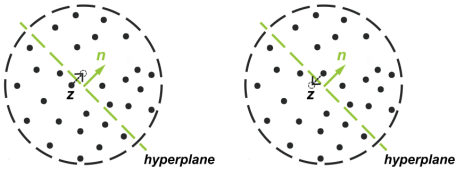

Figure 2. Manipulation of a semantic attribute of the synthesized data by moving the latent code z alongside the unit normal vector n of the hyperplane of the corresponding semantic feature. The synthesis will be either more positive ($\alpha > 0$; left) or negative ($\alpha < 0$; right).

Given the well-trained StyleGAN2 model for architectural imagery, we synthesize 300K images with randomly sampled 512-dimensional latent codes z, to pseudo exhaustively cover the learned distribution of the latent space. The aforementioned attribute predictor is used to calculate attribute scores for all synthesized images. For each attribute, the images are sorted by the corresponding scores. The 2,000 samples with highest scores are chosen as positive candidates and the 2,000 with lowest scores as negative samples, so as to avoid false prediction of ambiguous candidates as the pre-trained attribute predictor might not be entirely accurate. 70% of the selected candidates are randomly chosen as training set to train a linear support vector machine (SVM), bringing forth a binary classification decision boundary, namely the aforementioned separating hyperplane of each semantic attribute. The other 30% of the selected samples are used to verify the performance of the SVM. The inputs for the SVM training are the initial latent codes z for image synthesis, while the binary labels are acquired using the attribute predictor, indicating the presence of a target attribute in the corresponding synthesized image. The normal directions of all learned semantic attribute boundaries are normalized to unit normal vectors for further attribute manipulation experiments of the synthesized images.

3.1. DISENTANGLEMENT OF HIERARCHICAL SEMANTIC ATTRIBUTES

As we have previously discussed, deep generative models taking in layer-wise latent codes can spontaneously embed the semantics of the learned latent

space in a hierarchical manner from various abstract levels, which facilitates disentanglement of semantic features and manipulation of the synthesis process (Yang et al. 2020). To interpret the hierarchical semantics embedded in the learned generative representations for architectural image synthesis, 22 attributes relevant to architectural design are selected from the original 102 attributes of the SUN database (Patterson et al. 2014) and collected into five categories based on their characteristics (Table 1).

Table 1. Selected attributes relevant to architectural design categorized into five categories.

Characteristic	Attributes
Configuration	vertical_components, horizontal_components, symmetrical, cluttered_space
Openness	open_area, semi-enclosed_area, enclosed_area
Texture	glossy, matte, sterile, rugged_scene, rusty, moist, dry
Senses	soothing, stressful, warm, cold, man-made,natural
Material	brick, tiles, concrete, metal, wood, glass

We synthesized a series of images using the well-trained deep generative model with identical initial latent code z while moving z across a set of specified attribute boundaries (Figure 3). The outputs have verified that it is possible to controllably manipulate the synthesis process with specified attributes.

Figure 3. Synthesized samples of manipulating specified attributes with the same latent code z using the deep generative model trained on the architectural image dataset.

Figure 4 further illustrates some synthesized samples with distances close to and away from the learned attribute boundaries. For each row of samples, the middle one is the original synthesis with initial latent code z, while the left and right are synthesized results by moving z alongside the negative and positive direction of the unit normal vector n of the learned attribute boundary respectively. Each step indicates one unit distance away from the attribute boundary.

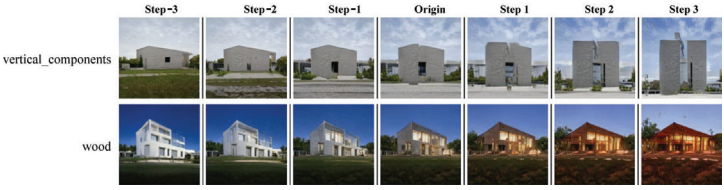

Figure 4. Synthesized samples manipulated at two specified attributes with distances close to and away from the learned attribute boundaries.

As previously mentioned, StyleGAN2 possesses a more disentangled latent space W based on the latent space Z of conventional deep generators which feeds

the latent code $w \in W$ to every convolutional layer with varied transformations; There are a total of 14 convolutional layers in the generator of the well-trained StyleGAN2. To measure the relevance level of each variation factor concerning every layer, attributes are re-scored per layer to quantify the correlation between the layer-wise representation and the corresponding semantic attribute. The normalized score shows that the layers of the generator are specialized to synthesize attributes hierarchically: Layers close to the input layer determine the configuration and openness of the architectural image, layers closer to the output layer control the attribute-level variations, and the material scheme is mostly rendered at layers closest to the output layer (Figure 5). This sequence is fairly consistent with a human architect's perception of the design process.

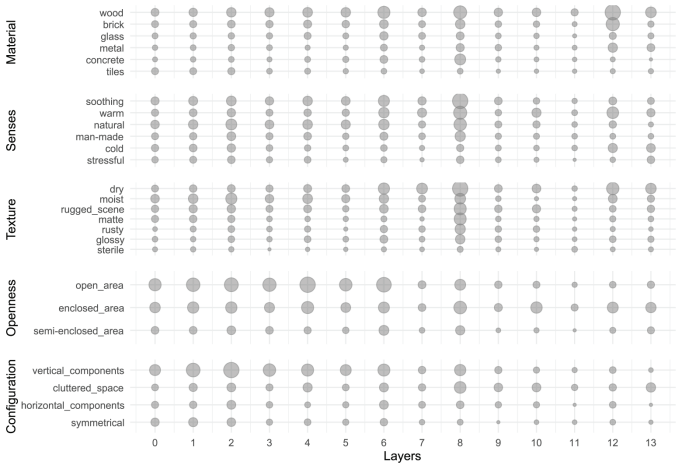

Figure 5. The correlation level between the layer-wise representation and the semantic attributes of synthesized images, the attributes in each characteristic group are sorted in descending order based on the overall level of relevance of the corresponding attribute.

3.2. DISENTANGLEMENT OF CORRELATED SEMANTIC ATTRIBUTES

As can be seen from the previous section, the manipulation results of some attributes are somehow intertwined with each other. It would be ideal to manipulate certain target attribute of the synthesis while keeping other attributes unchanged, which requires disentanglement of correlated semantic attributes. According to the previous discussion, different semantics s could be disentangled only when $\mathbf{\Sigma s}$ is a diagonal matrix and the unit normal vector of the separating hyperplanes of each semantic attribute $\{n_1, \ldots, n_m\}$ are orthogonal (linearly independent) with each other. Semantics violating this condition are correlated with each other and their entanglement level can be measured with $n_i^T n_j$.

As aforementioned, the latent space W of StyleGAN2 is not restricted to any predefined distribution and can learn a more disentangled representation, which enables layer-wise manipulation of the identified semantic features and can thus

provide controllable attribute editing. By layer-wise manipulating the latent code alongside certain semantic boundaries, we can visually examine how the synthesis varies at different layers. Figure 6 shows some synthesized samples with initial latent code z moving across specified semantic boundaries at the bottom, lower, upper, and top layers. These turn out to be mostly consistent with the conclusion drawn in section 3.1: 'vertical_components' can be significantly manipulated at bottom layers but have less impact at later levels of the model, whilst 'natural' can be best controlled at upper layers. Manipulating the latent code at less relevant layers can also lead to a change of image content. However, the change may be irrelevant to the expectation, f.i., manipulating the 'wood' attribute at any layers changes the synthesized image content, but the changes at middle layers relate to the building facade's configuration, the changes at upper layers relate to the texture of the facade, while the top layers contribute to the colour scheme. An interesting inference can be deduced from the observation: As the wood attribute can be relevant to both the texture and colour of the building facade, it might be possible to further decompose a singleton attribute feature based on its intrinsic definition.

To further quantify the correlation between different attributes, two metrics are adopted from Shen et al. (2020). First, the cosine similarity between two attribute normal vectors is defined as $\cos(n_1, n_2) = n_1^T n_2$, where n_1 and n_2 stand for the unit normal vectors. A value of zero indicates that the two unit normal vectors are orthogonal with each other, namely, they are fully disentangled. The cosine similarity matrix of the attribute boundaries of the learned latent feature space (Figure 7 left) can help to explain some of the observed phenomena, f.i., 'wood' attribute is relatively highly correlated with 'rugged_scene' with cosine similarity value 0.22, which can explain why manipulating the 'wood' attribute at middle layers can change the configuration of the building facade (Figure 6), considering that 'rugged_scene' has high correlation level at middle layers (Figure 5).

Figure 6. Synthesized samples with latent codes moving alongside the unit normal vector of two specified attribute boundaries at the bottom, lower, upper, and top layers of the well-trained model respectively.

Second, to examine the correlation of the synthesized attribute distribution, each attribute score is treated as a random variable, and the attribute scores obtained from all 300K synthesized images are used to calculate the Pearson correlation coefficient of every two semantic attributes respectively (Figure

7 right). We note the high correlation of ‘soothing’ and ‘natural’ attributes (correlation coefficient 0.79), ‘warm’ and ‘dry’ (0.79), and ‘glass’ and ‘glossy’ (0.77). The correlation among different attributes is similar for both metrics, which indicates that the adopted supervised approach for disentangling semantic attributes in the learned latent space is effective and accurate.

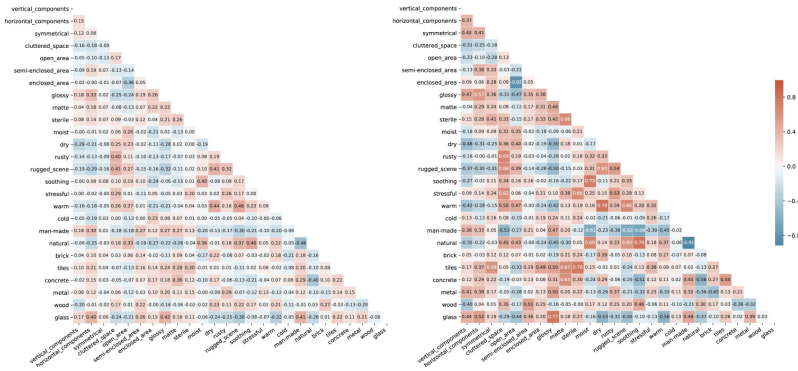

Figure 7. Cosine similarity matrix of the learned attribute boundaries (left) and correlation matrix of synthesized attribute distribution (right) for the well-trained deep generative model.

4. Discussion and summary

We have examined the potential capabilities of different representation learning-related techniques for latent architectural design space interpretation, and have demonstrated the multifaceted possibilities of leveraging representation learning to manipulate the exploration of architectural design alternatives controllably. This study’s long-term goals are to advocate a generic epistemic shift for more diverse and manipulatable design alternative generation and to promote interactive toolsets permitting user control over the synthesis process given that any physically expressible design codes can be intaken. This epistemic perspective might also be able to tackle the generalization issue of conventional generative design paradigms. Moreover, by coupling representation learning with optimization algorithms, it can be promising to achieve a more robust and efficient design space interpretation and exploration system.

Last but not least, the fact that the adopted attribute prediction model is not customized for architectural image recognition has hindered the accuracy and relevance of the attribute boundary retrieval task during the design space interpretation process. It would be worthwhile to develop an attribute predictor with an orientation of architectural design in the future. In addition, although it would be easy to expand the list of attributes for the predictor as assistance for latent design space interpretation, it is difficult to exhaustively explore the entire latent semantic space in a supervised manner. As such, it can be beneficial to introduce unsupervised approaches to disentangle the semantic features of latent architectural design solution space in future works.

Acknowledgements

The computational work for this article was partially performed on resources of the National Supercomputing Centre, Singapore (https://www.nscc.sg).

References

Bau, D., Zhu, J.Y., Strobelt, H., Zhou, B., Tenenbaum, J.B., Freeman, W.T. and Torralba, A.: 2020, "On the Units of GANs (Extended Abstract)" . Available from <https://arxiv.org/abs/1901.09887>.

Bengio, Y., Courville, A. and Vincent, P.: 2013, Representation learning: A review and new perspectives, *IEEE transactions on pattern analysis and machine intelligence*, **35**(8), 1798-1828.

Brock, A., Donahue, J. and Simonyan, K.: 2019, "Large Scale GAN Training for High Fidelity Natural Image Synthesis" . Available from <https://arxiv.org/abs/1809.11096>.

Eastman, C. and Computing, D. 2001, New directions in design cognition: studies of representation and recall, *in* C. Eastman, W. Newstetter and M. McCracken (eds.), *Design knowing and learning: Cognition in design education*, Elsevier, 147-198.

Erhan, H., Chan, J., Fung, G., Shireen, N. and Wang, I.: 2017, Understanding Cognitive Overload in Generative Design-An Epistemic Action Analysis, *Proceedings of CAADRIA 2017*.

Goodfellow, I., Pouget-Abadie, J., Mirza, M., Xu, B., Warde-Farley, D., Ozair, S., Courville, A. and Bengio, Y.: 2014, Generative adversarial nets, *Advances in neural information processing systems*, 2672-2680.

Gui, J., Sun, Z., Wen, Y., Tao, D. and Ye, J.: 2020, "A Review on Generative Adversarial Networks: Algorithms, Theory, and Applications" . Available from <https://arxiv.org/abs/2001.06937>.

Han, Z., Shang, M., Liu, Y.S. and Zwicker, M.: 2019, "View Inter-Prediction GAN: Unsupervised representation learning for 3D shapes by learning global shape memories to support local view predictions" . Available from <https://arxiv.org/abs/1811.02744>.

Heusel, M., Ramsauer, H., Unterthiner, T., Nessler, B. and Hochreiter, S.: 2017, Gans trained by a two time-scale update rule converge to a local nash equilibrium, *Advances in neural information processing systems*, 6626-6637.

Karras, T., Laine, S. and Aila, T.: 2019, A style-based generator architecture for generative adversarial networks, *Proceedings of CVPR 2019*, 4401-4410.

Karras, T., Laine, S., Aittala, M., Hellsten, J., Lehtinen, J. and Aila, T.: 2020, Analyzing and improving the image quality of stylegan, *Proceedings of CVPR 2020*, 8110-8119.

Patterson, G., Xu, C., Su, H. and Hays, J.: 2014, The sun attribute database: Beyond categories for deeper scene understanding, *International Journal of Computer Vision*, **108**(1-2), 59-81.

Shen, Y., Gu, J., Tang, X. and Zhou, B.: 2020, Interpreting the latent space of gans for semantic face editing, *Proceedings of CVPR 2020*, 9243-9252.

Sönmez, N.O.: 2015, Architectural layout evolution through similarity-based evaluation, *International Journal of Architectural Computing*, **13**(3-4), 271-297.

Tsai, Y.H.H., Liang, P.P., Zadeh, A., Morency, L.P. and Salakhutdinov, R.: 2019, "Learning Factorized Multimodal Representations" . Available from <https://arxiv.org/abs/1806.06176>.

Woodbury, R.F. and Burrow, A.L.: 2006, Whither design space?, *Artificial Intelligence for Engineering Design, Analysis and Manufacturing: AI EDAM*, **20**(2), 63.

Xiao, Z., Yan, Q. and Amit, Y.: 2019, "Generative Latent Flow" . Available from <https://arxiv.org/abs/1905.10485>.

Yang, C., Shen, Y. and Zhou, B.: 2020, "Semantic Hierarchy Emerges in Deep Generative Representations for Scene Synthesis" . Available from <https://arxiv.org/abs/1911.09267>.

Zagoruyko, S. and Komodakis, N.: 2017, "Wide Residual Networks" . Available from <https://arxiv.org/abs/1605.07146>.

A GRAPH THEORETIC APPROACH FOR THE AUTOMATED GENERATION OF DIMENSIONED FLOORPLANS

KRISHNENDRA SHEKHAWAT
[1]*Department of Mathematics, BITS Pilani, Pilani Campus, India-333031*
[1]*krishnendra.shekhawat@pilani.bits-pilani.ac.in*

Abstract. The automated generation of architectural layouts is an intensively studied research area where the aim is to generate a variety of (initial) layouts for the given constraints which can be further modified by designers and architects. From a mathematical perspective, one of the well-known constraints is given in the form of an adjacency graph which represents the adjacency relations of the given rooms and problem is to generate multiple layouts satisfying the adjacency relations. In the literature, the adjacency graph is usually taken as a bi-connected planar triangular graph. In this paper, we present the results of a prototype GPLAN that generates multiple dimensioned layouts for any given planar graph. The larger aim of this work is to develop software that can produce a variety of architecturally acceptable floorplans corresponding to the given constraints.

1. Introduction

From 1970s, a good amount of work has been done in the domain of computer-aided architectural design, where the prime focus is to automatically generate floor-plan layouts, so that these layouts are regarded as preliminary layouts by architects/designers and can be further modified and adjusted by them (Steadman 1973, Mitchell et al. 1976). If we restrict ourselves to the generation of floorplans corresponding to a given adjacency graph, a few of the relevant work in this direction is as follows:

The automated generation of architectural layouts using graph theory began with the generation of rectangular floorplans (RFP). It was first proposed by Levin 1964 in the early 1960s. Then in 1970s, many researchers proposed graph-theoretical algorithms for the enumeration or construction of rectangular layouts (Lynes 1977, Gilleard 1978, Baybars and Eastman 1980). During 1980s, Roth et al. 1982, Rinsma 1987 and Rinsma 1988 developed efficient graph algorithms for the construction of dimensionless and dimensioned RFPs with some restrictions on the input graph.Then in early 1990s, researchers realized that there are graphs for which RFPs do not exist (Rinsma et al. 1990, Yeap and Sarrafzadeh 1993). Liao et al. 2003 gave a linear time algorithm for constructing a dimensionless orthogonal floorplan (OFP) for any planar triangulated graph (PTG). Jokar and Sangchooli 2011 used the concept of face area of a graph for the construction of dimensionless OFPs for given PTGs. Eppstein et al. 2012 gave an

PROJECTIONS, Proceedings of the 26th International Conference of the Association for Computer-Aided Architectural Design Research in Asia (CAADRIA) 2021, Volume 1, 141-150.

algorithm for finding an area universal RFP for the given adjacency requirements whenever such layout exists. Wang et al. 2018 gave the automated regeneration of well-known existing dimensionless RFPs while considering underlying adjacency graph of the existing floorplan. In the same year, Shekhawat 2018 enumerated all possible maximal RFPs without considering dimensions of the rooms. Recently, Upasani et al. 2020 developed a prototype for generating dimensioned RFPs for any drawn rectangular arrangement, satisfying adjacency, size and symmetric requirements. In the same year, Wang and Zhang 2020 extended GADG (Wang et al. 2018) for generating dimensioned OFPs corresponding to user-specified design requirements.

It can be observed from the literature that the construction of floorplans is restricted to bi-connected planar triangulated graphs only while for many architectural layouts the underlying graph is either 1-connected or non-triangulated. In this work, we present the results of prototype GPLAN that generates floorplans for any given planar connected graph. The obtained floorplans are categorized into two forms: the one having the rectangular boundary and other ones having the non-rectangular boundary.

2. Terminologies

In this section, we present the definitions related to adjacency graph and floorplans, which will be used further in the next Section.

A floor plan is a polygon, the plan boundary divided by straight lines into component polygons called rooms. If the boundary as well as rooms of a floorplan are rectangular it is called rectangular floorplan (RFP). If the boundary is rectangular while some rooms are rectilinear, it is called orthogonal floorplan (OFP). In a non-rectangular floorplan (NRFP), boundary is rectilinear while the rooms can be rectangular or rectilinear. For an illustration refer to Figure 1, where RFP, OFP and NRFP are shown.

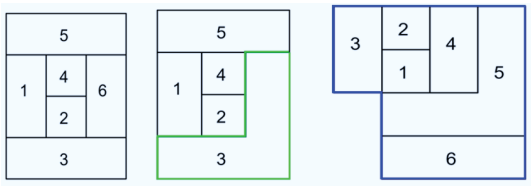

Figure 1. Floorplans Characterization.

Corresponding to a floorplan, there always associates a graph known as dual graph which can be constructed by taking each room as a vertex and drawing an edge between two vertices if and only if corresponding rooms share a wall or a part of a wall (see Figure 2).

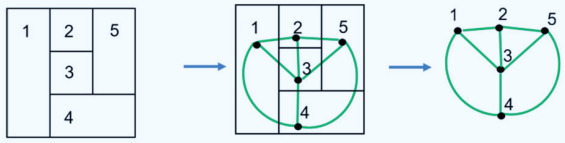

Figure 2. Constructing dual graph of a floorplan.

Moving from a floorplan to a graph is trivial but constructing a floorplan for a given graph is not easy and therefore, we will discuss it in detail in the next section. For example, consider the graph in Figure 3 for which constructing a floorplan is not trivial by hand and an algorithm is required to deal with such graphs having a large number of vertices.

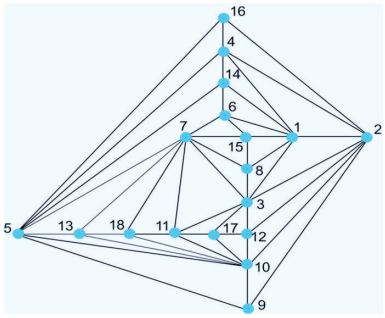

Figure 3. An adjacency graph for which constructing a floorplan manually is not easy.

A connected graph is said to be planar if it can be drawn in plane with edge crossings. A plane graph is a planar graph with an embedding that divides the plane into connected components called faces/regions. The unbounded region is called external face. Except for the external face, all other faces are internal faces. A planar triangulated graph (PTG) is a planar graph having all of its faces triangular. For example, the graph in Figure 4a is not planar while in Figure 4b is a PTG.

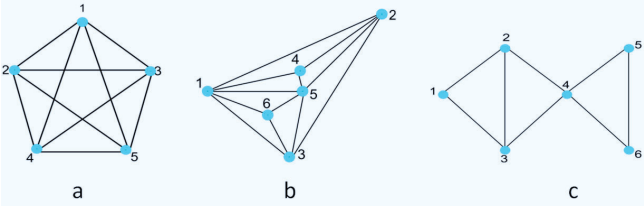

Figure 4. Illustrating planarity and connectivity of a graph.

A graph G is said to be 1-connected if it has a cut-vertex where a vertex v is a cut-vertex if its removal disconnects the graph. A graph G is said to be bi-connected if it has no cut-vertex. For example, the graph in Figure 4c is 1-connected (vertex 4 is the cut-vertex) while the graph in Figure 4b is bi-connected having no cut-vertices.

Since a floorplan itself can be regarded as a planar connected graph, therefore from here onwards an adjacency graph refers to a planar connected graph.

3. Methodology

In this section, we present the construction of dimensioned floorplans for any given adjacency graph G that are produced using the prototype GPLAN. It is important to note here that G mainly represents the adjacency relations among the rooms. At the same time, G also serves the following two purposes which are not directly visible:

- The geometry of the rooms: We are not asking for the room geometries as an input but they are derived based on the adjacency relations, i.e. in order to satisfy the given adjacencies, the rooms can be rectangular or rectilinear. For example, for the graph in Figure 5, at least one of the room in the corresponding floorplan needs to be rectilinear for satisfying the given adjacencies. In the floorplan in Figure 5, room 1 is of T-shape .
- Adjacency with the exterior: While drawing an adjacency graph, the user has a choice to keep any of the rooms in the interior or at the exterior. For example in Figure 5, rooms 1, 2 and 3 are interior rooms while 4, 5 and 6 are exterior rooms.

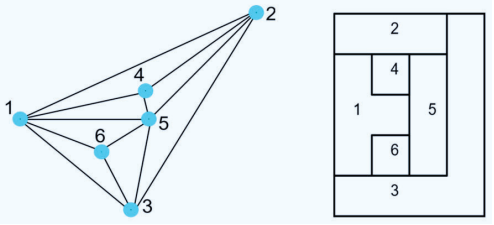

Figure 5. Illustrating geometry of the rooms and their relation with the exterior.

To proceed further, we consider the following cases based on the nature of the given graph G:

- 1. If the given graph G is planar, bi-connected and triangulated

In this case, it is always possible to construct a floorplan with rectangular boundary but the rooms can be rectangular or rectilinear. For example, GPLAN construct the required floorplans in Figure 6 where there exists a RFP for the first graph but RFP does not exist for the second graph and therefore OFP has been illustrated. Also in the RFP, all rooms are adjacent to the exterior while in the OFP, only room 5 is at the interior.

For the construction of a RFP, a linear time algorithm has been developed which is core of all the results of the paper, i.e., modifying this algorithm, floorplans in the consequent steps have been obtained.

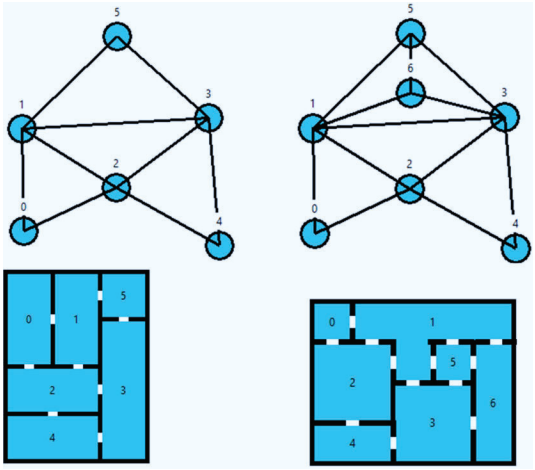

Figure 6. RFP and OFP corresponding to given graphs.

As mentioned in the Introduction, most of the work is restricted to planar bi-connected and triangulated graphs and it is covered in Step 1. Now in the coming steps, we address the construction of floorplans where the input graph is neither bi-connected nor triangulated.

- 2. If G is a planar bi-connected graph but not triangulated

If the graph is not triangulated, it means there exists at least a cycle of length greater 3 in the graph. Architecturally it is interesting to note that a cycle of length greater than 3 in a graph represents a corridor, i.e., to satisfy given adjacencies, corridors need to be introduced in the corresponding floorplan (see Figure 7C).

If the graph is not triangulated, the first step is to triangulate it by adding new edges (the graph in Figure 7A is not triangulated which is further triangulated in Figure 7B by adding 3 new edges). Now because of the new edges, we have two floorplan representations as follows:

- Floorplans with corridors: After triangulation, the floorplan F can be obtained as in Step 1. Now in the obtained floorplan F, if the additional edges or connections are removed, then we get a floorplan with corridors corresponding to the given graph as shown in Figure 7C. Clearly, in Figure 7A, there are two cycles of length greater 3 which leads to the generation of two corridors as shown in Figure 7C.
- Floorplan with and without doors: Also in the obtained floorplan F, the original adjacencies can be represented by doors while the new added adjacencies can be represented by the walls as shown in Figure 7D. For example, since room 1 and room 3 are not adjacent in Figure 7A, there is no door between them in Figure 7D while there is a door between rooms 0 and 3. This representation can be used when corridors are not required and floorplans need to be more compact and flexible.

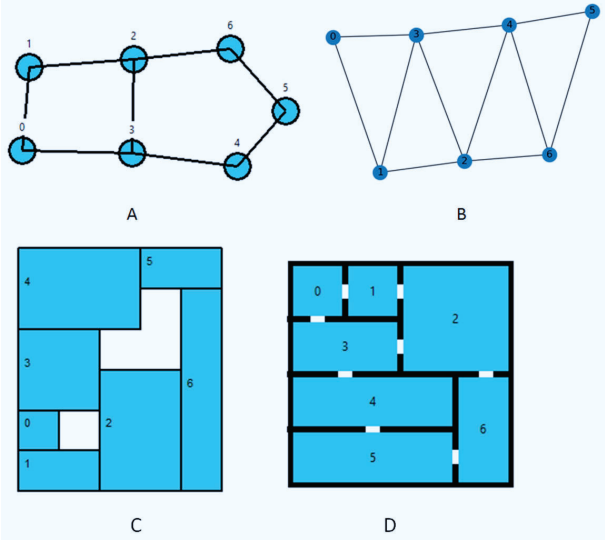

Figure 7. Corresponding to a given non-triangulated graph, a floorplan with corridors and a floorplan with doors.

- 3. If G is a planar 1-connected triangulated graph

In this case, we first add extra edges to make the graph G bi-connected and obtain a floorplan F using Step 1. For example, for the graph in Figure 8A, which is 1-connected, corresponding bi-connected graph is shown in Figure 8B. Now again added connections can be removed from F to have a floorplan with corridors or added connections can be represented by walls in F as done in Step 2 (refer to Figure 8C and 8D respectively).

The 1-connected graphs are helpful in representing different blocks of a building. For example, in Figure 9B, rooms 0, 1, 2 and 3 form a block which is adjacent to other block of building via room 3. Also, using 1-connected graphs, it is easy to represent rooms which requires isolation or a minimum connectivity. For example, in Figure 10C, room 5 is only adjacent to room 2.

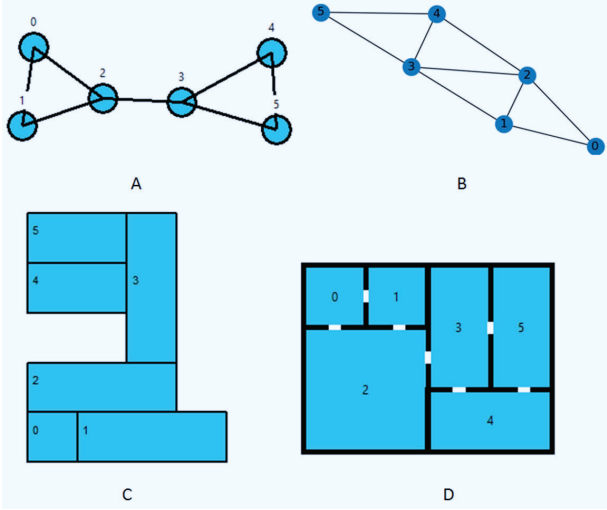

Figure 8. 1-connected graph and corresponding floorplans.

- 4. If G is a planar 1-connected graph and not triangulated

In this case, we first make G bi-connected and then triangulate it. Then using the concepts of Steps 2 and 3, we will have required floorplans. For example, refer to Figure 9A where the given graph is non-triangulated and 1-connected and floorplans corresponding to it are illustrated in Figures 9B and 9C.

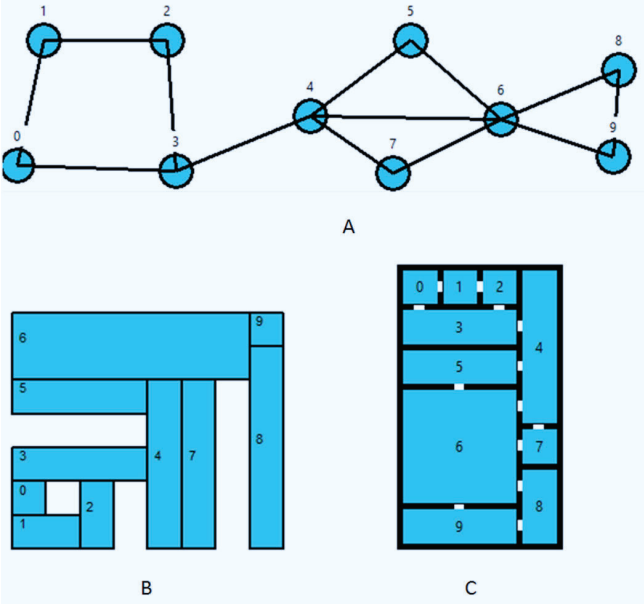

Figure 9. A 1-connected non-triangulated graph and corresponding floorplans.

- 5. Dimensioned floorplans

Once we obtain the required floorplans, the dimension of each room is taken as input in the form of minimum and maximum width along with minimum and maximum area. For example, refer to Figure 10B where dimensional constraints are illustrated. A dimensioned floorplan for the graph given in Figure 10A is shown in Figure 10C.

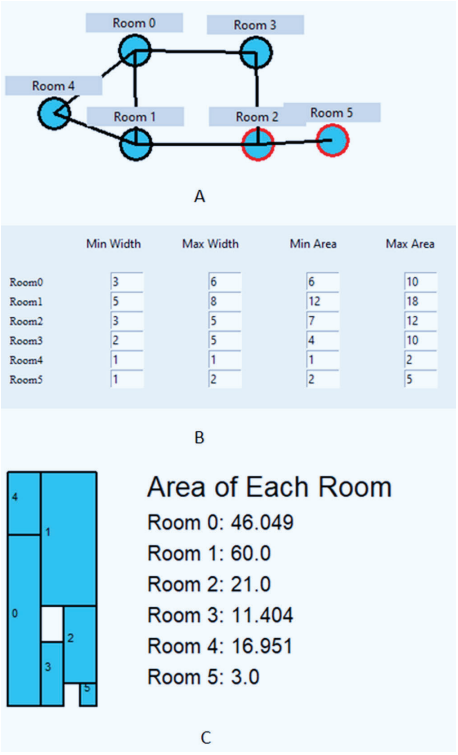

Figure 10. Dimensioned floorplan for the given graph.

Remark. In Figures 7, 8 and 9, we have proposed two floorplan representation for the given adjacency graph. In both the representations, all adjacency relations are satisfied but in the second one, the boundary is always rectangular and empty spaces are not allowed (see Figures 7D, 8D and 9C) while in the first one, empty spaces as well as non-rectangular boundary are considered (see Figures 7C, 8C and 9B). Architecturally each one has its importance as discussed above but mathematically, they differ on the basis of compactness.

4. Conclusion and Future Work

In this paper we have presented the results of an operational software GPLAN where the purpose is to generate dimensioned floorplans for a given graph. It can be found in the literature that the most of the work is restricted to planar

bi-connected triangulated graph, i.e., the 1-connected graph and non-triangulated graphs were neglected which are quite crucial for representing some interesting features of architectural layouts. For example, non-triangulated graphs directly shows the requirement of corridors while 1-connected graph represents different blocks that are connected through a cut-vertex.

Furthermore, GPLAN can also be regarded as a tool for regenerating existing floorplans by considering the dual graph of existing floorplan. For example, in Figure 11, Villa Trissino has been regenerated using GPLAN.

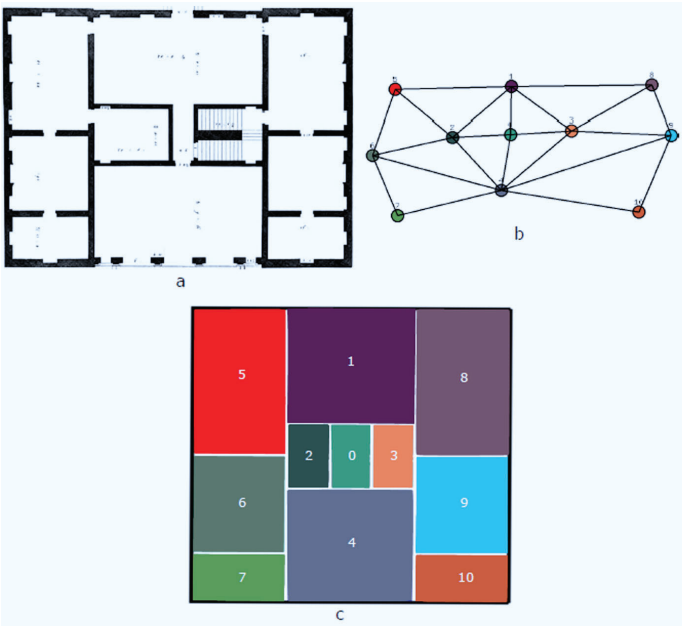

Figure 11. Regenerating Villa Trissino.

At this stage, many important components are not covered by GPLAN, few of them are circulations, boundary constraints, daylight constraints etc., which we are planning to cover in near future. Also, we agree that the proposed designs at this stage may not be architecturally acceptable and therefore we are thinking of introducing data-driven approaches (Hu et al. 2020) to GPLAN so that GPLAN provides multiple initial layouts to designers which can be further modified.

References

Baybars, I. and Eastman, C.: 1980, Enumerating architectural arrangements by generating their underlying graphs, *Environment and Planning B*, **7**, 289-310.

Eppstein, D., Mumford, E., Speckmann, B. and Verbeek, K.: 2012, Area-universal and constrained rectangular layouts, *SIAM Journal on Computing*, **41**(3), 537-564.

Gilleard, J.: 1978, Layout - a hierarchical computer model for the production of architecturalfloor plans, *Environment and Planning B*, **5**, 233-241.

Hu, R., Huang, Z., Tang, Y., Matias, O., Kaick, V., Zhang, H. and Huang, H.: 2020, Graph2Plan:

learning floorplan generation from layout graphs, *ACM Transactions on Graphics*, **39**(4), 1-14.
Jokar, M.R.A. and Sangchooli, A.S.: 2011, Constructing a block layout by face area, *The International Journal of Advanced Manufacturing Technology*, **54**(5-8), 801-809.
Levin, P.H.: 1964, Use of graphs to decide the optimum layout of buildings, *The Architects' Journal*, **7**, 809-815.
Liao, C.C., Lu, H.I. and Yen, H.C.: 2003, Compact floor-planning via orderly spanning trees, *Journal of Algorithms*, **48**(2), 441-451.
Lynes, J.A.: 1977, Windows and floor plans, *Environment and Planning B*, **4**, 51-55.
Mitchell, W.J., Steadman, J.P. and Liggett, R.S.: 1976, Synthesis and optimization of small rectangular floor plans, *Environment and Planning B: Planning and Design*, **3**(1), 37-70.
Rinsma, I.: 1987, Nonexistence of a certain rectangular floorplan withspecified areas and adjacency, *Environment and Planning B*, **14**, 163-166.
Rinsma, I.: 1988, Rectangular and orthogonal floorplans with required room areas and tree adjacency, *Environment and Planning B: Planning and Design*, **15**(1), 111-118.
Rinsma, I., Giffin, J. and Robinson, D.: 1990, Orthogonal floorplans from maximal planar graphs, *Environment and Planning B: Planning and Design*, **17**(1), 57-71.
Roth, J., Hashimshony, R. and Wachman, A.: 1982, Turning a graph into a rectangular floor plan, *Building and Environment*, **17**(3), 163-173.
Shekhawat, K.: 2018, Enumerating generic rectangular floor plans, *Automation in Construction*, **92**, 151-165.
Steadman, P.: 1973, Graph theoretic representation of architectural arrangement, *Architectural Research and Teaching*, **2(3)**, 161-172.
Upasani, N., Shekhawat, K. and Sachdeva, G.: 2020, Automated generation of dimensioned rectangular floorplans, *Automation in Construction*, **113**, 103149.
Wang, X.Y., Yang, Y. and Zhang, K.: 2018, Customization and generation of floor plans based on graph transformations, *Automation in Construction*, **94**, 405-416.
Wang, X.Y. and Zhang, K.: 2020, Generating layout designs from high-level specifications, *Automation in Construction*, **119**, 1-12.
Yeap, K.H. and Sarrafzadeh, M.: 1993, Floor-planning by graph dualization: 2-concave rectilinear modules, *SIAM Journal on Computing*, **22**(3), 500-526.

DEEP-PERFORMANCE

Incorporating Deep Learning for Automating Building Performance Simulation in Generative Systems

SHERMEEN YOUSIF[1] and DANIEL BOLOJAN[2]
[1,2]*Florida Atlantic University*
[1,2]*{syousif|dbolojan}@fau.edu*

Abstract. In this study, we introduce a newly developed method called Deep-Performance, to enable automatic environmental performance simulation prediction without the need to perform simulations, by integrating deep learning strategies. The aim is to train neural networks on datasets with thousands of building design samples and their corresponding performance simulation. The trained model would offer performance prediction for design options emerging in generative protocols. The research is a work-in-progress within a broader project aimed at automating buildings' environmental performance evaluations of daylight analysis and energy simulation, using deep learning (DL) models. This paper focuses on the implementation of a supervised DL method for automating the retrieval of daylight analysis metrics, targeting successful daylight design and higher building enclosure efficiency. We have further improved a Pix2Pix model trained on 5 different datasets, each containing 6000 paired images of architectural floor plans and their daylight simulation metrics. In the inference phase, the model was able to accurately predict the daylight simulation for unseen sets of floor plans. For validation, two quantitative assessment metrics were followed to assess the predicted daylight performance against the daylight performance simulation. Both assessment metrics showed high accuracy levels.

Keywords. Deep Learning; Artificial Intelligence; Deep-Performance; Automating Building Performance Simulation; Generative Systems.

1. Introduction

In the last few decades, performance-driven generative design (PDGD) systems have assisted designers in achieving higher building environmental efficiency. Yet, despite their increasing applications, PDGD frameworks still present many challenges. One challenge is the required level of expertise and technical skills that architects and engineers are expected to possess (Touloupaki and Theodosiou, 2017). Architects are concerned with the environmental performance of their building designs yet are not necessarily familiar with the building performance

PROJECTIONS, Proceedings of the 26th International Conference of the Association for Computer-Aided Architectural Design Research in Asia (CAADRIA) 2021, Volume 1, 151-160.

simulation (BPS) and optimization methods required to achieve higher building performance. Overall, BPS is a dynamic multidisciplinary method requiring in-depth understanding and requires accuracy in performing the modeling tasks, with science and engineering expertise (Bazjanac, 2008). Such complexity can be related to the multiplicity of the inter-related variables required for the environmental simulation tasks (Nguyen et al., 2014). A second challenge is that BPS methods are still computationally expensive, particularly in generative protocols when thousands of design alternatives are explored. Importantly, a third issue is the designer-system interaction, which remains problematic in terms of the ease with which designers operate such frameworks[2] (Harding and Brandt-Olsen, 2018). Although research attempts to develop methods that integrate performance simulation seamlessly in generative protocols are conducted, e.g. (Schwartz et al., 2017), such work is still time and computationally expensive, and requires domain expertise to perform the simulation protocol. Ideally, it would be beneficial for designers to retrieve automatic real-time building performance evaluation for each design option generated in the design process. This becomes crucial in early design phases to inform decision-making that could highly impact the designs' environmental performance (Hemsath, 2013).

A potential solution to offer automated real-time performance simulation is to employ artificial intelligence (AI) strategies. For performative design aspects, since AI can process, learn, and synthesize data, it can assist designers in effective decision making by enabling prediction of environmental metrics of their designs (Spacemaker, 2020). This could be a game-changer in design research. Generative Adversarial Networks (GANs) are DL-based models that enable the machine to learn structures and semantics from observing input datasets (Goodfellow et al., 2016). One model of the GANs family is Pix2Pix, authored by Philip Isola (2016). The model is an image-to-image translation method, able to learn mapping from an input to an output image in an effective manner, synthesizing and reconstructing data in a conditional (supervised) approach (Isola et al., 2017). This work is part of a broader research project focused on developing a framework that incorporates DL models to tackle different building systems and predict building environmental performance evaluation. As an initial phase, this paper focuses on the use of a DL model to predict multiple daylight simulation metrics. As a supervised process, the Pix2Pix model facilitates accurate image-to-image translation and therefore provides real-time visual feedback without the need for additional operations to be performed on the analysis grid. This supports seamless integration of daylight prediction into generative systems. The model, provided with examples of building floor plans, will generate daylight predictions. We pursued developing a system we call "DeepPerformance" (DP), demonstrated in a fully working method that successfully offers real-time predictions of daylight simulations for designs produced within generative protocols. In the development phase of the DP system, the following protocol was required: (1) generative modeling and daylight simulation (2) deep learning model training, and (3) validation, as explained in greater details in the Research Methods section. In the application phase (user centered interaction) users will simply integrate the trained model into their generative protocol where the algorithmic package (of the DP system) will offer

automatic real-time daylight analysis for generated floor plan designs (Figure 1).

The research significance lies in the framework's ability to automate simulation tasks and to offer a designer-centered system that enables real-time feedback on design performance. It is targeted for a larger audience of lay-designers and architects with no domain expertise. Such a designer-centered approach will facilitate exploration while achieving higher efficiency in performance-driven generative systems, at a minimum computation and time expense. Our research contributes to the transition from simulation-based to prediction-based design performance methods. This approach of prediction models is also known as surrogate models, defined as models that imitate the behavior of simulation models as closely as possible while being less expensive computationally (Bamdad et al., 2020). We believe that the introduced system is capable of "augmenting" the designers' decision-making by offering a collaborative human-machine interaction to enhance the design process. Embedded here is our preference for an "open-loop" of back and forth feedback between the designer and the machine rather than the "closed-loop" of input-output frameworks. The paper is structured as follows. In the background section, an overview of related research is offered and discussed, in addition to describing the most important concepts and methods relevant to this work. The methods section describes in detail the research methodology, the overall framework, a test-case application, and validation procedures. Next, an overall discussion is offered, and in the last section, conclusions and future work are highlighted.

2. Background

Despite the fact that performance-driven generative systems were introduced in the last two decades, and although many methods have been developed for simulation and performance optimization, the applications of those methods are still less outspread in the architectural domain. While the introduction of AI in performance-driven frameworks is still experimental, the approach has the potential to leverage and more importantly enact designers' successful exploration of the design space while achieving higher performance. When it comes to seamless real-time retrieval of environmental performance, computational and time expense issues still arise in PDGD (Rahmani Asl et al., 2017). Since the introduction of GANs into architectural design research occurred (5 years ago), employing AI strategies to performative aspects of building systems is still limited. Relevant methods to this project have been found in projects such as the Energy Model Machine (EMM) that targets automating energy consumption (Rahmani Asl et al., 2017), and the project of "Wind-flow Prediction through Machine Learning", developed by the research team at the Austrian Institute of Technology (Galanos et al., 2019). A more recent work is the Space Allocation Techniques developed by Nirvik Saha as a design optimization toolset (DOTS) for Grasshopper (Saha, 2020). The tool utilizes reinforcement learning methods to automate space allocation problems at both urban and building scales. AI's integration into fabrication has been also investigated in the work of Thomsen et. al. where the authors sought for using ML strategies to adapt fabrication data in real-time within the fabrication processes (Thomsen et al., 2020). Research

attempts to automate daylight analysis are still experimental, such as the work of (Shaghaghian and Yan, 2019) where Convolutional Neural Network (CNN)s were used for shape classification and Auxiliary Classifier GAN (AC-GAN) was implemented for generating light and shadow patterns of windows and walls based on daylight performance. In Ngarambe et al. 's work (2020), a comparative analysis of 5 machine learning (ML) algorithms was pursued to explore potentials of ML to perform daylight illuminance studies. Another study that attempts to investigate predicting illuminance values in office buildings using artificial neural networks is the study of (Kazanasmaz et al., 2009). All of those attempts represent preliminary experimentation and do not offer yet a fully working method designed for generative systems.

Our argument of augmented seamless human-machine collaboration is supported by multiple references. In cognitive science, Margaret Boden reinforces the concept of using artificial intelligence to "augment" the user's creativity (Boden, 2004, Boden, 2007). In her work, Boden discusses both AI and human creativities, addressing that AI is capable of producing combinational creativity and possibly exploratory creativity-two of her three models of creativity. Computers "can come up with new ideas and help people do so" (Boden, 2007, p. 12). Also, the idea of human-machine collaboration has been argued for by Garry Kasparov who describes it as "Human-Plus-Machine" (Kasparov, 2017). For him, machines perform a supplementary task, supporting cognitive functions such as memory, and we can add this powerful machine capacity to process otherwise overwhelming datasets into a human-plus-machine mode. This human-plus-machine mode of collaboration benefits us and makes us stronger. We can "...use information technology as a tool to enhance human decisions instead of replacing them with autonomous AI systems" (Kasparov, 2017, p. 215). Given this background information, the issue of developing a method with real-time feedback on daylighting design and offering a designer-centered framework remains unsolved, which was the motivation of conducting this research. Next, we describe the process of developing our Deep-Performance system, in addition to offering definitions and explanations of the important related methods that we implemented.

3. Research Methods

The research methodology involves experimentation with incorporating DL methods into a PDGD framework, prototyping the proposed system, application and testing, and verification methods. After thorough investigation and experimentation with DL methods, in this study, we demonstrate our "Deep-Performance" system in a fully working prototype. In the development phase (authors developing the prototype), the prototypical workflow included processes of (1) creating a performance-driven parametric generative design model with daylight simulation, (2) developing and training the DL model, and (3) performing validation studies.

In the application phase (users of DP), the system is defined as a two-step workflow, (1) a generative process (e.g. generation of floor plan designs) and (2) a real-time simulation prediction model, allowing for daylight evaluation of

hundreds/thousands of design options. The full diagram (Figure 1) demonstrates the development and application phases of the method. The framework prototype consists of a series of novel generative and prediction tools, organized as a Grasshopper add-on, soon to be released. To apply the Deep-Performance system and test its functionalities, the following test-case experiment was carried out.

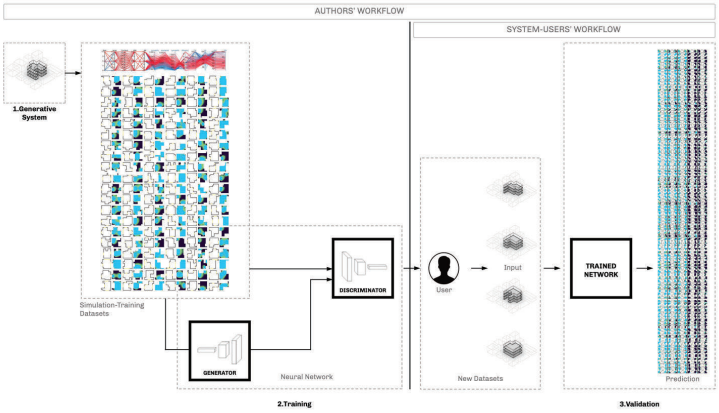

Figure 1. The workflow of the proposed DP framework, real-time daylight performance evaluation predictions using deep learning.

3.1. TEST-CASE APPLICATION

For the framework development, various interfaces and methods were leveraged for respective stages of dataset generation, preparation, training, and validation of the models. Rhino/Grasshopper® was used to create a generative model that produces floor plans and windows configurations. Ladybug® and Honeybee® add-ons, developed by (Roudsari, 2014), were used to perform 5 different types of daylight metric simulations. PyTorch® and Tensorflow® deep learning packages were used within the PyCharm environment for data preparation, augmentation, and for the development/training of the neural networks.

3.1.1. Generative Modelling and Daylight Simulation

In Experiment 1 (orthogonal layouts), a daylight performance simulation experiment was integrated into a generative system that produced 3000 orthogonal floor plan design options. Every generated design option was evaluated against 5 annual daylight simulation metrics of spatial Daylight Autonomy (sDA), Direct Daylight Access (DLA), and Useful Daylight Illuminance ranges of UDLI(0-100), UDLI(100-2000), and UDLI(2000_more) in lux. This has led to a total of 3,000 pairs of floor plan-daylight simulation images for each daylight simulation metric, to be used as a training dataset. We ran the simulation with a grid resolution of 0.2m and at 0.76m a working plane height. A labeled dataset was generated by defining 3 main classes/labels: light gray color representing the floor area class,

black label for the wall class and yellow color for the window class, as depicted in both Figures 2 and 3. While the yellow color saturation defines the window height (in this test-case, we used one height, ceiling-to-floor), different intensities of gray were used to define functional types e.g. office, retail etc. In this experiment, the floor plan was considered an open layout for an office building program. We followed a common convention in daylight simulation studies to analyze office spaces as open floor plans where partitioning walls are not included (Reinhart, 2002). Curating the datasets, we divided each dataset of the 5 metrics into 90% training and 10% testing sets, thus we used 2700 training and 300 testing for each.

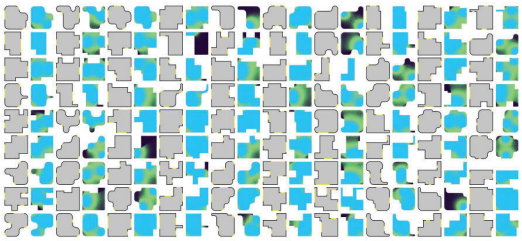

Figure 2. A sample of the training datasets in pairs of 90 paired images representing floor plans and one of their daylight simulations (in this case the spatial Daylight Autonomy).

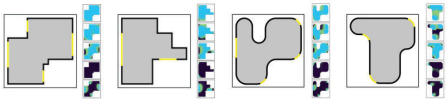

Figure 3. A sample of 4 design options evaluated against 5 daylight simulation metrics of sDA, DLA, UDLI(0-100), UDLI(100-2000) and UDLI(2000_more).

3.1.2. DL Model Training

The network architecture is based on the Pix2Pix model that allows for supervised Image-to-Image translation (Isola et al. 2017), yet we made further improvements to the networks' filters in order to create feature-maps that summarize well the detected features in the input (Figure 4). All experiments were trained for a total of 400 epochs. Adam optimizer was used with an initial learning rate of 0.0005 for the first half of the training and was reduced linearly to a rate of 0.0000 over the remaining iterations. The optimizer momentum term was set to 0.65 for both generator and discriminator networks. The input and output resolution was set to 1024x1024 pixels; due to GPU training device memory constraints we used a batch size of 40 and we normalized the input layer with batch normalization (Ioffe and Szegedy, 2015). The discriminator network used a basic network architecture 70x70 PatchGAN, and the generator network uses a RESNET 9blocks network architecture. To reduce the model's oscillation, we used a pool size of 50 (Shrivastava et al., 2017). Each network's layer is followed by instance

normalization and a ReLU layer.

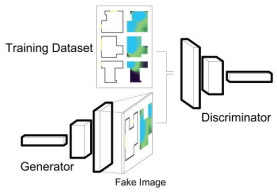

Figure 4. Pix2Pix Architecture - Paired dataset.

3.1.3. Results and Validation

In the testing phase, the results confirmed the expected performance of the DL algorithm to successfully predict daylight simulation when new floor plan designs are introduced in the testing process. The accuracy of the predicted results of the surrogate model has been assessed against the actual (real) simulation results of Honeybee. In one of the assessment experiments, we tested the accuracy of the predicted Direct Daylight Access (DLA) values against the actual DLA simulation. Presented with a new batch (unseen by the trained model) of 50 floor plan options, the network predicted the DLA metric, in the testing phase, with an average prediction accuracy of 90%, as shown in Figure 5. Compared to the Honeybee daylight simulation results that took 3 minutes for each simulation run, our surrogate model was able to offer a comparable accuracy of 90%, taking less than 0.3 second for each prediction. In a generative design process, when exploring 6000 design options, it would take 3*6000=18000 minutes, equivalent to 12.5 days to retrieve daylight simulation results using Honeybee or Diva, in contrast to 0.3*6000=1800 seconds, equivalent to 30 minutes using the surrogate model. Quantifying the accuracy comparison between the surrogate model and the simulation model, we plotted the two results to display where the accuracy of the two results converges. Figure 5 exemplifies this accuracy comparison of the DP-predicted DLA values (represented in light gray lines) and the Honeybee simulation DLA values (represented in black line). When the curves converge, this means the accuracy of the DP-prediction is at its highest value, and the margin of difference is within 15%. Additional evaluation methods were used such as, the SSIM and Perceptual Similarity, explained in the following subsections.

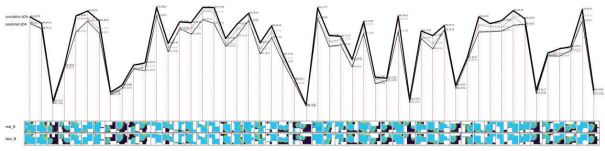

Figure 5. Prediction results - comparison between daylight simulation DLA values and DP-Prediction DLA values.

- SSIM and Perceptual Similarity

Following Goodfellow et al. 's approach which emphasizes human judgment (2016), the first validation study we conducted was the Structural Similarity Index Measure or SSIM (Wang et al. 2004). SSIM is a method for image quality assessment that involves extracting structural information and measuring the degradation of the structural data for the images under analysis. For this procedure, the predicted daylight simulation results were evaluated against the Honeybee simulation, and the results show an average similarity value of 0.94 with an overall similarity value range of 0.84 - 0.96.Perceptual Similarity (PS) is another method we used that was developed to evaluate the effectiveness of deep learning-produced images similar to the way humans perform perceptual judgements (Zhang et al., 2018). For this PS assessment method, the lowest value retrieved was 0.89 and the highest value was 0.98. Figure 6 illustrates a sample of eight cases of the testing process assessed by the SSIM and PS measure. The two rows (with two pairs in each) depict the DP-predicted (synthetic) and Honeybee simulation (real) images of two daylight metrics, with the lowest SSIM/PS values to the left and the highest SSIM/PS to the right (Figure 6).

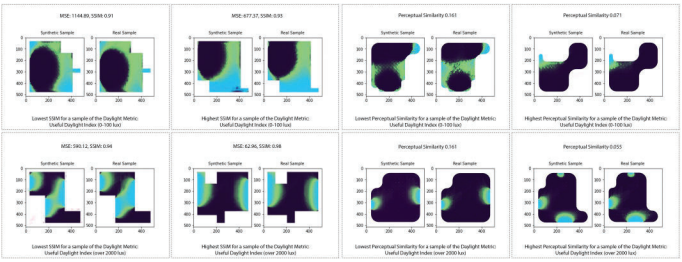

Figure 6. Eight cases of the testing dataset of synthetic-real pairs assessed by the SSIM and PS Measure for UDLI(0-100) and UDLI(2000_more).

4. Discussion of Test-Case Experiment

In the experiment, the proposed DP framework was demonstrated in a fully working prototype, applied to a generative model with daylight simulation data, and a modified Pix2Pix model was trained with the design-simulation datasets to predict daylight simulation results. As presented, our DP framework is capable of offering high accuracy levels for daylighting predictions. More importantly, this test-case application has shown promising results towards the automation of other environmental performance objectives as well. Such a surrogate model offers automatic prediction, which becomes beneficial in early design phases to inform decision-making. The DP prediction model coupled with design generation is depicted in Figure 7 where 3 design models are shown in the upper part, and their two copies in the lower part. For each floor plan design, a predicted daylight mesh is represented. In inference phase, the DP framework will enable designers to explore a manifold of design options, while evaluating in real-time design performance. The significance of retrieving predicted daylight evaluation lies in its impact on morphology and associated design decisions.

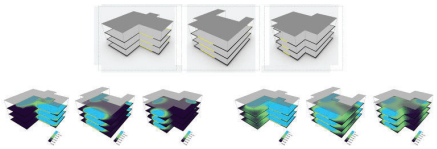

Figure 7. Three building design options and automatic prediction presented in the daylight simulation meshes for each floor plan.

5. Conclusions and Future Work

In our project, we aim for AI applications that encompass the complexity of building systems. Such integration of AI in architecture research can be targeted at developing upon the paradigm shift discourse of system thinking as introduced by Christopher Alexander (Menges and Ahlquist, 2011, p. 11). Presented in this paper is a method to incorporate a deep learning model to facilitate and enhance generative design protocols. This was accomplished by offering real-time predictions of daylight performance. The results provide evidence of the potential to implement deep learning methods to automate other building performance simulation tasks. In-progress is our experimentation to automate the whole building energy simulation by integrating DL networks into generative protocols. The project requires thorough investigation to tackle the complexity of the inter-related parameters of thermal modeling. As a future work, the surrogate model will enable designers to explore a plethora of design options in an articulated design space. Additional AI models will be required to sort out successful design options with higher performance to facilitate the overwhelming task of sorting through thousands of designs. Additional improvement will be targeted at creating a designer-friendly interface that will be assessed by lay architects in empirical procedures, in order to provide feedback on limitations of the DP framework. Future work also includes developing a cloud-based interface for the Deep-Performance framework.

References

Bamdad, K., Cholette, M.E. and Bell, J.: 2020, Building energy optimization using surrogate model and active sampling, *Journal of Building Performance Simulation*, **13**(6), 760-776.

Bazjanac, V.: 2008, IFC BIM-Based Methodology for Semi-Automated Building Energy Performance Simulation, *ICIT 2008*.

Boden, M.A.: 2004, *The creative mind: Myths and mechanisms*, Psychology Press.

Boden, M.A.: 2007, Creativity in a nutshell, *Think*, **5**(15), 83-96.

Galanos, T., Chronis, A. and Vesely, O.: 2019, "Wind Flow Prediction Through Machine Learning" . Available from <http://cities.ait.ac.at/site/index.php/2019/05/29/wind-flow-prediction-through-machine-learning/>.

Goodfellow, I., Bengio, Y. and Courville, A.: 2016, *Deep learning*, MIT press.

Goodfellow, I., Pouget-Abadie, J., Mirza, M., Xu, B., Warde-Farley, D., Ozair, S., Courville, A. and Bengio, Y.: 2014, Generative adversarial nets, *Advances in neural information processing systems*, 2672-2680.

Harding, J. and Brandt-Olsen, C.: 2018, Biomorpher: Interactive evolution for parametric design, *nternational Journal of Architectural Computing*, **16.2**, 144-163.

Hemsath, T.L.: 2013, Conceptual energy modeling for architecture, planning and design: Impact of using building performance simulation in early design stages, *13th Conference of International Building Performance Simulation Association*, 376-384.

Ioffe, S. and Szegedy, C.: 2015, Batch normalization: Accelerating deep network training by reducing internal covariate shift, *arXiv preprint arXiv:1502.03167*, **CiteSeerX**, 1-11.

Isola, P., Zhu, J.Y., Zhou, T. and Efros, A.A.: 2017, Image-to-Image Translation with Conditional Adversarial Networks, *IEEE Conference on Computer Vision and Pattern Recognition (CVPR)*, 5967-5976.

Kasparov, G.: 2017, *Deep thinking: where machine intelligence ends and human creativity begins*, Hachette UK.

Kazanasmaz, T., Günaydin, M. and Binol, S.: 2009, Artificial neural networks to predict daylight illuminance in office buildings, *Building and Environment*, **44**(8), 1751-1757.

Menges, A. and Ahlquist, S.: 2011, *Computational design thinking: computation design thinking*, John Wiley & Sons.

Ngarambe, J., Irakoze, A., Yun, G.Y. and Kim, G.: 2020, Comparative Performance of Machine Learning Algorithms in the Prediction of Indoor Daylight Illuminances, *Sustainability*, **12**(11), 4471.

Nguyen, A.T., Reiter, S. and Rigo, P.: 2014, A review on simulation-based optimization methods applied to building performance analysis, *Applied Energy*, **113**, 1043-1058.

Rahmani-Asl, M., Das, S., Tsai, B., Molloy, I. and Hauck, A.: 2017, Energy Model Machine (EMM)-Instant Building Energy Prediction using Machine Learning, *eCAADe*, **2017**, 277-286.

Reinhart, C.: 2002, Effects of interior design on the daylight availability in open plan offices, *Proceedings of the 2002 American Council for an Energy Efficient Economy (ACEEE) Summer Study on Energy Efficiency in Buildings*, **3**, 309-322.

Roudsari, M.: 2014, "Ladybug Tools" . Available from <https://www.ladybug.tools/about.html>.

Saha, N.: 2020, "DOTS: design optimization tool set" . Available from <https://github.com/nirvik00/DOTS>.

Schwartz, Y., Raslan, R., Korolija, I. and Mumovic, D.: 2017, Integrated Building Performance Optimization: Coupling Parametric Thermal Simulation Optimization and Generative Spatial Design Programming, *15th International Building Performance Simulation Association Conference, San Francisco, CA, Aug*, 7-9.

Shaghaghian, Z. and Yan, W.: 2019, Application of Deep Learning in Generating Desired Design Options: Experiments Using Synthetic Training Dataset, *arXiv preprint arXiv:2001.05849*, **2019**, 1-10.

Shrivastava, A., Pfister, T., Tuzel, O., Susskind, J., Wang, W. and Webb, R.: 2017, Learning from simulated and unsupervised images through adversarial training, *Proceedings of the IEEE conference on computer vision and pattern recognition*, 2107-2116.

Spacemaker, initials missing: 2020, "Early stage planning Re-imagined" . Available from <https://www.spacemakerai.com/>.

Thomsen, M., Nicholas, P., Tamke, M., Gatz, S., Sinke, Y. and Rossi, G.: 2020, Towards machine learning for architectural fabrication in the age of industry 4.0, *International Journal of Architectural Computing*, **2020**, 1478077120948000.

Touloupaki, E. and Theodosiou, T.: 2017, Performance simulation integrated in parametric 3d modeling as a method for early stage design optimization—a review, *Energies*, **10**(5), 637.

Wang, Z., Bovik, A.C., Sheikh, H.R. and Simoncelli, E.P.: 2004, Image quality assessment: from error visibility to structural similarity, *IEEE transactions on image processing*, **13**(4), 600-612.

Zhang, R., Isola, P., Efros, A.A., Shechtman, E. and Wang, O.: 2018, The unreasonable effectiveness of deep features as a perceptual metric, *Proceedings of the IEEE conference on computer vision and pattern recognition*, 586-595.

HIERARCHICAL (MULTI-LABEL) ARCHITECTURAL IMAGE RECOGNITION AND CLASSIFICATION

JIELIN CHEN[1], RUDI STOUFFS[2] and FILIP BILJECKI[3]
[1,2,3]*Department of Architecture, National University of Singapore*
[1]*chen.jielin@u.nus.edu* [2,3]*{stouffs|filip}@nus.edu.sg*

Abstract. The task of architectural image recognition for both architectural functionality and style remains an open challenge. In addition, the paucity of well-organized, large-scale architectural image datasets with specific consideration for the domain of architectural design research has hindered the exploration of these challenging tasks. Drawing upon images from the professional architectural website Archdaily®, and leveraging state-of-the-art deep-learning-based classification models, we explore a hierarchical multi-label classification model as a potential baseline for the task of architectural image classification. The resulting model showcases the potential for innovative architectural discipline-related analyses and demonstrates some heuristic insights for visual feature extraction pertaining to both architectural functionality and architectural style.

Keywords. Image recognition; hierarchical classification; multi-label classification; architectural functionality; style.

1. Introduction

The emerging awareness, and pertinent discussion, regarding the application of machine learning techniques is permeating the architectural discipline of both its methodology and epistemology. Architectural image classification models with high performance show potential as informative tools for a series of architecture-related tasks. For example, classifying the functionality of individual buildings can be useful for urban utility planning and population density mapping at a finer level of urban intrinsic scale (Kang et al. 2018; Hoffmann et al. 2019); identifying visual features of building instances can assist the investigation of the impact of built environment characteristics (Nguyen et al. 2018; von Platten et al. 2020); and recognition of emerging architectural styles can provide novel insights into the trend of modern architectural design practice. Nevertheless, architectural image classification can deviate from conventional image recognition tasks due to the convoluted inter-class relationships between different architectural categories and styles (Xu et al. 2014), as there is no standard criterion regarding the definition of architectural types and styles concerning visual features, and some architectural types and styles can be interdependent and the corresponding latent features may not be identically distributed. Hitherto, only limited efforts have been made to address the task of individual building instance classification

PROJECTIONS, Proceedings of the 26th International Conference of the Association for Computer-Aided Architectural Design Research in Asia (CAADRIA) 2021, Volume 1, 161-170.

(Kang et al. 2018). Meanwhile, although existing architectural style-focused datasets can be adapted to some interesting machine learning-based applications such as style transformation, the predefined styles involved in existing datasets are mostly of historical significance and might have limited application potentials in real-world design scenarios. Although it would be worthwhile to explore the variety of modern architectural styles that are somehow ill-defined in current architectural literature, few previous studies have explored the task of architectural style prediction with a perspective of modern architectural design practice.

Thus, the task of architectural image recognition for both architectural functionality and style remains an open challenge. However, the paucity of well-organized, large-scale architectural image datasets has hindered the exploration of these challenging tasks. Even though there are generic data banks available with tagged images, it can still be tricky to find specific datasets of architectural images for various purposes and the quality of images is not guaranteed with respect to architectural design. Hence, there is a necessity for new large-scale architectural image datasets with hierarchical labelling and different levels and details of annotations, which could be useful for the training of deep neural networks or other machine learning techniques for architectural design research. Shalunts et al. (2011) have collected a small dataset with 400 building facade images labelled by architectural styles for the classification task of cultural heritage buildings. Llamas et al. (2017) have compiled a publicly available dataset with more than 10,000 images sorted in 10 types for classifying architectural elements of interest in imagery of heritage buildings. Xu et al. (2014) have extracted and fine-tuned an architectural style dataset from Wikimedia with 25 architectural style classes tailored for architectural style classification, and each class has images ranging from 60 to 300 with a total number of roughly 5,000. Recently, Kang et al. (2018) have built a dataset to facilitate the training and evaluation of building instance classifiers using street view images, while using geographic information retrieved from online map services for labelling. The dataset has a training set of size 17,600 and a test set of 2,058. However, the dataset only possesses 8 classes, and the environmental context of the images retrieved from street view websites is somehow homogeneous, which has made the image dataset limited pertaining to the level of diversity.

We compiled an architectural image database called AIDA, short for Annotated Image Database of Architecture, composed of building imagery with high-diversity and high-coverage for general-purpose deep learning-based model training. The new dataset provides an enhanced platform for the evaluation of the performance of existing deep learning-based models, as well as encouraging the creation of new ones. We also offer a series of multi-label architectural image classifiers with integrated classification labels, including scene classes (indoor and outdoor-street-level) and architectural functionality categories. The obtained architectural image classifier showcases the potential for many innovative architectural discipline-related analyses. Also, it provides some heuristic insights with respect to visual feature extraction in the context of architectural design research.

2. Construction of AIDA

To ensure the quality of imagery concerning architectural design and satisfy the requirement of a broad spectrum of coverage, images are retrieved from professional architectural website Archdaily®, an architecture projects broadcasting website with probably the largest online repository of architecture projects worldwide. The crawled images, one image per architectural project, have been manually filtered to meet specific requirements for training tasks for architectural design research: the photos need to be real-world photography and need to be focused on the architecture. Unqualified or irrelevant images have been discarded. Images retrieved from Archdaily® have been annotated with ground truth category labels acquired from the website. To ameliorate class imbalance, architectural categories with too few or too many images have been omitted to compose a condensed image database. Images are further categorized into two scene classes: outdoor-street-level and indoor, with 25 architectural categories each (image samples are shown in Figure 1). The number of images in each architectural category of each scene class varies from 20 to 1,400, and the total number of images in AIDA is 14,659 (Figure 2). Noticeably, the underlying inter-relationships between different architectural categories might distinguish the newly collected database from conventional scene classification datasets.

Figure 1. Image samples from two scene classes, outdoor-street-view and indoor, and various architectural categories of AIDA (source: https://www.archdaily.com/).

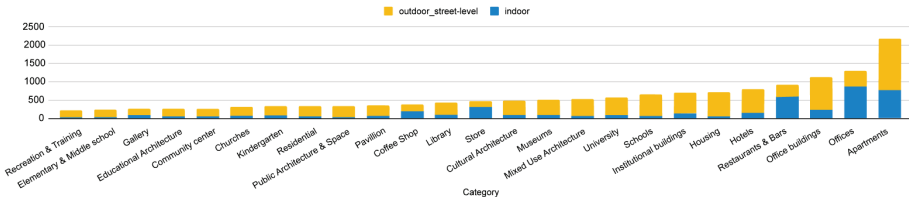

Figure 2. Number of images per category in AIDA, sorted in ascending order; AIDA contains 14,659 images from 25 architecture categories.

3. AIDA-CNNs: hierarchical (multi-label) architectural image classification

Compared with flat classification tasks, hierarchical classification can be a more efficient approach to organize the enormous amount of information involved and can be cast to more real-world applications; classes are pre-established as different levels of hierarchy, either a tree or a directed acyclic graph (DAG) structured class taxonomy (Silla & Freitas 2011). The AIDA database has a DAG class taxonomy as each child class—architectural category—can be directed back to more than one parent class—scene class. Hence, the hierarchical classifier might be more suitable for the AIDA database compared with flat classifiers.

Most approaches in the context of hierarchical classification can be regarded as multi-label classification and categorized into local or global classifiers. Local classifiers explore the class structure in a top-down manner with a series of classifiers; global classifiers employ a single classifier dealing with the entire class structure (Silla & Freitas 2011). The local classifier per parent node (top-down) approach adopts one multi-label classifier for each parent class in the hierarchy to distinguish between its child classes or, alternatively, a multi-label classifier for each hierarchical level. Instead, the global classifier approach takes into account the dependencies between classes in a more straightforward way and a single yet relatively complex classification model is constructed, treating the class hierarchy as a whole for a single run of the classification algorithm (Freitas & Carvalho 2007). Compared with the modularity for local training of the classifier, global classifiers have the advantage of learning a global model for all the classes in a single run yet adding complexity to the adopted model.

To fuse the scene classification and architectural category classification as an integrated task, we adopt a global classifier in the context of hierarchical classification as the basic, multi-label classification framework. Figure 3 illustrates the proposed hierarchical image classification model framework: an integrated CNN model as the global classifier takes in the labeled architectural images and produces predicted labels of both the scene classes and the architectural categories, which are then separately interpreted as two hierarchical classifiers.

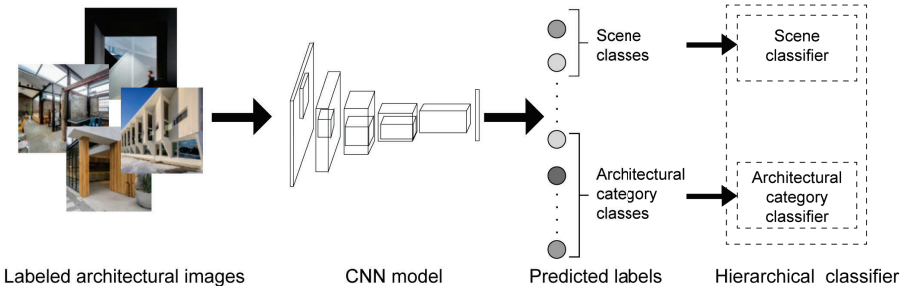

Figure 3. The proposed hierarchical image classification model framework.

3.1. TRAINING

We chose two state-of-the-art CNN architectures for image classification tasks, namely ResNeXt (Xie et al. 2017) and DenseNet (Huang et al. 2017), to construct the baseline CNN models. While adopting the basic model structure of ResNeXt and DenseNet, the output layers of both models are modified using a sigmoid function for the output layer to suit the multi-label classification task. Such modification also enables the analysis of inter-relationships of architectural classes probabilistically and offers a latently rational explanation of the gradual transition and mixture of visual architectural features with soft probabilistic assignments.

The image database is still not sufficiently large to properly train the selected models with over millions of parameters from scratch; at least an order of magnitude more instances relative to the trainable parameters of the model would be sufficient (Google Developers, n.d.). Therefore, the convolutional layers of the networks have been trained using the transfer learning approach. Fine-tuning a pretrained CNN for new training tasks with novel datasets has been proven to be efficient, as local features like edges and corners generated by the bottom layers of the neural network are usually similar for different types of imagery. In contrast, the high-level features extracted by the top layers are task-dependent. For the model training, 11,730 images from the dataset have been randomly selected for training and 2,929 for testing, while 20% of images from the training samples have been selected as validation data to monitor the training status of the networks. For the experimental implementation, we chose the corresponding network version of the ResNeXt and DenseNet models with relatively better performance based on the evaluation provided by PyTorch (Paszke et al. 2019), respectively, ResNeXt-101 and DenseNet-161, where the numbers 101 and 161 in the nomenclature denote the depth of the specific version of the network models.

Both networks are initialized with corresponding model checkpoints provided by PyTorch, which were pre-trained on the ImageNet database (Deng et al. 2009), and the output layers were initialized in a random manner by adopting a uniform distribution. The training adopted a batch size of 32 and used the adaptive moment estimation algorithm (Kingma & Ba 2014) with a learning rate of $\alpha = 10^{-3}$, exponential decay rate for the first moment estimates $\beta_1 = 0.9$, exponential decay rate for the second-moment estimates $\beta_2 = 0.999$, and $\epsilon = 10^{-8}$ for training. The binary cross-entropy loss function was used and a drop out rate of 20% was adopted for the neurons of fully connected layers. Data augmentation was used for the training data with the following settings: (a) random crop size of 224×224 pixels with resize range of 0.8-1.0 of initial input size 256×256 pixels; (b) random rotation with a range from -15 to 15 degrees; (c) random horizontal flip with a probability of 50%. All training and testing were performed with PyTorch (Paszke et al. 2019) on 2 Nvidia Tesla V100 32GB GPUs.

Three classification accuracy metrics have been calculated using scikit-learn (Pedregosa et al. 2011), including weighted precision, weighted recall and weighted F1 score, which are typically used metrics for multi-label targets. The nomenclature "weighted" indicates that the averaging performed on the calculated metric is weighted by the number of true instances of each label, which accounts

for the impact of latent label imbalance. Precision p = *true positive* / (*true positive* + *false positive*) is the ratio of true positive predictions to the total predicted positive instances. Recall r = *true positive* / (*true positive* + *false negative*) is the ratio of true positive predictions to all instances in the corresponding class. F1 score $F_1 = 2(rp)/(r+p)$ is the weighted average of precision and recall, and considers both false positive and false negative instances, which can be useful if the class distribution is uneven. As can be seen from the calculated accuracy metrics in Figure 4, both networks have fluctuations for the weighted F1 score at the early stage, plausibly caused by the uneven distribution among different classes. Meanwhile, DenseNet-161 has outperformed ResNeXt-101 based on the three accuracy metrics (weighted precision, weighted recall and weighted F1 score) calculated over different training epochs.

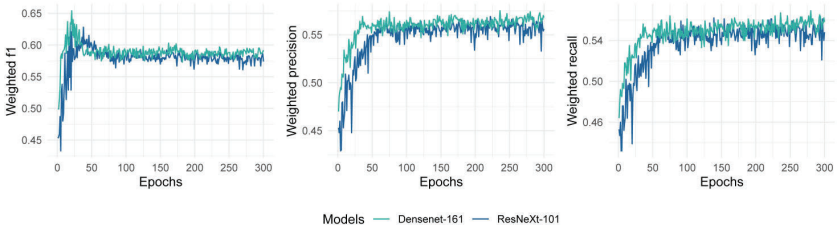

Figure 4. DenseNet-161 obtains slightly higher accuracy compared to ResNeXt-101.

3.2. TESTING

To testify the model performance on the two hierarchical levels, we further evaluate the trained classifiers on the scene classes and architectural categories separately using the test set. Figure 5 illustrates the corresponding overall accuracy and accuracy of each scene class at different training epochs of ResNeXt-101 and DenseNet-161. DenseNet-161 achieves slightly better performance on the scene classification task with 96% accuracy compared to ResNeXt-101 with 95% accuracy.

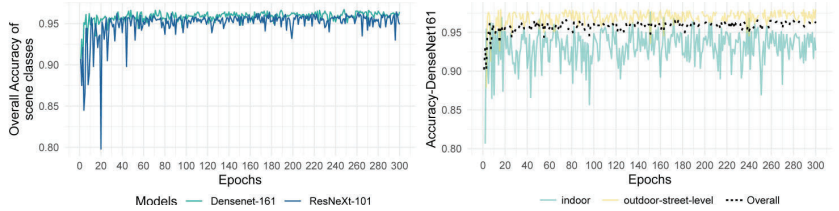

Figure 5. Comparison of the overall accuracy of the scene classes between ResNeXt-101 and DenseNet-161(left) and accuracy of each scene class of DenseNet-161 (right).

A comparison of the overall accuracy of the architectural categories between ResNeXt-101 and DenseNet-161 (Figure 6 left) shows that DenseNet-161 also slightly outperforms ResNeXt-101 on the architectural image classification task.

It is worth noting that the overall accuracy of architectural category classification fluctuates at early epochs, plausibly caused by the divergent accuracy value among different architectural categories during initial epochs (Figure 6 right). The discrepancy of accuracy between different architectural categories gradually decreases as the number of epochs increases, which might also contribute to the fluctuation phenomenon of the weighted F1 score over all target classes at the early stage.

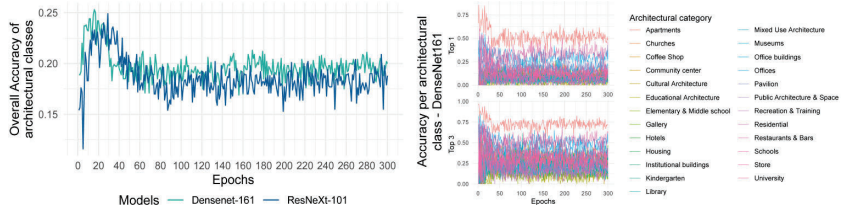

Figure 6. Comparison of the overall accuracy of architectural categories between ResNeXt-101 and DenseNet-161 (left) and top-1, top-3 accuracy per category of DenseNet-161 (right).

To further examine this phenomenon, the mean and standard deviation of the accuracy per architectural category are calculated for both ResNeXt-101 and DenseNet-161 (Figure 7). The mean accuracy per architectural category increases while the standard deviation decreases with the increase of the number of epochs as anticipated. DenseNet-161 has a higher mean and lower standard deviation of accuracy per architectural category during the early training epochs, while the difference gradually eliminates as the number of epochs increases.

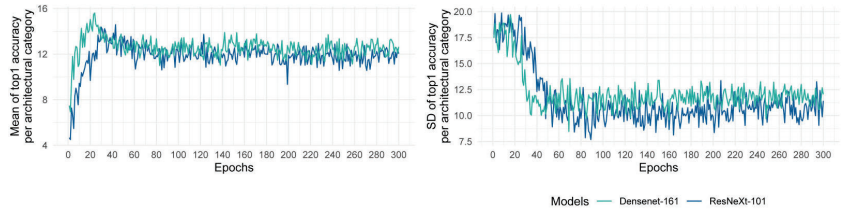

Figure 7. Comparison of the mean (left) and standard deviation (right) of top-1 accuracy per architectural category between ResNeXt-101 and DenseNet-161.

3.3. EVALUATION

Table 1 uses t-SNE (Van der Maaten & Hinton 2008) to visualize the high-dimensional space of the image classification manifolds by giving each predicted datapoint a location in a two-dimensional map. We demonstrate the predicted class projection via t-SNE with DenseNet-161 trained at different epochs using the full dataset and the test set respectively: the separation between different classes becomes gradually more pronounced as the number of epochs increases. The separation between the two scene classes is already distinguishable after 30 epochs, while for the architectural categories, the situation is more convoluted.

Table 1. Predicted class projection via t-SNE with DenseNet161-based hierarchical multi-label classifier trained at different epochs using the full dataset and the test set of AIDA.

	Epoch 10	*Epoch 30*	*Epoch 50*	*Epoch 70*	*Epoch 90*
Scene class	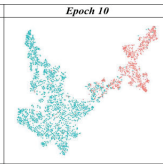	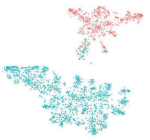	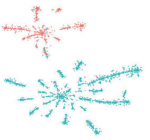	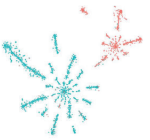	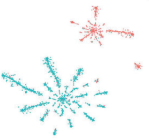
Architectural class			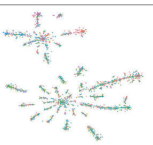	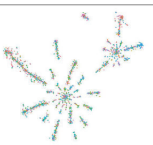	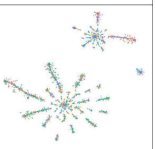

To examine the disentanglement between architectural categories, the normalized confusion matrix is plotted based on the AIDA test set evaluated with DenseNet-161 trained at epoch 70 (Figure 8). Some pairs of architectural classes have entangled relationships with each other, indicating the complex inter-class relationships between different architectural categories, as mentioned in the introduction.

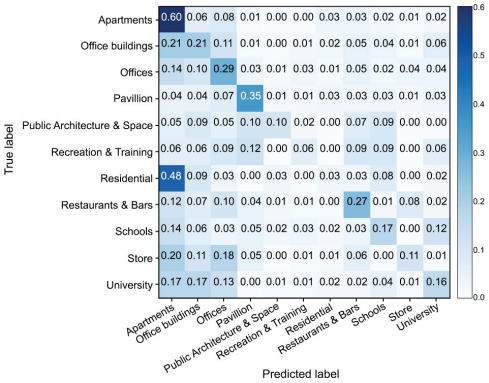

Figure 8. Normalized confusion matrix for architectural category prediction with DenseNet-161 trained until epoch 70 (showing only 11 selected categories), demonstrating the convoluted inter-class relationships between different architectural categories.

To further examine the latent stylistic relationship between architectural categories, we projected the prediction of each image of the "Apartments" category in the test dataset with DenseNet-161 at epoch 70 using t-SNE and examined a series of images from different prediction clusters. Surprisingly, the projected prediction mapping reveals some latent inter-class style relationships. We used the Gradient-weighted Class Activation Mapping (Grad-CAM) proposed by Selvaraju et al. (2017) to produce coarse localization maps with highlights of important discriminative regions of the image which correspond to the predictive decision of interest. Red regions of the heatmap correspond to high scores for class prediction significance (Figure 9).

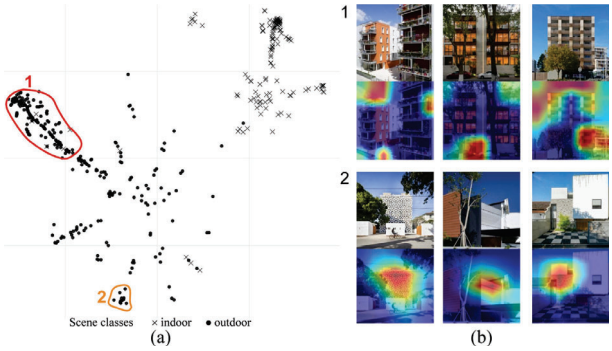

Figure 9. (a) Prediction of "Apartments" category with DenseNet-161 at epoch 70 projected using t-SNE; (b) Sample images with feature activation maps produced using Grad-CAM: images from clusters 1 have been correctly classified as "Apartments", while images from clusters 2 have been incorrectly classified as "Offices".

We note that the architectural category classification has an intrinsic relationship with some stylistic characteristics of the corresponding architectural image: the images mistakenly classified as another architectural category in clusters 2 are in possession of some common visual features, such as the solid white cubic geometry recurring in cluster 2. Meanwhile, the images which are correctly classified are also in possession of some similar visual features, such as the grid pattern of images from cluster 1.

4. Discussion and summary

We explored two multi-label architectural image classifiers with integrated classification labels, including scene classes and architectural functionality categories, trained on a new architectural image dataset with hierarchical labelling. The resulting model showcases the potential for innovative architectural discipline-related analyses.

The latent stylistic relationship between different architectural categories has revealed heuristic insights with respect to visual feature extraction in the context of architectural design research. The architectural image classification models can capture some deeper representations of higher-level visual features which can be related to the interpretation of architectural stylistic characteristics. Such property can be leveraged for architectural style identification and induction. The classification models can also be leveraged to develop an architectural style relationship network and provide architectural style analysis for individual buildings, which might distinguish itself from existing architectural style classification models relying on predefined historical styles with limited application potentials in real-world design scenarios.

5. Data availability statement

Some or all data and code that support the findings of this project are available from https://dataverse.harvard.edu/dataverse/AIDA_AIDA-CNNs.

References

Deng, J., Dong, W., Socher, R., Li, L.J., Li, K. and Li, F.F.: 2009, Imagenet: A large-scale hierarchical image database, *2009 IEEE conference on computer vision and pattern recognition*, 248-255.

Google Developers, initials missing: n.d., "The Size and Quality of a Data Set" . Available from <https://developers.google.com/machine-learning/data-prep/construct/collect/data-size-quality> (accessed 1st November 2020).

Freitas, A. and Carvalho, A. 2007, A tutorial on hierarchical classification with applications in bioinformatics, *in* D. Taniar (ed.), *Research and trends in data mining technologies and applications*, IGI Global, 175-208.

Hoffmann, E.J., Wang, Y.Y., Werner, M., Kang, J. and Zhu, X.X.: 2019, Model fusion for building type classification from aerial and street view images, *Remote Sensing*, **11**(11), 1259.

Huang, G., Liu, Z., Van Der Maaten, L. and Weinberger, K.Q.: 2017, Densely connected convolutional networks, *Proceedings of the IEEE conference on computer vision and pattern recognition*, 4700-4708.

Kang, J., Körner, M., Wang, Y., Taubenböck, H. and Zhu, X.X.: 2018, Building instance classification using street view images, *ISPRS journal of photogrammetry and remote sensing*, **145**, 44-59.

Kingma, D.P. and Ba, J.: 2014, Adam: A method for stochastic optimization, *arXiv preprint arXiv:1412.6980*.

Llamas, J., M Lerones, P., Medina, R., Zalama, E. and Gómez-García-Bermejo, J.: 2017, Classification of architectural heritage images using deep learning techniques, *Applied Sciences*, **7**(10), 992.

Van der Maaten, L. and Hinton, G.: 2008, Visualizing data using t-SNE, *Journal of machine learning research*, **9**(Nov), 2579-2605.

Nguyen, Q.C., Sajjadi, M., McCullough, M., Pham, M., Nguyen, T.T., Yu, W.J., Meng, H.W., Wen, M., Li, F.F. and Smith, K.R.: 2018, Neighbourhood looking glass: 360º automated characterisation of the built environment for neighbourhood effects research, *J Epidemiol Community Health*, **72**(3), 260-266.

Paszke, A., Gross, S., Massa, F., Lerer, A., Bradbury, J., Chanan, G., Killeen, T., Lin, Z., Gimelshein, N. and Antiga, L.: 2019, Pytorch: An imperative style, high-performance deep learning library, *Advances in neural information processing systems*, 8026-8037.

Pedregosa, F., Varoquaux, G., Gramfort, A., Michel, V., Thirion, B., Grisel, O., Blondel, M., Prettenhofer, P., Weiss, R. and Dubourg, V.: 2011, Scikit-learn: Machine learning in Python, *the Journal of machine Learning research*, **12**, 2825-2830.

von Platten, J., Sandels, C., Jörgensson, K., Karlsson, V., Mangold, M. and Mjörnell, K.: 2020, Using Machine Learning to Enrich Building Databases—Methods for Tailored Energy Retrofits, *Energies*, **13**(10), 2574.

Selvaraju, R.R., Cogswell, M., Das, A., Vedantam, R., Parikh, D. and Batra, D.: 2017, Grad-cam: Visual explanations from deep networks via gradient-based localization, *Proceedings of the IEEE international conference on computer vision*, 618-626.

Shalunts, G., Haxhimusa, Y. and Sablatnig, R.: 2011, Architectural style classification of building facade windows, *International Symposium on Visual Computing*, 280-289.

Silla, C.N. and Freitas, A.A.: 2011, A survey of hierarchical classification across different application domains, *Data Mining and Knowledge Discovery*, **22**(1-2), 31-72.

Xie, S., Girshick, R., Dollár, P., Tu, Z. and He, K.: 2017, Aggregated residual transformations for deep neural networks, *Proceedings of the IEEE conference on computer vision and pattern recognition*, 1492-1500.

Xu, Z., Tao, D., Zhang, Y., Wu, J. and Tsoi, A.C.: 2014, Architectural style classification using multinomial latent logistic regression, *European Conference on Computer Vision*, 600-615.

REINFORCEMENT LEARNING FOR ARCHITECTURAL DESIGN-BUILD

Opportunity of Machine Learning in a Material-informed Circular Design Strategy

CHIEN-HUA HUANG
[1]*Institute of Architecture, University of Applied Arts Vienna*
[1]*chienhua.huang91@gmail.com*

Abstract. This paper discusses the potentials of reinforcement learning in game engine for design, implementation, and construction of architecture. It inaugurates a new design tool that promotes a material-informed design-build workflow for architectural design and construction industries that achieves a comprehensive circular economy. As a proof of concept, it uses the project "Reform Standard", a machine-learning-based searching system that designs new shell structures composed of existing wasted materials, as a demonstration to discuss how reinforcement learning, machine vision and automated searching algorithm in the game engine can promote a material-aware design and converts wastes into construction materials. The demonstrator project sorts and transforms irregular chunks of wasted broken plastics into a new form. Instead of recycling those wastes in an energy-intensive process, the game engine is capable of finding the intricacy and new machine-oriented aesthetics in those otherwise neglected wastes. Furthermore, future research directions such as robotic-aided construction are discussed by exposing the potentials and problems in the demonstrated project. Finally, the future circular strategy is discussed beyond the demonstrated tests and local uses. The standardization of material, legislation and material lifecycle needs to be comprehensively considered and designed by architects and designers during conceptual design phase.

Keywords. Reinforcement Learning; ML-Agents; Unity3D; circular design; geometric analysis.

1. Introduction

Machine learning (ML) has been rapidly advancing and becoming accessible for design practice. Plugin packages such as RunwayML for web-based platforms, ML-Agents kit for Unity, and Owl for Grasshopper allow designers to utilize computational power for computational design and modeling. Examples of applications of artificial intelligence (AI) and ML in the architectural field have recently emerged. ArchiGAN, for instance, is a generational tool based on

PROJECTIONS, Proceedings of the 26th International Conference of the Association for Computer-Aided Architectural Design Research in Asia (CAADRIA) 2021, Volume 1, 171-180.

supervised learning algorithms for generating building plans (Chaillou, 2020). ML is now also being used in the engineering field to optimize structural configuration (Aksoez and Preisinger, 2020). Reinforcement learning (RL), a subcategory of ML, is also increasingly being explored in the design industry due to its interactive characteristic. RL, as defined by Howley and Mousavi (2018), 'involve[s] the strategy of learning via interacting (sequences of actions, observations, and rewards) with the environment' (p. 426). ML not only enhances efficiency and improves effectiveness but also opens up opportunities for innovative design practice.

In computational design, it implies that RL can play an increasingly significant role in material-informed design due to its ability to shift 'from a mere instrument of production to an agent of heuristic advancement' (Witt, 2016, p. 115). Hence, it may be able to build a comprehensively circular design strategy to reinforce the 'cradle-to-cradle' strategy, which perceives by-products and wastes as resources for other products (McDonough, 2002). Specifically, design can start from thinking of the whole design-build cycle and taking into account the massive fragments of waste and materials. Hence, architects' design criteria and responsibility can be expanded toward the full perspective of the circular strategy. Several works have demonstrated the need for and possibility of designing with waste and non-standard materials, such as in projects like Blob Wall by Greg Lynn, Mind the Scrap by Certain Measures, and Branch Formations by Conceptual Joining. However, these examples barely expand beyond its very specific function and styles. The challenge is caused by the computational-consuming analysis and design of complex geometries, which is time-consuming for designers. Instead of implementing an additional energy-intensive recycling strategy to reduce construction waste, a new ML-driven design workflow that directly reuses waste materials with irregular geometries as design inputs can significantly reduce waste production and potentially inaugurate new machine-oriented aesthetics.

This paper presents such new workflow, which takes advantage of RL for a material-informed design method to achieve a comprehensive circular strategy. The research in this paper discusses the potentials of RL in game engines for the design, implementation, and construction of an architecture that contributes to a comprehensive zero-waste design-build strategy and feasible construction affordance are discussed. A plastic structural shell is used as a demonstrator project to illustrate the potentials, problems, and methods involved. The paper concludes with the potential, limitations, and further research directions of RL/ML and the material-informed design strategy to address their application in creative design and production, thus providing diverse design outputs that take into consideration environmental concerns.

2. Methodology and Fabrication

2.1. OVERVIEW

The demonstrator project is an experiment on the design and assembly of a structural shell composed of wasted broken plastic chips. A method developed with multiple platforms, such as Rhinoceros, Grasshopper, Unity, and Reality

Capture, was applied to set up the comprehensive workflow. It consisted of inputs, a digital RL-based solution-searching program for assembling structural shells and outputs of instructions for the construction of each fragment and for the overall construction (Figure 1). In this paper, the digital workflow and ML-Agents, a Unity plugin for training intelligent agents via RL (Juliani et al., 2018), are presented in this project to showcase the power of RL in finding the shell assembly with the best structural performance, and thus to showcase its potential in promoting a material-informed circular strategy.

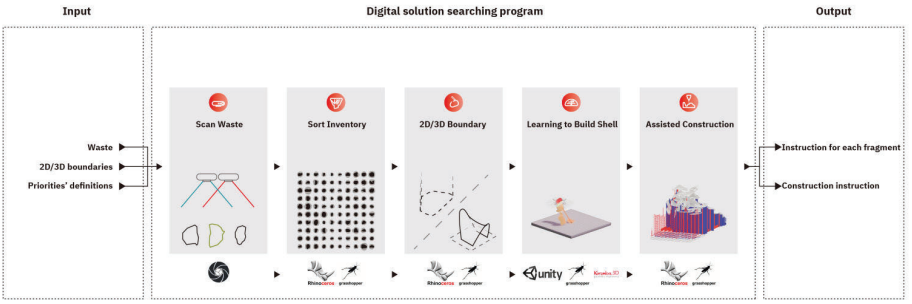

Figure 1. Diagram illustrating the program workflow.

2.2. SCAN WASTE

The first digital workflow process requires architects' first input sets of waste geometries, which are digitized with RealityCapture (RC) so they can be analyzed in Rhinoceros and Grasshopper. Figure 2 shows the setup for photogrammetrically scanning the target with the highest possible resolution to build a precise 3D model resembling its physical counterpart. High-resolution scanning can ensure proper geometrical analysis and digital assembly (Figure 3).

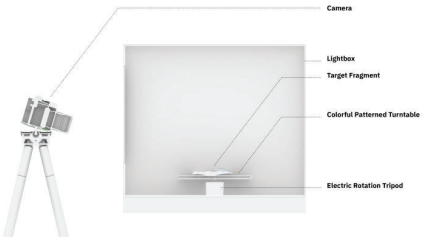

Figure 2. Setup for photogrammetry.

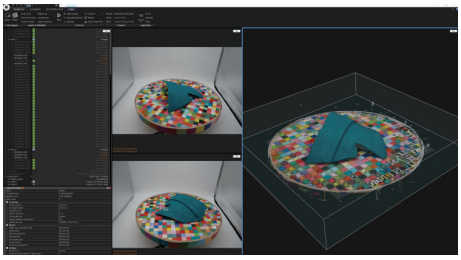

Figure 3. RealityCapture screenshot showing the photo samples and the digital model of one plastic fragment built via photogrammetry.

2.3. SORT THE INVENTORY

In the second step, each geometry is analyzed and sorted to enable sequential assembly in the searching process as the Unity program can place only one fragment at a time. Through Grasshopper, different data are extracted from each fragment for their implementation in future processes (Figure 4). Specifically, projection areas are used to define the maximum boundaries of the assembling procedure. The surface areas, HU invariants, number of control points, and erosion maps‘ areas are multiplied with different weights to sum them up into one number for every fragment so as to sequence the inventory. The skeleton’s midpoint and end points are exported to Unity so that ML-Agents can act according to the respective geometries’ topologies. To sum up, such data mitigate the burden on RL so that Unity does not need to encapsulate the computation-consuming sorting strategy.

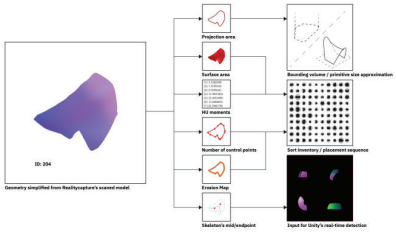

Figure 4. Diagram illustrating the types of data analyzed and their implementation in the following processes.

2.4. DEFINE THE 2D / 3D BOUNDARY

A 2D perimeter or a 3D volume is defined as a boundary for constraining the fragments‘ positions during the learning process. The boundary can be directly inputted by the user as a closed polyline or a closed brep. In the first case, unlimited height is allowed for the assembly within the regions. As for the 3D bounding geometry, the program resembles the solution of bin-packing problems with random geometries. The boundary is set to control the possibility of assembly

within a reasonable range. If the boundary is notably larger than the sums of all the fragments' projection areas or volumes, the efficiency of RL will remarkably diminish. Therefore, the boundary resembles the site perimeter and regulates the overall forms, which helps control design and avoid unnecessary learning time.

2.5. MACHINE LEARNING SEARCHING

After the above-mentioned conditional setup, all the sorted fragments and optimized boundaries are inputted into Unity for an assembly simulation test to search for the best structural shell. The most important benefit of introducing RL in ML-Agents is that the complex methodology of constructing a structural shell with various criteria does not need to be exclusively developed by architects. Rather, designers merely input priority criteria to direct ML-Agents. ML-Agents summarizes the data collected from the previous steps and learns to build a method that can construct a shell with different priorities defined by the users. Eventually, the method can be saved as a neural network model (NN-model), a model resembling a brain, to control the agents' behavior (Arthur et al., 2018).

In the Unity scene, each episode loads the fragment in sequence from the sorted inventory, finding a position to assemble the fragment onto the ground or other fragments, and developing a way to construct a structural shell through the observation of its environment (Figure 5). The game starts with the agent (controlled by AI) moving and rotating the fragment to find the best position based on its observation. The fragment is allowed to be assembled only if it fits all the criteria for a joint resembling a real physical connection (Figure 6). After the assembly, positive and negative rewards are assigned according to the evaluation results of the structure, height, and other performances defined by the users. Then the agent evaluates all the rewards and observation data to adjust the method for the next actions. Six major types of data are observed to train ML-Agents to assemble according to the performance of such priorities (Figure 7). These data are obtained via the cross-platform synchronization of shell model and analysis. Among the six types of observation data, the structural stability is evaluated via Karamba analysis in Grasshopper. Rhinoceros and Grasshopper are connected to Unity through a user datagram protocol (UDP) connection. The geometries are streamed from Unity to Grasshopper for Karamba structural analysis. Karamba is a Grasshopper plugin for finite element analysis that can provide real-time feedback. The analysis result is then streamed back to Unity through UDP for rewards stating. Other observation data, such as floor areas and thermal dynamics, are obtained using a camera within the game and RGB distribution analysis.

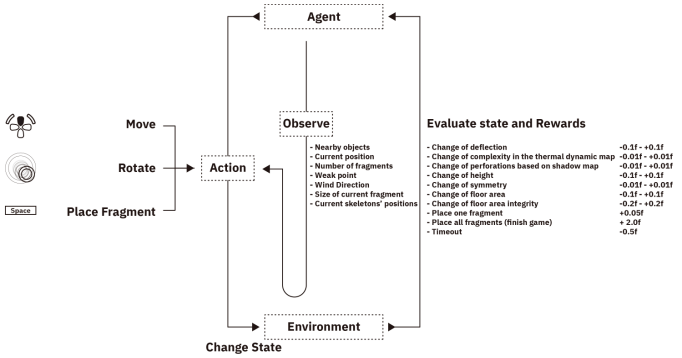

Figure 5. Diagram illustrating the processes, control, observation, and reward setup of the game for ML-Agents to learn assembly.

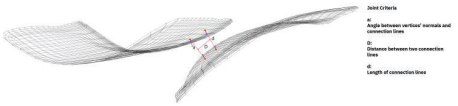

Figure 6. Diagram showing the conditions of the connection of two fragments.

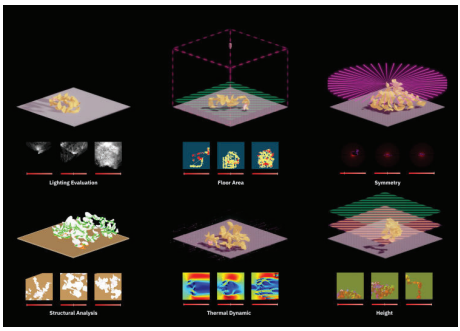

Figure 7. Diagram showing the maps and axonometric models of Unity observing the lighting variety (top left), floor area (top middle), symmetry (top right), structural stability (bottom left), thermal dynamic variety (bottom middle), and height (bottom right).

After the assembly simulation, the model of all the finished shells, their six scores, and an NN-model are saved. One shell can be selected to proceed based on the scores and the users' choices. The multiple reward evaluations and weights open up options for the users to curate their priorities according to their programs' needs (Figure 8). However, the nature of the evaluation may bring about results different from the users' expectations. The problem is caused by the different non-linear training trajectories used to obtain better scores for different evaluations. For instance, structural stability is much harder to achieve than area coverage as the former requires more data observations, detections, and

explorations. In the demonstrator project, a shell with the best structural stability was selected to proceed to the construction phase.

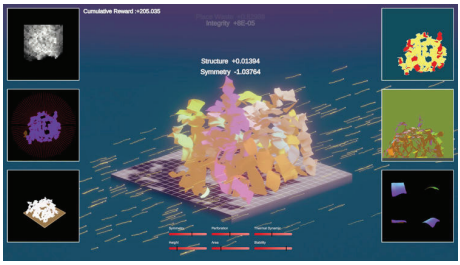

Figure 8. Unity screenshot of a training session.

2.6. ASSISTED CONSTRUCTION

After a decision is made by the user and the machine, the workflow will generate guidance on how to treat each fragment. This will aid the assembly of each fragment and ensure control and precise sequence. First, the connection points, drilling points, and their connection IDs indicating the fragments to be jointed are projected and marked on the geometry to exclude the digital devices' dependency (Figure 9). Plastic blind rivets were chosen as the joint because they are efficient for assembly purposes, homogeneous to plastic fragments, and lightweight (Figure 10 and 11). Despite the construction simplification, however, unexpected difficulties may arise when the assembly sequence is changed due to the need for temporary support. Thus, the whole procedure requires a fixed sequence.

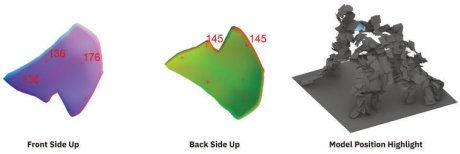

Figure 9. Rhinoceros screenshot of individual instructions for a sample fragment (left and middle) and its position in the model (right).

Figure 10. Under construction: Projection and marking (left), drilling (middle), and connecting (right).

Figure 11. Under construction: assembling and labeling.

3. Discussion and Future Researches

The successful design-build experiments on the workflow and the workflow's geometrical analysis, structural analysis, RL searching, and assembly prove the feasibility of further applying this process to other structural design practices. Figure 12 presents the final model in the demonstrator project. The design of the model subsequently prioritizes structural stability, floor area, and height among the six given types of observation data. The model was efficiently assembled even with only manual labor. However, several deficiencies occurred in the workflow experiment presented herein due to resource and technological limitations. First, the structure had around 2% deviations in width and length and an around 10% deviation in height from the digital model. This was caused by the imprecision of manual assembly, the unmatched material quality between the Karamba analysis results and the plastic fragments, and the different gap widths between Unity and the structural model. Second, not all the actions in the RL implementation can be rationally explained due to the nature of trial-and-error solution searching. Thus, RL can provide only solutions that seem intuitive, in which the reasons for some actions cannot be given. For example, in the final model, the columns have various types of composition, but the efficiency and stability of such columns cannot be compared within the RL framework. Nevertheless, RL implementation offers powerful insights and possibilities for architects that can be further optimized and edited.

Figure 12. Result: The model's front-perspective view.

To further expand the realm of the circular design strategy with materials as inputs, the future researches can expand the application of the workflow through three major aspects: robotic fabrication to replace manual work, introduction of the composition of mixed materials, and an online inventory to enable efficient mass collaboration and fabrication.

3.1. ARTISANAL ASSEMBLY VIA ML AND ROBOT

By combining ML and robotic assembly, architects can adopt an individual artisanal assembly approach. In the demonstrator project, the workflow outputs instructions for complicated manual construction, but robotic arms have the potential to handle such a complex assembly. Additionally, RL can enable robotic behavior and can interact with the environment (Kober et al., 2013). As such, it can be made part of the ML input so that during the design, the robotic movement can become a design parameter. Specifically, after the digital assembly phase, the program can train the robot to find an assembly strategy, proceed to physical control, and perform a task similar to digital simulation. Robotic fabrication for such an assembly can be beneficial and efficient due to robots' capacity for cooperation and possible involvement in the early design phase (Parascho et al., 2018). Therefore, future experiments with robotic assembly in the digital environment will ensure the profitability of the workflow and will contribute to the industrialization of this procedure.

3.2. MIXES OF MATERIALS AND JOINTS

The mixed assembly of different materials is feasible by allowing the use of other types of joints, which offers a wider variety of building types. The double-pin joints in the demonstrator project can already be applied to a significant number of materials, such as metal sheets and planks. To come up with a complex structure, a mix of different joint types may be necessary to enable other structural systems. Hence, future researches should investigate the method and reward systems in RL to search for multi-joint solutions.

3.3. MATERIAL AND COMPUTATION E-CROWDSOURCING

The digital production of the design algorithm promotes a potential new mass collaboration method through e-crowdsourcing. The potential new ways of practice through e-crowdsourcing are significantly beneficial as "the ideas of permanent variability, parametric mass customization, and digitally driven mass collaboration that designers test drove during the age of the first digital turn are now spreading in all areas of contemporary society, economy, and politics" (Carpo, 2017, p. 75). The inventory of fragments for design inputs can ideally be scanned, stored, shared, and delivered everywhere. As such, the users do not need to scan all the objects found. Rather, they can order the wanted construction materials from the web inventory and build a desired geometry from the selection. This will eventually help the users build more comprehensive structures with various textures and programs, which can help build a more comprehensive inventory that considers all kinds of non-standard resources.

4. Conclusion

When the difficulties of fitting geometry to design are dissolved by shifting the design cycle and applying RL searching, significant opportunities are opened up in a new realm of practice and design, especially the possible circular strategy. The nature of the workflow reinforces designers' responsibility to take into account the complex material reality in the environment. "Reform Standard" demonstrates how architectural design can implement ML in a design−build cycle and prioritize the material inputs. Despite the current limitation of computation power and RL's nature of unexplainable rationale, the workflow can effectively and smartly assemble complex geometries whose massive data are beyond a human designer's capacity to understand. Various future research potentials are unfolded by this workflow, which makes the sustainable design more industrially applicable, intelligent, and efficient. "Reform Standard" thus illustrates that RL has the potential to give rise to a material-informed design method and to fully sustainable building practices.

Acknowledgements

This research was based on a master thesis titled "Reform Standard" completed in June 2020 at Studio Greg Lynn, Institute of Architecture at the University of Applied Arts Vienna (die Angewandte), under the supervision of Prof. Greg Lynn and with the assistance of Bence Pap, Kaiho Yu, Maja Ozvaldic, and Martin Murero. Special thanks are extended to Lisa-Marie Androsch, Martin Lai, Wing Yan Joyce Lee, Yi Jiang, Yu Zhao, and Zach Beale.

References

Aksoez, Z. and Preisinger, C. 2020, An Interactive Structural Optimization of Space Frame Structures Using Machine Learning, *in* C. Gengnagel, O. Baverel, J. Burry, M. Ramsgaard Thomsen and S. Weinzierl (eds.), *Impact: Design With All Senses*, Springer, Cham, 18-31.

Arthur, J., Berges, V.P., Vckay, E., Gao, Y., Henry, H., Mattar, M. and Lange, D.: 2018, "Unity: A General Platform for Intelligent Agents" . Available from <https://www.researchgate.net/publication/327570403_Unity_A_General_Platform_for_Intelligent_Agents>.

Carpo, M.: 2017, *The Second Digital Turn. Design beyond intelligence*, MIT Press.

Chaillou, S. 2020, ArchiGAN: Artificial Intelligence x Architecture, *in* P. Yuan, M. Xie, N. Leach, J. Yao and X. Wang (eds.), *Architectural Intelligence, Selected Papers from the 1st International Conference on Computational Design and Robotic Fabrication (CDRF 2019)*, Springer, Singapore, 117-127.

Kober, J., Bagnell, J.A. and Peter, J.: 2013, Reinforcement Learning in Robotics: A Survey, *The International Journal of Robotics Research*, **32**, 1238-1274.

McDonough, W.: 2002, *Cradle To Cradle : Remaking the Way We Make Things*, North Point Press, New York.

Mousavi, S., Schukat, M. and Howley, E.: 2018, Deep Reinforcement Learning: An Overview, *Proceedings of SAI Intelligent Systems Conference (IntelliSys) 2016*, 426-440.

Parascho, S., Kohlhammer, T., Coros, S., Gramazio, F. and Kohler, M.: 2018, Computational design of robotically assembled spatial structures, *Conference: Advances in Architectural Geometry 2018*, Gothenburg.

Witt, A.: 2016, Cartogrammic Metamorphologies; or, Enter the Rowebot, *Log Journal of Architecture*, **36**, 115-124.

EXTRUDED POLYHEDRON MORPHOLOGY RESEARCH

HUADONG YAN[1] and ZIYU TONG[2]
[1,2]*Nanjing University School of Architecture and Urban Planning*
[1]*mg1836028@smail.nju.edu.cn* [2]*tzy@nju.edu.cn*

Abstract. An extruded polyhedron is a kind of geometry obtained by extruding the edges of a polyhedron along the normal line of its face. The interior of this geometry is a polyhedron-shaped space, and each polyhedron has a corresponding extruded polyhedron. Extruded polyhedrons formed by different polyhedrons have different properties; certain extruded polyhedrons are stable, while others are highly variable. Different variable extruded polyhedrons also have greatly different degrees of freedom. Based on previous studies, this paper thoroughly explores the deformation logic of complex extruded polyhedrons.

Keywords. Extruded polyhedron; Deformation of the logic.

1. Introduction

Researchers have always maintained great interest in the art of origami in the fields of materials, structures, nodes, etc. Structures inspired by special origami patterns have special mechanical properties, that are not present in traditional structures. Current research on origami mainly focuses on the creases in origami forms. Through special creases and crease treatments in the application process, the development of special structures can usually be realized, which is especially important in the research of deployable structures (Schenk & Guest 2013; Wei et al. 2013).

Modular origami breaks the limitation of a single paper in traditional origami art, folding multiple sheets of paper into modules; then, these modules are connected to each other to form a component. Certain forms are capable of large-scale shape transformations, making them ideal sources of inspiration for creating metamaterials, dynamic structures and components with tuned mechanical properties (Yang 2017).

The original source of extruded polyhedron geometries is a modular origami technique called Snapology. This origami technique invented by Heinz Strobl opens a new door to the study of geometry and provides a unique feature: strips are used to represent the faces and edges of polyhedrons (Strobl 2010; Goldman 2011). The extruded dodecahedron in Figure 1 is made using Snapology.

PROJECTIONS, Proceedings of the 26th International Conference of the Association for Computer-Aided Architectural Design Research in Asia (CAADRIA) 2021, Volume 1, 181-190.

a Polyhedron b Extruded Polyhedron

a from:https://loft-concept.ru
b from:https://artekusudama.blogspot.com

Figure 1. Snapology.

The variability of extruded polyhedrons and the application potential of modular origami methods are two important reasons for the introduction of extruded polyhedrons into scientific research. Horboman (2014) considered the extruded cube as an example for related application patents. The properties of extruded polyhedrons are completely dependent on the core polyhedral space, some of which can be deformed, while others are static. Variable extruded polyhedron coincides with the definition of an expandable structure to a certain extent (De Temmerman 2007). This is also a focus of our research.

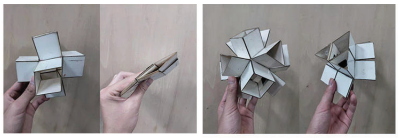

a Deployable b Undeployable

Figure 2. Deployable structure.

Compared to the history of research on modular origami, research on extruded polyhedron, which are a special type of modular origami, remains in the exploration stage. Overvelde et al. (2017) introduced an extruded cube into the study of materials science and used it as a basic unit to perform array transformation in space. Since each unit can be deformed, the formed material can also be deformed along a predetermined path. Following this idea, the team introduced more extruded polyhedrons for research, and studied their deformation characteristics after being arrayed (Figure 3). Research has also been performed on extruded polyhedron dynamic nodes, which can be used in furniture, architecture and other applications (Yan et al. 2020).

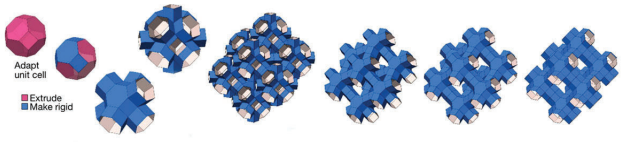

Unit and Array
from:《Rational design of reconfigurable prismatic architected materials》

Figure 3. Polyhedral array.

However, there are few theoretical studies of the deformation characteristics of a single expandable structure. At present, the extruded cube has been studied

in detail from a mathematical point of view, and the deformation characteristics of the extruded cube are expressed by the Angle relation between the three edges located at the same vertex of the cube (Overvelde et al. 2016).

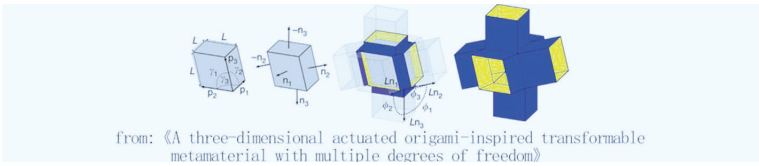

Figure 4. Extruded hexahedron deformation.

An extruded cube presents the simplest variable extruded polyhedron, and the logic of its deformation has been described relatively completely. This deformation logic uses the concepts of vectors and angles, and can clearly express the deformation state of the extruded cube using formulae. However, these formulae also have limitations. The three edges of an extruded cube have a vertical relationship at the starting position, and its computational complexity is low. If this logic is applied to a more complex extruded polyhedron, the spatial relationship between points, edges, and faces becomes more complex, which greatly increases computational complexity. This article proposes a logically clear, cognitively simpler method to describe the deformation of complex extruded polyhedrons.

The purpose of studying these deformation characteristics is to better understand the deformation principle of extruded polyhedron and to provide theoretical support for future research of the applications of extruded polyhedron, which have potential as dynamic nodes and structures.

2. Research strategy

There are many types of polyhedrons, among which the most common are Platonic polyhedrons and Archimedes polyhedrons (Peraza-Hernandez et al. 2014). The polyhedrons we encounter in daily life can generally be classified as one of these two types. The prototype of the research object in this paper is also one of these two types of polyhedrons, and the selected polyhedrons have a certain degree of complexity and representativeness.

In our research, we set an element that can affect the deformation of an extruded polyhedron as a degree of freedom. This element is called a degree of freedom element in this article. For example, in an extruded cube, the motion of three edges at the same vertex can control the deformation of the entire cube. Then, we can say that these three edges represent three degrees of freedom. When we select three vertices, the extruded cube can deform when the positions of the three points change; thus, the three vertices can also represent three degrees of freedom. In Figure 5, points, edges, and face methods are shown as examples of degrees of freedom.

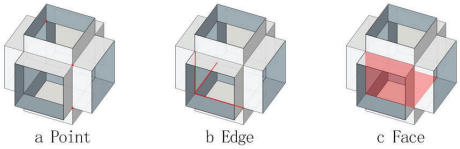

Figure 5. Degrees of freedom in different elements.

Using the angle between edges to represent the deformation characteristics of the entire extruded cube has been realized in previous research led by the Harvard University Graduate School (Overvelde et al. 2016). In this study, we discuss the deformation of extruded polyhedrons in a spherical coordinate system, where the determination of a position requires the joint action of two angles: the angle between the line and the axis between the point of interest and the origin, and the angle between the line and the plane. For convenience, the Z axis and the plane XOZ are used as references (Figure 6).

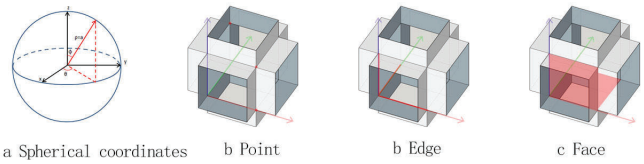

Figure 6. spherical coordinates and application.

For the three types, namely, points, edges and surfaces, the largest difference is the degree of integration of elements. One surface can integrate many points and edges, while an edge can integrate two points, and the points are scattered. The lower the degree of integration of an element, the worse the correlation between the element and other elements; the number of calculations increases accordingly. A high degree of integration of the elements will inevitably lead to a correlation between the front and back calculations; thus, the results of the previous calculations can lay the foundation for subsequent calculations, reducing the amount of calculations that must be performed.

We decided to abandon the method of using edges as degrees of freedom when investigating the logic of complex polyhedron deformation and adopted the surface method instead. Another advantage of this method is that it can divide the deformation logic into two layers. First, edges or points are used to derive the deformation of the surface, and then the deformation of the surface is used to derive the deformation of the extruded polyhedron.

3. Case study

3.1. EXTRUDED TRUNCATED-OCTAHEDRON STUDY

In this chapter, we use an extruded truncated octahedron to verify. In geometry, a truncated octahedron is a semi-regular polyhedron composed of eight hexagonal faces and six quadrilateral faces, with a total of 14 faces, 36 sides, and 24 vertices.

The deformation logic of an extruded truncated octahedron is more complex than that of an extruded cube. The face is of course the most important element of freedom. Nevertheless, the edges and points that make up the face will still run through the whole logic. Therefore, the mixed logic method dominated by surface elements is more convenient for description or calculation. The method is divided into two major steps: determine the surface, and determine the elements that are not on the surface. It is necessary to understand the role of these elements in the entire movement of the truncated octahedron. In our description system, we take the surface as the main element, and other elements are used to illustrate the shape and position of the surface.

3.1.1. .Hexagon deformation

We know that the cross section of the branches of the extruded truncated octahedron is composed of many aquadrilateral and hexagons.Obviously, the control force of the quadrilateral is far less than the control force of the hexagon to the entire extruded truncated octahedron. Then in this geometry, We use the hexagon as the degree of freedom element that controls the entire extruded truncated octahedron.

Mark the six sides as es1˜es6 , es1 is set as a fixed edge, the angle between es2 and es1 on the x0y plane is denoted as a, a in [0, π], the angle between es3 and es2 is b ,b in [π-a, π], the angle of c will cause the linkage change of the three angles d, e, f, when es5 is parallel to es6, c is at the minimum, when es5 When parallel to es5, c is at the maximum. And when c is determined, the shape of the hexagon can be directly determined.(Figure 7(a))

We will calculate the range of values of c in different values of a and b:

$$b1 = \frac{\pi - a}{2} \tag{1}$$

$$b2 = \frac{2 \cdot b + a - \pi}{2} \tag{2}$$

$$u^2 = 2 \cdot (2 - \cos a) \tag{3}$$

$$v^2 = 1 + u^2 - 2 \cdot u \cdot \cos a \tag{4}$$

$$C\min = \arcsin\left(u \cdot \frac{\sin(b2)}{v}\right) + \arccos\left(\frac{v^2 + 3}{4 \cdot v}\right) \tag{5}$$

$$C\max = \arcsin\left(u \cdot \frac{\sin(b2)}{v}\right) + \arccos\left(\frac{v^2 - 3}{2 \cdot v}\right), , a \in [0, \pi], b \in [\pi - a, \pi] \tag{6}$$

These two formulas represent the maximum and minimum values of c indifferent a and b, but the range of these two formulas will make the Angle between two edges of a hexagon bigger than 180°, so some restrictions need to be made.

When c is bigger than 180°, the minimum value formula of c is calculated according to the following formula, and the values of b1,u, and v in the formula

refer to the above formula

$$f1 = \frac{\pi + a}{2} \tag{7}$$

$$b2 = \arcsin\left(\frac{\sin(f1)}{2}\right) \tag{8}$$

$$b3 = b - b1 - b2 \tag{9}$$

$$w^2 = 1 + v^2 - 2 \cdot v \cdot \cos(b3) \tag{10}$$

$$C\min 1 = \arcsin\left(v \cdot \frac{\sin(b3)}{w}\right) + \arccos\left(\frac{v^2 - 3}{2 \cdot v}\right), a \in [0, \pi], b \in [\pi - a, \pi], \tag{11}$$

When the maximum value of C is bigger than 180°, the maximum value of C is directly set to 180°

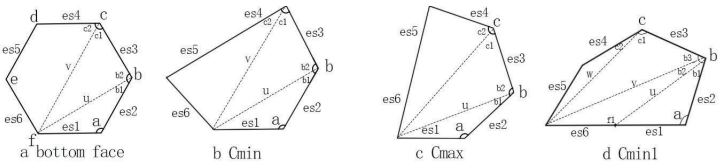

Figure 7. bottom face deformation.

By determining the position of three angles or four sides, we can determine the shape of a hexagon. In this way, we have a deep understanding of the shape of this face. The next step is to explore the influence of the parts other than the face on the entire extruded polyhedron, which is the edge or point we mentioned above.

3.1.2. other elements in deformation

After accurately describe the deformed posture of the hexagon, we use six edges to further determine the shape of the extruded truncated octahedron. However, we can also find that the interrelationship formed by these six edges determines only the other three hexagonal faces.

First, we put a hexagon on the plane XOY. For convenience, one of the sides coinciding with the X-axis and is set to be static. We thus restrict the movement of certain elements for the calculation. However, this does not affect the deformation results. For the bottom hexagon, f1 can move in the XOY plane based on the law of motion summarized in the previous section. The purple edge in Figure 8a is an element of the degree of freedom that determines the shape and position of hexagon f4 opposite to f1. Because some of the edges in the truncated octahedron are always parallel, we have optimized the choice of edges in order to facilitate the calculation because we must determine only the planes of the three faces f2, f3, and f5 to determine the position of the edge. As shown in Figure 8b, the edges are denoted e1˜e5.

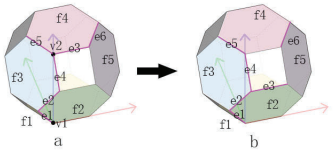

Figure 8. deformation setting.

In the coordinate system, the angle between e1 and the z axis is α, and the angle between the projection on the plane XOY and the counterclockwise phase of the XOZ plane is β. With the vector e1 = (a*sinα*cosβ, a*sinα*sinβ, a*cosα), where α in [0, 0.5 π), β in [0, π), this edge can move on the surface of the hemisphere (Figure 9). This vector is going to be used to represent the position of the f2 plane right here.

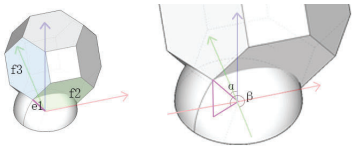

Figure 9. step 1.

When determining e1, the two edges of e1 and ex1 are sufficient to determine the plane of f2. We can calculate the range of motion of e2 and e3 on plane f2. We convert the standard plane to plane f2 when we calculate the law of motion of the edge on f2 (Figure 10). When determining e4, e5, and e6, we also need to convert the standard plane. The angle between plane f2 and plane XOZ is θ, and the included angle d1 between e1 and edge ex1 can be expressed by the known α and β:

$$\theta = \arccos\sqrt{\frac{\cos^2\alpha}{\sin^2\alpha\cdot\cos^2\beta+\cos^2\alpha}} \tag{12}$$

$$d1 = arc\cos\left(\sin\alpha\cdot\sin\beta\{r\in\mathbb{R}|0\le\alpha\le 0.5\pi\pi\}\square\{s\in\mathbb{R}|0\le\beta\le 2\pi\}\right. \tag{13}$$

Where the range of angle d2 is in [π-d1, π], and the range of angle d3 can be calculated with d1 and d2. When we obtain the exact values of these three angles, hexagon f2 can be determined.

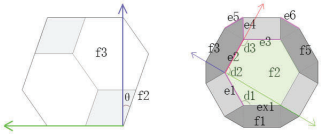

Figure 10. step 2.

When we determine the position of the edge, the shape of the entire hexagon is

also determined. Therefore, this method of mixing elements can also be considered as if points and edges elements were used to determine the surface, and then the surfaces were used one by one to determine the deformed shape of the entire extruded truncated octahedron.

The determination of face f3 requires four edges. Edge ex3 is parallel to the bottom edge ex1, thus, edge ex3 has been determined. Similarly, the position of e2 has also been determined. Therefore, the angle between ex3 and e2 is already a certain angle and can be represented by r, s, and d2. The position of the face f3 is also related to the three angles r, s, and d2. Taking the edge e2 as a vector, the distance and direction from the origin to the vertex of e2 can be obtained, and the e2 vertex can be obtained, which is also the origin of the f3 plane.

In the face f3, the positions of e4 and e5 can also be determined by the limited range of angle values; e2 and ex3 have been determined in the previous edge motion; and d4 is also a given value. Thus, the range of d5 on face f3 is in [π-d4, π], and the range of d6 remains more complex and must be substituted into the range calculation formula for c shown in Section 3.1.1.

The final edge that must be determined is on face f5. At present, there are three edges that have been determined for f5 in Figure 11b, and the shape of a hexagon needs to be determined by four edges. We choose e6. The first three edges of f5 are determined in the process of determining the three faces of f1, f2, and f3. Then the range of the angle between e6 and e4 can still be calculated using the value range of c in the previous section.

Finally, through the shape of a hexagon and the position of the six edges, we determined the specific shape of the extruded truncated octahedron. From another perspective, the determination of f1 and the position of the six edges essentially determines the shape and plane of the four hexagonal faces f1, f2, f3, and f5.

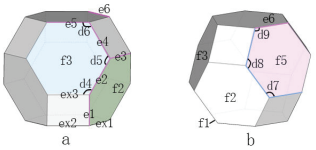

Figure 11. step 3,4.

3.2. SUMMARY

The process proposed in our research is to transform a monolithic deformation into a series of operations. By extracting elements with freedom of transformation, ignoring subordinate elements, we can determine the order of motion of the former elements, assign the constraints of the movement of the previous elements to the latter elements, and perform a stepwise analysis.

We also discovered that the final determination of our edges is in the shape of a hexagon. We can thus conclude that four hexagons can determine the shape of an extruded truncated octahedron.

To demonstrate the proposed method, we use the calculated values from our

calculation process. To make it easier to understand the state of the extruded truncated octahedron, we use a table to represent a certain state. The presentation of table information is divided into two levels. The first level is the surface, and the second level comprises the three angles between the edges and the edges in the plane. The determination of each hexagon requires a spatial plane position and three angle values. Four hexagons can completely describe the shape of an extruded truncated octahedron.

In this table, each group of angle values corresponds to a shape. Except where f1 is set on the XOY plane, the locations of the planes of other polygons do not require additional explanation. The plane position of the hexagon is unique and definite. It is subject to the angle limit within the hexagon, which indicates that when we determine these angles, the plane position of the polygon and the shape of the entire geometry are definite and unique.

Table 1 Cases presentation

Table 1. The relationship between angle and form.

Plane	Anglular name	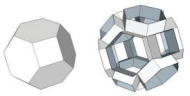	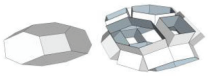	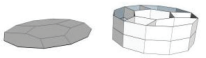
	∠α	35.31°	65.31°	90°
	∠β	240°	120°	150°
f1	∠a	120°	120°	120°
	∠b	120°	120°	120°
	∠c	120°	120°	120°
f2	∠d1	120°	76.27°	150°
	∠d2	120°	141.87°	60°
	∠d3	120°	76.27°	150°
f3	∠d4	120°	76.27°	150°
	∠d5	120°	141.87°	60
	∠d6	120°	76.27°	150°
f5	∠d7	120°	76.27°	150°
	∠d8	120°	141.87°	60
	∠d9	120°	76.27°	150°

The table gives an example of the corresponding shape of an extruded truncated octahedron corresponding to each group of angles. The plane here can be understood as a hexagon of the plane. For the specific position, please refer to Section 3.1.2.

4. Conclusion and Prospect

This article mainly discusses the deformation logic of a complex extruded polyhedron, which we describe with mathematics in detail. However, due to the complexity of the shape, there remains a lack of precise mathematical calculations

for some aspects of the shape, especially the accuracy of the plane where f3 and f5 are located. The purpose of this article is also to provide an initial understanding of a complex extruded polyhedron, which is usually considered difficult to describe, can be explained with clear logic.

It is necessary to conduct in-depth research on the deformation logic of more extruded polyhedrons, and explore the possibility of extruded polyhedrons in real applications, especially in combination with professional expertise, and how this kind of movable component can be combined with construction-related industries.

acknowledgement

This research was supported by National Natural Science Foundation of China (51578277).

References

Goldman, F.: 2011, *Using the Snapology Technique to Teach Convex Polyhedra*, CRC Press.

Hoberman, C.: 2014, Deployable structures based on polyhedra having parallelogram faces, *no source given*, Provisional US Patent Application, 62/023.

Overvelde, J. T. B., De Jong, T. A. and Shevchenko, Y.: 2016, three-dimensional actuated origami-inspired transformable metamaterial with multiple degrees of freedom, *Nature communications*, 7: 10929.

Overvelde, J. T., Weaver, J. C., Hoberman, C. and Bertoldi, K.: 2017, Rational design of reconfigurable prismatic architected materials, *Nature*, **541(7637)**, 347-352.

Peraza-Hernandez, E. A., Hartl, D. J., Malak Jr, R. J. and Lagoudas, D. C.: 2014, Origami-inspired active structures: a synthesis and review, *Smart Materials and Structures*, **23(9)**, 094001.

Strobl, H.: 2010, "Special snapology" . Available from <http://www.knotology.eu/PPP-Jena2010e/start.html>.

De Temmerman,, N.: 2007, Design and analysis of deployable bar structures for mobile architectural applications, *Vrije Universiteit Brussel*.

Wei, Z., Guo, Z. V., Dudte, L., Liang, H. Y. and Mahadevan, L.: 2013, Geometric mechanics of periodic pleated origami, *Physical review letters*, **110(21)**, 110(21).

Yan, H., Tong, Z., Park, D. and Lu, H.: 2020, A reconfigurable joint based on extruded polyhedrons, *25th International Conference on Computer-Aided Architectural Design Research in Asia, CAADRIA 2020*, 455-464.

Yang, Y. and You, Z.: 2017, Geometry of Modular Origami Metamaterials, *41st Mechanisms and Robotics Conference. Cleveland, Ohio*, USA.

EXPLORING OPTIMAL WAYS TO REPRESENT TOPOLOGICAL AND SPATIAL FEATURES OF BUILDING DESIGNS IN DEEP LEARNING METHODS AND APPLICATIONS FOR ARCHITECTURE

VIKTOR EISENSTADT[1], HARDIK ARORA[2],
CHRISTOPH ZIEGLER[3], JESSICA BIELSKI[4],
CHRISTOPH LANGENHAN[5], KLAUS-DIETER ALTHOFF[6] and
ANDREAS DENGEL[7]
[1,2,6,7]*German Research Center for Artificial Intelligence (DFKI)*
[1,2,6,7]*{viktor.eisenstadt|hardik.arora|klaus-dieter.althoff|andreas.dengel}@dfki.de*
[3,4,5]*Technical University of Munich*
[3,4,5]*{c.ziegler|j.bielski|langenhan}@tum.de*

Abstract. The main aim of this research is to harness deep learning techniques to support architectural design problems in early design phases, for example, to enable auto-completion of unfinished designs. For this purpose, we investigate the possibilities offered by established deep learning libraries such as TensorFlow. In this paper, we address a core challenge that arises, namely the transformation of semantic building information into a tensor format that can be processed by the libraries. Specifically, we address the representation of information about room types of a building and type of connection between the respective rooms. We develop and discuss five formats. Results of an initial evaluation based on a classification task show that all formats are suitable for training deep learning networks. However, a clear winner could be determined as well, for which a maximum value of 98% for validation accuracy could be achieved.

Keywords. Deep learning; spatial configuration; data representation; semantic building fingerprint.

1. Introduction

First approaches for computational support in solving architectural design problems were based on systems theory, which concentrated on design rules, but could not exhaustively represent the complexity of architectural designs (McCullough et al., 1990). Therefore, the second generation of the design methodology movement in the 1970s, represented by Horst Rittel among others, conceived of design not procedurally as the fulfillment of requirements, but rather as an individual process that can only be incompletely described.

In the research project Metis-I (2013-2016), we investigate approaches for the early conceptual design phases of architecture that can cope with the vagueness of architectural design problems. In this context, we investigate deep learning (DL)

PROJECTIONS, Proceedings of the 26th International Conference of the Association for Computer-Aided Architectural Design Research in Asia (CAADRIA) 2021, Volume 1, 191-200.

approaches for auto-completion of spatial configurations building on previous findings on search for design references from the research project Metis-II (2020-2023). After sketching first ideas of the the spatial configuration, rooms and their connections are suggested for completion to support the early ideation process. We envisage auto-completion to be helpful for architects to overcome their own design bias, by offering design options as an inspiration and to evaluate variants of the possible final results for deeper understanding of their own design decisions. Both projects are supported by German Research Foundation (DFG).

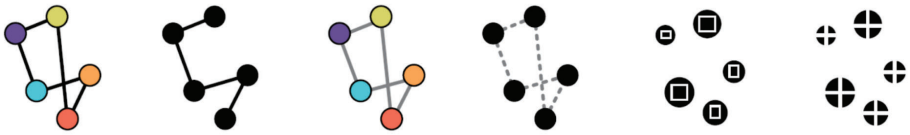

Figure 1. Examples of semantic building fingerprints (SBF). With topology (1-4): semantic spatial graph, through-path-graph, semantic spatial connection graph, spatial distance. Without topology (5, 6): envelope area, center of room.

Spatial information from the architects' sketches needs to be formalized to allow computational methods, such as DL, processing it. One approach for formalization is provided by the Semantic Building Fingerprint (SBF) (Langenhan 2017). It is comparable to the set of characteristic features in friction ridges of a human finger used for identification of human beings. SBFs are graph-based, rooms are mapped as nodes and the relationships between rooms, e.g. direct connections through doors, are represented by edges. Several SBFs with and without typology were developed (see Figure 1). For each SBF, a suitable representation for DL has to be elaborated. In this paper, we investigate such representations based on the common concept "relation map" for the most complex SBF with the strongest set of semantic information, the so called *semantic spatial connection graph*. This SBF takes rooms and their names as node labels for the graph as well as their connection between each other e.g. by a wall or door as edge labels of the graph into account. In contrast to raster graphics of e.g. floor plans, the semantic information in SBFs is directly accessible, which is especially useful for semantic tasks in DL in the domain of architecture.

However, semantic information encoded as an SBF graph needs to be converted for processing with DL, as this AI discipline makes use of uniformly preprocessed data to draw conclusions based on the features detected in this data. That is, for an optimal use within a DL approach, e.g. an artificial neural network (ANN), spatial configurations need to be turned into specific numerical or textual representations. These DL-compatible representations of SBF should be designed to allow reversible conversion from DL to SBF. This makes sure that deep learning results can be visualized for domain users such as architects or urban planners.

We explore how SBF-based spatial configurations can be represented optimally in DL approaches for architectural design, especially in the state-of-the-art ANNs. We propose five types of the DL-compatible representation "relation map" and evaluate three most promising using a straightforward classification task.

2. Research Context and Related Work

Currently, the most applied generic tasks of DL methods include classification (assignment of predefined classes to a new data entity, e.g. recognition of objects in an image), sequence learning (e.g. completion of natural language sentences), and generative methods (e.g. "deep fakes"). Nowadays, deep learning has become a common tool for computer science applications and is used in many knowledge-intensive domains as the solution of choice to help in decision making (e.g., in the financial sector) or security enhancement (e.g. face recognition). However, for the domain of architectural design, deep learning methods and approaches are still not common and not widely applied as for the other domains.

Existing DL approaches in architecture mostly make use of images of floor plans in the form of raster or vector graphics, for example, for retrieval of similar designs (Sharma et al., 2017), design style manipulation (Newton, 2019), or 3D room layout estimation (Sun et al., 2019). While this might be the most obvious way of using floor plans in DL, such pure image-based data might not allow for recognition of the relevant semantic information, such as relational dependencies between the rooms that make up the purpose of the spatial configuration. Thus the images do not allow for easy and flexible selection of semantic features that should be taken into account for learning of a DL model.

This problem became visible during our work on an AI-based prototype for support of early phases in architectural design, for which a number of DL approaches should be developed that make use of relevant semantic information contained in the SBFs. For example, the aforementioned intelligent auto-completion of spatial configurations with ANNs is one of these approaches. The data available for these approaches missed a suitable representation of spatial layouts for DL as the data was put together from different sources and had only GraphML as a common SBF representation format. However, this XML-based format does not provide a numerical tensor format required for the modern DL libraries such as TensorFlow or PyTorch. These libraries implement the standard DL methods that need to be evaluated for the research project goals of auto-completion to either use them, evaluate other libraries, or develop new DL methods for the domain of architecture. For graphs, it is possible to use a dedicated deep learning library, such as *Deep Graph Library* DGL, that functions as an abstraction layer to other DL frameworks extending them with deep learning methods for graphs that have already shown promising results (Zhang et al., 2020). However, DGL does not provide architecture-specific methods or representations as well, making use of generic representations, such as adjacency matrices that also do not allow for selective application of relevant SBF features.

As a practical approach for using GraphML data for DL, methods to construct a floor plan image based on the adjacency graph of the spatial configuration using graph theory tools and rulesets can be used (Shekhawat et al., 2019; Roth, 1982). However, these methods do not make use of semantic information as well and produce rectangular and orthogonal spatial layouts concentrating on the geometry, that is currently not considered by any DL approach of the AI-based prototype (but is encoded in SBFs like envelope area or center of the room, see also Figure 1).

3. Data Representation: Relation Map

In search of an optimal solution to the problem described in the previous section, we developed a number of representations, which are all based on a tensor data structure called "relation map". Before introducing the representations this chapter introduces the general underlying concept of the relation map.

A relation map is a tensor that represents *the modified adjacency matrix of the topology* of a spatial configuration encoded in a graph. Each row of the matrix represents *a particular room* and *its outgoing relations* to other rooms. Unavailable relations between the existing rooms and geometrical features of the building design are not considered. Initially, relation maps take inspiration from architectural morphospaces (Steadman and Mitchell, 2010) and geometry maps (De Miguel et al., 2019). Adjacency matrices have been already used as representation means of spatial layouts (Hickman and Krolik, 2009), however, the structure proposed by Hickman and Krolik only indicates if direct paths (connections) between the rooms are available (or not), making no use of any other semantic information.

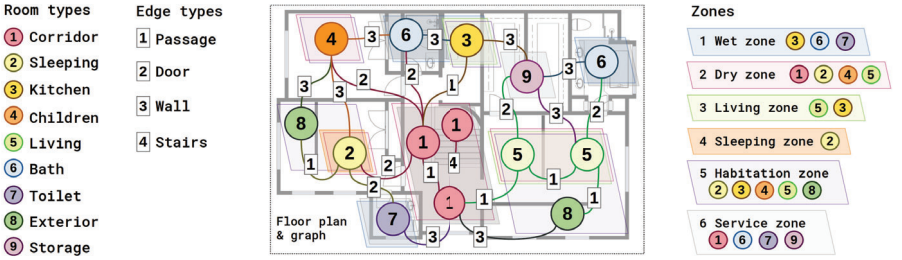

Figure 2. Basic topology for relation maps. An example of an SBF derived from a real spatial configuration graph shows how this typology can represent the semantic features.

As the relation maps make use of the semantic information rather than of the geometrical or raster graphics features, a specific typology of node and edge labels is required that can be used for standardized representation of the features. As mentioned in the introduction to this paper, the paramount features of the SBF semantic spatial connection graph, that we selected to work with, are its room and room connection types that correspond to nodes and edges of the room graph. However, generally, applying semantic typology for data that can be used as a graph it is possible to represent any type of information either as a node, an edge or their properties. In Figure 2, an example of such semantic typology is shown, in its basic version it consists of a number of room and relation types, each encoded with a specific number. The typology is flexible and can be easily complemented, extended, or reduced if required. For example, it can be reworked in a way that only an abstract categorization of rooms (e.g. habitable space) and connections (open or closed) is represented. An additional advantage, which is crucial at least for our research context, is that using the typology the relation map can be reconstructed back to GraphML or other graph representation format.

3.1. SIMPLE AND ZONED RELATION MAPS

The basic type of a relation map is a *simple relation map* that uses three numerical slots to encode the room type relations available in the SBF. Each relation between two rooms can be represented by a specific *relation code* and placed in the row that represents the room from which the connection goes out. For example, in the relation code 562, **living** (5) has an outgoing connection to **bath** (6) using a **door** (2). While such tensors are lightweight and easy to create, there are also limitations of their use caused by the occasionally repeating codes. The simple maps were integrated in a design augmentation approach (Arora et al., 2020) based on generative adversarial nets and related to the architectural design generation (As et al., 2018) and House-GAN (Nauata et al., 2020).

An improvement of the simple map is the *zoned relation map* that adds information on the architectural zones available in the SBF, making the maps more versatile and the relation codes rarely repeating. Architectural zones (Langenhan 2017) represent the taxonomy of categories for room types, grouping them by their functionality (see Figure 1). The room types can be part of multiple zones, for each room type a primary zone can be selected. Using a specific number, the primary zone can be used in the relation code. For example, the code 35162 represents **kitchen** (3) from the **habitation** zone (5) connected to **corridor** (1) from the **service** zone (6) by a **door** (2). Zoned maps were evaluated in the floor plan retrieval pipeline of the aforementioned AI-based prototype to provide contexts for the current search process (Eisenstadt et al., 2020).

3.2. MULTILAYER MAP

While the simple and the zoned type of relation map make use of a (basic) typology, in some cases the situation can occur when the dataset typology is not available. To use such datasets without typology, an approach is required that nevertheless is able to extract and encode semantic information to get relation maps for DL. To solve this case, we developed a specific type of relation map, the *multilayer map*, whose map conversion methods guarantee that the semantic information on room types and relations can be properly transformed into a relation map.

The basic approach of the multilayer map is the conversion based on hashing of values detected as possible room and relation types (e.g., via an attribute) rather than making a lookup in the typology. Based on cryptology techniques, hashing decodes byte information into a string of symbols of predefined size, e.g. to ensure that two files are identical, i.e. produce the same hash using the same hashing function. Applying the hashing methods to the room and relation semantics, given that the data is properly unified or was created with the same method, will result in the same string hashes for the same semantic entities. The hashes can then be decoded into integer or float values. For example, the MD5 hashing function always produces a hexadecimal string that can be converted into a decimal fraction.

A simple example of such conversion is the connection **living** <- **door** -> **bath** whose MD5 hash and the subsequent conversion from hexadecimal to decimal float will result in an array [0.89, 0.277, 0.637]. For the use in DL, a multi-layered 3D map can be constructed where the source room layer, target room layer, and

the relation type layer provide a separate matrix for each of these semantic entity types. This relation map type is inspired by the color scheme channels in an RGB image. For DL purposes, the original 3D, as well as 2D representation of the map (where source, target, and connection values are accumulated into one value) can be used. Figure 3 shows an example of conversion of an SBF to a multilayer map.

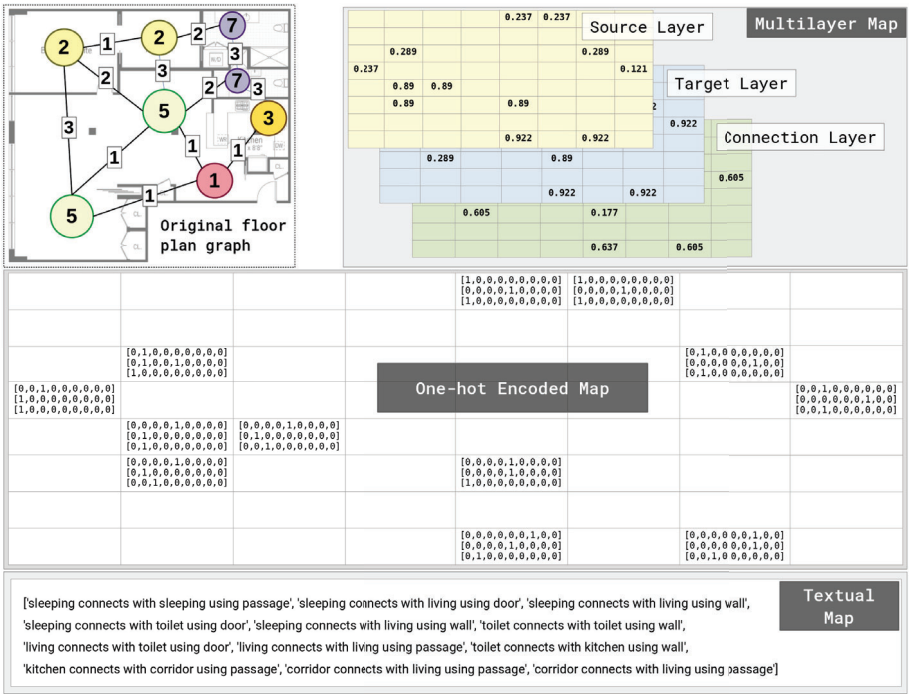

Figure 3. Original floor plan SBF and its conversions into multilayer map, one-hot encoded map, and textual map.

3.3. ONE-HOT ENCODED MAP

The conversion methods presented so far encode categorical data into numerical data and simple and zoned maps always summarize several pieces of semantic information in one numerical value. Depending on the position further left or further right in that number, the coded information has a larger or smaller influence on the numerical value. For example, in the current order of encoding in a simple relation map, the most significant digit encodes the source room, and the least significant digit encodes the relation. A change of the source room has a greater influence on the numerical value than a change of the relation. Also, there exists a risk that the assignment of categories to digits can be interpreted by the DL network as a ranking and a similarity measure for categories. In this case, using the typology shown in Figure 2, the difference between **storage** (9) and **corridor** (1) would be greater than between **toilet** (7) and **kitchen** (3), i.e. 9-1=8 vs. 7-3=4.

We introduce another representation, which is based on the classic *one-hot encoding* technique for categorical data (see Figure 3). In its simplest form, it is based on the simple relation map. Each field of the simple relation map is represented by three vectors, each of which encodes the category of the source room type, the target room type, and the relation type, respectively. Each vector has as many elements as there are categories for the entity type (room or relation type) with the highest amount of categories as required by DL. Each position in the vector corresponds to a category and can have either the value 1 (belongs to the category) or 0 (does not belong to the category). In each vector, the value 1 can appear exactly once because rooms and connections are uniquely assigned to categories. For this representation, the discussed influences do not play a role.

3.4. TEXTUAL RELATION MAP

The deep learning representations for spatial configuration presented in the previous sections try to encode the semantic information and varied room types as numerical values or as one-hot encoded vectors. The above-stated representations are usable as input tensors for a deep learning approach, but at the same time, these representations can be highly sparse and unadaptable. The text-based representation is designed to be adaptable to change in the number of room type or edge type categories while preserving the original shape of the tensors. Since the representation is text-based, different deep learning approaches such as text classification and sequence learning can also be applied to these representations.

The textual relation map is inspired by the simple relation map. In this representation, instead of encoding the semantic information using numerical values, sentences are used to represent a connection between two different rooms. For example, if two rooms are connected through a wall, then the textual formulation would be, **A connects with B using wall**. This representation also solves the problem of sparsity as for representing unavailable connection between two rooms instead of using 0 as the encoding, **'no connection'** is used. Figure 3 shows an example conversion of a spatial configuration into a textual relation map ('no connection' omitted due to limited space).

4. Evaluation

To explore optimal data representations in deep learning for topological and semantic features of a SBF, a preliminary *two-phase evaluation* using the straightforward classification task was performed. Using classification of data samples was selected for the evaluation due to an array of reasons. It is easier to perform classification, instead of more complex tasks such as data generation or sequence learning, and also easier to evaluate the performance of the models due to the presence of a labeled dataset and the built-in evaluation methods in the DL libraries. Additionally, the results can be used to help reduce the computational cost of searching for similar floor plan contexts in the AI-based prototype.

A total of 200 housing floor plans were initially at our disposal, while for training a DL model, larger amounts of data are required. Due to the lack of such amounts of data, it was decided to generate variations of the already present

spatial configurations using total of 15 different variation rules suggested by architecture domain experts. For example, the room types ‘sleeping’, ‘living’ and ‘room’ (the generic flexible type) can be freely exchanged in a one room apartment. The variationally generated floor plans were then checked by a specifically developed rule-based floor plan consistency checker to ensure that they adhere to the architectural rules removing from the final dataset those that do not pass the check. A total of 2544 housing floor plans made it to the final dataset.

For evaluation, the data set was labeled using a set of specific rules for the typology suggested by the architecture domain experts from the research project. The labels were divided in two different categories. The first category indicates the *number of habitable spaces* (i.e., sleeping, living, children, working, and room) in a spatial configuration. Again, the space ‘room’ was used a generic room to represent flexibility in the data. The second part indicates if the spatial configuration is *open* or *closed*, identified by whether there is *a passage between the kitchen and the living room*. Due to the above-stated labeling approach, it can be concluded that the floor plans have a strong correlation with the classes. The data set was separated into training and testing subset in relation 75% to 25%.

From the data representations presented in this paper, the multilayer map, one-hot encoded map, and the textual map were selected for the evaluation, as they were specifically developed for classification tasks using similar DL models and also make their debut in this paper. Other two map types (simple and zoned) were already evaluated before as mentioned in their respective sections.

In the first phase of the evaluation, a *multi-label classification* was performed using a total of 7 unique classes. Each spatial configuration of the dataset was assigned two labels, a number of habitable spaces, and if the layout is open or closed (e.g., “2 open”). In the second phase, a total of 10 unique classes was used for a *single-label classification* and the categories were combined into one single label for each building graph, resulting in, for example, “3closed”. The idea behind performing two runs for the classification using a different number of labels was to observe if the deep learning model can learn different semantic features for different graph types and how the number of labels influences the performance of the corresponding representation.

For both phases, a common deep learning model in the form of a convolutional neural network (CNN) using the out-of-the-box Keras API in the TensorFlow framework was constructed. All representation variants of this common model differed only in the dimensions of the input layer and the rest of the DL model structure was identical for all three of them: 1 Conv2D layer, 1 BatchNormalization, 1 MaxPooling2D, 1 Dropout, 1 Flatten, and 2 Dense layers. However, through some tuning phases, hyperparameters, such as the learning rate, batch size, or the number of epochs, were set optimally for each representation to ensure the best performance. For example, the number of epochs of 100, 1000, 1500 and the batch size of 128, 24, 24 were used in the single-label evaluation for the one-hot encoded map, the multilayer map, and the textual map, respectively.

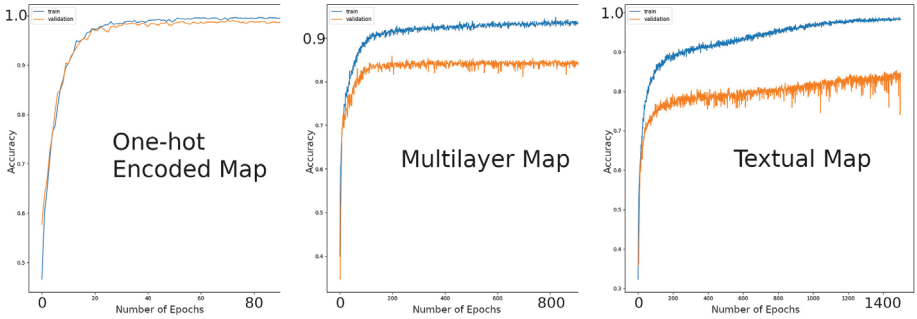

Figure 4. Results of the DL model training for the single-label classification. Blue curves represent the training accuracy, the orange ones the validation accuracy.

To evaluate the results of the model training it was decided to use the built-in evaluation methods implemented in the TensorFlow framework. In particular, the training and validation accuracy, as well as the training and validation loss were selected as the main performance metrics, as they provide the optimal overview of the stability and consistency of the models.

The results of both steps of the experiment revealed that the one-hot encoded map performed best in both classification phases and for all applied metrics. For the multi-label classification it achieved **96%** / **95%** on training and validation accuracy, in the single-label classification these values increased to **99%** and **98%** respectively (see Figure 4). The multilayer and textual maps performed worse in the multi-label classification: **90%** / **84%** for the multilayer and **90%** / **74%** for the textual map. During the single-label classification, the values improved: **93%** / **83%** for the multilayer map and **98%** / **83%** for the textual map (see Figure 4).

In terms of the loss calculation, the comparison of the representations provided a similar picture: the one-hot encoded map performed best and achieved the least loss value in both phases of the experiment. For the multi-label classification, this value was **1.4197** for training and **1.4876** for validation of the model. The multilayer map achieved the loss values of **1.5304** and **2.7472**, the textual map-based model achieved **1.4244** and **2.5508** accordingly. For the single-label evaluation phase, the one-hot encoded map could improve and achieve even lesser values: **0.0085** training loss and **0.0638** validation loss. However, other two models were able to improve as well: **0.0997** / **0.7089** for the multilayer map and **0.0382** / **1.0620** for the textual map.

One of the most significant observations of the evaluation was that the one-hot encoded map performed stable during the entire classification process, while the multilayer and the textual map representations provided different grades of instability during the training process (see Figure 4). Overall, it can be concluded that the one-hot encoded map performed better than the other two evaluated representations, achieving the first place in the first evaluation phase and confirming its performance in the second phase. On the high level, a tendency towards recognition of relevant semantic features within SBF-based relation maps could be observed, indicated by the overall training and validation numbers.

5. Conclusion and Future Work

In this paper, five different data representations for SBFs for use with common DL frameworks, all based on the common tensor-based structure "relation map", were presented. A classification task was performed to evaluate three of them. The results indicate that the DL models in the form of CNNs are able to process and understand the latent structure of the selected relation map types and the information contained in them. A max. validation accuracy of 98% was achieved for the winning type, the one-hot encoding map. For public use, the conversion methods are published under *https:github.com/metis-caad/roomconf-converter*.

In the upcoming experiments (to be submitted, e.g., to eCAADe 2021), relation maps will be much more comprehensively evaluated on further deep learning tasks (e.g., sequence learning or data augmentation) and examined on data not available in training or testing datasets. It is expected that there is no one-fits-all representation for all DL tasks, but the pros and cons of different relation map types for certain DL tasks can be outlined. We also intend to publish the data consistency checking methods used for the evaluation and discuss their limitations.

References

Arora, H., Langenhan, C., Petzold, F., Eisenstadt, V. and Althoff, K.D.: 2020, METIS-GAN: An approach to generate spatial configurations using deep learning and semantic building models, *ECPPM-2020/21*.

As, I., Pal, S. and Basu, P.: 2018, Artificial intelligence in architecture: Generating conceptual design via deep learning, *International Journal of Architectural Computing*, **16**(4), 306-327.

Eisenstadt, V., Langenhan, C., Althoff, K.D. and Dengel, A.: 2020, Improved and Visually Enhanced Case-Based Retrieval of Room Configurations for Assistance in Architectural Design Education, *ICCBR 2020*.

Hickman, G. and Krolik, J.L.: 2009, A graph-theoretic approach to constrained floor plan estimation from radar measurements, *IEEE transactions on signal processing*, **57**(5).

Langenhan, C.: 2017, Datenmanagement in der Architektur, *Doctoral diss., TU München*.

McCullough, M., Mitchell, W. and Purcell, P.: 1990, The Electronic Design Studio: Architectural Knowledge and Media in the Computer Era, *CUMINCAD*.

de Miguel, J.: 2019, Deep Form Finding-Using Variational Autoencoders for deep form finding of structural typologies, *CUMINCAD*.

Nauata, N., Chang, K.H., Cheng, C.Y., Mori, G. and Furukawa, Y.: 2020, House-GAN: Relational Generative Adversarial Networks for Graph-constrained House Layout Generation, *arXiv preprint arXiv:2003.06988*.

Newton, D.: 2019, Deep Generative Learning for the Generation and Analysis of Architectural Plans with Small Datasets, *CUMINCAD*.

Roth, J., Hashimshony, R. and Wachman, A.: 1982, Turning a graph into a rectangular floor plan, *Building and Environment*, **17**(3), 163-173.

Sharma, D., Gupta, N., Chattopadhyay, C. and Mehta, S.: 2017, Daniel: A deep architecture for automatic analysis and retrieval of building floor plans, *2017 14th IAPR ICDAR*, 420-425.

Shekhawat, K., Duarte, J.P. and thers, initials missing: 2019, A Graph Theoretical Approach for Creating Building Floor Plans, *CAAD Futures*, 3-14.

Steadman, P. and Mitchell, L.J.: 2010, Architectural morphospace: mapping worlds of built forms, *Environment and Planning B: Planning and Design*, **37**(2), 197-220.

Sun, C., Hsiao, C.W., Sun, M. and Chen, H.T.: 2019, Horizonnet: Learning room layout with 1d representation and pano stretch data augmentation, *IEEE CVPR*, 1047-1056.

Zhang, Z., Cui, P. and Zhu, W.: 2020, Deep learning on graphs: A survey, *IEEE Transactions on Knowledge and Data Engineering*.

SKETCH WITH ARTIFICIAL INTELLIGENCE (AI)

A Multimodal AI Approach for Conceptual Design

YIFAN ZHOU[1] and HYOUNG-JUNE PARK[2]
[1,2]*School of Architecture, University of Hawaii at Manoa*
[1,2]*{yifanz|hjpark}@hawaii.edu*

Abstract. The goal of the research is to investigate an AI approach to assist architects with multimodal inputs (sketches and textual information) for conceptual design. With different textual inputs, the AI approach generates the architectural stylistic variations of a user's initial sketch input as a design inspiration. A novel machine learning approach for the multimodal input system is introduced and compared to other approaches. The machine learning approach is performed through procedural training with the content curation of training data in order to control the fidelity of generated designs from the input and to manage their diversity. In this paper, the framework of the proposed AI approach is explained. Furthermore, the implementation of its prototype is demonstrated with various examples.

Keywords. Artificial Intelligence; Stylistic Variations; Multimodal Input; Content Curation; Procedural Training.

1. Introduction

Various media have been employed in the process of making conceptual design developments: sketches, drawings, physical or digital models, textual descriptions, and so on. The importance of sketches to delineate a design concept or its description has been highly appreciated by masters in architecture (Graves, 1977, Schildt, 1989, Moore, 2000). Furthermore, diversity of the media involved in the conceptual design augments the creativity and productivity of a designer. Sketches and textual descriptions have been instrumental for applying the implicit (tacit) and explicit knowledge in the conceptual design.

Based upon the premise that Artificial Intelligence (AI) is able to recognize qualitative patterns in data, various AI applications in design exploration have been developed for generating the design variations and suggesting the alternatives to meet given design goals with enhancing the adaptability, productivity, and quality of given input. The common processes of utilizing the AI applications are 1) data collection, 2) establishing artificial neural network (ANN) for machine learning, and 3) performing the training processes through the networks. As an ANN with multiple layers of generation and discrimination in deep machine learning process, Generative Adversarial Network (GAN) is developed for discerning

PROJECTIONS, Proceedings of the 26th International Conference of the Association for Computer-Aided Architectural Design Research in Asia (CAADRIA) 2021, Volume 1, 201-210.

subtle patterns in the given dataset. This pattern recognition extends the application of AI to the generation of 2-D and 3-D design alternatives (Russell and Norvig, 2002, Goodfellow et al., 2016).

Current AI-based design applications show their potential to learn from the dataset and extrapolate its learning into the creation of new alternatives in many design-related disciplines. The applications in architecture have been developed for the generation of 2-D images in plan and facade, and for their stylistic variations. With Pix2pixHD, a modified version of GAN, the neural network is trained to recognize the architecture plan drawings and generate the architecture plan based on the input color pattern diagram (Huang and Zheng, 2018). Chaillou further applies Pix2pix with supervised learning of selected architectural precedents to generate the variations of the floor plans of the precedents according to their program changes (Chaillou, 2019). Also, four stylistic variations (Baroque, Manhattan Unit, Suburban Victorian, Row-House) of the plans have been generated. The stylistic generation of a specific architect's residential plan and facade is performed using GAN (Newton, 2019). With a deep convolutional neural network (DCNN) model, the classification of various design projects is performed according to different architects (Yoshimura et al., 2019). Furthermore, the application of AI in design has been employed for augmenting a user's imagination by generating semi-abstract 'visual prompts' as emergent shapes for a human designer to use them as a starting point of design development (Schmitt and Weiß, 2018). Also, Google quickdraw research showcases the ability of artificial intelligence to automatically recognize various sketch inputs by the users and generate coherent sketch drawings (Ha and Eck, 2017) and could offer drawing refinement suggestions through the auto draw platform (Motzenbecker and Phillips, 2017).

In this paper, sketches and textual descriptions in conceptual design process are employed as multimodal inputs for generating AI's reproduced visions through a proposed procedural training as the visual prompts for a user's design inspiration. 70,000 architectural images are collected from the Internet, and 10,000 images from the collection are labeled according to architect, building category, and so on. Pix2Pix with a U-net structure (Isola et al., 2017), a conditional generative adversarial network (cGAN), is combined with procedural training for generating the variations of its predicted image. The stylistic variations have experimented with 1) sketch & single textual attribute, and 2) sketch & multiple textual attributes. The outcomes of the proposed training model are also compared to two existing GAN models in terms of the image quality and the versatility in the stylistic variations (Isola et al., 2017, Zhao et al., 2019) within the given dataset.

2. Multimodal Interactive AI Application

The proposed multimodal AI approach is composed of three parts: 1) Dataset, 2) Content Curation + Procedural Training, and 3) Sketch & Textual Input + Predicted Image Output.

2.1. DATASET

Different from the traditional Von Neumann computer system, machine learning is a science of training and learning models based on data (Samuel, 1959). The quantity and quality of the initial dataset are critical for the reliability of the outcomes from machine learning. A small dataset may lead to overfitting problems and a poor-quality dataset leads to poor outcomes.

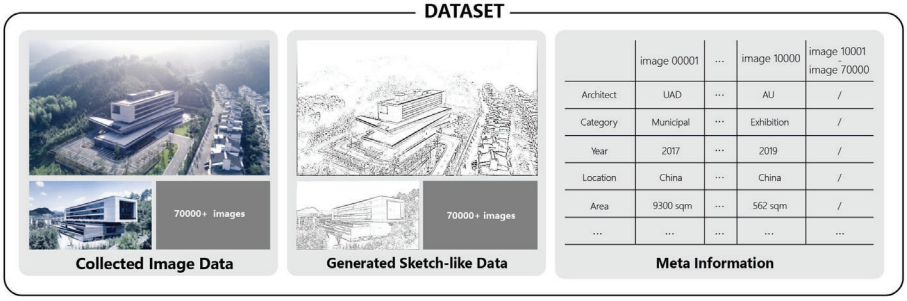

Figure 1. Dataset diagram.

In this paper, the pair of image datasets are prepared. One is the dataset of the images collected from the websites of various architect offices (Foster + Partners, GMP, Perkins and Will, Zaha Hadid Architects) by a python scripted web crawling system. The total number of images reaches 70,000. The other is the sketch-like line drawings paired with the collected images. In order to mimic the sketch input of an architect, the paired sketch-like line drawings are generated using XDog: Extended Difference-of-Gaussians (Sangkloy et al., 2017, Winnemöller et al., 2012). Though generated images using XDog are somehow different from what human sketches are, they still represent similarity to human sketches which often focus on the silhouette and outline of the objects. On the premise that the XDog images could somehow represent human sketches, at this moment, this research uses XDog images to represent human sketches. Human sketch uniqueness like distortion, deformation, and personal style of the sketch will be studied based upon the extended collection of human sketches in the future.

70,000 pairs of images are prepared for updating the parameters of the generator and discriminator at phase one training procedure of the proposed approach. 10,000 out of 70,000 initial pairs are labeled with textual attributes such as architect, building type, project year, project size, project location, and filtered through phase two training procedure. The dataset is randomly split into a 99% portion for training and a 1% portion for validation.

2.2. CONTENT CURATION + PROCEDURAL TRAINING

Our proposed procedural training is performed in a unique dataset pipeline with content curation. The proposed training is divided into two procedures. Both training procedures are performed using Pix2Pix with U-net structure. Phase one training procedure is to make sure the generator and discriminator get a global

understanding of the translation from sketch-like data to colored image. The phase one training takes all the images into the Generator and Discriminator and does the backpropagate(Rumelhart, Hinton et al. 1986). The parameters of the generator and discriminator like weights and biases are updated according to the loss calculated on the training dataset. After 20 epochs of training, parameters are restored. Phase two training procedure is to empower the generators with stylistic variations presented in Section 3. During the phase two training, a dataset filtering algorithm in the dataset pipeline shown in Figure 2 is introduced to curate the data input of the neural network. The dataset filtering algorithm divides the dataset into several categories according to textual attributes. Replicas of the restored parameters of the phase one training are prepared for each curated category. Parameters in each replica are only updated based on the corresponding curated dataset. After 100 epochs of training, parameters of each replica are restored. Currently, the curation of the dataset takes five different attributes (architect, building category, project size, project year and project location) into consideration. The combination of the attributes is scalable such as (architect), (architect + building category) and so on. Therefore, with the extension of the dataset and attributes, more complex textual training is possible.

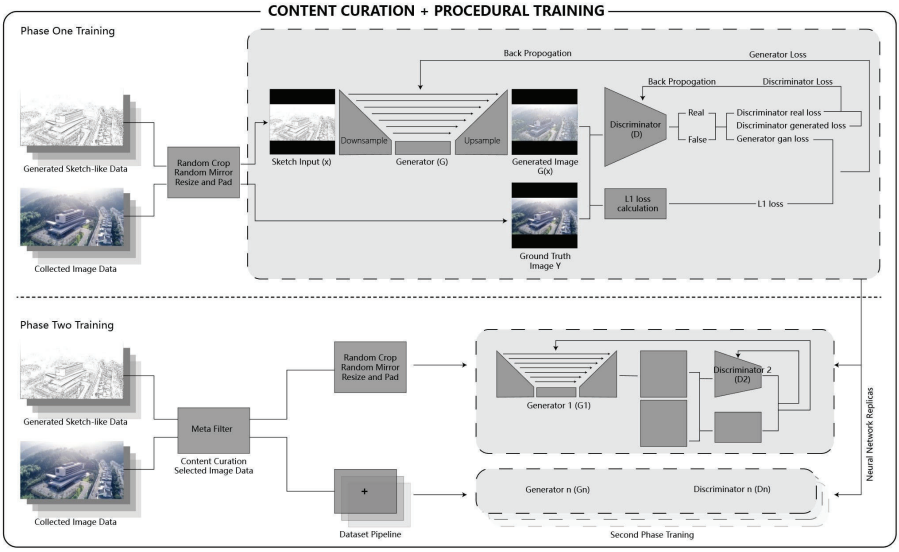

Figure 2. Content curation and procedural training.

Both collected image data and its sketch-like line drawing data are standardized as a [256,256,3] tensor for the input of the generator network. Through the down sample process and up sample process with skip connections, the generator G could output a [256,256,3] tensor as a predicted colored image G(s). The discriminator D takes the generated image G(s) or the ground truth image as the input [256,256,3] tensor and makes true or false judgment through a series of down sample processes. Through the adversarial training process, the generator tries to

fool the discriminator and the discriminator tries to tell the predicted image from the ground truth image. The phase one training procedure uses the recommended learning rate 2*10-4 and the phase two training procedure does a lower learning rate to ensure the stability of the general GAN training process. The updated parameters (weights and biases) through the backward propagation at the phase one training procedure will be recorded as the starting parameter for the phase two training procedures. And the parameters of the proposed approach are restored separately according to the curated data in the phase two training procedure. Loss metrics and inference results in both training dataset and validation dataset will be monitored during the training process to make sure if the training is functional.

2.3. SKETCH & TEXTUAL INPUT + PREDICTED IMAGE OUTPUT

The multimodal inputs (sketch and text) in the conceptual design process are available for generating stylistic variations of a predicted input image with Pix2Pix (Isola et al., 2017) with U-net structure through the content curation and two-step procedural training. Currently, contour-like line drawings or freehand sketches are used as a sketch input. Textual inputs are defined by the content curation of the 10,000 images with labeling. The supported attributes of the curation include architect, building category, and the combination of the architect and building category. Different textual attributes will lead the sketch translation into various results. The results are shown in section 3 Stylistic Variations.

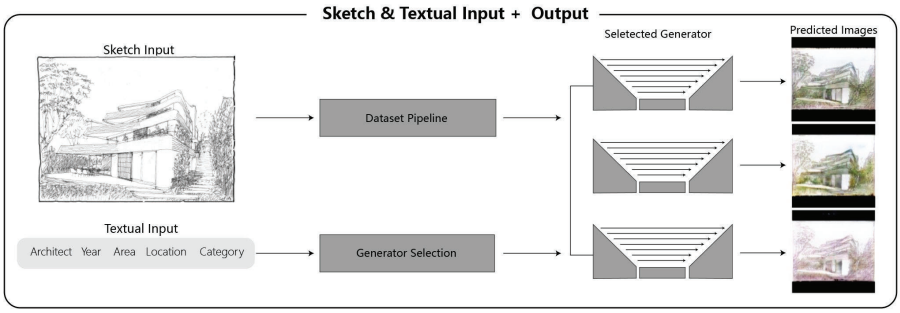

Figure 3. Sketch and textural input and output.

3. Stylistic Variations

The stylistic variations of the input sketch are generated with 1) single attribute of the textual input and 2) multiple attributes. The first experimentation of the single attribute of the textual was performed with the “Architect” attribute. The second was with “Building Type.” “Architect” and “Building Type” attributes are combined for the experimentation of the multiple attributes. Also, the different detail levels of the same input sketch are tested for the stylistic variations. The outcomes of the proposed training model within the given dataset are compared to two existing GAN models as a benchmark.

3.1. SINGLE ATTRIBUTE: ARCHITECT

In this single attribute stylistic variation experimentation, the authors take four representative architects (architecture offices) for instance, which are Foster + Partners, GMP, Perkins and Will, and Zaha Hadid Architects. The generator of the 4 attributes is trained on the 70000 images during the first phase of the procedural training process. For the second phase training, each of them is trained with selected data with the corresponding architect attribute information. As shown in Figure 4, different architect attributes lead to the various predicted styles accordingly. Visual prompts from different color inclinations, material combination preferences, and lighting effects could be observed in the following results. Multiple predicted results provide the user with quick conceptual design direction references.

Figure 4. Single attribute: architect.

3.2. SINGLE ATTRIBUTE: BUILDING TYPE

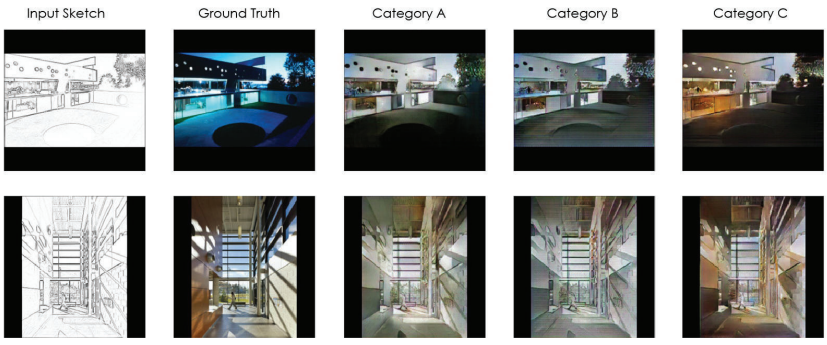

Figure 5. Single attribute: building type.

At the early stage of architectural design development, the comparative approaches of building types also provide an innovative starting point for testing different

architectural nuance. Manipulating the building type information could lead the design into different directions. Three typical categories are selected for highlighting the proposed approach's potential in predicting the colored image with the textual input. In figure 5, category A represents the house interiors and apartment interiors. Category B represents renovation projects. Category C represents hotels and restaurants. The emergent visual prompts from the changes could be also observed from the selected results.

3.3. MULTIPLE ATTRIBUTES: ARCHITECT + BUILDING TYPE

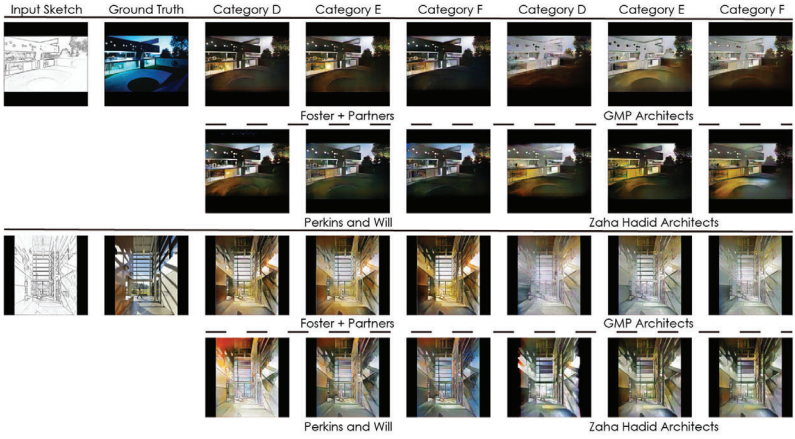

Figure 6. Multiple attributes: architect + building type.

The multiple attributes (Architect & Building Type) are performed with four architect choices and three building types. The outcomes show the scalability of multiple attributes that allows a user to build more complex textual input combinations with extended sets of attributes in the future. The versatility of the stylistic variations is demonstrated with category D (housings & hotels), category E (cultural building), and category F (pavilions and others) in Figure 6.

3.4. BENCHMARK

The existing machine learning models such as Pix2pix with U-net structure (Isola et al., 2017) and GAN techniques (Zhao et al., 2019) perform well on the CelebA dataset (Liu et al., 2015), including the images of prototypical figures such as human faces. This research reproduces the network and training strategy employed in the previous researches (Isola et al., 2017) (Zhao et al., 2019) and compares their results with the one from our method. The pix2pix network (Isola et al., 2017) is conditioned on the input image only. Thus, the network itself does not take the textual information as an input. Its predicted image's variation is led by dropout function in the U-net structure. As shown in Figure 7, its image quality is sharp while the variation led by its dropout function does not cover enough range of

design references. The GAN network structure (Zhao et al., 2019) takes the textual input in addition to a conditional image input. Figure 7 shows the versatility of the GAN network in making variations. However, the sharpness quality of its outcomes does not reach the one from the result of the pix2pix network. The proposed approach takes multimodal inputs such as image and textual information. The textual information is used to select the parameters of generator G to empower its stylistic generations. The comparison made in Figure 7 shows the advantage of our method in terms of the quality and versatility in the stylistic variations within a given dataset.

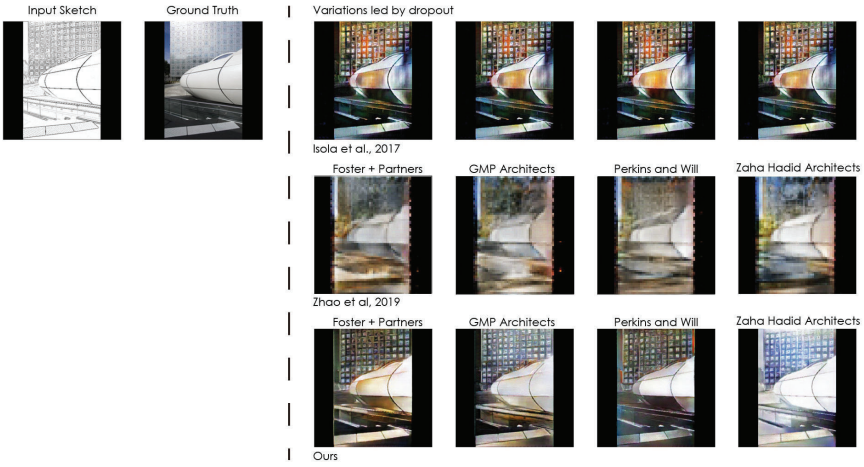

Figure 7. Benchmark with Pix2Pix (Isola et al., 2017) and GAN (Zhao et al., 2019).

3.5. DETAILS OF SKETCH INPUT

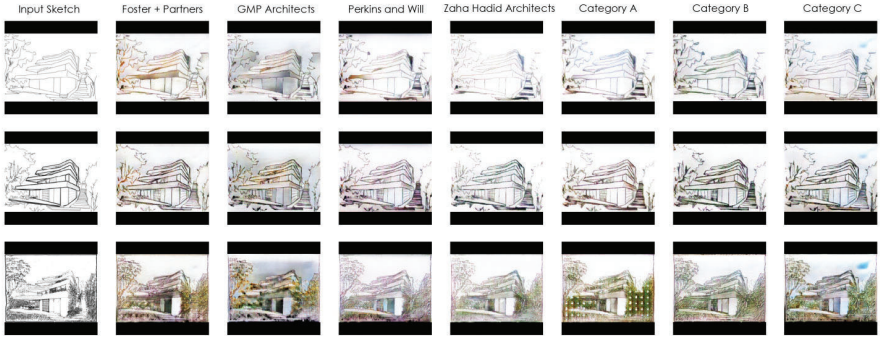

Figure 8. Comparison of sketch detail's influence on the predicted outcomes.

In real practice, architects might not come up with detailed sketches during the conceptual design phase. The different detail levels of sketch inputs are tested for finding the influence of the input details on the predicted images. As shown in Figure 8, in order to fully utilize the generator of the current approach, more detailed sketch input is encouraged for generating convincing images or more human sketches are needed to be collected in the future.

4. Discussion

In the process of making conceptual design developments, design inspiration comes from unexpected design changes as an emergent shape or ambiguous outcomes as a visual prompt (Mothersill and Bove, 2019). This proposed multimodal approach allows a user to engage in the design process with making stylistic variations as its feedback. In terms of conceptual design development, AI augmented visual prompts could act as a quick validation of the conceptual sketch, which could be used in the design discussion within the team or with the client. The versatility in the stylistic variations of the proposed approach could help architects with conceptual inspiration with multiple possible choices suggested by AI when they draw sketches at the early stage of design.

The two phases procedural training models with the content curation employed in this multimodal approach provides a way to manage the quality and diversity of the generated variations within the given dataset. The benchmark results show that the improvements from two existing GAN models in terms of quality and versatility in the stylistic variations have been realized in the proposed approach.

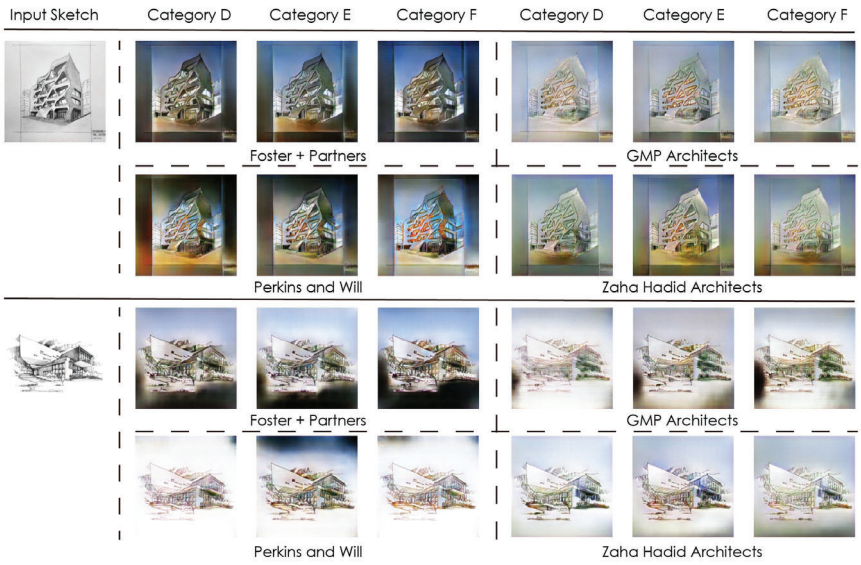

Figure 9. Predicted image based on sketch.

The results on the rough hand drawings in Figure 9 will be further improved by increasing the size of the dataset for the pairs of hand-drawing sketches and colored images in the future. Building up a platform for collecting the hand drawing sketches and colored images pair will be developed further.

References

Chaillou, S.: 2019, *AI + Architecture | Towards a New Approach*, Master's Thesis, Havard Graduate School of Design.

Goodfellow, I., Bengio, Y., Courville, A. and Bengio, Y.: 2016, *Deep learning*, MIT press Cambridge.

Ha, D. and Eck, D.: 2017, A Neural Representation of Sketch Drawings, *arXiv preprint*, arXiv:1704.03477.

Huang, W. and Zheng, H.: 2018, Architectural Drawings Recognition and Generation through Machine Learning, *Proceedings of the 38th Annual Conference of the Association for Computer Aided Design in Architecture (ACADIA)*.

Isola, P., Zhu, J.Y., Zhou, T. and Efros, A.A.: 2017, Image-to-image translation with conditional adversarial networks, *Proceedings of the IEEE conference on computer vision and pattern recognition*.

Liu, Z., Luo, P., Wang, X. and Tang, X.: 2015, Deep learning face attributes in the wild, *Proceedings of the IEEE international conference on computer vision*.

Michael, G.: 1977, Necessity for drawing-tangible speculation, *Architectural Design*, **47**, 384-394.

Moore, K.: 2000, Between the Lines: drawing, creativity and design, *Environments by Design*, **3**, 35-58.

Mothersill, P. and Bove, V.M.: 2019, Beyond Average Tools. On the use of 'dumb' computation and purposeful ambiguity to enhance the creative process, *The Design Journal*, **22**, 1147-1161.

Newton, D.: 2019, Generative Deep Learning in Architectural Design, *Technology| Architecture+ Design*, **3**, 2.

Rumelhart, D.E., Hinton, G.E. and Williams, R.J.: 1986, Learning representations by back-propagating errors, *Nature*, **323**, 533-536.

Russell, S. and Norvig, P.: 2013, *Artificial intelligence: a modern approach*, Pearson Education Limited.

Samuel, A.L.: 1959, Some studies in machine learning using the game of checkers, *IBM Journal of research development*, **3**, 210-229.

Sangkloy, P., Lu, J., Fang, C., Yu, F. and Hays, J.: 2017, Scribbler: Controlling deep image synthesis with sketch and color, *Proceedings of the IEEE Conference on Computer Vision and Pattern Recognition*.

Schildt, G.: 1989, *Alvar Aalto, the Mature Year*, Rizzoli, New York.

Schmitt, P. and Weiß, S.: 2018, The Chair Project: A Case-Study for using Generative Machine Learning as Automatism, *32nd Conference on Neural Information Processing Systems (NIPS 2018)*.

Winnemöller, H., Kyprianidis, J.E. and Olsen, S.C.: 2012, XDoG: an extended difference-of-Gaussians compendium including advanced image stylization, *Computers & Graphics*, **36**, 740-753.

Yoshimura, Y., Cai, B., Wang, Z. and Ratti, C.: 2019, Deep learning architect: classification for architectural design through the eye of artificial intelligence, *International Conference on Computers in Urban Planning and Urban Management*.

Zhao, J., Xie, X., Wang, L., Cao, M. and Zhang, M.: 2019, Generating photographic faces from the sketch guided by attribute using GAN, *IEEE Access*, **7**, 23844-23851.

ARCHITECTURE, LANGUAGE AND AI

Language, Attentional Generative Adversarial Networks (AttnGAN) and Architecture Design

MATIAS DEL CAMPO
[1] *Taubman College of Architecture and Urban Planning, University of Michigan*
[1] *mdelc@umich.edu*

Abstract. The motivation to explore Attentional Generative Adversarial Networks (AttnGAN) as a design technique in architecture can be found in the desire to interrogate an alternative design methodology that does not rely on images as starting point for architecture design, but language. Traditionally architecture design relies on visual language to initiate a design process, wither this be a napkin sketch or a quick doodle in a 3D modeling environment. AttnGAN explores the information space present in programmatic needs, expressed in written form, and transforms them into a visual output. The key results of this research are shown in this paper with a proof-of-concept project: the competition entry for the 24 Highschool in Shenzhen, China. This award-winning project demonstrated the ability of GraphCNN to serve as a successful design methodology for a complex architecture program. In the area of Neural Architecture, this technique allows to interrogate shape through language. An alternative design method that creates its own unique sensibility.

Keywords. Artificial Intelligence; Machine Learning; Artificial Neural Networks; Semiotics; Design Methodology.

Figure 1. Attentional Generative Adversarial Network - Sample of Result.

PROJECTIONS, Proceedings of the 26th International Conference of the Association for Computer-Aided Architectural Design Research in Asia (CAADRIA) 2021, Volume 1, 211-220.

1. Problem

When Walter Gropius, at the beginning of his career, started to work in Peter Behrens office, he kept a terrible secret: he could not draw (Wigley 1998). He struggled with this deficiency in the environment of the Behrens office but famously became proficient in dictating drawings to his collaborators, demonstrating the ability of language to describe the complex material and spatial relationships in an architectural project (Führ, 1997). Synonymously Sol LeWitt expanded the concept of description into an entire career, dedicated to the efficacy of language (as instructions) and foreshadowing the emergence of programming and scripting as a means of artistic and architectural expression (Miller, 2016). So, what is the relationship of language to architecture?

An answer to this question could fill tomes. Therefore, for the sake of an appropriate length of the paper, the authors would like to rely on an abbreviated discussion on language, semiotics, semantics, and the implementation of language in machine learning (ML) processes. On a simple level language is capable of producing both the symbolic and social dimension of spaces, aiding in the calcification of these dimensions in the form of the built environment. To give the reader more background please allow for a brief excursion into Semiotics and its meaning for the project presented in this paper. Breaking down language means observing its constituting parts first: signs. A sign can be defined as a physical subject that carries meaning and is formed by the combination of signifiers manifesting a phonological image of the world. In addition, it contains a conceptual image of the world which can be described as its *signification*. In order to understand the meaning of other signs, it is necessary to untangle its structural relationships (Peirce, 1977) - akin to the structural performance of a building.

This base gave rise to two distinct branches of interrogation: the semiotics of communication and the semiotics of signification (Xanthos, 2010) - both of which play a distinct role in the application of AttnGANs (fig.1) in general. The former -semiotics of communication- is concerned with the exploration of the signs within the domain of communication and thus centers around aspects of human language. The latter -semiotics of signification- considers that any phenomenon that signifies anything can be considered part of the domain of semiotics, in doing so it covers a far larger territory than language alone. A territory that includes symbolic cultures that expand into material cultures (de Landa, 2016): Brand Logos, Instagram Images, YouTube videos, TikTok, memes, paintings, sculptures, architectures. This has been exemplarily laid out by Roland Barthes in his writings on the semiotics of signification which discusses the plurality of meaning in language as well as concepts of denotation and connotation. With this background in mind, we can expand this idea to the nature of the dataset used in the example presented in this paper. The database, Microsoft COCO (Common Objects in Context) was used to generate the images that resulted in the basic 3D models of the project. The database was primarily created not with architecture in mind, but for object recognition. As discussed in the previous section -sign, signifier, signification (Barthes, 1968) - language contains the toolset for recognizing the world. With this in mind, we have to consider in addition that an object is part of a scene - and thus to achieve a better object recognition, scene recognition is key (Xu et al,

2018). COCO achieves this by collecting images of everyday scenes that contain common objects contextualized in their natural environment. These objects are then labeled using per-instance segmentation in order to be able to localize the object in the scene more precisely. Microsoft employed a crowd worker (Jäger et al, 2019) approach in order to create more than 2.5mio labeled instances in 328.000 images which included instance spotting and instance segmentation. Project 24 Highschool (Fig.2) used this database in an alternative fashion. Instead of using it for the detection of objects in an image - for example for facial recognition, traffic control, object sorting, or the likes, we used the database in a generative role, reversing the flow of information in order to create images rather than analyzing them with the help of the labeled database. In order to do so, we employed an AttnGAN.

Figure 2. The PE center and dorms of the 24 Highschool. This image shows the distinct hand of the GraphCNN in full color. The coloration created by the process was embraced and forms a distinct feature of the project.

2. Methodology

In order to describe our materials and methods, we will rely on the example of the proof-of-concept project 24 Highschool Shenzhen. It was important for the authors to demonstrate the efficacy of the approach by implementing it into a demanding design process. The practice SPAN (Matias del Campo & Sandra Manninger) was invited to participate in a competition for the realization of a large new Highschool with 110.000m2 providing space for around 3000 Students. The program included classrooms, multipurpose hall, laboratory building, fab lab, physical education building, dorms, canteens and outdoor sporting grounds. The structural engineering was done by Bollinger & Grohmann. A project of this size demands a considerate positioning within the urban texture. The site is located in the northwest outskirts of Shenzhen and is in close proximity to the sea. The wedge-shaped site has its highest point in the northwest corner, eight-meter above sea level, and slopes from there towards the southeast.

2.1. INITIAL MODELING

In a first step a series of raw massing models were generated in Maya, in order to explore various primary design directions. A decision was reached very quickly to position the masses of the school along a North/South axis, with a set of classroom clusters strewn along the south border of the site. Making use of the natural topography of the site helped to avoid building under the water table, thus implementing the requested underground parking without the costs of building under the water table. The natural slope of the site was accentuated by positioning the tallest volumes (the dorm towers) on the highest point of the site. This model provided the possibility to implement the competition rules, site boundary restrictions and height restrictions to a pragmatic model in order to make sure to comply with FAR rules, local building code and the competition program. In a future step plans are in place to apply this modeling step with the aid of a parametric model in order to increase the speed up the time needed to check the model for its viability. While one group in the office was working on the raw massing, another team was working on images created with the AtnnGAN.

2.2. ATTNGAN

Generating images automatically based on natural language descriptions is a fundamental problem in many applications, such as in computer-aided design and art generation, and serves as a propellant in multimodal learning research and inference across vision and language, as evidenced by the increased research activities in this area of inquiry (Zhang, 2017). Attentional Generative Adversarial Network (AttnGAN) allow attention driven, multi-stage refinement for fine-grained text-to-image generation. Attention in Neural Networks imitates the way that humans are able to concentrate on particular aspects of their sensory input and blend out the rest around them. The architecture of the AttnGAN consists of two components. component one is an attentional generative network (Xu, 2018) that contains an attention mechanism that draws different sub-regions of the image. The focus is on words that are most relevant to the sub-region being

drawn. The generative network uses initially a global sentence vector to generate a low-resolution image. Subsequently, it uses the image vector in each sub-region to query word vectors by using an attention layer to form a word-context vector. The regional image vector is then combined with the corresponding word-context vector to form a multimodal context vector. These form the basis on which the model generates new image features in the surrounding sub-regions, which results in higher resolution pictures with more details at each stage. Component two in the AttnGAN is a Deep Attentional Multimodal Similarity Model, (DAMSM). Using both the global sentence-level information and the fine-grained word-level information, the DAMSM can compute the similarity between the generated image and the sentence. Therefore, an additional fine-grained image-text matching loss for training the generator is provided by the DAMSM. Co-author Alexa Carlson translated the AttnGAN algorithm to operate with the COCO database. The sentences used with the AttnGAN Algorithm were a combination of sentences derived from the program of the buildings and descriptions of the activities in these buildings. For example:

- Multipurpose hall: It can be used as a theater to hold lectures and events.

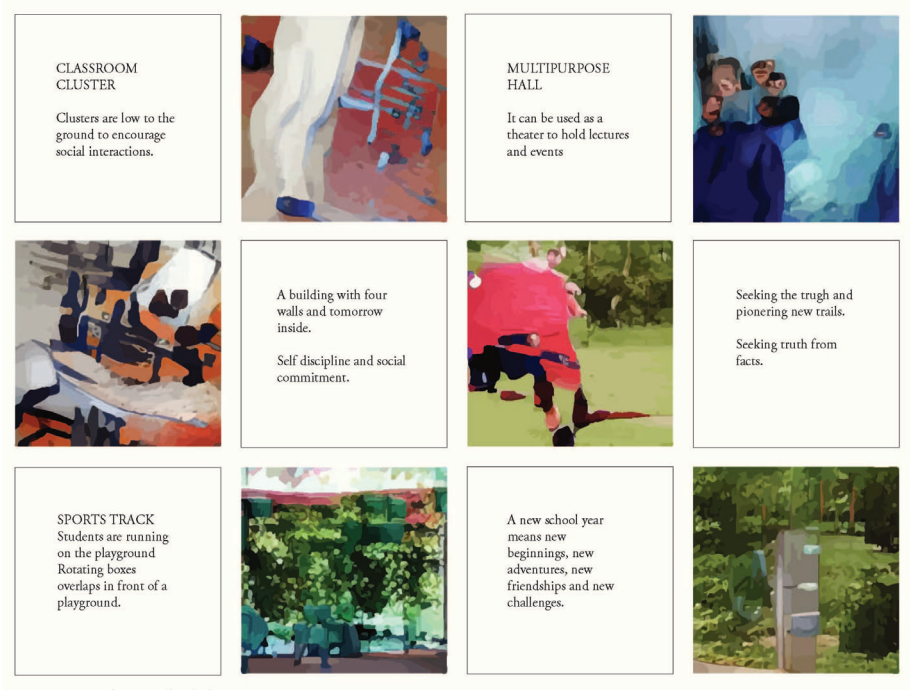

Figure 3. Examples of results of the AttnGAN.

2.3. GRASSHOPPER 3D

The results of this process can be seen in figure 3 these various images were used to inform the function and aesthetics of the buildings on the site. Using Grasshopper 3D the images were analyzed with the image mapper and subdivided into color patches. These color patches provided the blueprint to subdivide the larger 3D volumes that were created in the first round of modeling. An automated distribution pattern provided the vertical position and extrusion height of the volumes. Several passes of volume subdivision were employed in order to find the right balance between different scales and resolutions of the subdivision scheme. This step is certainly something that needs further exploration as it includes a portion of top-down design methodology, which contradicts the ambition to use an entirely emergent approach to design.

3. Discussion

3.1. CONTEXT OF THE DESIGN

The Northwest of Shenzhen is currently under rapid development and provides the larger population for this school project. The trapezoid shaped site has a longer side facing south and a short side facing north. The highest point of the site is in the Northwest corner. It falls from there towards south and east. The design team made an intentional decision to use the given topography of the site in the best possible way. It is best visible in the section (fig4) of the North South Axis:

Figure 4. Section .

The resulting design draws its qualities from the interplay of a well-balanced overall design, and the architectonic considerations put into each and every building. Although the building morphologies are distinctly different, and driven by its inherent programmatic needs, all of them together form a larger whole that provides students, faculty, administration and staff with a state-of-the-art school environment, that responds to the educational needs of this specific population. In addition, it provides a point of identification. Circling back to the conversation in the introduction of this paper it can be stated that this project complies with the semiotics of signification, which considers that any phenomenon that signifies anything can be considered part of the domain of semiotics, in doing so it covers a far larger territory than language alone. Thus the project demonstrates the ability of a Machine Learning processes to provide semiotic meaning to architecture through the use of language as design input.

Figure 5. Axonometry of Project.

4. Results

The use of AttnGAN (fig.6)as an architectural design technique is in its nascent state, thus it is difficult to position this project within a particular set of projects. Rare examples of computationally savvy architects testing the waters of AttnGAN exist, such as the works of Miloš Ilić (Silic, 2020) Much more common than the use in architecture is the application of AttnGAN in the arts (Amaya, 2020) and in fashion (Yi, 2019) though to describe them as common might be quite a stretch generally speaking. More successful would be an approach to contextualize the work along the lines of the use of language as a design environment. As a placeholder for a larger discussion on language and architecture, the authors will only mention Christopher Alexander - who is to this day notoriously unpopular with architects (Wright Steenson, 2017). This launches us directly back to the discussion on Semiotics in the introduction to this paper. Why is Semiotics of interest when discussing design methods based on Artificial Neural Networks? (For the record AttnGANs belong to the family of Artificial Neural Networks) Exactly because Semiotics can be considered a prime example of a theory of the artificial and thus occupies a central position in understanding phenomena of design. The differentiation between the analytic and the synthetic is akin to the liaison between design and semiotics, thus semiotics strives to talk about the environmental element of design which is so essential to narratives of architecture design based on symbolic cultures (signs, scripts, code, signifier, etc.). These conversations ultimately have to turn towards aesthetics, in order to conduct a

survey of emerging milieus. In the frame of the conversation within this paper aesthetics is connotated (Berrio-Zapata et al, 2015) with the parallel mapping of the environment, the articulation of the environment, and the alternative nature of any design process - leading to the assumption that within Neural Architecture (fig.7), design and aesthetics take the same position and value. In conclusion, this also means that signs can be artificial, or rather that signs can be considered theories of constructed meaning, which includes design. There is a long history in the relationship of semiotics and design - not only in design methodologies but also in its pedagogy. This is for example evidenced in the way that Max Bill conducted his studios at Ulm (Betts, 1998), the pedagogical alternatives to the Beaux-Arts methodologies established in France and Italy post-1969 (Holt, 2017), the long-standing enamoration of Umberto Ecco with architecture and urbanism (Leach, 1997), Roland Barthes interrogation of fashion (Barthes, 2006), Anne Beyaer-Geslin's research on semiotics, design, and aesthetics (Beyaert-Geslin, 2012), and so on and so forth. The common denominator for a design theory gravitating around ideas emerging from Semiotics is the search for a language of design (Holt, 2017).

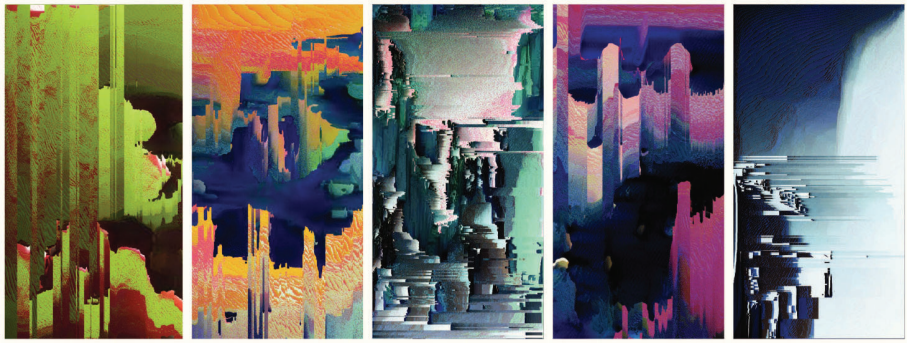

Figure 6. Result from the AttnGAN.

Figure 7. Translation into 3D models.

The results of the approach presented in this paper can be positioned exactly

along this line of thinking. The search for a language of design based on the artificial creation of signs and signifiers. The major finding of this paper is -apart from the creation of a theoretical basis for the application of language in a NN driven design method - the proof of concept that this approach can produce viable architectural designs. The presented method still needs major work. For example: the design method primarily creates either exteriors or interiors, but not both at once and interdependently. Steps such as the initial massing modeling, the exact nature of the plans and details of the 3D models are introduced in a top-down method. It would be of interest to explore in further research the possibility to automatize more of the process, in order to interrogate the emergent properties of the artificial creation of signs. As stated above, Semiotics is a perfectly fitting thinking school in regard to its consideration of the artificial.

We started the paper with the story of Walther Gropius and his terrible secret: the inability to sketch anything. He overcame this problem by describing his ideas in a lingual fashion to others around him who converted his language into images. We presented in this paper a possibility to convert this terrible secret into a design weapon. One that oscillates between the interrogation of language, inquiries aspects of the artificial, and its role in contemporary design culture. One that creates images somewhere between abstraction and the surreal full of instances of estrangement and defamiliarization in an architecture that can be described as something different, alien, strange and wonderfully beautiful - maybe the first genuine 21st century architecture.

Figure 8. An example of Neural Architecture: Laboratory Building.

References

Amaya, N., Nieman, N., Prakash, R. and Rahman, F.: 2020, “Generating Album Artwork from Lyrics” . Available from <https://medium.com/@nickn9715/generating-album-artwork-fro

m-lyrics-699b7d57a92d> (accessed 13th December 2020).
Barthes, R.: 1968, *Elements of Semiology*, New York: Hill & Wang, New York.
Barthes, R. and Stafford, A.: 2006, *The Language of Fashion*, Berg, Oxford.
Berrio-Zapata, C., Moreira, F.M. and César Gonçalves, R.: 2015, Barthes' Rhetorical Machine: Mythology and Connotation in the Digital, *Bakhtiniana: Revista de Estudos do Discurso*, **10**(2), 135-157.
Betts, P.: 1998, Science, Semiotics and Society: The Ulm Hochschule Für Gestaltung in Retrospect., *Design Issues*, **14**(2), 67-82.
Beyaert-Geslin, A.: 2012, *Sémiotique du design*, Presses Universitaires de France, Paris.
Führ, E.: 1997, Werk Räume, *Wolke Magazin – Architektur Sprache*, **2.JG**(Heft 2), 56-67.
C. S. Hardwick and V. Welby Gregory (eds.): 1977, *Peirce, C. S., and Welby-Gregory, Victoria (Lady Welby), Semiotic and Significs: The Correspondence between C. S. Peirce and Victoria Lady Welby*, Indiana University Press, Bloomington and Indianapolis.
Holt, M.: 2017, Semiotics and design: Towards an aesthetics of the artificial, *The Design Journal*, **1**, 332-341.
Jäger, G., Zilian, L.S. and Hofer, C.: 2019, Crowdworking: working with or against the crowd?, *Proceedings of the J Econ Interact Coord 14*, 761–788 .
de Landa, M.: 2016, *Assemblage Theory*, Edinburgh University Press, Edinburgh, UK.
N. Leach (ed.): 1997, *Rethinking architecture : a reader in cultural theory*, Routledge, London.
Michela, D. and Zingale, S.: 2017, Semiotics in Design Education. Semiotics by Design,, *The Design Journal*, **20**(1), 1293-1303.
Miller, M.: 2016, Code Art Rooted in An Unlikely Era: The 1960's,, *Fast Company*, **Innovation by Design**, 43-56.
Reed, S., Akata, Z., Mohan, S., Tenka, S., Schiele, B. and Lee, H.: 2016, Learning what and where to draw., *ICML*.
Reed, S., Akata, Z., Yan, X., Logeswaran, L., Schiele, B. and Lee, H.: 2016, Generative adversarial text-to-image synthesis., *ICML*.
Silic, M.: 2020, "AI-Architecture-AtnnGAN" . Available from <http://spacecollective.org/milosilic/9169/Ai-Architecture-AttnGAN> (accessed 13th December 2020).
Wright Steenson, M.: 2017, *Architectural Intelligence – How Designers and Architects Created the Digital Landscape*, MIT Press, Cambridge, Massachusetts.
Wigley, M.: 1998, Whatever Happened to Total Design?, *Harvard Design Magazine*, **2**(No.5), 52-63.
Xanthos, N.: 2012, Wittgenstein, *Signo*, **1**, 23-32.
Xu, T., Pengchuan, Z., Huang, Q., Zhang, H., Gan, Z., Huang, X. and He, X.: 2018, AttnGAN: Fine-Grained Text to Image Generation with Attentional Generative Adversarial Networks, *Proceedings of the 2018 IEEE/CVF Conference on Computer Vision and Pattern Recognition*, 1316-1324.
YI, Z.: 2019, *Text-to-image Synthesis for Fashion Design*, Master's Thesis, KTH.
Zhang, H., Xu, T., Li, H., Zhang, S., Wang, X., Huang, X. and Metaxas, D.: 2017, Stackgan: Text to photo-realistic image synthesis with stacked generative adversarial networks, *ICCV*.

MULTI-OBJECTIVE OPTIMISATION OF A FREE-FORM BUILDING SHAPE TO IMPROVE THE SOLAR ENERGY UTILISATION POTENTIAL USING ARTIFICIAL NEURAL NETWORKS

XIN ZHAO[1], YUNSONG HAN[2] and LINHAI SHEN[3]
[1,2,3]*School of Architecture, Harbin Institute of Technology; Key Laboratory of Cold Region Urban and Rural Human Settlement Environment Science and Technology, Ministry of Industry and Information Technology, China*
[1]*20S034010@stu.hit.edu.cn* [2]*hanyunsong@hit.edu.cn*
[3]*forestoshen@qq.com*

Abstract. Optimisation of free-form building design is more challenging in terms of building information modelling and performance evaluation compared to conventional buildings. The paper provides a "Photogrammetry-based BIM Modelling - Machine Learning Modelling - Multi-objective Optimisation" framework to improve the solar energy utilisation potential of free-form buildings. Low altitude photogrammetry is used to collect the building and site environmental information. An ANN prediction model is developed using the control point coordinates and simulation data. Through parametric programming, the multi-objective algorithm is coupled with the ANN model to obtain the trade-off optimal building form. The results show that the maximum solar radiation value in winter can increase by 30.60% and the minimum solar radiation in summer can decrease by 13.99%. It is also shown that the integration of ANN modelling and photogrammetry-based BIM modelling into the multi-objective optimisation method can accelerate the optimisation process.

Keywords. Multi-objective optimisation; Artificial neural network; Free-form shape building; Solar energy utilisation.

1. Introduction

Solar radiation is one of the most important factors in building design as it directly affects the heating and cooling energy demand. Solar radiation is even more critical in free-form building design as self-occlusion significantly affects solar energy utilisation. The optimisation of free-form buildings is more time-consuming than that for conventional buildings (Jin and Jeong, 2014) and new optimisation methods are expected to be adopted in the early stages of design.

Multi-objective optimisation models could identify the trade-offs between different and conflicting aspects of potential solutions and provide scientifically sound decision support (Asadi, Silva and Antunes, 2014). There were many studies focused on multi-objective optimisation of buildings. Jin and Jeong

PROJECTIONS, Proceedings of the 26th International Conference of the Association for Computer-Aided Architectural Design Research in Asia (CAADRIA) 2021, Volume 1, 221-230.

(2014) explored the applicability of optimisation methods to minimise the external thermal load of free-form buildings using a genetic algorithm. Zhang, Zhang and Wang. (2016) developed a multi-objective optimisation model to maximise solar radiation and space efficiency and minimise the shape coefficient of a free-form building located in the severe cold region of China. Camporeale and Mercader-Moyano (2019) applied a multi-objective genetic algorithm to modify the high-rise building shape and reduce energy consumption. Ciardiello et al. (2020) proposed a multi-objective approach to optimise the building envelope and reduce energy demand. It is found that building performance can be improved by multi-objective optimisation. However, the process of multi-objective optimisation using simulation data is very time-consuming, particularly when several variables are involved.

Since 2010, many researchers have shown that a machine learning-based model can predict building performance more efficiently than simulation software. In order to reduce the time requirements of the optimisation process, work has been carried out on combining the machine learning model with multi-objective optimisation algorithms. Si et al. (2019) applied different multi-objective optimisation algorithms with ANN models to a newly built tourist centre to improve the indoor thermal comfort and minimise energy demand. Sun, Liu and Han (2020) implemented a multi-objective optimisation design method based on ANN on a public library to improve daylighting, lower energy and operating costs. Seyedzadeh et al. (2020) employed a Random-Forest (RF) model combined with a multi-objective optimisation (MOO) algorithm to predict building heating and cooling loads. Bagheri-Esfeha, Safikhanib and Motahar. (2020) performed multi-objective optimisation using ANN to minimise the heating and cooling loads in a residential building integrated with phase change materials (PCM). These works showed how, with the aid of machine learning models, the process of multi-objective optimisation can be accelerated considerably. However, these examples generally relate to residential buildings which are usually in regular form and there is very limited research focused on the optimisation of free-form buildings. Research that combines multi-objective optimisation and artificial neural networks with solar energy utilisation in severe cold areas is also limited. Moreover, there is still an issue with the heavy time requirements for BIM modelling and the accuracy of this process cannot be guaranteed.

The purpose of the paper is to develop a novel multi-objective optimisation method combining photogrammetry-based BIM modelling, machine learning modelling and multi-objective algorithms to improve the solar radiation utilisation of a free-form building.

2. Methodology

The framework of the proposed method consists of the three steps as shown in Figure 1. The first step is photogrammetry-based BIM modelling. Low altitude photogrammetry is used to collect the building and site environmental information, and a parametric model of the built environment is generated in Grasshopper.

The second step is ANN-based prediction modelling. The structure of the ANN

model is proposed according to the optimisation objective and decision variables. Latin Hypercube Sampling (LHS) is used to generate the input dataset used to train the ANN model. The simulation tools calculate the solar radiation for each group of input datasets, providing the output from the ANN-based prediction model. The ANN is then trained, validated and tested based on the input and output datasets generated in the above steps.

The third step is the performance-driven optimisation process. The multi-objective engine, Wallacei, is launched to conduct the multi-objective optimisation and calculate the optimal solutions coupled with the ANN model.

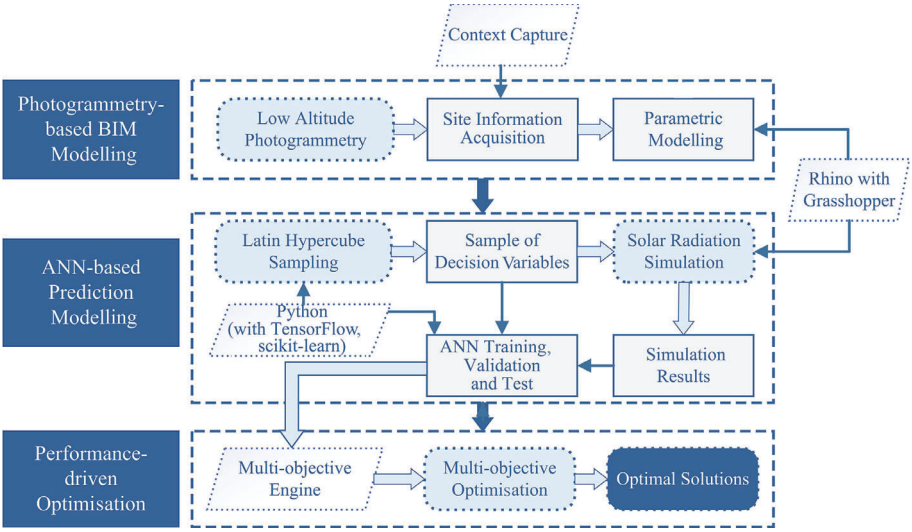

Figure 1. The framework of the proposed method.

2.1. LOW ALTITUDE PHOTOGRAMMETRY AND BIM MODELLING

An Unmanned Aerial Vehicle (UAV) mounted with a camera is used to collect the building and site environmental information. A point cloud can be extracted from the photographs taken by the UAV. A triangular mesh model of the photographed area is then generated, consisting of the surroundings, the target building and the square models. A parametric model of the target building is developed in Rhino and Grasshopper, allowing the coordinates of the main curves (the control points) to be modified to optimise the shape of the building.

2.2. ARTIFICIAL NEURAL NETWORKS

The structure of the ANN used in this work is characterized as a feedforward MLP network. The control-point coordinates are selected as the optimisation variables, and these are also the input variables to the ANN model. A total of 39 input variables are used to represent the variation of the six curves' control points. In order to reduce the size of the training and test dataset while retaining

the characteristics of the data, Latin hypercube sampling (LHS) is used to generate small representative data samples. In this study, 5000 sets of data are generated, each consisting of 39 numbers ranging from 0 to 1.

2.3. MULTI-OBJECTIVE OPTIMISATION

2.3.1. Optimisation objectives

The two optimisation objectives are the maximum solar radiation in winter and the minimum solar radiation in summer, which are contradictory in nature. As the reference building is located in the severe cold zone of China, the maximum solar radiation in winter has a higher weighting.

2.3.2. Decision variables and constraints

The decision variables are the variation of coordinates of the control points which define the main curves and determine the shape of the surfaces.

For a free-form building in the severe cold region, the constraints may arise from the environment which includes the climate and the social conditions including government regulations and standards. The domains and the steps selected for the variation of the variables need to be considered carefully since the appropriate values enable the optimisation process to proceed smoothly and in a reasonable shape.

2.4. PLATFORM

A UAV model is constructed on the Context Capture platform, and the BIM model is built in Rhino and Grasshopper. LHS is implemented using Python. The simulation data used as the output data for the ANN is acquired with the help of Ladybug. The ANN is trained, validated and tested with Python coupled with TensorFlow and the scikit-learn module. The saved ANN model is then loaded into Grasshopper with the help of GH_CPython and the multi-objective optimisation engine, Wallacei is used to calculate the Pareto frontier. The experiments are performed on a computer with a Windows 10 operating system (16 core 3.0GHz processor, 48G RAM).

2.5. REFERENCE BUILDING

The building referenced in this case study is the Harbin Opera House, designed by MAD Architects and located on the Cultural Centre Island of Harbin, China. The building form is composed of free-form surfaces. The distribution of solar radiation on the surface changes with the undulation of the free-form surfaces and is affected by the surrounding environment.

3. Results and discussion

This section illustrates how the proposed method is used to maximise the solar radiation gain in winter and minimise it in summer.

3.1. RESULTS FROM PHOTOGRAMMETRY-BASED BIM MODELLING

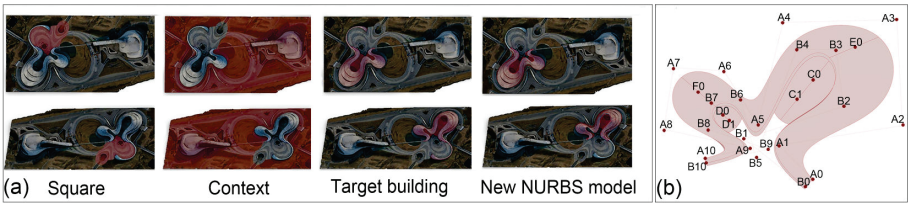

Figure 2. Different parts of photogrammetry-based BIM model and control points of the reference building a) different parts of photogrammetry-based BIM model, b) control points of the reference building.

Table 1. The steps and domains for the movement of the control points.

Curve	Control points	Step			Domain					
		Xstep	Ystep	Zstep	Xmin	Xmax	Ymin	Ymax	Zmin	Zmax
A	A0	1	1	0	20	10	-5	10	——	——
	A1~A8	1	1	0	-25	25	-25	25	——	——
	A9	1	1	0	-25	25	5	10	——	——
	A10	1	1	0	0	20	0	10	——	——
B(points on Curve B move along the vectors between points on Curve A and original points on Curve B)	B0~B4		1			-20			20	
	B5		1			-20			-10	
	B6~B9		1			-25			25	
	B10		1			0			20	
C	C0~C2	——	——	1	——	——	——	——	-30	30
D	D0~D2	——	——	1	——	——	——	——	-10	10
E	E0	——	——	1	——	——	——	——	-30	30
F	F0	——	——	1	——	——	——	——	-10	10

Through low altitude photogrammetry and 3D reconstruction, the UVA model is built. As illustrated in Figure 2, it is divided into three parts on the Rhino and Grasshopper platform, namely the target building, the square and the context, and a new NURBS (non-uniform rational basis spline) surface is modelled. The model is defined by 6 curves with a total of 39 control points. The variation of the points provides the input variables to the ANN and the decision variables for multi-optimisation. The steps and domains for the variation of the control points are shown in Table 1.

3.2. RESULTS OF ARTIFICIAL NEURAL NETWORK MODELLING

3.2.1. Data acquisition and pre-processing

Through LHS and data pre-processing on the Grasshopper platform, random numbers are mapped to the range of each of the optimisation variables and they are used as the input data for the ANN. All of the simulation cases are run in Grasshopper using Ladybug. The simulation of the 5000 cases took around a day. The results of the simulation are written to an Excel file and used as the output data for the ANN training and validation set.

3.2.2. Artificial neural network training, validation and testing

In this study, the ANN is composed of 39 neurons in the input layer, which consists of the variations of the control points, one hidden layer, and one output layer composed of 2 neurons which are the data of the solar radiation.

The input data is scaled to a smaller range using Z-score standardisation defined as follows:

$$Xscale = \frac{x - \mu}{\sigma} \tag{1}$$

where μ and σ represent the average and standard deviation of the input data. The three layers use ReLU as the activation function and the training process uses the Adam optimisation algorithm to update weights.

The dataset is split into 3000 datapoints for training, 1000 for validation and 1000 for testing. The mean squared error (MSE) function is used to evaluate the predictive accuracy of the ANN model defined as follows:

$$MSE = \frac{1}{m}\sum_{i=1}^{m}(y_i - \hat{y}_i)^2 \tag{2}$$

where m = the size of the test set, y_i = the solar radiation simulation value and $\hat{y}_i$ = the predicted value of ANN.

The coefficient of determination(R^2) is used to assess the strength of the correlation of the prediction values and the simulation values, and this usually ranges from 0 to 1. The closer R^2 is to 1, the greater the correlation between the predicted value and the simulated value. R^2 is generally defined as follows:

$$R^2 = 1 - \frac{\sum_{i=1}^{m}(y_i - \hat{y}_i)^2}{\sum_{i=1}^{m}(y_i - \overline{y})^2} \tag{3}$$

where y_i and $\hat{y}_i$ have the same meanings as in (2), and $\overline{y}$= the average value of the set of y_i.

3.2.3. ANN results and discussion

After tuning the parameters on the validation set, the final parameters for training are determined as follows: the number of hidden units is 20, and the dropout rate for both the hidden and the output layer is 0.2, the learning rate is 0.001, epochs are 400, and the batch size is 10. The ANN model reached its goal after approximately 300 epochs, and the final MSE and R^2 values for the training, test and validation sets are shown in Table 2. The final MSE and R^2 for the validation set are 0.299 and 0.992, and the final MSE and R^2 for the training set are 0.303 and 0.992. The MSE and R^2 for the test set are 0.286 and 0.829.

The learning curve demonstrating the MSE and R^2 trends during the training process and the regression between the ANN predictions and the simulation data are illustrated in Figure 3. A good match between the prediction and the simulation data can be seen. To further illustrate the accuracy of the ANN model, Figure 4 compares the 1000 prediction values generated by the ANN model with the winter and summer simulation values. It can be seen that the two data sets are very similar

in both winter and summer.

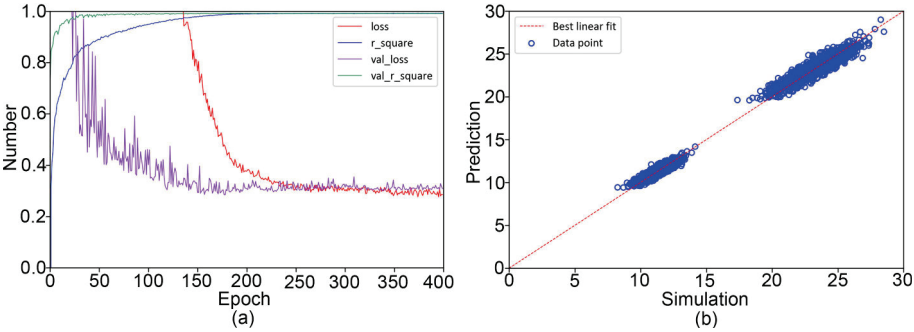

Figure 3. The learning curve and the linear regression between the simulation and prediction values. a) The learning curve, b) Linear regression between the simulation and prediction values.

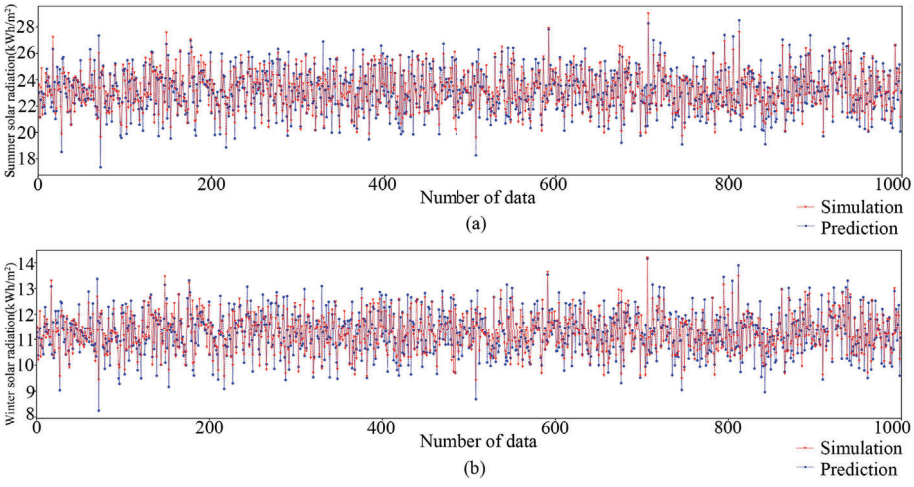

Figure 4. Comparison of ANN prediction and simulation values in summer and winter. a) summer solar radiation, b) winter solar radiation.

Table 2. The final MSE and #R^2# values for the training, test and validation sets.

	MSE	R^2
Training set	0.299	0.992
Validation set	0.303	0.992
Test set	0.286	0.829

3.3. MULTI-OBJECTIVE OPTIMISATION

3.3.1. Multi-objective optimisation settings

After evaluation and testing, the ANN model is used to predict the solar radiation of the reference building for optimisation. For this case, the following GA parameter values are set as shown in Table 3. The generation count is 100, the generation size is 50, crossover probability is 0.9 and mutation probability is 1/r where r represents the number of variables, 39 in this case. The mutation rate is 0.4 and elitism is also 0.4.

Table 3. The GA parameters.

Genetic algorithm parameters	Generation count	Generation size	Crossover probability	Mutation probability	Mutation rates	Elitism	Iteration
Value	100	50	0.9	1/39	0.4	0.4	100

3.3.2. Optimisation results and analysis

With the acceleration of the ANN model, multi-objective optimisation took 6.42 hours. This is considerably less than when just using the simulation data as the optimisation objectives. After 100 iterations, 473 non-dominated solutions are generated. In theory, all of the solutions on the Pareto frontier can be used as final design solutions. To balance the two objectives, 6 non-dominated solutions are chosen for analysis. The results showing the optimised shapes and solutions are shown in Table 4. Solution 5 and Solution 6 have the maximum and minimum solar radiation in summer and winter respectively, and Solutions 1 to 4 are somewhere in between. The solar radiation is 23.59 kWh/m^2 in winter and 11.17 kWh/m^2 in summer for the initial state. The solar radiation in winter is 14.95 kWh/m^2 for Solution 5, which is 30.60% higher than the pre-optimisation state, and value in summer is 30.10 kWh/m^2, 27.60% higher than the initial state. The solar radiation in winter for Solution 6 is 9.69 kWh/m^2, a drop of 12.25%, and the solar radiation in summer is 20.29 kWh/m^2, a reduction of 13.99%. Solutions 1 to 4 are similar. With Solution 1 as an example, solar radiation is 26.07 kWh/m^2 in summer, 10.50% above the initial state while lower than the value for Solution 5, and 12.91 kWh/m^2 in winter, 15.58% higher than the initial state and again lower than Solution 5.

The change in solar radiation varies for the selected solutions, and so does the form of the building. The shape tends to expand both in plan and section to reduce self-occlusion and receive more solar radiation. In the optimisation, the two objectives are contradictory, as lower summer radiation gains results in lower winter solar radiation too. As this reference building is in a severe cold zone in China, the maximisation of winter solar radiation is more important. Hence, a solution with a greater increase in solar radiation in winter and summer, such as Solution 4, is more likely to be selected in a practical application. During the process of optimisation, the variables are modified dynamically to achieve a more reasonable shape. The optimisation process automatically shifts the form in different directions and this can provide support during the early stages of design.

Table 4. Optimisation results and solutions.

solutions		Summer	Winter
	initial state	23.59kWh/m^2	11.17kWh/m^2
1	Area 26726.76m^2	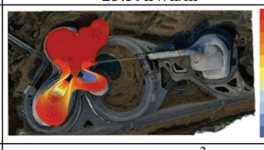	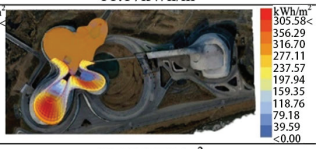
	Radiation value	26.07 kWh/m^2	12.91 kWh/m^2
	Comparison with initial state	10.50%	15.58%
2	Area 32930.87m^2	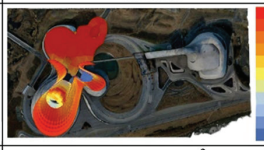	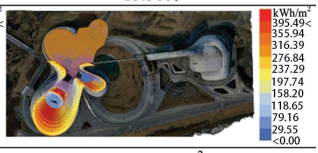
	Radiation value	25.07 kWh/m^2	11.34 kWh/m^2
	Comparison with initial state	6.27%	1.50%
3	Area 27553.18m^2	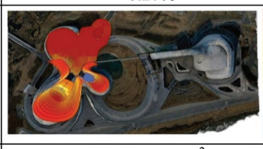	
	Radiation value	24.79 kWh/m^2	12.38 kWh/m^2
	Comparison with initial state	5.09%	10.83%
4	Area 28368.53m^2	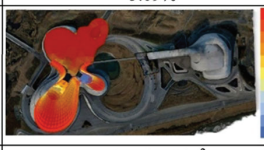	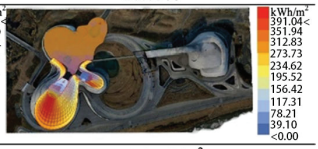
	Radiation value	28.13 kWh/m^2	14.18 kWh/m^2
	Comparison with initial state	19.25%	26.94%
5	Area 29498.04m^2	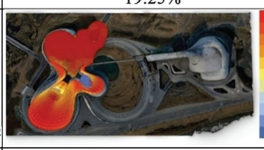	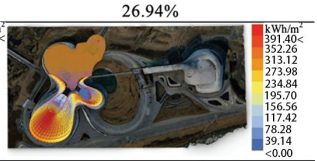
	Radiation value	30.10 kWh/m^2	14.95 kWh/m^2
	Comparison with initial state	27.60%	30.60%
6	Area 27809.81m^2	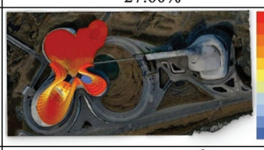	
	Radiation value	20.29 kWh/m^2	9.69 kWh/m^2
	Comparison with initial state	-13.99%	-12.25%

4. Conclusion

The research demonstrates an original multi-objective optimisation method for improving the solar energy utilisation potential of a free-form building. The results show that with the aid of ANN and low altitude photogrammetry, the optimisation time can be reduced considerably. In comparison with the initial

state, the maximum solar radiation value in winter increases by 30.60% and the minimum solar radiation in summer is reduced by nearly 13.99%.

The framework applied in this study can accelerate the optimisation process. It offers support to designers and enhances the decision-making process in the design of free-form buildings. The method can be used for future design of free-form buildings and improves the solar energy utilisation potential. It can also be extended to other similar performance-driven design processes.

Acknowledgments

This work was supported by National Natural Science Foundation of China (grant number 52078157); National Natural Science Foundation of China (grant number 51938003); The China Postdoctoral Science Foundation Funded Project (grant number 2017M621276) and the Heilongjiang Postdoctoral Science Foundation (grant number LBH-Z17076). The corresponding author of the article is Yunsong Han (hanyunsong@hit.edu.cn).

References

Asadi, E., Silva, M., Antunes, C., Dias, L. and Glicksman, L.: 2014, Multi-objective optimization for building retrofit: A model using genetic algorithm and artificial neural network and an application., *Energy and Buildings*, **81**, 444-456.

Bagheri-Esfeh, H., Safikhani, H. and Motahar, S.: 2020, Multi-objective optimization of cooling and heating loads in residential buildings integrated with phase change materials using the artificial neural network and genetic algorithm, *Journal of Energy Storage*, **32**, 1-11.

Camporeale, P.E. and Mercader-Moyano, P.: 2019, Towards nearly Zero Energy Buildings: Shape optimization of typical housing typologies in Ibero-American temperate climate cities from a holistic perspective, *Solar Energy*, **193**, 738-765.

Ciardiello, A., Rosso, F., Dell'Olmo, J., Ciancio, V., Ferrero, M. and Salata, F.: 2020, Multi-objective approach to the optimization of shape and envelope in building energy design Adriana, *Applied Energy*, **280**, 115984.

Jin, J. and Jeong, J.: 2014, Optimization of a free-form building shape to minimize external thermal load using genetic algorithm., *Energy and Buildings*, **85**, 473-482.

Seyedzadeh, S., Rahimian, F.P., Oliver, S., Glesk, I. and Kumar, B.: 2020, Data driven model improved by multi-objective optimisation for prediction of building energy loads, *Automation in Construction*, **116**, 103188.

Si, B., Wang, J., Yao, X., Shi, X., Jing, X. and Zhou, X.: 2019, Multi-objective optimization design of a complex building based on an artificial neural network and performance evaluation of algorithms, *Advanced Engineering Informatics*, **40**, 93-109.

Sun, C., Liu, Q. and Han, Y.: 2020, Many-Objective Optimization Design of a Public Building for Energy, Daylighting and Cost Performance Improvement, *Applied Sciences*, **10**, 2435.

Wong, S., Wan, K. and Lam, T.: 2010, Artificial neural networks for energy analysis of office buildings with daylighting., *Applied Energy*, **87(2)**, 551-557.

Zhang, L., Zhang, L. and Wang, Y.: 2016, Shape optimization of free-form buildings based on solar radiation gain and space efficiency using a multi-objective genetic algorithm in the severe cold zones of China, *Solar Energy*, **132**, 38-50.

AN EVOLUTIONARY APPROACH FOR TOPOLOGY FINDING IN FLEXIBLE AND MODULAR HOUSING

ÖZLEM ÇAVUŞ[1], HIZIR GÖKHAN UYDURAN[2], DELARA RAZZAGHMANESH[3] and IMDAT AS[4]
[1,3,4]*Istanbul Technical University*
[1,3,4]*{cavus19|razzaghmanesh|ias}@itu.edu.tr*
[2]*Yıldız Technical University*
[2]*gokhanuyduran@gmail.com*

Abstract. Today, the living environment is much more complex due to rapid urbanization and cities hardly can bear increasing crowds. This evolving environment together with the change in living habits, put a strain on the shoulders of architects and engineers to find faster and more effective solutions towards flexible and responsive design in future city scenarios. Modular design is one of the most suitable solutions since it is based on interchangeable components that facilitate different combinations and activities responding to emerging needs and demands without demolishing a whole edifice. There are many available algorithms defining rules for the automated generation of modular building units but mainly designed for top-down solutions. This paper proposes an evolutionary approach aiming to find topological relations among the units based on a specific architectural program concerning environmental performance. Environmental conditions define the rules for the growth of units on site. The algorithm produces an automatic layout through a set of positioning rules for units organized around a core depending on a branching system. In this sense, this paper contributes to showing how rule-based modular growth on-site is shaped with environmental and architectural concerns for future city scenarios.

Keywords. Modular Housing; Affordable Housing; Future City; Branching Structure; Evolutionary Approach.

1. Introduction

Housing is a fundamental need for every human being to live in one form or another either as a homeowner or a tenant in an enclosed space. Today, cities hardly can bear increasing crowds and have difficulties in meeting the demands of the citizens because of rapid urbanization, increase in housing prices, and the change in living habits such as co-living. Cities will require a good amount of affordable housing to cater to the large middle and lower-income demographic. Thus, the design, configuration, orientation, heating, flexibility, spaciousness, or lack thereof impacts the physical and mental health of people and can shape the life of entire societies. However, part of the existing housing stock suffers from

PROJECTIONS, Proceedings of the 26th International Conference of the Association for Computer-Aided Architectural Design Research in Asia (CAADRIA) 2021, Volume 1, 231-240.

heating problems due to insufficient insulation, and about 23% of houses do not get direct sunlight, and only 5.8% of homeowners in Turkey are very pleased with where they live, whereas in the EU this number is at 33.4% (Aydin, 2019). There is a gap in satisfactory housing availability, and a vast demand for good quality, affordable housing solutions in Turkey. This paper is intended to explore to tackle this problem with a flexible and modular housing approach which is exemplified on a future city project site located in Esenler, which is one of Istanbul's densest districts, with 70,000 people per km2, and a population of 454,569 inhabitants. The challenge is to re-envision high-density housing solutions in a fast and reliable way concerning environmental impacts such as daylighting.The above-stated facts reveal the significance of customized generative systems offering quick and feasible solutions considering environmental performance as well as flexibility in use from the very beginning of the design processes. Particularly, repeatable use of structures in different scenarios without demolishing existing buildings is very valuable both in engineering and architecture. Therefore, modular design is one of the most suitable solutions as it offers interchangeable components that can come together in different combinations allowing to hold different activities. In this regard, modular systems can respond to emerging needs and demands without demolishing the whole system.In innovative housing approaches such as the participatory housing solution proposed by Aravena (URL-1) and Sidewalk Labs Future City Project in Toronto (URL-2), modularity is a key term delivering flexibility, user participation, and economic gains for the occupants. Flexibility is particularly crucial to meet and adapt to changing needs and demands as fast as possible. Therefore, the design should respond to different building configurations together with allowing fast delivery of services systematically, so hierarchical distributions of functions are required. The success of Aravena's social housing project depends on user-centric participatory design. In combination with the expert knowledge, assigning users active roles in the design making process creates customization and democratization of the planning processes (Sandercock, 2005). Housing projects in future city scenarios can be expensive, so affordability maintaining the desired level of living conditions for lower-income citizens is a significant concern in social housing projects. In this regard, the concept of shared housing instead of owning (Shamsuddin & Srinivasan, 2020) and the role of given subsidy before the project starts can be the solution. However, low-income housing subsidies can also increase the occupied housing stock, so tenant-based housing programs can be more effective (Sinai & Waldfogel, 2005). Another key term playing an important role in sustaining affordability is the efficient use of resources. As Jiboye (2012) argued, sustainable and affordable housing is the optimal utilization of limited resources to provide housing for the masses as well as for future generations. Hence, future cities require systematic and holistic design approaches. For instance, the design proposal for Toyota Woven City in Japan offers a smart grid as an organizer of both infrastructure and superstructure giving priority to connectivity (URL-3). It should be stressed how mereological relations between housing units and the other city domains are synthesized to create a whole system. Unless units/parts are designed concerning inter-relations in land use scenarios, implementations cannot effectively answer design problems.

Therefore, it needs a certain level of adaptability and flexibility to implement the required living conditions, and to cope with deconstruction and reconstruction of existing implementations over and over. These relations among the units should be well-defined in regards to architectural and environmental criteria, in this sense.Many rule-based solutions automatically generate adaptable and flexible housing proposals through modular design. For example, cellular automata are created by the local communication between cells over time by simple rules of the neighborhood (Wolfram, 1984). This approach can provide interesting experimental results in land use scenarios controlling density, however, it does not address specific requirements of architectural design. It usually involves a response to a design summary and constraints, and existing environments (Herr & Kvan, 2007). Another rule-based design solution is shape grammars, which can produce designs through known and finite rules that generate new shape compositions by their repeated application of basic building blocks (Stiny & Gips, 1971). Also, branching systems are widely used for hierarchical organization. The branch structure is a basic topological growth mechanism that maximizes the surface area of a tree limb, human lung, or coral algae, and sends out resources, and responds to structural forces (Park & Lee, 2019). Hierarchical branching can be used as an organizational tool for ordering information, space, resource flow, or even software logic (Jabi, 2013). All these rule-based solutions should be encouraged by environmental and architectural criteria to function efficiently in real-life scenarios. Thus, it needs optimization for efficient use of sources sustaining fitness criteria.There are two types of optimization problems working with single-objective or multi-objective functions. In the former, the fitness of a solution is equal to its objective function value, yet the optimization of multiple contradictory objectives is hard (Deb, 2014). The latter can particularly be useful for real-world problems offering a set of optimal solutions as it considers several conflicting objectives simultaneously (Deb, 2014). Among many other evolutionary techniques, genetic algorithms have been used in architecture as optimization methods. They operate on a population of possible solutions and searches by randomly sampling within an optimization solution space. Then, stochastic operators are used to directing a process based on objective function values (Goldberg, 1980).Taking into account the above-stated discussions on existing studies, there is still a need for customized tools for topology finding in modular design towards future city scenarios. Instead of relying on rule-based guidance in design generation, relations among modules, branching systems, and environmental conditions should be in dialogue with architectural fitness criteria. The main difference of this paper from similar past approaches responding to housing solutions, is that it proposes a semi-automated generative design approach that deals with a flexible configuration where rules are defined respecting architectural needs and environmental performances in future city scenarios. This paper presents an evolutionary approach that aims to define associative relations among the units and the site according to performance-based criteria.

2. Methodology

The offered evolutionary approach aims to define relations between parts i.e. the way components can come together, concerning optimal use of resources and energy performance of each module. Topology is defined as the way the parts are organized or connected, it is the relation among the spaces as invariant properties of the layout under any geometrical transformation (Damski & Gero, 1997). In this paper, the term topology finding encapsulates base unit generation comprising a specific architectural program and defining part relations between the generated base unit(s). The organization of the whole system is based on a branching structure which is described as multi-layered hierarchical systems containing modules within modules. The reason to use a branching system is that 'branch structure' is a basic topological growth mechanism that maximizes the surface area and thus generates flexibility for the building (Park & Lee, 2019). Therefore, it is questioned how the relations between parts can come together in the hierarchical branches from a holistic point of view.The research method is two-fold as module level and site level which are evaluated over a set of simulations. The former focuses on the generation of the base unit as a mass-based on any specific architectural program. The latter, on the other hand, evaluates the base unit(s) following a specific branch(es) on a given project site. This evaluation intends to find optimum relation which defines how units can come together according to environmental performances.The algorithm of the simulation attempts to produce a semi-automated layout by a set of positioning rules that follow requirements. The units are plugged in each other and organized around cores. These cores are indeed associated with the grids connecting to each other with a branching system. The units encapsulate residential, common, and commercial spaces whose contexts are defined by any specific architectural program. These spaces can also be categorized as private, semi-private, and semi-public. Regardless of the categorization, they are organized in the branches hierarchically.The first order of the hierarchical program distribution on the branching system is the core which serves as a distribution channel bounding main spaces. This channel is indeed associated with a smart grid in future city scenarios such as Toyota Woven City Project. The second-order focuses on the main spaces that can be regarded as housing and shared spaces. According to the needs of the residents, the units can be plugged-in or out to have bigger or smaller units. Their organization is determined by an evolutionary algorithm based on environmental analysis.The reason to use evolutionary algorithms is that the size and non-linear nature of search space in building-related problems, classical optimization techniques are not usually suitable (Kiss, 2020). Indeed, genetic algorithms tend to perform better as the size of search space increases (Tuhus-Dubrow, 2009; Wetter, 2004). The form generation workflow that tries to find topological relations among the units, consists of 4 main stages as indicated in Figure 1. The first stage creates the initial base unit as a response to a specific architectural program. Taking into consideration the standards and living habits of distinct user groups, the size of the base unit should be suitable enough to meet certain architectural criteria. Once the size of the base module(s) is determined, the second stage shows the way how these units connect with each other. Connection rules are significant since they also

define assembly rules and have an impact on the environmental performance of each individual unit. The third stage focuses on the accommodation of the units on a given terrain. This accommodation is in line with the grids i.e. core with respect to the slope of the terrain. The fourth stage depicts an evolutionary approach for finding optimum connection rules between individual units and their organization on-site regarding the results obtained from the environmental analysis. In fact, these interrelated four stages may help to construct a holistic view of an integrated design process for future city scenarios. In this sense, the proposed approach shows how to find topology-based solutions that respond to the changing needs and environmental performances from the very beginning of the design processes. In light of the above-stated research flow, a case study is developed with reference to a branching system composed of a network of grids. These grids are associated with the distribution of functions which exemplifies hierarchical organization. The simulation is developed in Rhino 6, and Grasshopper using Magnetizing to create each layout based on the needs of residents, Galapagos for single-objective optimization in the generation of a base unit, Wasp to assemble discrete units, Ladybug Tools to evaluate energy and daylight performances, and Wallacei to decide assembly rules by NSGA-II genetic algorithm.

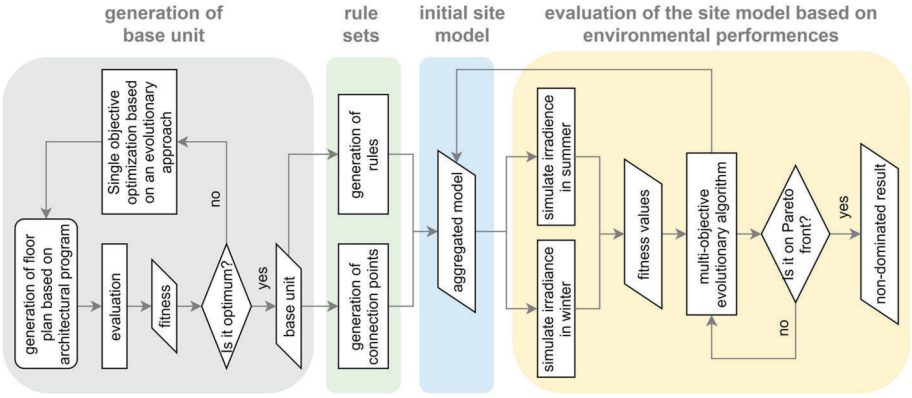

Figure 1. The flow of the Research Method.

3. Case Study

The case study exemplifies how topology findings among base units are determined by an evolutionary approach concerning environmental performances. Within this context, a simulation is developed and explained following the research flow in Figure 1. Accordingly, a layout of a base unit is firstly generated according to an architectural program. Note that the aim of this paper is not to offer an ideal architectural layout nor design an algorithm in future city scenarios. Rather, it tries to define associative relations among the units and the site according to performance-based criteria. Otherwise, predetermined rules control the whole aggregation on the site which are mainly disregarded with the social and environmental aspects. Therefore, two base units regarded as housing

and common are created as an example based on an architectural program, and their connection rules are determined by an evolutionary solver. In the formation of base units, plan generation is performed based on bubble diagrams tagged with area and room name in Magnetizing. The principle behind Magnetizing depends on the fitness of the architectural program for given boundary conditions. It tries to fit all the given rooms according to the program as much as it can. In case the boundary is not adequate enough to comprise all the list, its definition needs to be reconsidered. Hence, it is further evaluated over a single objective optimization based on the evolutionary approach in Galapagos. The single objective is the placement of the entire program in the given boundary condition. Its fitness criteria are the maximization of room numbers that are placed in the boundary. Genomes are related to the number sliders defining the location of the corner points of the boundary frame. In this regard, all the program is encapsulated and then fitted in a bounding box to obtain a base unit. Once the base unit is obtained, the assignment of the connection rules should be defined. Wasp functioned with the rules based on shape grammars to aggregate discrete elements. Two inputs should be assigned to initiate the aggregation: modules to be connected and connection points and guidelines on the faces of the modules. Connection rules are strings that define how one module is connected to another recognizing the given names to the modules and id of the connection points (Figure 2). Four different rules are set for each guideline and these rules are selected by genetic algorithms to choose modules and id from a gene pool.

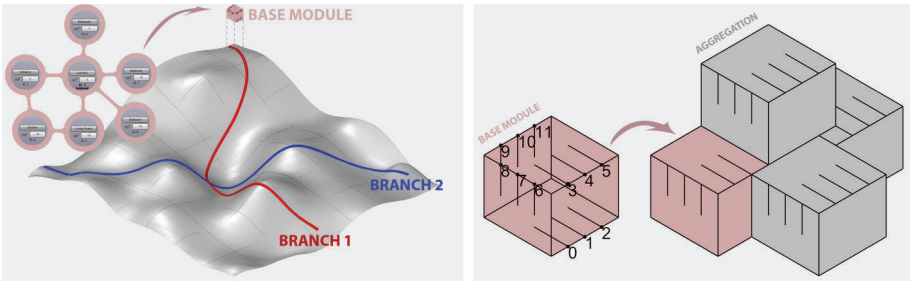

Figure 2. Left: Base Unit Generation. Right: Definition of Part Relations in Assembly Connections.

Multi-objective optimization based on environmental analysis is performed to select the way units should be connected. Performance criteria are selected as irradiance on module surfaces in winter and summer, creating a trade-off between objectives to balance the effect of the obtained sunlight. Ladybug tools are used to calculate irradiance on surfaces. The multi-objective optimization based on the Pareto method (Figure 3 on the top) is aimed to decrease the solar irradiation in summer to decrease overheating and heat gains while increasing the irradiation in winter for better daylight performance and decrease heating loads (Figure 3 on the bottom). The genetic algorithm evaluates the population size of 50 and a generation size of 50 (Figure 4).

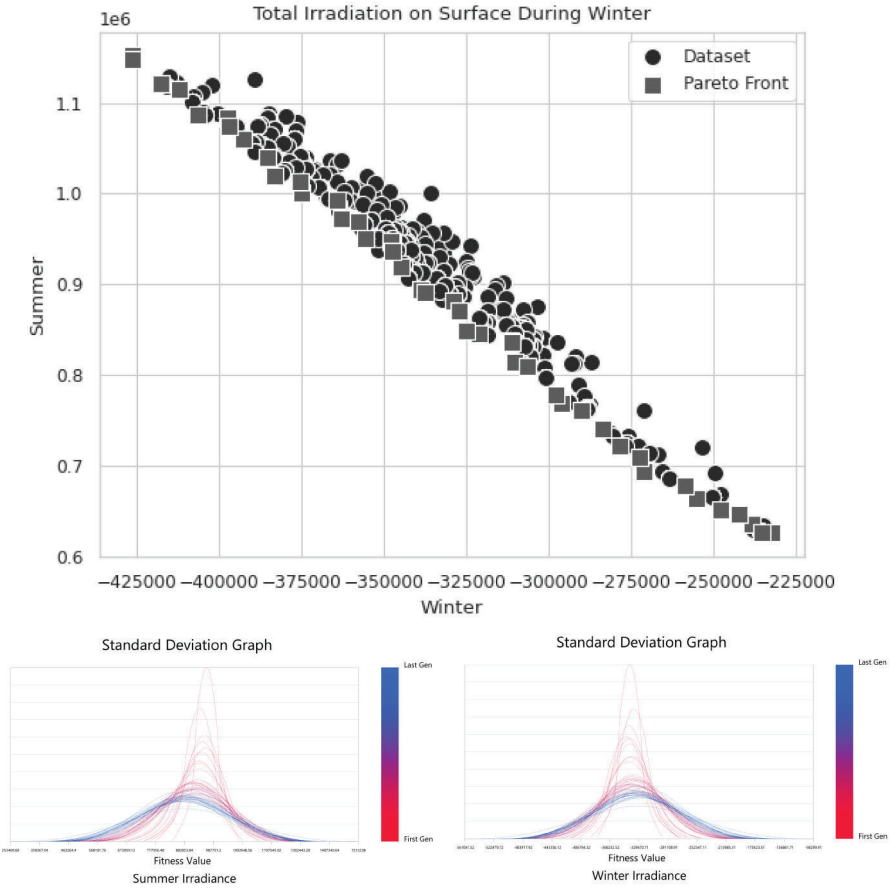

Figure 3. Top: Pareto Graph. Bottom: Standard Deviation Graphs.

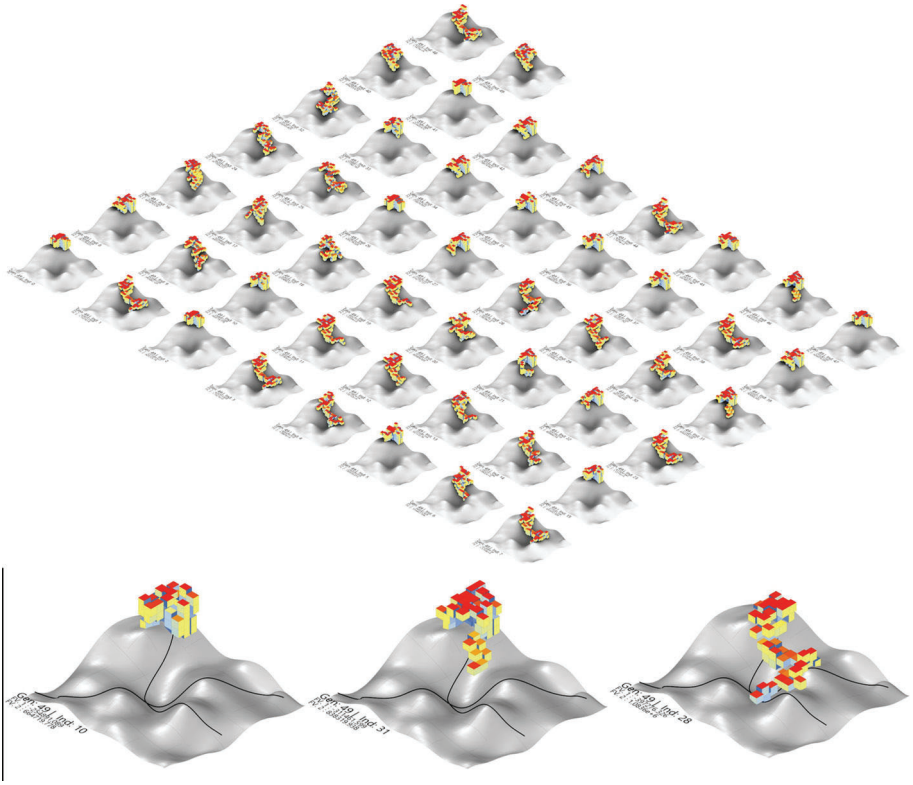

Figure 4. Optimal Aggregation of Units on Site.

By multi-objective optimization relations among units and site are defined. It is based on enhancing the daylight performance in winter and summer and the units are arranged according to the slope and the defined path lines (branches) of the site. The result of the optimization shows the optimal solution which is the best arrangement and the connection of the units on the site.

4. Results and Discussion

This study shows how rule-based design solutions can be developed through various architectural criteria and environmental performances. The genetic algorithm created rules that moved modules together to decrease solar irradiation for the summer months and separated them to increase solar irradiation for the winter months. We evaluated three optimal solutions on the project site as indicated in the Pareto Graph seen in Figure 4. This research extends to the third-order defined as an assembly level. Assembly level defines components that can be plugged-in or out within the base module. These components can be wet spaces, staircases, separation walls and slabs, and balconies. For instance, a wall can serve as a separator to create open and semi-open spaces based on telescopic movement. It can retract to create a passage between units and to

extend the living spaces forward. Besides, the connection of physical elements such as walls, slabs, and staircases together with their different configurations can be embedded in the base unit design. Also, the relation between parts like core and utility services or wet spaces and base units should also be considered. In addition, further studies can be evaluated over organization criteria of structural elements or utility services. For instance, the distribution of utility services can be associated with a structural system based on branch theory. This methodology can be used in other locations in order to add further layers of exploration based on the local construction habits and architecture styles. Recently, due to covid-19, our living habits are also transforming into new typologies, where for example home offices are added to housing programs. These new mixed-use concepts trigger discussions on private and public domains in future home designs. This transformation of use case scenarios can be incorporated into new architectural programs, e.g. the level of privacy. Indeed, our approach can create intermediate social zones, where new social paradigms can melt with novel environmental and physical aspects of future home design.

Acknowledgments

This paper has been produced benefiting from the 2232 International Fellowship for Outstanding Researchers Program of TÜBİTAK (Project No: 118C284). However, the entire responsibility of the paper belongs to the owners of the paper. The financial support received from TÜBİTAK does not mean that the content of the publication is approved in a scientific sense by TÜBİTAK.

References

"URL-1" : no year given. Available from <https://www.dezeen.com/2016/04/06/alejandro-aravena-elemental-social-housing-designs-architecture-open-source-pritzker/>.

"URL-3" : no year given. Available from <https://www.toyota.co.nz/about-toyota/toyota-news/2020/june/toyota-woven-city/>.

"URL-2" : no year given. Available from <https://www.sidewalktoronto.ca/>.

Aydın, K.: 2019, Türkiye, *Sociology*, **39**(2), 277 - 301.

Damski, J. C. and Gero, J. S.: 1997, An evolutionary approach to generating constraint-based space layout topologies, *CAAD futures 1997*, 855-864.

Deb, K.: 2014, *Multi-objective optimization*, Springer, Boston, MA.

Goldberg, D. E.: 1989, *Genetic algorithms in search, optimization, and machine learning*, Addison-Wesley, Reading, MA.

Herr, C.M. and Kvan, T.: 2007, Adapting cellular automata to support the architectural design process, *Automation in Construction*, **16**(1), 61-69.

Jabi, W.: 2013, *Parametric design for architecture*, Laurence King Publishing.

Jiboye, A. D.: 2011, Achieving sustainable housing development in Nigeria: A critical challenge to governance, *International Journal of Humanities and Social Science*, **1**(9), 121-127.

Kiss, B. and Szalay, Z.: 2020, Modular approach to multi-objective environmental optimization of buildings, *Automation in Construction*, **111**, 103044.

Park, J. E. and Lee, H.: 2019, Parametric design model of urban collective housing, *SIGraDi 23*, 385-392.

Sandercock, L.: 2005, The Democratization of Planning: Elusive or Illusory?, *Sandercock, L. (2005). The Democratization of Planning: Elusive or Illusory?*, **6**(4), 437-441.

Shamsuddin, S. and Srinivasan, S.: 2020, Just Smart or Just and Smart Cities? Assessing the Literature on Housing and Information and Communication Technology, *Housing Policy*

Debate, **3**, 1-24.
Sinai, T. and Waldfogel, J.: 2005, Do low-income housing subsidies increase the occupied housing stock?, *Public Economics*, **89**, 11-12.
Stiny, G. and Gips, J.: 1971, Shape grammars and the generative specification of painting and sculpture, *Information Processing 71*.
Tuhus-Dubrow, D. and Krarti, M.: 2009, Comparative analysis of optimization approaches to design building envelope for residential buildings, *ASHRAE Transactions*, 554-563.
Wetter, M. and Wright, J.: 2004, A comparison of deterministic and probabilistic optimization algorithms for nonsmooth simulation-based optimization, *Building and Environment*, **39**(8), 989-999.
Wolfram, S.: 1984, Cellular automata as models of complexity, *Nature*, **311**, 419-424..

SWARMBESO: MULTI-AGENT AND EVOLUTIONARY COMPUTATIONAL DESIGN BASED ON THE PRINCIPLES OF STRUCTURAL PERFORMANCE

DING WEN BAO[1], XIN YAN[2], ROLAND SNOOKS[3] and YI MIN XIE[4]
[1]*School of Architecture & Urban Design, RMIT Architecture | Tectonic Formation Lab and Centre for Innovative Structures and Materials, School of Engineering, STEM College, RMIT University*
[1]*nic.bao@rmit.edu.au*
[2]*Center of Architecture Research and Design, University of Chinese Academy of Sciences and Centre for Innovative Structures and Materials, School of Engineering, RMIT University*
[2]*yanxin13@mails.ucas.ac.cn*
[3]*School of Architecture & Urban Design and RMIT Architecture | Tectonic Formation Lab, RMIT University*
[3]*roland.snooks@rmit.edu.au*
[4]*Centre for Innovative Structures and Materials, School of Engineering, STEM College, RMIT University*
[4]*mike.xie@rmit.edu.au*

Abstract. This paper posits a design approach that integrates multi-agent generative algorithms and structural topology optimisation to design intricate, structurally efficient forms. The research proposes a connection between two dichotomous principles: architectural complexity and structural efficiency. Both multi-agent algorithms and Bi-directional evolutionary structural optimisation (BESO) (Huang and Xie 2010), are emerging techniques that have significant potential in the design of form and structure.This research proposes a structural behaviour feedback loop through encoding BESO structural rules within the logic of multi-agent algorithms. This hybridisation of topology optimisation and swarm intelligence, described here as SwarmBESO, is demonstrated through two simple structural models. The paper concludes by speculating on the potential of this approach for the design of intricate, complex structures and their potential realisation through additive manufacturing.

Keywords. Swarm Intelligence; Multi-agent; BESO (bi-directional evolutionary structural optimisation); Intricate Architectural Form; Efficient Structure.

1. Introduction

This research posits an innovative design methodology that establishes a complementary relationship between topological optimisation and behavioural

PROJECTIONS, Proceedings of the 26th International Conference of the Association for Computer-Aided Architectural Design Research in Asia (CAADRIA) 2021, Volume 1, 241-250.

generative design algorithms. The research explores and evaluates the application of topology optimisation and multi-agent algorithms in a form-finding design process. It demonstrates the process of integrating these two algorithms to establish a real-time structural feedback loop in the process of designing intricate forms. It describes a hybrid of architectural and structural behaviours through the integration of swarm systems and BESO methods.

This approach, termed swarmBESO (see figure 1), creates a negotiation between concerns of architectural design and structural engineering in a simultaneous generative approach. This is a fundamental shift from the normative sequential workflows that either inform generative approaches with structural analysis or operate sequentially to optimise the structure of complex geometries already created within generative processes. The swarmBESO algorithm is demonstrated here through two- and three-dimensional cantilevered structure examples.

The future application of swarmBESO to architectural design will enable the creation of complex, the expressive architectural form which is highly efficient in terms of material and structural performance. The complexity and intricacy of the geometry generated through this process are expected to become increasingly feasible through the rapid development of building-scale additive manufacturing approaches.

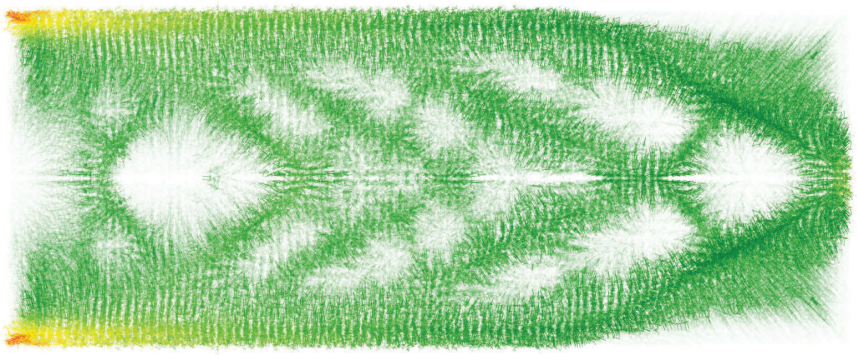

Figure 1. SwarmBESO.

2. Swarm Intelligence and Behavioral Formation

Swarm intelligence examines the emergent behavior of systems that self-organise through the interaction of autonomous agents. This behavior is evident within the natural world through systems such as flocks of birds, schooling of fish, and social insects' interaction.

The phenomena of swarm intelligence can be simulated and generated through multi-agent algorithms - a computational logic that dates to John von Neumann's work with cellular automata in the 1940s. Multi-agent algorithms operate through

the local interaction of computational agents. This interaction of agents creates a self-organising behavior at the meta, or global, scale. These algorithms establish a non-linear relationship where each agent responds to the neighbouring agents without hierarchical, or top-down, control.

The development of generative design processes based on multi-agent algorithms has been emerging for twenty years within experimental architectural practices and academia. One pioneering approach, Behavioral Formation, has been developed by Roland Snooks that builds on the computational boids research of Craig Reynolds. (Reynolds 1987).

Behavioral Formation is a generative design approach that draws from swarm intelligence logic and operates through a multi-agent algorithmic process (Snooks 2014). Through this approach, the architectural intention is encoded within computation agents. The interaction of which creates a self-organised design intention and generates emergent proto-architectural form.

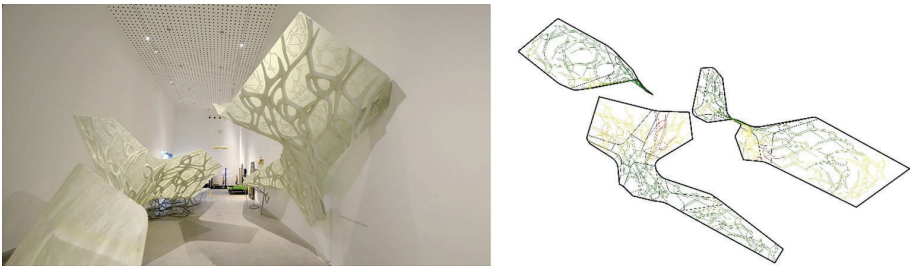

Figure 2. Composite wing by Studio Roland Snooks.

The exclusively local interaction of multi-agent systems creates self-organising behaviour at the expense of global, or meta, awareness. This global ignorance limits the capacity of multi-agent design strategies to respond to global conditions such as topology, enclosure and structure. A strategy has previously been proposed by Roland Snooks in response to this, termed *agency of structure*, which operates through a heuristic approach to local structural behaviors that respond to global structural analysis. Agency of structure "operates by iteratively testing agent-based geometry, such as a network of members or bundle of strands, using a finite element structural method. Finite element methods analyse the entire structural topology and return information pertaining to each individual node or agent (see figure 2). The agent adapts its behavior in response to this information based on heuristic structural rules designed to resist the load. Through this strategy, agents respond to the local implication of global conditions and, in doing so, re-form the global conditions, setting up a continuous feedback loop." (Snooks 2014, p131-132)

3. Bi-directional Evolutionary Structural Optimisation Method

Topology optimisation techniques have been widely used in structural fields. Conventional optimisation methods are always aimed at achieving the single purpose of maximising the structural performance. Due to the potentials for

generating elegant and light-weight structures with high structural performance, topology optimisation has gained extensive attention and experienced considerable progress over the three decades. Topology optimisation aims to find an initial structural configuration which meets a predefined criterion, and occasionally it gives a design that can be completely new and innovative. Several notable topology optimisation methods have been widely developed in topology optimisation field, e.g. the homogenisation method (Bendsoe 1989; Bendsoe and Kikuchi 1988), the solid isotropic material with penalisation (SIMP) method (Bendsoe and Sigmund 1999; Bendsoe and Sigmund 2004), the evolutionary structural optimisation (ESO) (Xie and Steven 1993; Xie and Steven 1994), the bi-directional evolutionary structural optimisation (BESO) (Huang et al. 2007; Huang and Xie 2007) (see figure 3) and the level-set method (LSM) (Wang et al. 2003; Allaire et al. 2004). Among others, BESO method has been proved to be a reliable optimisation technique, which has been successfully applied in many engineering and architectural design (Zhao et al. 2018; Yan et al. 2019; Burry et al. 2005).

Figure 3. Bi-directional Evolutionary Structural Optimisation (BESO).

Although most topology optimisation techniques aim at achieving the most optimised solution, the structural layout with the highest performance may contradict the functional requirements and aesthetic designing concepts in real problematic practices. Therefore, some modification methods based on conventional topology optimisation are explored widely to solve specific application problems. In 1992, Mike Xie and Grant Steven proposed a numerical method for topology optimisation Evolutionary Structural Optimisation (ESO) (Xie and Steven 1993; Xie and Steven 1994), and later Mike Xie and Xiaodong Huang developed the Bi-directional Evolutionary Structural Optimisation (BESO). BESO method allows the material to be removed and added simultaneously. In BESO method algorithm, The initial research on BESO was conducted by (Yang et al. 1999) for stiffness optimisation. “In their study, the sensitivity numbers of the void elements are estimated through a linear extrapolation of the displacement field after the finite element analysis. Then, the solid elements with the lowest sensitivity numbers are removed from the structure, and the void elements with the highest sensitivity numbers are changed into solid elements.” (Huang and Xie 2010, p17). Two unrelated parameters determine the numbers of removed and added elements in each iteration: the rejection ratio (RR) and the inclusion ratio (IR), respectively. “In their BESO algorithm, elements with the lowest von Mises stresses are removed, and void elements near the highest von Mises stress regions are switched on as solid elements. Similarly, the numbers of

elements to be removed and added are treated separately with a rejection ratio and an inclusion ratio, respectively." (Huang and Xie 2010, p17).

4. SwarmBESO Methodology: BESO Logical Multi-agent System

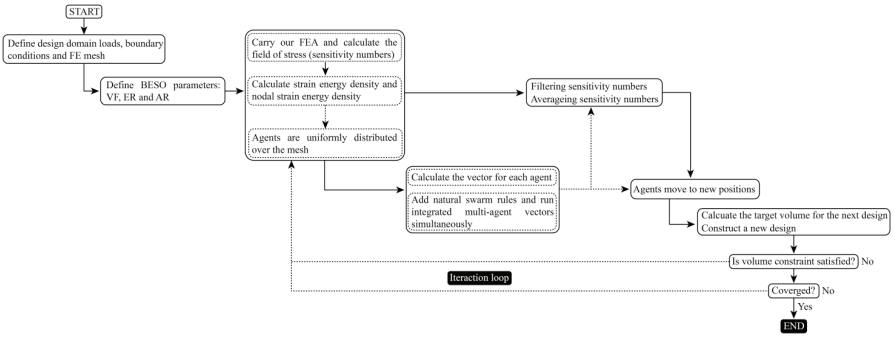

Figure 4. Flowchart of the SwarmBESO method.

The swarmBESO approach involves iterative feedback where the results of an FEA analysis drive structural behaviour within a multi-agent generative algorithm, which in turn re-forms a structural mass. Each step of the agent triggers this recursive process such that a constantly updating structural model drives every step. The multi-agent generative algorithm negotiates between these structurally driven behaviours and non-structural design behaviours, to create forms that are generated by architectural design intention while being near-optimal structural solutions (see figure 4).

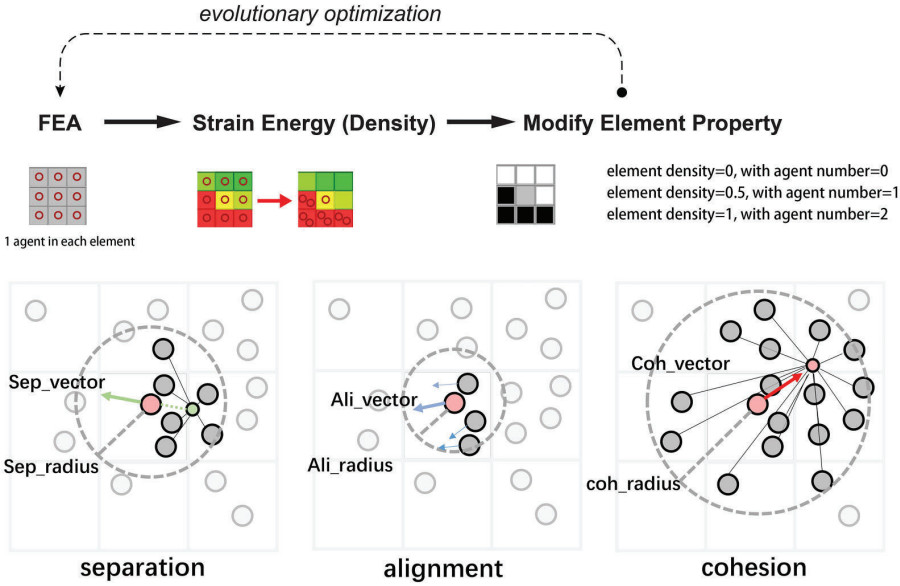

Figure 5. The logic of SwarmBESO method.

The agent number in each FEA element is connected with the relevant element material property, which means the element will be given a softer material with less Young's modulus value in the next iteration if it has fewer agents inside. As the diagram shows (see figure 5), a strain energy field is generated based on the whole structure FEA result in each iteration. Every agent can be assigned an initial velocity according to the strain energy field, and this velocity represents the structurally driven behaviour. Furthermore, some essential swarm-rule-based modifications, such as separation, alignment and cohesion, are introduced to modify the initial agent velocity. As a result, with the modified velocities, agents will make movements inside the FEA mesh and change the next FEA process's material properties.

4.1. 2D CANTILEVER

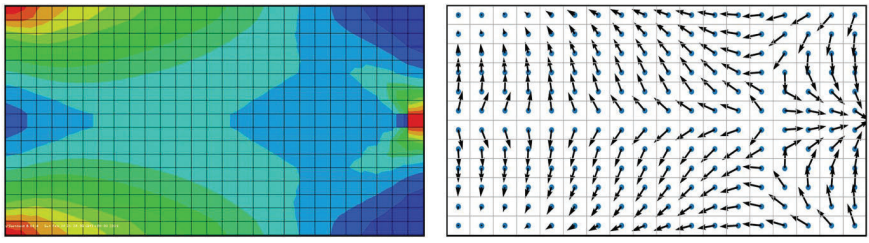

Figure 6. 2D Cantilever in FEA platform (left) and initial generated velocity field (right).

The 2D cantilever model is a classic analysis model in structural optimisation. The plate model is fixed around the left side and subjected to a concentrated load at the middle point on the right side (see left in figure 6). With swarmBESO method, the strain energy field and initial structurally driven velocity field are generated like the illustration (see right in figure 6). After several iterations, the agent can be re-located as the diagram shows (see figure 7), and this result is similar to the conventional topology optimised result.

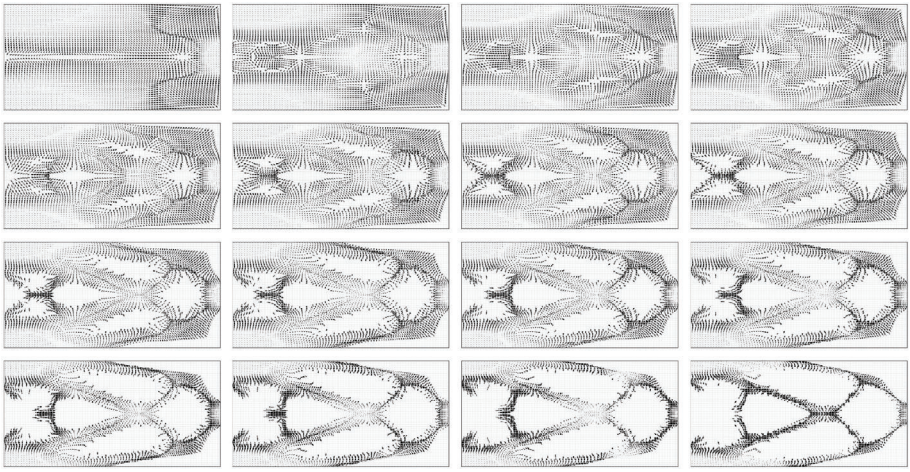

Figure 7. 2D evolutionary result.

The new method has also been tested on the 2D long beam structure (see figure 8). The colourful cloud pictures are the visualization result of analysed data in finite element method. The green figures are the normal BESO result. The multi-agent figures are the swarmBESO result, they are respectively iteration 10 (see left in figure 8) and iteration 35 (see right in figure 8). In comparison, the swarmBESO results both achieve structural performance and have more complex & diverse forms.

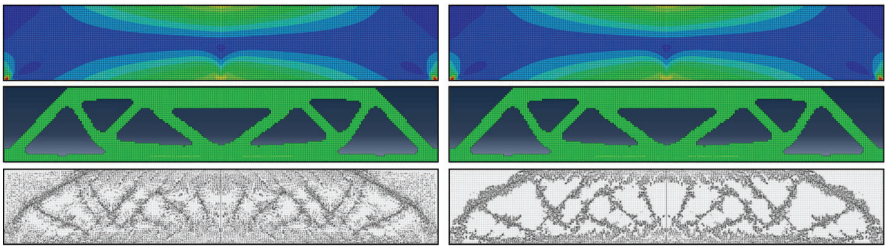

Figure 8. BESO and swarmBESO result comparison.

However, because of the single element layer, the 2D model may be faced with some local blocking during the evolution process. In the 3D model, the situation

will be averted as there are multi-movement strategies for an agent to bypass the local obstacles.

4.2. 3D CANTILEVER

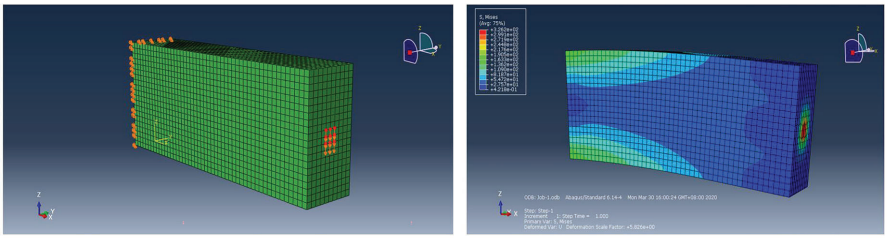

Figure 9. The 3D cantilever in FEA platform.

Initially, a simple 3D cantilever (solid element) is tested for swarmBESO algorithm in the FEA platform Abaqus (see figure 9). After setting up the boundary conditions, the finite element method analyses the entire structural surface, and return the information of the field of stress and strain energy density (SED) among the whole structure. A certain number of agents are uniformly distributed over the entire structure to represent the material distribution.

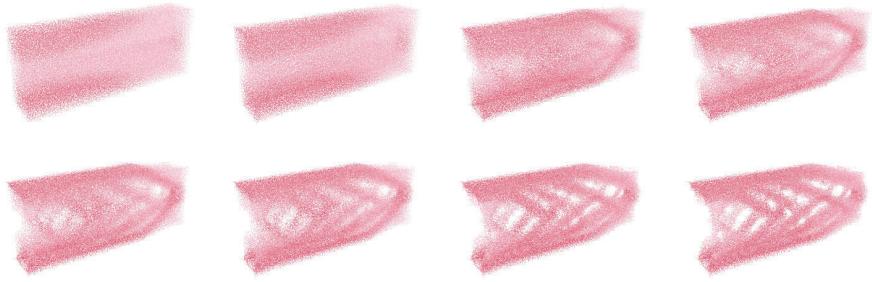

Figure 10. Real-time SED information feedback and iterations.

Based on the returned information of the field of stress and SED, the initial vector will be applied to each agent. At the same time, three basic swarm rules are applied to the agents (see figure 10).

The agent adapts its new modified behaviour in response to this integrated information of vector and starts to move to a new position. Based on the logic of BESO (Huang and Xie 2010), the material distribution will be kept updating in each loop iteration until it reaches a certain volume fraction.

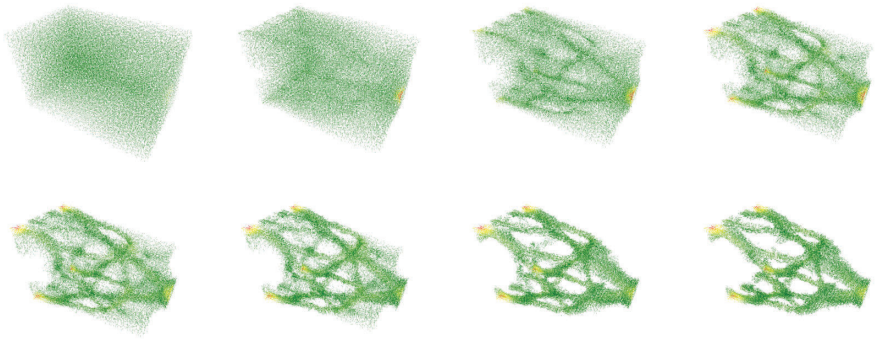

Figure 11. 3D evolutionary process.

In each step of the iteration, the information of structural performance will be returned and reviewed. The information can be analysed by checking the strain energy density distribution. Thus, the structural logic-based swarm evolutionary method is applied and tested. From the above diagram (see figure 11), it is evident that the swarmBESO generations are less than conventional topology optimisation methods. In swarmBESO, all the agents are motivated based on local rules at the same time rather than just some certain areas are changed in other traditional methods. As a result, it may be difficult for swarmBESO to find the globally optimised structure, but it can generate diverse results with similar structural performance.

5. Conclusions

The integration of multi-agent generative algorithms and structural topology optimisation creates a simultaneous process of architectural and structural generation. This approach has the potential to develop a closer working collaboration between architects and structural engineers in the early stages of design and to avoid the structural rationalisation of unfeasible architectural forms. The next steps in this research are to demonstrate the capacity of this algorithmic tool through the design of several prototypical projects and to embed the logic of additive manufacturing techniques within the swarmBESO algorithm. While the simple cantilever examples illustrated here to demonstrate the operation of swarmBESO, the real potential in this approach lies in the capacity of this algorithm to create highly complex and intricate architectural tectonics that are structurally efficient.

References

Allaire, G., Jouve, F. and Toader, A.-M.: 2004, Structural optimisation using sensitivity analysis and a level-set method, *Journal of Computational Physics*, **194**, 363-393.

Bendsoe, M.P.: 1989, Optimal shape design as a material distribution problem, *Structural Optimization*, **1**, 193-202.

Bendsoe, M.P. and Kikuchi, N.: 1988, Generating optimal topologies in structural design using a homogenisation method, *Computer Methods in Applied Mechanics and Engineering*, **71**, 197-224.

Bendsoe, M.P. and Sigmund, O.: 1999, Material interpolation schemes in topology optimisation, *Archive of applied mechanics*, **69**, 635-654.

M.P. Bendsoe and O. Sigmund (eds.): 2003, *Topology optimization: theory, methods, and applications*, Springer, Berlin Heidelberg.

Beni, G. and Wang, J.: 1993, Swarm Intelligence in Cellular Robotic Systems, *NATO Advanced Workshop on Robots and Biological Systems, Tuscany1989*, Italy, 703-712.

Burry, J., Felicetti, P., Tang, J., Burry, M. and Xie, Y.M.: 2005, Dynamical Structural Modeling: A Collaborative Design Exploration, *International Journal of Architectural Computing*, **3**, 27-42.

Huang, X. and Xie, Y.M.: 2007, A new look at ESO and BESO optimisation methods, *Structural and Multidisciplinary Optimization*, **35**, 89-92.

X. Huang and Y.M. Xie (eds.): 2010, *Evolutionary Topology Optimization of Continuum Structures*, John Wiley & Sons, Chichester, UK.

Huang, X., Xie, Y.M. and Burry, M.C.: 2007, Advantages of Bi-Directional Evolutionary Structural Optimization (BESO) over Evolutionary Structural Optimization (ESO), *Advances in Structural Engineering*, **10**, 727-737.

Reynolds, C.W.: 1987, Flocks, Herds, and Schools: A Distributed Behavioral Model, *SIGGRAPH Conference Proceedings 1987*, California, 25-34.

R. Snooks (ed.): 2014, *Behavior formation Multi-agent algorithmic design strategies*, RMIT University.

Wang, M.Y., Wang, X. and Guo, D.: 2003, A level set method for structural topology optimisation, *Computer Methods in Applied Mechanics and Engineering*, **192**, 227-246.

Xie, Y.M. and Steven, G.P.: 1993, A simple evolutionary procedure for structural optimisation, *Computers & Structures*, **49**, 885-896.

Xie, Y.M. and Steven, G.P.: 1994, Optimal design of multiple load case structures using an evolutionary procedure, *Engineering with Computers*, **11**, 295-302.

Yan, X., Bao, D.W., Cai, K., Zhou, Y. and Xie, Y.M.: 2019, A New Form-finding Method for Shell Structures Based on BESO Algorithm, *Proceedings of IASS Annual Symposia 2019*, Barcelona, 1-8 (8).

Yang, X.Y., Xie, Y.M., Steven, G.P. and Querin, O.M.: 1999, Bidirectional Evolutionary Method for Stiffness Optimization, *AIAA/USAF/NASA/ISSMO Symposium on Multidisciplinary and Optimization 1998*, St. Louis, MO, 1483-1488.

Zhao, Z.-L., Zhou, S., Feng, X.-Q. and Xie, Y.M.: 2018, On the internal architecture of emergent plants, *Journal of the Mechanics and Physics of Solids*, **119**, 224-239.

SPATIAL FINDINGS ON CHILEAN ARCHITECTURE STYLEGAN AI GRAPHICS

TOMAS VIVANCO LARRAIN[1], ANTONIA VALENCIA[2] and PHILIP F. YUAN[3]
[1]*Pontifical Catholic University of Chile, Tongji University*
[1]*tvivancol@uc.cl*
[2]*Pontifical Catholic University of Chile*
[2]*arvalencia@uc.cl*
[3]*Tongji University*
[3]*philipyuan007@tongji.edu.cn*

Abstract. The use of StyleGAN algorithms proposes a novel approach in the investigation of architectural images. Even though graphical outcomes produced by StyleGAN algorithms are far from being architectural spaces, they might become a starting point in the creative process of architectural projects. By creating a database of specific categories of architectural images located in certain contexts, significant findings might emerge regarding their categorization in accordance to the 'style of a culture.' This research analyzes the architectural images that result from implementing StyleGAN algorithms in a database of images of Chilean houses built between the years 2010 and 2020 and selected as finalist of the ´Project of the Year´ from international viewers and curators of the most viewed architectural website of the world. Our findings suggest that Chilean houses have two distinctive elements strongly influenced by human bias: the proportion of voids in the architectural-like generative volume and the integration of vegetation or landscape.

Keywords. StyleGAN; Chilean architecture; artificial intelligence; spatial findings.

1. Introduction.

Recent advances in the area of computer science have allowed for the integration of new procedural tools in the design process. Designers and computer scientists have found common ground in exploring and creating new formal possibilities, building a three-dimensional creative space to navigate within its latent vector.

Conceptually, ideas exist due to the fact that we can represent them, and in turn, representation implies the use of known or trained tools or methods that make the idea explicit. At the same time, a new creative idea is driven by intuition, which cannot be understood or described employing logical operations that only become visible when it can surprise an observer or user, generating a certain degree of novelty. Therefore, a new creative idea lies in the recipient of that idea.

PROJECTIONS, Proceedings of the 26th International Conference of the Association for Computer-Aided Architectural Design Research in Asia (CAADRIA) 2021, Volume 1, 251-260.

From the perspective of the creator, ideas are produced by connections that are not necessarily rational or logical, originated by three sources of information. The first is inherited prior or genetic knowledge; the second is knowledge acquired through feelings and perceptions, or senses; and the third is knowledge gained throughout the creator's life.

These three sources of information nourish our massive database–the place where we explore all the knowledge that feeds into our unique and creative design processes. From this perspective, we then ask ourselves: is it possible to explore the limits of our creativity through the generation of databases of information or images?

Considering the origin of ideas as a starting point for the creative development of design processes questions the idea of creative freedom, as it challenges the notion that an idea is the interconnection of a non-logical organization of senses (Baars, 1988), experiences, learned knowledge and genetics.

On the one hand, computational technologies, specifically Artificial Intelligence, represent a significant advance towards the development, optimization and automation of processes; on the other, there is a large and emerging debate (Boden, 199) about their ability to replace or extend human creativity. Understanding the information that fuels our creativity as "manageable" and "arrangeable" allows for the possibility of generating new images or patterns without direct human intervention (Bechtel & Abrahamsen, 2002) and designing with images or formal references previously known and with which we consciously and unconsciously operate. So, can an algorithm navigate or operate within creativity? Alternatively, perhaps, are algorithms able to explore some of the formal attributes of existing architectural buildings in specific contexts that influence us and define, in an unconscious manner, a local style or attributes?

This research explores and analyzes synthetic images that result from implementing StyleGAN algorithms with a database of images of 1,500 Chilean houses between the years 2010 and 2020 in order to identify spatial attributes that suggest a particular architectural style present in Chilean houses.

1.1. GENERATIVE ADVERSARIAL NETWORKS.

Generative Adversarial Networks (GANs) are generative Artificial Intelligence techniques based on a networked algorithm that recognizes patterns and generates relationships between a large amount of data, similar to the way neural networks work in the brain (Brock, 2019). The input information is processed in layers of algorithms, recognizing patterns and generating associations between them in order to generate a result. If the result is similar to the original, the network learns from it and generates a new result, ensuring that the generated outcome is novel compared to the original database.

GANs are composed of two neuronal networks that 'compete' in order to produce these original images: a bottom-up generator which generates images, and a top-down Discriminator that evaluates the generated images. Somehow, the Generator takes the role of the artist and the Discriminator of the critic (Leach,

2019), as the former has to constantly 'surprise' the latter. In this process of 'competition,' the generator must produce realistic images until the Discriminator is unable to distinguish them from the given dataset.

1.2. GENERATOR AND DISCRIMINATOR STYLEGAN

The Generator and Discriminator are two basic components that enable GAN's functioning. Both components are models of Neuronal Networks that are constantly operating.

The function of the Generator (Figure 1) is to generate fake results from random noise or from an aleatory input given by real data. The Discriminator is the algorithm that distinguishes real data from fake data before re-entering that data to the Generator. This process is called the Epoch.

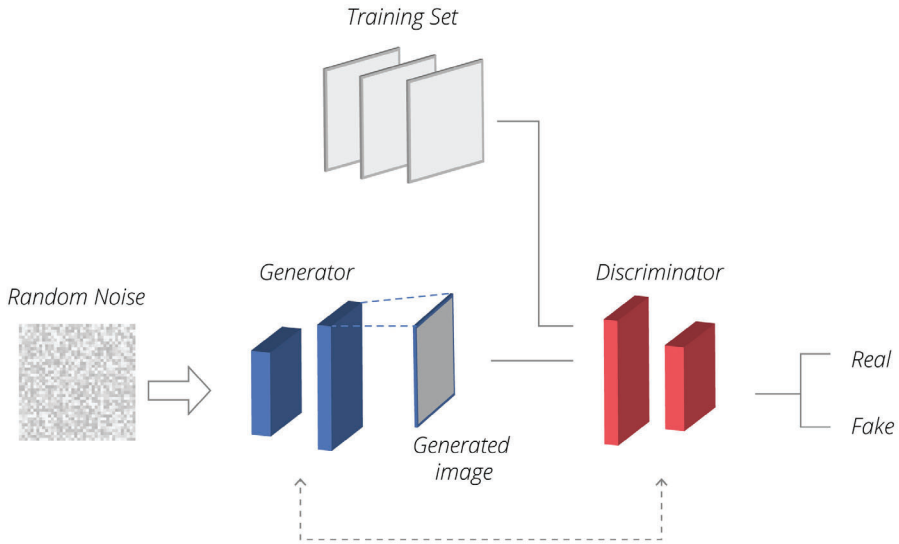

Figure 1. Generator and Discriminator of a Generative Adversarial Network.

1.3. STYLEGAN

Presented by Nvidia in 2018, it occupies the structure of a Generative Antagonist Network (GAN) with the main purpose of generating new images of faces, from a database of images of real faces modified with noise and interference. Two "neural" networks constantly interact, where one proposes new options, and the other evaluates their level of authenticity.

Similar to the process when humans learn a specific architectural style or geometric element (del Campo, Manninger, 2020), neural networks are trained with as many images as possible–at least a thousand–to recognize the differences between elements and styles.

Suppose the process of computing a large number of images to recognize motifs

(Priore, 2001) and to produce new stylish images with those patterns are similar to the human process of observing, classifying and creating. In that case, computers through AI algorithms might become, in a way, as creative as humans or at least become a supportive tool with which to navigate through creativity in an extended and collaborative way.

Human Learning and Machine Learning applied to the analysis of images are similar processes based on the detection of significant patterns. The main difference between these two processes is that AI-based learning is an automatized algorithm (Shalev-Shwartz, 2014) that transforms previous experiences into specific know-hows without knowing what the symbolic, cultural and functional purposes of the analyzed object are. Hence, it cannot make any relationships or functional associations with other objects or generate any results outside the input trained data.

2. Methods and processes.

The human-machine learning design methodology allows the designer to take the role of curator. Co-designing with machine intelligence involves an exploratory territory where the outcome cannot be predicted, and thus involves tweaking specific parameters and objectives to turn a human design process into a human-machine conversation.

The main objective of this research is to generate synthetic architectural images using a StyleGAN algorithm and analyze those images to detect main objects or elements that emerge as a suggestion of style or attributes. To achieve this objective, StyleGAN2 and Object Detection algorithms from Runway ML app were trained to generate the images and to detect objects and elements from them. Four steps composed the process (Figure 2) to accomplish the results and findings:

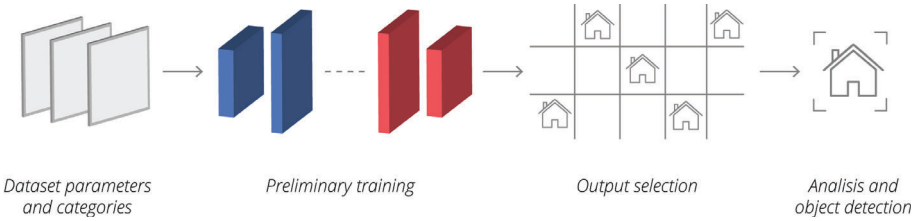

Figure 2. Four steps methodology used on the presented research.

RunwayML is an Artificial Intelligence tool for creators that allows them to discover, create, and use artificial intelligence in creative work. Creativity is being subjected to a revolution with human and machine interactive co-design by allowing creators to use this new tool and explore the boundaries of creation. Designers with no coding experience may take into consideration new design questions and objectives, encouraging experimentation with pre-trained models.

The images were chosen from ArchDaily´s ´Building of the Year´ database from the category of Chilean houses build between 2010 and 2020, each project was selected by their community- with round 160 million views per month- and

global curators composed by architects and designers. This means, there is a crossed, wide and blind selection of each house without any intervention from the authors, giving a global and local validation of their architectural attributes.

2.1. DATASET PARAMETERS AND CATEGORIES

The first step to train a custom model for the generation of StyleGAN based images is to gather a dataset that will serve as the input to train the model. It is crucial to elaborate an organized, clean and robust database and later pre-process it. These steps consist of a collection of around 1,500 images (Figure 3), ensuring that they are representative and exemplify the target image, and that undesired elements are removed.

The database is classified in categories and subcategories to unify it and make it more effective. Considering the role of the designer in the human-machine learning process, the realization of a robust and organized dataset will explain a work strategy, a database classification topology, and the parameters needed to achieve the results.

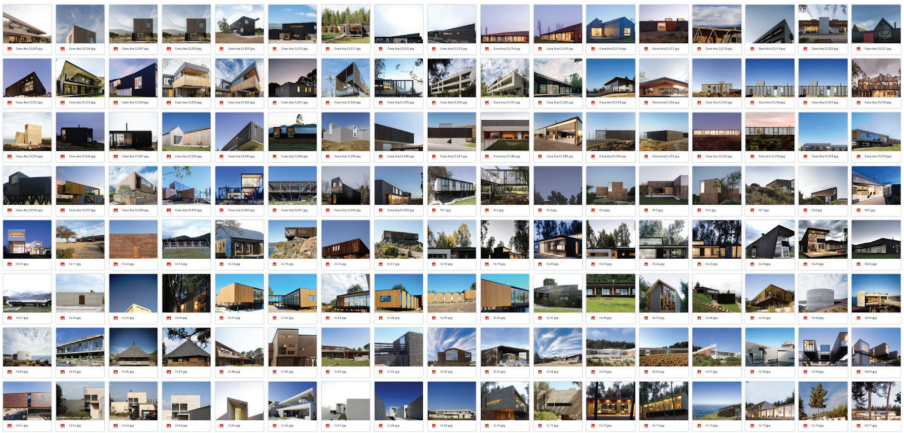

Figure 3. Dataset topology of 1.500 Architectural Chilean Houses facades retrieved from ArchDaily database.

The images were selected from Archdaily's database; each are photographs of the facade of houses built in different regions in Chile. Renowned local architects designed each house, and curators from Archdaily selected them and published them on their platforms. Many of them were published in different national and international architectural magazines. The main characteristic for the selection of images consists of generating a diverse but pre-worked dataset from a diverse range of designs, including houses in urban, rural and seaside contexts, as well as two volumetric strategies: boxed or 'Mediterranean' volume with a minimum roof slope, and triangular volume or Colonial-Chilean house with a steep roof slope. Each image showed a centred facade, showing the surroundings of the house, meaning the image needed to show where the house was built; also, it must show the entire facade, and the volumes needed to be fully visible in the perspective of

elevation views.

2.2. PRELIMINARY TRAINING

The first training of the StyleGAN model was carried out after obtaining a robust and pre-worked database. First, it began with the choice of a pre-trained model to generate faces from the Flickr database, to then set the number of training steps and refine specifications. Once the pre-processing was ready, a latent space allowed the navigation from an extensive arrangement of 512 dimension vectors (Figure 4), each one of them offering infinite possibilities of synthetic images. The possibilities are endless, and curatorship takes a critical role in evaluating the outcomes.

Figure 4. A generative vector space grid as a result of the training process.

The algorithm was trained under 2,000 steps, each one of them understood as an epoch. As can be seen in Figure 4, the pre-trained model 'forgot' about human faces and only selected facades, ensuring a high-performance result and a generation of a clean image.

Truncation and sampling distance mark the variability of the output images within the 512 dimension vectors. An increment in the sampling distance generates a more diverse set of facades, resulting in a more significant distinction between picture and picture in the latent space. Truncation, on the other hand, determines how "realistic" the output image will be. The closer the number is to 0, the closer it approximates to the original dataset (Table 1). For example, using an input vector of an image as the centre of the starting point (of the latent space), and lowering down the truncation-psi and the sampling distance, results in the effect of detail variation under a similar input shape.

Table 1. Variation of truncation and sampling distance with an input vector as a starting point in the latent space. Images represent the difference between each selected stop in the parameters and the effect on the generated images.

2.3. OUTPUT SELECTION

As previously stated, the database is a critical piece that feeds the system. Using clear and concise input criteria will provide thorough work for the outcome images. In some way, the input criteria are the borders where the generated images cannot pass. The cognitive process of selecting input images and evaluating the outcomes based on specific classifications identified in the generative process means an unconscious but culturally constructed bias that controls the process.

Why does one image pass the filter, and another does not? What does the designer consider when selecting an image that represents the style of Chilean architectural facades? The act of analysis and selection is essential, as those parameters affect the meta-designer/curator level and final selection.

The vector latent space images were selected under three objective criteria based on the dataset topology: first, the clarity of the image, where the edges of the house-like volumes were clean and straight, this because all the images from the datasets showed volumes straight lines; second, clear boxed or 'Mediterranean' volumes; and third, Chilean colonial house type volumes with steep roof slopes.

To the human eye, each selected outcome image presented some evident characteristic that defined standard classification criteria, suggesting the definition of a particular "style" of a Chilean house over others, from which, after analyzing the dataset and the generated images, two main criteria were observed:

(1) Incidence of vegetation in the image as an architectural element.

(2) Relationship between voids and solids of the images, with a strong tendency to voids.

2.4. ANALYSIS AND OBJECT DETECTION

From the latent vector space, 1,000 synthetic images were selected after finishing the first training. The selection of each image depended on the clarity of the architectural volume, vegetation as an external but integrated element, and voids inside the architectural volume (Figure 5).

With those three elements, an Object Detection algorithm (pre-trained to detect different objects or elements in images) was firstly trained with the original dataset to recognize three types of elements: vegetation, windows or façade voids, and volumes (Figure 6). A second training was done using the vectors of the generated synthetics images, and, at last, each synthetic image was analyzed to recognize and meet the previously established criteria.

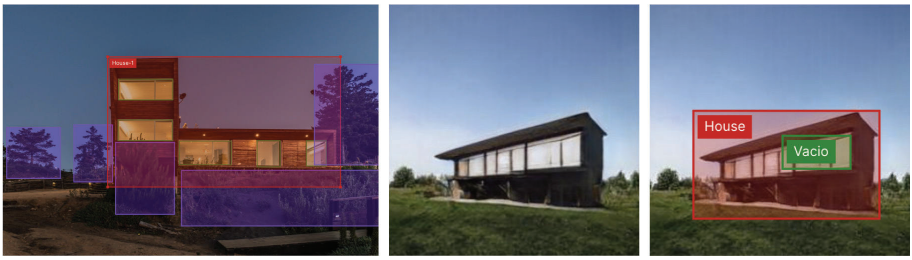

Figure 5. Object detection model trained to identify the classified elements that compose a Chilean architectural facade: presence of vegetation, and proportion of empty v/s full and identify a house.

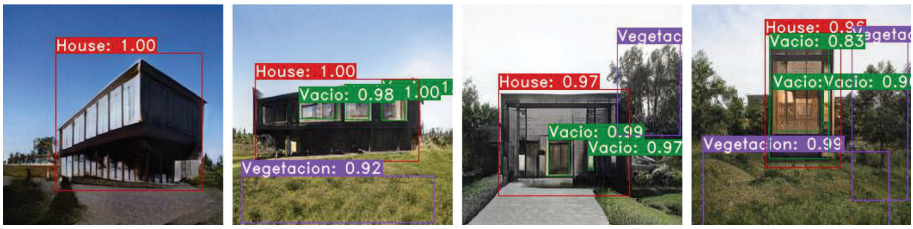

Figure 6. Selected images by the object detection algorithm based on criteria.

3. Final training images and results.

The results of the StyleGAN2 algorithm are images that look like houses, even though they were just the combination of pixels with supposedly no spatial relationship.

Nevertheless, two main spatial standard features that emerged from the process are the integration of landscape and nature, and the proportion of the volume-void relationship. Both characteristics serve to analyze the generated images and to define a specific Chilean Houses Architectural Style characteristics (Figure 7).

Figure 7. Final Synthetic images after the analysis of the classification criteria.

4. Discussion.

Considering all the variables that architectural projects must integrate to become a physical spatial solution, this StyleGAN image generation process is only successful in allowing users to explore new graphic relationships and configurations of recognizable elements in a pixel arrangement. This is generated by the limited relationships between pixels that configure images, given within the limits of what is possible. However, the database frames what the algorithm knows or learns, which means that nothing that has not been previously accepted or selected by the designer or curator can emerge as an outcome, consciously or not.

The use of Machine Learning as part of the creative process affects how the designer communicates and makes design decisions influenced by different aspects of the outcome form. Not only does it affect the images, but it also influences the narrative behind the final results. Creativity is subject to a series of parameters and historical data that is interpreted by technology. Nevertheless, decisions are still under the responsibility of the designer, now acting as the conductor of the orchestra.

The lack of architectural ornaments or historical architectural styles from the chosen images that compose the input database supports the fact that neither of the analyzed synthetic images had a particular or singular element. Generating homogeneous and global criteria of the resulting images that suggest the Chilean architectural house style or characteristics.

Because of the common and homogeneous spatial language of the synthetic images, attributable to the ‘real´ images of the original database, and due the selection of those houses was made by a select group of international curators, along with the website visitors from around the world who recognized relevant architectural design contributions to the field, architectural languages is strongly influenced by their bias, but at the same time, influences the authors of those houses build between 2010 and 2020 selected a ´Project of the Year´ finalists. Building a common and homogeneous spatial and formal architectural language, opening the possibility that a synthetic image could compete in a design or architectural competition with equal footing with ´real’ buildings.

Further research from this investigation could rely on quantifying the relationships between void and solid, advances in the detection of specific architectural elements like columns, and the measurement of the proportion of

the theoretical three-dimensional volumes.

References

"ArchDaily | Broadcasting Architecture Worldwide" : 2020. Available from <www.archdaily.com>.

Baars, B.: 1988, *A Cognitive Theory of Consciousness*, Cambridge University Press.

Bechtel, A.A.a.: 2001, *Connectionism and the Mind*, John Wiley & Sons.

Boden, M.A.: 1998, Creativity and artificial intelligence, *Artificial Intelligence*, **103**(1-2), 347-356.

Brock, A., Donahue, J. and Simonyan, K.: 2018, Large Scale GAN Training for High Fidelity Natural Image Synthesis., *International Conference on Learning Representations.*.

Bátfai, N.: 2011, Conscious Machines and Consciousness Oriented Programming., *arXiv*.

del Campo, M.M.: 2020, A Question of Style - Style, Artificial Intelligence and Architecture, *Architectural Intelligence*.

Karras, T., Laine, S. and Aila, A.: 2019, A Style-Based Generator Architecture for Generative Adversarial Networks, *IEEE/CVF Conference on Computer Vision and Pattern Recognition (CVPR)*.

Leach, N.: 2019, Do Robots Dream of Digital Sleep?, *Proceedings of ACADIA 19:Ubiquity and Autonomy*.

Priore, P., G'omez, A., Pino, R. and Rosillo, R.: 2014, Dynamic scheduling of manufacturing systems using machine learning: An updated review, *Artificial Intelligence for Engineering Design, Analysis and Manufacturing*, **28**(1), 83-97.

Shai Shalev-Shwartz, S.B.D.: 2019, *Understanding Machine Learning*, Cambridge University Press.

Building Information Modelling, Structural and Environmental Performance

INTEGRATING DIGITAL DESIGN AND ADDITIVE MANUFACTURING THROUGH BIM-BASED DIGITAL SUPPORT

A decision support system using Semantic Web and Multi-Criteria Decision Making

CHAO LI[1] and FRANK PETZOLD[2]
[1,2]*Technical University of Munich, Chair of Architectural Informatics, Munich, Germany*
[1,2]*{chao1.li\petzold}@tum.de*

Abstract. Additive Manufacturing in Construction (AMC) envisions a possible alternative for predominantly manual construction with various benefits. In addition to the well-known extrusion-based implementations of AMC, other techniques have been developed to meet various visual and functional requirement. However, the application of Additive Manufacturing (AM) into construction projects has to be carefully evaluated, especially during the early phases of architectural design when important decisions are made. From this point, this work devised an AMC-Oriented Design Decision Support System (DDSS) to identify suitable building components which can be manufactured with specific AM methods. In such a DDSS, knowledge base and decision-making strategy are both critical. To this end, principle of leveraging Semantic Web techniques and Multi-Criteria Decision Making (MCDM) methodologies will be addressed. At the current stage of our research, pre-printed building components using concrete material are considered during the decision support process.

Keywords. Additive Manufacturing in Construction; BIM; Design Decision Support System; Multi-Criteria Decision Making; Semantic Web.

1. Introduction

Conventional construction processes are commonly labour-intensive, material-inefficient, time consuming, and in some cases dangerous. As an alternative, the emerging AMC is able to lower material and labour cost, offer faster building rate, and enrich novel shapes (Ghaffar, Corker and Fan, 2018). Among the industrial practices of AMC, extrusion and particle-bed processes are most representative when dealing with concrete materials (Paolini, Kollmannsberger and Rank, 2019). Apart from that, many researchers are investigating further on the underlying AM methods (Lowke et al., 2020) (Kloft et al., 2020). Furthermore, different reinforcement strategies have been proposed

PROJECTIONS, Proceedings of the 26th International Conference of the Association for Computer-Aided Architectural Design Research in Asia (CAADRIA) 2021, Volume 1, 263-270.

to improve the mechanical performance of printed elements (Asprone et al., 2018) (Matthäus et al., 2020).

In consequence to versatile industrial practices in AMC, the decision-making of specific AM methods is becoming more complicated, but important. (Sacks et al., 2018, p. 180) illustrates that the early design greatly impacts on the overall functionality, costs and benefits of the building project, thus a preferred design process should put more effort into it. Accordingly, the influences of adopting AMC needs to be analysed in early design phases to minimize expensive changes or corrections of the plan. Nonetheless, inadequate knowledge of AMC by the architects and engineers impedes its consideration during decision-making processes of early-phased design.

It is known that Building Information Modelling (BIM) has significant potential to modernize the conventional AEC business model and brings advantages to the entire range of the building life cycle. Nowadays, it is a de-facto methodology applied in AEC industry (Sacks et al., 2018). Gradeci and Labonnote (2020) state that, although in-depth research studies have been done on both BIM and AM, the integration of BIM into AM is very scarce. They exploited the joint value creation potential of AM and BIM for concrete structures. Among those, the synergy of AM and BIM advantages the design process with greatest potential value. In recent years, BIM-based design decision support draws attention of researchers from various domain. However, it still faces a dilemma as formal description of the underlying knowledge bases receive limited consideration.

We believe that a critical step to advance the AMC is to establish a knowledge-based decision support system which helps architects and engineers determine the feasibility of AM methods given an interoperable building design. So far, research works have hardly covered a comprehensive framework that utilizes decision-making support for the integration of AM into BIM-based design. Within the scope of the collaborative research centre ‘Additive Manufacturing in Construction - The Challenge of Large Scale’ (TRR 277 2020) funded by ‘Deutsche Forschungsgemeinschaft (DFG)’, our research unit is dedicated to bridge this gap. As we are in an initial phase of the research period, this paper will propose a preliminary concept of a DDSS and focus on the formalized knowledge base containing capabilities and constraints of AM methods. Based on that, future work will introduce multiple design criteria and explore the potential of combining simulations with such a knowledge base during decision-making processes. To prove our concept, the system will firstly concentrate on the decision-making of concrete printing in scale of individual building components.

2. Related work

2.1. INTEGRATION OF BIM WITH AM SYSTEMS

Several research studies have demonstrated the integration of BIM with AM systems. Among those, Davtalab, Kazemian and Khoshnevis (2018) introduced a comprehensive framework which seamlessly integrates BIM and Contour Crafting. In their study, the named POCSAC software extracted geometry and material information from the BIM design using IFC data schema. Next, the

software output an optimized tool path in graphical form. With the architectural and structural requirement specified in building design, a following laboratory test was mandatory to determine proportions of the printing mixture by considering fresh and hardened concrete properties. Finally, G-code was automatically generated for the control of construction robot. In the aforementioned process, the retrieval of material and geometry information from IFC remains implicit. On the other hand, Smarsly et al. (2021) proposed 'Printing Information Modelling' (PIM) as a BIM-based meta-modeling approach to facilitate the concrete printing in terms of data flow from BIM to AM. A PIM model comprises three abstract classes of data which are necessary to describe the AM methods in aspects of process, material and geometry. Smarsly et al. successfully mapped material and geometry information from an IFC formatted design into the PIM, while process parameters have to be fed in manually. The specialized PIM application then generated corresponding CNC code controlling a gantry concrete printer. Both of the practices evidenced the possibility of integrating BIM-based design with AMC, but still faced with a problem between architectural design and the adoption of AM methods, which would be tackled by the proposed DDSS.

2.2. DFAM KNOWLEDGE BASES

Dinar and Rosen (2017) emphasized the importance of AM-specific design guidance system and correspondingly formalized a Design for Additive Manufacturing (DFAM) (Rosen, 2007) knowledge base using Web Ontology Language (OWL). They explained the advantages of choosing ontology over direct use of traditional database in several aspects, mainly: expressiveness to model knowledge, pertinency to tutoring system, and integration to web technology. Similarly, but more in detail, Kim et al. (2019) presented a profound DFAM knowledge base by explicitly structured DFAM knowledge conceptually into three categories: part design (design feature and geometry parameters), manufacturing features and process planning (material and process parameters). In their work, design and manufacturing features were loosely coupled by parameters. Based on that, manufacturability was evaluated by applying design rules on the knowledge base, which is defined using Semantic Query-Enhanced Web Rule Language (SQWRL).

2.3. MCDM METHODOLOGY IN BIM AND AM

Established decision support systems using MCDM have been presented for both AM and BIM. Wang, Zhong and Xu (2018) introduced a posteriori MCDM system for informed decision support to tackle the complexity of choosing a specific AM method. Different from the typical MCDM system, their system allowed users to explore and refine the option space defined by technical, economic and indirect criteria. Such an exploration feature is considered as 'design-by-shopping' (Yannou and Akle, 2017), which is deemed to be helpful in optimizing user's satisfaction of a decision support system. Jalaei, Jrade and Nassiri (2015) applied MCDM approach on a BIM-based design to assist users in selecting sustainable building components. Interestingly, the authors invited a group of attendees to weight the criteria matrix and leveraged Entropy Method to emphasize consensus

among different opinions. Afterwards, TOPSIS method was deployed to rank the alternatives for LCC analysis.

3. DDSS Integrating AM into BIM

An overarching goal of the DDSS is to allow a maximum of design freedom by converting resulting design into actually constructible entities. To this end, knowledge needs to be acquired in advance from a number of experts and then formally described for its use in decision support process. DDSS should then apply such a compensating knowledge base to verify feasibility of printing building components selected from a BIM-based design.

3.1. SYSTEM WORKFLOW

In our proposed decision support workflow (see Figure 1), BIM-based design, DDSS and AMC-related knowledge base are organized as in-parallel but interconnecting components. With this manner, knowledge can be maintained without greatly changing the logic behind the DDSS, meanwhile, DDSS is able to provide a close-looped decision support to the architect. Sequentially, five activities are involved:

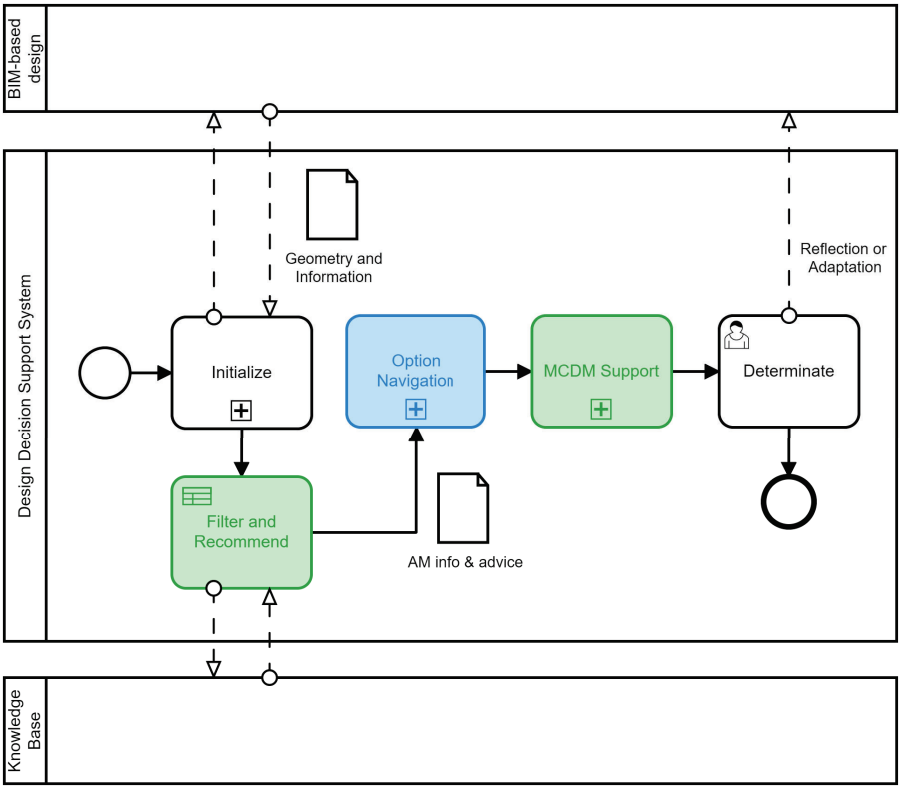

Figure 1. Workflow of DDSS.

1. *Initialize*: It is when an architect chooses working mode, selects building components and sets primary constraints. Correspondingly, the DDSS will read geometry and semantics of selected building components.
2. *Filter and Recommend*: The DDSS builds an option space by reasoning and querying feasible options from the knowledge base. Notably, the generated AM information and recommendation will be kept for use in subsequent decision-making processes. This process is enabled by an embedded inference engine and a specific API for knowledge access.
3. *Option Navigation*: In first instance, this activity asks the architect to pick multiple criteria from an existing list, then computes an optimal set of AM methods to form an option space. Afterwards, the architect is allowed to interactively explore and constrain the option space at will.
4. *MCDM Support*: A posteriori MCDM approach will consider multiple criteria selected by the user for the informed decision support. Ranked alternatives could be generated from this step.
5. *Determinate*: Based on the ranked alternatives and recommendations of design adaptation, the architect now either chooses a feasible AM method or adjusts the design. Once a certain AM method is determined, pre-defined and parameterized object types, hence, "families", will be automatically imported into and configured inside the BIM-based design.

Through this decision-making process, we could foresee the improvement of the Level of Development (LOD) with information obtained from the knowledge base, such as U-value, internal filling method, mechanical strength, etc. Evenmore, upcoming simulation and analysis procedures could also benefit from the given detailed information.

3.2. PRINCIPLE OF KNOWLEDGE FORMALIZATION

Domain-specific knowledge base usually serves as a backbone in a Knowledge-Based System (KBS). Due to the collabrality among various research groups, the knowledge base of proposed DDSS has to be formalized in an extensible, reusable and interoperable manner. Formal Knowledge Representation (KR) methods such as semantic network, frame, production rule and logical representations have their own strengths and limitations, while the paradigm in context of Sematic Web merges both rules and logical representations in form of logic programming and descriptive logic (Patel and Jain, 2018). Concretely, AMC-specific classes, rules and facts can be conceptualized with Web Ontolgoy Language (OWL), defined using Semantic Web Rule Language (SWRL) and queried through Simple Protocol and RDF Query Language (SPARQL). Furthermore, reasoning can be supported by various inference engines which are compatible to the aforementioned languages.

In our research, the specific ontology and design rules of AMC should be conceptualized to build a knowledge base (see Figure 2). The ontology needs to capture a series of information from the following perspectives:

- Method's know-how: The combined use of materials, process parameters and machine systems distinguishes the AM methods from each other. Apparently, characteristics of used material are decisive to the behaviors of printed

components. Machine systems' building envelope and mobility directly constrain the scale of the printed components. Process parameters, on one hand, are determined through experiments given specific materials and machine systems. On the other hand, greatly influence the printed component's form and function. Note that an AM method could have multiple candidate materials, machine systems and process parameters.

- Boundary Condition: AM method's boundary conditions indicates the thresholds of method's capabilities (mechanical performance, geometric freedom, etc.) and are often conditioned with AM's proprietary features. For example, the minimum down-sink angle for a printable overhang is captured in AM method's boundary conditions, given by the type of AM method, material, printing path and machine's degree of freedom.
- Design Intention: Building component's material, geometry and function directly reflect the architect's design intentions. Therefore, all decision support activities in the proposed DDSS stem from these aspects. In addition to exterior geometry, the infilling pattern has also been taken into account during construction, as it is closely related to functional performances. Functions such as load-bearing and thermal comfort are in turn described using specific parameters.
- Parameters: Parameters are attributes that represent the above aspects, which can be conceptualized as classes or data properties for individual instances.

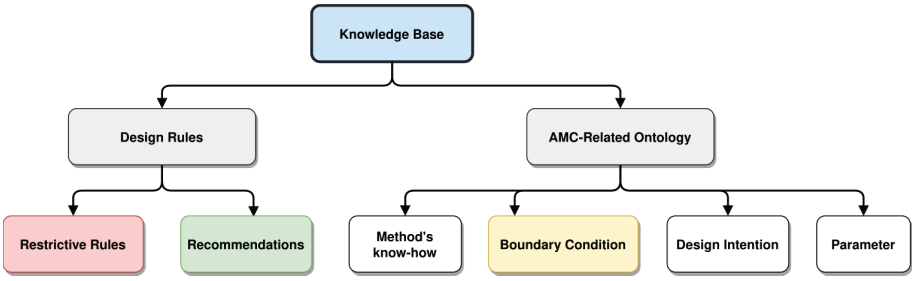

Figure 2. Knowledge Base Structure.

Figure 3 further illustrates the AMC-related ontology by denoting relations among conceptualized classes. Considering the combination of process parameters, material and machine system, experts set AM methods' functional and geometrical boundary conditions, which in turn constrain the evaluated building component. It is worth noting that there could be multiple AM methods that can print a given building component, according to the design rules.

Design rules, on the other hand, provide insights into manufacturability considering constraints in relation to design, process and material (Jee and Witherell, 2017). As far as AMC is concerned, design rules can stipulate various restrictions to apply AM methods, such as manufacturability, transport regulations, building codes requirement, etc. In addition to these restrictive rules, (Kim et al., 2019) utilized design rules for recommendations of overhang support structure and design adaptations. A simple design rule recommending design adaptation, in plain words, may state that: "IF the down-sink angle of the overhang feature

is smaller than the corresponding limit in boundary conditions of specific AM method, THEN it is recommended to adjust the overhang to this limit". With the same antecedent, an additional recommendation for support structure can be stated.

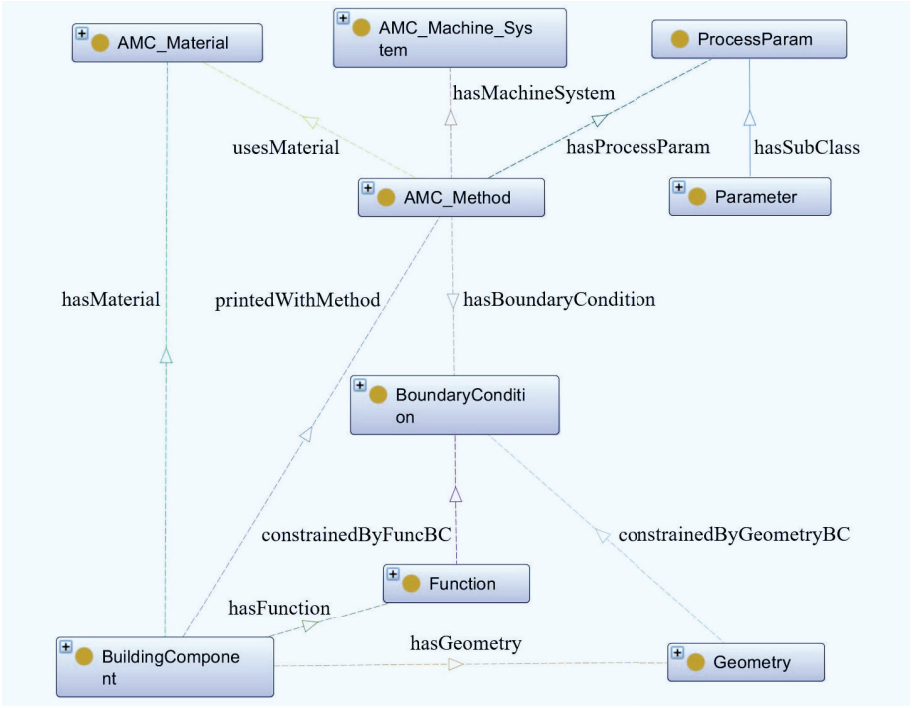

Figure 3. Simplified AMC Ontology (Top Level).

4. Conclusion and future work

This paper proposed an AMC-Oriented decision support system for BIM-based architectural design which aimed at integrating AM methods into BIM using Semantic Web technology and MCDM approach. We had also insight into the knowledge base with respect to its domain ontology and design rules. Since we are in the first phase of a four-year research period, this paper conservatively reveals our research rationality and initial findings. Sequentially, future work will attempt to tackle the difficulties in manufacturability validation and formalize the knowledge base. Afterwards, the knowledge base will be integrated into a BIM authoring system. Multiple decision-making criteria and MCDM approaches will then be studied, adapted and merged into the DDSS workflow. Next, the proposed DDSS will be extended to incorporate simulations processes with assistance of a feedback mechanism.

References

"TRR 277" : 2020. Available from <https://www.tu-braunschweig.de/trr277> (accessed 24th November 2020).

Asprone, D., Menna, C., Bos, F.P., Salet, T.A.M., Mata-Falcón, J. and Kaufmannd, W.: 2018, Rethinking reinforcement for digital fabrication with concrete, *Cement and Concrete Research*, **112**, 111-121.

Davtalab, O., Kazemian, A. and Khoshnevis, B.: 2018, Perspectives on a BIM-integrated software platform for robotic construction through Contour Crafting, *Automation in Construction*, **89**, 13-23.

Dinar, M. and Rosen, D.W.: 2017, A design for additive manufacturing ontology, *Computing and Information Science in Engineering*, **17**(2), 1-9.

Ghaffar, S.H., Corker, J. and Fan, M.: 2018, Additive manufacturing technology and its implementation in construction as an eco-innovative solution, *Automation in Construction*, **93**, 1-11.

Gradeci, K. and Labonnote, N.: 2020, On the potential of integrating building information modelling (BIM) for the additive manufacturing (AM) of concrete structures, *Construction Innovation: Information, Process, Management*, **20**(723611), 321-343.

Jalaei, F., Jrade, A. and Nassiri, M.: 2015, INTEGRATING DECISION SUPPORT SYSTEM (DSS) AND BUILDING INFORMATION MODELING (BIM) TO OPTIMIZE THE SELECTION OF SUSTAINABLE BUILDING COMPONENTS, *Information Technology in Construction*, **20**, 399-420.

Kim, S., Rosen, D.W., Witherell, P. and Ko, H.: 2019, A Design for Additive Manufacturing Ontology to Support Manufacturability Analysis, *Computing and Information Science in Engineering*, **19**(4), 1-10.

Kloft, H., Krauss, H.w., Hack, N., Herrmann, E., Neudecker, S., Varady, P.A. and Lowke, D.: 2020, Influence of process parameters on the interlayer bond strength of concrete elements additive manufactured by Shotcrete 3D Printing (SC3DP), *Cement and Concrete Research*, **134**(106078).

Lowke, D., Talke, D., Dressler, I., Weger, D., Gehlen, C., Ostertag, C. and Rael, R.: 2020, Particle bed 3D printing by selective cement activation – Applications , material and process technology, *Cement and Concrete Research*, **134**(106077).

Matthäus, C., Kofler, N., Kränkel, T., Weger, D. and Gehlen, C.: 2020, Interlayer Reinforcement Combined with Fiber Reinforcement for Extruded Lightweight Mortar Elements, *Materials*, **13**(4778).

Paolini, A., Kollmannsberger, S. and Rank, E.: 2019, Additive manufacturing in construction: A review on processes, applications, and digital planning methods, *Additive Manufacturing*, **30**(100894).

Patel, A. and Jain, S.: 2018, Formalisms of Representing Knowledge, *Procedia Computer Science*, **125**, 542-549.

Rosen, D.W.: 2007, Design for Additive Manufacturing: A Method to Explore Unexplored Regions of the Design Space, *18th Solid Freeform Fabrication Symposium*.

Sacks, R., Eastman, C., Lee, G. and Teicholz, P.: 2018, *BIM Handbook BIM Handbook Rafael Sacks*, John Wiley & Sons.

Smarsly, K., Peralta, P., Luckey, D., Heine, S. and Ludwig, H.M.: 2020, BIM-Based Concrete Printing, *The International ICCCBE and CIB W78 Joint Conference on Computing in Civil and Building Engineering*.

Wang, Y., Zhong, R.Y. and Xu, X.: 2018, A decision support system for additive manufacturing process selection using a hybrid multiple criteria decision-making method, *Rapid Prototyping*, **9**, 1544-1553.

Yannou, B. and Akle, A.A.: 2017, Information visualization for selection in Design by Shopping, *Research in Engineering Design*, **28**, 99-117.

PARTICIPATORY HOUSING: DISCRETE DESIGN AND CONSTRUCTION SYSTEMS FOR HIGH-RISE HOUSING IN HONG KONG

CHUN YU MA[1] and JEROEN VAN AMEIJDE[2]
[1,2]*The Chinese University of Hong Kong*
[1]*kelvin.ma@link.cuhk.edu.hk* [2]*jeroen.vanameijde@cuhk.edu.hk*

Abstract. There has been a recent increase in the exploration of mereological systems, speculating on how digital design, assembly and reconfiguration of "digital materials" (Gershenfeld, 2015) enables digitally informed physical worlds that change over time. Besides opportunities for construction and design automation, there is a potential to reimagine how multiple stakeholders can participate in the computational decision-making process, using the benefits of the "mass customization of logistics" (Retsin, 2019). This paper presents a research-by-design project that applies a digital and discrete material system to high-rise housing in Hong Kong. The project has developed an integrated approach to design, construction, and inhabitation, using a system of "discrete parts" which can be assembled in various apartment configurations, to incorporate varying occupant's requirements and facilitate negotiations and changes over time.

Keywords. Participatory Design; Generative Design; Adaptable Architecture; High-rise Housing.

1. Introduction

High-rise housing in Hong Kong is highly standardized, to optimise design and construction costs. As the layout of an apartment defines the social relations and possible patterns of user behaviour (Hanson, 1998; Hillier, 1996), the over-optimisation of floorplans limits the freedom of choice of activities and discriminates against people with non-standard lifestyle requirements. Previous studies into the evolution of building typologies in Hong Kong public housing (Kitahara & Shinohara, 2014; Deng, Chan, & Poon, 2016) show that while the quality and environmental aspects of housing projects have improved, the amount of space and layout has not changed over the years. While new estates since 2004 adopt a 'non-standard' planning approach, the apartment layouts are in fact based on a standardised catalogue that offer no alternatives to the strategic arrangement of rooms. To optimise space, living rooms double up as circulation spaces to access bedrooms located at the perimeter, resulting in a high degree of unavoidable social interaction between household members.

This study employs a topological approach to the planning of apartment layouts, proposing different configurations of room locations and connections

PROJECTIONS, Proceedings of the 26th International Conference of the Association for Computer-Aided Architectural Design Research in Asia (CAADRIA) 2021, Volume 1, 271-280.

to offer different possibilities for social networking. We argue that this is an appropriate and necessary evolution in design thinking about housing, in a time when society is no longer characterised by standard nuclear families and regular work/live patterns. New technologies and cultural changes have increased demand for new forms of co-living and working from home, requiring new types of apartment layouts for a wide range of lifestyles.

Following the introduction of analytical descriptions for social structures in architecture by Hillier & Hanson (1984), ‘’space syntax‘’ methodologies have been widely adopted by researchers worldwide. The logic of defining spatial hierarchies and relationships has also been developed as a design methodology (Al-Jokhadar, 2017; Nourian, 2017), using generative computational methods to create apartment layouts based on network configurations. Layouts can be arranged in ways that enable more independent activities for different household members, or to offer them more freedom in choosing when or how to engage in social interactions.

Our study employs a configuration based design methodology (Fig. 1), generating apartment floor plans based on residents’ desired lifestyles. It explores possibilities for the introduction of mass-customised apartments, as we assume that many different households would have different requirements. As personal living requirements are open to change, and buildings will see different people move in and out over time, we also explore strategies for making layouts adaptable, using a building system that allows for the easy reconfiguration of apartment structures.

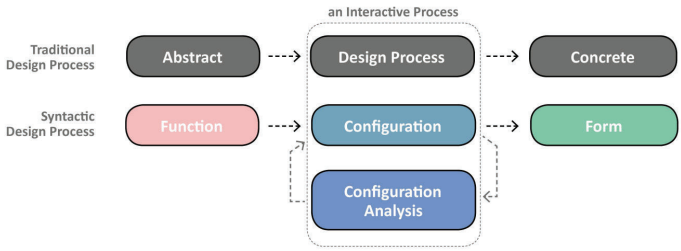

Figure 1. Configuration-based design processes (based on Nourian, 2017).

2. Generative Floor Plan Layout Design

For this research-by-design project, a unit layout configuration script was created to generate room clusters and relationships, based on a circle packing system and real-time physics simulation following on from Nourian (2017). The Rhino/Grasshopper plugin ‘’Wallacei‘’ (Makki, Showkatbakhsh and Song, 2019) was used to enable a multi-objective optimisation process, evaluating complex and contradictory requirements such shared circulation, building structure, daylight access and views.

As inputs to the script, end-user defined parameters are used including the number of required rooms, their function and size, and the desired connectivity

between them. The inputs are translated into an automatically generated spring model that creates a closest packing solution by translating desired connectivity into higher spring stiffness parameters. Reverse relationships (maximising distance between rooms) can also be applied. The circle packing solution is translated into an orthogonal floor plan by using a standardised grid system relating to furniture element dimensions and building components (Fig. 2).

Figure 2. Design mechanism for generative apartment layouts.

The computational workflow was further developed to negotiate between several units on one floor, incorporating shared unit boundaries and their connection to vertical circulation. To test a hypothetical scenario with different apartments having to configure around a shared core, four different types of households requirements were used and a number of optimisation criteria were introduced to generate the collective floor plan layout. The four main fitness objectives used were daylight access, views, floor plate geometry complexity, and internal circulation. These objectives are analysed when floor plate geometries are generated using an expanded version of the circle packing method describes above, highlighting how some objectives may align in certain solutions while others are contradictory. Maximising views from all rooms, for instance, creates a more irregular floor plan outline, while optimising geometry complexity (which indicates construction costs) results in a more compact and simple outline. The nature of the multi-objective optimisation process is that several optimal solutions are presented to the stakeholders, giving insight in the consequences of prioritising certain parameters and allowing the users to make an informed decision in negotiation with each other (Fig. 3).

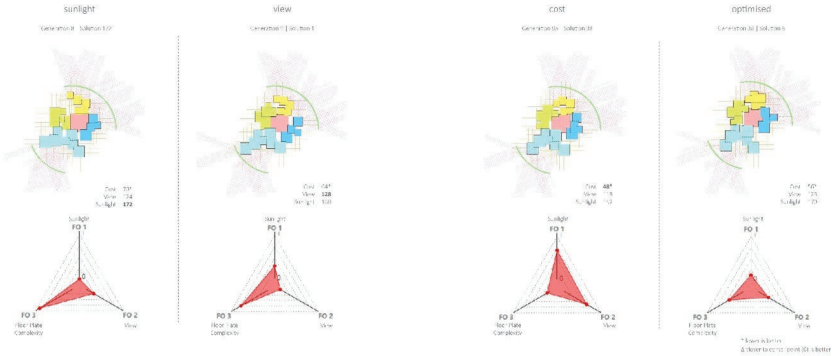

Figure 3. Layout optimisation based on daylight, views, complexity and circulation.

3. Optimisation Criteria for Multi-apartment Floor Plans

The generative algorithm incorporates minimum requirements for daylight access, to ensure that all rooms have access to light and ventilation in accordance with Hong Kong's planning standards and guidelines. In addition to measuring daylight access into all rooms, the algorithm incorporates a minimum distance of ten metres to another parallel façade element, to avoid privacy issues between neighbouring apartments. This distance could be adjusted by the residents, to fit different sites or cultural requirements.

To maximise views, which contributes to quality of living and to the value of the apartments in Hong Kong's high-density urban environment, sight-lines at 40-degree view angles (left and right) are projected from a row of points on the outer facades, checking for intersections with other parts of the floorplan geometry. A hypothetical context was added to test how layouts can be optimised in relation to attractive views in the surroundings, or to avoid view obstructions from adjacent buildings.

As construction cost is one of the major pressures on the design of housing projects in Hong Kong, the methodology used in this study incorporates several measures to rationalise the complexity of the generative solutions and improve their affordability. A key aspect is the integration of the characteristics of a modular construction system, assuming an assembly process of industrially prefabricated spatial units. The modular grid sizes for this system are optimised so that a large amount of different apartment configurations can be achieved with a small set of different modules. Using a process of 'snapping' to this construction grid, the algorithm can prevent non-standard modules and count the number of components needed to enclose the desired area of apartment floor space. The ratio between these values indicates the construction efficiency, while further data regarding the costs of different types of modules could be added, to give more specific feedback to the users. At the overall floor plate level, the script aims to reduce the total complexity of the floor plate geometry to reduce cost, assembly time and improve environmental performance.

Using the genetic algorithm functions in the multi-objective optimisation process, a large number of shape variations (phenotypes) are generated based on the same topological relationships (genotypes). All solutions are evaluated against the above fitness criteria and new generations of solutions are created by adding mutations to the best performing phenotypes of each generation. The desired number of rooms and their connections are achieved in all solutions, while presenting different options to the users that represent a different balance between views, daylight access and floorplan compactness. For the purpose of illustrating the potential outcomes of the generative design method, a series of 'non-standard' household and lifestyle scenarios was entered into the workflow, and the resulting apartment layouts and their spatial qualities were visualised (Fig. 5).

Figure 4. Iterative snapshots of floorplan layouts based on optimisation towards daylight and views, in relation to surrounding buildings.

Figure 5. Diverse life style requirements resulting in non-standard apartment configurations.

4. Integration Between Digital Participatory Design and Construction Systems

In parallel and in dialogue with the development of the generative design process for spatial layout solutions, a materialisation system was developed based on the premise of a fully prefabricated system of modular building elements. Following the desire to develop an adaptable apartment configuration system that would be open to changes in users, or user requirements over time, an interchangeable set of elements was developed based on the idea of ‘’discrete materials‘’ (Retsin, 2016). The discretised parts were developed by adapting existing modular elements used in Hong Kong’s public housing.

Since the first prefabricated systems developed in the 1930’s and 40’s by Wachsmann, Gropius and others, factory made elements have evolved from panel systems to volumetric systems, known as PPVC (Prefabricated Prefinished Volumetric Construction) or MIC (Modular Integrated Construction). These systems use cost-effective, high-quality elements to enable rapid assembly on site. Recent systems also integrate various services and finishes, further reducing the needs for specialist trades and processes on site.

The concept of digital materials as introduced by Gerschenfeld, Sanchez (2014) and Retsin, offers a new perspective on the integration between digital design and construction systems, using generative computational processes to optimise physical structures that have the same organisational logic as their digital counterparts. Discrete assemblies of elements can be tested and evaluated by designers and stakeholders alike in a collaborative process, before deciding which version would be materialised. Example projects by Retsin and others explore universal elements that avoid a classification between structural and non-structural, taking advantage of the multiple combinatory possibilities of the pieces to create flexible compositions of prefabricated elements (Retsin, 2017).

Dry connections that are reversible extend the lifespan of the elements, connecting the materials systems to a philosophy of reusable and adaptable products, reducing environmental impact and use of natural resources.

The discrete materials systems in their pure form result in redundancies and inefficiencies when dealing with structural performance requirements at larger scales, which is contradicting with current practice in Hong Kong's high-rise tower construction, where separate building systems are highly specialised and optimised. Therefore for our study, we have focused on a composite system that combines a non-flexible internal tower structure and a reconfigurable ''discrete'' apartment construction system. This is similar to current practices in Hong Kong housing construction where in-situ cast concrete cores are supplemented by prefabricated elements that form partitions, stairs, bathrooms, and facades (HKHA, 2011).

5. Discrete Material Systems in Highrise Construction

Following the aim of providing a reconfigurable construction system that allows for participatory housing design, the building is divided into three systems which are designed according their different levels of adaptability. The permanent vertical structure combines a circulation core and moment frame to provide structural stability to the entire tower, as well as a framework against which to connect the housing modules (Fig. 6).

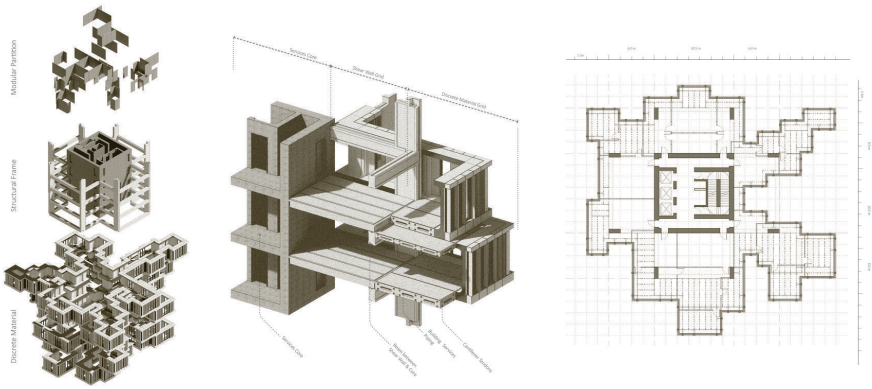

Figure 6. Combined system of permanent tower structure and adaptable apartment configurations.

The second system consists of the ''discrete'' spatial modules that form floor slabs and outer façade elements of the apartments, using a limited family of types with modularised dimensions. As individual apartments should be able to be reconfigured without affecting neighbouring units in all directions, apartments are cantilevered from the internal structure using post-tensioning cable systems. The steel framed modules would be designed to have efficient weight to strength ratios and have interlocking connection joints to create watertight enclosures. The third

system consists of the internal partitions, which are light steel infill panels that are easily reconfigurable by the users. The different systems have different rates of change: apartments could be expected to be altered once every 3-10 years while interiors might be changed more frequently.

While some international research on discrete material systems speculates on the automation of construction and adaptation using robotics, this study assumed a near-future scenario where the changes in apartment configurations could be implemented using conventional contractor services and equipment. The key innovative aspect around the system is the control and negotiation around customised housing configurations as part of a participatory and collaborative community process, facilitated through a user-friendly mobile application. The role of the architect is expanded towards the design of these processes, including guidelines and mentorship to assist residents with their decision making. The algorithms tested in this study could be further developed to provide a comprehensive forecasting service on the consequences of residents proposals, running background performance calculations while visualising the desired or even better solutions, to create better living environments for all members of the community.

6. Conclusions

This research has explored the conceptual possibilities of introducing a customisable and adaptable construction system into the highly constrained practice of high-rise housing design. Through the development of a case study tower design, and a number of prototypical assemblies, several potential configuration states have been illustrated, describing an ever-changing and user-driven housing community. The use of multi-objective optimisation processes and computational performance analysis could help to facilitate the ‘’democratic‘’ process of finding a balance between the desires of individuals and the interests of the collective, through their ability to indicate opportunities and help mediate conflicts of interest through a data-driven design approach.

The study aims to demonstrate the potential of architectural systems and processes that don’t produce housing that is conceived as finished when construction has completed, but instead construct open-ended systems that evolve with the changing living requirements of their inhabitants. The continuous collection of performance and user data throughout the life of the community, can provide feedback for continuous updating and improving the physical environment. This interactive process establishes a new definition of participatory and bottom-up design. The digital model of the building is more than a duplicate version of physical tower, as it serves as a virtual testing, visualisation and negotiation platform for residents. The resulting interactions blur the boundaries between digital and physical systems, not only supporting the construction of customised housing, but also to document and communicate the benefits and balance between different spatial, environmental and building performance criteria. Most importantly, this interactive process facilitates informed collaborative participation and negotiation assisted by the power of computation.

Future research could be used to further developed the technical aspects of implementing the conceptual notions around ‘’digital material‘’ systems towards the complex typology of high-rise housing in Hong Kong. As housing is one of the most significant factors in the experience of urban living, more effort should be devoted to innovation, using a more critical and user-centric approach to ensure that designs are fit for purpose. As design and construction processes are already becoming increasingly digitised, it is time to futher explore the value and capacity of digital systems to actively respond to the demands of residents, contributing to a better quality of life and help to promote a sense of belonging. While this approach is capable of disrupting the doctrine of standardisation and repetition in housing in Hong Kong, it may also offer opportunities to rethink scenarios of inhabitation in many other types of buildings and locations across the world.

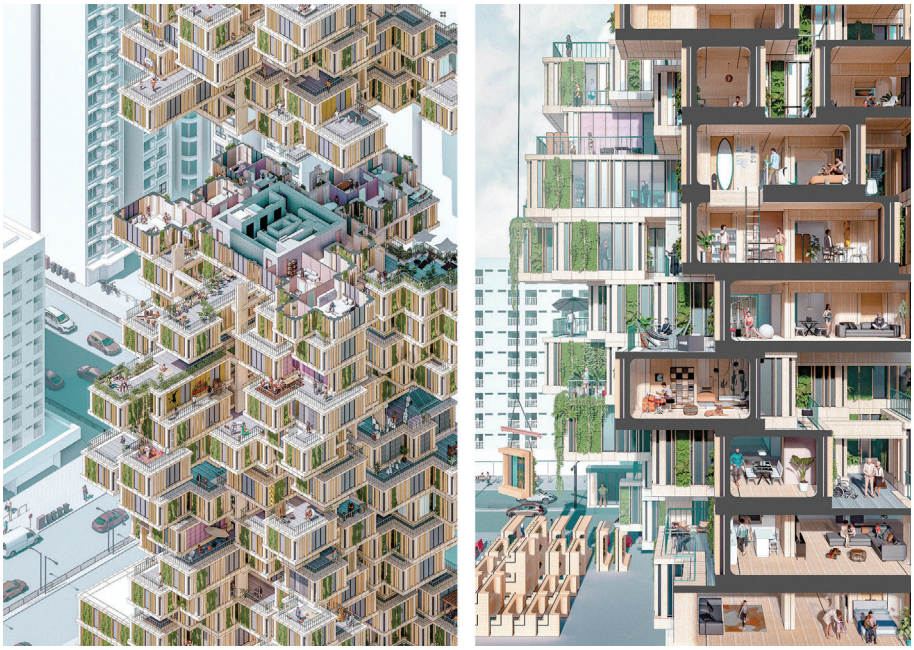

Figure 7. Diverse living configurations within participatory housing.

References

Al-Jokhadar, A. and Jabi, W.: 2017, Qualitative Representation and Spatial Reasoning in a Rule-Based Computational Design Model, *ECAADe RIS.*.

Deng, Y., Chan, E.H.W. and Poon, S.W.: 2016, Challenge-driven design for public housing: The case of HongKong, *Frontiers of Architectural Research*, **5**, 213 - 224.

Gerschenfeld, N., Carney, M., Jenett, B., Calisch, S. and Wilson, S.: 2015, Macrofabrication with Digital Materials: Robotic Assembly, *Architectural Design*, **85**(5), 122-127.

Hanson, J.: 1998, *Decoding homes and houses*, Cambridge University Press, Cambridge, New York.

Hillier, B.: 1996, *Space is the Machine: A Configurational Theory of Architecture*, Cambridge

University Press., Cambridge.
Hillier, B. and Hanson, J.: 1984, *The Social Logic of Space*, Cambridge University Press, Cambridge.
HKHA, D.C.D.: 2011, *Planning, design, and delivery of quality public housing in the new millennium*, Hong Kong Housing Authority, Hong Kong.
Kitahara, R. and Shinohara, S.: 2014, A Study on the Floor Planning in Public Rental Housing by Hong Kong Housing Authority, *AIJ Journal of Technology and Design*, **20**(46), 1053-1058.
Nourian, P., Rezvani, S. and Sariyildiz, S.: 2017, Designing with Space Syntax - A configurative approach to architectural layout, proposing a computational methodology, *ECAADe RIS*.
Retsin, G.: 2016, Discrete Assembly and Digital Materials in Architecture., *Herneoja, Aulikki; Toni Österlund and Piia Markkanen (eds.), Complexity & Simplicity - Proceedings of the 34th eCAADe Conference-Volume 1*, University of Oulu, Oulu, Finland, 22-26 August 2016, 143-151.
Retsin, G.: 2019, Toward Discrete Architecture: Automation Takes Command, *ACADIA 19:UBIQUITY AND AUTONOMY [Proceedings of the 39th Annual Conference of the Association for Computer Aided Design in Architecture (ACADIA) ISBN 978-0-578-59179-7]*, The University of Texas at Austin School of Architecture, Austin, Texas 21-26 October, 2019, 532-541.
Sanchez, J.: 2014, Post Capitalist Design: Design in the Age of Access, *Gerber, D and Ibanez, M (eds) 2014, Paradigms in Computing, Evolo*, New York.

A FRAMEWORK FOR MULTIVARIATE DATA BASED FLOOR PLAN RETRIEVAL AND GENERATION

KIHOON SON[1] and KYUNG HOON HYUN[2]
[1,2]*Department of Interior Architecture Design, Hanyang University, Republic of Korea*
[1,2]*{gnswn00|hoonhello}@hanyang.ac.kr*

Abstract. Spatial designers explore various design references in the design process. These design references significantly impact the quality of design outcomes and the process. Therefore, it is crucial to provide useful designs through the retrieval or generation process to spatial designers. To do this, a methodology must be developed to identify and quantify the floor plan's multivariate design data. Through quantifying various design data, the retrieval and generation process can provide appropriate designs in many ways. This study proposed a new floor plan design framework for retrieval and generation with newly quantified design data. For validation of this framework, we conducted a floor plan retrieval and generation process. Newly quantified design data show usability in both processes. We also compare our framework with previous studies for validation. The comparison results show that our framework utilizes the most diverse design data of the floor plan.

Keywords. Design quantification; Multivariate data; Floor plan design; Design retrieval; Design generation.

1. Introduction

Given that a design is the outcome of a complex design process, spatial design results contain various design data (Sönmez, 2018). Thus, spatial designers are also familiar with exploring design solutions from previous design references (Maher & Silva Garza, 1997). However, the design reference has a significant impact on the results (Goldschmidt, 2011). Therefore, it is crucial to provide the spatial designer with an appropriate design for the situation through the design retrieval and generation process. To do this, a methodology of identifying and quantifying multivariate design data in a spatial design should first be established.

In this context, floor plan design retrieval and generation studies have been conducted. For example, Ahmed et al. (2014) and Son et al. (2020) proposed a floor plan retrieval system a.SCatch and C-Space. These two systems retrieve designs by calculating the similarity of floor plan design data. On the other side, EASE (Dino, 2016), SPG (Das et al., 2016), and Graph2Plan (Hu et al., 2020) generate new floor plan designs through a genetic algorithm and convolutional neural networks (CNNs). These systems use quantified design data as a design constraint when generating new floor plans. Many design data of floor plans

PROJECTIONS, Proceedings of the 26th International Conference of the Association for Computer-Aided Architectural Design Research in Asia (CAADRIA) 2021, Volume 1, 281-290.

have been used in the retrieval and generation process. However, previous studies insufficiently used design data, such as a room's shape and relationships crucial in floor plan design (Arvin & House 2002). For more accurate and efficient retrieval and generation results, more various design data should be quantified and utilized.

Upon this background, this study suggests a new multivariate framework of floor plans by identifying and quantifying new design data. To this end, we conducted three tasks: 1. Identifying and quantifying floor plan design data (Room shape layout, Room shape, Adjacency & Connectivity of rooms); 2. Image processing of 2101 actual floor plans to extract quantified design data. 3. Performing design retrieval and proposing new generation methods based on quantified design data.

2. Related works

2.1. DESIGN QUANTIFICATION

A spatial designer considers various design data to create a design. According to Sönmez (2018), the design contains data describing a complex and ambiguous design process. He therefore emphasized the quantification of data from design references to support designers. Many researchers have conducted design quantification studies. Hekkert et al. (2003) suggested design style quantification by identifying a style's design component. Likewise, Hyun & Lee (2018) quantified a car's design data and calculated the similarity between car designs. Through this, they analyzed each car brand's trend as a marketing strategy. In architectural design, Langehan & Petzold (2010) conducted floor plan retrieval by calculating the similarity of design data. Dino (2016) conducted floor plan generation through quantification of design data. As seen in previous studies, design quantification is an essential process for analyzing, retrieving, and generating designs. Thus, as more design data are quantified, more accurate design analysis, retrieval, and generation are possible.

2.2. FLOOR PLAN RETRIEVAL

In architectural design, floor plan retrieval studies were conducted to provide designers with appropriate floor plan designs. Spatial designers consider topological and geometrical design data to create a floor plan (Arvin & House, 2002). Topological data include the relationship of rooms, and the geometrical elements include the shape and size of the rooms. Langehan & Petzold (2010) proposed a retrieval method using the floor plan design's semantic fingerprint data. a.SCatch (Ahmed et al., 2014) is a sketch-based floor plan retrieval system that applies this semantic fingerprint concept. They extracted each room's type and the direct/indirect relationship data from the floor plan into one graph query. However, the query has no location data considering cardinal direction and room shape data. Son et al. (2020) also proposed a C-Space that retrieves floor plan design. C-Space uses the number of rooms, direct connectivity of rooms, and the floor silhouette data. However, C-Space does not consider the room's shape and adjacency data. For an accurate and appropriate design retrieval process, it is necessary to increase the search dimension by quantifying various design data.

2.3. FLOOR PLAN GENERATION

To support spatial designers, floor plan generation research has been conducted. EASE (Dino, 2016) and SPG (Das et al., 2016) are systems that set design constraints with design data, such as the room's width, height, center point, number, and size. They generate a floor plan design with quantified design data and optimize it through a genetic algorithm. Wu et al. (2019) and Hu et al. (2020) generate a floor plan by learning the actual floor plan design based on the Convolutional Neural Network (CNN). They optimized the walls' location in the floor plan to avoid wrong designs. However, as in floor plan retrieval studies, generation studies did not sufficiently consider the room's shape and relationship data. To generate useful and accurate floor plan designs, these data should be sufficiently considered. Therefore, in this study, we quantify the room's shape and adjacency/connectivity design data.

3. Methodology

3.1. IDENTIFYING AND QUANTIFYING DESIGN DATA

Son et al. (2020) used 16 grids and aspect ratio information of a bounding box to quantify the floor silhouette. These 16 grids are the shape's area occupying ratio for each grid. In this study, developing this method, the shape's grids were generated as binary array data depending on whether the shape exists in the grid's center point. Also, to improve the grid resolution, we make 32*32 grids (Figure 1-a). The relationship between spaces is crucial topological design data in the floor plan (Arvin & House, 2002). Hu et al. (2020) quantified all rooms' adjacency relationships in a graph by node and edge (Figure 1-b). Using this method, we quantify the direct and indirect relationship between rooms as an adjacency and connectivity graph.

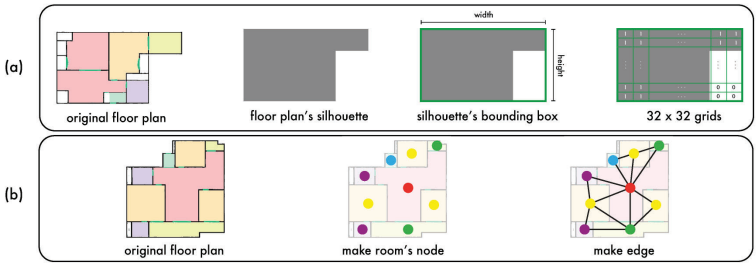

Figure 1. Floor plan's 32*32 grids and adjacency graph.

3.1.1. Room shape layout

Room shape layout (RSL) data indicate the shape and location of rooms on a floor plan. Floor plan design is often conducted within a fixed floor silhouette. Using RSL data, designers can retrieve or generate floor plan designs in any shape and location within a given silhouette. We conducted quantification in the following way. First, we create a bounding box based on a floor silhouette. Next, we make

32*32 grids in this bounding box (figure 2-b). Finally, the width, height of the bounding box, 32*32 grids, and area ratio data of the room are extracted. These data are saved in JSON format. We created RSL data of each room type (figure 2-c).

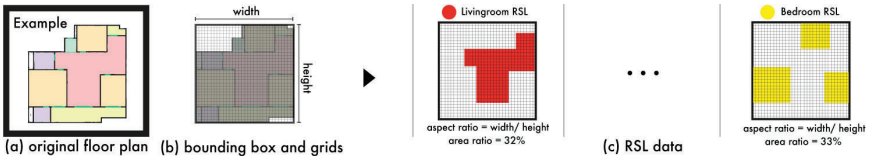

Figure 2. Room shape layout (RSL) quantification process.

3.1.2. Room shape

Room shape (RS) is the shape data of one room. The design data, unlike the room layout, are created with a bounding box for one room. With RS data, it is possible to retrieve or create the room's shape regardless of the floor silhouette. For RS quantification, we extract the 32*32 grids, the corner points and aspect ratio of the bounding box, the area ratio of room, and the room type and ID information (Figure 3).

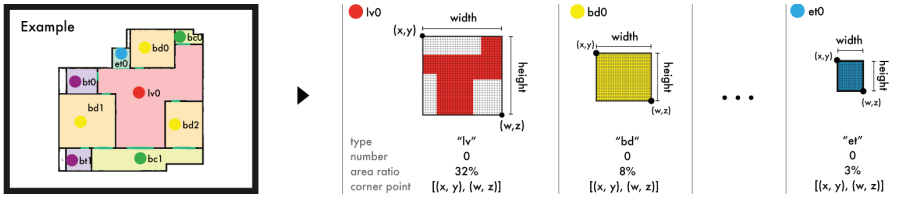

Figure 3. Room shape(RS) quantification process.

3.1.3. Room adjacency and connectivity graph

In the adjacency graph of Hu et al. (2020), the room's direct and indirect relationships are included without distinction. The direct connectivity between rooms is significant in a floor plan design (Arvin & House, 2002). Son & Hyun (2021) created the relationship graph of rooms by separating the direct connectivity and adjacency data (figure 4). In addition, an adjacency graph (figure 4-a) was created by adding the relationship with a cardinal direction. In this study, we use these graphs to conduct the floor plan retrieval and generation.

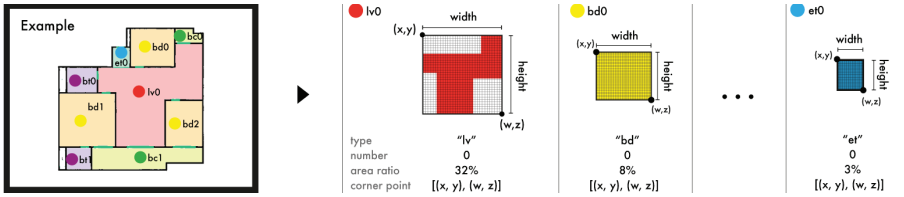

Figure 4. Adjacency and connectivity of room quantification process.

3.2. SIMILARITY CALCULATION METHOD

3.2.1. Room shape layout

RSL contains the 32*32 grids, aspect ratio (width/height) of the bounding box, and area ratio data for each room type. To calculate the similarity of RSL, we utilized these three data. Assuming that two RSL a and b are compared, grid vectors (GV_a and GV_b) are obtained by converting 32*32 grids into one vector. AS_a and AS_b are the aspect ratio, and AR_a and AR_b are the area ratio values of a and b. We use cosine similarity and subtract the result value from 1 (Eq 1) for comparing two GV data. The aspect ratio (AS) represents a scaler of a bounding box. For example, a square and a rectangle have the same 32*32 grids but differ in AS. To reflect the AS difference, we calculated this difference (Eq 2). We also considered the difference in area ratio (AR), which means the relative area (Eq 3). To adjust each value from 0 to 1, we normalized the AR and AS values to their respective maximum and minimum values. Also, to reflect the importance of each element, we multiplied weight values (W_{GV}, W_{AR}, W_{AS}). The final RSL similarity is obtained by averaging the three similarities. This RSL similarity calculation method reflects the rooms' static occupied grid shape, orientation, scale, and relative size, per room type.

$$Similarity_{GV} = \left\{1 - \text{cosine similarity}\left(\vec{GV_a}, \vec{GV_b}\right)\right\} \times W_{GV} \tag{1}$$

$$Similarity_{AR} = |\text{norm}(AR_a) - \text{norm}(AR_b)| \times W_{AR} \tag{2}$$

$$Similarity_{AS} = |\text{norm}(AS_a) - \text{norm}(AS_b)| \times W_{AS} \tag{3}$$

3.2.2. Room shape

The RS similarity is calculated in the same way as the RSL similarity calculation method (Eqs 1, 2, 3). The difference is that RS data are made by creating a bounding box on a room's shape (Figure 3). However, to calculate the RS similarity of a room and a floor plan, or between two floor plans, the RS similarity calculation process should consider the number of rooms to be compared. If the designer inputs two bedrooms, a and b, the floor plan design with only one bedroom cannot obtain RS similarity (Figure 5-a). On the other hand, in the floor plan with two bedrooms (d, e), as shown in Figure 5-b, we can obtain combinations of similarity (a-d, b-e; a-e, b-d). To obtain the final RS similarity value, we calculated the minimum Euclidean distance among the possible similarity

combinations. This method can select the two most similar bedrooms, even in a floor plan with more than three bedrooms (Figure 5-c).

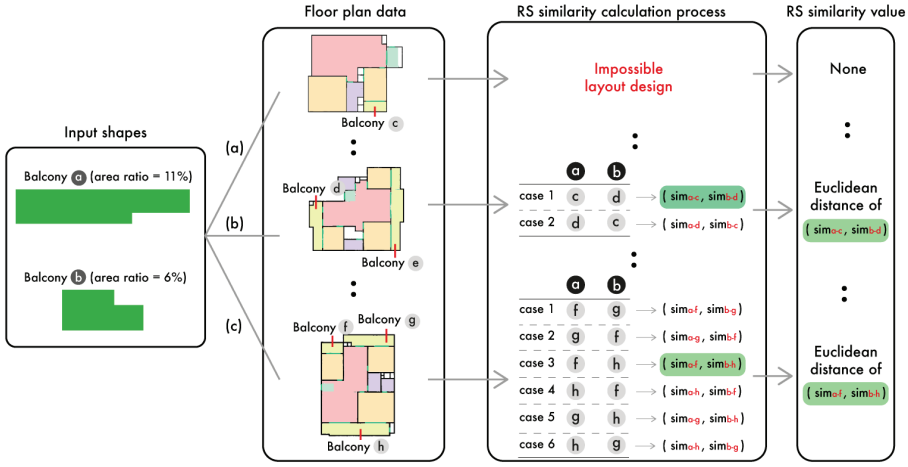

Figure 5. Room shape(RS) similarity calculation process.

3.2.3. Room adjacency and connectivity graph

To calculate the similarity between two graphs, we used the Bipartite Graph-Edit Distance (Riesen et al., 2007). Originally, Graph-Edit Distance (GED) calculates the minimum number of corrections to make the two graphs equal. However, since the original GED based on the A^* algorithm has a huge computational cost, it is difficult to calculate the similarity in real-time. Thus, to solve this problem, Son & Hyun (2021) conducted the graph similarity calculation with bipartite GED. Bipartite GED is a method that applies graph edit distance to an assignment problem. In this study, we used the Bipartite GED of GMatch4py (https:github.com/Jacobe2169/GMatch4py), a Python library.

4. Implementation and Discussion

In this study, we extracted six design data (Figure 9) from the actual 2101 floor plans. Furthermore, we implemented the multivariate framework for the retrieval and generation process, and validated the usability of the proposed design data.

4.1. FLOOR PLAN DESIGN RETRIEVAL

4.1.1. Room shape layout

By using the RSL data, 2101 floor plan design retrievals were conducted. In similarity calculations, W_{GV}, W_{AR}, and W_{AS} were set to 1. The outputs are the top 4 among the 2101 floor plans (Figure 6). The RSL similarity-based retrieval process shows the results reflecting the rooms' location and shape in the floor silhouette.

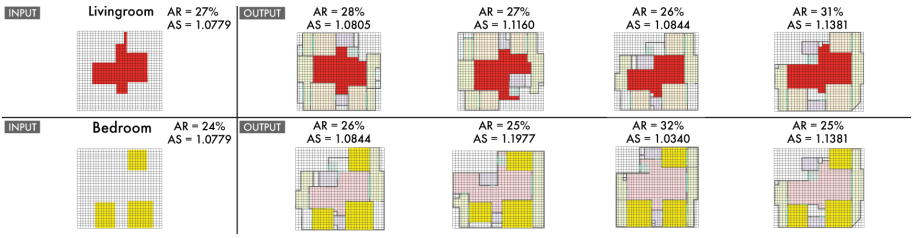

Figure 6. Room shape layout(RLS) retrieval result.

4.1.2. Room shape

RS similarity-based retrieval was performed with one living room and two balconies (Figure 7). Unlike RSL, the RS retrieval result does not consider the position within the floor silhouette. Although all weight values are set to 1, the retrieval system in future work should consider that designers can adjust the weight values according to their situation.

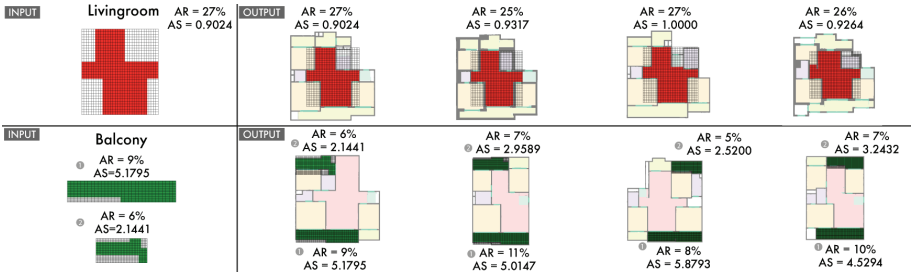

Figure 7. Room shape(RS) retrieval result.

4.1.3. Room adjacency and connectivity

The results of the room adjacency graph and connectivity graph retrieval are presented in figure 8. Since the room adjacency graph considers the cardinal direction, all the rooms' locations show similar results (Figure 8-a). However, room connectivity graphs consider only direct connectivity between rooms. Thus, the result also contains a different room layout, as in the 4th result (Figure 8-b).

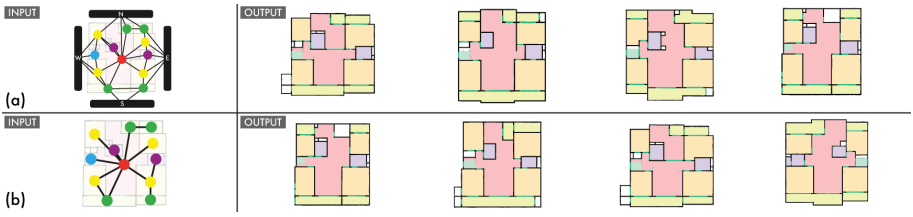

Figure 8. Adjacency & Connectivity graph retrieval result.

4.2. FLOOR PLAN DESIGN GENERATION

4.2.1. Switch and change method

The switch method is a way to generate a new floor plan design by changing all design data of two rooms. When the two rooms are changed, all floor plan design JSON data change except for the number and floor silhouette (Figure 9; 10-a). Unlike the switch method, the change method changed the type of room (Figure 10-b). When changing the type of one room, all design data except the floor silhouette are changed.

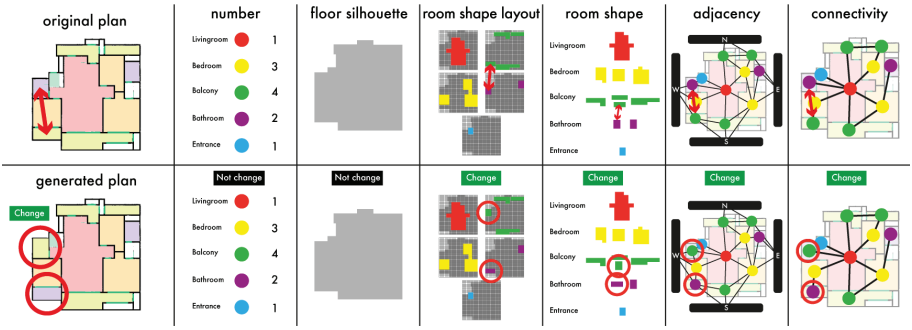

Figure 9. An example of the floor plan data editing process (Switch).

4.2.2. Result

The generated floor plan designs through switch and change are presented in figure 10. These methods are the most straightforward and precise way to use the floor plan's JSON data. When applied to the design system, these methods could also perform generation according to the design constraints. However, the floor plan design data should be further supplemented in the following way. Since the currently quantified information is focused on the room's shape and relationships, the wall and the door are not considered. If the wall and door design data are quantified and represented in the design, a more accurate floor plan image could be generated, unlike Figure 10-(b). It is also possible to create a new room shape and freely add or delete it from the floor plan. Therefore, these additional quantifications should be conducted in future work.

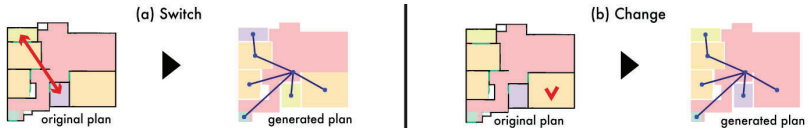

Figure 10. Floor plan design generation result.

4.3. DISCUSSION

A floor plan is a design that contains multivariate data. It is necessary to quantify various design data to retrieve and generate more accurate and useful floor plans. For validation of our framework, we compared design data from the previous floor plan design retrieval and generation research (Table 1).

Table 1. Comparison of our framework with previous studies.

Frameworks (Retrieval / Generation) \ Floor plan's design data	room type & number	floor silhouette	location of rooms	connectivity of rooms	adjacency of rooms	area ratio	cardinal directions	shape of rooms	using previous designs
Langehan & Petzold (2010)	˅			˅	˅				
Ahmed et al. (2014)	˅			˅	˅				
Sabri et al. (2017)	˅			˅	˅	˅			
Son et al. (2020)	˅	˅		˅					
Dino (2016)	˅	˅	˅			˅	˅		
Das et al. (2016)	˅	˅			˅	˅			
Wu et al. (2019)	˅	˅	˅						˅
Hu et al. (2020)	˅	˅	˅		˅	˅			˅
Our framework*	˅	˅	˅	˅	˅	˅	˅	˅	˅

In the retrieval framework, various retrieval methods must be provided to obtain the desired result (Kim & Lee, 2017). The floor plan consists of many design data, but some data have not been used. Thus, quantifying new design data corresponds with increasing the search dimension. Through higher search dimensions, the designer can retrieve a floor plan design with higher accuracy. As shown in Table 1, our framework uses the most diverse design data of the floor plan. Unlike previous retrieval studies, we quantified adjacency and connectivity as different topological design data. Also, the design data related to room shapes are new data. Likewise, the generation framework needs various design data for an accurate generation. EASE (Dino, 2016) and SPG (Das et al., 2016) are likely to create wrong designs if design constraints are not sufficiently considered with various design data. Wu et al. (2019) and Hu et al. (2020) reduced this weakness through learning from actual floor plans. However, Wu et al. and Hu et al. did not consider room shape and connectivity data sufficiently. Thus, it is difficult to generate floor plans that meet various design constraints. To solve these problems, our framework utilizes the most diverse quantified design data while using an actual floor plan's data. Our generation methods use most of the actual floor plan data (Figure 9). These methods can be applied to the spatial remodeling process in which a large amount of spatial design data is maintained.

5. Conclusion

This study proposed a new multivariate floor plan design framework by quantifying design data. The floor plan retrieval process showed the results that well reflected the characteristics of each design data. In the generation, a new floor plan was generated using the switch and change method. These retrieval and generation methods can be applied immediately to a spatial design support system. As a result, our framework utilizes the most diverse design data than the framework of previous studies. However, for more accurate and various generation methods, design data such as walls and doors will need to be quantified. In future work, we will study additional quantifications and new generation methods.

Acknowledgement

This work was supported by the National Research Foundation of Korea(NRF) grant funded by the Korea government(MSIT) (NRF-2020R1C1C1011974).

References

Ahmed, S., Weber, S., Liwicki, M., Langenhan, C., Dengel, A. and Petzold, F.: 2014, Automatic analysis and sketch-based retrieval of architectural floor plans, *Pattern Recognition Letters*, **35**, 91-100.

Arvin, S. A. and House, D. H.: 2002, Modeling architectural design objectives in physically based space planning, *Automation in Construction*, **11(2)**, 213-225.

Das, S., Day, C., Haymaker, J. and Davis, D.: 2016, Space plan generator: Rapid generationn & evaluation of floor plan design options to inform decision making, *Proceedings of the 36th Annual Conference of the Association for Computer Aided Design in Architecture 2016*.

Dino, I. G.: 2016, An evolutionary approach for 3D architectural space layout design exploration, *Automation in Construction*, **69**, 131-150.

Goldschmidt, G.: 2011, Avoiding design fixation: transformation and abstraction in mapping from source to target, *The Journal of creative behavior*, **45(2)**, 92-100.

Hekkert, P., Snelders, D. and Van Wieringen, P. C.: 2003, 'Most advanced, yet acceptable': Typicality and novelty as joint predictors of aesthetic preference in industrial design, *British journal of Psychology*, **94(1)**, 111-124.

Hu, R., Huang, Z., Tang, Y., van Kaick, O., Zhang, H. and Huang, H.: 2020, Graph2Plan: Learning Floorplan Generation from Layout Graphs, *ACM Transactions on Graphics*, **39**, 4-18.

Hyun, K. H. and Lee, J. H.: 2018, Balancing homogeneity and heterogeneity in design exploration by synthesizing novel design alternatives based on genetic algorithm and strategic styling decision, *Advanced Engineering Informatics*, **38**, 113-128.

Kim, S. J. and Lee, J. H.: 2017, A study on metadata structure and recommenders of biological systems to support bio-inspired design, *Engineering Applications of Artificial Intelligence*, **57**, 16-41.

Langenhan, C. and Petzold, F.: 2010, The fingerprint of architecture-sketch-based design methods for researching building layouts through the semantic fingerprinting of floor plans, *International electronic scientific-educational journal: Architecture and Modern Information Technologies*, **4(13)**, 1-12.

Maher, M. L. and de Silva Garza, A. G.: 1997, Case-based reasoning in design, *IEEE Expert*, **12(2)**, 34-41.

Riesen, K., Neuhaus, M. and Bunke, H.: 2007, Bipartite graph matching for computing the edit distance of graphs, *International Workshop on Graph-Based Representations in Pattern Recognition*, 1-12.

Sabri, Q. U., Bayer, J., Ayzenshtadt, V., Bukhari, S. S., Althoff, K. D. and Dengel, A.: 2017, Semantic Pattern-based Retrieval of Architectural Floor Plans with Case-based and Graph-based Searching Techniques and their Evaluation and Visualization, *In Proceedings of the 6th International Conference on Pattern Recognition Applications and Methods*.

Son, K., Chun, H., Park, S. and Hyun, K. H.: 2020, C-Space: An Interactive Prototyping Platform for Collaborative Spatial Design Exploration, *In Proceedings of the 2020 CHI Conference on Human Factors in Computing Systems*, Honolulu, Hwai, 1-13.

Son, K. and Hyun, K. H.: 2021(submitted), What's Your Design Move? Design Support System with Real-Time Feedback based on Dynamic Linkography to Augment Spatial Design Process, *Advanced Engineering Informatics*.

Sönmez, N. O.: 2018, A review of the use of examples for automating architectural design tasks, *Computer-Aided Design*, **96**, 13-30.

Wu, W., Fu, X. M., Wang, Y., Qi, Y. H. and Liu, L.: 2019, Data-driven interior plan generation for residential buildings, *ACM Transactions on Graphics*, **38(6)**, 1-12.

DEVELOPING AN AUTOMATIC CODE CHECKING SYSTEM FOR THE URBAN PLANNING BUREAU OF HUANGPU DISTRICT IN SHANGHAI

CHENGYU SUN[1], MENGTING LI[2] and HANCHEN JIANG[3]
[1,2,3] *Tongji University*
[1] *ibund@126.com* [2] *dreamstop1204@163.com* [3] *jhc975@qq.com*

Abstract. As Chinese cities entering a so-called 'organic renewal' era, building projects runs with much more constraints from high-density and high-rise surroundings. Such a situation makes the technical review in any urban planning bureau time-consuming and error-prone, which conflicts with the developer's profits and citizen's rights. This study introduces a preliminary system being developed for the planning bureau of Huangpu District, Shanghai. It has covered 21 code items among 44 computational ones of the local planning codes last year, which automatically generates technical reviews upon developer's submissions. Due to the feasible level of BIM application in domestic projects, a set of strategic approaches, such as the standardization of CAD drawings and the reconstruction of an internal building information model, are adopted rather than developing the system on any BIM platform directly. Two examples of technical reviews about distance-checking between buildings and length-checking of facades are demonstrated, in which officers reached confidential judgments in seconds rather than several days conventionally.

Keywords. Planning Constraints; Code Checking; 3D Reconstruction; Design Automation; Building Information Model.

1. Introduction

In a so-called 'organic renewal' era (Zhou 2019), to keep both the citizen's rights and the developer's profits in high-rise and high-density urban surroundings, every Chinese city authorizes its urban planning bureau to make technical reviews on all the building projects according to its local planning codes from the very beginning. On one hand, the technical officers have complex code items to check carefully, which is a time-consuming and error-prone duty. On the other hand, they have to reach the final judgment as soon as possible to keep the business efficiency of the whole city for the developers. Suffering from such a situation in the last decades, the planning bureau of Huangpu District, Shanghai, appointed our team to develop an automatic code checking system for them to raise efficiency and to avoid errors.

A preliminary system has been developed since the winter of 2019. Currently, twenty-one items of the forty-four computational items in the planning codes are covered. Although a BIM platform always comes to mind immediately to support

PROJECTIONS, Proceedings of the 26th International Conference of the Association for Computer-Aided Architectural Design Research in Asia (CAADRIA) 2021, Volume 1, 291-300.

such a system, the current system is still developed to accept CAD drawings with a set of strategic approaches, such as the standardization of CAD drawings and the reconstruction of an internal building information model. It keeps the system feasible in real domestic projects nowadays and makes the algorithms migratable to any BIM platform in the future.

2. Reviews On Automatic Code Checking

2.1. BIM-PLATFORM-BASED METHODS

The popular BIM platforms can provide inborn data for automatic code checking through object properties and geometric features of a building. Thus, most existing researchers follow this method.

FORNAX is the first automatic code checking platform based on IFC (Industry Foundation Class) model. The platform is a C++ object library. Programmers don't need to develop algorithms for retrieving the required information from the IFC model, but only need to use the FORNAX object and its member functions to 'interpret the rules written in natural language into a programming language' (Eastman et al. 2011). The disadvantage is the lack of openness, and that the user can only program to customize the rule according to specific needs and write system.

Solibri Model Checker (hereinafter referred to as SMC) has the largest user group, which is a desktop application based on JAVA language. It only supports IFC model, which can complete clash check and find out the violation of regulations in the model. These detections are all based on a 'detection rule set'. SMC provides some 'rule sets' in various fields and it has been developing and improving. Due to different local standards, users can modify these 'rule sets' to meet localization needs (Eastman et al. 2011). At the same time, SMC is the first to realize pre-checking to validate that the data needed for checking is available from the model to improve the checking efficiency (Ding et al. 2004).

SMARTcodes can realize semi-automatic interpretation from written language regulations to computer code through IECC dictionary, using a dictionary of domain-specific terms and semi-formal mapping methods (Martins and Monteiro 2013). However, the current system focuses on checking easily-obtained or easily-derived attributes, rather than simulating complex situations based on various model views (Ke 2016).

2.2. CAD-DRAWING-BASED METHODS

On the contrary to the BIM-platform-based methods, CAD-drawing-based methods can only describe the building in a 2.5D way with distributed data, from which the object properties and geometric features are hard to extract. However, due to its long history in the design industry, CAD drawings and data sheets are still adopted by some researchers for automatic code checking development in real projects.

The earliest effort named 'CORENET' was led by Singapore, who started considering code checking on CAD drawings in 1995. The initial method of code

checking in this project was to use artificial intelligence and feature-based CAD technology to check the floor plans of buildings, thus developing the BP-Expert application. Due to the limited coverage of regulations, the inability of processing inconsistent or wrong data, and the instability of the overall performance, the program was not successful, but it provides some great learning experience for the follow-up code checking program e-PlanCheck based on IFC model (Khemlani 2005).

At the end of the 20th century, starting from Shanghai, Guangzhou, Shenzhen, and other cities with huge amount of urban planning management business, China also began research on online approval and automatic code checking systems, with a batch of commercial software emerging. For example, Urban Planning Results Management System developed by the Guangzhou Urban Information Research Institute; Urban Planning CDS developed by Luoyang Zhongzhi Software Company; Planning Management Information System developed by Hongye Technology; Santong Software developed by the Guangzhou Urban Planning Automation Center including 'Baojian Tong','Xiuxiang Tong', 'Yanshou Tong' (Tang 2013).

These systems require huge and redundant data input by designers and extra extraction algorithms to work. Almost all of them rely on a concept of 'block' popular in CAD platforms, with which geometric features and object properties are bound. Designers have to input a large number of additional block attributes manually and the programs require extra algorithms to extract data from these distributed files with high redundancy. It comes with unnecessary workflow and it makes coherence problem easily.

In summary, in the field of automatic code checking, there are two camps, namely "BIM-platform-based method" and "CAD-drawing-based method". Obviously, the former is much more popular. However, the domestic design industry in China has not yet fully entered the era of BIM-based design, which means submission with a set of BIM documents is infeasible. Instead, the methods based on "CAD drawings + data sheets" fit the current situation. The only problem is that the existing methods relying on the concept of 'block' in CAD still require many manual operations, and are not able to support complex geometric algorithms.

3. Methodology

3.1. A REVISED CAD-DRAWING-BASED METHOD

"CAD-drawing-based method" and "BIM-platform-based method" are essentially two ways to describe a building. The following are their pros and cons.

A CAD-drawing-based method: It uses 'CAD drawings + data sheets' to describe a design project comprehensively from the general plan, each floor plan, elevation, profile and other views, which is still the absolute mainstream at present in China. Such a method can efficiently describe those buildings with horizontal ground and orthogonal exterior walls and roofs (see Figure 1, the first row and the second row). It makes the scale of the submitted files smaller and makes files convenient to check and transfer. Meanwhile, the CAD drawing platforms have a

much larger user group than BIM platforms have in China currently. It can also seamlessly connect to the existing descriptions of planning codes printed on paper. The disadvantage is that when describing non-vertical (such as folded surface, curved surface) wall (see Figure 1, the third row), or non-horizontal (such as folded surface, curved surface) roof, the method is inefficient and approximative through a large number of section drawings with huge redundancy to cause errors.

A BIM-platform-based method: It inherits all the advantages from the integration of building data, which means that the object properties and geometric features can be easily extracted by algorithms of automatic code checking (Sun and Ke, 2016, p.145). It can describe buildings of various shapes efficiently and accurately without redundancy. However, due to the design of current BIM platforms, the method runs through a much larger file set, which is difficult to transfer for the submission. Meanwhile, its user group is much smaller than the CAD camp in China, which means huge money for better computers and numerous training hours make such automatic code checking system too expensive to run. Furthermore, the current 2D version of planning codes has to be upgraded into a 3D version through a legal process. All these issues make the BIM-platform-based method infeasible currently in China.

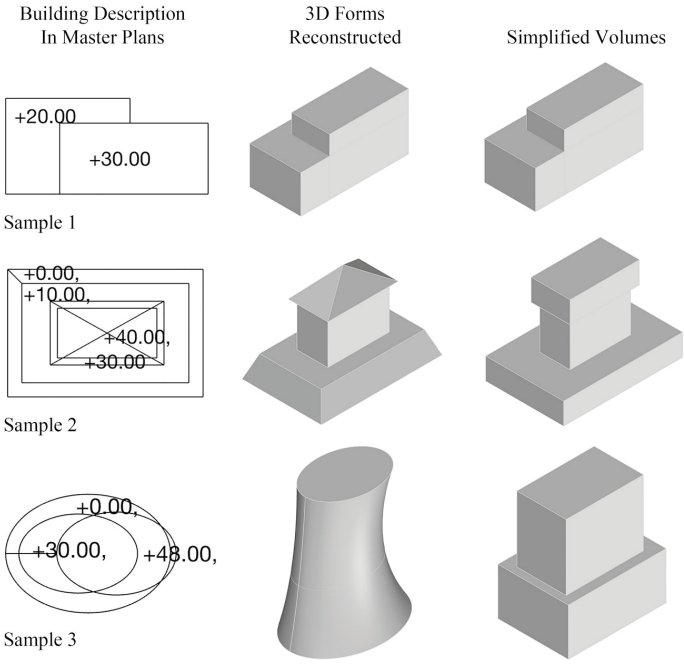

Figure 1. Three Samples of Building Description.

Obviously, neither of the above methods is suitable for the current requirements from the Planning Bureau of Huangpu District. Thus, a revised CAD-drawing-based method is proposed for the real projects running in Shanghai,

China.

First, it uses a combined building description comprised of layers with specific names, 2D outlines on specific layers, and text objects on specific layers (Figure 1, the first column), to define a 3D face belong to any building object, such as a piece of wall or roof. In the CAD drawings, a 'nearest principle' and a 'leading line rule' are designed to automatically establish the relationship between 2D outlines and text objects. And the layer name of any graphic object defines its properties. The binding mechanism is based on relationships between objects and the layers they located rather than 'blocks', which is closer to designers' daily operations.

Next, any 3D building object is defined by a set of 3D faces, which enables the revised method to reconstruct any complex 3D building form (Figure 1, the second column) even with non-vertical walls or non-horizontal roofs. A set of 'automatic face complementation rules' is designed to make designers' CAD drawing as simple as possible, with which algorithms generate all the faces according to a few 2D outlines in master plans (Figure 1, the first column) rather than all the edges of the object.

Last, the 3D forms reconstructed from the lines in master plans will be simplified as volumes with vertical facades furtherly (Figure 1, the last column), which matches the building concept currently described in the planning codes.

3.2. A COMPATIBLE STRATEGY WITH BIM-PLATFORM-BASED METHODS

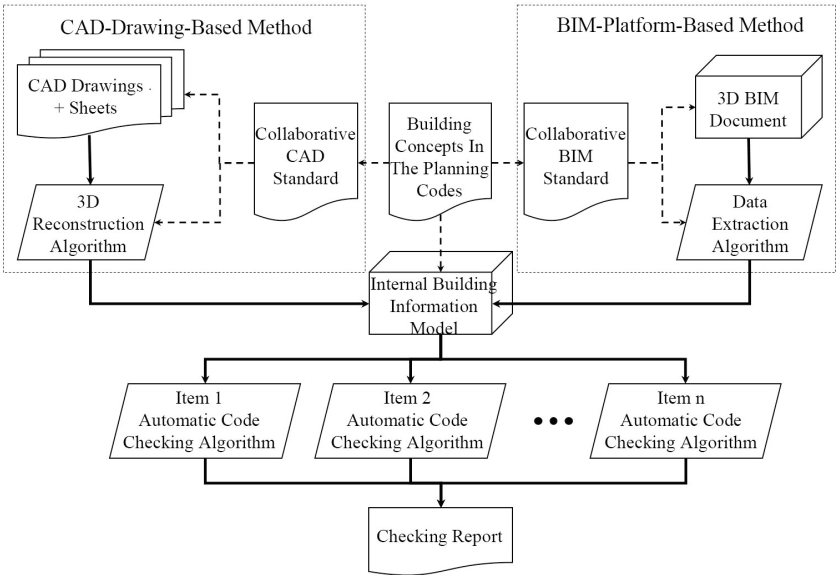

Figure 2. A Compatible Strategy.

In order to keep the automatic code checking algorithms of the revised method compatible with BIM platforms in the future, an internal building information

model is designed. Firstly, CAD drawings and data sheets are compiled according to a specific CAD standard. They are converted into an internal building information model by a 3D reconstruction algorithm. The model supports any data extraction as a conventional BIM platform does (see Figure 2). Actually, all the code checking algorithms are developed item by item based on this model. When BIM platforms are adopted everywhere in China, the current automatic code checking algorithms can be immigrated to any of them seamlessly. That is the compatible strategy.

3.3. WORKFLOW OF AUTOMATIC CODE CHECKING

The workflow of automatic code checking is divided into two major parts, conducted by 'A Project Developer' (Figure 3, the left part) and 'A Planning Bureau Officer' (Figure 3, the right part).

- A Project Developer

Step 1: Prepare documents in accordance with format requirements. For a long time, because the CAD drawings only require 'looks correct', but it is very difficult for machine identification, so it is necessary to put forward certain format requirements for the submissions (see 'Result A' in Figure 3). The Developer shall follow this requirement for document preparation.

Step 2: Check the format of the submissions automatically by computer. This 'Self-Check Tool' (see 'Result B' in Figure 3) is an automatic verification program to check whether the submissions meet the preparation requirements. The Developer can use this tool to check the format of the submission to reduce the possibility of submission being returned.

Step 3: Submit documents online or offline. And the management preventing version tampered should be provided.

- A Planning Bureau Officer

Step 1: Check the format of the submissions again. Use 'Self-Check Tool' again (see 'Result B' in Figure 3) to conduct a second check on the documents submitted to ensure that they meet the requirements before proceeding to the next step of checking.

Step 2: Check Visually in way of human-computer interaction (optional). The 'Visual-Check Tool' (see 'Result C' in Figure 3) can display as classified regions in the CAD submissions, which is convenient for the management department to conduct a semi-automatic visual check to avoid malicious traps. In this way, in the initial stage of implementation, it's also helpful to find loopholes in self-check logic to continuously improve the algorithm.

Step 3: Check various regulations automatically (see 'Result D' in Figure 3). The computer automatically calculates the content of the submissions according to the designation of the officer, and the results are displayed both in the two-dimensional and three-dimensional windows, and detailed reports are used to facilitate on-site confirmation and subsequent review. If there is any problem, it will be returned to the Developer.

Step 4: Follow up other approval tasks. After obtaining the reports of automatic code checking, officers can not only carry out other regulation checking that has not yet been automatic, but also make various 'judgments' based on the detailed reports immediately, and finally complete the checking process.

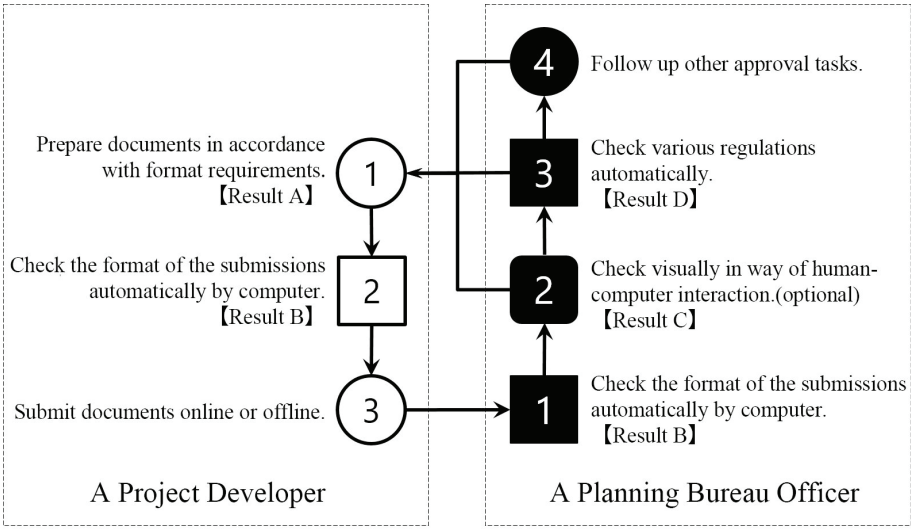

Figure 3. Workflow of Automatic Code Checking.

4. Two Examples of Technical Reviews

According to the above method, a preliminary system has been developed since the winter of 2019. Currently, twenty-one items of the forty-four computational items in the planning codes are covered. Among them, the length-checking of facades and the distance-checking between buildings are the most popular items for daily review, which are demonstrated in the following.

4.1. LENGTH-CHECKING OF FACADES

First, the officer selects the building outlines in a master view in Rhino and clicks 'Start' toggle to run the program in Grasshopper. The system analyses the building outlines and text objects on the specific layers. An internal building information model depicting the simplified building volumes are reconstructed. All these buildings are divided into multi or low-rise groups, or high-rise groups, according to the adjacency between any two volumes.

Secondly, taking each group as a unit, bounding boxes are calculated along all the axis directions hinted at by segments of the outlines in the group. The box with the minimum volume is recognized as the presenting box of the group. Its height and length are extracted as the key parameters for the group. Group by group, the algorithm checks these parameters according to the height-length formula in the item of planning codes to make the judgment.

Finally, as a kind of visualized report, a rectangle at the top of each building group indicates the checking result through a Rhino view. The height and size of a group hint at its bounding box. Its color hints at the result: pass in green and fail in red. (Figure 4, the bottom part). Meanwhile, detailed reports in text are also provided through the interface in Grasshopper (Figure 4, the top part). The officer can read the text in detail after a quick visual confirmation in the 3D view.

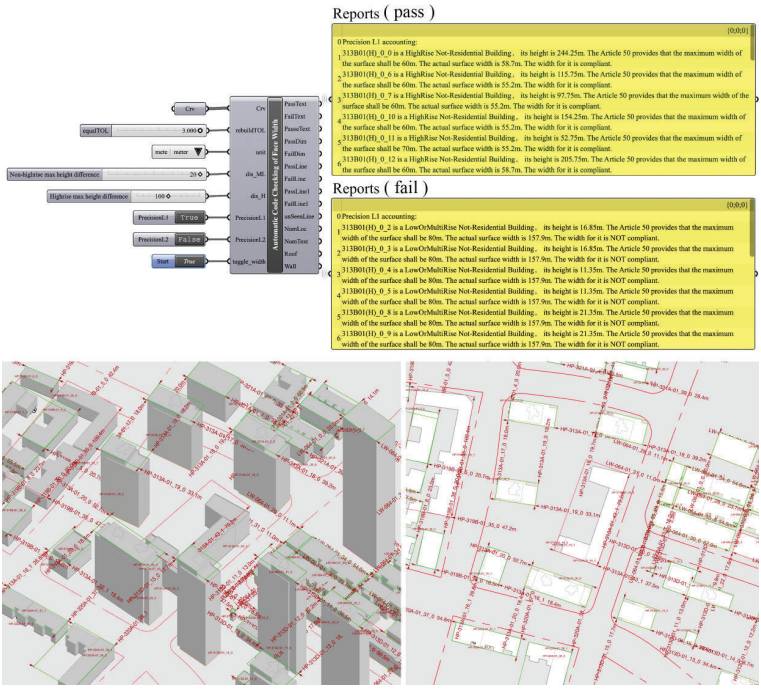

Figure 4. Length-checking of facades (top: system interface embedded in Grasshopper; bottom: graphic interface embedded in Rhino).

4.2. DISTANCE-CHECKING BETWEEN BUILDINGS

First, the officer selects the building outlines in a master view in Rhino and clicks ‘Run It’ toggle to run the program in Grasshopper. The system reads the required data including building outlines and text objects according to their layers. The 3D form of any 3D building volume is reconstructed from an outline and figures in text objects bound to it indicating its elevation and height.

Secondly, the system checks the distance between any two 3D volumes according to the planning codes. There are two precision levels during the checking. At a lower level, a volume is converted into a box first, which means any complex volume is treated as four pieces of facades. While at a higher level, every piece of façade is calculated. For each two volumes, the system actually checks the distances between their pieces of facades. The size, orientation, elevation, and

building type are used in a formula of acceptable distances.

Finally, the building volumes with the distance dimensions annotated as visualized results are displayed in a Rhino view. The color of the volume hints at the result: pass in grey and fail in red (Figure 5, the bottom part). Meanwhile, the detailed reports including specific items of the planning codes are presented through the interface in Grasshopper (Figure 5, the top part). The officer can read the text in details and make the final decision after a quick visual confirmation in the 3D view.

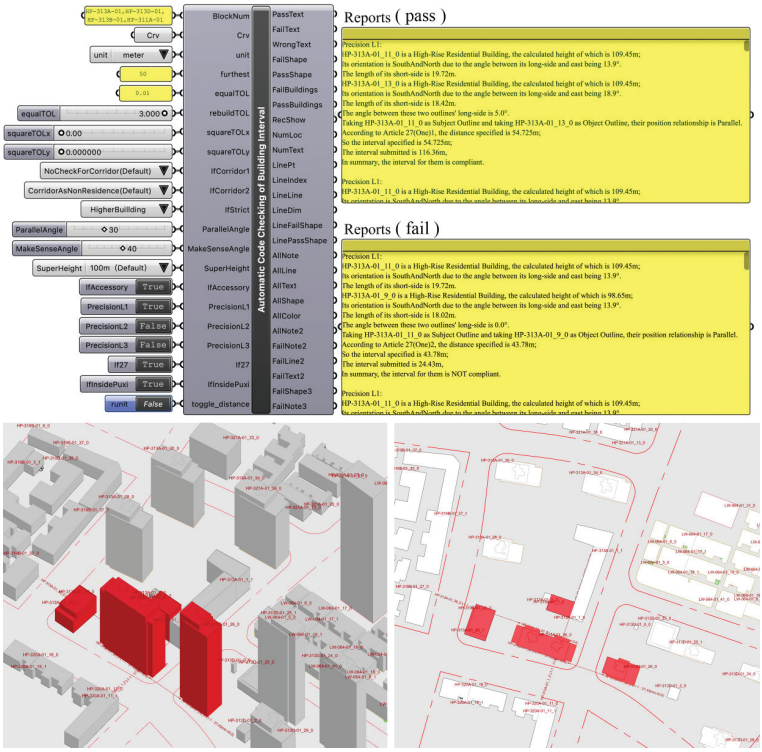

Figure 5. Distance-checking between buildings (top: system interface embedded in Grasshopper; bottom: graphic interface embedded in Rhino) .

5. Conclusions & Future Work

By the end of 2020, the above preliminary system has been tested in 14 building projects submitted to the Planning Bureau of Huangpu District, Shanghai. The conventional technical review period reduces from weeks to seconds, which keeps the citizen's right in an efficient way and even makes negotiations between government and developers possible in an acceptable schedule.

The development does not stick to the popular BIM platform as many other existing systems did, due to a deep understanding of the real level of BIM

application in China. Feasibility in the daily workflow is concerned in the first priority. A revised CAD-drawing-based method is proposed to realize the automatic code checking and keep the compatibility with BIM platforms in the future.

Although the length-checking of facade and the distance-checking between buildings are two main issues in the daily review, many other code items are still on the way in our development. With these explorations, some problems from the code itself have come to the surface. The object model of buildings is found out of fashion seriously. For example, free forms can't be interpreted by the current codes. The team believes that a systematic revision of the codes should be done in the near future.

Acknowledgements

The research was supported by a project of Natural Science Foundation of China titled 'An internet-plus-based approach of crowd simulation for public buildings' (no. 51778417), a project of Shanghai Science and Technology Committee titled 'Study and application of 3D modeling technologies in urban renewal regions' (no. 19DZ1202300).

References

Ding, L., Drogemuller, R., Jupp, J., Rosenman, M.A. and Gero, J.S.: 2004, Automated Code Checking, *Clients Driving Innovation International Conference*.

Eastman, C., Lee, J. and Jeong, Y.: 2009, Automatic rule-based checking of building designs, *Automation in Construction*, **18(8)**, 1011-1033.

Ke, X.: 2016, *Study on BIM-based Building Code Checking Method: Taking Subway Station As An Example*, Master's Thesis, Tongji University.

Khemlani, K.: 2005, "CORENET e-PlanCheck: Singapore" . Available from <http://www.novacitynets.com/pdf/aecbytes_20052610.pdf> (accessed 19st November 2020).

Martins, J.P. and Monteiro, A.: 2013, LicA: A BIM based automated code-checking application for water distribution systems, *Automation in Construction*, **29(JAN.)**, 12-23.

Sun, C. and Ke, X.: 2016, Method of automatic design code checking for BIM models, *BUILDING SCIENCE*, **32(4)**, 140-145.

Tang, M.: 2013, *Research on Urban Planning Assistant System and Urban Master Planning Data Standard based on GIS*, Master's Thesis, Central South University.

Zhou, M.: 2019, New Thoughts on Urban Planning Management under 'Principle of the Second Man'——Review Elaborated Planning of Historical Streets: A New Perspective on Organic Urban Regeneration in Shanghai, *Time+Architecture*, **2019(5)**, 170-171.

DATA-DRIVEN ANALYSIS OF SPATIAL PATTERNS THROUGH LARGE-SCALE DATASETS OF BUILDING FLOOR PLAN

HOYOUNG MAENG[1] and KYUNG HOON HYUN[2]
[1,2]*Department of Interior Architecture Design, Hanyang University*
[1,2]*{roach555|hoonhello}@hanyang.ac.kr*

Abstract. This paper introduces a unique quantitative analysis method and results that are differentiated from those in existing studies. We analyzed five types of information in floor plan images: the silhouette, number of rooms, room area, and direct and indirect room connectivity. Furthermore, the analysis used a large-scale apartment unit dataset consisting of 33,892 units. We present convincing and objective spatial pattern analysis results of Korean apartments by quantitatively analyzing a large-scale dataset. It is expected that the analysis results will clarify the characteristics of the residential environment of Korean apartments. The results suggest that changes in lifestyles lead to the modularization of bedrooms, increased numbers of private bathrooms and balconies with corridors as junctions, and the diversification of room layouts.

Keywords. Floor Plan Analysis; Design Quantification; Residential Layout; Spatial Pattern Analysis; Semantic Fingerprint.

1. Introduction

According to Statistics Korea (2020), apartments account for 51.1% of residential space in South Korea. Researchers have been actively investigating residential styles in Korea to understand apartment floor plan features (Bae et al. 2001; Choi 2003), to identify the effects of apartment units on lifestyles (Choi et al. 2004), and to infer residents‘ social and cultural structures from their spatial structures (Choi et al. 2004). Researchers have identified that Korean apartments’ floor plans are undergoing diversification over time, mainly in terms of the number of rooms or the functions of the rooms (Bae et al. 2001; Choi, 2003; Choi et al., 2004). However, previous studies were limited in terms of the number of datasets and were thus unable to show apartment trends over the longer term. Moreover, they organized their datasets manually. Thus, this study aims to propose a computer-aided data-driven analysis to provide a better understanding of the spatial patterns of apartments and to generate accurate and reliable results based on large-scale datasets. To do this, our study analyzes apartment units from the following three perspectives: 1) A morphological analysis of apartment floor plans (silhouette); 2) An analysis of the number of rooms, sizes of rooms and their types (room components); and 3) an analysis of floor plan layouts (room connectivity). Custom-made software was used to compile the dataset from an

PROJECTIONS, Proceedings of the 26th International Conference of the Association for Computer-Aided Architectural Design Research in Asia (CAADRIA) 2021, Volume 1, 301-310.

online real estate database (r114.com) consisting of floor plan images and 28 types of textual information. We conducted quantitative analyses of the silhouette, room components, and room connectivity data and examined the spatial structures of apartment floor plans over time.

2. Related Works

2.1. ANALYSIS OF UNIT FLOOR PLANS IN KOREAN APARTMENTS

Previous studies researched only partial spatial structures of Korean apartments. Bae et al. (2001) and Choi (2003) manually investigated 129 and 128 floor plans in the early 2000s in an effort to determine numbers of rooms and typical room layouts. Other researchers made attempts to quantify the connectivity of floor plans with the space syntax. Choi et al. (2004) collected 2,833 floor plans from 1966 to 2002 and quantified the minimum path from one room to another. Choi et al. (2014) compared the concept of spatial centrality with 60 floor plans. Given these studies, we can find three main aspects for a better analysis of apartment unit plans. The first is a larger dataset. We collected the most extensive data on 42,984 apartments and 5,890 floor plan images from 1970 to 2020 in Seoul. The second aspect is a perspective from a more thorough analysis that ensures an advanced understanding of the spatial structure of floor plans. The third aspect is automation of the recognition and data extraction process. Thus, we focused on these three developments to propose a novel method.

2.2. COMPUTER-AIDED QUANTITATIVE ANALYSIS OF SPATIAL STRUCTURES

Researchers that invented recognition systems for floor plan components were investigated. Ahmed et al. (2014) classified the features of floor plans using line thicknesses, recognized walls and openings, and extracted the semantic structure. However, his method is inadequate if applied to floor plans with various wall thicknesses. Liu et al. (2017) integrated a convolutional neural network and integer programming to distinguish floor plans' components, showing an accuracy rate of 94.7%. Given that the machine-learning dataset of Liu et al. (2017) mainly consists of square-oriented floor plans, there is a limit to interpreting curved or diagonal floor plans. The deep multi-task neural network developed by Zeng et al. (2019) uses an advanced method to recognize walls and types of rooms separately. This network learned diverse residential floor plans, specifically 1,047 with various wall thicknesses, including those with curved and diagonal wall lines, providing an improved floor plan recognition rate compared to that by Liu et al. (2017). In our study, to improve on the manual floor plans analysis methods in previous Korean apartment studies, a novel method was developed considering the aforementioned literature.

3. Methodology

This paragraph introduces five types of data extracted from the floor plan images. The first is the floor plan's silhouette, as it is possible to observe how the appearance of the apartment unit shape has changed. The second and third

types are the number and area of the rooms. The room in the unit is a general index which can be used to discover changes in floor plan and is therefore the most fundamentally investigated aspect in the existing literature. The fourth and fifth types are direct and indirect connectivity based on the semantic fingerprint concept of Langenhan & Petzold (2010). We aimed to determine changes in the relationship between rooms and the layout of the floor plan over time. Various types of images were collected. Considering the investigation subjects, we excluded 3D renderings that were not appropriate floor plans and multi-floor units that were not in the standard Korean apartment format. Consequently, we studied 5,355 2D floor plan images and 33,892 instances of metadata to generate the five types of information. A custom-developed software package referring to the Grid-Based (GB) descriptor by Rodrigues et al. (2017), the floor plan recognition network of Zeng et al. (2019), OpenCV, and the NetworkX libraries were used for the information extraction process. Our system has the following differences with these earlier methods. Rodrigues et al. (2017) conducted a study to find a descriptor with high accuracy in cluster classification by comparing digitizing floor plans' silhouettes with labeled data. Zeng et al. (2019) focused on devising advanced machine learning networks capable of accurately recognizing the walls, doors, and types of rooms in floor plans. We aimed to extract various types of representable information from floor plans compared to those in previous studies. This approach is novel in that it allows more than 5000 floor plan silhouettes to be classified into clusters of an appropriate number and facilitates the quantification of the diversification, relationships, and connectivity aspects of rooms.

3.1. PREPROCESS

It was barely possible to extract information with a single image analysis system due to the various styles that existed. Therefore, to unify all of the images into the same format, unnecessary elements were manually trimmed. Simultaneously, 1,297 of 5,890 floor plans with different interior textures were modified into one drawing style with five color schemes for the living room, bedroom, toilet, balcony, and entrance (Modified Plan in Figure 1). After this alteration, we converted the images into pixel images in the 'Boundary Plans, format consisting of walls, doors, and windows, using a method developed by Zeng et al. (2019) (Figure 1). It processed input floor plans into three outputs - wall lines, connection parts (walls and windows), and room pixels - with different colors for each room type. Because the room types that were extracted by Zeng et al. (2019)'s method were significantly different relative to actual room types, we used only the wall lines and connection parts to generate Boundary Plans, in which black pixels represent wall lines and green pixels represent doors and windows. As illustrated in Figure 1, we unified the drawing style into a Modified Plan after removing external sections. We created Boundary Plans that express only the walls and openings from the Modified Plans in the preprocessing step, after which we performed the extraction process with our novel system.

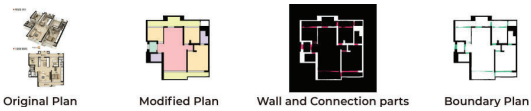

Figure 1. Preprocess steps.

3.2. SILHOUETTE EXTRACTION OF FLOOR PLANS AND SILHOUETTE CLUSTERING

Each Modified Plan image was changed into grayscale with white inside and a black background to obtain the corresponding silhouette. Because the transformed images contain large-scale pixel information of different sizes, the next step was to create a reduced binary image of an identical size. We utilized GB descriptor by Rodrigues et al. (2017) to do this (Figure 2). GB descriptor created a square with the floor plan located in the center and drew 28x28 equally spaced grids by dividing the square. If a grid's center is located inside the floor plan, the value is 1, and if the center is located outside the floor plan, the value is 0. It was necessary to classify silhouette data to check the morphological changes of apartment units over time. However, the floor plans' directions were not unified, meaning that even the same floor plans could be classified into different clusters. Using only GB descriptor without any processing, identical L-shaped floor plans simply rotated 90 degrees will be recognized as two different floor plans. Thus, it was necessary to acknowledge the two as the same L-shaped floor plan to find only the shape changes of the silhouette. Thus, floor plans undergo two processes so that we can standardize the directions. First, we rotate floor plans so that the long side is always in the vertical position. Second, we rotate the floor plans so that areas with more black pixels, i.e., empty segments, are located at the top. Afterward, the standardized GB described 28x28 matrices were transformed into 784 binary data in one-dimensional matrices. Subsequently, we classified clusters by means of the K-means method. The silhouette score and elbow method helped determine the optimized number of clusters.

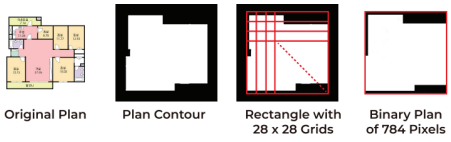

Figure 2. GB descriptor execution of the original floor plan.

3.3. ROOM COMPONENTS DETECTION

Boundary Plans are pixel images drawn into black wall lines and green-colored openings, and each room has individual contours based on the doors and walls. Our system selects the Modified Plan's color located in the centroid of each room contour of the Boundary Plan to assign room types to the contours in the Boundary Plan. After recognizing the room type, it colors each contour of the Boundary

Plan with the corresponding color. For example, if the center of a contour is orange in the Modified Plan, the contour will then be colored orange (Figure 3). However, the network devised by Zeng et al. (2019) could not draw the doors well compared to the walls, leading to errors. Occasionally, in poorly generated Boundary Plans, two or more rooms were recognized as one contour because the door was incomplete. In such cases, error detection was possible when two or more room centroids designate an identical contour. Our system searched for problematic door pixels close to an overlapped contour and extended these pixels in the direction of the longer side until the line hit the closest wall to become a proper door. The repair process was repeated until all of the contours marked only one room in each case. The system was completed, but some errors cases had multiple doors that were too close such that the system recognized two or more doors as one. We filtered these out according to their abnormal ratio for a door from the colored Boundary Plan and manually altered the doors given that our system could not identify overlapped doors separately. This left only valid walls, doors, and rooms in the colored Boundary Plans. Our system then stored the number and area of rooms depending on the number of colored contours and pixels.

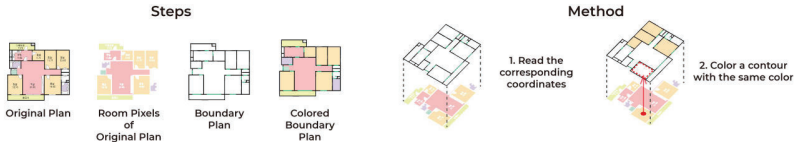

Figure 3. Colored Boundary plan generation steps and method.

3.4. ROOM CONNECTIVITY ANALYSIS

Room connectivity was analyzed using colored Boundary Plans. The system recognized the doors by color and selected two coordinates located at a certain distance in a direction parallel to the short side of the doors. If coordinates at both ends are located in different rooms, this indicates that the two rooms are connected through the door; i.e., direct connectivity is established. Meanwhile, there could be a colorless (empty) room between the rooms. The designated room types had their color assigned and, the colorless room in this case is either a closet or an extra room, such as a walk-in closet with no assigned color. The former did not influence the connectivity because it was open to a single room. However, the latter was open to multiple rooms and acted as a corridor between rooms. We defined the corridor as a new room type for the latter cases. If a corridor candidate (colorless room) has more than two doors connected to other rooms, the system colored the candidate in cyan (Figure 4). Our system newly stored the number and area of corridors in the room components data. Because floor plans were drawn in different standards, in some cases it was necessary manually to modify direct connectivity after our system filtered out possible errors. Depending on the style, floor plans had a shower booth and bathroom connected through a door or without a door. In such a case, the system recognizes these elements

as separate bathrooms. Considering this, we removed the shower booth doors after checking visually whether two or more bathrooms were actually connected. We were thus able to generate correct direct connectivity and colored Boundary Plans with added corridors. With regard to indirect connectivity, room pixels in the colored Boundary Plans were dilated to exceed the wall thickness, and the overlapping rooms were indirectly connected (Figure 4).

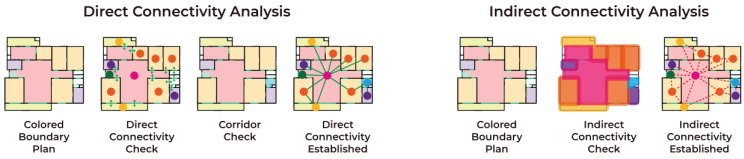

Figure 4. Direct and indirect connectivity analyses.

After the generation of the direct and indirect connectivity graphs, the degree centrality, the betweenness centrality, and the closeness centrality were calculated. The definitions of and equations for each centrality are as follows: degree centrality refers to how many rooms are connected to each room ($C_D = \sum E_w$; E_w: the set of edge connected to the node), closeness centrality refers to the closeness of all rooms in the floor plan to each other ($C(u) = \frac{n-1}{\sum_{v=1}^{n-1} d(v,u)}$; n: the number of nodes, d(v, u): the shortest path from v to u), and betweenness centrality refers to how many times the shortest paths pass through each room ($C_B(v) = \sum_{s,t \in V} \frac{(s,t|v)}{(s,t)}$; V: the set of nodes, σ (s, t): the number of shortest(s, t) -paths, σ (s, t|v): the number of shortest (s, t) -paths passing through some vertex v other than (s, t)).

4. Implementation Results

4.1. CLASSIFICATION OF FLOOR PLANS

We classified floor plans into five sizes by referring to Seoul's apartment-application deposit criteria. These are denoted here as Small (S) (-60m2), Small-medium (SM) (60-85m2), Medium (M) (85-102m2), Medium-large (ML) (102-135m2), and Large (L) (135m2 and larger). The numbers of floor plans by size were as follows: S: 1,462, SM: 2242, M: 220, ML: 948, and L: 483. The move-in year of the apartment units investigated in this study ranged from 1976 to 2020. Choi et al. (2004) noted that data reorganization by period based on events that affected the apartments is a very effective method when discussing socio-cultural phenomena via a spatial analysis. We reconstructed the years into several periods by referring to Choi et al. (2004). These are Period 1 (P1) (1976-1985), Period 2 (P2) (1986-1989), Period 3 (P3) (1990-1997), Period 4 (P4) (1998-2002), Period 5 (P5) (2003-2010), and Period 6 (P6) (2011-2020).

4.2. SILHOUETTE CLUSTERING

We grouped the silhouettes by size and investigated how the shapes of the units changed over time. The optimal numbers of clusterings for each size were S: 3; SM: 4; M: 6; ML: 4; and L: 3. Table 1 presents representative images of two versions of each cluster. The first image shows the average value obtained by adding the 28x28 binary silhouettes and dividing this value by the number of images in the cluster. The second representative image is a binary image of the first image. It can be inferred that the apartment unit's silhouette is standardized in several typical shapes, regardless of the size. Rectangle, rounded rectangle, L, mirrored L, and square shapes appeared in common, and the proportion of changes over time appeared to be similar. As a result, silhouettes varied the most in P5 and P6, which means that some diversification occurred in the 2000s and 2010s.

Table 1. Silhouette clustering of floor plans.

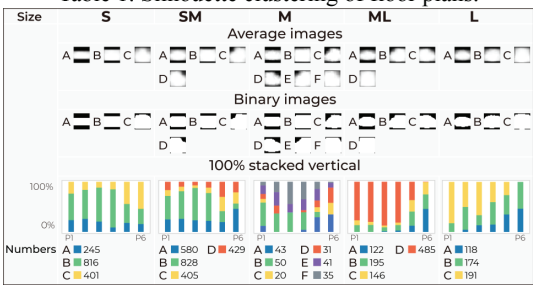

4.3. ANALYSIS OF THE NUMBER AND AREA OF ROOMS

Figure 5 illustrates the average of each room area's sum and the number of rooms excluding the living room according to the size over the period. The number of rooms increased to P5 overall, and all values decreased in P6. On average, the number of rooms increased from 7.3 for P1 to 9.2 for P6. We expected that the increase in the number of rooms would reduce the area of the rooms. However, the room area scarcely changed at most sizes, and L even increased up to P5. The fact that the room area did not decrease implied a decrease in the living room area. Next, we examined in more detail the room types. The numbers of bedrooms changed individually for each type; the number increased in S; there was little change in SM, M, and ML; and it decreased in L. The number of bathrooms for the L size increased from 2 to 2.5, and the number also increased in other sizes, settling at 2. Corridors showed slight increases in the number in general. The number of balconies increased up to P5, apart from the L size, and this number eventually decreased in P6. The areas of the bedrooms, bathrooms, and balconies were inversely proportional to their numbers, but both values decreased for the P6 balconies, representing less preference for balconies in the 2010s. Only the number of corridors and the corresponding area increased simultaneously, and the area expanded remarkably from P3, indicating growing demand for this element.

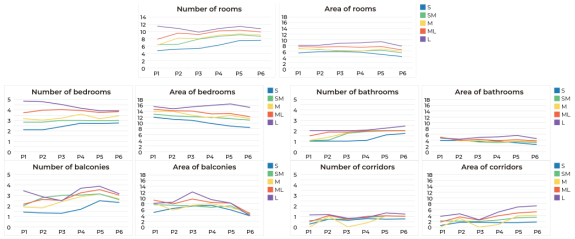

Figure 5. Number and area of rooms by period.

4.4. ANALYSIS OF DIRECT CONNECTIVITIES

In this section, we analyzed the direct connectivity of rooms. The average graphs for rooms shown in Figure 6 illustrate the average for the degree, closeness, and betweenness centrality of the rooms by period, excluding the living room in each case. With regard to the degree, even if there is a difference in P1, it converges to 1.5 at P6. Because closeness is a value that declines when the number of rooms or the depth of the space increase, S is largest and L is smallest. Betweenness increased the most for the SM size, and the other sizes similarly showed gradual increases. Next, we studied the centrality of each room in more detail (Figure 6). The degree and betweenness values for bedroom increased but closeness decreased, suggesting that bedrooms are becoming modularized and individualized over time due to the following reasons. First, while the bedroom's degree value increased, the numbers of balconies and bathrooms both increased (Figure 5) with decreases in their degrees. The first reason implies that added balconies and bathrooms over time are open to bedrooms only. Second, the betweenness value for bedrooms increased, indicating that bedrooms became an intermediate node between other rooms. These situations indicate increases in the numbers of private balconies and bathrooms. Except for a sharp decrease in P3, the corridor is the only room type for which the closeness value increased, as corridors serve as the bridge between bedrooms and private balconies or bathrooms. In rooms other than a corridor, the closeness value decreased due to the presence of modularized bedrooms, which means the minimum distance to other rooms grew. However, the betweenness value for corridors increased, as these elements served as the main junction in the modularized bedrooms.

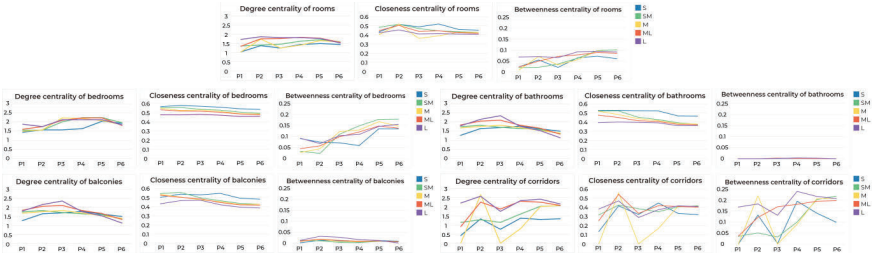

Figure 6. Degree centrality, closeness centrality and betweenness centrality of rooms by period

4.5. ANALYSIS OF ROOM LAYOUTS

In this section, we analyzed the indirect connectivity. Indirect connectivity is a component indicating the shape of the floor plan, similar to a silhouette (Section 4.2), as it connects nearby rooms. However, unlike silhouettes, which are represented by pixels, the layout information is identified by converting a floor plan into a network by examining the indirect connectivity between adjacent rooms. We utilized the graph edit distance (GED) to indicate how floor plans have become more diversified with Python's GMatch4Py library. GED was calculated by pairing two of the floor plans with the same size classification, and the average value was illustrated over time (Figure 7). As a result, we found that GED increased over time, implying that the diversification of the layout became more active over time. The larger sizes had larger GED, implying that a large area allows the diversification of the layout. It was able to describe the change of layouts in more specific values than the silhouette clusters in Table 1.

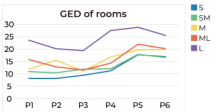

Figure 7. Graph edit distance (GED) values of rooms by period.

5. Discussion and Conclusion

P4 contains data from 1998 to 2002, a period of "The 1997 Asian Financial Crisis" in Korea. During the restoration period, P5, various apartments were designed to increase the construction volume with pump-priming by, for instance, financial support and deregulation. Furthermore, this socio-cultural background explains the peculiarity of the analyzed data in P5. We find a vigorous improvement in the number of cluster types, the number and area of rooms, modularization of bedrooms, and the diversity of layouts. Our method's limitation stems from the fact that floor plans available online vary in terms of the level of detail, the residential type, and the expression style. For example, whether the furniture is represented in the floor plan; the use of a non-constant wall thickness; and definitions of the range of room types, such as bedrooms, master bedrooms, bathrooms, shower booths, balconies, utility rooms, corridors, and walk-in closets depends on the architect or reader. Therefore, it was challenging to recognize floor plans completely without manual manipulation, and it was inevitable that we needed manual manipulation between the processes. A limitation in the results is that there is a significant difference in the number of floor plans for every period and size. Thus, the unevenness in the number of data instances led to the unintentional stressing of a specific situation. In P3 for the M size, there are relatively few samples, and corridors are absent in all 18 units. Accordingly, the dropped values in Figures 5 and 6 stood out. In future studies, data on more apartment units will be collected to secure data diversity.

This study quantitatively examined the historical changes and diversification of Korean apartment units from various perspectives through large datasets.

There are several important results. First, the silhouettes of the apartments were similar for all sizes, and the distribution by period changed similarly. Second, the number of rooms increased, and the area was maintained. Third, individualization and modularization of bedrooms were noted. Fourth, corridors are both evidence and a catalyst of the third finding above, and the preference for corridors increased over time. Fifth, the degree of layout diversity increased up to P5 and then declined. This study's crucial contribution is that employing large datasets for floor plan investigations quantitatively to analyze spatial patterns in morphological, numerical, and semantic criteria is important. Further research will explore more specific correlations between current values and conduct rigorous analyses with regions, prices, and nearby traffic conditions and convenience facilities.

Acknowledgement

This work was supported by the Ministry of Education of the Republic of Korea and the National Research Foundation of Korea (NRF-2019S1A5A8034285).

References

"Real Estate 114" : 2019. Available from <https://www.r114.com/> (accessed 6th November 2019).

"Statistics Korea.: 2020, 2019 Population and Housing Census" : 2020. Available from <https ://kostat.go.kr/portal/korea/kor_nw/1/2/2/index.board?bmode=read&bSeq=&aSeq=384690&pageNo=1&rowNum=10&navCount=10&currPg=&searchInfo=&sTarget=title&sTxt= > (accessed 25th September 2020).

Ahmed, S., Weber, M., Liwicki, M., Langenhan, C., Dengel, A. and Petzold, F.: 2014, Automatic analysis and sketch-based retrieval of architectural floor plans, *Pattern Recognition Letters*, **35**, 91-100.

Bae, J.M., Jung, Y.S. and Yoon, J.S.: 2001, A Study on Characteristics of Apartment Housing Unit Plans, *Journal of the Korean Housing Association*, **12**, 1-12.

Choi, E.H.: 2003, A Study on the Characteristics of Unit Plan Composition according to Sizes in Public Housing : Focused on the Residential Apartments built after 1999 and occupied from 2001, *Journal of the Korean Institute of Interior Design*, **38**, 134-142.

Choi, J.P., Cho, H.K., Park, I.S. and Park, Y.S.: 2004, A Spatial Analysis of the Apartment Unit Plans from 1966 to 2002 in Seoul, *OURNAL OF THE ARCHITECTURAL INSTITUTE OF KOREA Planning & Design*, **20**, 153-162.

Choi, J., Kim, Y., Kang, J. and Choi, Y.: 2014, Comparative Analysis of the Spatial Structure of Apartment Unit Plans in Asia - Apartments in Korea, Vietnam, and Kazakhstan -, *Journal of Asian Architecture and Building Engineering*, **13**, 563-569.

Langenhan, C. and Petzold, F.: 2010, The fingerprint of architecture-sketch-based design methods for researching building layouts through the semantic fingerprinting of floor plans, *International electronic scientific-educational journal: Architecture and Modern Information Technologies*, **4**, 1-8.

Liu, C. and Kohli, P.: 2017, Raster-to-vector: Revisiting floorplan transformation, *Proceedings of the IEEE International Conference on Computer Vision (ICCV) 2017.*

Rodrigues, E., Rodrigues, D., Sampayo, M., Gaspar, A., Gomes, A. and Antunes, C.: 2017, Clustering of architectural floor plans: A comparison of shape representations, *Automation in Construction*, **80**, 48-65.

Zeng, Z., Li, X., Yu, Y. and Fu, C.: 2019, Deep Floor Plan Recognition Using a Multi-Task Network With Room-Boundary-Guided Attention, *Proceedings of the IEEE/CVF International Conference on Computer Vision (ICCV) 2019.*

ICE STEREOTOMY

A Case Study of Free-Form Ice Shell

JINGWEN SONG[1], YUETAO WANG[2], PING CHEN[3] and HAO ZHENG[4]
[1,2]*School of Architecture and Urban Planning, Shandong Jianzhu University, Jinan, China*
[1]*anwenarch@foxmail.com* [2]*wyeto@163.com*
[3]*School of Architecture, Harbin Institute of Technology, Harbin, China*
[3]*chenping543@163.com*
[4]*Stuart Weitzman School of Design, University of Pennsylvania, Philadelphia, USA*
[4]*zhhao@design.upenn.edu*

Abstract. The free-form ice shell is the most challenging type in the design and construction of free-form buildings due to the regional and temporary nature of its materials. This paper presents a case study of the integration of design and fabrication of free-form ice shell. Taking the computational design and robotic fabrication of the ice shell as the main object, we discuss that combines the form-finding of the shell structure of graphic static with the tessellation technology of stereotomy, and propose a new method and workflow for the integration of discrete free-form ice shell design and construction. In the end, we built a free-form ice shell consisting of 116 discrete ice blocks. Practice has proved the feasibility of the integrated method of discrete free-form ice shell design and construction in the article.

Keywords. Ice shell; Graphic statics; Digital stereotomy; Form-finding; Robotic fabrication.

1. Introduction

1.1. RESEARCH BACKGROUND

During the Renaissance, and due to the emergence of printing, Leon Battista Alberti believed that design drawings were the final output form of the architect's work, and the building was merely a repetition of that work. This triggered a change in how the work of architects was understood and drove the formal separation of architectural design and fabrication. Since then, architects have needed to rely on two-dimensional drawings to convey three-dimensional design information (Evans et al. 1997).

The development of computer-aided design has made it possible for architects to use parametric modeling and quantitative analysis to design non-orthogonal

PROJECTIONS, Proceedings of the 26th International Conference of the Association for Computer-Aided Architectural Design Research in Asia (CAADRIA) 2021, Volume 1, 311-320.

free-form buildings. The separation of design and fabrication led to the geometry of buildings becoming more complex, leading to problems such as long construction periods and the need for a large amount of construction material (Garcia 2013). When French architects built the church dome, they used the masonry surface as the reference surface from which the geometry was defined. This method was to allow precise cutting of construction materials (Plaza 2006). The form was also based on projection drawings executed throughout the process of design and fabrication. The generation mechanism of computer-aided design is able to reconnect design and fabrication.

1.2. PROBLEM STATEMENT

The free-form ice shell is the most challenging type of free-form building to design and fabricate because of the regional availability and temporary nature of its materials. In Figure 1a is the stretched nylon double-curved subsurface sprayed with water to form an integral ice shell at McGill University in 1975 (Sijpkes 2009). Figure 1b shows how the inflatable mesh rope fixed on the snow and ice foundation was then covered with a two-dimensional film bag to construct a three-dimensional template. A one-centimeter layer of ice and snow covered the film, and water was sprayed to make it freeze naturally to form an integral ice shell (Kokawa 2012). The methods commonly used for designing and building ice shells are the inflatable membrane method, the upside-down method, and the fluid form method. These methods have two shortcomings: artificial form-finding methods cannot accurately control the shape of the ice shell, and ice composite materials damage the original material properties of ice and snow-transparency. Both the Igloo and the Gothic masonry vault display the natural aesthetics of stone and ice (Figure 1c).

Figure 1. (a) Water sprayed on stretched double-curved subsurface (Sijpkes 2009). (b) Application of snow and water (Kokawa 2012). (c) Igloo under construction (Masterson 2009).

Stereotomy allows the natural aesthetics to be transformed from an artistic characteristics to technical realization. The application of stereotomy is extended to the design and fabrication of ice shells. With the aid of digital-fabrication technology, ice material can be cut to compensate for the error of manual shape finding. At the same time, the ice material is prefabricated in discrete units to retain the permeability of water freezing to become a real ice shell.

1.3. PROJECT GOAL

The ultimate goal of our research is to create an integrated method of computational design and robotic fabrication for free-form buildings. The scope of application of the design method is no longer limited to conventional materials such as concrete but is extended to ice and snow materials under extreme conditions. we work through the geometric origin and development of digital stereotomy and graphic statics. Digital stereotomy and graphic statics are integrated with computer technology tools to perfect the concept of projective cast proposed by Robin Evans and provide a theoretical basis for the integrated method of computational design and digital fabrication. And we propose a computational workflow, introducing it for the design and fabrication. In computational design, to realize the unity of the external shape and internal force of the shell, graphic statics is used for form-finding, and the duality principle guides the design of discrete elements. In digital fabrication, discrete ice blocks are prefabricated using the principles of digital stereotomy.

2. Digital stereotomy and graphic statics

2.1. THE GEOMETRIC DEVELOPMENT OF STEREOTOMY AND GRAPHIC STATICS

Stereotomy is the art and science of cutting three-dimensional objects into specific shapes (Sakarovitch 2003). An arch building of stone and wood materials with high spatial complexity is constructed by defining the geometric rules, and corresponding relations between the arch system and the discrete units (Andrusko 2014). Giuseppe Fallacara first proposed "Digital stereotomy" and three invariants in 2003. This research lays a solid foundation for the design and fabrication of digital stereotomy (Fallacara 2006).

The research on graphic statics and architectural design methods in the last twenty years is the basis of the rise to the emergence of the field of architectural design. In 2009, Philippe Block of MIT used the characteristics of projection geometry to analyze the limit state of masonry structures using thrust lines (Block 2009.). Block has since established the Block Research Group laboratory at ETH Zurich to continue to study the free-form design of graphic statics (Block 2014). This research was combined with the force density method for form-finding to develop RhinoVault, which has developed into an effective tool for designing arched space structures.

2.2. INTEGRATION OF STEREOTOMY AND GRAPHIC STATICS

The concept of projective cast was originally derived from the work of Robin Evans, who believed that architects design and depict buildings in a projective way, where the diagram and space project each other. Space is perceivable by people. The projected object, the map, and the building bear the task of expressing space in two-dimension and three-dimension (Evans 2000). Although he provided an extensive formal analysis of architecture, he did not propose a clear method for design and fabrication based on geometry.

Stereotomy is a method of drawing and geometric cutting in the first of these projection relationships from imagination to picture to architecture. The method for drawing between horizontal and vertical sections is considered to be the embryo of descriptive geometry. Theories about drawing methods have gradually improved since the second half of the 18th century. Descriptive geometry makes designers pay attention to the drawn expression of abstract concepts. Jean-Victor Poncelet summed up projective geometry as based on descriptive geometry (Calvo-Lopez 2011). Jacques Hyman initiated the study of structural performance-based design based on the duality principle of projection geometry and the invariable cross ratio (Garcia-Ares 2015). Graphic statics is a typical representation of structural geometry. However, since the second half of the 18th century, descriptive geometry made designers pay more attention to architectural-perspective drawings and other drawing expressions. Ignoring the positioning and description of shapes in actual construction through a series of geometric operations led to the stagnation of stereotomy. Technology in actual construction has stagnated. The development of computer technology, stereotomy, and graphic statics, fused with computationally aided design and parametric-design tools, addresses the separation of architecture and structure and promotes the integration of design and fabrication.

3. Methodology

3.1. COMPUTATIONAL WORKFLOW

Figure 2 describes the integrated process of free-form architectural design and fabrication based on the projective cast concept. The fusion of graphic statics and stereotomy provides theoretical support for computational design and digital fabrication. Computational design includes form-finding, reference-plane geometric division, and discrete element design. Digital fabrication includes two techniques of discrete unit prefabrication.

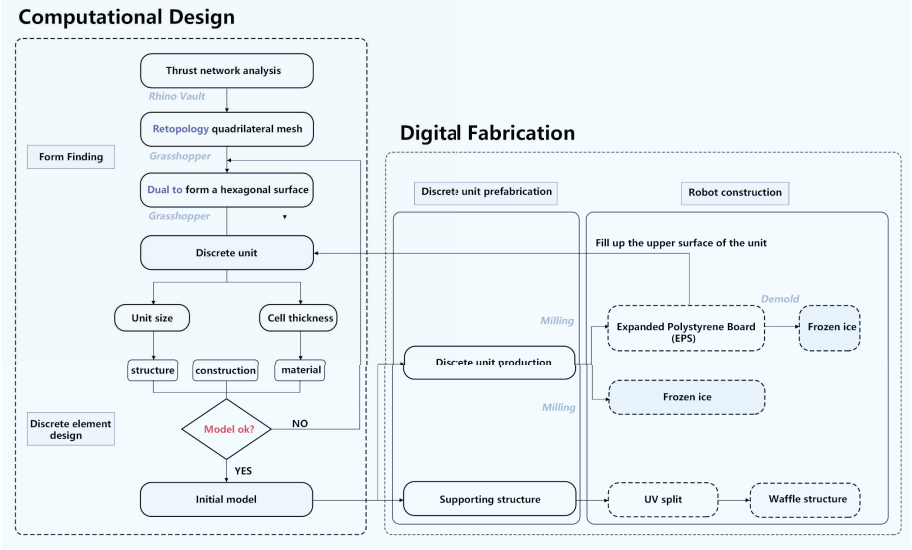

Figure 2. Computational Workflow.

3.2. COMPUTATIONAL DESIGN

3.2.1. Form finding

The ice-shell is a gathering place where the three directions of people flow are gathered. Its planar shape is shown in Figure 3a. The direction of the horizontal thrust in the RhinoVault thrust grid is derived from three-dimensional target geometry and structural features. The form diagram (Figure 3b) and the force interaction diagram (Figure 3c) are used to find the equilibrium state of the shell structure on the horizontal projection (Block et al. 2007). In the form-finding process, the stable shape produces a static balance that requires horizontal loads to ensure that all loads are transferred to the base. The vertical load is applied to make the thrust grid appear three dimensional. The generated thrust grid can be converted into a grid surface, which can then be used as the middle surface of the ice shell.

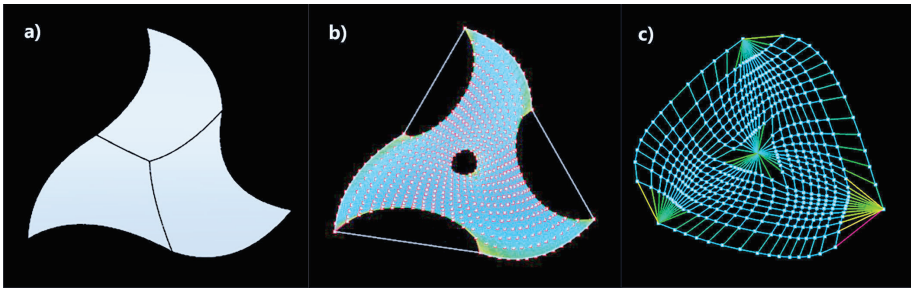

Figure 3. (a) Plane form. (b) Form diagram. (c) Force diagram.

3.2.2. Discrete element design

After the computational form-finding design stage, the digital stereotomy method is used to geometrically divide the thrust-grid reference surface just generated. This is done to construct the three-dimensional shape and precise proportions of each component of the shell before the actual construction and implementation of robotic processing. The mesh surface (Figure 4a) is retopologized into a triangular mesh surface (Figure 4b). Using the dual algorithm in projection geometry, the triangle-mesh faces evenly becomes a polygon; the number of sides is determined by the number of triangles connected to a vertex. The advantage of using triangular meshes for duality is that the generated polygons are extruded to form a compression-only structure (Figure4c). The stress flow of the triangular surface is internalized to the shape itself.

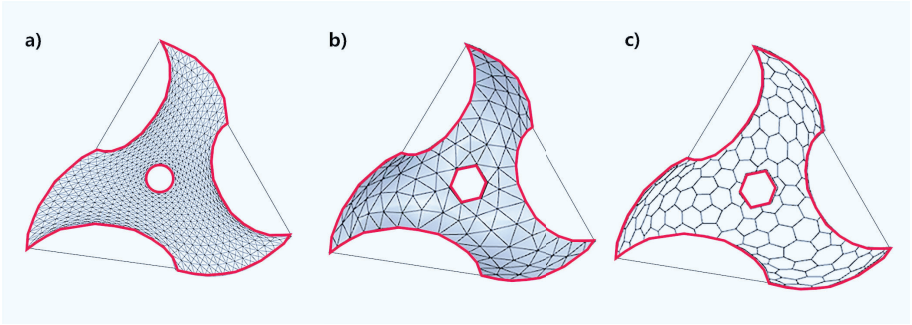

Figure 4. (a) Quadrilateral grid. (b) Triangular mesh. (c) Polygon.

The discrete element of the free-form surface is transformed from a plane figure to a thick polyhedron by using the method of translating the thrust grid along the normal vector (Oval et al. 2019). The enclosing of the body occurs through inlay processing. First, the span of the ice shell is 7.1m. The thrust line is calculated along the axial direction of the curved surface using the compressive strength of the ice material and the relationship between volume and weight. The optimal ice thickness under this scheme and scale is obtained. The thickness of the support is 6cm, and the thickness of the highest point of the unsupported arch is 4cm. Second, this measurement is fed back to the offset grid surface ice, and a three-dimensional boolean operation is carried out to enclose a composite body in the form of a discrete unit body with a corresponding thickness. This unit body realizes the internal shape of the ice crust and unity of force. Third, each discrete unit body generated is placed on the datum plane according to the uniform coordinate, and the units numbered from west to east.

3.3. DIGITAL FABRICATION

3.3.1. MCT milling of EPS template

MCT technology is mainly applied to the milling of templates for the discrete units. The position, processing speed, processing path, and other parameters of each

ice-unit model are set using the SprutCAM platform (Dunn 2012). The simulation module includes automatically optimized motion-path and collision detection. By transferring the NC-code output to the KUKA robot for the fully automatic milling process, the discretized EPS unit template is realized.

Furthermore, the expansion coefficient of ice is 52.0 (Fukusako 1990). In the preliminary experiment, water was directly poured into the EPS-unit template to freeze. It was found that the ice and EPS could not be separated after freezing. We learned from the concrete demoulding method, and plastic was poured into the EPS template plastic filmand fixed all around with paper clips (Figure 5). Before pouring water, one side of the paperclip was removed to ensure that the plastic wrap remained completely attached to the template under the action of water flow.

Finally, the processed discrete unit molds are placed uniformly outside at a temperature below -20°C according to the label, and frozen under natural conditions for more than 40 hours. No water flow inside was observed, indicating that the ice was completely frozen and can be used as a unit to build.

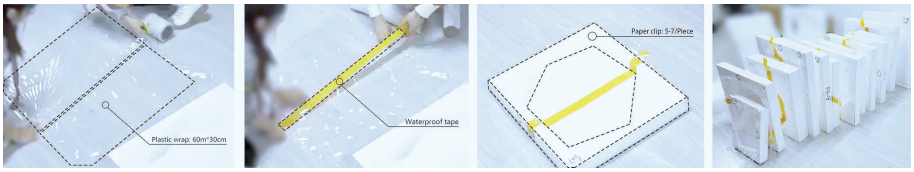

Figure 5. (a) Plastic film. (b) Waterproof tape for bonding plastic film. (c) Paper clip fixed to EPS. (d) Sorted by serial number.

3.3.2. MCT milling ice

The key to MCT milling of ice blocks is the fixation of the ice blocks. Preliminary attempts were made using two fixing methods: the suction cup and the physical shield fixing methods. The advantage of the suction-cup method is that there is only one contact surface between the suction and the ice block, the processing constraint is 1, and the other surfaces can be processed directly. However, in the actual milling process, it was found that the sucker was controlled by the air compressor and that the pulling force of the milling speed, stepping width, cutting depth, and bit speed on the ice block was greater than the friction force of the sucker on the ice block, which made the ice block offset 15° counterclockwise. The sucker-fixing method was not applicable to the milling ice block. The second, shielded physical fixation method, can only provide processing on one side, and the processing constraint is 5, which is suitable for milling ice blocks (Figure 6).

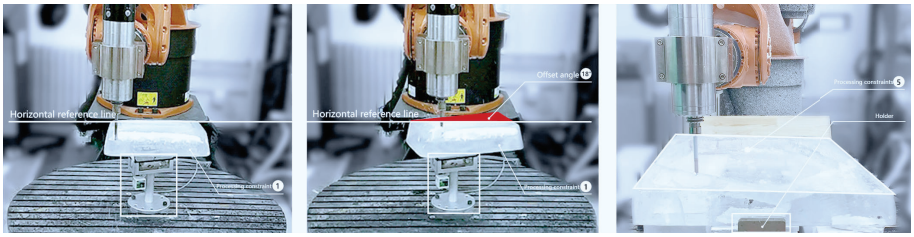

Figure 6. The suction cup fixing method and the shielding physical fixing method.

The logic of milling ice blocks is that the original ice blocks are inverted. A circle of contour lines is drawn on the original ice blocks with a drill bit, and the excess ice blocks milled out. The milling surface is the lower surface, and the upper surface is the plane. The milling logic of ice blocks is opposite to that applicable to EPS boards. The problem introduced to the process of milling by the shielded physical fixation method is that the processing constraints are too high and the method inflexible. Therefore, it is necessary to manually detach and remove the ice from the milling part in time to prevent the ice from coagulating with the standard ice. The advantage of directly milling ice is that standard ice can be used, which saves time on freezing ice. Therefore, the ice blocks with H>11 in this experiment were made using MCT-milled ice blocks.

4. Results

The on-site assembly of the ice shell takes place in sequence in three stages: the base, the support grid, and the discrete unit body. The base is positioned using the 1:1 drawing method, with the accurate CAD drawing being printed on white paper and then covered with a transparent plastic protective film. Six standard ice bases with a size of 0.75m*1.55m*0.5m were placed by forklift on the positions corresponding to the drawings. Wooden planks were used to define the boundary area, and water poured into the area to freeze the base and the ground as a whole and to prevent the base from being displaced during the construction process.

The discrete unit ice blocks were placed on the support grid in a spiral manner and directly in contact with the wooden board; there is no other material between the two. The precise machining by the robot makes the inner surface of the discrete unit a curved surface, which has the same curvature as the support grid, and achieves a precise fit if there is accurate positioning. The gap between the first layer of ice and the ice base was filled with crushed ice, slag, and snow, and water poured in after filling. After the first layer of ice blocks and the base were frozen into one body, the ice blocks were placed layer by layer and frozen with water after every two layers of ice blocks were attached. When the discrete units were prefabricated, a layer of plastic wrap was laid in the EPS template to make the inner surface of the ice block smoother. The increase in smoothness has a negligible impact on fabrication, and the use of plastic wrap makes it very convenient to demold the ice. The EPS template can also be reused.

5. Conclusion and discussion

This article combined stereotomy and graphic statics to develop a free-form shell-design method and process that was applied to the ice shells. A discrete unreinforced ice shell design was constructed using architectural geometry and digital fabrication. An experimental building process accommodated the precise positioning of the free-form ice block and the permeability of the material while expanding the application range of stereotomy and graphic statics. Using the concept of projective cast proposed by Evans and taking advantage of the evolution of the architectural-drawing method, stereotomy, and graphic statics were recombined. The projection mold from Evan's concept was transformed into a practical principle and design method, and the theory of projective cast advanced (Figure 7).

Figure 7. Real view of the ice shell during the day.

The combination of computer-aided design and parametric tools allowed for the emergence of a parametric design method for free-form buildings based on the projective cast. Traditional design methods and fabrication techniques were combined with computer-aided design and parameterization tools to take advantage of and develop traditional theories in the context of digital technology.

In cold climates, ice and snow are used as local materials, and water is easy to fetch and transport. As the temperature rises, temporary ice and snow buildings melt into water and then re-enter the natural water cycle. Materials are easy to obtain and sustainable. In digital fabrication, the robot milling template and ice respond differently. One approach to this is to use templates that can be recycled. The other approach is to cut standard ice directly, which is suitable for large-scale ice fabrication. These two different digital fabrication methods and the previous computational design form a set of precise fabrication and allow the recycling of the model of the ice-shell structure. This model provides new ideas for

people living in severely cold areas to quickly build ice and snow buildings with short-term wind and cold resistance and to be able to easily model and view those structures. The model also provides more diversified directions for development in the construction of ice and snow buildings in the more severe climates of the Arctic, and Antarctic.

Acknowledgement

This research is the result of the "Computational Design 2019" workshop organized by the Computational Design Committee of the Architectural Society of China. The author expresses gratitude to the Computational Design Committee of the Architectural Society of China and the workshop organizers.

References

Andrusko, P.A.: 2014, Stereotomy: Stone Architecture and New Research by Giuseppe Fallacara, *Nexus Network Journal*, **2**(16), 501-504.

Block, P.: 2009, *Thrust network analysis: exploring three-dimensional equilibrium*, Ph.D. Thesis, Massachusetts Institute of Technology.

Block, P. and Lachauer, L.: 2014, Three-dimensional (3D) equilibrium analysis of gothic masonry vaults, *International Journal of Architectural Heritage*, **8**, 312–335.

Block, P. and Ochsendorf, J.: 2007, THRUST NETWORK ANALYSIS : A NEW METHODOLOGY FOR THREE-DIMENSIONAL EQUILIBRIUM, *Journal-International Association for Shell and Spatial Structures*, **48**(3), 167-173.

Dunn, N.: 2012, *Digital fabrication in architecture*, Laurence King.

Evans, R.: 2000, *The projective cast: architecture and its three geometries*, MIT press.

Evans, R., Difford, R. and Middleton, R.: 1997, *Translations from drawing to building and other essays*, Architectural Association London.

Fallacara, G.: 2006, Digital stereotomy and topological transformations: reasoning about shape building, *Proceedings of the second international congress on construction history*, 1075-1092.

Fukusako, S.: 1990, Thermophysical properties of ice, snow, and sea ice, *International Journal of Thermophysics*, **11**(2), 353-372.

Garcia, M.: 2013, Emerging technologies and drawings: The futures of images in architectural design, *Architectural Design*, **83**(5), 28-35.

Kokawa, T.: 2012, Building techniques for ice shell as temporary structure, *Proceedings of IASS-APCS*.

Calvo Lopez, J.: 2011, From Mediaeval Stonecutting to Projective Geometry, *Nexus Network Journal*, **13**(3), 503-533.

Oval, R., Rippmann, M., Mesnil, R., Van Mele, T., Baverel, O. and Block, P.: 2019, Feature-based topology finding of patterns for shell structures, *Automation in Construction*, **103**, 185-201.

Plaza, B.: 2006, The return on investment of the Guggenheim Museum Bilbao, *International journal of urban and regional research*, **30**(2), 452-467.

Sakarovitch, J. and Huerta, S.: 2003, Stereotomy, a multifaceted technique, *Proceedings of the First International Congress on Construction History*, 24th.

Sijpkes, P., Barnett, E., Angeles, J. and Pasini, D.: 2009, The architecture of phase change at McGill, *Leadership in Architectural Research*, **2009**, 241.

FUZZY LOGIC IN BENDING-ACTIVE GRIDSHELL DESIGN

SINING WANG[1] and XINCHEN ZHAO[2]
[1,2]*School of Architecture, Soochow University*
[1]*snwang@suda.edu.cn* [2]*527434032@qq.com*

Abstract. Performance-based design is encouraging designers to carry out quantitative-oriented research, sometimes indifferent to qualitative matters that concern social, cultural, and even psychological aspects. Design requirements related to humans' subjective value and decision-making ought to be properly addressed. This paper begins with the discussion of architectural complexity about its ill-defined design problems. Human's linguistic variables contain the ambiguous yet uncertain value that seemingly unfit for today's precise digital design approaches. Hence, this paper involves the idea of fuzzy logic and its inference system, presents a soft computing method using membership functions to describe qualitative parameters. It then uses MATLAB Fuzzy Logic Toolbox, as an auxiliary design tool apart from Rhinoceros Grasshopper, to grade design options of a bending-active gridshell from an undergraduate design studio.

Keywords. Fuzzy logic; digital architecture; linguistic variable; bending-active gridshell.

1. Introduction

This presented work selects a bending-active gridshell project from an undergraduate design studio where students were asked to work with NURBS modelling tool and physics simulation engine in long-space architecture design. Performance-based design approaches already came to the forefront of architectural discourse, so that pioneering architects, designers, and researchers are keen on carrying out quantitative form-finding designs based on data extracted from such as environment, material behaviour, and fabrication capacity. However, this emerging trend of digital paradigm may jeopardise a designer's conscious decisions made to his/her projects. Matters like spatial experience, cultural reflections, and aesthetical pursuits etc. are impossible to measure using conventional data strings. The very nature of architectural design must include complex design problems insofar as it urges today's architects to consider multi-variate factors when they are looking for design solutions. Hence, this reveals necessity to investigate potential means of transforming humans' ambiguous expression to measurable outcomes so that both quantitative and qualitative design variables can be rationally integrated.

PROJECTIONS, Proceedings of the 26th International Conference of the Association for Computer-Aided Architectural Design Research in Asia (CAADRIA) 2021, Volume 1, 321-330.

2. Architectural complexity

Peter Rowe (1987) categorised two types of design problems: well-defined and ill-defined. The former ones normally prescribe articulate goals and work towards expected results. Its problem-solving trajectory is relatively linear with few uncertainties. For example, the modern architectural industry used to pursue a Fordian mode of design and production by standardising building forms, component details, and implementing techniques. By doing so, one may evade latent risks caused by intricate design requirements but, at the same time, weaken a project's persona. Ill-defined design problems, on the other hand, can never be comprehensively described at the beginning of a project (Lawson, 2005). Lawson believes most of today's architectural and urban design practices belong to the latter one. This is because, firstly, new design requirements may emerge anytime without formulations; secondly, the problem-solving process may last more than expected; and thirdly, the problem-solution may be diverse from case to case.

2.1. FLEXIBLE DESIGN PROBLEMS

Lawson created a 'completed model of design problem' to describe the intricacy of an architectural project, which contains the problem's generator, nature, and category. From these three dimensions, the model illustrates design problems of their contained variables and corresponding rigidity. For example, practical requirements from legislator ought to be rigid since they often refer to strict matters such as building codes and site-specific restrictions. Comparatively speaking, questions about building forms and geometries usually play a less decisive role in architectural practice therefore are more flexible. These design requirements always involve qualitative variables from designer, stakeholder, and user.

However, there is no clear boundary between 'rigid' and 'flexible' design problems. What architects are pursuing within a design space is so-called 'trade-offs', while it is well acknowledged that there is never an optimal outcome without compromise made over certain aspects. Given this, architects usually rely on their pervious project experience and expertise to make the judgment call on the best design solution. With emerging digital advances, we may now be able to integrate both quantitative and qualitative needs until discovering a feasible design solution space.

2.2. LINGUISTIC VARIABLES IN ARCHITECTURAL DESIGN

Some qualitative design problems are not defined with articulate rules but are verbally described based on human experience. For example, a client may ask for 'proper colour', 'sufficient lighting', or a 'large room'; and an architect may also respond with an 'asymmetrical shape' or 'positive space'. Here, neither 'proper', 'sufficient' and 'larger' nor 'asymmetrical' and 'positive' encompass precise meaning that can be mathematically programmed with design tools. Conventional hard computing approach may appear short-handed since a 'high degree of precision is usually incompatible with a high degree of complexity,' says Oguntade and Gero (1983).

Hence, the vague messages from one human being to another need to be

interpreted before they become intelligible to a computer. Design requirements like 'large' and 'asymmetrical' are linguistic variables which possess uncertain qualities (Talašová and Achten, 2009). These 'soft' forms of data, according to Ottchen (2009), reveal aesthetical, socio-cultural, historical, and even political dimensions that should not be left out by architects while making design decisions. He suggests architects to look at a bigger picture where these qualitative variables are parameterised, constrained with domains, assigned with weight and integrated in order via building information models. Soft computing is capable of handling the architectural complexity of its inexactness and imperfection, which therefore suits architecture's ill-defined characteristic.

3. Fuzzy logic

Introduced by Lotfi Zadeh in 1965, fuzzy logic is one of the soft computing methods providing alternatives to classic bivalent hard computing. In order to describe linguistic variables or human mind per se, fuzzy logic reveals an inference system that models nonlinear functions of vagueness and complexity then transforms into a desired degree of precision. In a traditional crisp set, there are only two types of relationships exist between a variable x and a universe A: membership ($x \in A, A(x) = 1$) or no membership ($x \notin A, A(x) = 0$). Contrary to a traditional crisp set that builds on two-valued logic, a fuzzy set adopts partial membership to accommodate imprecise expressions. Its mathematical expression can be illustrated as μA(x)=[0,1] (Cox, 1992).

3.1. FUZZY LOGIC IN ARCHITECTURE

This multi-valued expression allows designers to deal with qualitative design problems, which allows them to map an input space to an output space. Fuzzy logic was initially used for boiler design, in which the valve status has been determined by a range of temperature from 'cold' to 'hot'. Likewise, such soft data operation may also be applied to the architectural and urban domain so that multi-variate requirements are appropriately addressed. Within the realm of the fuzzy set, the problem-solving trajectory is no longer linear. For instance, if one divides the domain of a ceiling height into three subsets: 'tall', 'medium', and 'low', value h=3.2 m may belong to the 'low' and 'medium' subset at the same time.

In architecture, fuzzy logic is mainly used for design analysis and post-design interpretation. Talašová and Achten (2009) utilised fuzzy logic to evaluate the spatial composition of a villa design by Adolf Loos; Koutamanis (2001) has noticed the capacity of fuzzy logic representing human's vague expression, so he applied it in transforming architect's hand sketch into a digital model; Çekmiş (2016) created an evaluation method for the planning project of a residential community. However, only a few examples illustrated fuzzy logic's contribution to design generation: Wierzbicki-Neagu and Wilfred de Silva (2012) applied the idea to a folding structure design where they combined the soft-computing operation with genetic algorithm.

3.2. FUZZY LOGIC TOOLBOX AND DIGITAL DESIGN

Commonly used fuzzy logic control systems include Mamdani, Tsukamoto, Sugeno and Larsen. This project chose MATLAB Fuzzy Logic Toolbox with Mamdani inference system as an auxiliary design tool apart from Rhinoceros Grasshopper. It includes three general steps: 1) 'fuzzification' translates linguistic yet inexact variables into membership sets; 2) 'inference' creates a series of 'if-then' rules to integrate multi-dimensional design problems and to set their relative weights; and 3) 'defuzzification' adopts a centroid (centre of gravity) approach to extract a final solution from the output space.

The combination of Fuzzy Logic Toolbox and Grasshopper aimed to explore a pragmatic method addressing qualitative matters. A project's digital model reveals a fundamental design logic, in which its composition is secured with a series of parametric parent-children relations. By defining input parameters, an architect also articulates the boundary for fuzzy inference. In the gridshell design discussed below, this project regards Fuzzy Logic Toolbox as an analytical tool that grades project variations. By adopting Fuzzy Logic Toolbox, the student was able to transform her linguistic demands into computationally intelligible meanings, then combine with other measurable criteria in order to finalise the shape of a bending-active gridshell.

4. Fuzzy logic in gridshell design

The research of bending-active gridshell started from Frei Otto, a German structural engineer and architect who dedicated his life to designing lightweight flexible architectures. Gridshells are curved framework gains structural integrity from bending-active rod elements and rigid joints. 'Flatbed' is a typical gridshell construction method which gradually bends a planar grid that prefabricated on-site into shape (Crolla, 2018). Renowned built projects adopted this method include Mannheim Multihalle (1975) by Frei Otto, Japan Pavilion (2000) by Shigeru Ban, and Weald and Downland Gridshell (2002) by Cullinan Studio.

With emerging computational design and implementation technologies, people began to revisit gridshell practice and liberate this structure type from its typological cliché. Most importantly, off-the-peg simulation tools allow today's designers to quickly generate forms, offer them significant advances comparing to Otto's classic hanging-chain method. However, comparing to design data such as bending force and material properties, qualitative factors including space efficiency and construction difficulty remain unmeasurable. This project investigates the possibility of adopting Fuzzy Logic Toolbox to assist gridshell design.

4.1. A GRIDSHELL DESIGN STUDIO

This project chooses one student's design to illustrate the use of Fuzzy Logic Toolbox and design selection. The concept is a multi-purpose building with an equilateral gridshell that occupies an area of around 140 metres long and 90 metres wide, and the maximum structural height should be less than 30 metres. The building's program includes a theatre and several indoor basketball courts

which demand a vertical space more than 10 to 15 metres. With the algorithmic modelling tool Rhinoceros Grasshopper and the real-time physics simulation engine Kangaroo, gridshell design concepts are created from a planner grid and anchored to several edge profiles. The project selects 6 different design options for evaluation via Fuzzy Logic Toolbox (Figure 1).

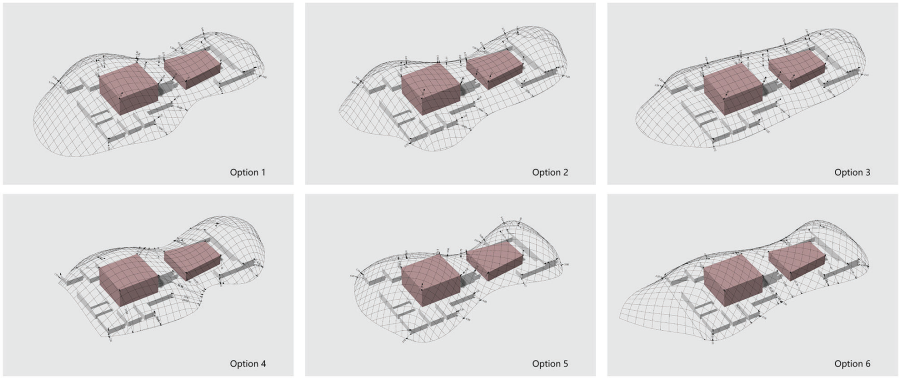

Figure 1. Gridshell design variations.

4.2. FUZZY LOGIC SETUP

Fuzzy Logic Toolbox is an individual plug-in of MATLAB, which uses data from a design's parametric model and transforms into fuzzy sets according to the inference rationale mentioned above. The project sets 4 types of data that concern structural integrity, space rationality and efficiency. Figure 2 shows several checking points that measure the distances between the roof structure and the programs inside. Coloured spheres are the indication of Gaussian curvatures at structure joints. For each gridshell design option, the programme boxes (in red) remain unchanged and whose corresponding 'Preference (P)' score is calculated from these variables below:

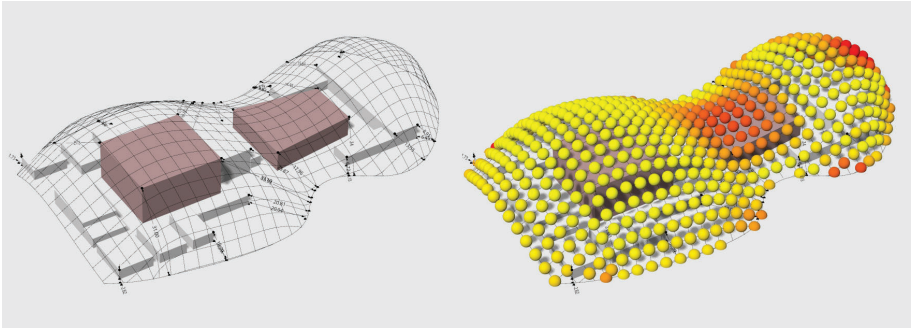

Figure 2. Gridshell checking points and Gaussian curvature indication.

1. The minimal (Hmin) and the maximum height (Hmax) of vertical space between a gridshell surface and the checking points. These distances (measured in metre) reveal the space efficiency inside a structure meanwhile evaluate if the overall structural height matches the requirement (neither too short nor too high). Both input variables are divided into 3 fuzzy sets based on designer's common knowledge: namely 'short', 'medium', and 'large'. For Hmin, these domains are [0, 2.5], [1, 3.5], and [2.5, 5]; and they are [0, 13], [10, 20], and [17, 30] for Hmax;
2. The horizontal space between internal walls and the gridshell surface, which is illustrated using minimal width (Wmin) and maximum width (Wmax). A proper distance shall neither be too narrow for a pedestrian walkway nor too tight for a public space. Thus, Wmin contains 3 fuzzy sets: [0, 1.5], [1, 3], and [2.5, 4], while Wmax's domains include [1, 8], [6, 14], and [12, 20], all units are in metres. The ranges of 'short', 'medium' and 'large' are defined according to human scale and common dimensions.
3. Structural and implementing rationality are represented using Gaussian curvatures. From the design's digital model, the study extracts three types of data including the tightest positive curvature (K+), the tightest negative curvature (K-), and the percentage of tightest curvatures to all (K%). Based on material test and gridshell construction experience, the study defines [-0.005, -0.003] and [0.003, 0.005] as 'high' curvature; [-0.0035, -0.0015] and [0.0015, 0.0035] as 'medium' curvature; and [-0.002, 0.002] as 'low' curvature. As shown in Figure 2, the range of curvatures is visualised with a colour gradient from red to yellow where red spheres represent 'high'.
4. A gridshell's total area (A) also influences the space efficiency. Thus, the project also categorises this parameter into 3 fuzzy sets: 'small', 'medium', and 'large' area (m2). The domain is appointed as [8000, 10000], [9000, 11000], and [10000, 12000] according to site conditions.

4.3. INFERENCE RULES AND EVALUATION

Fuzzy inference rules are the key to integrating these qualitative design requirements that are seemingly disconnected or even conflicting. All these input variables are influenced by the gridshell geometry. For example, an 'efficient' building plan layout may result in a high percentage of 'high' curvatures in the roof structure; or the vertical and horizontal space cannot be 'large' or 'small' at the same time. With the Mamdani fuzzy inference system, the project defined in total 16 rules (Figure 3) subject to the input values and the corresponding design problems the value represented. Design options are graded using 'preference (P)' where 'not preferred' range from 0 to 40, 'medium preferred' range from 30 to 70, and 'preferred' range from 60 to 100.

Each rule shares the same weight insofar as it equally affects the final score of a design option. More than half of the rules (rule No.1 to No.12) describe the designer's concern about spatial quality. For instance, rule No.1 says 'if Hmin is short while Hmax is large and A is small, then a gridshell is preferred.' On the contrary, rule No.8 indicates 'if Wmin is large and Wmax is short or A is large, then a gridshell is NOT preferred.' These are 2 rules that interpret a designer's demand for 'proper' space. Also, rule No.13 to No.16 follow rigid structural requirements. For example, rule No.13 clarifies 'if both K+ and K- are low and K% is low, then

a gridshell is preferred,' but rule No.15 argues 'if either K+ or K- is high and K% remains medium, then a gridshell is 'medium preferred.'

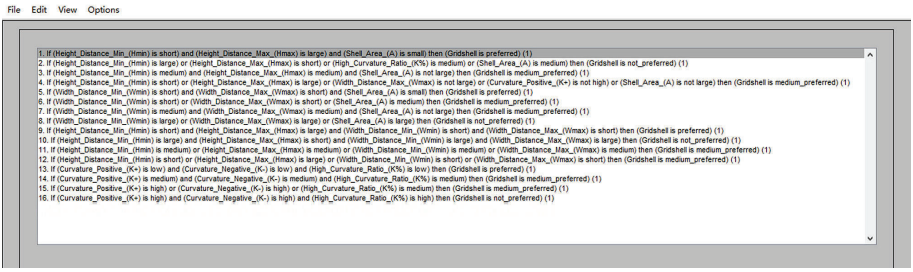

Figure 3. Inference rules created in Fuzzy Logic Toolbox.

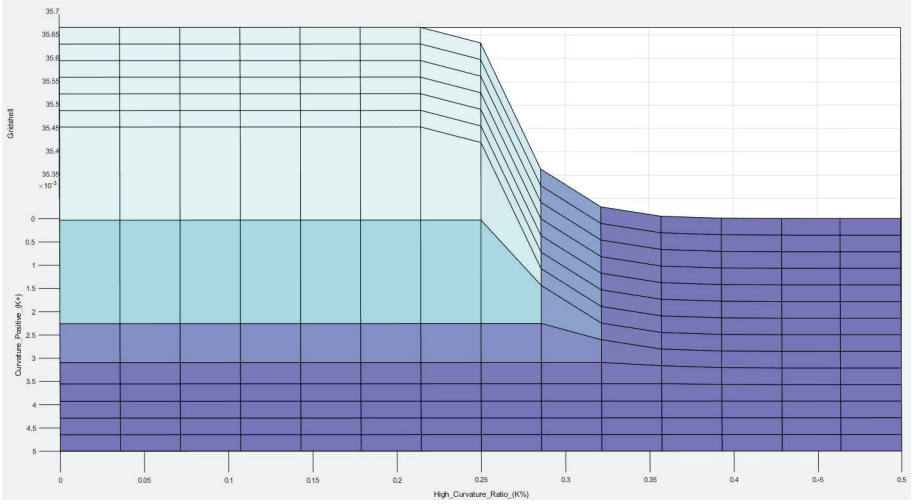

Figure 4. A 3-dimentioanl relation of 'K+' and 'K%'.

These 16 rules establish a non-linear analytical system that helps the designer to sort design options. Figure 4 illustrates the non-linear relation of 'K+' and 'K%' under rule No.13 to No. 16. For each design option, the project extracts 30 values from the gridshell's digital model and converts which into 8 types of fuzzy sets. Final grade 'P' is calculated through a centroid defuzzification method (Figure 5). In the end, Option 4 gets the lowest score (35.4 = 'not preferred') while Option 6 is relatively higher than the others (43.2 = 'medium preferred').

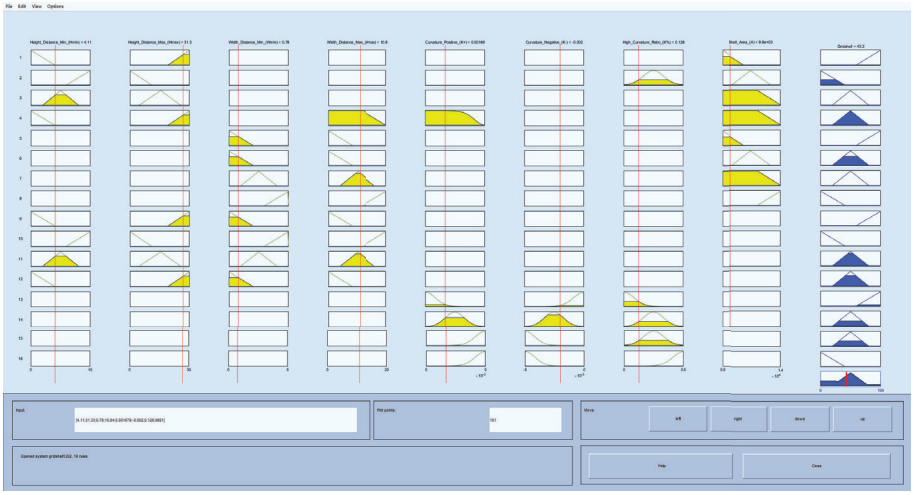

Figure 5. Option 6 fuzzy inference and defuzzification.

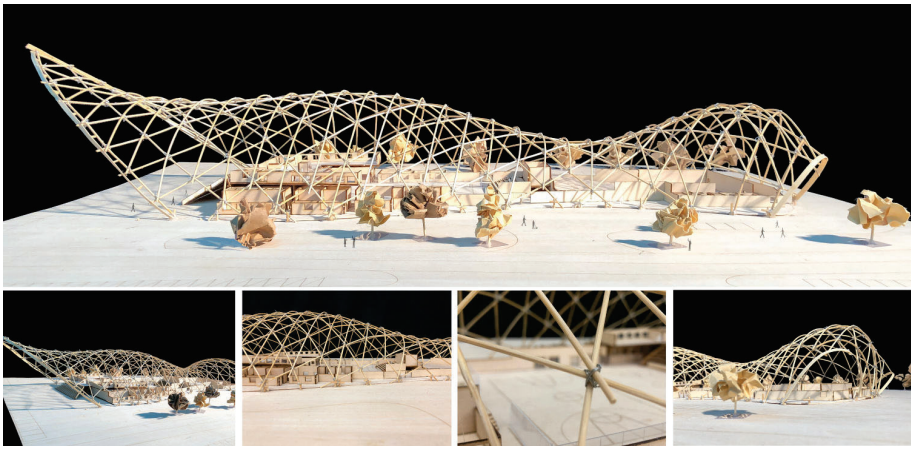

Figure 6. Physical model of option 6.

Just by visually comparing Option 4 and 6, the designer will not be able to tell the reason why one gridshell is better than the other. This makes Fuzzy Logic Toolbox interesting media for architects and engineers to approach complex design problems. In this case, the project helps the student to choose the best yet pragmatic shape out of 6 bending-active gridshells. The chosen outcome is tested through physical modelling (Figure 6).

5. Conclusion

This project uses a bending-active gridshell design to demonstrate the feasibility of fuzzy logic in assisting design decisions. The introduction of fuzzy logic may

reduce the negative impact of traditional hard computing since, in this project, the chosen parameters for soft computing combine common design knowledge, human scale, material properties, and designers' conscious demands. The author believes that fuzzy logic is not only suitable for post-design evaluation, but also can be used for design generation as an optimisation tool.

Integrating soft computing into architectural decision-making aims to reduce architects' bias and increase design rationality. Fuzzy logic provides a mathematical approach for describing linguistic variables as these qualitative design requirements often play an essential role in shaping a design trajectory. With the rapid development of computational intelligence, questions emerge: how to address 'humanity', or the uncertainties, ambiguities, and comprehensiveness in other words, in today's digital workflow? What is the appropriate collaboration mode between human and machine? Through a preliminary experiment, this project postulates fuzzy logic as one way to help architects resolve ill-defined design problems, to sort multi-variate variables, and eventually to mathematically transform qualitative needs into a design-solution space. Its further applications may appear in urban-scale analysis and design as well.

Acknowledgements

The presented work is part of the research project 'Monitor and Adapt Construction Deviation - A Case Study of Bending-active Gridshell' funded by the Natural Science Foundation of the Higher Education Institutions of Jiangsu Province (Project No. 20KJB560022).

References

Cox, E.: 1992, Fuzzy Fundamentals, *IEEE Spectrum*, **29**(10), 58-61.

Crolla, K.: 2018, Bending Bamboo Rules: Beyond Century-Old Typologies, *Journal of Architectural Education*, **72**(1), 135–145.

Crolla, K.: 2018, *Building Simplexity: The 'more or Less' of Post-Digital Architecture Practice*, Ph.D. Thesis, RMIT University.

Iancu, I. 2012, A Mamdani Type Fuzzy Logic Controller, *in* E. Dadios (ed.), *Fuzzy Logic - Controls, Concepts, Theories and Applications*, InTech Croatia Rijeka.

Koutamanis, A.: 2007, Fuzzy modelling for early architectural design, *International Journal of Architectural Computing*, **5**(4), 589–610.

Lawson, B.: 2005, *How Designers Think: The Design Process Demystified*, Architectural Press, Abingdon.

Oguntade, O. and Gero, J.: 1983, Architectural Complexity and Contradiction: A Fuzzy Set-Theoretic Basis and Viewpoint, *Design Studies*, **4**(4), 202–207.

Ottchen, C.: 2005, The Future of Information Modelling and the End of Theory: Less Is Limited, More Is Different, *Architectural Design*, **79**(2), 22-27.

Otto, F.: 1974, *IL 10: Gitterschalen*, Institute for Lightweight Structures, Stuttgart.

Du Peloux, L.: 2017, *Modeling of bending-torsion couplings in active-bending structures: application to the design of elastic gridshells*, Ph.D. Thesis, Paris Est Univeristy.

Rowe, P.G.: 1987, *Design Thinking*, MIT Press, Cambridge.

Talašová, Z. and Achten, H.: 2009, Fuzzy Rule Bases as a Tool of the History of Architecture - Application to the Analysis of Villas Designed by Adolf Loos, *Proceedings of 27th ECAADe Conference*, Computation: The New Realm of Architectural Design, 705–712.

Wierzbicki, M. and de Silva, C.: 2007, Design Tools for Foldable Structures with Application of Fuzzy Logic, *International Journal of Architectural Computing*, **5**(4), 645–662.

Zadeh, L.: 1965, Fuzzy sets, *Information and control*, **8**(3), 338–353.
Çekmiş, A.: 2016, Fuzzy Logic in Architectural Site Planning Design, *12th International Conference on Application of Fuzzy Systems and Soft Computing*, Vienna, Austria, 176–182.

EXPANDING BENDING-ACTIVE BAMBOO GRIDSHELL STRUCTURES' DESIGN SOLUTION SPACE THROUGH HYBRID ASSEMBLY SYSTEMS

CHUN YU MA[1], YAN YU JENNIFER CHAN[2] and KRISTOF CROLLA[3]
[1,2] *The Chinese University of Hong Kong*
[1,2] *{kelvin.ma|jennifer_chan}@link.cuhk.edu.hk*
[3] *University of Hong Kong*
[3] *kcrolla@hku.hk*

Abstract. This paper discusses the development and testing of a novel design method for the low-tech construction of bending-active bamboo gridshell structures. It expands this typology's current design solution space by combining and building up on two common production methods for light-weight shell structures: 1) the "lay-up" method, typically used in bamboo architecture in which members are added one at a time, and 2) the "flatbed" method, in which a prefabricated equidistant flat grid without shear rigidity is propped up and deformed into its final doubly curved shape. The novel methodology expands the system's design solution space by incorporating singularities within the grid topology and by layering multiple separate grids. This allows for spatially radically different building geometries without loss of implementation workflow efficiency. A demonstrator design project, tested through a large-scale prototype model, is described to illustrate the possible spatially engaging architectural design opportunities presented by the novel approach.

Keywords. Bending-active structures; Bamboo architecture; Shell structures; Low-tech fabrication; Form finding.

1. Introduction

The combination of bamboo construction and digital design technology enables radically unique and spatially versatile architectural solutions rooted in local culture and sustainable building practices. This design research project builds on earlier fundamental research on the digital design and implementation of bending-active bamboo shell structures and expands its concept design methods, leading to more diverse design outcomes. The study combines research in architectural design with digital physics-simulation engines and prototyping for low-tech, light-weight construction systems and uses demonstrator design studies as proof of concept (see Fig. 1, 11).

PROJECTIONS, Proceedings of the 26th International Conference of the Association for Computer-Aided Architectural Design Research in Asia (CAADRIA) 2021, Volume 1, 331-340.

Figure 1. Close-up of the 1:20 scale demonstrator physical prototype.

Bamboo is a material of high environmental and socio-cultural importance. It is one of the fastest growing, widely available, low-cost, carbon-sequestering natural resources suitable for direct implementation in construction. It has globally been part of vernacular construction for centuries. Expanding its design solution space with contemporary answers will positively impact the development of the built environment.

Bending-active shells are amongst the most material-efficient, hyper-light-weight structures. They rely for strength and construction implementation on the overall geometrical double curvature and elastic bending properties of their components. Their nonstandard geometries provide unique spatial design opportunities, and their material efficiency results in a reduced need for natural resources. Two types of bending-active gridshell structures exist. 1) "Flatbed" structures employ initially flat, prefabricated, regular grids with no shear rigidity, and elastically deform and brace those into place. 2) The "lay-up" method additively bends and joins individual members into a final shape onsite. Both types present important opportunities and restrictions. Prior research illustrates that computational tools considerably facilitate their development (Crolla, 2017, 2018); yet, no scholarly study exists on further typologies or hybrid structures, and limited research exists on bamboo applications.

This study illustrates that a wider and spatially more versatile and practically applicable solution space exists for this eco-friendly mode of construction.

2. Background

2.1. BENDING ACTIVE GRIDSHELL STRUCTURES

Bending-active gridshells are material performance-driven structures defined by a doubly curved grid with a shell-like behaviour. It requires minimal amounts of materials for making large spans. Applications typically use the rapid and cost-effective deployable flatbed construction method, in which an initially flat

regular grid with no shear rigidity is elastically deformed and braced (see Fig. 2). The advantages of this shaping process are savings in construction cost and erection time, as the structural members do not need individual bending and the grid can be prefabricated flat on the ground. Yet, few bending-active shell structures have been built outside of academic research lab environments. This can be ascribed to two issues. Firstly, the related design-analysis processes are historically notoriously cumbersome. Until recently, only analogue form-finding methods were available to define a specific geometry's appropriate boundary conditions, grid patterns, and bearing positions (Bächer et al., 1978). Today, parametrically controllable digital design simulation tools absorb most of this heavy lifting in form-finding (Tamke and Nicholas, 2013), allowing architects to focus their attention on other design criteria, such as spatial development and programmatic or contextual response. Secondly, flatbed grid systems leave very little room for geometry deviation, heavily restricting the architectural designs flexibility required by professional design practice. To capitalise on the system's benefits, expanded typologies need to be explored in search of more flexible spatial solutions that include appropriate methods for efficient onsite implementation.

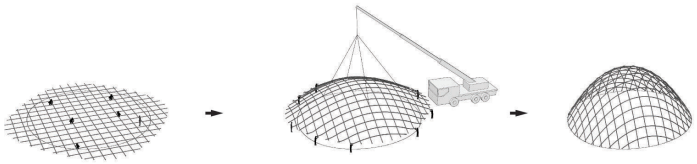

Figure 2. Deployable "flatbed" structures prefabricate an initially flat regular grid with no shear rigidity and elastically deform and brace it into place.

2.2. BAMBOO ARCHITECTURE

The demand for eco-friendly architectural practice is continuously increasing. Sustainable, regionally accessible and renewable materials play an essential role in reducing the overall carbon footprint of global building production, particularly in the world's most rapidly urbanising regions. Bamboo is one of the fastest growing natural construction materials, locally available in most of the developing world (Hidalgo-López, 2003). It is becoming increasingly popular amongst contemporary architects. Certain giant bamboo species can be used in their raw form in construction, grow up to a metre a day, and can be harvested in three-to-five-year cycles, making bamboo far more sustainable than any wood species. Yet, despite its century-old use in vernacular architecture, natural unprocessed bamboo is hardly incorporated as a viable structural material in today's construction.

The plant's unique cellular build-up results in a highly efficient section profile very suitable for use not only in compression or tension, but also when bent. Yet, when used in construction, bamboo is most commonly used in its processed form or as a replacement for traditional wood or steel members (Minke, 2012). Common

bamboo architecture rarely fully absorbs the plant's most unique natural bending properties. Limited research has been done on the applications of bamboo as a structural material in bending-active gridshells from the viewpoint of professional practice. This knowledge gap has only recently begun to be addressed.

David Rockwood's book "Bamboo Gridshell" presents fundamental work on bamboo gridshells using the 'flatbed' method (Rockwood, 2015). Building on work by the Institute for Lightweight Structures (Dunkelberg, 1985), he touches on the design and construction challenges when using bamboo in gridshells produced with the flatbed method in an academic context. Typical 'flatbed' methods turned out to be ill-suited for e.g. traditional Cantonese bamboo craftsmanship, which involves building structures one stick at a time in a lay-up method (see Fig. 3). This traditional way of working was successfully combined with a computation-driven design and implementation methodology in the ZCB Bamboo Pavilion - a thirty-seven-meter spanning temporary pavilion built in Hong Kong in 2015 using this method (Crolla, 2015). This method provides more geometric design freedom, allowing better architectural response to site, context, and programme. However, its challenges are its labour-intensive nature, and the management of errors and deviation associated with manual construction.

This study seeks to advance knowledge towards implementation of a hybrid system that combines benefits of both the flatbed and lay-up approach.

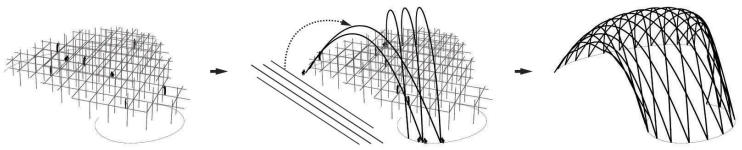

Figure 3. The "lay-up" method additively bends and joins individual members into the final shape onsite. Both types present important opportunities and restrictions.

3. Computational Design System

This study was driven by the development of a series of digital and physical bending-active bamboo gridshells prototypes aimed at iteratively increasing the typology's spatial variety and overall geometric complexity. The bamboo models operated as analogue form-finding computers relying on material properties and physical model constraints. The digital computation models mimicked this approach in McNeel's 3d NURBS modeller Rhinoceros 6® with procedural modelling plugin Grasshopper®, interactive simulation live physics engine Kangaroo®, and parametric structural engineering engine Karamba 3D®. The physics simulation engine abstracts forces at play in the analogue material prototypes by applying corresponding vector forces to discretised curve networks represented by a spring-particle system. Each curved member in this interconnected network aims to maintain its original length and attempts to straighten itself by pushing against its anchor points. Macrolevel behaviour can

then be perceived similar to what is found in physical models and comparable geometries emerge as all virtual forces balance out in equilibrium.

Further data can be derived from these digital setups. Geometry data, such as member curvature, can straightforwardly be derived and structural engineering engines can apply actual material properties and real-world physical loading scenarios to extract structural performance properties like overall displacement and compression or tension forces. Additional building model information can be extracted to facilitate construction: the equidistant parts of the curve network can be relaxed into their respective orthogonal flat grids, while the laid-up members can be individually unrolled into straight lines with their intersection points with other members mapped out onto them. Such notational information becomes crucial in facilitating a straightforward and low-tech construction and/or fabrication of the prototypes.

4. Design Research

4.1. DEMONSTRATOR 1: HYBRID SYSTEM

The design study started with the production of a basic shell structure to test the concept of a hybrid system between both flatbed and lay-up methods. Its design consisted of a half-elipsoid-like shell made from a triangulated bamboo grid. From this grid, 2 of the 3 member directions defined an equidistant bent grid that was "popped" into place using the flatbed method. The third member direction was added using the lay-up method (see Fig. 4).

A 1:6 scale model was built from bamboo splits and metal wire to first test the implementation strategy. Following this, a larger prototype was built at 1:1 scale using 2.5mm diameter round bamboo sticks and plastic zip ties. In both prototypes, the flat, equidistant, rectilinear grid was first pre-assembled and then converted into a domed-shaped surface by pushing the centre point upwards while pulling the edges down and anchoring them onto a ringbeam. For the full scale prototype, the digital design model accounted for properties like material thickness and stick overlaps, and the orientation of the connection ties was predefined to allow for easy hinging in the predicted digitally-simulated direction.

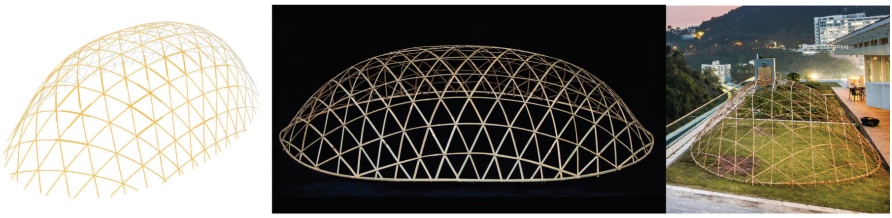

Figure 4. Tectonic study model: digital model, 1:6 scale prototype (1.6m x 1.0m x 0.4m), 1:1 scale prototype (9.6m x 6.2m x 2.8m). .

The final emerged geometry of both prototypes deviated slightly from the digital model as variables like uneven forces during the pop-up process, variations in bamboo diameters, inaccurate joints locations, etc. couldn't be anticipated

precisely in the digital simulation engine. This, however, was allowed for and seen as an inherent part of the system. The overall behaviour and outcome of the demonstrator successfully proved its concept.

4.2. DEMONSTRATOR 2: EXPANDED DESIGN SOLUTION SPACE

A second demonstrator was then developed with as main goal to expand the design solution space associated with the workflow tested in demonstrator 1 and to a bring this beyond the typical "bubble" shaped architecture solutions found in projects like the Mannheim Multihalle (Otto et al., 1975). The approach relied on the precise and strategic inclusion of singularities within the continuous grid to allow for directional changes in the grid and overall geometry (see Fig. 5).

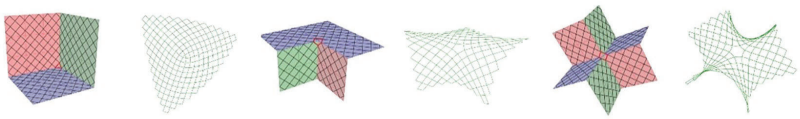

Figure 5. 3, 5, and 6-sided singularity inclusion into a continuous, equidistant, quadrilateral bending-active system.

To this idea, a multi-layered system of different grids was added, recomposing the system's primary structural tectonic layer from three distinct quadrilateral grid layers. The outer layers from this system could then be "peeled-off" from the primary layer to become single-layer grids that define stiffening geometries, like a support column structure or an upward "eye-lid" that could allow light to come down into the structure (see Fig. 6). To allow for this, three pentagonal singularities were inserted into the quadrilateral grid system around the points of deflection. This flexible system expanded the design solution palette of further project designs (see Fig. 7).

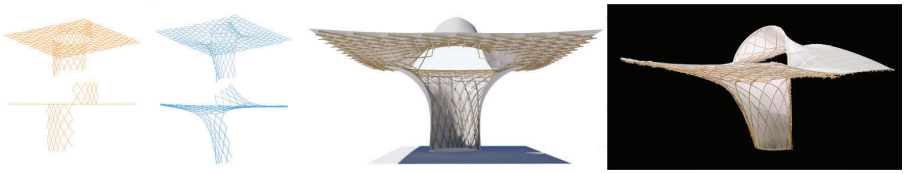

Figure 6. Topology, digital simulation, and 1:20 physical prototype .

In further design developments, an additional layer was added to the central rectangular grid to form a hexagonal grid system. This further expanded design opportunities, as the rectangular nature of the earlier central grid constrained the orientation of columns and openings. A multi-axial symmetric topology instead permits rotating column and eye-lid features in multiple directions, allowing spatial alternatives underneath while simultaneously further reinforcing the structural system. In this hexagonal system, openings were also six-sided and relied on the inclusion of two heptagon singularities around the points of deflection.

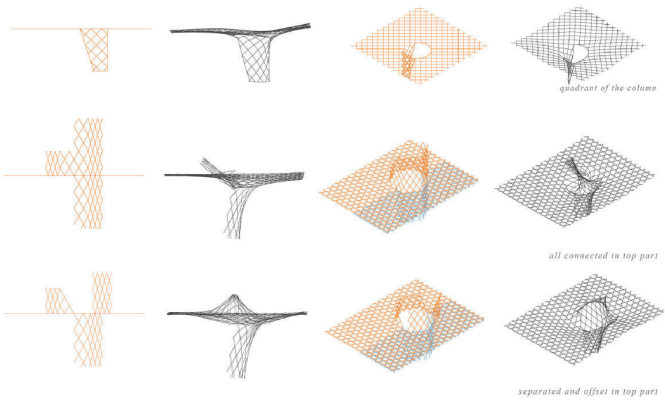

Figure 7. Variations on input grid layering and topology producing various opening & column strategies.

4.3. DEMONSTRATOR 3: DESIGN APPLICATION

Finally, applicability of the overall tectonic system was tested through the conceptual design of an architectural intervention. The selected design brief and programme requested a temporary outdoor music performance space cover with three stages and a central bar area.

The design's primary structural tectonic system consisted of a hexagonal grid that overlapped with the quadrilateral grids of three bent half-columns and one large column placed in the centre (see Fig. 8, 11). The multiple overlaid structural systems were designed and linked together to work in symbiosis, strengthen one another, and secure overall structural integrity. Grid layouts were positioned and combined to allow the generation of a continuous, undulating roof surface that was distorted and pulled down at points of de- and inflection created around the support columns. These features were then link to the architectural programme and specified stage and bar areas.

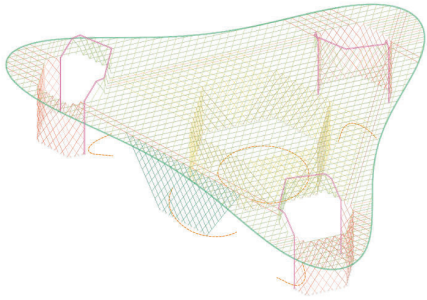

Figure 8. Design topology input diagram.

Figure 9. Simulation and analysis: displacement under gravity, structural utilisation, and curvature.

Once activated, the digital simulation setup allowed for the real-time evaluation of properties like displacement under gravity and loading, material utilisation, and curvature analysis (see Fig. 9). Constructability of the demonstrator was then tested through the production of a large 1:20 scale bamboo study model that was assembled following a process similar to a possible actual large-scale construction sequence (see Fig. 10, 11). Round bamboo sticks with a 2mm diameter were used for their behaviour was deemed comparable to bamboo culms at full-scale. To represent the manual ties found in traditional bamboo architecture, standard zip-ties were used as these allow for a similar level of flexibility and rotation. The first fabrication step involved the production of the several equidistant quadrilateral flat grid layers Three half-columns were bent into shape and joint to the main top grid, to which the skylight openings and central support column were added. An edge ring beam was added to stiffen the perimeter. Then, additional diagonal members were added using the lay-up method to turn the top grid into a hexagonal grid, adding stiffness to the overall shell by locking the quadrilateral grid into place. Overall, the geometry gradually formed and stiffened up as different layers of the structure were joined. Finally, the model was covered in a translucent elastic fabric as a representation of a glassfibre-reinforced membrane cover as found in the ZCB Bamboo Pavilion.

Figure 10. Fabrication process of physical model.

5. Discussion and Evaluation

5.1. ARCHITECTURAL DESIGN EVALUATION

The final design outcome portrayed a dramatic departure from the typical bubble-shaped geometries often associated with bending-active gridshell structures, or from the typically planar geometries found in traditional bamboo architectures that use the straight members as column, beam, or screen elements. Instead, a fluid and elegant continuous surface emerged from the setup in response to all the internal forces finding their equilibrium. The system allowed a spatially unique design response to site and programme, while maintaining the material's high environmental and socio-cultural importance and benefits.

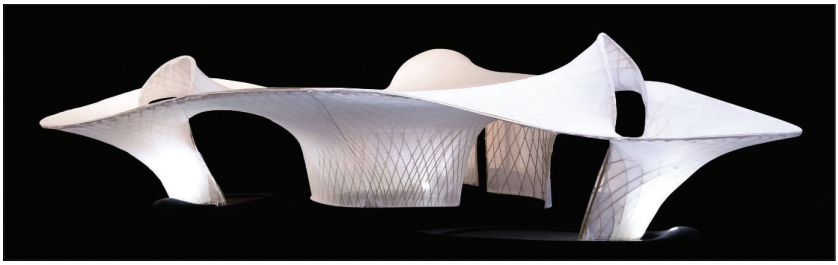

Figure 11. Final 1:20 scale physical prototype (2.4m x 2 m x 0.5m).

5.2. FUTURE CRAFT

Similar to how the ZCB Bamboo Pavilion commenced with a conceptual 1:20 scale bamboo model to inform its novel structural system, here too physical scale models are used as analogue material computers to point towards possible future directions for bamboo architectural construction (Crolla, 2017). While many items and challenges will need to be resolved in far greater detail before the project's actual construction could become possible, a clear and novel pathway is identified.

The demonstrator prototypes showcased that the developed approach can merge complex geometrical form with low-tech construction methods: computational simulation and building information modelling techniques significantly reduced the complexity of construction of the final non-standard building form. Possible future ways to further reduce the construction complexity associated with the developed methodology may involve introduction of new implementation strategies beyond the annotation and labelling systems developed earlier for projects like the ZCB Bamboo Pavilion. Augmented and mixed reality technology provide very interesting opportunities to reduce the complexity of the whole construction process even further, while simultaneously opening doors for continuous information feedback from and into the digital model during construction for further development or analysis. This will be a topic of study for future research projects.

6. Conclusion

This paper demonstrates that the industry has far from reached the limitations of the architectural design and construction solution spaces found in low-tech building contexts without access to advanced computer-controlled fabrication equipment or that employ natural, unprocessed materials like raw bamboo culms. Through the strategic integration of computation and digital simulation in century-old crafts and building traditions, a world of design opportunity can be opened up without substantially increasing construction complexity. In response to the urgent call to find more environmentally sustainable alternatives to our current wasteful methods of construction, this study highlights the vast future potential of bamboo as a construction material.

Figure 12. Physical prototype of bending-active bamboo gridshell.

Acknowledgements

This research was supported by a grant from the Research Grants Council of the Hong Kong Special Administrative Region China: Project Ref No. 14604618, Project Title: Bending-active bamboo shell structures: methods and guidelines for best architectural design practice.

References

Bächer, M.a.x., Burkhardt, B. and Otto, F.: 1978, *IL13 - Mannheim Multihalle. Stuttgart*, Institut für Leichte Flächentragwerke.

Crolla, K.: 2017, Building indeterminacy modelling – the 'ZCB Bamboo Pavilion' as a case study on nonstandard construction from natural materials, *Visualization in Engineering*, **5:15**, -.

Crolla, K.: 2018a, Bending Bamboo Rules: Beyond Century-Old Typologies, *Journal of Architectural Education*, **Volume 72 - Issue 1: A / To Project**, 135-145.

Crolla, K.: 2018b, *Building Simplexity: The*, Ph.D. Thesis, RMIT University.

Dunkelberg, K.: 1985, *IL31 – Bamboo. Bambus als Baustoff Bauen mit pflanzlichen Stäben.*, Stuttgart: Institut für Leichte Flächentragwerke.

Grasshopper3D, : 2019, *Available from www.grasshopper3d.com*, Robert McNeel and associates.

Hidalgo-Lopez, O.: 2003, *Bamboo: The Gift of the God*, Oscar Hidalgo-López.

Kangaroo, : 2017, *Available from www.food4rhino.com/app/kangaroo-physics*, Robert McNeel and associates.

Karamba3D, : 2019, *Available from www.rhino3d.com*, Karamba3D.

Minke, G.: 2012, *Building with Bamboo*, Basel: Birkhauser.

Rhinoceros3D, : 2019, *Available from www.rhino3d.com*, Robert McNeel and associates.

Rockwood, D.: 2015, *Bamboo Gridshells*, New York: Routledge.

Tamke, M. and Nicholas, P.: 2013, Computational Strategies for the Architectural Design of Bending Active Structures, *International Journal of Space Structures*, **28**(3-4), 215-228.

ASYMPTOTIC BUILDING ENVELOPE

Combining the benefits of asymptotic and principal curvature layouts

EIKE SCHLING[1], CHIH-LIN HSU[2] and MUYE MA[3]
[1,3]*The University of Hong Kong, Department of Architecture*
[1]*schling@hku.hk* [3]*muye.ma.1991@gmail.com*
[2]*National Taiwan University of Science and Technology, Department of Architecture*
[2]*D10713010@mail.ntust.edu.tw*

Abstract. This paper presents current research on low-cost, high-performance doubly curved building envelopes that benefit from a curvilinear layout along an isothermal web on minimal surfaces. We investigate the geometric symbiosis of an elastic lamella mullion system that follows the asymptotic curves combined with panelization strategies along the principal curvature lines in order to simplify fabrication and enhance the structural performance. We present a digital and physical setup of a full-scale prototypical asymptotic façade substructure. In collaboration with the construction industry, we evaluate the complete design and construction process, including digital modeling, fabrication planning, computer-aided manufacturing and logistics, prefabrication, and assembly. Both digital and physical prototypes are used to investigate cladding solutions. Our studies are specifically looking at developable-elastic and planar-rigid tessellations, which utilize a principal curvature layout. We conclude by highlighting flat-sheet fabrication, high structural resilience, and assembly time and tolerances, as primary potentials and challenges of this design strategy.

Keywords. Asymptotic Curves; Principal Curvature Line; Double Curvature; Building Envelope; Elastic Construction.

1. Introduction

There is an urgent need for innovative building construction methods that combine high structural efficiency with design freedom and integrate well into the built environment. Great potential lies in double-curved systems, such as gridshells. These form-active structures enable a spatial load transfer via compression and tension, allowing for optimal use of material to create lightweight, transparent building envelopes. Nonetheless, their application in architecture remains rare and specialized, as their free-form geometry creates high costs in the fabrication and assembly of individual and spatially complex parts. To achieve a shell-load-transfer, a consistent double curvature and tangential supports are

PROJECTIONS, Proceedings of the 26th International Conference of the Association for Computer-Aided Architectural Design Research in Asia (CAADRIA) 2021, Volume 1, 341-350.

necessary, which constraints the design and often lacks to integrate with the urban environment.

The research branch of **Architectural Geometry** (Pottmann et al. 2015) has produced fundamental insights on topology optimization for curved structural grids (Bo et al. 2011; Bartoň et al. 2013; Pellis and Pottmann 2018) as well as curved building skins (Liu et al. 2006; Huard et al. 2015; Eversmann et al. 2016) with the goal to simplify fabrication and allow the use of planar or developable building elements.

Figure 1. Asymptotic lamella gridshells. A: The Inside/Out Pavilion at the Technical University in Munich. B: The Intergroup Hotel Canopy in Ingolstadt.

Recent research on elastic gridshells has presented **asymptotic curves** (AC) (following the path of vanishing normal curvature), as beneficial network for lamella construction, as they facilitate simple fabrication from straight and flat elements with repetitive orthogonal nodes (Schling 2018). Asymptotic lamella networks allow for a simple, self-forming erection process, where the weak axis of the lamellas is elastically bent and twisted to form the design shape, while the strong axis creates high resilience against external loads (Schikore et al. 2019). This system thus combines the structural benefits of a gridshell and grillage, offers a versatile design from curved to flat, and allows smooth integration into the urban environment. However, this design method has only been used for free-standing sculptural projects without a cladding solution (Figure 1). The potential for integrated building skins has not been investigated.

Figure 2. Double-curved facade paneling following the principal curvature directions. A: The Strasbourg train station. B: The Eiffel Tower Pavilions. C: The Schubert Club Band Shell.

In opposition to the asymptotic layout, research on doubly curved building skins has promoted **principal curvature lines** (PCL) (following the max/min normal curvature), which encode the path of vanishing geodesic torsion and thus allow rectangular, planar-quad (PQ) and developable panels (Pottmann et al. 2008; Pottmann et al. 2010; Tang et al. 2016). Such methods have been applied in the

construction of building envelopes (Figure 2), f.e. looking at cylindrical glass panels (Strasbourg train station, Eiffel Tower Pavilion) or planar quadrilateral panels (The Schuber Club Band Shell).

This paper presents a novel construction system for doubly curved curtain wall systems, which combines a structural layout along the AC with a cladding layout along the PCL. Both networks are combined in an **isothermal web on a minimal surface** (Pottmann et al. 2007, p. 648) bisecting each other and thus creating reciprocal benefits for structural bracing and façade connections. We first present our digital design method for a curtain wall corner module. We introduce a novel construction strategy and describe the manufacturing, prefabrication, assembly and erection process, highlighting the benefits and challenges of elastic, asymptotic construction. Finally, we present three cladding solutions driven by the principal curvature direction.

2. Digital Method

Both ACs and PCLs create quadrilateral networks, but never align with each other. There is, however, a geometric sweet spot in the form of minimal surfaces in which both networks form almost quadratic cells and can be defined with the same intersection points. Such a layout is called an **isothermal web**. (Due to the tight paper-restriction of 10 pages max, the computational method to model minimal surfaces, ACs and PCLS in an isothermal web was omitted from this paper. More details can be found in the dissertation of Eike Schling (Schling 2018)).

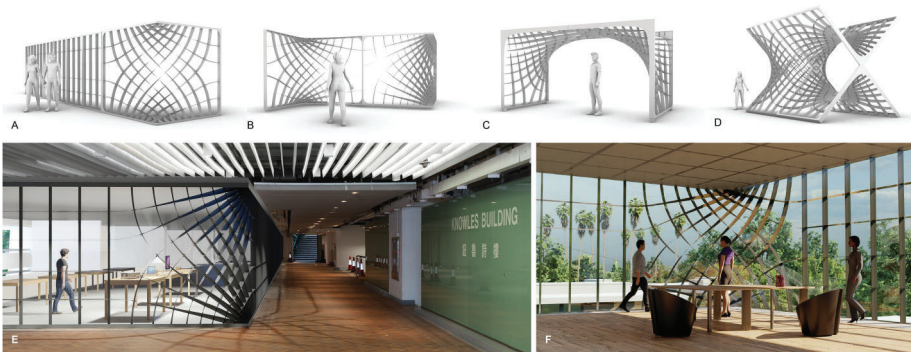

Figure 3. Asymptotic Scherk module. The corner module allows smooth integration into existing mullion and transom systems (A), and may be combined to create modular building envelopes (B and C) or even periodic continuous network typologies (D). We anticipate integrating this construction technology into the built environment to allow a smooth transition from a standard, curtain-wall systems into a diagonal, doubly curved layout.

Modular design. The Scherk singly periodic cell was used as basis for our façade prototype (Figure 5), as it can be positioned as a corner module into any rectangular building type (A), but also be combined to create multiple architectural scenarios, in which modules tie smoothly into one another (B and C) or even create a periodic minimal surface network (D). The façade module exhibits a

smooth transition from a straight and regular transom-and-mullion-typology to the distinctive, diagonal, and twisted asymptotic network. We aim to take advantage of this transition to integrate a curved expressive corner module in a standard curtain wall system (E, F).

3. Asymptotic Substructure

The constructive development of the substructure builds upon knowledge from previous projects (Figure 1), looking at double-lamella bolted construction (A) (Schling et al. 2018), and single lamella welded construction (B) (Schikore et al. 2020). Both systems work with a slotted connection to interlace two families of lamellas within one level. This strategy allows for a simple assembly of the lamellas as flat segments on the ground and a subsequent deformation into the designed doubly curved shape. Once the final geometry is generated, the joints are fixed in their final 90-degree-position. There is room for improvement: Handling the single strips of steel is precarious, as the slots create weak spots, which are prone to develop kinks during assembly. Once the structure is completed, the lamellas are weakest between two joints in their lateral direction. Here, we can observe a buckling behavior along the lines of Euler Case 2 (hinged on top and bottom), where the slotted joints act as hinges, resulting in a buckling length similar to the joint-to-joint distance ($s_k = h$). This behavior has a direct effect on the buckling stress and deflections under compression.

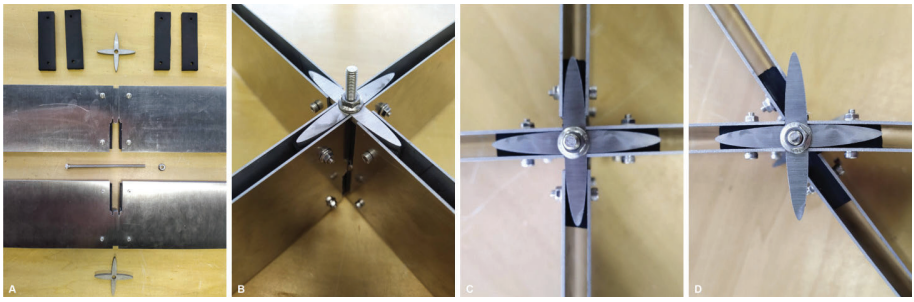

Figure 4. Composite joint system from two 1.5mm stainless steel strips with 8mm rubber inlays (A). The joints are designed to allow up to +-30° rotation freedom during assembly (D) and lock at 90 degrees once the rounded star-washers are fixed (B, C).

3.1. JOINT SYSTEM

The construction development was focused on creating more resilient lamellas for the assembly and the load-bearing structure. The novel joint system is created from two stainless steel strips of 1.5 mm (and 100 mm height) and rubber interlays of 8 mm, and is prefabricated into composite elements with 11 mm thickness (Figure 8). The rubber reinforces the slotted steel to prevent kinks and allow for a continuous elastic behaviour. Within the joints, the rubber-and-steel-composite acts like cartilage-and-bone-system, in which the rubber is a flexible mediator between two intersecting lamellas and allows for up to +- 30° rotation of the scissor

joints (Figure 8, D). This is necessary to facilitate the transformation of the lamella grid from flat to curved geometry. Once the final shape is created, the star-shaped washers are fastened to enforce the 90° angle, while the rounded sides of the stars still allow for continuity in curvature (Figure 8, C). This reinforcement through rubber and star-washer aims to create a rigid connection, thus shifting the buckling mode towards Euler Case 4 (clamped on top and bottom) and reducing the buckling length to 0.5 ($s_k = 0.5h$).

3.2. PLANNING, FABRICATION AND LOGISTICS

All strips are fabricated straight and flat with a standardized joint detail. The only information needed from the 3D model is the distances between joints and the chamfer-angles at the end of each strip to fit the outer steel frame. Their geodesic curvature creates a slight variation in length between the inner and outer strip within one lamella (Figure 9). Therefore, the joint distances are measured individually for each strips. To produce the 2D drawings, we simply draw straight parallel strips, mark the intersections, copy the standardized slot-detail to each intersection marker, and finally add the chamfered ends. The 3D lamellas are modeled and unrolled as control geometry.

The double symmetric network of our design has only five different lamella geometries. There are two families of lamellas, one on the bottom, with slots pointing up, and one on top, with slots pointing down, and each lamella consists of two metal strips. This creates a total number of 20 individual strips, each produced twice. They are labelled with a 3-digit-system by number (1-5), family (top or bottom) and position within the lamella (left or right). Laser-cutting and shipping benefit greatly from the straight geometry of lamellas, creating almost no offcuts of the rectangular stainless steel sheet material and minimal packing size (Figure 10).

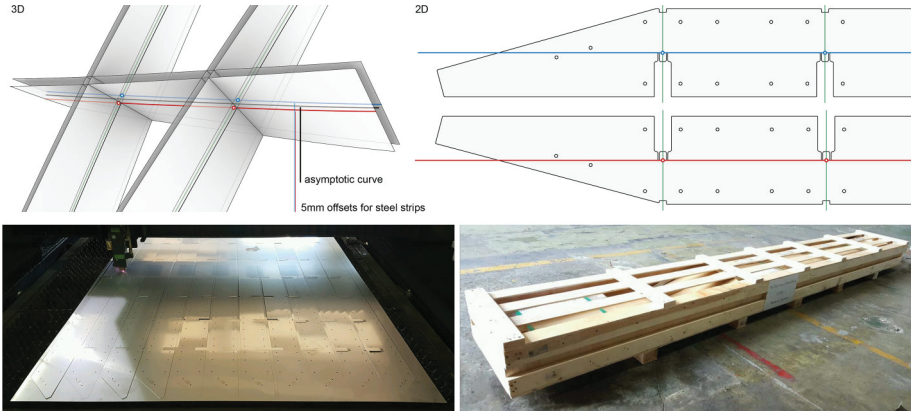

Figure 5. Fabrication. Top: The joint-to-joint distance and chamfered edges are measured individually for each metal strip. Bottom: The straight steel lamellas can be cut from sheet metal with virtually no waste material and packed and shipped efficiently.

3.3. CONSTRUCTION

The construction process consists of prefabrication of lamellas, assembly of the grid, deformation of the grid, fastening of the joints, and finally, fixture within the rigid frame.

The composite-lamellas are **prefabricated** by hand in the workshop (Figure 11, A, B). Two rubber pieces are placed left and right of each slot-joint and fastened with two rivets each. This process embeds the geodesic curvature into the lamellas and makes them resilient to kinks. The grid of lamellas is **assembled** flat on the ground (C, D). The star-washers are not yet fastened, as the joints need to be able to accommodate up to 30° rotation. The assembled grid is placed on a cross-shaped frame and **elastically formed** into its curved design shape (E-H) without the need for form-work. The final geometry is confirmed simply by measuring the diagonal distance at the top and bottom. This deformation adds geodesic torsion within the lamellas. Once the final geometry is completed, the **star-washers are fastened** to fix the 90° angle and align the lamellas into one level. This process was most challenging, as lamellas and stars had to be aligned with some force, and the bolts had to overcome high friction in the joints. Finally, the curved grid is bolted to the **rigid steel frame** (K-L), which acts as a supporting beam. The final module weighs approximately 300 kg, including the 6 mm steel frame. It is used in the following research as substructure for different panelization strategies.

Figure 6. A-D: Prefabrication. E-H: Elastic formation. I-L: Completed module.

4. Double Curved Envelope Strategies

The digital and physical substructure was used to investigate multiple cladding options (Figure 12). In this section, we will focus on triangulated, planar-quad, and developable strips, as they take geometrical advantage of the isothermal web.

4.1. TRIANGULATED FAÇADE

The triangulated typology visualizes clearly the possible reading of layouts (Figure 13). It can be created with horizontal (A) or vertical (B) folds resulting in regular joints, supporting six adjacent glass panels. Such panelizations read as discrete strips similar to the developable façade (4.3). An alternative approach is to alternate horizontal and vertical folds (C), creating alternating joints with either 4 or 8 glass panels. Here, the effect of our isothermal network becomes visible, as the clusters of 4 triangles naturally lie within one plane and read like a planar quad. We propose a simple point bracket for frameless glazing with silicon joints (D).

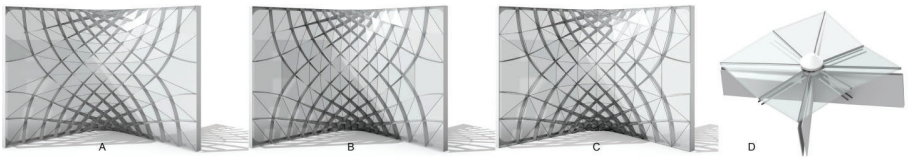

Figure 7. Three possible triangular layouts, along the horizontal (A), vertical (B) or alternating (C) directions.

4.2. PLANAR QUADS

The principal curvature directions encode the path of vanishing geodesic torsion. A quadrilateral mesh along these directions will consist of planar faces (Figure 14). The isothermic network creates nearly square panels which allows efficient fabrication (minimal offcuts) and a homogenous visual pattern. The panels are positioned diagonally to the asymptotic layout (A). They are fixed at four joints and cover a fifth. As the asymptotic lamellas exhibit no normal curvature, their joints are planar so that the x-shaped lamella intersection neatly nestles with the panel above. We fabricated a proof-of-concept for the prototype using quasi-square acrylic glass panels (B). An alternative fixing system was developed by Marilies Wedl (Wedl 2020) at the Technical University in Vienna. Wedl proposes a four point bracket at every alternate joint on a laminated timber structure (C). Her 1:1 prototypical model beautifully illustrates the subtle anticlastic folds between four planar glass panels, following the principal curvatures (D).

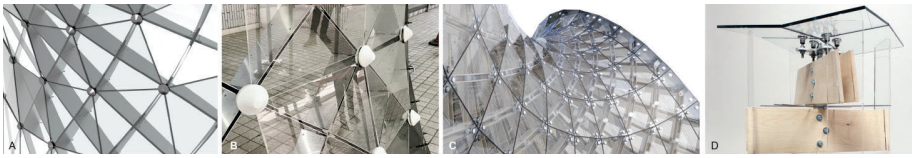

Figure 8. Planar-quad glazing along the principal curvature directions in steel (A,B) and timber (B,C) (Wedl 2020).

4.3. DEVELOPABLE STRIPS

Tangential developable strips are nothing but an infinitely dense set of planar quads (Liu et al. 2006) and may be designed along one family of PC-lines. Such a semi-discrete panelization beautifully translates the design language of elastic strip construction into the building skin (Figure 15). In this case, the panels are not planar but create a singly curved geometry that is either convex (A) (bending away from the substructure) or concave (B) (bending towards the substructure). For a concave layout, an additional offset at each connection joint is needed to prevent the acrylic glass from colliding with the diagonal lamellas. We propose aluminum strips to fix the panels and offer structural bracing through triangulation (D). We fabricated a proof-of-concept (C) for a concave layout, creating a vertical cover.

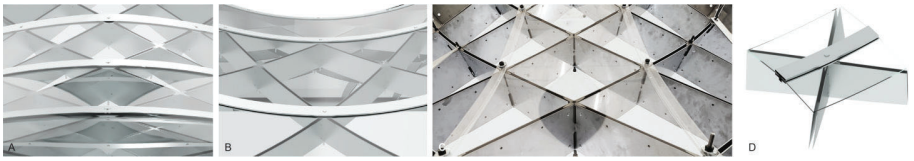

Figure 9. Developable strip facade along the principal curvature directions.

The physical testing of the cladding strategies revealed tolerances of up to 10 mm between the digital model and the physical prototype. The panels were remeasured and fitted individually.

5. Conclusion

This paper presents a design method for low-cost, high-performance, doubly curved building envelopes. The method relies on the geometric sweet-spot of isothermal webs on minimal surfaces, creating a quasi-square layout of both asymptotic curves and principal curvature lines bisecting each other at 45°. We design a versatile cubic 2.4 m prototype that can be integrated into existing buildings to create smooth transitions from curved to a flat curtain wall system. The asymptotic grid is used as the steel lamella substructure. This allows for a simple fabrication of slender, flat and straight steel strips, producing minimal offcuts. We prefabricate single-curved, composite lamellas using rubber inlays to improve the elastic and structural performance during assembly and load-bearing state. After flat assembly, the lamella grid is deformed into double curvature and fixed to the rigid rectangular steel frame. The slender lamellas enable an elastic erection while maintaining high resilience against normal loads, such as wind, typical for curtain walls. Finally, both digital and physical models are used to develop cladding strategies along the principal curvature lines, diagonal to the asymptotic substructure. We give an overview of options and present a triangulated, planar square and elastic developable system, comparing their functional and aesthetic quality, offsets and fixtures.

5.1. INSIGHTS

The isothermal design combines simple fabrication and assembly, and high structural resilience for the asymptotic substructure, with geometric benefits, namely planar-quad and developable layouts, for the cladding. The cubic prototype presented here is a first attempt to digitally and physically combine these qualities and test the fabrication workflow for both substructure and cladding. The main challenges of this technique are the tolerance and friction which arise from an elastic construction. Tolerances specifically need to be kept at a minimum to allow for accurate high quality cladding.

5.2. FUTURE RESEARCH

The computational tool to draw asymptotic and principal curvature lines are well developed. The isothermal web, however, is created individually by hand. An automated process would speed up the design process immensely. The fabrication and assembly of the steel substructure were carried out over the course of approx. 8 hours. Optimizing the details of the slot to avoid friction of rubber and steel might speed up the assembly and fixing process. Furthermore, we anticipate testing other materials, like GRP and aluminum, to lower the total weight of the façade module. The strategies for cladding are yet in an experimental design stage. Here, a further investigation of material, scale, tolerances, maintenance and functionality in weather conditions is of utter importance.

Acknowledgements

Our gratitude goes to GOMORE Building Envelope Technologies, who generously sponsored the material, fabrication and shipment of the prototype substructure. We specifically thank Hou-Yang Chen, who completed the digital fabrication planning and logistics. We also want to express our thanks to Prof. Shen Guan Shih and Tiago Costa from the Architectural Department of the National Taiwan University of Science and Technology for their collaboration and inspiration. We would like to thank all students involved in the prefabrication and assembly of the Asymptotic Building Envelope prototype, foremost our Research Assistants Nuozi Chen, Wesley She and Fai Lam Chung. The investigations and visualizations of cladding strategies were conducted by Sherene Ng (Triangulated glass façade), Vivian Wang (Planar quadrilateral glass panels) and Fai Lam Chung (Developable acrylic strips). We are grateful for their creativity, diligence and commitment.

References

Barthel, R. 2005, Natural Forms - Architectural Forms, *in* W. Nerdinger (ed.), *Frei Otto - Complete Works. Leightweight construction - natural design*, Birkhäuser, Basel, 16–30.

Bartoň, M., Shi, L., Kilian, M., Wallner, J. and Pottmann, H.: 2013, Circular Arc Snakes and Kinematic Surface Generation, *Computer Graphics Forum*, **32**(2pt1), 1-10.

Bauer, A.M. and Längst, P.: 2019, "Kiwi3d! Meshfree, Isogeometric FE Analysis integrated in CAD" . Available from Chair of Structural Analysis, Technical University Munich<https://www.kiwi3d.com/> (accessed 27.05.2020).

Bo, P., Pottmann, H., Kilian, M., Wang, W. and Wallner, J.: 2011, Circular arc structures, *ACM Transactions on Graphics*, **30 (101)**(DOI: 10.1145/1964921.1964996), 1-11.

Eversmann, P., Schling, E., Ihde, A. and Louter, C.: 2016, Low Cost Double Curvature. Geometrical and Structural Potentials of Rectangular, Cold-bent Glass Construction, *K. Kawaguchi, M. Ohsaki, T. Takeuchi (Eds.): IASS Annual Symposium 2016*, Tokyo.

Huard, M., Eigensatz, M. and Bompas, P.: 2015, Planar Panelization with Extreme Repetition, *Philippe Block, Jan Knippers, Niloy J. Mitra, Wenping Wang (Eds.): Advances in Architectural Geometry 2014*, London, 259–279.

Kiendl, J.: 2011, *Isogeometric Analysis and Shape Optimal Design of Shell Structures*, Ph.D. Thesis, Chair of Structural Analysis, Technical University Munich.

Liu, Y., Pottmann, H., Wallner, J., Yang, Y.L. and Wang, W.: 2006, Geometric modeling with conical meshes and developable surfaces, *ACM Transactions on Graphics*, **25 (3)**(DOI: 10.1145/1141911.1141941), 681.

Oberbichler, T.: 2019, "Bowerbird. Plug-In for Grasshopper" . Available from Chair of Structural Analysis, Technical University Munich<https://github.com/oberbichler/Bowerbird> (accessed 19.11.2020).

Pellis, D. and Pottmann, H.: 2018, Aligning principal stress and curvature directions, *Lars Hesselgren, Karl-Gunnar Olsson, Axel Kilian, Samar Malek, Olga Sorkine-Hornung, Chris Williams (Eds.): Advances in Architectural Geometry 2018*, Gothenburg, 34-53.

Pottmann, H., Asperl, A., Hofer, M. and Kilian, A.: 2007, *Architectural Geometry*, Springer & Bentley Institute Press, ISBN: 978-3-211-99765-9.

Pottmann, H., Eigensatz, M., Vaxman, A. and Wallner, J.: 2015, Architectural Geometry, *Computers and Graphics*, **47**(DOI: 10.1016/j.cag.2014.11.002), 145-164.

Pottmann, H., Huang, Q., Deng, B., Schiftner, A., Kilian, M., Leonidas, G. and Wallner, J.: 2010, Geodesic Patterns, *ACM Trans. Graphics*, **29 (4)**(DOI: 10.1145/1778765.1778780), 1-10.

Pottmann, H., Schiftner, A., Bo, P., Schmiedhofer, H., Wang, W., Baldassini, N. and Wallner, J.: 2008, Freeform surfaces from single curved panels, *ACM Transactions on Graphics*, **27(76)**(DOI: 10.1145/1360612.1360675), 1-10.

Schikore, J., Bauer, A.M., Barthel, R. and Bletzinger, K.U.: 2019, Large torsion on elastic lamella grid structures, *Carlos Lázaro, K.-U. Bletzinger, Eugenio Oñate (Eds.): FORM and FORCE 2019*, Barcelona, 807-814.

Schikore, J., Schling, E., Bauer, A.M. and Oberbichler, T.: 2020, Kinetics and Design of Semi-Compliant Grid Mechanisms, *Olivier Baverel, Helmut Pottmann, Caitlin Mueller, Tomohiro Tachi (Eds.): Advances in Architectural Geometry 2020*, Paris, (to be published).

Schling, E.: 2018, *Repetitive Structures. Design and Construction of Curved Support Structures with Repetitive Parameters*, Ph.D. Thesis, Chair of Structural Design, Technical University of Munich (DOI: 10.14459/2018md1449869).

Schling, E., Hitrec, D. and Barthel, R.: 2017, Designing Grid Structures using Asymptotic Curve Networks, *Klaas de Rycke, Christoph Gengnagel, Olivier Baverel, Jane Burry, Caitlin Mueller, Minh Man Nguyen et al. (Eds.): Design Modelling Symposium 2017*, Paris, 125-140.

Tang, C., Kilian, M., Bo, P., Wallner, J. and Pottmann, H.: 2016, Analysis and design of curved support structures, *Sigrid Adriaenssens, Fabio Gramazio, Matthias Kohler, Achim Menges, Mark Pauly (Eds.): Advances in Architectural Geometry 2016*, Zurich, 8-23.

Wedl, M.: 2020, *Ein Beitrag zur Erstellung einer Gitterschale unter der Verwendung asymptotischer Kurven auf Minimalflächen*, Master's Thesis, Technischen Universität Wien, Vienna. Fakultät für Architektur und Raumplanung.

THE INFINITE LINE ACTIVE BENDING PAVILION: CULTURE, CRAFT AND COMPUTATION

VERNELLE A. A. NOEL[1], NILOOFAR NIKOOKAR[2], JAMIESON PYE[3], PHUONG 'KAREN' TRAN[4] and SARA LAUDEMAN[5]
[1]*University of Florida*
[1]*vernelle.noel@ufl.edu*
[2]*Carnegie Mellon University*
[2]*nnikooka@andrew.cmu.edu*
[3,4,5]*Georgia Institute of Technology*
[3,4,5]*{jpye7|ptran44|slaudeman3}@gatech.edu*

Abstract. Active bending projects today employ highly specialized, complex computer software and machines for design, simulation, and materialization. At times, these projects lack a sensitivity to cultures limited in high-tech infrastructures but rich in low-tech knowledges. Situated Computations is an approach to computational design that grounds it in the social world by acknowledging historical, cultural, and material contexts of design and making, as well as the social and political structures that drive them. In this article, we ask, how can a Situated Computations approach to contemporary active bending broaden the design space and uplift low-tech cultural practices? To answer this question, we design and build "The Infinite Line"- an active bending pavilion that draws on the history, material practices, and knowledges in design in the Trinidad Carnival - for the 2019 International Association for Shell and Spatial Structures (IASS) exhibition in Barcelona, Spain. We conclude that Situated Computations provide an opportunity to integrate local knowledges, histories, design practices, and material behaviors as drivers in active bending approaches, so that structure, material practices, and cultural settings are considered concurrently.

Keywords. Situated Computations; craft; wire-bending; active bending structures; Trinidad Carnival; dancing sculptures.

1. Introduction

Active bending structures are an approach to creating three-dimensional (3D) curved geometry and forms from two-dimensional (2D) planar or linear elements using stresses and elastic deformations in the materials (Lienhard, Alpermann, et al., 2013; Nicholas and Tamke, 2013). The close relationship between geometry, material properties, and forces in these structures make predictive modeling very complicated. Vernacular structures based on active bending usually take

PROJECTIONS, Proceedings of the 26th International Conference of the Association for Computer-Aided Architectural Design Research in Asia (CAADRIA) 2021, Volume 1, 351-360.

a behavior-based approach that is intuitive (Lienhard, 2014). Because of their complexity, most active bending projects today employ highly technical, complex computer software and machines for design, simulation, and materialization. For example, the ICD/ITKE pavilion made from thin birch plywood strips used finite element method (FEM) simulations and robotic manufacturing; the AA Hybgrid project used special software built for design and analysis of fiber-composite strips; the twisted-arch plywood structure used special algorithms, FEM analyses, and CNC precision milling (Laccone et al., 2020); and Isoropia which used Isogeometric Analysis (IGA), a physics solver, and CNC knitting (Tamke et al. 2019). Some projects more sensitive to local material practices and skills include the ZCB and TOROO bamboo pavilions that use physical prototyping and hand-tied knots (Crolla, 2017, 2020), and an installation "Timespace," that employed mesh optimization, physics simulation and weaving of polycarbonate pipes for construction (Huang, Wu and Huang, 2017). Software subscriptions, computational power, technical knowledge, and training required for engagement with contemporary active bending projects can limit the design space and who participates.

1.1. SITUATED COMPUTATIONS

Situated Computations is an approach to computational design that grounds it in the social world by acknowledging the historical, cultural, and material contexts of designing and making (Noel, 2020). The approach asks that we not remain ignorant of the social and political structures that drive design. It facilitates an understanding of cultures, people, and traditions; creates design spaces for interactions between different people and knowledges; and amplifies the stories, histories, and innovations of groups and cultures often left out of computational discourses. Our active bending project is framed within a Situated Computations approach with "The Infinite Line" pavilion demonstrating what this might mean for research and practice in active bending structures.

1.2. THE TRINIDAD CARNIVAL

Carnival in Trinidad and Tobago was borne in the 1780s when French planters introduced it to Trinidad. Enslavement of Africans started in Trinidad in the 17th century, but after its abolishment in 1834, the formerly enslaved reinvented the Carnival, making it a space to release psychological tensions from oppression and violence at the hands of white systems of control (Liverpool, 1998). In this reinvented Carnival, people showcased their creativity by using easily accessible materials to make elaborate costuming.

1.3. DESIGN AND MAKING IN CARNIVAL IN TRINIDAD & TOBAGO

People and communities continue to create dynamic dancing sculptures for Carnival with easily accessible materials for performance in public squares and streets during parades and design competitions (Noel, 2017). Skills and embodied knowledges from art, crafts, dance, and design make these artifacts a reality. One integral craft is wire-bending, in which wire, fiberglass rods, rattan, and other

linear elements are bent and shaped to create 2D and 3D structures (Noel, 2015). Wire-bending inscribes a milieu of interactions between community, senses, and the moving body while designing and making with static and dynamic linear materials for concurrent expressions of each in three-dimensional space (Noel, 2020). Most tools and machines used are manual and include hacksaws, hammers, adhesive tapes, pliers, and drills (Fig. 1). Fiberglass rods are used in the making of elaborate and dynamic costuming. In 1984, carnival designer and artist Peter Minshall used fiberglass rods for an active bending approach to dancing sculptures by inserting them into the hems of t-shirts, creating textile hybrid costuming (Fig. 1). He continued this design method for the Barcelona and Atlanta Olympic opening ceremonies in 1992 and 1996, respectively.

Figure 1. Tools used in Carnival and dancing mobile by Minshall in 1984.

In this study, we employ Situated Computations to design and construct a lightweight structure built on the culture of Carnival for an innovative structures exhibition at IASS 2019 in Barcelona, Spain. The design brief called for an experimental installation of max. dimensions 4x4x4 meters, resting on the ground with all materials fitting into max. six (imaginary) boxes of max. dimensions 1x0.75x0.65 m per box, each box weighing max. 32 kg (70 lbs.) for transportation by airplane. In this paper, we investigate how a Situated Computations approach to active bending might amplify rich social and cultural practices of people with limited access to high-tech infrastructures. We design, build and exhibit an active bending pavilion that acknowledges and amplifies the historical, cultural, and material contexts of design and making in the Trinidad Carnival.

2. Situated Computations Framework for Active Bending Structures

Our framework for a Situated Computations approach that grounds active bending structures in their context is shown in Figure 2. It begins with understanding traditional and contemporary knowledges in a setting, the materials available, and cultural design and making practices in which communities engage. Based on this understanding, we can develop design interventions that connect local material practices with active bending and culture. After design, simulation is required to get feedback on the geometry, structural behavior, and material properties. In regions with limited, highly technological resources, simulation might involve physical prototyping for feedback that informs structural decisions. In areas with high levels of technological infrastructures and resources, structural simulation software and custom algorithms can be used and developed by those with expert

knowledge. Materialization of active bending structures in a low-tech setting might involve manual and hand-powered fabrication and assembly methods. In contrast, a high-tech community might apply advanced fabrication techniques and robotics.

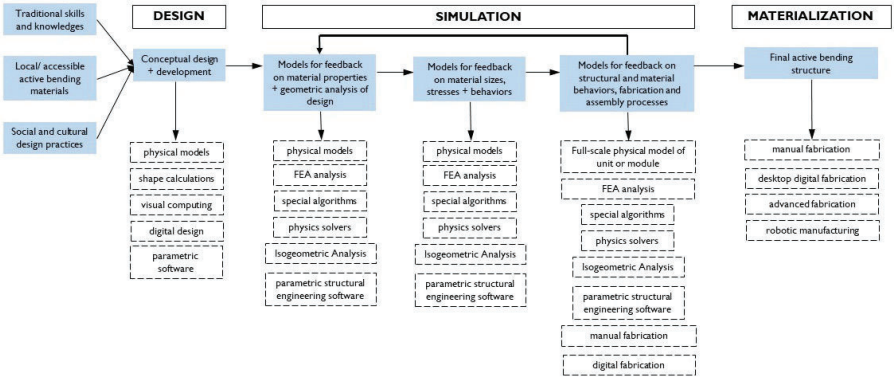

Figure 2. Situated Computations Framework for Active Bending Structures.

3. Materials and Methods

Our motivations in this project were: (1) employing knowledges in the Trinidad Carnival context; (2) creating an active bending structure with limited high-tech infrastructures; (3) using materials, tools, and techniques in wire-bending for fabrication; and (4) designing for easy assembly, disassembly, transportation, and reuse. The Infinite Line's design emerged from an analysis of a previous pavilion built by our team (Noel, 2019). The project was made using a CNC wire-bender, hand tools, wire, fiberglass rods, and adhesive tapes - industrial strapping tape and industrial duct tape. Based on that study, we took an active bending approach to this proposal due to the potential advantages of material behavior, packaging, curved geometries, structural stability, and transport. We used fiberglass rods because of their local accessibility, availability, affordability, their ties to costuming in the Trinidad Carnival, and their use in wire-bending.

3.1. PHYSICAL FORM-FINDING

3.1.1. Conceptual Design model

Since limited access to complex computer software and machines would inform our approach, physical modeling was our primary method for design, simulating appearance, material behaviors, fabrication and assembly processes, and failures. We took a geometry-based approach by creating and manipulating circular geometries from clear polycarbonate rods. We used the computational design method shape grammars to calculate design possibilities visually (Knight, 1991). Four of the 12 design studies are shown in Figure 3.

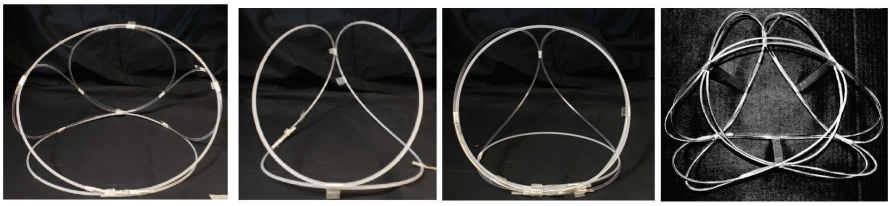

Figure 3. Conceptual designs and form-finding. (L-R): 3A, 3B, 3C, 3D.

3.2. PHYSICAL MODELS #2 (1/6TH SCALE)

Based on our conceptual studies, we explored two designs at 1/6th scale and made from 1/8" diam. fiberglass rods to observe how our ideas behaved at larger scales (Fig. 5A). After analyzing their design, behaviors, and geometries, we proceeded with the design in Figure 3D, which comprised three modules that we called "pringles" (Fig. 4). In the design, each module is rotated 120 degrees from each other. This design was selected for its modularity, geometric simplicity, and coiling possibilities for packaging and transportation.

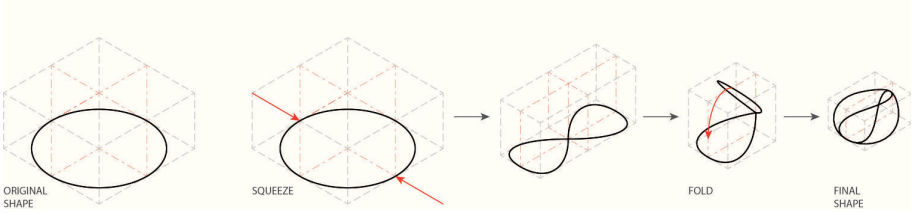

Figure 4. Steps for construction of the 'pringle' module.

3.3. PHYSICAL MODELS #3 AND #4 (1/4TH SCALE)

We built our third model at 1/4 scale with two 1/4" diam. fiberglass rods bundled together. At this scale, the rods' stresses were very high, requiring extra force to control them during taping, bending, and compressing. The high flexural stiffness caused rods to buckle and crack. After analyzing its material failures, stiffness, and assembly, we built a fourth model of same scale. This fourth model was made using bundles of two 3/16" diam. fiberglass rods, and resulted in a less stressed, easier to assemble model (Fig. 5C). After feedback from the models on sectional diameter, we built one pringle module at full-scale.

3.4. DIGITAL MODELS AND SIMULATION

While building physical models, we also employed digital modeling and simulation methods with Rhino 3D and the Kangaroo2 plugin. Minshall's textile hybrid costumes and our models were reminiscent of minimal surface geometries. Our digital models leveraged this similarity and were constructed from a series of rods and surfaces contracted together to approximate the physical model. Using

the Kangaroo2 plugin, we employed a minimal surface method for modeling and applied a pre-tensioned mesh to discretized rods pulling them into shapes approximating the physical prototypes, and based on the internal tension of the rods and the minimal surface bounds of the mesh. Three of these forms were intersected to match the physical model. Due to complexities involved in digitally modeling these structures, we decided to construct ours so that: (a) each pringle was modeled independently such that there was no structural relationship between the three; (b) bundled rods behaved like a single rod of the same diameter, and (c) the flexural modulus was constant at 6.0x10ˆ6 psi. Construction of the digital model in Kangaroo2 mimics the physical method with rods independently folded, assembled, then joined. The second and third decisions helped simplify the modeling process. However, by modeling bundled rods as a single rod, we exclude potential internal friction forces within bundled rods.

3.5. PHYSICAL MODEL #5 (FULL-SCALE SINGLE MODULE)

We bundled four 10-foot long 1/4” diam. rods for a one-inch sectional diameter to build our full-scale pringle module. This allowed an understanding of material and geometric behavior and stresses and our fabrication and assembly strategies (Fig. 5D).

Figure 5. Figure 5. (L-R) 5A: 1/6 scale model (left); 5B: 1/4 scale model from 2 No.1/4“ diam. rods; 5C: 1/4 scale model from 2 No.3/16” diam. rods; and 5D: full-scale ‘pringle’ model (right).

4. Fabrication and Assembly

One 10 ft. rod was placed beside another with both ends at each other’s midpoint. This process of placing and securing one rod beside the other to form a pair was continued until the entire length measured 80 ft. After two sets of paired 80’ bundles are fabricated, both pairs are bundled together to create an 80’ long bundle of four rods. We used 1/2” wide industrial strapping tape and 2” wide industrial duct tape for bundling, since they performed best during our tensile experiments (Noel, 2019). Industrial strapping tape was wrapped 12”-16” apart, and industrial duct tape at 5’-0” apart. After fabricating the four-rod bundle, we built the circle and followed the steps shown in Figure 4. To reduce sliding and slip between rods, tape is first wrapped around one rod with some excess, then adhered to itself before wrapping it around the adjoining rod and securing both. This strategy was employed for all bundles, i.e., bundles of two and four, using both the strapping and the duct tape.

5. Full-scale pavilion

After fabricating and assembling the three full-scale pringle modules, and building the pavilion, we observed the structure sagging under its own dead load. To counter this, we created three structural members made from fiberglass rods. Each was a circle of circumference of 25 ft. built from two 1/4" diam. rods. These circles were secured with industrial strapping tape at the tops and bottoms of the pavilion at three locations 120 degrees apart. We then squeezed these 8' diam. circles to apply upward forces to the structure and further stabilize it (Fig. 6). Only a partial understanding of the effects of dead loads was possible with one module of the design. A fuller understanding through physical modeling could only be achieved after building the entire pavilion.

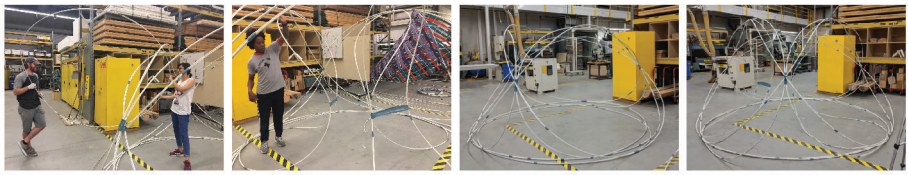

Figure 6. Installation of tensile struts to resist dead loads.

6. Results

Circular geometry allows us to leverage the flexural properties of the fiberglass rods, linking the physical form to the material properties, permitting experimental determination of 3D forms, which in turn inform the developing digital model. We used a 32" diam. base drum case to pack and transport our structure and additional rods should replacements be necessary (Fig. 7). After fabricating, installing, and testing our pavilion in Atlanta, GA., we de-installed, disassembled, and packaged it for our flight to Barcelona, Spain (Fig. 7B). The entire process - unpacking, bundling pairs, assembly, and erection in Spain - took approximately three hours, with the whole pavilion weighing less than 30 kg (66 lbs.). This mode of travel supports the mobile, temporary nature of Carnival with quick construction, disassembly, exhibition, and transportation of its artifacts.

Figure 7. 7A: Coiled pavilion structure in drum case (left); 7B: Drum case at the airport (middle); and 7C: Pavilion in Barcelona, Spain (right).

Communities come together to make artifacts from locally accessible materials for Carnival. By developing this active bending pavilion with a Situated Computations approach, people can make active bending structures as architecture and costuming for the Carnival. Second, children, adults, crafts persons, and other professions can come together to design and fabricate these structures that include traditional craft and costuming skills embedded in the Carnival. Third, through these structures, communities can showcase their creativity as they have done since the 1830s. Fourth, the ability to repurpose and create multiple design options using modular units ties back to the histories and innovations of people who use ordinary materials in extraordinary, creative ways. Figure 8 shows a rendering of the pavilion during the Carnival celebrations.

Figure 8. Render of Infinite Line pavilion during Carnival in Trinidad & Tobago.

7. Analysis & Discussion

We investigated how a Situated Computations approach can broaden the design and research space into active bending structures by computationally designing and building an active bending pavilion from local techniques in wire-bending,

available materials, and design in the Trinidad Carnival. Our results show that by bringing together traditional crafts, cultural practices, and shape computation, we can develop novel approaches to active bending structures and contribute to scholarship. One practical challenge encountered in physical modeling was that feedback on deformation from dead loads was only observable when the entire structure was assembled at full-scale. This underscores a shortcoming of our digital model as it did not indicate a need for additional supports. Two limitations are that this structure was exhibited inside and did not have to resist external wind loads. Second, continuous coiling and uncoiling of rods for disassembly and packaging weakens rods over time.

Employing a finite element method and other advanced software and computational resources for digital design, simulation, and fabrication may have given extra information for predicting behavior. However, these methods turn a blind eye to the social, cultural, and technical knowledges of its setting. Second, they limit who can participate in design and scholarship by catering mainly to experts. Third, they restrict the fields and practices in which active bending can be explored with preference given to those largely resourced. Emphasis on highly technological methodologies limits advancement in design and research at the intersection of active bending, computational design, and cultural making practices. Although this project focuses on employing low-tech approaches to designing, simulating, and materializing active bending structures in a specific social, cultural, and technological context, other computational methods can be integrated for a hybrid approach. Parametric software can be used to generate design possibilities (Fig. 9), digital design and 3D printing technology can be used to fabricate connectors like previous projects (Noel, 2016, 2017), and structural simulation software in Rhino and Grasshopper can be combined with physical modeling for material and geometric feedback and analysis.

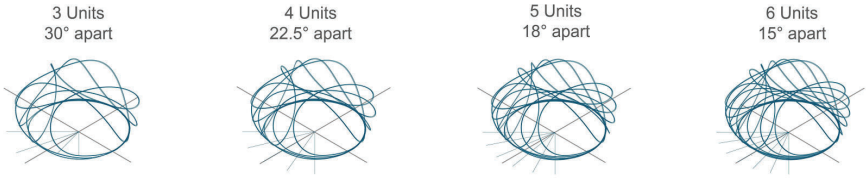

Figure 9. Digital designs of variations.

By building on existing knowledges and skills in Carnival, and facilitating creative expression using tools and materials at hand, a Situated Computations approach can (1) strengthen social and cultural connections, (2) link and advance culture, craft, and computation, and (3) employ the tensions and elastic deformations in society and materials to drive and generate form. A Situated Computations approach in active bending provides an opportunity to integrate local knowledges, design practices, and material behaviors as drivers in active bending approaches, so that structure, sociality, material practices, and cultural settings are considered concurrently. Future studies will continue to develop low-tech computational methodologies for design, simulation, and materialization

in active bending discourse. Situated Computations opens the design space so that research in active bending is not driven solely by highly technological tools and skills but includes low-tech computational tools and knowledges and creates practices where both can work together and engage in mutual learning.

Acknowledgment

Special thanks to the Ventulett NEXT Generation Fellowship from the School of Architecture at the Georgia Institute of Technology for funding this research. Grateful acknowledgment is given to students and colleagues at Georgia Tech. Digital Fab. Lab for their support.

References

Ahlquist, S. and Lienhard, J.: 2013, Physical and Numerical Prototyping for Integrated Bending and Form-Active Textile Hybrid Structures, *Rethinking Prototyping: Proceedings of the Design Modelling Symposium*, Berlin.

Crolla, K.: 2017, Building indeterminacy modelling – the "ZCB Bamboo Pavilion" as a case study on nonstandard construction from natural materials, *Visualization in Engineering*, **5**(1).

Huang, W. and Wu, C.: 2017, A Weaving Structure for Design & Construction of Organic Geometry, *Proceedings of the IASS Annual Symposium 2017*, Hamburg, Germany.

Laccone, F., Malomo, L., Perez, J., Pietroni, N., Ponchio, F., Bickel, B. and Cignoni, P.: 2020, A bending-active twisted-arch plywood structure: computational design and fabrication of the FlexMaps Pavilion, *SN Applied Sciences*, **2**(9), 1505.

Lewis, W.: 2013, Modeling of Fabric Structures and Associated Design Issues, *Journal of Architectural Engineering*, **19-2**(doi: 10.1061/(ASCE)AE.1943-5568.0000097), 81-88.

Lienhard, J.: 2014, *Bending-active structures□: form-finding strategies using elastic deformation in static and kinetic systems and the structural potentials therein*, Ph.D. Thesis, University of Stuttgart.

Lienhard, J., Alpermann, H., Gengnagel, C. and Knippers, J.: 2013, Active Bending, A Review on Structures where Bending is used as a Self-Formation Process, *International Journal of Space Structures*, **28**(3/4), 187-196.

Nicholas, P. and Tamke, M.: 2013, Computational Strategies for the Architectural Design of Bending Active Structures, *International Journal of Space Structures*, **28**.

Noel, V.A.A.: 2015, The Bailey-Derek Grammar: Recording the Craft of Wire-Bending in the Trinidad Carnival, *Leonardo*, **48**, 357-365.

Noel, V.A.A.: 2016, Crafting as Inquiry into Computation - Exploring wire-bending in traditional practice and design education, *Proceedings of the 34th eCAADe Conference - Volume 1*, Oulu, Finland.

Noel, V.A.A.: 2017, From Costuming and Dancing Sculptures to Architecture: The Corporeal and Computational in Design and Fabrication of Lightweight Mobile Structures, *Future Trajectories of Computations in Design CAAD FUTURES 2017*, Istanbul, 22-41.

Noel, V.A.A.: 2019, Reviving a Craft through Architecture: Computational Making of a lightweight pavilion based on wire-bending techniques, *Form and Force. International Association for Shell and Spatial Structures Annual Symposium 2019*, Barcelona, Spain, 563-570.

Noel, V.A.A.: 2020, Situated Computations: Bridging Craft and Computation in the Trinidad and Tobago Carnival, *Dearq*, **27**, 62-75.

MATERIAL (DATA) INTELLIGENCE

Towards a Circular Building Environment

ANNA BATALLE GARCIA[1], IREM YAGMUR CEBECI[2], ROBERTO VARGAS CALVO[3] and MATTHEW GORDON[4]
[1,2,3,4]*Institute for Advanced Architecture of Catalonia*
[1,2,3,4]*{annabatalle|iyagmurcebeci|robert.en.var|mattjosephgordon}@gmail.com*

Abstract. The integration of repurposed material in new construction products generates resiliency strategies that diminish the dependency on raw resources and reduce the CO2 emissions produced by their extraction, transportation, and manufacturing. This research emphasizes the need to expand preliminary data collation from pre-demolition sites to inform early design decisions. Material (data) Intelligence investigates how the merging of artificial intelligence and data analysis could have a crucial impact on achieving widespread material reuse. The first step consists of automating the process of detecting materials and construction elements from pre-demolition sites through drone photography and computer vision. The second part of the research links the resulting database with a computational design tool that can be integrated into construction software. This paper strengthens the potential of circular material flows in a digital paradigm and exposes the capability for constructing big data sets of reusable materials, digitally available, for sharing and organizing material harvesting.

Keywords. Computer vision; material database; automation; reclaimed material; digitalization.

1. Introduction

At present, the construction industry is the 'number one' consumer of global raw materials (World Economic Forum and The Boston Consulting Group, 2016, p. 12) while being one of the biggest producers of waste in the EU, where it accounts for approximately '25% to 30% of all waste generated' (Construction and demolition waste - Environment - European Commission, 2019). The construction industry is facing a waste management issue compounded by a near-future resource scarcity problem; consuming more than what we can sustainably produce. On average, humans use more than '1,5 times the resources that the planet can provide' (Jensen and Sommer, 2019, p. 24). This fact questions current material flows and supports the use of obsolete buildings as a source of second-life high-value assets and materials.

PROJECTIONS, Proceedings of the 26th International Conference of the Association for Computer-Aided Architectural Design Research in Asia (CAADRIA) 2021, Volume 1, 361-370.

Changing the linear material flow into a circular one will increase the material recovery rate, which is only 'one-third' worldwide at the moment, (The Ellen MacArthur Foundation, 2013, p. 17) while simultaneously reducing overall demolition and construction waste (DCW). Several medium to large scale demonstrators and frameworks of secondary use materials and circular design are being constructed, including the *Buildings as Material Banks* pilot projects in Germany (Buildings As Material Banks (BAMB2020) 2020), and *Ressource City* in Denmark (Ressource City 2020); indicating the interest in eco-innovation of the European Union with long-term programs like *EU Circular Economy Action Plan* (EU Circular Economy Action Plan 2020) and projects like *Reflow* (Reflow Project 2019).

Parallel to these developments, various digital platforms have been created for secondary use materials marketplaces; matching suppliers and buyers like *Opalis* in Belgium and *Oogstkaart* in the Netherlands. Platforms like *Building Material Scout* in Germany have put in place a more robust system connecting architects, planners, auditors, investors, manufacturers, contractors, and user operators to create integrated assessments and certifications on future projects for the use of reclaimed materials. These processes start with the data acquisition of the physical environment, creating databases where all the relevant information and specifications of the materials and components are collected and organized. However, the methods used to build up this framework require a more robust infrastructure and a highly qualified workforce presenting a challenge to the sector. Therefore, to increase the feasibility of these practices more digital workflows need to be implemented.

The data acquisition could be performed through a digitally recorded model with the aid of 3D-scanning technologies into a 3D point cloud, such as in the 'Machine Vision for Reassembly' project (TU Darmstadt, 2020), where concrete elements were extracted by geometrical properties. However, the project does not implement any automated methods for the point cloud reconstruction or segmentation process, or further considerations for material database generation. With this in mind, this work aims to bring greater automation and scale for these workflows, as well as to connect their data naturally into the design process.

Lastly, a more unconventional and contemporary approach to reuse appears in the work developed by Brandon Clifford and Wes McGee in 'Cyclopean Cannibalism, a Method for Recycling Rubble' (Clifford and McGee, 2018). The project investigates new ways of bringing back concrete and off-cut stone to the construction stream instead of crushing the material into gravel. The rubble is scanned to create a point cloud, then used to run an algorithm that finds the best fitting polygon within the overall design. Apart from formal considerations, the algorithm takes into account structure limitations and fabrication constraints. The prototype was a method based experiment that set up guidelines on how to approach the process of integrating obsolete material into new and digital construction systems. The paper presents this workflow, from digitizing data acquisition to design. It establishes a new approach that opens and integrates technological advances to demolition companies' and designers' processes to maximize material reused.

2. Methods

The process that has been developed is organized into two parts, initially focusing on generating datasets of available materials from pre-demolition sites using geometric reconstruction and automatic localization techniques, to be used both as a process and a product in a new circular market. Collections of site photography from automated drone flights are first run through image localization algorithms, detecting the presence of relevant materials and their rough locations. Simultaneously, these images are used to reconstruct the site using photogrammetry; first as a rough mesh and then as data-defined building elements. These are combined with the earlier localization data to create a mapping from which material volumes, accessibility analysis, and demolition timeline planning can be obtained. The gathered data is stored in a material database and displayed in a user interface.

The second stage employs this database with a computational prototype design tool that can be integrated into the design process for architects and construction companies. The system both matches designed components with relevant stored materials by their design requirements, as well as providing suggestions for design changes. The proposed iterations aim to optimize repurposed material utilization and cost.

3. Data Capture

Initial reality capture from the demolition site is performed in three main stages. These cover the physical collection of data, the creation of mesh representations of this data, and the localization of useful materials within these digital representations.

While higher accuracy could be found with terrestrial laser scanning systems, our method used a photogrammetry workflow, both for cost and for path planning practicality. The state of debris or clutter in a pre-demolition site would impede ground vehicles robots, while consumer-level drones can cover ground more freely.

The photogrammetry reconstruction was tested with *Agisoft Metashape* (Agisoft Metashape 2006). Among the tested area, around 200 photographs were used to reconstruct a single-height space of approximately 500 square meters, interspersed with concrete columns. To extract usable geometry, *Cloud Compare* was used for its plane fitting and shape detection features to ultimately create a mesh representation of the scanned area.

As this workflow employed 2d imagery as an intermediate step, this presented an immediate data source for use by categorization and image localization algorithms. These material-localized images can then be mapped into the mesh representation for final material estimations.

Figure 1. Images from the building inspection analyzed by Larger Sliding Kernel.

Localization is performed by combining many small image classification jobs on a sliding subpatch, producing a localization map at roughly 25% the resolution of the original image, where the patch size matches the standard resolution of the training set. The classifier uses a Stacking Ensemble Learning system, combining the results of a Bag of Visual Words (BoVW) classifier with simpler Local Binary Pattern and Hue/Saturation based classifiers, which helps avoid weaknesses in each individual classifier's result. The BoVW system uses the GFTT feature detector and BRISK descriptor algorithm for generating descriptions of a patch. At the training stage, a representative subsample of all found descriptions were clustered into 512 codewords; for which each classification has an expected histogram concentration. Classification is then performed by comparing the codeword histograms between the image patch and each category.

The Local Binary pattern analysis uses 24 input points at a diameter of 8 pixels, resulting in a simple histogram of patterns present used as input for a Support Vector Machine model. Likewise the Hue and Saturation channels are reduced to size 16 histograms and used with a separate SVM model.

Table 1. Categories and training scores.

Category	Brick	Concrete	Metal	Wood	None
f-1 Score	0.96	0.97	0.96	0.94	0.94

F-scores for categorization among the test set is shown above. While the model performs well against the compiled dataset, presently there are still issues with generalization and noisy results when recombining patches into a localized result. Improvement of the compiled dataset is ongoing, as most existing publicly available image sets don't include imagery relevant to our categories, and image sets that do include more material categories (such as MINC) focus on interior finishes and fit out rather than the structural layer.

4. Material localization environment

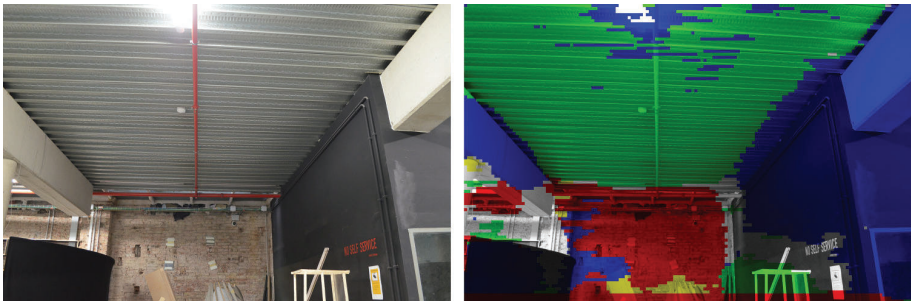

Figure 2. Material Localization.

After the image-based material localization is performed (see Fig 2), the imagery is reconstructed into a color coded point cloud (see Fig 3). The subsequent dense cloud is overlaid and measured in proximity with the reconstructed textured mesh and component segmentation, creating associations between e.g. the ceiling plane and the metal category (See Fig 3). Looking at the back wall element for instance, we look at the percentages of the material-representative colors in their mapped textures, with red for bricks, green for metal, blue for concrete, yellow for wood, and grey implying no classification. For this wall the percentage of materials in the element was as follows (with a threshold of 0.5 for each color): bricks: 48.8%, metal: 7.6%, concrete: 5.3%, wood: 7.2% and others = 31.1%.

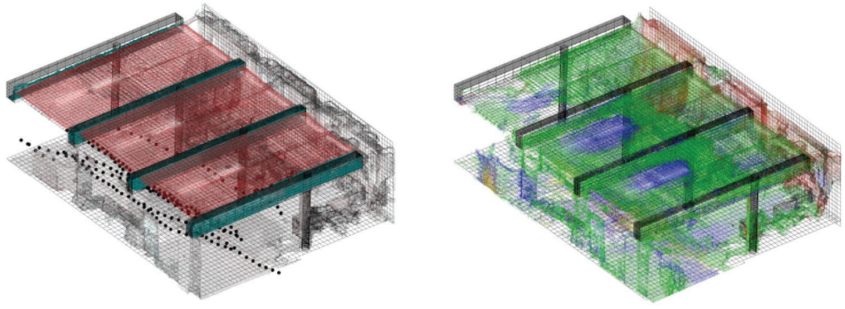

Figure 3. The isometric drawing on the left shows the original point cloud, camera locations from the imagery, reconstructed cleaned quad mesh and component segmentation. The drawing on the right shows the dense point cloud from the color coded image localization images.

Lastly a user interface was built to have more control over the information gathered. This interface includes a search bar for components and materials, once, for example, a “brick wall” is found, several information appears at the side bars (See Fig 4), showing the geo-located photographs and material localization imagery related to that material, along with other types of data like area, volume,

quantity and precision of the localization for that particular searched material. This tool can potentially be applied in demolition companies to further develop deconstruction processes creating a better building material report.

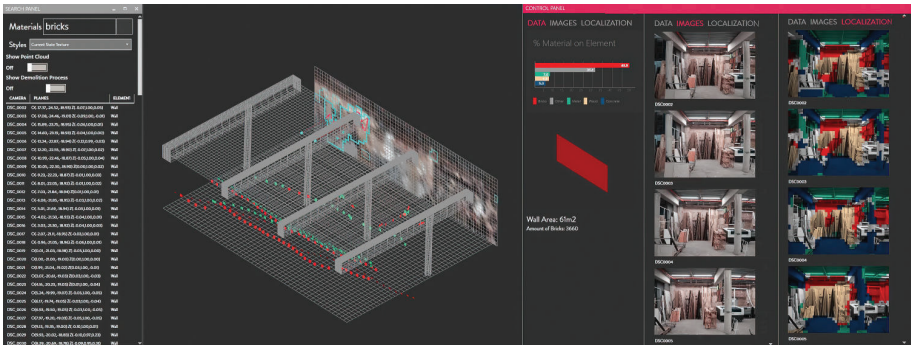

Figure 4. The user interface serves as a three dimensional environment displaying all the dataset gathered during the data acquisition from the building.

5. Design from scarcity

Once a system of data gathering and storage has been instituted, this work proposes methods for integrating, access, and previewing of this information into the computer design workflow.

The system for the design tool has been built specifically for a case study that speculates on recovering wooden beams from the "Institute for Advanced Architecture of Catalonia" (IaaC) roof structure and incorporates the recovered material in a new solar protection system for facades.

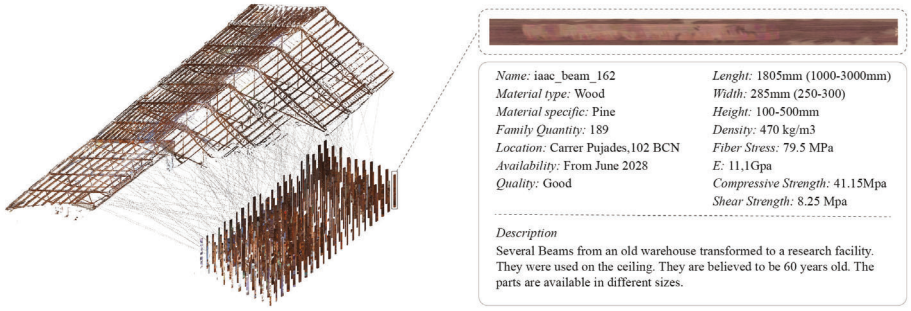

Figure 5. IaaC Roof Dataset.

In the first step the designer inputs an adaptable design and chooses a specific range of data to use in their project, adjusting the applied slice based on several constraints. The material interface focuses on presenting spatial features for geometric constraints, material specifications for structural performance analysis, and site localization for shipping cost estimation. The chosen subset is previewed

live as the user adjusts parameters.

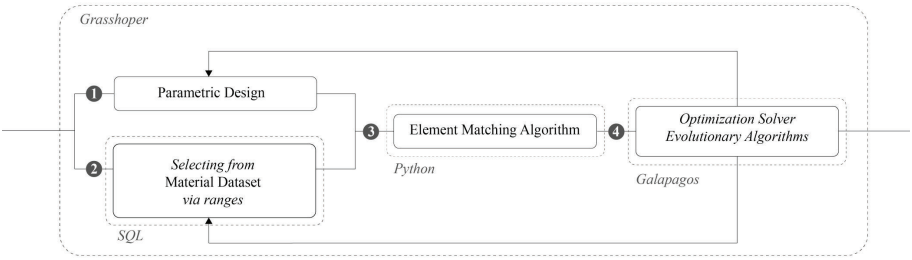

Figure 6. Circular Design Workflow.

The second step is the development of a matching algorithm. Using the Grasshopper computational design environment, a system was developed that reviews stored materials in the library and matches them with the design requirements. As each element in the design is compared with the dataset, there are three possible results: First, it may find a direct match within a certain tolerance. Alternatively, a larger piece may need to be cut down to match, and the resulting cutoff added back to the dataset. Finally, the dataset may be unable to provide the necessary element and a new-stock element will need to be procured.

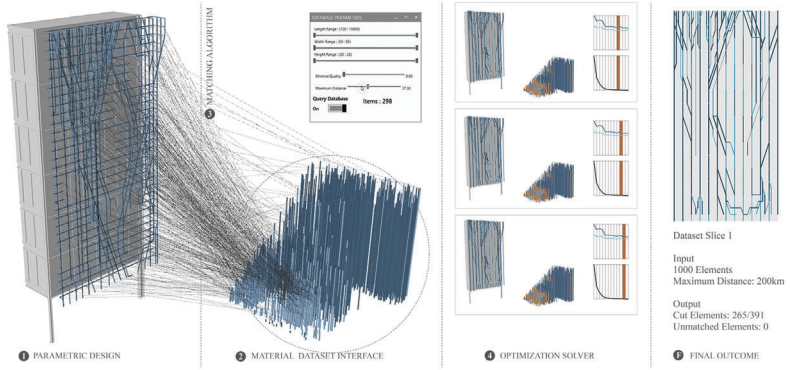

Figure 7. Case Study Process.

With the goal of an optimal density of reused material, the design approach features a degree of flexibility by adjustment of certain parameters. When an iteration of the design is submitted to the system, the materials calculated for its construction are matched up with the available items from the material dataset. The efficiency of this mapping, along with a resulting structural simulation of the resulting configuration, is used as a guiding fitness value for gradually adjusting and optimizing the design.

Finally, for the optimization, a three-dimension genetic algorithm applies small

translations to the geometric inputs of the facade and minimizes a total fitness value calculated from the previous analysis. Inputs are weighted to favor efficient reuse first, with the structural results only disqualifying an iteration if the system proves to be very unstable.

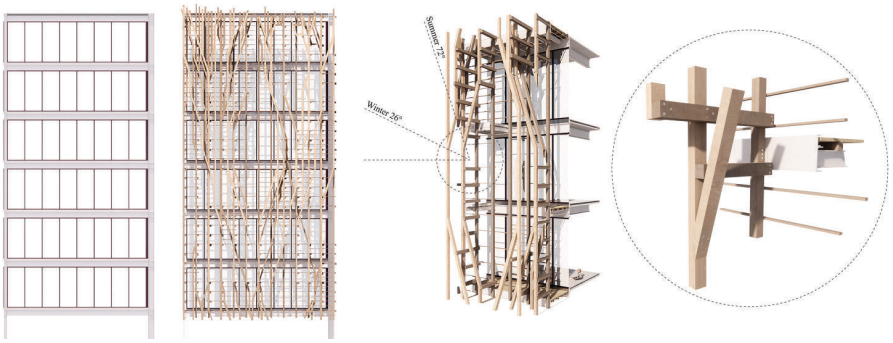

Figure 8. Existing facade and new solar protection system made with recovered wood.

6. Results and Discussion

6.1. MATERIAL DETECTION

Currently our material detection is trained for four common and generic categories: wood, concrete, steel, bricks. Ideally, the classes will be split further based on the specific of recovery, e.g. wooden flooring vs wall studs.

There are also common false-positive situations that should be trained against - e.g. concrete masonry units would occupy their own reuse profile not currently in our system, but to a computer vision system share common features both with cast concrete and brick elements.

6.2. MATERIAL ANALYSIS

The material analysis developed for the case study is composed mainly by visual inspection. Initial research towards material analysis is currently being performed using computer vision and depth camera systems to identify features such as knots, fractures and nail holes, and locate degraded areas based on surface roughness.

In most cases, post processing of the materials is necessary to remove their connective elements (e.g. nails, mortar, bolts). Automated systems for this processing would require specifically developed workflows in sensing and actuation for each type of connection.

6.3. DESIGN APPROACH

The current test-case of using rectangular extrusions with very few irregularities with dimensional data creates a proof of concept for the overall desirable system. This study case clearly relates a sparse and locally defined dimensional dataset from upcycle wood pieces to a generative design workflow. Further

explorations into this particular workflow can create a need for different types of assemblies novelty in design for disassembly strategies when shape recognition and shape matching come to play in the dataset. Lastly, as more factors such as environmental impact or recovery cost are calculated, more specific machine learning tools would also be incorporated to help the user analyze the breadth of information and meaningfully appraise the results.

6.4. LIFE-CYCLE AND MATERIAL VALUE

While the study case of the research specializes in the utilization of wood for the design prototype for the sake of speed of the tests and machinery available, the value of other materials are recognized similarly in ecological and economic potential impact. The value of a reinforced concrete wall element is some '50 times higher per ton than the value of the gravel' into which it is currently broken down when buildings are demolished (Jensen and Sommer, 2019, p. 24), because of the cost of new labour and energy (extraction, transportation, manufacturing and assembly) needed to build a new component.

When repurposing material it should be taken into account the different materials layers, for example differentiate the guidelines for the use of recycled concrete on the material level, and create an approach for reuse on the component level. At the same time a tracking system should be implemented to monitor when a material changes its location, product finish or where repairs might be needed to secure its quality when being reused in a new construction. This active monitoring will give the best status of the current state of the material increasing the robustness and durability of the system. This implies a systemic change, going from an analog categorization and assessment of pre-demolition or ready-to-disassemble sites to an intelligent planning tool that documents the quality and reliability of the components and assemblies for reuse, thereby verifying an endured market value of the buildings assets.

7. Conclusion

In developed countries, '85% of the buildings that will still be standing in 2050 have already been built' (Jensen and Sommer, 2019, p. 7), proving there is a significant need for more robust protocols for material digitalization of the already constructed environment, and most specifically, buildings. Through this research, a more intelligent and resilient system has been proposed for selective and partial disassembly of building components.

The architecture and construction sector has not presented a thorough investigation on how to use technological advancements to extract material information from existing buildings before considering the development of new ones. This research adds critical knowledge towards acquiring and using currently available assets within an automated data collection that could be plugged into existing powerful second-life material sharing platforms. The presented workflows complement each other; starting from the scanning of the physical demolition site, to data collection and elements organization, and finally its connection to a new design. Within this investigation, it has been demonstrated

that a relationship can be established between a dataset and the design principles of reusability. The proposed workflow is an exchange between generative design options and upcycled resources availability, constantly evaluating the designer intent and the building performance. The overall configuration follows a scarcity from local specificity, adding new information towards the challenge of form follows sparse availability.

Lastly, the paper displays a set of tools that can support redefining material flows in the construction industry. Following through the whole design and construction process the problem has been holistically approached by merging technologies in the process of detecting, sorting, manipulating, and reusing the recovered material.

Acknowledgments

This research was developed during the *Master in Robotics and Advanced Construction (2019-2020)* in the *Institute for Advanced Architecture of Catalonia*. We would like to recognize the support we received from the faculty, especially our mentors *Alexandre Dubor*, *Aldo Sollazzo* and *Mathilde Marengo*.

The structure analysis is performed employing *Karamba* and the evolutionary solver implemented is *Galapagos* created by *David Rutten*.

References

"Agisoft Metashape" : 2006. Available from <https://www.agisoft.com/> (accessed 2020).

"Towards the Circular Economy Vol. 1" : 2013. Available from <https://www.ellenmacarthurfoundation.org/assets/downloads/publications/Ellen-MacArthur-Foundation-Towards-the-Circular-Economy-vol.1.pdf.>.

"Ressource City" : 2014. Available from <https://ressourcecity.dk/> (accessed 2020).

"Shaping the Future of Construction A Breakthrough in Mindset and Technology" : 2016. Available from <http://www3.weforum.org/docs/WEF_Shaping_the_Future_of_Construction_full_report__.pdf>.

"BAMB – Buildings As Material Banks" : 2016. Available from <https://www.bamb2020.eu/> (accessed 2020).

"EU Construction & Demolition Waste Management Protocol and Guidelines" : 2018. Available from <https://ec.europa.eu/environment/waste/construction_demolition.htm> (accessed November 2020).

"Reflow Project" : 2019. Available from <https://reflowproject.eu/> (accessed 2020).

"Additional tools EU Circular Economy Action Plan" : 2020. Available from <https://ec.europa.eu/environment/circular-economy/> (accessed November 2020).

Cliffor, B. and McGee, W.e.s.: 2018, Cyclopean Cannibalism. A method for recycling rubble, *ACADIA 2018*, 404-413.

Merrild, H., Jensen, K.G. and Sommer, J.: 2016, *Building a Circular Future*, GXN.

Rosebrock, A.: 2015, "'Content Based Image Retrieval', 'Image Classification and Machine Learning', 'Local Binary Patterns with Python & OpenCV'" . Available from <https://www.pyimagesearch.com/2015/12/07/local-binary-patterns-with-python-opencv/> (accessed 25th November 2020).

Rutten, D.: 2014, "Karamba3D" . Available from <https://www.karamba3d.com/> (accessed 2020).

Wibranek, B., Braumann, A., Martinovic, L., Sysoyeva, N. and Tessmann, O.: 2020, "Machine Vision For Reassembly. [video]" . Available from <https://proximities.acadia.org/m/5f909dbfe7280855b0e934fe> (accessed 25th November 2020).

WASTED ... AGAIN

Or how to understand waste as a data problem and aiming to address the reduction of waste as a computational challenge

M. HANK HAEUSLER[1], ANDREW BUTLER[2],
NICOLE GARDNER[3], SAMAD SEPASGOZAR[4] and SHAN PAN[5]
[1,3]*UNSW / Computational Design*
[1,3]*{m.haeusler|n.gardner}@unsw.edu.au*
[2]*Cox Architecture Sydney*
[2]*andrew.butler@cox.com.au*
[4]*UNSW / Construction Management*
[4]*Sepas@unsw.edu.au*
[5]*UNSW / Information Systems and Technology Management*
[5]*shan.pan@unsw.edu.au*

Abstract. The global construction industry is the single largest consumer of materials on the planet. Of that material consumption anywhere between 10-20% will end up in landfills as waste. Currently, there are three approaches to tackle this problem - reduce, reuse, and recycle. Concentrating purely on the challenge of reducing waste this research aims to address the problem of waste in the construction industry by addressing it in the preliminary design stage. It does so by asking the research question if computational design offers opportunities towards lean construction or to achieve Zero Waste by understanding waste as a data management challenge. For our research materials are specified in databases outlining geometrical and quantitative information either in material supplier databases (homepage) or in architecture and construction databases via Revit or Grasshopper. Consequently, one can collect via web scraping, investigate via databases, inspect and compare via Grasshopper and Python these databases to understand if one can transform data into information towards material use and consequently into knowledge on waste production and reduction. This investigation, its proposed hypothesis, methodology, implications, significance, and evaluation are presented in the paper.

Keywords. Construction industry; waste reduction; databases; web scraping; computational design.

1. Background and motivation

Rapid growth in construction activities in Australia in recent years has led to increased generation of construction and demolition (C&D) waste (Shooshtarian

PROJECTIONS, Proceedings of the 26th International Conference of the Association for Computer-Aided Architectural Design Research in Asia (CAADRIA) 2021, Volume 1, 371-380.

et. al, 2019). Ibid. argues that, according to the latest statistics (NWR, 2018), about 20.4 Mt of C&D waste was generated across Australia during 2017- 2018. That is equal to 30.5% of the total waste generated, from which 33% is disposed of in landfills. With the existing rate of migration and population growth (ABS, 2018), it is expected that C&D waste generation will continue to grow steadily in the coming years. To give a general background the paper wants to present a few figures in order to give the research a sense of the magnitude of the problem. The Australian Bureau of Statistics (ABS, 2020) lists in 2020 recent report with a reference period for the 2018-19 financial year that Australia generated 75.8 million tonnes of solid waste in 2018-19, which was a 10% increase over the last two years (since 2016-17). Over half of all waste was sent for recycling (38.5 million tonnes), while 27% was sent to landfill for disposal (20.5 million tonnes). Sectors generating the most waste were:

- Manufacturing: 12.8 million tonnes (16.9%)
- Construction: 12.7 million tonnes (16.8%)
- Households: 12.4 million tonnes (16.3%)
- Electricity, gas and water services: 10.9 million tonnes (14.4%)

Showcasing that construction waste in the above-cited years ranks higher as a waste producer than households. In providing industry insights the same report states that construction with its 16.8% contribution of total waste has with masonry materials (8 million tonnes) the largest supply (35%) of all masonry material waste. The construction industry has spent AUS$2 billion on waste services and the construction waste increased by 22% since 2016-17. With these figures in mind, construction waste is further classified by the EPA (2020) who provides information for demolition and excavation companies, builders, contractors, project managers, and property developers. Ibid. states that construction and demolition activities can generate a wide range of different waste materials. This waste is not just rubbish and unwanted material, but based on type, the construction debris is classified into excavation debris, roadwork debris, demolition debris, and complex debris (CDRecycler, 2020).

- **Excavation debris** is further segmented as vegetable soil, soil, sand, gravel, rock, and clay.
- **Roadwork debris** includes debris generated by activities such as construction, demolition, and renovation of roads, railroads, airports, and runways. This includes concrete, broken asphalt, paving stone, sand, pebble, railway traverse, and ballast.
- **Construction debris** generated by the building and demolition of industrial and residential buildings, hospitals and schools such as concrete with iron, concrete without iron, roofing, tiles, bricks, wood, stucco, gypsum and ceramic are included in demolition debris.
- **Complex debris** such as plastics, metals, ceramic, paper, and cartons are considered separately.

For our research we concentrate solely on (3) construction debris with an extension to (4) complex debris, as (1) excavation debris not necessarily is harmful in landfills, and its reduction is not covered in the research, similar to (2) roadwork

debris. In terms of material, construction debris is segregated into wood, metal, shingles, asphalt brick and concrete (ABC) debris, packaging debris, ceramics, gypsum, plastic, and others.

- **Wood waste** includes plywood, manufactured wood, painted wood, pallets and crates, and treated wood.
- **Metal waste** includes ferrous and nonferrous metals.
- **ABC debris** includes asphalt, bricks, concretes and composites.
- Toilets, sinks, and tiles are included in **ceramic debris**.
- Plastic pipe, vinyl siding, and other plastics are considered **plastic waste**.

The outlook on waste is dire as the volume of construction waste generated worldwide every year, according to a report from Construction Waste Market (2016) will nearly double to 2.2. billion tons by the year 2025 confirming the importance to address this research.

Literature on addressing waste in the construction industry lists the following. The Australian Government suggests three approaches to minimising waste as the three 'Rs' of waste minimisation: reduce, reuse, recycle (YourHome, 2020).

- **Reduce** consumption of resources by building smaller houses that are better designed for your needs. This is the most effective way to conserve precious resources for use by future generations and reduce waste. It also lowers costs. Improve the accuracy of your ordering so that materials are not wasted nor sit around a site for long periods where they can become damaged.
- **Reuse** existing buildings and materials in order to reduce demand for resources, lower waste volumes, and save money. A lot of energy and resources go into the materials used to construct a home and due to the mixed nature of these materials most end up in landfills. The following graph shows that the emissions from the energy of the materials required to construct a typical house are nearly equal to the emissions from the energy required to heat or cool that house over a typical 50-year life. Consider renovating an existing house, rather than demolishing the old and building from scratch as very little of the demolished house is recycled or reused.
- **Recycle** resources that are leftover or have reached the end of their useful life. This reduces the demand for new materials and lowers the volume of waste going to landfills. Use materials with high recycled content to create a market for recycled resources. It raises the price paid by recyclers for recovered resources and increases the viability of recycling.

In computational design research investigating waste as a data management challenge, we concentrate on the first point to reduce waste. This is further motivated also computational designers primarily work in offices in design, documentation, and communication stages of a building where they are in a position to reduce waste in design or documentation and not on construction sites. Further one can argue that any waste not produced contributes to the solution of reducing waste. Hence the following source (United Rental, 2018) suggests the 8 Ways to Reduce Construction Waste (only the first three are listed due to their relevance for this research).

- Reduce construction mistakes

- Order the right amount of materials
- Get the right-size materials for the job

Yet while a reduction of waste is arguably a topic worth pursuing given the above-stated problem, research that investigated if and how architects can prevent waste production paints a dire picture. When investigating *'Architects' perspectives on construction waste reduction by design'* (Osmani et al., 2006, 2008) the author's research revealed that waste management is not a priority in the design process. Additionally, their research unveiled that architects seemed to take the view that waste is mainly produced during site operations and rarely generated during the design stages; however, about one-third of construction waste could essentially arise from design decisions (Ibid.). The authors conducted a questionnaire survey based on specific and interrelated organisational waste minimisation issues conducted with architects and contractors and revealed that very few attempts are made to reduce waste during the design process. On the other hand, the results show that contractors are pursuing a more proactive approach to manage on-site waste production through the development of environmental and waste management policies. The results reveal that poorly defined responsibilities are leading to confusion regarding who should control and monitor waste management. Both architects and contractors are constrained by internal and external factors, such as 'waste accepted as inevitable' and lack of interest from clients (Ibid.).

2. Research Question, objectives and outcomes

Research in Computational Design as a discipline following pragmatist concepts (Gardner et al., 2019) suggests that computational design research offers the opportunity to use and apply new methods and tools to 'old problem'. Through the literature review above we have identified waste in the construction industry as one 'old problem' suitable to pursue through a computational lens. Hence asking the core research question of waste can be understood and investigated as a data management challenge and consequently assists in understanding better how much waste is produced in the design phase and if waste can be reduced.

Objectives. As part of this research the paper aims to introduce a different way of thinking about waste. In the work presented the researchers thought about buildings, their designs, and their materials as series of databases, starting and applying seven observations. (1) Architecture is made out of industrial designed products (i.e. plasterboards) that companies manufacture and sell; (2) Industrial design products are often only partially used to build a building - some of them are turned into Waste; (3) EACH product is defined as data through their dimensions, material, costs, carbon footprint, etc.; (4) Data that defines these products are stored in a database (Excel / REST framework online); (5) Architects define through their drawings which product is used, in which quantity, and if the single object is used in its whole or only in parts (no waste/waste per item). BIM families defining elements used for walls, facades, floors; (6) IF databases in (4) and (5) exists one, therefore, compare both databases to identify waste. If this assumption is correct one would be able to understand how much waste is produced during

design, and (7) This could allow the establishment of a WASTE BUDGET during the design phase (ignoring the reuse of offcuts).

Outcomes. The research project presents a proof of concept study in which we used web/HTML scraping to source products data from suppliers homepages (over 1400 products over one week trial), stored in REST frameworks, and connected these with GH scripts defining the geometry (residential/commercial floor plan, facades, and roof) and allowing an optimisation of the geometry towards using products as a whole while at the same time understanding how much waste will be produced as a consequence of design, in the first five minutes of design.

3. Methodology

The research project was conducted as part of a 2nd-year course at the Bachelor of Computational Design at the University of New South Wales, Sydney in engaging students in setting up data structures and writing robust interoperable code in Grasshopper and Python. The project applied action research methodology (Sein et. al, 2011) to create a frame that focuses, informs, and guides the work undertaken to ensure that the previously stated aims are met, and the questions sufficiently answered. The research project applied the concept of 'Upstreaming Information' as a main theoretical framework, arguing that information as digitised data exist within a current or past project (i.e BIM data) and outside a project (i.e data on homepages such as planning regulation or environmental). While these data can exist in various stages of a design project at a current stage we aim to 'upstream' them to the 'first five minutes of design'. This is motivated and influenced by the 'MacLeamy curve' developed in 2004, as discussed by Daniel Davis in blog and Ph.D. (2020). The MacLeamy curve outlines, according to Davis (Ibid.), "a pretty self-evident observation that architectural projects become more difficult to change the more developed it becomes". Consequently, the curve visualises the ability to impact a project and the cost of design changes during the duration of a project from predesign to construction. The idea of 'Upstreaming' argues that one can take digitised information and move them up and down across different stages in a linear progression of a construction project (predesign to construction). While there is various digitised information that has the potential to be 'upstreamed' in this research we concentrate on material information to reduce waste in the first five minutes of the design process. In order to do so, we needed to source data using Web/HTML scraping, storing data in a REST (Representational State Transfer) framework, and linking the stored data to a Grasshopper model. All concepts explained in the following.

4. Literature Review

Other than the previously discussed literature review outlining the current thinking and research on waste in the construction industry the paper briefly aims to introduce the following technical concepts which provided a base for the investigation.

Web or HTML scraping is a technique or term used to describe the use of a program or algorithm to extract and process large amounts of data from

the web. As the internet hosts arguably the greatest source of information many disciplines such as data science, business intelligence, or other forms of investigative reporting benefit from collecting and parsing raw data from websites. In the case of the research, we argued that nearly all material suppliers for the construction industry will offer their products on websites. Hence information about this product such as data through their dimensions, material, costs, the carbon footprint can be accessed as raw data via web scraping. In our research, we used 'Beautiful Soup' a Python library for parsing structured data (Realpython, 2020). Beautiful Soup allows you to interact with HTML in a similar way to how you would interact with a web page using developer tools. Beautiful Soup exposes a couple of intuitive functions you can use to explore the HTML you received. Following the tutorials, on realpython.com (Realpython, 2020b) the research team builds a web scraper that fetches Software Developer job listings from the 'Monster' job aggregator site (2020). Our web scraper parsed the HTML to pick out the relevant pieces of information and filter that content for specific words (in our case material information). When inspecting our data source, we explored the website, decipher the Information in URLs, and inspect the Site Using Developer Tools. This was followed by the second part in which scraped HTML Content From a Page (we used mainly Bunning's homepage, Bunnings is a large Australian hardware store which sells most building products used for small scale residential developments, yet went as well to other producers such as tile manufacturer) using Python. Here we were getting the site's HTML code into our Python script so we could interact with it, using Python's 'requests' (2020b) library. Depending on the website type one would face either static HTML content. In this scenario, the server that hosts the site sends back HTML documents that already contain all the data you'll get to see as a user. Alternatively, a hidden website contains information that's hidden behind a login or dynamic websites where the server might not send back any HTML at all. For ease, we mainly targeted static websites. The third and last task was then to parse HTML Code with Beautiful Soup to parse lengthy code responses with Beautiful Soup to make it more accessible and pick out the data we were interested in.

A **Representational state transfer (REST)** is a software architectural style that defines a set of constraints to be used for creating Web services. Web services that conform to the REST architectural style, called RESTful Web services, provide interoperability between computer systems on the internet. In our research, we used Django REST (2020) framework, a powerful and flexible toolkit for building Web APIs.

Postman Collaboration platform. In order to collaborate as a team we used 'Postman' (2020) a collaboration platform for API development. Postman is a popular API client that makes it easy for developers to create, share, test, and document APIs. Via Postman users can create and save HTTP/s requests needed in the case of the research to combine various material information. When copying a URL into Postman and run a sent one can see the source code and returns information to the user. When linking this to a database one can write requests into Postman to list various components useful for the later task. This enabled us to generate a joint database. Making a 'Post' request allows us to feed data

into the joint database. All information is stored in a joint Google sheet which was overtime populated with ˜1500 material/product information within one week (the duration of a specific task in class) from various suppliers offering building products.

5. Project

The proof of concept research project was conducted as part of class CODE2120 - Building Data course as the Bachelor of Computational Design in mid-2020. As part of a ten-week course, students were given the above in Chapter 2. Research Question, Objectives, and Outcomes listed seven observations to address in three assignments. Please see the following URLs with Video clips of student works showcasing work in the assignments:

- Scarlett Rogers - www.youtube.com/watch?v=cOFqCnC3qSQ&feature=youtu.be
- Luka Jovanovic - www.youtube.com/watch?v=130RGnbON0A&feature=youtu.be
- Eddie Azzi - www.youtube.com/watch?v=KSOOlyf2xKQ&feature=youtu.be

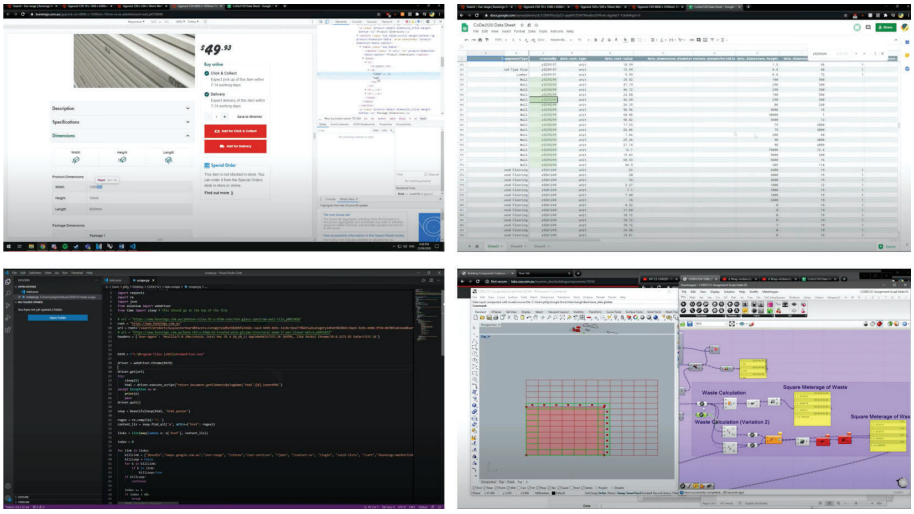

Figure 1. Screenshots from Video Eddie Azzi - HTML-scraped homepage (top/left), Google database (top/right), pythonscript (bottom/left), and grasshopper script (bottom/right).

Assignment 1: Understanding operability Here we outlined to students that building material data are stored in various online databases that sell products such as Bunnings Warehouse (a large Australian supplier of building material) and many others with information about dimension and many more. In this first assignment, students were asked to identify database systems for Building material data and sourced, scraped, stored them in the order as listed in the literature review. During the exercise, students learned how to set up databases and define agreed formats in how data are sorted and listed.

Assignment 2: Automating tasks in architectural workflows By the end

of the first assignment students have established a database for the materials (with dimensions and other information). This information now needs to be brought together with architectural geometry. As outlined above in Observation 5 architects define through their drawings which product is used, in which quantity, and if the single object is used in its whole or only in parts (no waste/waste per item). Here, and this is simplified - if one draws the floor plan of a room and the room is surrounded by walls defined via a BIM family with i.e plasterboards our script is able to do the following calculation. If the wall is 5100mm long and the plasterboard would come in a length of 1250mm then one would require 5 plasterboards with a total length of 6250mm of which one only uses 5100mm and 1150mm would become waste. Ignoring the fact that one can use the left-over plasterboard elsewhere for the moment the design has produced significant waste with 18.4% of the material going to landfill. When moving the wall by 100mm one could use exactly 4 plasterboards and create 0% waste. This calculation is easily done in this example but harder on a whole building - but not for a computer. In the following task, students were asked to script a shape (L, S, T, U, I shape) so the computer knows what shape the presented one is either clockwise or counter-clockwise shapes. This is essential to do in the following advanced tree manipulation in Grasshopper.

Assignment 3: Waste in construction The last task asked students to combine the material database and the Grasshopper models to return a calculation similar as the one outlined when talking about the plaster board. Naturally, as this was done computationally one could do the calculation on as all walls on each floor of a building and get a result.

6. Evaluation, conclusion and next steps

In evaluating the above-listed method of extracting information using web scraping, storing jointly collected data in one database, and connecting this database with grasshopper models one can conclude the above as success. Students were able to draw a simple building outline ((L, S, T, U, I shape) with parametric heights representing design stages in a 1:200 scale, the Grasshopper script generated a simplified floorplan (walls and room purpose) and the python script returned quantities of the selected material used and waste produced for each building outline. Given the limited timeframe of ten weeks for the experiment while learning Beautiful Soup, Django, Postman amongst others from scratch and using students as developers for the experiment one can clearly state that the presented approach has seeds worthwhile further development. The Python scripts could estimate the amount of waste produced and communicate to designers in an early design stage the quantity of waste. If nothing else a script like this might raise much-needed attention onto the topic - which too often ignored as research by Osmani et al (2006, 2008) has proven. Yet the presented research has obviously room for improvements and the presented research understands itself as a position paper aiming to raise attention in the CAAD community to the issue of waste in the construction industry and that one can contribute in addressing the problem through computational skills. The results motivated the team to continue the research and we are planning to investigate:

- **Developing a tool for waste reduction.** As currently we only have a proof of concept script the first step is in developing a robust tool based on Python and/or C languages that will be hosted on the Giraffe Technology platform (2020). We envision that future users can model rooms as the smallest item in the AEC industry on Giraffe and the platform will send our tool geometry information we can process, connect with to material and BIM database and return a result. Yet other steps are needed as well.
- **Extracting information out of BIM.** In 2.1 Objectives we state that architects define the characteristics of walls, floors, or ceilings via BIM families and that these families contain information that needed to be linked to an extended material database as the one explained above. Hence future research will be conducted to understand the data structure of BIM families to (i) allow the future user to upload their RFA (family) files and RFT (family template), (ii) storing material-related information in a separate database to match with the material database. In parallel, we are already working on Natural Language Processing (NLP) as we assume that each BIM user names its families and products differently and NLP has, in our research so far, proven to be successful.
- **Extending material database.** While our proof of concept was able to collect ˜1500 material via web scraping, we are planning to extend this exercise to source five to six-figure numbers of material concentrating first on products used in Australia.
- **Experiments in machine learning and multi-objective optimisation.** While we know how much waste one might produce, we do not offer yet a solution to the problem. Hence research will be undertaken to investigate how a machine can offer design solutions that reduce waste. The focus here can be on a solution that reduces waste on specific material types i.e with high embodied carbon or materials that are not biodegradable to name but two examples.
- **AI-enabled mentoring on waste.** How and when in the design process is the human informed by the machine on waste? What interaction happens, how is the information communicated, how does the human react and act upon receiving the information?

We hope to address these questions and topics for future research to reduce waste in the construction industry in the first five minutes of design.

References

"Construction Waste Market" : 2016. Available from Construction Waste Market: Global Industry Analysis, Size, Share, Growth, Trends and Forecast 2017-2025<https://www.transparencymarketresearch.com/construction-waste-market.html> (accessed 09. December 2020).

"NWR" : 2018. Available from Australian National Waste Report 2018. Department of the Environment and Energy<https://www.environment.gov.au/protection/waste/publications/national-waste-reports/2018> (accessed 09. December 2020).

"ABS" : 2018. Available from Australian Demographic Statistics. In: STATISTICS, A. B. O. (ed.). ENVIRONMENT AND COMMUNICATIONS REFERENCES COMMITTEE 2018. Never waste a crisis: the waste and recycling industry in Australia. In: SENATE, T. (ed.). Commonwealth of Australia 2018.<https://www.aph.gov.au/Parliamentary_Business/Committees/Senate/Environment_and_Communications/WasteandRecycling/Report> (accessed 09. December 2020).

"United Rental" : 2018. Available from 8 Ways to Reduce Construction Waste<https://www.unitedrentals.com/project-uptime/expertise/8-ways-reduce-construction-waste#/> (accessed 09. December 2020).
"Postman" : 2020. Available from Collaboration platform for API development<https://www.postman.com/> (accessed 09. December 2020).
"Monster" : 2020. Available from Software Developer Job Listing<https://www.monster.com/jobs/search/?q=Software-Developer> (accessed 09. December 2020).
"ABS" : 2020. Available from Waste Account Australia Experimental Estimates<https://www.abs.gov.au/statistics/environment/environmental-management/waste-account-australia-experimental-estimates/latest-release> (accessed 09. December 2020).
"EPA" : 2020. Available from Waste / Industrial Waste / Construction Demolition<https://www.epa.nsw.gov.au/your-environment/waste/industrial-waste/construction-demolition> (accessed 09. December 2020).
"CDRecycler" : 2020. Available from Global Volume Construction Demolition Waste<https://www.cdrecycler.com/article/global-volume-construction-demolition-waste/> (accessed 09. December 2020).
"Realpython" : 2020. Available from Beautiful Soup Web Scraper Python<https://realpython.com/beautiful-soup-web-scraper-python/> (accessed 09. December 2020).
"YourHome" : 2020. Available from Waste Minimisation<https://www.yourhome.gov.au/materials/waste-minimisation> (accessed 09. December 2020).
"UN SDGs" : 2020. Available from UN Sustainability Development Goals<https://www.un.org/sustainabledevelopment/sustainable-consumption-production/> (accessed 09. December 2020).
"Django" : 2020. Available from Django Rest Framework<https://www.django-rest-framework.org/> (accessed 09. December 2020).
"Giraffe Technology platform" : 2020. Available from Giraffe is a json editor with map of world to model and an app store to upload tools<https://www.giraffe.build/> (accessed 09. December 2020).
"Mirvac" : 2020. Available from Mirvac releases its plan for zero waste<https://www.mirvac.com/about/news-and-media/mirvac-releases-its-plan-for-zero-waste#> (accessed 09. December 2020).
"Davis" : 2020. Available from Daniel Davis Blog - Macleamy curve<https://www.danieldavis.com/macleamy/> (accessed 09. December 2020).
"Realpython" : 2020b. Available from Python requests<https://realpython.com/python-requests/> (accessed 09. December 2020).
Gardner, N. and Haeusler, M. H. 2019, Introduction: Computational Design - From Promise to Practice, *in* N. L. Gardner, M. H. Haeusler and Y. Zavoleas (eds.), *Computational Design: From Promise to Practice*, avedition, Ludwigsburg, Germany, 7-15.
Osmani, J., Glass, J. and Price, A. D. F.: 2006, Architect and contractor attitudes to waste minimisation, *Proceedings of the Institution of Civil Engineers - Waste and Resource Management*, **159**(2), 65-72.
Osmani, M., Glass, J. and Price, A. D. F.: 2008, Architects' perspectives on construction waste reduction by design, *Waste Management*, **28**(7), 1147-1158.
Sein, M., Henfridsson, O., Purao, S., Rossi, M. and Lindgren, R.: 2011, Action Design Research, *MIS Quarterly*, **35**(1), 37-56.
Shooshtarian, S., Maqsood, T., Khalfan, M., Wong, P. and Yang, R.: 2019, Construction and Demolition Waste Management in Australia: Review of Differences in Jurisdictional Regulatory Frameworks, *CIB World Building Congress 2019*, Hong Kong SAR, China, 1-11.

OPTIMISATION DESIGN STRATEGY OF RURAL BUILDING FORMS FOR A HEALTHY MICROCLIMATE ENVIRONMENT

YUQING ZHANG[1], QINGLIN MENG[2] and BIN LI[3]
[1,2,3]*South China University of Technology*
[1,3]*{771901995|445453185}@qq.com* [2]*arqlmeng@scut.edu.cn*

Abstract. The paper based on microclimate environment of the site takes the optimized design of rural building form to help the rural revitalization and sustainable development. The reconstructed house project in Baihua Village of Tangchi Town in Anhui Province is taken as the research case to discuss the form optimization strategies. Based on the principle of passive priority and active optimization, the building in Baihua Village is analyzed by field investigation and numerical simulation. First, the outdoor environment is interpreted by using Weather Tool software to offer a building form proposal. Then, with the drawing software CAD, ecological building simulation software Ecotect, and green building analysis software PKPM, the optimization strategy analysis of healthy building form was carried out to verify the optimal solution of building form based on China's national standards. Finally, this paper summarized and improved the rural building optimization design system for a healthy microclimate environment. The results of this paper are hoped to use for the contemporary rural architectural form design.

Keywords. Building form; Healthy environment; Design optimization; Software analysis.

1. Introduction

In 2017, "Healthy China" became China's national strategy. However, the majority of the rural population in China has been attracted by the rapid and efficient development of cities in recent decades. From the countryside to the city, the urban architectural form, function, and cultural characteristics have been brought back to the countryside and grafted into the development and reform of the countryside. Rural renewal and construction not only improve the living quality of rural residents but also directly or indirectly affect the traditional building microclimate environment that has been formed in rural areas for a long time. It is one of the strategies to solve the contradiction between rural tradition and modern development to explore the form of rural architecture that is conducive to the creation of a healthy microclimate environment.

The primary significance of the architectural form is to improve the natural climate and create a comfortable indoor environment, and the diversity of the microclimate creates the diversity of the architecture. Natural ventilation can

PROJECTIONS, Proceedings of the 26th International Conference of the Association for Computer-Aided Architectural Design Research in Asia (CAADRIA) 2021, Volume 1, 381-390.

enhance human comfort (Li, B., et al., 2020). New houses can be simulated and analyzed with the help of local wisdom (Li, B., et al., 2020). Scholars have determined that appropriate building forms provide better passive results for shading and natural ventilation (Olgyay, A., et al., 2015). The reflectivity and emissivity of the surface of the corridor on the influence of solar radiation will have different rules (Maragno, G.V. and Roura, H.C., 2010). Solar energy and wind energy can be used to realize the effective operation and increase energy saving of buildings with variable forms (Schumacher, M., Schaeffer, O., and Vogt, M., 2010). In addition to the discussion of technical analysis means, the focus on regionalism and practicality is also an important factor to realize the optimization of architectural form. Therefore, under the background of fully analyzing the traditional microclimate environment and combined with the modern lifestyle, this paper discusses the optimization design strategy of the rural architectural form.

2. Object and methods

2.1. OBJECT

Baihua village is located in Tangchi town, the westernmost part of Lujiang County, Hefei City, Anhui Province, in central China. It covers an area of 9 square kilometers. Baihua village is a mountainous village with undulating terrain and mountainous mountains from east to west, which also has a fundamental influence on the layout and form of buildings in the village.

The architectural form of Baihua Village is dominated by strip buildings. The single building with grey tiles, rammed earth walls, and stone foundations as the main structural materials (Figure 1). Among them, rammed earth wall architecture, an important architectural form of Baihua Village, is based on the raw earth that can be recycled and used locally as the main raw material. Rammed earth wall houses have good thermal performance and high indexes of thermal resistance and thermal inertia, so rammed earth buildings have an excellent thermal insulation effect, which will make the indoor warm in winter and cool in summer. The porous nature of rammed earth walls has a particular regulating effect on indoor humidity. Based on the original building materials and forms of Baihua Village, it is crucial to find the appropriate analysis means and realize the optimization of the new building form.

Figure 1. Status Quo of Grey Tile, Pitched Roof and Rammed Earth Wall.

2.2. METHODS

Weather Tool is a sub-software in Autodesk Analysis Ecotect software. It is widely used in the field of building ecological environment simulation and analysis, which can effectively improve energy efficiency and assist sustainable design. The Weather Tool reads and transforms a range of commonly used Weather data formats, including TMY (Typical Weather Year), TMY2, and DAT (Data), in a graphical visual representation. It contains hourly meteorological parameters commonly used in most performance-based building simulations.

In the early stage, meteorological data were analyzed through the Weather Tool to offer the design proposal. After that, the drawings made by software CAD based on field study. Then ecological building simulation did by software Ecotect to analyze the indoor natural lighting performance. And the software PKPM analyzed the indoor wind environment and air quality to verify whether the building form is healthy enough or not based on the relevant standards.

3. Results

3.1. CLIMATE ANALYSIS

3.1.1. Orientation and Solar Radiation analysis

The best orientation is calculated based on the amount of local solar radiation during the overheating and supercooling periods throughout the year. The optimal orientation of buildings in Hefei is due south, while the appropriate orientation is due south by west 5° and due south by east 15°, so the orientation should not be due west. It can be seen that the annual average solar radiation amount in the Hefei area is most in the direction of 25° South by east, 7.5° South by east in the period of subcooling, and 10° East by 10° South in the period of overheating.

Solar Radiation refers to the analysis and comparison of annual Solar Radiation on the facade facing all directions. From the figure, it shows the overheating period in the red zone is from late May to early September in Hefei. The supercooling period in the blue area is from late November to early March. The thick yellow line represents the annual average solar heat gain due south (Figure 2).

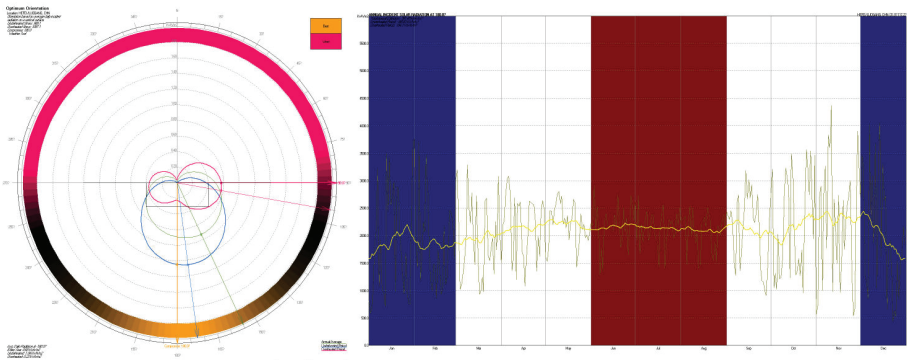

Figure 2. Solar Radiation and it's Optimal Orientation.

Through comparative analysis, the solar radiation heat of each facade is obtained during the overheated period and the under cold period in a year, and the relative optimal architectural orientation for the design of the building plane and facade is summarized, to meet the optimal effect of building lighting and sunshine.

3.1.2. Enthalpy analysis

Enthalpy is a quantity of energy in a matter, a parameter representing the state of the matter in units of K.J. or K.J.kgˆ-1. Enthalpy and Humidity figures are used in ventilation and air conditioning engineering to determine the state of air, including temperature, moisture content, atmospheric pressure, and the relationship between water vapour pressure and thermal environment. Generally, Enthalpy and Humidity diagrams are used in the process of climate design to intuitively analyze and determine the cold, hot, dry, and wet conditions of the indoor and outdoor climate of the building, as well as the deviation degree from the comfort zone. The horizontal coordinate of the Psychrometric Figure is the dry bulb temperature (unit: Degrees Celsius); The ordinate is absolute humidity (unit: g.kgˆ-1); The oblique line with different slope indicates wet bulb temperature (unit: Degrees Celsius); The parallel slash represents Enthalpy in K.J.kgˆ-1. The comfort zone in the Enthalpy Figure is determined by air temperature, relative humidity, airflow velocity, and ambient radiation temperature.

The annual time range of Hefei is selected for analysis (Table 1) - using software prediction, simulation, and quantitative expression functions. Six passive technologies were selected: passive solar heating, high heat capacity material applications, night ventilation, natural ventilation, direct evaporation cooling, and indirect evaporation cooling. It can be seen from Table 2 (a-f) that the measures suitable for improving the thermal comfort of the local climate in Baihua Village are as follows: adopting high-heat melt enveloping material to increase heat storage capacity, strengthening nighttime and natural ventilation, and indirect evaporation cooling. Compared with other measures, passive solar energy and direct evaporation cooling methods are slightly less effective. The main reason for this phenomenon is that Baihua Village is in the subtropical monsoon climate zone, and the solar radiation intensity is not high.

Table 1. Total Annual Solar Radiation (MJ/mˆ2) in Major Cities of China in 2001.

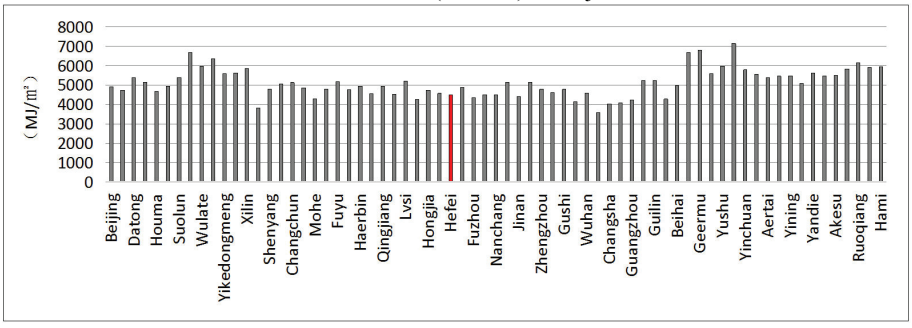

Table 2. Comparison of Passive Measures Before and After Use.

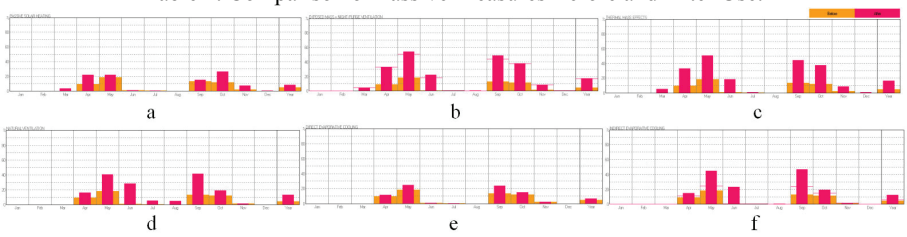

3.1.3. Wind analysis

The Wind Analysis figure includes Wind frequency (colour depth), Wind direction (circular coordinate), and Wind speed (vertical coordinate) (Figure 3). The figure shows the Wind environment of Hefei in 12 months, and the comprehensive Wind environment of the whole year. It can be judged from the figure that the perennial wind direction of Hefei is the southeast wind in summer, south wind and east wind in a transitional season, and northwest wind prevails in winter with obvious seasonality. The architectural design can guide the use of the dominant wind in summer and transitional season to prevent and weaken the prevailing wind in winter, to achieve natural ventilation, dehumidification, and cooling.

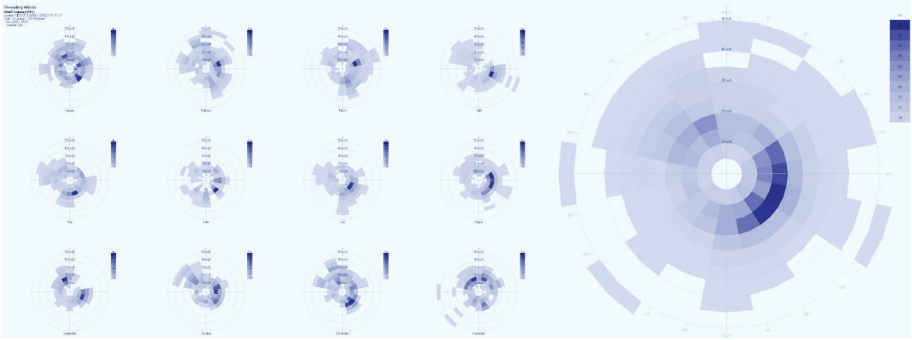

Figure 3. Wind Environment in 12 Months and the Whole Year of Hefei.

3.2. FORM OPTIMIZATION

3.2.1. Shape

The sloping roofs, courtyards, and single shapes of the original village buildings have become the key reference objects for the new buildings in Baihua Village. The architectural shape elaboration is shown in Figure 4: According to the status quo of the base boundary, conduct site slope finding treatment (a); Limit the scope of new buildings and level off the site (b); Determine the body block area and limit the height (c); Divide the block according to the optimal orientation and site form (d); Set the location of the air shaft and the height of the wind guide wall to create ventilation conditions (e); Set the way to enter the building, use the space in the

west direction and the space in the north direction, and minimize the occupancy of the lighting resources in the south direction (f); The bottom is raised on stilts to form a ventilation corridor (g); Build a semi-climatic landscape platform between the blocks (h); Rammed earth envelope, independent block (i); External balcony, separated from the main load bearing system (j); Select sloped roof elements and place solar water heaters (k); Assist the roof of the north-facing slope to avoid direct sunlight and build a roof rest platform with full climate (l).

3.2.2. Function

The best orientation of Baihua Village is due south, and the accommodation and other main functions are set in this area according to the topographic characteristics of the base. The meeting room and reception room are designed to face the southeast. Combined with the traditional architectural features of Baihua Village, courtyard space and landscape platform are added to assist the main building in ventilation and lighting. The surrounding scenery of the project is pleasant. The interactive experience between humans and nature is fully considered in the design, and the visual effect is also considered (Figure 5).

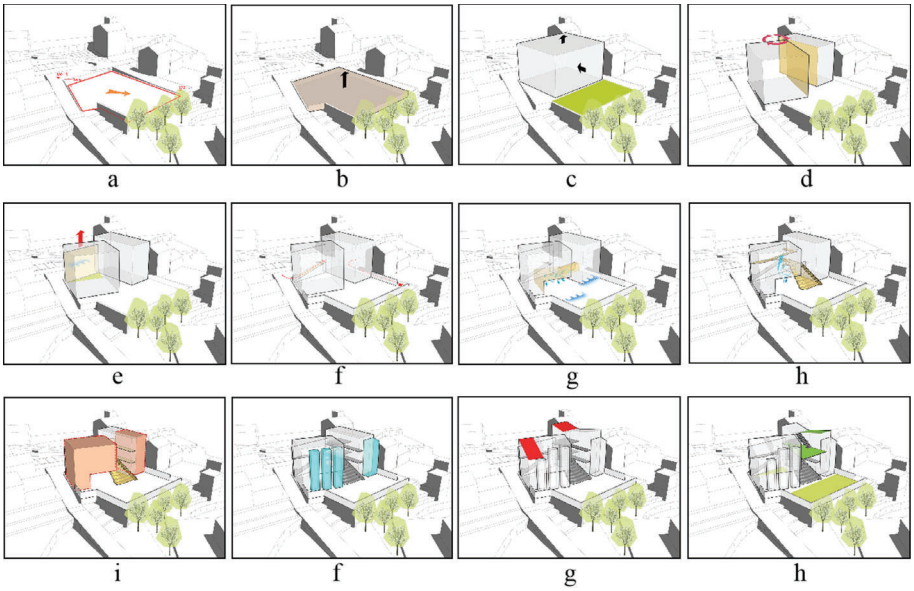

Figure 4. Healthy Building Technology Deduces Building Form.

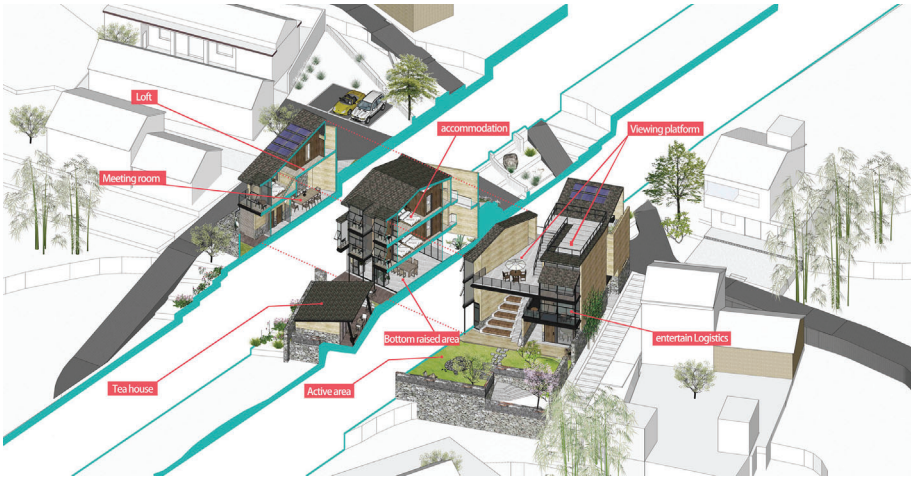

Figure 5. Planar Function Configuration.

3.2.3. Facades

This building facade selects the contemporary curing agent rammed earth enveloping material. This material overcomes the defects of the traditional rammed earth wall, effectively increases the load-bearing capacity of the wall, and is convenient for construction with low cost. Besides, the annual solar radiation of the base is sufficient, the summer rainy season rainfall is large, and the natural water resources outside the base are abundant. So, auxiliary facilities such as wind guide patio, solar thermal equipment, balcony without heat bridge, and rainwater collector are set to realize the optimization of the building form (Figure 6).

Figure 6. Configuration Optimization Technique Tests the Integration.

3.3. OUTDOOR SHADOW RANGE

Hefei city is located in north latitude N31°49' 21.30". Under sunny conditions, the intensity of solar radiation energy and ultraviolet radiation received on the surface of the earth is directly proportional to the sine of the solar altitude angle. The lower the latitude, the higher the altitude Angle of the sun, the more solar radiation energy the earth receives, and the higher the relative temperature. It can be seen from the shadow range that the sun's altitude Angle is the largest in a day at noon, is larger in summer than in winter, the maximum at the summer solstice and the minimum at the winter solstice. According to the outdoor shadow range of different period to set the Angle of solar photovoltaic system equipment and its distribution form, to get the best slope and orientation of slope roof (Figure 7).

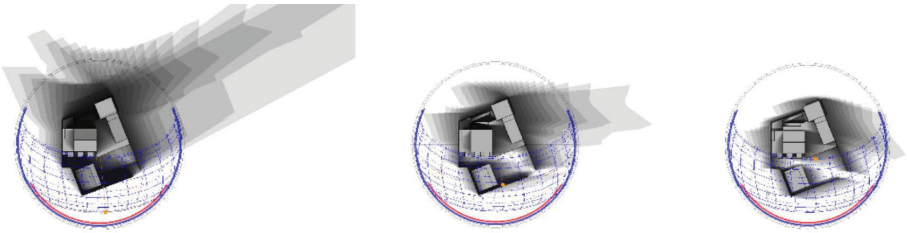

Figure 7. Shadow Range in Winter, Transition Season, and Summer.

3.4. INDOOR MICROCLIMATE

3.4.1. Natural lighting

Existing national norms, for different attributes of the building to the use of an indoor natural light area, lighting coefficient, and other aspects to make detailed provisions. Ecotect V5 software was used to simulate the daylight lighting situation of the design building, and daylight elements were divided into 11 visual levels from 0 to 5.5%. We can see from the graph, the main bedroom room is north-south facing, have a better daylighting condition. The partial function uses a room, like toilet, because to daylighting requirement is not high, did not design the daylighting effect of the large area. If there is a need for functional replacement in the later stage, the optimization design can be carried out by partially adjusting the size of the window (Figure 8).

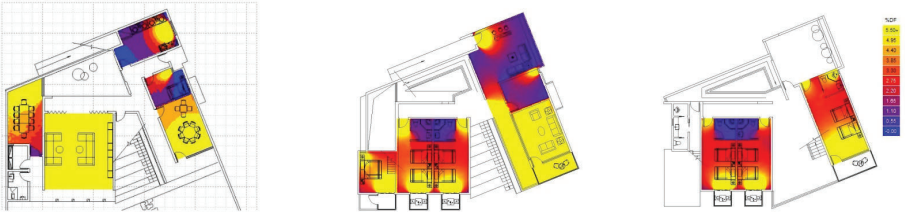

Figure 8. Daylighting Simulation Results on the First, Second and Third Floors.

3.4.2. Natural ventilation

The indoor ventilation effect of the building is a direct reflection of the optimization quality of the architectural form. The building wind environment is simulated with the help of PKPM-CFD green building software. It can be seen from Figure 9 that the building space on the first floor has a better ventilation environment due to the overhead ground floor and the installation of air Wells. The second-floor space is set south, north to the door, and the window only opens 1/3, the visible ventilated effect is not very good. As a contrast, the North-South Windows of the three floors with similar layout were all opened, and the bathroom was opened, and the ventilation effect was significantly improved. It can be seen that a good indoor wind environment can be controlled only with the help of opening Windows to guide natural ventilation (Figure 9).

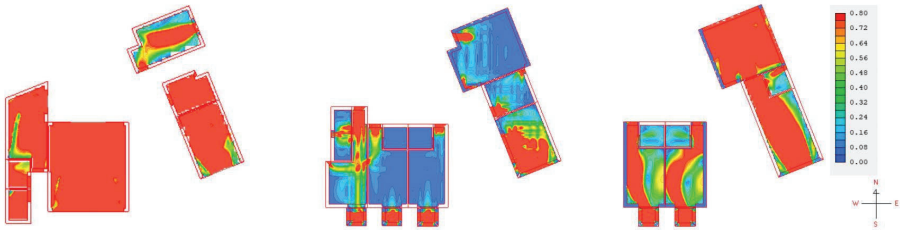

Figure 9. Plane Wind Speed Simulation Results on the First, Second and Third Floors.

3.4.3. The air age

The air age can reflect the time of air particles from entering the room to arriving at a certain point in the room, and it can also reflect the freshness of indoor air. Generally, it is used to measure the ventilation effect of the room, which is an important index for the evaluation of indoor air quality. Green building software PKPM was used to simulate the indoor environment of the building. It can be seen from Figure 10 that the blue area occupies 98% of the indoor space. Blue represents the state of zero air age. The younger the air age is, the fresher the air at this point is, the better the air quality is.

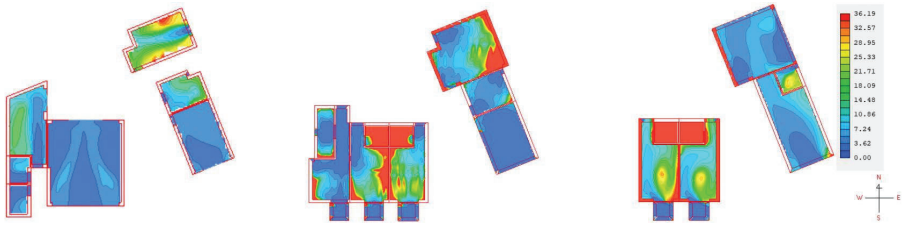

Figure 10. Plane Air Age Simulation Results of the First, Second, and Third Floors are Shown.

4. Discussions and conclusions

First of all, the paper extracts the architectural form characteristics of Baihua Village and finds the relevant elements of the microclimate environment. It is concluded that the most exposed to radiation is the winter-summer 172.5 ° east by south and east by south 100 ° according to Weather Tool software on a comprehensive interpretation of Baihua village building external environment. The simulation also revealed by enhancing dominant wind in summer and transition seasons, cut off winter prevailing winds to optimize construction form, and selects high melt palisade structure and building additional components to improve ventilation at night. Second, better solutions of different architectural forms are obtained by interpreting the results. With the help of software, the optimization strategy analysis of healthy building form in the early stage was carried out to obtain the optimal solution of building form. Third, according to the latest published healthy building standards, the simulation analysis and verification were carried out on the indoor microclimate environment such as wind, light, and heat after the optimization of the building form, to ensure the rationality of the optimized design of the building form. This paper presents the feasibility of comprehensive analysis methods and design strategies and illustrates the role of normative standards in analysis and verification. The research method of this paper has reference value in other rural areas of China and can be used to explore the combination of rural building form optimization and simulation software. In the following research, genetic algorithm (GA) and finite element analysis (FEA) methods will be considered to make the research methods and tools more scientific and reasonable, and provide a reference for other similar research.

Acknowledgments

This research was supported by “Anhui Horizon Architectural Design Co., LTD., China”; The results won the Excellence Award in the professional group of the “2020 First National Green Building Design Competition” in China and were recognized by “The School of Architecture of Southeast University”, “The School of Architecture of Tianjin University”, and “China Construction Technology Group Co., LTD”.

References

Li, B.i.n., Guo, W., Schnabel, M.A. and Moleta, T.: 2020, Feng-Shui and Computational Fluid Dynamics (CFD): Analyzing Natural Ventilation and Human Comfort, *Proceedings of the 25th International Conference of Computer-Aided Architectural Design Research in Asia*.

Li, B.i.n., Guo, W., Schnabel, M.A. and Zhang, Y.: 2020, Virtual Simulation of New Residential Buildings in Lingnan using Vernacular Wisdom, *Proceedings of eCAADe 2020.*

Maragno, G.V. and Roura, H.C.: 2010, Impacts of form - design in shading transition spaces: The Brazilian veranda, *Conference on Central Europe towards Sustainable Building*.

Olgyay, A., Lyndon, D., Olgyay, V. W., Reynolds, J. and Yeang, K.: 2015, *Design with Climate: Bioclimatic Approach to Architectural Regionalism - New and, expanded Edition*, Princeton University Press.

Schumacher, M., Schaeffer, O. and Vogt, M.: 2010, *Move: Architecture in Motion-Dynamic Components and Elements*, Princeton: Princeton Architectural Press.

THE INFLUENCE OF SPATIAL GEOMETRIC PARAMETERS OF GLAZED-ATRIUM ON OFFICE BUILDING ENERGY CONSUMPTION IN THE HOT SUMMER-WARM WINTER REGION OF CHINA

JIE DING[1] and KE XIANG[2]
[1,2]*School of Architecture, South China University of Technology*
[1]*dingjie_jessica@163.com* [2]*xiangke@scut.edu.cn*

Abstract. To investigate the influence of the spatial geometric parameters of glazed-atrium on building energy consumption, this study established a prototypical office building model in the hot summer-warm winter region in China, and simulated the effect of energy consumption of six selected factors based on orthogonal experimental design (OED). Through the statistical analysis, the results showed that the floor height and the skylight-roof ratio were the most important parameters affecting the total energy consumption, with the contribution rates of 55.5% and 18.2%, followed by the section shape parameter and the plane orientation. In addition, the floor height and the section shape parameter were closely related to the cooling load and the lighting load, respectively, and both energy consumption could be reduced to a lower degree when the atrium inner interface window-wall ratio was 60%. Finally, the optimized parameter combination and energy-saving design strategies were proposed. This study provides architects with a simplified energy evaluation of atrium spatial geometric parameters in the early design stage, and it has an important guiding significance for the sustainable development of office buildings in the future.

Keywords. Energy consumption; Spatial geometric factors; Glazed atrium; Office building; Hot summer–warm winter region.

1. Introduction

With the development of urban construction and the continuous improvement of people's requirements for building environments, building energy consumption presents an obvious rising trend. The data show that the proportion of building energy consumption in China's total social energy consumption fluctuates between 17% and 21% at present, and this proportion is expected to increase in the coming years (CABEE, 2018). Due to the characteristics of large building areas and long-running times, office buildings have huge energy consumption demands, accounting for about 20% of the total energy consumption of public buildings (Lu, 2020). Hence, it is urgent to integrate energy-saving strategies into the design of office buildings to minimize building energy consumption.

In recent years, glazed atriums have been widely used in office buildings due to their highly transparent spatial characteristics. According to the layout

PROJECTIONS, Proceedings of the 26th International Conference of the Association for Computer-Aided Architectural Design Research in Asia (CAADRIA) 2021, Volume 1, 391-400.

configurations, a glazed atrium can be divided into single, double, three, and four-sided type (Saxon, 1986). All kinds of atriums could not only provide high-quality indoor public communication space but also serve as buffer zones. Based on natural light utilization and ventilation strategies, an atrium can be used as an important passive design method to adjust indoor comfort as well as reduce artificial lighting loads and air conditioning operating times.

The influencing factors for the energy-saving design of an atrium have been a matter of concern for many researchers, mainly when using the methods of energy investigation, typical model simulation, and data analysis. It has been shown that changing an atrium's plane and section shape (Aldawoud, 2013; Zhao et al., 2017), area and volume (Nasrollahi et al., 2016; Fan and Zhang, 2020), glazing form and material (Laouadi et al., 2002; Tabesh and Sertyesilisik, 2016), and shading configuration (Palma, 2014) will have a significant impact on building thermal efficiency and ventilation efficiency, thus affecting various energy costs. In addition, only a few studies have investigated the effect of atrium geometric parameters (WI, PAR, SAR) on lighting performance (Ghasemi et al., 2016).

To date, studies on the impact of atrium spatial geometric parameters on energy performance from the perspective of passive design have been quite limited. The greatest potential of building energy conservation derives from the early design stage (Zhang et al., 2019). Hence, the early spatial design parameters closely related to the architectural forms determined by the architects, such as orientation, height, and plane aspect ratio not only affect the internal dimensions and spatial experience of an atrium but also lead to a substantial increase in energy consumption due to improper design (Wang et al., 2017; Vujošević and Krstić-Furundžić, 2017). Furthermore, the inner physical environment of an atrium is determined by multi-factors, and sometimes there may be conflicts between the design requirements corresponding to different energy-saving goals. Thus, it is necessary to consider not only the relevance of a single factor but also the coupling relationship between multiple variables and the overall energy consumption.

The aim of this paper is to fill the aforementioned research gaps. In this study, a prototypical office building in a hot summer-warm winter region was taken as an example, and combined with orthogonal experiment and variance analysis, to examine the effects of the spatial geometric factors of a glazed atrium on building energy performance and its influence degree. Additionally, the optimal parameter combination was proposed. The results show a simplified and universal energy evaluation method for the reasonable design by architects in the early design stage, and also provide a reference for passive design strategies related to the atrium spatial geometric parameters, which has important practical significance for the energy conservation of office buildings in the future.

2. Simulation experiment methods

2.1. SPACE GEOMETRY DESIGN PARAMETERS

This simulation was set in a hot summer-warm winter region in China (taking Guangzhou as an example). This area has high temperatures and relative humidity

throughout the year, as well as strong and sufficient solar radiation. Generally, the energy-saving potential of the glazed atrium in this area mainly came from reducing the cooling load and the lighting load.

With the consideration of the literature review and corresponding climate characteristics, six spatial geometric factors for double-sided atriums of general office buildings (less than 20,000 m^2) were proposed as the simulation independent variables, namely, atrium plane orientation (A), plane aspect ratio (B), skylight-roof ratio (C), floor height (D), section shape parameter (E), and Inner interface window-wall ratio (F). To analyze the effective range of these factors, 50 actual projects in nine representative cities in hot summer-warm winter regions were investigated in this study. The summarized defining characteristics are shown in Table 1.

Table 1. Design characteristics of the office building in the hot summer-warm winter region.

Design characteristics		Typical value range
Basic Building Information	Standard floor area	1500-3500 m^2
	Floor number	4F-6F
	Floor–floor height	3.6 m-4.5 m
	Outside window-wall Ratio	0.25-0.65
Atrium Design Parameters	Plane orientation	N, S, E, W
	Plane shape	rectangular, circular, polygon
	Section shape	rectangular-shaped, A-shaped
	Plane aspect ratio	1/1-1/3
	Skylight form	Horizontal
	Skylight–roof ratio	≤20% (according to GB 50189—2015)
	Inside window-wall ratio	0.4-0.8

2.2. PROTOTYPICAL MODEL SETTING

According to the above survey results, for the convenience of calculation and modeling, the final prototypical model in this study was established as shown in Figure 1. The total building area was 12,500 m^2 (2500 m^2 / floor), with a square plane that was 50 m in length and width and a double-sided atrium. The model was assumed to have five floors. The fenestration of each facade was set as the horizontal windows with a window-to-wall ratio of 0.3, and each floor was divided into three air-conditioned open zones by virtual partitions in the software.

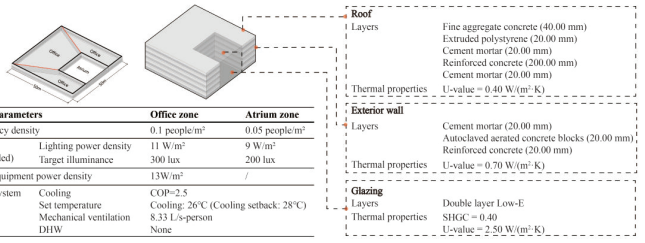

Preset parameters		Office zone	Atrium zone
Occupancy density		0.1 people/m²	0.05 people/m²
Lighting (Suspended)	Lighting power density	11 W/m²	9 W/m²
	Target illuminance	300 lux	200 lux
Office equipment power density		13W/m²	/
HVAC system	Cooling	COP=2.5	
	Set temperature	Cooling: 26°C (Cooling setback: 28°C)	
	Mechanical ventilation	8.33 L/s-person	
	DHW	None	

Figure 1. Model's envelope materials and thermal properties/other parameters setting.

In this study, an annual energy consumption simulation was performed by using the DesignBuilder (Version 6.1, EnergyPlus simulation engine, CSWD meteorological data of Guangzhou) and the calculation time was one year (8760 h). This study focused on the comparative examination of the simplified models

of general office buildings. Thus, to further reduce other influencing factors, the surrounding buildings and the shading configuration were not considered. The materials and thermal properties of the model's envelope, as well as the assumptions for the interior loads' parameters and HAVC system were determined according to the design standards of GB 50189-2015 and 2015 green building guideline in Guangzhou. The preset values are also shown in Figure 1. One should be noted that the energy influence on the heating and DHW was not included in this simulation, and only the cooling, lighting, and office equipment energy consumption was considered. The cooling period lasted from May 1 to October 31, and the common schedules for weekdays are shown in Figure 2.

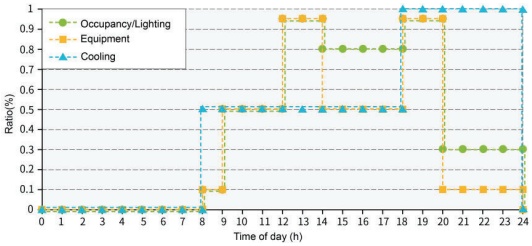

Figure 2. Schedules for occupancy, lighting, equipment, and cooling for weekdays.

2.3. ESTABLISHING ORTHOGONAL EXPERIMENT

The orthogonal experiment is an effective way to investigate the multi-factor coupling relationship by using balanced sampling and typical tests instead of comprehensive tests. In this study, $L_{27}(3^{13})$ was chosen from the standard orthogonal array to arrange the experiment. The six atrium spatial geometric variables and three change levels are displayed in Figure 3-a. It also included three error columns and two interaction columns, namely, plane orientation and plane aspect ratio (AxB), plane aspect ratio and floor height (BxD).

As shown in Figure 3-b, 27 cases needed to be simulated in total. The previous data suggested that the annual unit energy consumption of general office buildings in Guangzhou was between 60 and 90 kWh / (m^2·yr). According to the simulation, the results of all the models were within this range, and through the examination of the monthly and hourly distributions of the energy consumption, it was shown that there was no continuous overheating in the indoor temperature of the office area during the selected working period. Hence, the output results of the typical model were reasonable and could be used for further comparative analysis.

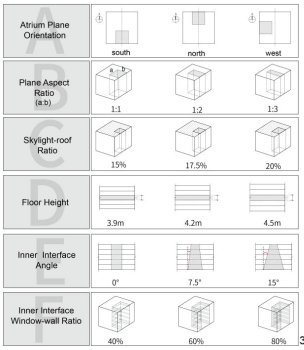

3-a

NO	1	2	3	4	5	6	7	8	9	10	11	12	13	Combination
1	1	1	1	1	1	1	1	1	1	1	1	1	1	A1B1C1D1E1F1
2	1	1	1	1	2	2	2	2	2	2	2	2	2	A1B1C2D2E2F2
3	1	1	1	1	3	3	3	3	3	3	3	3	3	A1B1C3D3E3F3
4	1	2	2	2	1	1	1	2	2	2	3	3	3	A1B2C1D1E1F2
5	1	2	2	2	2	2	2	3	3	3	1	1	1	A1B2C2D2E2F3
6	1	2	2	2	3	3	3	1	1	1	2	2	2	A1B2C3D3E3F1
7	1	3	3	3	1	1	1	3	3	3	2	2	2	A1B3C1D1E1F3
8	1	3	3	3	2	2	2	1	1	1	3	3	3	A1B3C2D2E2F1
9	1	3	3	3	3	3	3	2	2	2	1	1	1	A1B3C3D3E3F2
10	2	1	2	3	1	2	3	1	2	3	1	2	3	A2B2C1D2E3F1
11	2	1	2	3	2	3	1	2	3	1	2	3	1	A2B2C2D3E1F2
12	2	1	2	3	3	1	2	3	1	2	3	1	2	A2B2C3D1E2F3
13	2	2	3	1	1	2	3	2	3	1	3	1	2	A2B3C1D2E3F2
14	2	2	3	1	2	3	1	3	1	2	1	2	3	A2B3C2D3E1F3
15	2	2	3	1	3	1	2	1	2	3	2	3	1	A2B3C3D1E2F1
16	2	3	1	2	1	2	3	3	1	2	2	3	1	A2B1C1D2E3F1
17	2	3	1	2	2	3	1	1	2	3	3	1	2	A2B1C2D3E1F1
18	2	3	1	2	3	1	2	2	3	1	1	2	3	A2B1C3D1E2F2
19	3	1	3	2	1	3	2	1	3	2	1	3	2	A3B3C1D3E2F1
20	3	1	3	2	2	1	3	2	1	3	2	1	3	A3B3C2D1E3F2
21	3	1	3	2	3	2	1	3	2	1	3	2	1	A3B3C3D2E1F3
22	3	2	1	3	1	3	2	2	1	3	3	2	1	A3B1C1D3E2F2
23	3	2	1	3	2	1	3	3	2	1	1	3	2	A3B1C2D1E3F3
24	3	2	1	3	3	2	1	1	3	2	2	1	3	A3B1C3D2E1F1
25	3	3	2	1	1	3	2	3	2	1	2	1	3	A3B2C1D3E2F3
26	3	3	2	1	2	1	3	1	3	2	3	2	1	A3B2C2D1E3F1
27	3	3	2	1	3	2	1	2	1	3	1	3	2	A3B2C3D2E1F2
Layout	A	AXB	B	AXB	C	D	E	F	e	BXD	BXD	e	e	A:Plane orientation B: Plane aspect ratio C: Skylight-roof ratio D: Floor height E: Section shape parameter F: Inner interface window-wall ratio e:error column

3-b

Figure 3. Six spatial geometric parameters (three change levels) and simulation arrangements.

3. Results and discussion

3.1. IDENTIFICATION OF THE SIGNIfiCANCE OF EACH PARAMETER WITH THE ORTHOGONAL METHOD

Range analysis and variance analysis (ANOVA) are commonly used to analyze the results of an orthogonal test. In this study, SPSS software was adopted to combine these two methods to examine the annual cooling, lighting, and total building energy consumption per unit area of different cases. The simulation results are presented and discussed in this section.

3.1.1. Influence of six parameters on the cooling energy consumption

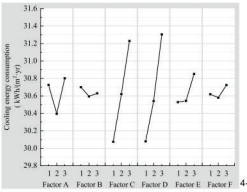

4-a

Factor	III Sum of square	F-value	P-value	Contribution rate	significance
Plane orientation (A)	0.84	30.72	0.001	5.62%	**
Plane aspect ratio (B)	0.05	1.86	0.235	0.34%	
Skylight–roof ratio (C)	6.00	220.02	0.000	40.23%	***
Floor height (D)	6.89	252.60	0.000	46.19%	***
Section shape parameter (E)	0.60	21.97	0.002	4.02%	**
Inner interface window–wall ratio (F)	0.10	3.70	0.090	0.68%	
Plane orientation (A) x plane aspect ratio (B)	0.27	4.90	0.042	1.79%	*
Plane aspect ratio (B) x floor height (D)	0.09	1.61	0.286	0.59%	
Influence degree sequence	D>C>A>E>AXB>F>BXD>B				

4-b

Figure 4. (a) Trend analysis and (b) ANOVA of influencing factors of the cooling load.

Figure 4-a shows the influence trend of six factors on the cooling load based on the range analysis. It can be seen from the figure that when the multiple parameters worked together, the impact of the plane orientation (A), skylight-roof ratio (C), and floor height (D) on cooling energy was greater than other parameters. This was because different orientations greatly affected the thermal environment and the indoor temperature of the main building, as the double-sided atrium has two solar radiation receiving surfaces, the top surface and the side. Thus, the west-facing atrium received the strongest solar radiation and had the highest cooling load. Similarly, when the skylight-roof ratio increased from 15% to 20%, the upper space had a larger heating area and the cooling load also showed an increasing trend, at 30.075 kWh / (m^2·yr) and 31.229 kWh / (m^2·yr), respectively.

Furthermore, when the floor height changed from 3.9 m to 4.5 m, the atrium indoor temperature was distributed unevenly in the vertical directions. Consequently, the cooling load increased accordingly to achieve an appropriate average temperature.

Figure 4-b presents the analysis of variance and statistical significance (P-value) of the experimental results when $\alpha = 0.05$. The results suggested that the effects of factors A, C, D, E, and AxB were statistically significant, with P-values of 0.000, 0.000, 0.001, 0.002, and 0.042, respectively. The F-value indicated the relative importance of each factor. Accordingly, for the cooling energy consumption, the influences of the six atrium spatial geometric factors were ranked as D > C > A > E > F > B. The contribution rates of factors D and C were as high as 46.19% and 40.23%, while factors A and E are secondary influencing parameters, and the interaction between BxD is not obvious.

Additionally, previous studies suggested that for the central atrium, the cooling load simulation results were narrow-shaped atrium > square-shaped atrium (Aldawoud, 2013). However, In this study, for a double-sided atrium with mixed effects of multiple factors, the cooling load was narrow-shaped (south-north) < square-shaped. This was because the decrease of the atrium plane aspect ratio in the east-west direction meant the increase of the south-north depth, that is, the width of the external heating surface decreased instead, which ultimately led to the reduction of the cooling load. Hence, in the initial stage of design, it is better for architects to minimize the width of an atrium outside interface that is unnecessarily exposed to direct sunlight to reduce the cooling energy consumption accordingly.

3.1.2. Influence of six parameters on the lighting energy consumption

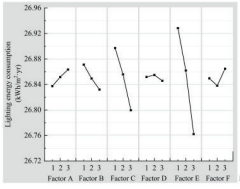

5-a

Factor	III Sum of square	F-value	P-value	Contribution rate	significance
Plane orientation (A)	0.003	1.255	0.350	1.62%	
Plane aspect ratio (B)	0.007	2.779	0.140	3.58%	
Skylight-roof ratio (C)	0.043	17.411	0.003	22.46%	**
Floor height (D)	0.000	0.146	0.867	0.19%	
Section shape parameter (E)	0.126	50.806	0.000	65.52%	***
Inner interface window-wall ratio (F)	0.003	1.303	0.339	1.68%	
Plane orientation (A) x plane aspect ratio (B)	0.001	0.252	0.898	0.65%	
Plane aspect ratio (B) x floor height (D)	0.001	0.167	0.948	0.43%	
Influence degree sequence	E>C>B>F>A>AXB>BXD>D				

5-b

Figure 5. (a) Trend analysis and (b) ANOVA of influencing factors of the lighting load.

Figure 5-a presents the trend analysis of influencing factors of the lighting load. In contrast to the variation rules of the cooling load, the result of the lighting load did not show a significant difference with the influence of the floor height (D). The plane aspect ratio (B), skylight-roof ratio (C), and section shape parameter (E) had a greater impact on the lighting load, among which the factors C and E were significantly negatively correlated with the lighting load. This was because the space close to the atrium side interface made the best use of natural light. With the increase of the skylight-roof ratio and the change of the inner interface angle from 0° to 15°, both sides of the atrium and the ground space could receive more direct sunlight, ultimately reducing the need for artificial lighting.

In the same way, the atrium plane aspect ratio decreased from 1/1 to 1/3, which was equivalent to expanding the available natural lighting depth of the

functional areas, so its impact on the lighting load was consistent with the variation trends of factors C and E. This result was similar to the study of Boubekri et al.(1994), that is, increasing the plane width-length ratio was an effective method for gaining side-lighting. Therefore, the narrow-shaped plane was better than the square-shaped plane in reducing the lighting load of the atrium.

According to the F-value and the P-value (figure 5-b), it could be determined that factor E had the most significant impact on the lighting energy consumption, followed by factor C, with the contribution rates of 65.5% and 22.5%, respectively, and other factors were general influencing factors. As a result, for atrium design in hot-humid climate areas, the A-shaped section design was superior to the rectangle-shaped section design, especially when the ratio of width to length was relatively large, the significantly reduced lighting energy consumption could be expected when the skylight-roof ratio and floor height were designed properly.

3.1.3. Influence of six parameters on the total annual energy consumption

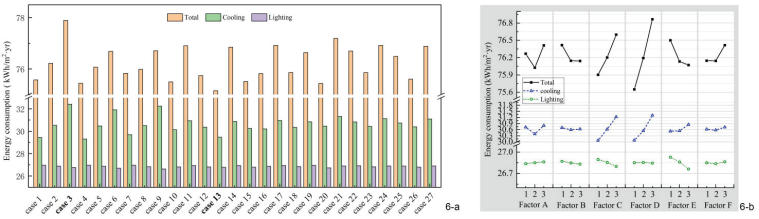

Figure 6. (a) Energy consumption simulation results of 27 cases. (b)Trend analysis of influencing factors of the total/cooling/lighting load.

Figure 6-a displays the simulation results of 27 cases in the three-level variation range of the six factors. We found that the total energy consumption per unit area was the highest in case 3 and the lowest in case 13. The difference in the total energy consumption between the two cases was about 3.5%. Generally, the increase in the cooling load was mainly responsible for the increase in the total energy consumption in all models. However, when the increase of cooling energy consumption was less than the decrease in lighting energy consumption, the total energy consumption was also expected to decrease.

As shown in Figure 6-b, the total energy consumption trend graph was added to the cooling and lighting energy consumption trend graph. Although the lighting load decreased with the increase of the skylight-roof ratio, the cooling load increased sharply due to the influence of solar radiation on the top interface, which eventually led to a substantial increase in the total load. This changing trend also applied to factor D. In contrast, changing the atrium section shape parameter was not very effective in reducing the cooling load, but it helped to reduce the lighting load, so the total load decreased with the increase of the atrium side interface angle. Furthermore, the results showed the inner interface window-wall ratio had little impact on the building energy consumption, but when the ratio was 60%, the annual cooling load and the lighting load could both reach lower values. Thus, a

reasonable design of the inner interface window-wall ratio could not only promote ventilation, but also contribute to the utilization of the natural light to achieve the goal of reducing the building energy consumption to some certain extent.

As can be seen from table 2-a, under the joint effect of the six spatial geometric parameters, the degree sequence of their influence on the total building energy consumption from high to low was floor height > skylight-roof ratio > section shape parameter > plane orientation > plane aspect ratio > inner interface window-wall ratio. The floor height and the skylight-roof ratio were particularly significant influencing factors, with contribution rates of 55.5% and 18.2%, respectively. Among the other factors, the contribution rates of the plane orientation and the section shape parameter ranged between 5% and 8%, while the plane aspect ratio and the inner interface window-wall ratio had less influence on the total energy consumption, with the contribution rate being less than 4%. Moreover, the interaction between AxB and BxD did not seem to be significant.

Table 2. (a) ANOVA and (b) Interaction analysisof influencing factors of the total load.

Factor	III Sum of square	F-value	P-value	Contribution rate	significance
Plane orientation (A)	0.677	6.251	0.034	5.63%	**
Plane aspect ratio (B)	0.445	4.108	0.075	3.70%	*
Skylight–roof ratio (C)	2.183	20.163	0.002	18.17%	***
Floor height (D)	6.667	61.587	0.000	55.51%	***
Section shape parameter (E)	0.969	8.952	0.016	8.07%	**
Inner interface window–wall ratio (F)	0.435	4.018	0.078	3.62%	*
Plane orientation (A) x plane aspect ratio (B)	0.204	0.942	0.500	1.70%	
Plane aspect ratio (B) x floor height (D)	0.107	0.494	0.742	0.89%	
Influence degree sequence	D>C>E>A>B>F>AXB>BXD				

2-a

AXB	Plane orientation (A)			
		A1	A2	A3
Plane aspect ratio (B)	B1	76.562	76.368	76.491
	B2	76.067	76.049	76.325
	B3	76.176	**75.836**	76.420

BXD	Plane aspect ratio (B)			
		B1	B2	B3
Floor height (D)	D1	75.764	75.596	**75.590**
	D2	75.764	76.491	76.674
	D3	77.169	76.694	76.732

2-b

3.2. OPTIMAL SPACE DESIGN PARAMETERS FOR ATRIUM ENERGY-SAVING

According to the analysis described in Section 3.1 and the interaction results (table 2-b), the optimal combination of the six parameters to obtain the lowest energy consumption was determined as $A_2B_3C_1D_1E_3F_2$. This combination was characterized by the north atrium, with a plane aspect ratio of 1/3, a skylight-roof ratio of 15%, a floor height of 3.9 m, an inner interface angle of 15°, and an inner interface window-wall ratio of 60%. After the further simulation, it was confirmed that the optimized design model could be more energy-saving, with the unit cooling energy consumption of 28.996 kWh / (m^2·yr), and the unit total energy consumption of 73.659 kWh / (m^2·yr). By comparison, the optimal model could save up to 10.52% more cooling load than the highest model could, and the difference of the total energy consumption between the two could reach 5.4%. It is worth noting that the step difference between the floor height and the skylight-roof ratio in this study was set to be small, so when the value range is further expanded, it would produce a higher difference in the energy-saving effect.

Finally, through the investigation and comprehensive consideration of the influencing factors, we proposed the energy-saving design strategies for glazed atriums in a hot summer-warm winter region. First, with the condition of a certain floor area, reducing the floor height can significantly improve the energy-saving effect. Second, since solar penetration might seriously influence the physical environment of the functional areas, thus affecting various energy costs, the design of the double-sided atrium should give priority to the north side. Moreover, based on meeting the actual lighting needs, it is better to reduce the skylight-roof ratio

as much as possible and to place shading devices or vertical skylights to avoid direct sunlight. Third, the architects should consider a specially-shaped atrium in combination with passive design strategies, such as adopting an A-section atrium, which is conducive to natural ventilation, and appropriately reducing the plane aspect ratio to achieve the goal of energy conservation.

4. Conclusion

Based on the orthogonal experiment and variance analysis, in this study, the influence of glazed atrium spatial geometric parameters on the energy consumption of office buildings in the hot summer-warm winter region of China was investigated. The conclusions are as follows:

1) The atrium spatial geometric parameters are important factors to be considered in passive design. Generally, the influence of the cooling load on the total energy consumption is greater than that of the lighting load.

2) When the six spatial geometric parameters listed in this study worked together, the influence degrees sequence on the total annual building energy consumption per unit area were ranked as floor height > skylight-roof ratio > section shape parameter > plane orientation > plane aspect ratio > inner interface window-wall ratio. The contribution rates of the floor height and the skylight-roof ratio were 55.5% and 18.2%, respectively. In addition, the floor height and the skylight-roof ratio had a greater influence on the cooling load, while the skylight-roof ratio and section shape parameters were more important to the lighting load. When the atrium inner interface window-wall ratio was 60%, these two kinds of energy consumption could be reduced to a lower degree. Hence, a better energy-saving effect can be achieved by reducing the floor height as well as adopting a smaller skylight area and reasonable section shape.

3) With the comprehensive consideration of the energy influence of the six parameters, an optimal parameter combination with minimum cooling and the total load was presented. That is, the north atrium with a plane aspect ratio of 1/3, a skylight-roof ratio of 15%, a floor height of 3.9 m, a section shape parameter (inner interface angle) of 15°, and an inner interface window-wall ratio of 60%. By comparison, the differences in cooling load across the considered models could be up to 10.5%, and the total load difference could reach 5.4%. This study provides architects with a simplified energy impact evaluation in the early design stage, which could be applied to the simulation analysis and passive design strategy research for some similar climates and different types of buildings in the future.

4) Limitations and future work. First, there were five thermal design zones in China, and this study was limited to the hot summer-warm winter region. The influence of a glazed atrium on the cooling and heating load will vary greatly in different climatic areas. Hence, for these areas, a designer would need to balance the effects of the two loads when making a reasonable design. Second, the results of this study are only applicable to specific assumptions. Changes of parameters that would have a great impact on the simulation, such as the glazing type and comprehensive efficiency of the cooling system would significantly alter the conclusion. In addition, in the early stage of design, architects need

to consider various factors, including building form, economic cost, technical difficulty, thus, the ranking and optimization of spatial geometric factors provide only a preliminary decision-making reference for architects to evaluate the energy consumption impact. Indeed, the selection of design parameters at the present stage was not comprehensive, only the basic parameters with great influence were adopted. Based on the typical model established in this study, in future work we hope to utilize computational power to simulate more spatial design parameters with higher analysis standards, such as different glazed atrium types, plane shapes, and skylight forms to obtain more comprehensive results.

Acknowlegements. This research was supported by National Key R&D Program of China (no. 2017YFC0702309).

References

Aldawoud, A.: 2013, The influence of the atrium geometry on the building energy performance, *Energy and Buildings*, **57**, 1-5.

Boubekri, M. and Anninos, W. Y.: 1996, Daylighting Efficiency of an Atrium: Part 1-The Four-Sided Type, *Architectural Science Review*, **39**(2), 75-81.

China Association of Building Energy Efficiency, C.: 2019, China energy consumption report, *architecture*, **02**, 26-31.

Fan, Z.Y. and Zhang, Y.H.: 2020, Numerical Investigation of key design parameters impact on energy consumption of commercial complex distributed atrium in cold area of China, *IOP Conference Series: Earth and Environmental Science*, 012024.

Ghasemi, M., Kandar, M. Z. and Noroozi, M.: 2016, Investigating the effect of well geometry on the daylight performance in the adjoining spaces of vertical top-lit atrium buildings, *Indoor and Built Environment*, **25**(6), 934-948.

Laouadi, A., Atif, M. R. and Galasiu, A.: 2002, Towards developing skylight design tools for thermal and energy performance of atriums in cold climates, *Building and Environment*, **37**(12), 1289-1316.

Lu, Y.R.: 2020, Study on Energy Consumption of High-rise Office Buildings in Zhengzhou Based on Design Builder Simulation, *Journal of Shandong Agricultural University (Natural Science Edition)*, **51**(02), 355-359.

Nasrollahi, N., Abdolahzadeh, S. and Litkohi, S.: 2015, Appropriate geometrical ratio modeling of atrium for energy efficiency in office buildings, *Journal of Building Performance*, **6**(01), 95-104.

Palma Rojas, D.: 2014, Atrium building design: key aspects to improve their thermal performance on the Mediterranean climate of Santiago de Chile, *International Journal of Low-Carbon Technologies*, **9**(4), 327-330.

R. Saxon (ed.): 1983, *Atrium Buildings: Development And Design*, Architectural Press, LONDON.

Tabesh, T. and Sertyesilisik, B.: 2016, An investigation into energy performance with the integrated usage of a courtyard and atrium, *Buildings*, **6**(2), 1-20.

Vujošević, M. and Krstić-Furundžić, A.: 2017, The influence of atrium on energy performance of hotel building, *Energy and buildings*, **156**, 140-150.

Wang, L., Huang, Q., Zhang, Q., Xu, H. and Yuen, R. K.: 2017, Role of atrium geometry in building energy consumption: The case of a fully air-conditioned enclosed atrium in cold climates, China., *Energy and Buildings*, **151**, 228-241.

Zhang, Z., Li, W.Z. and Ying, X.Y.: 2019, Research on Parameterization for Shape of Standard Floor of Office Buildings under a Low-Energy Consumption Target, *South Architecture*, **2019**(01), 76-81.

Zhao, W., Kang, J. and Jin, H.: 2017, Influence Of Architectural Factors On Physical Environment In Atria, *Architecture Technology*, **48**(07), 779-782.

BIO-ENERGY MANAGEMENT FROM MICRO-ALGAE BIO-COMPUTATIONAL BASED REACTOR

FARAHBOD HEIDARI[1],
MOHAMMAD HASSAN SALEH TABARI[2],
MOHAMMADJAVAD MAHDAVINEJAD[3], LISS C. WERNER[4] and
MARYAM ROOHABADI[5]
[1]*Ph.D.Student in Architecture,Department of Architecture,Tarbiat Modares University, Tehran, Iran*
[1]*f-heidari@modares.ac.ir*
[2]*Master of Bionic Architecture,Pars University of Art and Architecture, Tehran, Iran*
[2]*saleh.tabari@gmail.com*
[3]*Professor of Department of Architecture, Tarbiat Modares University, Tehran, Iran*
[3]*mahdavinejad@modares.ac.ir*
[4]*Professor of Bio-Inspired Architecture and Sensoric, Institute of Architecture ,Technische Universitat Berlin,Berlin,Germany*
[4]*liss.c.werner@tu-berlin.de*
[5]*Master of Architecture, Department of Architecture, Tarbiat Modares University, Tehran, Iran*
[5]*roohabadimaryam@Modares.ac.ir*

Abstract. Microalgae are a sustainable source of unique properties with potential for various applications. Biofuel production has led to the use of them as bioreactors on an architectural scale. Most of these efforts cannot manage the output due to the lack of intelligent control and monitoring over environmental micro-scale growth. This research presents the possibility of control and monitoring over the bio-energy retrieved through micro-organisms in bio-reactors, specifically the growth environment's computation. To achieve monitoring, three dimensions of the medium culture captured by cameras, and with the advantage of image processing, the picture frames pixel values measured. In this process, we use the Python OpenCV Library as an image processing reference. Finally, a specifically developed algorithm analyses the calculated 3d-matrix. By changing the environmental parameters, control happens by directly recognizing changes in density and outputs. This research's computational process has proposed a novel approach for controlling particle-based environments to reach the desired functions of microorganisms, This approach can use in a wide range of cases as a method.

Keywords. Bio-Computation; Monitoring; Image Processing; Pattern Recognition; Multi-Functional Bio-Materials.

PROJECTIONS, Proceedings of the 26th International Conference of the Association for Computer-Aided Architectural Design Research in Asia (CAADRIA) 2021, Volume 1, 401-410.

1. Introduction

Microalgae are photosynthetic microorganisms that live in the aquatic medium culture and can tolerate environmental conditions changes. They can be growth in the medium culture as a group or individually, which changes their unique properties during the growth steps. Microalgae are an essential source of carbon dioxide and various biological products widely used to produce biofuels, food industry, pharmaceuticals, and wastewater treatment (Barsanti et al.2008;Das et al.2011;Brennan and Owende .2010). This materials can be used for a wide range of applications, such as Architectural Component, the use of bio-materials for large scale architectural and engineering applications is still underdeveloped (Benyus 1997; Vincent 2012). In recent years, micro-algae has received much attention as a bioreactor to be embedded into buildings to produce renewable energy (Pasquero and Poletto,2020). In most of these efforts, two main and fixed methods use to cultivate algae: Raceway pond systems and photobioreactors (PBRs). "A typical raceway pond comprises a closed loop oval channel, w0.25e0.4m deep, open to the air, and mixed with a paddle wheel to circulate the water and prevent sedimentation (Ponds are kept shallow as optical absorption and self-shading by the algal cells limits light penetration through the algal broth). In PBRs the culture medium is enclosed in a transparent array of tubes or plates and the micro-algal broth is circulated from a central reservoir. PBR systems allow for better control of the algae culture environment but tend to be more expensive than raceway ponds "(Slade and Bauen 2013). These methods apply for biological fuel production and air purification with limited architectural scale forms. Energy generation through micro-algae is divided into two main phases. In the first step, the biomass that is created by them will collect. In a second step, the biomass is converted into renewable energies through multiple-stages processes such as thermochemical or bio-chemical, which are utilizing expensive equipment with low efficiency (Singh and Sharma,2012). In these processes and methods, parameters such as oxygen and light use to control the growth and outputs efficiency, which is controlled by the timing of oxygen injection or the quantity of light in laboratory environments with limited computing infrastructure. At the architectural scale, due to the reality of various forms and structures and different environmental conditions, the parameters affecting growth perform a more critical role that cannot be calculated with limited laboratory infrastructures. To use personalized bioreactors on the architectural scale, industrialization and, mass customized production, we need to use methods beyond the individual controlling parameters (Haidari et al.2017;Heidari et al.2018;Bitaab et al.2018). That can adapt to different environmental conditions, and in an intelligent interface, it can compute changes with a multitude of parameters. On the other hand, the use of multi-stage energy production methods at the architectural scale, due to various forms, limit the use of this type of sustainable mechanisms in mass production and slow down its development process. When living materials is used in a structure, there are various ways to guide those to the designer's specific goals. In addition, to direct control by DNA and determining their behavior, this control can be done by controlling environmental parameters. Due to various forms on the architectural scale, environmental parameters are set in different

situations and typologies relative to microorganisms. These multiple behaviors with computations in the ideal environment by the handy tools have significant gaps, such as determining microorganism's real-time behavior relative to input parameters and their output efficiency. The lack of integrated biocomputational infrastructure in architecture has led to the lack of development of microorganisms in this area to achieve the goals defined by the architects and designers. These constraints have made bioreactors on an architectural scale limited to specific forms and positions and added to the buildings as separate components. They can additionally identify as building and Form. These restrictions will lead to the lack of development of creative approaches in this field and the death of ideas at the scale of biology and architecture laboratories due to the inability to develop them industrially. To fill these gaps, we need to monitor and control the medium culture designed as a bioreactor to directly change the medium culture growth environment by changing the environmental parameters. These analyses provide the ability to controlling outputs and recognizing, including biological energy, particle movement detection, density, and diffusion.

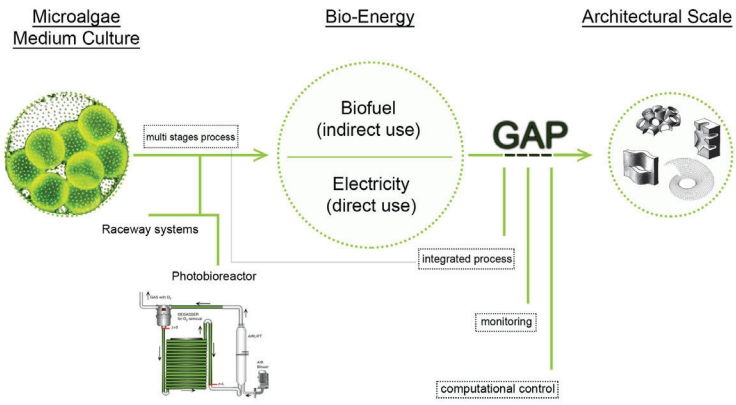

Figure 1. The Gap between biological functions in laboratory and mass customization in architecture.

2. Research Structure

The Western tradition of prioritizing mind over matter, along with the long time governed architectural discourse, developed in the sixteenth century by Leon Battista Alberti, draws a clear distinction between the responsibilities of the architect and those of the builder, separating the mental labor of design from the physical labor involved in materials and construction. (Cardoso Llach,2015). It is important to define the difference between bio-inspired and bio-integrated design.

Biomimicry is defined as imitating or taking inspiration from nature's forms and processes to solve human problems (Benyus, 1997). To use bioreactors as an architectural component, there is a need to design them in various forms, with the ability to control and detect micro-scale particles in them and eliminate the multiple-stages of energy production. In most past efforts, the medium culture's control done through various detection modules, including ultrasonic, thermal modules, or lighting. Due to the real-time changes in the density and diffusion of microorganisms in the growth medium, this sensors and modules methods have computational faults and cannot evaluate at the micro-scale and cover a large diffusion volume. On the other hand, libraries of these modules limit to specific commands that will not support various environmental conditions on an architectural scale. This research's primary focus is on controlling and monitoring the medium culture and their output, which implement the growth process of the specific type of micro-algae called "Spirulina." The multi-stages energy production process is eliminated and performed directly by the electrodes from the medium culture to produce energy connected with microorganisms' growth. Three cameras are placed in three dimensions to implement the monitoring through image processing (top, left, right) to capture the medium culture. The medium culture was captured for four days, with an interval of 15 minutes. To control the growth environment, oxygen used as a critical parameter, If we assume that the flow of oxygen injected into the medium culture on the first day is 1 liter per minute, 1 liter per minute is added to its flow rate daily, and finally, on the fourth day of capturing, it reaches 4 liters per minute, so that the effect of this process changes in output growth and energy. The medium culture's nutrient, including light, temperature, humidity, and the cameras' distance from the medium culture, is fixed and does not change during the capturing days.

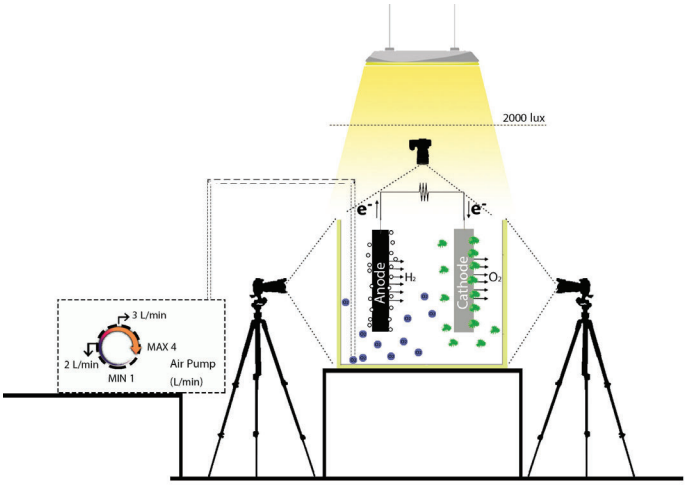

Figure 2. Overview of Project.

3. Material and Methods

3.1. IMAGE PROCESSING

When we talk about image processing, we want to analyze an image's numerical matrix. Matrices in images are the same pixels that make them up, this reason, the capturing resolution of our different dimensions determines the number of pixels and, finally, our matrices' formation. In a two-dimensional image, the pixels are positioned in the x and y directions, each with a numeric value determined by RGB. This value in each image is directly related to the camera settings, which must also be set to RGB. After completing the Image processing in different dimensions, we have a set of medium culture images in triplicate at certain times, which generally determines our microorganism's growth graph at specific intervals. We use the Thresholding method to binary these images and convert them into two colors in black and white. In general, with this method, the images are remapped to the numeric range 0 and 1.

3.1.1. Pre-Processing

Before this round, we need a pre-process to remove the noises from the images. In this project, three steps define to reach this goal. Due to the presence of micro-algae microorganisms in the medium culture, its color composition is in the green range; in the first step, we filter the green color in binary images. After this stage, the image contrast increases, and microorganisms appear in the medium culture. This process changes the triple numeric arrays between the initial 0 to 255 of the images to our regular range, and these high-contrast images can measure by Thresholding.

Noises are pixels with specific numerical values whose value of RGB is unbalanced with the Context RGB value. After increasing the contrast of the images, noises appear in it, and due to the microorganisms' micro-scale, they are known as noise. We use the "Gaussian Function" to remove noises. "Gaussian Function" averages each pixel's numerical values with the surrounding pixels in a two-dimensional range and normalizes them in a specific command. Because of the very small scale of microorganisms, they themselves are also known as noise. We must prevent them from being removed during the Gaussian process. To prevent the removal of microorganisms from images, we use the dispatcher or exclude function. To perform this process, we write a function that, when filtering, Separate pixels whose RGB value is close to the RGB of our particles and put them in those categories, and finally executes the "Gaussian Function" for the unused pixels.

3.1.2. Thresholding

After performing the Gaussian Function and removing the noise, our images are placed close to each other in a specific numerical matrix and ready for the main Thresholding process. In this section, like the Gaussian process, we use the OpenCV library. Before starting the main Thresholding process, the image needs to be Gray style and form the main color handle with values 0 and 1 in the images. Because Thresholding analyzes based on white and black colors, by

doing Gray style, we have helped this process one step to increase its accuracy. Finally, black-and-white images and quantification fall into two general areas of context and particles, the black parts being the same medium culture and the white parts being the same microorganisms. A set of matrix shapes of numbers 0 and 1 shows the density of white parts in black, which is the same as the growth of microorganisms in different time intervals. Furthermore, it shows the growth trend in terms of density. Total density (WS) at time T is the total of two-dimensional densities in three dimensions divided by 3.

3.2. BIOLOGICAL-PROCESS

In this research, to eliminate multiple stages of energy production, a new approach has been used to directly generate electrical energy from an electrolyte solution through copper and aluminum electrodes. The oxygen parameter is injected into the medium culture through an air pump with a maximum transfer capacity of 4 liters per minute. To analyze the effect of environmental parameters on growth and the amount of energy output, the oxygen parameter has been selected as a sample. Its effect on growth rate can be seen through our defined computational process. The ambient temperature is 25 to 28 degrees Celsius, and the amount of direct light in the environment is 2000 lux. The culture medium is a cube with dimensions (20cm * 20cm * 30cm) with 12000 liters of solution. Ingredients of the culture medium, general light, distance of cameras to the culture medium are considered. Details of the ingredients of the culture medium can be seen in full in Table 1.

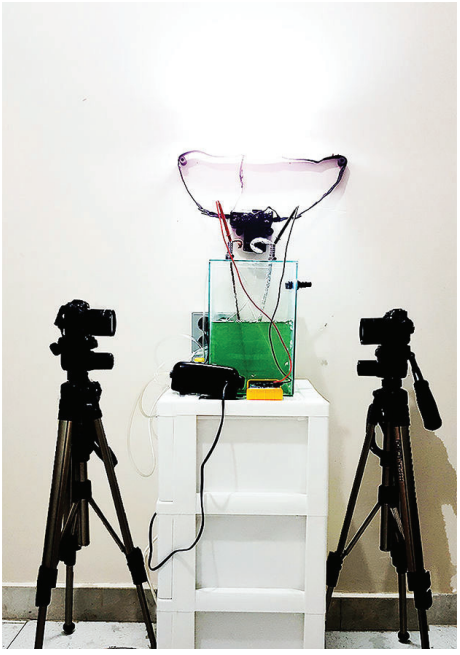

Figure 3. Real-Environment Details.

Table 1. Medium Culture and Environment Condition.

Component	Amount	PH	Temperature	Oxygen Supply	Target Tank Volume	Environmental Light	Microorganism	Medium Culture Amount
Nacl	1g	7	25-28c°	Max: 4 L/min Min: 1 L/min	20*20*30 cm 12000 ml	2000 Lux	Spirulina Algae (6000 ml)	6g
Magnesium sulfate	0.2g	5.5-6.5						1.2g
Sodium bicarbonate	16.8g	8.4						100.8g
Phosphate	0.5g	9.8						3g
Sodium nitrate	2.5g	5.5-8						15g
Potassium sulfate	1g	5.5-7.5						6g
Calcium chlorid	0.04g	5.5						0.24g
Ferrous sulfate	0.01g	2						0.06g
EDTA	0.08g	4-6						0.48g
Solotion A	1ml	7						6ml
Solotion B	1ml	7						6ml

4. Data Analysis

Based on the monitoring process, it is illustrated that as flows increased in a specific time the bacteria density is increased. From the monitoring system, during an independent day, it is achieved that bacteria have a steady growth rate on their own. The bacteria growth ratio is in an increment as the colony density is enhanced and the environment parameters are adjusted to the comfort setting. However, the interesting behavior demonstrated here from the colony is that the growth range will accelerate as the oxygen flows within the vitro. So, the fluctuation of the growth rate is represented here in the graph is because of that. The secret part is that how we can reduce this fluctuation and drive it in a sharp increment way. Thus, we did some controlled periodic flow and trying to set it with the other vitro parameters. The results will be discussed in our future works to use them in analysis phases.

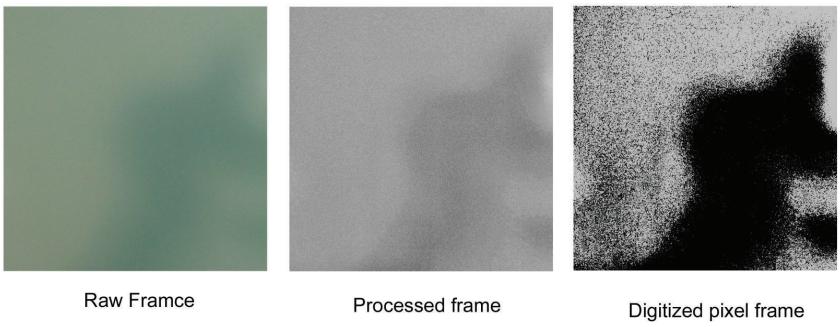

Figure 4. Filtering and Pre-Processing.

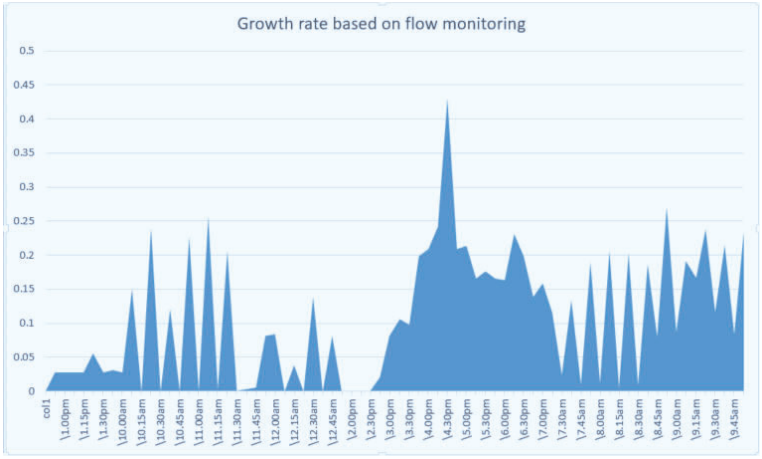

Figure 5. Sample of Growth Rate-December 9th.

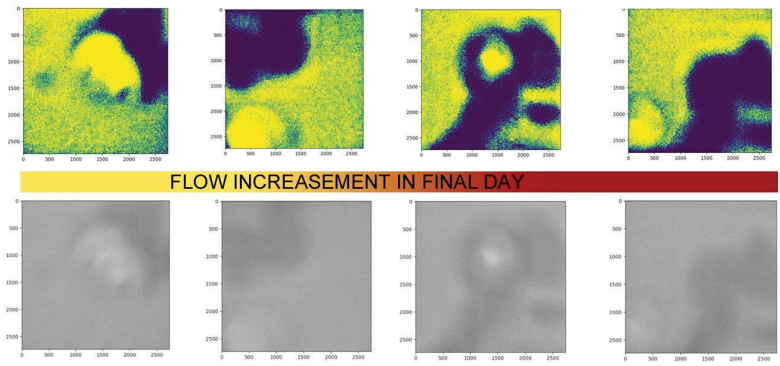

Figure 6. The effect of Oxygen flow during 4 days - An analysis of the maximum density at the end of each day.

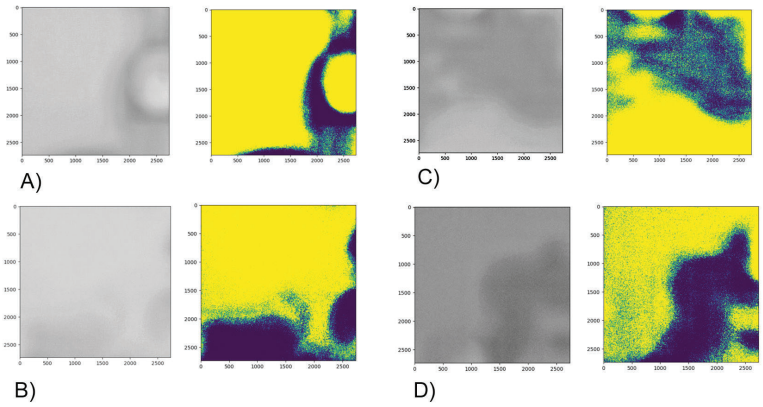

Figure 7. sample of different diffusion of microorganisms at the medium culture.

5. Conclusion

The main purpose of this study is to create a new approach to monitoring and controlling the medium culture of microorganisms with the aim of using different functions of them in the architectural scale, which has been done using image processing tools. The process defined in the computational part of this project is a method of controlling and monitoring the function to use them in the architectural scale. In the example of this project Spirulina microalgae and its biological energy have been applied as an output function on the medium culture. By using this process in monitoring the growth of microorganisms daily and in general over 4 days Recorded at any time, which grows over a period of time and shows the behavior of microorganisms with changes in environmental parameters. These behaviors allow us to observe the effect of the type of inputs and their amount on growth and ultimately its effect on output performance and achieve the desired output by changing the inputs relative to the microorganism's behavior. In this study, oxygen was considered the determining input parameter. By changing the amount of injection on different days, its effect on growth and diffusion, and finally, the biological energy of the output was investigated, both of which had an upward trend towards increasing oxygen injection Generally.

6. Outlook

This research can be performed as a method on other microorganism samples to achieve the desired functions. By eliminating the problem of monitoring and precise control of microorganism's growth environments, a platform has been provided for their use with different applications in architecture. Due to this process's micron accuracy, and behavior in the growth environment for changes in environmental parameters can be identified. On the other hand, if we want to change the genetics of microorganisms to create a function in architecture, with the method proposed in this research, the subsequent behaviors of genetic changes can

be controlled, and a step further, it will also optimize its behavior. On a small scale, by creating a platform for dynamic imaging in different parts of the building, this process will be able to be implemented simultaneously in the form of an intelligent central core in the building. This method has removed the limitation in using different forms with desired functions on an architectural scale by monitoring and controlling the microorganism's growth environment.

References

Barsanti, L., Coltelli, P., Evangelista, V., Frassanito, A.M., Passarelli, V. and Gualtieri, P.: 2008, Oddities and curiosities in the algal world., *Algal toxins: nature*, **-**, 91-353.

Benyus, J.M.: 1997, *Biomimicry: Innovation Inspired by Nature*, Quill, New York.

Bitaab, N., Heidari, F. and Khadivi Golestani, N.: 2018, Investigating Strategies for Creating Healthy Cities with Sustainable Development Approach, *European Journal of Research*, **1**, 34-44.

Brennan, L. and Owende, P.: 2010, Biofuels from microalgae- a review of technologies for production, processing, and extractions of biofuels and co-products, *Renewable sustainable energy*, **14**, 77-557.

Cardoso, L. and lach, D.: 2015, *Builders of the vision : software and the imagination of design*, Routledge, New York.

Das, P., Aziz, s.s. and Obbard, J.P.: 2011, Two phase microalgae growth in the open system for enhanced lipid productivity, *Renewable energy*, **36**, 8-2254.

Gajda, I., Greenman, J., Melhuish, C. and Ieropoulos, I.: 2015, Self-Sustainable Electricity production from algae grown in a Microbial Fuel cell System, *Bio-mass and Bio-Energy*, **82**, 87-93.

Heidari, F. and Mahdavinejad, M.: 2017, High-performance Sonitopia (Sonic Utopia): Hyper intelligent Material-based Architectural Systems for Acoustic Energy Harvesting, . *Proceedings of the 2nd International Conference on Green Energy Technology*.

Heidari, F., Mahdavinejad, M. and Sotodeh, S.H.: 2018, Renewable energy and smart hybrid strategies for high-performance architecture and planning in case of Tehran Iran, *Proceedings of the 4th International Conference on Environment and Renewable Energy*.

Pasquero, C. and Poletto, M.: 2016, *Cities as biological computers*, Cambridge University Press, Cambridge .

Pasquero, C. and Poletto, M.: 2020, Bio-digital aesthetics as value system of post-Anthropocene architecture, *International Journal of Architectural Computing*, **18**, 120-140.

Singh, R. and Sharma, S.: 2012, Development of suitable photobioreactor for algae production–A review, *Renewable and Sustainable Energy Reviews*, **16**, 2347-2353.

Slade, R. and Bauen, A.: 2013, Micro-algae cultivation for biofuels: Cost, energy balance, environmental impacts and future prospects, *Journal of Biomass and Bio-Energy*, **53**, 29-39.

Vincent, J.: 2012, *Structural Biomaterials*, Princeton University Press, Princeton.

De Wilde, P.: 2014, 'The gap between predicted and measured energy performance of buildings: A framework for investigation, *Automation in Construction*, **41**, 40-49.

FORECASTING PERFORMANCE OF SMART GROWTH DEVELOPMENT WITH PARAMETRIC BIM-BASED MICROCLIMATE SIMULATIONS

JONG BUM KIM[1], JAYEDI AMAN[2] and
BIMAL BALAKRISHNAN[3]
[1,2,3] *University of Missouri Columbia*
[1,2,3] *{kimjongb|ja2qm|balakrishnanb}@missouri.edu*

Abstract. Smart Growth is a fast-growing urban design and planning movement developed by the United States Environmental Protection Agency (EPA). These regulations control urban morphologies such as building form, position, façade configurations, building materials, road configurations, which have an explicit association with the microclimate and outdoor comfort. This paper presents an urban modeling and simulation framework that can represent the urban morphology and its impact on microclimate shaped by Smart Growth. First, we created urban models using custom parametric objects and a building component library in BIM. Then we integrated parametric BIM and multiple performance simulations, including wind analysis, solar accessibility, and energy use. For implementation, a case study was carried out using two Smart Growth regulations in the Kansas City metropolitan area. The paper elaborates on the findings from simulation results, challenges in implementation, and limitations of the proposed framework to manage a large number of regulation variables in simulation.

Keywords. Smart Growth Regulations; Building Information Modeling (BIM); Parametric Simulation; Microclimate Simulation; Computational Fluid Dynamics (CFD).

1. Smart Growth and its impact on microclimate

Smart Growth is a fast-growing urban design and planning strategy initiated by the United States Environmental Protection Agency (EPA) (Smart Growth America, 2019). In 2005, the EPA launched the Smart Growth Implementation Assistance (SGIA) program to revise traditional planning regulations that caused high car-dependency and suburban sprawl. The program has led to the adoption of design-based planning regulations. The conventional land-use and zoning focused on land-use distribution, but the Smart Growth regulations prioritize sustainable development using prescriptive design requirements and standards. These regulations control urban morphologies and building design such as building use, position on the parcel, façade configurations, exterior building materials, public landscapes, and street configurations. These design variables are inarguably

PROJECTIONS, Proceedings of the 26th International Conference of the Association for Computer-Aided Architectural Design Research in Asia (CAADRIA) 2021, Volume 1, 411-420.

associated with local microclimate, outdoor thermal conditions, and human comfort.

Smart Growth is growing fast. As of 2017, over 650 municipalities have adopted Smart Growth regulations, driving a remarkable shift in community and regional planning (Borys, et al. 2017). Strong design controls from the early planning stage become a phenomenon critical for urban modeling and simulation research. As urban regulations use more design controls, we can infer that they will have significant implications for sustainability and environmental footprints. Still, forecasting the environmental impact of planning regulations is challenging due to the complexity in regulation interpretation, urban modeling, and urban simulation. Many studies investigated various modeling and simulation methods, such as building stock models for fast urban modeling (Dascalaki et al., 2011), energy demand prediction using historical energy use data (Sandberg, et al. 2016), and assessment of the environmental footprints and greenhouse gas emissions (Ballarini, 2014). Many of these studies obtained the dataset of existing urban and building settings from Geographic Information System (GIS). While GIS has comprehensive data for spatial and attributes data sets, it is limited to envisioning the development scenarios for future community development.

This paper presents a simulation and visualization framework that can represent the urban morphology shaped by Smart Growth regulations and assess these regulation's potential impact on microclimate. We integrated parametric BIM and a multi-criteria microclimate simulation centered on pedestrian wind analysis and outdoor thermal comfort, building on our research projects on BIM-based performance simulation and visualization (Kim et al., 2020, 2019). We implemented the simulation framework through case studies of Smart Growth regulations in the Kansas City metropolitan area, including Overland Park Downtown FBC (City of Overland Park, 2018) and City of Mission's West Gateway Form-based Code (The City of Mission, 2014). Kansas City has pursued sustainable community development and downtown revitalization based upon rigorous planning efforts such as Smart Growth and Smart City initiatives. Two cases have a similar regulation structure, a similar climate condition, and different site topologies. In this case study, we explored what-if scenarios of the potential community development governed by Smart Growth regulations.

2. Parametric BIM-SIM framework for microclimate simulations

This section describes the proposed Parametric BIM-SIM framework for microclimate simulations. Figure 1 presents a workflow of parametric BIM-SIM framework development for microclimate. We conducted four research phases: (1) a data collection for modeling and simulation from Smart Growth regulations (A1); (2) parametric modeling in Building Information Modeling (BIM) (B1); (3) software prototyping for microclimate simulations (C1-C6); and (4) analysis and visualization of simulation results (D1). The overall process and methods for the regulation analysis (A1) and the parametric modeling (B1) are described in our previous research papers (Kim et al., 2020, 2019).

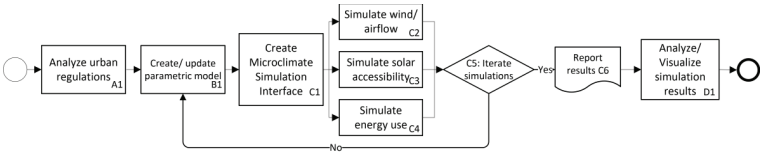

Figure 1. A workflow of Parametric BIM-SIM framework.

To create a microclimate simulation interface (C1), we connected BIM models with visual programming based simulation tools. To feed regulation variables into the simulation, we identified the required simulation variables, located relevant regulation provisions (A1), and stored them as custom parameters in BIM (B1). This mapping process is illustrated in Section 2.2. The research envisions a better understanding of the association between Smart Growth regulations and microclimates. In this context, the parametric simulation iteration (from B1 to C5) is significant to test a range of regulation variables collected in A1.

2.1. REPRESENT SMART GROWTH REGULATIONS WITH PARAMETRIC BIM

The main components for our modeling and simulation were as follows:

- Regulating Plan: District map, Transect in the Plan indicates streets, blocks, building positions, and the types of each design standards
- Building Envelope Standards (BES): Controls building height, sectional configurations, and use
- Architectural Standards: Controls façade configurations, materials, and styles
- Public Space Standards: Provides requirements for traffic lanes, pedestrians, and open space design

Regulating Plan is similar to a land-use and zoning map, providing parcel/block information, setback positions for each parcel, and Transect types. The transect is a unique classification system in Smart Growth regulation, assigning the allowed configurations of public landscapes, traffic lanes, pedestrians, building use, building typologies, and building facades. The requirements for each category are listed in streetscape standards, building envelope standards, and architectural standards. We created parametric models in BIM as a three-dimensional representation of Regulating Plan. The parametric district model consists of multiple objects, representing blocks, streetscapes, open spaces, and buildings. The building objects can variate their scales with parameter value changes. For modeling, we used Autodesk Revit and Revit API (Application Programming Interface).

2.2. DATA MAPPING FROM REGULATION VARIABLES TO SIMULATION VARIABLES

Microclimate simulation needs multi-domain performance analyses, often making input processes complicated and inaccurate. BIM database is expendable to store both regulation and simulation variables. It is also interoperable with various simulation platforms. Besides, CFD simulation demands higher computing power than other simulations do. In this context, our priorities were (1) mapping

regulation variables into simulation variables, (2) the use of the BIM database for modeling and simulation, (3) reliable simulation iterations, and (4) smooth communication between BIM and microclimate simulations. Figure 2 presents a relationship between Smart Growth regulation components, simulation variables, and microclimate simulations.

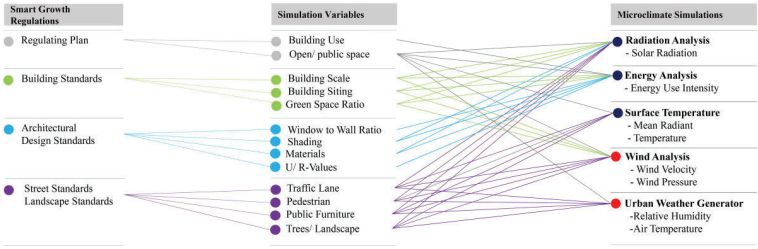

Figure 2. Parametric BIM-SIM Workflow .

Smart Growth regulations have a wide range of regulation variables associated with microclimate simulations. For example, Regulating Plan indicates the configurations of subdivisions, traffic lanes, pedestrians, building facades, public furniture, and landscapes. In our framework, we used parametric BIM as a database to store regulation variables so that the simulation interface can read such information from BIM. To do so, we identified a list of input variables from the simulation engines, collected the relevant variables from Smart Growth regulations, and stored these variables as custom parameters in BIM. Due to the different semantics between the regulations and simulations, we carried out a mapping process in the simulation interface (C1). Table 1 presents an example of the data mapping process for energy use simulation, Energy Use Intensity (EUI), in this paper.

Table 1. An example of data mapping in parametric BIM-SIM framework.

Regulation components (A1, A2 in Fig.1)	Regulation variables (A1, A2 in Fig.1)	Parametric BIM (B1 in Fig.1)	Simulation variables (C1, C3 in Fig.1)
• Regulating Plan*	• Block/ parcel information	• Building use parameters	• Wall area
• Building Standards*	• Required Building Line (RBL)	• Building parameters (height, setback, etc.)	• Window area
• Architectural Standards*	• Building section configuration	• Opening ratio parameter per building types	• R-Value
	• Façade configuration (Minimum and maximum opening requirements)	• Material properties	• U-Value

Note: *These are typical names of regulation components and sections in Smart Growth regulations.

We identified (1) building types (building-use) from Regulating Plan, (2) sectional configurations from Building standards, and (3) required opening ratios for each building type. Most Smart Growth regulations require a vertical mixed-use with varying façade requirements, which can variate each building's opening ratio. For example, fenestration control in Overland Park Downtown

Form-based Code is as follows: "Ground Story Fenestration shall comprise between 33% and 70% of the Facade...." (City of Overland Park, 2018). In BIM, we added custom parameters of the opening ratio and façade material information. To calculate total window and wall area, the simulation interface obtained the surface areas and their opening ratio parameters from BIM. Then the interface calculated the opaque wall and window areas for individual masses. As shown in Formula 1, we calculated the total window area, Awin, and wall area Awall where a building has n surfaces, the individual surface area is Sn, and the opening ratio is ORn.

$$f(\text{Awin}) = \int_1^n Sn \cdot ORn \tag{1}$$

$$f(A\text{wall}) = \int_1^n Sn \cdot (1 - ORn) \tag{2}$$

This data mapping approach minimized the hard coding input process within the simulation interfaces and enabled the simulation modules reusable for varying regulations.

3. Case Study

This section describes the implementation process explained Figure 1. For implementation, we carried out a case study of two Smart Growth regulations of Overland Park Downtown Form-based Code and City of Mission's West Gateway Form-based Code. They are suburban cities of the Kansas City Metropolitan Area. Kansas City is a few cities that actively participated in both Smart Cities and Smart Growth planning movements. Kansas City was selected in the Smart City Initiative program and has integrated information and communication technology (ICT) and sensor-based data collection through private and public collaborations. To promote the revitalization of old communities, many cities in the Kansas City Metropolitan area have adopted Smart Growth regulations. It provides Kansas City with a unique context and significance for urban planning and design research.

City of Mission and Overland Park are southern cities of Kanas City Metropolitan along highway I-35 and Metcalf Avenue. Vision Metcalf Plan is a comprehensive master plan to revitalize multi cities' downtown corridors along Metcalf Avenue. It has driven successful economic development, including $270 million of new developments, approximately 14% of the total revenue growth (City of Overland Park, 2018, 2017). Overland Park FBC is a part of the Vision Metcalf Plan, and we focused on Downtown Form District. West Gateway FBC was adopted to revitalize the 130 acres downtown district. The district's westbound is Metcalf Avenue. The two regulations have the same weather conditions, similar formats, and structures. It enabled a comparison of the impact of urban morphology of Smart Growth development on microclimate performances.

Based on the modeling method (Section 2.1), we created two district models in parametric BIM having blocks, parcels, and building objects. They have custom parameters for regulation variables and a part of simulation variables to provide inputs to microclimate simulations. Next, we parameterized simulation variables

within the parametric objects and their custom parameters. Handling simulation variables in parametric BIM had the following advantages. In Smart Growth, many regulation variables had a range of maximum and/or minimum requirements. These requirements varied over the parcels and blocks. It could make the simulation input process time-intensive and inaccurate. The parametric BIM provided various simulation variables from parcel-level mass geometry and block typologies. The building component library in BIM stored a range of material properties for energy simulations. We coupled simulation variables with material properties for each parcel and fed them into simulation modules. It minimized direct inputs to simulation modules, eliminating redundant and time-intensive input processes.

3.1. PARAMETRIC BIM-SIM INTEGRATION

The framework integrated parametric BIM, microclimate simulations, and bespoke software to handle a large set of parameter values. We focused on smooth communication with parametric BIM and multiple simulation platforms. Three performance simulations were performed for Mean Wind Velocity, Radiation Accessibility, and Energy Use Intensity (EUI). Figure 3 illustrates the main steps of our parametric BIM-based microclimate simulation.

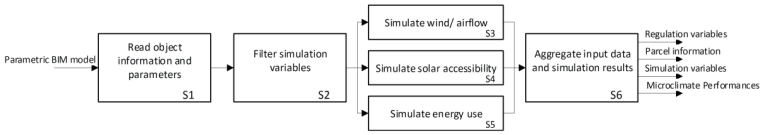

Figure 3. A Workflow of Parametric BIM and Microclimate Simulation .

3.1.1. Wind analysis

Smart Growth regulations control the design of streets, public spaces, landscapes, and building facades, associated with intricate airflow patterns in public areas. We measured average wind velocity in the outdoor space along the main corridor and public plaza area for two cases. Figure 4 shows the wind simulation workflow in our framework.

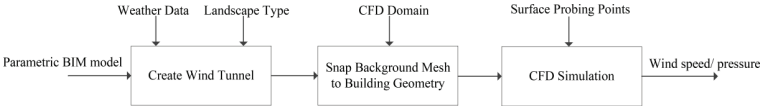

Figure 4. Wind simulation Workflow.

We used Butterfly, a CFD analysis plug-in using OpenFOAM. The first step was to create a wind tunnel depending on wind direction in the local microclimate. The level of accuracy is associated with the configuration of wind mesh and its resolutions. To create the wind tunnel, we built a hexahedral mesh with additional refinement though multiple geometrical criteria and the cell density. We applied the settings used in previous studies (Mackey et al., 2017, Hammod et al, 2011).

The top boundary was placed at the level of 2×maximum building heights. The lateral extension was approximately 3×maximum building heights. The landscape roughness was considered as 'Rough (Z0 = 0.25m). Next, a polyhedral mesh was created using the building geometries, snapped from the background mesh. Last, we assigned the mesh of building geometries to obtain outdoor wind speed and wind pressure. For validation, we used the surface probing points with a minimum normalized residual number, 1×10−4.

3.1.2. Solar accessibility

Smart Growth regulations control block layout, building typology, and façade configuration, associated with solar accessibility. Figure 5 presents the solar radiation simulation process. First, the simulation module read the object information and parameters in BIM. Then the geometries were proceeded for solar radiation calculation based on local sky condition and weather data. Finally, we executed solar radiation simulation on building envelope surfaces for 24 hours of the Summer Solstice. For solar radiation, we used Ladybug, a Grasshopper plug-in. Our previous study investigated BIM and solar radiation integration using Revit and Ladybug (Kim, et al. 2020).

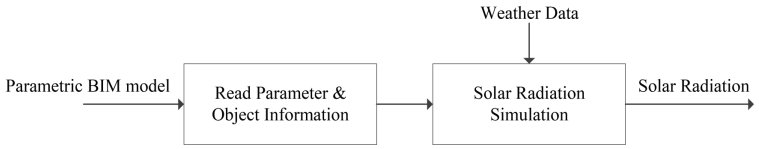

Figure 5. Solar Radiation Simulation Workflow.

3.1.3. Energy use

Forecasting energy supply and demand is an essential step for resource management in Smart Growth. We performed EUI to understand whole building energy consumption shaped by Smart Growth regulations, as shown in Figure 6.

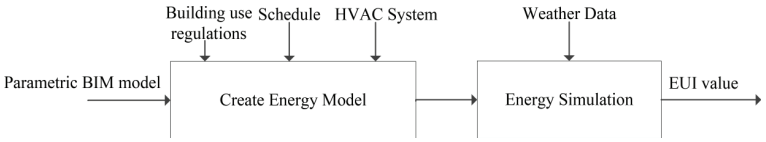

Figure 6. Energy Simulation Workflow.

The first step was creating thermal zones based on the Mixed-use building type. Simulation variables were collected from the Smart Growth regulations, such as building use, materials, facade configurations, and opening ratios. Then, we assigned standard values for schedules and systems that are not included in the regulations. Lastly, the simulation module calculated heating, cooling, and lighting loads and divided the total loads with the gross floor area obtained from the Revit model. For EUI simulation, we used Honeybee, a Grasshopper plug-in.

3.1.4. Simulation iterations

In the simulation, parametric BIM models provided regulation variables, simulation variables, and spatial information of development scenarios. The first step was loading the simulation interface from Revit. We employed Rhino.Inside plug-in (McNeel, 2019) to connect Revit and Grasshopper platform. This connection enabled to access BIM information, extract subsets of object information, update BIM parameters, and execute performance simulations through the Grasshopper platform. Three plug-ins used in this research enabled the use of validated simulation engines of Radiance, EnergyPlus, and OpenFOAM (Jasak, Jemcov, & Tukovic 2007). We used TMY3 weather data of Kansas City, Kansas (724460). Simulation iterations were critical to producing a comprehensive dataset of regulation variables and multi-criteria performances. Simulation iterations were automated by the Colibri plug-in (CORE studio, 2017).

Table 2. Parameter sets for simulation iterations.

Parameters	Unit	Values	Iterations
Building Height (T1)	ft	34 to 70 (24, 52, 70)	3
Setback (T1)	ft	5 to 10	2
R-Value (T1)	ft2·°F·h/BTU	15 to 25	2
Opening Ratio (T1)	-	0.26-0.70	2
Building Height (T2)	ft	34 to 70 (24, 52, 70)	3
Setback (T2)	ft	5 to 10	2
R-Value (T2)	ft2·°F·h/BTU	15 to 25	2
Opening Ratio (T2)	-	0.3-0.8	2
Total Iteration		$(3 \times 2 \times 2 \times 2)^2 =$	**576**

4. Visualization and analysis of simulation results

We produced comprehensive simulation results from the simulation iterations. The results include visualizations of wind pressure, wind velocity, EUI, and solar radiation. The parametric model provided development capacity information such as block area, parcel area, ground coverage, gross floor area, and Floor Area Ratio (FAR). The statistical analysis is in progress to reveal the relationship between regulation variables and microclimate simulation results. The following figures are examples of simulation result visualizations. Figure 7 shows the color-coded renderings of solar radiation simulations for two cases.

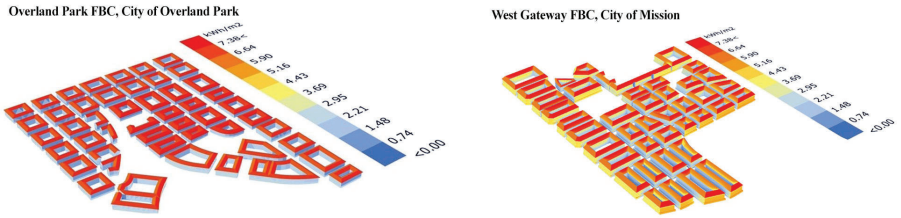

Figure 7. Solar radiation renderings of two cases.

Figure 8 visualizes wind velocity (left) and wind pressure (right) near Overland Park FBC's central plaza. 2-5 story mixed-use buildings surround the plaza. The ground level is allowed for retails, and the upper floors are available for offices and apartments. The wind speed maps show higher airflow along the corridors between south side buildings.

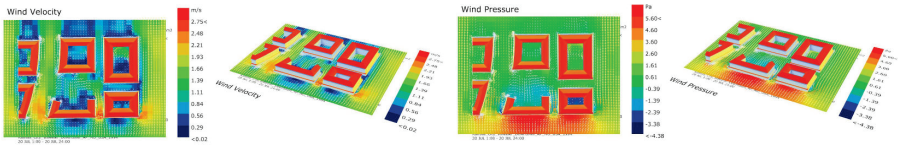

Figure 8. Visualization of wind analysis for wind velocity (left) and pressure (right) .

Figure 9 is a data visualization of Overland Park simulation results. Each plot shows the combined data series of simulation variables and simulation results. The three columns from the right side are solar radiation, EUI, and wind velocity, respectively. A dispersed distribution of simulation results indicates a weak relationship with the regulation variables.

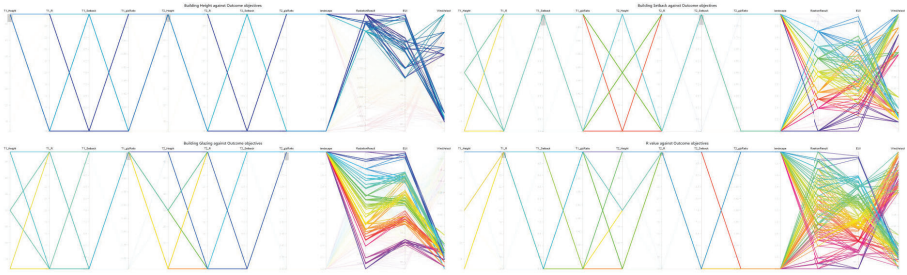

Figure 9. Data visualization of Overland Park simulation results. Note: (Top left) Building height impact, (Top right) Building setback impact, (Bottom left) R-value impact, (Bottom right) Window Ratio impact.

The top left plot presents simulation results when the maximum building height is assigned. We can infer that solar radiation (The third column from the right) is more sensitive to building height than other simulations.

5. Conclusion

This paper presented the parametric BIM-SIM framework to understand Smart Growth regulations' impact on the local microclimate. We explored parametric BIM-based urban modeling, integration of BIM and multi-criteria simulations, and simulation result visualizations. To test the framework, we performed case studies of two Smart Growth regulations.

Parametric modeling and BIM database were critical in the modeling process. Custom parameters could store a range of regulation and simulation variables in BIM. It eliminated the redundant input processes for multi-criteria simulations. However, when considering the number of regulation variables, the current

modeling approach has limitations. Further studies on data structure and schema will improve interoperability and maintainability in regulation modeling and simulation research. Our framework connected BIM with multiple simulation interfaces of validated simulation engines. It provided external validity, but visual programming-based software development often makes validation and maintenance difficult. We will carry out validations with base-case models for each simulation.

Level of details and level of scale are inherited challenges in urban modeling simulation. In our simulation, CFD demands extensive computing time. We noticed that CFD is highly sensitive to the mesh properties, but high-density meshes made simulation slow down further. The interaction between Revit and Grasshopper tools made the simulation iterations even slower. To drive more convincing results, it was required to increase the number of iteration. However, we drastically reduced the number of regulation variables due to the extensive computing time. The microclimate performance is associated with multi-criteria simulations, but individual methods were developed independently with varying scopes. It increases ambiguity in understanding simulation results and creating holistic recommendations. These constraints bring attention to limitations and challenges in urban simulations.

Acknowledgments. This research was supported by University of Missouri Research Council Fund and Richard Wallace Faculty Incentive Grant Award of University of Missouri Columbia.

References

"Overland Park, Municipal Code. Downtown Form-Based Code" : 2016. Available from <http ://online.encodeplus.com/regs/overlandpark-ks/doc-viewer.aspx#secid-7098>.

"Smart Growth America: Improving Lives by Improving Communities" : 2020. Available from <https://smartgrowthamerica.org/>.

Borys, H., Talen, E. and Lambert, M.: 2019, "The Codes Study, The web" . Available from <ht tp://www.placemakers.com/how-we-teach/codes-study/>.

Dascalaki, E.G., Droutsa, K.G., Balaras, C.A. and Kontoyiannidis, S.: 2011, Building typologies as a tool for assessing the energy performance of residential buildings – A case study for the Hellenic building stock, *Energy and Buildings*, **43**(12), 3400-3409.

US EPA, O.: 2013, "Codes That Support Smart Growth Development" . Available from <https ://www.epa.gov/smartgrowth/codes-support-smart-growth-development>.

Hammond, D.S., Chapman, L. and Thornes, J.E.: 2012, Roughness length estimation along road transects using airborne LIDAR data, *Meteorological Applications*, **19**(4), 420-426.

Jasak, A.: 2007, OpenFOAM: A C++ Library for Complex Physics Simulations, *International Workshop on Coupled Methods in Numerical Dynamics*, IUC, Dubrovnik, Croatia.

Kim, J.B. and Balakrishnan, B.: 2019, Visualize Smart Growth Development with Parametric BIM: A Case Study of Columbia Unified Development Plan, *CAADFutures19*, Daejeon, Korea.

Kim, J.B., Balakrishnan, B. and Aman, J.: 2020, Environmental Performance-based Community Development, *Proceedings of CAADRIA 2020*, Hong Kong.

Mackey, C., Galanos, T., Norford, L. and Roudsari, M.S.: 2017, Wind, Sun, Surface Temperature, and Heat Island: Critical Variables for High-Resolution Outdoor Thermal Comfort, *Proceedings of the 15th IBPSA Conference*, San Francisco, CA, USA, 985-993.

SIMULTANEOUS EFFECT OF FORM MODIFICATIONS AND TOPOLOGY OF THE BRACING SYSTEM ON THE STRUCTURAL PERFORMANCE OF TIMBER HIGH RISE BUILDING

Introducing an innovative approach using parametric design

SABA FATTAHI TABASI[1], MATIN ALAGHMANDAN[2] and HAMID REZA RAFIZADEH[3]
[1,3] *Tehran University*
[1,3] *{Saba.fth92|h.rafizadeh}@gmail.com*
[2] *Shahid Beheshti University*
[2] *m.alaghmandan@gmail.com*

Abstract. Topology optimization is a tool that minimizes the material consumption in a structure, while at the same time provides us design alternatives integrating architectural and structural engineering concepts. However, topology optimization is a structural engineering subject and its known methods are required professional knowledge of engineering to be used. In this article, the mutual effect of form modifications and topology of the bracing system in a 9-story timber exoskeleton high-rise building regarding the governing wind load and seismic load is examined. What differentiates this study from former ones and in fact its main purpose is introducing an innovative approach towards structural topology optimization using parametric design. In this innovative approach, the possibility of moving for each central node of bracing systems in defined ranges independently and the possibility of the existence or absence of each bracing member is provided. This parametric model will enable architects to optimize the topology of the structural elements which are part of their architectural design by themselves. The CMA-ES-algorithm-based optimization is done to minimize both "total mass of structure per unit area" and "the horizontal displacement of the top floor". For modeling, optimizing cross-sections and structural analysis, Grasshopper and its plug-in called Karamba are utilized.

Keywords. Topology optimization; Form finding; Parametric design; Timber tall buildings; Exoskeleton structures.

1. Introduction

Environmental advantages, building performance, and speed of timber construction on one hand, and the need for high rise building caused by the growing population and lack of land, on the other hand, rationalize the increasing attention towards timber high rise buildings all around the world. ''In recent

PROJECTIONS, Proceedings of the 26th International Conference of the Association for Computer-Aided Architectural Design Research in Asia (CAADRIA) 2021, Volume 1, 421-430.

years, the wood industry has developed new engineered timber products such as glue-laminated wood, laminated veneer lumber (LVL), and cross-laminated timber (CLT). These products were developed to increase the strength of the structural members, provide a more precise and consistent product, and to provide more effective use of natural resources'' (Hein and Baldassarra,2015, p.5). ''Between 2008 and 2016, the height of modern buildings using engineered timber increased from the nine-story Stadthaus building in London to TallWood at Brock Commons building in Vancouver'' (Foster, Ramage and Reynolds, 2017, p.28). Because of the fact that structural behavior is most influenced by the geometric form, the highest potential for structural efficiency and a balance of design goals occurs when determinative decisions are made in conceptual design. In field of form modification of high-rise buildings, some studies have been done. In the study of Moon (2011) parametric structural models are used to investigate the impacts of variation of important geometric configurations of complex-shaped tall buildings utilizing diagrid system, such as the rate of twisting and angle of tilting. In the paper of Ardekani et al. (2019) the effects of form parameters including tapering and changing plan shape as two commonly used modifications on the structural efficiency of tall buildings are investigated by generating a parametric platform. Mirniazmandan et al. (2018) focuses on studying the effect of both geometric modification of tall building and the angle of diagrid structure to improve the efficiency of tall buildings. In research of Alaghmandan et al. (2014) a design method of tall buildings considering integrated architectural and structural strategies, and reducing the along wind effect is presented to achieve the minimum weight of the structure as one of the main parameters of the efficiency. ''Researchers have previously developed many computational optimization tools for design optimization, in which the goal is to reduce the cost or material usage in a structure while satisfying specific design criteria. Among these tools, there are the cases of size optimization, shape optimization, genetic algorithms, topology optimization, and others'' (Beghini, 2013,p.18). ''Topology optimization has been recognized as one of the most effective tools for least-weight and performance design. It has undergone a remarkable development in both academic research and industrial applications. Various approaches have been proposed, such as density-based methods, evolutionary procedures, and level set methods'' (Xia, 2016, pp.4-8). In regards to topology optimization, several different studies have been done over the years. The research of Baldock (2007) has focused on structural topology optimization of steel building frameworks and has investigated three distinct methods. Symmetry constraints, rules for element removal and addition, and also some aesthetic requirements are considered in this study. Paper of Baldock and Shea (2006) presents a genetic programming method for the topology optimization of steel bracing systems that aims to create optimal design solutions. Liang (2007) utilizes the performance-based optimization (PBO) technique to investigate the effects of continuum design domains on the layouts and performance of multistory steel bracing systems under lateral loads. In this system, underused finite elements are gradually removed to obtain optimal bracing systems. Former the other similar study was done by Liang, Xie and Steven (2000). In the study of Mijar, et al. (1998) a continuum

structural topology optimization formulation is presented for the concept design optimization of structural bracing under lateral-wind and seismic loading. In research of Balling, Briggs and Gillman (2006) simultaneous optimization of size, shape, and topology of skeletal structures, including trusses and frames is done through a genetic algorithm that is presented. Considering the fact that this is a well-documented field of research So what is the need for a new study? Firstly, ‘’the spatial arrangement of material, often known in the literature as the layout problem, is of key importance for the design and usability of many engineering products. Specifically, in building design, the manner in which material is distributed is significant for engineers to develop a lateral bracing system or create a conceptual design for structural members. While topology optimization is a very powerful tool for design, often the resulting topologies produced consist of complex geometries and poor material layouts which are of limited value to real-world problems due to expense and ease of manufacturing‘’ (Stromberg et al., 2010, p.165). So considering a manufacturing constraint on the size of members in a study will make the result more valuable. Of course, this issue has been paid attention to in some of the former studies but still, there is potential for more progress. Secondly, topology optimization is a specialized field of civil engineering so its known methods are required the knowledge of engineering and are not easy to understand by architects. The purpose of this study is to introduce an innovative methodology and in fact, a parametric model that enables architects to do the structural topology optimization of their design by themselves. Needless to say, these elements are parts of architecture too. In other words, they will affect the structure and architecture at the same time. So, using this approach allows the architect to choose from a wide range of architectural options resulted from the optimization process and also makes them sure that their choice is structurally efficient too. Or, it will enable them to design their desired structure in the parametric model and check it structurally. Moreover, in this study, the effect of form modification and topology of bracing systems is examined simultaneously and in a timber exoskeleton structure, unlike most of the former works that choose steel or concrete as their main material. These new considerations can bring novel interesting results.

2. Methods

2.1. FORM MODIFICATION

To find the general form of the building, the diameters of the two ellipses, which were created as the initial top plan and initial base plan to form the initial total volume, were considered as variables in the optimization process. In fact, by changing these diameters, different forms of tall buildings can be achieved. (Figure.1) In this research, the range of changes of each diameter is defined between 24 to 40 meters, as a result of which we will have 81 different forms. This range of change is determined according to the importance of effective daylighting for spaces. So that considering the defined fixed central core in the structure with a diameter of 16 meters, the lease span will be between 4 to 12 meters. ‘’Leasing depth or lease span is the distance of the usable area between the exterior wall and the fixed interior element, such as the core or the multi-tenant corridor.‘’(Sev

and Ozgen, 2009, p.75) The maximum lease span varies from region to region but some countries have determined it. For example, in Germany, the maximum leasing depth cannot be more than 8.0 meters, but in Japan it is typically 18.0 meters. In the United states buildings with a lease span of 17.0 meters can be found (Sev and Ozgen, 2009).

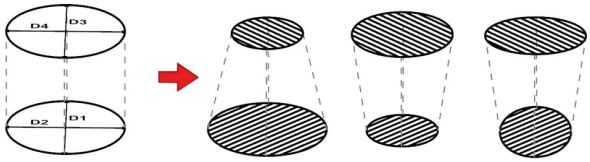

Figure 1. General form modifications of the building with changes in the diameters of the base ellipses.

What is defined as the main top plan and main base plan in this study, is the polygons inscribed in the described ellipses. In the parametric model (modeled in Grasshopper), a situation is provided that allows the formation of any polygon (from triangle to circle) in the base ellipses. So that it is even possible to define the top plan and base plan differently. (Figure 2) But, in this study, to simplify the model and to examine the effect of optimization variables on the results as accurately as possible, the top plan and base plan were both considered as 30-sided (close to a circle). However, as described, it is possible to examine more complex forms in future studies.

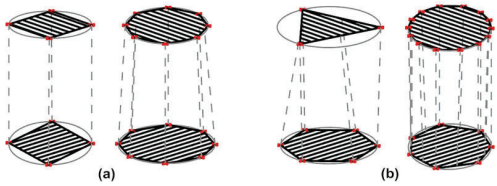

Figure 2. Some forms that their formation is possible in the parametric model. The similarity in top plan and base plan (a), The difference in top plan and base plan (b).

In the parametric model, it is possible to change the number of columns in certain ranges, in fact, it is possible to consider this number as a variable in the optimization process. But for this study, according to the mentioned reasons, the fixed number of 30 columns located at the vertices of the polygon is defined. Also, for braced frames, a fixed height of 3 floors (equivalent to 12 meters) is considered.The procedure to study the topology of these bracing members is shown in Figure 3. As shown in Figure 3, the possibility of moving for each central node of bracing systems is provided in defined ranges independently. Moreover, the possibility of the existence or absence of each bracing member is provided. So, there are 32 different modes of formation for each frame “independently”. All these modifications are done randomly and based on seed in the grasshopper plugin. Some possible modes of formation of exoskeleton structure on the façade are shown in Figure 4.

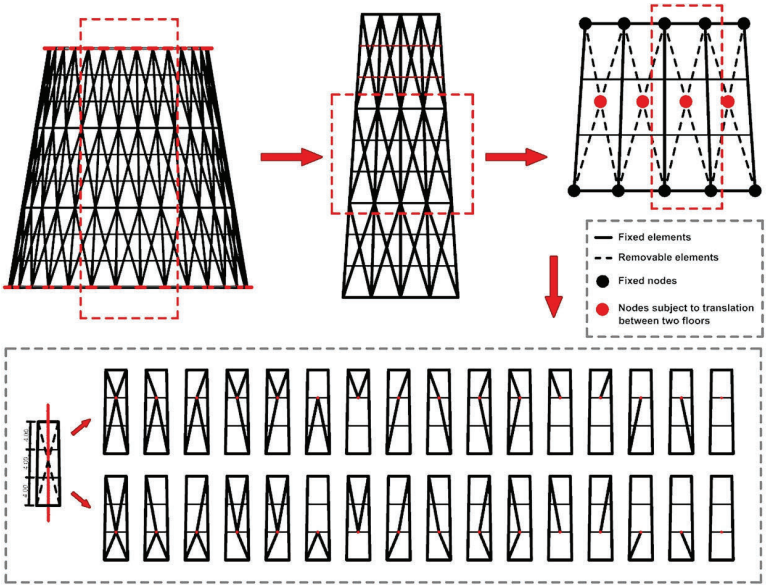

Figure 3. The procedure to study the topology of the bracing members.

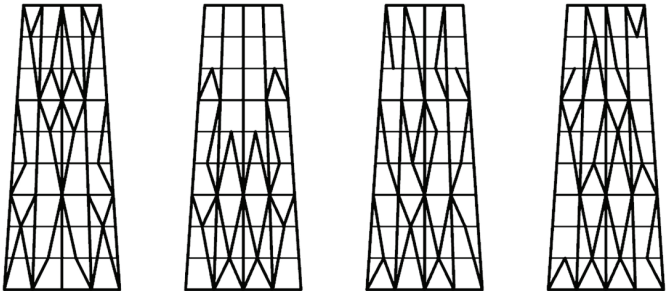

Figure 4. Some possible topologies of bracing members.

After modeling the members of the exterior structure parametrically, other structural members were also modeled to transform the model into a stable integrated structure. In this research, the considered structure includes 1- Central core (fixed position and fixed diameter), 2- Radial beams (fixed number, variable and parametric length), 3- Peripheral beams (fixed number, variable and parametric length), 4- Exoskeleton structure (fixed number, variable and parametric length for columns- variable and parametric number and length for bracing members).

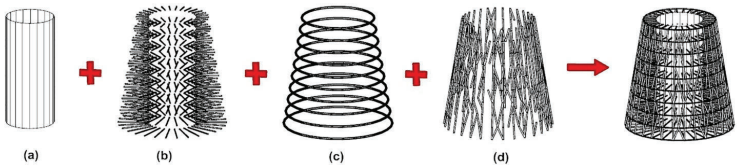

Figure 5. Considered structure in this study: Central core(a), Radial beams (b), Peripheral beams (c), Exoskeleton structure (d).

2.2. FINITE ELEMENT MODEL OF STRUCTURE

To convert modeled members into the structure and to analyze the final structure, the Karamba plugin (FE method) is utilized. ‘’Finite Element Method (FEM) is a computational technique used to obtain approximate solutions of boundary value problems in engineering (Bialkowski and Kepcyznska-Walczak, 2015, p.2).‘’ The loads considered for structural analysis in this study are:1-gravity load, 2-totally live load and dead load on each floor (8kn/m2 on each floor), 3-wind load, 4-seismic loadThe calculation of wind load and seismic load is done based on CBC (Canada’s building code), Iran National Building Regulations provisions, and Iranian Seismic Code 2800.

2.3. STRUCTURAL ANALYSIS AND OPTIMIZATION

After the formation of integrated structure and applying horizontal and vertical loads, in the initial step for structural analysis, optimized cross-section tool of Karamba is used to limit the maximum displacement -based on (AISC)- to (H/500=0.072, H= the total height of the building) by changing Cross-section dimensions of structural members (peripheral and radial beams and also exoskeleton structure) in defined ranges. Table 1 reports details about building elements. When cross-sections are chosen, and structural analysis is completed, some structural information such as maximum displacement and mass are extractable. In fact, these steps (includes 1- formation of structural members based on variables, 2- formation of integrated structure, 3- optimization of cross-sections, 4- analysis of structure, 5- extraction of structural information) repeat during the optimization process. One example of structural analysis in Karamba under defined horizontal and vertical loads is shown in Figure 6. In this study, the objective of the optimization is minimizing both “total mass of structure per unit area” and “the horizontal displacement of the top floor”. To do this optimization a CMAES-algorithm-based optimizer called Opossum is implemented. ‘’Covariance Matrix Adaptation Evolution Strategy (CMA-ES) developed by Nikolaus Hansen is an evolutionary algorithm for difficult non-linear non-convex black-box optimization problems in continuous domains. The CMA-ES is considered as state-of-the-art in evolutionary computation and has been adopted as one of the standard tools for continuous optimization in many research labs and industrial environments around the world that is proved to converge at optimal solution in very few generations, thus, decreasing the time complexity ‘’ (Gagganapalli, 2015,p.13).

Table 1. building elements details.

Building elements	Cross section	Fixed dimensions	Variable dimensions	Material
Core	Shell const	Diameter: 16m Thickness: 15cm	-	Wood material E:1050[kN/cm2] G12:360[kN/cm2] G3:360[kN/cm2] gamma:6[kN/m3] alphaT:5.0E-6[1/C°] fy:1.3[kN/cm2]
Radial beams	Solid rectangle	-	Cross section height:10-100cm Cross section Width:10-100cm Length: Around 4-12m	
Peripheral beams	Solid rectangle	-	Cross section Height:10-100cm Cross section Width:10-100cm Length: Around 2.5-4m	
Columns	Solid rectangle	Length: Around 4m (each floor)	Cross section Height:15-95cm Cross section Width:15-95cm	
Bracings	Solid rectangle	-	Cross section Height:15-95cm Cross section Width:15-95cm Length: Around 4-4.5m	
Slabs	Shell const	Thickness: 15cm	Diameters: 24-40m	

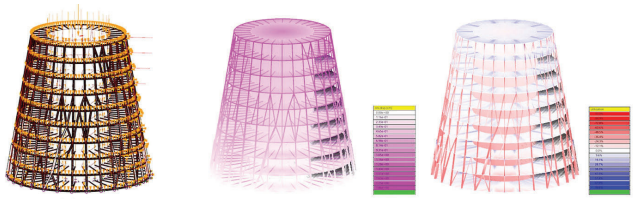

Figure 6. One example of the structure under defined horizontal and vertical loads (a), Displacement in structural members after structural analysis (b), Utilization in structural members after structural analysis (c).

3. Results and discussion

During the optimization process, about 39,000 different alternatives were investigated. Form modification results and information about maximum displacement and mass/area of the first 15 optimal results are shown in Figures 7 and 8. As shown in the graphs, the most appropriate form according to the objectives set for optimization is the top plan with radiuses of 17 and the base plan with radiuses of 20. Figure 9 shows the results of topology optimization in the first 3 optimal alternatives. In this figure, the different sides of each optimized result are displayed according to their position relative to the wind. It should be noted here that the parametric model described is under development and it is expected that a more complete and flawless version of it be presented in future studies. In such a way that more regular results can be reached and stronger conclusions can be made. Also, if this study is done on a building with a higher height, the effect of wind force on the formation of the topology of bracing members on different sides will be more visible. But as mentioned before, the main purpose of this research is not to achieve the most optimal answer, but to introduce a simple and easy-to-use platform that enables the architect to study the topology of the structure and the form modification in a building. This is even more important when the considered structure is an exterior structure. Because in exoskeleton structures, the facade of the building and the structure are practically the same and no boundary can be drawn between them. Using this parametric model, the architect is able to create

a favorable form as well as an architecturally desirable pattern with the structural members and evaluate its structural performance. An example of patterns that can be created with this model and their structural performance is shown in Figure 10. As it is clear, these structures, while meeting the architectural needs, are structurally acceptable.

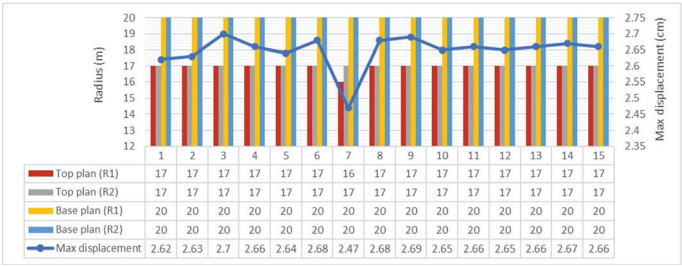

	1	2	3	4	5	6	7	8	9	10	11	12	13	14	15
Top plan (R1)	17	17	17	17	17	17	16	17	17	17	17	17	17	17	17
Top plan (R2)	17	17	17	17	17	17	17	17	17	17	17	17	17	17	17
Base plan (R1)	20	20	20	20	20	20	20	20	20	20	20	20	20	20	20
Base plan (R2)	20	20	20	20	20	20	20	20	20	20	20	20	20	20	20
Max displacement	2.62	2.63	2.7	2.66	2.64	2.68	2.47	2.68	2.69	2.65	2.66	2.65	2.66	2.67	2.66

Figure 7. The radius of the top plan and base plan vs. max displacement.

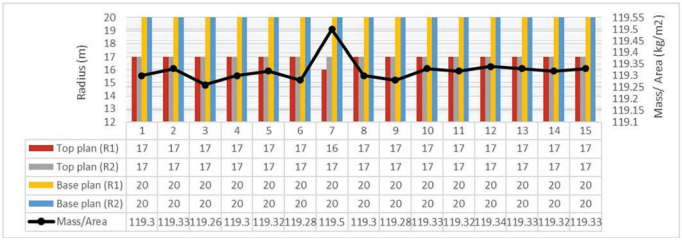

	1	2	3	4	5	6	7	8	9	10	11	12	13	14	15
Top plan (R1)	17	17	17	17	17	17	16	17	17	17	17	17	17	17	17
Top plan (R2)	17	17	17	17	17	17	17	17	17	17	17	17	17	17	17
Base plan (R1)	20	20	20	20	20	20	20	20	20	20	20	20	20	20	20
Base plan (R2)	20	20	20	20	20	20	20	20	20	20	20	20	20	20	20
Mass/Area	119.3	119.33	119.26	119.3	119.32	119.28	119.5	119.3	119.28	119.33	119.32	119.34	119.33	119.32	119.33

Figure 8. The radius of the top plan and base plan vs. Mass/Area.

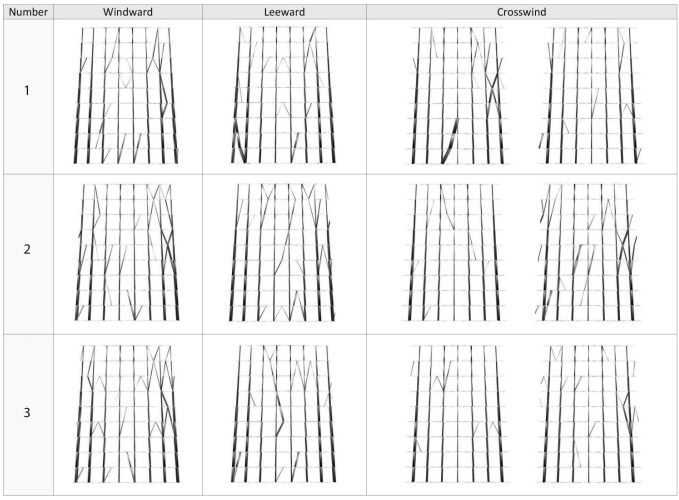

Figure 9. Results of topology optimization in the first 3 optimal alternatives.

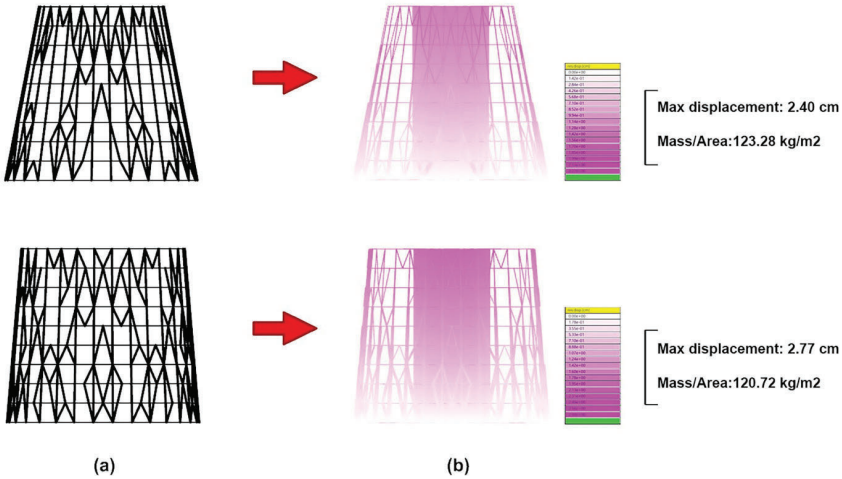

Figure 10. Some patterns that can be created by the architect in the parametric model (a), Displacement in structural members after structural analysis (b).

4. Conclusion

The study was done to propose an innovative method that makes form-finding and also modifying the topology of the bracing system in a timber exoskeleton structure possible. In this innovative approach, unlike the past works, some bracing elements are defined, and the possibility of relocating and even eliminating them is provided. In fact, the central nodes of these elements are able to move in defined ranges to find their best location according to the objectives of the optimization or desires of the architect. Of course, it should be noted that this study does not seek to downplay the role of the structural engineer or eliminate it, because this is certainly not possible, and naturally the design of an optimal building is the result of the interaction between the architect and structural engineer. The purpose of this study is to empower the architect as much as possible to propose designs consistent with engineering principles. This method opens up new perspectives on the role of computational design and parametric design in the future of architecture.The methodology although helpful has some limitations. Making the locating of nodes independently which has increased the number of variables, on one hand, dependence on randomness, and seed, on the other hand, Extends optimization time. This will be more obvious when the topology of a higher tall building is going to be investigated. It is expected that the more developed parametric model in the futures studies provides us more specific results. Considering some constraints like symmetry constraint that decreases the number of variables is a suggestion.

References

Alaghmandan, M., Elnimeiri, M., Carlson, A. and Krawczyk, R.: 2014, Optimizing the Form of Tall Buildings to Achieve Minimum Structural Weight by Considering along Wind Effect, *Proceedings of the Symposium on Simulation for Architecture & Urban Design*.

Ardekani, A.R., Dabbaghchian, I., Alaghmandan, M., Golabchi, M., Hosseini, S.M. and Mirghaderi, S.R.: 2019, Parametric design of diagrid tall buildings regarding structural efficiency, *Architectural Science Review*, **63**, 87-102.

Baldock, R.: 2007, *Structural optimization in building design practice: case-studies in topology optimization of bracing systems*, Ph.D. Thesis, Cambridge University.

Baldock, R. and Shea, K. 2006, Structural Topology Optimization of Braced Steel Frameworks Using Genetic Programming, *in* I.F.C. Smith (ed.), *Intelligent computing in engineering and architecture : revised selected papers*, Springer, Heidelberg, 54-61.

Balling, R.J., Briggs, R.R. and Gillman, K.: 2006, Multiple Optimum Size/Shape/Topology Designs for Skeletal Structures Using a Genetic Algorithm, *Structural engineering*, **132**(7), 1158-1165.

Beghini, L.L.: 2013, *Building science through topology optimization*, Ph.D. Thesis, University of Illinois at Urbana-Champaign.

Bialkowski, S. and Kepcyznska-Walczak, A.: 2015, Engineering Tools Applied in Architecture – Challenges of Topology Optimization Implementation, *eCAADe 2015*, Vienna, 261-268.

Foster, R., Ramage, M. and Reynolds, T.: 2017, Rethinking CTBUH height criteria in the context of tall timber, *CTBUH journal*, 28-33.

Gagganapalli, S.R.: 2015, *Implementation of And Evaluation of CMA-ES Algorithm*, Master's Thesis, North Dakota University.

Hein, C. and Baldassarra, C.: 2015, Debating tall: Tall timber in 10 years?, *CTBUH journal*, 5.

Liang, Q.Q.: 2007, Effects of continuum design do-mains on optimal bracing systems for multistory steel building frameworks, *5th Australasian Congress on Applied Mechanics*, Brisbane.

Liang, Q.Q., Xie, Y.M. and Steven, G.P.: 2000, Optimal Topology Design of Bracing Systems for Multistory Steel Frames, *Structural engineering*, **124**(7), 823-829.

Mijar, A.R., Swan, C.C., Arosa, J.S. and Kosaka, I.: 1998, Continuum topology optimization for concept de-sign of frame bracing systems, *Structural engineering*, **124**(5), 541-550.

Mirniazmandan, S.A., Alaghmandan, M., Barazande, F. and Rahimianzarif, E.: 2018, Mutual effect of geometric modifications and diagrid structure on structural optimization of tall buildings, *Architectural science review*, **61**, 371-383.

Moon, K.S.: 2011, Diagrid Structures for Complex-Shaped Tall Buildings, *Procedia Engineering*, **14**, 1343–1350.

Sev, A. and Ozgen, A.: 2009, Space Efficiency In High-Rise Office Buildings, *METU Journal of the Faculty of Architecture*, **26**, 69-89.

Stromberg, L.L., Beghini, A., Baker, W.F. and Paulino, G.H.: 2010, Application of layout and topology optimization using pattern gradation for the conceptual design of buildings, *Structural and Multidisciplinary Optimization*, **43**, 165-180.

Xia, L.: 2016, *Multiscale Structural Topology Optimization*, ISTE Press & Elsevier.

CO-EVOLUTIONARY SPATIAL-STRUCTURAL BUILDING DESIGN OPTIMISATION INCLUDING FACADE OPENINGS

HERM HOFMEYER[1], THIJS DE GOEDE[2] and SJONNIE BOONSTRA[3]
[1]*Eindhoven University of Technology*
[1]*h.hofmeyer@tue.nl*
[2]*Alba Concepts, The Netherlands*
[2]*thijs@albaconcepts.nl*
[3]*ABT Consulting Engineers, The Netherlands*
[3]*s.boonstra@abt.eu*

Abstract. Within co-evolutionary building design simulations, a spatial design can be automatically transformed into a structural design, and its structural performance can lead to modifications of the spatial design, after which a new cycle starts. This paper presents two procedures to include facade openings in these simulations, to allow for future simulations that include lighting. The first procedure reassigns a fixed pattern of facade openings to the spatial design each cycle, whereas the second procedure only assigns a pattern at the start, and modified spaces inherit their openings. For structural peformance, it is concluded that deterministic vertical opening patterns, with a low facade opening ratio, lead to a reduction of the number of stories, and consequently optimise the structural design. Also, it is shown that the first procedure maintains facade opening ratios during simulations, whereas the second procedure leads to decreasing openness, and more unconnected spaces. As such the first procedure is considered for an upcoming project, where spatial-structural-thermal-lighting building optimisation is investigated, including non-rectangular spatial designs.

Keywords. Spatial-Structural Optimisation; Co-evolutionary Design; Structural Design; Facade Openings.

1. Introduction

State-of-the-art design support tools, if used for multi-disciplinary building optimisation, often start with a fixed Building Spatial Design (BSD), which includes building spaces and their locations. However, a predefined BSD may exclude optimal (domain specific) solutions, and it can be shown that allowing a BSD to be modified during discipline related optimisation will allow for better performing designs (Boonstra et al, 2018). A suitable approach to obtain BSD modification is the application of co-evolutionary design (Maher, 2000), which iteratively explores both a problem and solution space. Co-evolutionary design has been implemented for design support and optimisation of BSDs and their

PROJECTIONS, Proceedings of the 26th International Conference of the Association for Computer-Aided Architectural Design Research in Asia (CAADRIA) 2021, Volume 1, 431-440.

structural and thermal designs (Boonstra et al, 2018). However, although the structural designs may involve (implicit) openings, so far facade openings have not been considered explicitly. But for future research, including functionality and lighting, openings must be taken into account. Here, two procedures will be introduced to include and manage facade openings in co-evolutionary building design simulations. The first procedure (re)assigns a fixed pattern of facade openings to the spatial design each cycle, whereas the second procedure only assigns a pattern at the start, and modified spaces inherit their openings. Then, a case study investigates these procedures for an application of co-evolutionary building design simulation to spatial-structural optimisation.

2. Related research

In the field of Architecture, Engineering and Construction (AEC), it shows to be very time-consuming to design even a single BSD in the conceptual design phase (Flager et al, 2009). This aspect has a significant effect on the quality of the final building, for all subsequent design phases rely strongly on the conceptual design decisions, and major redesign efforts cannot be made later in the process (Okudan and Tauhid, 2008).

Single Disciplinary Optimisation (SDO) can support (conceptual) design, by finding better solutions with respect to e.g. energy consumption or structural design (Fuyama, Law and Krawinkler, 1997). However, the time-consuming search for trade-offs between the disciplines still has to be made (Machairas, Tsangrassoulis and Axarli, 2014). Multi-Disciplinary Optimisation (MDO) provides a solution, by optimising either a weighted sum of the objectives (e.g. Chantrelle et al, 2011), or conceiving a so-called Pareto Front Approximation (PFA). The latter offers a ranking of design alternatives (only), e.g. for the structural and daylight optimization of classrooms (Flager et al, 2009). Another well known type of optimisation is the use of genetic algorithms (Evins, 2013; Beume, Naujoks and Emmerich, 2007). Heuristic algorithms use intuitive judgement to find design solutions, and although their functioning can be difficult to track (Verhagen et al, 2012), optimal solutions may be found (Evins, 2013). Heuristic algorithms can explore design search spaces during conceptual spatial design (Stiny, 1980) and structural design (Geyer, 2008). Most of the aforementioned approaches, except co-evolutionary design (Maher, 2000) use a predefined design search space, thus limiting the creativity and reach of the design solutions.

A so-called BSO Toolbox has been developed to study the optimisation of BSDs and their discipline designs (Boonstra et al, 2018): An initial BSD is extended with domain specific designs (e.g. a structural and a thermal design); these designs are evaluated; and the BSD is modified. How this approach relates to e.g. a multi-fitness solver, using evolutionary algorithms, is shown in Boonstra et al (2021).

3. Methodology

3.1. BSO TOOLBOX

The BSO Toolbox is an open source C++ library for BSD design and optimisation (Boonstra and Hofmeyer, 2020). The BSD is represented by the "Building design", shown in figure 1 on the left, which consists of spaces, these spaces made by surfaces, in turn consisting of edges and points.

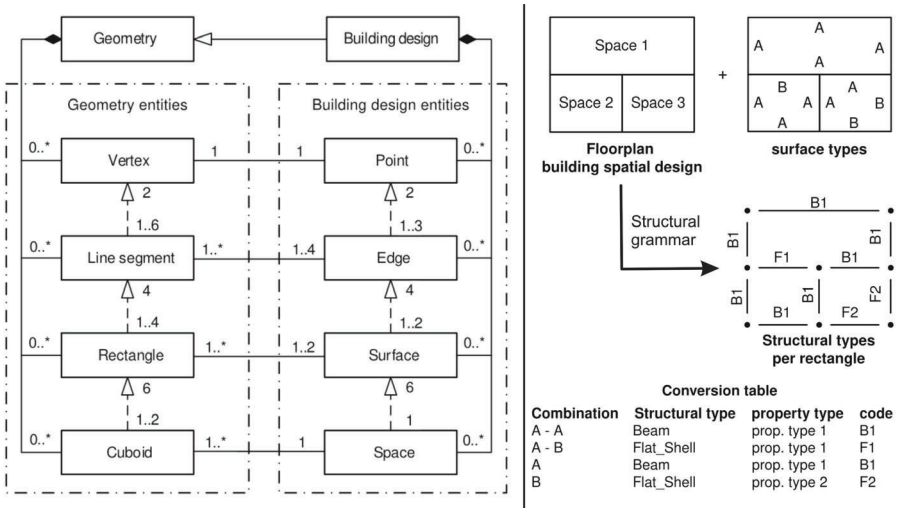

Figure 1. On the left UML of ConFormal (CF) representation, on the right a structural grammar.

Another used representation is the ConFormal (CF) model, shown in figure 1 by "Geometry". At the geometry level, cuboids are formulated, which are made of rectangles, line segments, and vertices. By a process defined as conformation, these cuboids are generated such that they can be seen as building blocks for the spaces, with their vertices not intersecting any line segments, rectangles or cuboids. For the CF model, so-called design grammars are defined that generate domain-specific models for the evaluation of domain-related objectives. Relevant in this paper are the structural grammars that generate a structural design consisting of (1) structural components, (2) loads, and (3) constraints. Practically, the structural grammar works as shown in figure 1 on the right. The BSD has spaces, for which the surfaces may have been assigned with surface types. The structural grammar follows the conversion table (on the bottom right of figure 1) and generates structural types and properties (e.g. the Young's Modulus) for the rectangles corresponding to the surfaces. Hereafter, each rectangle is provided with structural components (trusses, beams, or flat-shells) as a function of the structural type (Boonstra et al, 2018).

In Boonstra et al (2018) the BSO Toolbox is used for the spatial-structural optimisation of BSDs, where BSD modification is carried out by Scale & Subdivide: After adding to the BSD a structural design, for each structural

component the strain energy [Nmm] is determined. Then a selected number of spaces that contain the structural components with the lowest strain energy are deleted, and these spaces are brought back into the design by splitting the spaces with the highest strain energy in half across their longest side (width or depth). Lastly, the BSD is scaled horizontally such that the original volume is restored. Here, this type of optimisation will be used for the demonstration of facade openings.

3.2. FACADE OPENINGS

To introduce facade openings, the BSO Toolbox has been extended by an additional property for the rectangles in figure 1, namely the face type, which can be "open" or "closed". Also layers of rectangles have been introduced. For a BSD a single set of horizontal layers is generated, in which each layer consists of all rectangles with the same height position of their centre point. For vertical layers, four sets of layers are made, one set for each direction (north, east, south, west), as shown in figure 2 at the bottom right. For instance, each of the six layers (x = 1 to 6) within the north set contains all facade rectangles that face north, with the same position of their centre point in east-west direction. Six facade opening patterns have been tried, as shown in figure 2 at the top left. Deterministic Horizontal (DH) defines the face type of rectangles in a certain horizontal layer (all around the building) all "open" or "closed", based on the facade opening ratio [0 to 1], which is the number of open layers over the total number of layers. As can be seen in figure 2 at the top right, for the same opening ratio this offers several possibilities if the first position of the pattern and the number of equal layers (open or closed) is varied: All possibilities will be used in the parameter study in section 4. Deterministic Vertical (DV) and Diagonal (DD) function in a similar fashion. Stochastic Horizontal (SH) and Vertical (SV) still assign "open" or "closed" to all rectangles of a layer, but whether a specific layer is "open" or "closed" is determined randomly, however, still assuring the opening ratio. Finally, Stochastic Rectangle (SR) randomly assigns "open" or "closed" to the rectangles, but again keeping track of the opening ratio, now defined as the number of open rectangles over the total number of (facade) rectangles. Finally, note that the opening ratio applies to each set of layers (so horizontal, north, east, south, west) separately. See for more details De Goede (2019).

3.3. LOAD PANEL

In section 3.1 it was explained that the structural grammars provide each rectangle with structural components. In this paper, for rectangles with face type "closed" a flat-shell component is generated. For rectangles that are "open", no structural components should be generated, for in practice the "open" rectangles will contain a transparent facade system, which does not contribute to the structural performance of the building. However, the facade transfers wind loads to the structure. Therefore, still a flat-shell structural component is added to the "open" rectangles, but now having a very low stiffness, and is consequently defined as a "load panel". In a validation study it was found that if the load panel's Young's Modulus is multiplied by 1E-5 compared to the normal flat-shells, wind loads are

transferred correctly, while the contribution to the building's structural behaviour is negligible (De Goede, 2019).

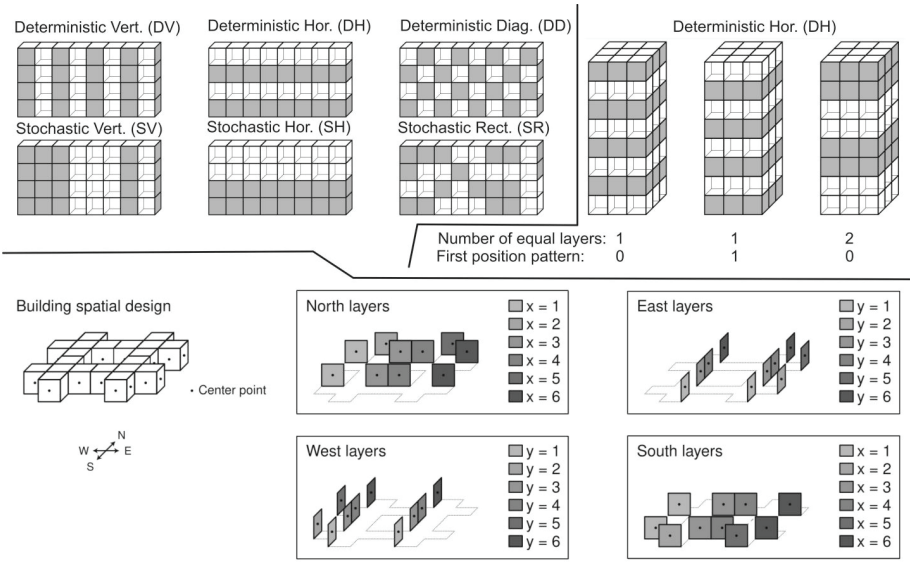

Figure 2. Facade opening patterns (top left), different options for one pattern (top right), four sets of vertical rectangle layers (bottom row).

3.4. ASSIGNMENT OF OPENINGS DURING SIMULATIONS

When the BSD is modified during the co-evolutionary design simulations, as explained in section 3.1, the opening patterns (see section 3.2) have to be managed, for which two procedures have been developed. For the first procedure, "inheritance", for each space surface the surface type (see figure 1, conversion table) is at the start manually defined as open or closed. Subsequently, a rectangle associated with one or two surfaces inherits this information, and is then by conversion rules defined as open or closed. If a particular space is deleted during the simulation, the associated rectangles and their face type (open or closed) are deleted, however, if a space is split into two spaces, these two spaces inherit the surface types of the initial space, and the associated rectangles are then also open or closed. Note that as such the facade opening ratio cannot be controlled. The second procedure, "reassignment", simply reapplies the steps in section 3.2 on every modified version of the BSD, so the facade opening ratio is assured. However, it is possible that the new BSD lacks the number of layers to assure the ratio exactly (e.g. 1 layer with a ratio equal to 0.5), and then the simulation is stopped.

4. Parameter study

A parameter study is performed to demonstrate the effects of facade openings on the spatial-structural optimization of BSDs (via the simulation of a co-evolutionary design process). Two initial BSDs are used, A and B, as shown in figure 3 at the top left, subject to $2\times3\times6\times2=72$ simulations that span all combinations of the following settings: (a) inheritance (IN) or reassignment (RE), see section 3.4; (b) facade opening ratio = 0.25, 0.50, or 0.75; (c) the 6 different patterns in figure 2; (d) design A or B.

4.1. STRUCTURAL DESIGN SETTINGS

As mentioned earlier, each rectangle with face type "closed" is modelled with a flat shell component. The thickness of this component is 150 mm, the Young's modulus equals 30000 N/mm^2, Poisson's ratio is 0.3, and each component is meshed by 3×3 shell finite elements. The open rectangles follow the same approach, but for these the Young's Modulus equals 0.3 N/mm^2. Horizontal line segments that are located at or below ground level ($z \leq 0$) are constrained for each displacement direction (*x*-, *y*-, and *z*-direction). For each assessment of the structural design, five load cases are applied on the structure via BSD properties: a live load on the horizontal rectangles equal to 0.005 N/mm^2, and for each direction (north, east, south, west) a wind load with either a normal pressure of 0.001, a wind shear equal to 0.0004, or a wind suction equal to 0.0008 N/mm^2, as a function of the rectangle orientation. For each load case the sum of the strain energy over all finite elements is calculated and the total strain energy (the performance) is the sum of the five energy values. Also for each structural component its contribution to the total strain energy is calculated.

4.2. SIMULATIONS

For this parameter study, each simulation consists of 19 cycles, in which for each cycle four spaces, out of 72 (design A) or 80 (design B), are deleted and brought back by splitting other spaces. Minimal dimensions for a space are prescribed, namely 750 mm for either the width or depth. If splitting the best performing space would violate these constraints, the next-best space is tried. Finally, due to space deletion and splitting, BSDs may occur that show (groups of) spaces that are not connected to the ground. To prevent this situation, the BSD is tested by meshing each component with 1 finite element, and applying to this finite element model a single value decomposition, which reveals structural instability (Smulders and Hofmeyer, 2012) and so the unconnected (groups of) spaces. These spaces are neglected for the subsequent finite element simulation, and the first to be deleted in the next cycle. Each simulation is evaluated by: (a) the average structural design's performance over all cycles, (b) the best achieved performance; (c) the performance after the final cycle. All are normalised with respect to the initial performance and concerning the strain energy, for which a lower value is better (a more stiff structure). Also, the average facade opening ratio over all cycles is calculated, and again normalised for its initial value.

4.3. RESULTS

About one fifth of the simulations ended before finishing the 19 cycles, because of (i) in the case of reassignment, using design B, and for a deterministic horizontal pattern, the opening ratio could not always be assured, see section 3.4. Secondly, at the time of the research, (ii) numerical imprecision sometimes led to intersected spaces, which could not be handled by the implementation. Not ending simulations prematurely, it also happened that unconnected spaces did not trigger the single value decomposition, which led to a dramatic increase of the compliance, in which case that value was neglected. This issue and problem (ii) were solved after the research presented here. Figure 3 at the bottom shows a typical simulation, for design A with deterministic vertical reassignment, and an opening ratio 0.5. The graph at the top right shows that structural performance first decreases (i.e. higher strain energy), but thereafter improves beyond the initial value.

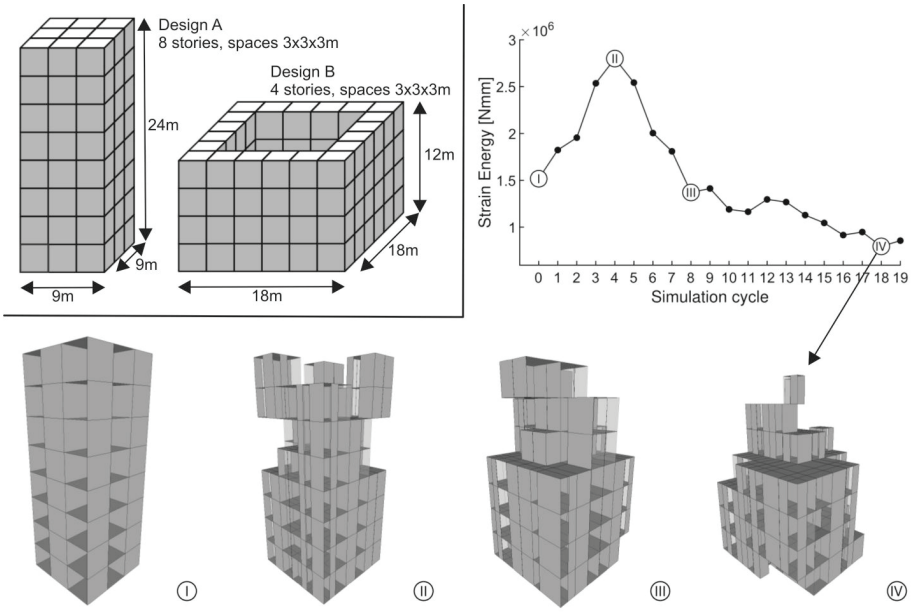

Design A with reassignment, opening ratio 0.5, and deterministic vertical pattern, at cycles 1 (I), 4 (II), 8 (III), and 18 (IV).

Figure 3. Case study designs on the top left, typical simulation shown at the bottom with graph on the top right.

For all 72 simulations the measurements, as presented in section 4.2, are presented in box plots, see figure 4. Normalised average performances show that vertical patterns and the lowest opening ratio (on average across the cycles) perform better than other options. Reassuringly, best performance (within each simulation) plots show that the simulations always lead to better performance, showing they are useful for optimisation. Furthermore, using facade openings allows for better structural performance than for a completely closed building (red dots) and this regardless the use of inheritance or reassignment. End of simulation

performance shows a lot of scatter and thus stresses the need for monitoring the simulation process, rather than to trust the final answer. Not displayed here, for inheritance the openness decreased, whereas for reassignment the openness kept reasonably constant, as expected (De Goede, 2019). Results show that inheritance led to 86% of the simulations corrected by the singular value decomposition procedure, whereas for reassignment this was only 46%. The hypothesis here is that reassignment leads to the continuation of more regular patterns along the cycles, and so a more regular pattern of space deletion, whereas inheritance leads to an increasingly free formed opening pattern during the simulations, promoting unconnected spaces. Finally, it should be noted that even the best peformance may be a local minimum, due to the heuristic search. Global search (e.g. with an evolutionary algorithm) may reveal global minima.

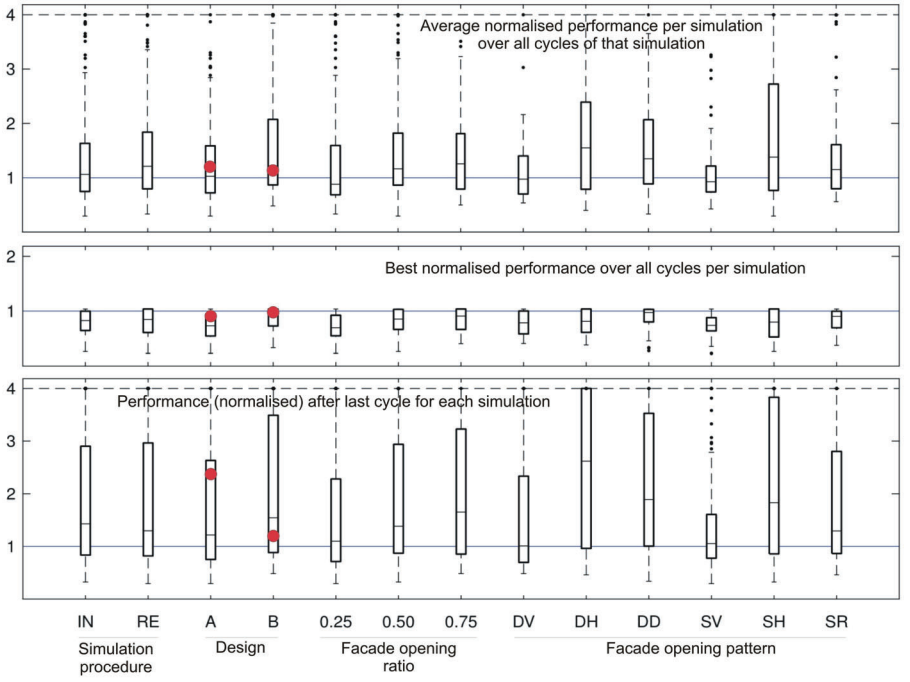

Figure 4. Results of all simulations shown in box plots. Red dots indicate reference simulations with no openings at all.

4.4. DISCUSSION

In the parameter study, only one structural grammar has been used. Other structural design types, made possible by different grammars, could change the outcomes of the study significantly. The same applies to variations of simulation settings, i.e. the number of cycles per simulation, the number of spaces deleted per cycle, and the minimal space dimensions.

Data not presented in this paper show that a decreasing facade opening ratio leads to more improvement of structural design performance over the cycles, due to the reduction of building storeys. It appears that openings "weaken" a space as they do not allow for structural components at the opening, and so surrounding components are strained more, leading to a higher strain energy for the space. Spaces with openings are thus less likely selected for deletion. Besides, in each cycle 4 spaces are deleted, less than a storey for both design A and B, and thus spaces will be left at the top floor. Also it can be shown that if the opening ratio is higher, these left spaces at the top floor will have more open rectangles, thus increasing the strain energy, and avoiding deletion, and thus the reduction of storeys.

For designs without openings, sometimes spaces directly under the spaces at the top floor are deleted, leaving some top floor spaces cantilevered. This increases the strain energy in these top floor spaces significantly, once again avoiding the reduction of the number of storeys. This indicates the importance of selecting the appropriate number of spaces to be deleted, or the need for more globally operating design variables.

In this research, only the effects of facade openings on the structural performance of a BSD have been investigated. However, the facade openings have been introduced first of all to include lighting and improve thermal performance assessments in future co-evolutionary building design simulations. However, for lighting and thermal performance the effects have not been studied yet, and some designs as shown in this paper may not be useful from the perspective of these disciplines.

5. Conclusions

An existing toolbox, which among others can be used to simulate co-evolutionary spatial-structural building design processes, has been extended by (i) the inclusion of facade openings in the building representation; (ii) a generator to design facade opening patterns; (iii) two procedures to manage the facade openings during modifications of the spatial design; (iv) a load panel to transfer wind loads on the facade "openings" to the structure.

A parameter study has been carried out to study the effect of facade openings on spatial-structural building optimisation via co-evolutionary design simulations. All combinations of settings (BSD, opening management, opening pattern, opening ratio) have been simulated. It is shown that vertical facade opening patterns with a limited opening ratio improve spatial-structural optimisation, by enabling the number of storeys to be reduced. Inheritance did not give control over the opening ratio, and led to many cases of unconnected spaces.

The research has shown that the number of spaces to be deleted in one cycle of the simulations is critical for the results, and more global operating modifications should be studied.

The reassigment procedure is considered for an upcoming project, where spatial-structural-thermal-lighting building optimisation is investigated, including non-rectangular spatial designs. This will allow for the investigation of the effects

of facade openings on structural, thermal, and lighting design. Furthermore, multi-disciplinary optimised BSD's can be found, and related design processes can be supported.

Acknowledgements / authors statements

This research has been carried out by Thijs de Goede, who was supervised by Herm Hofmeyer, Sjonnie Boonstra, and Arjan Habraken. Arjan is highly acknowledged for his expertise and supervision during the project.

References

Beume, N., Naujoks, B. and Emmerich, M.T.M.: 2007, SMS-EMOA: Multiobjective selection based on dominated hypervolume, *European Journal of Operational Research*, **181**, 1653-1669.

Boonstra, S., van der Blom, K., Hofmeyer, H. and Emmerich, M.T.M.: 2021, Hybridization of Evolutionary Algorithms and Simulations of Co-evolutionary Design Processes for Building Design and Optimization, *Automation in Construction*, **124**(103522), 1-18.

Boonstra, S., Van der Blom, K., Hofmeyer, H., Emmerich, M.T.M., Van Schijndel, A.W.M. and De Wilde, P.: 2018, Toolbox for super-structured and super-structure free multi-disciplinary building spatial design optimisation, *Advanced Engineering Informatics*, **36**, 86-100.

Boonstra, S. and Hofmeyer, H.: 2020, "BSO Toolbox" . Available from Open Source Repository, doi: 10.5281/zenodo.3823893<https://github.com/TUe-excellent-buildings/BSO-toolbox> (accessed November 23, 2020).

Chantrelle, F.P., Lahmidi, H., Keilholz, W., El Mankibi, M. and Michel, P.: 2011, Development of a multicriteria tool for optimizing the renovation of buildings, *Applied Energy*, **88**, 1386-1394.

Evins, R.: 2013, A review of computational optimisation methods applied to sustainable building design, *Renewable and Sustainable Energy Reviews*, **22**, 230-245.

Flager, F., Welle, B., Bansal, P., Soremekun, G. and Haymaker, J.: 2009, Multidisciplinary process integration and design optimization of a classroom building, *Journal of Information Technology in Construction (ITcon)*, **14**, 595-612.

Fuyama, H., Law, K.H. and Krawinkler, H.: 1997, An interactive computer assisted system for conceptual structural design of steel buildings, *Computers & Structures*, **63**, 647-662.

Geyer, P.: 2008, Multidisciplinary grammars supporting design optimization of buildings, *Research in Engineering Design*, **18**, 197-216.

De Goede, T.Y.: 2019, *Co-evolutionary Building Design Simulation for Structural Optimization with Facade Openings*, Master's Thesis, Eindhoven University of Technology, Department of the Built Environment.

Machairas, V., Tsangrassoulis, A. and Axarli, K.: 2014, Algorithms for optimization of building design: A review, *Renewable and Sustainable Energy Reviews*, **31**, 101-112.

Maher, M.L.: 2000, A model of co-evolutionary design, *Engineering with computers*, **16**, 195-208.

Okudan, G.E. and Tauhid, S.: 2008, Concept selection methods–a literature review from 1980 to 2008, *International Journal of Design Engineering*, **1**, 243-277.

Smulders, C.D.J. and Hofmeyer, H.: 2012, An automated stabilisation method for spatial to structural design transformations, *Advanced Engineering Informatics*, **26**, 691-704.

Stiny, G.: 1980, Introduction to shape and shape grammars, *Environment and Planning B: Planning and Design*, **7**, 343-351.

Verhagen, W.J.C., Bermell-Garcia, P., van Dijk, R.E.C. and Curran, R.: 2012, A critical review of Knowledge-Based Engineering: An identification of research challenges, *Advanced Engineering Informatics*, **26**, 5-15.

OFFICE BUILDING DESIGN IN HONG KONG ISLAND THROUGH SHAPE OPTIMIZATION

MARINELLA CARALLO
[1]*Politecnico di Milano*
[1]*10687885@polimi.it*

Abstract. Dealing with crucial decision-making process has led to the development of many different methods of multicriteria assessments, especially optimization methodologies. This work is mainly focused on the integration of advanced computational design and digital methods, to design a complex building shape resulting in a performance-based approach through optimization methodologies. The project consists of the design of a skyscraper in Hong Kong Island made through parametrically controlled shape and evaluated respect to light and wind to reduce Urban Heat Island phenomena and enhance liveability. The aim is to find out a unique methodology that can be applied to different cases by making small adaptations regarding the parametrization and the parameters involved. The design is divided into two stages that need to arrange the methodology at different levels throughout the workflow. For this reason, it is mandatory to adapt inputs to the algorithm according to the goal. The result is a skyscraper placed in the financial district of Hong Kong, which has both the features of a Grade A Office building and can mitigate the UHI effect thanks to its particular and optimized shape.

Keywords. Shape optimization; Computational design; Genetic Algorithm; UHI effect; ventilation.

1. Introduction

Designers can use several techniques to discover an "optimal" solution including parametric analysis, genetic algorithms, multi-objective optimization, and even "passive" optimization. "Passive" optimization is what many designers are doing by creating three or four options, mentally testing them against past experience, and then intuitively determining a "best" solution; but in most of the cases it leads to an inaccurate prediction; moreover, it is not easy to consider more than one variable at the same time. For this reason, the most efficient method consists in the use of parametric analysis coupled with a genetic algorithm.

In their article Sun Lee, Ki Jun Han and Jae Wook Lee, compares the conventional "passive" approach, which depends on a designer's sense of judgment with the approach which uses genetic algorithms, to create optimal indoor lighting conditions by adjusting louvre shapes and window patterns. (Lee, et al., 2016).

PROJECTIONS, Proceedings of the 26th International Conference of the Association for Computer-Aided Architectural Design Research in Asia (CAADRIA) 2021, Volume 1, 441-450.

Martins, Adolphe and Bastos searched for the adaptation and evolution of existing building stock blocks into 'positive energy' neighbourhood, by adjusting urban morphology elements. The optimization of solar energy incident on building outer surface is proposed, aiming at enhancing local energy production and minimizing potential solar gains. (A.l. Martins, et al., 2014)

Y. K. Yi and A. M. Malkawi explain the workflow of their research about optimizing building form; they introduce new methods to control building forms by defining a hierarchical relationship between geometry points to allow the user to explore the building geometry without being restricted to a box or simple form. Their methodology succeeds in generating an optimized site-specific building form by integrating advanced simulation and optimization algorithm. (Kyu & Malkawi, 2009)

It is impossible to reduce the environmental factors that impact a building to a single parametric relationship. The factors that affect a building, its envelope and its ability to serve as an effective system of climate control, are multi-dimensional. Parametric simulators can aid in understanding variation in environmental performances of a single parameter but are unable to optimise adequately all the involved factors. As a consequence, in building design, commonly, there is more than one objective function for optimization, then a multi-criteria optimization problem arises.

Genetic Algorithm is different from other optimization algorithms because it requires no skilled mathematical knowledge and is easy to apply. It aims to obtain superior genes via multiple generations, which is similar to a biological evolutionary process. The basic idea is to generate a new set of designs (population) from the current set such that the average 'fitness' of the population is improved. Thus, a superior 'gene' provides a more optimal shape. (J.T.Jin, et al., s.d.)

This paper proposes a computational approach for the design of the shape of an office building in Hong Kong Island. This approach offers an optimized workflow that focuses on two stages: first on the plan optimization and secondly, the location of six sky gardens is carried out. To implement a Pareto curve, it is fundamental the use of visual programming language with a 3D modelling tool for the improvement of passive design practices by showing alternatives and optimizing parameters. The different methods are tested and implemented by Grasshopper together with its plug-in dealing with both building simulations (*Ladybug, Honeybee, Eddy3D*) and genetic algorithms (*Galapagos* and *Octopus*).

2. Methodology

2.1. CONTEXT ANALYSIS

The first step in the design process is to analyse the environment to have clear what issues must be solved and what possible strategies can be implemented in the building. This becomes even more important talking about Genetic Algorithms. The role of the designer is fundamental to change the building's features and goals according to the specific site and problems.

Despite being a highly competitive global city, a leading financial centre and an

attractive tourist destination; Hong Kong only has moderate performances in terms of liveability and innovation, which must be enhanced. Particularly the problems of Urban Heat Island and quality of spaces are addressed.

The temperature difference within urban areas compared to the surrounding countryside is known as the 'Urban Heat Island' (UHI) phenomenon and the main causal factors for this must be considered.

Solar exposure, affecting urban radiant temperature, is most directly influenced by building density but also by land-use zoning allocation of the built mass as well as the charter of vegetation cover on open ground. The building density is manifested in the extent of ground coverage, the allowable floor area ratio, and the ratio of the height of buildings to the width between them. This influences the shading of the solar heat during the day affecting gain and radiative heat loss at night due to the related parameter of sky view factor.

An appropriate solution to UHI effect is reached by designing adequate solar exposure, vegetation, natural ventilation; in addition, high albedo or high solar reflectance materials in urban areas can reduce this problem. This can be done at three scales: building group scale, building scale and building component scale.

The case study is located in Murray Road landmark site. It was the first commercial plot to be released in Central since 1996; for this reason, it got the attention of local developers. Henderson Land Development is going to turn the 31,000 sq ft site into a single landmark Grade A office building with around 35-floors by 2022. The car-park is going to be transformed into a "landmark building" in Hong Kong's downtown business district with the contribution of Zaha Hadid Architects, which presented their project last November. Adding a central atrium and sky gardens it is possible not only to exploit cross ventilation for heat gains reduction but to increase liveability and daylight exposure.

2.2. PROCESS DESCRIPTION

To simplify the process, the design was divided into two main phases. First, the plan optimization was conducted and then, when the best plan shape was fixed, the sky gardens' position were parameterized and optimized. The parameters involved in the two phases were different, changing according to the goal of each analysis, but the logic behind the process was the same.

In general, the process is made by the following steps:

1. Develop a geometrical representation connected to the parametrized plan and the fixed height.
2. Run simulations
3. Run again to compare the performances. The more runs are done the more it is possible to understand which variable impact the most.

The whole iterative process is then automized thanks to the optimization component. Reading the results for each trial problems can be highlighted and fixed. At the end of the workflow, it was possible to establish the best methodology and the final most efficient shape.

Before starting the simulation, for both stages, it was fundamental to define the

geometry (Genome) and the parameters to test (Fitness), then the analysis process started.

2.3. STAGE ONE: PLAN OPTIMIZATION

To run the optimization component, it was first necessary to parametrize the plan to define the 'Genome' of the analysis. Three different plan parametrizations were tested to find out the one able to stay within the constraints.

Together with the performance-based approach, represented by the optimization workflow, it was fundamental to keep in mind the limitations given by prescriptive Regulations; in fact, the first stage of the parametrization was to check Hong Kong's Standards. According to Sustainable Building Design Guidelines, APP-152 establishes the design requirements regard the continuous projected façade length (Lp), Separation Distance (S) and Permeability (P). (BuildingDepartment, 2016)

Putting together the limits given by standards and design features stated by the designer, the project's constraints are summarized in:

- - Fixed building height: 180 m
- - Fixed floor to floor height: 5 m
- - Building setbacks from APP-152
- - Permeability: min level of 20% per each Assessment Zone from APP-152
- - Maximum and minimum GFA from APP-152

The next step consisted of the parameter's definition. They were assessed considering how these affect the performances of the building and how to implement them on Grasshopper to be linked to the Genetic Algorithm software.

The main features to consider in the early design phases were grouped in daylight availability, sky exposure and natural ventilation. To perform these variables a preliminary analysis permitted to define the best method to implement them in the software. Summing up this preliminary phase, the defined parameters were: hours of sun and radiation, regarding the daylight availability; Sky View Factor and Quality View Factor (view on the harbour) for the sky exposure; and permeability and wind velocity ratio related to natural ventilation.

Moreover, to work with a unique variable instead of different scores for each analysis point, a post-process of the quantities was necessary. *Figure 1* shows an example of radiation analysis on a shoebox, displayed as the value per point on the left and with the coloured mesh generated by *Ladybug*, on the right.

The goal of this first stage was to test different methods to assess which algorithm performs better dealing with multi-criteria optimization. Thus, three methods were carried out, each giving some pros and cons permitting the designer to define limitations and to find a way to solve them and improve the workflow.

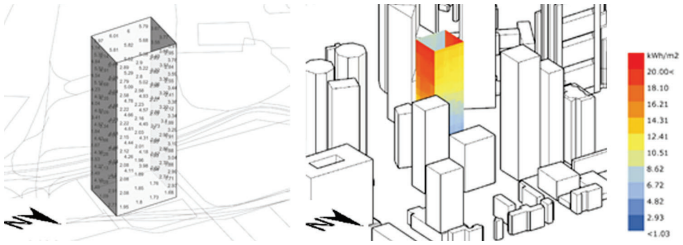

Figure 1. Radiation analysis on a shoebox. Value in each point (left), coloured mesh (right).

The tested variables changed throughout the workflow according to limitations emerged during the trials. Going form Method 0 to 3, the number of parameters involved increased and the software complexity with it. Method 0 consisted of a preliminary test on a shoebox, which enables the designer to assess the limitation of the site and critical areas and values to work on. Then, Method 1 was the fastest way to automatically test different orientations thanks to a tool integrated into the analysis components (radiation, sunlight-hours and view analysis), of *Ladybug* itself, which lets the user study the relationship between the orientation of the building and the amount of incident solar radiation or sunlight hours. In this study, it was applied to the Radiation component. It does not permit to test different geometries and the number of orientations is limited to the value input by the designer.

For these reasons, Method 2 involved a Genetic Algorithm using the plug-in *Galapagos*. This software looks for maximising or minimising a variable, resulting in several 'optimized' results displayed in the software's panel. The main problems of this method were related to the parametrization, which exceeded the site boundary, and to the number of parameters considered. These drawbacks were solved thanks to Method 3, both using a multi-criteria GA plug-in (*Octopus*) and changing the plan's parametrization.

The last method was carried out in different trials, in which the change of plan's parametrization and of the number of parameters were necessary.

The fourth, last, trial involved a four-parameters optimization trying to:

- - Maximise Gross Floor Area
- - Minimize Radiation
- - Maximise Sky View Factor
- - Maximise Quality View factor.

Octopus' results were displayed both on a three-dimensional graph and on a parallel one (*Figure 2*) in which the phenotypes were normalized on the four axes. In the second one, it is easier to read the non-dominated solutions, which are represented with thicker and darker lines, tending to minimize their value and to move towards the left of the diagram. The selected solutions are highlighted in yellow, and the corresponding values are reported in *Table 1*.

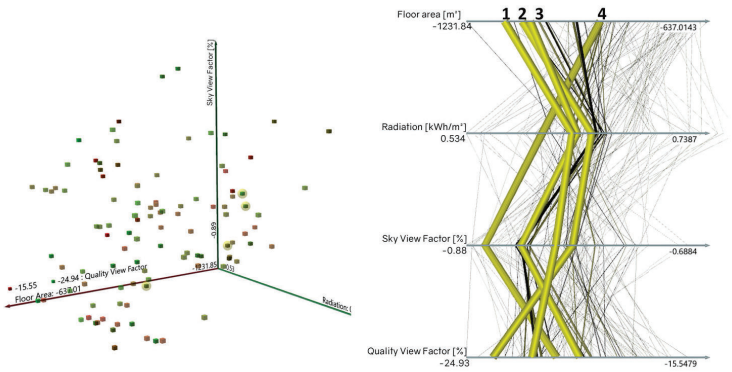

Figure 2. Three-dimensional results‘ graph (left), parallel axis results’ (right) from Octopus. Stage 1.

Looking at these four options, the role of the designer is to evaluate the results, using both his knowledge and comparing them in terms of other useful parameters. In this project, a comparison in terms of natural ventilation on the first three solutions, displayed in *Figure 3*, permitted to assess the final best shape.

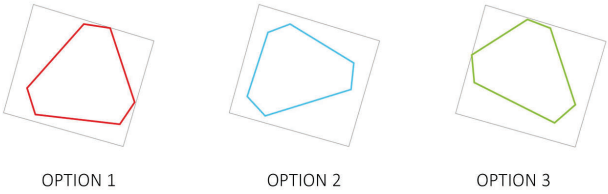

Figure 3. First three best options’ plan geometry.

To evaluate which plan configuration can reduce stagnant area and increase the natural ventilation at the urban level both prescriptive and performance-based approaches given by Hong Kong’s standard were used. First, referring to APP-152 (BuildingDepartment, 2016) the permeability of each configuration was evaluated. After that, considering the Air Ventilation Assessment Guidelines (AVA), the Velocity Ratios, both at Spatial and Local level were maximised. (Ng, 2009) To evaluate these values, a CFD analysis on the site was run, thanks to the *Grasshopper* plug-in *Eddy3D*.

In *Table 1* the final results are collected to point out that the best plan shape is given by Option 3.

Table 1. Summary of results. Stage 1.

Solution	Description	Floor Area [m2]	Total Rad [kWh/m2]	SVF [%]	QualVF [%]	Tot perm. [%]	Tot wVR [-]
1	Octopus: four-criteria opt.	1129.96	9059.27	30.65	22.17	156	0.76
2	Octopus: four-criteria opt.	1061.62	9085.45	30.87	20.17	157	0.85
3	Octopus: four-criteria opt.	1082.39	9150.29	30.55	23.83	163	0.95

2.4. STAGE TWO: SKY GARDEN OPTIMIZATION

A characteristic feature of this design is the presence of sky gardens connecting the external environment with an atrium in the middle of the geometry. The five-storey gardens, which are located at different levels and directions, provide fresh air into the central atrium, which acts as a natural ventilation chimney for the building. Moreover, central atrium and the triangular shape of the building plan help to create a zone with negative pressure, which itself causes the building's natural ventilation.

The second stage of the optimization methodology consisted of the design of the sky gardens' location. Differently from the first stage, the methodology applied was the same (Method 3 / Octopus multi-criteria optimization), but the parameters involved changed from Method 1 to Method 2 due to considerations carried out throughout the process.

The 'Genome' for the algorithm were six sliders corresponding to the height of the sky gardens. These were set according to Regulation's constraints given by the Practice note N.01, regarding green features to be exempted from the GFA. (BuildingDepartment, 2014)

Considering the geometry to design, the first step was to state the parameters ('Fitness') to take into account. Indeed, Method 1 aimed to maximise the radiation hitting on the internal façade to increase the buoyancy effect due to the increased surface temperature, minimizing the external radiation and maximizing the overall SVF. Nevertheless, designing an atrium geometry, the contribution given by the reflected light in the atrium well is fundamental, and a big limitation of *Ladybug* tool is that it does not include the light's indirect component.

For this reason, Method 2 conceived the use of *Honeybee*, which works with Radiance and Daysim tools which better represent the reality. Moreover, a deeper analysis of the internal daylight was carried out executing a dynamic daylight analysis at four significant floors. The parameters involved were UDI (Useful Daylight Index), customized UDI evaluating the percentage of time with lux in a comfort level (office buildings: 300-1000lux) and sDA (spatial Daylight Availability). Lastly, the 'Fitness' parameters for *Octopus* were: Radiation on the internal façade to maximise, and customized UDI to maximise.

Big limitations to this method were given by a series of assumptions taken to design a parametric thermal zone and the time needed to obtain a consistent result. For these reasons the parameters involved were just two, but a longer and deeper evaluation may consider more parameters and a more detailed model containing information regarding all the floors and the precise materials and glass' definition.

Given the parameters and the 'genotype' of the analysis, a two-dimensional

optimization was run. The first three solutions, showed in *Figure 4*, were evaluated also in term of sDA, UDI and internal radiation and their coloured mesh helped to identify critical areas of each geometry. An example of the comparison of the four floors behaviour in the three geometries is reported in *Figure 5*; it represents the percentage of time that points are hit by less then 300lux, thus the red area corresponds to the critical one, with poor light exposure.

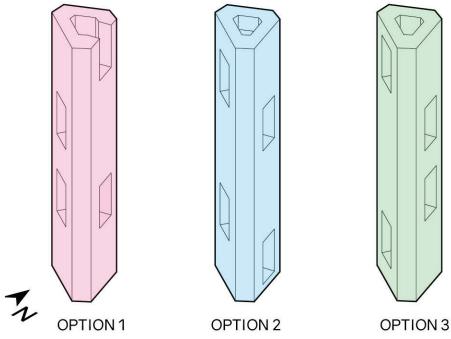

Figure 4. First three best options' sky gardens locations.

These values were also reported in *Table 3* to better compare the results. In conclusion, Option 2 was selected as the best shape and its geometry is reported in *Figure 4*.

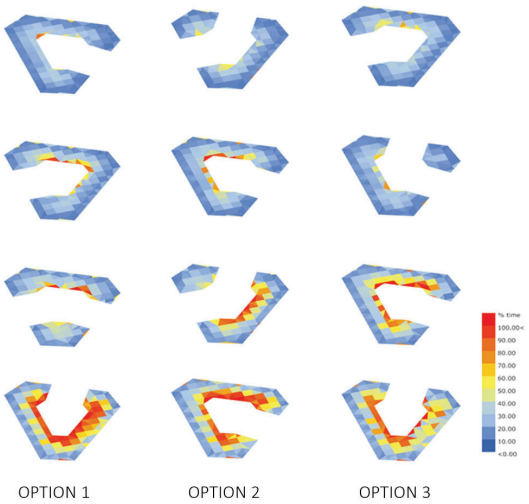

Figure 5. UDI<300lux evaluated at the four selected floors in three best sky gardens configurations.

Table 2. Summary of results. Stage 2.

Solution	Description	Tot Internal Rad [kWh/m²]	Total External Rad [kWh/m²]	UDLI [%]	UDI [%]	sDA [%]	Avg Floor Rad[kWh/m²]
1	Octopus: two-criteria opt.	75.73	274.59	31.82	86.83	78.20	16.81
2	Octopus: two-criteria opt.	76.73	269.04	30.51	86.53	99.97	15.60
3	Octopus: two-criteria opt.	77.55	272.17	31.29	86.93	80.28	17.06

3. Results

A final stage consisted of running a CFD analysis for the final optimized shape, to confirm that it permits to increase cross-ventilation along the building atrium. A vertical plane along the main wind direction was considered and the coloured arrows, displayed in *Figure 6* clearly show how this geometry permits to reduce the stagnant areas on the leeward side. The bottom openings help on the windward side facing the prevailing wind direction, while the upper openings help to increase the stuck ventilation.

The result presented contribute to prove the effect of cross ventilation, whose goal is to promote sustainable development as a countermeasure to the UHI effect.

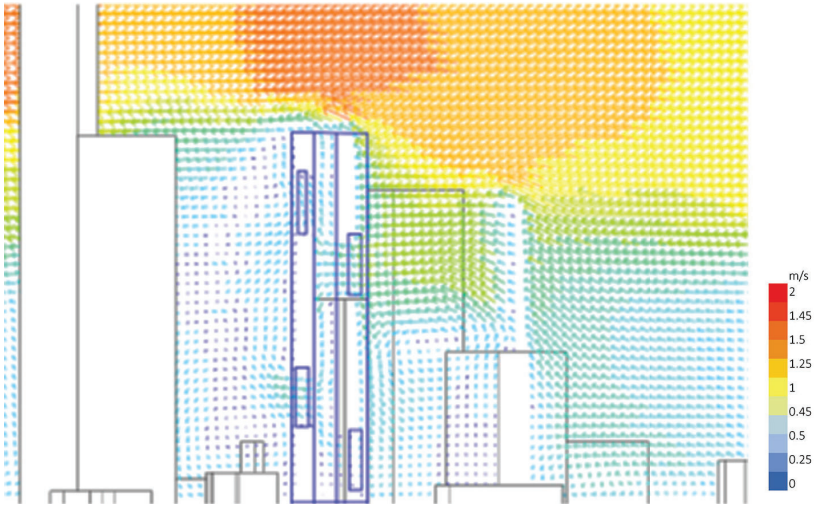

Figure 6. CFD analysis along the main wind direction plane.

4. Discussion

Thanks to the workflow presented it was possible to assess the best shape to lower the UHI effect and increase liveability. The method is a combination of performance-based approaches, given by the Genetic Algorithm, and a prescriptive ones used both to fix the design constraints and, in the last phase, to assess the permeability of each option. The focus of this project was the optimization methodology for both the stages conceiving different constraints.

For each simulation, it was necessary to define the 'Genome' and 'Fitness', that changes with the goal of the analysis. Regarding the first stage, the 'Genome' was the plan shape, including all the parametrized sliders which make it change. The 'Fitness' varied among the different trials. Focusing on the third method, which turned out to be the best one, this involved the use of Octopus plug-in, able to run a multi-criteria optimization.

Especially the second stage was characterized by big restrictions given by the software. These were mainly related to the model definition and the level of detail of the analysis. It was necessary to accept many approximations to make the analysis faster. Nevertheless, these limitations can be easily solved increasing the time necessary to define the model and run the optimization tool. According to the needs of the project, the model can be more or less detailed, and even more parameters can be included in 'Fitness'.

One of the advantages of using *Octopus* is the ability to define multiple objectives that can be evaluated simultaneously. The result, after several iterations, is a pool of optimized design alternatives that meet the objective function set. Nevertheless, although it is a user-friendly method, it cannot be a substitute for the designer. His role is to adjust 'Genome' and 'Fitness' according to the project's needs.

Moreover, these algorithms are not able to assess only one optimal solution. The Pareto curve proposes many non-dominated solutions looking to minimize the fitness parameters involved, but the more criteria are inserted the more complicated is to find out an exceptional solution. On one side it does not help designers in finding a unique solution but it still represents great support in decision-making stages that must be followed by a deeper analysis of the results.

Optimization methods are mainly used in the preliminary design phases of a new building or for building retrofit. If a methodology of sensitivity analysis is applied in the early stages, it is possible to identify the most important parameters about building performance and the expert judgment can be used to simplify the optimization problem and reduce the size of the solutions each space.

References

D. Building (ed.): 2014, *Practice Note for Authorized Persons, Registered Structural Engineers and Registered Geotechnical Engineers APP-151*, Building Department HKSAR.

D. Building (ed.): 2016, *Practice Note for Authorized Persons, Registered Structural Engineers and Registered Geotechnical Engineers APP-152*, Building Department HKSAR.

T Jin, T. J., J Cho, J. C. and W Jeong, W. J.: 2018, Optimization of Freeform Building Shape Using Genetic Algorithm, *Department of Architectural Engineering*, **1**, 1-8.

Kyu, Y.Y. and Malkawi, A.M.: 2009, Optimizing building form for energy performance based on hierarchical geometry relation, *Automation in Construction*, **18**, 825-833.

Lee, K.S., Lee, K.S. and Lee, K.S.: 2016, Feasibility study on parametric optimization of daylighting in building shading design, *Sustainability (Switzerland)*, **8**, 12.

Martins, T.A., Adolphe, L. and Bastos, L.E.: 2014, From solar constraints to urban design opportunities: Optimization of built form typologies in a Brazilian tropical city, *Energy and Buildings*, **76**, 43-56.

Ng, E.: 2009, Policies and technical guidelines for urban planning of high-density cities - air ventilation assessment (AVA) of Hong Kong, *Building and Environment*, **44**, 1478-1488.

THE SYNERGY OF BUILDING MASSING AND FACADE

An Evo-Devo approach for performance-based design optimization combining facade design with building massing

HAN ZHANG[1], LIKAI WANG[2] and GUOHUA JI[3]
[1,2,3]*School of Architecture and Urban Planning, Nanjing University*
[1]*han_mail@foxmail.com* [2]*wang.likai@outlook.com* [3]*jgh@nju.edu.cn*

Abstract. One of the problems lies in performance-based architectural design optimization is the separation of building massing design and facade design. The separation of design processes significantly weakens the synergizing of building massing and facades for more progressive performance improvement. In order to overcome this weakness, this paper presents a performance-based design optimization workflow combining facade with building massing design using an Evo-Devo approach. This workflow enables architects to make a rapid design exploration of different façade design schemes incorporating building massing design optimization. For demonstration, a case study is presented to show how this approach can facilitate early-stage architectural design exploration, and how the combination of the two factors can outperform the results produced by separated design processes.

Keywords. Evolutionary development; building massing; performance-based design optimization; adaptive facade design.

1. Introduction

In performance-based architectural design, building massing and facades are the two critical elements that have great impacts on various building performance related to energy efficiency, daylighting, passive cooling/heating, and ventilation. Over the last decade, a growing amount of research and designs have started applying computational optimization to exploit the potential in building massing or facades for more desirable performance. However, no matter in conventional architectural design or the design with computational optimization, the design processes of building massing and facades are typically separated, where façade design is being scheduled after the building massing being finally determined (either by computers or architects). The separation of design processes significantly weakens the synergizing of building massing and facades for more progressive performance improvement.

In order to overcome the drawbacks mentioned above, this study applies an Evo-Devo approach to integrate the facade design into a building massing design

PROJECTIONS, Proceedings of the 26th International Conference of the Association for Computer-Aided Architectural Design Research in Asia (CAADRIA) 2021, Volume 1, 451-460.

generation procedure. This approach consists of a parametric model that generates building massing design and a bespoke algorithm for façade development. While the building massing design is controlled by external parameters, the facade development is defined by a performance-related property associated with the generated building massing. This approach can be included in an optimization process that allows the optimization to search for solutions that can maximize the building performance by synergizing the building massing and façade design at the same time. Furthermore, architects can use this approach to explore the interdependent relationship between different façade design schemes and building massing design and become more performance-aware and informed in the design process.

To place this research into context, we first discuss the progress that has been made related to the evolutionary development approach. In section 2, we propose the workflow based on the Evo-Devo approach, which integrates façade and building massing design into optimization processes, followed by a case study and a comparison study to demonstrate its efficacy. We conclude the study by discussing the advantages of the facade-integrated processes over the separated design processes and how this approach can help in architects' early-stage design exploration and promote the incorporation of building massing and facade for performance-based architectural design.

1.1. APPLICATION OF EVO-DEVO IN ARCHITECTURAL DESIGN

Getting inspiration from nature in architecture has a long-standing tradition in history. It began with mimicking nature form in the 19th century. Later on, inspired by natural processes and systems, research on biomimicry-based adaptive design rise gradually. According to John Frazer (1995), architects should evolve rules (relations) for generating form, rather than the forms themselves, which explained the adaptive design (in his words, responsive architecture) well. Soon after that, evolutionary developmental biology science (Evo-Devo) was on the horizon, bringing new insight into the design field. Michael Weinstock (2013), who recognized and adopt Evo-Devo strategies in the architectural field, was considered the initiator of the related works by Navarro and Cocho (2020).

Evolutionary developmental design (Evo-Devo-Design) is a design method that combines complex developmental techniques with an evolutionary optimization technique (Janssen et al. 2011). In the architectural field, Evo-Devo approach is often used in design generation. Navarro has explored the generative capacity to integrate patterns and flows analogous to Evo-Devo strategies to develop emergent proto-architecture with great diversity in forms (Navarro and Cocho 2020). Such diversity was valuable but from the perspective of architectural design practice, hardly can this be useful for real-world design tasks.

In contrast, Evo-Devo approach also has been applied to performance-based building design optimization, where façade design is treated as a developmental change to create design variants with high diversity and environmental responsiveness. Janssen has presented design approaches using Evo-Devo approach involving façade development with a simple shading and fenestration

pattern (Janssen et al. 2011). Although this can be of greater relevance to practice, the approach simply integrates façade design into a linear workflow but without additional design consideration such as comparing different façade schemes. In real-world design scenarios, building facade is rarely determined at the outset of design, so that iterative design exploration of different façade schemes is often undergone to achieve an acceptable compromise among aesthetics, performance, budget, etc. Thus, this paper takes a step further through leveraging Evo-Devo approach for early-stage design exploration by including and synergizing building massing and different façade design schemes at the same time.

2. Method

As stated in section 1, this study applies an Evo-Devo approach for building design generation which can simultaneously combine the building massing and façade design in performance-based design optimization. Rather than merely searching for optimal solutions, this study is also aimed to facilitate architects' early-stage design exploration in regards to building massing and façade schemes, thereby, promoting a systematic investigation of the interactive relationship between them. This approach includes three steps, massing generation, simulation, and façade development.

First, the building massing generation procedure is based on an additive form generative algorithm, which is provided by EvoMass (Wang et al 2020a), a Rhino-Grasshopper plug-in. This algorithm creates the building massing by accumulating several mass elements, allowing the generated design to have high variability. The generated building massing design variants can be controlled by altering initial parameter settings, such as plane size, orientation, target area, etc. The strength of this algorithm is that it can be used for different types of building massing design, which, as a result, renders the proposed generation workflow high versatility beyond the presented building design task. Once the settings are defined, the generated design will be used as the basis for the following facade development.

Next, a simulation is conducted to calculate a performance-related attribute of the generated building massing. The attribute is affected by the building massing itself and the surrounding urban environment, which results in a large differentiation for the attribute of each façade surface. In this study, the simulation is executed by DIVA (Jakubiec and Reinhart 2011) relating to the solar irradiation. After the simulation, the generated building massing and the performance-related attribute will be sent to the next step.

The final step is facade development. With a predetermined facade design scheme, specific façade patterns are generated based on the corresponding building massing's surface and controlled by the performance-related attribute adherent to the surface. From the perspective of Evo-Devo, this step can be viewed as the building massing grows itself an adaptive skin in response to its surrounding environment.

The above design generation procedure can be included in an optimization process and evolved for high-performing design variants (Figure 1). Architects

can not only use these optimal design variants for further design development but also extract useful information and performance implication from the result (the elites' building massing, façade, and the performance indicator), which can be helpful for decision-making and design ideation.

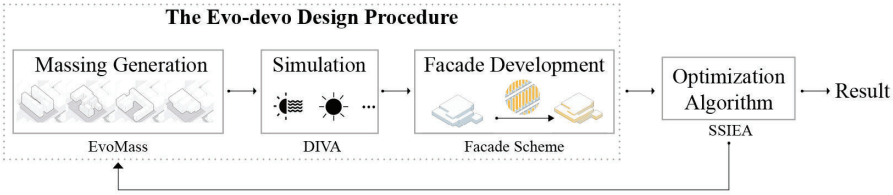

Figure 1. The proposed Evo-Devo design generation workflow.

3. Case study

3.1. DESIGN SETTING

For demonstrating the efficacy of the proposed workflow based on the Evo-Devo approach, a case study of performance-based building design optimization is presented. The target building of the case study is a 7-story building located in Wuhan, China (Figure 2). This region is characterized as a typical subtropical climate, which results in heavy cooling loads in summer due to excessive solar irradiation (SI) received.

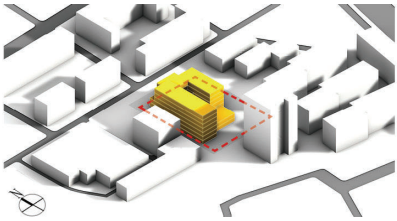

Figure 2. Case study design settings.

As shown in Figure 2, the selected site is situated in a complex urban environment with several high/middle-rise buildings, which leads to a complex micro-climatic condition. On the one hand, the surrounding buildings can cast shadows on the building plot, preventing certain parts of the building from being over-heated. But on the other hand, they also jeopardize daylight harvesting. Such a complex micro-climatic environment makes environmental factors (irradiation and daylighting) to be of great importance and can produce differences in the SI received on the façade surfaces. In this case, the façade's responses to the environment can be a significant factor in building performance.

3.2. BUILDING MASSING GENERATION AND FACADE DEVELOPMENT

First, building massing design is created by the generative algorithm. The main initial settings are 7 additive mass units, a 6-meter sized plan span(12×16), 7 floors with 4.5 meters in height each, and a target area of 15000 square meters. Second, due to the specific climatic conditions in Wuhan, solar heat gain is a more dominant factor affecting building performance than daylighting. Thus we conduct a simulation to calculate the solar irradiation (SI) received on the surface of the building massing, and use this to differentiate the feature of each facade surface.

Next, we define and encode three self-adjusted façade generative algorithms based on commonly-seen façade design schemes with distinguishing characteristics (Figure 3). These include a grille pattern (vertical shading), a sunshade pattern (vertical-horizontal mixed shading), and a fenestration pattern. Each pattern's generative algorithm remaps the SI intensity to a corresponding facade's attribute (density, depth, and numeric variation). With this attribute, an adaptive skin is grown from the generated building massing in response to the façade's thermal condition.

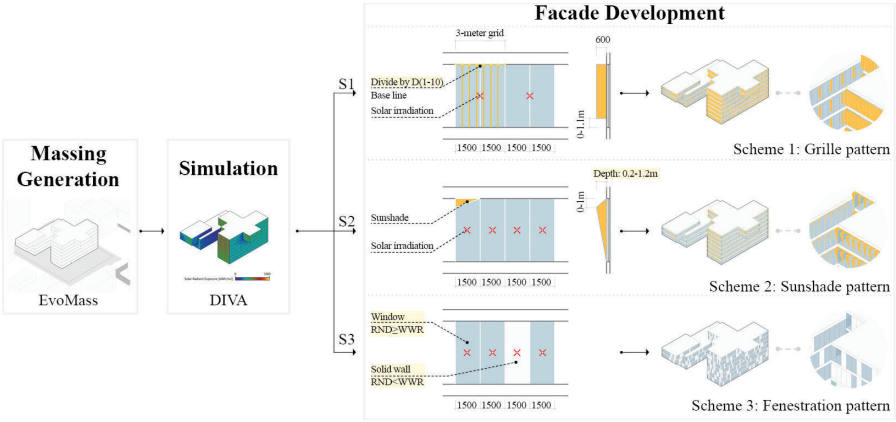

Figure 3. Three façade development schemes based on solar irradiation intensity received on the surface of the building massing.

Scheme 1 is a grille pattern with a density variation. First, the façade is divided into a 3-meter-width surface unit, and the SI data closest to the unit's central point is extracted for calculating the density of the grills in this façade unit. Then, the algorithm remaps the data of SI to an integer (D) between 1 and 10, and D defines the number of grilles in the façade unit. Thus, the grilles are denser where SI is higher. To make this pattern more influential, the length of grilles in the vertical direction also changes with SI intensity.

Scheme 2 is an external sunshade device with a depth variation. First, the façade is divided into a 1.5-meter-width surface unit. Next, an extruded triangular shading device is generated, while using the SI data closest to the unit's center as the basis for the sunshade's depth. The sunshade device has a greater depth

in places with higher SI. To enhance the sun-shading capability of the device, the height of the sunshade's extruded peak is also changing with SI intensity.

Scheme 3 is a fenestration pattern with a numeric and Boolean variation. Similar to Scheme 2, the façade is first divided into a 1.5-meter-width surface unit. Next, the SI data closest to the unit's center is used to convert to the wall-to-windows ratio (WWR), and each unit is assigned a unique random value (RND). If RND is smaller than WWR, then the unit will be defined as solid walls between windows, otherwise, glazing curtain walls. Consequently, the window opening ratio is lower where the SI intensity is higher.

3.3. OPTIMIZATION PROCESS

The proposed generation workflow with different façade patterns' developmental algorithm is included in an optimization process to explore the solution with maximized daylighting quality and the reduced SI to avoid over-heating. After the generation process, the final design variant is evaluated against the daylighting and SI performance. The performance indicator of daylighting (sDA) and irradiation (SI) is used to calculate the fitness for the optimization process. Regarding the optimization process, SSIEA (Wang 2020b) is used, which is a diversity-guided evolutionary algorithm provided by EvoMass. Three optimization processes (S1, S2, S3) are carried, based on the three façade patterns respectively.

For the optimization processes, the total number of iterations was 3,150, concluding 5 subpopulations. It means that there will be 5 elites winning after 3150 rounds of calculation. The optimization objective is to minimize SI and to maximize sDA, which are formulated into a single-objective fitness function as below:

$$\text{fitness} = \left(sDA - \frac{\text{SI}}{10000}\right) \times \left(1 - \left|\frac{S_A - S_T}{S_T}\right|\right) \tag{1}$$

The fitness is calculated by subtracting indoor solar heat gain through the façade (SI) from the daylighting indicator (sDA). Thus, high-performing design variants receive lower SI while gaining higher daylighting. In addition, a target gross area of the building (S_T=15000 m²) is set and served as a penalty function so that the design variants (with the actual gross area of S_A) failing to satisfy the gross area requirement is punished by reducing the fitness value.

4. Result

In this case study, the five highest-ranking design variants (elites) from three optimization processes (S1, S2, S3) with different façade schemes are retrieved. Each process took about 35 hours to calculate. Figure 4 summarizes the elites and their performance indicators. Table 1 provides the average of each indicator of the elites from S1, S2, S3.

For optimization S1, it achieves the best average fitness among these three optimization processes. From the architectural perspective, the elites show the east-west strip shape with a small depth in floor plans, which is favorable for daylighting quality. It is because that the grille pattern is more efficient in blocking

sunlight; therefore, the compromise on daylighting is trivial.

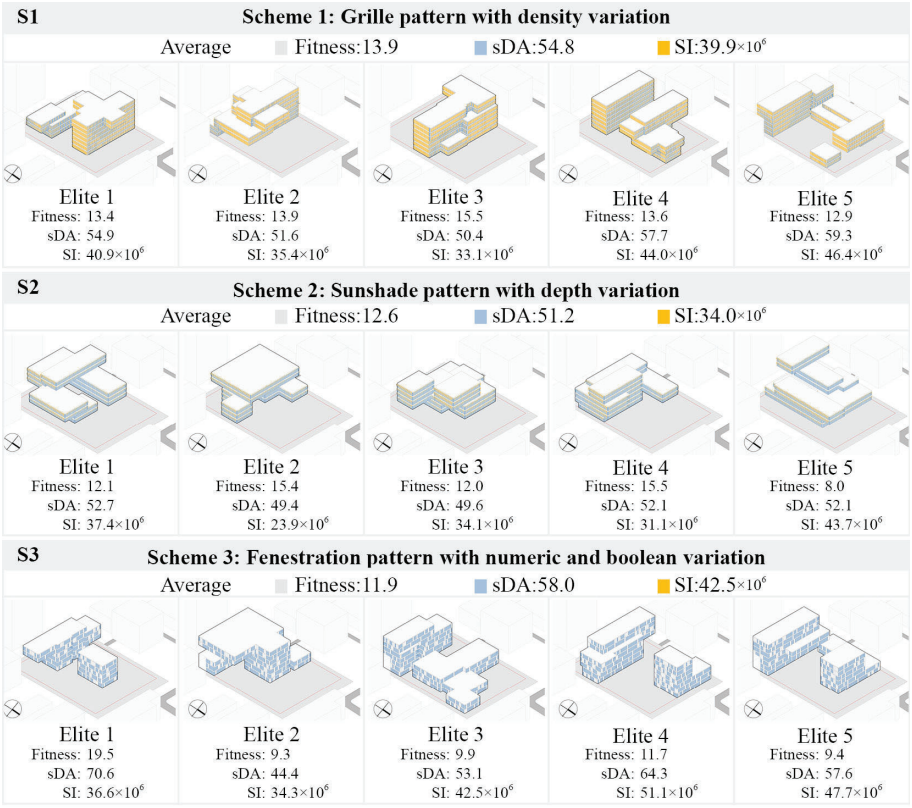

Figure 4. Five highest-ranking design variants(elites) from the three optimization results of the case study (Total number of tests:3150 for each).

For optimization S2, the elites show a tendency of self-shading with a greater depth in the floor plan than those in S1. It reveals that the triangular shading element is relatively weak in blocking SI, while reducing the adverse effect on daylighting. Thus, the weaker shading effect, in turn, requires the building massing to play a greater role in avoid over-heating. Thus, it also results in a significant compromise on daylighting than in S1 indicated by the average sDA value.

For optimization S3, it gets the lowest average fitness. The elites feature scattered and separated massing, and the massing in the north are generally higher than those in the south to achieve a mutual blocking of sunlight. This is to compensate for the incompetence of the shading effect, for this pattern can only respond to SI through varying the wall-to-windows ratio. However, it achieves the best average sDA due to less daylight obstruction when there are no extra shading devices.

Table 1. The average of each indicator of the elites from optimization S1, S2, S3 (SI:×10^6kWh).

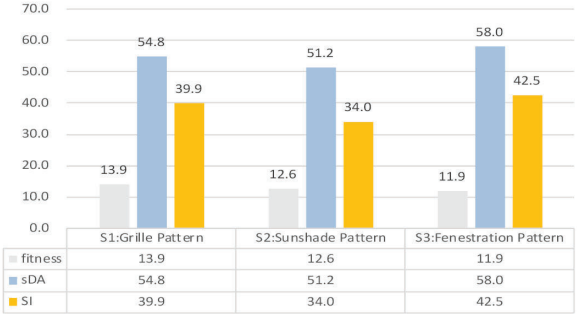

5. Comparison study

The optimization results show different compromises between SI and daylighting when using different façade schemes. It raises the question of how the design responds to the environment without these adaptive building skins, and whether the facade-integrated design process has an advantage over the non-integrated one. In light of this, a comparison study is conducted to test out whether the integration of the façade development would make a difference in the optimization.

Firstly, an optimization process (C0) is carried out to optimize the design without any self-adjusted façade generation scheme but with the same settings as the case study, which serves as an example of the conventional facade-separated design process to be the control group for the former experiments (Figure 5, S1, S2, S3). Since SI is the main influencing factor, the elites from the control group (C0) show concentrated shapes in the south with a large depth, to minimize the heat gain by taking advantage of the shadow created by the high-rise building in the south.

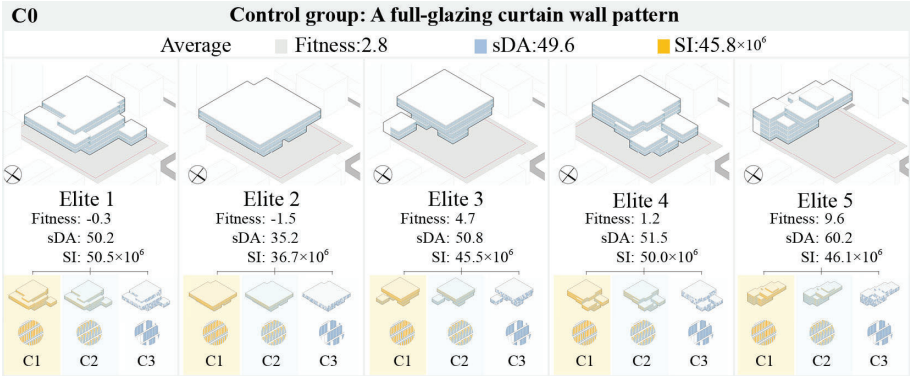

Figure 5. Optimization C0's result and groups of the generative results (C1, C2, C3) with façade scheme 1 to 3 respectively.

According to the results of these four optimizations, demonstrated in Table 2, elites from facade-integrated design processes (S1, S2, S3) significantly outperform those in the C0. Additionally, the building massing demonstrates distinctive differences, as shown in Figure 4 and Figure 5. Both become evidence of the great influence of façade design on building performance.

Next, the five elites' building massing designs from C0 are also incorporated with the three façade schemes, resulting in 15 final designs, which are marked C1, C2, C3 to present 3 groups of the results with Schemes 1 to 3 respectively. This generative step simulates the conventional design processes, where facade design is being scheduled after the building massing is finally determined.

As shown in Table 2, the average fitness of S1, S2, S3 generally outperforms the ones from C1, C2, C3, which further validates the efficacy of the proposed generation workflow. By comparing the average of sDA and SI, it is notable that integrated ones (S1, S2, S3) unexpectedly outperform in sDA but underperform in SI, it may be because that building massing in C0 contributes more to SI reduction than façade. Lastly, the separated design process drives the optimization search for solutions in one direction and results in one type of building massing design, thus killing the diversity of the final results. In contrast, with different design schemes, the proposed approach diversifies the optimization searching direction and, thereby, stimulate architects' design exploration..

Table 2. The average of each indicator of the elites in optimization S1, S2, S3, C0, C1, C2, C3, showing the difference between the façade-integrated design processes and the non-integrated ones (SI:×10^6kWh).

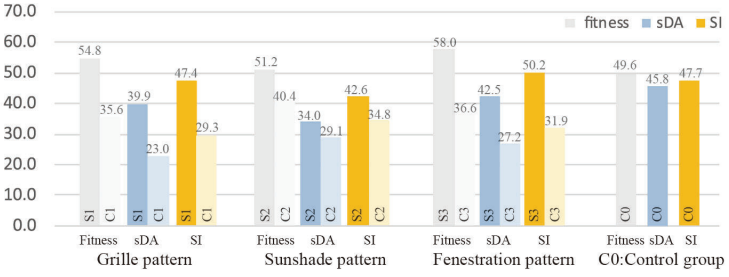

6. Discussion and conclusions

The results of the case study demonstrate that with different façade schemes, the produced optimal building design shows different characteristics in terms of the building form and performance. In addition, the comparison study also highlights the necessity of the proposed integrated design workflow based on the Evo-Devo approach comparing with the non-integrated one. Thus, incorporating façade design into the performance-based building massing design is rewarding.

With the proposed workflow combining EvoMass, architects can make an early-stage design exploration of different façade schemes by comparing the feature of design variants, from which, they can extract information about façade and building massing design. For façade design, this exploration helps to reveal

underlying performance implications about different façade schemes and their impact on building massing design. This can inform architects' decision-making when considering other design concerns such as aesthetics and cost. For building massing design, this exploration discloses how the building responds to the environment with different skins. Consequently, such exploration provides architects a larger picture of the design problem and stimulate design ideation.

Beyond its implication of practical applications, this study also promotes research on the façade design's impact on building performance. This topic is not new in research, and there have been many studies that consider façade design as an important factor influencing building performance, such as Lee's research of façade shading (Lee 2017). However, the limitation is that they typically use rooms as the analysis unit, rather than from the perspective of the whole building to compare the advantages or disadvantages of different facade designs. This may be misleading when considering the overall design.

To conclude, this paper proposes an integrated building design optimization workflow that can synergize the strengths of building massing and façade design at the same time. The advantages will encourage architects to apply design optimization exploration to the early-stage design and make architecture become a more responsive and adaptive agent in shaping our future built environment. Future research will consider more factors in the optimization objectives, such as ventilation, cost, and energy consumption, to meet the requirements of complex real-world design scenarios. Furthermore, more detailed and sophisticated façade schemes can be considered in the façade development step, including varying sizes, orientations, angles, materials, which will increase the practicality and enhance performance improvement.

References

Frazer, J.: 1995, *An Evolutionary Architecture*, AA Publications, London,UK.

Hensel, M., Menges, A. and Weinstock, M.: 2013, *Emergent technologies and design: towards a biological paradigm for architecture*, Routledge.

Jakubiec, J.A. and Reinhart, C.F.: 2011, DIVA 2.0: Integrating daylight and thermal simulations using Rhinoceros 3D, Daysim and EnergyPlus, *Proceedings of building simulation*, 2202-2209.

Janssen, P., Basol, C. and Chen, K.W.: 2011, Evolutionary developmental design for non-programmers, *Ecaade 2011*, **Respecting Fragile Places**, 245-252.

Lee, K.S., Han, K.J. and Lee, J.W.: 2017, The impact of shading type and azimuth orientation on the daylighting in a classroom–focusing on effectiveness of faccade shading, comparing the results of DA and UDI, *Energies*, **10**(5), 635.

Navarro-Mateu, D. and Cocho-Bermejo, A.: 2020, Evo-Devo Strategies for Generative Architecture: Colour-Based Patterns in Polygon Meshes, *Biomimetics*, **5**(2), 23.

Wang, L., Chen, K., Janssen, P. and Ji, G.: 2020, ALGORITHMIC GENERATION OF ARCHITECTURAL MASSING MODELS FOR BUILDING DESIGN OPTIMISATION - Parametric Modelling Using Subtractive and Additive Form Generation Principles, *CAADRIA 2020*.

Wang, L., Janssen, P. and Ji, G.: 2020, SSIEA: a hybrid evolutionary algorithm for supporting conceptual architectural design, *Artificial Intelligence for Engineering Design, Analysis and Manufacturing: AIEDAM*, **34(4)**, 458–476.

Robotics & Digital Fabrication in Construction

A TOOL FOR SEARCHING ACTIVE BENDING BAMBOO STRIPS IN CONSTRUCTION VIA DEEP LEARNING

XUYOU YANG[1] and WEISHUN XU[2]
[1] *1 Design Lab*
[1] *xuyou.yang.92@gmail.com*
[2] *Zhejiang University*
[2] *xuweishun@zju.edu.cn*

Abstract. As an alternative material for construction, the structural use of bamboo in architecture is commonly associated with active bending. However, as natural material, the deformation of unprocessed bamboo strips is affected by the distribution of nodes, whose impact on deformation is difficult to precisely programme for each individual case and thus often causes discrepancies between generic digital simulation and construction. This research proposes a tool for searching active bending bamboo strips via deep leaning based on a multi-task neural network. The tool is able to predict both the number and locations of nodes suggested on bamboo strips according to a target curve as tool input. By approximating the prediction, users can find a strip that is most likely to deform into the desired geometry.

Keywords. Neural network; active bending; neural architecture search (NAS); bamboo; material behaviour.

1. Introduction

1.1. BAMBOO AS AN ALTERNATIVE BUILDING MATERIAL

As well known, bamboo, with a simple and fast production process, is a sustainable, economic and structurally efficient material (Van der Lugt et al., 2006). As an alternative building material, bamboo construction consumes far less energy when compared to the use of conventional building materials such as concrete or steel of the same size (Janssen, 1988) .

Earlier life cycle assessment studies show that among different types of bamboo-based construction, the use of raw bamboo including bamboo poles and strips has the lowest environmental impact (Escamilla and Habert, 2014; Escamilla et al., 2018). In traditional architectural practices, structural use of raw bamboo is commonly associated with systematic choreography of active bending (Dunkelberg, 1985; Lienhard et al., 2013).

1.2. DIGITAL SIMULATION OF ACTIVE BENDING

Bending-active structures are often formed by rod elements that deform in bending, and are usually light-weight and resilient, due to the fact that elastic bending in

PROJECTIONS, Proceedings of the 26th International Conference of the Association for Computer-Aided Architectural Design Research in Asia (CAADRIA) 2021, Volume 1, 463-472.

the material allows for flexing instead of breaking and buckling (Cuvilliers et al., 2018). The lightness and adaptability of bending-active structures have been of spatial and technical interest to architects such as Frei Otto (Nerdinger and Barthel, 2005).

The deformation of material in bending-active structures can usually be described by analytic geometry following the rules of the elastica (Lienhard, 2014), which offers a mathematical basis for its form-finding regardless of materiality. In the digital age, form-finding simulation methods are actively developed to accommodate architectural designers' interest in bending-active structures in the design stage (Bauer et al., 2018). For instance, by reducing the degree of freedom of a spatial node from 6 to 3 (Adriaenssens and Barnes, 2001), Kangaroo Physics, a plug-in for the digital modeling software Rhinoceros, applies dynamic relaxation method to simulate bending-active behavior of an elastic rod (Piker, 2013; Cuvilliers et al., 2018).

1.3. INACCURATE SIMULATION OF NATURAL MATERIALS

Despite the wide adoption of digital simulation solutions for bending-active structures, it has been difficult to accurately design and construct bending-active bamboo structures in the contemporary digital design context. One major reason has to do with the inaccuracy of commonly adopted digital form-finding process when applied to natural materials such as bamboo, thus creating a gap between the design and subsequent construction.

Two major reasons cause the difficulty to accurately simulate and construct the designed form of bamboo strip structures. First, the structural performance of bamboo strip bending displays non-linear characteristics due to its foam-fibre composite structure (Obataya et al., 2007; Zhou et al., 2012), which renders the form-finding process of bending bamboo strips rather difficult through commonly used design software. Also, the compression and tensile modulus of the material are different from each other, causing more complex material behaviour (Dongsheng et al., 2013). Second, the distribution of bamboo nodes has a complicated impact on compression during the bending process and therefore impact the deformation (Meng and Sun, 2018). Due to the uniqueness of unprocessed bamboo strips, it is much laborious to precisely programme the impact on deformation for each individual case.

The inaccuracy of digital simulation for material behaviour of bending raw bamboo strips is particularly pronounced when node distribution is involved in real world, as shown in an earlier study (Chen and Hou, 2016). In a preliminary one to one scale simulation-construction test (Figure 1) conducted by the authors in the early stage of this research, extra lateral supports had to be added to the bending-active structure in order to respond to the obvious deviation from the simulated geometry caused by unpredictable distribution of nodes, thus effectively rendering the load condition different from the intended design.

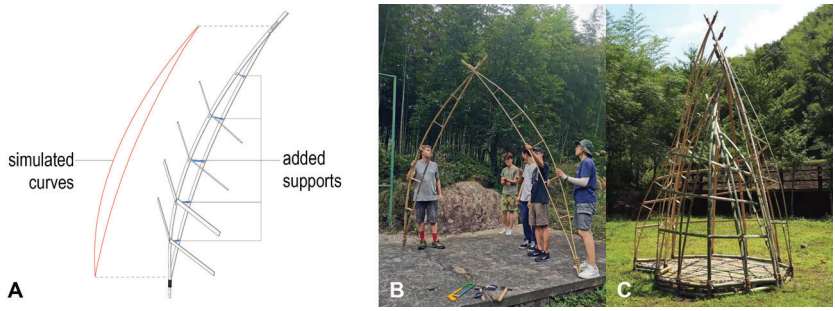

Figure 1. The preliminary one to one scale simulation-construction test. A: extra lateral supports added to respond to the deviation from simulation; B: construction process; C: final outcome .

1.4. MACHINE LEARNING'S RECENT DEVELOPMENT IN ARCHITECTURE

In the recent years, enabled by the rapid growth of computational power, machine learning techniques emerge quickly and have been globally implemented in many disciplines such as autonomous driving, biological diagnose, privacy protection and so on. It has also been increasingly deployed in architectural studies to solve various problems including material behaviour prediction (Luo et al., 2018; Chen et al., 2019; Wu et al., 2019) that were previously difficult to approach through conventional structural modelling. One important advantage of machine learning in solving material behaviour problems is that it is data-driven instead of computing the outcomes following structural formulas, which paradoxically have difficulties in describing the behaviour of natural materials as introduced in section 1.3.

Among all machine learning subfields, neural network (NN) makes up the backbone of deep learning. Early NNs can date back to the 1960s or even earlier and gained their popularity in the new millennium (Schmidhuber, 2015). Usually, a neural network takes numerical input, and can be used for regression and classification problems.

1.5. PROPOSED SOLUTION

This research proposes a handy tool which could predict a specific number and locations of nodes required on a bamboo strip in order to better deform the bamboo strip into a desired shape in construction via deep learning. Architects or builders can search for such a bamboo strip by approximating the prediction. This tool closes the gap between digital simulation and subsequent construction of a design. It also helps designers avoid confronting simulation software with structural knowledge as the tool bypasses programming structural rules by using machine learning techniques.

A neural network model is chosen to build up the tool because of its powerful nonlinear fitting ability, and the model is trained and tested with a dataset collected by the authors.

2. Methods

2.1. DATA COLLECTING

In this research, a series of bamboo strip bending experiments are conducted. A set of original data is collected from the experiments and processed automatically with the help of computer vision algorithms.

2.1.1. Preparation of Bamboo Strips

A batch of 40 bamboo strips of the same species purchased from the same supplier are used for the experiments to minimise the impact of unmeasured parameters such as fibre quality or node structure. Each bamboo strip is about 4,000 mm in length, 50 mm in width measured from the bottom end and 10 mm in thickness. Due to the nature of the species chosen, the strips are rather even in width and thickness distribution. Because each node occupies a tiny visual proportion in the environment, to enhance the apparentness of nodes, each node on the bamboo strips is marked with bright red elastic tapes before the bending experiments. The experiments are finished within two weeks in order to minimise the potential material behaviour change caused by bamboo dehydration and preservation conditions.

2.1.2. Bending Platform and Environment Setup

A pair of two Kuka KR120 R2500 six-axis industrial robots placed 3,200 mm apart from each other measured from the canter points of the base are used to form the bending platform. The bending platform is placed in an indoor lab with ample artificial lighting. However, the lab has a few large skylights that cannot be blocked, creating a changing lighting environment throughout the day. Due to the limited experiment time window, a few bending and video shooting sessions have to be executed during the day. A large piece of black fabric, along with a few pieces of black PVC boards have to be placed behind and around the bending platform to reduce the impact of the natural light. However, the lighting environment change is still visible from the videos taken.

The end effectors of the bending platform are designed to freely rotate in order to minimise torque from the holding positions. A pair of QT-120 steel ball lock tool quick change system are used as its base, and an NSK sliding bearing are placed as its core. The position of the bearing is locked onto the flange by four M10 bolts, and the journal of the bearing is subsequently connected to a round stainless-steel platform on top of which two adjustable rubber clamps are mounted. The rubber clamps are marked with blue paint for segmenting the holding positions through computer vision method.

2.1.3. Bending Experiments

The free-rotation setup of the end effectors allows the operation of only one robotic arm. A fixed route-following algorithm generated in Grasshopper is used on different bamboo strips for half of the bending and video shooting sessions. To add to the randomness of the data sample, for the other half, the robotic arm is

manually operated through the teach pendant. In both cases, as demonstrated in Figure 2, the end effectors are placed in a surface perpendicular to the camera direction. An iPhone XS placed 5000 mm from the center-to-center line of the bases of the industrial robots and 1250 mm above floor level is used for shooting videos. Subsequently, the movement of the end effector is controlled to be around the same height and refrained in the same plane 4000 mm from the camera. During the bending experiment, most bamboo strips are held at three different positions to allow for different node distribution patterns, and for each position, the robot arm moves along at least two route settings to obtain different bending curves. Along each route, three to five distinguishable bending curves are saved by extracting frames from the videos. Finally, a total number of 1100 images are collected with 40 bamboo strips.

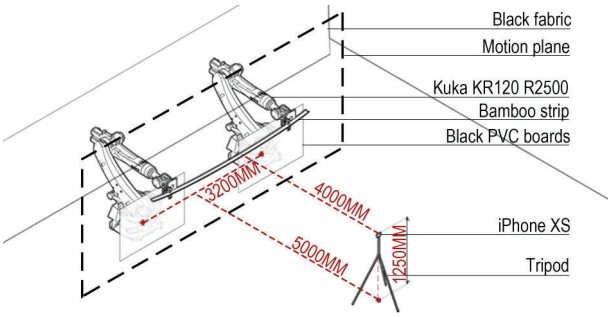

Figure 2. The bending experiment .

2.1.4. Computer Vision Processing of Images

Because of the visible light changes across images, in order to guarantee a uniform quality of the images and obtain a more accurate colour segmentation result, each bamboo node is marked again in Adobe Photoshop before processing with a computer vision algorithm. However, this extra marking step can be avoided by recording the videos in a fully light-controlled condition.

The computer vision algorithm separates bamboo strips and nodes from the background. In details, for every input image, pixels of the bamboo strip are segmented and converted into a curve lying in the centre of the bamboo strip in a Cartesian coordinate system. Then the curve is discrete into 1000 points so that each point can be assigned a probability of being a node. Secondly, the X and Y values of the node centroids in the coordinate system are computed. Thirdly, the Euclidean distance between each node centroid and its adjacent points on the curve is calculated. Probabilities of being a bamboo node for the 1000 points are assigned according to this distance and are normally distributed around the node centroids. Compared to labelling a few specific points as bamboo nodes, assigning points with node probabilities is more feasible for training the neural network introduced in later sections. Finally, a 1002-line text file is generated. The first 1000 lines document the coordinate values of each point on the curve and their corresponding probabilities of being a node. The last two document the total number of nodes

and the indexes of them respectively. With the 1100 images mentioned in section 2.1.3, a same number of such files are generated. Figure 3 demonstrates an original image and the output of the computer vision algorithm.

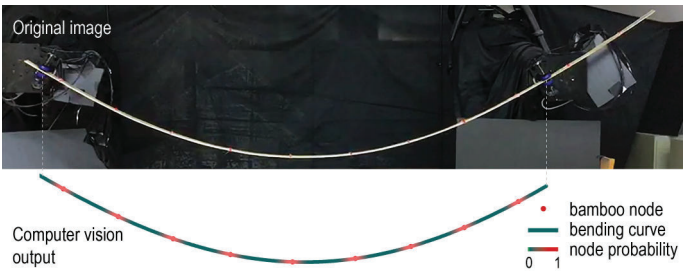

Figure 3. An original image and the computer vision output.

2.2. THE NEURAL NETWORK

This tool is established based on an artificial neural network. In construction, to better achieve a particular form through bamboo strip active bending, one can input the designed curve to the neural network model, which can then predict the node distribution of a bamboo strip that can most probably deform into the designed curve.

2.2.1. Dataset

The dataset contains 1100 files introduced in section 2.1.4, representing different combinations of bamboo strip node distribution and bending curve. Regardless of the actual length of the curves in reality, the coordinate values are all normalised to the range between 0 and 1. Among the files, randomly 1000 are used for training the neural network, and the rest 100 are used for testing.

2.2.2. Basic Neural Network Architecture

The neural network has a multi-task learning architecture consisted of an input layer, backbone, node number branch and node location branch as Figure 4 shows.

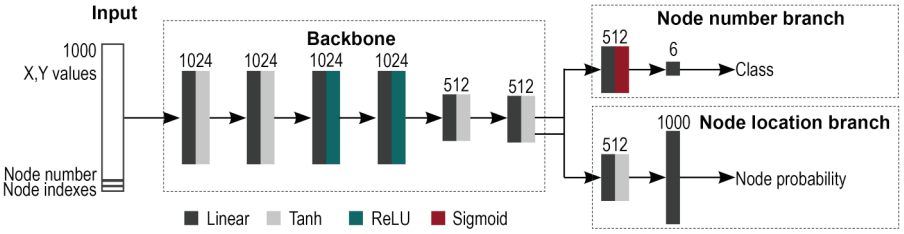

Figure 4. Architecture of the neural network.

The backbone plays the role of extracting features shared by the node number branch and node location branch. It contains 6 layers: the first 4 layers have 1024

channels, and the width of the last 2 layers is 512. This particular architecture is chosen via automatic neural architecture search which will be introduced in section 2.2.3. In this research, predicting the number of nodes is considered as a classification problem where each type of node number is seen as one class. As in the current dataset the number of nodes ranges from 6 to 11, there are 6 classes in total. Accordingly, the node number branch outputs 6 classification probabilities. The node location branch contains 1000 output units. Each unit outputs the node probability of a curve point.

The neural network was originally designed as one single branch predicting the probabilities of the 1000 points being a node. Consequentially, the number of nodes is calculated according to the number of probability peaks. However, this method could not provide accurate result because it is very complicated to denoise the probabilities without knowing the exact number of nodes. Since it is necessary to obtain both the number of nodes and the 1000 probabilities, it is then considered as a multi-task learning problem. The performance of the neural network dramatically improves when the architecture is modified to consist the truncated node number branch and node location branch.

2.2.3. Neural Architecture Search

As manually developing the architecture of neural networks can be time-consuming and inefficient, automatic neural architecture search (NAS) (Elsken et al., 2019) is increasingly deployed in various machine learning tasks. This research uses the Neural Network Intelligence (NNI) v1.9, a toolkit developed by Microsoft to automatically search the backbone architecture of the neural network that could best perform the tasks.

There are three major parameters in the search space, namely, depth of the neural network, types of activation functions, and number of channels in each hidden layer. Specifically, the depth of the network can range from 2 to 6, and every linear layer is followed by an activation function of Tanh, Sigmoid or ReLU. The channel of each layer can vary among 256, 512 and 1024. In a prediction, if the number of nodes does not match the ground truth, this prediction is considered as an error. The total number of errors is reported to the NNI tuner to be minimised.

Within the allowance of computational power and research period, 1020 different backbone architectures are tested in the search space. Figure 5 displays the search trials where the backbone architecture introduced in section 2.2.2 is chosen from.

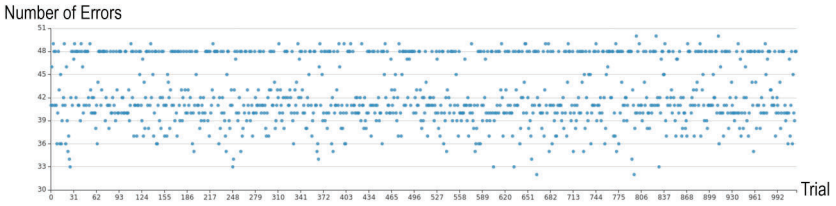

Figure 5. Neural architecture search trials.

2.2.4. Training

To train the neural network model, an initial learning rate of 1e-3 is adopted with a Cosine learning rate decay limited to 1e-8 as minimum. An Adagrad optimiser (Duchi et al., 2011) is used. There are two different types of loss functions applied to the number of nodes and the locations of them. For the number of nodes, it uses cross entropy loss, while for the locations of nodes, mean squared error loss is adopted. The total loss equals to the location loss summed with a dynamically weighted node number loss whose weight increases from 0.1 to 0.3 from the first epoch to the last. The total epochs are 1500 when training the network whereas to accelerate the NAS, the number of epochs is set to only 360 during the search. The batch size is 16.

3. Result

Through testing, 74% of the node number predictions are accurate, within which the average discrepancy of node locations equals to only 3.66% of the length of a bamboo strip. Among the inaccurate predictions of node numbers, the average discrepancy is only 1.2 nodes. This is considered as just acceptable as having one node different would not affect the deformation dramatically. The result demonstrates a decent accuracy of the tool in both node number and location prediction tasks. Figure 6 demonstrates some of the prediction results.

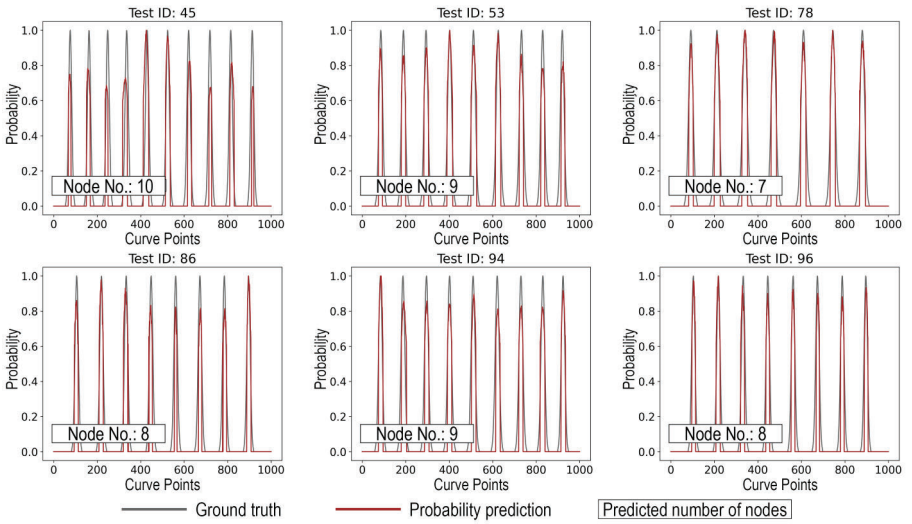

Figure 6. Predictions of the neural network compared with ground truths .

4. Future Line of Research

The current dataset contains a small number of samples. For the following two reasons, it is critical to expand the dataset to improve the performance of the tool and obtain more useful applications. First, as the deformation of bamboo strips is

affected by many other factors than nodes, it can be valuable to develop a much larger dataset of bamboo strips to involve factors such as species, humidity, age and so on, and use them all as machine learning features. In this way, the model can be extended to practical use under varied conditions. Second, a larger dataset with more evenly distributed number of nodes can help achieve a higher overall accuracy, since the current dataset has a very biased amount of data in each class.

The current computer vision algorithm uses colour segmentation to extract node locations. This makes it very prone to light conditions when the images are taken and is very likely to be affected by other contents within the image. However, using object detection to detect nodes could avoid these disadvantages.

As of applying the findings in this research to actual construction, future exploration should also include how an integrated workflow can be setup from establishing a digital material database to design and subsequent material allocation. Due to the dynamic nature of bending-active structure construction, real-time feedback of the construction with technologies such as augmented reality should also be considered.

5. Conclusion

This research is a primary study of utilising machine learning techniques to predict natural material behaviours which are difficult to simulate with conventional architectural design software. A dataset of bamboo node distribution patterns and bending curves is created, based on which a tool for users to search bamboo strips that can better deformed into the desired shape is developed via multi-task learning method. It achieves a very promising accuracy when applied to the range similar to the current dataset. However, it needs to be further developed to suit a wider range of applications.

Acknowledgement

The authors sincerely thank Yucheng Zhao for his advices on machine learning and computer vision. The authors also thank Yiyao Guo, Sijia Gu, Shengzhang Pan, Liquan Zheng, Yang Luo, Xinchang Chen, Yijiang Zhu, Jiale Huang, Fan Yu, who are architecture students from Zhejiang University, for helping with the data collection.

References

Adriaenssens, S. and Barnes, M.R.: 2001, Tensegrity spline beam and grid shell structures, *Engineering structures*, **23**(1), 29-36.

Bauer, A.M., L”angst, P., La Magna, R., Lienhard, J., Piker, D., Quinn, G., Gengnagel, C. and Bletzinger, K.U.: 2018, Exploring Software Approaches for the Design and Simulation of Bending Active Systems, *Proceedings of IASS Annual Symposia 2018*, Boston, USA, 1-8.

Chen, I.C. and Hou, J.H.: 2016, Design with bamboo bend: Bridging natural material and computational design, *Proceedings of the 21st CAADRIA Conference*, Melbourne, Australia, 125-133.

Chen, D., Luo, D., Xu, W., Luo, C., Shen, L., Yan, X. and Wang, T.: 2019, Re-perceive 3D printing with Artificial Intelligence, *Proceedings of the 37th eCAADe/23nd SIGraDi Conference*, Porto, Portugal, 443-450.

Cuvilliers, P., Yang, J.R., Coar, L. and Mueller, C.: 2018, A comparison of two algorithms for the simulation of bending-active structures, *International Journal of Space Structures*, **33**(2), 73-85.

Dongsheng, H., Aiping, Z. and Yuling, B.: 2013, Experimental and analytical study on the nonlinear bending of parallel strand bamboo beams, *Construction and Building Materials*, **44**, 585-592.

Duchi, J., Hazan, E. and Singer, Y.: 2011, Adaptive subgradient methods for online learning and stochastic optimization., *Journal of machine learning research*, **12**(7), 2121-2159.

Dunkelberg, K., GaB, S., Drüsedau, H. and Hennicke, J.: 1985, *IL 31 Bambus Bamboo*, Karl Krämer Verlag Stuttgart.

Elsken, T., Metzen, J.H. and Hutter, F.: 2019, Neural architecture search: A survey, *Journal of Machine Learning Research*, **20**, 1-21.

Escamilla, E.Z. and Habert, G.: 2014, Environmental impacts of bamboo-based construction materials representing global production diversity, *Journal of Cleaner Production*, **69**, 117-127.

Escamilla, E.Z., Habert, G., Daza, J.F.C., Archila, H.F., Fern'andez, J.S.E., Trujillo, D. and Archilla, H.F.: 2018, Industrial or traditional bamboo construction? Comparative life cycle assessment (LCA) of bamboo-based buildings, *Sustainability (Switzerland)*, **10**(9), 3096.

Janssen, J.J.: 1988, The importance of bamboo as a building material, *Bamboos: Current Research, Proceedings of the Engineering and Utilization International Bamboo, Workshop*, Cochin, India, 14-18.

Lienhard, J.: 2014, *Bending-active structures: form-finding strategies using elastic deformation in static and kinetic systems and the structural potentials therein*, Ph.D. Thesis, University of Stuttgart.

Lienhard, J., Alpermann, H., Gengnagel, C. and Knippers, J.: 2013, Active bending, a review on structures where bending is used as a self-formation process, *International Journal of Space Structures*, **28**(3-4), 187-196.

van der Lugt, P., van den Dobbelsteen, A. and Janssen, J. J.: 2006, An environmental, economic and practical assessment of bamboo as a building material for supporting structures, *Construction and building materials*, **20**(9), 648-656.

Luo, D., Wang, J. and Xu, W.: 2018, Applied Automatic Machine Learning Process for Material Computation, *Proceedings of the 36th eCAADe Conference*, Łódź, Poland, 109-118.

Meng, J. and Sun, D.: 2018, Effects of node distribution on bending deformation of bamboo, *Journal of Tropical Forest Science*, **30**(4), 554-559.

Nerdinger, W. and Barthel, R.: 2005, *Frei Otto: Complete Works: Lightweight Construction, Natural Design*, Birkhäuser Switzerland.

Obataya, E., Kitin, P. and Yamauchi, H.: 2007, Bending characteristics of bamboo (Phyllostachys pubescens) with respect to its fiber–foam composite structure, *Wood science and technology*, **41**(5), 385-400.

Piker, D.: 2013, Kangaroo: form finding with computational physics, *Architectural Design*, **83**(2), 136-137.

Schmidhuber, J.: 2015, Deep learning in neural networks: An overview, *Neural networks*, **61**, 85-117.

Wu, N.H., Dimopoulou, M., Hsieh, H.H. and Chatzakis, C.: 2019, Rawbot-A digital system for AR fabrication of bamboo structures through the discrete digitization of bamboo, *Proceedings of the 37th eCAADe/23nd SIGraDi Conference*, Porto, Portugal, 161-170.

Zhou, A., Huang, D., Li, H. and Su, Y.: 2012, Hybrid approach to determine the mechanical parameters of fibers and matrixes of bamboo, *Construction and Building Materials*, **35**, 191-196.

OPTIMAL DESIGN OF WOODEN PAVILION GRIDSHELL STRUCTURES IN THE CONTEXT OF ARCHITECTURAL AND STRUCTURAL COLLABORATION

EWELINA GAWELL
[1] *Warsaw University of Technology, Faculty of Architecture*
[1] *ewelina.gawell@pw.edu.pl*

Abstract. In the article two interacting aspects of collaborative design are described: shaping of the form and the rational use of materials. Form shaping will be analyzed on the basis of pavilions. The material aspect of this paper is concerned with the use of wood in contemporary construction. The first goal is to analyze the selected technical parameters related to the use of wood in the optimal shaping of gridshell structures in architecture. The second goal is to identify new opportunities for architectural and structural engineering cooperation in the context of generative digital tools. The possibility of creating new plugins for the existing generative modeling programs to improve the quality of collaboration will also be discussed. The paper is concerned with elementary research. I was able to achieve the set goals by means of theoretical analyzes based on the known literature as well as the analysis of the created objects and the accompanying research. The background for the work is a description of the selected trends of using natural wood as load-bearing elements in contemporary architecture and case studies of the selected objects that express the idea of form and material eco-efficiency.

Keywords. Wooden structures; structural detail; bionic models.

1. Introduction

Architecture is the art of building in confrontation with many issues - technical as well as sensational. The overarching goal of architectural design emerges from the antagonism of all of the elements involved in the process of creating the work. The need to express the beauty of the form - its composition, proportions, materials - confronts the author with a reality, which manifests itself, among others, in construction technologies, building law and design standards, etc. The knowledge of the matter and tools of the trade is essential in the process of creating architectural work, but the idea requires sensitivity, reflection and deliberateness. The basis for architectural design is therefore the search for spatial forms whose structural beauty is in symbiosis with the physical forces which affect them. The words of Jordan Woodson (an engineer working at the Arup studio) may be helpful in understanding the issues of the design of structural forms: "To understand how something stands up you have to understand how it might fall down". The state in which the structure would fail reveals the "uncertainty" of the structure, which

PROJECTIONS, Proceedings of the 26th International Conference of the Association for Computer-Aided Architectural Design Research in Asia (CAADRIA) 2021, Volume 1, 473-482.

allows to infer how to safely design a load-bearing structure. Such analysis is particularly valuable for young architects in training.

Due to the contemporary sustainable development trends in architecture, rational design of structural forms is becoming more and more important. The growing interaction between architecture and structural design indicates the logical direction for creative explorations. In the search for effective solutions inspiration can be found in the technologies developed by Nature. Bionic inspirations often take the form of recreating the structure of living organisms. In this context, the use of wood in architecture is a natural choice - due to its material characteristics and anisotropic properties. Optimal design of wooden structures requires an understanding of those properties. Bionic solutions are also visible in the analysis of the flow of physical forces in structures and designing them in such a manner as to reduce unnecessary geometry [P. Charest, A. Potvin, C. Demers, S. Menard, 2019]. This is facilitated by the use of timber as a structural material - which is further supplemented by, among others, the dynamic development of formative construction technologies, e.g. related to the use of CNC machines for the production of load-bearing gridshell elements [A. Menges, B. Sheil, R. Glynn, M. Skavara, 2017].

Modern directions for the developments in architecture are connected with multi-criteria rationalization of technical solutions, aimed at reducing the investment costs as well as the negative impact on the environment. Eco-efficiency became an important part of construction and it finds its expression, among others, in minimizing building material and energy consumption, using materials that can be reused or the production speed of construction elements. At the same time, the search for new artistic quality in architecture is still an unchanging determinant of the design process and the criterion for assessing the work.

2. Architectural and structural design in the context of material properties

In contemporary wooden architecture, designers strive to design innovative solutions, structurally logical and visually attractive. A technical answer to an aesthetic creation can be found in the structural form, an example of unity between technique and art [Siegel, 1974]. The same applies to structural connections. The joint is a special place for transferring physical forces and the power of visual expression - it combines technology and art in one solution. The essence of design exploration is not to design an architectural form that would cover structural elements. Its purpose is to show the beauty of the structure and achieve synergistic solutions [Gawell, 2018]. This perception of architecture is a modern direction, rooted in bionic thinking. One of the main assumption of this trend is the pursuit of eco-efficiency understood as the rational use of material. This is related to the reduction of material consumption (minimum weight of structural material used). In the case of wood it is particularly due to the effective use of its natural properties. An example of such a design is the roof structure of the Mannheim Pavilion designed in 1975 by Otto Frei (in collaboration with two architects: Carlfried Mutschler and Winfried Langner), see Figure 1 and [I. Liddell, 2015]. The unconventional roof consists of a double-curved four-layer square wooden grid, the shape of which is based on a chain model. The layers of the grid allowed to obtain the appropriate stiffness (important due to the height of the structure)

while maintaining the lightness of the form both visually as well as the actual total weight and material consumption. Canadian hemlock wood laths with a cross section of 50x50mm every 0.5 m were used for the construction. Its widest span is 60m (while the longest is 85m) and the height is 20m. The detail of the joints is particularly noteworthy. During the construction of the pavilion, the bolt connecting the four layers of laths allowed for free movement. After determining the target position of all the mesh elements, the bolts were tightened to prevent the sliding of individual layers of wood. Additionally, every sixth node was tied with a steel cable with a 6mm diameter. The logic of the form and the design of the structural detail of this pavilion inspires to search for beauty and engineering quality in simple materials and solutions. However, this requires an understanding of the structure of the material and the forces acting on it.

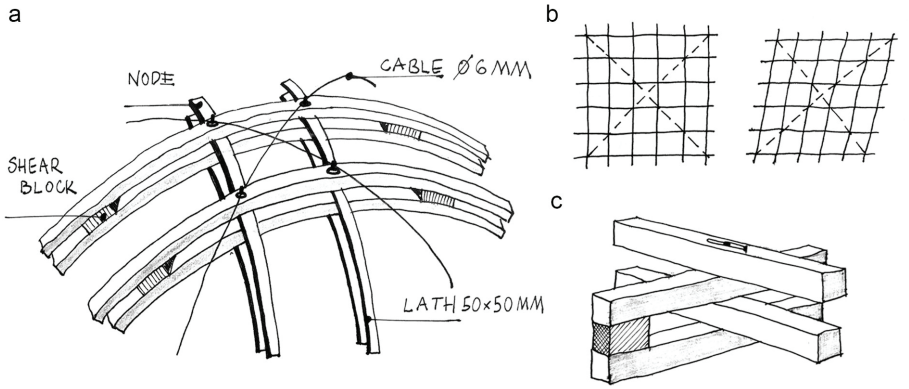

Figure 1. The Mannheim Pavilion – designed by Otto Frei, Germany, 1975; a) sketch of structural detail; b) lattice distortion; c) joint system.

Another example of rational design of a wooden structural form is the Savill Building designed by Glenn Howells Architects, built in 2006 in Windsor Great Park in Great Britain. The distinctive feature of the building is its corrugated barrel vault roof which creates an approximately 90 x 25 m free plan. The gridshell is based on an orthogonal structural mesh made out of larch and oak obtained from the Crown Estate forests. The rational design of the form is continued in its structural connections which benefit from the material properties of wood used for their creation. Just like in the previous example, the laths overlap at nodes and "slide" to allow rotation. This required the use of timber shear blocks fixed between the layers of the orthogonal mesh [D. Naicu, R. Harris, C. Williams, 2014]. This allows the laths to be curved and to obtain the appropriate shape using simple engineering solutions.

The first timber gridshell in Britain - The Weald & Downland Open Air Museum, in Downland (1996-2002) is another example of effective use of materials. The building was created as a result of the cooperation between the architect Edward Cullinam and engineers from Buro Happold and the carpenters from Green Oak Carpentry. The corrugated vaulted roof creates an unsupported

space that is 48m long and 11-16m wide. It was made of green oak harvested locally (Normandy region - northern France) [D. Naicu, R. Harris, C. Williams, 2014]. Initially, the orthogonal 1,0x1,0m mesh (in places densified to 0,5x0,5m) was assembled flat from 50x35mm laths . The grid was then bent to the final shape of the gridshell using the elasticity of the freshly cut raw material. The Weald & Downland Open Air Museum is a remarkable example of sustainable architecture - as it minimizes material and energy consumption. The examples mentioned above show the synergy of solutions that arise from multi-disciplinary cooperation - the exchange of knowledge and experience in working with building materials.

2.1 From form to material

Form dominates architectural design - other elements such as function, ergonomics and technical solutions affect its shape, but as a rule, conceptual analyses begin with the form. Cooperation between architectural and structural design begins at the stage of preliminary technical verifications. Issues related to structural shaping of the form (span of the load-bearing elements, types of connections, etc.) and the selection of material solutions are the basic background for inter-branch cooperation. Nowadays, the cooperation is more and more often facilitated through the use of BIM. It is based on the refinement of building information on a single model (for many related disciplines). Nevertheless, the order of tasks remains the same - structural engineers analyze the spatial form designed by the architects. The usage of BIM enables the improvement of tools - it accelerates the exchange of information, detects collisions, etc. However, it does not change the way of thinking in the search for the new quality of this cooperation. Algorithmization of the architect's digital work tools provides more and more interesting parametric modeling opportunities - it allows architects to shape complex systems of urban and environmental connections, or to create complex geometries [G. T. N. Brígitte, R. C. Ruschel, 2018]. This in turn forces the current dynamic development of numerical programs to be able to verify the construction of such solutions. Referring to Patric MacLeamy's research - "MacLeamy Curve" (inspired by Boyd Paulson's work), an architectural design becomes more difficult to change the more it develops. The concept of early optimization - Integrated Project Delivery (IPD) aims to reduce the costs related to the optimization of the structure [S. Talebi, 2014]. The awareness of this dependency means that the cooperation of architects and structural engineers begins at an increasingly earlier stage of the project.

A contemporary example of cooperation between architecture and structure using digital design tools is the research done for the Modular Timber Structure - a roofing designed by Bastien Thorel, see Figure 2 and [Nabei, Weinand & Baverel, 2011]. The designer created a form of structural arches connected in a parallel system, and as a result, four types of simple flat modular interlocking elements were used. The concept was that flat elements would overlap and stiffen each other - this assumption required numerous structural analyses. As a result of simulations, it was found that the distribution of stress concentrates at the place where the flat elements are joined. Further design (changes resulting from the need to strengthen the connections) was made in cooperation between the architect and the civil engineer. This object is an interesting example of optimal shaping of

the form and structural detail. Nevertheless, the form dominates the material - the structure of this roof could as well be made of a different material. This is also evident from structural analyses that focus on general issues and do not take into account, for example, the anisotropic features of wood. From an engineering point of view this kind of structure, made from simple elements, creates a very complex stress pattern which may trigger fracture, crushing, surface interaction, and other types of nonlinear material and geometrical effects. Probably, none of the currently available computational models for wooden materials can handle this properly, neither with respect to deformation nor safety. To utilize the potential for creativity and good design of timber structures, more effort should be put into numerical modeling of wooden materials as numerical modeling is the design tool of the future.

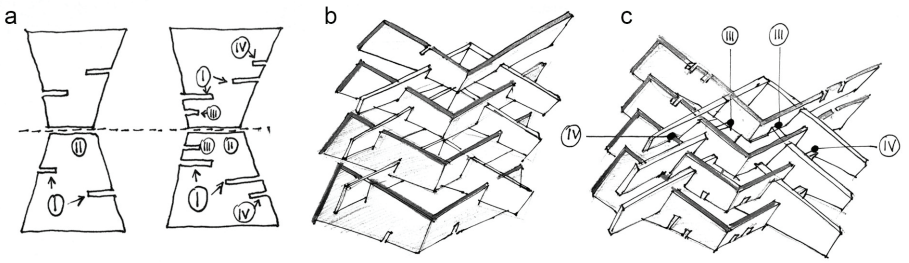

Figure 2. Modular Timber Structure – designed by B. Thorel, Germany, 2008-2009; Two geometrical configurations of structural detail; a) connection variants - plans; b) basic variant – perspective sketch; c) optimization variant – perspective sketch.

2.2 From material to form

Eco-efficient structural and material solutions are not a tendency, but a challenge facing us today. Contemporary generative modeling programs enable form shaping in line with the idea of 'form follow forces', which aims at the reduction of unnecessary structural geometry. An example of which is form finding. It uses the methods of transient stiffness, force density and dynamic relaxation [W. J. Lewis, 2008]. One of the computational tools for the modeling of gridshell structures using the dynamic relaxation method is the Kangaroo Live Physics program developed by Daniel Piker. This type modeling leads to construction based on digital fabrication, where the materials with a homogeneous structure, such as concrete, steel etc. are most often used. In this context, wood as a building material is reduced to repeatable boards, strengthened beams, or it is processed to such an extent that it can be printed (laywood). The material is modified, simplified in terms of structural structure, to allow for the creation of complex forms. Contemporary digital tools do not provide one effective form-finding program in which one could analyze a material with a heterogeneous structure. Carrying out analyses in terms of the strength of wood, including the determination of limit states due to damage, requires a separate design study. The individual analyses have to be performed in stages, using several different digital programs. However, the constantly developing technologies also lead to greater

respect for the known, simple technologies. Moreover, advanced technologies are more often used to increase the effectiveness of natural materials and solutions.

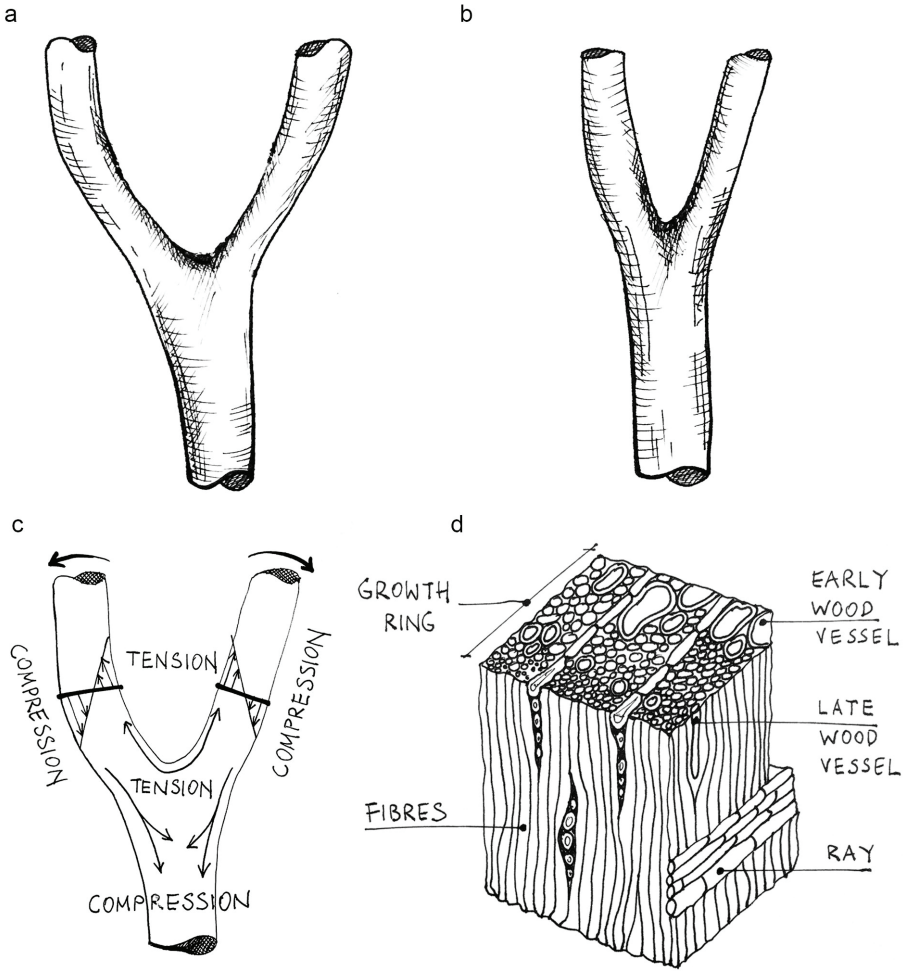

Figure 3. Type of branches used in the Robotically Fabricated Wood Chip Barn – designed by AA School of Architecture, 2015-2016: a) tension fork; b) compression fork; c) stress diagram in tension fork; d) structure of wood.

For instance, there is a concept of scanning natural tree branches to build architectural objects from those elements [M. Self, E. Vercruysse, 2017]. Natural knots (tree branches) are not the most effective structural solution for architectural buildings - this is due to the difference in the load model (Figure 3). Different forces act on the branches in the tree's natural environment and in a structural form. Nevertheless, the activities outlined below are an interesting example of structured exploration and cross-industry cooperation. The Design + Make

program at the Architectural Association satellite campus out in Hooke Park, Dorset aims to educate students in structural design by experiencing wood as a natural material in its ”growing” phase. In this case, the study of wood means the haptic experience of the forest - the environment in which this material is formed. The assumption of the Design + Make program is the digital analysis of the anisotropic structure of wood and the use of natural properties of the material in architecture. This approach to wooden construction sets new directions in design, but also in cooperation between architecture and structural engineering. The result of this approach and the students' work is a robotic barn, the structure of which was made of local trees. An arched vierendeel truss structure that supports the roof consists of 25 forked beech branches. Elements were selected on the base of the preliminary criteria, harvested and scanned into a 3D model. Then the students, in collaboration with the engineers from ARUP, used an optimization script to set the final ”forks”. Milling robots drilled holes along the ”structural branches” into which steel fasteners were inserted.

3. Wood properties in the context of structural analysis

Wood is an attractive structural material, easily available and easily shaped, a highly sustainable material storing large amount of greenhouse gases. As an organic material, wood is produced by Nature - through a growth process whose rate depends on climatic conditions, as well as water and sunlight availability. The anatomy of wood is close to being cylindrical in the cross section of the stem due to the growth taking place only at the exterior (Figure 3). The internal structure of wood can be simply described as formed by [clusters of tubes] [aligned channels?] (straws) glued together and arranged in the form of rings. Annual rings are varied and depend on the growth rate - this has an impact on the properties of the material. Wood is a naturally grown composite structure, strong and stiff in the direction of the tubes but distinctly weaker in the other directions [M. Self, 2017]. The weakest properties of wood are its tensile strength (towards the grain) and shear stress resistance between the annual rings. As a rule, the cracks that form as a result of these stresses occur along the direction of the fibers where the strength is the lowest. The vulnerability to cracking is one of the biggest challenges for the use of wood in construction. Furthermore, strong anisotropy is problematic in the context of using parametric modeling tools.

Carrying out detailed computer analyses for wood requires a digital database of strength properties. The creation of such a catalog for various species of conifers (mainly those used in load-bearing structures) is an essential element in the development of digital tools for the work of structural engineers. Currently, the available programs are insufficient for detailed wood analysis [Y. Weinand, 2017]. Programs such as Revit or Robot Structural Analysis use standards and catalogs of wooden profiles available in them (or imported by users). However, it is a simplification consisting of averaged strength parameters, as for a material with a homogeneous structure. Analysis of the connections allows to explore the issues related to the diverse structure of wood. Nevertheless, these constitute the scope of a very narrow structural specialization based on original research and optimization processes. Architectural and structural cooperation usually takes place at the stage of form conceptualization. In the case of conventional modeling tools, the

architectural model is usually simulated from loads and modified based on the suggestions of the civil engineer (Figure 4).Using generative modeling tools, it is possible to initially automatically verify the variants generated by an algorithm. However, this requires individual modifications: creating an original script and introducing matrices relating to the properties of a given material [G. Stellmacher 2017]. Another direction of possible research is the creation of an accurate database for each specific material. The material then becomes the starting point for further work - such as form shaping. This design path is, however, closely related to fabrication technologies. The adoption of precise research tools at the start of the design process usually indicates unconventional material solutions. An alternative to the modification of natural wood is a deeper understanding of the strength characteristics of wood depending on the species of the trees, their growth conditions, or the phenomenon of the so-called wood programming [J. Burry, B. Sheil, R. Glynn, M. Skavara, 2020]. An example of such thinking is the Urban Tower, designed and constructed by engineers from the University of Stuttgart (ICD + ITKE). The form is the result of a non-energy-intensive process of predicting how the wood will shrink as it dries out. This design contains clear elements of a scientific experiment. The solution proposed by the designers for the "processing" of CLT panels (allowing them to deform under the influence of moisture) seems to contradict the logic of the material itself. The main goal of the cross-laminated wood technology is to eliminate these deformations [R. Brandner, 2013]. On the other hand, minimizing the energy built into material processing, which controls this process, as well as the method of shaping of the form, are an interesting example of cooperation between architecture and structure. Such designs also show possibilities in the development of material and manufacturing technologies.

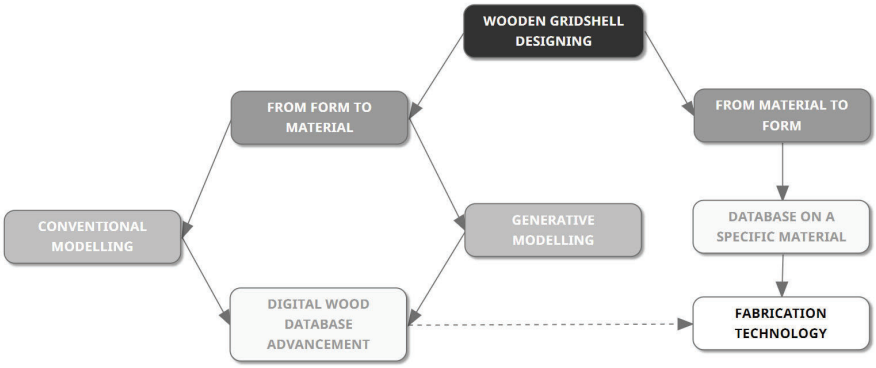

Figure 4. Diagram of stages for the design of contemporary wooden structures .

4. Summary

The collaboration of architects and structural designers is an interesting field in the development of digital modeling tools. In the era of widespread digitization,

an indispensable element of building design is the creation of both a model of the architectural form and a structural model (loads, supports, material, etc.). Regardless of the chosen method of search, invariably it is about the flow of information, as well as the method of its recording. In the case of wood, which is a material with a heterogeneous structure, a key element in the development of computer programs is the creation of a digital database for different types of wood. This issue applies both to structural analysis programs as well as programs for the optimization of joints.

An interesting trend is the return to the simple material processing technologies, the aim of which is to conserve energy. Using the natural properties and form of modernized wood or carpentry connections are just some of the inspirations that architects reach out for. An important role in increasing the quality of eco-efficient solutions is the use of broadly understood fabrication technologies that support the entire process of the formation of architecture (material analysis, design, construction). The search for synergistic structural solutions will indicate new directions for the development in material technologies. This requires the continuous broadening of knowledge and skills from all of the involved disciplines, which can be achieved through practical cooperation between the designers.

References

Brandner, R.: 2013, Production and Technology of Cross Laminated Timber (CLT): A state-of-the-art Report, *Conference: Focus Solid Timber Solutions - European Conference on Cross Laminated Timber (CLT); Volume 1*, Graz.

Tomczinski Novellini Brígitte, G. and Coeli Ruschel, R.: 2018, Identification of applicable patterns to algorithmization in BIM to explore solutions in the design stage of Social Housing, *Proceedings of the 22nd Conference of the Iberoamerican Society of Digital Graphics - ISSN: 2318-6968*, Brazil, São Carlos , 68-73.

Charest, P., Potvin, A., Demers, C. and Menard, S.: 2019, Assessing the Complexity of Timber Gridshells in Architecture through Shape, Structure, and Material Classification, *Timber Gridshell Architecture*, **14(1)**(DOI: 10.15376/biores.14.1.1364-1378), 1364-1378.

Gawell, E.: 2018, The structuralism of contemporary architectural details in generative modeling methods, *In Defining the Architectural Space - Rationalistic or Intuitive Way to Architecture, vol.4*, Crakov, 63-72.

Lewis, W.J.: 2008, Computational form-finding methods for fabric structures, *Proceedings of the Institution of Civil Engineers – Engineering and Computational Mechanics*, Coventry, 139-149.

Liddell, I.: 2015, Frei Otto and the development of gridshell, *Case Studies in Structural Engineering*, **4**(DOI: https://doi.org/10.1016/j.csse.2015.08.001), 39-49.

Menges, A., Sheil, B., Glynn, R. and Skavara, M.: 2017, *Fabricate. Rethinking design and construction*, UCL Press, London.

Nabei, S., Weinand, Y. and Baverel, O.: 2011, Geometrical description and structural analysis of a modular timber structure., *International Journal of Space Structures, vol. 26, No 4*, 321-330.

Naicu, D., Harris, R. and Williams, C.: 2014, Timber gridshells: design methods and their application to a temporary pavilion, *WCTE 2014 - World Conference on Timber Engineering*, Quebec City, Canada.

Self, M. 2017, Applications for timber in its natural form, *in* A. Menges, T. Schwinn and O. D. Krieg (eds.), *Advancing Wood Architecture. A computational approach*, Routledge, New York, 141-153.

Siegel, C.: 1974, *Formy strukturalne w nowoczesnej architekturze*, Arkady, Warsaw.
Stellmacher, G. 2017, The Timber Seasoning Shelter at Hooke Park, *in* A. Menges, T. Schwinn and O. D. Krieg (eds.), *Advancing Wood Architecture. A computational approach*, Routledge, New York, 155-167.
Talibi, S.: 2014, Exploring advantages and challenges of adaptation and implementation of bim in project life cycle, *2nd BIM International Conference on Challenges to Overcome*, Lisbon.
Weinand, Y. 2017, Timber fabric structures, *in* A. Menges, T. Schwinn and O. D. Krieg (eds.), *Advancing Wood Architecture. A computational approach*, Routledge, New York, 61-72.

FUTURE COASTAL CITIES WITH BIOROCK INFRASTRUCTURE

Alternative Coastal Futures with Biodesign

JENNIFER GAUTAMA[1], CHRISTINE YOGIAMAN[2] and KENNETH TRACY[3]
[1,2,3]*Singapore University of Technology and Design*
[1]*jennifer_gautama@yahoo.com* [2,3]*{christine_yogiaman|kenneth_tracy}@sutd.edu.sg*

Abstract. Despite having the potential of being a durable building material, Biorock, a form of calcium carbonate formed by the electro-accumulation of minerals dissolved in seawater, has never been applied on an architectural level due to its slow accretion process. This paper aims to plays out the possible narrative of this slow accruing material process in the incrementally submerged coastline of Jakarta, to empower local marginalized communities to self-construct a "new city" for habitation using Biorock, especially where building material resources may be limited. Urban cores with basic communal, housing and aquaculture facilities will be established using Biorock as the main building structure, which would be harvested in response to the gradual sea level rise.

Keywords. Biorock; Accretion; Aggregation; Coastal Floods; Biodesign.

1. An Introduction: Sinking Jakarta

Currently, Jakarta now stands at the threshold of climate change with 40% of the city predicted to be completely submerged by 2050 (Kimmelman & Haner, 2017). Instead of finding solutions to save Jakarta from further damage, giant sea walls are simply being erected and plans have even been made to move the capital to Borneo (Gorbiano, 2019). Jakarta currently sits around 3m below sea levels and is prone to coastal floods.

1.1. CAUSE: SEA LEVEL RISE AND LAND SUBSIDENCE

The two main causes of coastal floods are 1) sea level rise and 2) land subsidence. For Indonesia, the general rise of sea level in 2030 will reach 15cm to 18cm. In 2050, sea level could increase by 25cm to 30cm, 40cm to 48 cm in 2080, and finally 50cm to 60cm in 2100 (Sofian, 2010). However, sea level rise accounts for only a small % of why the capital city may be submerged. The bigger reason behind the sinking capital is attributed to its rapid subsidence. There are four factors contributing to land subsidence in Jakarta, namely - excessive groundwater

PROJECTIONS, Proceedings of the 26th International Conference of the Association for Computer-Aided Architectural Design Research in Asia (CAADRIA) 2021, Volume 1, 483-492.

extraction, pressure from building and construction, natural consolidation of alluvium soil and tectonic activities. Jakarta is sinking at an average rate of 7.5cm a year, in some places up to 17cm (Bakker, Kishimoto, & Nooy).

1.2. CURRENT SOLUTIONS AND THEIR INFECTIVENESS

To combat the issue at hand, the Giant Sea Wall Jakarta was constructed as part of The National Capital Integrated Coastal Development program (NCICD). It commenced in 2014 and is expected to materialize by 2025 (Bakker, Kishimoto, & Nooy). However, this might not be sustainable in the long run. Firstly, the construction of the outer sea wall in Jakarta Bay will have a profound impact on the fishing communities in North Jakarta. A Rapid Environmental Assessment, conducted by the Danish Hydraulic Institute in 2012, estimated that due to the current reclamation, 586.3 hectares of aquaculture area in Jakarta Bay will be lost, causing ten of thousands of people to lose their livelihoods (Bakker, Kishimoto, & Nooy). Besides, there have been reports of constant leaking. The sea wall has also collapsed several times in 2007 and 2019, giving way to sudden coastal floods that inundated neighborhoods for days. In these scenarios, flood levels can reach up to a height of 0.4m to 2.0m.

2. Design Methodology

This clearly shows that the sea wall is not a reliable solution in the long run. Not only is it ineffective, but is also detrimental to communities around. This paper instead seeks to explore alternative methods of living through an enduring fabrication of a new living system that will eventually evolve into a sanctuary for communities to live in against unpredictable climatic conditions. “Biodesign fiction” (Camere & Karana, 2018) which has gained traction over the years would be used as a speculative design approach to envision how biology could be useful in future, provocative scenarios. This paper will specifically delve into the Biorock process which involves marine electrolysis and its potential to grow limestone building components, exploring how nature and human can design a co-produced space in an urban context.

2.1. INTRODUCTION TO BIOROCK

Biorock refers to the cement-like substance formed by electro-accumulation of minerals dissolved in seawater. The process, developed by Wolf Hilbertz, was patented in 1979. It was determined that a low voltage would accrete aragonite, a form of calcium carbonate suitable as a building material (Goreau, 2012). The material is three times harder than Portland concrete, becomes stronger with age and have self-repairing properties (Goreau, 2014). Until today, it has been mainly used for the restoration of coral reefs which do not maximize the strength of this material. Despite the technical breakthrough, little exploration has been done to employ Biorock as a construction material.

There is yet an architectural scale application of this promising material accretion methodology due to its slow accretion process. The dependency of accretion on natural cycles renders this process into a speed that is not typical

to current material production standard practice. With low voltage, the Biorock can only grow up to 2cm per year. However, in the context of marginalized and informal communities, this natural material accretion can be a sustainable procedure to gain building material resources.

2.2. APPLICATION

The study plays out the possible narrative of this slow accruing material process in the incrementally submerged coastline of Jakarta (Takagi, Esteban, Mikami & Fujii, 2016). Economic gridlocked and dis-empowered governess create the inevitable reliance on community and alternative source of funding infrastructure development. Hence, the implementation of Biorock infrastructures becomes a feasible solution to "grow" a new city.

The research simulates over a period of 100 years the process of accretion and unit aggregation based on relationships and rules referenced from water access based on the changing water levels. Wireframes are first harvested and left to accrete Biorock to achieve structural components within substantially deep waters, in the initial coastline of Jakarta. To identify where the components would be harvested, ocean current directions during the spring and monsoon seasons are first determined, as currents are essential in the accretion of Biorock to happen. The intersection of current direction during the two seasons are taken as harvesting nodes (Figure 1).

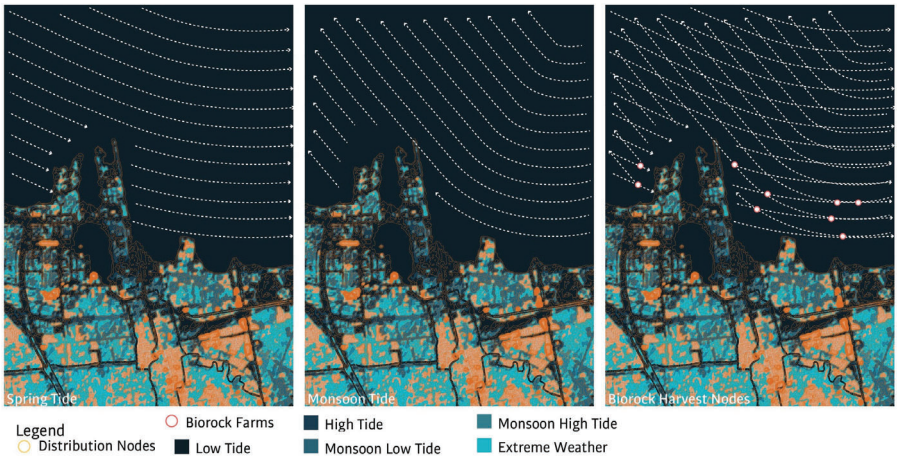

Figure 1. Left to Right: Ocean current direction in Spring, Ocean current direction in Monsoon, Potential Harvesting Nodes.

The components are then transported to various sites to be assembled. The changes in tidal conditions would cause different levels and areas of submergence daily, monthly and yearly. Due to both sea level rise and land subsidence, it can be said that Jakarta is sinking at approximately 10cm per year. Daily, tidal heights vary by about 1m. During the monsoon, tides may increase by 1-2m and up to 5-8m during extreme weather events. Due to the constantly changing

floodplains, specific routes for the transportation of Biorock will be mapped out to reach selected cores by 2050 (Figure 2). These cores may then further extend out to create branching networks.

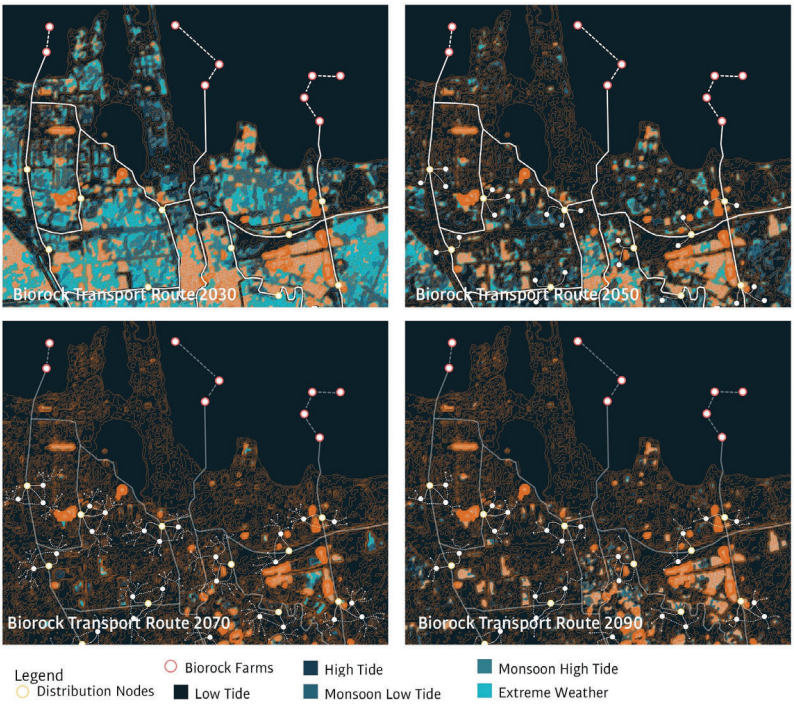

Figure 2. Biorock transport routes Year 2030, Biorock transport routes Year 2050, Node Expansion 2070, Node Expansion 2090.

In both Figure 1 and Figure 2, the orange areas represent plots of unaffected dry land, whereas the different shades of blue represent areas inundated due to sea level rise. The darkest shade of blue represents the areas covered at low tide during the non-monsoon season. During high tide, monsoon season and extreme weather conditions, increasing amount of land become inundated, as represented by the different shades of blue.

It is important to note that while these cores may not necessarily be the first few pieces of land to be completely submerged first, they are at least submerged daily at high tide in the initial years. Firstly, this allows the components to be transported when connecting water bodies are created to the selected cores at specific times of the day. Secondly, the fact that these areas are not submerged all the time also allows the communities to further add on components during moments of low tide much more efficiently as compared to when the area is submerged. Finally, these components can further accrete daily to create a strong structural foundation for the urban cores during high tide.

2.3. UNIT GEOMETRY

The modules are 3-Dimensional T shapes of varying heights and lengths (Figure 3). The angle of the T shape may vary which allows either square-shaped or diamond-shaped enclosures to be formed when joined together. The modules may be connected to one another at the edges and on top of one another. The module is broken down into two main parts - it would mainly be composed of a wireframe surface that allows the accretion of Biorock to occur (Figure 4). However, edges where the modules may connect would be made of a metal that would not allow accretion to happen.

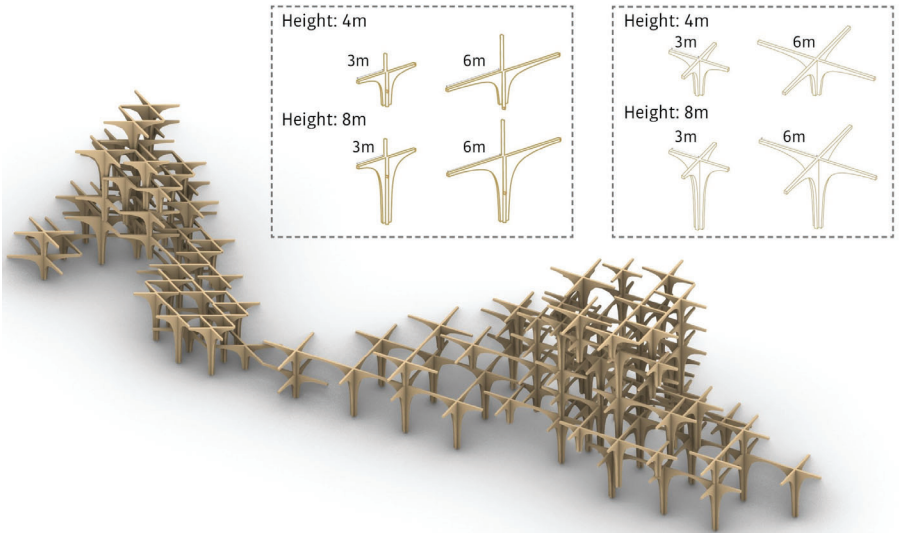

Figure 3. Catalogue of various modules and basic aggregation of square and diamond enclosures.

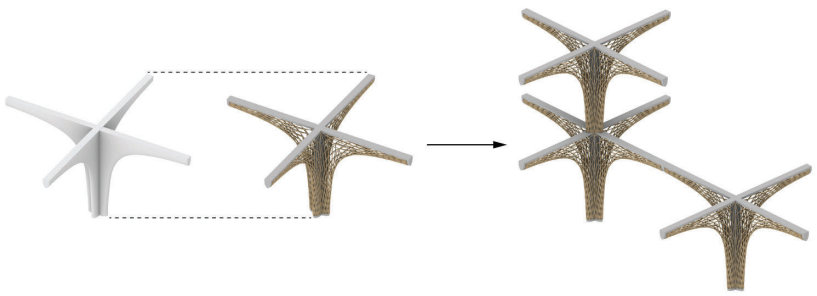

Figure 4. Detailed breakdown of module.

Depending on the amount of time left to accrete Biorock, the components

would have different strengths and densities (Figure 5). With this, components that have more accretion may be used as the building foundation, while lighter components are stack towards above it.

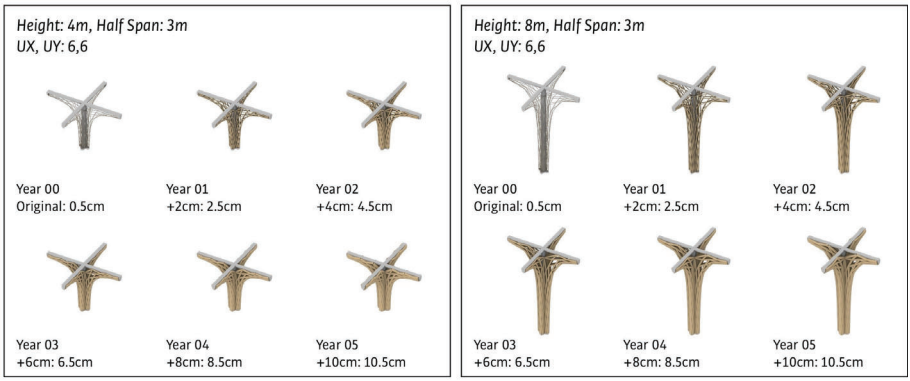

Figure 5. Accretion on wireframes over a period of 10 years.

However, it is also acknowledged that Biorock may not accrete uniformly on the wireframes, hence affecting the overall stability of the structure. Currently, there is not a solution for this. However, if the structures do indeed have significant irregularities, post processing of the wireframes may take place. For example, where accretion on certain areas of the wireframes are lacking, concrete may be added as a substitute. For wireframes with accretion that are too irregular to be post processed, they may be use for the restorations of coral reefs and marine life around the submerged Jakarta.

Currently, there is also lack of information available on the implementation of Biorock as a construction material. Hence, it is uncertain how the proposed wireframe structure, in addition to the accretion build-up on it, may work. While it would be most ideal to conduct physical one-to-one scale studies with the proposed structure, the structural feasibility of the wireframes and the accretion of the Biorock on the modules, may also be analyzed using Karamba (on Grasshopper), which allows us to input information on materials' volume, strength and density. With this analysis, one would be able to better understand the minimum and maximum accretion build-up on the wireframes necessary to construct various structural configurations on site.

Another important component of the infrastructure would be wooden floors and walls that would subsequently be added to the infrastructure after the wireframes Biorock modules have been aggregated (Figure 6). The walls would be placed in between the axis of the Biorock components connection points as shown in the exploded axonometric in Figure 6. This creates a variety of room configurations. Walls may also be designed to be removable to allow for different uses of space to happen from time to time.

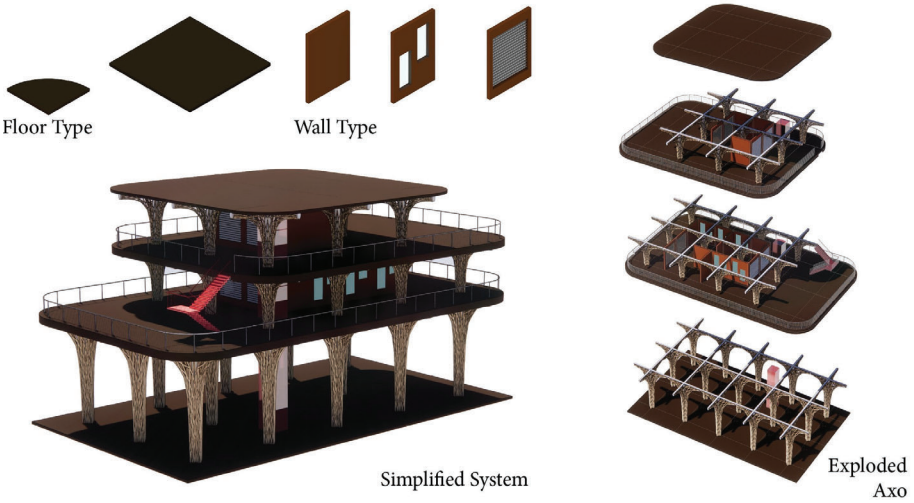

Figure 6. Basic wireframe modules aggregations with walls and floors.

3. Coastal Futures: Final Massing

Wasp, an aggregation Grasshopper computational tool, is used to simulate a time-based build-up of the large scale slow growing infrastructure. Wasp, allows one to input components and their connection points, that are to be aggregated within a volume or line of path. Using this logic, aggregation may be applied within existing buildings using areas of volumes as a constraint. On the urban landscape, aggregation would occur along predetermined paths that accounts for existing urban conditions, essentially creating an elevated walkway and connecting buildings that remain above the floods.

Selected nodes, where the Biorock were transported to initially, will become urban cores and are characterized by the dense, large and high build-up of the modules. These cores would usually surround urban buildings left behind. They would be made of square-like modules of various sizes. The core urban nodes would initially comprise mainly of housing, communal facilities and domestic industries. As these urban cores develop over time, they may also grow outwards, creating a branching network system that supports other programs such as aquaculture, a program that would be an ideal addition given the fact that the entire landscape would be fully submerged eventually (Figure 7). While this paper only shows the potential form of one potential Biorock island at one site, there will be numerous similar islands replicated throughout Jakarta at the selected nodes highlighted in the mapping in Figure 2.

While it was mentioned earlier on that Wasp is used to simulate an urban build-up, it has its limitations in attempting to control the overall output geometry it may form. If the singular units as shown are left to aggregate, very random geometries would be generated, as shown in Figure 3. While some degree of randomness is acceptable, one would like to be able to control the infrastructural

system that would be formed eventually. This is especially so for the aquaculture system. Hence, to have a greater degree of control over the aquaculture system, initial forms representing routes and various types of aquaculture hubs are first designed from the singular diamond shapes units in Figure 3. These larger units are then aggregated to form a branching network extending for the communal and housing core. On the other hand, the communal core can be aggregated using the initial singular units as the spaces created could be more informal.

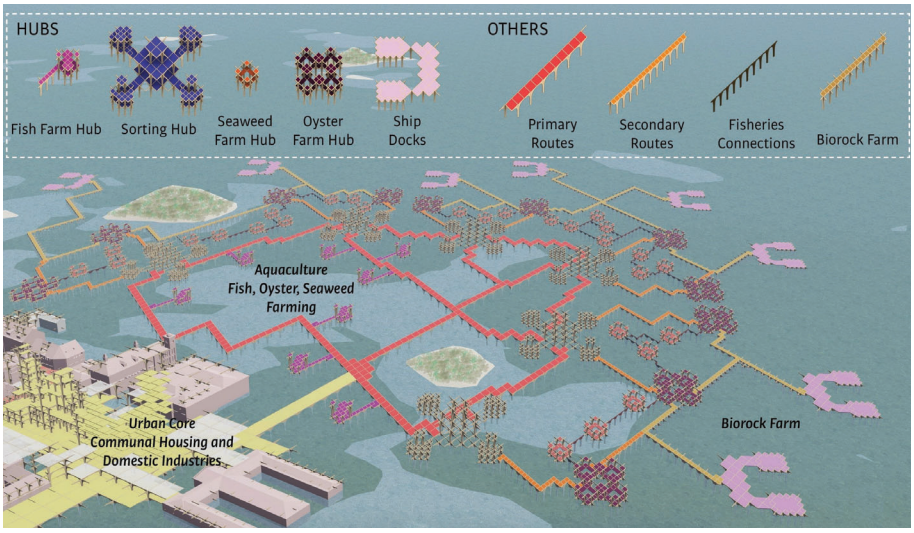

Figure 7. Aerial View and Components.

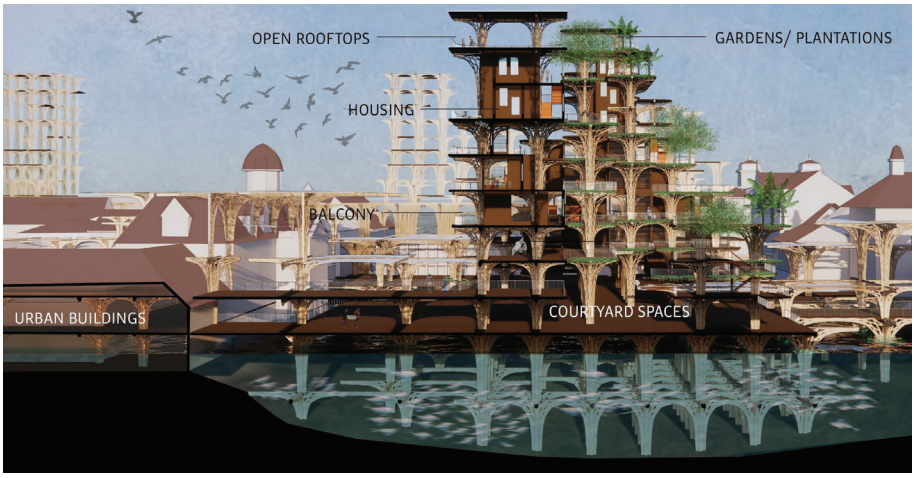

Figure 8. Section of urban core highlighting various spaces.

Within the dense communal housing nodes, large volumes would also be

identified, which would be inputted into the script to disallow modules from being aggregated within those selected areas. This would create another layer of spatial quality within the urban landscape. These large volumes of spaces within the dense cores may be identified as large communal spaces (Figure 8 and 9 and 10). On the other end, towards the edges of the aggregation, the aggregated modules will change from its square-shaped formation to diamond-shaped, which signals the dispersal of the "Biorock" islands towards the edges (Figure 9).

Figure 9. Various Views.

Figure 10. Perspective view - high tide conditions in 2050.

4. Conclusion: Future Self Sustaining Systems

Finally, while developments in the initial phases would be focused on building infrastructure to create spaces to live and work for communities, the building system may eventually expand to support more complex programs such as water harvesting, intensive aquaculture and even energy production. Biorock not only have benefits as a building component, but have also been proven to be able to increase the productivity rate of aquaculture and even produces hydrogen gas, as a potential energy source. With all these potential functions and their outputs, a self-sustaining ecosystem may be developed to support communities living in future flooded landscapes (Figure 11).

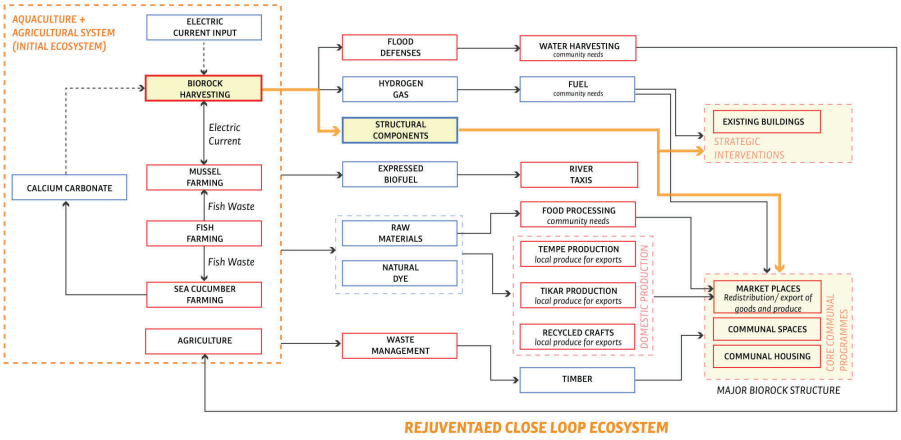

Figure 11. Potential Self Sustaining System.

References

Bakker, M.B., Kishimoto, S.K. and Nooy, C.N.: 2017, *Social justice at bay. The Dutch role in Jakarta's coastal defence and land reclamation project.*, Both ENDS, SOMO, TNI.

Camere, S.C. and Karana, E.K.: 2018, Fabricating materials from living organisms: An emerging design practice, *Journal of Cleaner Production*, **186**, 571-584.

Gorbiano, M.I.G.: 2019, "BREAKING: Jokowi announces East Kalimantan as site of new capital" . Available from <https://www.thejakartapost.com/news/2019/08/26/breaking-jokowi-announces-east-kalimantan-as-site-of-new-capital.html>.

Goreau, T.J.G.: 2014, *Biorock Benefits*, Ph.D. Thesis, BIOROCK TECHNOLOGY INC..

Goreau, T.J.G. 2012, Marine Electrolysis for Building Materials and Environmental Restoration, *in* J.K. Janis Kleperis (ed.), *Electrolysis*, IntechOpen.

Kimmelman, M.K. and Haner, J.H.: 2017, "Jakarta Is Sinking So Fast, It Could End Up Underwater" . Available from <https://www.nytimes.com/interactive/2017/12/21/world/asia/jakarta-sinking-climate.html?mtrref=www.google.com>.

Sofian, I.S.: 2010, Scientific Basis: Analysis and Projection of Sea Level Rise and Extreme Weather Event, *Indonesia Climate Change Sectoral Roadmap ICCSR*, Indonesia.

Takagi, H.T., Miguel Esteban, M.E., Mikami, T.M. and Fujii, D.F.: 2016, Projection of coastal floods in 2050 Jakarta, *Urban Climate*, **17**, 135-145.

BIO-MINERALISATION AND IN-SITU FABRICATION OF IN-DUNE SPACES: CASE STUDY OF THAR DESERT

MEDHA BANSAL[1] and ELIF ERDINE[2]
[1,2]*Architectural Association*
[1]*medhabansal18@gmail.com* [2]*Elif.Erdine@aaschool.ac.uk*

Abstract. Desertification has made large productive landscapes in the South-west Thar desert redundant, subjected people to migration and induced a constant influx of sand into the region (Singhvi and Amal, 2014). The abundance of sand creates an opportunity to adopt an existing technique, Bio-mineralisation, to develop a sand based composite material which, when treated with a construction binder like sodium alginate, can be used for engineering purposes. The paper sets a theoretical framework to develop a fabrication mechanism with microbial-grout injections and propose the development of in-dune/underground assembly of habitable spaces. Each of the sub-components of material system, fabrication mechanism and In-dune structures are detailed, and evaluated to devise a hierarchy between them. Their interdependencies together inform design strategies, a phasing plan and global time scale for overall terrain transformation.

Keywords. Bio-mineralisation; Bio-grouting; In-dune fabrication; Tool path algorithms; Micro-climate analysis.

1. Introduction

Desertification, being a global problem, has made large productive landscapes redundant and subjected people living in these areas to migration. Amidst the adversities, there are opportunities to procure the abundant resources in a desert and combine them with traditional and modern mitigating interventions.

The Thar desert is the easternmost extension of the vast Sahara- Arabian deserts in the horse latitudes. The desert is dominated by the south-west monsoon, which controls both the wind vector and the vegetation cover. Dearth of rain in this region is a result of configuration of atmospheric dynamics and sinking air masses which increase the surface pressure and temperature significantly (Bryson and Baerreis, 1967).Absence of any substantial vegetation cover and agricultural activities, coupled with high wind velocity has increased the vulnerability to sand movement in the region through erosion and depositional processes.

Abundance of sand can cater to the development of a material system that can be used locally by hardening the sand. While within the realm of geotechnical engineering conventional production methods are not economical, alternative biological approaches including microbial injection and by-product precipitation

PROJECTIONS, Proceedings of the 26th International Conference of the Association for Computer-Aided Architectural Design Research in Asia (CAADRIA) 2021, Volume 1, 493-502.

have been investigated. The presented research specifically details and adopts the application of microbial induced polymers or biopolymers as a new type of construction binder.

The material system of the research is founded on a case study conducted in TU Delft in 2009 (Van Paassen et al., 2009) The objective of the study has been to test the scalability of bio-grouting in order to verify the potential of the method in ground improvement. As an ex-situ experiment inside a laboratory, biopolymers are mixed with sand and water and cast in a mould. In another ex-situ experiment set-up bio grouts are injected to containers filled with soil of volumes 1 m3 and 100 m3 through injection wells. Progression from casting 10 cm3 of sand to injecting 1 m3 and 100 m3 of sand as single point and grid of injections has directed the research to study the flow lines of the bio grout fluids, control the forms and pattern generated along these lines, control inlet and outlet locations of injection and observe pressure difference inside the sand.

The current experiment thus in turn also focuses on controlling the uniformity and structural properties of the hardened mass. The experiment resulted in achieving unconfined compressive strength from 0-15 MPa. The increase of stiffness from precipitation of carbonate in subsurface can also be quantified as function of the volume of injected grouting agents and its dry-density. Observations and conclusions from the bio-grouting experiments done at TU Delft suggest the scalability of the technique.

Biopolymers are the most viable environment friendly option (Chang, Im and Cho, 2016). Once added to the soil, they form a stable gel matrix that synergies with ecosystem locally and does not damage it. Combined with their water retaining properties in soil, biopolymers are thought to be capable of promoting vegetation growth. Furthermore, the use of cross-linking for biopolymers may provide a more powerful soil stabilizing method. Cross-linking is a technique used to greatly improve the properties of a specific material by introducing an agent that promotes interactions between separate polymer chains, thereby enhancing their overall strength. Addition of calcium to the biopolymer and sand makes the composition gain strength and repel water solubility. About 5% Sodium Alginate and sand mixture can attain an unconfined compressive strength of 1550 KPa, 96 % of which is attained in 14 days (Zdruli,Cherlet and Zucca, 2017).

2. Research and Development

This research is founded upon existing applied research in the field, with existing machine definitions / limitations, as well as applied research on material composite studies. The innovation of this research is how it brings together research on material composites and large-scale fabrication with environmental and climatic considerations.The material system discussed in the previous section has the potential to be adapted and coupled with a fabrication mechanism to propose a new morphology of habitation spaces in Thar Desert. The current section details several components of the fabrication mechanism and evaluates them for their environmental performance.

2.1. SCALING UP FABRICATION MECHANISM

2.1.1. Single Point Injections and Matrix Jnjections

In order to harden a vast dunal land mass, bio-grouting should be carried out such that large sections of the terrain are hardened at once with some local variations. Single point injection has shown its industrial success and ability to stabilise ground, however the impact of its application is local and limited to a small area. By building on the observations and conclusions from the TU Delft experiment discussed in the previous section (Van Paassen et al., 2009), the limitations of single point injection are aimed to be resolved by proposing an extension to this technique. The proposal comprises replacement of a single point injection with a matrix of injections, which can harden a larger portion of subsurface at once (figure 1).

The customised injection grid can be mounted onto a grouting machine which can freely run over the dunal fields. It is beyond the scope of this work to digitally simulate the grout spread of individual injections, and the density of the injections in the matrix can only be determined on site by observing the net grout spread. For the following experiments, it is assumed that the grout spread by each injection is uniform so that the net grout spread from all the injections can collectively cover the entire surface homogeneously without leaving any traces of loose unhardened portions or overly injected portions within that patch.

2.1.2. Machine Specifications

The selected machine should be able to withstand the load of the injections, manoeuvre over the undulating field and inject into varying depths and at different angles. In order to meet these objectives, the mobile injection grouting drill KR 807-7G by Klemm- Bohrtechnik is selected. Long and heavy drilling masts are mountable so that the maximum depth the mast can travel is up to 15000mm and can attain stability while taking challenging drilling positions. The machine is designed with enhanced inherent stability such that its manoeuvring and setting up times are significantly less. Machine's crawler base's oscillating ability (from +12.5° to -7°) and the mast's automated positioning within ±5° from the vertical in all directions (K Bohrtechnik, 2018) maximise its area of impact (figure 1).

The jig/extension that can be attached to hold the injections has a dimensional constraint of 3m X 3m, indicating that the machine can harden patches in multiples of 9 m2. These start to define the physical constraints of fabrication and have a direct impact on the profile of in-dune habitable units, which will be further discussed in the following sections.

2.1.3. Machine Positions

Having the ability to rotate the mast, the machine can inject in all the planes between two orthogonal planes. Injecting in orthogonal planes enables the machine to develop a vertical, horizontal and inclined injection system(figure 1), each having a different area of impact.

2.2. MACHINE TOOL PATHS

While the machine allows injection in 3 orthogonal planes and increases the scope of developing multiple tool paths, by injecting horizontally a large portion of vertical surface remains unhardened (figure 1). On the contrary, while injecting vertically, the machine can harden the entire 15m depth uniformly. This narrows down the focus to development of vertical injection systems and compel further development of tool path algorithms in the global x-y plane.

The propagation path of the machine can define the hardening pattern of the surface. During the injection process, there is a possibility that the hardened patches can either overlap or be separated by a distance. Either of these cases make the resulting hardened surface inefficient, for there is wastage of material in overlapping, and weakening and erosion of sub-surface in separation. Considering the prime objective of a compact packing of 3m X 3m patches, tool path algorithms are developed in two stages. The first stage formulates the trajectory type for machine's propagation based on mathematically defined 1°, 2° or 3° curves. Stage 01 rules out the possibility of the innumerable tool paths that can be developed by the machine's unconstrained ability to manoeuvre in x-y plane. In additional to the compact packing of hardened patches, it is essential that the time to harden multiple patches is also reduced. Due to the crawler base's turning capability, more than one patch can be injected from the same machine position (figure 2). This could reduce the time lost in moving and parking the machine for next injection position. The second stage leads to computational form-finding of specific tool paths based on machine's turning radii, injection positions and the selected trajectory type from Stage 01.

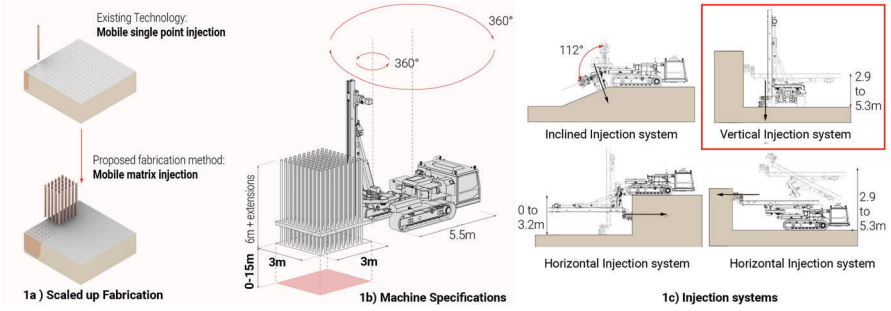

Figure 1. Scaling-up Fabrication Mechanism.

Stage 01- Tool Path Trajectory type and Direction of Propagation

If the machine were to run in the trajectories as demonstrated in figure 2 and inject at the intervals of 3m, only the trajectories based on mathematically defined 1° curves (polynomial equations with highest power as 1) meet the objective of compact packing. Hence, a series of tool paths are further developed based on 1° curves. Furthermore, running of the machine or other heavy equipment over pre-hardened patches can cause cracking due to differential settlement of sand. The tool paths are therefore developed as unidirectional so that there is no

cross-routing for machine.

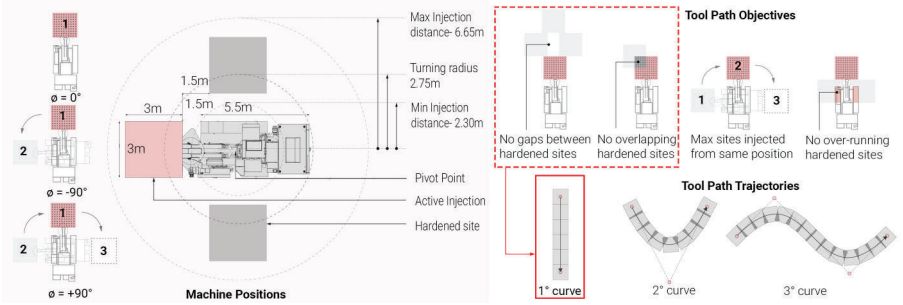

Figure 2. Machine Position and Tool Path Objectives.

Stage 02- Tool Path algorithms

Mathematically there are three variables involved in defining the tool paths of the machine- the local co-ordinates (x and y) of the machine's pivot position and the turning radii of the machine, ø (figure 2). Combinations of rotation and pivot positions can computationally generate a series of tool paths. For the experiments, a test area of 12m X 24m has been selected.

For hardening the selected site of 12 m along x-axis and 24m along y-axis, machine trajectory is defined such that it first completes hardening one row along x direction before shifting to next position in y-direction at steps of 3m and repeating the hardening pattern. For a given y co-ordinate we consider the machine to inject in increments of 1.5 m along x-axis. Total number of variables along x-axis = 5 (-6.0 to +6.0). Similarly, as trajectories based on 1° curves are opted for, ø can only vary in multiple of 90°(ranging between -90° and +90°). Total number of variables for rotation = 3.

Total number of variables in injecting 12m width (1st row) = 8.

Total number of combinations that can be formed= $\Sigma\ {}^{n}_{r}C$ (here n=8 and r= 1 to 8)= 246

A total of 246 tool paths are developed. Some of them are shown in figure 03.

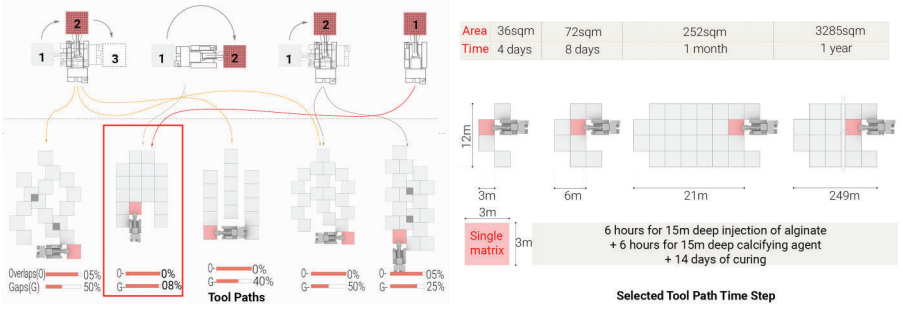

Figure 3. Tool Paths and Time Step.

2.3. TOOL PATH TIME SCALE

The selected tool path has no overlaps and gaps within the hardened patches. The selected tool path has a width constraint of 12 m and hardens 36 m2 area in first cycle of complete injecting before moving to the next row (figure 3). Multiple machines injecting with the same rate and at the same time need to be deployed on different parts and steps of the dunal section to escalate the stabilisation procedure for the entire terrain. Development of the site starts with identification of dune valley to be developed to accommodate 2250 people. Based on selected tool/path and rate of injection, it is estimated that it would take 25 years to develop the entire terrain. The continual procedure of injection for over 2 decades demands for construction of pathways for machines' circulation around the dune profile and establishment of a machine maintenance area at the centre(figure 4).

Figure 4. Multiple injections on site and Global Time Scale.

3. In-Dune Structures

The development of the material system and fabrication system is followed by the elaboration of an assembly of in-dune habitable spaces. The ability of the injections to inject at different depths can create volumetric enclosures within the dune. Occupying the interiors of a dune can demonstrate several environmental and functional benefits which can enhance living conditions in relation to the arid biome. The adaptation can facilitate heat exchange between the structure and dunal sub-soil, which in turn can significantly lower the temperature of inhabited spaces. In-dune habitation minimises the area exposed to the hot winds and sedimentation caused by their dropping velocity.

3.1. COMPONENTS OF IN-DUNE HABITABLE UNITS

In the adopted matrix injection system, injecting at different levels within the 3m X 3m grid is proposed. The construction of foundations and walls comprises the application of multiple injections and single point injections at different depths respectively (figure 5). Locally procured secondary material is used to stack additional floor slabs and roof over the pits.

3.2. LIVEABILITY IN IN-DUNE STRUCTURES: MICRO-CLIMATE ANALYSIS

A shoe-box microclimate analysis is conducted to simulate the liveability of excavated habitable spaces in terms of thermal comfort based on the relationship between parameters such as depth of excavation, peripheral wall thickness, soil temperature and value of sub-soil's thermal conductivity. Openings on the pits influence the convective capacity of the space's air volume due to its exposure

to direct solar radiation. Thermal mass and opaque conductivity regulate the nature and degree of heat transmission through the peripheral wall assemblies. The same wall properties of the hardened sand (in figure 06) work with low U-values to inhibit high degrees of thermal exchange and permit more regulated living conditions for the occupants.

Experiment: The experiment aims to record the range of temperatures inside an excavated pit for varying wall thickness and depth. Controlling these parameters alter the thermal transmittance or u-value of the subsoil and bring significant changes to micro-climate. The evaluation is based on the combination of depth and wall thickness (figure 6) that modify the air temperature such that it falls under the comfort band of Jaisalmer for respective seasons (with reference to ASHRAE 55). The machine constrainting injecting depth to 15 m marks the limit to test these variations (ranging 0.1m-15m). The wall thickness is ranging 0.3m-1.5m. The study is conducted separately for summer and winter.To record the temperature variations, the surface temperature of the surrounding soil are calibrated based on precedent data (Gupta, 1986) for both the seasons. (figure 6)

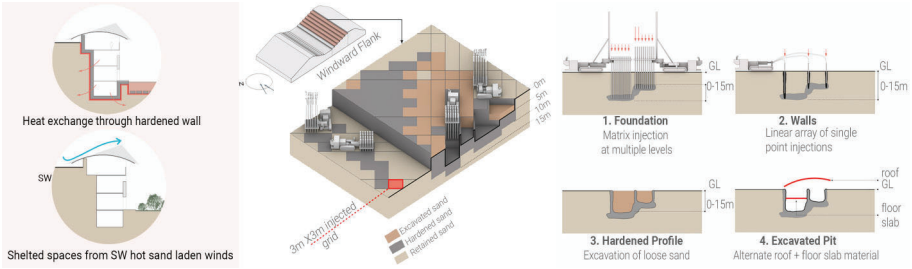

Figure 5. Fabrication strategy and components of in-dune structure.

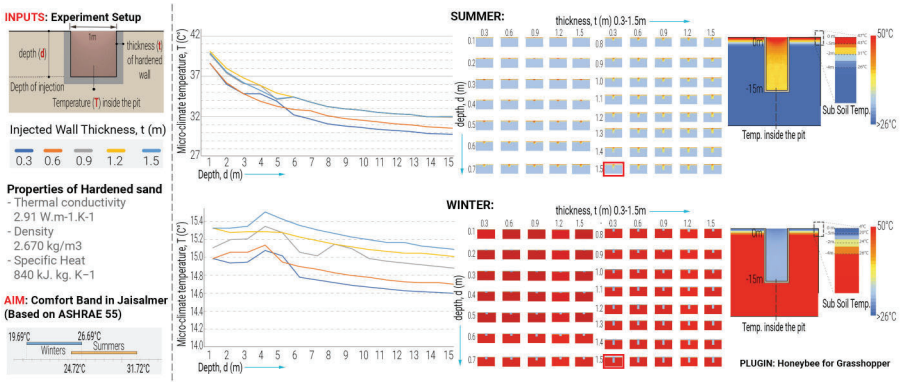

Figure 6. Shoe-box Micro-climate analysis.

Observations & Conclusions: Ground coupling serves as a proficient thermal comfort enduring technique. The technique shows significant difference for summer, for there is a flow of heat from interiors of the pit to subsoil. When the

temperature outside during harsh summers is 50°C, a drop of 20°C can be achieved inside the pit. As shown in the graphs above, the temperature is observed to start equalising after a depth of 9-12m . Hence, despite having injecting capability up to 15m, the injection depth of the machine can be limited to 12m to save time and material. For winters, there is a reverse flow of heat from subsoil to the interiors of the pit. This increases the temperature of the pit instantaneously to about 10-12°C (figure 6)when the outside temperature is 4°C but shows no significant variation across different depths. The temperature variations brings the micro-climate of the excavated pit within the comfort band for both the seasons.

3.3. FABRICATION OF DIFFERENT PROFILES BASED ON FUNCTIONS

While the material and fabrication mechanism enable the construction of in-dune spaces, the shoe-box thermal analysis indicates liveability. It also limits the depth of these pits to 12 m and peripheral wall thickness to 0.3 m. Constraint of machine width and injection depths start defining the sizes of the spaces that can be created and determine the functions they could transform into (figure 7). The shapes and sizes of these components play a critical role in developing sand stabilisation and deflection mechanism and will be further elaborated in another publication.The fabrication of these different profiles begin with piling and flattening of the sloped dune face. First the slope is retained by sheet piles or fences before cutting. Injection on these loose stepped profiles are carried simultaneously near the sheet piles on each step to maintain the homogeneity of the retaining wall. Once the surfaces have attained strength (after 14 days of injection), the loose sand is excavated and the hardened mass is either shaped or filled with fertile soil based on the profile's purpose.

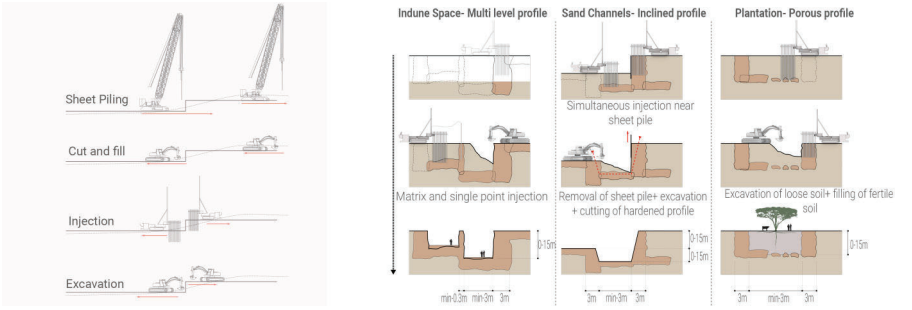

Figure 7. Fabrication of different profiles.

3.4. EVALUATION OF FABRICATION METHODOLOGY AT CLUSTER SCALE

The shoe-box micro-climate experiment done in Section 3.2 suggest favourable temperature variations in summers and winters inside these pits and set the parameters/physical constraints for the fabrication of in-dune spaces. The following experiment is another micro-climate analysis carried on the design proposal of a cluster of open, semi-open and closed spaces inside a dunal stretch (figure 08). These spaces are an output of a series of multi-objective optimisation

experiments carried out previously and will be further expanded in another publication. The results from this micro-climate analysis will evaluate liveability for the in-dune inhabitants in open and closed spaces.

Experiment Setup: A smaller portion from the cluster is extracted and it is assumed that the spaces within this portion are separated from the rest of the cluster by an adiabatic wall so that there is no heat loss or gain within this selected portion from the entire dunal stretch. Considering that the foundation slab and walls are made of bio-mineralised sand and stacked floors of wood, temperature variations are stratified for outdoor and indoor spaces during summers and winters. We input the same material properties as defined in previous experiment.

Observations & Conclusions: It is observed that in summers when temperature peaks to 50°C there is a significant drop of 10-12°C at both indoor and outdoor spaces. In winters however no significant rise in the temperature is observed. The outdoor spaces rather witness a minor temperature drop, making them less favourable to use. In comparison to the shoe-box experiment of section 3.2, the cluster here has greater surface area exposed to the sun versus the volume of the pit , facilitating faster dissipation of heat. There is greater thermal mass within the cluster. It can be concluded that while the proposed material system having a high thermal mass regulates the temperature of a given space to human comfort, the high surface area to volume ratio does not allow the heat to be trapped within the pit. The dimensional constraints from the proposed fabrication methodology supports the usability of in-dune spaces for mainly in summers.

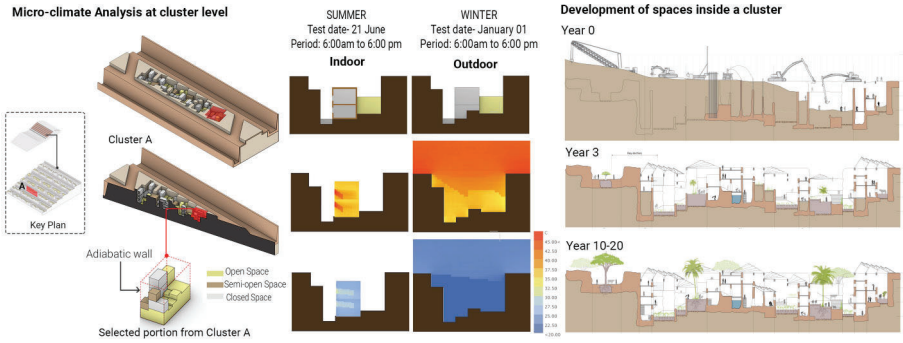

Figure 8. Cluster Scale Micro-Climate Analysis.

4. Conclusion and Analysis

The paper marks a clear hierarchy between the material system, fabrication process, and habitable spatial organisation to propose a highly sophisticated and interdependent complex methodology. Their interdependencies together inform design strategies, a phasing plan and global time scale for overall terrain transformation. Heavy ground manipulation needs a radical shift in adapting to fabrication mechanism and habitation of in-dune spaces. Every subsystem has its own limitation in the scope of application and some deprecated impact on

the neighbouring terrain. Scaling up their applicability across the dunal field would also mean scaling up the limitations. Inclusive of all the advantages and disadvantages, these systems can build an ecosystem which has the potential to be resilient to desertification in western Thar.

Microbial injecting into sand to develop habitable spaces and other components in different profiles has been proposed based on the compressive strength that homogeneously cast composite brick attains. While it is assumed that the grout spread is uniform inside the sand, the actual spread should be tested physically. The results from the tests would start defining the attainable surface textures, wall thicknesses, undulations, permeability and load bearing capacity. The arrangement of spaces has been directed by micro-climate analysis only, the strategy should be coupled with structural tests. For the difference in hardening time of different components for varying injection depths, profiles and volume of required grout, the fabrication strategy and time estimations for development of each phase should be revisited. Monolithically casted each wall would behave like a load bearing structure. While core-cutting is proficient to make small openings in such structures, its ability to make bigger openings for doors and windows need to be practically tested. The developed climate conscious architecture finds its applicability in dunal regions which are severely affected by desertification and shifting sands. The schemes can be adopted and adapted based on the effected regions' dune morphology, wind pattern, demographics, ground fabric, availability of resources like water and other infrastructural support.

Acknowledgement

This work is a part of the graduate thesis completed at AA, London in 2019-20 by Medha Bansal, Saumil Nagar and Kai Yeh, under the supervision of Dr. Michael Weinstock and Dr. Elif Erdine. Special thanks to Patrick Lawrence Monfort for conducting the environmental performance simulations.

References

Bohrtechnik, K.: 2018, "Drill Rigs: KLEMM Bohrtechnik GmbH" . Available from <https://www.ecanet.com/uploads/files/Resources/KR-807-7G_7GP.pdf> (accessed 10th May 2019).

Bryson, R.A. and Baerreis, D.A.: 1967, Possibilities of Major Climatic Modification and their Implications: Northwest India a Case for Study, *American Meterological Society*, **48**, 136-142.

Chang, I., Im, J. and Cho, G.C.: 2016, Introduction of Microbial Biopolymers in Soil Treatment for Future Environmentally-Friendly and Sustainable Geotechnical Engineering, *Sustainability*, **8**, 251.

Gupta, J.P.: 1986, Moisture and thermal regimes of the desert soils of Rajasthan, India, and their management for higher plant production, *Hydrological Sciences Journal*, **31**, 347-359.

Van Paassen, L.A., Harkes, M.P., Van Zwieten, G.A., Van Der Zon, W.H., Van Der Star, W.R.L. and Van Loosdrecht, M.C.M.: 2009, Scale up of BioGrout: A biological ground reinforcement method, *Proceedings of the 17th International Conference on Soil Mechanics and Geotechnical Engineering*, Alexandria.

Singhvi, A.K. and Amal, K.: 2014, The aeolian sedimentation record of the Thar desert, *Journal of Earth System and Science*, **113**, 371–401.

Zdruli, P., Cherlet, M. and Zucca, C. 2017, Mapping Desertification: Constraints and Challenges, *in* R. Lal (ed.), *Encyclopedia of Soil Science*, CRC Press.

THE F8LD MASK

Parametrized on-body design for personal protection.

ANDREI NEJUR[1] and SZENDE SZENTESI-NEJUR[2]
[1] *Université de Montréal*
[1] *andrei.nejur@umontreal.ca*
[2] *Technical University of Cluj-Napoca*
[2] *szende.szentesi@arch.utcluj.ro*

Abstract. The present research introduces a novel parametric approach for the construction of PPE, a face mask inspired from takeaway food packaging and kirigami techniques. The technique requires only foldable planar material with no gluing or binding. The design is customizable to the user's face using an augmented reality application and automatic processing in the Grasshopper environment. Using the proposed workflow, a personal mask can be constructed from a cutting and folding pattern printed on any household 2d printer. This makes it one of the most affordable and fast techniques for artisanal PPE existent now.

Keywords. Folding; ar; mask; parametric; on-body design.

1. Introduction and Problem Statement

The Covid-19 crisis has brought about many changes. People wearing masks everywhere trying to avoid contamination is probably on of the most visible ones. Through the first half of 2020 the procurement of PPE (Personal Protection Equipment) has been an important objective. Next to social distancing, PPE has been identified as the best modality to protect against SARS-COV-2 infection. The medical or artisanal mask is now a strong recommendation or a requirement in most countries touched by the pandemic. The sudden high demand has caught PPE producers off guard and has severely disrupted supply chains. The big demand has driven prices for PPE and especially masks to record highs and has depleted stocks everywhere. Until the industry managed to scale up to the demand users had to adapt. Besides conservation strategies employed for the healthcare industry (Livingston, Desai and Berkwits, 2020) a series of DIY initiatives have risen to the challenge of helping communities stay safe (Maia Chagas et al., 2020; Richterich, 2020). Different desktop fabrication techniques have been employed to replace or repair the missing equipment. The initiatives can be divided in two categories based on targeted users or used techniques. First there are the initiatives supporting the healthcare industry and that use a more standardized approach and digitally driven processes. Second, there are the artisanal and craft-based initiatives that used very basic techniques and target the general public.

PROJECTIONS, Proceedings of the 26th International Conference of the Association for Computer-Aided Architectural Design Research in Asia (CAADRIA) 2021, Volume 1, 503-512.

In the first category the most popular technique, due to its wide spread availability and adaptability, was additive manufacturing (AM) (Belhouideg, 2020). It found use for ventilator parts including helmets (Erickson et al., 2020), face shields (Flanagan and Ballard, 2020), masks (Swennen, Pottel and Haers, 2020; Tarfaoui et al., 2020), door handle grabbers and many others. CNC cutting of planar materials (often used in conjunction with AM) was also very popular due to very fast turnover times, simplicity and cost-effectiveness of used materials (Chaturvedi et al., 2020).

In most of the cases falling in the first category, the digital fabrication techniques were used as a substitution to industrial mass production means. They represent also a digitally assisted way of partially circumventing broken or sub-dimensioned distribution networks. In general, the digitally assisted fabrication techniques allow for the mass customization of the produced result based on design intent but more importantly on the targeted user's biometric data. Recent developments in orthosis design attest to that (Sharma et al., 2020). In the initiatives linked to the pandemics however, this aspect of customization is often very limited due to multiple reasons. The most important one is that the fabrication process is not as distributed as the users' biometric data. The mentioned fabrication processes don't have access to biometric data and more important they have no way of matching that data with the actual targeted individuals. As a result, they need to constrain themselves to small subsets of extrapolated median values and embrace a one-size-fits-all type of mentality in hope of covering as much of the user spectrum as possible.

The second category groups a set of very different approaches that make use of analogous very simple techniques for the manufacture of PPE like sewing and tailoring. Of interest here is the use of digital dissemination techniques and the distribution of the design rather than of the physical product to enhance the impact. This is possible due to the inherent simplicity of the used techniques and the wide availability of the tools and materials required for crafting the products. To give a bit of perspective, one of the most viewed tutorials for making a fabric mask has over 54 million views in 7 months on YouTube. Many studies comparing the effectiveness of artisanal and industrial PPE (Mueller et al., 2020; O'Kelly et al., 2020) avoid taking this reach aspect into consideration.

One of the advantages of the initiatives in the second category is also one of their shortcomings. The simplicity of analogous techniques ties the success of the product and its ability to do its job to the crafting abilities of the user. There is in fact very limited help from the digital technologies when it comes to making a mask. Beyond the tutorials and examples, the user is on its own when it comes to making the product and especially when adapting the design to its own measures. This often limits the reach and the effectiveness of the technique.

The problem, as it emerges from our small survey above, is that when it comes to nonindustrial PPE production and especially to masks, reach, effectiveness and cost seem to be competing metrics. With none of the initiatives being able to score in all.

2. Solution

A solution to the problem stated above is to empower the final user to produce its personal protection equipment with widely available materials and simple, prevalent household tools while also making use of the technological achievements of the 21st century for fabrication. In this context the production of a PPE mask using cutting and folding sheet material emerges as a very interesting alternative able to leverage simplicity, customization, cost and digital distribution. Even though at the time of writing this we haven't been able to find similar approaches towards making PPE masks, variants of this technique are already used on larger scales (Baerlecken et al., 2014; Vergauwen, De Temmerman and Brancart, 2014) with different degrees of computational assistance. One healthcare initiative using folding that stands out is the Apollo3 Isolation Hood (Ross et al., 2020).

In this paper we present a parametric solution that creates a disposable mask from sheet material using cutting and folding. The process works in 4 steps: 1. User face model acquisition using a smartphone's frontal camera with optional custom fitting of mask feature points. 2. Face mesh import in the CAD application Rhinoceros and automatic pattern generation. 3. Pattern printing using a 2d printer. 4. Mask creation by cutting and folding of the pattern.

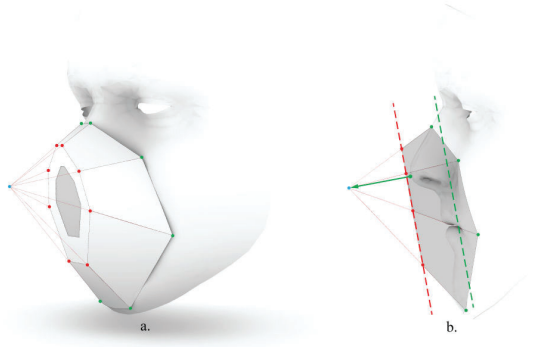

Figure 1. Geometric attributes and relation with the face for the F8LD mask.

The parametric design is based on an initial mask object (called the F8LD) created through an analogous process in the CAD software Rhinoceros. The F8LD is a disposable paper mask made from a precut sheet of material that requires only folding and no glue or fasteners for the assembly. Only a 2d printer and a paper knife or a pair of scissors are required to make the mask. The parametric version of the mask uses the features of the analogous design and extends it through mass customization. In the following paragraphs we will first present the design steps for the analogous design. After that we will elaborate on the features and enhancements brought by the parametric workflow.

3. Analogous implementation

The design is based on the polyhedral shape of an octagonal truncated pyramid. The apex of the pyramid is placed about 4 cm away from of the tip of the nose and its base points are resting on the face itself. In Figure 1 the green dots represent the feature points chosen on the scan of the face, the blue point is the apex of the pyramid. The apex is determined in several steps. First the best fit plane of the 8 feature points (the green dots excluding the nose point) picked on the face is constructed (in Figure 1.b represented as a dashed green line). Secondly the picked point representing the tip of the nose is moved in the direction of the fitted plane normal for about 4 cm to find the apex (Figure 1.b the blue dot). The red lines connecting the apex with the feature points on the face are the generatrixes of the pyramid. The top base of the truncated pyramid is constructed by intersecting a plane (in Figure 1.b represented as a dashed red line) with the generatrixes. The plane parallel with fitted plane of the face points is positioned so that the resulting truncated pyramid fully covers enclosed face features. The folding process of the mask from a planar pattern gives an overview of the design steps. The most important states of the folding process are presented in Figure 2.

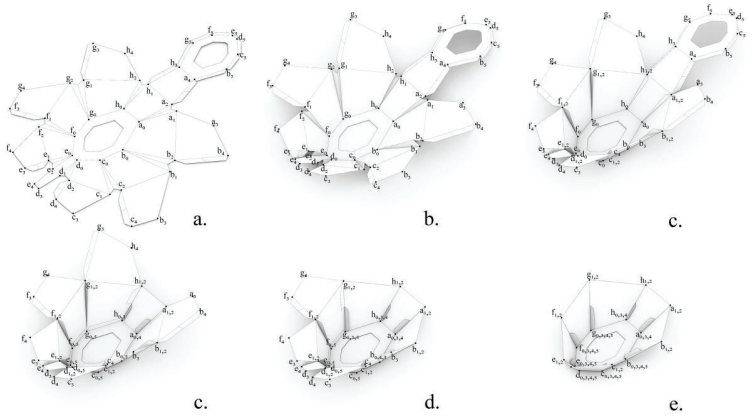

Figure 2. Screen grabs from the augmented reality application constructed to fit the mask to the face.

The fully unfolded model, presented in Figure 2.a, is an eight-arm star-shaped planar pattern containing each face of the truncated pyramid exactly twice in two concentric rings. The pattern includes several flaps and fold-in bellows. The flaps are used to keep the folded form in its shape and the bellows ensure the surface continuity in the folded state. The process reveals how folding doubles each face of the mask thus ensuring a continuous layer of material throughout the folded shape. Each vertex has a unique tag composed of a letter from a to h and a number. The letters correspond to nodes in the octagonal polygon that is the base of the pattern. The numbers denote the relationship between the points connected to the same octagon vertex but part of different folded faces.

The process starts from the flat, pre-creased pattern visible in Figure 2.a. First the bellows are folded inside to achieve the general shape of the volume. This corresponds to joining vertices with numbers *1* and *2*. This brings the faces in the first ring around the octagonal base, like *face(a0,a1,b2,b0)*, at the correct dihedral angle with the base *face(a0,b0,c0,d0,e0,f0,g0,h0)*. The process is visible in Figure 2.b and 2.c. At this step the form is not stable. The natural elasticity of the material is fighting the folds in the shape and if no force is exerted from the outside the object tends to revert to its flat version. This is resolved by folding the flattened bellows on the sides of the volume as shown in Figure 2.c. *Fold(a0,a1,a2)* and *fold(h0,h1,h2)* are bent over the *face(h0,h1,a2,a0)* and *face(h1,h3,a4,a2)* is folded over them to fix them in place as seen in Figure 2.d.

The same folding action brings down *face(a4,b5,c5,d5,e5,f5,g5,h3)* over *face(a0,b0,c0,d0,e0,f0,g0,h0)*. The folding process continues along the perimeter in two directions with *face(a1,a3,b4,b2)* and *face(g0,g1,h2,h0)* as seen in Figure 2.e. It is important to note that the mentioned faces will fold over the flaps connected to *face(a4,b5,c5,d5,e5,f5,g5,h3)* but also over the flaps connected to *face(h1,h3,a4,a2)*. The flaps connected to the latter are split and only half of them remain under the face folded next (the top half) while the other half sticks out. This ensures that consecutive folded faces like *face(g1,g3,h4,h2)* and *face(h1,h3,a4,a2)* ensure each others folded stability through a reciprocal mechanism. Figure 2.f shows the completed process with all faces folded and flaps tucked in or sticking out according to the rule.

One important, albeit optional feature of the design is the possibility to include a filtering material between the double faces of the base of the truncated pyramid. Between the folding actions shown in Figure 2.c and 2.d, a patch of filtering material can be inserted between *face(a4,b5,c5,d5,e5,f5,g5,h3)* and *face(a0,b0,c0,d0,e0,f0,g0,h0)*. The octagonal cut-out in the two faces is designed to facilitate the flow of air, through the filter. Presently one singular cut-out is designed but this can be replaced with an array of smaller holes that help to better secure the filtering material in place.

4. Evolution and parametric approach

The first iteration of the design makes for a very inexpensive and easy to distribute product either as a digital download or a precut pattern. But in this simplicity also lies one of its most important shortcomings, its lack of adaptability. Because faces come in many shapes and sizes a one-size-fits-all kind of approach does not do well, especially with semi rigid objects that need to be worn so close to the skin. The downloadable pattern can be scaled prior to printing but this in not enough to adapt it to a wide range of face shapes. In the following paragraphs we will present the additional steps undertaken to make the design parametric and customizable.

4.1. FACE MODEL ACQUISITION

The first step deals with acquiring a representation of the user face to be used for the parametric construction of the mask. In order to make the scanning process as accessible as possible we decided to use as scanning device a Time of Flight (ToF)

camera. The ToF technology is present in many of today's consumer electronics and most of the new smartphones. Using ToF information the embedded software of the smartphone can construct a topologically constant but geometrically adapted model for the face of the user each time it is in view of the camera. The model is topologically constant because the constructed mesh will always have the same number of vertices and the same vertex interconnectivity, regardless of the viewed face and regardless of the face's pose. The geometry of the produced face mesh is always adapted to the user's face and represents a close 3d depiction of its features. The accuracy of the mesh compared with the real face makes possible its use as a biometric test granting access to the phone contents.

Figure 3. Screen grabs from the augmented reality application constructed to fit the mask to the face.

We propose to use this feature of modern smartphones to extract the 'scanned' face as a mesh and use it to construct our parametric mask model on it. In order to achieve this, we leverage the game engine and application development environment Unity3d with its extension for augmented reality ArFoundation. The use of Unity3d allows the construction of a custom application that can run on modern iOS or Android phones and can extract the 3d mesh representation of the user's face.

In our current workflow the application works in 3 stages. First, the application leverages, through arFoundation, Apple's arKIT and extracts a dynamic mesh very closely fitted to the user face. The mesh matches de dimensions and features of the face and can mimic all expressions (the gray overlay in in Figure 3). Second, inside the application the user can modify the eight placeholders (the red spheres in Figure 3) corresponding to the eight corners of the base of the truncated pyramid resting on the face. The transformation is done with a simplified augmented reality preview of the mask model visualized on the face of the user. In the last stage the mesh and sphere positions are exported as .obj and .txt files.

4.2. PARAMETRIC MODEL

The second step in our workflow is the automatic creation of the geometry of the mask in both its constructed (folded) state as well as in its planar pattern (unfolded) state. The scope is to construct a model that accurately and completely simulates

the folded model of the mask and then use unfolding routines to make it flat. For reasons pertaining to the tools required to handle the unfolding process, the Grasshopper visual scripting environment attached to Rhinoceros was chosen as a work environment for this step.

The face mesh is imported into Rhinoceros and referenced into Grasshopper together with the eight landmarks saved with the .obj file. The landmarks are saved as a text file containing eight integer values referring to the indexes of the eight mesh vertices used as positions for the mask corners. Based on the eight positions the truncated pyramid is constructed following the same steps as the ones detailed in the solution section. The model of the truncated octagonal pyramid is constructed as a mesh that starts with 24 vertices and 16 faces. The 24 vertices correspond to the two bases of the truncated pyramid 8 on the face, 8 for the small base extending away from the face and the last 8 in the middle of the small base to define the hole for the filter. From the 16 initial faces eight are quad faces between the generatrixes of the truncated pyramid and 8 are quad faces composing the small base and fanning around the hole at its center.

In order to achieve the exact model of the mask required for unfolding, all the faces in the model need to be doubled and multiple flaps and bellows need to be added. For this scope the number of vertices is increased. In Figure 2.a the reader can follow the process and identify the individual vertices in the unfolded state as well as the multiplied vertices in the partially folded and fully folded states. The vertices defining the small base *a0* to *h0* are tripled thus producing the sets with numbers *3*,*4* and *5*. The vertices that rest on the face or set *a1* to *h1* are doubled to produce the similar set with number *2*. The multiplied vertices are necessary for the construction of the double faces in the 3d model of the folded mask. The construction of the doubled faces and thus the topology of the mesh model of the mask can be similarly followed in Figure 2. In addition to the named vertices visible in the same Figure, several other vertices are necessary for the construction of flaps. For example the flap linked to *edge(g1,g3)* is created through a 5 mm offset of the edge in the plane of the *face(g0,g1,h2,h0)* in the folded state presented in Figure 2.e. The offset line is then scaled to 80% length and connected to *edge(g1,g3)* to create the flap. The *bellow(a0,a1,a2)* is created using the geometric positions of *edge(a0,a1)* and *edge(a0,a2)* in the unfolded state shown in Figure 2.a. The fourth point of the bellow is found using the formula $\frac{a1+a2}{2} \cdot 0.8 + a0 \cdot 0.2$. All other flaps and bellows are created in a similar manner.

4.3. UNFOLDING

The flat pattern is the result of unfolding the constructed mesh of the mask object on a plane. For unfolding we are using the Grasshopper add-on Ivy (Nejur and Steinfeld, 2016, 2017) that can unfold 2-manifold meshes of the most diverse configurations for subsequent fabrication from flat sheet materials. The add-on represents the mesh as a graph where each mesh face is a node in the graph and each 2-manifold mesh edge is an edge in the graph. The graph is a dual of the input mesh. The algorithms in Ivy make the mesh unfold by converting the constructed

graph of the mesh from a graph with cycles into a tree graph. This happens by removing graph edges based on metrics chosen by the user (like dihedral angles between faces or face area). If the mesh is representable as a tree graph one can start from any mesh face and rotate neighboring faces around the common edge to have a 180-degree angle with their neighbor. If this process is followed for each subsequent neighbor, it yields an unfolded version of the mesh with no dimensional distortion.

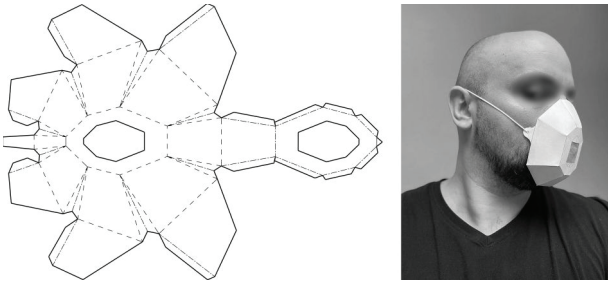

Figure 4. Fully unfolded pattern and image of a fabricated prototype being used.

For the final 2d pattern, to help the user cut and fold, we represent each edge of the unfolded mesh with a different line-type according to its role in the construction process for the mask. Cut edges are continuous, mountain edges have a dash pattern, valley edges use a dash-dot pattern while flat edges have no 2d representation. Figure 4 shows the final pattern and an image depicting the use of a prototype affixed to the face with an elastic string.

5. Discussion.

The design presented in this paper brings a new approach for the construction of nonindustrial PPE and of masks in special. It brings notions from packaging design, and tools used for geometry rationalization at the architectural scale and uses them for the creation of wearable protection. The presented design offers many advantages over the classical PPE masks in four main areas: Availability, Ecology, Cost and Adaptability.

5.1. ADVANTAGES

Availability. Since it can be delivered as a digital download all supply chains are bypassed. Getting a mask can be as fast as the time required to cut and fold the pattern from the printed sheet of paper. The materials and production tools are generally available in a typical household. **Ecology**. The typical material for the creating the mask is paper. This makes this mask biodegradable or recyclable depending on post-use decisions. Other materials can be used for the mask especially if the pattern is cut with a numerically controlled tool like a laser cutter. If more durable materials are used, like polypropylene or PET-G sheets, the mask can be used as a reusable one. **Cost**. The main cost of a mask is the cost of a printed sheet of paper. Event though our approach does not rely on industrial processes and large quantities to drive down cost it can compete in terms of cost with any

PPE mask solution currently being offered. **Adaptability**. The parametric version takes most of the advantages of the original design and adds customization. The proposed process creates a fitted mask for any user with the possibility for custom adjustment. Each mask is fitted based on individual biometric data.

5.2. LIMITATIONS.

While the parametric version improves in several areas the analogous approach, it also introduces an important shortcoming that cuts into the advantages of the original design through the required use of a commercial CAD platform to perform the creation of the unfolded pattern. For the limited scope of running the script that generates the pattern, acquiring a commercial program and the minimal skills required to use it will be too expensive and time consuming for the average intended user. Additionally, the current data exchange procedure via files can cumbersome and further cuts into the advertised advantages.

6. Conclusion and Next steps.

In this paper we have presented a parametric approach for the construction of a personal protection mask created from flat sheet material. The design is based on a scan of the user face, easily obtainable with the help of a modern smartphone fitted with a ToF camera. In the smartphone app the user can customize the position of the mask on the scan of the face and export the scan and the set positions to the Rhino/Grasshopper scripting environment. Here the complete 3d model of the mask is constructed and unfolded into a flat pattern. The pattern can be directly printed on a sheet of paper cut and folded to obtain the mask. The mask can be delivered in different ways. It can be made by the user at home from paper. It can be offered as a service that includes custom fitting by a business. It can be delivered (digitally or physically) as readymade patterns pre-tailored to a few typical face sizes. The design is open-source and the GitHub repository (Nejur, 2020) offers the work under a GPL3 licence to anyone willing to use or improve the design.

For the parametric process our next step would be to create a full integration of the mask construction and unfolding process inside the smartphone application. This would remove the requirement for a CAD framework to handle the flat-pattern creation and will improve significantly the availability and cost metrics for our proposed design. For the design, some transformations to the geometry generation process to ensure a better seal around the nose area will be undertaken. Currently due to the straight edges of the base octagon of the mask, areas of high concavity can produce gaps and partially compromise the seal of the mask to the face. We plan to address this by looking into curved folds and/or curved cuts for the base of the mask resting on the face. For the material study we plan to experiment with other flat sheet materials like PP (Polypropylene) or PET-G (Polyethylene terephthalate glycol) to test designs that can turn the mask into a reusable one. We plan to test the design on several metrics like airtightness and filtration as part future developments of the research.

References

Baerlecken, D., Gentry, R., Swarts, M. and Wonoto, N.: 2014, Structural, Deployable Folds — Design and Simulation of Biological Inspired Folded Structures, *International Journal of Architectural Computing*, **12**(3), 243-262.

Belhouideg, S.: 2020, Impact of 3D printed medical equipment on the management of the Covid19 pandemic, *The International Journal of Health Planning and Management*, **35**(5), 1014-1022.

Maia Chagas, A., Molloy, J.C., Prieto-Godino, L.L. and Baden, T.: 2020, Leveraging open hardware to alleviate the burden of COVID-19 on global health systems, *PLOS Biology*, **18**(4), 1-17.

Chaturvedi, S., Gupta, A. and Bhat, A.K.: 2020, Design, usage and review of a cost effective and innovative face shield in a tertiary care teaching hospital during COVID-19 pandemic, *Journal of orthopaedics*, **21**, 331-336.

Erickson, M.M., Richardson, E.S., Hernandez, N.M., Bobbert, D.W., Gall, K. and Fearis, P.: 2020, Helmet Modification to PPE With 3D Printing During the COVID-19 Pandemic at Duke University Medical Center: A Novel Technique, *The Journal of Arthroplasty*, **35**(7, Supplement), S23-S27.

Flanagan, S.T. and Ballard, D.H.: 2020, 3D Printed Face Shields: A Community Response to the COVID-19 Global Pandemic, *Academic Radiology*, **27**(6), 905.

Livingston, E., Desai, A. and Berkwits, M.: 2020, Sourcing Personal Protective Equipment During the COVID-19 Pandemic, *JAMA*, **323**(19), 1912-1914.

Mueller, A.V., Eden, M.J., Oakes, J.M., Bellini, C. and Fernandez, L.A.: 2020, Quantitative method for comparative assessment of particle removal efficiency of fabric masks as alternatives to standard surgical masks for ppe, *Matter*, **3**(3), 950-962.

Nejur, A.: 2020, "F8LD Mask repository" . Available from Publication Title: F8LD<https://github.com/andrei-nejur/f8ld>.

Nejur, A. and Steinfeld, K.: 2016, Bringing a Weighted-Mesh Representation to Bear on Generative Architectural Design Applications, *ACADIA 2017*.

Nejur, A. and Steinfeld, K.: 2017, Ivy: Progress in Developing Practical Applications for a Weighted-Mesh Representation for Use in Generative Architectural Design, *ACADIA 2018*.

O'Kelly, E., Pirog, S., Ward, J. and Clarkson, P.J.: 2020, Ability of fabric face mask materials to filter ultrafine particles at coughing velocity, *BMJ open*, **10**(9), e039424.

Richterich, A.: 2020, When open source design is vital: critical making of DIY healthcare equipment during the COVID-19 pandemic, *Health Sociology Review*, **29**(2), 158-167.

Ross, A., Smith, A., Kumar, A. and Yang, A.: 2020, "Apollo3 Patient Isolation Hood" . Available from Publication Title: Harvard GSD<https://research.gsd.harvard.edu/maps/portfolio/pih/>.

Sharma, N., Welker, D., Cao, S., von Netzer, B., Honigmann, P. and Thieringer, F.: 2020, An Interactive, Fully Digital Design Workflow for a Custom 3D Printed Facial Protection Orthosis (Face Mask), *International Conference on Additive Manufacturing in Products and Applications*, 26-36.

Sturgess, B.N. and Carey, F.T. 1987, Trilateration, *in* R.C. Brinker and R. Minnick (eds.), *The Surveying Handbook*, Springer US, 340-389.

Swennen, G.R.J., Pottel, L. and Haers, P.E.: 2020, Custom-made 3D-printed face masks in case of pandemic crisis situations with a lack of commercially available FFP2/3 masks, *International Journal of Oral and Maxillofacial Surgery*, **49**(5), 673-677.

Tarfaoui, M., Nachtane, M., Goda, I., Qureshi, Y. and Benyahia, H.: 2020, 3D printing to support the shortage in personal protective equipment caused by COVID-19 pandemic, *Materials*, **13**(15), 3339.

Vergauwen, A., De Temmerman, N. and Brancart, S.: 2014, The design and physical modelling of deployable structures based on curved-line folding, *4th International Conference on Mobile, Adaptable and Rapidly Assembled Structures, MARAS*, 145-56.

BRANCHING INVENTORY

Democratized Fabrication of Available Stock

KEVIN SASLAWSKY[1], TYLER SANFORD[2],
KATIE MACDONALD[3] and KYLE SCHUMANN[4]
[1]*University of Stuttgart*
[1]*ksas123@gmail.com*
[2]*University of Tennessee*
[2]*tsanford0514@gmail.com*
[3,4]*University of Virginia / After Architecture*
[3,4]*{kmacdonald|schumann}@virginia.edu*

Abstract. Branching inventory is a construction methodology demonstrated through a full-scale structural prototype that reduces the waste inherent in milling lumber and celebrates natural variation by making complex form the efficient result of irregular material. The processing of wood into standardized components embeds waste and intensive energy consumption into timber construction. This work reimagines the utility of raw materials, using computational feedback to place natural form in dialogue with design intent – creating a dialogue between technology, material, and designer. A custom workflow synthesizes a network of branches into a specific, structural form, shaped by the thicknesses and curvatures of the stock material as well as design input. Building on work using machine visioning in fabricating non-standard timber by others – most of which relies on elaborate and cost-prohibitive 3D scanning and robotic fabrication systems – branching inventory demonstrates a low-fidelity, democratized version of such approaches, using standard wood and metal-working tools and in which the available material stock contributes to design possibilities.

Keywords. Digital Design; Digital Fabrication; 3D Scanning; Material Agency; Democratized Technology.

1. Introduction

During Industrialization, wood construction became standardized through the milling of logs into dimension lumber. Subtractive part reduction, repeated at forest, sawmill, and construction site, produces material and energy waste. Amid an escalating environmental crisis, dimension lumber faces new lifecycle questions and overextended supply chains. The potentials of computational imaging in fabricating non-standard timber have been both discussed (by Mario Carpo and others) and demonstrated in built projects (at AA Hooke Park, University of Michigan, Aarhus, and elsewhere) over the last several years (Carpo,

PROJECTIONS, Proceedings of the 26th International Conference of the Association for Computer-Aided Architectural Design Research in Asia (CAADRIA) 2021, Volume 1, 513-522.

2017; Devadass et al, 2016; Self and Vercruysse, 2017; Von Buelow, 2018; Larsen and Aagaard, 2019). Most of this work relies on elaborate and cost-prohibitive 3D scanning and robotic fabrication systems. This paper describes a democratized take on such approaches, developing a novel construction methodology which reimagines the utility of raw logs, using computational feedback to place natural form in dialogue with design intent. The workflow makes use of low-cost, consumer-grade and industry-standard software, and fabrication relies on simple welds and either a waterjet or jigsaw.

This methodology creates a dialogue between technology, material, and designer that reduces the waste inherent in milling lumber and celebrates natural variation by making complex form the efficient result of irregular material. A custom workflow synthesizes a network of branches into a specific, structural form, shaped by the thicknesses and curvatures of the stock material as well as design input. Because material eccentricity informs design geometry, minimal part reduction must be performed, in turn decreasing construction energy and waste during harvesting, production, and on-site construction.

The workflow is demonstrated through the construction of a full-scale structural prototype, a wall ten meters in length and three meters in height. Invasive plant species – specifically the bradford pear – are explored as a potential non-traditional, but rapidly-renewable natural material stream for construction. This effort attempts to incentivize the removal of such species (through harvesting) and in turn remediate the environment at a regional scale. The bradford pear, which was popularized in yards and parking lots due to its natural ornament and fast growth, is prone to losing branches due to its weak, acutely angled forks and numerous limbs originating from the same point. The built prototype collects and makes use of these fallen branches. Irregular branches are collected, scanned, inventoried, and sorted across a curved surface using a smartphone 3D scanning app and custom parametric workflow, matching natural curvature to the designed model and locating stronger branches near the base of the assembly. The parametric model outputs unique steel joint templates which program the overall geometry within each node.

This paper presents a built research investigation but describes a methodology that is globally transferrable – a democratized workflow between common tools that can be adapted to local material supplies and craftsmanship. The success of the prototype points to the possibility that imaging and computation, coupled with non-traditional material streams, can reconsider the default practice of standardization and part reduction in timber construction.

2. Methods

Branching inventory develops a hybrid analog/digital workflow from which many types of structures can be designed and built, which will vary in form according to material inputs and design intent. A system diagram illustrates the components and relationships in the process, which mediates designer, material, computation, and physical fabrication (Figure 1). The following project methodology is described in five main steps: collection and scanning, inventorying and analysis, branch and

surface sorting, programmed joints, and physical assembly.

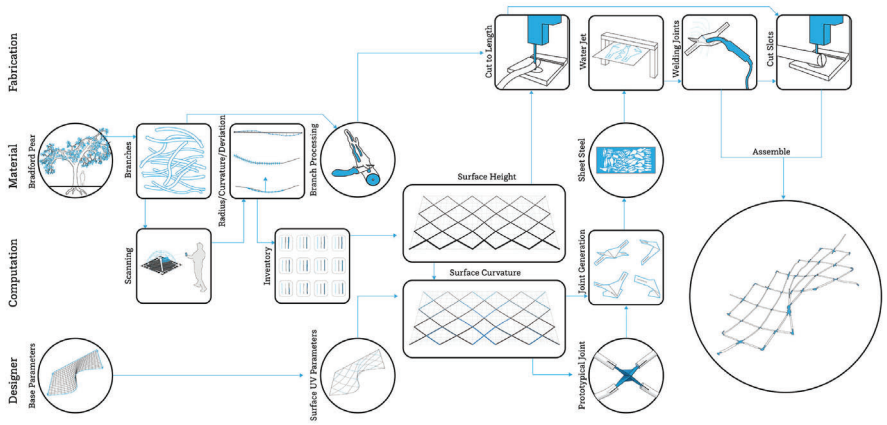

Figure 1. System Diagram.

2.1. COLLECTION AND SCANNING

The project aims to make use of material that is too irregular to be milled into traditional lumber. In this case, a desire to use material from invasive plant species led to the project team selecting the bradford pear, a tree with irregular branches and weak forks but otherwise quality wood that is popular for woodturning pens and other small objects. The team harvested all material for the project from a single bradford pear tree, resulting in a collection of sixty branches, each approximately one meter in length.

To extract physical qualities from the irregular material which can inform a design, a reliable 3D scanning method was required. Several 3D scanning methods were tested, from consumer-grade smartphone apps to high-end industrial 3D scanning hardware and software systems. These were assessed based on scan accuracy, usability, file size, and cleanliness of the digital model. Ultimately, a user-friendly smartphone app, Qlone, was selected. Qlone is a photogrammetry scanning software that uses a printed calibration grid as the surface on which an object is scanned. This surface can be printed at any scale and isolates the digital model from all background material, meaning that no post processing of the resulting digital mesh is required – this was a significant advantage over other smartphone scanning apps. An augmented half dome is viewable around the object as it is scanned to direct the user to views and angles yet to be photographed.

This method produced scans that were clean, immediately usable, and of high enough resolution to be processed using the project workflow. Since a joinery method (described below) was developed that does not require accurately machining the branches themselves, the selected scanning method was more than sufficient. This approach sets itself apart from other projects that rely on extremely accurate 3D scans to generate 3D toolpaths for intricate joinery. Additionally,

the use of a smartphone app democratizes the approach, replacing 3D scanners which retail for tens of thousands of dollars with software that costs a few dollars. The resulting digital meshes are also significantly smaller in file size, making manipulating dozens at once within a single Rhinoceros file possible on a standard laptop. It is also worth noting that this method is limited by the resolution of the smartphone camera, and resolution does not scale with larger objects. This is due to the nature of the photogrammetry method used in the software, which requires the same number of photographs be taken of an object, regardless of scale.

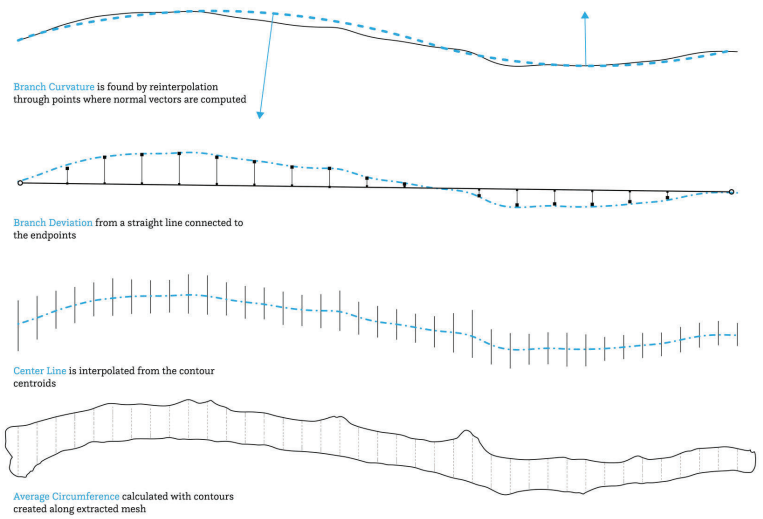

Figure 2. Branch Analysis.

2.2. INVENTORYING AND ANALYSIS

This step of the process functions as the digital link between designer and material. First, the inventory was prepared for analysis, with the goal of extracting specific understandings of the branches' inherent eccentricities, such that they can be used to the designer's advantage. Once all sixty branches were scanned, they were numbered to match their physical identity, compiled into an organized grid in a single Rhinoceros file, and oriented uniformly lengthwise. The data extracted (including values of curvature and average radius) is crucial to understand and determine how the irregular material can be used accurately in predictably modeling and fabricating a structure (Figure 2).

The first operation performed on each 3D mesh was a simple contouring along the length of the branch, serving as a base for many other operations. Connecting the centroids of each contour curve results in an interpolated curve representing the centerline of the branch – a spatial delineation that can be further refined

by interpolating circles over each of the contoured sections, in effect smoothing out branches with small protruding geometries. The generated centerlines are linked to each individual branch and stored in the corresponding place within the inventory. The interpolated circles also serve to measure and calculate the average circumference and radius of each branch – a set of values that are likewise added to the growing data inventory.

Using the new inventory of centerline curves, a set of curvature values are determined for each branch. First, the length of each branch curve is reparameterized from zero to one, and three points are positioned at 0.3, 0.5, and 0.7. A circle is then interpolated from these three points, representing the overall curvature of the branch. The radius of this circle is stored as the curvature value for each individual branch. The radius, also visualized as a vector, is used later on in determining the orientation of branches within the structure.

With these four components (average circumference, centerline curve, curvature value, and curvature vector) generated and saved, they are linked to their corresponding scanned meshes and constitute the complete inventory.

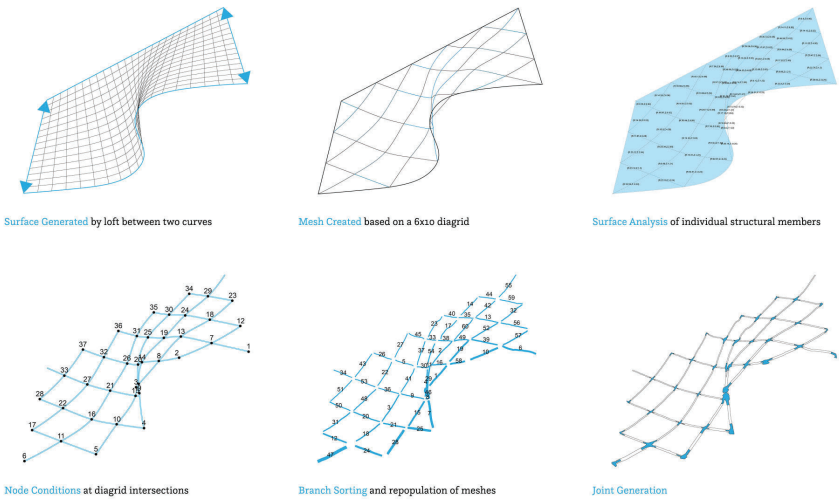

Figure 3. Surface Design and Analysis.

2.3. BRANCH AND SURFACE SORTING

Having scanned and analyzed an inventory of branches, the next step is to correlate this material inventory with a designed form. The form was designed as a lofted surface between a straight and an undulating curve, resulting in a vertical, wall-like structure that is serpentine at ground level and straight along the top.

With the form designed, branch sorting can begin. The designed mesh contains embedded information in each of its UV division curve edges that is similar to the information gathered in the branch inventory described previously. Each mesh

edge has a particular associated curvature and has its own Z-height relative to the ground. These two values are evaluated and inventoried across the surface (as was done with the branches). These new mesh values are compared to the branch values in a best fit system as follows (Figure 3):

First, the branches are sorted by average circumference and assigned to an appropriate horizontal section of the mesh according to Z-Height values – heavier branches are kept toward the bottom of the structure and lighter branches are located toward the top. Next, beginning with the most extreme curvature values, branches are matched to the mesh edge with the most similar curvature value. After all branches have been located across the surface, the surface is reauthored based on the curvature values of the branches.

This reauthoring of the surface requires the designer to yield some degree of authorship to the eccentricities of the material. Each branch has its own texture and smaller scale surface variations – data not captured through the scanning process. These irregularities result in variability within the finished structure. If the process is performed again on a different set of physical branches, or branches from a different tree species, for example, the resulting geometry would be reshaped based on the peculiarities of the new inputs.

2.4. PROGRAMMED JOINTS

After the branches are located across the structure, a joinery method is implemented to physically fabricate the structure. Rather than relying on highly specific joints that must be machined into the ends of the branches (and therefore require high-fidelity 3D scans), a joint system was developed that could connect the ends of branches where they meet at the nodes on the surface. Joint design anticipated low skill fabrication methods and was aimed at expedient manufacturing and assembly. Finally, the joints were customized for each node by programming each with the overall geometry of the structure. The joint design made a large scaffolding or template unnecessary for assembly, since angles of intersection and positioning were inherent to joint geometry.

Multiple joint iterations were developed and tested, ranging in scale and complexity. Initially, joints anticipated the overlapping and capturing of branch ends, but this was deemed too visually clunky and complex. Instead, the final joint design required the branches terminate just short of intersection, slotting into a node made of two intersecting pieces of steel sheet and forming a thin joint that does not distract visually from the legibility of the best fit system.

To model and fabricate the joints, two planar surfaces were generated using the points of intersection between four branches, intersecting with each other at the center of the joint. Two triangles were created to hold the surfaces together for welding accurate angles and to reinforce the joint. Once the joints were adapted to the geometry of each node in the structure, they were cut from a 14-gauge steel sheet and welded manually using triangular alignment pieces. Cutting the joints can be performed by either a CNC water jet or plasma cutter in a typical digital fabrication workflow or, in a more low-tech, democratized approach, by hand using printed paper templates and a metal bandsaw or jigsaw. Joints at the

edges of the assembly are generated with the same process with slight variation: the bottom joints connected to the ground are made with the two metal planes folded and welded back-to-back, while the elbow joints on the ends and top edges are simply bent to the correct angle to hold the edge pieces in place.

Figure 4. Assembled Structure.

2.5. PHYSICAL ASSEMBLY

With the branch and joint inventory complete, the joints were fabricated, and the branches were trimmed to length. To attach the metal joints to the wood branches, six centimeter kerf cuts were made in the ends of each branch to accept the joint. With the metal joint inserted, two holes were drilled through both the branch and joint through which bolts hold the assembly together and prevent rotation.

The digital model was referenced to guide the correct orientation of the branches during kerf cutting. The photographic data gathered during 3D scanning aided in this alignment process, but it proved to be the most tedious part of fabricating the structure. Future work should consider the use of augmented reality systems to aid in proper and precise alignment of end slots.

All joints and branches were assembled sequentially working in rows from the bottom to top of the structure. The bottom joints were anchored to the ground with a foundation of cement pavers. Once fastened, the programmed geometry of the joints accurately positioned the branches in the correct orientation within the overall assembly, meaning that assembly was easily completed in its correct upright orientation by a team of two individuals without the use of scaffolding or any large scale alignment templates (Figure 4).

3. Results

The 3D scanning method proved accurate enough to complete the project and was affordable and data efficient compared to more advanced systems. Some discrepancies were experienced in the process that could be designed around in future work. Since the object being scanned sits on top of a flat registration image, the underside of the object is obscured from view and thus interpolated. This reduced accuracy of the scan for the bottom side of each branch and produced some geometrical discrepancies during branch analysis. Future work should explore mounting of the branch within a simple armature for scanning, such that it is elevated, and the bottom is more visible. Finally, Qlone produces scans with no measurable scale, meaning that scans were manually resized. Future work can use of a physical scaling object to calibrate the resultant digital model.

Orienting the branches for slot incision presented challenges. Methods exist and have been proven by others to accomplish this step by robotically locating the branches in space. Such techniques, while effective, would dilute the democratized approach of this project. Alternatively, consumer-grade augmented reality headsets may provide better guidance in the future to match branch orientation more accurately to the digital model.

Several challenges arose during fabrication of the metal joints. In particular, the CNC water jet that was planned for fabrication suffered an unrelated technical problem and was unavailable for use. As a result, the team successfully implemented the low-tech joint fabrication option, using full-scale printed paper templates to cut joints manually with a metal bandsaw and jigsaw. The incorporation of triangular templates for accurate welding of angles was effective. The 14-gauge steel that was selected for the joints, while enabling a freestanding installation, resulted in some flexibility in the structure. Future versions would benefit from thicker steel and further stiffening of the metal joints by permanently integrating the triangular angle templates.

4. Discussion

This research contributes to a body of work that advances applications of irregular, non-standard materials in the production of architectural structures, in particular projects using the irregularities of raw material to impact the form of an assembly (MacDonald et al, 2019). Ideas around material agency and minimization of waste in digital fabrication processes resonate with Bandsawn Bands, a project in which the natural form of a tree flitch generated a three-dimensional topographic surface, while ideas about scanning and building with logs offer alternative approaches to the process developed for making use of tree forks in Tree Fork Truss (Johns and Foley, 2014; Devadass et al, 2016). Techniques aimed at minimizing part reduction build on the approach developed to make use of concrete debris in Cyclopean Cannibalism (Clifford and McGee, 2018). Branching Inventory contributes to this area of scholarship by proposing and demonstrating the transformation of such methods to readily available democratized technologies – no prohibitively expensive scanning or robotic fabrication equipment is necessary. The approach is globally transferrable, usable by anyone with a smartphone,

laptop, Rhinoceros/Grasshopper, and a few basic manual tools.

Figure 5. Variability of branches produces visual distortions in assembly.

The project also advances an ecological narrative through the use of material that is essentially landscape waste and would not otherwise be usable in architectural applications. Specifically, the use of material harvested from invasive species, whose existence is typically a nuisance, demonstrates the utilization of such material and incentivizes their removal and the subsequent remediation of native ecosystems.

The bradford pear was selected for the demonstration of this workflow due to its tendency of breaking at joints during storms and losing branches that are otherwise hardy lumber. The project methodology is established in such a way that in future work, other invasive or non-invasive tree species can be used by simply substituting these new materials as the scanned inputs. Since the formal qualities of the scanned material influences the final form of the structure, each species will yield a different geometry (Figure 5). The process mediates authorship in the realization of architectural form: it grants agency to the material and requires the designer to relinquish some degree of formal control. Technology is used to span the gap presented by eccentric material qualities that are typically avoided altogether, with a cohesive process of 3D scanning, digital inventorying and analysis, and form found optimization through a best fit system.

Finally, scaling the system from a pavilion-scale installation toward a more traditional architectural scale with building enclosure is conceivable. Projects using similar scanning strategies have demonstrated that building-scale structures are possible (Mollica and Self, 2016). In this case, the reliance on low-tech,

accessible technologies must be considered in scaling the work, possibly drawing upon the inherent knowledge within vernacular building traditions (Watson, 2020). Barriers to widespread use (codification, permitting, etc.) remain, but as recent developments in public policy enabling mass timber construction in the American northwest show, such changes are possible if technologies and material systems can be adequately demonstrated and tested at scale. Structural testing of input materials would be a first step in developing a precise understanding of the material's capacities, such that digital simulations could prove the performance of structural assemblies. This work intends to question the role of standardized materials in architectural production, presenting an accessible workflow to bring irregular natural materials into contemporary building.

Acknowledgements

The installation presented was developed by Kevin Saslawsky and Tyler Sanford for the 'Material Misbehavior' studio taught by Katie MacDonald and Kyle Schumann at the University of Tennessee. The authors would like to thank Jason Young, Director of the School of Architecture, for supporting the project with materials funding.

References

Von Buelow, P., Torghabehi, O.O., Mankouche, S. and Vliet, K.: 2018, Combining parametric form generation and design exploration to produce a wooden reticulated shell using natural tree crotches, *Proceedings of the International Association for Shell and Spatial Structures (IASS) Symposium 2018: Creativity in Structural Design*, Cambridge.

Carpo, M.: 2017, *The Second Digital Turn: Design Beyond Intelligence*, MIT Press, Cambridge.

Clifford, B. and McGee, W.: 2018, Cyclopean Cannibalism: A Method for Recycling Rubble, *ACADIA 18: On Imprecision and Infidelity, Proceedings of the 38th Annual Conference of the Association for Computer Aided Design in Architecture*, Mexico City, 404-413.

Devadass, P., Dailami, F., Mollica, Z. and Self, M.: 2016, Robotic Fabrication of Non-Standard Material, *ACADIA 2016: Posthuman Frontiers: Data, Designers, and Cognitive Machines; Proceedings of the 36th Annual Conference of the Association for Computer Aided Design in Architecture*, Ann Arbor, 206-213.

Johns, R.L. and Foley, N.: 2014, Bandsawn Bands: Feature-Based Design and Fabrication of Nested Freeform Surfaces in Wood, *Robotic Fabrication in Architecture, Art and Design*, Ann Arbor, 17-32.

Larsen, N.M. and Aagaard, A.K.: 2019, Exploring Natural Wood: A workflow for using non-uniform sawlogs in digital design and fabrication, *ACADIA 19: Ubiquity and Autonomy, Proceedings of the 39th Annual Conference of the Association for Computer Aided Design in Architecture*, Austin, 500-509.

MacDonald, K., Schumann, K. and Hauptman, J.: 2019, Digital Fabrication of Standardless Materials, *ACADIA 2019: Ubiquity and Autonomy, Proceedings of the 39th Annual Conference of the Association for Computer Aided Design in Architecture*, Austin, 266-275.

Mollica, Z. and Self, M.: 2016, Tree Fork Truss: Geometric Strategies for Exploiting Inherent Material Form, *Advances in Architectural Geometry 2016*, Zurich, 138-153.

Self, M. and Vercruysse, E.: 2017, Infinite Variations, Radical Strategies, *Fabricate: Rethinking Design and Construction*, Stuttgart, 30-35.

Watson, J.: 2020, *Lo-TEK: Design by Radical Indigenism*, Taschen, Cologne.

THE ACOUSTIC PAVILION

Prototyping Alternatives for Gypsum based Construction

RACHEL DICKEY
[1]*University of North Carolina Charlotte*
[1]*rdickey4@uncc.edu*

Abstract. Gypsum is one of the most commonly used building materials today and prevalent in architectural acoustics. However, despite its ubiquitous appropriation, few domains of research or practice seek to provide opportunistic approaches for its acoustical application. This paper outlines the computational design and fabrication processes for the development of a pavilion that explores alternative acoustic applications for gypsum. It demonstrates how sound performance can drive the conceptual agenda for a project by articulating the conditions of spatial experience through the design of architectural surface.

Keywords. Fabrication; computational design; acoustics; reflective surfaces; diffusive surfaces.

1. Introduction: Gypsum and Acoustics

Everyday architectural applications for sound quality often rely on quick material additions rather than acoustically designed solutions. Added layers of sound attenuated batt insulation help reduce sound leakage and additional layers of gypsum wallboard aid in mitigating transfer (Healey, 2014). Even the gypsum-based popcorn ceiling, which emerged in the 1930s, acts as a sound absorbing buffer by muffling noise with its increased surface area produced from the spray-on process. Gypsum is one of the most commonly used building materials today and prevalent in architectural acoustics. However, despite its ubiquitous appropriation few domains of research seek to provide opportunistic design approaches for its acoustical application.

Recognizing that designs are often constrained by preconceived ideas of building materials and their traditional applications, this research began by asking, how might methods for gypsum-based fabrication inform the design of sound based environments? This project avoids a purely building science or physics understanding of acoustics in favor of investigating sound qualities and their relationship to the perception of space. Surfaces, their materiality, density, and form, all affect the way sound propagates space. Considering these effects, the Acoustic Pavilion explores how sound performance can drive the conceptual agenda for a project by articulating the conditions of spatial experience through the design of acoustically informed surfaces, as seen in Figure 1.

PROJECTIONS, Proceedings of the 26th International Conference of the Association for Computer-Aided Architectural Design Research in Asia (CAADRIA) 2021, Volume 1, 523-532.

Figure 1. Pavilion exploring alternative acoustical applications for gypsum.

2. Spatial Audio

The relationship between space and acoustics has a long history, with the vaulted ceilings of Gothic cathedrals and the domed interiors of the Baroque (Libera and Klein, 2012), designers have directed sound in buildings as means for expanding upon the auditory conditions of human experience. After the completion of the construction of the Salzburg cathedral in 1628, musicians playing wind instruments, percussionists, string orchestras, and a choir, strategically positioned themselves in and around the nave of the cathedral in order to enhance the audience's auditory experience (Klein, 2012). Later in 1881, Clement Ader experimented with spatial audio by setting up microphones in the front of the Paris Opera Hall, with their audio outputs running to a series of headphones in a room nearby (Davis, 2007). Ader's experiment demonstrated the ability to construct various audio configurations based on the listener's location in space.

Today, spatial audio technologies provide a similar multidimensional approach to sound. With the electroacoustical control of sound to various positions, headphones distribute digital soundtracks to left and right ears and surround sound systems disperse sound in a room by playing multichannel digital tracks to a set of speakers. The pavilion project outlined in this paper explores digital and material conditions of spatial audio with integrated speakers and surfaces directing and diffusing sound.

The project presents a design opportunity to articulate the unseen boundaries of space through subtle acoustical variations in the environment. It does so through collaborative efforts with a sound designer (name omitted for blind peer review) in order to compose various corresponding tracks played from different channeled speakers embedded in key geometrically altering sound panels, to generate a unique auditory experience based on the guests' proximity in and around the pavilion, as seen in Figures 2 and 3. The intent is not only to explore physical acoustical parameters, but also to develop material and fabrication strategies that expand the perception of auditory performance.

Figure 2. Speaker integrated in Acoustic Pavilion.

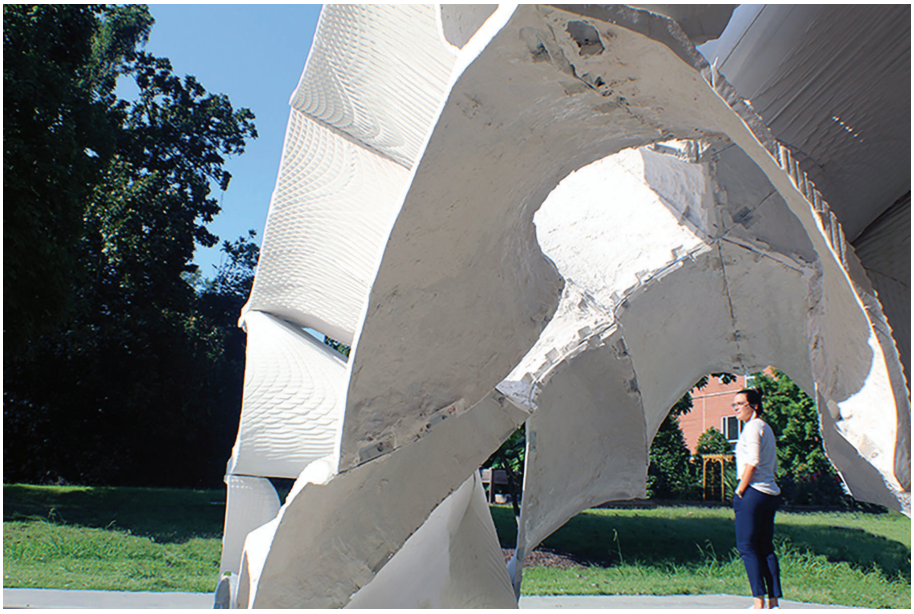

Figure 3. Pavilion visitor walking in and around pavilion discovering various acoustic conditions.

3. Diffusive Surfaces and Reflective Forms

Often the discussion of controlling sound in buildings refers to sound reduction (Cowan, 2007). However, in the case of the pavilion, the intent is to preserve and direct elements of sound from the speakers through reflection, while also reducing exterior noise through diffusion. These components provide a design opportunity to use acoustical tendencies as a means to articulate space through change in sound volume and quality.

The two acoustical tools that manipulate the conditions of spatial audio in the pavilion design include surface diffusion and form based reflection. Surface based diffusion aids in controlling harsh sound reflections, through variation in geometry, size and depth of surface patterns that correspond to sound waves (Ajlouni, 2017). The production of a series of ray tracing simulations, which describe the way sound scatters after contacting diffusive surfaces, aid in the design of the diffusing surface texture, as seen in Figure 4. The simulations characterize sound behavior with scattering coefficient measurements, which measure the amount of sound scattered away by comparing the ratio between non-mirrored and mirrored acoustic energy. In other words, a set of vectors projected toward the designed surface hit the surface and then the simulation provides a comparison between the vectors that directly bounce back as a mirrored condition with those that scatter based on the surface geometry.

These ray-tracing simulations aid in the design process and provide a way for the team to examine the reflection patterns from a variety of different surface

conditions. These models help to produce an approximation of the scattering coefficient, which is well adapted for use in geometric room prediction methods (Cox, 2006). While the tests provided a basic understanding of the performance, a true scattering coefficient varies based on frequency and understanding of the wave nature of the sound (Cox, D'Antonio, and Embrechts, 2006), which is not accounted for in the design team's simulations. Instead, the predictions provide an approximation of the performance of the surface by comparing the behavior of rays that reflect secularly and diffusely. Also, the predictions show the smaller texture size with increased depth increases the degree of scattering. In order to accommodate a spectrum of sound wavelengths, the surface includes a range of scale in surface texture, depths, and angles to provide a range of diffusive qualities. Variation of these characteristics is optimal for diffusing a range of frequencies (Ajlouni, 2017). The parameters mapped in the model allow for flexibly based on size, depth and angle to accommodate a variety of surface inputs for testing. The method also provides a way to address specific design problems by adjusting input surface conditions to match acoustical preferences.

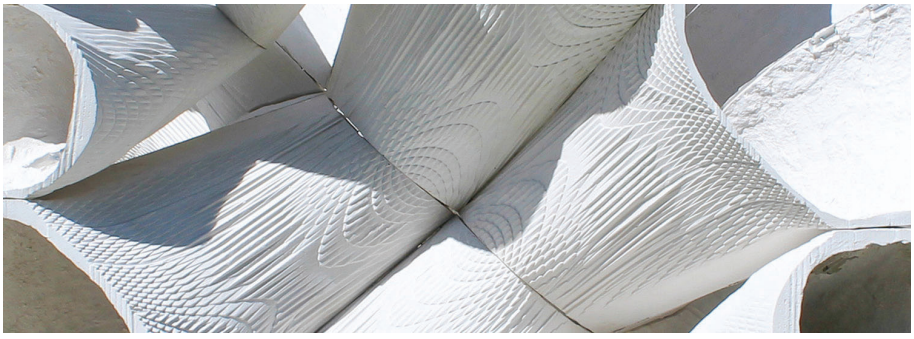

Figure 4. Diffusive sound surface texture.

The second acoustical component of study for the pavilion involves preservation and intensification of sound through form based reflection. Similar sound intensification projects include Anish Kapoor's Untitled, a stainless steel installation at the High Museum, Marirena Kladeftira's Whisper Dishes, and Zackery Belanger's Slumped Glass. The key to the pavilion's use of reflection is to avoid echoes and resonance, while also directing sound with curved surfaces. Specifically the project uses concave surfaces to focus sound energy from the speakers, while the convex sides of the panels with the surface texture diffuse sound from outside sources. The concave reflective surfaces create heightened auditory spaces with concentrated sound and lighter auditory spaces with less sound (Belanger, McGee, and Newell, 2008).

The configuration of individual panels into a larger system provides a means for aggregating the various sound conditions. Importantly, the design team avoided prototyping by adding the diffusing and directive panels to a typical wall or ceiling in order to generate auditory-based spaces delineated by a continuous surface. The panels vary in degrees of curvature and configuration in order to provide a range of

results. The scale of the body informs the scale and aggregation logic of the panels. As seen in Figure 5, the location of directive panels varies based on human height for increased emphasis and at time face downward to cause additional directional emphasis toward the visitor. The central interior space provides the most even distribution of all the sound channels from the speakers, while the exterior focuses and reflects various tracks. The panels collectively send sound to spaces in and around the pavilion by enhancing sound through reflections, encouraging the visitor to experience, the composition in different ways based on their location. The shifting position of the visitor exposes the formalized acoustical environment with the different in qualities of the space and variations in sound composition.

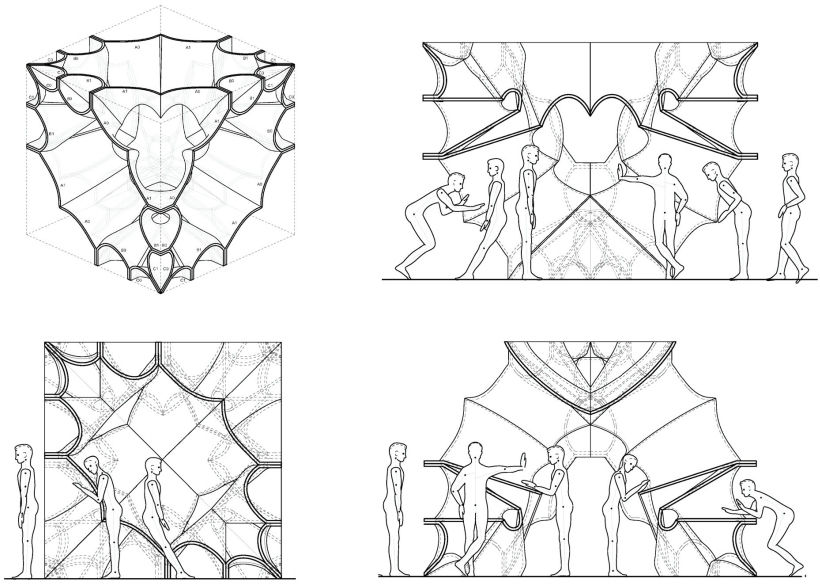

Figure 5. Scale drawings depicting scalar relationship of the configuration of panel to the body.

.

4. Design and Fabrication Methods

The project strives to strike a balance between material, form, fabrication, and acoustical performance. It does so by allowing material and fabrication procedures to inform and influence the design decisions along the way. The fabrication procedures for each panel involve the production of a CNC milled foam positives used to produce negative molds with a two-part silicon and fiberglass support shell. The silicon aids in capturing texture on the panel and allows for easy demolding, while the fiberglass shell supports the silicon and maps the overall panel form. A set of plywood ribs matching the sectional geometry of the panel support the fiberglass shells to avoid flexibility and ensure the molds maintain their form during the casting process. These rib supports negate deflection of mold during

the casting process.

The diffusive surface design also takes into account the machine procedures of subtractive processes. It does so by optimizing the amount of time spent carving the foam positive, by accounting for the incremental carving procedure and using it as an expressive quality of the surface, which also acts as the sound diffusive surface texture of the resulting cast, as seen in Figure 6. Since the subtractive methods and step down texture directly relate to the form of the surface, the design team 3D modeled the incremental machine carved texture in order to compare optimized machine time with diffusive sound performance of the texture. The model parametrically adjusts to included variable depth of the texture to correspond to the cutting part of the milling bit and its plunge depth (i.e., how far the bit goes down into the material during the subtractive process). The other condition of the surface texture includes the scale, which directly relates to the curvature of the surface. (i.e., the tighter the curvature on the surface the smaller the texture). This direct relationship between surface geometry and texture also accommodates the relationship to the incremental carving process. The resulting step down surface design provides a balance between acoustical performance and optimization of fabrication processes to decrease overall machine time.

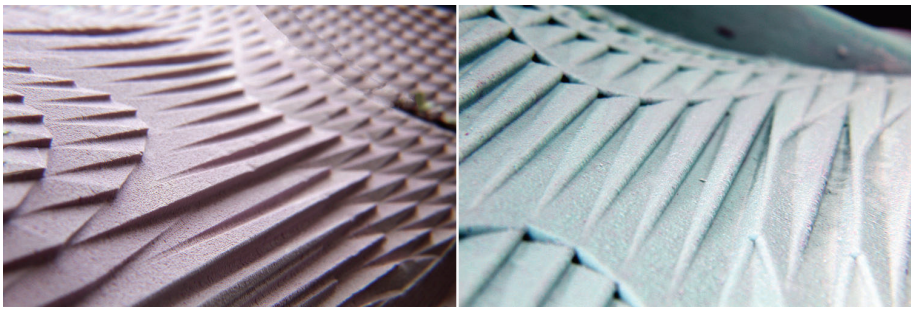

Figure 6. Image of positive foam texture (left) and silicon mold texture (right) based on step down procedures of the CNC mill.

The production of the pavilion integrates material and fabrication processes in the design evaluation by considering the optimization of machine time during subtractive processes and with the redundant use of molds. The fabrication procedures for redundant use of the molds, which are capable of producing three hundred casts, influence the design of the aggregation of panels by using a design assembly that involves aggregating similar panels in three-dimensional space with variable relationships between them, as illustrated in Figure 7.

This technique of aggregation differs from traditional parametric design approaches, which boast of variation from unique parts through mass customization. For instance, the production of the glass fiber reinforced concrete panels for the Heydar Aliyev Centre by Zaha Hadid uses a similar mold process; however, each mold was unique and therefore the fabricators only used the mold for a single cast before discarding. The approach for the pavilion achieves variation from repetition, which is similar to methods of combinatorial design.

Combinatorial methods study “discrete finite sets of units and their possible arrangement by an algorithmic or intuitive process” (Sanchez, 2016, p. 52). Combinatory design not only offers a means for exploring configurations, but also provides a fabrication strategy capable of producing multiple parts from a single mold. Such methods permit a similar approach to architecture as those used for advanced manufacturing strategies of automobiles, where complex geometry is efficient due to the quantity of parts produced from a single mold.

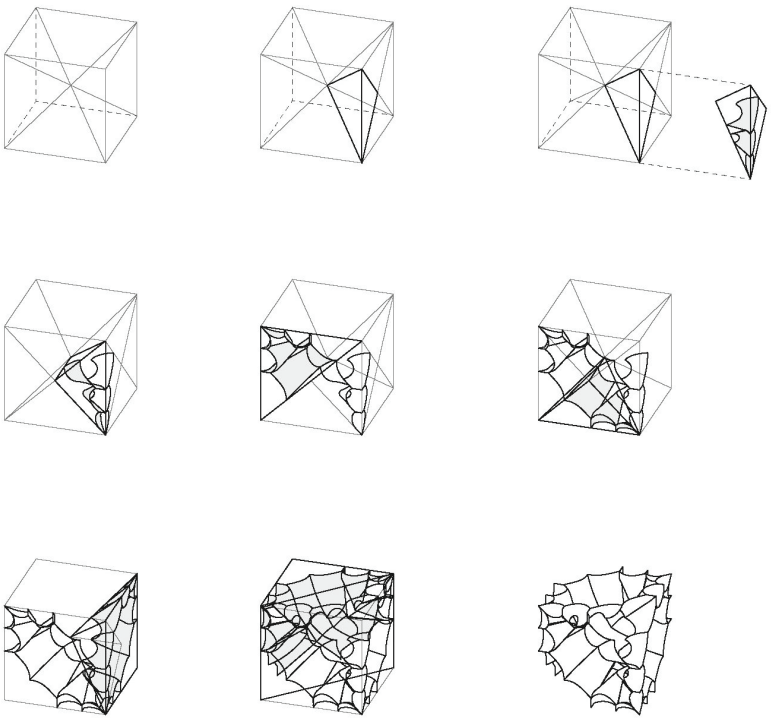

Figure 7. Diagram illustrating the design process for redundant panels that share variable relationships in three-dimensional space.

5. Conclusion

In order to render acoustical conditions as an architectural material, the investigation purposely generates a variety of inhabitable sound configurations for guests to perceive. The site and exhibition of the pavilion took place at (omitted for blind peer review) as demonstration of combined research and design activity between architecture and acoustics. The exhibition also involved two sound based performances. The first of which included the embedded speakers where the panels geometrically intensifies portions of sound tracks corresponding to different locations of the pavilion to generate a unique auditory experience related to space.

The second performance involved two members of (omitted for blind peer review), playing trumpet and trombone from within it the pavilion, strategically shifting their bodies and instruments to tune portions of their musical performance. Many of the pavilion visitors sensed the variations of the acoustical environment and called attention to the difference in sound qualities.

With industrialization, mass production of building materials, and stylistic concerns of the simple and sparse brought on by modernism, today there is a proliferation of large flat interior surfaces covering building frames and structures. Acoustician Trevor J. Cox writes, "There is a need for scattering surfaces that complement contemporary architecture in the way statuary coffered ceilings and relief ornamentation complemented classical architecture" (Cox and Peter D'Antonio, 2004, p.105-106). The uninterrupted oblique surfaces resulting from the abundance of banal architectural boxes that surround us are the source of the strong specular sound reflections and do little to diffuse unwanted noise in our everyday environments. A true consideration of sound performance in buildings, requires alternative fabrication and material approaches to contemporary architecture. Rather than layering on excess material or decorating the interior of our box buildings, perhaps we can design solutions that draw upon both the art and science of acoustics manifested from human perception of sound.

Acknowledgements

The Acoustic Pavilion was produced in collaboration with Alex Cabral, Drake Cecil, Hana Maleki, Margaret Martin, Jarrod Norris, Robby Sachs, and Hunter Sigmon.

References

Ajlouni, R.: 2017, Simulation of Sound Diffusion Patterns of Fractal-Based Surface Profiles, *Disciplines and Disruption: Proceedings of the 37th Annual Conference of the Association for Computer Aided Design in Architecture*, Cambridge, 52-61.

Belanger, Z., McGee, W. and Newell, C.: 2018, Slumped Glass: Auxetics and Acoustics, *Recalibration on Imprecision and Infidelity: Proceedings of the 38th Annual Conference of the Association for Computer Aided Design in Architecture*, Mexico City, 244-249.

Bradely, D., Snow, E.O., Riegel, K.A. and Nasipak, Z.D.: 2014, Numerical Prediction of Sound Scattering From Surfaces with Fractal Geometry: A Preliminary Investigation, *Proceedings of Meetings on Acoustics 12 (Acoustical Society of America)*, Seattle, 2-9.

Cowan, J. 2007, Building Acoustics, *in* T. Rossing (ed.), *Springer Handbook of Acoustics*, Springer, New York, 387-425.

Cox, T.J. and D'Antonio, P.: 2004, *Acoustic Absorbers and Diffusers: Theory, Design and Application*, Taylor & Francis, New York.

Cox, T.J., D'Antonio, P. and Embrechts, J.J.: 2006, A Tutorial on Scattering and Diffusion Coefficients for Room Acoustic Surfaces, *Acta Acustica united with Acustica*, **92**, 1-15.

Davis, M. 2007, Audio and Electroacoustics, *in* T. Rossing (ed.), *Springer Handbook of Acoustics*, Springer, New York, 746.

Healey, R.: 2014, Investigations into the Sound Absorbing Properties of Gypsum Wall Board, *Journal of the Acoustical Society of America*, **135**, 2204.

Leitner, B. 2012, Sound as Building Material: Bernhard Leitner in conversation with Eugen Blume, *in* M. Michał Libera and L. Klein (eds.), *Making the Walls Quake As If They Were*

Dilating with the Secret Knowledge of Great Powers, Zachęta National Gallery of Art, Warsaw, 64-74.

Wai Ma, K., Ming Mak, C. and Wong, H.M.: 2020, Development of A Subjective Scale for Sound Quality Assessments in Building Acoustics, *Journal of Building Engineering*, **29**, 101.

Sanchez, J.: 2016, Combinatorial Design, *Posthuman Frontiers: Data, Designers, and Cognitive Machines, Proceedings of the 37th Annual Conference of the Association for Computer Aided Design in Architecture*, Ann Harbor, 44-52.

A MULTI-SCALE WORKFLOW FOR DESIGNING WITH NEW MATERIALS IN ARCHITECTURE: CASE STUDIES ACROSS MATERIALS AND SCALES

Case studies across materials and scales

FARZANEH OGHAZIAN[1] and ELENA VAZQUEZ[2]
[1,2]*The Pennsylvania State University*
[1,2]*{fxo45|emv10}@psu.edu*

Abstract. In this paper, we present a workflow developed for designing with and scaling-up new materials in architecture through an iterative cycle of materialization and testing. The framework establishes a connection between design requirements and form, taking advantage of different scales in new materials known as micro, meso, and macroscale in the process of design/manufacture. Different scales when dealing with material systems-especially in those that possess some level of uncertainty in their behavior from the formation process-make it challenging to deal with the different material variables controlled at each scale. This paper presents a brief review of existing design workflows centered on material properties. We then discuss case studies and argue for a multi-scale approach for design. Finally, we present the workflow. By implementing the workflow on two case studies, we answer how we can include material scales and their embedded properties as the central part of the design/manufacture process to aid in implementing new materials in architecture. The case studies are a responsive skin system and a free-standing tensile structure incorporating 3D printed wood filament and knitted yarn as the primary material.

Keywords. Material computation; material-based design; wood 3D printing; knitting; multi-scale workflow.

1. Introduction

With the development of new materials in textile design, material science, and related disciplines, architects have become increasingly interested in a material-centered research approach for incorporating new materials at an architectural scale. Researchers argue that the advent of digital design and fabrication has enabled the integration of structure, material properties, and form in novel computationally enhanced processes (Vazquez and Duarte, 2019). Nevertheless, incorporating new architectural design materials and scaling them up to the building scale is not without its challenges.

PROJECTIONS, Proceedings of the 26th International Conference of the Association for Computer-Aided Architectural Design Research in Asia (CAADRIA) 2021, Volume 1, 533-542.

One of the challenges is transferring material knowledge from other fields into architectural design. The challenge comes from the fact that different material scales exist: micro-, meso, and macroscale that have corresponding material behavior. The translation becomes even more challenging when designing with materials that possess some level of uncertainty in their behavior derived from material formation processes. Furthermore, the area of expertise of these different disciplines also varies in scale. While material scientists are usually concerned with the configuration of materials at a microscopic scale, architects are used to dealing with measurements from millimeters and up. This paper forms part of a broader research agenda concerned with leveraging material knowledge from other fields and successfully translating them into architectural design. From the micro-scale of material making to the macroscale of architectural elements, there must be a coherent material logic to take advantage of new materials' embedded material properties. This paper formulates a multi-scale workflow for designing and scaling-up new architectural design materials through an iterative making cycle of materialization and testing, considering the making process an informative asset of designing with new materials. The workflow is derived from a review of the theoretical approaches of material-centered design in the literature and the critical examination of existing research in textiles and additive manufacturing that identifies strategies and multi-scale approaches.

The first section of the paper describes the theoretical design models that argue for a material-centered approach that favors the emergence of forms from the material properties. We then identify design and manufacturing strategies in the literature on textiles and additive manufacturing, where we argue for the need of a multi-scale approach. In the following section, we present a workflow for incorporating and scaling up new architectural design materials. Finally, we examine two case studies incorporating the previous section's workflow. The first case study is developing a responsive skin system by 3d printing a wood-based composite material. The second case study aims to create a free-standing tensile structure using a knitting technique and fibers. In the case studies, the starting points are a filament for 3d printing and a yarn. By comparing the iterative development cycles of both case studies, this paper describes a workflow in which the material's characteristics across the scales are used to articulate fabrication, design, and functional material properties.

2. Background Studies

2.1. MATERIAL-CENTERED DESIGN

This section reviews theoretical approaches of material-centered design to set the foundation for a workflow centered around material properties across scales. (Oxman, 2010) introduces a theoretical approach called Material-based Design Computation, where the form results from material properties and their structuring according to performance requirement. The design methodology that emerges from this theoretical foundation is called the Variable Property Design environment (VPD). This methodology is associated with the modeling, simulation, and fabrication of the materials corresponding to the variable

functional constraints. The model presented by the author is abstract enough that researchers can apply it to design with materials at different scales and with other requirements. The author presents a generalizable approach where the form results from several interrelated material variables.

Similarly, (Ahlquist et al., 2013) introduce a framework for design and computational thinking for complex material systems. Their framework, shown in Figure 1, illustrates how computational rules and material logics are generated through the physical prototyping and discrete experimentation of practical methods and simulations. In the framework, one can identify two levels that appear to refer to different scales, the left-hand side that contemplates discrete experiments at a smaller scale and the right-hand side that prototypes at a larger scale. On the left-hand side, the framework considers that combining experimental methods such as manufacturing and simulation studies allows researchers to understand material behavior. At the right-hand side, the framework describes prototyping at a larger scale by developing spatial material systems. The authors consider the approach to be iterative, where material systems are developed in increasing complexity levels, as new material parameters and rules are established.

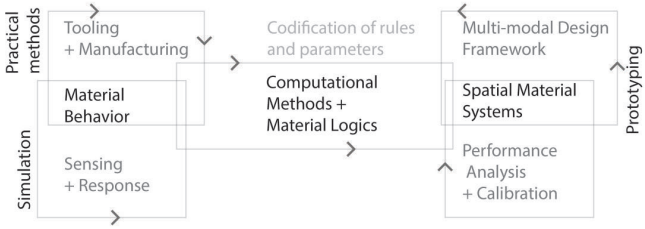

Figure 1. A material-based framework. Redrawn from (Ahlquist et al., 2013).

2.2. DESIGN FOR MANUFACTURING

Additionally, several design methodologies developed for additive manufacturing (AM) could inform design approaches for new materials in architectural design. Design for additive manufacturing is a well-consolidated field of research that seeks to take advantage of this novel manufacturing system. In this context, the structures are designed considering the possibilities and constraints of additive manufacturing methods, informed by the process and material properties. An example of an AM design methodology is proposed by (Yang and Zhao, 2015), summarized in Figure 2. The authors present a design workflow that considers the correlation between functional requirements, manufacturing constraints, and physical attributes, incorporating process knowledge and structural optimization into the design for better performance and functionality. One drawback of the proposed model is that it does not consider the design feedback loops at different design stages. Nevertheless, the workflow presents insights into designing a new manufacturing process, designing for this novel material process. A similar approach could be implemented when designing a novel material, where some comparable steps and constraints can shape the process.

Thus far, we have discussed three theoretical approaches that provide insights on a methodology for designing with new materials in architecture. Oxman (2010) sets the basis for a material-based design, where material properties and functional requirements are a priori of any shape or form. Ahlquist et al., (2013) present a methodology for a complex material system, identifying two scales of action and an iterative process. Finally, we discussed how design methodologies for a novel manufacturing process such as AM provide design requirements to take advantage of the material process's opportunities. One aspect of designing with novel materials that we want to address in this research is the existence of different scales that designers and researchers must consider to take full advantage of the new material.

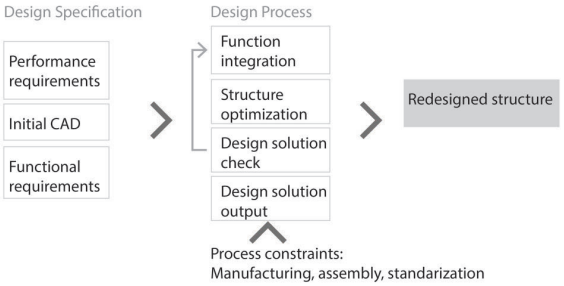

Figure 2. A design-based AM methodology- Redrawn from (Yang and Zhao, 2015).

2.3. CASE STUDIES: IDENTIFYING STRATEGIES AND MULTI-SCALE APPROACHES

In this section, we explore some strategies applied for integrating new materials at different scales related to AM and knitted material in the industrial, textile, and architectural fields. By analyzing the existing research on these two materials, we intend to extract common strategies for introducing new materials at an architectural scale.

Knitted textile material has been a dominant material in the garment industry for many years; however, knitted textile and the knitting technique are new material and processes in architecture. One of the advantages of knitted materials is that the knit's unique structure allows integrating other new materials into their structure and offers many architectural application opportunities. Additive manufacturing processes have also started to permeate architectural practice in recent years; the process allows for the generation of unique complex shapes and the introduction of new materials to architecture. Architects can utilize novel materials in building construction with the various AM technologies such as thermal processes and material extrusion.

There are three interconnected scales associated with AM materials and knitted textiles, namely micro, meso, and macroscale. In most studies, explorations on the material's behavior and characteristics are restricted to the mesoscale due to the manufacturing, simulation capabilities, and cost limitations. Manufacturing

limitations refer to the size and volume restrictions that the machines themselves have. At the same time, computational capabilities limit the accuracy of digital studies that can simulate material behavior.

In terms of scale, while textile designers mostly focus on the micro-and mesoscale properties of the knitted material, architects are typically concerned with applying the material at a macroscale. At the micro-and mesoscale, researchers usually investigate material properties from a small patch of the material. For example, the correlation between textile opacity and shape change of the material under the specific load is studied for a small textile piece by (McKnelly, 2015). In their study, a simplified mesh-based method is also introduced for the digital simulation of knitted textile material's overall shape. Similarly, (Çapunaman et al., 2017) illustrate scaled-up material properties at the mesoscale for a given general form using the crocheting method. The study explores the effect of a single material variation in the overall geometric result, touching upon the micro-scale (yarn thickness) and mesoscale (patch size). Along those lines, (Baranovskaya et al., 2016) explored the correlation between the material's local and global characteristics. The authors developed rules for top-down and bottom-up approaches to design pattern configurations. The study illustrates how researchers can utilize rules at different scales to transition from one scale to another.

Literature shows that two strategies have been implemented so far to study knitted textiles. The first is prototyping at the mesoscale by architect designers to learn about the behavior of the material. This approach also entails modeling the textile's exact shape and structure comprising the loops, their intersection, twist, and mechanical characteristics of the yarn and textile itself by textile designers to investigate the textile's structural performance. The second strategy is to incorporate digital simulations and substitute stitches with simple mesh geometries to implement the material in large-scale and complex architectural forms.

Similar issues of scale arise when designing AM processes for an architectural scale. For instance, (Hojati et al., 2018) discuss challenges in designing toolpath for concrete printing, considering the mixes' rheological aspects. Explorations at the toolpath level, which can be regarded as the meso or even micro-scale, are typical among concrete printing research. (Ashrafi et al., 2020) develop an experimental study at this scale to predict the deformation of material at different layers in concrete printing. The careful analysis and design of toolpaths for additive processes are at the core of current research in the area, which indicates the multitude of scales in introducing printed materials at the building scale.

Another research approach into additive manufacturing for architectural purposes consists of producing prototypes at the mesoscale, in a feedback loop that improves the manufacturing systems‘ accuracy. For instance, (Craveiro et al., 2020) present a method for printing functionally graded material and demonstrate their system by printing functionally graded parts. The research also delved into a different scale. While imaging analysis software analyzed cork particles' presence in the prototypes at the micro-scale, 3d scanners captured the printed geometries at the mesoscale to compare them with CAD models. Researchers have also recognized that different problems occur at different scales. Small-scale

prototypes can provide insights for mesoscale toolpath design considerations, but full-scale constructions present their unique challenges (Ahmed et al., 2016).

The studies discussed in this section highlight the need to develop a framework that considers the different scales involved when introducing new materials to architectural design. New materials processes such as knitting and additive manufacturing entail thinking not only on the overall shape-but also on the mesoscale of the patterns or toolpaths and the micro-scale of the material. Knitted materials and AM processes are similar because the knitting pattern or the toolpath configuration determines the micro and meso scales. Also, the geometries at different scales that have their unique representation strategies: At the macroscale, geometries can be simplified into meshes, at a meso and micro-scale, lines and paths represent the manufacturing coordinates.

3. Proposed Workflow

This section proposes a design workflow that builds upon the available frameworks in material-based design systems while adopting a multi-scale approach. We emphasize the role of material properties at three micro, meso, and macro scales as the core part of the design-manufacturing process when dealing with new materials and their implementation in architecture. Therefore, the proposed framework establishes a connection between requirements (material performance, function, aesthetics, etc.), form, and scale. However, the non-linearity between architectural requirements and structural performance and the uncertainty of material behavior at different scales makes the implementation of the new materials more challenging. This is why the proposed framework reflects the non-linearity through feedback loops in the process.

The workflow comprises two main directional processes, design and manufacturing. In the design direction, the main concern is about applying the material at the macroscale for an overall shape and architectural scale. Designers are typically concerned with the application aspect of new materials; consequently, these applications require thinking about form and function at the architectural scale. Therefore, the direction of the design process is shown from the macro to the micro-scale. In the manufacturing direction, the focus is on the smallest units of the material, determining the material's properties at the other scales. This is why the manufacturing direction is shown from the micro-scale to the macroscale. The three scales of material characteristics known as micro, meso, and macroscale are interconnected and embedded elements at the center of the workflow. Digital simulation and physical modeling are also considered as strategies in the workflow. While these can be applied at different scales, physical modeling is a strategy that can inform initial explorations at the micro and mesoscale and increment in size with the iterative loops. Additionally, digital modeling and simulation can inform initial studies at the macroscale to speculate on different applications' full-scale appearance with the new materials. The correlation between the main elements of the proposed workflow is presented in Figure 3.

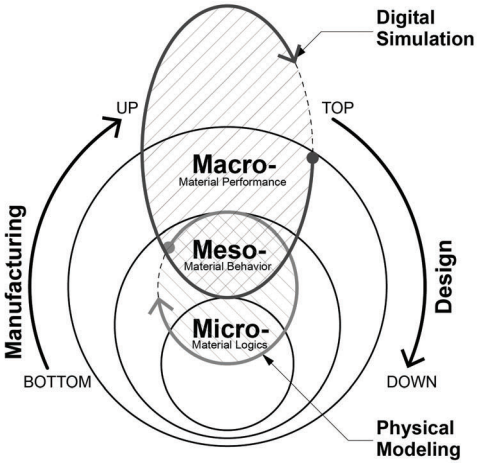

Figure 3. Proposed multi-scale workflow for design and manufacture with new materials in architecture.

The starting point for researchers can be at any of the three scales. One option starts from the mesoscale, which is placed between design and manufacturing. At this scale, one can identify material rules getting informed from other scales. Here a top-down approach will entail thinking about the full-scale form. At the same time, a bottom-up study will explore the material logic and material behavior at the micro and mesoscale and build up from there. At this step, the making process is a principal tool of discovering and characterizing material properties. The emergent shapes, forms, and material behaviors through the making process help categorize the rules that satisfy the macroscale requirements.

4. Case Studies

This section shows how we implemented the multi-scale approach in two case studies. The two case studies are a responsive skin system and a free-standing tensile structure that incorporate 3D printed wood filament and knitted yarn as the main material. Table 1 shows the details related to the 3D printed wood filament and knitted textile characteristics and structure. It also shows material/design/manufacture variables related to the material properties and material formation that can be controlled at different scales. For a more detailed discussion of the case studies themselves, readers can refer to previous studies on hydro-active skin systems (Vazquez et al., 2020)

As illustrated in Figure 4, by having the first imagination about the overall form, one can experiment with the mesoscale's material behavior (step one). Explorations at the mesoscale will be informed by performance analysis results and design requirements at the macroscale (step two). To satisfy the macroscale requirements, we change and manipulate the micro-scale's material variables to develop a new material configuration with specific characteristics at the mesoscale (step three).

Table 1. Variables of Material/Design/Manufacturing for case stidies.

	Microscale	Mesoscale	Macroscale
Characteristics			
Knitted Textile Structure (Outdoor Hypar Canopy)	- One loop/ Stitch	- Combination of loops for a piece of fabric/ pattern generation	- Combination of knitted pieces in a specific pattern to construct overall Hypar form
3D Printed Shading (Responsive skin system)	-Toolpath design for a single layer	-Combining layers of toolpath design within kirigami geometry	-Repeating unit in a specific pattern to construct a skin system
Variables			
Knitted Textile Structure	Materials: Yarn type (thickness, elasticity, strength) Design: Type of stitch Fabrication: Tension, speed	Design: Adjacency of stitch types (Patterns), looseness and stiffness, the distance between stitches	Materials: Connection between pieces (with joint or seamless) Design: Sequence of knitting, boundary shapes, and size
3D Printed Shading	Materials: filament type Design: bead distance, toolpath geometry Fabrication: printing settings (temperature, speed)	Design: Layer count, layer distance, geometry type.	Materials: connections and frame materials. Design: Number of units, gradients between units, connections, attachments, frames.

For example, in a free-standing tensile structure, we understand that we need to control the knitted textile's strength at the edges and around the support points against the strain from the form-found and structural analysis models. Additionally, displacement of the structure under the load requires to have a material that resists unusual displacements. Having this structural information from the overall form's critical analysis, we examine the material's behavior at the mesoscale for different pattern types and different knitting directions. There are multiple possibilities of developing patterns when choosing stitch types at the micro-scale and manipulating their adjacencies at the mesoscale. However, we systematically narrow our design space to the options aligned with the overall design and manufacturing requirements. In addition to the structural performance, other architectural requirements must be met as well. The process can be iterated multiple times to develop various patterns with determined characteristics that satisfy multiple requirements. The macroscale product could be a seamless knitted structure with different patterns, opacities, and direction of knitting at different structure sections.

In the responsive skin system, the mesoscale's starting point is to characterize the shape change of the hydro-active material to satisfy a daylight requirement at the macroscale. By conducting a series of experimental studies at the mesoscale, one can determine the effect certain variables have on the shape-changing behavior and study the use of different geometries to design the skins. These variables at the micro-scale, such as bead distance in the toolpath design, significantly affect the hydro-active response. Therefore, we can systematically study the effect these variables have in samples constructed at the mesoscale to select which of these variables can be optimized. Moreover, the experiments conducted at the mesoscale studied kirigami geometries' potentials in amplifying the shape morph

of the prototypes. Simultaneously, daylight analysis informed the mesoscale's explorations by providing performance information on how the shape change should be. Table 1 summarizes the material, design, and manufacturing variables for both case studies at the three scales.

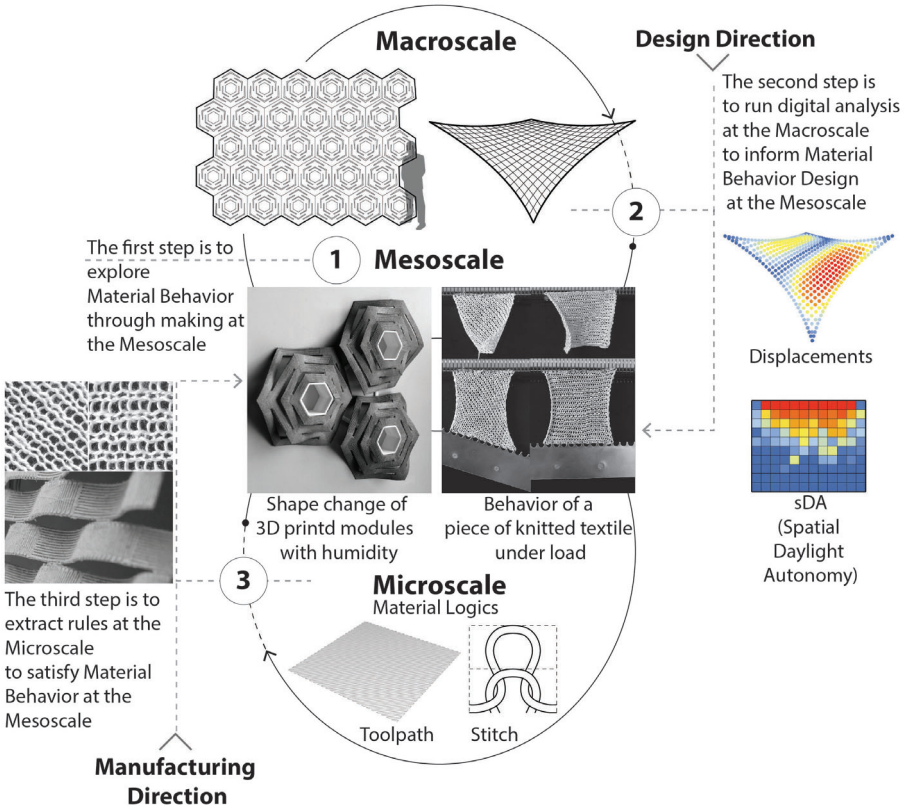

Figure 4. Case studies: 3D printed shading system and knitted Hypar tensile structure.

5. Conclusion

The application of new materials in architecture comprises the integrated design process with the new materials and design of material behavior itself. However, uncertainty in the behavior of new materials at different scales makes it difficult and unpredictable when we apply them in developing architectural forms. In this research, we introduced a multi-scale workflow to enhance the integration of new materials in architecture. The main elements of the proposed workflow are: design/manufacturing requirements, form, and scale. The three material scales are known as micro-, meso-, macro, which sit at the center of the workflow. We showed how we can systematically control and introduce new materials to the architectural scale through an iterative process of manipulating, making,

and simulating within two case studies. The process entails the manipulation and creation of new material logics at the micro-scale, the emergence of the new material behavior during the formation process at the mesoscale, and the translation of that behavior into a digital environment at the macroscale. The framework developed in this research is general enough to be incorporated at the first steps of design and manufacturing with other new materials that possess uncertainty in their behavior for developing architectural forms. However, it should be mentioned that there is no restriction in categorizing the three scales of new material as we did for knitted tensile structures and wood 3D printed responsive skin. Even in case studies introduced here, a mesoscale in one project can be macroscale in another project. The important point is to take advantage of the three scales in a way that helps designers control mesoscale behavior by manipulating microscale characteristics of the material for a macroscale performance.

References

Ahlquist, S., Newell, C., Thün, G. and Velikov, K.: 2013, Toward a Pedagogy of Material Systems Research, *TxA INTERACTIVE*.

Ahmed, Z.Y., Bos, F.P., Wolfs, R.J.M. and Salet, T.A.M.: 2016, Design considerations due to scale effects in 3D concrete printing, *8th International Conference of the Arab Society for Computer Aided Architectural Design (ASCAAD 2016)*, London, United Kingdom, 1-10.

Ashrafi, N., Nazarian, S., Meisel, N.A. and Duarte, J.P.: 2020, Experimental prediction of material deformation in large-scale additive manufacturing of concrete, *Additive Manufacturing. https://doi.org/10.1016/j.addma.2020.101656*.

Baranovskaya, Y., Prado, M., Dörstelmann, M. and Menges4, A.: 2016, Knitflatable Architecture- Pneumatically Activated Preprogrammed Knitted Textiles, *eCAADe 34 MATERIAL STUDIES | Concepts, 1*.

Capunaman, Ö B., Bingöl, C. K. and Gürsoy, B.: 2017, Computing Stitches and Crocheting Geometry, *CAAD Futures 2017 Communications in Computer and Information Science*.

Craveiro, F., Nazarian, S., Bartolo, P. J. and Duarte, J.P.: 2020, An automated system for 3D printing functionally graded concrete-based materials, *Additive Manufacturing*, **33.doi:10.1016/j.addma.2020.101146**.

Hojati, M., Nazarian, S., Duarte, J. P., Radlińska, A., Ashrafi, N., Craveiro, F. and Bilén., S.: 2018, 3D Printing of Concrete: A Continuous Exploration of Mix Design and Printing Process, *42nd IAHS World Congress on The housing for the dignity of mankind*, Naples, Italy.

Knight, T. and Stiny, G.: 2015, Making Grammars: From Computing With Shapes To Computing With Things, *Design Studies*, **41**, 8-28. doi:10.1016/j.destud.2015.08.006.

McKnelly, C. L.: 2015, *Knitting Behavior: A Material-Centric Design Process*, Master's Thesis, Massachusetts Institute Of Technology.

Oxman,, N.: 2010, *Material-based Design Computation*, Ph.D. Thesis, Massachusetts Institute of Technology.

Vazquez, E. and Duarte, J.: 2019, Computational tools for designing shape-changing architectures, *ARCC Conference*.

Vazquez, E., Gürsoy, B. and Duarte, J.P.: 2020, Formalizing shape-change: Three-dimensional printed shapes and hygroscopic material transformations, *International Journal of Architectural Computing*, **18**(1), 67-83.

Yang, S. and Zhao, Y.F.: 2015, Additive manufacturing-enabled design theory and methodology: a critical review, *The International Journal of Advanced Manufacturing Technology*, **80**, 327-342.

DISCRETE ELEMENT DESIGN FOR MYCELIUM COMPOSITE USE IN CIRCULAR ASSEMBLY SYSTEMS

Strategising Geometric Treatment of Biomass Composites for Viable Assembly and Construction Systems

CINDY WITONO[1], CHRISTINE YOGIAMAN[2] and KENNETH TRACY[3]
[1,2,3]*Singapore University of Technology and Design*
[1]*cindy_witono@mymail.sutd.edu.sg* [2,3]*{christine_yogiaman|kenneth_tracy}@sutd.edu.sg*

Abstract. This paper presents a construction strategy for topologically interlocking mycelium composites as replaceable structural modules that could be periodically replaced, extending the lifespan while varying the architecture. Concepts of discrete fabrication would drive the methodology. The research will be carried out in two scales; (a) at the scale of the 'part' such as foundation, column, beam, joint, and floor slab component, which would be studied to form a set of interlocking geometry that allow for easy installation and de-installation process; and (b) an investigation on aggregating 'whole', whereby elements are aggregated using Wasp to generate bays of walls, flooring and cantilever roof. The elements are to be aggregated to the point of redundancy, which would support replacement of components by providing standby structural system. This will integrate repair and recondition processes as part of the building life cycle.

Keywords. Mycelium Composite; Topological Interlocking; Redundancy; Digital Fabrication.

1. Introduction

With rising urgency to reduce construction and materials waste, the built industry has been working on achieving a circular, grounded in the pursuit of closed-loop manufacturing and design systems. Under this motivation, builders and designers are urged to employ Cradle-to-Cradle (M. Braungart & W. McDonough, 2002) concepts by extending the product's lifespan through reuse, repair, and reconditioning of its parts.

A more effective circular economy system occurs when the entire loop is localized and produced out of biocompatible materials. When the resources, manufacturing, and labor are localized, the system encourages the community and site to be self-sufficient, and the energy in transportation is conserved. Using biomaterials also ensures that the system is cleaned thoroughly compared to

PROJECTIONS, Proceedings of the 26th International Conference of the Association for Computer-Aided Architectural Design Research in Asia (CAADRIA) 2021, Volume 1, 543-552.

a circular production system comprised of synthetic materials. Biocomposite components could be constructed quickly in low energy, zero waste, fabrication process. A circular economy built out of agricultural resources could elevate the results and effectiveness of cradle-to-cradle design research.

With this motivation, the research would focus on using Mycelium as a biocompatible building resource. Mycelium composites have stood out as a type of organic material suitable for various building and structural uses. Existing projects (Figure 1) have shown mycelium composite capabilities as a substitute for synthetic building material. Such performance is made possible by optimizing its self-standing structural ability and strategically designing the parts' geometry. As mycelium composites are fibrous, the structural design tends to adopt compression-only formal strategies. By carefully manipulating forces' equilibrium through the geometry design, soft materials could perform structurally while also embodying aesthetic purpose.

Figure 1. (Left) Hy-Fi Tower by The Living + Ecovative Design and (Right).

Mycotree by KIT Karlsruhe + ETH Zürich + Singapore-ETH Centre are examples of built structure using load-bearing mycelium composites.

The logistic of repair and reconditioning in this economy could be made efficient by discretizing building elements. In Digital Manufacturing, Structures made of these discrete elements are reversible; they can be re-assembled and reconfigured into other types of structures. Using these elements enables the architecture to be treated in modular parts and at the human scale. Repair and reconditioning can be done without compromising the whole structure by isolating components to assemble. The formal exploration carried out in this research would be driven towards appropriating discrete elements for disassembly and reassembly processes.

2. Evaluating Material Characteristic and the Appropriate Design and Structural Methodology

Mycelium is the root structure of mushrooms, known as hyphae, which feeds on plant-based waste to flourish. It digests the nutritious waste and grows into a network of fibres that bind the mixture compact. Through processes such as inoculation and fermentation, mycelium composite could form a durable, leather-like material that is resistant to fire, water, and harsh climate (Jones, et al. 2018).

With these capabilities, mycelium has been widely studied and used in product design. As technology develops across the years, mycelium's application has expanded from small-scale use in packaging or product design to large scale architectural implementation.

As mycelium composite possesses a relatively softer and more fibrous composition than most building materials, it requires a different attitude towards its geometric strategy to ensure structural integrity and logistic efficiency. The performance of mycelium composite, as an organic material, could be optimized with an appropriate design strategy.

2.1. INTERLOCKING GEOMETRIC DESIGN METHODOLOGY

Literature reviews done as a precedent study to this research have shown that mycelium composite holds the density of 0.1-0.4 g/cm3 varying from non-pressed, cold-pressed to heat-pressed process. Such numerical characteristic sets the material comparable in density with softwoods and forms. Wood composite has a density of about 0.5-1 g/cm3, and foams usually come in a density of 0.05-0.3g/cm3. Similarly, the bending strength, stiffness, and brittleness of Mycelium could also be comparable to that of foams, the former ranging between 0.04- 0.24 MPa in tensile strength. (Appels, et al. 2019)

Building with organic material that is considerably delicate in tension and bending requires an emphasis on achieving equilibrium through contact forces and compression only. Appropriating the geometry is essential to guarantee good transfer of loads through surfaces.

An interlocking assembly principle is adapted to develop mycelium composite geometry with lock-key ends. This design principle will ensure replaceability while also possessing structural integrity. Interlocking assemblies are capable of remaining firmly in-tact and withstand destabilizing forces (Tessman, 2012). The discrete components are force-locked onto each other's contact surface and would be kinematically compressed in place. With this system, parts of the building can be disassembled by sliding it out of its surrounding locking geometry when a replacement is required.

2.2. REDUNDANT STRUCTURAL METHODOLOGY TO ENSURE CONSISTENT STABILITY

While structural stability could be achieved through geometric optimization, it should also be considered that mycelium composite's relative brittleness would require frequent replacement. In a discrete element system, assembly and disassembly could be done in isolated sections. Carrying these out would need the rest of the structure to remain intact while repair and replacements are being carried out. Hence, it is necessary to set up a structural composition that allows redistribution of load transfers when parts of the structure are assembled and disassembled, ensuring stability during parts replacement. This can be done by having the components cluster to the point of redundancy.

The concept of redundant part refers to the idea that if the said part is detached from the structure, it will not compromise the stability of the system. The existence

of the part within the structure does not directly impact the structural performance, hence rendering it 'redundant.' Such a point of redundancy can only be attained after achieving a certain amount of optimal density, thickness, or contact force within the structure.

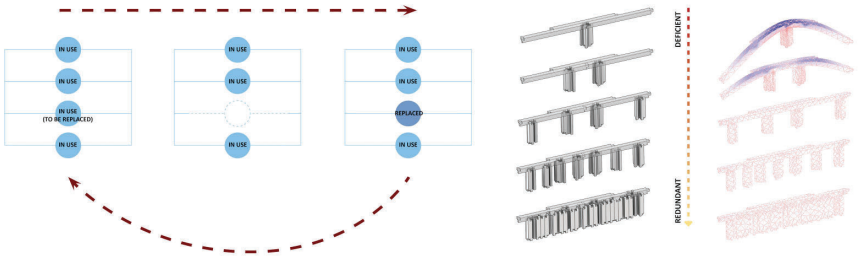

Figure 2. (Left) A system diagram that mimics a parallel circuit system, whereby the displacement of one part would not disconnect the flow of electricity flowing through the circuit and would merely make the other components perform at a higher voltage. (Right) Redundancy in structure can be represented in quantity or density.

3. Design Strategy for Disassembly and Replaceability

The ensuing geometric strategy from concepts explained above would consider the logistics of disassembly and assembly processes. Firstly, building components with an interlocking assembly system would be discretized to a human scale. Parts would possess contact forces that allow discrete elements to be kinetically interlocked without permanently binding them together. This way, the repair and replacement process could be made convenient and done in isolated sections. Secondly, the parts would be aggregated to achieve redundancy to have parts acting as standby components in the structure. By incorporating redundant elements, expected removal of parts could go on as loads are shifted onto standby parts, and the structure would remain stable.

This research would be carried out within the conventional context of building construction. A column-beam system is used due to its high flexibility, as the system is comprised of vertical and horizontal components of a building structure.

Parts would be digitally aggregated with the Grasshopper tool Wasp, which simulates the process of assembly based on contact surfaces (A. Rossi & O. Tessmann, 2019). The Grasshopper plug-in Wasp is a tool that enables designing with discrete components based on a set of rules and defined quantity of parts. It takes the information of the geometry and generates quick iterations of self-assembly using surface planes as connections. Discrete elements can be aggregated stochastically or field-driven, which direct the aggregation to be within a curve path, a region, or a volume. The tool also functions to simulate decision making on aggregating infills of walls or structures. Utilizing Wasp to create

simulations helps ensure adequate and extensive aggregation results possible from designed module parts.

3.1. ASSEMBLY PROCESS BASED ON RATE OF CHANGE

The process of architectural construction is done such that the most structurally integral components are built first. The skeletal frames of the building function as the main path of loads through the building. Beyond that, elements such as plastered walls, surface tiles or veneers, window frames, and partition walls are secondary to its structure. Such parts are hence expected to hold a shorter life expectancy than that of the structure.

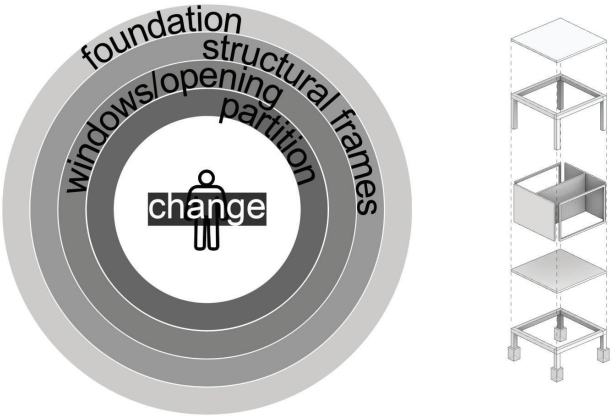

Figure 3. Sections of a building discretised according to its susceptibility to change.

According to its expected rate of change, the relationship between sections varies depending on other neighboring parts. If a part is expected to be more prone to change, its logistics for disassembly would be more straightforward. Such part might be independent of other neighboring elements in the aspect of structural performance, and its detachment would not affect the rest of the structure. The opposite could be said for parts that could be more long-lasting. These parts would probably be interlocked between neighboring parts, requiring more disassembly steps and dependent on others for structural stability.

The foundation laid out on-site would be built to form the field boundary in which spaces could create using the other parts. The foundation parts directly connect to the ground and require a more synthetic material that would be resistant to change or decay caused by natural factors.

The most transient layer in the architecture would be parts that define the program and spatial division of the spaces, both of which would be expected to change according to the user's need and future damages. In most architecture, the

walls are most directly exposed to environmental factors when acting as façade or partition. In the proposed construction system, the loadbearing, insulating walls are made of aggregated discrete pieces, while partition walls are made of simple detachable boards. These parts would be made of mycelium composites.

The beams and slabs are layers directly dependent on the load-bearing vertical components and act as roof or floor components. Although it is also equally exposed to environmental factors, these parts would not be as prone to changes as the columns or partition. They do not necessarily change according to the space program. As they remain used within the architecture, they would merely shift around following the walls. The horizontal components would be made out of timber parts, which would require higher energy emission and longer time for fabrication, although it is more long-lasting.

3.2. INTERLOCKING JOINT OF PARTS

Woodworking joints were used as applied case studies of kinetically force-locked surfaces. 'Bridle' joint, 'Tongue and Groove' joint, and 'Lap' joint are traditional joint systems commonly used to overlap planar surfaces into an interlock. These joints could be assembled and disassembled from both lateral and vertical directions, hence imposing flexibility in the user interface during the construction process.

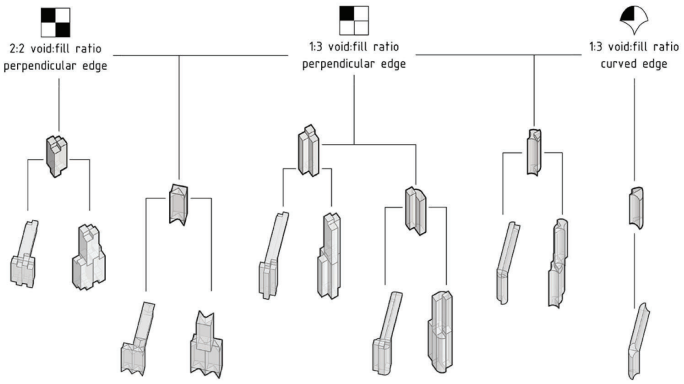

Figure 4. Exploration of tesselating and interlocking geometry, through evaluation of vertical to horizontal joinery.

Planar surfaces tend to be more versatile in creating connection planes. It possesses a more straightforward set of point data, such as straight edges, connecting points on 2-dimensional planes, and is asymmetrical in most aspects. Furthermore, working with platonic volumes give more possibilities in multi-plane

aggregation.

3.2.1. DESIGN OF WALL PARTS

Loadbearing wall parts, which are expected to experience more wear and tear, are discretized into an L-base column in which the edges are either identical or exactly twice the length of the other. This relationship allows the surfaces to always overlap onto each other, edge to edge, or edge to center. With the 'L' shape as its base, the columns could be rotated and still suitable as a locking piece. The geometry offers extensive locking combinations, which would always result in exterior surfaces where an extension is possible.

The partition is discretized into panels with connecting arms on the sides, made up of male-female connections. This connection allows aggregation on a singular partitioning plane that creates a division between the load-bearing walls of column parts. It could be connected to the load-bearing walls using frames that fit in between the column parts.

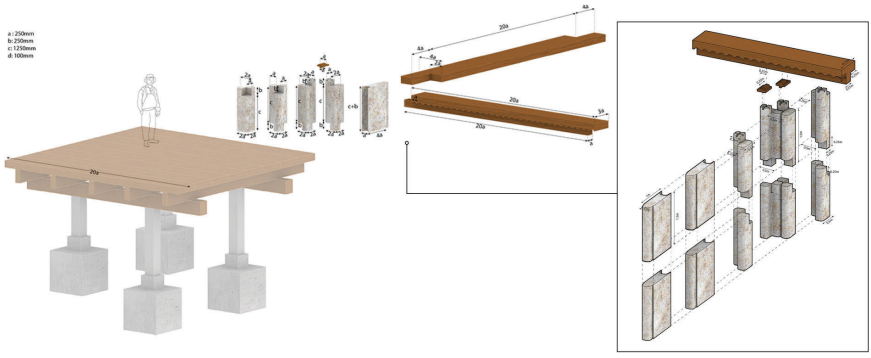

Figure 5. Parts dimensions are in increments of each other to ensure continuity at joints and are designed to be proportionate to the ground connection and human scale.

Its size was set to mimic the standard building column, usually built to be 0.75-1m thick and 3m-6m tall. It is assumed that there would at least be two 'L' shaped column stacked together at any location to form a locking part. For two beams to achieve 0.75-1m thickness, one beam should be 0.5m thick while considering overlapping. To maintain human scale in the production and construction process, the column and partition panels are discretized to components of the height of 1.5m. As mycelium composites are fibrous, there's a risk of degradation by scraping on the edges. To avoid this, the geometry is chamfered and smoothed out at its long edges.

3.2.2. DESIGN OF FLOOR AND ROOF COMPONENTS

While the columns create vertical pieces that aggregate into wall systems, the beams and slabs become horizontal part that make up the flooring/roof systems.

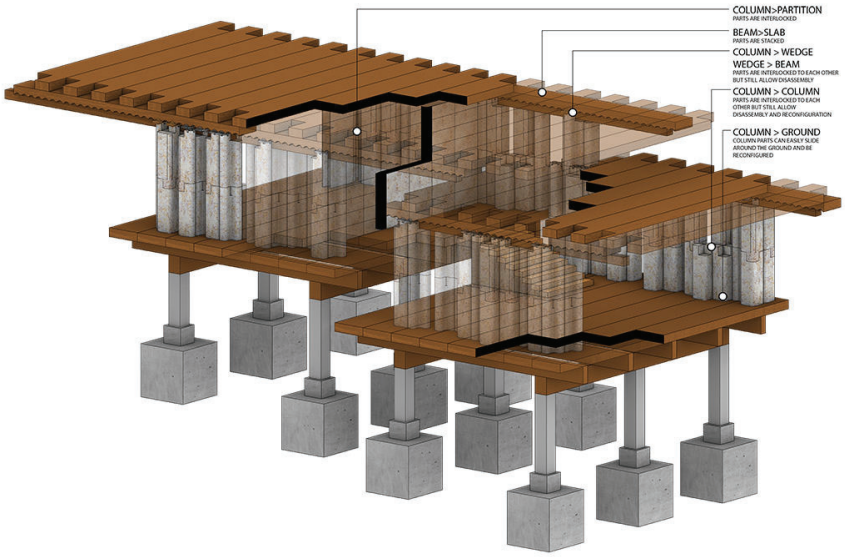

Figure 6. Configuration of parts.

The beam is a construction part supported by multiple columns at once, acting as a connecting horizontal piece to the vertical columns. Its design has to complement the top of the columns and make it so that three column pieces are required to support the beam minimally. The column pieces create valleys above it, which is complementary to the T-shaped cross-section of the beam. Columns are interlocked onto the beam from the sides and underneath while also linking onto other neighboring columns. Being in contact with the beam on its bottom surface ensures stable support against any main load-bearing forces onto the columns.

Similarly, the floor slab piece is designed to overlap onto the top surface of multiple beams at once. Instead of having large parts, the slab is further discretized into plank-like pieces. These planks are then oriented perpendicular to the length of the beam.

The horizontal parts are designed with assembly and disassembly in mind, which prompts a need for an additional joinery part that acts as a wedge that could lock the pieces in place during assembly and let the pieces be looser and quickly pulled out during disassembly. This geometry is designed to eat into the beam and column parts, interlocking onto both. It also fits onto the beams' ridges so as not to cause any sliding motion on the column parts.

Figure 7. Assembly process of vertical to horizontal component.

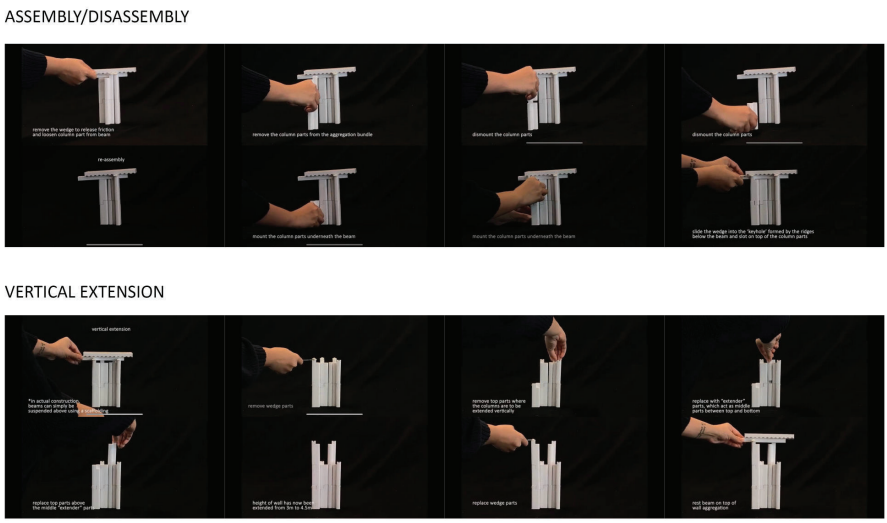

Figure 8. Assembly, Disassembly and Extension construction process.

4. Aggregation Simulation and Assembly Possibilities

As the design and connection of discrete elements are defined, they become factors that would determine possible variation in randomly aggregated massing. Different connectivity rules would offer local decisions within a field boundary, which could obtain coherent and functional configuration. In the case of the project, the potential formation would be in increments of the component dimensions.

Within the horizontal plane, spaces could be formed with depths of 4m, 8m, and their respective multiplications. This is because the beam and slabs span 8m and 12m in length. In vertical planes, the spaces' height would be multiples of 1.5m following the height of the column and partition wall parts. Hence, the room heights would be 3m, 4.5m, 6m, and 7.5m.

Space-making using the kit of parts designed in this research allow flexible iterations. The variations are only limited with a set of dimension rules that keep the parts usable, replaceable or reconfigurable on the human scale.

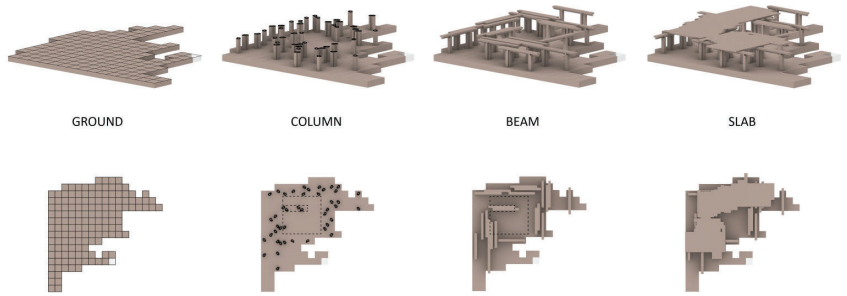

Figure 9. Space making, presented in layers.

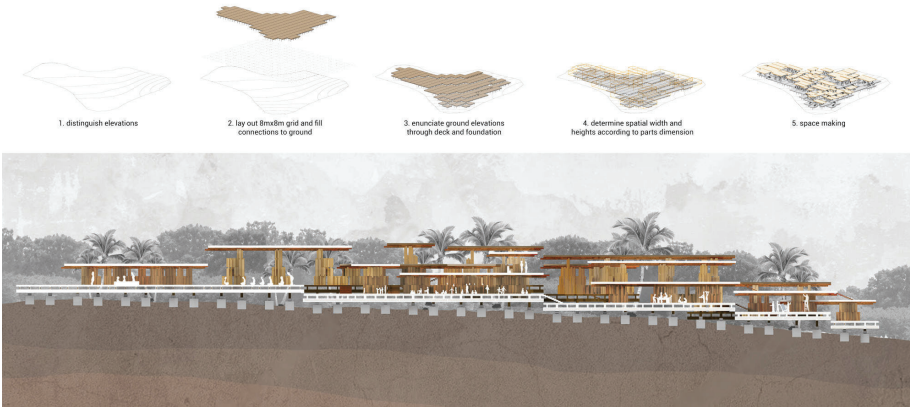

Figure 10. Implementation of modules on site allow for spaces of varying heights and widths.

References

Appels, F.V., Camere, S., Montalti, M., Karana, E., Jansen, K.M., Dijksterhuis, J., Krijgsheld, P. and Wösten, H.A.: 2019, 'Fabrication factors influencing mechanical, moisture- and water-related properties of mycelium-based composites, *Materials & Design*, **161**, 64-71.

Braungart, M. and McDonough, W.: 2002, *Cradle to Cradle: Remaking the Way We Make Things*, Farrar, Straus and Giroux, London.

Jones, M., Bhat, T., Kandare, E., Thomas, A., Joseph, P., Dekiwadia, C., Yuen, R., John, S., Ma, J. and Wang, C.H.: 2018, Thermal Degradation and Fire Properties of Fungal Mycelium and Mycelium - Biomass Composite Materials, *Scientific Reports*, **8**(17583), -.

Jones, M., Huynh, T., Dekiwadia, C., Daver, F. and John, S.: 2017, Mycelium Composites: A Review of Engineering Characteristics and Growth Kinetics, *Journal of Bionanoscience*, **11(4)**, 241-257.

Rossi, A. and Tessmann, O.: 2019, From Voxels to Parts: Hierarchical Discrete Modeling for Design and Assembly, *ICGG 2018 - Proceedings of the 18th International Conference on Geometry and Graphics*, 1001-1012.

Tessmann, O.: 2012, Topological interlocking assemblies, *Digital Physicality: Proceedings of ECAADe 2012*, 211-219.

DEPLOYABLE RECIPROCAL FRAME STRUCTURES: DEPLOYABLE MODULE

Deployable Module

SAYALI SHAH
[1]*Department of Masters in Digital Architecture, MKSSS Dr.Bhanuben Nanavati College of Architecture,Pune, Pune University*
[1]*sayaliishah@gmail.com*

Abstract. This study contains new results concerning several aspects of reciprocal frame research. The paper intends to induce portability and deployability in reciprocal structures using straight bars. A complex grillage, when created as an assembly of units, which is a self-standing 3d structure is Reciprocal Frames(RF) Structure. While these structures are attractive reflecting their simplicity, beauty, and ease of assembly, disassembly, deployment, and reuse of elements; creating such structures, however, is difficult. Straight bars encourage its use in building the RF structures which further led to the study of the Deployable Reciprocal Frame Structure. An attempt is made to design a structure that has the potential of being converted into a Deployable Emergency Module that offers protection after natural disasters.

Keywords. Reciprocal, deployable, straight bars, habitable space, emergency module.

1. Introduction

A span greater than its own length covered with a combination of balanced structural elements is Reciprocal Frames Structures(RF). Mutually supported elements which are placed in a cyclic manner establish balance and equilibrium. At least three elements are must to obtain the stability in the RF unit. (See Figure 1). The characteristic of these RF structures is that they do not intersect at the elements' longitudinal extensions but meet along the supporting length at the centre of the assembly. These systems had also proved to be very useful in the ancient period when material availability was scarce. (Godthelp, 2019)

PROJECTIONS, Proceedings of the 26th International Conference of the Association for Computer-Aided Architectural Design Research in Asia (CAADRIA) 2021, Volume 1, 553-562.

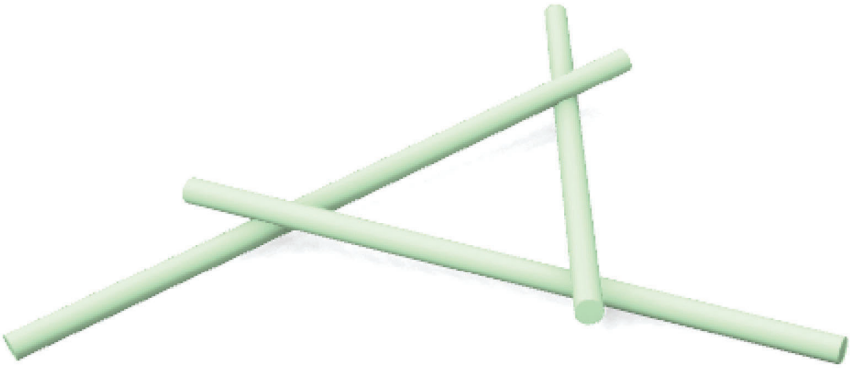

Figure 1. Reciprocal Frame Structure Component. (Source: Author).

1.1. HISTORY AND TIMELINE OF THE USE OF RECIPROCAL FRAME SYSTEM:

The reciprocal frame concept can be traced to prehistoric building types through the archaeological record and surviving traditions' observations. Similar systems appear in archetypes. (See Figure 2.1a) (See Figure2.1b) show the timeline of Reciprocal Frame Structure Systems used. The reciprocal frame structure is categorized to the different topologies as 1D (Leonardo da Vinci's bridge), 2D (Leonardo da Vinci's grid), and 3D(Pugnale, 2014). Simple rules for pattern generation are used for both 2D and 3D reciprocal frame structures, where a very different result is generated using the same pattern for 3D reciprocal frame structure. Hence, this inspires the study of a 3D reciprocal frame structure that can achieve complex forms using simple rulesets. (Parigi, 2014). Modern RF systems have introduced the new use of these systems. (See Figure 2.2)

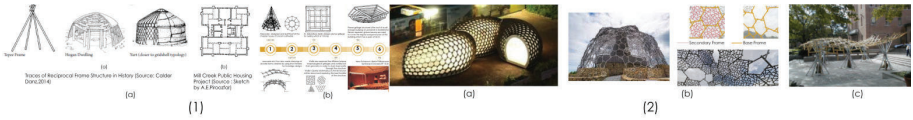

Figure 2. 1(a): History of Reciprocal Frames 1(b): Timeline of the Use of Reciprocal Frame Structure System (Source: Author) 2(a) Kreod Pavilion (Source: Ed Kingsford) 2(b)Rokko-Shidare Observatory (Source: O-Popovich-Larsen -2014) 2(c)Experimental Pavilion. (Source: Rice Gallery).

2. Need for the study:

Using straight bars, different possible morphologies of deployable structures with an approximation of habitable space using an independent unit repeated

can assemble by using component aggregation. To expand the horizon of RF structures, a new study is exploring its application for deployability and portability and further looking towards the component aggregation where this system can be modularly used. The efficiency of structure development, deployability, and easily tuneable properties raise the need for new attention to this concept. The paper attempts to approach the portability and deployability of the system.

3. Brief:

The paper aims to achieve a component aggregation using a Reciprocal Frame Structure Component that is stable and deployable, which in the future can be used as a deployable emergency module.

4. Methodology:

For a component generation, the RF component's anatomy and the types of method to generate them were studied. Different components were generated computationally as well as using bamboo struts. The height of the component and its stability were the filtration criteria to shortlist the components. The components were further aggregated with different rule sets that were analyzed for deployability. A module was then built to the scale that was deployable and used as an emergency module.

4.1. COMPONENT GENERATION:

After studying the RF component's anatomy, various struts components were generated computationally and physically to understand further possible aggregation. Later studying the RF component (See Figure 3a), a computational script was developed to design the RF components (See Figure 3b). The components were generated to understand further possible aggregations and forms. (See Figure 3b) After generating the components, they were also studied to understand the height to the radius ratio. (See Figure 3b)

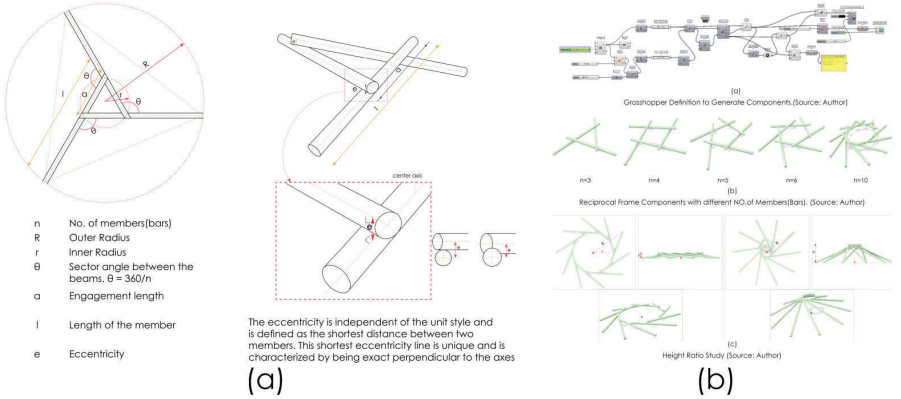

Figure 3. (a)Anatomy of Reciprocal Structure Component. (Source: Author) (b)Study of Reciprocal Frame Component(Source: Author).

In (See Figure 3b), where "R" represents the outer radius of the component, and "r" represents the inner radius of the component, the following points are observed and concluded:

- The scaling factor and point height determine the beam height.
- The smaller the inner radius of the polygon higher is the height of the component and vice versa.
- The height of the RF component is inversely proportional to the inner radius of the RF component.

The existing 2d patterns generated using the RF component are studied, and the rule sets are analyzed which were applied on shells for demonstration. Computational and analogue models were made. (See Figure 4a). A delta in height of the shells was observed despite of using same length struts while fabricating the physical model. Additionally, the four strut aggregation was rigid as compared to the other aggregations making it less likely for further experiment

While these physical models were made, the process helped to understand that each bar is placed at a certain angle depending on the number of struts used in that component. To extend the study, components and their internal angle were studied systematically, and hence the rotation angle was achieved. Rotation Angle of the Joinery Depends on the internal angle of the RF component. The following table helps to understand the same. (See Figure 4b).

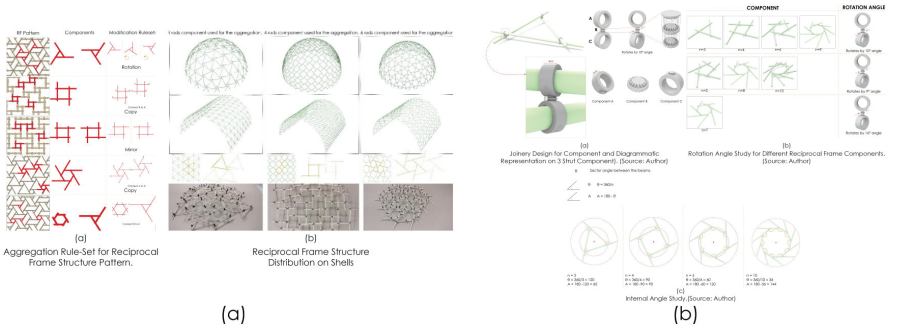

Figure 4. (a): Aggregation Rule-Set Pattern and its Distribution on Shells (Source: Author) (b): Component Joinery Design and Its Study (Source: Author).

4.2. DEPLOYABLE MECHANISM STUDY:

Different deployable mechanism study was initiated, and it was found that there are majorly two types in which the deployable mechanism is classified.

4.2.1. Strut Structures.

Structures made using struts where the members act as the compression, tension, or bending members connected by hinge or joints are strut structures. Types of the deployable mechanism used for these structures are:

- Scissor - Hinge Mechanism
- Sliding or Umbrella Mechanism.
- Hinged -Collapsible Strut Mechanism.

4.2.2. Surface Structures.

Structures where the surfaces carry or act as stress members are surface structures. These surfaces act as the compression or tension members of the structures. Types of the deployable mechanism used for these structures are:

- Telescopic Mechanism.
- Inflatable Mechanism.
- Foldable Mechanism.

4.3. PARAMETERS TO CONSIDER FOR DEPLOYABLE STRUCTURES:

The following diagram explains clearly the parameters to consider while designing deployable structures. (See Figure 5)

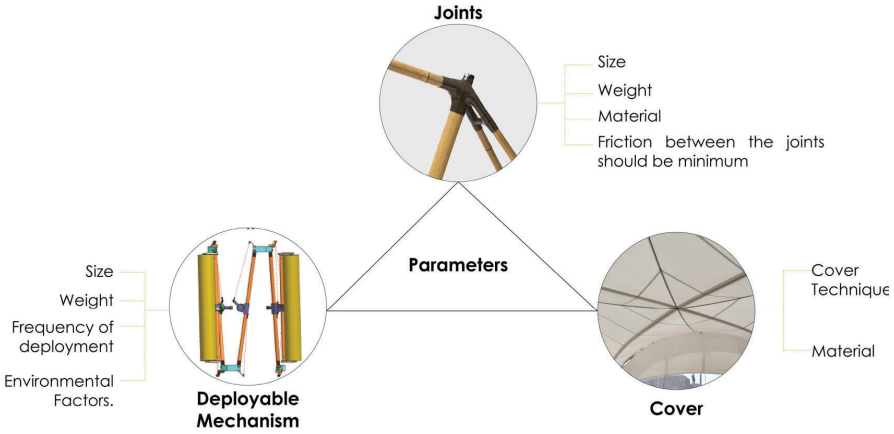

Figure 5. Parameters for Deployable Structures. (Source: Author).

4.4. AGGREGATION AND DEPLOYMENT OF RF STRUCTURES:

Small Bamboo sticks were used for the study of RF aggregation and their possible deployable techniques. The exercise is carried out of 3 strut components, 5 strut components, and 6 strut components. The growth pattern and their deployable output were studied, but the further focus was on the enclosure growth pattern, as a result, demanded habitable space (emergency module). (See Figure 6b). The aggregation studies in two patterns:

- Linear Growth Pattern: The aggregation rule set for different components varies depending on the number of members used to generate a component. Once the aggregation was developed, deployable points were identified, and the aggregation was deployed to check its limit. (See Figure 6a)

- Enclosure Growth Pattern: The aggregation rule set for different components varies depending on the number of members used to generate a component. Once the aggregation was developed, deployable points were identified, and the aggregation was deployed to check its limit. (See Figure 6b)

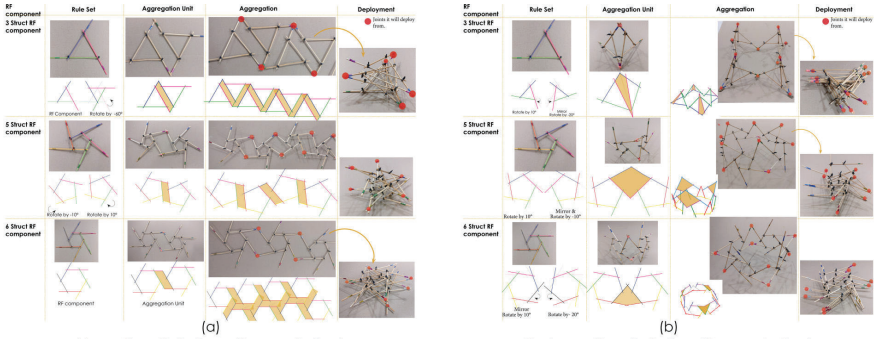

Figure 6. Aggregation Growth Patterns (Source: Author).

4.5. DEPLOYABLE JOINERY DESIGN AND BASE CONNECTION DETAIL:

Once the deployable points were identified, common deployable joinery suitable for all RF components is designed. The joinery is designed to allow the structure to deploy easily, keeping in mind the notch-free joint design criteria. This helps to save bamboo from damage, and also, the life span of the bamboo increases. Joinery is designed to rotate easily at a 360-degree angle in the plan, and 180-degree in front elevation, making the deployable movement flexible. (See Figure 7a) Also.3D printed prototype for the same was created. (See Figure 7a).

Every component creates an angle different from the ground when placed. Hence the need for customizing joints for the individual component is needed. (See Figure 7b). For module aggregation of each component's base angle will be the same. (Figure 7b). Also, in the 5 strut component, the component rests on two struts, and hence the two separate base angles will be designed. Also.3d printed prototype for the same was created. (See Figure 7b).

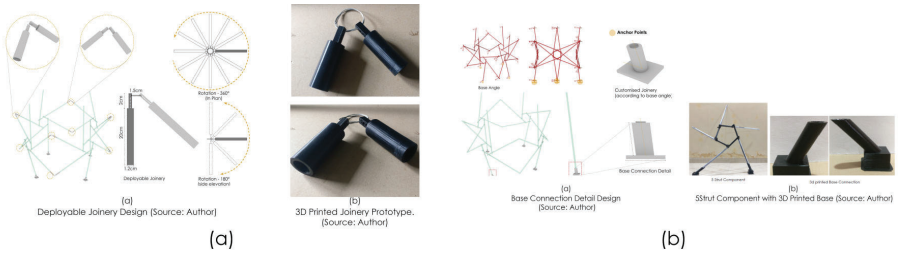

Figure 7. (a): Deployable Joinery Design for Aggregation and 3D printed prototype of the Joinery. (Source: Author) (b): Base Connection Detail and 3D printed prototype of the Base. (Source: Author).

4.6. COMPARISON OF DIFFERENT AGGREGATION.

A comparative study of different enclosure aggregations of 3 strut, 5 struts, and 6 struts was studied keeping the number of components in the strut's aggregation and length constant. (See Figure 8a) shows that the 5 strut aggregation is most suitable as the area of enclosure to the height. The aggregation fulfils the basic requirement of habitable space. Further, the modules are also tested against the pressure where the wind speed is 15m/sec. (See Figure 8b) shows that wind pressure on the 5 strut aggregation is comparatively less. Hence 5 strut aggregation shortlisted for further studies.

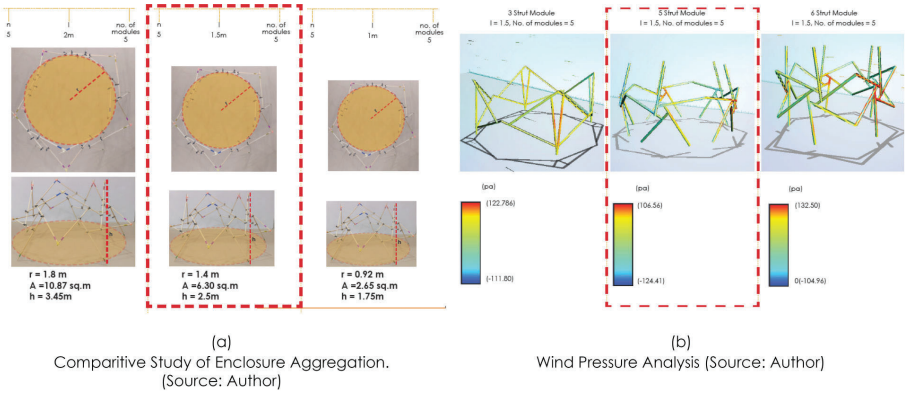

Figure 8. Comparative Study of Enclosure Aggregation and Wind Pressure Analysis on the Aggregation. (Source: Author) .

4.7. COMPARISON OF 5 STRUT AGGREGATION WITH DIFFERENT MEMBER'S LENGTH.

Further, keeping 5 strut aggregation and the number of components used in aggregation constant, the member's length was changed, and then the length to area ratio of the aggregation was studied. (See Figure 9a) shows that when the

member's length is 1.5m, the length to area ratio is apt. The habitable space can be easily deployed.

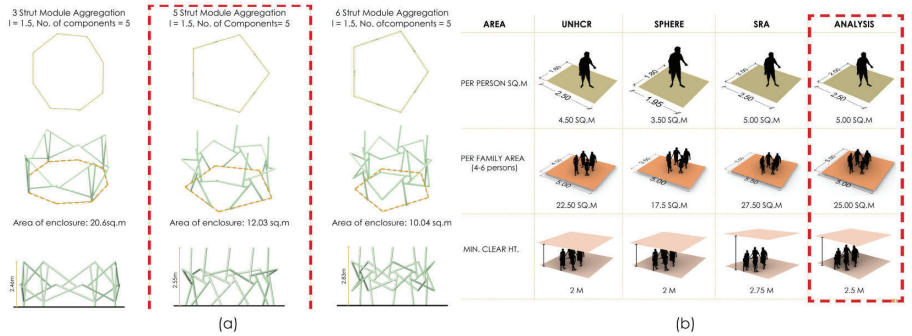

Figure 9. (a): Comparision of 5 strut Aggregation with different Member's Length (Source: Author) (b): Space Matrix (Source: Author).

5. Design Proposal:

The shelter is the basic need of humans, but natural calamities like earthquakes, floods, and people left out homeless lead to the emergency shelter. The deployable emergency modules can offer protection after natural calamities.

5.1. SPACE MATRIX AND HABITAT DESIGN (UNIT DESIGN): :

Minimum space requirement laws for emergency shelter are studied from UNHCR and SPHERE, compared with SRA norms, and is analyzed to give the best possible habitat area. (See Figure 10b)

The components were designed so that each component is individually stable, and when aggregated, the module (unit) is also stable. The study concluded that the number of components added to design a unit is directly proportional to the enclosure area. (See Figure 10a) Rhinoceros and Grasshopper were used for the aggregation. The following script shows the development. (See Figure 10b). The following study represents number of components used to area of enclosure and number of the person, it could cater. (See Figure 10c)

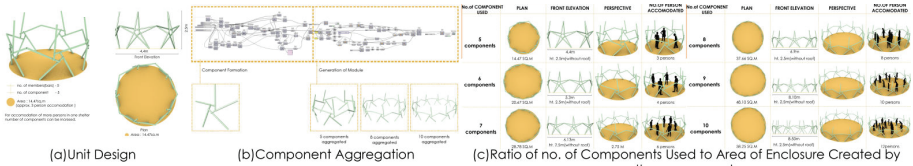

Figure 10. Habitable Unit Design Process (Source: Author).

6. Fabric Study:

Mainly 3 types of fabrics are used for the external covering:

- Polyester
- Polycotton
- Cotton.

Advantages and disadvantages of these fabrics were studied on the basis of comparing their positive and negative points. It was concluded that polycotton, since it's a combination of polyester and cotton, befitted both materials, making it the aptest material for the unit's external covering. (components and roof).

6.1. UNIT AND ROOF COVERING AND ROOF COVERING CALCULATION AND ITS MATRIX:

5 strut component was considered, area to cover the component and the roof is marked and the fabric required is calculated. Through the diagram and physical model, the covering method is explained below. For demonstration, a tensile cloth is used. (See Figure 11.1). Area of enclosure + area of the triangle x no of components added to the aggregation.The calculation for Fabric required for a few module aggregations is shown below. (See Figure 11.2)

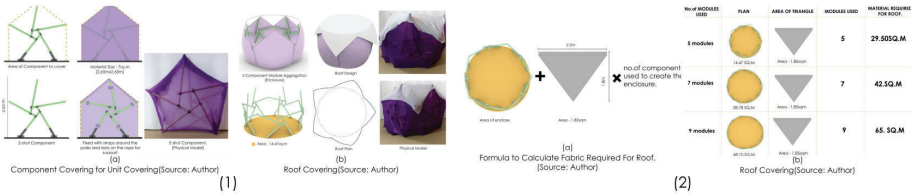

Figure 11. (1): Fabric Covering Technique Study (Source: Author) (2)The Calculation for Roof Covering and Roof Covering Matrix (Source: Author).

7. Scaled Prototype and Visual Representation: :

A scaled prototype was made using conceal pipe and 3d printed joints to check the structure's stability. The member was 2 feet(0.60m) long, with diameter 20mm. (See Figure 12(a)(b)(c)) shows all steps of prototype construction. Visual representation showcases its use. (See Figure 12d) can be used as an emergency module after natural disasters. In the current scenario where the world faces the COVID pandemic, these structures can be constructed easily and used as isolation centres on open grounds or any flat land.

Figure 12. (a): Construction of Component. (b): Construction of Aggregation Unit (c): Deployed form. Scale Prototype (Source: Author) (d): Visual Representation (Source: Author).

8. Discussion and Conclusion:

Reciprocal Frame structures are lightweight structures. This reciprocal structure technique of making small adjustments for fine-tuning the loaded structures or quick repair of the members without damaging the complete structure is possible. The design of these structures can prove to be an essential feature for up-coming generation in mechanical and Civil Engineering. The feature of deployable reciprocal structure offers operational and portability advantages. Using this technique, many structures can be built, which can be permanent structures or temporary structures. A wide range of emergency structures can build in emergencies as these structures can be easily and quickly built. Component aggregation for reciprocal structures can prove to be an on-site built system, where components can be transported to the site and then connected, and space is created.With mass design being minimal, the structure's efficiency increases. Since these structures deploy in one direction, they are easier to manage than the structures deploying in different directions. Hence, this also increases the efficiency and demand of these structures for use now and in the future.

References

Cullen, J.M.C.: 2012, *Sustainable materials: with both eyes open*, Originally published.

Danz, C.D., Danz, C.D. and Danz, C.D.: 2014, *Reciprocal Frames, Nexorades and Lamellae*, Master's Thesis, University of Washington.

Godthelp, T.G.A.J.: 2019, *TIMBER RECIPROCAL FRAME STRUCTURES*, Master's Thesis, Eindhoven university of technology.

Larsen, O.P.: 2008, *RECIPROCAL FRAME*, Architectural Press.

Mellado, N.M.: 2014, Computational Design and Construction of Notch-Free Reciprocal Frame Structures, *Conference: Advances in Architectural Geometry*, London.

Mimendi, L.M. and Lorenzo, R.L.: 2020, Digitisation of bamboo culms for structural applications, *Department of Civil, Environmental and Geomatic Engineering, University College London, London, UK*, **Journal of Building Engineering** (29:101193), 29.

parigi, D.P. and Pugnale, A.P.: 2014, Three-dimensional reciprocal structures: morphology, concepts, generative rules, *Conference: IASS-APCS-2012 symposium: "From spatial structures to space structures "*, Seoul.

Popovic, O.P.: 1996, *RECIPROCAL FRAME STRUCTURES"*, University of Nottingham, England.

Tunç, E.T.: 2015, Shaping a timber reciprocal frame structure, *Delft University of Technology, Department of Architecture*.

ROBOTIC COLOR GRADING FOR GLASS

Additive Manufacturing of Heterogeneous Color and Transparency

SOFIA MICHOPOULOU[1], RENA GIESECKE[2],
JONAS WARD VAN DEN BULCKE[3], PIETRO ODAGLIA[4] and
BENJAMIN DILLENBURGER[5]
[1,3]*Master of Advanced Studies ETH in Architecture and Digital Fabrication*
[1,3]*{michopoulou.s|jonas.vandenbulcke}@gmail.com*
[2,4,5]*Digital Building Technologies, Institute for Technology in Architecture, ETH Zurich, 8093 Zurich, Switzerland*
[2,4,5]*{giesecke|odaglia|dillenburger}@arch.ethz.ch*

Abstract. This paper presents a new additive manufacturing method for color grading of glass. Color-graded elements, ranging from product design to architectural scale, could filter light and view in a novel way through locally differentiated color and opacity, and produce color effects in space. Existing methods for manufacturing multi-colored glass are either not economic for building due to labor intensity, limited to surface applications or small scale objects made of resins or plastics. To allow for automated color grading of glass in two-and-a-half and three dimensions we propose a robotic multi-channel process. The multi-channel tool mounted on a Universal Robot consists of four compartments, containing red, yellow, blue and transparent glass granules. Colors can be mixed on the fly by implementing varying flow rate ratios along the print path. Loose granules are fused in a kiln at high temperature into color-graded glass elements. The goal of this research is to lay the basis for color-graded elements of larger size and volume with higher pattern differentiation for functional and aesthetic purposes.

Keywords. Color grading; robotic fabrication; multi-channel printing; glass.

1. Introduction

Traditional manufacturing of multi-colored glass for cultural and household objects dates back to antiquity (Wight 2011) including several methods such as kiln fusing, stained glass, and Murrina & Millefori or Vetro Pezzato (Chambers and Oldknow 1999). Kiln fusing, the oldest technique for making glass artifacts, was invented by the Egyptians around 2000 BC and relies on fusing small glass pieces under high temperature in a kiln. Glass pieces are manually assembled according to a pattern or the artisans design idea and fused into a three-dimensional or multi-colored glass artifact (Reynolds 1987). The artisan craft of stained

PROJECTIONS, Proceedings of the 26th International Conference of the Association for Computer-Aided Architectural Design Research in Asia (CAADRIA) 2021, Volume 1, 563-572.

glass, developed in ancient Rome, enables the manufacture of multi-colored glass elements of larger size suitable for buildings. The process consists of manually cutting and joining glass pieces of different colors into figurative or abstract patterns using metal joinery (The Metropolitan Museum of Art 2000). Resulting elements can perform as illuminated wall decorations and windows in churches. While the glass is colored inherently by adding metal oxides to the glass mixture, glass surfaces can also be painted by manually applying acrylic enamel paint onto the surface of glass (Wylie and Cheek 1997). Due to the labor intensiveness of these processes, the manual production of multi-colored glass and glass painting techniques are primarily used for exclusive luxury objects or in restoration projects until today. Contemporary techniques of adding color onto glass include silkscreen and ceramic digital printing onto glass. For the silkscreen printing process, a decorative layer of ceramic ink is applied through a screen mesh onto the glass. This technique is durable and suitable for application in building projects as realized in the Ricola building by Herzog de Meuron in 1993 (Herzog & de Meuron 1996). Digital ceramic printing onto glass is an automated technique for applying ceramic inks onto flat glass with a multi-head process (Hoffmann 2012). This technique is automated, but it remains a surface application of color onto glass that is not material-inherent or applicable to locally varying properties within a volume. On the other hand, latest multi-material printing shows the potential to locally vary material-inherent properties, colors and transparencies, within artifacts. Stratasys Objet Connex printers can produce high-resolution, geometrically complex, and materially heterogeneous 3D printed objects at product scale by locally jetting and curing drops of photo-curable resin as demonstrated in the Vespers II Series (Doubrovski et al. 2015). Nevertheless, multi-material printing methods are either limited to plastics (Grigoriadis 2018) or restricted in size due to the extremely high machine and material costs of resin-based multi-jetting techniques; thus not economic for application at architectural scale. Previous research for *Color and Transparency Grading in Glass* (Giesecke 2018) has demonstrated the potential for material-inherent color grading of granular glass according to computed gradient patterns. In summary, existing methods are either labor-intensive, limited to surface application of color or not suitable for up-scaling due to economic constraints. As a continuation of *Color and Transparency Grading in Glass* the goal of this research is to allow for the concept of color grading and multi-color printing to enter architectural scale and application enabled by an automated multi-channel printing process. We present a method for additive manufacturing of multi-colored glass elements with material-immanent color grading in two-and-a-half and three dimensions.

2. Methods

The research consists of the following steps:

1. Material Research and Kiln Fusing
2. Multi-channel Tool and Robotic Setup
3. Computational Modeling of Three-dimensional Color Gradients
4. Tool Path Generation for Multi-channel Grading
5. Grading Tests

2.1. MATERIAL RESEARCH AND KILN FUSING

When composed of its basic ingredients sand, soda ash and limestone, soda-lime glass is transparent. By adding different metal oxides one can add color. To fuse glasses of different colors, their compatibility needs to be assured. Compatibility is related to glass type, expansion coefficient, viscosity during the heating process and the types of metal used for coloring. Incompatibilities in metal oxides can evoke reactions that lead to unexpected coloring results. As a first proof of concept, we use off-the-shelf *Bullseye* and *Farbglas* glass which use non-reactive metal oxides and provide compatibility charts. Red, yellow, blue and transparent glass are chosen as exemplary channel inputs based on the traditional color wheel for mixing of physical colors (Baty 2017), from which secondary colors can be mixed and according to their intensity. These inputs can be varied in relation to the desired output. To test the color logic a set of manual tests is conducted to establish the color spectrum attainable with the primary colors. Transparent base granules of 3.3 - 5 mm ø and coloring granules of 0.5 - 1mm ø results in fine coloring resolution and high potential transparency. The maximum amount of colored granules used in a given location is 16% (see Figure 1, central triangle). The ratio of the 3 base pigments alternates with pure red, blue and yellow along the edges with a minimum of 4% of one type of pigment added.The color palette produced (see Figure 1) demonstrates that pigments do not share the same intensity. Red is clearly more dominant, mixing red with blue results in unexpectedly dark tones. Consequently, colors are dosed depending on their relative dominance: red is dosed at 1:6 parts, blue at 1:4 and yellow at 1:3 ratio. The local maximum saturation is reduced from 16% to the lowest percentage of color within the testing setup, 4% in further tests.

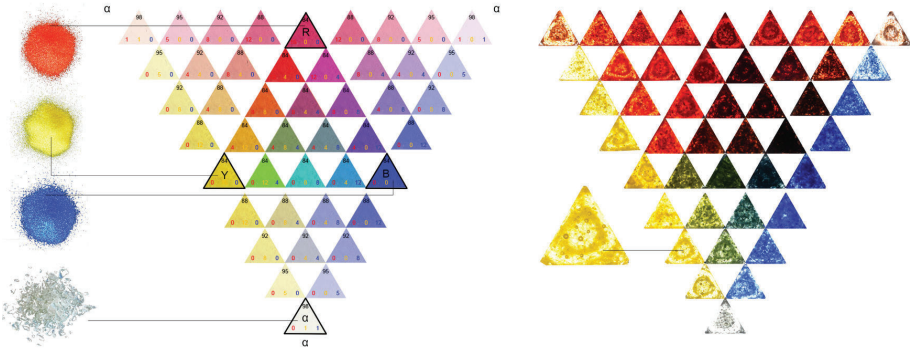

Figure 1. Exemplary color palette RYBα visualization of mixing ratios (left) and resulting materialized color spectrum in glass (right).

For identifying a suitable logic for the automated layering process in relation to the resulting coloring output. Alternating colored and transparent layers of glass granules facilitate transparent properties of resulting artifacts. From these tests is concluded that depositing dense layers of colored granules without transparent

glass in between results in opaque optics while alternating colored layers of small granules and transparent large granules allow for light to pass through the artifacts. To fuse glass granules, they are placed in the kiln at room temperature (see Figure 2) and fused along a specific heating and annealing curve (see Figure 3), depending on the glass product and type used (Griffith 2014). The firing duration is related to the thickness and volume of the glass object. The fusing process fuses the granules, while the annealing process releases stress from the glass.

Figure 2. Loose granules robotically placed before kiln fusing (left) and after fusing in the kiln (right).

2.2. MULTI-CHANNEL TOOL AND ROBOTIC SETUP

For the automated distribution of red, yellow, blue and transparent granules a multi-channel-dispenser is designed. The multi-channel tool attached to a UR robot consists of a dispenser body with four compartments, each containing glass granules of a different color (see Figure 3). An inverse-pyramid shape of the tool enables the collection of granules from different channels in the bottom center and refilling of the channels from the top. Vertical customized conveying screws transport and dose the granules (see Figure 4). To minimize the collection area, the screws are slightly tilted inwards. Every compartment consists of a container with a metal tube at the bottom, through which the granules pass. Each screw is connected to a stepper motor on top of the cartridge. The tubes, combined with the conveyor screw, create a section small enough for the granules to start packing. Their flow is enabled by spinning the conveyor screws. For the small granule color channels transporting granules of 0.5-1mm size off-the-shelf Ø 5mm steel drill bits are used, for the large granules of 3.3-5mm size a costume 3D printed plastic conveyor screw was designed in an iterative process. This iterative process includes testing various helix diameters and steepness to ensure dispensing process without clogging resulting in a 20mm screw diameter and 30° helix steepness. For both granule sizes, the relationship between tube size and screw shape is identified in calibration tests. Depending on the revolution speed of the motor more or less granules can be dispensed over time allowing the different colors to be mixed in specific ratios along the robotic tool path.

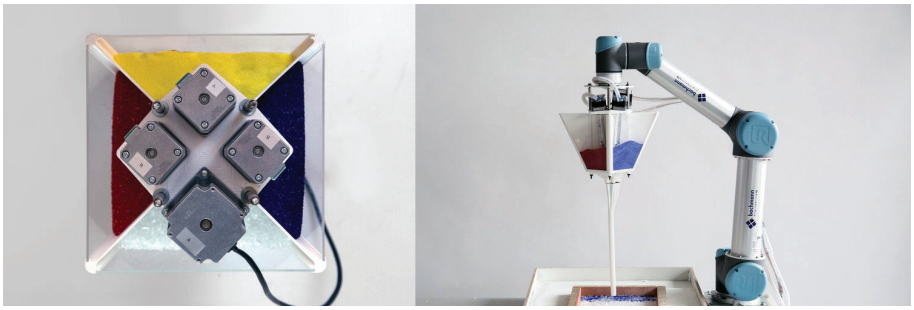

Figure 3. Top view (left) and elevation (right) of multi-channel tool and robotic setup.

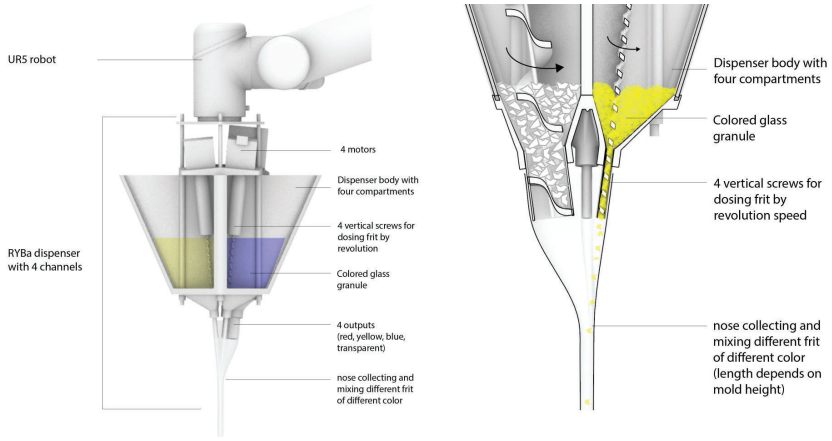

Figure 4. Multi-channel tool (left) elevation and detailed section (right).

2.3. COMPUTATIONAL MODELING OF THREE-DIMENSIONAL COLOR GRADIENTS

To model linear color gradients in plane and in volume, an axial grading model is set up using distance functions, with the start point of every axis being transparent (α) and the end point a primary color (RYB). Initial two-dimensional grading tests use the X- and Y-axis, while for the volumetric tests the same modeling logic is also applied to the Z-axis. To visualize a design, the volume of the object is discretized into dots/voxels for which the matching RYBα values are calculated. Those are then translated into RGBα using the color transformation matrices as found in *Paint Inspired Color Mixing and Compositing for Visualization* (Gossett 2004) values which are then rendered through Rhino's Grasshopper plugin.

2.4. TOOL PATH GENERATION FOR MULTI-CHANNEL GRADING

The computed volumetric design is sliced into layers. Based on this information a tool path is generated for each layer and the robotic movement is defined by a set of movement frames. Those frames provide sampling points to generate the RYBα

values along the tool path. These RYBα values are then translated into GCode to operate the stepper motors of every color channel. For the final output, based on a range of process parameters identified through various tests (see Table 1), the time intervals for both the robotic movement and stepper motors are synchronized. The revolution of every screw corresponds to the ratio of each color channel at a specific location. Both the communication with the stepper motors driven by an Arduino board flashed with GRBL (Motion Control for Makers), and the UR5 robot is done in Grasshopper using GHPython components and the *Robots* plugin. Two different dispensing methods are identified to achieve grading the discrete process and the continuous process. In a discrete process, the robot moves from one point to the next, dispensing different amounts of color at each point (see Figure 5a). In the continuous process, the robot dispenses the required quantity of color along a continuous path allowing for the inscription of sharp lines (see Figure 5b) as well as for creating smooth gradients (see Figure 5c). When using the discrete method the amount of color can be varied by the amount dispensed in one spot. The continuous method allows for varying color intensity by changing robot speed, thus for producing smooth gradients at a higher speed.

Table 1. Process parameters.

Parameter		Min.	Typ.	Max
Robotic movement speed		10 mm/s	35 mm/s	150 mm/s
Path spacing		5 mm	10 mm	25 mm
Layer thickness		2 mm	5 mm	15 mm
Nozzle-surface-distance		2 mm	10 mm	50 mm
Channel pipe diameter	Color channels	-	6 mm	-
	Transparent channel	-	22 mm	-
Granule size	Color channels	0.5 mm	-	1 mm
	Transparent channel	3.3 mm	-	5 mm
Spindle speed	Color channels	0.05 rev/s	0.5 rev/s	6 rev/s
	Transparent channel	0.1 rev/s	0.3 rev/s	0.5 rev/s
Corresponding mass/time	Color channels	0.07 g/s	0.26 g/s	0.66 g/s
	Transparent channel	8.6 g/s	10.4 g/s	13.2 g/s

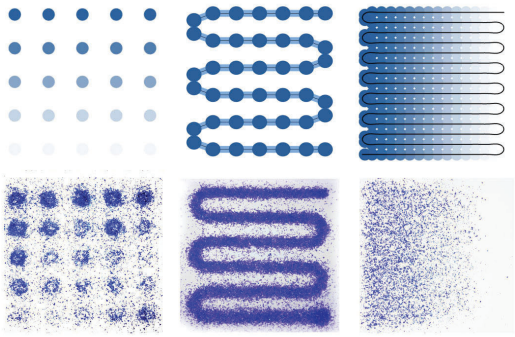

Figure 5. Dispensing a) discrete dots b) along a continuous curve c) along a continuous curve with varying speed and decreased distance.

2.5. GRADING TESTS

Material research and tool design allow for the gradation between two (transparent to blue), three (transparent to blue to yellow) and four properties (transparent to blue to yellow to red). As a first proof of concept, linear grading is tested in two-and-a-half dimensions. The loose granular material is distributed within reusable limitation ledges, reusable molds, consisting of coated vermiculite plates, and then fused in the kiln. Tiles of 15x15x1cm size and cubes of 10x10x10cm size are fabricated demonstrating the possibility to fabricate linear gradients, smooth transitions between color properties (see Figure 6) made from *Bullseye* (see Figure 6b) and *Farbglas* glass (see Figure 6c). The quality of the colors also depends significantly on the primary colors and the granule size used. Samples made from *Farbglas* and *Bullseye* glass result in different physical properties and aesthetics differing in resolution, color intensity, and transparency. Volumetric grading of cubes (see Figure 7) follows the same process logic as the linear grading of tiles. Layers with 2D grading patterns are built up vertically to fill the volume of the mold. The glass volume is compressed vertically by 45% throughout the fusing process. When layering the granules such shrinkage in volume can to be taken into account within the modeling and fabrication process. Fused cubes show a heterogeneous deformation with proximity to the edge caused by friction with the mold. Non-homogeneous deposition or taking these deformations into account in the computational model could mitigate this issue. Furthermore, the colors deviate slightly from the intended result, especially red is still dominating. This issue can be resolved by updating the current color modeling translation matrix used for translating the RYBa to RGBa.

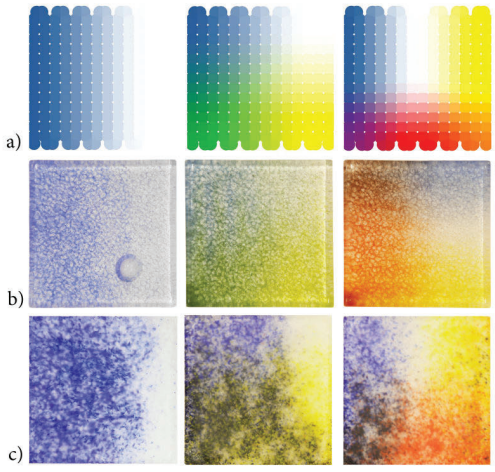

Figure 6. RYBα tiles from top to bottom (a) digital visualization (b) in Bullseye glass and (c) in Farbglas color spectrum.

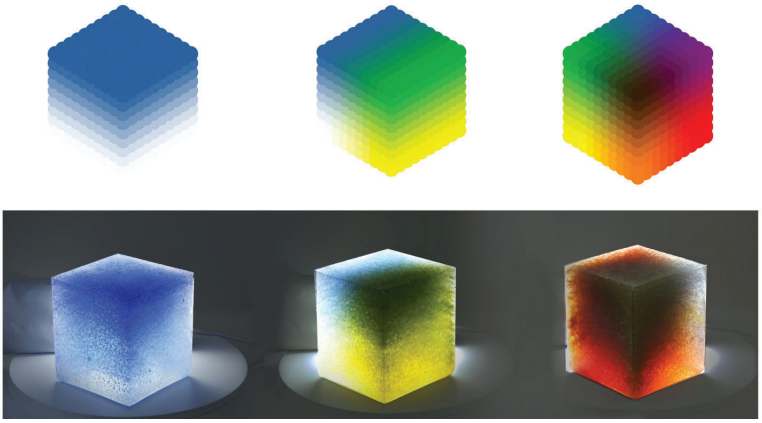

Figure 7. Color gradient visualization (top) and color graded glass cube (bottom).

3. Results

Grading tests (see Figure 8) provide a small scale proof of concept for *Robotic Color Grading of Glass*. The following list will summarize and critically reflect the research contributions made:

Material system. As widely used material with a long history in multi-colored objects and architectural applications such as stained glass windows, glass has great potential for automated color grading. Further research could expand the knowledge on using recycled glasses or testing cheaper glasses for their compatibility.

Multi-channel tool. Augmenting the robot with a multi-channel tool opens up new possibilities for various multi-property printing processes. The presented tool remains a first iteration and requires further development in terms of robustness, precision and variability of grain sizes.

Precision. Colors showed deviations from the intended results which require updating the color translation matrix. The precision of the process is lower than the one of multi-material printing processes due to the spreading of granules. This material behavior requires either further calibration of process parameters (e.g. surface distance) or the intentional implementation of process parameter dependent material behavior as part of a design tool.

Computational modeling. The computational methods applied allow for modeling and fabricating gradients between two or more properties and linking the digital and physical color model of the glass through a translation matrix. Deviations described above will require small adjustments of this translation. The use of other computational modeling techniques will allow the method to expand beyond printing of gradients to other multi-coloring approaches.

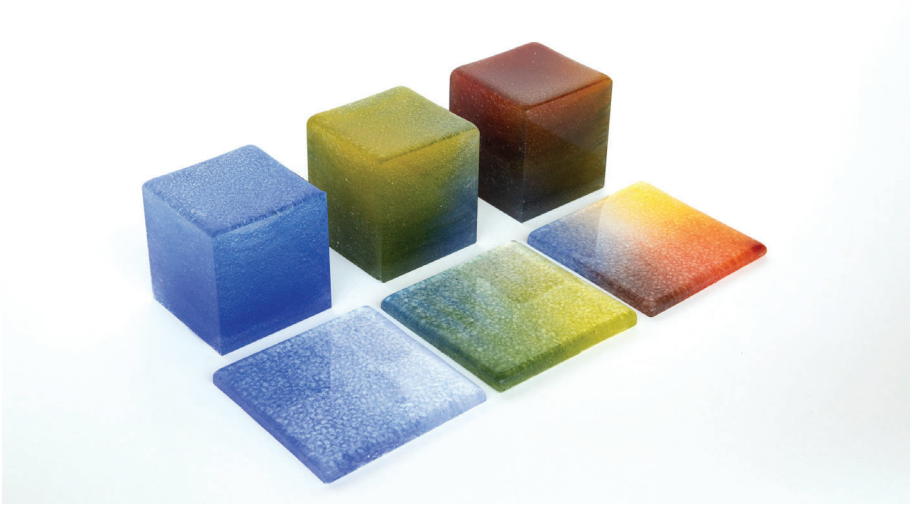

Figure 8. Tile and cube prototypes.

4. Discussion

The current results present a first small scale proof of concept for the possibility to automate the process of color grading. However, as the long-term goal of this research is to provide a manufacturing process for large scale applications, several steps need to be taken:

Material research. Glass research in a larger kiln will evaluate if the method is scalable to large elements with the current material system used, or if a change in glass type or size is required.

Molding. The process requires reusable ledges to keep the granular material in place during printing; further research will tackle mold-free printing.

Tool adaptation. Augmenting the robot with a multi-channel tool opens up new possibilities for various multi-property printing processes. The presented tool is a first iteration and requires further development in terms of precision, robustness and compartment size.

Computational design. Color patterns and color-form relationships can be explored in addition to process parameters and their implementation in a simulation tool.

Cost and accessibility. The fabrication process can be executed with a low cost tool attached to a motion system or universal robot and a conventional glass kiln. For up-scaling, further material and market research could contribute to more economic solutions for glasses and decrease cost.

Speed. The relatively high speed of the process increases the probability of applying it at large scale.

Architectural application. This research opens up a wide design space that could include facade elements, windows or interior separations.

The steps above could lead to large architectural elements that filter daylight and view through locally differentiated properties such as colors and opacity in an unprecedented manner, animate architectural space dynamically through controlled light conditions and produce sophisticated color effects in space.

5. Authorship Information Statement

Giesecke and Michopoulou are both equally first authors of this paper as they contributed equally to the written content including abstract, introduction, methods, results and discussion. Giesecke has provided the research framework based on initial material research executed, formulated the research topic, and supervised the experiments and tool development. Michopoulou has provided further material research and tool development. W. Van den Bulcke has developed the tool and computational workflow, and provided the process parameters. Odaglia supervised the research experiments and provided the electro-mechanical components of the tool. Dillenburger has contributed to the contextualization of the research and edited the text.

Acknowledgements

1. Dr. Mathias Bernhard, ETH Zurich, Computational modeling consulting
2. Erna Piechna-Sotherby, Creative Glass Volketswil, Technical coaching for glass

References

"Herzog & de Meuron: Ricola-Europe SA, Production and Storage Building Mulhouse-Brunstatt" : 1996. Available from <www.herzogdemeuron.com/index/projects/complete-works/076-100/094-ricola-europe-production-and-storage-building.html> (accessed 18th July 2020).

"The Metropolitan Museum of Art: Stained Glass in Medieval Europe" : 2000. Available from <http://www.metmuseum.org/toah/hd/glas/hd_glas.htm> (accessed 22nd September 2020).

Baty, P.: 2017, *Anatomy of Color. The Story of Heritage Paints and Pigments*, Thames & Hudson, London.

Chambers, K. and Oldknow, T.: 1999, *Clearly Inspired: Contemporary Glass and Its Origins*, Pomegranate Communications, San Francisco.

Doubrovski, E. L., E.Y., T., D., D., Geraedts, J. M. P., Herr, H. and Oxman, N.: 2015, Computer-Aided Design Voxel-Based Fabrication through Material Property Mapping: A Design Method for Bitmap Printing, *Computer-Aided Design*, **60**, 3-13.

Giesecke, R.: 2018, "Grading Color and Translucency in Glass" . Available from <https://dbt.arch.ethz.ch/research-stream/grading-material/> (accessed 3rd May 2020).

Gossett, N. and Chen, B.: 2004, Paint Inspired Color Mixing and Compositing for Visualization, *Proceedings of the IEEE Symposium on Information Visualization*, 113-118.

Griffith, B.: 2014, *Kiln-formed Glass: Beyond the Basics*, Lark Crafts, New York.

Grigoriadis, K.: 2016, *Mixed Matters: A Multi-material Design Compendium*, Jovis, Berlin.

Hoffmann, B.: 2012, Ceramic Digital Printing - Customized Glass Facade Design, *Challenging Glass 3*, 943-955.

Reynolds, G.: 1987, *The Fused Glass Handbook*, Hidden Valley Books, Arizona.

Wight, K.B.: 2011, *Molten Color: Glassmaking in Antiquity*, Springer, Los Angeles.

Wylie, E. and Cheek, S.: 1997, *The Art of Stained and Decorative Glass*, New Line Books, New York.

ROBOTIC WEAVING OF CUSTOMIZABLE FRP FORMWORKS FOR LARGE-SCALE OPTIMIZED STRUCTURE

GUANQI ZHU[1], YA OU[2], DINGWEN BAO[3] and DAN LUO[4]
[1,4]*School of Architecture, The University of Queensland, St Lucia, Queensland 4072, Australia*
[1]*guancizhu66@gmail.com* [4]*d.luo@uq.edu.au*
[2]*School of Civil Engineering, Central South University of Forestry and Technology, Changsha 410004, China*
[2]*ya.ou@uqconnect.edu.au*
[3]*School of Architecture and Urban Design, RMIT University, Melbourne, Victoria, 3000, Australia*
[3]*nic.bao@rmit.edu.au*

Abstract. This research presents a novel method of robotic fabrication for customizable fiber-reinforced polymer (FRP) tubular formworks, which also function as reinforcements for large-scale structural components. This process is achieved by the spatial weaving of FRP fabric driven by a robotic arm, and calibrated with the fast-cure resin which is applied on the fabric and cures during the weaving process so the fabricated structure is self-supporting and the structure is formed in an additive manner. With this method, structural members with changing sections can be customized and fabricated rapidly with off-the-shelf materials, following a system of structural reinforcement that has been widely adopted in the construction industry and promotes new applications of construction robotics.

Keywords. Robotic fabrication; fiber reinforced polymer; structural topology optimization.

1. Introduction

Continuous studies in the structural design and topology optimization bring out the demand for the fabrication of customized structural components. Rapidly and cost-effective production of structural components have become increasingly important for the implication of optimized or formally dynamic structure systems in construction.

In the current construction projects, most of the non-standard components are fabricated via customized formworks. Time and financial cost of customizing formworks and the additional burden of transportation limit its general application. Additive manufacture, such as 3D printing, provide mass customization of non-standard components without formworks. However, as an emerging method, 3D printing faces great challenges in the process of being integrated into the workflow of the traditional construction industry. The disassociation between 3D

PROJECTIONS, Proceedings of the 26th International Conference of the Association for Computer-Aided Architectural Design Research in Asia (CAADRIA) 2021, Volume 1, 573-582.

printing technology and traditional construction technology makes 3D printing difficult to be applied to large-scale traditional construction projects with the current workflow.

Based on the FRP arch bridge system developed by the University of Queensland (Burnton et al. 2019), this paper proposes a fabrication method via an additive process FRP wrapping. In this arch bridge system, the prefabricated FRP tubes serve both as formwork for concrete casting, but also provide structural reinforcement. Based on the analysis of this constructed structure, this study explores the implementation of an industrial robotic system to explore the potential of FRP fabrication in terms of both geometrical freedom and flexibility for on-site fabrication, including improving the material efficiency and increasing the compatibility with the existing system. At the same time, cost and time are also important to consider.

Compared with existing construction method like 3D printing, it has the following advantages:

1. The wrapping path is planned and controlled by the robotic arm, allowing the components with diversified curvature and unconventional sections manufactured via the same process and cost.
2. Using FRP fabric role instead of FRP fiber strings effectively improves the fabrication efficiency. On the basis of the same knitting operation mode, the increase of material area also means more areas can be covered in a short time.
3. In the fabrication of large-scale components, the combination of cured FRP mold with epoxy resin offers additional reinforcement to the casted structure, and the bearing range is larger than 3D printing mode, which indicates the better mechanical performance of materials.
4. The fabricated FRP formwork is developed from an established construction system. Comparing with 3D printing, the compatibility of components fabricated by FRP is more feasible, and the assembly process will be effectively reduced.
5. FRP braided formwork will also act as a part of reinforcement after concrete casting, which avoids the waste of traditional formwork and improves the efficiency of materials.
6. The application of the industrial robot allows the possibility of on-site fabrication so as to reduce the transportation cost and avoid the transportation risk to a certain extent.

In this research, as a preliminary feasibility study, we used a Kuka KR900 robotic arm to fabricate two prototypes, Figure 1, proving the capacity of this method to additively manufacture formworks with a non-uniform cross-section and dynamic flow of profiles. With the two prototypes, we have in principle established the feasibility and flexibility of this system, which will lead to the future development of more elaborate prototypes in full-scale architecture.

2. Background

FRP has been widely used in the construction process at this stage. It is an established technology to rap and laminate FRP fiber to the surface of components for strengthening the original structure (Trung et al. 2015). Recently,

concrete-filled FRP tubes (CFFTs) are becoming a common construction method shown in Figure 2 (Yu et al. 2006; Wong et al. 2008). In CFFTs, concrete-filled with the FRP section plays the role of structural reinforcement. In the load-bearing system, the concrete and FRP reinforcement compensate each other in terms of material properties. At the same time, FRP tubes also serve as a corrosion-resistant protective layer to effectively extend the life-span of concrete, and this characteristic is widely applied in bridge piers, offshore piers, etc. (Qasrawi et al. 2015; Fam and Mandal 2006).

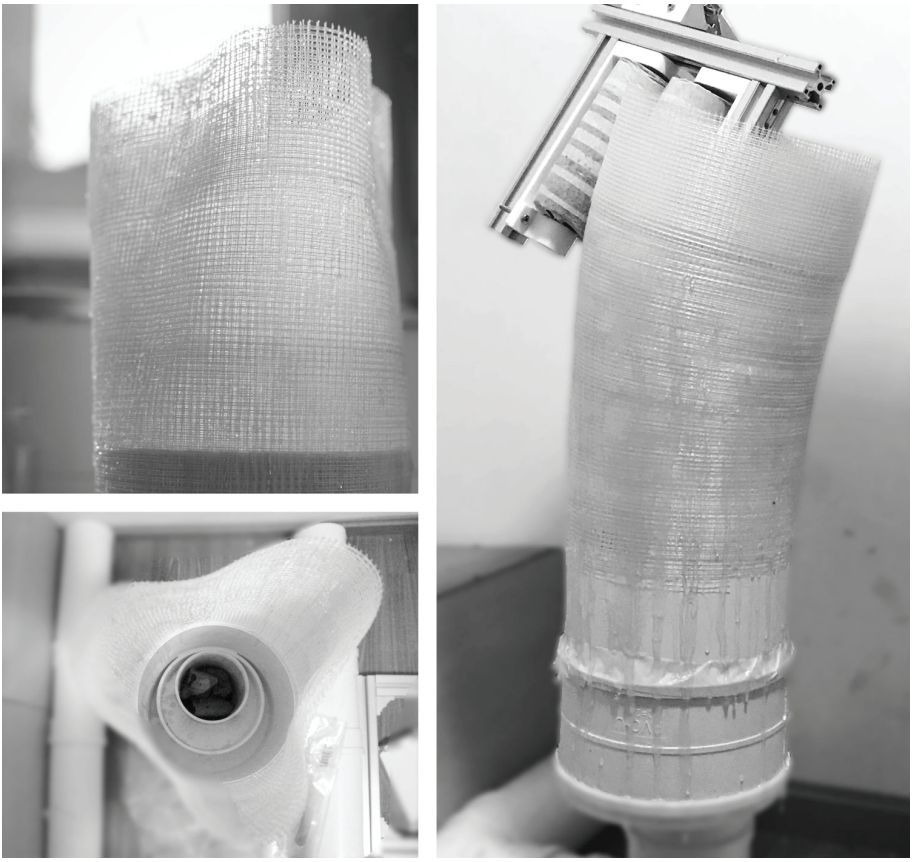

Figure 1. Left: prototype B, a tube with changing section. Right: prototype C, a tube with changing direction. .

Recent studies on structural optimization have proven that the material efficiency can be significantly improved by using topologically optimized irregular sections in replacement of the conventional sections. Within the last decade, a dynamic approach using the Finite Element Analysis (FEA) has been developed for structural optimization. This technique seeks the most efficient use of material by altering the shapes and topology and geometries of the buildings

and their structural components. The optimized structures are featured with non-uniform cross-sections along the member span or height, such as the tree-like structure exhibited at 2019 IASS Form & Force Expo (Bao et al. 2019). FRP is found to be a promising material for irregular profiles because of its flexibility. However, as concluded above, fabrication of irregular structural components with conventional manufacturing techniques remains a challenge.

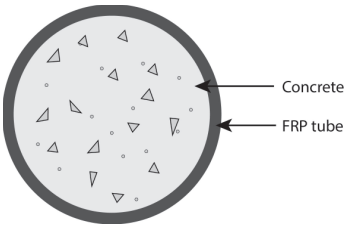

Figure 2. Cross-section of the concrete-filled FRP tubes (CFFTs).

The customized large-scale components have been intensively studied with the emerging technology of 3D contour crafting (Lloret and Shahab et al. 2015). However, in addition to the restriction of cost and speed, many of the current concrete printed components are restricted in terms of structure strength due to the difficulty in reinforcement and joinery. In term of compatibility with current construction process, fabricating formwork for concrete casting has significant advantage over direct 3D printing. Brian Peters from Kent State University has investigated a method of using patented fused deposition modelling (FDM) for fabricating formwork (Peters 2014). His research exposed the challenging aspect of expanding from small scale to large structure scale formwork due to hydrostatic pressure exerted by the concrete. Submillimetre Formwork project (Burger and Lloret et al. 2020) from ETH Zurich provide another alternative of using typical FDM robotic printing to fabricate formwork while simultaneously casting into it. However, the formwork in those cased serves as a means to the end for casting concrete, raising the challenge of material efficiency and integration.

Following the concept of additive fabrication and the precedence in FRP weaving, this paper presents a novel fabrication method for the mold/mandrel-free FRP tubular sections, providing a feasible method for on-site fabrication of customizable formwork for optimized structure members with non-uniform cross-sections.

3. Experiment workflows design

This experiment mainly focused on challenging two unconventional FRP forms: variable cross-section and variable mandrel, which are the two major types of non-standard form. The outcomes are able to propose the possible construction solution strategy of the BESO structural analysis result.

3.1. ROBOTIC SYSTEM DESIGN

3.1.1. End effector / working radius

In this experiment, a KUKA KR900 robot was deployed and it's working area can meet the size requirement of the final outcomes (300mm * 300mm * 800mm), Figure 3. An end-effector was developed to guide the fabric waving and to carry the GFRP roll. In this preparation phase, the size of the end-effector is designed to carry a 50m long, 100mm wide fiber fabric roll, which is enough to extrude an 500mm tall column with an average diameter of 200mm. The current end-effector requires a 120mm clearance on the inner side of the tube to operate, which restricts the minimum diameter of the column to be 120mm.

At the left side of the end-effector, a pair of passive sponge rollers were set to rotating along the outer side for positioning and ensuring the accuracy of sections, and one supporting aluminum profile is designed to hold the fiber fabric in a passive way. By adjusting the gap between two sponge rollers can tighten the fabric and provide pressure on the newly-weaved fabric, so it is fully appended to the previous layers and socked with the resin.

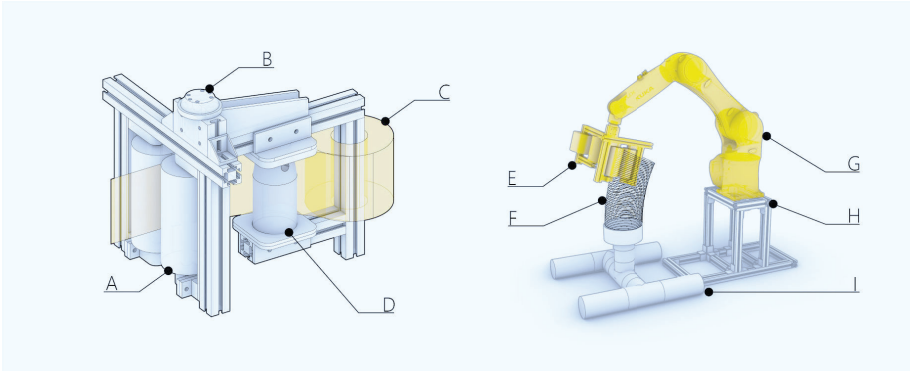

Figure 3. The end-effector and working environment. (A) Passive roller. (B) Head of the end-effector, connected to KUKA. (C) FRP roll. (D) Epoxy resin dispenser. (E) End-effector. (F) Path for wrapping FRP. (G) KUKA KU6 R900. (H) Base for robotic arm. (I) PVC platform.

In the middle of the tool, a bottle fixed to the aluminum profiles was set to hold the resin and gluing the fiber belt by three small holes automatically. So, when the fiber belt slide forward to the sponge rollers, it will pass through the resin storage bottle and will be gradually tainted by resin. The big hole on the top of the bottle was designed to refill the resin quickly.

3.1.2. Endless axis

The working path of the weaving end-effector demands a dedicated designed path. It has to be ensured that there is no collision with the surrounding work environment, the existing FRP tubular, and the KUKA robot itself. Besides, the working process of weaving FRP seems like wrapping up the fracture patient,

which means the trail of the fiber belt should be a continuous trail rotating around the mandrel. Therefore, the A6 axis of the robot arm was set to the endless mode so as to break the normal angle limitation between +175 and -175 degrees. Figure 4 demonstrates the FRP weaving process.

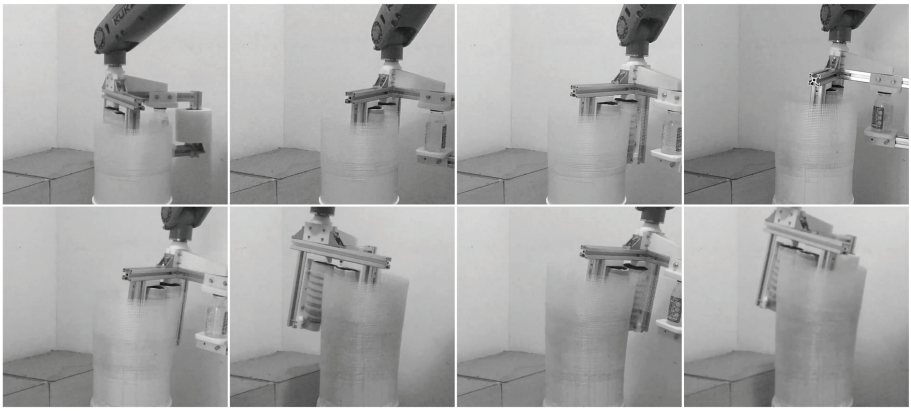

Figure 4. The sequential process of the robotic weaving method.

3.2. CRAFT TECHNIQUES

3.2.1. Calibration

The experiment is a continuous process, where the fiber fabric was rotating along the mandrel from beginning to end. Even a little error or fault will lead to the accumulation of errors, Figure 5. Normally, the deviations come from two aspects: the end-effector of the robotic arm and the platform in the working environment. The first one is able to be calculated and calibrated by the preset program in the robotic arm, just following the guide in the controller one by one manually. However, the latter one is hardly noticeable in the working space, where the floor may not precisely horizontal and the platform may not parallel to the KUKA robot. All the deviation is inconspicuous that is hard to be noticed by eyes- maybe just several degrees. Thus, an efficient way to fix the problem is remapping the coordination of the physical world to the digital model. By detecting three points along the outside of the PVC pipe, a series of coordination will be input in the Rhino so as to define a circle with a plane. When exporting the path-planning program for the KUKA robot, the deviation that comes from the ground slopes will be calculated. Therefore, before the experiment, the calibration of the end-effector is significant to the accuracy of the final outcomes. In order to test the accuracy of the system setting and the tool calibration, a circle drawing program was applied to test.

3.2.2. Platform

The fabrication platform was made of PVC pipes with two diameters. The 110mm one was used for the platform support, and the 200mm one was used for connecting

with the FRP as the foundation of the tubular. The PVC pipes and the relevant accessories such as the tee-junction are easy to achieve from the construction material market and convenient to assemble according to the design paper. The structural performance of the PVC pipes is strong and it is able to be replaced effortlessly after one of the experiments is finished. However, the lightweight of the PVC pipes is not firm enough to provide an immovable foundation, so the interior of the pipes was full filled with cobblestone.

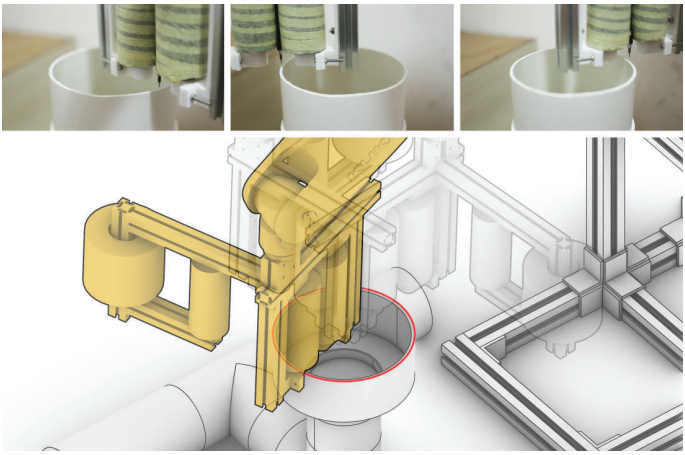

Figure 5. calibration and detection.

The PVC pipes only serve as a platform for the beginning part, which is similar to the brim layer in the normal 3d printing and it will be removed from the FRP after weaving. The cured resin is hard and strong, so the fret saw was used to split these two parts.

3.3. MATERIAL PROPERTIES

Commercial bidirectional glass fiber fabric with 100mm width and 150 g/m2 was used for this study. The fabric has a plain-woven structure with a count of 3 threads/cm in both warp and weft directions. The mix ratio used in this experiment was 100: 2 by weight for the epoxy resin and hardener. The prototype was fabricated in the indoor environment with a temperature of 15 degrees, a 100g resin was used in each mix, and the pot life (working time) was about 20 mins before the viscosity of the mix is too large to be applied by brush. When fabricating a cylindroid form, all the fiber fabric is spread on the mold neatly. However, the fiber fabric is not an elastic material. So, when wrapping a non-standard form, the gaps between layers are obvious, resulting in a deviation from the final outcomes, Figure 6.

Besides, the number of fabric layers at each cross-section of the tube is critical for the success of the fabrication process. When the layers are not enough, the stiffness of the tube would be too small to hold the top layers during weaving, while if too many layers of fiber are used, the fabrication time would be prolonged

and the material efficiency is reduced. In this application, a series of trials have been conducted to find the balance between the construction speed and section stiffness. A result of 15 layers of GFRP fabric in each standard section was found to provide adequate support for the upper layers.

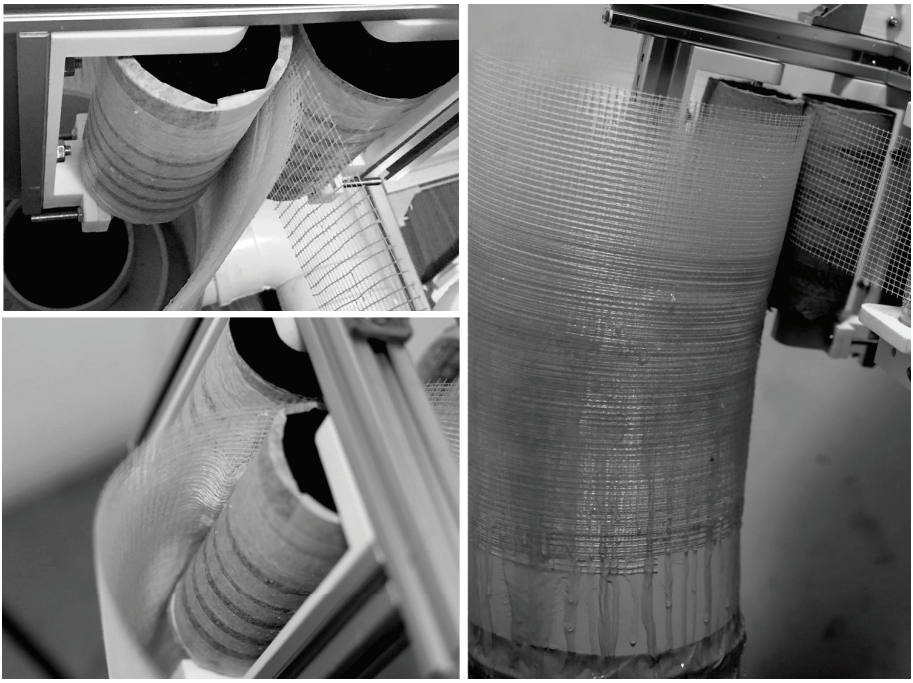

Figure 6. Left top: Gaps between layers. Left bottom: Deviation accumulated. Right: The uneven finished surface .

3.4. EXPERIMENT SUMMARY

A series of tests have been carried out with two non-standard FRP form components that were fabricated to explore an appropriate combination of resin curing time, speed of movement, and the number of layers. Based on the experiments, several limitations are concluded for FRP robotic fabrication:

1. The resin cure time will influence the efficiency of the experiment. In the normal room temperature of approx. 25 degrees, the new wrapped fabric should be cured for approximately 45mins. However, the temperature is changing in a day, so the cure time varies from 30mins - 60mins. Especially in the variable cross-section experiment, the experiment will stop waiting for the resin cure at three significant transformation points. Therefore, how to decrease-curing time of resin should be explored in the future.
2. The size of the end-effector and the height of the fiber fabric affect the variation of the variable cross-section FRP. It is as same as the concept of “DPI” which is commonly used to define the detail level of the screen. A smaller roller on the

inner side of the tubular will generate more details. So, the height of the fiber fabric is similar to the "height of layer" in 3d printing.

3. The ideal finishing surface should be smooth and shiny with an evenly applied resin. However, the uncured resin will flow down due to gravity, resulting in a rough outside surface of FRP, Figure 6.
4. The feasible FRP form for fabrication is limited because as a non-framework system, the stability during the weaving process is based on the weaved and cured FRP part.

4. Application in the fabrication of customizable structure component

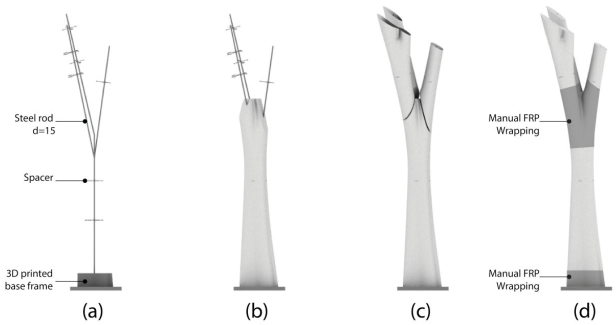

Figure 7. Assembly sequence: (a) inner structure, (b) weaving of the base, (c) assemble the branches, and (d) reinforcement with manual wrapping at the joint and base.

The robotic fabrication for customizable FRP formworks technology integrated with the BESO method has the potential to serve the building industry due to its capability of producing large-scale customizable structural components with high performance and low cost. Recently, the general solutions to fabricate the complicated surface in the practical architectural field are casting, planarization or 3d printing, etc. However, both of the methods mentioned above have their challenges. The planarization is often used in the double-curved curtain wall, but it is not self-supported because normally the panels are fixed to the metal support system. Although the 3d printing technologies have developed rapidly in recent years -many materials were employed in the research prototypes including concrete, PETG, or clay - the structural performance is still limited. So, the spatial FRP waving system proposed in this paper has more potential in the practical application, comparing with the other method.

Inspired by the tree branch shape columns in Sagrada Familia Basilica, the Bi-directional Evolutionary Structural Optimization (BESO) method offers the opportunities to mimic the morphology of biological structural system with a direct and rational connection between form and material (Mattheck 1998). Figure 7 shows the possible construction method of the tree branch system optimized by BESO algorithm.

5. Conclusion

This paper explores an innovative additive manufacturing technology to construct customizable FRP formworks for building structure, by integrating the advanced robotic fabrication and the dynamic FRP wrapping technique. In this research, two preliminary prototypes were fabricated and verified, proving the fabrication feasibility. This method will be extremely beneficial for the construction of topological optimized structures.

As a representative scenario, the experiment also demonstrates how the new digital design and robotic fabrication process collaborated together could effectively increase the cost, time, and material efficiency, while allowing more flexibility in the fabrication of the highly optimized non-standard structure. The proposed method is developed based on an established construction system and has the potential benefit of incorporating it into the existing construction process with minimum adaptation effort.

References

Bao, D.W., Yan, X., Snooks, R. and Xie, Y.M.: 2019, Design and Construction of an Innovative Pavilion Using Topological Optimization and Robotic Fabrication, *Proceedings of IASS Annual Symposia*, 1-8.

Burger, J., Lloret-Fritschi, E., Scotto, F., Demoulin, T., Gebhard, L., Mata-Falc'on, J., Gramazio, F., Kohler, M. and Flatt, R.J.: 2020, Eggshell: Ultra-Thin Three-Dimensional Printed Formwork for Concrete Structures, *3D Printing and Additive Manufacturing*, **7**(2), 48-59.

Burnton, P. and McDonnell-Arup, D.: 2019, Design and Construction of a Hybrid Double–Skin Tubular Arch Bridge, *Australian Small Bridges Conference, 9th, 2019, Surfers Paradise, Queensland, Australia*.

Burry, J., Felicetti, P., Tang, J., Burry, M. and Xie, M.: 2005, Dynamical structural modeling: a collaborative design exploration, *International Journal of Architectural Computing*, **3**(1), 27-42.

Fam, A. and Mandal, S.: 2006, Prestressed concrete-filled fiber-reinforced polymer circular tubes tested in flexure, *PCI journal*, **51**(4), 42.

Lloret Kristensen, E., Gramazio, F., Kohler, M. and Langenberg, S.: 2013, Complex Concrete Constructions–Merging Existing Casting Techniques with Digital Fabrication, *Computer-aided design*, **60**, 40-49.

Mattheck, C.M. and Mattheck, C.: 1998, *Design in nature: learning from trees*, Springer Science \& Business Media.

Peters, B.: 2014, Additive formwork: 3D printed flexible formwork, *ACADIA 14: Design Agency [Proceedings of the 34th Annual Conference of the Association for Computer Aided Design in Architecture]*, **60**, 40-49.

Qasrawi, Y., Heffernan, P.J. and Fam, A.: 2015, Performance of concrete-filled FRP tubes under field close-in blast loading, *Journal of Composites for Construction*, **19**(4), 04014067.

Trung, V.A.N., Le Roy, R. and Caron, J.F.: 2015, Multi-reinforcement of timber beams with composite materials: Experiments and fracture modeling, *Composite Structures*, **123**, 233-245.

Wong, Y., Yu, T., Teng, J. and Dong, S.: 2008, Behavior of FRP-confined concrete in annular section columns, *Composites Part B: Engineering*, **39**(3), 451-466.

Yu, T., Wong, Y., Teng, J., Dong, S. and Lam, E.: 2006, Flexural behavior of hybrid FRP-concrete-steel double-skin tubular members, *Journal of Composites for Construction*, **10**(5), 443-452.

AUTOMATIC ASSEMBLY OF JOINTED TIMBER STRUCTURE USING DISTRIBUTED ROBOTIC CLAMPS

POK YIN VICTOR LEUNG[1],
ALEKSANDRA ANNA APOLINARSKA[2], DAVIDE TANADINI[3],
FABIO GRAMAZIO[4] and MATTHIAS KOHLER[5]
[1,2,3,4,5]*ETH Zurich*
[1,2,3,4,5]*{leung|apolinarska|tanadini|gramazio|kohler}@arch.ethz.ch*

Abstract. This paper presents a novel robotic assembly method for timber structures with integral timber joints, specifically, crossed-half-lap joints. The proposed method uses a set of custom-built, remote-controlled, high-force robotic clamps to operate in collaboration with an industrial robotic arm to overcome challenges of robotic timber joint assembly, such as providing large assembly forces and correcting misalignments. This method enables automatic assembly of non-repetitive and spatially connected timber structures. We developed custom software for modelling, visualization and feasibility-checking for structures compatible with the proposed assembly method. As a proof of concept, we designed and robotically assembled a spatial frame structure (4.8 x 3.0m footprint, 3.4m tall) comprising 40 pieces of 100x100mm profile timber elements.

Keywords. Robotic Assembly; Spatial Timber Structure; Wood Joints; Distributed Robots.

1. Introduction

Robotic timber assembly concerns the use of easily-programmable robots for placing and joining timber elements. It is a rapidly advancing field in academia and industry that aims to construct timber components and structures through the use of programmable assembly robots. This paper focuses on the assembly of bespoke (aka. non-repetitive), spatial (aka. non-planar) timber structures with integral timber joints, in particular, crossed-half-lap joints.

Integral timber joints were used extensively in pre-industrial timber structures (Zwerger, 2015; Sobon 2002; Coaldrake et al 2006; Sato and Nakahara, 1998) and are still used today in large scale timber structures (SBA Tamedia, 2013). These connections are often spatially joined in different directions to create a stable structure. In the past few decades, industrial automatic joinery machines (Wieloch and Porankiewicz, 2010) had substantially lowered the cost of the otherwise labour intensive process of cutting intricate timber joints. These machines can be digitally programmed to cut different joint geometries at different locations along the length of the timber element. However, the assembly of these digitally machined timber components had so far been performed manually.

PROJECTIONS, Proceedings of the 26th International Conference of the Association for Computer-Aided Architectural Design Research in Asia (CAADRIA) 2021, Volume 1, 583-592.

Recent researches in robotic timber assembly often use robotic arms to manipulate timber elements to achieve spatial placement of timber elements (Thoma et al, 2018). The connections used in these precedence research tend to avoid form closure and instead use glue (Kohlhammer et al, 2017), screws (Thoma et al, 2018; Robotic Pavilion, 2016) and nails (Apolinarska et al, 2016). This research focuses on the assembly of integral timber joints without fasteners and addresses the following challenges:

1. **Large assembly force to overcome joint friction.** Timber joints are often designed to be tight-fitting to ensure structural rigidity. However, when the parallel faces of the lap joint rub against each other during joint closure, a large frictional resistance is created. This friction can vary widely due to surface roughness or misalignments, and can result in jamming. Traditional solutions to this problem include tapering the mating faces (avoid parallel faces) so that the contact on both sides is deferred to the very last moment.
2. **Simultaneous assembly of multiple joints.** The risk of jamming is particularly common when multiple tight-fit joints need to be inserted at the same time, e.g. one beam is joined to two or more others, in a kinematically constrained trajectory.
3. **Local and global accuracy.** The position of two mating elements have to be precisely aligned at the mating joint during assembly. Within a small range, this alignment can be guided by a chamfer at the expense of increased friction. However, in the case where multiple joints need to be aligned, the structure may have displaced or deformed in different directions, making large friction unavoidable.

2. State of the Art

Many researchers have demonstrated the versatility of a 6-axis robotic arm for spatial manipulation of long elements. Thoma et al. (2018) made use of two robotic arms mounted on linear axes for constructing modular timber houses. One arm can be used for temporarily supporting unstable elements, while another arm continues the assembly. Leder et al. (2019) used distributed robots to collaboratively transport and assemble timber elements, by attaching the robots to the partially-built structure, and using the timber elements as part of the robot's kinematic chain.

There have only been a few publications on robotically assembling tight-fitting joints. Robeller et al. (2017) used a 6-axis robotic arm to assemble tight-fitting tenon joints along the edge of cross-laminated wood veneer panels. However, they have only limited success using the robotic arm alone for the assembly and various external help (including a vibration device) was needed. They also experimented with a tapering angle and observed a reduction in assembly force. Apolinarska et al. (2020) applied reinforcement learning techniques to control robot arms for timber joint assembly based on contact forces. Their trained models allowed the controller to automatically adjust insertion movement strategy in reaction to collisions and friction.

3. Prototypical Setup

Our approach to solve the above mentioned challenges is to make use of distributed robotic clamps to apply a large clamping force at each mating joint in a synchronized motion. This approach separates the task of applying large assembly force from the task of manipulating timber elements in space. This allows the use of a low-payload robotic arm to perform spatial manipulation and in collaboration with as many robotic clamps as necessary to assemble an element with any number of joints. Below we explain our prototypical setup.

3.1. ROBOTIC CLAMPS

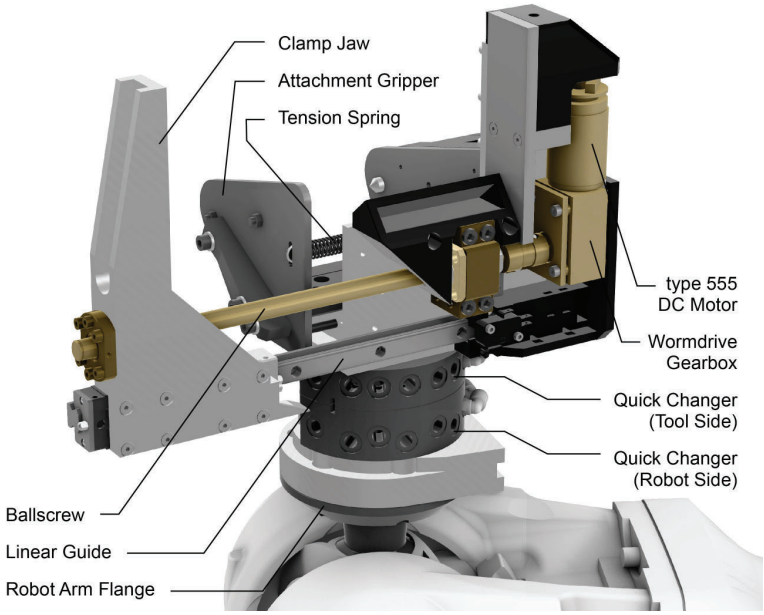

Figure 1. Major mechanical components of the clamp. The motion powertrain is highlighted in brown.

Each clamp is essentially a single-axis robot with a high force actuator that pushes a pair of lap joints together, and can be re-positioned by a robotic arm. Because different joints types (e.g. lap joints, tenon joints and splice joints) require very different clamping directions, they require different clamp designs. In this paper we focus on clamps for in-plane lap joints. The main features of the proposed clamps are wireless operation, ability to produce large force, synchronize to a motion profile, have a small size and low weight. In our demonstration, our clamps can produce 3kN force, move at 2mm/s and weight 4.9 kg.

The mechanical components of our demonstration clamp are shown in Fig.1. A spring-loaded mechanism allows the clamp to attach to the timber element by itself, allowing the robotic arm to detach from it (Fig.2a-b). The clamp jaw is

positioned across the lap joint and pushes on the opposite element. To enable non-standard structures, the clamp can accommodate joint angles from 25° to 90°, a mirror copy of the clamp accommodates angles 90° to 155°.

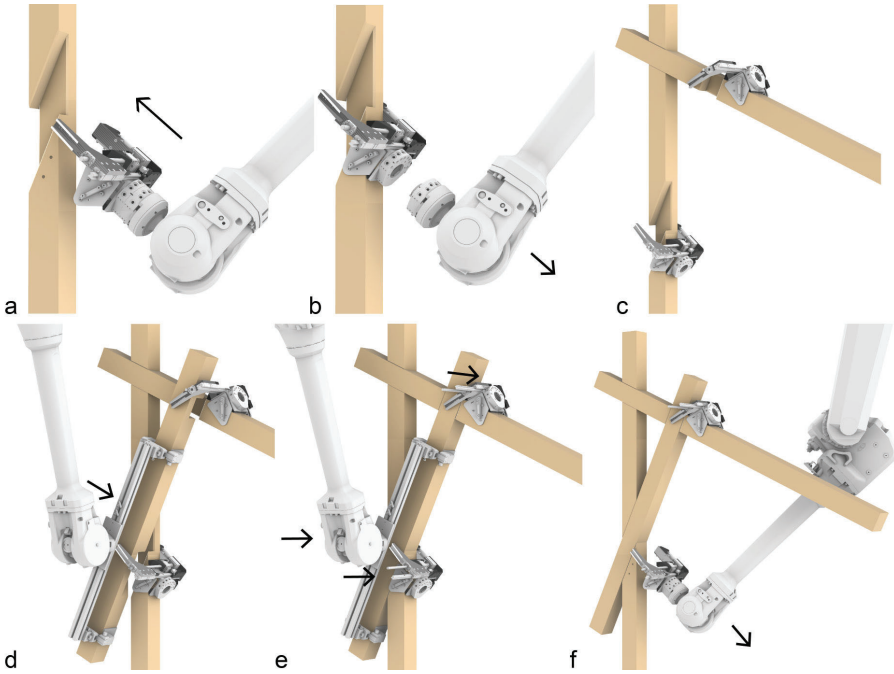

Figure 2. Robotic arm moving clamp to joint. (b) Clamp detach from arm. (c) As many clamps as necessary are placed. (d) Robotic arm brings a new element in the clamp jaw using a gripper. (c) Element assembled by arm and clamps. (e) Clamps removed by robot, one at a time.

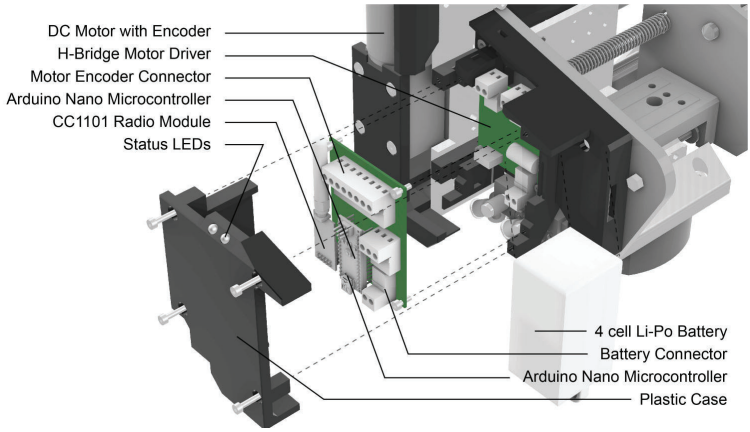

Figure 3. Major electrical components at the back side of the clamp.

In order to allow synchronized motion between multiple clamps and the robotic arm, the clamps are controlled by an Arduino Nano microcontroller (Fig.3). It drives a brushed DC motor with encoders for position feedback. To enable adaptive force output against variable resistance, the motor current is controlled by a 100Hz PID controller that minimizes instantaneous positional error to a motion profile. The wireless communication is based on a CC1101 digital radio transceiver operating in the 433MHz ISM band frequency for its ability to band around obstacles. All the clamps can be controlled from one computer equipped with the same transceiver to execute motions.

3.2. ROBOTIC ARM AND GRIPPER

The proposed assembly process requires a robotic arm with a reachability that covers the construction area (e.g. mounted on a gantry) and a tool changing system for changing between grippers and clamps. In our demonstration, we used an ABB IRB 4600 robotic arm, mounted on a custom 3-axis Güdel gantry system (operating within 8 x 8 x 6 meters envelope) and a Schunk SWS040 robotic tool changer. The robotic arm is programmed to be compliant in case of small misalignment. To pick and hold the timber elements, we used two grippers (500mm and 1m long), each containing two PGN-plus 100 parallel grippers with sandpaper lined fingers.

3.3. ASSEMBLY PROCESS

Elements are placed one at a time. For every element, the robotic arm places the clamps on the partially-built structure at every joint that needs to be connected to the next element (Fig.2c). After all the clamps are placed, the gripper is attached to the robotic arm, picks up the next timber element and places it into the jaws of the clamps (Fig.2d). The arm and the clamps then move synchronously to insert the element (Fig.2e). During this movement, the arm supports the weight of the element while following the assembly trajectory and the clamps provide the necessary force locally at each mating joint to overcome the resistance. This step repeats for all the subsequent elements after the arm relocates the clamps to the next joints (Fig.2f).

3.4. LAP JOINT DETAIL

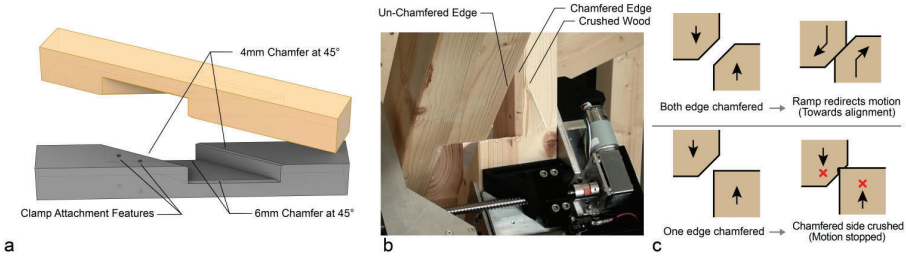

Figure 4. (a) Joint chamfer details used in our demonstration. (b) Photo showing failed attempt with crushed wood when only one side is chamfered. (c) Diagram showing misaligned edges being clamped together, highlighting the undesirable crushing behaviour.

To guide insertion in the event of misalignments, we chamfer the edges of first contact by 4mm and 6mm at 45° (Fig.4a), this amount is determined empirically to correct up to 6mm of misalignment. Note that it is not sufficient to chamfer only one side, as the "sharper" un-chamfered corner can crush the wood on the opposite side (Fig.4b-c).

4. Process Constraints and Computer-Aided Design

4.1. ELEMENTS, JOINTS AND SEQUENCE

In order to design structures that can capitalize on the proposed assembly method, considerations have to be made for (1) joint angles, (2) assembly sequence, (3) insertion direction (includes the orientation of the lap joint) and (4) room for collision-free robotic manipulation of clamps and timber elements. These decisions are interdependent problems and two approaches can be taken to ensure agreement between assembly sequence and the joints' design. The first approach ("Auto-sequence", Fig.5a) is to first design the structure with all joint geometry, and then derive feasible assembly sequence. The second approach ("Auto-joint", Fig.5b) is to design the structure by specifying the assembly sequence, and the insertion direction and then derive the joint geometry.

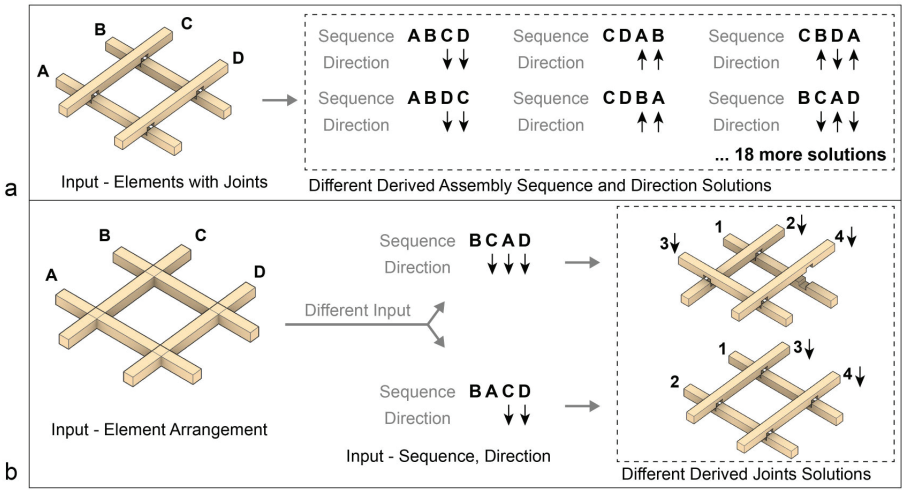

Figure 5. (a) Auto-sequence approach: Given elements arrangement and joints, different assembly-sequence-and-direction are possible. (b) Auto-joint approach: Given the same elements arrangement but different assembly sequence and direction, resulting in different joint geometry.

We opted to use the second approach for our demonstration because we find it more intuitive. In either method, there might be either none or multiple solutions. In case of no solution, the sequence or member arrangement have to be changed. In case of multiple solutions, one can be chosen based on structural requirements and robot accessibility.

4.2. PATH PLANNING

The timber elements can be grasped by the gripper from all four sides and at many possible locations along the element's length. These two decisions affect the pose of the robot when holding the element for assembly. Furthermore, each clamp can be attached to a joint in two possible orientations. For every joint and element that needs to be clamped, the robot arm requires a continuous path that goes through the following key waypoints without collision between the robot arm, the tools, the already-placed timber elements and the element in motion.

- **Attach each clamp:** (1) Clamp storage approach, (2) target, (3) retract, (4) Clamp attachment location approach, (5) target and (6) retract.
- **Attach timber element:** (1) timber pickup approach, (2) target, (3) retract, (4) timber approaching clamp, (5) placement inside clamp jaw, (6) assembled, (7) empty gripper retract.
- **Detach each clamp:** Reverse sequence of attaching clamp.

4.3. SOFTWARE SETUP FOR DESIGN AND FABRICATION

To assist the design process, we developed custom software to run in Rhinoceros 6 using the COMPAS 0.16 framework (Van Mele 2021). A designer can model timber elements with the Rhino user interface and specify their assembly sequence, assembly direction, attachment position of clamps and grasp pose for grippers. It allows designers to visualize different steps of the assembly process by displaying the partially assembled structure, the active element being assembled and tools involved. The software checks at design-stage if assembly is feasible (all parts are insertable without collisions, given the sequence and joint geometry). Next, it calculates continuous motion paths for the robotic arm by using the path planning functionality of the COMPAS FAB (2018) library. If no valid path is found, the designer can then choose to modify the location of timber elements, the assembly sequence, selecting a different clamp attachment orientation or a different grasp pose.

5. Demonstration

As a proof of concept, we designed a spatial frame structure (4.8 x 3.0m footprint, 3.4m tall), featuring lap joints at different angles (25°-155°). It comprises 40 pieces of 100x100mm profile elements, ranging from 1.7 to 3.4m in length, made of GL24h grade glue-laminated spruce (Fig.6), produced by a Hundegger ROBOT-Drive joinery machine.

5.1. STRUCTURAL DESIGN

The structure consists of seven structural frames (in parallel, vertical planes) that are 700mm apart, each consisting of five elements, and cross-braced in the opposite direction. All joints are modelled as stiff connections and supports can only transfer compression to the ground. We applied self-weight and lateral (e.g. wind) load from 24 different horizontal directions. The joints are assumed to withstand bending moments up to 1kN.

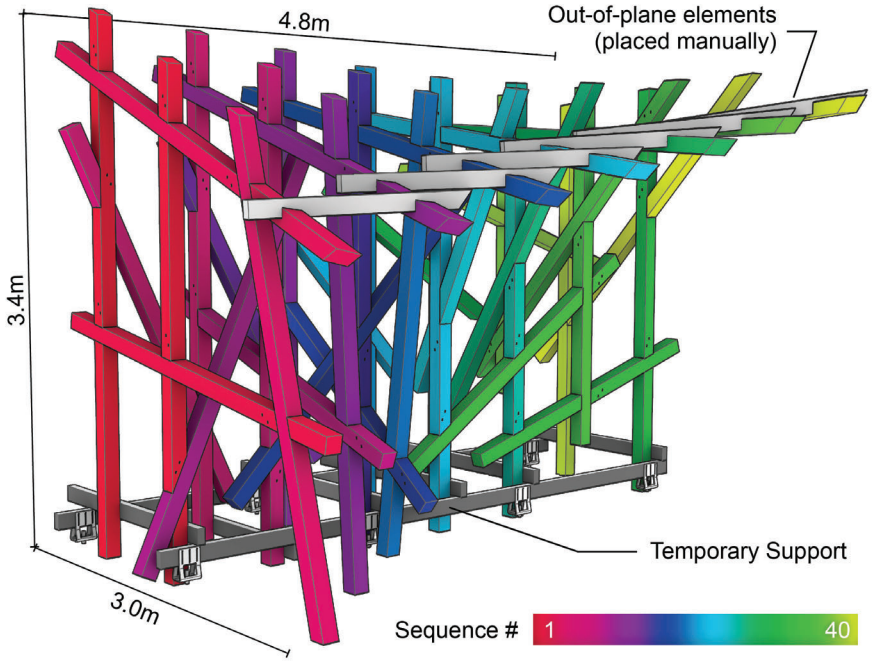

Figure 6. Diagram showing the demonstration pavilion, the colours represent the sequence of assembly; Six non-structural elements that are not robotically assembled (light grey); Temporary foundation during assembly (dark grey).

5.2. EXECUTION

The assembly process is executed by a desktop computer streaming pre-computed movement waypoints to the robotic arm, the gantry system and the clamps over a ROS network created by COMPAS FAB. For the joint closure movement that requires synchronization between the robotic arm and the clamps, the computer schedules the movements commands at the same time and constantly monitors the position of the two systems.

We manually placed the timber into the gripper, performed the tool change and attached carpentry clamps between the structure and the temporary foundation. This allowed us to reduce our experiment setup time. At the current stage, we also placed the clamps manually, with the aim to robotize this process in near future. The entire structure was assembled in a total of 24 work hours (Fig.7a), 4 hours of which involved machine operation (approximately 6 minutes per element).

5.3. OBSERVATION AND DISCUSSIONS

During the execution, we have recorded the power output of the clamp (proportional to the force output) and the instantaneous position error. As an example, Fig.7b shows the recorded data for three clamps during the assembly

of one element. The small error (<0.1mm) yet high spike in output power (>2 times) shows the adaptive power control is able to keep the clamps in sync despite changes in friction.

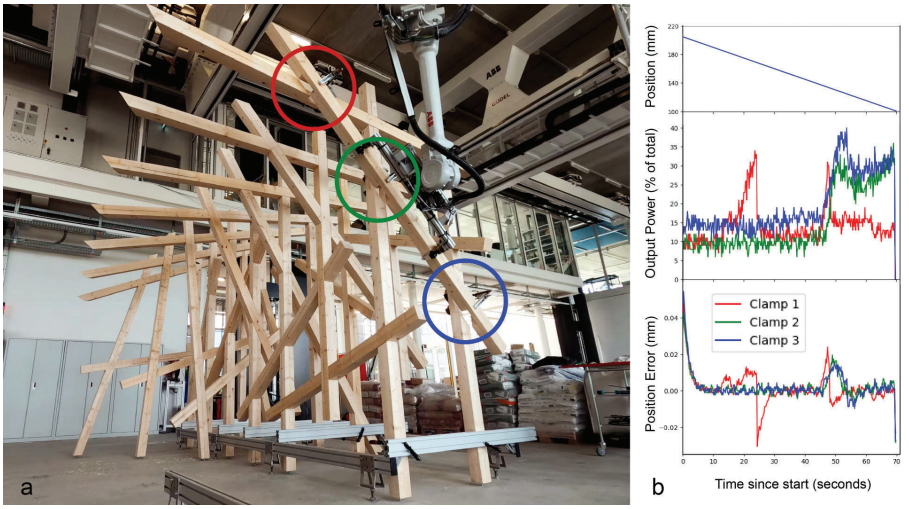

Figure 7. (a) Photo showing the final (40th) element being assembled. (b) Corresponding graph showing the clamp jaw position (left), power output (middle) and instantaneous error (right) during joint insertion.

The misalignment errors were larger than expected (> 6mm) at the beginning of the assembly. We believe this is caused by low joint stiffness, weak connection to the temporary foundation and insufficient cross-bracing. After the first two frames (12 elements) were assembled, misalignment amount falls within the ±6mm as predicted. Future work should attempt to improve the initial stiffness.

We have encountered a few collisions during assembly. Some are caused by a discrepancy between the real world and the digital model, specifically the temporary platform and the temporary clamps. Future work should be more diligent about their correct representation in the digital space. One collision is caused by an insufficiently high resolution setting in the motion planner. Two collisions are caused by the cable of the robot tangling with the structure.

6. Conclusion

We have demonstrated for the first time robotic assembly of spatial timber structures with tight-fitting joints using distributed robotic clamps, and showed that automated construction can extend to complex, non-standard structures. We have illustrated the decisions that need to be considered during the design stage and showed how it can be assisted by computational tools.

The concept of distributed, synchronized robotic clamps effectively addressed the problems of assembling integral, tight-fitting joints. In future works, the clamp design can be further developed to make them more universal and the remaining

manual tasks can be automated. This allows a designer to design, plan and execute an entire timber structure in a digitally streamlined process.

Acknowledgements

This research is supported by a doctoral fellowship in ETH Zurich and the Swiss National Centre of Competence in Research (NCCR) Digital Fabrication. We would like to thank Frederic Brisson for leading the design of the demonstration pavilion as part of his MAS Thesis (Brisson, 2020). We would like to thank Matteo Pacher, Yijiang Huang, Michael Lyrenmann, Philippe Fleischmann, and Gonzalo Casas for their technical assistance.

References

"SBA Tamedia" : 2013. Available from <http://www.shigerubanarchitects.com/works/2013_tamedia-office-building/> (accessed 1st September 2020).

"Robotic Pavilion" : 2016. Available from <http://gramaziokohler.arch.ethz.ch/web/e/lehre/309.html> (accessed 1 September 2020).

"COMPAS FAB: Robotic fabrication package for the COMPAS Framework" : 2018. Available from <https://github.com/compas-dev/compas_fab/> (accessed 1 September 2020).

Apolinarska, A.A., Knauss, M., Gramazio, F. and Kohler, M. 2016, The sequential roof, *in* A. Menges, T. Schwinn and O.D. Krieg (eds.), *Advancing Wood Architecture: A Computational Approach*, Routledge.

Apolinarska, A.A., Pacher, M., Li, H., Cote, N., Pastrana, R., Gramazio, F. and Kohler, M.: 2020, Robotic Assembly of Timber Joints using Reinforcement Learning, *Automation in Construction*, in press.

Brisson, F.: 2020, *Pushing the boundaries of integral joints in robotically assembled timber structures*, Master's Thesis, ETH Zurich.

Coaldrake, W.H., Seike, K., Yobuko, Y. and Davis, R.M.: 2006, *The Art of Japanese Joinery*, Monumenta Nipponica.

Kohlhammer, T., Apolinarska, A.A., Gramazio, F. and Kohler, M.: 2017, Design and structural analysis of complex timber structures with glued T-joint connections for robotic assembly, *International Journal of Space Structures*, **32**, 199–215.

Leder, S., Weber, R., Wood, D., Bucklin, O. and Menges, A.: 2019, Distributed Robotic Timber Construction: Designing of in-situ timber construction system with robot-material collaboration, *ACADIA 2019*.

Van Mele, T. and surname missing, initials missing: 2021, "{COMPAS}: A framework for computational research in architecture and structures." . Available from <http://compas.dev>.

Robeller, C., Helm, V., Thoma, A., Gramazio, F. and Kohler, M. 2017, Robotic Integral Attachment, *in* A. Mengen, B. Sheil, R. Glynn and M. Skavara (eds.), *Fabricate 2017*, UCL Press.

Sato, H. and Nakahara, Y.: 1998, *The Complete Japanese joinery*, Hartley and Marks Publishers.

Sobon, J.A.: 2002, *Historic American Timber Joinery: A Graphic Guide*, Timber Framers Guild.

Thoma, A., Adel, A., Helmreich, M., Wehrle, T., Gramazio, F. and Kohler, M.: 2018, Robotic Fabrication of Bespoke Timber Frame Modules, *Robotic Fabrication in Architecture, Art and Design*.

Wieloch, G. and Porankiewicz, B.: 2010, Computerised production line of carpentry products–processing centre Hundegger K-2, *Annals of Warsaw University of Life Sciences-SGGW*, **72**, 438-443.

Zwerger, K.: 2015, *Wood and Wood Joints: Building Traditions of Europe, Japan and China*, Birkhauser Architecture.

A DISTRIBUTED AGENTS APPROACH FOR DESIGN AND FABRICATING PROCESS MANAGEMENT AMONG PROTOTYPING PRACTICE ENVIRONMENT

CHI-FU HSIAO[1], CHING-HAN LEE[2], CHEN CHUN-YEN[3] and CHANG TENG-WEN[4]
[1,2]*College of Future, National Yunlin University of Science & Technology*
[1,2]*{chifu.research|chinghanglee}@gmail.com*
[3,4]*Dept. of Digital Media Design, National Yunlin University of Science & Technology*
[3,4]*{m10635013|tengwen}@gemail.yuntech.edu.tw*

Abstract. This paper develops a design and fabrication process management platform for prototyping practice environments using a robot operating system (ROS) framework, which we refer to as a fabricating operating service (FOS). The FOS executes a sequence of fabrication workflow that goes from materials handling, positioning, fabrication simulation, executing process to parts assembling. Each work phase is considered a different activity in the execution phase and a compact printed circuit board node to send and receive physical data. These nodes are registered onto an FOS cloud master, which distributes the node-to-node communication and links up the entire sequence of the workflow map. We propose FOS given that its loose, coupled, and distributed computation framework allows the fabrication team to visualize and record data using sharable ROS package structures. The FOS provides the advantage of easily creating additional tools, configurations, and automated scripts, and it increases the fabrication capabilities by simplifying and providing solutions for future robotic-aided fabrication development.

Keywords. ROS; prototype; node; fabrication workflow; .

1. Introduction

The process of prototyping helps fabrication teams communicate with one another. It's an efficient method for designers to use physical or virtual models to transform abstract ideas into concrete understanding. However, the development of a prototype practice environment (PPE) usually remains in the exploratory phase due to ill-defined design methods, implementation technologies, or experimental mechanisms. Thus, initial prototype production is relatively slow, and the development of a prototype process for subsequent versions will be even more time consuming.

The importance of prototyping speed according to the "seeing-moving-seeing" design thinking model is that a real-time feedback interface can help designers

PROJECTIONS, Proceedings of the 26th International Conference of the Association for Computer-Aided Architectural Design Research in Asia (CAADRIA) 2021, Volume 1, 593-601.

purify their ideas quickly and exchange experiment results and ideas with each other more easily (Schon and Wiggins, 1992).

Wesugi proposed another co-existing PPE experiment for interactive representation (shown in Figure 1[a]), called an Interactive Spatial Copy Wall (ISCW). An ISCW provides interplay movement tracing from virtual to reality via visual display processes. This early mix-reality (MR) PPE explains the design potential clearly, integrates designer behaviors, and design a mechanism details with immersive interplay workflow (Wesugi et al., 2004).

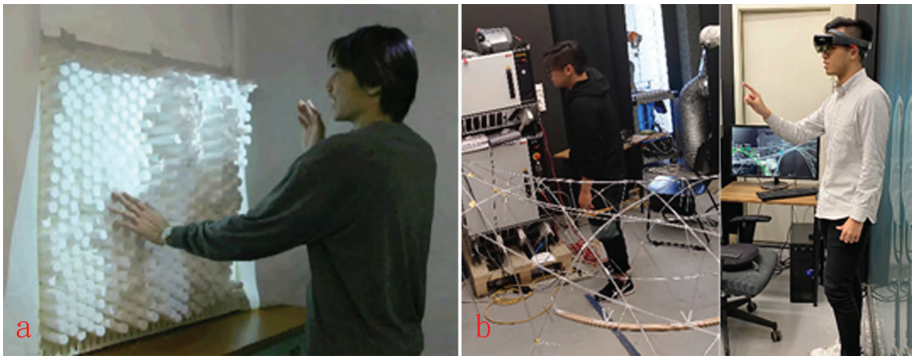

Figure 1. (a)ISCW, a physical interplay PPE(Wesugi et al., 2004), (b) Cofabs, gesture sensitive PPE.(Hsiao et al., 2020).

In order to accelerate development and manufacturing in digital design fabrication projects, Tsai-Ling Hsieh proposed the design-fabrication-assembly (DFA) system to help fabrication teams integrate designers‘ ideas and strengthen workers’ understanding. The DFA attempts to merge the fabrication phase and design decisions, enable team members to participate in the design process, and help the designer take control of PPE management (Huang et al., 2017).

As a conceptual framework, DFA uses a rapidly produced blueprint mechanism to help participators communicate with each other. Hsiao further applies an interactive co-existing PPE method based on digital twin, which is called the Cofabs method and is shown in Figure 1(b). Cofabs uses HoloLens to project the digital twin model (DTM) for users, it identifies designer gestures to command machine prompt scripts, and it generates future predictions for designers. This MR phase connects designer ideas and fabrication tools, which aligns virtual database and reality space with coordinators’ remapping systems. Furthermore, Cofabs not only records the recursive workflow of prototyping, but also provides the potential for optimizing the prototyping workflow (Hsiao et al., 2020).

In the Cofabs fabrication process, the prototype is physically divided into several nodes that are connected to each other so that the whole structure will morph when users change the position of even one node. Based on the Cofabs framework, nodes are calculated with a clearly matching, limited problem space and are able to share the same computing server. Because Cofabs pre-defined weaving fabrication as a simplified, clear, and predicable progress. However,

systems like ISCW, DFA, or Cofabs are not able to consider several practical variables, such as material handling, fabrication positioning, executing signals, the duration of parts assembly, etc. After all, Cofabs retrieves a real-time digital prototype with an immersive perspective, but it still requires more information from each node to complete the entire PPE fabrication sequence.

2. Distributed architecture of robot operating system (ROS)

To address the limitations presented in the last section, this paper proposes another agent-based fabrication process management platform for PPE based on the robot operating system (ROS) framework. The ROS framework is a kind of network architecture composed of distributed processing as agents, which uses sharable communication nodes and implements loosely coupled P2P network connections between functional micro control units.

The early ROS development team has presented the architecture philosophy of ROS as containing the following (Quigley et al., 2009):

1. A peer-to-peer communication system: The ROS encourages fanout messages between each node component. Although there are master mechanisms for coordinating and distributing information, the ROS preserves its loose coupled status to ensure the flexibility and adaptation of the system.

2. Multi-lingual development: The ROS is based on common basic grammar and uses neutral interface definition language (IDL) to achieve communication between different nodes, which helps nodes in the system connect with each other via different programming languages.

3. Tools-based: The ROS connects each smallest activity node modular, and each node is capable of communicating the distributed computing results to the master server.

4. Light-weighted: The ROS framework encourages the construction of modular tasks in the source code, and it uses CMake to encapsulate the complex mechanisms of all tasks in the client library.

5. Open-Source: The ROS encourages all users to share their own data kits for application in various working environments to improve adaptability.

Kousi applied the ROS framework and the DTM in automotive industry management, enhancing the synergy between the working environment and human behavior using a virtual interface and sensing mechanisms. He uses a variety of work state messages to communicate with mobile robotic arms and updates the status of the overall working environment using sensing components to improve supervision of the entire assembly pipeline (Kousi et al., 2019).

Kousi suggests that the integration of the ROS and the DTM in a practical manufacturing process indeed helps managers evaluate the efficiency of the staff. However, tasks that involve human-decision making are difficult to integrate into machine executing reflecting.

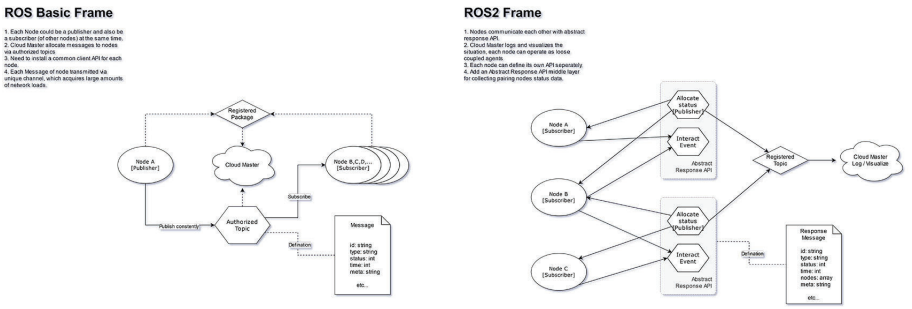

Figure 2. The different architecture between ROS and ROS2 framework.

In order to improve human and machine synergy in a real-time feedback chain, the ROS group has presented a new architecture called ROS2. The main differences between ROS1 and ROS2 are shown in Figure 2.

ROS2 cancelled the master server to improve the agent mechanism reflexing time and specifically attempted to enhance real-time performance by bridging the gap between prototypes and products. However, in Casini's compositional performance analysis (CPA) task, they modeled an ROS2 multiple callback chain and measured the underlying data distribution service (DDS) communication delay every time the network was crossed. They determined that ROS2 works fine in a stable operation, but in a continuously developing environment such as PPE, they suggest that ROS users implement complex communication primitives like the long-running and high-level actions from ROS1 relatively (Casini et al., 2019).

3. Fabricating operation service framework

The ROS framework is composed of a distributed processing architecture that uses sharable communication agents (referred to as nodes in the ROS concept) to implement loosely coupled P2P network connections between functional micro control nodes in PPE. Under this ROS architecture, we define a set of topics namespace, called a fabricating operation service (FOS), to aid the fabrication workflow sequencing in PPE, including materials handling, positioning, fabrication simulation, executing process, and parts assembly.

Each node in the FOS needs to be registered in a cloud server to set up node-to-node communication for PPE activities and update the states. Nodes can also send or receive messages in publish or subscribe mode using WebSocket protocol, and these messages can contain sensor data, G-code commands, state changes, specific coordinate positions, or anything else that is within the node's capability.

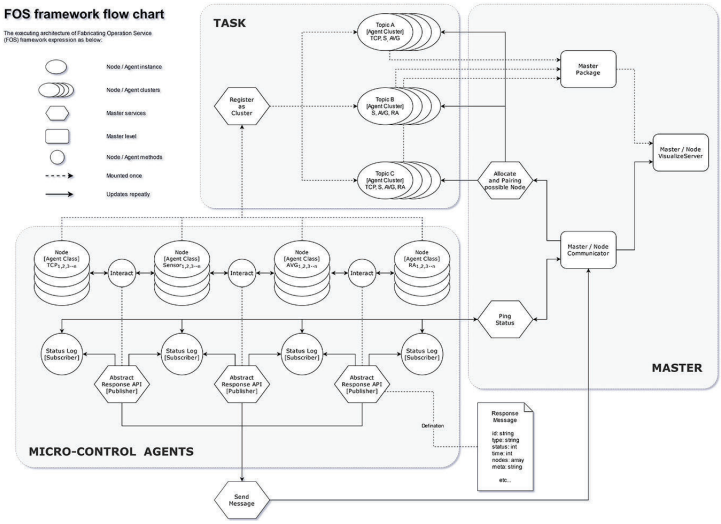

Figure 3. The FOS framework.

In the FOS, we defined the following three-node cluster thread to manage the fabrication PPE, as shown in Figure 3:

1. Physical nodes: include various 2D or 3D sensor elements and use ID and location tags for position determination. The sensor node cluster follows publish and subscribe protocol to provide notification on different topics and is capable of generating possible path planning for requesting resource.

2.Task nodes: include users, arms, various work sequences, etc. Each node defines different working conditions, includes global settings, and contains coordinate, path information or various custom action settings.

3. Master node: uses the DTM to classify the collision or contact state of assembled parts, then visualize the situation and help users update the execution status of the workspace.

The FOS provides a visualization interface for users to take care of nodes' cooperation situation based on a workflow design and fabrication perspective. The developed FOS is a computation graph framework that allows fabrication teams to visualize and record data in sharable ROS package structures.

4. Nodes in FOS

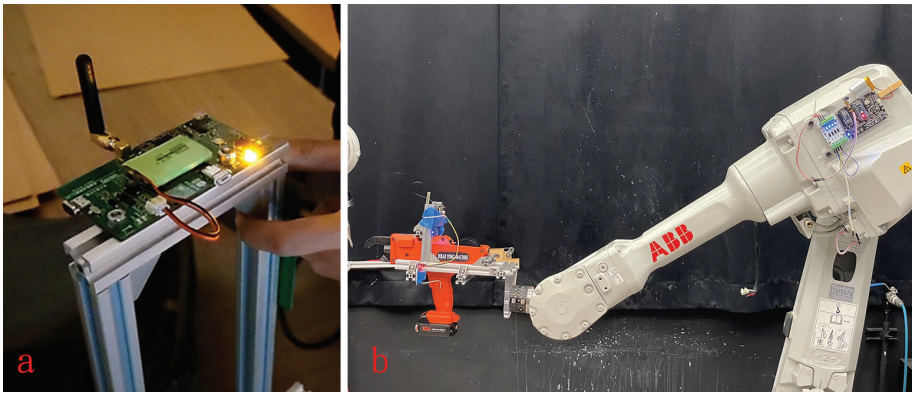

Figure 4. (a) Extendable universal PCB with wireless transmitting / receiving and power input module, (b) micro-controller nodes installed on robotic arm and tool head.

- Micro-controller with extendable physical nodes:

In the development of the FOS, we need to use a variety of different micro-controller modules for transmitting, computing, and receiving data. We physically installing them on the sensors, robotic arms, tool head, or automatic vehicle. Generally, there should be reference to micro-controller modules with various capacities, such as Ardunio, HC-12, DHT-22, HMI, etc. As the framework of the ROS, each micro-controller node must be connected, wired, and rewired based on its own required program. Therefore, we organized the requirements of the FOS and designed a universal module on a printed circuit board (PCB) layout unit, which can expand the capability of Ardunio by including an onboard button/slider, wireless transmission/receiving, an HMI human-machine interface, and wearable battery/external power (shown in Figure 4).

- Relative time stamp between task nodes:

In the FOS, each sensing node has different coordinate systems, and its status requires a mechanism for frequent comparison and conversion between its own respective coordinate and the world coordinate system. In order to avoid difficulties in troubleshooting and the loss of transmission packets, we further applied the ROS architecture's time-based transformation service into a node processing thread by adding the standard message header time stamp comparison task and correlating the before/after schedule within the server thread. This enables each publish/subscribe node cluster to ensure the synchronicity of the overall system.

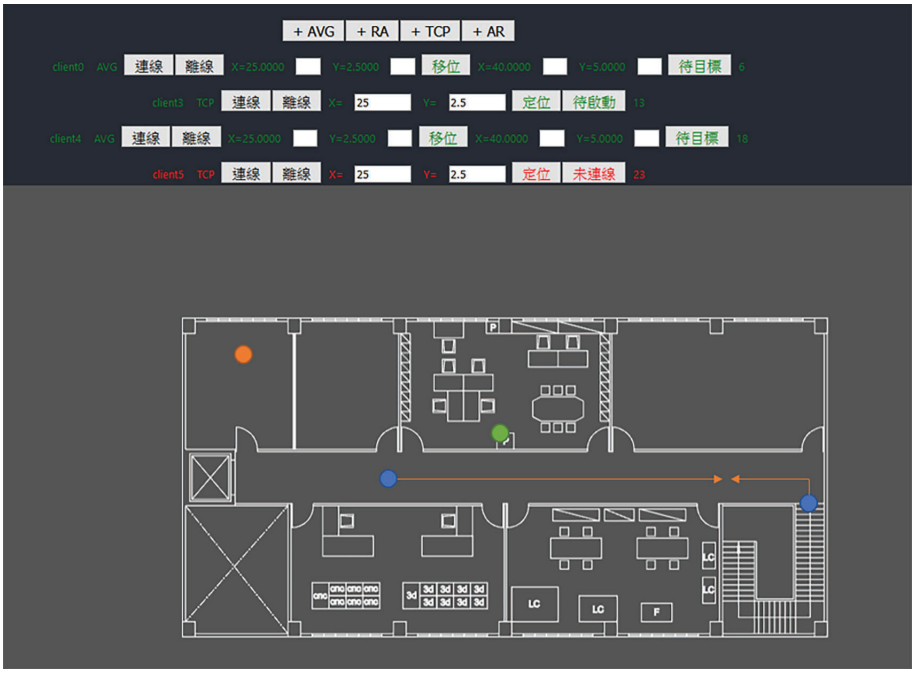

Figure 5. The FOS represents the node communication result via monitor ROS master and graphical remapping of the allocation of nodes.

- GUI of FOS master node:

We established and visualized FOS nodes, activities, statuses, and the field mapping interface to project the relativity of the virtual and physical situation of the PPE. The FOS was built using JavaScript and can be accessed by PPE users through an intranet, which will typically represent the node communication result in the ROS master. To improve the ROS built-in master system, the FOS not only provides naming and registration messages with text lines, but also provides a graphical mapping interface to identify the relative states. After users execute the FOS, a master server will launch and monitor the task workflow simultaneously. This GUI is responsible for keeping track of the nodes; when new nodes are executed and come into the system, they cannot communicate until the FOS master notifies the nodes of one others' existence. Thus, we provide a dynamic allocation mechanism for connections, and the FOS also determines the connection state or the major prompt command that a node executes. A simple example is shown in Figure 5.

- Pipeline arrangement of thread callback:

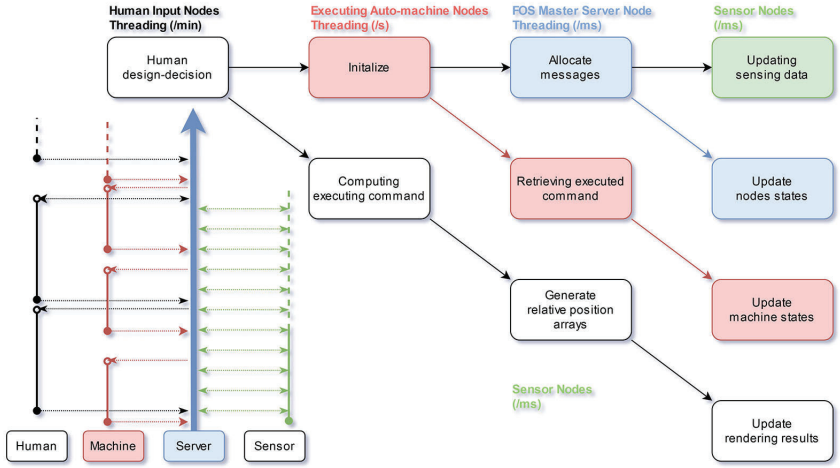

Figure 6. FOS callback thread pipeline arrangement.

The architecture of human-machine collaboration mainly uses software framework (SWF) planning, which divides the workflow into response times based on the cognitive response of human-computer interactions. This can result in well-defined, independent behavior modules that ensure performance.

Thus, the FOS divides the processing threads of the fabricating module into simulation and debugging, fault tolerance, security adjustment, usability and support interface, etc. While the ROS1 architecture needs to be coordinated by the master to distribute information transmission between multiple nodes, the FOS rearranges the node thread callback mechanism with the pipeline shown in Figure 6.

5. Discussion and Conclusions

This paper proposed an FOS based on the ROS framework that integrates services designed for a multifarious computer cluster, such as low-level embedded micro controllers, implementation of robotic arm controlling, message communication between execution threads, and log package supervision and management.

The FOS uses sharable communication WebSockets to implement nodes to connect physical PCB units in a piratical prototype environment. We have also planned a layout sequence for fabrication workflow, which includes materials handling, positioning, fabrication simulation, execution process, and parts assembly. Each node in the FOS is registered into a master server, setting up node-to-node communication messaging for prototype activities and updates on the states. The messages can use per-settled .msg files to transmit/receive sensor data, G-code commands, state changes, specific coordinate positions, or anything else according to the node's own capability. The FOS also provides a visualization interface for users to develop the agent cooperation situation under the design/fabrication workflow perspective.

The developed FOS is a computation graph framework that allows fabrication teams to visualize and record data in sharable ROS package structures. We propose FOS for its ability to easily create additional tools, configurations, and automated scripts, and its ability to increase fabrication capabilities by simplifying and providing solutions for future robotic-aided prototyping and fabricating environments.

References

CASINI, D., BLAï, T., UTKEBOHLE, I. L. and BRANDENBURG, B.: 2019, Responsetime analysis of ROS 2 processing chains under reservation-based scheduling., *ECRTS 2019*, 1-23.

HSIAO, C.-F., LEE, C.-H., CHEN, C.-Y. and CHANG, T.-W.: 2020, A Co-existing Interactive Approach to Digital Fabrication Workflow, *CAADRIA 2020*, 105-114.

HUANG, H.-Y., CHANG, T.-W., WU, Y.-S. and CHEN, C.-Y.: 2017, Collective Fabrication A Responsive Dynamic Skin Design Case, *CAADRIA 2017*, 99-100.

KOUSI, N., GKOURNELOS, C., AIVALIOTIS, S., GIANNOULIS, C., MICHALOS, G. and MAKRIS, S.: 2019, Digital twin for adaptation of robots' behavior in flexible robotic assembly lines, *Procedia Manufacturing, 28*, 121-126.

QUIGLEY, M., CONLEY, K., GERKEY, B., FAUST, J., FOOTE, T., LEIBS, J., WHEELER, R. and NG, A.: 2009, ROS: an open-source Robot Operating System, *ICRA Workshop on Open Source Software. 3*.

SCHON,, D. A. and WIGGINS, G.: 1992, Kinds of Seeing and their Functions in Designing, *Design Studies*, **13**, 135–156.

WESUGI, S., ISHIKAWA, K., SUZUKI, N. and MIWA, Y.: 2004, Interactive spatial copy wall for embodied interaction in a virtual co-existing space, *13th IEEE International Workshop on Robot and Human Interactive Communication*, 265-270.

ROBOTIC 3D PRINTING OF MINERAL FOAM FOR A LIGHTWEIGHT COMPOSITE FACADE SHADING PANEL

PATRICK BEDARF[1], DINORAH MARTINEZ SCHULTE[2], AYÇA ŞENOL[3], ETIENNE JEOFFROY[4] and BENJAMIN DILLENBURGER[5]
[1,5]*Digital Building Technologies, ETH Zurich*
[1,5]*{bedarf|dillenburger}@arch.ethz.ch*
[2]*Master of Advanced Studies ETH in Architecture and Digital Fabrication*
[2]*dschulte@student.ethz.ch*
[3]*Complex Materials, Department of Materials, ETH Zurich*
[3]*senola@student.ethz.ch*
[4]*FenX AG*
[4]*etienne.jeoffroy@fenx.ch*

Abstract. This paper presents the design and fabrication of a lightweight composite facade shading panel using 3D printing (3DP) of mineral foams. Albeit their important role in industrial construction practice as insulators and lightweight materials, only little research has been conducted to use foams in 3DP. However, the recent development of highly porous mineral foams that are very suitable for extrusion printing opens a new chapter for development of geometrically complex lightweight building components with efficient formwork-free additive manufacturing processes. The work documented in this paper was based on preliminary material and fabrication development of a larger research endeavor and systematically explored designs for small interlocking foam modules. Furthermore, the robotic 3D Printing setup and subsequent processing parameters were tested in detail. Through extensive prototyping, the design space of a final demonstrator shading panel was mapped and refined. The design and fabrication process is documented and shows the potential of the novel material system in combination with fiber-reinforced ultra-high performance concrete (UHPC). The resulting composite shading panel highlights the benefits of using mineral foam 3DP to fabricate freeform stay-in-place formwork for lightweight facade applications. Furthermore, this paper discusses the challenges and limitations encountered during the project and gives a conclusive outlook for future research.

Keywords. Robotic 3d-printing; mineral foam; lightweight construction; concrete formwork; facade shading panel.

1. Building with Foam

During the last two decades, large-scale additive manufacturing (AM) in construction gained considerable momentum in the research community and in

PROJECTIONS, Proceedings of the 26th International Conference of the Association for Computer-Aided Architectural Design Research in Asia (CAADRIA) 2021, Volume 1, 603-612.

industry (Lim et al. 2012; Delgado Camacho et al. 2018). These new fabrication technologies can contribute to more sustainable and lean construction processes. Most advancement has been reported in the field of 3D printing (3DP) for load-bearing applications with cementitious materials. However, the availability of sustainable materials in construction 3DP that address other important building-physical properties such as thermal insulation or water permeability remains limited. Only a few researchers investigated porous foam-like materials for this purpose. Expanding polyurethane foam was used to 3DP stay-in-place formwork for a dome structure (Keating et al. 2017) and a single-storey residential building (Furet, Poullain, and Garnier 2019). Other researchers printed with cement foams on existing masonry walls to improve their insulation performance (Lublasser et al. 2018).

Porous materials and in particular foams have a great legacy in architecture and construction because of their lightweight and thermal insulating properties. Already our Neolithic ancestors used natural porous materials like pumice and clay to insulate their dwellings. By the beginning of the 20th century the plastic revolution transformed the building industry with new high-performance materials such as synthetic foams (Engelsmann, Spalding, and Peters 2010; Faircloth 2015). Today synthetic foams such as polystyrene and polyurethane represent more than 41% of the European insulation market. However, synthetic foams come with considerable environmental and health concerns because they are based on finite resources and are highly flammable. In contrast, inorganic solutions such as aerated concrete and mineral foams are more suitable for environmentally friendly and safe construction. Novel sustainable solutions were developed recently and it was demonstrated that they can be used for 3DP (Minas et al. 2016; Dutto 2019).

2. Motivation and Project Focus

Most application methods of foams in contemporary construction practice are time and labor demanding, geometrically limited, and very wasteful. 3DP however, offers a lot of opportunities for automated fabrication of complex objects without extra cost, formwork, and production specific tooling. These advantages can be transferred into construction. This enables for instance geometrically complex freeform building elements made of foam that are impossible or unfeasible to produce with any other technique. The design space of modular foam blocks for architectural envelopes and formwork could be considerably extended. Furthermore, custom foam shapes would be traditionally manufactured with subtractive methods from large blocks, which produces a lot of waste. 3DP of foams would allow to increase the resource-efficiency through the formwork-free direct production of objects with a much higher degree of geometric complexity. The approach of large-scale 3DP with mineral foams in construction opens new perspectives for architectural design and sustainable construction. It fosters not only resource-efficiency but also the invention of novel lightweight building components. The combination of different densities as composite with foam as functional formwork makes building elements lighter and more versatile for different use cases.

Against this background, this project was conceived as a student design thesis

and investigated the use of mineral foam 3DP for fabricating brick-sized modules that can be assembled into an architectural-scale structure as lightweight facade application. Key research questions concerned the design of the assembly and modules as well as how the material and fabrication system can be leveraged as paramount design drivers. How can discretization and combinatorics inform modular architectures? How can the modules be joined, interlocked and reinforced? How does the 3DP and post-processing influence the design space? What kind of geometric limitations exist and how could they be overcome? The methods consisted of empirical exploration through prototyping and a final demonstrator. Iterative cycles of experiments combined design and fabrication with qualitative evaluation of the print results. After assessment, the print metrics, material and post-processing routines were optimized and module designs further refined. The evaluation of prototypes was of qualitative nature due to the available equipment, short project period, and anticipated result of a visually impressive architectural-scale demonstrator.

3. Material and Fabrication System

The mineral foam was fabricated based on the formulations developed by FenX AG. Industrial waste-based fly ash particles were mixed with water and modifiers. The resulting suspension was then vigorously foamed using a household mixer. After five minutes mixing, the foam was inserted into printing cartridges. Eventually, foams with wet densities ranging between 500 and 550 kg/m3 were obtained. After printing, the printed elements were dried at room temperature for a minimum of 48 hours and then hardened by sintering in a ceramic kiln. The sintering process consisted of a burnout period (450 °C for 2h) and a sintering period (1100 °C for 3h). The elements were then cooled down to room temperature.

For the robotic 3DP setup (Fig. 1, left), an existing stationary custom syringe extruder was used, which was developed during preliminary extrusion experiments with mineral foam. Decoupling the extruder from the robot allowed for developing it independently without payload or movement constraints. The 6-axis robotic arm used throughout prototyping and final fabrication was an ABB IRB 120 with a maximum reach of 580 mm and a payload of 3 kg. A 400 x 400 mm platform was mounted as a print bed end-effector with the fifth robot axis advantageously oriented downward for maximum payload performance (Fig. 1, right). Furthermore, durable 300 x 300 x 5 mm recrystallized silicon carbide (R-SiC) sintering plates were placed on the print bed for transport and furnace processing. They were chosen for their low weight since other conventional cordierite sinter plates resulted in exceeding the robot payload limitations during printing.

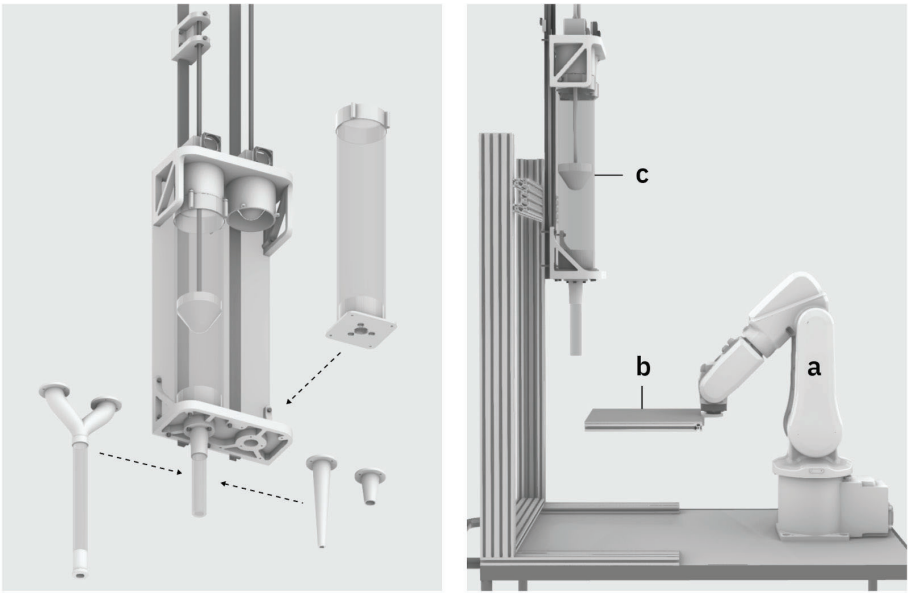

Figure 1. Left: dual syringe extruder with replaceable cartridges and nozzles. Right: robotic fabrication setup with a) ABB IRB 120, b) print bed end-effector, and c) stationary syringe extruder.

The stationary syringe extruder was a custom made tool for the controlled extrusion of batch-processed material. The development was inspired by many examples that can be found in the research literature of paste extrusion *(Seibold et al. 2019; Kontovourkis and Tryfonos 2020)*. Executed as a double syringe that is actuated by two independent linear drives, the extruder allowed for precise flow rate control and operations involving one or both material chambers. Each of them measured 90 mm in diameter and 500 mm in height with a volume of 3.2 L. The motors were controlled by an Arduino microcontroller and all extruder operations executed with a GUI application written in Java. No IO signals were sent or interpreted from the robot controller. The robot movement was programmed using the COMPAS framework and the COMPAS_RRC extension for online non-realtime control *("COMPAS" 2020)*. Target frames were generated as a JSON file from the CAD software Rhinoceros3D through a custom Grasshopper Python script. A central script was responsible for establishing the online connection to the robot controller, parsing the JSON robot targets, sending them to the controller and waiting for feedback.

4. Prototyping Observations

On the outset of this project, the empirical data about the capabilities and limitations of the material and fabrication system was limited. Mineral foams are a new material group in large-scale 3DP so far. During three consecutive prototyping phases with specific objectives and methods, the design space for the individual 3D-printed foam modules could be explored and mapped.

The first prototyping phase focused on the individual filament quality and surface artifacts of printed objects (Fig. 2, first row). Identifying the most suitable resolution for the application in this project was the primary objective at this step. To achieve this, different nozzle sizes and print parameters such as extruder flow rates, robot speeds, layer heights and resulting layer widths were tested and evaluated. All nozzles were 3D-printed from PLA on conventional desktop 3D-printers and could be quickly interchanged by loosening three screws at the bottom bracket of the extruder. The first nozzle diameter tested was 10 mm, which resulted in a layer height of 7 mm and width of 15 mm with an extruder flow rate of 3 ml/s and a robot speed of 50 mm/s. These print settings resulted in over-extrusion and a rough surface texture. The second nozzle diameter chosen was 12 mm, which resulted in 8 mm layer height and 18 mm layer width with 1 ml/s flow rate and 10 mm/s robot speed. Here, the results were more promising with less disturbances of the material microstructure, an improved filament quality and a more smooth surface finish. The last nozzle diameter tested was 16 mm, which resulted in 10 mm layer height and 25 mm layer width with 1 ml/s flow rate and 9 mm/s robot speed. Those parameters resulted in the best printing quality. The slow robot movements also avoided vibrations and dragging of the filament. Fabrication speed could be neglected because of the small print sample sizes.

The second prototyping phase targeted to maximize the print height of elements with a footprint of 15 x 25 cm while minimizing elastic buckling of the fresh material (Fig. 2, center row). Methods to achieve this were geometric reinforcement strategies such as adaptive wall thickness and internal bracing structures. First, overlapping filament paths in the form of a double wall were tested and resulted in plastic deformation and tapering. Second, corrugation of the filament path was explored, which led to an improved layer built up until 8 consecutive layers and a final element height of 8 cm without plastic deformation. However, elastic buckling resulted in several print failures and collapses. Third, intersecting filament paths were explored with different cellular print layouts. They were based on triangular and square patterns and the most successful approach for the objective of maximizing height in this prototyping phase.

The third prototyping phase focused on reducing internal material stresses in the 3D-printed cellular foam modules to avoid cracking during drying and sintering. First, square-based cellular patterns with different layer built ups were tested. One foam element was printed with three consecutive layers resulting in 30 mm height and only half of the pattern was continued on top with additional three layers resulting in 60 mm height. Cracks occurred in sharp filament turns and between areas of three and six horizontally deposited layers because of asymmetric loading of the material (Fig. 2, bottom row). Second, circle-based cellular patterns were printed with intersecting and overlapping horizontal layers and a vertical built up of six layers. It could be observed that cracks occurred only in areas where layers did not overlap sufficiently. Third, filament pathing around the circle-based cellular patterns was optimized for sufficient layer overlap of 50 % width and resulted in crack-free foam elements after drying and sintering. The design of the foam modules was iteratively developed throughout the three prototyping phases.

Figure 2. Prototyping evolution. Top row: improving surface quality. Middle row: maximizing print height. Bottom row: reducing cracks.

5. Full-scale Demonstrator

Based on the maximum print heights achievable during prototyping, the design decision was taken for a surface-like assembly of interlocking cellular foam modules that would be bound together by casting fiber-reinforced ultra high performance concrete (UHPC) in between them. This application resembles a lightweight composite panel for a second skin facade that controls light and ventilation. Here, using 3DP allows for the unique customization of the geometrical features of the shading panel in a resource-efficient and waste-free fabrication process. Moreover, mineral foams are particularly suitable because of their low weight and can be used as lost formwork in combination with the strength of cast concrete.

Figure 3 illustrates the design steps for the full-scale demonstrator. The overall dimensions of the facade panel were determined by the available fabrication time: 6 modules could be produced per week, which resulted in 24 modules in 4 weeks. Circles were chosen as the base unit for the cellular module pattern. First, a generative design tool based on circle-packing was used that distributed a global circle pattern within the design boundary of 500 x 1000 mm. Second, the circle radii parametrically varied as a function of the distance to an arbitrary attractor curve. This allowed to program the permeability of the facade panel for light and ventilation control. Third, the same distance function also affected the print heights from 3 to 6 layers of the circle units. Lastly, the circles were bundled into clusters for individual foam modules with maximum dimensions within the print bed. This step further refined the circle packing scheme and updated path distances for crack-free bonding of overlapping print paths.

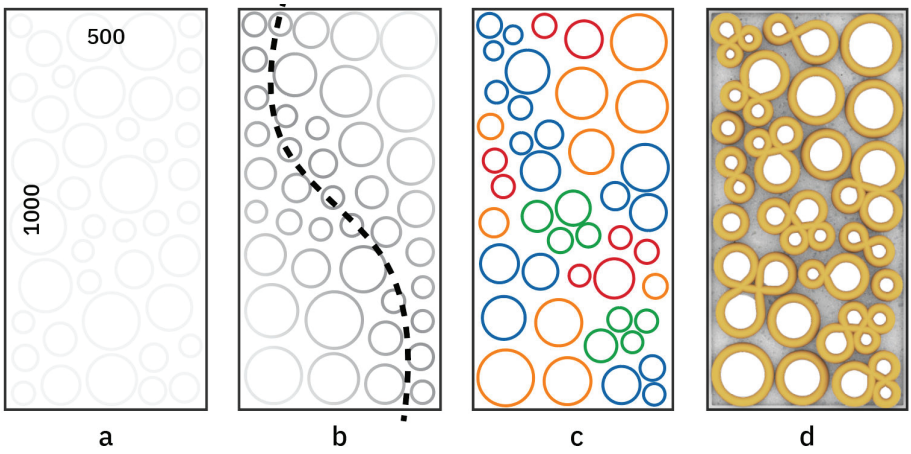

Figure 3. Design steps of final demonstrator: a) boundary condition, b) circle packing, c) module clustering, and d) toolpath bundling .

All 22 cellular foam modules could be produced during the fabrication period of 4 weeks with staged intervals for printing, drying and sintering. The module sizes varied between 60 to 280 mm in diameter and 30 to 60 mm height, which equals 940 mm (3 layers height) to 5060 mm (6 layers height) print path length and 0.2 to 1.2 L of print material. Printing times varied between 8 to 15 minutes with an average of 6 minutes per module. An overall volume of 12.4 L mineral foam was printed. The final step of casting UHPC between the printed foam modules consolidated the composite assembly (Fig. 4). For that, a boundary frame made from 30 x 30 mm steel L-profiles with reinforcement pins served as formwork and could be left in place as a finished edge with mounting details. The resulting panel weighs 15.7 kg, which is comparable to other lightweight ceramic facade claddings. Furthermore, approximately 6.2 kg are printed mineral foam, 6.7 kg UHPC and 2.8 kg steel frame.

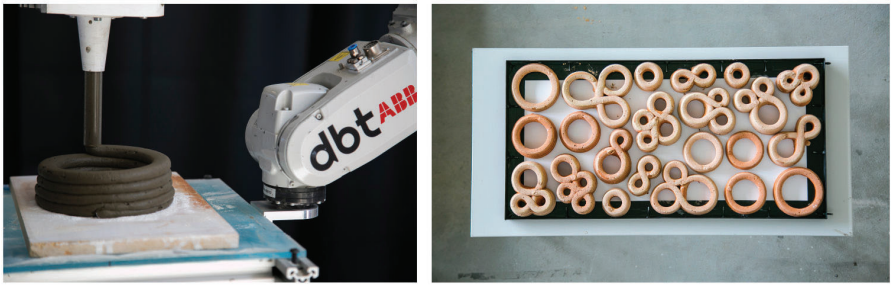

Figure 4. Fabrication of the final demonstrator. Left: 3DP of one module. Right: assembly of sintered modules in steel frame before casting of UHPC.

6. Conclusions & Outlook

The main advantages of the proposed 3DP procedure are the simplicity of the foaming process and the applicability of mineral foams as ink material in construction scale. There are still many process parameters to work on, in terms of the 3DP setup and material system, which could enable easier processing and better material quality in the print results. In particular, the energy-intensive consolidation process of sintering in a ceramic kiln impacts the sustainability of the material system dramatically. Furthermore, the drying and sintering processes showed an increased sensitivity for cracking. Both steps are time demanding and slow down the fabrication speed. Improvements in the print setup could include the transfer of the ink in a continuous manner from foaming to printing, instead of filling a cartridge. Similarly, a moving printing plate could be detrimental for the shape retention, which eventually limits the printable height. Of course, further integration of the extruder tool head with the mechanical system e.g. industrial robot would facilitate the real-time control and synchronization of both and increase the process robustness.

Figure 5. Full-scale demonstrator. Overall impression and closeups.

Large-scale 3DP with mineral foam for freeform construction is a novel approach with promising applications for sustainable, resource-efficient and innovative building elements. For the first time this project showed how mineral foam 3DP can be used for an architectural scale object that leverages the advantages of the automated formwork-free fabrication method for bespoke freeform geometries (Fig. 5). All 3D printed foam components that composed the

demonstrator in this study are unique. Consequently, the significance of mineral foams for lightweight architectures could be shown to be extended with 3DP particularly in the domain of bespoke facade elements that are designed for a specific local building context. Beyond that, mineral foams exhibit a very high thermal resistance and can be used with 3DP for freeform insulating building elements in future research. The empirical exploration of the design space with the current material and fabrication setup is an important contribution to future research. Furthermore, an architectural outlook as a building-scale application based on the demonstrator shading panel was proposed (Fig. 6). For this preliminary design and fabrication study, sintered mineral foams were used as stay-in-place functional formwork and UHPC was used as a filler. Considering the high cement content in this concrete, a more sustainable option would be a cement-free material. This opens a new chapter for future sustainable construction with 3DP of functionally graded mono-material building elements made entirely from mineral foams - *a new kind of monolithic.*

Figure 6. Visualization of a building-scale application of the shading panel.

7. Authorship

This project was part of a larger research collaboration between Digital Building Technologies at ETH Zurich and FenX AG. It was briefed as a 10-week long design thesis for the ETH Master of Advanced Studies in Architecture and Digital Fabrication. The work presented in this paper is the thesis project of Dinorah Martinez Schulte in collaboration with Patrick Bedarf (tutor), Ayça Şenol and Etienne Jeoffroy (material development). All photographs were taken by Dinorah Martinez Schulte.

References

"COMPAS" : 2020. Available from https://github.com/compas-dev/compas<https://compas.dev/> (accessed 1st September 2020).

Camacho, D.D., Clayton, P., O'Brien, W.J., Seepersad, C., Juenger, M., Ferron, R. and Salamone, S.: 2018, Applications of Additive Manufacturing in the Construction Industry – A Forward-Looking Review, *Automation in Construction*, **89**, 110-119, 9.

Dutto, A.M.: 2019, *3D-Printing of Mineral Foams Made from Clay Towards Sustainable Thermal Management in Buildings*, Master's Thesis, ETH Zurich.

Engelsmann, S., Spalding, V. and Peters, S.: 2010, *Plastics in Architecture and Construction*, Walter de Gruyter.

Faircloth, B.: 2015, *Plastics Now - On Architecture's Relationship to a Continuously Emerging Material*, Routledge.

Furet, B., Poullain, P. and Garnier, S.: 2019, 3D Printing for Construction Based on a Complex Wall of Polymer-Foam and Concrete., *Additive Manufacturing*, **28**, 58–64, 6.

Keating, S.J., Leland, J.C., Cai, L. and Oxman, N.: 2017, Toward Site-Specific and Self-Sufficient Robotic Fabrication on Architectural Scales, *Science Robotics*, **2**.

Kontovourkis, O. and Tryfonos, G.: 2020, Robotic 3D Clay Printing of Prefabricated Non-Conventional Wall Components Based on a Parametric-Integrated Design, *Automation in Construction*, **110**, 103005.

Lim, S., Buswell, R.A., Le, T.T., Austin, S.A., Gibb, A.G.F. and Thorpe, T.: 2012, Developments in Construction-Scale Additive Manufacturing Processes, *Automation in Construction*, **21**, 262-268, 6.

Lublasser, E., Adams, T., Vollpracht, A. and Brell-Cokcan, S.: 2018, Robotic Application of Foam Concrete onto Bare Wall Elements - Analysis, Concept and Robotic Experiments., *Automation in Construction*, **89**, 299–306, 7.

Minas, C., Carnelli, D., Tervoort, E. and Studart, A.R.: 2016, 3D Printing of Emulsions and Foams into Hierarchical Porous Ceramics, *Advanced Materials*, **28**, 9993-9999, 6.

Seibold, Z., Mhatre, S., Alhadidi, S., García del Castillo y López, J.L. and Bechthold, M.: 2019, Janus Printing: Coextrusion Based Multi-Material Additive Manufacturing for Ceramics, *Proceedings of ACADIA 2019*, 576-585, 9.

EXPANDING THE ROLE OF ELECTRO-THERMAL ACTUATORS BASED ON CARBON NANOTUBES WITHIN THE FABRICATION OF PRE-PROGRAMMED MATERIAL COMPOSITES.

EREZ EZRA[1] and SHANY BARATH[2]
[1,2]*Technion, Israel Institute of Technology*
[1]*arch.erezezra@gmail.com* [2]*barathshany@technion.ac.il*

Abstract. Taking a cue from research at the crossroads between chemistry, material science, and nanotechnology this paper examines the role of material-driven fabrication methods that enable the integration of pre-programmed geometrical expression onto customized thin-film composites from within a design mindset. Recent developments in electrothermal actuators (ETAs) have demonstrated low cost and ease of fabrication with relatively high precision deformation capabilities. We, therefore, explore ETAs based on Carbon Nanotubes (CNT) capable of reversible actuation in a controlled fashion by external stimuli. Our interest focuses on the ability to pre-program deflection through intervention with the CNT application and composite layer configuration as well as exploring affordable and relatively accessible fabrication methodologies. These adaptive mechanisms displaying; controllable movements, unique actuations, and high thermal insulation suggest affordable and responsive opportunities for developing design applications capable of expanding the role of material agency in the physical context.

Keywords. Material computation; Pre-programmed geometry; Electro-thermal actuation; Carbon Nanotubes; Composite fabrication.

1. Introduction

The re-invention of materials through the assimilation of new technologies has been essential to the way that architecture has evolved in form, expression, and performance over the centuries. Such impact can be demonstrated through early concepts of adaptive and responsive architecture that evolved in the '60s and '70s, mainly due to the developments in cybernetics, artificial intelligence, and information technologies (Kolarevic and Parlac, 2015). Ideas seeking spatial intelligence and adaptability through material novelty have been described by novelist James Graham Ballard in the 'plastex' as early as 1962. However, current alternatives addressing responsiveness through a material perspective have emerged due to technological advancements and automation processes that enable elaborated research into material performance and its possible integration into a spatial context. Shifting from an understanding of isolated architectural systems

PROJECTIONS, Proceedings of the 26th International Conference of the Association for Computer-Aided Architectural Design Research in Asia (CAADRIA) 2021, Volume 1, 613-622.

into a logic of integration and inclusiveness, we enter a context where materials themselves can be active and intentional. What does it mean to 'program' matter to fulfill architectural needs and adapt to a changing context and stimuli? How can a material agency become instrumental in the design of responsive systems?

Current exposure to new modes of production through advances in the fields of biotechnology, material science, and design computation have given architects access to intricate material resolution colliding new form-making techniques with new manufacturing procedures in order to optimize standard material applications and propose novel architectural expressions. Examples for such qualities include; Living materials that incorporate living organisms or ecosystems as essential components (Myers and Antonelli, 2018), Smart Sensor Technology that processes environmental data towards pre-programmed code specifying material behavior (Abhari and Abhari, 2019) as well as flexible actuators in Soft Robotics that have seen a revival of interest in recent years within architectural discourse due to parallel developments in the state of the art robotics and material research (Decker, 2015; Poppinga et al., 2018). The potential to blur the distinction between machine and material i.e. to 'program matter', entails the design of physical matter capable of changing form and/or function in a programmable manner (Tibbits, 2012). As the practice of material design expands, the ability of materials to interact with the environment and respond to external stimuli has become technologically possible (Kretzer, 2017). Following advancements in soft robotics addressing electro-thermal actuators (ETAs) based on Carbon Nanotubes (CNT), this paper explores the role of these actuators beyond the crossroads of chemistry, material science, and nanotechnology, infusing the fabrication of such pre-programmed composite structures towards design intent.

2. Flexible Actuators in Soft Robotics

Soft robotics has opened new perspectives for robot design and control by using highly compliant materials capable of high deformations during interaction (Laschi et al., 2012). Flexible actuators and materials which can vary their stiffness are used, and their control is partially embedded in the body morphology and in their capacity to interact with the environment (Brooks, 1991; Trivedi et al., 2008). New requirements for robots to deliver performance similar to natural motions (gripping, crawling, walking, etc.) have triggered research into soft materials avoiding heavy motors and rigid links that can be greatly attributed to the evolution of flexible actuators activated by various stimuli, such as light, magnetic field, pneumatic pressure and electric field (Yang et al., 2020). Within electrically activated actuation, electro-thermal actuators (ETAs) are considered active materials capable of producing different deformation motions without the use of printed circuit boards (PCBs) or embedded flexible printed circuits (FPCs) and can be activated from thermal expansion induced by the amount of joule heating and the coefficient of thermal expansion (CTE) of the material (Sun et al., 2019). Common bi-layer ETAs consist of a polymer carrier layer such as polyimide (Kapton), PDMS, polypropylene, and a flexible electrode layer. Once the voltage is applied, the electrode layer heats up and the actuator bends towards the material with the smaller thermal expansion. Parameters defining the actuation

deflection include the use of different polymers, electrical conductivity, flexibility, chemical and thermal stability of the electrode layer, and the expansion of the actuator composite structure with additional layers (Wang et al., 2013).

3. Electro-thermal Actuators based on Carbon Nanotubes

Within composite ETAs, Carbon nanotubes (CNTs) are highly compatible as an electrode layer since they can result in flexible films with sufficient electrical and thermal conductivity. They have a significantly lower CTE than many common polymers and are capable of visual transparency which makes them relevant for both optical and electrical applications (Wu et al., 2004; Kim et al., 2017). These qualities also suggest potential compatibility for spatial frameworks such as façade surface film applications and their possible extension towards increased human and environment feedback and interaction. Another advantage of the CNT composite actuator can be seen in its low-cost and ease of fabrication. Electrothermal actuators usually require easy fabrication processes, compatible with the standard Integrated Circuits (IC) and Micro-electromechanical systems (MEMS) and open a wide range of relatively accessible prototyping exercises (Tarun and Wang, 2012). Their integration within common devices and implementation within existing fabrication flows (Potekhina and Wang, 2019) enable us to test relevant prototype methods for composite film printing in relation to design applications.

Composite ETAs based on CNTs have been of particular interest in the research group of Prof. S. Magdassi at the Center for Nanoscience and Nanotechnology and the Institute of Chemistry in the HUJI. By reconfiguring a bi-layer CNT-Kapton soft actuator and adding a thermally triggered shape memory polymer (SMP), they have formed a tri-layer composite structure capable of extremely high bending curvature movements (300°) and reversible pre-programmed deformations (Sachyani Keneth et al., 2020). The successful restructuring of the bi-layer CNT-Kapton ETA enables exploring alternatives that lend themselves towards spatial performance. The width of research and application of carbon nanotubes in electronic devices (solar cells, electronic displays) along with their distinct qualities as conducting films, capable of transparency, motion flexibility, and integration within common fabrication processes, all serve as a starting point for our design experimentations.

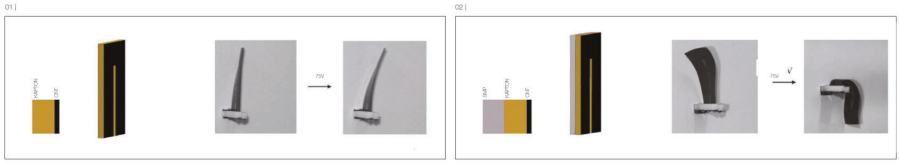

Figure 1. Composite ETAs based on CNTs (Sachyani Keneth et al. 2020), (1) Bi-layer CNT-Kapton (2) tri-layer CNT-Kapton-SMP.

4. Assembly and operation of fabrication workflow

Experiments were designed in order to test possible control of reversible pre-programmed geometrical displacements based on changes in the CNT deposition location, layering structure, and substrate dimensions. The following components were used in the laboratory experiments:

Kapton (Carrier layer): The polyimide film developed mainly for spacecraft and satellites, is used as a flexible yet durable carrier material capable of absorbing extreme temperatures (−269 to +400 °C.) without losing its material properties. (Dementyev et al., 2018).

Carbon Nanotube Ink (Electrode layer): CNT ink can be applied in several ways: Inkjet printer, Airspray, Brushing, or Painting. Ink quantity, application, and coverage on the carrier layer affect the actuator deflection as they reconfigure the material weight, flexibility, and energy consumption. Applying voltage between 5 and 200v on a CNT flexible electrode deposited onto polymeric films results in the heating of the electrode layer, and consequently, in actuation (Sachyani et al. 2017).

Electronic power supply (Activation source for laboratory experiments): Each actuator is activated by a stream of voltage from an external energy source. Two Horizon Dual DC power supplies were (50v) connected, in order to reach a maximum of 100v.

Digital model: Designing variations in electrical conductivity can be controlled through differentiation within the electrode layer. As the CNT application is responsible for the way the voltage is passed through the composite sheet the electrical heating of elements in different locations and distributions across the substrate has a major influence on the actuator shape-changing behavior. A 3D digital model is used to explore possible CNT layouts for defined geometrical deformations.

Composite fabrication: Experiments are assembled with a single Kapton film thickness of 50.8 microns (200 HN, Dupont, USA) cut to size and a homogeneous operable 4-micron electrode layer of brushed CNT ink (Sachyani et al., 2017). Draw-down was performed with an 8R Brush and dried using a hot electric plate (Goldline ALT-500, 82 celsius) between each layer application. The CNT layer used was post-treated with 70% nitric acid for 5 min, in order to improve conductivity similar to the experiments conducted at the Magdassi Lab. The power source is applied in a chain connection to the composite sheet using double-sided brass tape and attaching +- electrodes. Voltage is applied using a dimmer switch enabling a controlled range of power supply until 100v. Applying electricity equals turning on the system. The experiments were framed in two categories:

1. Geometrical deflection within the dimensions of the actuator; Testing the ability to create pre-programmed behavior through differentiated CNT application patterns.
2. Geometrical deflection beyond the dimensions of the actuator; Understanding the capability for actuation within a larger spatial configuration through the expansion of the carrier layer beyond the dimensions of the electrode layer.

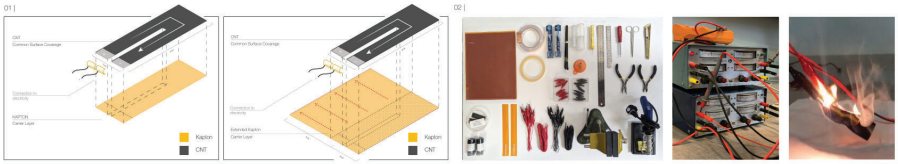

Figure 2. (1) Experiment setup diagrams within and beyond the actuator dimensions (2) Fabrication assembly equipment and initial operability testing .

5. Results

Geometrical deflection within the dimensions of the actuator:

Bending actuation (fig. 3.1): The common actuation mechanism of the basic bi-layer ETA is bending. We first tested the initial operability of actuation through the proposed fabrication workflow on a typical bi-layer . When applying a voltage through the actuator we achieved reversible bending. The actuator deflection is affected by a few parameters such as CTE differences, thermal conductivity, electrical voltage, electrical connectivity (i.e. tape used and electrodes connected), and mechanical properties. In the following experiments, we kept the same parameters of the initial bending actuation apart from the CNT distribution on the kapton. Our aim was to examine the dependency of area and location of heating patterns on bending angles and direction of deflection.

Twist actuation (fig. 3.2): The actuator bends in the direction of the CNT layer due to the CTE differences. Therefore in order to pre-program double bending deformation resulting in a twist at the edge of the actuator, we fabricated a tri-layer composite. CNT ink was applied on both sides of the kapton layer in strategic areas that would define opposite curvature directions of the kapton. However, when applying 100v through the actuator we achieved minor material deformation. We suspect that the edge width dimension of 20mm might have been a limiting factor and have expanded on this in experiment 4.3.

Bifurcation actuation (fig. 3.3): Continuing to test dual-direction curvature, the actuator was fabricated with a cut of 2cm at the loose edge of the carrier layer and positioned in the center of the layer width. CNT ink was once again applied on both sides of the carrier layer to form a tri-layer actuator. Our aim to actuate a reversible bifurcation of the composite was successful when applying a voltage through the actuator.

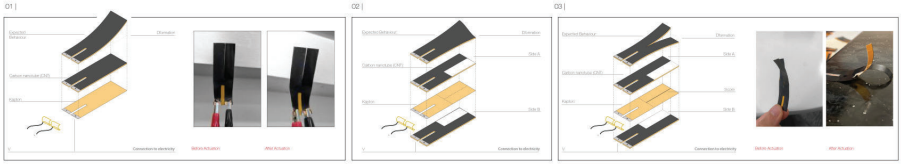

Figure 3. (1) Bi-Layer Bending (2) Tri-Layer Twisting(3) Tri-Layer Bifurcation.

Geometrical deflection beyond the actuator dimensions:

The next experiments examine larger geometrical configurations of singular and multiple actuation. In these experiments, we extend the carrier layer beyond the dimensions of actuation i.e. beyond the dimensions of the electrode layer, in an attempt to examine the impact of deformation as part of a continuous surface.

Surface Bending (fig. 4.1): Applying a standard CNT electrode layer of 20X60mm to an extended Kapton carrier layer 40X60mm. This setup demonstrated the ability of the Kapton surface to potentially amplify the geometrical deflection beyond its thermally activated dimensions. Another possibility that emerges from this setup is the ability of the Kapton extension to serve as a connection area with other materials without interfering with the electrical circuit.

Differentiated Surface Bending (fig. 4.2): Applying two standard electrode layers 20X60mm to the edge of a continuous carrier layer 80X60mm. This experiment requires separate connections to the power supply to enable two actuations on a single surface. Here we test the bending deformation of the full carrier layer when activated homogeneously from both edges and also by applying a different voltage on each edge to achieve gradient reversible curvature. In both experiments, we achieved the actuation of the full surface as predicted in the digital model and experiment setup.

Twisting Surface (fig. 4.3): Continuing with a double actuation setup CNT was applied on a continuous carrier layer 80X60mm on opposite sides of the Kapton). As the direction of deformation is towards the CNT layer due to the CTE differences with the kapton carrier layer we expected each edge to curve in the opposite direction resulting in multiple variations of twisted surfaces. When applying a voltage through the actuators the desired deformation was achieved.

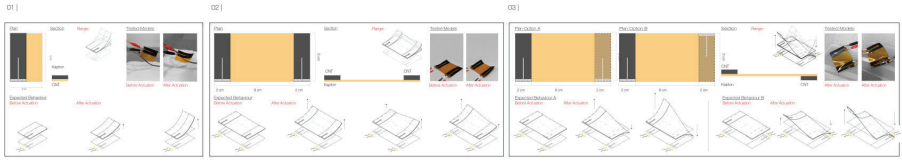

Figure 4. Gradient surfaces (1) Bi-Layer Bending Surface (2) Bi-Layer Dual Activation Bending Surface (3) Tri-Layer Dual Activation Twisting Surface .

6. Discussion

The aspiration for a material agency capable of robotic-like transformation is currently being explored widely within the design and manufacturing of architecture. The demonstration of inherent behavioural features achieved through variations in the fabrication of a tri-layer CNT-Kapton-CNT composite inspires a range of useful characteristics such as reversible actuation, shape modulation, direct interaction with the surroundings and the extension of these qualities within a continuous surface. Nonetheless, when reflecting on these characteristics towards significant spatial performance, questions of scalability and applicability arise regarding (1) Precision and impact of the achieved geometrical deflections

(2) Energy efficiency (3) Integration of the fabrication workflow within possible design applications and the inclusion of additional layers for material performance beyond geometrical deflection.

Geometrical tolerance: Surface articulation within digital architecture has enabled us to re-formulate the resolution of tectonic expressions, and therefore, it is important allowing such control intricacy within the proposed geometrical actuations. The ink deposition has a significant impact on the electrical conductivity and functional motion of the actuator. However, the application method tested enabled mainly aerial CNT layers or simple area divisions attributing mostly homogeneous heating schemes to the actuator and lacking possible enhanced tolerance of deformation through patterning (fig. 5.1). Increasing the application resolution of the CNT ink on the carrier surface would enable investigating ink patterning within the digital model similar to the applications of printed electronics (Heibeck et al., 2015), including potential parameters such as line weight and density (fig. 5.2). Differentiated CNT layer thickness has been demonstrated to influence the deflection of the actuator to a certain extent i.e. sheet resistance decreased with the increase in layer thickness (Sachyani et al., 2017) (fig. 5.3). These potential control variables suggest micro-variations of geometrical deflections that could potentially gain spatial presence through systemic multiplicity on extended surfaces.

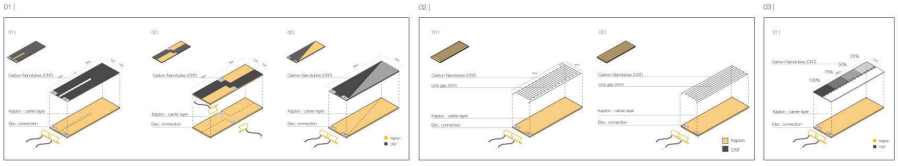

Figure 5. CNT Ink distribution digital inquiry: (1) Aerial (2) Patterned (3) Gradient .

Energy efficiency towards multi actuation surfaces: multiple actuations require exploring alternative power sources that can be incorporated within the extended structure for partial or full activation by environmental parameters (heat, light, etc.), also contextualizing activation in relation to environmental modulation. Possible directions can be seen in recent studies of solar actuation for electricity generation (Xiong et al., 2018) and in developments of printing processes within the photovoltaic solar industry such as Inkjet printing of thin-film solar cells that have also made the technology affordable and accessible (Rardin and Xu, 2011). Within these possibilities, we are able to reflect onwards towards larger configurations of multiple actuation surfaces. The framework needs to be further developed in order to integrate the electrical connectivity between actuations within the material system to avoid exposed wiring and external limitations of the surface deformation. Whereas rigid robotic systems typically employ central control, the use of conductive inks for printed electronics can be investigated in order to support a spatial network of material deformations, distinguishing between deposition of ink for material deformation and deposition of ink for electrical conductivity, defining resistive and non-resistive heating

patterns. Accordingly, we have designed an initial test for the fabrication of a multi-actuation surface setup (fig. 6) based on the presented bifurcation experiment. Here we plan to incorporate the two control systems on a single carrier layer in order to test selective control over material deformation and electrical conductivity.

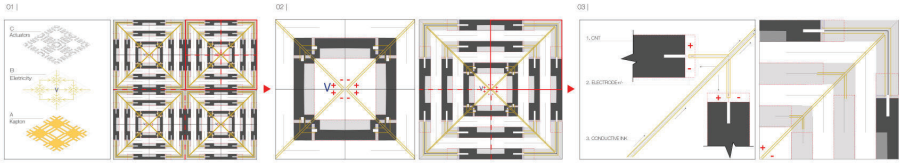

Figure 6. Multi actuation surface diagram (1) Surface layering structure defined through resistive and non-resistive heating patterns (2) Electrical distribution supports minimum connections to external power sources (3) conductive ink to support multiple activations .

Composite Film Printing: Currently, we have initiated the printing of CNT circuits by re-configuring Inkjet printer cartridges, thus testing the transfer of multiple CNT deposition variables from the digital model onto a carrier surface. Our initial tests examined printing articulated thicknesses and geometrical CNT configurations. Similar to applications enabled by printing processes in thin film solar cells and conductive electronics, this opens up potential possibilities for the scalability and integration of thin-film responsive composites based on distributed heat actuations for exterior and interior building surface applications. Multiple challenges are yet to be addressed within the printing process; (1) Compared to regular ink, a relatively thick layer is required to achieve high conductivity (Lin et al., 2013). (2) The possibility to deposit multiple inks both heat resistive and non-heat resistive through cartridge reconfiguration. Further reflections relate to additional layers that will be tested to introduce visual expression of the composite beyond geometrical deflection such as color and opacity modulation that are impactful within a spatial setting. Material composites demonstrating such behavior have been developed for epidermal sensors and on-skin interfaces (Kao et al., 2016; Shi et al., 2018) that are activated through contextual conditions (UV levels, temperature). The potential to extend such material expression through the fabrication of additional performative layers suggests highly intricate material agency within surface interfaces.

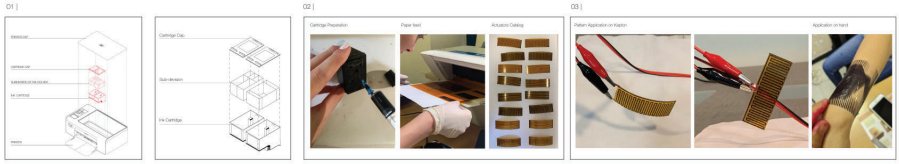

Figure 7. (1) Inkjet HP 1015 printer cartridge configuration(2) Printed CNT testing density & thicknesses (3) Initial printing tests on kapton and adhesive layer .

7. Conclusion

The development of smart materials and flexible systems, such as ETAs based on CNT ink, opens up mechanisms of movement and actuation that demonstrate a range of encouraging possibilities for both accessible and articulated composite behavior. In our explorative studies, we have demonstrated geometrical control through the direct application of CNT ink (electrode layer) on Kapton (carrier layer) expanding from a typical bi-layer to a tri-layer configuration and pre-defining assigned deformations beyond the actuator and onto a surface configuration. The affordable and relatively accessible fabrication methodology has been restructured into a printing method through the configuration of a standard Inkjet printer. We aim to increase control capability over ink thickness, density and type in order to test higher tolerance and threshold of applications. Potential spatial frameworks for expressive thin film composites include; Surface applications for human and environment stimulus-response control systems, Monitor coatings for screens and facades, and new media applications for standard and non-standard geometrical surfaces. The research into additional composite layers would enable the integration of new performance variables that can function as atmospheric and environmental indicators, i.e. the ability to detect PH level, temperature, or humidity conditions and translate them into programmable visual signals, color transformations, and/or opacity levels. Understanding the operability of material composites emerging from the crossroads of different scientific communities enables us to discover new narratives for material performance and explore how may their dynamic behavior be designed and experienced in the space of architecture.

Acknowledgment

We would like to thank Prof. Shlomo Magdassi and Ela Sachyani Keneth at the Magdassi Group,HUJI, for their knowledge and support. The students at the D.Dlab studio namely: Donia Ibraheem, Noa Einhorn, Lour Fahoum & Shireen Saad, and Mr. Kobi Kohai from CRML at the EE Department in the Technion - IIT.

References

Abhari, M. and Abhari, K.: 2019, Design with Perfect Sense: The Adoption of Smart Sensor Technologies in Architectural Practice, *HICSS 2019*.

Brooks, R.A.: 1991, New Approaches to Robotics, *Science*, **253**(5025), 1227-1232.

Decker, M.: 2015, Soft Robotics and Emergent Materials in Architecture, *eCAADe 2015 - 33rd Annual Conference 16th-18th September 2015*.

Dementyev, A., Qi, J., Ou, J. and Paradiso, J.: 2018, Mass Manufacturing of Self-Actuating Robots: Integrating Sensors and Actuators Using Flexible Electronics, *2018 IEEE/RSJ International Conference on Intelligent Robots and Systems (IROS)*, 6099-6104.

Heibeck, F., Tome, B., Della Silva, C.D. and Ishii, H.: 2015, uniMorph: Fabricating Thin Film Composites for Shape-Changing Interfaces, *28th Annual ACM Symposium on User Interface Software & Technology - UIST '15 Adjunct*, 233-242.

Kao, H.L.(, Holz, C., Roseway, A., Calvo, A. and Schmandt, C.: 2016, DuoSkin: rapidly prototyping on-skin user interfaces using skin-friendly materials, *Proceedings of the 2016 ACM International Symposium on Wearable Computers*, New York, NY, USA, 16-23.

Kim, C.L., Jung, C.W., Oh, Y.J. and Kim, D.E.: 2017, A highly flexible transparent conductive electrode based on nanomaterials, *NPG Asia Materials*, **9**(10), e438-e438.

B. Kolarevic and V. Parlac (eds.): 2015, *Building Dynamics: Exploring Architecture of Change*, Routledge, London ; New York.

Kretzer, M.: 2017, *Information Materials: Smart Materials for Adaptive Architecture*, Springer International Publishing.

Laschi, C., Cianchetti, M., Mazzolai, B., Margheri, L., Follador, M. and Dario, P.: 2012, Soft Robot Arm Inspired by the Octopus, *Advanced Robotics*, **26**(7), 709-727.

Lin, Z., Le, T., Song, X., Yao, Y., Li, Z., Moon, K.s., Tentzeris, M. and Wong, C.: 2013, Preparation of Water-Based Carbon Nanotube Inks and Application in the Inkjet Printing of Carbon Nanotube Gas Sensors, *Journal of Electronic Packaging*, **135**, 011001.

Myers, W. and Antonelli, P.: 2018, *Bio Design: Nature • Science • Creativity*, Thames and Hudson Ltd.

Onal, C., Wood, R. and Rus, D.: 2013, An Origami-Inspired Approach to Worm Robots, *Mechatronics, IEEE/ASME Transactions on*, **18**, 430-438.

Poppinga, S., Zollfrank, C., Prucker, O., Rühe, J., Menges, A., Cheng, T. and Speck, T.: 2018, Toward a New Generation of Smart Biomimetic Actuators for Architecture, *Advanced Materials*, **30**(19), 1703653.

Potekhina, A. and Wang, C.: 2019, Review of Electrothermal Actuators and Applications, *Actuators*, **8**(4), 69.

Rardin, T. and Xu, R.: 2011, Printing Processes Used to Manufacture Photovoltaic Solar Cells, *The Journal of Technology Studies*, **37**, 2.

Sachyani, E., Layani, M., Tibi, G., Avidan, T., Degani, A. and Magdassi, S.: 2017, Enhanced Movement of CNT-Based Actuators by a Three-Layered Structure with Controlled Resistivity, *Sensors and Actuators B: Chemical*, **252**, 1071-1077.

Sachyani, E. K., Scalet, G., Layani, M., Tibi, G., Degani, A., Auricchio, F. and Magdassi, S.: 2019, Pre-Programmed Tri-Layer Electro-Thermal Actuators Composed of Shape Memory Polymer and Carbon Nanotubes, *Soft Robotics*, **7**(2), 123-129.

Shi, Y., Manco, M., Moyal, D., Huppert, G., Araki, H., Banks, A., Joshi, H., McKenzie, R., Seewald, A., Griffin, G., Sen-Gupta, E., Wright, D., Bastien, P., Valceschini, F., SEITE, S., Wright, J., Ghaffari, R., Rogers, J., Balooch, G. and Pielak, R.: 2018, Soft, stretchable, epidermal sensor with integrated electronics and photochemistry for measuring personal UV exposures, *PLOS ONE*, **13**, e0190233.

Sun, Y.C., Leaker, B.D., Lee, J.E., Nam, R. and Naguib, H.E.: 2019, Shape programming of polymeric based electrothermal actuator (ETA) via artificially induced stress relaxation, *Scientific Reports*, **9**(1), 11445.

Tarun, A.P. and Wang, P.: 2012, Designing and building inexpensive flexible circuits, *TEI '12*.

Tibbits, S.: 2012, Design to Self-Assembly, *Architectural Design*, **82**(2), 68-73.

Trivedi, D., Rahn, C.D., Kier, W.M. and Walker, I.D.: 2008, Soft Robotics: Biological Inspiration, State of the Art, and Future Research, *Applied Bionics and Biomechanics*, **5**, 99-117.

Wang, C., Nosaka, T., Yost, B., Zimmerman, B., Sutton, E.D., Kincaid, E., Keberle, K., Iqbal, Q.A., Mendez, R., Markowitz, S., Liu, P., Alford, T.L., Chan, C.K., Chan, K.S. and O'Connell, M.J.: 2013, Printed Carbon Nanotubes on Polymer Films for Active Origami, *Materials Research Letters*, **1**(1), 13-18.

Wu, Z., Chen, Z., Du, X., Logan, J.M., Sippel, J., Nikolou, M., Kamaras, K., Reynolds, J.R., Tanner, D.B., Hebard, A.F. and Rinzler, A.G.: 2004, Transparent, conductive carbon nanotube films, *Science (New York, N.Y.)*, **305**(5688), 1273-1276.

Xiong, Y., Zhang, L., Weis, P., Naumov, P. and Wu, S.: 2018, A solar actuator based on hydrogen-bonded azopolymers for electricity generation, *Journal of Materials Chemistry A*, **6**(8), 3361-3366.

Yang, Y., Wu, Y., Li, C., Yang, X. and Chen, W.: 2020, Flexible Actuators for Soft Robotics, *Advanced Intelligent Systems*, **2**(1), 1900077.

TOOLPATH SIMULATION, DESIGN AND MANIPULATION IN ROBOTIC 3D CONCRETE PRINTING

LUCA BRESEGHELLO[1], SANDRO SANIN[2] and
ROBERTO NABONI[3]
[1,3]*CREATE - University of Southern Denmark, Section for Civil and Architectural Engineering*
[1,3]*{lucab|ron}@iti.sdu.dk*
[2]*University of Innsbruck*
[2]*sandro.sanin@icloud.com*

Keywords. 3D Concrete Printing; Robotic Fabrication; Additive Manufacturing; Toolpath Simulation; Toolpath Manipulation.

Abstract. *Digital fabrication is blurring the boundaries between design, manufacturing and material effects. More and more experimental design processes involve an intertwined investigation of these aspects, especially when it comes to additive techniques such as 3D Concrete Printing (3DCP). Conventional digital tools present limitations in the description of an object, which neglects material, textural, and machinic information. In this paper, we exploit the control of extrusion-based 3D printing via programmed layered toolpath as a design method for enhancing the control of the manufactured architectural elements. The paper presents an experimental framework for design, analysis and fabrication with 3DCP, developing a system for materializing interdependencies between geometry, material, performance. This is applied to a series of architectural artefacts which demonstrate the advantages and possibilities opened by the introduced workflow, expanding the design process towards higher control on the objects buildability, structural integrity and aesthetic.*

1. Introduction

3D Concrete Printing (3DCP) is a rapidly expanding technique, both in research and in the construction practice, promising high geometric freedom, reduced material consumption, and automation of construction. Most of its potential is yet to be fully exploited, mainly due to material limitations (Roussel 2018), and to a process that is still experimental (Suiker et al. 2020). Current studies on 3DCP are focusing on the performance and rheology of printing materials (Casagrande et al. 2020, Panda et al. 2019); the advancement in the printing technology (Craverio et al. 2020, Mechtcherine et al. 2019); the integration of reinforcements (Marchment & Sanjayan 2020, Bos et al. 2018); and the environmental and economical sustainability of the fabrication process (Mohammad et al. 2020, Kuzmenko et al. 2020). The complex interrelation of numerous parameters affects the printing outcomes, with unforeseen failures due to poor dimensional accuracy or mechanical performance (Wolfs, Bos and Salet 2018, Kruger et al. 2020). Limited research has been conducted to date on the design implications of

PROJECTIONS, Proceedings of the 26th International Conference of the Association for Computer-Aided Architectural Design Research in Asia (CAADRIA) 2021, Volume 1, 623-632.

3DCP, which demand specific modelling strategies for the manufacturing process (Carneau et al. 2019), compared to cast concrete elements.

Explorations in the design and control of the toolpath planning have been conducted, with a focus on different aspects. On the one hand, tools for controlling the printing process have been developed using agent-based path planning and printing simulation (Efthimiou, Grasser 2019; Stuart-Smith et al. 2020); implementing algorithms that output printing paths in static equilibrium (Bhooshan et al. 2018); and workflows for adaptive correction of the toolpath following geometric and fabrication constraints (Adilenidou et al. 2019). On the other hand, toolpath design strategies have been explored, focusing on emergent material patterns as an effect from the manipulation of the deposition speed (Mohite 2019); developing programmed patterns and surface articulation to demonstrate new material and aesthetic (Anton 2018; Westerlind, Vargas 2020). The existing research, however, does not provide instruments for quick and accurate printing simulation, analysis and visualization. In this work, we address this issue by introducing a modelling framework for 3DCP which allows designers to control and visualize the printing toolpath and the outcome of the printing process. This approach is used to enhance aspects of buildability, structural performance, and aesthetics during the printing process, where form and machining toolpaths are controlled simultaneously.

2. Methods

2.1. 3DCP WORKFLOW: DESIGN, MATERIALS, ANALYSIS, MACHINE

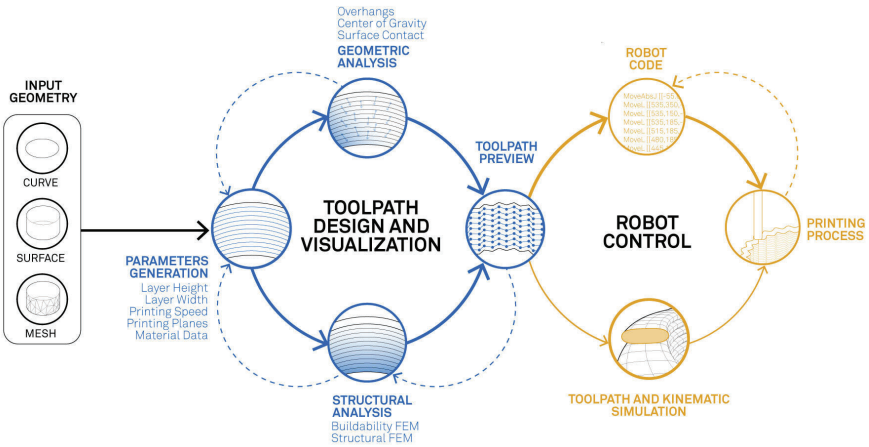

Figure 1. Design and Fabrication workflow for automated informed toolpath manipulation for 3DCP.

The standard 3DCP workflow includes the phases of design, the generation of a code for the printing machine, the preparation of a material mix and the printing process. The presented work builds on this by developing and integrating a set

of design and analysis tools into the process. This is divided into two phases: (a) Toolpath Design and Visualization; (b) Robot Control, where the toolpath parameters are translated into motion command and a kinematic simulation of the printing procedure (Fig. 1).

2.2. FRAMEWORK FOR TOOLPATH DESIGN, ANALYSIS AND SIMULATION

For this reason, a reliable and agile numerical and visual preview of the layers is relevant to control the various printing parameters, to ensure a direct evaluation and control of the layers that constitute a print, for mechanical, tectonic and aesthetic purposes.

Parameters Generation - When a 3D digital model is translated into a toolpath for the layered extrusion, an approximation of the original shape is necessary. To address this transformation, we developed a framework from input 3D design to machine-readable code where a fast visualization of the printed outcome allows for the control of its geometrical characteristics. Developed in C-sharp within Grasshopper and Rhino, the framework firstly tackles the translation of an input geometry (surface, BReps, meshes or curve) into polylines at defined distances, defining the height H_x of the printed layers. Optionally, a spiralization of the toolpath is applied, constantly increasing the vertical position without an abrupt movement to change layer. The specific cross-sectional shape of the filament is determined by a series of parameters: considering the nozzle diameter, material mix, and the volumetric material flow as constant, the defining parameters for the layer shape are the movement speed, the layer height, and nozzle orientation (Comminal et al. 2020). The width W_x and in turn the sectional shape of the layer are a resultant of the other variables. These also determine surface contact S_x (Fig. 2).

Geometric and Structural Analysis - Once the printing parameters and the toolpath are defined, a series of analysis can be performed. On the one hand, an analysis of print overhangs, the centre of gravity and resisting section are graphically visualized (Naboni, Breseghello 2020); on the other hand, a Finite Element Analysis (FEA) is performed on the geometry resulting from the toolpath generation using Karamba for Grasshopper. A buckling simulation for the early-age behaviour of the concrete during the printing process developed by Vos et al. (2020) is employed to have immediate feedback on the stability of the generated toolpath.

Toolpath Preview - Given the influence of the layer generation process onto the 3D model and the importance of the layer shape on the quality, performance, and aesthetics of the print, the framework integrates a fast preview of the filament shape determined by the above-mentioned parameters, including information about the print, i.e. printing time, layer printing time, material quantities. The tool transforms the curve generated through the slicing process into a low poly mesh with the minimum number of control points (v_y) to describe the filament section, and subsequently into a Subdivision Surface (SubD) object, a high precision spline that provides a smooth curvilinear object representation from a polygonal mesh input.

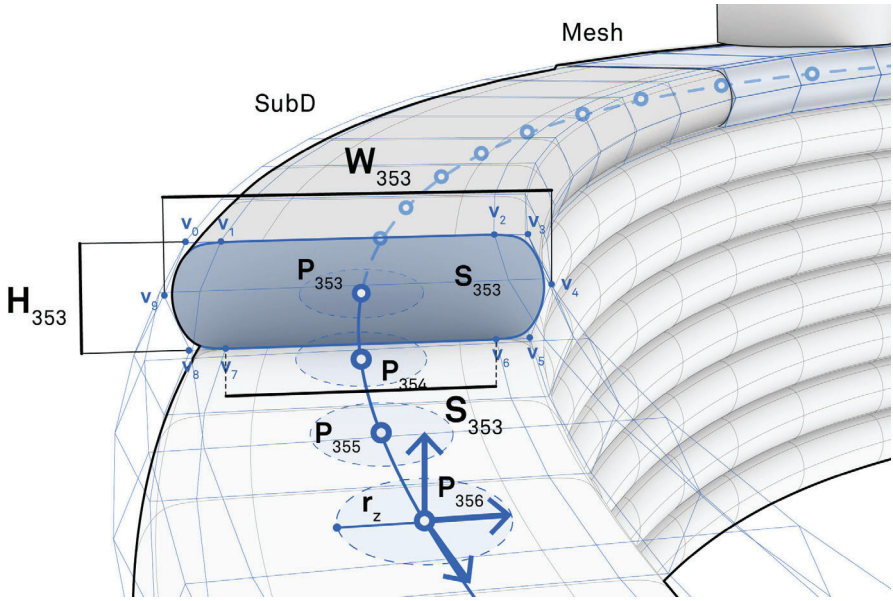

Figure 2. 3D preview of the toolpath and layer section with printing parameters and motion planes.

2.3. ROBOT CONTROL

Robot Code - The layer generation process outputs a set of 3D planes P_x that will serve as motion positions for the linear movement of the robot. The distance between these points is adaptive to the local curvature of the path with the goal of minimizing the number of planes and maintaining the closest fidelity to the input shape. The generated and analysed series of motion planes are then translated into a RAPID module file, integrating the printing speed, print zones(P_x), i.e. a parameter that determines the distance at which the robot computes the movement to the next point, and further additional movements for the pre and post-printing routine.

Printing Process - In parallel to the robot code generation, a kinematic simulation, as well as visualization of the final toolpath, are performed before being transferred to the robot controller. The presented framework is tested using the 3DCP facility of CREATE Lab at the University of Southern Denmark, which consists of an ABB 6650S industrial robot, a control unit and an extrusion system composed of a conveying pump and a circular printing head with a nozzle diameter of 25 mm. The employed cementitious material is based on a standard product for shotcrete with aggregates with a particle size of 2 mm and an addition of an accelerator with low content of calcium-chloride, and a small dosage of polypropylene fibres. The tests are run adding to the premixed powder 16.5% of water, 1.5% of accelerant admixtures and 0.1 % of fibres. The system is based on a batch-mixing process, where the accelerating admixture is added to

the mixer. This process provides a constant material composition but creates a defined printing timeframe where the material has optimal mechanical resistance and capacity to flow through the pumping system.

2.4. EXPERIMENTING WITH TOOLPATH DESIGN MANIPULATIONS

The developed framework is tested on a fabrication experiment, where multiple toolpath design manipulations are applied to the design of a 400 mm diameter hollow cylindrical elements. The goal is understanding the influence of different parameters variations on successfully printing a column with a height of at least 2 m. The column design and proportion highlight two highly recognized challenges of 3DCP: one the one hand, its slenderness stresses on a stability-driven failure mechanism, i.e. elastic buckling; on the other hand, the relatively small diameter of the element and the short printing time for every layer enables a strength-based failure mechanism, i.e. plastic collapse (Fig. 3). These mechanisms are influenced by the fabrication parameters, i.e. motion speed, layer section, accuracy and consistency, by the early-age material characteristics and its mechanical evolution in time, as well as by the shape of the printed object, its centre of mass, the overhangs and the consequent toolpath design. The modelling framework for the design and manipulation of the printing toolpath, is tested on the presented experiment, developing methods of increasing the buildability while printing, i.e. the capacity of a layer to support the subsequent layers, and the structural resistance of the printed object through a series of informed manipulations of the toolpath parameters.

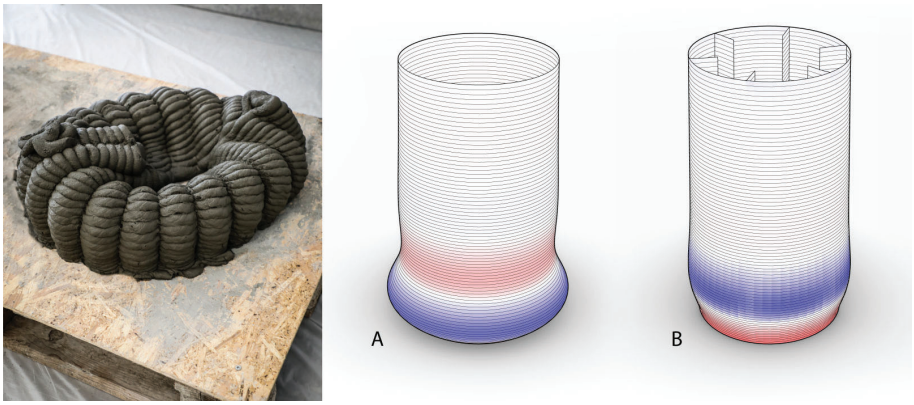

Figure 3. Collapsed 3D print (left) and FEM simulation highlighting the buckling effect on a plain column (A) and a ribbed column (B) (right).

The first developed manipulation method is based on the transformation of the target positions in the XY world plane (Fig. 4 - left). This strategy offers the chance to create ribs along the printing path by moving every n-th plane inward and outward according to the direction normal to the curve on the XY plane. Different parameters are here defined to control the manipulation: the resolution defines the distance between manipulated points; the amplitude defines the distance of the

new plane from its original position; the pattern defines which points are moved. This can result in very dense and short in-and-out movements as well as in a few, deep, ribs along the toolpath. A series of weaving patterns are generated by shifting the movement of the planes in consecutive layers and creating an interlocking print with the material collapsing onto the layer below. The second strategy (Fig. 4 - centre) takes advantage of the movement rate of the robot to vary the amount of material extruded at every portion of the toolpath. This allows to locally control the width of the layer without creating any additional movement to the path, in turn offering a punctual control over the section, larger when the movement is slowed down and thinner when the motion speed is increased. The third manipulation (Fig. 4 - right) logic builds on a gradual movement on the vertical axis that creates a variation in the layer height according to a defined pattern. On the one hand, a constant speed and the change of height of the layers are defining a change of width. On the other hand, it is possible to manipulate the speed to maintain a constant section along the toolpath. These manipulations can be gradually controlled by coupling their generative parameters to external inputs such as the above-mentioned structural analysis.

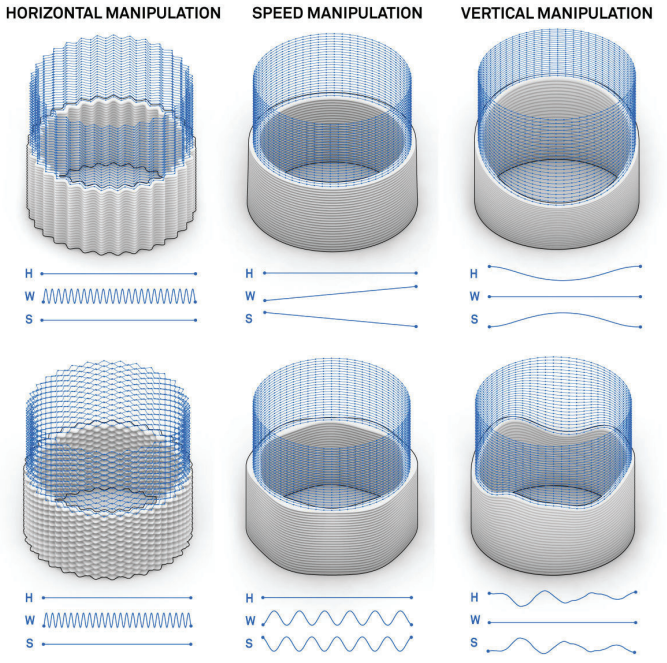

Figure 4. Toolpath variations applied to cylindrical columns: (left) transformation of target positions in the horizontal plane; (centre) variation of the robot's speed to deposit material when it is needed; (right) non-planar printing through variation in the vertical direction. The graphs are showing the evolution of layer height (H), print section width (W) and speed (S) during one layer of printing.

3. Results and Discussion

The work developed the proposed method of toolpath manipulation and visualization and tested it to improve the printing buildability of slender construction elements. The design manipulation and code generation workflow was tested practically by means of manufacturing a total of 17 columns with 9 different toolpath variations. Eight different circular elements with the same diameter and heights varying between 0.7 m and 1.70 m have been partially printed using different manipulations of the print path (Fig. 5). The process was interrupted due to the closing of the printing window, i.e. material too viscous to be pumped, or imperfections that caused layer adhesion problems. Other test columns presented failures throughout the process, either causing an interruption of the printing process and a partial result or a full collapse of the printed object.

Figure 5. Details of patterns from the C3DP columns designed through toolpath manipulation.

The highest column printed within the experiment's framework reached a height of 2.30 m, weighing about 280 Kg (Fig. 6). The toolpath presented a horizontal modulation shifted every second layer with variable amplitude in its height, starting from 150 mm at the first layer and linearly converging to zero and to a linear path. The column was printed at a constant speed of 300 mm/s generating an average layer time of approximately 4.5 s and a total printing time of around 10 minutes for the 230 layers. The layer size was defined as 10 mm height and 35 mm width. However, the shifted nature of the pattern generates an emergent variation of the section and an interlocking pattern between consecutive layers. The developed framework for the design and manipulation of printing toolpath for 3DCP provided a sufficiently accurate and agile tool during the design process, offering possibilities for control and variation of the toolpath given external inputs, e.g. structural analysis, as well as providing a fast visualization of the parameters in play and of of the printing process. The accuracy of the preview is limited to a geometric construct, approximating emergent physical and material behaviours in favour of responsive modelling feedback (Fig. 7).

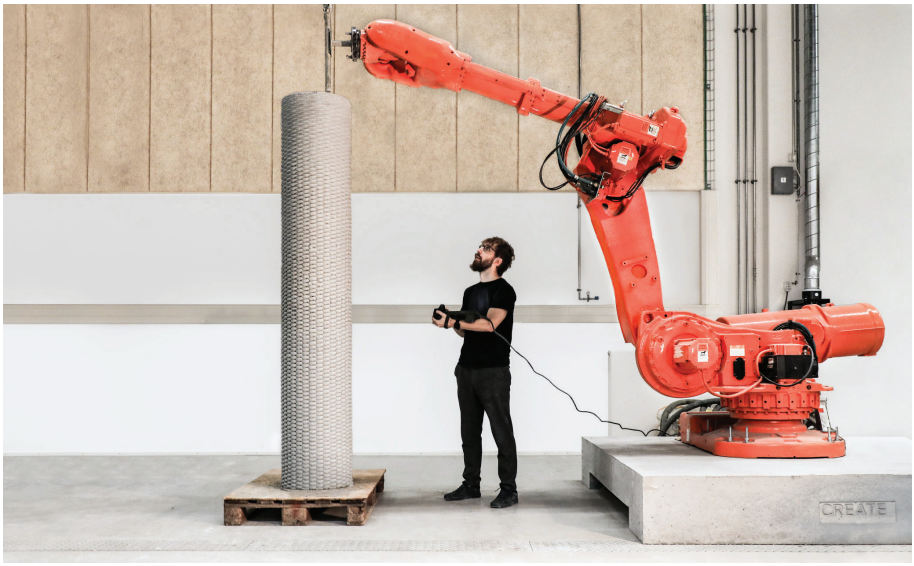

Figure 6. Concrete 3D Printed hollow column presenting an alternated XY toolpath manipulation.

Figure 7. Distance-based comparison between a 3D scanned C3DP column and its 3D digital model designed through toolpath manipulation.

4. Conclusions

This paper explored toolpath manipulations as a design method for 3DCP, based on agile digital tooling for controlling and visualizing the geometry of the print path. The presented framework proved the seamless integration of the manipulation and analysis operations within the design and fabrication process of concrete elements.

The work provides a base for the development of novel design solutions based on the manipulation of the toolpath, which could greatly benefit the fabrication process as well as generate novel aesthetic and performative solutions in the realm of construction. Future works will look into further development of the visualization tool, to provide anticipation of the dimensional features and physical behaviour of the layers for different printing and material conditions. The approach will be applied in future to the enhancement of buildability and structural properties in 3DCP, as well as applied in the design of specific aesthetic features.

Acknowledgements

This work was carried out at the CREATE Lab at the University of Southern Denmark - Section for Civil and Architectural Engineering, in cooperation with industrial partner Hyperion Robotics. The project has been developed with the help of Ashish Mohite, Anja Kunic and the students participating in the CREATE SDU Summer School 2020. The authors wish to thank the project partners Weber Saint Gobain Denmark (concrete material), Fosroc (concrete admixtures) and Danish Fibres (polypropylene fibres).

References

Adilenidou, Y., Ahmed, Z.Y., Bos, F. and Colletti, M.: 2020, Unprintable Forms, *eCAADe*, 168-177.

Anton, A. and Abdelmahgoub, A.: 2018, Ceramic Components - Computational Design for Bespoke Robotic 3D Printing on Curved Support, *eCAADe*, 71-78.

Anton, A., Yoo, A., Bedarf, P., Reiter, L., Wangler, T. and Dillenburger, B.: 2019, Vertical Modulations, *ACADIA 19*, 596-605.

Bhooshan, S., Van Mele, T. and Block, P.: 2018, Equilibrium-Aware Shape Design for Concrete Printing, *Design Modeling Symposium: Humanizing Digital Reality*, 493-508.

Bos, F.P., Ahmed, Z.Y., Wolfs, R. and Salet, T.A.: 2018, 3D Printing Concrete with Reinforcement, *High Tech Concrete: Where Technology and Engineering Meet - Proceedings of the 2017 fib Symposium*, **1**, 2484-2493.

Carneau, P., Mesnil, R., Roussel, N. and Baverel, O.: 2019, An exploration of 3d printing design space inspired by masonry, *Proceedings of the IASS Annual Symposium*, **6**(November), 1-9.

Casagrande, L., Esposito, L., Menna, C., Asprone, D. and Auricchio, F.: 2020, Effect of testing procedures on buildability properties of 3D-printable concrete, *Construction and Building Materials*, **245**, 118286.

Comminal, R., Leal da Silva, W.R., Andersen, T.J., Stang, H. and Spangenberg, J.: 2020, Modelling of 3D concrete printing based on computational fluid dynamics, *Cement and Concrete Research*, **138**(August), 106256.

Craveiro, F., Nazarian, S., Bartolo, H., Bartolo, P.J. and Pinto Duarte, J.: 2020, An automated system for 3D printing functionally graded concrete-based materials, *Additive Manufacturing*, **33**(January), 101146.

Efthimiou, E., Grasser, G. and Grasser, G.: 2018, Liquid rock – Agent based modeling for concrete printing, *Advances in Architectural Geometry*, 236-255.

Kruger, J., Cho, S., Zeranka, S., Viljoen, C. and van Zijl, G.: 2020, 3D concrete printer parameter optimisation for high rate digital construction avoiding plastic collapse, *Composites Part B: Engineering*, **183**(October 2019), 107660.

Kuzmenko, K., Gaudilliere, N., Dirrenberger, J. and Baverel, O. 2020, Assessing the Environmental Viability of 3D Concrete Printing Technology, *in* C. Gengnagel, O. Baverel, O. Burry, M. Ramsgaard Thomsen and S. Weinzierl (eds.), *Design Modeling Symposium*, Springer International Publishing.

Marchment, T. and Sanjayan, J.: 2020, Mesh reinforcing method for 3D Concrete Printing, *Automation in Construction*, **109**(June 2019), 102992.

Mechtcherine, V., Nerella, V.N., Will, F., Nather, M., Otto, J. and Krause, M.: 2019, Large-scale digital concrete construction – CONPrint3D concept for on-site, monolithic 3D-printing, *Automation in Construction*, **107**(August), 102933.

Mohammad, M., Masad, E. and Al-Ghamdi, S. G.: 2020, 3D concrete printing sustainability: A comparative life cycle assessment of four construction method scenarios, *Buildings*, **10 (12)**, 1–20..

Mohite, A., Kochneva, M. and Kotnik, T.: 2019, Speed of Deposition - Vehicle for structural and aesthetic expression in CAM, *eCAADe*, 729-738.

Naboni, R. and Breseghello, L. 2020, High-Resolution Additive Formwork for Building-Scale Concrete Panels, *in* F. P. Bos, S. S. Lucas, R. J. M. Wolfs and T. A. M. Salet (eds.), *Second RILEM International Conference on Concrete and Digital Fabrication - Digital Concrete 2020. DC 2020. RILEM Bookseries*, Springer, Cham.

Panda, B., Mohamed, N.A.N., Paul, S.C., Singh, G.V., Tan, M.J. and Savija, B.: 2019, The effect of material fresh properties and process parameters on buildability and interlayer adhesion of 3D printed concrete, *Materials*, **12**(13), 1-12.

Pham, L., Lu, G. and Tran, P.: 2020, Influences of Printing Pattern on Mechanical Performance of Three-Dimensional-Printed Fiber-Reinforced Concrete, *3D Printing and Additive Manufacturing*, **1**(February), 1-17.

Roussel, N.: 2018, Rheological requirements for printable concretes, *Cement and Concrete Research*, **112**(May), 76-85.

Suiker, A.S., Wolfs, R.J., Lucas, S.M. and Salet, T.A.: 2020, Elastic buckling and plastic collapse during 3D concrete printing, *Cement and Concrete Research*, **135**(January), 106016.

Vos, J., Wu, S., Preisinger, C., Tam, M. and Xiong Neng, N.: 2020, "Buckling Simulation for 3D Printing in Fresh Concrete" . Available from <https://www.karamba3d.com/examples/moderate/buckling-simulation-for-3d-printing-in-fresh-concrete>.

Westerlind, H. and Hern'andez, J.: 2020, Knitting Concrete, *RILEM Bookseries*, **28**(September), 988-997.

Wolfs, R., Bos, F.P. and Salet, T.A.: 2018, Early age mechanical behaviour of 3D printed concrete: Numerical modelling and experimental testing, *Cement and Concrete Research*, **106**(May 2017), 103-116.

OBJECT RECOGNITION AND USER INTERFACE DESIGN FOR VISION-BASED AUTONOMOUS ROBOTIC GRASPING POINT DETERMINATION

FANG-CHE CHENG[1], CHIA-CHING YEN[2] and
TAY-SHENG JENG[3]
[1,2,3]*Department of Architecture, National Cheng Kung University, Taiwan*
[1]*fccheng0902@gmail.com* [2]*ccyen@umich.edu*
[3]*tsjeng@mail.ncku.edu.tw*

Abstract. The integration of Robot Operating System (ROS) with Human-Machine Collaboration (HMC) currently represents the future tendency toward Autonomous Robotic In-Situ Assembly on Construction Sites. In comparison with the industrial environment, construction sites nowadays are extremely complex and unpredictable, due to the different building components and customized design.This paper presents a visual-based object recognition method and user interface enabling on-site robot arms to autonomously handle building components, to build specific designs without the influence of material, shape, and environment. The implementation is an object recognition approach that serves with KUKA industrial robotic manipulator along with an RGB-depth stereo camera in an eye-in-hand configuration to grasp and manipulate found elements to build the desired structure. Opportunities for using vision-based autonomous robotic in-situ assembly on construction sites are reviewed.

Keywords. Computer vision; robot operating system; object recognition; pose estimate; grasping point determination; human-robot collaboration.

1. Introduction

In the field of architecture and engineering, Robotic fabrication has been the predominant research subject recently. Robotic autonomous stands as a promising field for construction, it provides an efficient, more secure, and more precise way for processing architecture on-site resources, which allows extending more possibilities of creative and customizable architecture. While the autonomous robotic assembly has great benefits on the construction process definitely, there are still limits on the application in the projects of real construction. On-site robotic construction differs from robotics in the manufacturing industry should be taken into account the evolving, massive and unstructured environment of typical work sites. It is difficult to make robots adapt to the continually changing site without actively participating in the building process. The growing accessibility

PROJECTIONS, Proceedings of the 26th International Conference of the Association for Computer-Aided Architectural Design Research in Asia (CAADRIA) 2021, Volume 1, 633-642.

of closed-loop robotic fabrication, promises the industry a way to automate aspects of the construction process, either on- or off-site, that require feedback from the physical environment for their success (Tish, King, and Cote, 2020)

1.1. PRECEDENTS

Although the use of industrial robotic arms can improve the adaptability and accuracy of the automated transformation system, the traditional robotic arm processing path planning requires tedious and time-consuming point-to-point teaching through the teach pendant, so that the robotic arm can perform processing operations according to the planned path. Moreover, the operator usually does not have the professional skills in this area and must go through a prolonged period of training to use the teaching pendant to plan the processing path of the industrial robotic arm. More importantly, whenever the processing path needs to be re-planned, the entire production line will be interrupted as a result, causing losses to the manufacturer.

As the real construction environments are normally chaotic and unstructured, the posture of the object to be processed in the environment appears randomly, only using CAD-system to plan the path of the robotic arm cannot process objects with random poses. Therefore, it is no doubt that construction robotics applications need computer vision and other sensing mechanisms to supply the robot with real-time data and information of its physical environments. Giftthaler et al. presented that the stereo camera rig fixed on the base of the robot observes was can be tailored to very different sensing tasks by modifying their configuration and the subsequent image processing, cameras are the sensing modality with the highest potential for on-site robotic building construction. (Giftthaler et al. 2017). Feng et al. also presented vision-guided autonomous robotic assembly research that addresses these challenges and enables autonomous robotic assembly of freeform modular structures on construction sites (Feng et al. 2015). Other research has also show computer vision used to fabricating and assembling irregular components is controlled by sensor-enabled material selection. (Wu and Kilian 2016). In many of the projects described above, the computer vision system perceives the information of the working environment through the image sensor, thereby processing and analyzing the environmental information, allowing the robotics to autonomously complete more complex processing operations.

2. Related work

2.1. COMPUTER VISION

In the construction industry, computer vision has immense potential. The computer vision system was developed to detect the targets and estimate the robotic pose of unmarked construction objects in the work cell. The end-effector is equipped with an Intel RealSense D435 RGB-Depth camera. An active infrared stereo is used for the camera to build three-dimensional point clouds of its field of view and also includes an RGB color sensor. The depth accuracy of the D435 cameras is less than one percent of the distance from the object. The accuracy is about 2.0mm to 5.0mm if the D435 camera is located 1 meter above the object.

This camera provides a great field of view of approximately 10 meters, along with a global shutter on the depth sensor that is ideal for fast-moving applications and computer vision.

2.2. COORDINATE SYSTEM TRANSFORMATION AND HAND-EYE CALIBRATION

In computer vision with the robot arm, the hand-eye calibration problem (also called the robot-world calibration or robot-sensor problem) is an important issue of determining the transformation with a camera and end-effector or the robot base of the world coordinate system. The use of a camera in a robot control loop can be performed with two types of architecture: the camera is said eye-in-hand when rigidly mounted on the robot end-effector and it is said eye-to-hand when it observes the robot within its workspace (Fig. 1). These two schemes have technical differences and they can play complementary parts. The eye-in-hand one has a partial but precise sight of the scene whereas the eye-to-hand camera has a less precise but global sight of it (Gregory Flandin, Francois Chaumette & Eric Marchand, 2000). To allow the position of the camera to be flexibly changed, and to avoid the problem of the camera being blocked by the robotic arm, the configuration with eyes-in-hand is performed here.

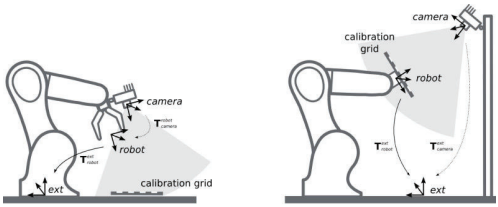

Figure 1. Two situations with hand (robot) eye (camera) calibration. Eye-in-Hand Calibration and Eye-to-Hand Calibration.

This paper, using the OpenCV library method to find the conversion matrix between the 2D image and the 2D coordinates of the robot tool. In the beginning, a color image containing a calibration chessboard is acquired through the camera, and then the robotic arm is manually controlled to locate the four corners of the board to record the results in sequence. Using OpenCV functions to find the actual positions of the four corners on the chessboard in the image (Fig. 2). With the coordinate position of the robotic arm tool PT and the position of the corner points of the image PC, it is necessary to find a 3x3 conversion matrix M and substitute it into the equation. Set Z value in the space as 1, and input any two-dimensional coordinate values to acquire the coordinate of the robot arm tool after matrices are multiplied. The formulas are as follow:

$$P_T = MP_C \tag{1}$$

$$\begin{bmatrix} p_1^x & p_1^y & 1 \\ p_2^x & p_2^y & 1 \\ p_3^x & p_3^y & 1 \end{bmatrix}_T = M \begin{bmatrix} p_1^x & p_1^y & 1 \\ p_2^x & p_2^y & 1 \\ p_3^x & p_3^y & 1 \end{bmatrix}_C \tag{2}$$

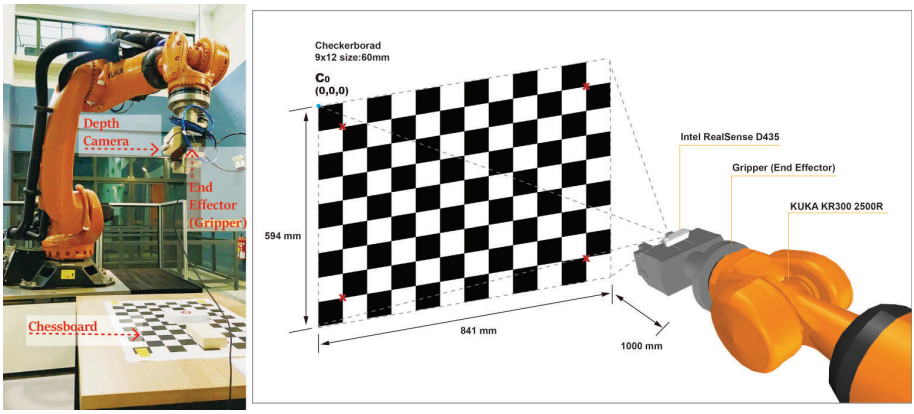

Figure 2. Combination of the robot arm and depth camera. Eye-in-hand calibration with depth camera and robot, and locate four corners of the Cali-chessboard.

This calibration method is more robust and easier to collaborate with different end effectors, the approach can be applied to the whole coordinates of workspace viewed through the lens to spatialize data in the coordinate system of the robot.

2.3. OBJECT RECOGNITION

Compared to the industrial environments, the construction sites are much more complex and unstable. There are two approaches to present as the object recognition system was developed: RGB-based object recognition and Depth image object recognition. According to the results, to make the object recognition system more stable and reduce the interference effect generated by the external environment, this recognition method discards RGB recognition and adopts depth recognition (Fig.3). As all of the targets and environment workspace were placed, the camera captures a 1280 x 720 resolution depth image above the platform 90° angle of depression and sets this position as a visual point. First, perform a threshold operation based on the depth value in the image to obtain the mask of the object -this method to get the mask is faster and more accurate. Second, blur the mask to remove noise and smooth the object boundaries of the mask. Third, introduce morphological closing operation to obtuse acute angles of the image, and maintain background areas that have a similar shape to this structuring characteristic. Last, detecting the shape of each object contours through open CV libraries, and check to determine if the approximate object in view. This depth recognition method allows the robot's detection system to solve the problem that objects may fail to detect when the object is in the same color background or due to the influence of light, and it also allows the program to detect targets of different colors or materials.

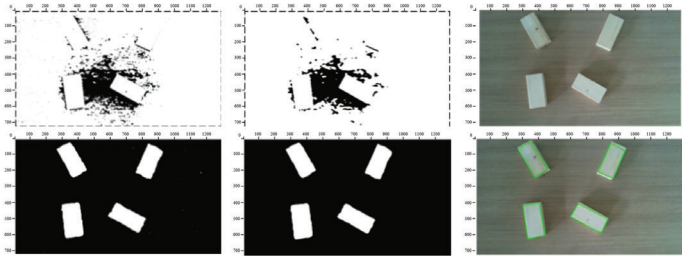

Figure 3. Comparison results of depth recognition and RGB recognition. The images above are HSV hue thresholding, and the bottom row is the results of depth image thresholding.

3. Autonomous robotic grasping system

3.1. SYSTEM CONTROL FLOW

To put the system into a construction application, this research developed an autonomous robotic recognition system (ARR), which can detect the design components and their properties without placing the robot in a controlled environment. Allowing it to automatically look for every available object in the view or raw materials, and it autonomously estimates the robot posture and target angle for the end effector to grasp. The user runs it on an online computer and is written in Python and reduces the requirements for control panel operations.

The Framework of the ARR comprises two systems, the object detection system and a grasping pose estimation system (Fig.4). Both systems depend on computer vision to work; first, the object detection system captures one RGB and one depth image from the working environment through the depth camera Intel RealSense D435. Thresholding the depth image to get the object's mask, then blur it to remove noise into smooth boundaries. The final output results through a closing operation to obtain the object image and contour information. Second, the grasping pose estimation system calculates the rotation angle and center point of the object through the four corners of the contour, and input the pick and place position to avoid collision between robot and objects.

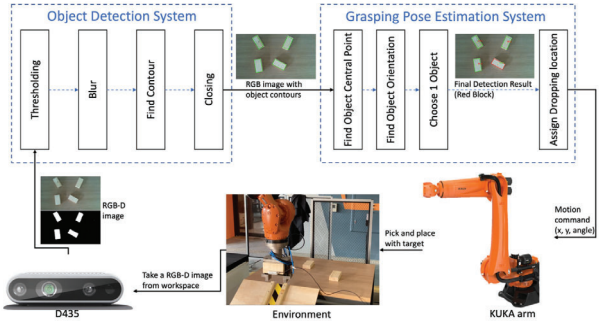

Figure 4. Closed-loop control flow diagram of the autonomous robot object recognition system.

As all the system data is completely collected, a sequence of motion outputs can be obtained. The robot arm processes the given action outputs in sequence and completes the grasping task in the working routine. Finally, we let the camera take images from the environment again and detect whether there are objects on the screen. If the environment is empty, stop the routine; otherwise, the system acquires a newly RGB-D image as the output of the object detection system and repeats the above steps until all objects in the working environment have been grasped to stop.

In the following text, there are more insight details about the object recognition algorithm to introduce the information with how it presents, which is helpful to understand the limitations and potentials of the system later.

3.2. POSE AND ANGLE ESTIMATION

With the contour frame of object identification now in hand, the next step is to estimate the grasping pose of the robotic arm. Thus, a motion planning algorithm was developed to find the optimal grasping position and plan a collision-free motion to deliver the target. The motion planning algorithm was based on the following:

(A) Object central pointMove the lens to the position of 90° angle of depression above the platform, using the contour of the object to find the four corner points of each, and use the average to calculate the center point of the object (Fig.5).(B) Angle of the detected objectSeeing as the object to be clamped in the experiment is a square, the vector of the long side and the short side can be calculated through the four corner points, and the long side vector is selected as the rotation angle of the object (Fig.5).(E) End effector rotationThus, the system generates the rotation angle of each target based on the vectors, this range of values is between -180 degrees and 180 degrees (Fig.5). (D) Grasping selectionAfter calculating the gripping pose estimations of all objects, we select the object with the lowest Y-axis position in the screen as the most preferred object to be gripped. The initially picked object is displayed in a red frame, and other non-target objects are displayed in a green frame.(E) Robot movementBy feeding the gripping posture and drop location of the target, we simulate robot behavior for each specified sequence of actions on all objects. Besides, we generated a plug-in for KUKA PRC in grasshopper to simulated and visualized robot path planning.

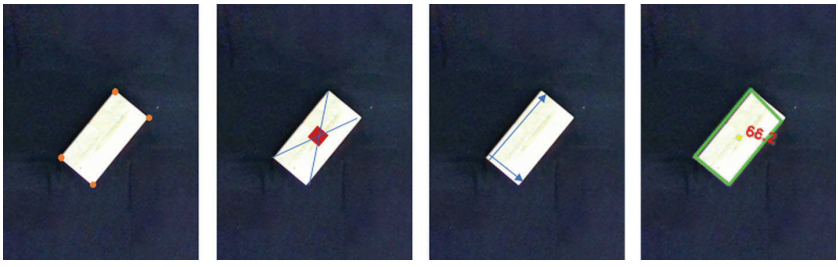

Figure 5. Object central point and angle estimate process.

3.3. HOME AND SYSTEM ROUTINE

For the robot to perform the assembly task, a list of sequential commands is generated as follows: (1) Positioning the camera above the workspace to capture the entire field of view and set the position to home Ph. Calculate the transformation matrix between the robot and camera based on a calibration chessboard. (2) The object detection system checks every object that is present in the view. (3) To avoid collision between robot and object, move the end effector to a position about 500 mm above the object. (4) Move slowly to target and rotate the end effector to the grasping through the angle and pose estimate algorithm. (5) Pickup and place the target to assembly. (6) Move back to Ph along the generated path, and the camera runs the object recognition routine (Fig.6).

After one object is placed, the control algorithm loops return to the robot's Home state to re-estimating object recognition, there are two reasons for this: first, there may be errors to use a single pose estimation for the robot arm to complete all the grasping postures. If the working environment changes, for instance, different numbers of objects or workspace, then the robot arm performs the grasping action according to the original detection result. However, this error may be corrected once the system re-estimates the grasping posture in every home state. Moreover, if a single detection failure results in the omission of some objects, then the system ignores it if the pose estimation is not performed again, making the grasping task incomplete. Another great advantage of re-estimating the pose is that the execution process can interact with the environment, such as manually adjusting the position of objects, removing or adding different ones, making the entire recognition process more flexible. In the meantime, we accomplished a pick and place test of the object recognition routine in Robot Aided Creation and Construction (RAC-Coon) of National Cheng Kung University.

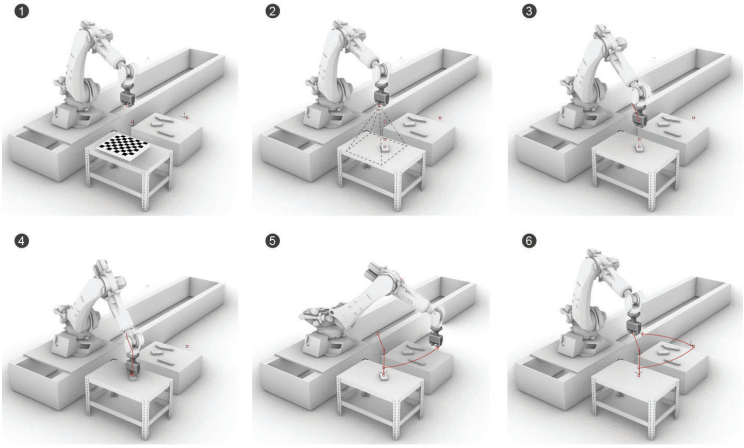

Figure 6. Visual-based autonomous pick and place workflow: 1. Home set and hand-eye calibration (this step only set at the beginning), 2. Object recognition and pose estimate (system routine), 3. Grasping position, 4. End effector angle and pick the target, 5. Place and assemble, 6. The robot moves to the home state and detects the environment again.

Figure 7. Images of pickup and feed to ramp process for the autonomous robotic recognition system in the laboratory.

4. Human-Robot Collaboration interface

To put the system into fabrication application, an autonomous construction workflow interface was designed, and then all the real-time information of the shapes and spatial properties are imported to a Human-Robot Collaboration (HRC) system. Allowing it to automatically find every target in the working environment either materials or shapes, and it can also achieve Computer in the Human Interaction Loop (CHIL) to choose the desired object.

The framework of the HRC interface consists of two systems, automatic object recognition, and a user manually control process (Fig.7). Both systems depend on this object recognition system to work. The automatic object recognition requires an environment image from the Intel RealSense d435 camera that is then displayed on the left screen, the screen will be updated in real-time during program execution. The screen on the right is the recognition result image, which includes the central point and pose angle, the depth recognition program automatically outputs the result as detected in every movement. The manual planner process allows the user to manually click on the selected object in the real-time screen, and then the robot moves to the specified position to grasp the target. This system not only provides user control of the workflow, but it also can test the program of the calibration results. The buttons in the bottom row are used to control the movement of the robotic arm in three-dimensional space and the on/off functions of the gripper through the program. Also, there is a "grasping" button, when the button is triggered, it can automatically detect objects on the screen and use this system to estimate the pose of the grasping. There is a text output function at the top of the screen, which describes what action the program is performing in the current state so that users can track the movement immediately.

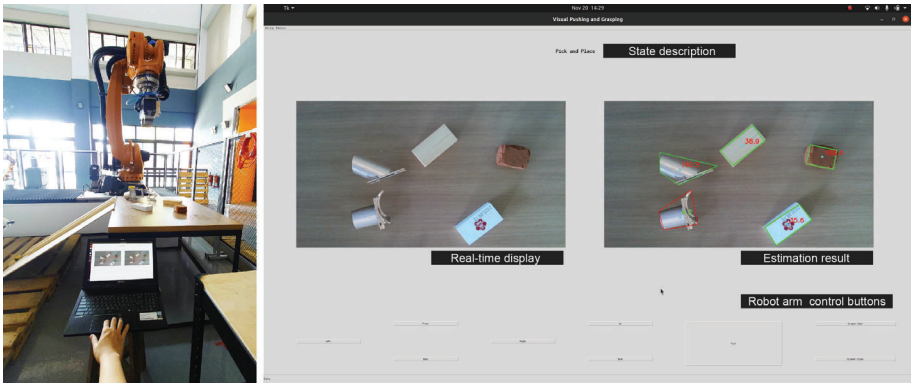

Figure 8. Image of human-robot collaboration and user interface.

5. Result and Discussion

To realize the possibility of intelligent construction in the future, the research here presents a highly accessible approach of open-source libraries and low-cost components. These open-source libraries can provide assembly processes with more stable and vision-guided robot fabrication for the construction industry. This system reduces some requirements for professional training in industrial robot control and can apply to off-site construction or even potential for on-site construction.

However, more tasks could be solved with robotic computer vision to improve the fabrication process and complex application. The object recognition system is developed based on 2D depth images; thus, it cannot effectively recognize 3D object information and activate the robot to complete more difficult assembly. In the real construction site, multiple spatial point clouds are required to be registered and edited into the recognition system. An effective way is to introduce additional cameras into the system to estimate the posture evaluation and angle results between the object and the robot in the three-dimensional space, it can provide more accurate targeting to increase the precision around. In addition, the integration of object recognition with the BIM models can improve the performance of robotic fabrication. In this framework, the BIM models of the project are the main base to drive the autonomous system, each of information on the building components can be provided and searched easily, and more design and requirements about the assembly process can be added in future experiments. It helps to record the details and tries to plan more effectively on-site for robot-to-construction.

6. Conclusion

Industrial robots are excellent at repetitive tasks in the controlled surrounding, but the opposite is true on construction sites. In-situ robots indeed require layers of sensing and intelligence to be able to adapt to the unstructured working environment and real-time variability with few to no reprogramming. The object

recognition developed in the research makes for robotic assembly construction processes to bring advantages with convenience, flexibility, and affordable recognition.

This research develops eye-in-hand coordinate spatial transformations, object recognition, and user interface required for pick and place assembly close-loop workflows through the depth-vision camera, integrating the object detection system and grasping pose estimation system into a Human-Robot Collaboration system for real-time robotic control. This object recognition system is constructed with Open-Source Computer Vision Libraries and low-cost components, permitting the accessible technology deployment in several applications.

It shows the great potential of the proposed system to be operated as an intelligent, sustainable, and efficient approach for on-site autonomous applications. Moreover, it allows more possibilities for robotic fabrication to achieve more complex and special design, exploring a new collaboration between humans and robots in the intelligent construction area.

Acknowledgments

This research is developed by Robot Aided Creation and Construction (RAC-Coon) of National Cheng Kung University and the Department of Architecture. We would like to thank Dr.Yi-Hsuan Tu provides the resource of computer vision and support, Dr. Yang-Ting Shen for advice on the human-computer collaboration, Dr. Sheng-Fen Chien for advice on the pose estimation, Ying-Syu Huang for providing the robotic coding, and Yu-Xun Chen for providing the method of calibration and coding.

References

Chuang, S.: 2019, *Picking of Stacked Workpieces by Robot Arm Based on RGB-D images*, Master's Thesis, National Chung Cheng University.

Dawod, M. and Hanna, S.: 2019, BIM-assisted object recognition for the on-site autonomous robotic assembly of discrete structures, *Construction Robotics*, **3**, 69–81.

Feng, C., Xiao, Y., Willette, A. and Kamat, V.R.: 2015, Vision guided autonomous robotic assembly and as-built scanning on unstructured construction sites, *Automation in Construction*, **59**, 123-138.

Flandin, G., Chaumette, F. and Marchand, E.: 2000, Eye-in-hand / Eye-to-hand Cooperation for Visual Servoing, *Proceedings - IEEE International Conference on Robotics and Automation 2000*, San Francisco, 2741-2746.

Giftthaler, M., Sandy, T., Dörfler, K., Brooks, I., Buckingham, M., Rey, G., Kohler, M., Gramazio, F. and Buchli, J.: 2017, Mobile robotic fabrication at 1:1 scale: the in situ fabricator. Constr Robot, *Construction Robotics*, **1**, 3-14.

Tish, D., King, N. and Cote, N.: 2020, Highly accessible platform technologies for vision-guided, closed-loop robotic assembly of unitized enclosure systems, *Construction Robotics*, **4**, 19-29.

Wu, C., Jiang, S. and Song, K.: 2015, CAD-based pose estimation for random bin-picking of multiple objects using a RGB-D camera, *Proceedings of ICCAS 2015*, Busan, South Korea, 1645-1649.

Wu, K. and Kilian, A.: 2016, Developing architectural geometry through robotic assembly and material sensing., *Robotic Fabrication in Architecture, Art and Design 2016*, Sydney, 240–249.

ROBO-SHEETS

Double-Layered Structure Based on Robot-Aided Plastic Sheet Thermoforming

LUFENG ZHU[1], BASTIAN WIBRANEK[2] and
OLIVER TESSMANN[3]
[1,2,3] *TU Darmstadt*
[1] *zlfatm@163.com* [2,3] *{wibranek|tessmann}@dg.tu-darmstadt.de*

Abstract. Computational design, in combination with robotic fabrication, allows the exploration of complex geometrical differentiation. Notably, thermoplastic sheet materials offer great potential for explorations in robotic fabrication due to their mailable qualities. However, the production of complex shapes from flat-sheet-thermoplastic materials usually depends on molds or on time-consuming procedures. This paper introduces a workflow for the design and fabrication of a double-curved surface made from plastic sheets, which develops a self-supporting structure through using robot-aided one-punch thermoforming. The thickness of a double-curved surface is optimized by applying the Finite Element Method. Notably, forming thermoplastic into a minimal surface strengthens its mechanical properties and this takes a relatively short period of time. According to the relationship between moment and stress in section, two connected minimal-surfaces form a three-dimensional I-profile, making it possible to construct a highly material-efficient structure. Unlike the normal form-finding process, the structure is not limited to compression-only geometry. Compared to thermoforming methods such as Single Point Incremental Forming (SPIF), our one-punch forming process described in this paper shows demonstrates high precision while being less time-consuming. Here, we present a one-to-one scale working prototype as proof of our approach.

Keywords. Robotic fabrication; Plastic sheet thermoforming; Lightweight structure; Self-supporting structure; Minimal surface.

1. Introduction

The research presented in this paper aims to discover the potentiality of thin thermoplastic sheets in double-layered light-weight structures through the employment of robot-aided plastic sheet panel thermoforming. Specifically, the structure was optimized digitally and fabricated on a one-to-one scale via advanced computational and robotic methods.

Double-layered structures were explored in different projects using sheet-materials such as metal and paper. These projects include investigations

PROJECTIONS, Proceedings of the 26th International Conference of the Association for Computer-Aided Architectural Design Research in Asia (CAADRIA) 2021, Volume 1, 643-652.

on incremental sheet forming of metal such as the bridge from CITA (Nicholas 2018). However, metal sheet incremental forming is a time-consuming process and requires much stronger equipment. That is why the light-weight structures with sheet metal expansion form AA (Erdine 2019) tried slicing off parts of the metal sheets to deform them more easily. Although this weakened the strength of the formed panels. And the team from RWTH formed only one layer of the structure for their light-weight construction (RWTH 2016). The Surface to Form project from University Innsbruck (Maleczek 2016) built a double-layered, self-supporting, light-weight structure with thin cardboards, which were folded and glued.

Traditional methods of plastic sheet thermoforming require a positive mold. This is done when the plastic sheet is heated above the glass transition temperature, which becomes pliable, the air is then drawn out and the sheet will develop the form of the mold. When the temperature of the plastic becomes lower than the glass transition temperature again, the plastic will harden and keep its form. One example project applying this method is the ArboSkin from ITKE University of Stuttgart (Knippers 2013). In this project, all the plastic elements had the same geometry as the mold. However, in cases with varying target geometries, different molds will then be required.

For surfaces with complex geometries, the internal stresses are usually ununiform, which indicates that the optimal structural thickness should not be uniform either. In this case, robot-aided plastic sheet panel thermoforming brings new opportunities.

The two most commonly used methods of robotic thermoplastic forming are Single-Point Incremental Forming (SPIF) and one-punch forming. The first method can create complex geometry but with relatively low accuracy and efficiency. One example project is the Single-Point Incremental Forming - Workshop from DADA in 2015 (ARA 2015). The second method creates only geometries like minimal surfaces but with relatively high accuracy and efficiency. One example of this approach is the wall panels-fabricated in the Extensile - Robotic Fabrication Workshop by the Chair for Computer-Aided Architectural Design (CAAD) at the ETH Zurich (CAAD ETHz 2015).

When a conventional I-beam is bent, the top and bottom skins bear tensile and compressive forces. Then, the expanded cones transfer shear forces, enabling the two skins to work in a composite manner. The value of stress follows this formula:

$$\sigma = \frac{M}{I} \cdot y \tag{1}$$

However, I-beams are only efficient for moments in one plane. For complex loading cases, a three-dimensional I-profile might be the solution (Fig. 1). According to the stress distribution along the section, two cones connected at the tipping point should be the shape of a three-dimensional I-profile. Considering the fabrication efficiency, a minimal surface was chosen as the basic geometry for thermoforming. Since two-dimensional bending can extraordinarily stiffen thin sheets (Pini 2016), the weakness of the hollow structure is compensated to some extent.

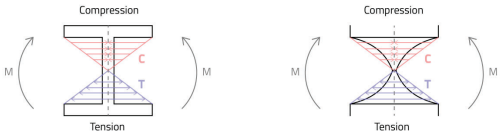

Figure 1. Bending moment and the internal stresses distribution in the section.

To test the entire workflow, a pavilion with double-curved geometry was fabricated and assembled in a one-to-one scale with a bounding box of 3 m width, 3 m length, and 2 m height. The location of the Pavilion is the gallery area of the Architecture Faculty of TU Darmstadt, Darmstadt.

2. Digital Design

2.1. FORM FINDING AND TESSELLATION

To obtain geometry with complex internal stress, four point-loads (three on the boundary and one at the center) were applied to the primary surface (Fig. 2) instead of reversed gravitational force. Usually, a double-curved geometry is not compression-only, so the inverse hanging method is applied for form-finding to acquire a compression-only geometry, which is optimal for materials such as concrete and brick. However, when more freedom is given to geometry design or other unexpected external forces are considered, the bending case will occur. In bending cases, strength against compression and tension is required, for example, the Elytra Filament Pavilion (Doerstelmann 2015). The geometry of the Pavilion determined that there will be significant tension on the upper surface and compression on the opposite. Material such as woven resin-soaked glass or carbon fibers is then required to bear both tensile and compressive stresses.

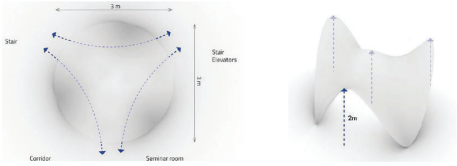

Figure 2. Design of the free-form shape.

The generated vault is 3 m wide and 2 m high and was discretized into smaller-sized elements for fabrication. The triangular mesh was chosen for tessellation to guarantee that the elements are planar. The aim of tessellation is to get triangular elements with proper sizes and proper angles to fit the original geometry as accurately as possible. To achieve this goal, the distances between every two vertices, the boundary and the distances between vertices and target surface were restricted in Kangaroo algorithm, resulting in a mesh with 336 elements (Fig. 3).

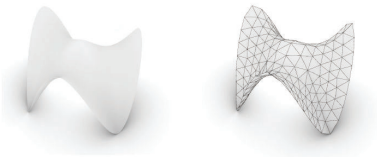

Figure 3. Target geometry and triangular mesh.

2.2. ANALYTICAL DESIGN PROCESS

The basic idea of this double-layer structure is to convert the bending moment into tensile and compressive stresses, which will be later translated into the heights of thermoformed plastic elements. In the elastic analysis, it is not allowed for the material's maximum stress to exceed its elastic limit. The elastic limit bending moment (yield bending moment) can be obtained with the following formula:

$$M_y = {}_yW \tag{2}$$

W is the section modulus of elasticity. For a rectangular cross-section (Fig. 4):

$$W = \frac{bh^2}{6} \tag{3}$$

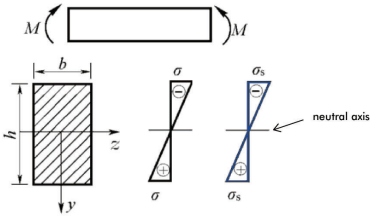

Figure 4. Relationship between moment and stresses in case of a beam with a rectangular section.

For the cross-section of other geometries, the yield bending moment and the section modulus can be obtained through the following two formulas:

$$\int_A \cdot dA = 0 \tag{4}$$

$$\int_A \cdot ydA = M \tag{5}$$

From these formulas, it is quite clear that less material is necessary near the neutral axis (where the stress is 0).

Minimal surfaces can provide a solution for this approach. Our one punch method thermoforming with a robotic arm was able to efficiently generate such geometries. The distribution of material increases with the distance to the neutral axis when two minimal-surface panels are connected at the tip side.

It is not difficult for one beam to calculate the moment by hand, but for a vault with double-curved geometry, the Finite-Element-Method is utilized. Karamba

implemented the Finite Element Analysis in this research. In Figure 5, blue indicates tension and red indicates compression. The higher the stress is, the darker the color will be. The illustration shows that there are compression-only parts (both surfaces are red) as well as bending parts (different colors on each surface).

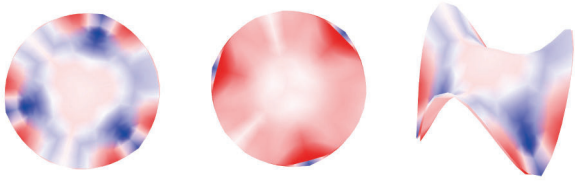

Figure 5. Top view, bottom view, and perspective view of the FEA result.

The thickness of the vault was calculated from the Finite element analysis. The mesh surface was translated into a double layer system in which the distance between the two layers indicated the stresses. Specifically, three hundred thirty-six triangles were offset using the normal vector for each triangle (Fig. 6). As the simple normal vector would create gaps, we instead calculated the weighted average normal vector considering all the vectors of the neighboring triangles. The weighting here was the area of each triangle. Based on this, the offset was created in both directions from the input mesh.

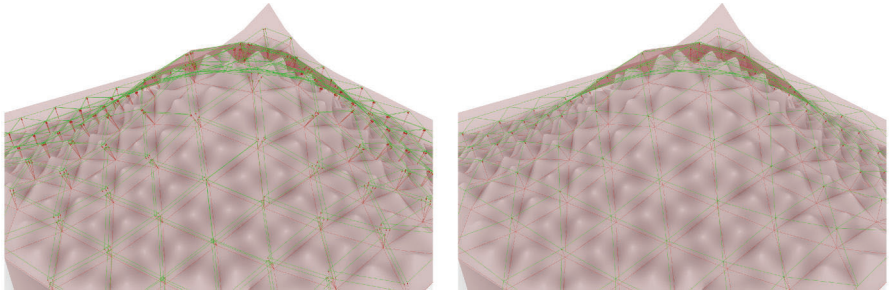

Figure 6. Offset along normal vectors (left) and along the weighted average normal vector (right).

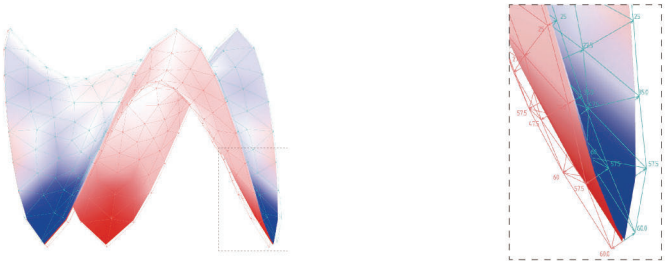

Figure 7. Double-layer meshes.

3. Robotic Fabrication

3.1. ADAPTIVE FRAME

For the thermoforming process, the edges of each panel had to be fixed. Since all the 672 triangular panels are slightly different, it was impossible to use a fixed frame. Instead, an adaptive frame with two adjustable side clips and a fixed bottom clip (Fig. 8) which can flexibly fit different triangular panels was used. For each side clip, there are two supports at the backside, against the punching force from the robot arm. Notably, the suitable angle ranges from 0 to 90 degrees, the suitable length of edge ranges from 0 to 500 mm and the clips were fixed manually for thermoforming (This process can also be automated if there are 2 more robotic arms with clipping tools).

Figure 8. The adaptive frame.

3.2. ROBOTIC THERMOFORMING

Thermoplastic is a plastic polymer material that becomes pliable or moldable at a specific temperature and solidifies again upon cooling. Because of this property, it is widely used in our daily life. The most common use is in PET bottles. Since the thermoforming process is repeatable for thermoplastic, they can be recycled. However, according to a report from WWF, only 20% of the plastic products were recycled.

For this research, PS (Polystyrene) sheets were chosen; PS has a glass transition temperature of approximately 100 °C and a melting temperature of approximately 200 °C. The relatively low temperature-resistance makes it unsuitable for civil engineering. Still, there is thermoplastic such as PAI with a glass transition temperature of approximately 260°C. With proper flame-treatment and further development in material science, thermoplastic could potentially become material for structural purposes.

In this research, it is crucial for thermoforming to maintain the temperature between 110 to 150 °C (Fig. 9). For heating, we used an electric radiator. The heating time was set to 70 seconds, and for cooling down, it was set to 60 seconds. The robotic arm's moving route was controlled parametrically by the Grasshopper plugin Robots developed by Vicente Soler (github.com/visose/Robots) (Soler 2016), and the only parameter controlling the process for each panel was the ID. The punching vector starts from the centroid of the fixed panel and ends at the middle point of the line, connecting this panel and its neighbor in another layer.

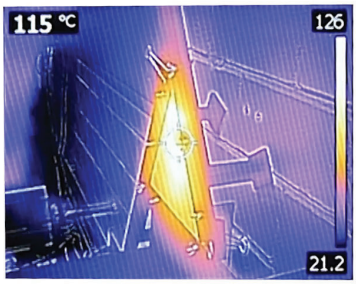

Figure 9. Thermal imaging of the forming process.

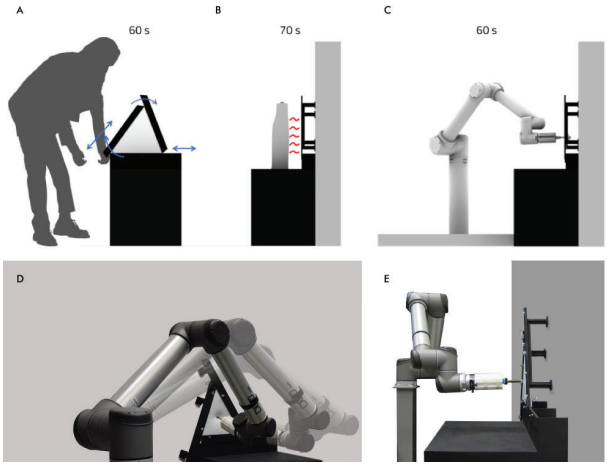

Figure 10. A: Adaptation of the frame; B: Heating procedure; C: Forming and Cooling procedure; D, E: different views of the forming procedure.

3.3. CONNECTION AND ASSEMBLING

The connection between the top and bottom layers should ensure the close touching of the neighbors in different layers. The connection of neighbor triangles in the same layer is more complex as there are angles between two panels, and the connection should bear the tensile stress caused by the bending moment. Two different connecting methods were tested. The first one connects the neighbors in the same layer on folding edges (Fig. 11); the advantage of that is that the folding edges bring more strength to minimal-surfaced panels on a local scale. Meanwhile, the disadvantage is that it needs approximately 450 seconds to fold the edges into precise angles, so it is much more time-consuming than thermoforming itself.

Figure 11. Connecting on fold edges.

The second connection is realized through strips using the wasted material cut from the plastic sheets. In the same layer, every two neighbors were connected by six R3045 nylon rivets and the strip, which allows some bending deformation to fit the angles on the two panels.

The different layers were connected by a set of M3 nylon screws and nuts (Fig. 12). This method requires almost no extra time for fabrication. The second method was chosen because of the time limit. However, it does need a more specific analysis by deciding the connection method. To get sufficient working space for rivets, the connection in the same layer had to be completed before connecting the panels in different layers. The entire structure was divided into six rings from inner to outer; the connection for an inner ring was completed before connecting to an outer one.

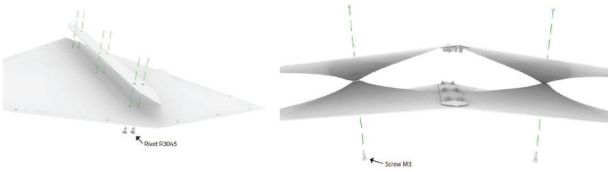

Figure 12. Connecting through strips.

In this research, minimal-surfaced thermoplastic panels were connected to build a double-layer structure like the microstructure of the beetles' shell (Fig. 13). The distances varied from vertex to vertex according to different internal stresses.

Figure 13. The double-layer structure consists of minima-surfaced thermoplastic panels.

3.4. THE GROUNDING

According to the tessellation result, all the weight will be applied on three tip points, which leads to significant extreme stresses there. To reduce the stresses at supports, the six bottom triangles were removed, and all 12 of their neighbors were adjusted to make them come into contact with the ground (Fig. 14). The offsetting vectors for the grounding points were modified to horizontal vectors instead of the weighted average normal vectors so that all 24 panels in top and bottom layers were in contact with the ground. For the ground connections, there were folding edges for these 12 relevant panels. In this way, the contacting area changed from three points to 12 surfaces, which tremendously reduced the stresses there, and the connection between folding edges and grounding plate became more stable.

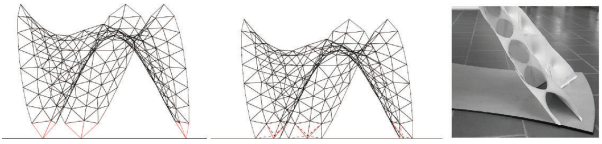

Figure 14. Grounding adjustment.

4. Discussion

This paper introduced a novel workflow of building a double-layered, light-weight structure with thermoplastic through the employment of robot-aided plastic sheet panel thermoforming. Robotic thermoforming makes it possible to form customized building elements without expensive molds. Notably, the one-punch process is especially efficient for forming minimal surfaces. It is possible to build a light-weight structure without any other secondary structure but thin thermoplastic sheets. This is done with the use of the two-dimensional bent thin plastic sheets' strength against both tensile and compressive stresses, together with FEM based elements optimization. However, thermoforming will change the thickness of the plastic sheet as the material loses strength when stretched too thin. To avoid this, the forming depth should influence the size of the triangle through tessellation. Besides, the relationship between the thickness and the mechanical properties of the thermoformed elements as well as the shape of connecting strips should be studied further by quantitative analysis, which will be part of future research.

Our approach highlights possibilities for efficient customization of building elements according to structural needs. Flat sheet thermoplastics offer great potential for robotic manipulation and might help us to design a more material-efficient built environment.

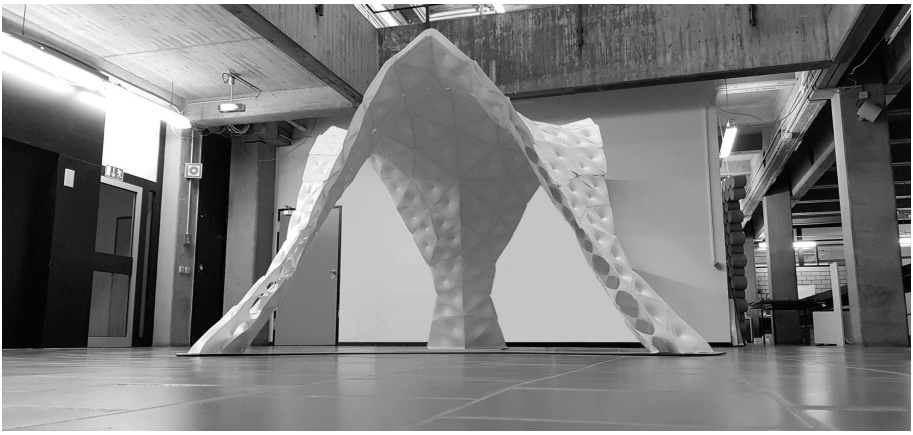

Figure 15. The Pavilion in one-to-one scale.

References

Association for Robots in Architecture, I.R.A.U.: 2015, “Single-Point Incremental Forming - Workshop @ DADA” . Available from <https://vimeo.com/132981872> (accessed November 11, 2020).

CAAD, E.: 2015, May/June, “Extensile – robotic fabrication workshop” . Available from <http://studioany.com/teaching/extensile/> (accessed November 11, 2020).

Doerstelmann, M., Knippers, J., Menges, A., Parascho, S., Prado, M. and Schwinn, T.: 2015, ICD/ITKE Research Pavilion 2013 14: Modular Coreless Filament Winding Based on Beetle Elytra, *Architectural Design*, **85(5)**, 54-59.

Erdine, E., Gianni, G., Moreira, A., Rodriguez, A., Song, Y. and Sungur, A.: 2019, Robot-Aided Fabrication of Light-Weight Structures with Sheet Metal Expansion, *10.1007/978-981-13-8410-3_24*.

Knippers, J. and Köhler-Hammer, C.: 2013, “ArboSkin, Stuttgart” . Available from <https://www.itke.uni-stuttgart.de/research/built-projects/arbo-skin/> (accessed November 05, 2020).

Maleczek, R., Scheiber, C. and Filz, G.: 2016, May 13, “Innovative Formen” . Available from Universität Innsbruck<https://www.uibk.ac.at/newsroom/innovative-formen.html.de> (accessed November 06, 2020).

Nicholas, P.(.: 2018, A Bridge Too Far, *Contribution to exhibition, ars electronica*.

Pini, V., Kosaka, P., Malvar, O., Calleja, M. and Tamayo, J.: 2016, How two-dimensional bending can extraordinarily stiffen thin sheets, *Scientific Reports*, 6.10.1038/srep29627.

Soler, V.: 2016, “Robots” . Available from <https://github.com/visose/Robots> (accessed December 11, 2020).

RWTH AAchen University, C.: 2016, November 11, “Manufacturing of Freeform Facade Elements as a Self-Supporting Structure Without Substructure of Stainless Steel by Means of Incremental Sheet Forming (IBU)” . Available from <https://trako.arch.rwth-aachen.de/cms/TRAKO/Forschung/Leichtbau/isbf/Faltstrukturen-aus-Feinblech/lidx/1/> (accessed November 12, 2020).

DEVELOPING A CORRECTING TOOL FOR INTERACTIVE FABRICATION PROCESS

YU-CYUAN FANG[1], TENG-WEN CHANG[2], CHI-FU HSIAO[3] and CHUN-YEN CHEN[4]
[1,2,3,4]*National Yunlin University of Science and Technology, Taiwan*
[1,2,3,4]*{liam.fc96|tengwen.chang|chifu.research|chunyan056}@gmail.com*

Abstract. This paper will propose the integration of multi-view stereo and time of flight technologies and components. Through the spatial point cloud sensor, the changes of objects in the space are converted into digital point clouds, which are feedback on the virtual interface. To make the virtual and physical will continuously communicate and feedback in space, which we established a correction tool for the integration of virtual and physical. The agent-based sensor computing method combines the fabrication process of visual sensors and behavior, from virtual object control to fabrication machines. In this tool, users can explain the reasons for design decisions by visualizing process and process-related information. It allows virtual and physical previews and feedback in real time, and finds out the differences between the two and makes real-time corrections. Solved the correction problem of coexistence.

Keywords. Digital fabrication; Digital Twin; Co-existing; Design process.

1. Introduction

The rapid development of digital fabrication tools has changed people's past creative modes, allowing machines to perform production and fabrication more quickly and conveniently. It is often pointed out that the interface bridging between the virtual and physical environment is useful for supporting personal fabrication design, but there are still differences between the virtual and the physical. Designers should continue to modify the process, increase the accuracy between the two and get closer to the appearance of both sides (Hsiao, Lee, Chen, & Chang, 2020). Currently, the real-virtual integration has attracted considerable attention in academic, industry and human-computer interaction. Many collaborative robots have been developed and integrated with these digital fabrication tools, such as automated operating systems using robotic arms and digital visual interfaces (W Huang, Williams, Luo, Wu, & Lin, 2018; WX Huang, Yan, Luo, & Li, 2016). The primary condition for human-machine collaboration is to integrate virtual and physical, as the preferred means of real-virtual integration. Digital twins (DT) have received extensive attention from industry researchers and

PROJECTIONS, Proceedings of the 26th International Conference of the Association for Computer-Aided Architectural Design Research in Asia (CAADRIA) 2021, Volume 1, 653-662.

practitioners through faster algorithms, enhanced computing power and available data (Dembski, Wössner, & Letzgus, 2019). It is a method of connecting virtual models and physical products. It is usually can be used in various physical assets, processes, personnel, places, digital replication systems and equipment for simulation. This method can also optimize the real-time control of products and production lines. The two can be integrated together so that the virtual object, and the physical product can be previewed in real time to find the differences and correct between them in time. It is effective Reduce fabrication errors and shorten production time (Caputo, Greco, Fera, & Macchiaroli, 2019).

During the experiment, we found that there is a difference in the presentation effect between the physical product in the real environment and the virtual model produced by the Mixed reality mobile, which leads to errors in the operation process(Okura, Kanbara, & Yokoya, 2015). Because the Multi-view Stereo (MVS) technology used it for environment establishment uses optical reflection to perform rapid multi-image overlay to obtain the calculation parameters of the environment model, and perform model establishment based on it (Chang et al., 2020). However, modeling through the difference in perspective will continue to deform the model in reverse due to the principle of perspective. When the deviation of the viewing angle is too large, the model level and the azimuth angle will be inaccurate. In this research, the digital twin will have a floating and uncertain state during execution. The time of flight (ToF) used by the Lidar point cloud sensor uses the principle of light wave reflection to detect reflected waves, and calculate the time difference to determine the location of the object as the basis for establishing the model (Sun, Zheng, Wang, Sun, & Ruiz, 2018). And computer-aided tools and digital fabrication are integrated to conduct research, and the problem of image errors caused by the implementation of virtual and physical integrated interactive tools is proposed, and solutions are found.

2. Literature Review

With the rapid development of digital technology, flat virtual images that originally existed only on computer screens have developed virtual environments, which can create more sensory experiences. This technology is changing the way people experience virtual and physical environments. The combination of virtual and physical requires the design of a human-machine interface, that can be sensed and controlled to establish a human-machine interactive operation method. Machines need to sense to identify the parameter information of the entity, and people need to use devices to understand the appearance of the virtual environment. By integrating the two, the barrier between human and machine can be crossed, so that the world of the machine can merge with the physical world to achieve completeness. Human-computer interaction model (Williams, Szafir, Chakraborti, & Ben Amor, 2018).

2.1. DIGITAL TWINS: DIGITAL MAPPING OF VIRTUAL AND PHYSICAL COEXISTENCE

The augmented reality (AR) in which the computer creates virtual objects or characters in reality combines people's perception of the physical world with the

virtual objects generated by the computer to develop a digital model of digital twins. The two-way connection between the environment and the physical world generates a more reasonable virtual and physical integrated fabrication process and precise production control methods to help realize intelligent fabrication (Qi, Tao, Zuo, & Zhao, 2018).

This technology brings unprecedented visual effects. In the past, the instructions can only be transmitted to the execution end through the tablet. And through the actual fabrication process to find the error, and then return to the input terminal for correction. Forcing the operator to repeat the alternate operation between the instruction and the assembly process, which greatly reduces the efficiency of the work process (Figure 1). However, virtual reality (VR) head-mounted displays have opened the door to these limitations, and the operation of performing system functions in a wearable manner overcomes these limitations. Head-mounted displays incorporating augmented reality technology have gradually appeared on the market, which can create virtual images in mixed reality (MR).

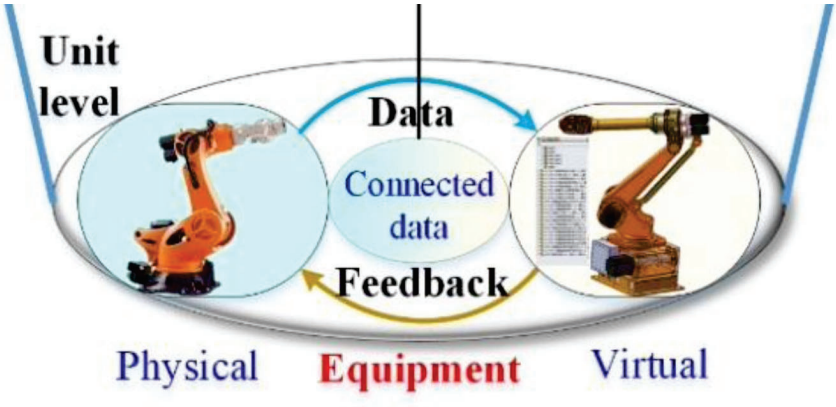

Figure 1. Digital twin in the virtual and real integration method of intelligent fabrication (Qi, Tao, Zuo, & Zhao, 2018).

2.2. DIGITAL FABRICATION TOOLS WITH VIRTUAL AND PHYSICAL COEXISTENCE

Mixed Reality is a technology application that allows users to experience navigation content. Through this technology, users can experience virtual visual effects in a real environment. Mixed reality creates new environments and visualizations through the integration of the physical world and the virtual world, in which physical and digital objects coexist and interact in real time. Mixed reality not only occurs in the physical or virtual world, it includes augmented reality technology that combines reality with virtual reality, and virtual reality real-time interaction technology. Today's mixed reality technology and application range have been extended to entertainment, interactive art, engineering, and medicine

are used in many applications (Tepper et al., 2017).

2.3. MULTI-VIEW STEREO OF MIXED REALITY MOBILE (MVS)

The MVS technology uses optical reflection images obtained from different viewing angles to quickly superimpose multiple images to calculate the image difference of the reference object, thereby performing 3D model creation. The multi-view manifestation technology originated from the human visual system. The brain builds a three-dimensional space through several high-frame-number images obtained by the eyes (Figure2). The MVS technology is to operate in this way, using lenses separated by a certain distance to obtain multiple images, by comparing the distance between each lens, and then calculating the distance of the object seen by each lens from the lens focal length to determine position of the object in space (Furukawa & Hernández, 2015).

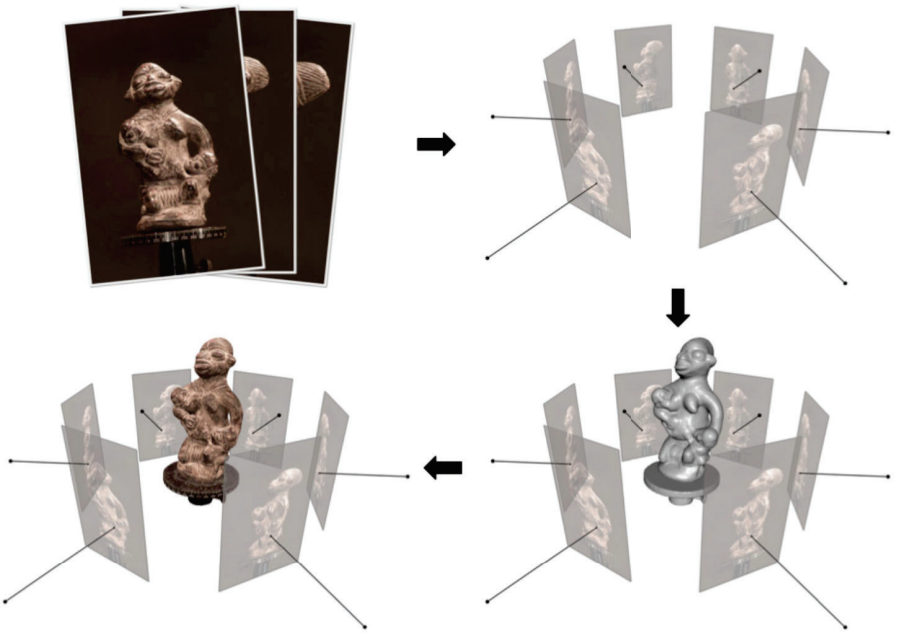

Figure 2. MVS image creation principle (Furukawa & Hernández, 2015).

2.4. TIME OF FLIGHT OF LIDAR SENSOR(TOF)

The space point cloud sensor technology can translate physical space objects into digital point clouds. The Lidar sensor uses this method to capture the parameter data of the physical space and is based on time of flight (ToF) Lightwave distance measurement, calculate the start and end signals of the flight time to get the distance, and then build the model (Li, Yang, Xie, Li, & Xu, 2018). Lidar uses

a sonar-like optical reflection mechanism to locate the point cloud, and uses the time difference between light wave emission and reception to calculate the position parameters of the physical object. Therefore, when the object is blocked, the distance of the blocked object can be obtained through reflection (Figure3).

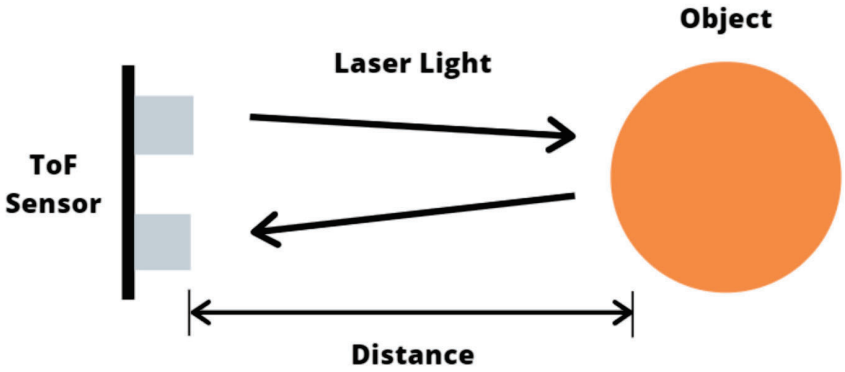

Figure 3. ToF lightwave ranging principle.

2.5. SUMMARY

Based on the above-mentioned literature discussion, the use of digital twin virtual and physical integrated fabrication tools requires the integration of that parameters. And virtual content needs to be presented to users with physical world devices, so that users can view the virtual environment from a realistic perspective. The physical environment also needs to be detected by the computer for identification by the sensor, so that the computer can know the appearance of the physical environment, so as to achieve the human-computer interaction where the virtual and physical coexist.

3. Materials and Methods

This experiment integrates the Lidar point cloud sensor time of flight (ToF) technology and the multi-view stereo (MVS) technology used by Mixed reality mobile in the establishment of the environment model. These two are different model results derived from sensing technology. In order to increase the accuracy between the virtual model and the physical environment, and apply it to the intuitive precision process control of the digital twin, so that the designer can more accurately view the fabrication process, so that the prototype can be corrected in real time when an error occurs (Chen, Chang, Hsiao, & Huang, 2019).

3.1. TOF AND MVS ENVIRONMENT MODELING

This technology first uses the ToF sensor Lidar to translate objects in space into digital point clouds, and feeds them back to the mixed reality mobile interface using the MVS module. In response to different sensing technologies in the

process, ToF and MVS will individually produce different digital models. This technical process is to examine the differences between these two virtual models to increase the accuracy of the virtual model and optimize it. Interactive workflow of the virtual and physical integration platform. In addition, this technology also expects to shorten the time for designers to fabrication and test prototypes by allowing designers to view and correct digital models more accurately and in real time, and to reduce problems that need to be corrected again after fabrication. First, we set up the ToF point cloud sensor in the space for sensing, and transmit the signal to the surroundings in a divergent manner. After sensing the physical object in the space, it will bounce back to the sensor to obtain the position information of each physical object, then convert it into a point cloud, and rearrange it in the software (Ouster Studio) to be in the virtual environment produced physical sensing model world (Figure4).

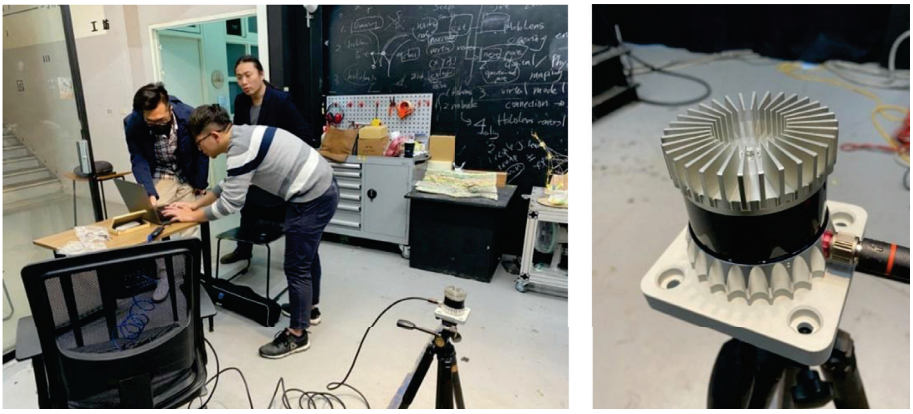

Figure 4. Use fixed ToF for environmental modeling pre-test.

When an object in physical space changes, the position of the bounced signal also changes. The signal is updated at 655,360 points per second to detect the change of the physical object in real time (Figure5).

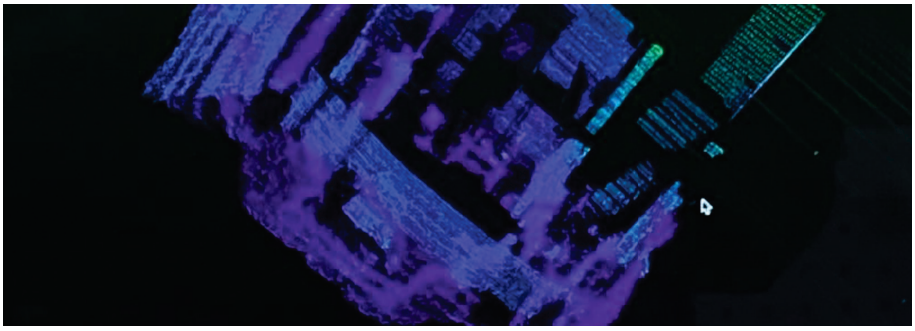

Figure 5. ToF point cloud model.

Then we set the initial origin in the MVS device, and use this origin as the base point of the virtual world and the origin in the computer-aided design software. The origin setting assists us in locating the space, fabrication equipment, and the relative position of the material (Figure6).

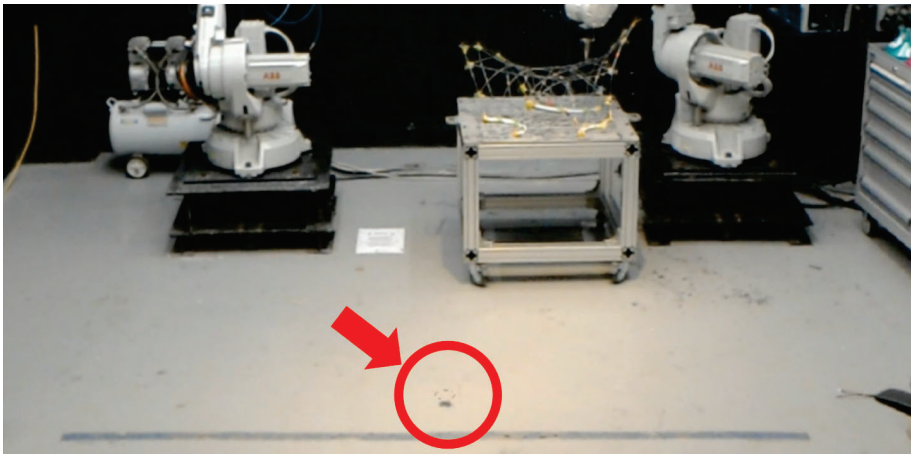

Figure 6. MVS positioning mechanism.

3.2. MVS AND TOF DIFFERENCE COMPARISON

In order to be able to analyze the point cloud, we will capture part of the point cloud and output it as a CSV, and then read the file by Grasshopper to generate the point cloud information in the computer-aided design software. However, after displaying the space model scanned by the mixed reality device (green) and the point cloud scanned by the sensor (red). We found a slight difference between the two. You can see the boundary of the space model scanned by the MVS, and the point cloud boundary of the ToF scan does not currently match in angle (Figure7).

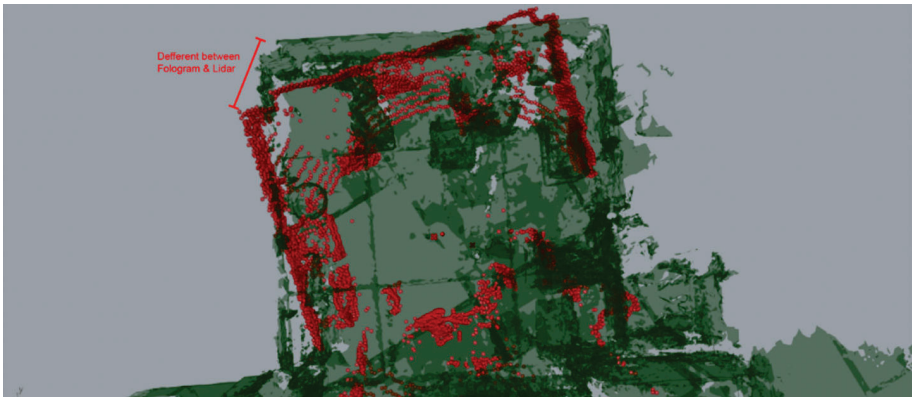

Figure 7. Differences in modeling results between MVS and ToF.

3.3. MVS AND TOF ERROR ADJUSTMENT

In order to make the two models match each other, we projected the origin of the MVS and the center of the ToF point cloud on the same reference center. The center point of the digital space formed by the point cloud is analyzed, and the center point is the position of the sensor. Since the sensor is mounted in the air, we connect the outermost point of the point cloud to form a frame, and use the center point of the bottom of the frame as the origin. Finally, the center point of the sensor and the origin of the mixed reality device are pasted together so that the spatial positions of the two are consistent (Figure8).

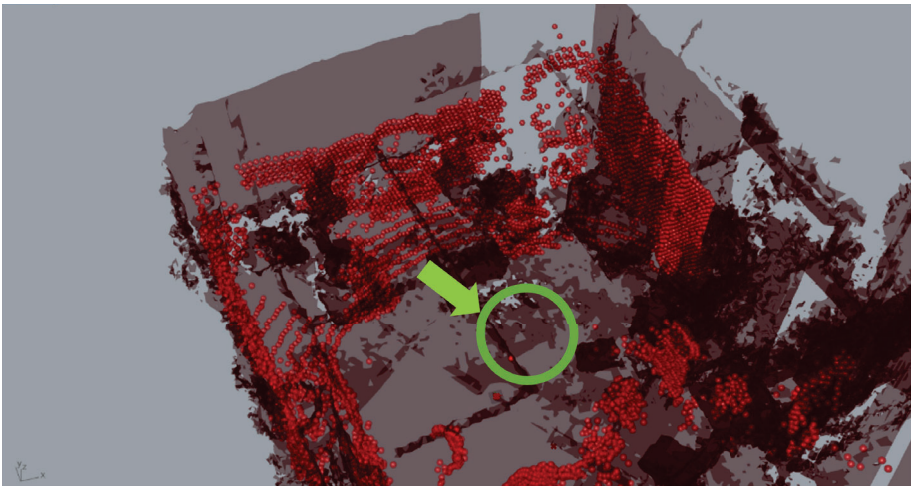

Figure 8. The MVS and ToF models are overlapped with a reference point and then the matrix transformation calculation is performed.

4. Result and Discussion

To enable the coexisting interactive fabrication tools to realize the physical and virtual interconnection, through the spatial point cloud sensor, the change of the object in the space is converted into a digital point cloud and feedback to the virtual interface. The two spaces of virtual and physical are constantly communicating and giving feedback, and the differences between virtual models and physical products are tested to optimize interactive design tools. We used two different sensing technologies to model the environment at different stages of the workflow, combined the advantages and disadvantages of MVS and ToF, and applied the two models derived from the algorithm for correction. According to the results of this experiment, it is recommended to digitally model the environment through the positioning ToF mechanism at the beginning of the work, and use it be a reference benchmark. And then continuously obtain it through the MVS of Mixed Reality Mobile Buffer model. The original reference object is calculated through digital reference and matrix transformation, and the comparison effect between the mixed reality mobile device and the point cloud sensor is further optimized.

After that, we also tried to use this interactive fabrication tool for the application of weaving structure. The weaving structure is widely used in the field of architecture, and the use of digital technology to construct a complex spatial curve model (Chang et al., 2020; Huang, Yan, Luo, & Li, 2016).We imported the physical data into the virtual system, and the environment construction used the optical correction tool of this experiment. It can be found that after this correction tool, the virtual image seen in Mixed Reality Mobile is close to the actual state, achieving a more complete digital twin effect (Figure 9). After the fabrication calibration system, the computer can obtain the environmental parameter values more completely and instantly. This system can help users greatly reduce errors when performing digital twinning, and more accurately view and operate the fabrication process. In the future, this system will be able to combine image recognition and machine learning to fully automate the operation of digital fabrication tools. This calibration mechanism provides rapid establishment of environment and object parameters, which helps the computer to establish an environment on the virtual side when performing automated settings later. And more importantly, users can accurately view the process through this system and can make real-time corrections.

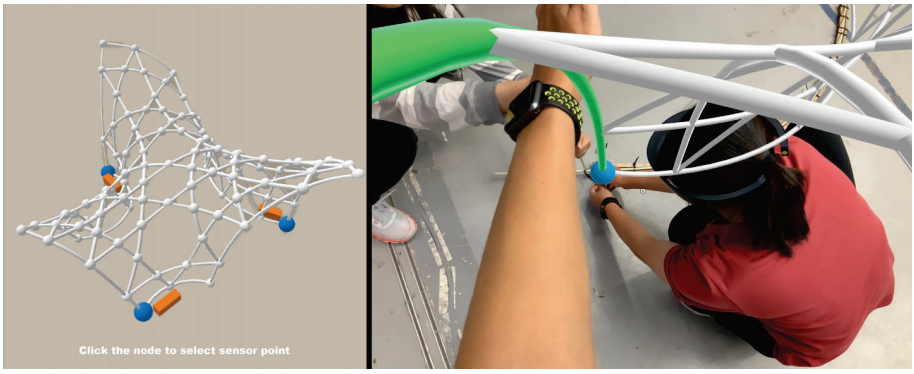

Figure 9. Use mixed reality mobile to manipulate the weaving structure of virtual models.

5. Conclusion

The ToF and MVS technologies are integrated to increase the accuracy of the digital tools that coexist with virtual and physical. In the process, it was discovered that the two technologies can be used to complement each other. ToF space point cloud technology Obtain the real space environment parameters to compensate for the errors caused by MVS in using different viewing angles to present images. In the experiment, we found that the models established through those technologies can be interactively compared and corrected, which can solve the inconsistency between the virtual space model and the physical space environment, when using the digital fabrication tools of Mixed reality mobile for work.

This technology can be applied to the building fabrication process, so that the virtual 3D model corresponds to the physical mechanical operation and can be

observed alternately at the same time. However, through experimental results, we believe that more automated calibration is needed to eliminate the need for manual adjustment during calibration. Therefore, a system to solve this problem can be established in the future. The system allows designers to execute directly on the device while viewing the virtual and physical environment. The virtual execution side can control and observe physical equipment to facilitate the fabrication process of digital buildings.

References

Caputo, F., Greco, A., Fera, M. and Macchiaroli, R.: 2019, Digital twins to enhance the integration of ergonomics in the workplace design, *International Journal of Industrial Ergonomics*, **71**, 20-31.

Chang, T.W., Hsiao, C.F., Chen, C.Y., Huang, W.X., Datta, S. and Mao, W.L.: 2020, Fabricating Behavior Sensor Computing Approach for Coexisting Design Environment, *Sensors and Materials*, **32**, 2409.

Chen, C.Y., Chang, T.W., Hsiao, C.F. and Huang, H.Y.: 2019, Developing an Interactive Fabrication Process of Maker Based on "Seeing-Moving-Seeing" Model, *The International Conference on Computational Design and Robotic Fabrication*, 312-321.

Dembski, F., Wössner, U.w.e. and Letzgus, M.: 2019, The Digital Twin-Tackling Urban Challenges with Models, Spatial Analysis and Numerical Simulations in Immersive Virtual Environments, *Proceedings of the 37th eCAADe and 23rd SIGraDi Conference*, 795-804.

Furukawa, Y. and Hernández, C.: 2015, Multi-view stereo: A tutorial, *Foundations and Trends® in Computer Graphics and Vision*, **9**(1-2), 1-148.

Hsiao, C.F., Lee, C.H., Chen, C.Y. and Chang, T.W.: 2020, A co-existing interactive approach to digital fabrication workflow, *Proceedings of the 25th International Conference of the Association for Computer-Aided Architectural Design Research in Asia (CAADRIA)*, Bangkok, Thailand.

Huang, W., Williams, M., Luo, D., Wu, Y. and Lin, Y.: 2018, Rsu X Tsinghua X Yuntech Weaving Structure And Interactive Space Workshop, *Proceedings of the 23rd International Conference on Computer-Aided Architectural Design Research in Asia (CAADRIA), Hong Kong*.

Huang, W., Yan, D., Luo, P. and Li, X.: 2016, Digital design and construction of a weaving structure, *The 8th International Conference on Fibre-Reinforced Polymer (FRP) Composites in Civil Engineering (CICE 2016), Hong Kong*.

Li, X., Yang, B., Xie, X., Li, D. and Xu, L.: 2018, Influence of waveform characteristics on LiDAR ranging accuracy and precision, *Sensors*, **18**(4), 1156.

Okura, F., Kanbara, M. and Yokoya, N.: 2015, Mixed-reality world exploration using image-based rendering, *Journal on Computing and Cultural Heritage (JOCCH)*, **8**(2), 1-26.

Qi, Q., Tao, F., Zuo, Y. and Zhao, D.: 2018, Digital twin service towards smart manufacturing, *Procedia Cirp*, **72**, 237-242.

Sun, C., Zheng, Z., Wang, Y., Sun, T. and Ruiz, L.: 2018, A Topological-Rule-Based Algorithm Converting a Point Cloud into a Key-Feature Mesh, *Proceedings of the 23rd International Conference on Computer-Aided Architectural Design Research in Asia (CAADRIA)*, Hong Kong, 597-606.

Tepper, O.M., Rudy, H.L., Lefkowitz, A., Weimer, K.A., Marks, S.M., Stern, C.S. and Garfein, E.S.: 2017, Mixed reality with HoloLens: where virtual reality meets augmented reality in the operating room, *Plastic and reconstructive surgery*, **140**(5), 1066-1070.

Williams, T., Szafir, D., Chakraborti, T. and Ben Amor, H.: 2018, Virtual, augmented, and mixed reality for human-robot interaction, *Companion of the 2018 ACM/IEEE International Conference on Human-Robot Interaction*, 403-404.

DIGITAL DESIGN AND FABRICATION OF A 3D CONCRETE PRINTED PRESTRESSED BRIDGE

QIANG ZHAN[1], XINJIE ZHOU[2] and PHILIP F. YUAN[3]
[1,2,3] *Tongji University*
[1,2,3] *{1932153|2032187|philipyuan007}@tongji.edu.cn*

Abstract. In recent years, additive manufacturing and 3D printing technologies have been increasingly used in the field of construction engineering. 3D Concrete printing is a kind of laminated printing method using concrete extrusion technique. Concrete has the advantages of high compressive strength, low deformation, and excellent durability, and has high application value in the construction field. However, as a brittle material, concrete has limited tensile and flexural strength. For beam like components, it is difficult to fully exert the compressive performance of the material relying solely on itself, so it is difficult to apply to the bending member. The experimental case introduced in this paper combined the prestressing system with concrete printing technology. A post-tensioning prestressing system suitable for prefabricated concrete 3D printing components, which combined the excellent tensile properties of steel bars with the compressive performance of the 3D concrete printed part was proposed.

Keywords. 3D concrete printing; Prestressed concrete; robotic fabrication; structural optimization.

1. Introduction

In concrete structures, formwork occupies a large part of the production cost, especially for components with complex shapes, with low formwork reuse rate. Additive manufacturing and 3D printing technologies that have emerged in recent years have been applied in the field of construction engineering, make it possible for the mass-customized production of building components. 3D Concrete printing technology is a template-free and mass customization construction method, which can effectively reduce the production cost of custom-shaped components, improve production efficiency and changes the traditional concrete construction method.

Recently, 3D printed concrete components have been gradually used in large-span structures. However, due to the weak layer bonding, it is difficult to transmit shear and tensile forces, and can only be used for purely compressed structures. Although ultra-high-performance material which shows better tensile performance have been developed for concrete printing (Li et al., 2020), the complex mixing pumping process and much higher material cost still make it difficult for mass production.

PROJECTIONS, Proceedings of the 26th International Conference of the Association for Computer-Aided Architectural Design Research in Asia (CAADRIA) 2021, Volume 1, 663-672.

The first all-concrete printing arch bridge with a span of 14.4m was built in Shanghai, China in 2019 by Weiguo Xu from Tsinghua University. The printing material is a fast-hardening sulphoaluminate cement-based mortar with PVA fibre, which has a compressive strength up to 65MPa. The total printing time for the entire bridge is 450 hours. (XU et al. 2020) Post-tensioning is firstly used in concrete printing component by TU Eindhoven in 2018 in a pedestrian bridge. The bridge has a length of 8m and a width of 3.5m, to improve the tensile and post-cracking capability. In the printing process, steel wires were implanted during the printing process. (A. M. Salet et al. 2020)

Figure 1. 3D concrete printed arch bridge by Tsinghua University 2019 (left) 3D concrete printed prestressed bridge by TU Eindhoven 2018 (right).

Post-tensioning technology delays structural cracking and improves load-bearing efficiency in concrete structures. If it is combined with the concrete 3D printing technology, the bearing capacity of the components can be effectively improved, so that the concrete 3D printing components can be used for the beam-like structure.

The experiment described in this paper combines post-tensioning prestressing technology with concrete 3D printing components and uses the cavity of the 3D printing components to place prestressed steel bars. The tensile strength of steel and the compressive properties of concrete was combined to form a lightweight beam-like structure with high load-bearing capacity. As shown in figure.2, the experiment process starts with material research. Several material tests were performed to obtain material performance parameters. Based on the material properties, the model was designed, optimized, and finally, a prestressed beam with a length of 4.7m and a width of 0.6m was printed and built.

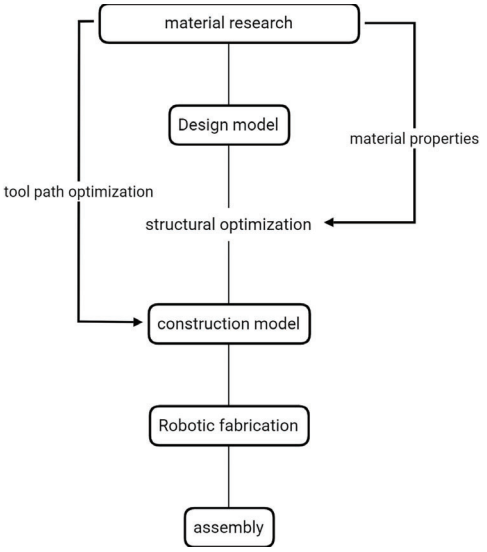

Figure 2. method and design process.

2. Research and Prototyping

2.1. MATERIAL AND MIXTURE DESIGN

A fibre-reinforced high-strength cementitious mortar was chosen as the primary printing material, and an alkali-free accelerator was added to control the set time. The major components of the mortar were list in table 1. P.W. I 52.5 White Portland cement is used as the main binder, which shows good compressive strength with silica fume. Metakaolin is used to make the mixture to reach the required thixotropy for extrusion and buildup (Zhang et al. 2018).

Table 1. Material and Mixture Design.

Material	**Quantity (kg/m^3)**
White Portland Cement (P.W I 52.5)	654
Silver Sand (0-1mm)	785
Silica Fume	65
Metakaolin	65
Water	229
Superplasticizer	0.65
PVA Fiber (13mm)	2.5

2.2. EXTRUSION TECHNIQUE

To simplify the dosing and mixing process. Dry powder of material was preblended and packed into 25kg bag ready mixed mortar according to the formula. And mix with water according to the proportion before printing. A continuous mixer was adopted to automatically add water and mix materials continuously. After the mixing process completed, the material was pumped to the print head for extrusion.

In order to reach the required pressure delivering the material from the ground to the nozzle with minimal pulsation, PCP (progressive cavity pump) was chosen as the pumping machine. However, there is certain inevitable pulsation for high-pressure PCP due to its mechanical properties. First, the material is pump from a high-pressure PCP to the buffer hopper of the print head and then extrude by a relatively low-pressure PCP to dampen the pulsation and reach a constant flow rate. An accelerator is added right before the mixture exit the nozzle. The general extrusion process is shown below.

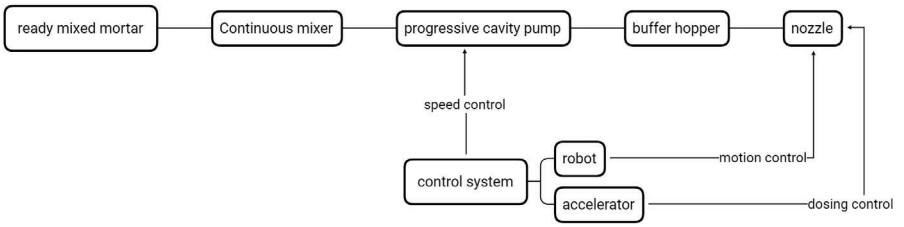

Figure 3. extrusion process.

2.3. MATERIAL PROPERTIES TEST

The shape adaptability and mechanical properties of printing materials are essential parameters that need to be determined before design. The experiments tested the maximum inclination angle of the toolpath, printing speed, and material properties.

2.3.1. Printing parameters test

The maximum overhang test generally bases on the method developed by ETH Zurich (Anton A. et al., 2020). The maximum overhang degree of this mortar was determined by test printing. The rib of the test concrete printed panel was inclined between 15° and 25°. Rib with the incline lower than 20° can buildup successfully, while the one greater than 20° cannot support itself. At the same time, the vertical buildup rate can be up to 1000mm/h to match the required set time of the mixture.

Figure 4. incline angle test 15°(left),20°(middle),25°(right).

The 3D printed component should keep in a full-section compression state by prestressing. So, the compressive strength and elastic modulus are the main design parameters to be determined. The 90° cross pattern was chosen to prevent the transverse split under pressure. After printing, samples were cured for 21 days following the standard curing process and sawed into cubic test block with an edge length of 70.7mm. The test was carried out according to "standard for test method of basic properties of construction mortar (JGJ／T 70-2009)". The test results are compared in parallel with the casting sample list in table 2. The average compressive strength of the print sample is 45.84MPa, 94% of the result of its casting sample. It shows that there is no significant strength loss caused by the printing process.

Figure 5. 90° cross pattern of test sample.

Table 2. compressive strength of print and cast samples.

Item	No.	1	2	3
Print samples	Length, mm	72.84	72.35	73.81
	Width, mm	71.46	70.77	71.95
	Compressive Strength, MPa	43.78	47.12	46.63
	Average, MPa		45.84	
Cast samples	**No.**	**1**	**2**	**3**
	Length, mm	72.92	71.42	71.66
	Width, mm	70.82	71.13	70.87
	Compressive Strength, MPa	47.64	50.59	47.53
	Average, MPa		48.58	

3. Computational design

The bridge body adopts a beam structure, two bundles of prestressed steel bars are placed at the lower part of the bridge body so that the printed components of the bridge body always maintain full section compression.

3.1. TOOLPATH OPTIMIZATION

The toolpath of the section was optimized according to the stress distribution. More material was distributed in the compressive part, which reduces the weight of the unit while ensuring the maximum section efficiency. Due to the pumping and extrusion methods, the printing process cannot start and stop in real-time. So the path of each layer is optimized to ensure each unit was printed in one continuous stroke.

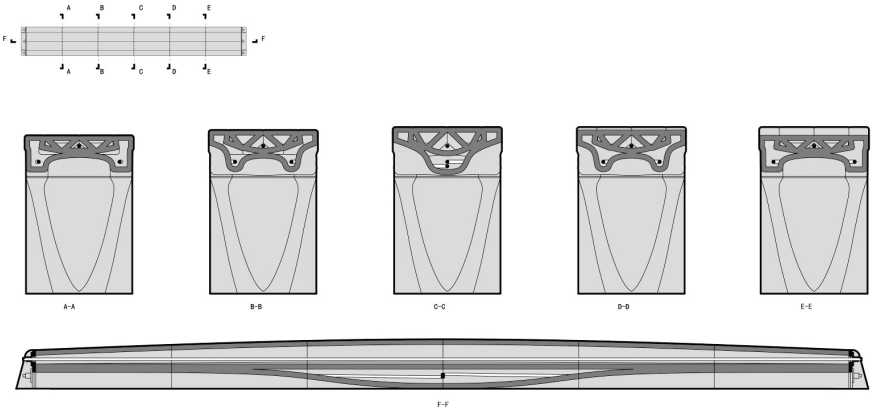

Figure 6. section drawings.

3.2. FEM ANALYSIS

Finite element analysis and simulation of the bridge were carried out to verify the design strategies and get the correct amount of prestressing. The structure diagram is as follow:

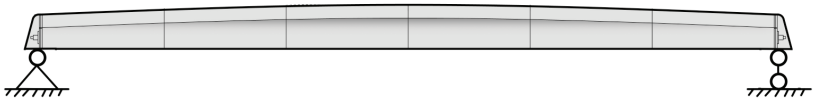

Figure 7. structure diagram.

Supports at both ends of the bridge are hinged. According to related regulation and the test result above, the material properties of the prestressed steel bars and the printed parts were listed as follows:

Table 3. material properties.

Material	**strength**	**Young's modulus**
Φ15 PSB 830 finish rolled rebar	830MPa (tensile strength)	200GPa
3D printed part	40MPa (Compressive strength)	20GPa

The steel bars were made of finished rolled rebar without longitudinal ribs, connected by rebar nuts on both sides, manually tightened by a torque wrench, and the amount of the tension is controlled by the wrenching torque. The live load of the bridge deck was set as 4.5kPa and calculate with the full span and half span load case.

Table 4. deformation of full span (left) and half span (right).

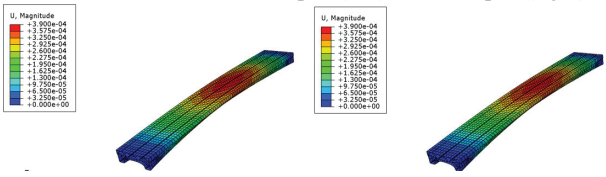

4. Robotic Fabrication

In order to reduce the difficulty of transportation and printing, the bridge section is divided into six equal-length units for printing. After 21 days of curing, the test

block is assembled on a simple bracket constructed by bricks. Finally, the bridge body is stretched and hoisted to the steel support.

Figure 8. workflow.

Due to the fast printing speed, the print head moving speed is up to 200mm/s. The traditional 3-axis printing platform has a heavy motion mechanism and a long acceleration and deceleration process, which is prone to jitter at the turning point. The print head discharge speed is difficult to achieve real-time adjustment. Thus effects the corner printing quality. The six-axis mechanical arm movement mechanism is light in weight and flexible in movement, which is more suitable for high-speed printing. The printing control system is based on rhino and grasshopper platforms. Based on the FuRobot system (Lu et al. 2020), computers can communicate with the robot in real-time and transmit the real-time position of the robot arm. The printing path is generated in real-time according to 3D model so that the printing path length is not limited by the file size. The robot's movement speed can be controlled in real-time based on external feedback.

Figure 9. printing process.

Due to the relatively lightweight of the components, six printing units, each weighing around 80-90kg, can be directly transported and assembled manually. The joints between components are filled with mortars to ensure the force transmission at the joints.

Figure 10. assembly.

Figure 11. final result.

5. Result and discussion

This bridge combines concrete 3D printing, post-tensioning, and robot fabrication technology. The printing process of the components only takes three days, and the assembly process only takes 2 hours. Fast and formless fabrication of customized components was achieved. At the same time, the total weight of the bridge is about 600kg. Compared with the solid beam structure, the printed components can optimize the material distribution in the section more freely, and make the structure lighter and more efficient.

Table 5. time comsumption.

	Time consumption of Fabrication	**Labor**
Printing	3 days	2
Curing	21 days	0
On site assembly	2 hours	3

References

Anton, A.n.a., Bedarf, P., Yoo, A., Reiter, L.e.x., Wangler, T., Flatt, R. and Dillenburger, B.: 2020, Concrete Choreography: Prefabrication of 3D-Printed Columns, *Fabricate 2020: Making Resilient Architecture*, 286-293.

Li, V.C., Bos, F.P., Yu, K., McGee, W.e.s., Ng, T.Y., Figueiredo, S.C., Nefs, K., Mechtcherine, V., Nerella, V.N., Pan, J., van Zijl, G.P. and Kruger, P.: 2020, On the emergence of 3D printable Engineered, Strain Hardening Cementitious Composites (ECC/SHCC), *Cement and Concrete Research*, **132**, 106038.

Ming, L.u. and Yuan, P.F.: 2020, A NEW ALGORITHM TO GET OPTIMIZED TARGET PLANE ON 6-AXIS ROBOT FOR FABRICATION, *Proceedings of CAADRIA 2020*, 393-402.

A. M. Salet, T., Y. Ahmeda, Z., P. Bos, F. and L. M. Laaglandb, H.: 2018, Design of a 3D printed concrete bridge by testing, *Virtual and Physical Prototyping*, **13**(3), 222-236.

Xu, W.: 2020, Fabrication and Application of 3D-Printed Concrete Structural Components in the Baoshan Pedestrain Bridge Project, *Fabricate 2020: Making Resilient Architecture*, 140-147.

Zhang, Y.u., Zhang, Y., Liu, G., Yang, Y., Wu, M. and Pang, B.o.: 2018, Fresh properties of a novel 3D printing concrete ink, *Construction and Building Materials*, **174**, 263-271.

TOWARDS SWARM CONSTRUCTION

YUHAN HOU[1] and PAUL LOH[2]
[1,2]*University of Melbourne*
[1]*yuhanh@student.unimelb.edu.au* [2]*paul.loh@unimelb.edu.au*

Abstract. Swarm intelligence has primarily been explored in architecture as a form-finding technique with resulting material articulation using advanced 3d-printing technology. Researchers in engineering have developed swarm robotics for construction and fabrication, typically constraints to small scale prototypes as the technology matures within the field. However, a few research explores the implication of swarm robotics for construction on the building or urban scale. This paper presents a novel swarm robotics construction method using mole-like digging technology to construct new architectural language using machine intelligence. The research discusses the role of swarm intelligence behaviours in design and synthesis such behaviour with machine logics. The paper addresses the conference theme through the speculative projection of future construction methodology and reflects on how automation can impact the future of construct and design.

Keywords. Swarm; Digital Fabrication; Robotic.

1. Introduction

The research proposed a novel robotic system that challenges the typical agent-based design techniques as form-finding (Snooks and Jahn, 2016) towards an agent-based fabrication system using swarm intelligence. The paper hypotheses on the use of multiple tunnelling swarm robots deployed to manipulate earthwork with resulting void spaces filled with self-compacting concrete to create structural form through design research methodology. Local communication with sensors (Schranz et al., 2020) allows swarm robotics to avoid colliding in the tunnel and generate feedback when implementing the staged earthwork. The swarm robotics works as a collective network instead of linear feedback, making the system robust, scalable and adaptable with the changing environment. Later part of the paper discusses the swarm robot design, including its control system and workflow in detail.

The research is tested through a series of construction scenarios as research outcomes through the synthesis of swarm behaviours with machine constraints and construction methodology. It demonstrates the potential to shape and challenge traditional construction cut and fill techniques in earthwork with application to create landscaping components striving for digital naturalism (Spuybroek, 2016).

PROJECTIONS, Proceedings of the 26th International Conference of the Association for Computer-Aided Architectural Design Research in Asia (CAADRIA) 2021, Volume 1, 673-682.

2. Background

2.1. RESEARCH GAPS: BEHAVIOUR, FORM, MOTION AND TECTONIC

Most of the swarm application in architectural design focuses on emergent characteristics of form. It mimics natural behaviour as a form of organicism (Spuybroek, 2016) with single robotic fabrication (Snooks and Jahn, 2016). These form seeking techniques tend to be self-referential in its data generation. The FIBERBOT (Kayser et al., 2018) designed at MIT Media Lab uses swarm robotics to build the tubular structure in emergent events and TERMES (Petersen et al., 2011) designed at Harvard University introduce an autonomous collective construction at a small scale. This paper intends to fill the gap of translating multi-agent algorithms directly to the collective swarm robotic construction. It is a novel design and construction system, from behaviour to form, and from form to motion, which informs the final tectonic outcome.

2.2. RESEARCH APPROACH: SWARM BEHAVIOUR STUDY

The research takes a systematic approach. The swarm behaviour is the fundamental principle of the system in generating form and defining robot movement. Based on the study of Craig Reynolds' theory (1987), in Figure 1, each agent or Boid's movement is defined by the basic forces as aligning, cohering and separating. The agent can be released with or without initial velocity. Vision radius (dashed circles) determines how far each agent can research its neighbour. This basic parameter decides the character of local behaviour which later inform the size and type of the global organisation.

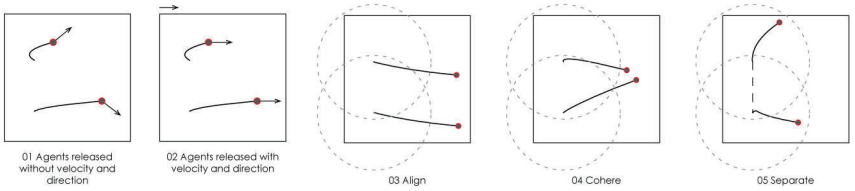

Figure 1. Basic swarm behaviour.

One type highlighted in this research is path tracking behaviour, which is used to generate later architectural geometry. It attracts agents to steer along a given path. Additional parameters further define tracking behaviour. As illustrated in Figure 2, projection distance refers to how fast agents move towards the path while the polyline radius determines the range of moving.

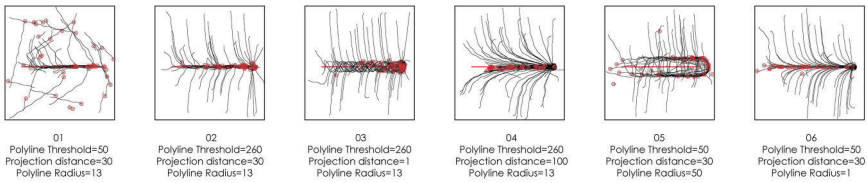

Figure 2. Path tracking behaviour.

Site surface datum levels (both existing and desired) are critical parameters that give the spatial organisation architectural meanings. Figure 3 shows one example of the serial architectural catalogues examined. The width and clearance of the road define the boundary of the interface. Groups of agents are released from or above the ground floor plane moving towards the path. The red spheres in figure 3a represent the individual agent's moving position while the black lines show the trajectories created with resulting geometry (Figure 3b). The moving slope decides the type of vertical elements such as column, staircase and ramps (Figure 3c). In this virtual prototype, the swarm technique proves its potentials in generating architectural elements via the site conditions. The new synthetic structure applied with swarm technique further facilitates the flood management on the site in the later urban landscape proposal.

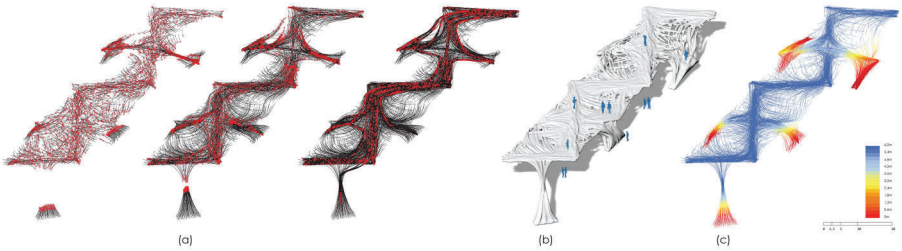

Figure 3. Architectural elements generated. (a) Generation process. (b) 3D outcome. (c) Height evaluation.

2.3. SUBTRACTIVE APPROACH - MOULD FOR CASTING CONCRETE

Figure 4 shows the logic of translating motion into tectonic outcome using a subtractive fabrication approach. The red sphere represents the individual robot that drills through the stock. Each trail generated in tracking behaviour is extracted to become the paths of the robots. The resulting void spaces become the mould for casting. So, the form generation process is directly translated into the fabrication process.

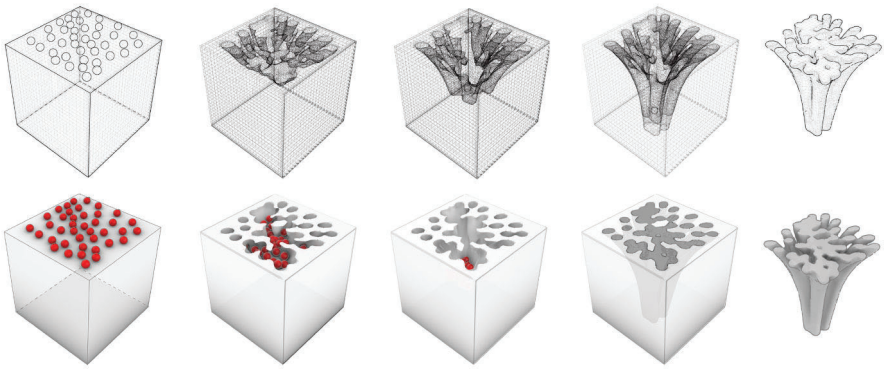

Figure 4. Translating swarm movement into tectonic outcome using the subtractive approach.

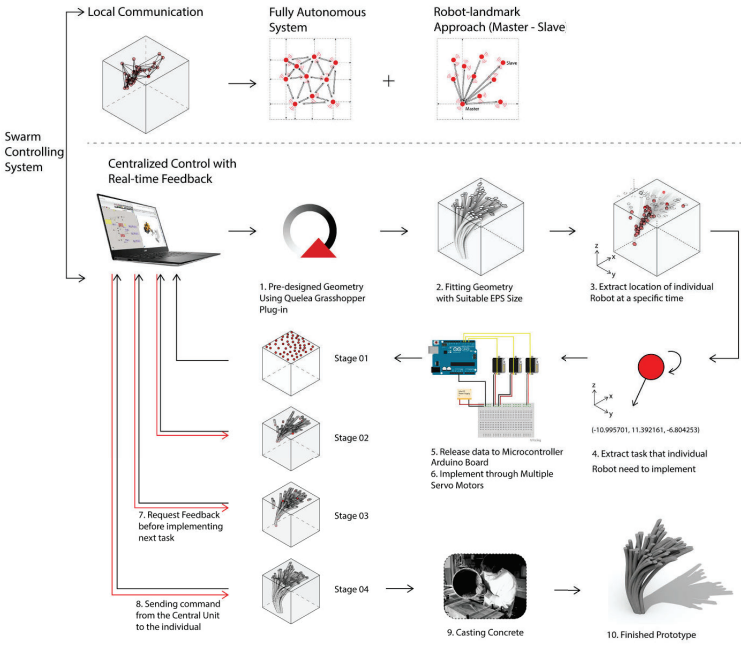

Figure 5. Swarm Controlling System.

2.4. SWARM CONTROLLING SYSTEM

Some researches identify decentralized decision making in swarm robotic application as a fundamental principle (Schranz et al., 2020). To maintain the agent's autonomy while reducing risk in real-time construction, the paper presents a new controlling system. The form-finding process is fully autonomous while the central unit with real-time feedback-controlled the fabrication procedure. To

be Specific, after geometry is generated with animated swarm behaviour, the X, Y, Z coordinate, velocity and moving directions are extracted and sent to the microcontroller of the individual swarm robot (see Figure 5). In each stage, the robots send the position to the central unit for calibration before implementing the next task.

2.5. COLLECTIVE CONSTRUCTION VS SINGLE ROBOTIC CONSTRUCTION

Swarm intelligence operates through simple behaviours to create emerging complex forms (Scribner, 2001). The simple mechanism makes the robot able to act independently and implement its own task. Under collective action, swarm robotics can generate a complex geometry. The project proposed a mole-like digging robot to perform the tunnelling action. Individual robots consist of microcontroller, senses, actuator and mobile power. Like Terms (Petersen et al., 2011), the complex structure can be built at a scale larger than an individual robot. With sensing capabilities, swarm robotics are interconnected and able to interact with each other and environment, which characterizes the system's main advantage as scalable, robust and adaptable. Compared with single robotic construction, having a collective of smaller and more mobile robots operating at the same time contributes to a faster and more efficient construction method.

3. Robotic System

3.1. DESIGN AND RESEARCH

The proposed swarm robot is based on Mole-like Drilling Robot (Lee, Tirtawardhana & Myung, 2020), which was originally designed for tunnelling through soil. The proposed design, titled Dig-bot, further expanded on the engineering design and adopted it for architectural purposes. As shown in Figure 6, it consists of the expandable drilling bit (01), forefoot (02) to remove soil, wheels (11) to manoeuvre and a pneumatic fibre mesh (13) to hold the soil. The paper will not explain the detail of the mechanism that has already been documented in engineering research (Lee, Tirtawardhana & Myung, 2020). Instead, the paper emphasis on the application of choosing mechanisms appropriate to architectural design and construction. The expandable mechanism using the rack and pinion system allows the drilling blade to expand and contract by rotating the inner shaft driven by the stepper motor. The soil removing mechanism is the design based on the scapula and humerus interaction of a mole. With a fixed point of connection, it can transform linear movement into the rotational movement to remove soil to the side. The fibre mesh attachment is able to inflate the plastic tubes lining inside through pneumatic pressure, similar to the Earthworm Soft Robot by Calderon et al. (2019).

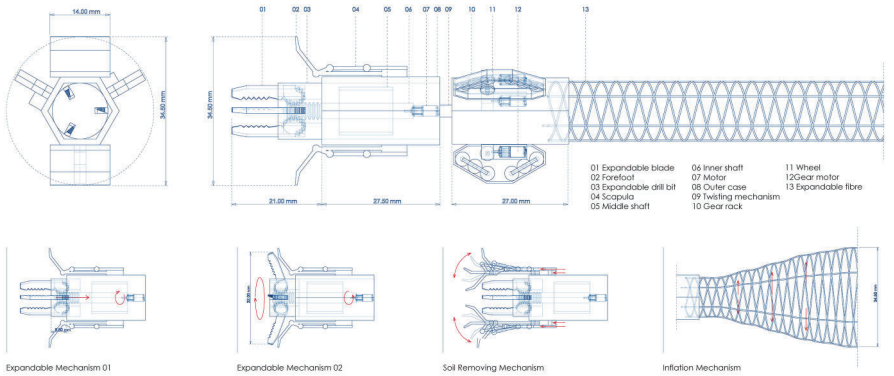

Figure 6. Mole-like swarm robotic component and key mechanism.

3.2. DIGGING PROCEDURE

Figure 7 illustrates the digging procedure starting with the initial position (7-A) where the forelimbs are located at the side of the robot. By rotating the motor counterclockwise, the folded drill bit moves forward, expanding the blade (7-B). The expanded blade keeps rotating to crush the soil while the robot advances forward (7-C). After a sufficient amount of soil is crushed, the motor rotates clockwise to retract the drilling bit to the starting position, providing enough space for soil removing (7-D). The forelimbs are pulled forward with linear actuators and spread left and right to remove soil to the side (7-E, F). After forelimbs are pulled back, the fibre mesh is inflated to hold the void space (7-G, H). While the same digging process is repeated, the waist mechanism allows the robot to change direction (7-I, J). The resulting void space will be supported by fibre mesh. This acts as a mould for concrete casting (7-K, L).

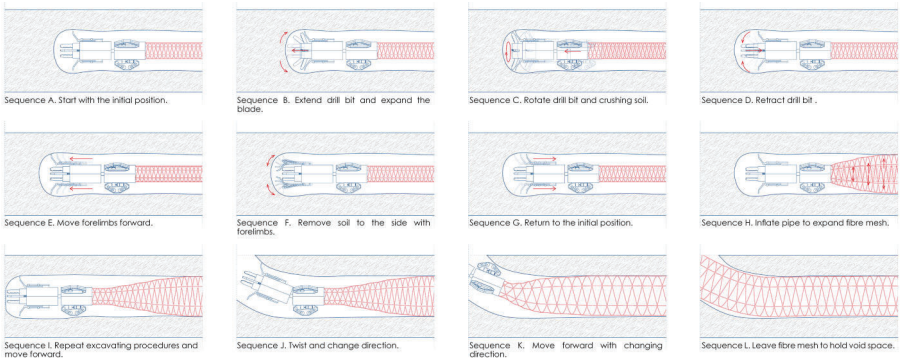

Figure 7. Digging process diagram of the system.

4. Urban Speculation

The performability of the swarm technique is tested in a speculative design, titled Digital Naturalism. The proposal is an infrastructure mediating flooding issue for a new university campus proposal. The site in consideration will be affected by increasing stormwater flooding due to climate changes. It is predicted that the site's mean sea level will rise by 0.8 meters by the year 2100 (Pty Limited et al., 2018). Facing the future challenge, the design emphasis on several water management strategies. The agent's flow is used to generate a water channel diverting rainwater from the bridge to the wetland (Figure 8). The structure indicates the procedure of swarm construction. Figure 9 also highlights the foundation shift on material and introduction of a new building type. As a passive structure to integrate with nature, the water and soil are considered as live elements of the system. The gravel with bio-resin fills in the gaps between structures which allow rainwater to flow through. Height difference in structure contributes to the varied depth of soil components, which allows the native ecosystems to coexist with the structure. The swarm becomes a technique to weave the form, material, ecology and infrastructural function together.

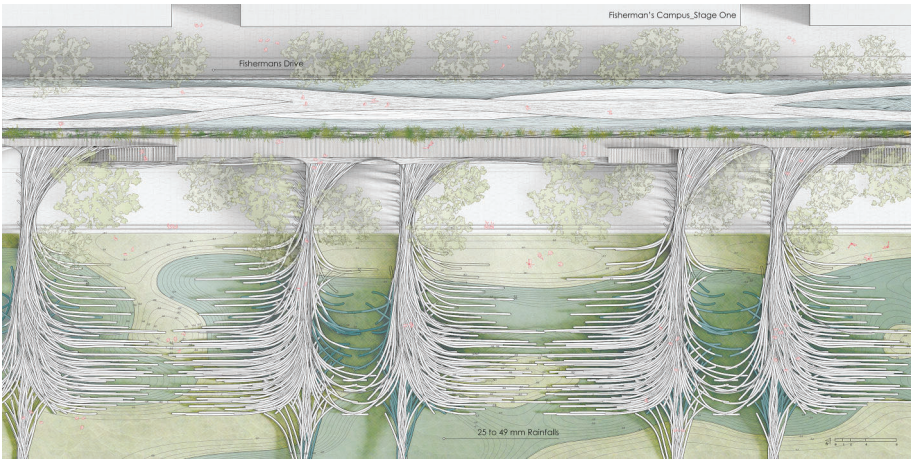

Figure 8. Plan: Proposed structure mediate flooding issue on Fishermans Bend site, Melbourne, Australia.

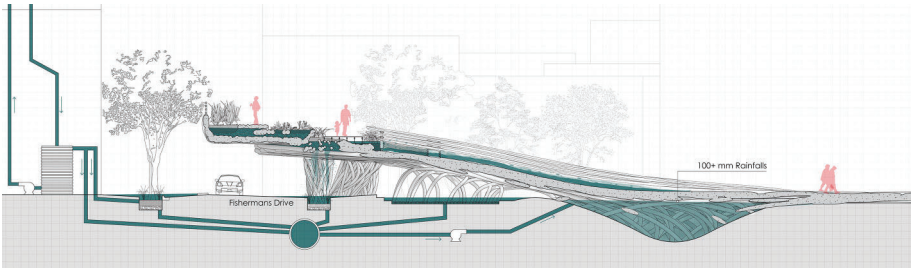

Figure 9. Section: Proposed structure mediate flooding issue on the test site.

Figure 10 highlights new swarm topography in the background of the existing urban environment and future university campus. The structure humbly sprawls from the ground and flows between the building and nature. The paper recognized that both nature and architecture are synthetic. The intent is to create a synthetic environment for nature and architecture to coexist, and facilitate each other overtimes, as a reinterpretation of naturalism in the digital age.

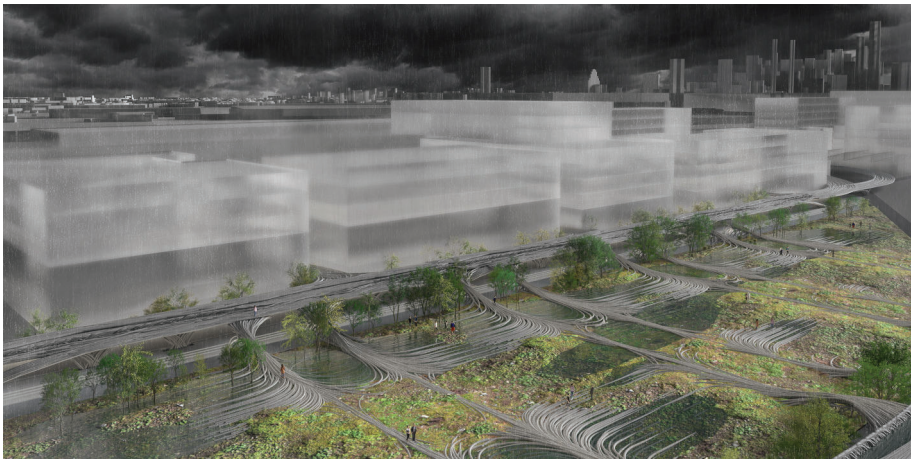

Figure 10. New swarm topography.

4.1. ON-SITE CONSTRUCTION

The project utilized the novel swarm robotic as an on-site collective construction (Figure 11). The construction procedures are designed largely based on existing construction systems with two sizes of the robot operate simultaneously. The swarm of Robot A constructs the primary structure, while the swarm of Robot B defines the surface texture. Soil is held in place using the standard Peri(TM) system, while earthwork is moved into place for robotic excavation (11-1). Swarm robots are released and tunnel inside the soil, leaving the fibre mesh to hold the void spaces (11-2). Self-compacting concrete with micro-reinforcement is pumped into the meshes and unifies all void spaces as one structure (11-3). After the concrete

is consolidated, most of the soil is removed with a hydro vacuum extractor, and some are left for planting (11-4).

Some researches also have examined the same casting technique. Montana's tippets rise art centre by Ensamble studio (2020) is a sculpture cast from the terrain. It traces the geological transformation process and is used as a way to reinterpret the terrain. The swarm construction proposed here also shared a similar aesthetic but with a unique automated construction process. As discussed in Section 2.5, collective construction provides high efficiency with small and simple robot working simultaneously. The same data used to generate form can be directly translated into the machine movement contributing to a high coherent workflow. The research project the future of design and construction, embedding the autonomy of natural system into form generation, using data to communicate between human and machine, machine and material, archiving a synthetic structure that facilitating an on-going mutual relationship between nature and architecture.

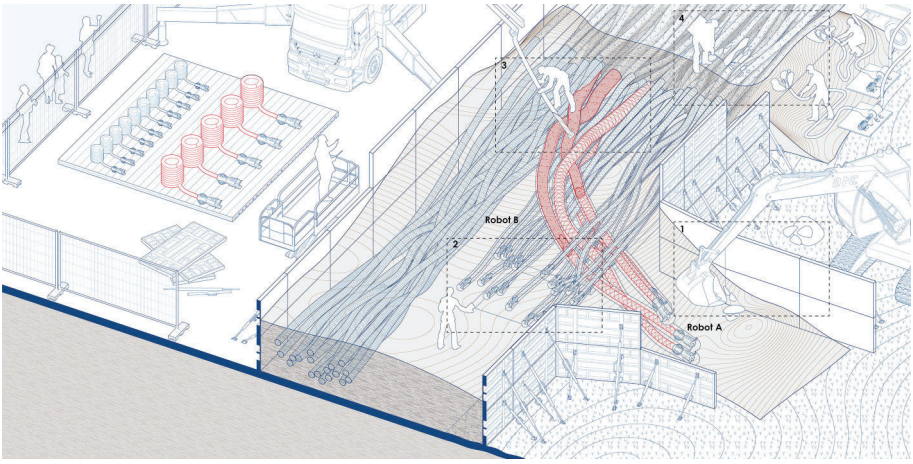

Figure 11. Swarm Robotic Construction on site.

4.2. ROUGHNESS - NEW AESTHETICS OF SWARM CONSTRUCTION

Roughness is a unique aesthetic highlight in this swarm construction. The research considers the notion of roughness as an approach to engage with nature. This thematic has been widely explored by architects such as Ensamble studio (2020), and Lina Bo Bardi (Veikos 2015). The rough quality of the surface records the process when the earth meets the concrete. The project presented in this paper extends the notion of roughness as surface quality and a digital construction strategy. In swarm construction, the robot's organization and routine are fixed while the tectonic outcome is not, allowing a certain level of change and imperfection. Besides, roughness also indicates the unfinished condition of the structure. The gaps created allow nature to infill over time, creating a live ecological system, constructing a synthetic environment for nature and

architecture to coexist.

5. Conclusion

In conclusion, the paper proposes a novel form-finding and collective construction method inspired by swarm intelligence. The research has a few constraints requiring future investigation, namely physical prototyping and the feasibility of designed robot. The autonomous construction system is also worth further exploration, particularly how the form emerges from the local communication through a central control interface. Overall, the paper finds its position in projecting the future design and construction informed by swarm intelligence. It proposed an implementation of a new digital naturalism - a condition where architecture and nature not just coexist but facilitate each other as one synthetic system in an on-going period.

References

"ENSAMBLE STUDIO" : 2020. Available from <https://www.ensamble.info/> (accessed December 12, 2019).

Calderón, A., Ugalde, J., Chang, L., Zagal, J.C. and Pérez-Arancibia, N.: 2019, An earthworm-inspired soft robot with perceptive artificial skin, *Bioinspiration & Biomimetics*, **14**(5).

Kayser, M., Cai, L., Bader, C., Falcone, S., Inglessis, N., Darweesh, B., Costa, J. and Oxman, N.: 2018, FIBERBOTS: Design and Digital Fabrication of Tubular Structures Using Robot Swarms, *ROBARCH 2018: Robotic Fabrication in Architecture, Art and Design*, 285-296.

Lee, J., Tirtawardhana, C. and Myung, H.: 2020, Development and Analysis of Digging and Soil Removing Mechanisms for Mole-Bot: Bio-Inspired Mole-Like Drilling Robot, *International Conference on Intelligent Robots and Systems*.

Pty Limited, K., Allen Williams, N., Attn, W., Bennett, S. and Shelley, D.: 2018, "AMENDMENT GC 81 EXPERT WITNESS SERVICES FISHERMANS BEND, VICTORIA City of Port Phillip & City of Melbourne" . Available from <www.ramboll.com> (accessed 2020-12-12).

Petersen, K., Nagpal, R. and Werfel, J.: 2011, TERMES: An Autonomous Robotic System for ThreeDimensional Collective Construction, *In Robotics: Science and Systems VII*.

Reynolds, C.: 1987, Flocks, herds, and schools: A distributed behavioral model, *14th Annual Conference on Computer Graphics and Interactive Techniques, SIGGRAPH*, New York, USA, 25–34.

Schranz, M., Umlauft, M., Sende, M. and Elmenreich, W.: 2020, Swarm Robotic Behaviors and Current Applications, *Frontiers in Robotics and AI*.

Scribner, S.J.: 2001, Emergence, *The Connected Lives of Ants, Brains*.

Snooks, R. and Jahn, G.: 2016, Closeness: On the Relationship of Multi-agent Algorithms and Robotic Fabrication, *Robotic Fabrication in Architecture, Art and Design 2016*.

Spuybroek, L.: 2016, *The Sympathy of Things*, Bloomsbury Academic, London.

Veikos, C.: 2015, *Lina Bo Bardi: 100: Brazil's Alternative Path to Modernism*, Hatje Cantz.

AN OPTIMIZATION METHOD FOR LARGE-SCALE 3D PRINTING

Generate external axis motion using Fourier series

MING LU[1], YIFAN ZHOU[2], XIANG WANG[3] and PHILIP F. YUAN[4]
[1]*Fab-Union*
[1]*andrealu2012@163.com*
[2]*Tongji University, University of Hawaii*
[2]*1732146@tongji.edu.cn*
[3,4]*Tongji University*
[3,4]*{18310021|philipyuan007}@tongji.edu.cn*

Abstract. With the increase in labor costs, more and more robot constructions appear in building construction and spatial structure fabrication. There are many robots working on large-scale objects. When the reach range of the robot cannot meet the requirements, so an external axis is needed. The external axis is usually a linear motion device, which can significantly increase the operating range of the robotic arm. In actual construction, it is also widely used. This article introduces a 3d printing coffee bar project. Because this project is of a large scale and needs to be printed at one time, the XYZ external axis was used in this project to complete the task. Inspired by this project, this article study several methods of optimizing the motion of external axes in large-scale construction. Finally, we chose to use the Fourier series as the most suitable method to optimize the printing path and programed this method as a component of FUROBOT for more convenient use. This article explains the principle of this method in detail. Finally, this article uses a 3D printing example to illustrate the precautions in actual use.

Keywords. Robotics; motion optimize; Fourier series; 3D printing; external axis.

1. Introduction

With the increase in labor costs, more and more robot constructions appear in build-ing construction (Chai,et al.2019)(Chen,et all.2019).There are a large part of robots are working for a large scale objects. When the reach of the robot arm cannot meet the requirements, you need to rely on the external axis for work. The architectural fabrication external axis is usually a linear motion device, which can greatly increase the operating range of the robotic arm. In actual construction, it is also widely used. This article introduces a real printed coffee bar (Figure 1), because this project has a large scale and needs to be printed at one time, so the xyz external axis was used in this project to complete the task. Inspired by

PROJECTIONS, Proceedings of the 26th International Conference of the Association for Computer-Aided Architectural Design Research in Asia (CAADRIA) 2021, Volume 1, 683-692.

this project, this article begins to study the problem of optimizing the motion of large-scale construction assisted by external axes.

Figure 1. coffee bar 3D-printing.

In the printing process using external axis, the movement of external axis can be controlled independently. Generally speaking, the programmer is required to formu-late the movement trajectory of the external axis, but if you encounter a large and complex project, this work is time-consuming and labor-intensive, and the manually planned movement path of the external axis is not necessarily reasonable. How to automatically generate the external axis motion path and generate a better path, these two problems are trying to solve this article.

2. Methodology

Usually, we use the spatial coordinate information of the target point to program the external axis. This example uses an object that is not very large for printing, for the convenience of demonstration (Figure 2).The robot is located on a single external axis.In this example, the biggest movement direction is y-axis.We need to complete the motion programming of the external axis in the y-axis direction.

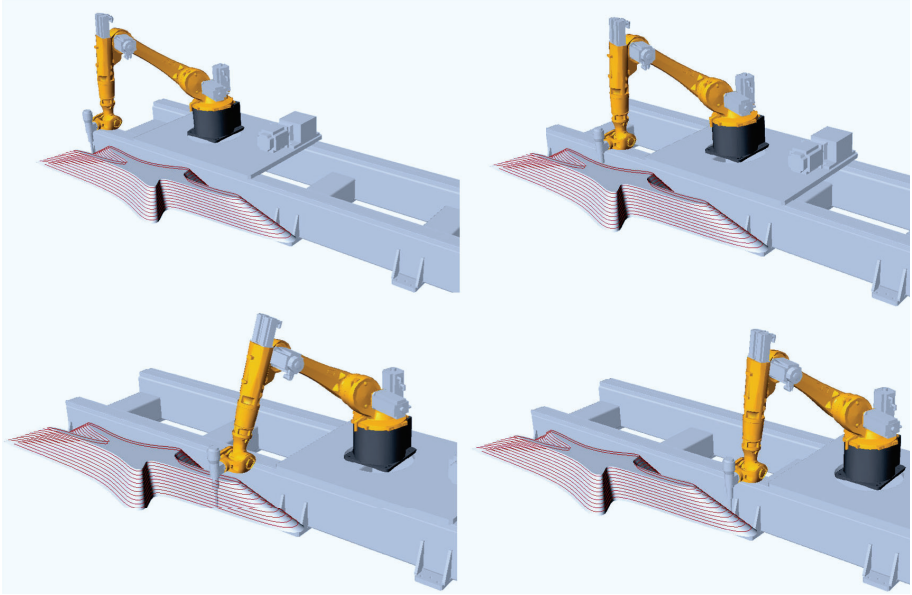

Figure 2. Simulation for 3D printing.

Programming directly with the target point data (Figure 3a), any change in the target point will directly affect the movement of the external axis, so it causes two problems:

- If there is a large and high-frequency position change between the target point and the point, it will cause vibration of the external axis, resulting in possible devia-tions in the work of the robot arm.
- Moving completely according to the target point will make the external axis move unnecessarily, and the movement will cause sway, so it is a more reasonable solu-tion to minimize the movement of the external axis and increase the motion of the robot to compensate.

If you use a manual method to straighten the motion curve, then some small excess motion will be drawn into a straight line and thus be deleted, so this method will produce a smoother path than the previous method. But the biggest problem with this approach is that it requires human participation (Figure 3b). At the same time, when the path undergoes the same drastic change, the external axis movement will also produce sharp abrupt changes. Of course, this problem can also be solved by manual adjustment again. This method is labor intensive, and this shortcoming limits the intelligent use of this method in general printing small builds.

So this article considers to solve the above problems directly from curve fitting. (Figure 3c).

Polynomial fitting can achieve this goal, , this method has ability to generate smooth curves, and easy to generate in algorithm and code. But the disadvantages obviously: this method is not suitable for generating periodic curves. If we increase the number of cycles of the curve, in order to better fit the target curve, we

have to increase the number of polynomials accordingly, which will bring a certain burden to the calculation and even cause memory overflow when programming. In actual print-ing, the number of cycles is the number of layers printed, generally there are thou-sands of layers, which is impractical to use polynomials.The same property exist in Bezier curve.

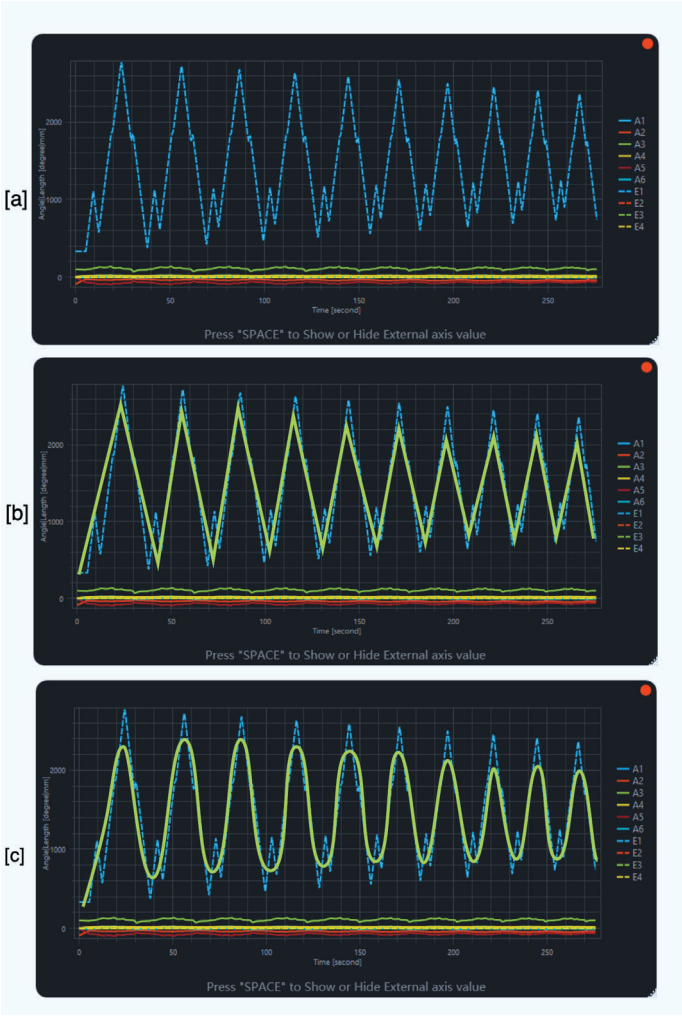

Figure 3. External axis visualization.[a]:Using target plane position .[b]: Using straight line to fit.[c]: Using a smooth curve to fit.

We need a method that can fit periodic curves,so we chose the fourier series(Lay,et al.2015).

2.1. PROJECTION

Before introducing Fourier series,it is necessary to talk about projection.

If there are two vector a and vector b, we need to find a coefficient so that after the coefficient is multiplied by the a vector, it can be as close to the b vector as possible. According to linear algebra, the following formula (1) can be used to find this scale coefficient:

$$c = \frac{b \cdot a}{a \cdot a} \tag{1}$$

So if multiply c to a, we can get $\hat{a} = c \cdot a$(Figure 4):

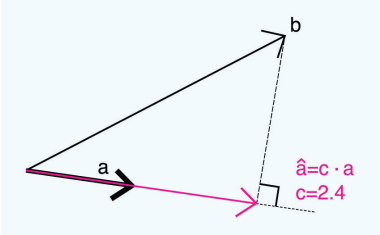

Figure 4. Projection.

This process is called projection.We can make an analogy between vector and function. We project the B function onto the A function and find a coefficient C such that the A function multiplied by C becomes the projection of the B function on the A function:

$$C = \frac{\langle B, A \rangle}{\langle A, A \rangle} \tag{2}$$

The expression $\langle A, B \rangle$ is called the inner product of the function A and B.As we all know,the definition of inner product of 2 vectors is:

$$v_1 = [x_1, y_1, z_1]^T, v_2 = [x_2, y_2, z_2]^T \tag{3}$$

$$v_1 \cdot v_2 = x_1 \cdot x_2 + y_1 \cdot y_2 + z_1 \cdot z_2 \tag{4}$$

As an anology,we define the inner product of one function $\langle A, B \rangle$ as:

$$\langle A, B \rangle = \int_a^b A(x)B(x)\,dx \tag{5}$$

We only need to find out the coefficients of our existing B function for several si-ne and cosine functions of different frequencies, and then we can use these sine and cosine functions to assemble this B function.

2.2. FOURIER SERIES

The intention of Fourier series is to decompose an arbitrary function into sine and cosine functions of different frequencies. With the helps of certain coefficients,all these trigonometric functions take a certain independent variable(such as x) and the sum of these harmonic functions is approximately equal to original function.

Firstly,we define the domain of harmonic function belongs to [0,2π],but in actual 3D printing,the number of target points are very large,usually tens of thousands of points.In order to be able to use this method,we first need to scale all target points to the interval of [0,2π].

We use this formula to coefficient:

$$\text{coeff} = \frac{2\pi}{\text{NumberOfPts} - 1} \tag{6}$$

Because fourier series consists of two parts, the cosine part and the sine part, we take the sine function as an example. Because we need to solve the Fourier series within[0,2π], we need to multiply the independent variable by the scale coefficient obtained in (6):

$$t = (\text{IndexOfPts}) \cdot \text{coeff} \tag{7}$$

We assume that there is a function: $\cos(t) t[0, 2\pi]$.If we divide $[0, 2\pi]$ into 5 equal parts,then we will have 6 points: $t_1 = 0, t_2 = \frac{2\pi}{5}, t_3 = \frac{4\pi}{5}, t_4 = \frac{6\pi}{6}, t_5 = \frac{8\pi}{5}, t_6 = \frac{10\pi}{5} = 2\pi$,and $d_t = \frac{2\pi}{5} = 1.2566$.

Add up each of them:$\cos(t_1) \cdot \cos(t_1) + \cos(t_2) \cdot \cos(t_2) + \cos(t_3) \cdot \cos(t_3) + \ldots + \cos(t_6) \cdot \cos(t_6) = \pi$

If we divide the domain into infinite small segments d_t,we also can get:

$$\int_0^{2\pi} \cos(t) \cdot \cos(t)\, dt = \langle \cos(t), \cos(t) \rangle = \pi, t > 0 \tag{8}$$

There exist strict proof of(8).Formula (8) represent inner product of function cosine.The same way to do sine function ,we can get:

$$\int_0^{2\pi} \sin(t) \cdot \sin(t)\, dt = \langle \sin(t), \sin(t) \rangle = \pi, t > 0 \tag{9}$$

We define:

$$a_n = \frac{1}{\pi} \sum_{t=0}^{2\pi} f(t) \cos(n \cdot t)\, dt, b_n = \frac{1}{\pi} \sum_{t=0}^{2\pi} f(t) \sin(n \cdot t)\, dt, n > 0 \tag{10}$$

From formula (12),when n=0,we can get: $\langle \cos(0), \cos(0) \rangle = 2\pi$ rather than π,therefore we must divide this coefficient of cosine part by 2, which is $\frac{a_0}{2}$,and the coefficient of sine doesn't exist when n=0.We can conclude:

$$f(x) = \frac{a_0}{2} + a_1 \cos(t) + b_1 \sin(t) + a_2 \cos(2t) + b_2 \sin(2t) + \ldots + a_n \cos(n \cdot t) + b_n \sin(n \cdot t) \tag{11}$$

Function (11) is the final function assembled by several sine and cosine function with different frequency.This function is also continuous,but in real case of 3D-printing,each data point is discrete,so we need to change the integral into a summation.

Harmonic function itself is a periodic function, which satisfies our need for

long-term periodic motion curve fitting. And you can set different orders for the Fourier series to obtain different smoothing effects (Figure 5). The order is actually "n" in function (11), which represent the highest frequency of the sine function and cosine function participating in the entire Fourier series.

After programming this method, the burden on the computer's cpu is small. After actual testing, the final calculation result can be obtained in real time.

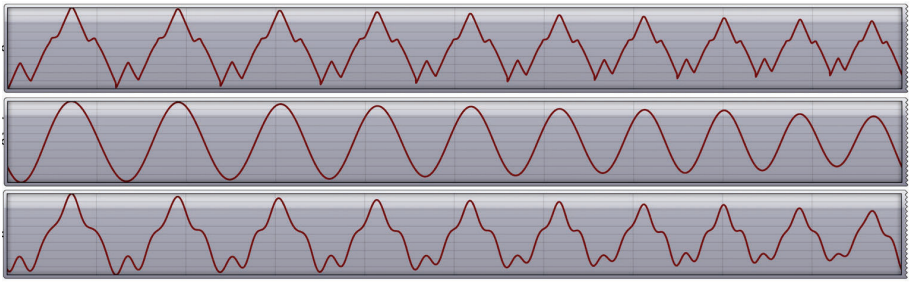

Figure 5. Top:original input sequence , Middle:order=15 ,Bottom:order=50.

3. Instructions

Because it is difficult for architects to apply these mathematical algorithms in their work, we wrote the above algorithms as a grasshopper component, which is built into FUROBOT for people to download and use for free.In specific usage, we only need to separate the xyz components of the target point separately by using "decompose point" component, and then find the Fourier series for each component. Then, on the obtained Fourier series, we can manually add an offset so that the robot is within the printing range of the object.

In detail, the two aspects of this paper that need to be solved:

1. Keep the external axis as stable as possible to avoid sudden curvature changes.
2. Minimize the length of the external axis movement path.

While satisfying these two requirements, it is necessary to ensure that the entire printing process does not occur such as joint limit, exceeding the printing range, etc., if the above phenomenon occurs, increase the order.

3.1. EXAMPLE

One example of the use of this method is demonstrated (Figure6), which uses XYZ three-axis external axis. This example verified by simulation and proved that this method is feasible and effective. Users can adjust the order number to get a smoother path curve, then check the reachability of TCP by this the path.

Figure 6. XYZ external axis.

In this example, first we have to find the smallest order, because the smaller the order, the better it can meet the above two requirements.In meeting the requirements of standard printing, we found that the minimum order in this example is 44, which happens to be the number of layers of the printed object 43 plus 1.Under this order, each layer is a period. At the minimum order, you can see that the trajectory of the external axis is an almost perfect ellipse(You can see that at the beginning of the print, it's not perfect because of the Gibbs phenomenon).The comparison of different orders:

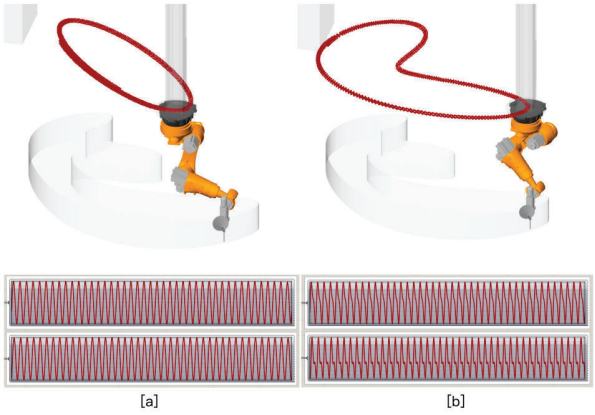

Figure 7. [a]:order=44, [b]:order=100.

When the order is 44, the external axis travels the least distance.In order to complete the same action, the robot needs to do more actions to compensate for the "lazy" external axis.At this time we will find that the A1 axis of the robot will rotate more than 180 degrees(Figure 8).For most robot, this is not a problem, because the limit of robot joint range can be lifted by setting.But if you encounter the problem of wire winding, you need to increase the order to avoid this problem.As long as the order is increased to a fixed value, the A1 axis of robot can keep stable in the whole process.

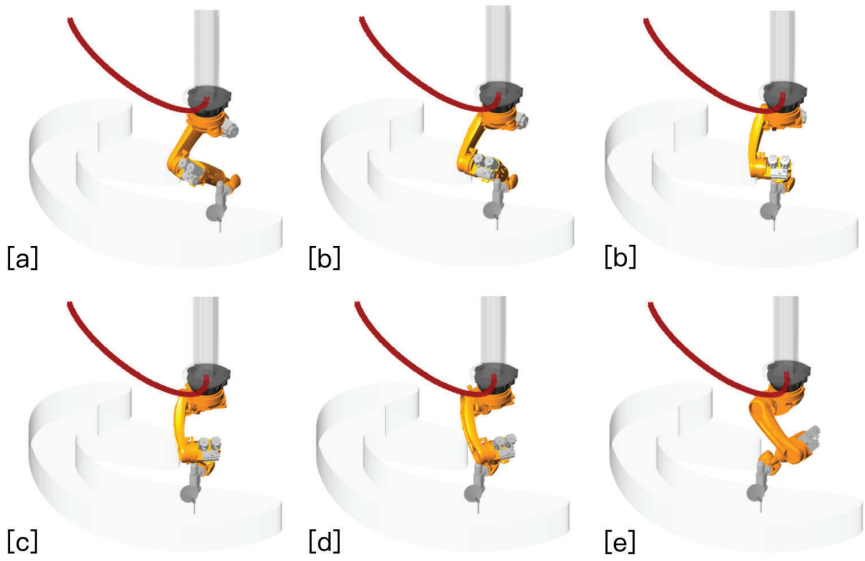

Figure 8. During the process from [a] to [e], the A1 axis rotated almost 180 degrees.

4. Conclusions

By introducing the Fourier series, this research contributes to the program of external axis movement. Printing stability and quality are improved with the proposed method. Furthermore, the proposed method is versatile and can be applied to various types of linear external axis programming.

- Add the acceleration control of the external axis to make the acceleration curve continuous,and control the acceleration value within a preset value(Spong,et al.2005)
- After obtaining the Fourier series, generally you can manually add an offset to each component so that the robot can print normally. This process can be improved by finding the position offset between the center of the target point cloud and the center of the external axis motion trajectory point cloud, and use this offset to replace the previous manual setting.

References

Chai, H.u.a., Zhang, L. and Yuan, P.F.: 2019, Advanced Timber Construction Platform:Multi-robot System for Timber Sturcture Design and Prefabrication., *In Proceedings of the 2019 DigitalFUTURES,edited Phil-ip.F.Y ,Yi.Min(Mike).X,JiaWei Y,Chao Y..Springer*, Shanghai, 303-311.

Chen, C.-Y., Chang, T.-W., Hsiao, C.-F. and Huang, H.-Y.: 2019, Developing and Interactive Fabrication Process of Maker Based on "Seeing-Moving-Seeing"Model., *DigitalFUTURES,edited Philip.F.Y ,Yi.Min(Mike).X,JiaWei Y,Chao Y .Springer.*, Shanghai, 312-321.

Lay, D.C., Lay, S.R. and McDonald, J.J.: 2016, *Linear Algebra and Its Applications*, Person.
Spong, M.W., Hutchinson, S. and Vidyasagar, M.: 2005, *Robot Modeling and Control*, JOHN WILEY & SONS, INC..
Yuan, P.F., Chen, Z. and Zhang, L.: 2019, Design Optimum Robotic Toolpath Layout for 3-D Printed Spatial Structures., *In Proceedings of the 2019 DigitalFUTURES,edited Phil-ip.F.Y ,Yi.Min(Mike).X,JiaWei Y,Chao Y .Springer.*, Shanghai, 322-330.

TWINNED ASSEMBLAGE

Curating and Distilling Digital Doppelgangers

KATIE MACDONALD[1] and KYLE SCHUMANN[2]
[1,2]*University of Virginia / After Architecture*
[1,2]*{kmacdonald|schumann}@virginia.edu*

Abstract. Recent developments in digital fabrication have made increasingly intelligent use of machine visioning and 3D scanning. These technologies enable ever-higher resolution digital models of physical material, and present opportunities for physical material to gain agency in the design process. Digital design workflows using such technologies require ever-greater computing power as the resolution of digitized models increases, and high-fidelity 3D scanning systems become cost-prohibitive, creating obstacles to widespread use. Twinned assemblage uses consumer-grade photogrammetry software, lowering the cost of equipment required, and presents a series of distillation methods that strategically reduce the fidelity of data digitally describing a physical object. Distillation methods discussed include reducing a mesh to a low-poly geometry, identifying the location and orientation of an object's largest faces, and creating 2D sections, among others. These methods can be designed intentionally to extract or highlight certain qualities in digital models, that in turn inform aggregation strategies generated through computational simulation. This paper presents several examples of such aggregations in a variety of materials, conveying benefits and challenges of the process. Such methods present opportunities for granting agency to physical materials in the design process, and for the democratized use of digitizing technologies.

Keywords. Authorship; Digitizing; Material Agency; Digital Design; Democratized Technology.

1. Introduction

Traditional authorship in architecture is exercised through a sequence in which the production of design documents precedes material acquisition and construction. Several recent projects including Tree Fork Truss at AA Hooke Park, Cyclopean Cannibalism at MIT, and elsewhere have reordered material's role within project delivery, beginning with raw logs and raw concrete fragments and shaping a designed form to fit and minimally reduce these inputs (Devadass et al, 2016; Clifford and McGee, 2018). Building on these developments, this paper examines how a physical collection of parts can be digitally documented, analyzed, indexed, and controlled, in particular how processes of distillation of the digital translation

PROJECTIONS, Proceedings of the 26th International Conference of the Association for Computer-Aided Architectural Design Research in Asia (CAADRIA) 2021, Volume 1, 693-702.

can grant objects agency within the design of an aggregate assembly – allowing parts to influence a whole in a dynamic give-and-take.

Found material collections are scanned and digitally aggregated using a series of low-cost, democratized simulation and modeling techniques. This methodology was performed by a group of collaborators working remotely, each of whom worked with a unique collection of found objects/materials. The workflow consists of curation and labeling of a physical collection, translation into a twinned collection of digital meshes using consumer-grade smartphone 3D scanning, distillation of digital meshes, and parametric aggregation strategies followed by physical assembly. Selective distillation of 3D scan data is employed as a principal strategy, allowing the designer to isolate characteristics of the objects that inform aggregation methodologies and develop parametric understandings of the meshes according to these biases.

Digitized collections were analyzed in Grasshopper using several methods to generate aggregations. Building on past scholarship using 3D scanning to optimize highly variable biomaterial parts, material eccentricity was embraced opportunistically (MacDonald et al, 2019). The aggregation strategies fell into three categories: 2D/3D packing, gravity physics simulation, and spring physics simulation, described in system diagrams that convey goals, techniques, and relationships. The methods are illustrated taxonomically in order to compare multiple variations of the approach. In all cases, the final physical aggregation was determined in part by the eccentricities of the collected objects.

2. Methods

The methods described herein lay out a series of steps in using twinned assemblage to generate digital aggregations that can be replicated physically. These steps include inventory curation, digitizing, distillation, aggregation through sorting and simulating, and physical assembly. Also discussed are the approach's implications on remote practices. Several example projects are described and shown, illustrating how the process can be adapted to different input materials and aggregation strategies.

2.1. INVENTORY CURATION

This research was developed and piloted through the serial curation of several collections of physical artifacts – found objects not created by the designer. Each collection ranges in selection criteria, from a common fabrication method to a shared biological or geological origin. Objects were inventoried with labels for referencing – a critical step to maintain a relationship between physical object and digital model, so that one can track where any single object is placed in an assembly.

The act of curation is viewed as a design problem and can be contextualized within a range of historical examples and precedents on collection. The late antiquity practice of spoliation, the sixteenth century *Wunderkammer*, and Sir John Soane's House collected and arranged architectural fragments and material objects, while the first open-air museum Skansen and a rich history of World's

Fairs collected and assembled entire buildings, both regionally and globally (Nilsson, 1906; Furján, 2004). Meanwhile, digital aesthetic culture has further seen the rise of collection, notably in James Bridle's New Aesthetic, which collected virtual tropes in a continually expanding Tumblr feed (Bridle, 2011). Within contemporary architecture, the collection and translation of digital objects into buildings is increasingly widespread: design leaders such as Mark Foster Gage kitbash digital models as a manifestation of Object-Oriented Ontology into architecture; in conventional professional practice, DIY open-source models on GitHub, ready-to-print models on Thingiverse, and product specification libraries in BIM packages such as Revit shape a built environment of assemblage (Gage, 2015).

The curation of a collection of materials to be digitized is important from a conceptual perspective, but also a practical one. The following distillation methods will be more accurate if the inventoried objects are of a similar form family, so that similar qualities can be extracted from the collection to inform aggregation methods.

2.2. DIGITIZING

Once each physical collection was curated and labeled, it was translated into a twinned collection of digital meshes using photogrammetry software (Figure 1). Professional 3D scanners (hardware and software systems that retail substantial sums) were tested but produced cumbersome data and large files that were difficult to share and open in Rhinoceros. Additionally, the high resolution produced was deemed unnecessary for this application. Instead, consumer-grade smartphone 3D scanning applications were found superior in meeting research objectives, with the authors settling on Qlone and Trnio for their efficiency, economy, and user-friendliness. Model resolution in scans produced using these apps was more than sufficient for current applications. Once scanned, digitized models were compiled into a single Rhino file, often arranged neatly in a grid with labels corresponding to the labels on the physical inventory.

2.3. DISTILLATION

Distillation methods are selected and implemented on a per-assembly basis and are aimed at two goals: reducing file size and computing time to use many digitized objects in a single file, and to analyze inputs to selectively isolate characteristics that inform aggregation methodologies and develop parametric understandings of the meshes according to these biases. These biases are constructed based on object properties and underlying orders such as geometry, volume, dimension, etc. and subsequently drive aggregation strategies. The term distillation is used here to describe both an act of reduction and a concentrating of certain qualities, building on Merriam-Webster's definition, 'to extract the essence of' (*Merriam-Webster*, 2020).

Figure 1. Physical and digital inventory data. Work by Kristin Pitts.

Distillation methods varied depending on which object qualities were needed to progress toward a certain aggregation strategy. Such methods were executed parametrically, and included simplifying a mesh to a low-resolution, low-poly geometry, identifying the location and orientation of the object's largest faces, reducing objects to critical 2D sections to use in packing simulations, and contouring models to interpolate centerlines, among others. If the number of undistilled models in a single Rhino file demanded too much computing power, models were distilled individually before being composed into an inventory within a single file.

Running physics simulations and evolutionary solvers with Grasshopper on one to two dozen 3D scanned meshes on average consumer-grade laptops often proved to be prohibitively slow, if not impossible. Distillation methods enable the creation and visualization of iterative results and allow the designer to control which qualities of the objects are primary factors in aggregation methods, described below.

2.4. AGGREGATION THROUGH SORTING AND SIMULATING

The distilled digital collections were analyzed in Rhinoceros using Grasshopper and a variety of plugins including Kangaroo, Galapagos, and Firefly, among others. Designers developed the methods for generating aggregations, but in all cases, the exact qualities of the final aggregation were determined in part by the irregularities of the collected objects – eccentricities highlighted through distillation.

Before objects were aggregated, they were computationally evaluated and sorted. Sorting criteria, like distillation methods, were assembly-specific and selected with a particular aggregation strategy in mind. Inventories were sorted according to qualities such as overall size (volume measurement), average circumference (section and area measurement), surface coloration (through scanned photographic data), or surface texture. Each sorting criteria was calculable using straightforward Grasshopper scripts. Objects were often positioned in 2D or 3D digital space according to sorting criteria before being aggregated through a digital simulation.

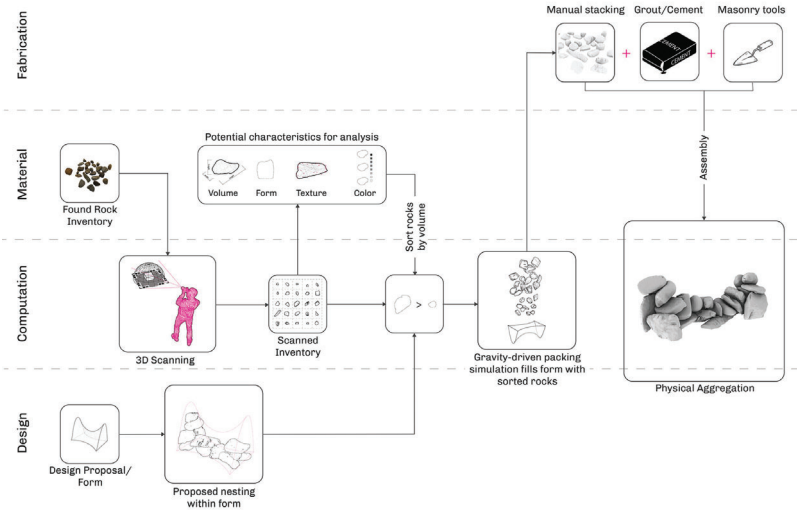

Figure 2. System diagram describes rocks scanned, sorted, and packed with a gravity simulation, that are then physically assembled with mortar. Work by Kristin Pitts.

Following in the vein of projects that use 3D scanning to optimize highly variable biomaterial parts, material eccentricity is viewed not as a barrier to aggregation but an opportunity (Devadass et al, 2016; Von Buelow et al, 2018). The aggregation strategies fell largely into three categories: object packing (2D or 3D), gravity physics simulation, and spring physics simulation. Aggregation strategies were described in relation to other steps in the process through system diagrams that outline contributors, relationships, processes, and negotiations (Figure 2). In each case, the aggregation strategy was enabled by and used data filtered or organized by the prior digitizing, distilling, and sorting techniques.

2.5. PHYSICAL ASSEMBLY

The final step in transitioning from computational model to physical aggregation is the design of the joinery between objects. For some, the objects themselves formed the joint – for example, the interlocking spines of pinecones, the tied laces of a collection of shoes, or the dry stacking of stones. In others, a secondary system of attachment was implemented – mortar, hot glue, melted wax, etc. The irregularity of each inventory and lack of a pre-defined method for joining objects posed the greatest challenge for implementing this approach. It was anticipated that distillation would produce discrepancies between physical objects and digital models, and the most successful assemblies took this into account when determining a joining strategy. Joinery method of the physical aggregation should be considered early in the digitizing process, so that decisions about distilling, sorting, and aggregating can be shaped accordingly. The use of a clear system diagram can aid in developing these relationships in different parts of the process simultaneously (Figure 2).

2.6. REMOTE PRACTICES

The methodology employed throughout was developed to allow multiple collections to be assembled remotely by designers during COVID-19, using consumer-grade technology rather than professional visioning and fabrication tools. Technology employed was limited to consumer-grade scanning and industry standard software, all run on personal laptops. The variety of collection types shows the adaptability of this approach. The leanness and distributed authorship of the resulting aggregations demonstrate how democratized visioning and parametric modeling can be deployed economically to produce bespoke physical assemblies of irregular parts.

Figure 3. Taxonomy of assemblies.

3. Results

Several distillation and assembly workflow examples are described. These and additional examples are illustrated taxonomically in order to compare multiple strands of a central approach – the orchestration of a complex group of physical objects via 3D scanning, distilling, parametric analysis, and simulation (Figure 3).

3.1. GRAVITY SIMULATION

A collection of round rocks was inventoried, sorted, and positioned in three-dimensional space based on size. Rock meshes were reduced by 50-75% to maintain formal definition but to reduce complexity for simulation. The digital collection was then packed into a form using a gravity and 3D object collision simulation with Kangaroo. The packing of rocks within the form was quickly iterated through many variations by editing the starting position of the rocks before being dropped (Figure 4).

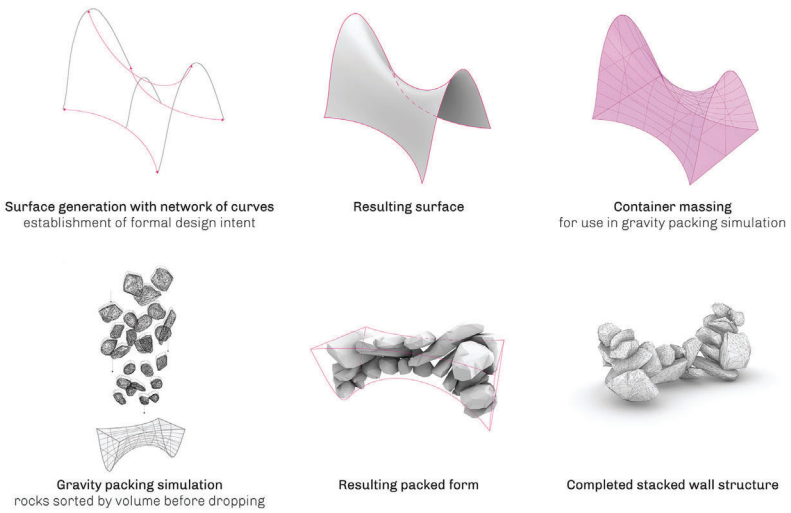

Figure 4. 3D packing with volume sorting and gravity simulation. Work by Kristin Pitts.

3.2. 2D SPRING SIMULATION

A collection of crushed aluminum cans was scanned and oriented uniformly within a grid in Rhino. Two longitudinal sections were cut through each can, each reducing the geometry to a single curve. These curves were aligned and pulled together into a stack using a 2D Kangaroo spring simulation. Iterations were developed by implementing a Galapagos evolutionary solver which attempted to create a stack of cans closely matching a goal curve drawn by the designer. Can stacking order was generated randomly, by cycling through the two different

sections of each object to determine its rotation, and iterating through many possible combinations to approach the geometry of the goal curve.

3.3. 3D SPRING SIMULATION

A collection of angular coal fragments was scanned. These were distilled by reducing object meshes to an extremely low-poly count (over 90% reduction in face count). The reduced meshes were then analyzed by measuring and identifying the largest flat faces. The corners of these faces became the endpoints of spring lines for a Kangaroo spring simulation that pulled and twisted the objects into arched forms (Figure 5).

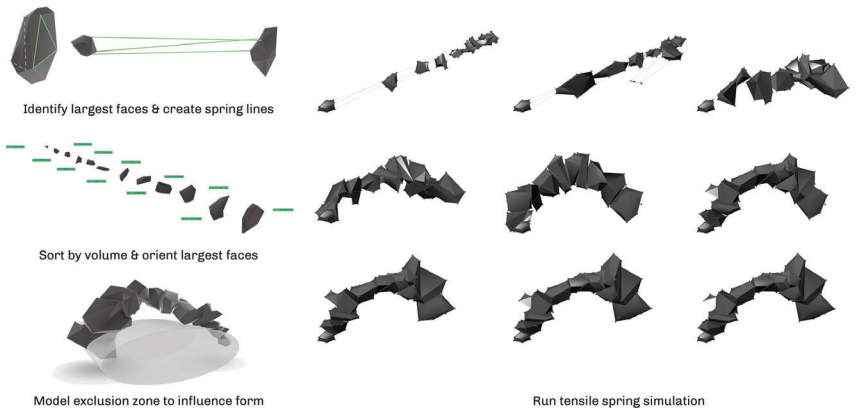

Figure 5. 3D assembly with face identification and tensile spring simulation. Work by John Michael Worsham.

3.4. PACKING AND FACE ALIGNMENT

A collection of slab-like rocks was scanned and inventoried. Each object in the inventory was relatively flat, allowing for the distillation process to reduce each rock to a simple straight extrusion using a section cut through the middle of each mesh. Distilled models were analyzed to measure the intersection angles of all edges, and the corners closest to 90 degrees were oriented together as the stones were stacked, forming a relatively consistent perpendicular corner within the stack.

4. Discussion

Techniques aimed at making digital copies of objects from the physical world have been underway for some time now – Mario Carpo describes the origins of digitizing methods: '[In the early nineties] several tools (some derived from medical instruments) were already available to scan and digitize all kinds of objects, regardless of their form, or formlessness. First, physical models had to be converted into their digital doppelgängers by scanning a sufficient number of their surface points. The digital process of design and manufacturing could

then take over' (Carpo, 2011, p. 37). Carpo goes on to describe Frank Gehry's early digitizing practices as a 3D pantograph, in which points are located in three-dimensional space on a physical object and translated to a digital model. Until now, the emphasis of such efforts has been placed on increasing the accuracy, resolution, and overall fidelity of such doppelgangers. The progression of visioning technology toward more identical digital copies is unending and certainly has its applications in complex machining.

As an alternative approach, this paper identifies opportunities to reduce and abstract the information captured and stored in the digital model. It places a digital lens on the physical world and reduces the complexity of form to contours, centerlines, tones, etc. (much in the lineage of architectural drawings which reduce landscapes to topographic lines, stones to profiles, and materials to hatches). It argues for selective use of data; similar to Gehry's digitization, some points or edges are more critical than others in describing the essential qualities of a particular form.

For widespread 3D scanning of material inputs to inform digital fabrication methods, designers must refine strategies to oscillate between digital models and physical objects. The work presented here argues against focusing on increasing resolution and computing power, instead proposing that an intentional distilling – an abstraction – of the digital mesh allows the designer to control which qualities of the object affect a design. The work contributes to an expanded understanding of authorship in architecture: it is rooted in Michel Callon and Bruno Latour's Actor Network Theory, which understands objects to have agency – in this case, to shape an architectural whole in dialogue with the designer (Latour, 1988; Leach, 2016). Rather than design a form and use materials to make that form, this approach grants agency to the curator of parts and the parts themselves; it collects objects and reconciles their characteristics with a looser design intention, choreographed through the development of an open-ended parametric workflow.

High fidelity digitizing methods have proven useful in the fabrication of full-scale structural assemblies. Twinned assemblage contributes to this landscape of projects through a new approach to digitized data that intentionally distills computational models in order to extract specific qualities that inform an assembly. This inevitably produces a discrepancy between the digital model and physical object, which presents a challenge to scaling up the work and applying it to one-to-one constructs. Future work will explore methods of maintaining an acceptable tolerance between digital and physical dimensions and develop joining or attaching methods that can accommodate such discrepancies. In this sense, the approach may be more easily transferrable to masonry construction, where mortar can forgive a certain tolerance, than highly precise machined connections in lumber that demand a close fit. In the latter case, a design problem is presented wherein the design of such joinery must be able to accommodate a certain tolerance; the ethos of twinned assemblage advocates for viewing this not as a limitation, but an opportunity. The deployment of this approach in the construction of a structural assembly will also require a thorough understanding of the structural qualities of the physical inputs which populate the geometry, leveraging heuristic, form-searching methods of structural simulation (Carpo, 2017).

The approach defined in this paper responds to and seeks an alternative to the copy-paste aesthetics that result from specification using building information modeling – a tendency toward assembling products repetitively and with uniform means. It draws from a rich architectural history in which physical objects are collected and combined (spoliation, *Wunderkammer*, etc.) and the more recent development of the kitbashed digital object collection. The resulting workflow establishes and demonstrates a method for the aggregation of physical parts, using computational modeling as an analytical intermediary between the physical object and the physical assemblage.

Acknowledgements

The work presented was conducted as part of the 'After Specification' seminar taught by the authors at the University of Tennessee. The authors would like to thank the students for their dedicated efforts in advancing the work: Rachel Crosslin, Matthew Crow, John Hooten, Julianna Olsen, Kristin Pitts, Watts Brown, Ryan Weaver, and John Michael Worsham, as well as Jason Young, Director of the School of Architecture, for his support of the work.

References

"Merriam-Webster" : 2020. Available from <www.merriam-webster.com/dictionary/distill> (accessed 27 November 2020).

Bridle, J.: 2011, "The New Aesthetic" . Available from <www.new-aesthetic.tumblr.com> (accessed 24 June 2020).

Von Buelow, P., Torghabehi, O.O., Mankouche, S. and Vliet, K.: 2018, Combining parametric form generation and design exploration to produce a wooden reticulated shell using natural tree crotches, *Proceedings of the International Association for Shell and Spatial Structures (IASS) Symposium 2018: Creativity in Structural Design*, Boston.

Carpo, M.: 2011, *The Alphabet and the Algorithm*, MIT Press, Cambridge.

Carpo, M.: 2017, *The Second Digital Turn: Design Beyond Intelligence*, MIT Press, Cambridge.

Clifford, B. and McGee, W.: 2018, Cyclopean Cannibalism: A Method for Recycling Rubble, *ACADIA 18: On Imprecision and Infidelity, Proceedings of the 38th Annual Conference of the Association for Computer Aided Design in Architecture*, Mexico City, 404-413.

Devadass, P., Dailami, F., Mollica, Z. and Self, M.: 2016, Robotic Fabrication of Non-Standard Material, *ACADIA 2016: Posthuman Frontiers: Data, Designers, and Cognitive Machines; Proceedings of the 36th Annual Conference of the Association for Computer Aided Design in Architecture*, Ann Arbor, 206-213.

Furján, H.: 2004, Scenes from a Museum, *Grey Room*, **17**, 64-81.

Gage, M.F.: 2015, Killing Simplicity: Object-Oriented Philosophy in Architecture, *Log*, **33**, 95-106.

Latour, B.: 1988, Mixing Humans with Non-Humans: Sociology of a Door-Closer, *Social Problems*, **35**(3), 298-310.

Leach, N.: 2016, Digital Tool Thinking: Object-Oriented Ontology versus New Materialism, *ACADIA 2016: Posthuman Frontiers: Data, Designers, and Cognitive Machines; Proceedings of the 36th Annual Conference of the Association for Computer Aided Design in Architecture*, Ann Arbor, 344-351.

MacDonald, K., Schumann, K. and Hauptman, J.: 2019, Digital Fabrication of Standardless Materials, *ACADIA 2019: Ubiquity and Autonomy, Proceedings of the 39th Annual Conference of the Association for Computer Aided Design in Architecture*, Austin, 266-275.

Nilsson, A. and Keyland, N.(.: 1906, *The Historical and Etnographical Department of Skansen: A Short Guide for the Use of Visitors*, The Northern Museum, Stockholm.

PUCCA 5.0

A framework for a digital system to aid informal self-construction

SURJYATAPA RAY CHOUDHURY
[1] *The University of Tokyo*
[1] *surjyatapa.rc@gmail.com*

Abstract. Assisted self-construction has been proclaimed by the UN Habitat as one of the most affordable methods of providing sustainable housing. Self-construction in informal settlements is analogous with incremental development, where design and construction occur in simultaneous waves. However, unassisted self-construction often produces housing of substandard quality owing to a lack of knowledge and resources. This paper hypothesizes that the core factor leading to substandard housing in informal self-construction is an information and communication gap in the existing process. In order to identify the gap, a mapping and analysis exercise is carried out that identifies the focal points where the informal system deviates from the formal, the decisions that influence these deviations, and the impact of these deviations on the overall output. The paper develops the framework for a smartphone-based, digital technical aid system, that fills this information and communication gap and provides construction guidance to owner-builders without compromising the nonlinear nature of incremental development.

Keywords. Informal Construction; Self-Construction; Digital Technical Assistance; Digital Fabrication.

1. Introduction

Self-construction is the practice of actively participating in the construction of one's own home. In informal settlements across the world, most homes are self-constructed incrementally, starting from a shelter built using temporary building materials such as bamboo and fabric, and gradually upgrading to a permanent dwelling [*Pucca in Hindi*] using bricks, stones, and reinforced cement concrete (Bredenoord and Lindert, 2014; Turner, 1977). While such practices match the socioeconomic and affordable limits of the dweller, the lack of construction-specific knowledge pertaining to materials, structural composition, and proper techniques often results in a substandard quality of the homes built (mHS Citylab, 2011; Turner, 1977). This led to the development of the concept of technical assistance, wherein organizations and institutions provide specialized knowledge and technical support to the owner-builders in the construction process (Harris, 1998).

PROJECTIONS, Proceedings of the 26th International Conference of the Association for Computer-Aided Architectural Design Research in Asia (CAADRIA) 2021, Volume 1, 703-712.

Although technical assistance caters to the knowledge gap in informal self-construction practices, it is limited in its capacity of achieving economies of scale and enforcing a faster rate of production of homes (Burgess, 1985). This limitation drives the adoption of other models of production of affordable housing, such as state-sponsored subsidized mass housing. However, standardized mass housing fails to address the varying socioeconomic and autonomous demands of the dweller (Turner, 1977). The need for a system of technical assistance that retains the autonomy of dwellers in self-construction while achieving a faster and economical rate of production can be developed with the application of digital technology. The economical aspect of such a system can be justified in the capacity of digital systems to achieve economies of production instead of scale, by replicating the process and not the product. To satisfy these constraints, this paper proposes a digital system of technical aid developed using ubiquitous and accessible technology such as smartphones.

Another limitation of current practices of technical assistance is its tendency to formalize the informal construction process (Burgess, 1985). Bredenoord and Lindert (2014, pp. 56-57) define the differences between formal and informal construction. Formal construction practices follow a linear process: planning and design are succeeded by construction activities followed by occupation by the dwellers. Informal practices, on the other hand, follow a non-linear process that begins by occupying vacant land followed by incremental upgrading and retrofitting to build a permanent dwelling. Burgess (1985) demonstrates how current practices of technical assistance tend to provide design-centric formal solutions that do not address the variable demands of informal dwellers. Moreover, such practices offer one-time assistance during construction, which limits its application in incremental development. This paper hypothesizes that the reason for multiple repairs and substandard quality of structures produced is an information and communication gap in the informal construction process. Instead of formalizing the existing process, this research examines the use of digital technology to fill the information and communication gap without changing the nature of incremental development.

This research, thus, aims to capture this non-linear nature of informal construction in a digital system of technical assistance that guides owner-builders in the self-construction process. The architecture for a low-cost, smartphone-based digital system is designed that gathers information from an owner-builder's environment, analyzes the information, and provides guidance to self-construct a quality output that is aligned with the owner-builder's requirement.

2. Related Works

This section reviews existing literature on digital technical aid systems, human-centered digital fabrication, and the application of smartphone sensors in position finding and communicating guidance with users. The proposed system builds upon the research reviewed here to develop the final system architecture.

2.1. DIGITAL TECHNICAL AID SYSTEM

While technical assistance for informal construction is a much researched area, there is very little work supporting a digital system of aid. Mehra et al. (2017) developed a digital project management system that provides information regarding material quantities, labor costs, and project timelines. The research focuses on supporting the lack of knowledge regarding material and labor costs. However, it does not provide construction activity related guidance to the workers. This paper builds on the above work and explores a system that can provide structural and spatial guidance in addition to material-specific knowledge.

2.2. HUMAN-CENTERED DIGITAL FABRICATION: GUIDED CONSTRUCTION

While most digital fabrication projects apply robotics in construction, a relatively new branch of study looks at the development of Human Computer Interface (HCI) systems to actively guide humans in construction. Yoshida et al. (2015) explores a digital system operating on real-time tracking and feedback using a depth camera and projection mapping. The system guides humans in an additive construction workflow. The proposed research builds on the concept of tracking and feedback applied in the above work to provide tailored guidance to owner-builders.

Additionally, in the field of active communication as construction guidance, Lafreniere et al. (2016) explore the use of wearable technology such as smartwatches in large-scale collaborative construction. In the field of Augmented Reality, interactive tools such as Fologram and state-of-the-art technology using a mix of visual and Inertial Measurement Unit (IMU) sensors have also been applied in guiding humans in construction (Gramazio Kohler Research, 2019; Newnham and Beanland, 2018). While most such studies use cost-intensive hardware that is not feasible in an informal context, this research adopts the technological concepts of the above studies in a low-cost setting.

2.3. ACCESSIBLE DIGITAL TECHNOLOGY

López et al. (2016) show how accessible, open-source technology such as ARToolkit can be used to gather positional information in digital fabrication systems. Such augmented reality applications are increasingly being developed for smartphones (Henrysson and Ollila, 2003). Additionally, Umek and Kos (2016) confirm the accuracy of smartphone gyroscopes to generate 6-degree coordinate information in a mobile biofeedback system. The system proposed in this research uses an array of smartphone sensors explored in the above works, such as camera and IMU sensors, to develop an accessible, low-cost hardware set-up.

3. Methodology

In order to develop a digital system that captures the non-linearity of the informal construction process, it is imperative to understand how the implicit decisions taken by owner-builders influence the construction process, and how it differs from the formal construction process. While Bredenoord and Lindert (2014) have highlighted the overall differences between the formal and informal process, this research focuses solely on the construction aspect. Foremost, a mapping

exercise is carried out that measures the informal construction process against the formal process to understand where deviations occur. Following that, the implicit decisions that build up these deviations are mapped.

While the system developed in this paper is generic and can be applied in any context, the local construction technology studied in this research is context-specific. For the purpose of this research, case examples from India were taken. To map the formal process, on-site visits of residential construction projects from the cities of New Delhi and Guwahati, India were undertaken. The projects were chosen based on a higher degree of application of local construction technology such as water levels, plumb bobs, etc., instead of high-end technology such as lasers. These local construction technologies most closely resembled the tools and construction technology applied in informal settlements, making the comparison more accurate.

For mapping informal construction, research on incremental construction done by Patel and Kunte (2011) in Mumbai, and King (2016) in Delhi were used as references. Additionally, pilot projects applying self-construction practices done by mHS Citylab (2011) were analyzed to understand the influence of local contractors and changes in family circumstances in the construction process.

Since the informal process is incremental in nature, information from one construction activity serves as feedback for the onset of a forthcoming activity. To best understand this process, the data gathered in the mapping exercise is analyzed through feedback loops to identify the information and communication gaps in the current process. These feedback loops also help analyze the non-linear (concurrent design and construction) nature of informal construction. This exercise is carried out using case examples from the work done by Patel and Kunte (2011), King (2016), and mHS Citylab (2011).

The analysis done using feedback loops helps develop the requirements for the digital aid system. The system architecture is then developed with the view of filling the information and communication gap in the current process, and provide structurally and spatially optimized, context-specific guidance to the owner-builder.

4. Mapping the Informal Construction Process

The studies on informal construction mentioned (see Section 3) show that socioeconomic conditions, lack of technological, material, and financial resources, and inadequate knowledge of construction are some of the major factors influencing informal construction. This mapping exercise identifies the focal points in the construction process where such factors intervene. The mapping exercise was done by breaking down the construction process into smaller modules such as marking reference levels for construction, excavating foundation, building walls, building roof and floor slabs, etc.

Table 1 presents the excavating foundation construction module. This module was chosen for illustration owing to the fact that in a formal construction process, this is the first step that deliberates on a target design. This marks the point where the informal process begins to clearly deviate from the formal process through the

implicit decisions taken by the owner-builders.

Table 1. Mapping the informal construction process for excavating foundation.

FORMAL		INFORMAL		
Construction Sequence	**Alignment and Traversing methods**	**Alignment and Traversing methods**	**Deviations from Formal Sequence**	**Decisions Leading to Deviations**
Mark functional areas on ground	Centre-to-centre distance marked using thread mesh	*Not Applicable*	Areas are not pre-determined, and built as required. Locations of all wet functions are not known	In incremental construction, different functions are added when there is availability of resources which limits prior planning
Calculate depth level of foundation from road level (reference)	Check digging level using water level	Inconsistent use of method	Inconsistent method. In some cases, road level is marked arbitrarily or eliminated all together	The method to mark and traverse level depends on the mason, and is sometimes done based on observations rather than accurate data
Stick 4 inch stakes on the ground	Check orthogonality by measuring diagonal with threads	Inconsistent use of method	*No deviation observed in construction sequence*	
Mark walls on the ground with chalk	*Not Applicable*	*Not Applicable*	*No deviation observed in construction sequence*	
Mark column centre	Thread mesh and plumb bob to determine centre	*Not Applicable*	Excavation is done for brick stepped footing. Columns are built at grade.	Knowledge gap: most masons are not aware of the techniques to construct a framed structure, and rely on existing practices.
Mark column footing profile using starter	*Not Applicable*	*Not Applicable*		
Excavate marked areas to required depth	Desired level of excavation measured using water level	*Not Applicable*		

As seen in Table 1, both the formal and informal process are broken down into two parts: the first column delineates the construction sequence while the second column captures the technology and tools applied for the measurement of construction elements. Capturing the data in this manner helps in understanding how to extract machine-readable data from the process. The construction output for every step, as well as human action involved, can be converted into machine-readable data using coordinate and sensory information.

For the informal process, the parts that deviate from the formal process have been mapped. The reason and external factors influencing each of these deviations are then demarcated (see Table 1, column 5). Identifying the focal point of deviation in the informal process and the factors causing the deviations help in understanding the method and type of information impacting informal incremental construction. To understand how this information, or lack thereof, impacts the overall outcome, the next section looks at the process through feedback loops.

5. Feedback Loops in Informal Construction

Feedback loops are a chain of causal connections within a system where some or all of the output produced in one part of the system returns as input information. In an incremental construction process, since subsequent layers of construction in

the form of upgradation or repairs always build on the construction output of a previous stage, it essentially functions as a feedback loop.

This section analyzes the informal construction process using feedback loops. Patel and Kunte (2011), and King (2016) demonstrate how the incremental self-construction process works. The incremental process begins with building a temporary shelter to occupy a vacant plot. This is followed by gradual upgradation when resources are available. Patel and Kunte (2011, p.58) highlight two types of incremental change: recurring changes from annual repairs and upgradation when there is a change in resources or family circumstances.

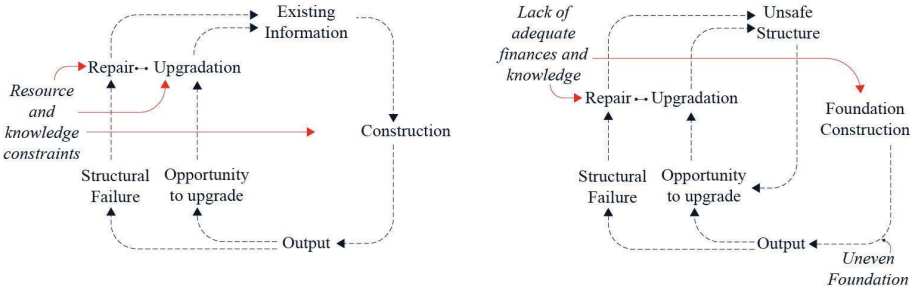

Figure 1. (Left) General feedback loop for incremental self-construction; (Right) Feedback loop for foundation construction.

Figure 1 (Left) shows the general feedback loop for incremental construction. The output that is affected by resource and knowledge constraints becomes the input for the next step of upgradation or repair. In this manner, a flaw in the structure in the initial stage of construction can lead to overall structural failure.

Figure 1 (Right) draws on a case presented by Patel and Kunte (2011, p.64), where uneven foundations laid by workers who lack construction knowledge crack easily. This creates a recurring expense for the dweller. Even in the case of repair, the persistent lack of knowledge would result in an unsafe structure that when upgraded would multiply the effect of the damage leading to overall structural failure.

Analyzing the informal construction sequence through such feedback loops highlights the impact of missing information in incremental development. This, coupled with the mapping of the informal process (see Table 1), forms a comprehensive roadmap for developing the digital system architecture.

6. Proposed System Architecture

From the analysis done in Section 4 and Section 5, it is evident that for any system to comprehensively capture the informal construction process, the following conditions are imperative:

1. Gather all information related to the construction process: construction method, tools and techniques, in addition to circumstantial information that can impact the process such as a change in family situation, lack of resources, and affordable

limits.
2. Analyze all information gathered simultaneously since it is evident from the feedback loop analysis that any part of the process affects the overall outcome.

Based on this analysis, contextual guidance can be generated by the digital system and provided to the owner-builder during construction.

6.1. SMARTPHONE INTEGRATION: FILLING THE INFORMATION GAP

The smartphone is the core part of the digital system that works as the communication medium between the worker and the backend analysis that computes and provides guidance. Smartphone sensors can be deployed to gather required information about the construction process and environment, as discussed in Section 2. Two types of data are required to comprehensively capture the entire construction environment:

1. **Point cloud data of construction elements**: Scanning all construction elements will enable the system to measure errors in spatial and structural composition. As seen in the case of Figure 1 (Right), scanning the foundation while constructing would capture the unevenness, and proper guidance could be delivered to eliminate this error. Camera sensors can be deployed to track construction elements using ARToolkit, to generate point cloud data. This method also ensures that only selected and necessary information is fed into the system, reducing the load on the backend analysis program.
2. **Sensory data related to owner-builder's activity**: Gathering data regarding the owner-builder's position, the rotation and angular motion of their hands used in construction can help gather information about activities undertaken. This information can be used to provide context-specific guidance. IMU sensors can be deployed to gather this data.

Additional information regarding circumstantial changes can be fed into a smartphone application interface in a boolean data format.

Guidance can be relayed to the owner-builder using inbuilt smartphone vibration sensors and Interactive Voice Response. Additionally, a layer of video-based guidance can reduce the knowledge gap further.

6.2. BACKEND ANALYSIS: PROVIDING CONTEXT-SPECIFIC GUIDANCE

In order to cater to simultaneous design and construction activity, the backend program needs to run a constrained analysis of the information gathered. This analysis should be run against the following three criteria:

1. **Procedure**: This criterion ensures that crucial steps of the process are not overlooked, such as measuring alignment and orthogonality, curing process for concrete, etc., by gathering relevant data regarding owner-builder's activity.
2. **Structure**: This criterion ensures the structural integrity of ongoing construction by gathering data on the alignment of structures, the structural composition of reinforcements, material composition, and interfacing elements.
3. **Spatial**: mHS Citylab (2011, pp. 13-14) highlights how self-constructed dwellings compromise on spatial quality. This criterion analyzes the quality of built spaces against configuration, functional layout, and environmental quality.

The role of the backend analysis is to generate guidance that is tailored to the construction activity. As such, a pre-established database comprising all types of local construction technology is required. Such a system would ensure that the guidance provided is not just for permanent construction, but also for spatial and structural optimization of temporary or other vernacular methods of construction.

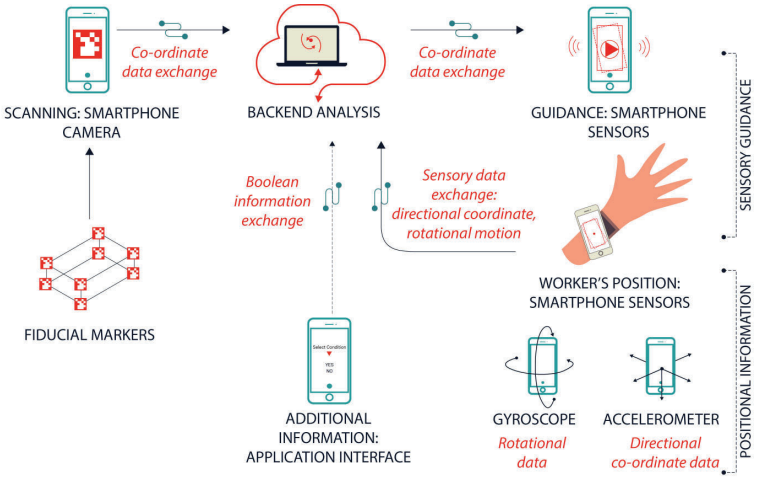

Figure 2. The System Architecture.

The overall system architecture is illustrated in Figure 2. The Backend Analysis is at the core of the system, which analyzes the information gathered from scanning construction output, the owner-builder's motion, and additional circumstantial information. The guidance is then relayed to the owner-builder through the smartphone.

7. Limitations

The research methodically develops a framework for the digital aid system based on the analysis of existing systems of incremental self-construction. In this section, the limitations of the research and implications for future work are discussed.

First, the data to map the construction process was primarily acquired through secondary methods. Since incremental construction takes considerable time to materialize and is dependent on external factors such as the availability of resources, it is difficult to capture the process first hand. Most such studies are based on interviews of the dwellers, and crucial information might be lost in the process.

Secondly, since the local construction techniques across the global south vary greatly, the study becomes highly context-specific. While the method of capturing data can be replicated, the architecture of the backend program may differ slightly based on the geographical location from where data is acquired.

Additionally, while the research builds upon a range of studies that demonstrate

the application of smartphone sensors in scanning and guidance technology, it does not test a prototype for the proposed system. As such, the physical limitations of the systems are yet to be determined.

8. Discussion

Despite the limitations discussed above, the contribution of this research in devising a method to actively aid informal self-construction without formalizing the construction process holds value. Most technical assistance practices and digital fabrication aimed to provide affordable housing is output-oriented. In order to minimize the error in the output, they tend to eliminate the information and communication gap in the process. While this ensures quality output, it offers one-time assistance that fails in an incremental setting. This research illustrates a process-oriented approach that fills the information and communication gap in the existing processes instead of eliminating it. Additionally, a digital system of aid ensures continued guidance that is independent of geographic and temporal constraints. The scope of future work for the system is discussed below:

Scaling across the global south: Since the backend program runs its analysis on a database of local construction technology, this model can be scaled and replicated across the global south by updating information on local technology pertaining to a specific location.

Applying Systems Theory: This research demonstrates a systems-based approach in identifying the information gaps in the existing scenario, by applying feedback loops to analyze the incremental process. This can be further amplified by exploring how actions at every step of the process affect the outcome and reinforcing the backend analysis to counter these actions to prevent failure in the output.

Training unskilled workers: This system can be used as a training module for unskilled workers. Since the proposed system is capable of identifying the knowledge capacity of workers by gathering information about the worker's activity, it can provide tailored guidance to train the workers.

9. Conclusion

This paper presents a framework for a smartphone-based, accessible digital aid system for informal self-construction that addresses a nonlinear, incremental method of construction. In the method presented here, design and construction occur concurrently, replacing the formal linear method of design preceding all forms of construction activity. The central argument of this paper is that while most forms of technical assistance for self-construction adopt a deterministic approach towards eliminating structural failures, this contradicts the principles of incremental construction and reduces the autonomy of the owner-builder in the construction process. Through an analysis of the informal process measured against formal processes, this research identifies that the primary cause of structural or spatial failures in the output is an information and communication gap in the construction process, that when filled can aid an incremental manner of development without compromising the quality of the output. To achieve a

real-time flow of information and communication in the construction process, the application of digital technology is sought. In order to deliver this, the paper proposes a framework for a digital system that explores the application of low-cost digital technology such as smartphone sensors to gather information from an owner-builder's construction environment, analyze it against three parameters: informed process, structural integrity, and spatial quality, and provide sensory guidance through a smartphone to guide the owner-builder in the construction process. The resultant system is a form of technical aid that ensures the non-linearity of incremental self-construction while maintaining quality output.

References

Bredenoord, J. and Lindert, P.V. 2014, Backing the self-builders, *in* J. Bredenoord and P.V. Lindert (eds.), *Affordable Housing in the Urban Global South: Seeking Sustainable Solutions*, Routledge; 1st edition (5 June 2014), 55-72.

Burgess, R.: 1985, The Limits of State Self–Help Housing Programmes, *Development and Change*, **16**(2), 271-312.

Harris, R.: 1998, The silence of the experts: "Aided self-help housing", 1939-1954, *Habitat International*, **22**(2), 165-189.

Henrysson, A. and Ollila, M.: 2003, Augmented reality on smartphones, *ART 2003 - IEEE International Augmented Reality Toolkit Workshop*, 27-28.

King, J.: 2016, *Incremental cities - Discovering the sweet spot for making town-within-a-city*, Ph.D. Thesis, London Metropolitan University.

L'opez, D., Charbel, H., Obuchi, Y., Sato, J., Igarashi, T., Takami, Y. and Kiuchi, T.: 2016, Human touch in digital fabrication, *ACADIA 2016: Posthuman Frontiers: Data, Designers, and Cognitive Machines - Proceedings of the 36th Annual Conference of the Association for Computer Aided Design in Architecture*, 382-393.

Lafreniere, B., Grossman, T., Anderson, F., Matejka, J., Kerrick, H., Nagy, D., Vasey, L., Atherton, E., Beirne, N., Coelho, M., Cote, N., Li, S., Nogueira, A., Nguyen, L., Schwinn, T., Stoddart, J., Thomasson, D., Wang, R., White, T., Benjamin, D., Conti, M., Menges, A. and Fitzmaurice, G.: 2016, Crowdsourced fabrication, *UIST 2016 - Proceedings of the 29th Annual Symposium on User Interface Software and Technology*, 15-28.

Mehra, R., Ferrario, M. and Janu, S.: 2017, Digital Tools for Low-Income Housing in Indian Cities, *Field Actions Science Reports. The journal of field actions*, **Special Issue 17**, 54-59.

mHS, C.: 2011, "Self construction: enabling safe and affordable housing in India" . Available from <http://www.mhscitylab.org/resources/> (accessed 16th March 2020).

Newnham, C. and Beanland, M.: 2018, Making in Mixed Reality, *ACADIA 2018: Recalibration: On Impercision and Infedility*, 2-11.

Patel, S. and Kunte, K.: 2011, "Incremetal A STUDY OF INFORMAL INCREMENTALITY, ITS IMPACTING FACTORS AND SUPPORTING SYSTEMS" . Available from <http://sparcindia.org/>.

Research, K.: 2019, "Augmented Bricklaying" . Available from <https://gramaziokohler.arch.ethz.ch/web/e/projekte/371.html>.

Turner, J.F.: 1977, *Housing by People: Towards Autonomy in Building Environments*, Pantheon Books.

Umek, A. and Kos, A.: 2016, Validation of smartphone gyroscopes for mobile biofeedback applications, *Personal and Ubiquitous Computing*, **20**(5), 657-666.

Yoshida, H., Igarashi, T., Obuchi, Y., Takami, Y., Sato, J., Araki, M., Miki, M., Nagata, K., Sakai, K. and Igarashi, S.: 2015, Architecture-scale human-assisted additive manufacturing, *ACM Transactions on Graphics*, 1-8.

PNEU-SKIN

A Haptic Social Interface with Inflatable Fabrics

YUJIE WANG[1] and MARCELA GODOY[2]
[1]*Massachusetts Institute of Technology, School of Architecture and Planning*
[1]*yujiew@mit.edu*
[2]*New York University Shanghai, Interactive Media Arts program*
[2]*mgodoy@nyu.edu*

Abstract. Wearable electronics endow us a great capacity to see clothing as an extension of our body and an interface to interact with our physical and social environment. The fashion industry is experimenting with new tectonics and materiality, however, few projects have explored wearables in the public and social domains and how it can dynamically respond to a wide range of interpersonal distances in social interaction. PNEU-SKIN is a pneumatic wearable that uses critical making as a research strategy to explore interactive and soft interfaces to create soft boundaries between private and public space. This paper proposes an embodied computation agenda and describes the design and prototyping process of a multi-sensory smart skin in response to varying social distance in interpersonal communication. By looking at adaptive behaviors in nature and the way that certain animal species respond to external stimuli by increasing their size and providing multi-sensory responses, PNEU-SKIN looks into how our clothing could become an adaptable skin to redefine interpersonal communication experience within everyday social interaction.

Keywords. Pneumatic Wearables; Interpersonal Communication; Embodied Computation; Critical Making; Sensory Feedback.

Figure 1. Final Design and Prototype of PNEU-SKIN.

PROJECTIONS, Proceedings of the 26th International Conference of the Association for Computer-Aided Architectural Design Research in Asia (CAADRIA) 2021, Volume 1, 713-722.

1. Introduction

Artists have been designing wearables to explore new relationships between body and space for a long time. For example, the fashion collection of Rei Kawakubo, Body Meets Dress, Dress Meets Body (1997), rethinks our perception of the human body by using filler and padding, altering the anatomical boundaries of it. Another example is the work of Lucy Mcrae who defines herself as a body architect, "speculates on the future of human existence by exploring the limits of the body". She understands the body as a combination of spaces and structures that can be reconstructed as an architectural space.

Figure 2. Rei Kawakubo. Comme des Garçons. Body Meets Dress–Dress Meets Body (1997).

Figure 3. Lucy McRae, Evolution (2008).

Technology is allowing us to see our clothing as an extension of our body and an interface to interact with our environment. Nowadays, wearable electronics are becoming everyday objects and designers found an opportunity in combining traditional techniques with technology to explore more complex ways of communication. As Sterlac observes, with the use of technology "the body has become an extended operational system, performing beyond the boundaries of the skin and beyond the local space that it inhabits." Artists, designers, and architects are now crossing disciplines to explore the realm of fashion, utilizing digital fabrication and electronics they are proposing new wearables from the point of view of performance, new tectonics, and materiality. Architect Behnaz Farahi exposes social issues such as gender and intimacy through the creation of robotic wearable technology. For example, her project Caress of the Gaze is a 3D printed actuated cape, which retracts and expands, changing its shapes according to external stimulus sessed by a camera embedded to the wearable. Another architect, Neri Oxman also uses technology in fashion stating "The future of wearables lies in designing augmented extensions to our own bodies that will blur the boundary between the environment and ourselves". The Mushtari is a 3D printed wearable that uses sunlight to generate consumable energy mimicking phenomena found in nature.

Figure 4. Caress of the Gaze: A gaze actuated 3D printed garment by Behnaz Farahi (2015).

Figure 5. Mushtari, Jupiter's Wanderer by Neri Oxman (2014).

As the fashion industry is experimenting with new tectonics and materiality, however, few projects have explored wearables in the public and social domains and how it can dynamically respond to a wide range of interpersonal distances in social interaction. In this paper, we describe the design and prototyping processes of PNEU-SKIN, a pneumatic wearable that uses critical making as a research strategy to explore interactive and soft interfaces to create soft boundaries between private and public space.

There is no doubt that men dominate the use of public space. In public transport, for instance, we often see that the space used by men is considerably more significant than the one used by women. Women are taught to make themselves small and be considerate of the space they occupy. Men, on the other hand, spread their bodies and invade others' personal space to make themselves comfortable. An example of this is "Manspreading", which is the practice of men sitting in public transport with legs wide apart, thereby taking up more than one seat. This kind of invasion of personal space is closely related to the study of Proxemics - human use of space in interpersonal communication. The most generally agreed taxonomy of human distances in space, according to Edward T. Hall, indicates that the interpersonal distances of man are categorized into four distinct zones-'intimate (<0.5m)', 'personal (0.5m-1.2m)', 'social (1.2m-4.0m)', and 'public (>4.0m)'. (Sussman and Justin 2015) These four interpersonal distances have their own uses and characteristics (Figure 6).

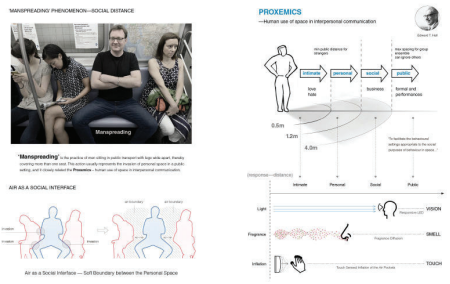

Figure 6. Manspreading Phenomenon on Public Transit and Critical Making Agenda with Sensory Feedback Integrated into Proxemics.

Leslie Kanes Weisman affirms "The appropriation and use of space are political acts. The kinds of spaces we have, don't have, or are denied access to can empower us or render us powerless." The relationship between power and space can be also found in nature. Species like pufferfish blow themselves up several times their normal size when they feel threatened by predators, while female toads inflate their bodies as a widespread mechanism to defend themselves from male toads and prevent them from mating with them. Like these two, several other species in the animal world can inflate their bodies, some of them use this ability to modify their sound and volume, but in general, the main purpose is a visual demonstration of prominence and power. In this study, the questions that emerge from this social issue are: What if our skin could respond to the invasion of our personal space redefining our anatomical perimeter? Would this empower women to reclaim their personal space? Digital technologies are used to design and fabricate a pneumatic wearable device that reacts to external stimuli through microcontrollers, sensors, and actuators. Utilizing a critical making approach and human-computer interaction concepts, this wearable acts as a reactive interface between the human body and the surrounding environment so that the bodily functions can be augmented, enhanced, and expanded.

The term Critical Making was introduced by Matt Ratto in 2008. It refers to a pedagogical practice and also a research strategy used to explore the intersection between critical thinking and hands-on practices to generate critical reflection about social issues. In Ratto's words, the emphasis of critical making is on "critique and expression rather than technical sophistication and function". (Ratto 2011) According to Ratto, a critical making project involves three stages: research, making, and reflection. The research stage implicates the study of relevant literature and the gathering of appropriate theories and concepts. The making stage involves the creation of material prototypes that are not focused on aesthetics, but in a conceptual exploration through fabrication to extend knowledge and skills in significant technical areas. The reflection stage involves an iterative process of exploration between different prototype alternatives where conversation and reflection begin. Architects and designers have been taking advantage of technology to communicate ideas better, design more efficiently, and reduce costs. However, the critical making approach steps back from this consumer-oriented culture and enables designers to reflect on social implications of the use of technology and practice design as a form of activism. Coming back to the idea of redefining human anatomy to reclaim personal space and empower women, the intention of creating a wearable as a second skin capable of interacting and reacting, is also an exploration of how art, design, and technology can reveal and challenge power relations in our society that emerge from the use of public spaces.

2. Method: Embodied Computational Workflow with Critical Making Agenda

We develop a critical making agenda with an embodied computational workflow through which sensory feedback is provided to form a haptic social interface responding to varying interpersonal distances.

Starting with ideating novel ways of social interaction, specifically, how our

design responds to varying interpersonal distances, we prototyped and tested with inflatable fabric modules and translated selected partial interaction to the body scale according to ergonomic principles. Through parametric patterning, digital fabrication, electronic interactive prototyping, and Arduino programming, we achieve the embodied computation agenda through system integration. A holistic approach is critical in this method as we intend to unify and synthesize the embodied computation agenda, sensory feedback mechanism, and inflatable material systems.

- **Material and Interactive Prototyping with Inflatable Fabrics** Material prototyping approaches the critical making agenda by conducting material experiments with inflatable fabric modules in different shapes and structures and testing various sensors and actuators in different sensory modalities. When activated with flowing air, inflatable fabric modules inflate and deflate in turn, and modules of different shapes and structures demonstrate different characteristics and behaviors. Iterations are made with selected pneumatic performance to achieve desired sensory responses.
- **Parametric Design and Patterning** Parametric design approaches the agenda by translating three-dimensional strategies on the body surface into a two-dimensional surface pattern. The pattern is determined by ergonomic Langer lines along which skin has minimum tension.
- **Digital Fabrication and Physical Prototyping** Digital fabrication approaches the agenda by laser cutting on nylon fabric materials for prototyping purposes. The cutting pattern is guided by ergonomic principles. This helps understand the actual material performance and behavior through interactive experiments.
- **Pneumatic Control and System Integration** Pneumatic control approaches the agenda by encoding how prototyped inflatable modules behave and provide sensory responses with simple hinging transformations and texture change in response to different interpersonal distances. The dynamic transformation of the garment can be achieved by controlling inflatable fabrics. The material layer, sensing layer, and the human body are integrated into a holistic system.

3. Results and Discussion: A Pneumatic Wearable Design Encoding Social Interaction

The proposed workflow was developed and tested in a design workshop the authors were instructed in Tongji University in 2018, taught by Behnaz Farahi and Jifei Ou. The authors designed and prototyped a pneumatic wearable that functioned as a haptic social interface that can provide sensory feedback to varying interpersonal distances.

3.1. MATERIAL EXPERIMENTS AND INTERACTIVE PROTOTYPING

PNEU-SKIN augments the body with novel interpersonal communication through enhancing sensory perception and feedback. Three types of sensory responses, namely touch, smell and vision, were mapped respectively to ‘intimate (<0.5m)’, ‘personal (0.5m-1.2m)’, ‘social (1.2m-4.0m)’ interpersonal distances according to Edward T. Hall’s Proxemics theory.Material experiments and inflatable module prototyping was then conducted. After cutting the non-sticky nylon fabric into

testing shapes, two nylon layers with one connector in between are stuck together with adhesive thermoplastic TPU through heat pressing. An air tube with another connector is then inserted into the air pockets. When activated with flowing air from a syringe, inflatable fabric modules inflate and deflate in turn, and modules of different shapes and structures demonstrate different characteristics and material behaviors. We also incorporated distance sensor (HC-SR04 ultrasonic distance sensor module) and touch sensor (TTP223B digital capacitive touch sensor) to detect interpersonal distances and touch behaviors. The touch sensor is small enough to be embedded inside the air pocket while the ultrasonic distance sensor is placed outside the air pocket. Responsive LEDs (WS2812B NeoPixel digital addressable RGB LED light strip) were placed inside the air pockets to provide visual cues through color and blinking patterns (faster blinking frequency in the closer distance) in response to interpersonal distance and perfume were also placed between fabric folds to provide olfactory feedback when inflated and deflated with inflatable modules. Through a series of material experiments and pneumatic tests, we selected the muscle-like inflatable module to develop further. It can expose the hidden layer when inflated (Figure 7).

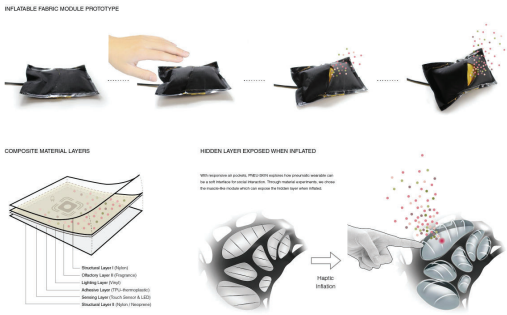

Figure 7. Inflatable Fabric Module Prototype with Touch and Distance Sensors.

The muscle-like module's inflatable layer is generated by a series of air pockets which are fabricated with two layers of Thermoplastic Polyurethane(TPU) and paper in between (Figure 8). TPU is a textile that can be fused by applying heat. The purpose of using paper is to allow only the edges to be fused and create an air pocket. The study introduces Box pleats on the TPU fabric to allow the pocket to grow in three dimensions. Pleating is a technique of folding fabric to create texture and changes in the shape of garments. Box pleats are made up of two knife pleats which are the most basic and commonly used techniques to pleat textiles. Knife pleats consist of two folds of equal width, a visible outside fold and a hidden inside fold. In a Box pleat, the two knife folds face away from each other. After developing a few prototypes, the pocket was made by the combination of two types of TPU fabrics; translucent for the inside fold and opaque black for the outside fold, so when the pockets inflate the translucent fabric is visible and also the light from LEDs placed behind the pockets.

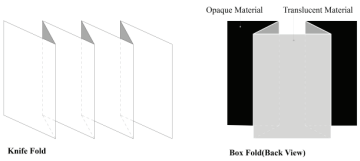

Figure 8. Fabric Pleat techniques used in the study.

3.2. PARAMETRIC PATTERNING AND DIGITAL FABRICATION

The three-dimensional body surface was unfolded into two-dimensional for pattern mapping and laser cutting. Voronoi patterns were laid out on the unfolded surface to accommodate the inflatable modules in procedural design software (Grasshopper) according to Langer lines, along which skin has minimum tension so that the patterns inform the air pockets and their form transformations (Figure 9). In this way, the pneumatic wearable reflects the architecture of the human body, as well as it is capable of being reconfigured according to the movement of the wearer's body. The resulting design was fabricated with a laser cutter in non-sticky nylon fabric materials for interactive prototyping and testing.

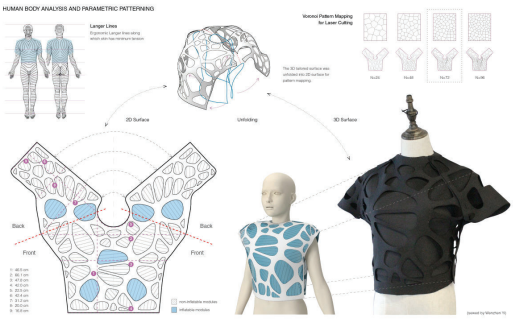

Figure 9. Body Tailoring, Parametric Patterning, and Laser Cutting.

The core structure containing the pockets is covered by two layers of Neoprene fabric, a synthetic rubber sandwich structured textile. The morphology of this fabric provides stability and maintains the flexibility needed for the wearable. The inside or base layer, facing the skin of the user, covers the pockets providing support for placing sensors, air pipes, and electronics. The front layer is designed in Grasshopper cutting out the air pockets to allow them to grow when the air is pumped in. The design of this piece is provided from the 3D model as one flat piece and cut precisely by using a laser cutter. Finally, the three layers (Figure 10) are assembled by the use of Double Sided Fusible Interfacing, a fusible fleece web that works like glue when it is heated. This layer was also laser cut, one with the shape of the outside layer and another one with the shape of the base layer.

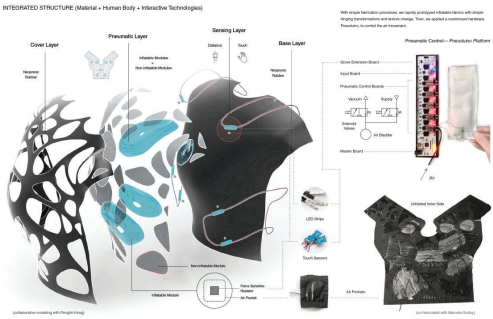

Figure 10. Material, Inflatable, and Electronic System Integration.

3.3. SOCIAL INTERACTION ENCODING, PNEUMATIC CONTROL, AND SYSTEM INTEGRATION

Three types of social interaction scenarios (Sussman and Justin 2015) were encoded into the pneumatic system's behavior and formed a novel embodied computation agenda. (Figure 11) PNEU-SKIN has no reaction at or beyond social distance (>1.2m). When someone approaches personal distance (0.5m-1.2m), the responsive LEDs turn on and inflatable modules will be slowly inflated to release perfume as a soft olfactory sensory response. The inflatable modules will be fully inflated as a strong haptic sensory response (Figure 12) when someone approaches an intimate distance (<0.5m) and touches the inflatable module.

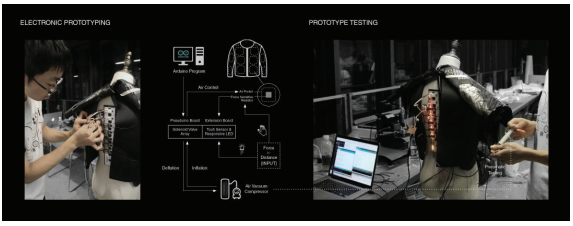

Figure 11. Electronic Prototyping and Testing.

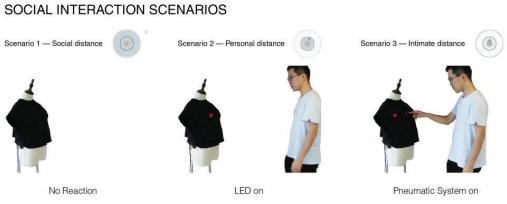

Figure 12. Social Interaction Scenarios and Interactive Prototype Testing.

The pneumatic system is primarily controlled by a customized modular hardware platform, the Pneuduino board (Yao et al. 2013) developed by MIT Media Lab Tangible Media Group, through Arduino microcontroller in order to control airflow and air pressure (Figure 4). The distance sensor and touch sensor were programmed in response to distance and pressure detection as mentioned above in Arduino IDE. Embedded with sensory technologies and elements, including responsive LEDs, distance and touch sensors, and perfume, PNEU-SKIN achieved original intentions of providing dynamic sensory feedback to varying interpersonal distance in social interaction and forms a soft boundary between private and public space (Figure 13).

Figure 13. Touch Sensed Inflation.

It is also important to note that, during the user testing, the noise caused by using the air pump has some negative impact on user experience, it could be improved with better insulation of the air pump with smaller noise in the future. The thickness of the fabric also weakened the sensitivity of touch detection of the touch sensor embedded inside the inflatable module, and it took several rounds of calibration with different types of fabric and interactive testing.

4. Conclusion

Unlike the common task-oriented approach to computational making, PNEU-SKIN goes beyond an investigation of HCI, soft robotics, and digital fabrication. As Neri Oxman states, “Digital technologies cannot and should not serve only our formal aspiration” (Dvir 2019), the project stimulates the neglected discussion and debate about gender and space. PNEU-SKIN explored wearables in the neglected public and social domains and how it can dynamically respond to a wide range of interpersonal distances in social interaction. Using critical making as a research strategy and embodied computation workflow, A pneumatic wearable was developed as an interactive and soft interface to create soft boundaries between private and public space. With easy access to digital fabrication, small electronics, and microcontrollers, this rapidly prototyped second skin speculates the limits of the human body and its implications of the relationships between body and space (Farahi 2016). Similar relationships in

nature served as inspiration for developing PNEU-SKIN. Reactions observed in animal skin for defense mechanisms are mimicked, postulating new attractive possibilities for human interaction.

Future Projections. Architecture is more than just designing buildings and spaces. It embodies the experiences of those who occupy them. In this regard, male domination in all spaces is undeniable, including professional, social, and intimate spaces, allowing us to reflect on the role of women in society. Consequently, it is crucial to contextualize architecture in relation to gender issues. Through the use of novel technologies, PNEU-SKIN presents a critical perspective on current practices and the norms of society. It advocates the critical making agenda and calls on greater awareness of gender inequality, power relationship in space, and other critical social issues in the computational making domain.

Acknowledgments

This research was supported by Tongji University College of Architecture and Urban Planning and developed in DigitalFUTURES Shanghai 2018 Workshop with team members Pengfei Kang, Wenzhen Yi, and Zhiyi Rong. The authors would like to express great appreciation to the instructors and teaching assistants of the workshop, specifically, Behnaz Farahi, Jifei Ou, and Yuqiong Lin. The authors would also like to extend grateful thanks to MIT Media Lab Tangible Media Group, whose work laid the hardware foundation of the case study and motivated the authors to do the research.

References

Dvir, B.: 2019, "Neri Oxman Is Redesigning the Natural World', Surface, July 26" . Available from <https://www.surfacemag.com/articles/neri-oxman-material-ecology> (accessed 18th September 2020).

Farahi, B.: 2016, Caress of the Gaze: A Gaze Actuated Garment, *36th annual Association for Computer Aided Design in Architecture conference*, Ann Arbor, Michigan, 352-361.

Hicks, J.: 2012, "no title given" . Available from <https://www.theverge.com/2012/9/14/3261078/meat-metal-and-code-stelarcs-alternate-anatomical-architectures> (accessed 18th May 2020).

Landry, L.: 2014, "'An MIT Professor Is Creating 3D 'Wearable Skin' to Help You Survive Outer Space'. The Business Journals, December 03" . Available from <https://www.bizjournals.com/boston/inno/stories/news/2014/12/03/an-mit-professor-is-creating-3d-wearable-skin-to.html> (accessed 16th September 2020).

Mallgrave, H.: 2013, *Architecture and embodiment: the implications of the new sciences and humanities for design.*, Routledge., London; New York.

Manne, K.: 2017, *Down Girl: The Logic of Misogyny*, Oxford University Press, New York.

Ratto, M.: 2011, Critical Making: Conceptual and Material Studies in Technology and Social Life, *The Information Society*, **27:4**(DOI: 10.1080/01972243.2011.583819), 252-260.

Rendell, J., Penner, B. and Borden, I.: 2000, *Gender space architecture: an interdisciplinary introduction*, Routledge, London.

Sussman, A. and Hollander, J.B.: 2015, *Cognitive Architecture: Designing for How We Respond to the Built Environment*, Routledge, New York.

Yao, L., Niiyama, R., Ou, J., Follmer, S., Silva, C.D. and Ishii, H.: 2013, PneUI: pneumatically actuated soft composite materials for shape changing interfaces, *26th annual ACM symposium on User interface software and technology (UIST '13)*, New York, NY, 13–22.

SISTEMA NERVI

Sustainable Production of Optimised Floor Slabs Through Digital Fabrication

OWEN OLTHOF[1], ANASTASIA GLOBA[2] and PAOLO STRACCHI[3]
[1]*Author*
[1]*owen.olthof@gmail.com*
[2,3]*Co-Author*
[2,3]*{anastasia.globa|paolo.stracchi}@sydney.edu.au*

Abstract. 'Sistema Nervi' (the Nervi System) invented by Pier Luigi Nervi greatly economised the production of complex concrete forms optimised in both material usage and structurally. However it did not translate well into other contexts due to labour and material considerations (Leslie, 2018). This paper explores novel methodologies of producing optimised floor slabs and concrete structures, using digital fabrication techniques, focusing on both labour economisation and sustainability principles. A module from the Australia Square lobby slab has been used as the set geometry and was reproduced using differing techniques of fabrication for a comparative study. The study was conducted at scale (1:20). The viability for production at full scale (1:1) for manufacturing is discussed. The assessment criteria for the tests are divided into four categories: Cost, Time, Performance, and Sustainability. 3D printing of PLA plastic and ceramic clay extrusion printing has been used to produce removable or degradable formworks. These technologies have been selected due to their current market availability and associated costs. This study hopes to introduce improved methodologies for producing optimized concrete forms, as well as the sustainability potentials of a degradable formwork such as ceramic clay. Both systems were ultimately able to produce workable formworks for optimised shapes and showed promise for reducing labour involved as well as presenting with material sustainability for discussion.

Keywords. Concrete formwork; Sustainability; Degradable formwork; Optimised concrete; Advanced fabrication.

1. Introduction

In pre-WW2 Fascist Italy, political embargoes limited Italy's access to steel. In a country without a rich natural supply of the material, what imports were allowed were directed to the production of armaments and munitions (Stracchi, 2019). In response to these conditions Nervi developed Ferrocement. This thin cement system with reduced steel reinforcement was developed in conjunction

PROJECTIONS, Proceedings of the 26th International Conference of the Association for Computer-Aided Architectural Design Research in Asia (CAADRIA) 2021, Volume 1, 723-732.

with the 'Sistema Nervi' (The Nervi System) to produce permanent formworks that could create optimised ribbed floor slabs that were greatly optimised in the use of materials as well as static loads (Antonucci and Nannini, 2019). The Nervi System proved a success in the context of 1940s Italy, with its limited access to steel and an abundance of cheap labour (Leslie, 2018).The process of the Sistema Nervi (Figure 1.1) requires several steps and mouldings to create the final permanent formwork (Seidler, Dupain and Williamson, 1969).This extended labour-intensive process, detailed below, is the main reason for the poor translation of the building technology into other contexts.

1.1. THE PROBLEM

Economic factors meant the Nervi System was not widely adopted. Optimised material usage provides us with economic and sustainability opportunities which are especially relevant today as we find ourselves in a similar position to Nervi with a need to reduce our material usage. Concrete and its production is a major contributor to global emissions. Slab structures are estimated to make up to 85% of a buildings weight (Georgopoulos and Minson, 2014) using portland cement, accounting for an estimated 5.2% of global CO2 emissions (J. Hawkins et al., 2016). Highly complicated, non unitized, systems such as 'Smart Slab' (Figure 1.2), developed by ETH Zurich which is an optimised ribbed slab system (not dissimilar to the outcomes from the Nervi system) have reduced the amount of concrete required by 70% compared to a standard floor slab (Aghaei Meibodi et al., 2018). However this requires an expensive methodology and complex digital fabrication systems. By employing modular formwork The Nervi System takes a much simpler approach to creating optimised ribbed structures and appeals to structural, aesthetic and sustainability needs. However, it currently falls short economically. 3D printing has been chosen as the technology to create formworks due to the its viability to be employed in current construction. The focus is on reducing the complexity of production and utilising 3D printing to lower the labour costs. 3D printing in PLA and ceramic clay have been identified as the materials due to their availability, cost and sustainability potentials.

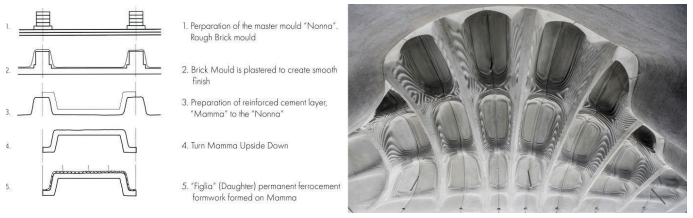

Figure 1. (Left to right) 1.1 Sistema Nervi Process, 1.2 Smart Slab (ETH Zurich 2018).

1.2. HYPOTHESIS

The hypothesis of this study is that PLA (Polylactic Acid) extrusion formworks and mouldings for permanent formwork will produce the most viable results. They are expected to be regular and have a high-quality finish but be more expensive

to produce. They will also be the least labour-intensive. Ceramic formworks are expected to be irregular, so problems with the 3D printed form and setting concrete will be encountered.

2. Case Study (Geometry)

The Nervi slab of Australia Square will serve as the case study and geometric focus for the purposes of this paper. The slab was designed and built in 1962-1967 and implements a system of seven repeating modules to manufacture the radial slab. These permanent formwork modules were then placed on site where additional reinforcement was added and concrete was poured into the formwork (Figure 2.1). A single module has been selected and reproduced for the purposes of this study (Figure 2.2).

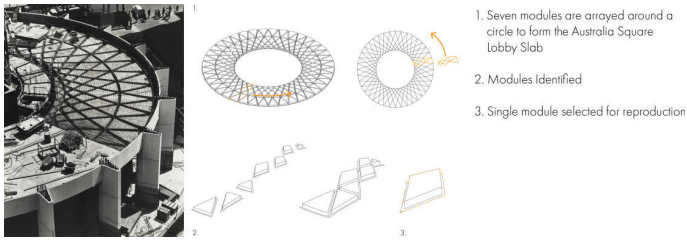

Figure 2. (Left to right) 2.1Construction of the Australia Square Nervi Slab (Dupain, 1967), 2.2 Selection of Module from Australia Square.

3. Methodology

To produce the selected module several methodologies were tested and the results have been analysed via a comparative analysis. The original methodology and output delivered in Australia Square acted as the control and final conclusions have been compared to this. The tests are divided into three groups:

1. PLA extrusion printing (Test group 1)
2. Ceramic print air-dried (Test group 2)
3. Ceramic print wet (Test group 3)

Each method was then analysed by the following criteria:

- Cost ($AUD)
- Time (Hr:Min:Sec)
- Performance (exterior finish and cracking)
- Sustainability (of formwork and printing material)

3.1. MOULD AND FORMWORK TYPES

Several forms of moulds and formwork types were explored to find a successful product. Maintaining a simple form was key as it would need to be scalable to remain viable. Cost and time implications were also very important for the viability of the method. Ultimately all the formworks were designed around having

a bounding volume with a negative of the module to be removed (Figure 3).

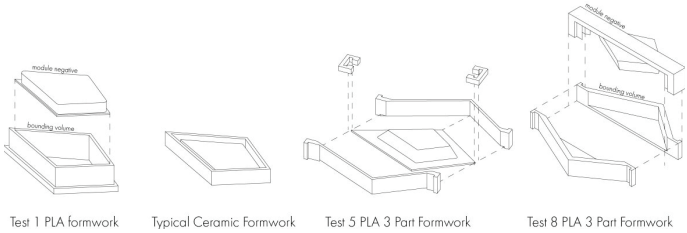

Figure 3. Typical 3D printed formworks.

3.2. FABRICATION OF MODULES

Modules were produced within a four-step process, pictured in figure 4:

1. Printing of formwork.
2. Cleaning of 3D prints.
3. Pouring Cement. (Ratio: 500g cement, 200g water, 5ml water reducing additive)
4. Demoulding.

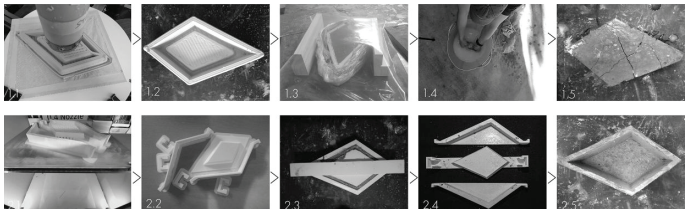

Figure 4. Process images, 1.1 Ceramic Printing , 1.2 Cleaned ceramic formwork, 1.3 Concrete pour and environmental control, 1.4 Washing and cleaning of module, 1.5 Outcome, 2.1 PLA printing, 2.2 3D formwork removal and cleaning, 2.3 Release agent application and Concrete pouring, 2.4 Demoulding, 2.5 Outcome.

4. Summary of Results and Discussion

The experiments have provided with two possible methods for creating formwork for optimised ribbed structures using digital fabrication. These were PLA with a multi part (3 or more) formwork design and release agent (as seen in experiments 5 and 8), and wet ceramic contained within a closed environment to control moisture (as seen in experiments 6 and 7). These methods will be the focus of the discussion and analysis of the comparative study criteria. Both presented methods with a low labour intensity and possibilities for reuse or recycling of the formwork material. The sustainability of these materials merits further study to draw conclusions about their true sustainability and recyclability. All other experiments experienced severe cracking or difficulties releasing from formwork. A full tabulated results list (table 1) of experiment images (section 4.01) and observations (section 4.02)

have been included. Production of mouldings for permanent formworks was not possible at the set experimental scale (1:20), but was trialled in experiment 2.

Table 1. Results tables (Left to right) 4.01 Experiment records in images, 4.02 Experiment observations and data.

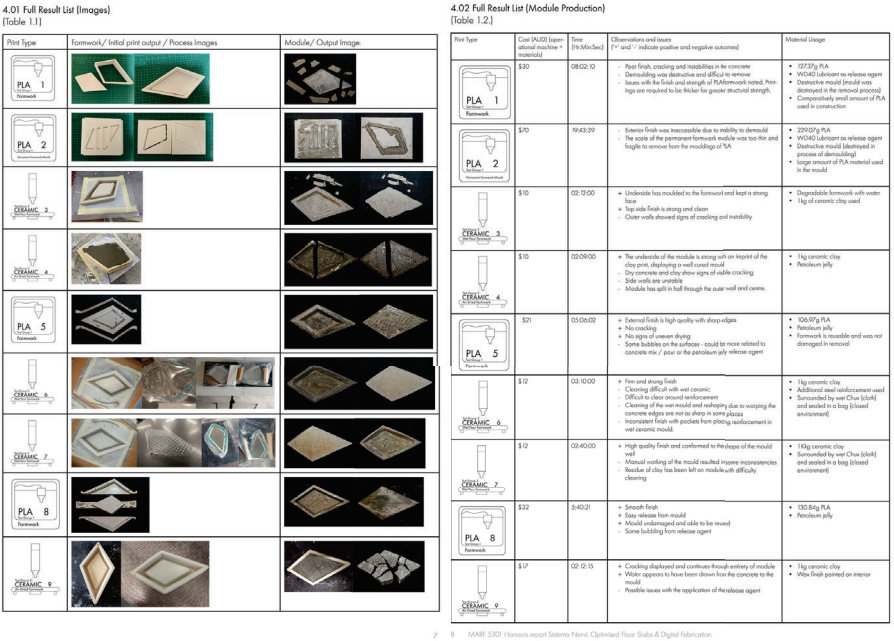

4.01 Full Result List (Images)
(Table 1.1)

Print Type	Formwork/ Initial print output / Process Images	Module/ Output Image
PLA 1 Formwork		
PLA 2 Permanent Formwork Mould		
CERAMIC 3 Direct Casting		
CERAMIC 4 Direct Casting		
PLA 5 Formwork		
CERAMIC 6 Direct Casting		
CERAMIC 7 Direct Casting		
PLA 8 Formwork		
CERAMIC 9 Direct Casting		

4.02 Full Result List (Module Production)
(Table 1.2.)

Print Type	Cost (AUD) (operational machine + materials)	Time (Hr:Min:Sec)	Observations and issues (+' and '-' indicate positive and negative outcomes)	Material Usage
PLA 1 Formwork	$30	08:02:10	- Poor finish, cracking and instabilities in tie concrete - Demoulding was destructive and difficult to remove - Issues with the finish and strength of PLAformwork noted. Printings are required to be thicker for greater structural strength.	• 127.37g PLA • WD40 Lubricant as release agent • Destructive mould (mould was destroyed in the removal process) • Comparatively small amount of PLA used in construction
PLA 2 Permanent Formwork Mould	$70	19:43:39	- Exterior Finish was inaccessible due to inability to demould - The scale of the permanent formwork module was too thin and fragile to remove from the mouldings of PLA	• 229.07g PLA • WD40 Lubricant as release agent • Destructive mould (destroyed in process of demoulding) • Large amount of PLA material used in the mould
CERAMIC 3 Direct Casting	$10	02:12:00	+ Underside has moulded to the formwork and kept a strong face + Top side finish is strong and clean - Outer walls showed signs of cracking and instability	• Degradable formwork with water • 1kg of ceramic clay used
CERAMIC 4 Direct Casting	$10	02:09:00	+ The underside of the module is strong with an imprint of the clay print, displaying a well cured mould - Dry concrete and clay show signs of visible cracking - Side walls are unstable - Module has split in half through the outer wall and centre.	• 1kg ceramic clay • Petroleum jelly
PLA 5 Formwork	$21	05:06:02	+ External finish is high quality with sharp edges + No cracking + No signs of uneven drying - Some bubbles on the surfaces - could be more relaxed to concrete mix / pour or the petroleum jelly release agent	• 106.97g PLA • Petroleum jelly • Formwork is reusable and was not damaged in removal
CERAMIC 6 Direct Casting	$12	03:10:00	+ Firm and strong finish - Cleaning difficult with wet ceramic - Difficult to clean around reinforcement - Cleaning of the wet mould and reshaping due to warping the concrete edges are not as sharp in some places - Inconsistent finish with pockets from placing reinforcement in wet ceramic mould.	• 1kg ceramic clay • Additional steel reinforcement used • Surrounded by wet Chux (cloth) and sealed in a bag (closed environment)
CERAMIC 7 Direct Casting	$12	02:40:00	+ High quality finish and conformed to the shape of the mould well - Manual working of the mould resulted insome inconsistencies - Residue of clay has been left on module,with difficulty cleaning	• 1Kkg ceramic clay • Surrounded by wet Chux (cloth) and sealed in a bag (closed environment)
PLA 8 Formwork	$32	3:40:21	+ Smooth finish + Easy release from mould + Mould undamaged and able to be reused - Some bubbling from release agent	• 130.84g PLA • Petroleum jelly
CERAMIC 9 Direct Casting	$17	02:12:13	+ Cracking displayed and continues through entirety of module + Water appears to have been drawn from the concrete to the mould - Possible issues with the application of the release agent	• 1kg ceramic clay • Wax finish painted on interior

7 8 MARF 5301 Honours report Sistema Nervi: Optimised Floor Slabs & Digital Fabrication

4.1. FABRICATION TECHNOLOGIES

A plethora of advanced fabrication technologies are available today and selecting the most appropriate systems for interrogation is important. Fundamentally the explored fabrication techniques needed to be be adaptable to custom products, have potential to reduce labour intensity from the current Nervi system, be readily available commercially and have possibilities for sustainability credentials in operation and material usage. For these reasons prefabricated systems such as waffled slabs and Holedeck, being unable to provide bespoke opportunities, were not explored. 3D printing of concrete has also been explored previously but is most commonly applied to simple unoptimized structures, with complex structures being possible but requiring highly complex and niche machinery (Zhang et al., 2019). CNC (computer numerical control) routers are readily available and the routing of foam is a fast method for formwork creation, but the foam and wastage of material were deemed unsustainable for the objectives of the study. Similarly, vacuum forming employed unsustainable non-recyclable Perspex. Wax printing has also been used to create formwork for optimised structures. The material was found to be unpredictable, (Oesterle, Vanteenkiste and Mirjan, 2012), (Hermann et al., 2018) and this technique was not able to be explored due to the availability of

wax printers. Both PLA plastic extrusion printers and ceramic printers are readily available in the market, relatively cheap, and the materials which they use are highly sustainable and low cost. Both materials are biodegradable, reusable, and recyclable. PLA printing was able to be used to explore the production of moulds for permanent formworks as well as removable formworks. Ceramic printing, due to its inherent limitation for creating self supporting, removable formwork was only able to be used to explore removable and degradable formworks. An 'Ultimaker 2+ connect' developed by 'Imaginables' (Ultimaker 2+ Connect, 2020) was the 3D PLA plastic printer used and a linear actuator, or, 'Potterbot extruder' by '3dpotter' (3DPotter, 2020) was the ceramic printer used.

4.2. FEASIBILITY OF SCALING

The 'Ultimaker' and 'Potterbot' are good case studies when operating at the 1:20 scale, but would not be viable for commercial production. Products made for industrial use or custom rigs would therefore need to be explored to draw conclusions on the feasibility for these methodologies. Commercial viability for large scale industrial ceramic printing has not been extensively explored. Experiments by Anya Gallacio have been developed as installations but would appear to exemplify the difficulties of printing wet medium at a large scale (Anya Gallaccio, 2015). It does however show that the creation of larger ceramic printers is possible, however accuracy is currently low. The method which produced the most viable outcomes using wet ceramic printed formwork required an enclosed environment. It could be difficult to provide these conditions on-site. Therefore a factory or controlled location would be needed to produce the formwork and concrete slab, then transport to site. The most successful test prints were the PLA test group. Large scale 3D printing of PLA and plastic structures has been commercially available for several years. Thinglab's 'Bigrep' series (Thinglab 2020), among other firms, produce industrial scale printers with print beds of above 1m3. Using a printer to produce a module for the Australia Square slab at 1:1 scale would require multiple interlocking pieces and could be a complex construction. However, if this complexity could be managed PLA has proven to be a good formwork for concrete structures and could become a commercially viable formwork for complex designs. It is assumed that the current method of outer bounding formwork with 3D printed complex formwork could be implemented at 1:1 scale as shown in figure 5.

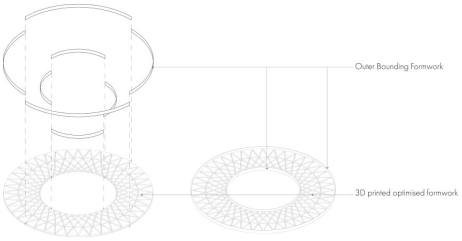

Figure 5. 1:1 scale technique implementation.

4.3. RESULTS OF ASSESSMENT CRITERIA

The test outputs were not of the same quality as the Australia Square slab. They did, however, indicate that an appropriate finish was achievable with the methods but may require more time and research into release agents, concrete composition and vibration to reduce cavitation. Cost, Time, Performance, and Sustainability can be discussed in context with the experiment but it is difficult to draw conclusions about the viability for the technologies in the current manufacturing industry without 1:1 experiments.

4.3.1. Cost

Ceramic prints for moulding formwork were significantly cheaper than the PLA prints (Figure 6.1), ranging from 14-50% of the total cost of some PLA prints. Both material and machine-use time were cheaper than the PLA printers. A note should be raised that because of the required operation and observation of the ceramic printer during use a labour cost could be included and alter results.

4.3.2. Time

Similarly, to cost calculations, a deeper understanding of, and comparison to, standard slab construction would help to situate the results. The time for production of ceramic extrusion prints ranged between 47minutes to an hour. PLA prints varied from approximately 4 hours to 10 hours (Figure 10.2). Ceramic prints required monitoring and machine calibration while the printing process was underway and thus were more labour intensive. The less labour-time intensive method was PLA printing but the faster overall time for production was ceramic printing.

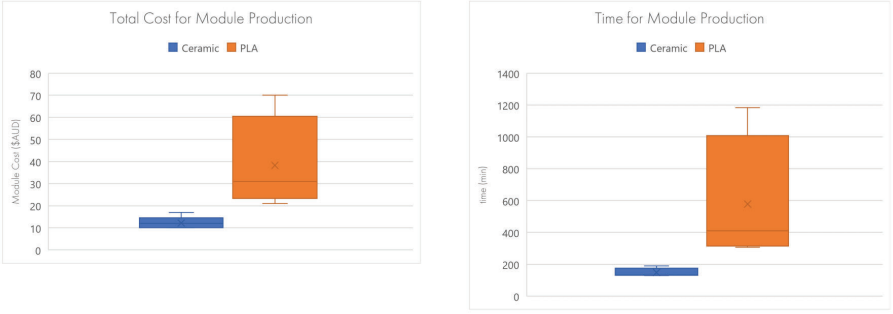

Figure 6. Box and Whisker Plot Results (Left to right) 6.1 Cost, 6.2 Time) .

4.3.3. Performance

The finish and consistency of PLA formwork were of higher quality in all aspects to Ceramic printing but lower than that of the existing Nervi System. PLA edges were sharper and faces were cleaner than that of the ceramic clay and the

final product from PLA prints were much more reliable and regular. This was largely due to the liquid nature of the ceramic clay causing inconsistencies and inaccuracies. Additionally, the manual calibrations of the 'Potterbot' contributed to inaccurate final products. Malformed prints required manual working to correct the alterations and reform some portions of the moulds. Ultimately, the manual work proved less consistent than the PLA formworks which required no interventions. There is room however for finer calibration and control of the 'Potterbot' to produce more uniform outputs and reduce the need for manual intervention, greatly increasing the performance and ability to produce regular formwork. Ultimately both systems showed promise, but PLA was the more immediately successful in the scope of the conducted experiments.

4.3.4. Sustainability

The Nervi system is well documented as reducing material usage by approximately 24% of a regular slab construction (Magan 2016) so in this aspect the system is clearly more sustainable. Sustainability is a blanket term that can cover many aspects of a product. For the purpose of this study it relates to materials. Specifically, the re-usability, recyclability and biodegradability of the materials which were printed. All clay used in the ceramic extrusion printing was able to be retained. This clay, however, had concrete chips dispersed through it and could not be directly reused through the printer. Cleaning and filtering of contaminants would be required to reuse the clay for printing. At a 1:1 scale it is expected that there would significant amounts of clay required for the formworks. PLA on the other hand could be used to produce the formworks with a much reduced volume of material. When used with appropriate release agent PLA formworks were able to be retained for reuse. The release agent would need to be removed from the formwork prior to its recycling and would need to have appropriate environmental credentials (being non toxic). PLA itself is biodegradable and technologies for recycling the plastic are available but in their early stages. Products such as Filabot's 'Filabot Reclaimer' (Filament Maker, 2020) granulates waste plastic and melts the resultant particles into new filament. This could be a viable method for recycling, however research into the effects of a release agent on the reclaimer machine would need to be explored. Commercial viability for the recycling and reuse of either of these materials is possible but would require further research into the feasibility for commercial use. Water use for the demoulding of ceramic formwork was extensive with each test requiring approximately 15L to remove the clay suggesting again that the intensive use of water for the formwork removal would be substantial for a full-sized slab.

4.4. LIMITATIONS

The study had three major limitations. Time, funding, and consequently scale. The time period set for the study was 4 months and the cost was to be below $350 (AUD). Due to these limitations the scale of the study was reduced and prohibited the investigation into permanent formworks. These constraints inherently limited the number of possible iterations and test subjects. The cost and time limitations this study was subjected to draw parallels with many projects. This is why these

limitations also helped to direct the study toward the most appropriate avenues for methods and technologies which would ultimately be viable for real world construction.

4.5. FUTURE STUDY AND WORK

Further study into the sustainability credentials of the materials used is needed. Whilst both appear to be recyclable or reusable more data is needed to draw a conclusion. Test prints at a larger scale are needed to gather a clearer indication of the costs for using these construction methods. Additionally, testing of the material strength is required to ascertain its viability for real world applications. Construction methodology including connections between the produced modules as well as an analysis of the structural qualities for the optimised rib slabs are targeted.

5. Conclusions

The study was set to explore possible methods to reduce the labour intensity of creating optimised floor flabs in the ilk of the Nervi System. The experiments suggest possible avenues for further study using the explored technologies. Both Ceramic and PLA extrusion printers were able to produce workable formwork for complex ribbed concrete structures. Wet ceramic formwork in a closed environment and PLA formworks with a release agent both showed promise as methods to reduce the labour intensity of creating optimised floor slabs. The methods have also presented opportunities for exploration for material sustainability with technologies for their reuse available, or biodegradability showing potential. Ultimately the PLA formwork when used in conjunction with a release agent yielded superior results, however the time for production was extensive. The table below summarises and illustrates what is a classical engineering/production dilemma: two processes with apposing costs of materials and labour (table 2).It is this authors opinion that the PLA technology is the more likely, with the results of further research, to be the more successful technology.The results of the study support the hypothesis that PLA would be the more successful method of production but also the more expensive, whilst ceramic clay would encounter problems with consistency and accuracy of printing.

Table 2. Conclusions Table.

	PLA	Wet Ceramic
Cost	• High cost of materials • Low cost of labour	• Low cost of materials • High cost of labour through high labour content to finished product
Time	• High print times • Low labour requirement • High design and computation time	• Low print times • High labour requirements
Performance	• High quality finish with use of release agent	• Lower quality finish due to manual interventions
Sustainability	• High embodied energy of the initial production of plastic • Biodegradable • Recyclable	• Biodegradable • Recyclable

References

"Bigrep Large Scale Additive Manufacturing" : 2020. Available from <https://thinglab.com.au /bigrep-3d-printers-australia/> (accessed 30 November 2020).

Antonucci, M. and Nannini, S.: 2019, Through History and Technique: Pier Luigi Nervi on Architectural Resilience, *Architectural Histories*, **7**, 1-8.

C. Chiorino, E.M. Nervi and T. Leslie (eds.): 2018, *Aesthetics and technology in building: the twenty-first-century edition*, University of Illinois Press, Champaign, Illinois.

Dupain, M.: 1967, "Construction Of The Australia Square Nervi Slab [image]" . Available from State Library NSW<https://www.sl.nsw.gov.au/stories/harry-seidler-collection/australia-square-sydney> (accessed 29 November 2020).

ETH, Z.: 2018, "Smart Slab [image]" . Available from <https://dbt.arch.ethz.ch/project/smart-slab/> (accessed Accessed 30 November 2020).

Filabot, c.o.: 2020, "Filament Maker - Recycle Filament For Any 3D Printer" . Available from Filabot Machine<https://www.filabot.com/> (accessed 30 November 2020).

Gallaccio, A.: 2015, "Beautiful Minds" . Available from <https://www.biennaleofsydney.art/artists/anya-gallaccio/> (accessed 30 November 2020).

Georgopoulos, C. and Minson, A.: 2014, *Sustainable Concrete Solutions*, Wiley-Blackwell, Chichester.

Hawkins, W., Herrmann, M., Ibell, T., Kromoser, B., Michaelski, A., Orr, J. and Pedre, R.: 2016, Flexible formwork technologies – a state of the art review: Structural Concrete, *Structural Concrete*, **17**, 1-5.

Hermann, E., Mainka, J., Lindermann, H., Wirth, F. and Kloft, H.: 2018, Digitally Fabricated Innovative Concrete Structures. In: International Symposium on Automation and Robotics in Construction, *ISARC*, Berlin, 1-10.

Imaginables, A.: 2020, "Ultimaker 2+ Connect" . Available from <https://imaginables.com.au/collections/3d-printers/products/ultimaker2plus> (accessed 3 December 2020).

Leslie, T.: 2018, *"Inevitably Translated:" Pier Luigi Nervi's Work In Australia*, Iowa State University.

Magan, C.: 2016, *Topology Optimization of a Concrete Floor Slab Guided by Vacuumatic Formwork Constraints*, Master's Thesis, TU Delft.

Aghaei Meibodi, M., Jipa, A., Giesecke, R., Shammas, D., Bernhard, M., Leschok, M., Graser, K. and Dillenburger, B.: 2018, mart Slab: Computational Design and Digital Fabrication of a Lightweight Concrete Slab, *ACADIA*, Mexico City.

Oesterle, S., Vanteenkiste, A. and Mirjan, A.: 2012, ero Waste Free-Form Formwork, *ICFF*, Zurich, 1-10.

3D Potter, initials missing: 2020, "Extruders For Ceramic 3D Clay Printers" . Available from < https://3dpotter.com/extruders> (accessed 3 December 2020).

Seidler, H., Dupain, M. and Williamson, H.: 1969, *Australia Square*, Horwitz Publications, Sydney.

Stracchi, P.: 2019, *Designed In Italy Made In Australia.*, The University of Sydney, Sydney.

Zhang, J., Wang, J., Dong, S., Yu, X. and Han, B.: 2019, A review of the current progress and application of 3D printed concrete, *Composites Part A Applied Science and Manufacturing*, **online**, 125-135.

GRADED KNIT SKINS

Design and fabrication of curved modular façade cladding panels

YING YI TAN
[1]*Singapore University of Technology & Design*
[1]*yingyi_tan@mymail.sutd.edu.sg*

Abstract. This paper presents the design and manufacture of lightweight membrane panels using a textile-rod system composed of bespoke multi-material knit membranes and bending-active rods. These two components come together to create cladding panels of non-standardised curved geometries. Moreover, this paper will explore how these two components can be designed to provide geometric control over the shaped panel. It will also demonstrate how these panels can be made into a modular system through the assembly of a 2x2 panel prototype.

Keywords. Knitted Textiles; Multi-material; Membrane panels; Textile Hybrid Systems; CNC Knitting.

1. Introduction

This paper demonstrates the design, fabrication and installation of modular façade cladding membrane panels. These are composed of bespoke knitted textiles and bending-active rods to form curved non-standardised geometries.

The motivation behind this research is the manufacture of non-standardised curved façade envelopes which present a challenge to be created economically on a building scale. Current methods used in practice to fabricate these geometries rely on Computer Numeric Control (CNC) milling to create a customised mould from large blocks of expendable material, such as EPS foam or timber (Henriksen, 2017). These moulds serve as a solid surface for either concrete casting or resin composite lamination.

However, this method is a costly and resource-intensive endeavor. This is primarily due to the nature of subtractive manufacturing where significant amount of material is consumed during the production of the moulds. These moulds are also mostly used for several instances before being discarded, further adding to the material waste generated from this method (Henriksen, 2017). Thus, there is a need for alternative materials and fabrication methods to create these forms in a resource-efficient manner.

PROJECTIONS, Proceedings of the 26th International Conference of the Association for Computer-Aided Architectural Design Research in Asia (CAADRIA) 2021, Volume 1, 733-742.

1.1. TEXTILE MEMBRANES IN CONSTRUCTION

One such strategy would be to use textiles to create these non-standardised curved forms for façade cladding applications (Paech, 2016). Its manufacturing process involves cut-and-join methods where fabricators cut out designated shapes from larger sheets of textile and join them together along their edges with sewing or welding methods. These are typically pulled taut onto a rigid structural frame to create the curved geometry.

Their low self-weight and ability to transfer tensile loads across their surfaces allows for large uninterrupted spans with minimal intermediate supports. These properties also reduce the size of the structural frames needed to support the membranes as compared to heavier concrete or composite façade panels (Kronenburg, 2015). Thus, this makes them a feasible substitute for façade panels made from stiffer materials.

1.2. IMPROVING STRUCTURAL MEMBRANES

This research seeks to improve upon the conventional design and manufacture of structural membranes by asking the research question: "How do we redesign (a) structural membranes and (b) its framing systems to create non-standardised curved geometries in a resource-efficient manner?"

For membranes, we propose the use of bespoke multi-material knitted textiles which offer variable and controlled elasticity to influence its shaped form. This research uses CNC weft knitting technology to design variations in stitch patterns from a combination of glass fibre and elastane yarns. This paper also proposes a design strategy to customise these textiles to control its geometry when shaped. Thus, we believe that the use of designed knitted textiles will allow fabricators to forgo the need for cut-and-join processes when forming non-standardised geometries.

The next part explores new a textile shaping and tensioning strategy premised on the principles of textile hybrid systems. The study shows how the interaction between an elastic linear rod inserted within a knitted membrane can create unique internally shaped panel geometries. This offers a straightforward way to shape a textile and negates the need for stiffer curved framing members which would require machinery to bend to a target curved profile.

The results from these studies will culminate to a 2x2 textile-rod panel prototype which demonstrates how multiple of these panels can be assembled as a continuous envelope. These will be affixed onto an aluminium pipe frame which serves as a makeshift load-bearing structure.

The objectives of this research are:

- Exploring the geometric range of multi-material textiles, knitted out of two stitch patterns, internally shaped by a bending-active rod;
- Implementing a textile design strategy to create graded knitted membranes based on an input geometry;
- Demonstrating how these textile-rod panels can be assembled together and mounted on a frame.

2. Literature Review

2.1. CUSTOMISING KNIT MEMBRANES

The choice of knitted membranes stems from its inherent elasticity and versatility in customisation, which is more so than woven textiles used typically as structural membranes. Knitted textiles have an intermeshed loop structure which can deform and shear to non-developable geometries with large surface curvatures without wrinkling - a problem faced when shaping stiffer woven textiles. Moreover, CNC (weft) knitting as a manufacturing process is more versatile than weaving. CNC knitting offers stitch-by-stitch control whereas customisation in weaving is limited to the yarns inserted the warp direction. The former technique allows for more minute variations of its internal microstructure (stitch patterns) and materials. Thus, CNC knitting provides the ability to create heterogeneity within the membrane by mechanically grading the textile via creating intermediate regions of elasticity and stretch capacity within a single piece of textile. Possible grading strategies include knitting with (i) differentiated stitch patterns and (ii) a secondary yarn material.

Designing with differentiated stitch patterns is a common textile design strategy in the production of graded knitted textiles. This changes the way the loops are being formed and a group of these loops creates a stitch pattern. These are essentially repeatable unit cells that are mapped within the membrane which influences its tensile elasticity/stiffness and elongation capacity. This strategy has been implemented by Tamke, et al. and Ahlquist, et al. in their installations of Isoropia (Ramsgaard Thomsen et al., 2019) and Mobius Rib-Knit (Ahlquist, 2015) respectively. Both designed their knits with different stitch patterns within the same membrane to alter its stretch capacity at designated regions, allowing it to conform to bent boundary rods or auxiliary tensioning elements.

Another strategy involves knitting a secondary yarn material that features a distinctly different mechanical performance from the base yarn material. This potentially changes the elasticity of the textile to greater extent than altering the textile's stitch patterns. While multi-material knits are more commonly featured in other fields to introduce functional properties to the textiles, few literature exists of designing multi-material textiles for geometric shaping. Sharmin & Ahlquist's research on textile-reinforced composites (Sharmin & Ahlquist, 2016) is the closest example, where they knitted stiffer and heavier synthetic yarns around a region of nylastic yarn. This difference in elasticity induced bending forces within the textile while it is being restrained and laminated with epoxy resin. These forces caused the cured composite panel to flex into different geometries after being released from its restraints.

In this research, we propose combining the above two strategies to create a multi-material stitch pattern using glass fibre and elastane yarns alongside a base pattern of glass fibre yarn. This grades the textile with localised regions of elasticities with the intention of providing control over the geometry when shaped, while maintaining a tensioned membrane surface. This also expands upon our previous work (Tan & Quek, 2019) with a revised method to map the different stitch patterns.

2.2. TEXTILE HYBRID SYSTEMS

Textile hybrid systems are structural configurations that consist of bending-active rods and tension-active knitted membranes. These two inherently elastic components depend on each other to resolve the internal forces to create a structurally stable system: the rods define a rigid curved boundary around the membrane which, in turn, restrains the bent rods and keeps them held in place (Ahlquist, 2015). This interaction effectively creates a shaping and tensioning system for structural membranes. This system has been also used with graded knitted membranes in architecture academia with two recent installations mentioned in section 2.1.

One way to use this system, that has yet to be experimented, would be to induce bending of the membrane's surface by inserting a central elastic rod. This strategy is akin to adding a ridge in the middle of the membrane to increase its curvature through out-of-plane deformation. In turn, this research hypothesizes that this interaction with the tensioned knitted membrane can cause rod to flex and create specific curve profiles. This results in the formation unique scalloped shaped shapes without the need for machine bending methods. Moreover, while these systems have been used primarily as stand-alone systems, there is potential in adopting textile hybrid systems as a panelling system. Scaling down to the size of discrete panels localises the load transfer from the entire membrane surface to the individual panel units. This also allows the panels to tesselate and conform to an input envelope geometry.

3. Multi-Material Knitted Textile

This research produces these bespoke textiles on the Shima Seiki MACH2 ®XS-153 WHOLEGARMENT flat-bed weft-knitting machine. These are composed of a base glass fibre (GF) yarn of 224 tex and a secondary elastane (E) yarn of 210d spandex wrapped with 75d*2 polyester and dyed blue. We chose these synthetic yarns to create structural membranes suitable for outdoor environmental conditions.

The textile features three main stitch patterns: (a) Interlock pattern knitted with GF yarns (GF_I); (b) Milano interlock pattern knitted with GF and E yarns (GFE_MI); (c) Modified tubular jersey pattern knitted with GF and E yarns. Pattern (c) creates continuous channels integrated as part of the textile and allows bending-active rods to be inserted through them. They have two variations of (ci) the horizontal and vertical boundary channels and (cii) an integrated channel that is knitted diagonally across the main body of the textile. Additionally, we perform uniaxial and biaxial stretching tests to characterise the tensile performance of the main body patterns of GFE_MI and GF_I.

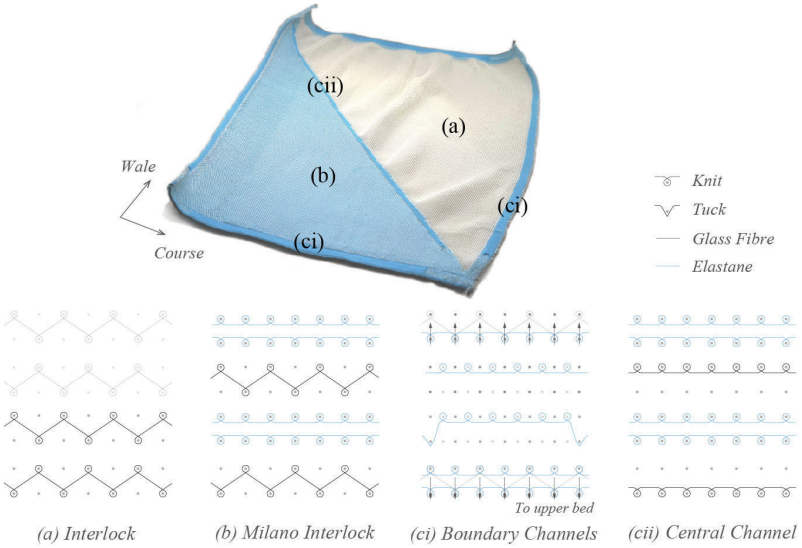

Figure 1. Different stitch patterns within the graded textile.

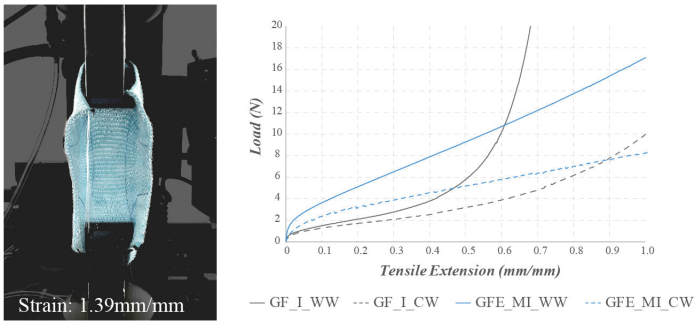

Figure 2. Uniaxial tensile tests of GF Interlock pattern and GFE Milano interlock pattern.

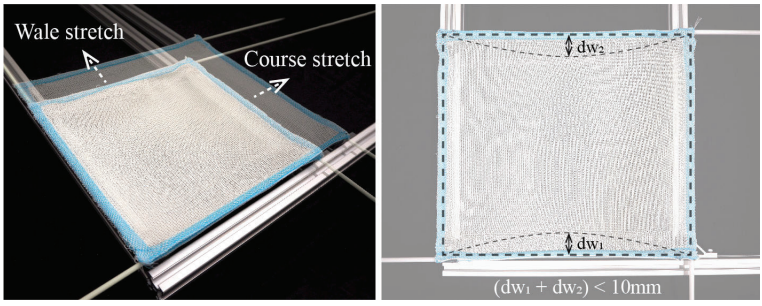

Figure 3. Biaxial stretching test set up.

Table 1. Biaxial stretching results.

		(i) Minimum Pretension				(ii) Maximum Pretension			
			Strain (mm/mm)		Area		Strain (mm/mm)		Area
Textile	Rod	Force	WW	CW	increase	Force	WW	CW	increase
GF_I	Delrin	*2.0N*	*0.17*	*0.28*	*1.50x*	*3.0N*	*0.32*	*0.47*	*1.94x*
	GFRP					*3.5N*	*0.37*	*0.55*	*2.12x*
GFE_MI	Delrin	*3.5N*	*0.09*	*0.25*	*1.36x*	*5.0N*	*0.19*	*0.47*	*1.75x*
	GFRP					*6.0N*	*0.26*	*0.62*	*2.04x*

WW: Walewise (longitudinal); CW: Coursewise (transverse)

(i) Minimum Pretension *- smallest area increase for ensuring membrane pretension;*
(ii) Maximum Pretension *- largest area increase before rods deflect excessively* ($dw_1 + dw_2 < 10mm$.

These tests demonstrate that GFE_MI pattern has a higher initial stiffness than the GF_I pattern. This results in a smaller area increase needed to pretension membranes knitted out of GFE_MI than GF_I, making it suitable as the smaller 'base' pattern. On the other hand, the larger loops of the GF_I pattern can be stretched out over a larger area, making it viable for areas experiencing increased elongation.

4. Internally Shaped Geometries

This section explores the geometric range achievable by inserting an elastic rod through the central integrated channel of the membrane. This is to assess how the parameters of rod and textile affect the geometry of the textile.

It uses three types of textiles design, one entirely knitted with the Milano interlock pattern (GFE_MI) and two being diagonally graded with interlock and Milano interlock pattern (G1, G2). The set up creates a 600 x 600mm textile-rod panel assembly with four stiff carbon fibre tubes as the boundary rods. We mount this assembly onto an aluminium frame using 3D printed joints and bolts, which isolates the membrane's bending to within its surface. We then fit the boundary members with 3D printed corner joints which house the tubes and set the start and end angles of the central rod. After installing the flat tensioned membrane, we insert Delrin rods of varying diameters (6/8mm) and lengths (900/1000/1100mm) through the central channel, causing the rod to flex and deform textile's surface.

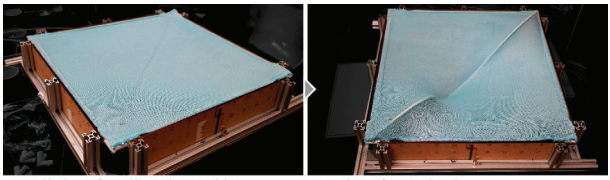

Installation of textile-rod assembly Insertion of central rod

Figure 4. Experimental set up for internally shaped geometries.

We scan each geometry using an Artec EVA 3D scanner, clean up and align the point cloud in its proprietary software and export the .STL mesh to Rhino. Using a Grasshopper script, we extract the profile of the curved rod and analyse its profile shape, assembly height in the z-axis, curvature and deviation from its intended plane. We scanned a total of 25 unique panel geometries.

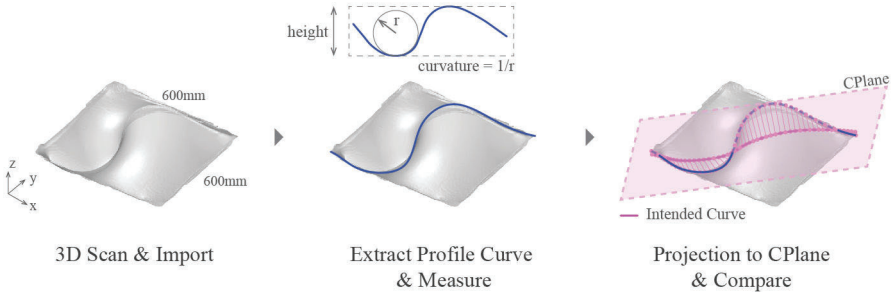

Figure 5. Scanning and parameter extraction.

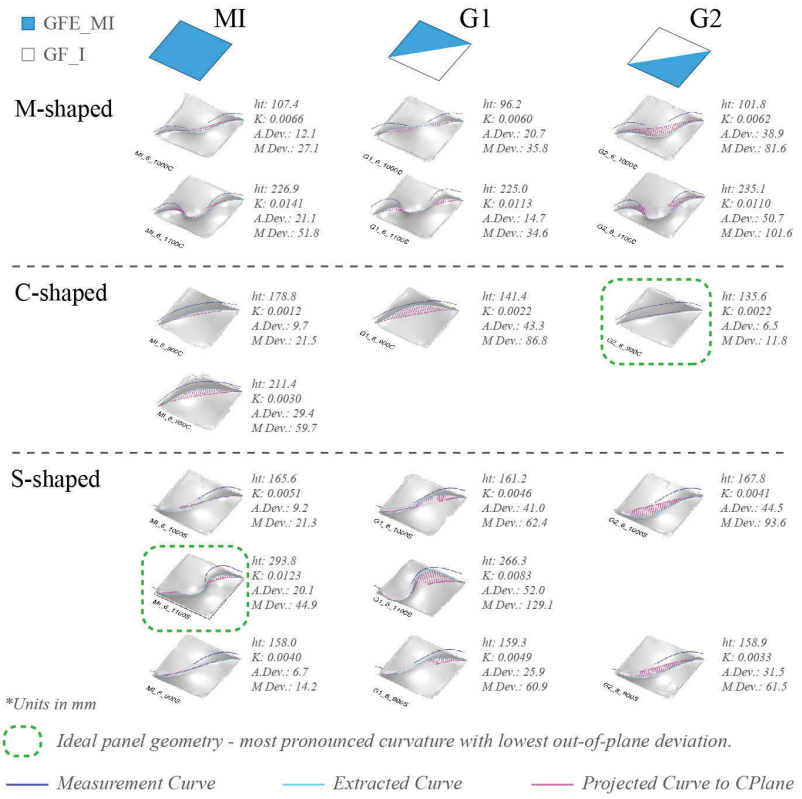

Figure 6. Several analysed internally shaped geometries.

These results reveal that the diameter of the Delrin rod has a significant influence over the curve profile and curvature. The smaller 6mm diameter rod allows longer rods to be inserted and this produces higher curvature, making it suitable to form S-shaped curves. However, its lower stiffness causes it to deflect under the tensile forces of the membrane to create M-shaped curves instead of C-shaped ones. On the other hand, 8mm diameter rods are stiffer and retain its shape to create C-shaped profiles.

The textile design primarily affects the deviation from the curve's intended plane. GFE_MI is the most suitable for forming S-shaped panels with low deviations. This could also be attributed to the symmetry of the pattern which causes the central rod to be tensioned equally on both sides. The graded patterns generally deflect the rod towards the stiffer GFE_MI side. This is beneficial for the formation of C-shaped panels in the case of G2 as it bends the 8mm rod into its intended plane.

5. 2x2 Panel Prototype

The next goal is to create a modular textile-rod panelling system that can be assembled into a larger continuous envelope. This section manufactures a 2x2 panel prototype mounted onto an aluminium pipe frame. This adopts the textile and rod parameters from the previous study to design these panels.

We referenced the four panel geometries from a segment of the preliminary design of a human-scale pavilion's envelope with 2 x C-shaped curved surfaces and 2 x S-shaped curved surfaces. These quadrilateral panels are bounded by stiffer GFRP rods and with a central Delrin rod inserted through the membrane's surface. The design strategy uses a revised Grasshopper script based on our previous paper (Tan & Quek, 2019) which dispatches stitch patterns based on a form-found quad mesh geometry. It scales down the textile based on boundary lengths and identifies which mesh faces have areas that exceed a certain percentage (185%) of the smallest mesh face. This value is derived from the biaxial stretching tests to ensure that the larger Interlock pattern is in tension when stretched to that size. If any mesh face elongates past this percentage value, it gets assigned the interlock pattern, while the remainder becomes the Milano interlock pattern.

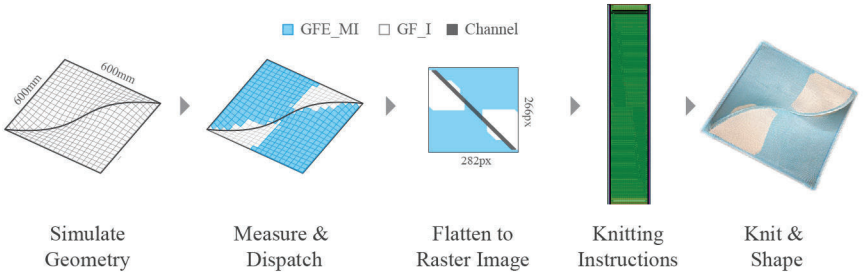

Figure 7. Stitch pattern mapping textile design strategy.

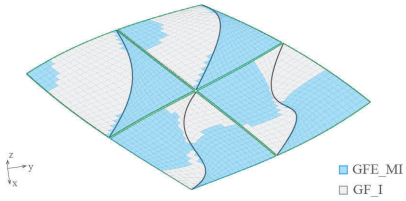

Figure 8. Mapped stitch patterns for 2x2 panel prototype.

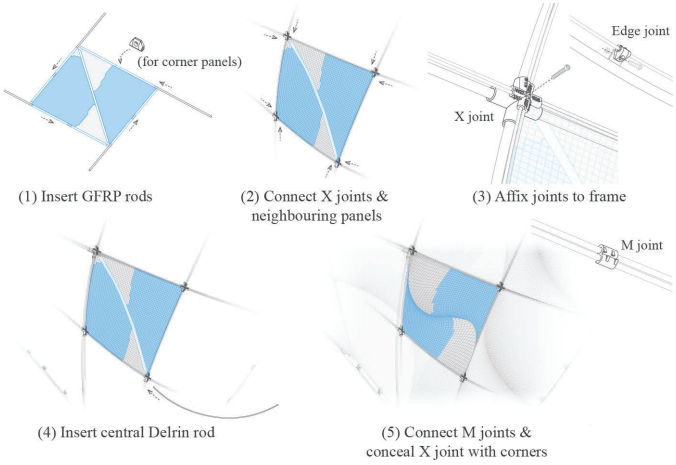

Figure 9. Assembly of the panels using customised 3D printed joints.

A group of three students and the author assembled the entire prototype over a few hours without much difficulty. The elasticity of these components provided a high installation tolerance and eased the assembly process and with all the four membranes being well in tension. The biggest obstacle was to fit the fourth and final panel. We had to prop up the frame to access the front and back of the panels to cover the central joint with the fabric corner. This is an issue that needs to be addressed when fitting the panels above ground level.

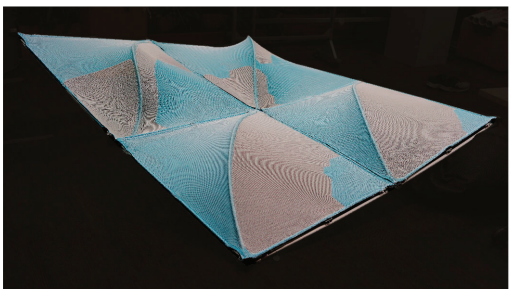

Figure 10. 2x2 panel prototype.

6. Conclusion & Future Work

In summary, this paper demonstrates the following:

- Knitting and mechanical characterisation of glass fibre and elastane knitted stitch patterns;
- Exploration of a shaping strategy using bending-active Delrin rods to internally shape knitted membranes and showing how the input parameters affect the outcome geometry;
- Testing a stitch mapping strategy to create bespoke multi-material textiles to match an input form-found geometry;
- Demonstrating how the textile-rod panelling system can be designed and interconnected as a 2x2 panel prototype assembly.

The next step works towards applying this modular system as an envelope skin for a human-scale pavilion. This pavilion will be covered in a future paper that details its design development, component manufacture and installation. As the final goal is to create an exterior membrane panelling system, we need to ensure weather proofing and long-term outdoor durability of our membranes. This can be improved by knitting glass fibre yarns coated with Telfon (PTFE) and evaluated by accelerated aging tests to determine the service life of our knitted membranes in a tropical climate.

Furthermore, this research broadens the potential of façade membranes to be used as dynamically actuated sunscreens. Flexing the Delrin rod by changing its start/end angles produces different curve profiles which alters the membrane's surface curvature. As such, we can pair this system with thermal sensors to modify the depth of the sunshade as a real-time response to recorded solar radiation.

Acknowledgements: This research was partially financed by a ZJU-SUTD IDEA grant and the Digital Manufacturing and Design (DManD) Centre. The author would also like to thank Kwan Wai Hin, Sruti Niranjan and Tim Yap Ming En for their kind voluntary assistance in this research.

References

Ahlquist, S.: 2015, Integrating Differentiated Knit Logics and Pre-Stress in Textile Hybrid Structures, *Design Modelling Symposium 2015*, 101-111.

Henriksen, T.N.: 2017, *Advancing the manufacture of complex geometry GFRC for today's building envelopes*, Ph.D. Thesis, TU Delft.

Kronenburg, R. 2015, Introduction: the development of fabric structures in architecture, *in* J.I. de Llorens (ed.), *Fabric Structures in Architecture*, Woodhead Publishing Limited, 22-42.

Paech, C.: 2016, Structural Membranes Used in Modern Building Facades, *Procedia Engineering*, **155**, 61-70.

Sharmin, S. and Ahlquist, S.: 2016, Knit Architecture, *ACADIA 2016: Posthuman Frontiers*.

Tan, Y.Y. and Quek, Y.H.: 2019, Graded Textile Shaping: Manufacture of curved Cladding Panels using Multi-material Knitted Preforms., *IASS 2019 Barcelona Symposium: Advanced Manufacturing and Non-Conventional Materials*, Barcelona.

Ramsgaard Thomsen, M., Sinke Baranovskaya, Y., Monteiro, F., Lienhard, J., La Magna, R. and Tamke, M.: 2019, Systems for transformative textile structures in CNC knitted fabrics – Isoropia, *Proceedings of the Tensinet Symposium 2019*, 95-110.

MIN-MAX: REUSABLE 3D PRINTED FORMWORK FOR THIN-SHELL CONCRETE STRUCTURES

Reusable 3D printed formwork for thin-shell concrete structures

MANIA AGHAEI MEIBODI[1], PIETRO ODAGLIA[2] and BENJAMIN DILLENBURGER[3]
[1] *University of Michigan*
[1] *meibodi@umich.edu*
[2,3] *ETH Zurich*
[2,3] *{odaglia|dillenburger}@arch.ethz.ch*

Abstract. This paper presents an approach for reusable formwork for thin-shell, double-sided highly detailed surfaces based on binder jet 3D printing technology. Using binder jetting for reusable formwork outperforms the milled and 3D printed thermoplastic formwork in terms of speed and cost of fabrication, precision, and structural strength against deformation. The research further investigated the synergy of binder jetting sandstone formwork with glass-fiber reinforced concrete (GFRC) to fabricate lightweight, durable, and highly detailed facade elements.We could demonstrate the feasibility of this approach by fabricating a minimal surface structure assembled from 32 glass-fiber reinforced concrete elements, cast with 4 individual formwork elements, each of them reused 8 times. By showing that 3D printed (3DP) formwork cannot only be used once but also for small series production we increase the field of economic application of 3D printed formwork. The presented fabrication method of formwork based on additive manufacturing opens the door to more individualized, freeform architecture.

Keywords. Binder Jet 3D Printing; 3D Printed Formwork; Reusable Formwork; Minimal Surface; GFRC (GRC).

Aghaei Meibodi, M., Jipa, A., Giesecke, R., Shammas, D., Bernhard, M., Leschok, M., Graser, K. and Dillenburger, B.: 2018, Smart Slab, *ACADIA 2018*.

1. 1 Introduction

Glass Fiber Reinforced Concrete (GFRC) is an ultra-strong and flexible composite that contains a cementitious matrix composed of cement, polymers, glass and water (Corey 2010). In the last 30 years, GFRC has contributed significantly to the construction industry. It has been a great candidate for freeform thin shell facade and envelope cladding, due to its lightweight, high mechanical performance, durability, versatility, and aesthetics. Because GFRC is significantly lighter than concrete (about 75% lighter than traditional concrete with rebar), it's

PROJECTIONS, Proceedings of the 26th International Conference of the Association for Computer-Aided Architectural Design Research in Asia (CAADRIA) 2021, Volume 1, 743-752.

easier to handle on construction sites and install as cladding. That means the building envelope will be much lighter and consequently requires significantly less support structure (minimizing the structural load) thus helping to reduce the overall material use in buildings. GFRC is also considered a sustainable construction material as it uses less cement than equivalent concrete and often uses high quantities of recycled materials such as a pozzolan, recycled glass, metals, and other recycled materials. Its life cycle is longer than traditional concrete.

While almost many contemporary architectural buildings could be realised with an exterior GFRC envelope, the current inability to produce formworks with the intended geometry and successfully casting the GFRC elements with an acceptable surface quality is a prevention (Henriksen 2017). Thin and architecturally exposed cast elements such as free-form thin-walled GFRC cladding panels often require double-sided formwork. In order to cast the exterior surface and the connection details for mounting the panels to the building structure on the backside. For one of a kind elements or elements in small lot sizes, the cost for fabricating such formwork using traditional methods is a challenge. Besides the cost, the geometric freeform and surface resolution and detailing of a thin GFRC element would be very constrained when using traditional fabrication methods for formwork.

Additive manufacturing is a game-changer as it could enable the fabrication of freeform formwork with less cost, higher precision, and higher geometric freedom compared to the traditional methods of formwork manufacturing. Several additive manufacturing technologies are explored for fabricating formwork such as FDM (Peters 2014), wax (Gardiner 2016), thin shell FDM (Aghaei Meibodi et al. 2020), and FDM for dissolvable formwork (Leschok 2019 and Aghaei Meibodi et al. 2020). This research focuses on Binder Jet 3D Printing (BJP) as it offers the largest geometric flexibility, finest resolution, and highest precision among large scale 3D printing methods. In BJP with sand, a liquid binding agent is selectively dropped on thin layers of particle material to bind it. Industrial printers, originally developed for printing molds for metal casting, can fabricate molds at a very high resolution, in the range of a tenth of a millimeter, and at a maximum volume of 8m3 (Aghaei Meibodi et al 2019).

BJP formwork (BJPF) has already been used for concrete casting for example for a concrete truss (Morel 2014). BJPF was used for a thin shell sprayed concrete structure (Dillenburger 2016), and for a lightweight concrete slab (Aghaei Meibodi et al 2018). In those examples, BJPF was used as single-use formwork, which would need to be destroyed after its use. So far, the reusability of BJPF for concrete and its use for thin-shell double-sided formwork applications with GFRC has not been tested.

2. 2 Method

This research investigates the application of binder-jetting for fabricating reusable and double-sided concrete formwork that will be used to cast freeform GFRC elements. It investigates the geometric limitation that such formwork imposes on the cast part, as the demolding direction needs to be taken into consideration

for the reusability of the molds. The performance of this fabrication method is compared to alternative fabrication methods (see Table 1). The investigation was carried through several small scale panels and a large scale demonstrator.

The first series of small-scale prototyping examined the potential of this approach for the production of high-resolution surfaces with geometrically complex detailing, surface finishing, and successful demolding of the cast part from the formwork. A series of panels with different geometric features that represent challenges for conventional milled molds were 3D printed. Those features are for example small concave features in the target part, which would require small convex features in the formwork. When fabricating such formwork with milling, this would lead to a long processing time and a large amount of material being subtracted (Figure 1 and 2). Successful demolding without chipping the cast or damaging the formwork was also a criterion that informed the design parameters for the detailing orientation of the parts. Another relevant parameter that informed the designed features and their orientation was the effective possibility to successfully demold the panels without chipping the cast or damaging the formwork

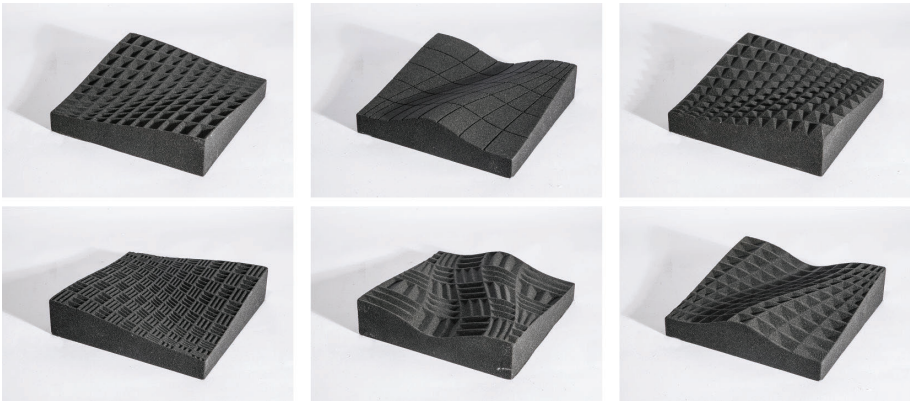

Figure 1. Series of 3d binderjet formwork tests with different surface characteristics (positive and negative features in different scale).

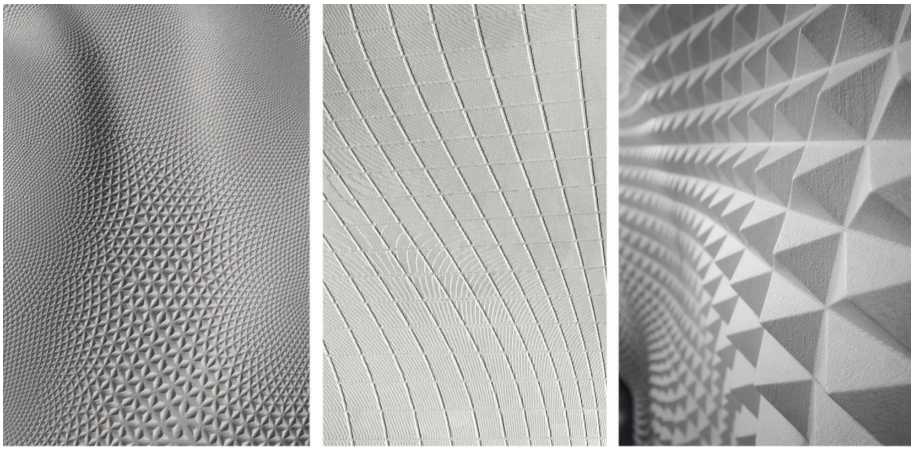

Figure 2. Resulting concrete casts of the first tests. Formwork could be removed non-destructively. The concrete shows all details down to the grains of the printed molds. In the middle sample, the structure of the 0.2mm high print layers is visible.

To evaluate the precision and accuracy of this method for large-scale GFRC freeform and thin envelope elements, we designed and fabricated a triply periodic minimal surface of the Schoen's "Batwing" family. Such a surface provides a valuable case study as it comprises sixteen equal quadrilateral parts, each of which sharing three edges with the neighboring ones and all meeting in one common point in the center of the assembly (Figure 3). This prototype was strategically designed in order to test the following criteria:

- ● Reusability
- ● Precision of interfaces
- ● Level of details of surface features
- ● Quality of freeform surface
- ● Fabrication time of the process

2.1. 2.1 FORM DESIGN

The design starts with Schoen's "Batwing" minimal surface. A minimal surface is a surface with a minimized total surface area for a given boundary. This surface can be adapted to several design possibilities. To describe the overall design, a computational method was developed to generate it as a NURBS. To obtain seamless adhering along the interfacing surfaces, an in-house bespoke function was developed that would take the designed surface as input and generate the thickness (Figure 3). The thickness was parametrically reformed for every feedback from physical prototyping to define the minimum thickness that can be successfully cast. A parametric subdivision method was developed on one side to showcase the level of details this formwork method allows.

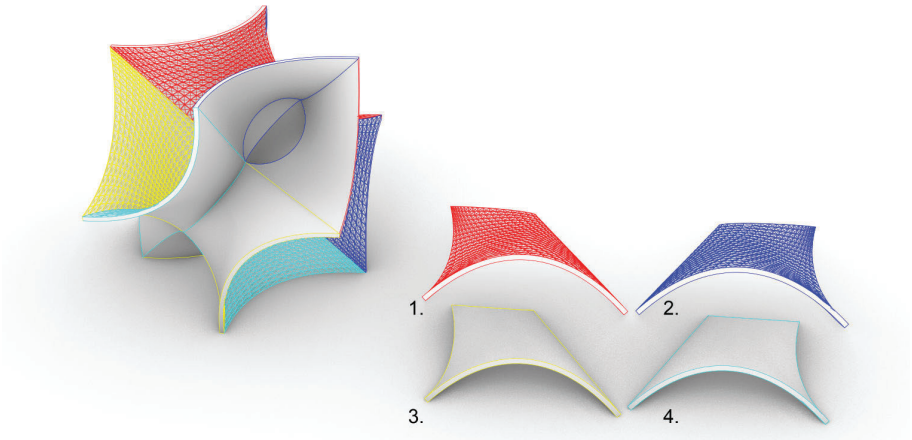

Figure 3. Segments of the concrete structure. The whole structure consists of one repetitive element and its mirrored copy; due to the ornamented details on one side of the surfaces, 4 different formworks had to be fabricated.

2.2. 2.2. FORMWORK DESIGN AND FABRICATION

The overall production required a total of four two-sided formworks, each composed of two elements assembled during the casting with the aid of a wooden frame: each part included bespoke connection details to ensure the precise relative positioning (Figure 4). To avoid potential occluded undercuts, we identified the optimal demolding direction using analysis tools provided by Solidworks which informed the design. Moreover, to overcome the brittle behavior of the 3D printed parts, each mold was infiltrated with epoxy resin.

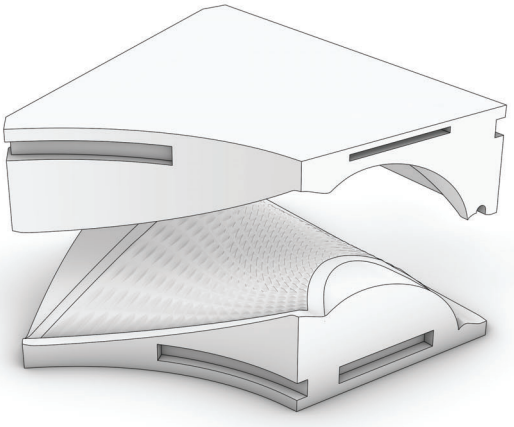

Figure 4. Schematic drawing of double-sided 3DP formwork with interlocking details.

The formworks were 3D printed using a commercial binderjet printer. The

eight individual formwork parts were nested to fit in only one print box, allowing to minimize the overall costs of production and the printing time to only 16 hours. This is about 90 times faster than FDM 3d printing and 20 times faster than Milling (Table 1).

Table 1. Comparison of different manufacturing methods for a single formwork part (dimensions 760x685x170 mm, volume ca. 25 l). Postprocessing time is not included.

	Binderjet Printer	**FDM**	**Milling of MDF (3 Axis)**
Software	Materialise / Netfabb	Ideamaker (Simulation)	RhinoCAM (Simulation)
Machine	ExOne S-Max	Raise3D Pro	Generic 3Axis Mill
Material	Sand/Furan	PLA	MDF
Specific Process Parameters		10% infill (2 shell 0.4 mm)	Tool diameter: 12 mm Feed: 4000/6000 mm/min Speed: 6000 RPM Cut depth (roughing): 20 mm Cut depth (finishing): 2 mm
Layer height	0.3 mm	0.3 mm	
Processing-time	2 h	180 h	40 h
Weight Material	1 kg/l	0.21 kg/l	0.7 kg/l
Weight Final part	25 kg	5.2 kg	17.5 kg

2.3. 2.3 CASTING

A company focusing on prefabricated concrete facades performed the casting using a mix of GFRC specifically tailored to ensure the complete filling of the thin void of the formwork, measuring only 18mm. The material was cast through the single inlet positioned at the bottom of each mold to avoid air trapping. The porosity of the printed formwork allowed the excess air to flow out of the casted volume. The selected material is frost resistance, freeze-thaw resistance, UV-Resistance, and qualifies as a facade material (Table 2). The advantage of fabricating the panels with an indirect printing method, compared to direct printing, is that the excellent properties of the cast material can be achieved. The below specifications of the selected cast material outperform current properties which can be achieved with 3D printing.

Table 2. Table 2. Selected characteristics of the cast GFRC concrete.

Property	Symbol	Unit	Characteristic	Norm
Density	ρ	kg/dm3	2.0	EN 1170-6
Compressive strength	f ck	N/mm2	60	EN 196-1
Limit of proportionality (LOP)	LOP	N/mm2	8	EN 1170-5
Flexural strength	MOR	N/mm2	10	EN 1170-5
Elongation	ε u	‰	1	EN 1170-5
Elasticity	E	kN/mm2	30	EN 1170-5
Water Vapor Diffusion	μ		> 50	DIN 4108-4
Waterproofing	c ws	m2 h	< 10	EN 772-11
Thermal Conductivity		W/mK	0.8	EN 12664
Coefficient of thermal expansion	αT		10 x 10-6	DIN 51045

2.4. 2.4. ASSEMBLY

Due to the high precision rendering of the geometry enabled by BJP, the assembly of the single casted parts was performed with the auxilium of simple wooden frames. The parts were glued together by applying a two-component epoxy glue along the interfacing surfaces, and no significant post-processing was needed (Figure 5).

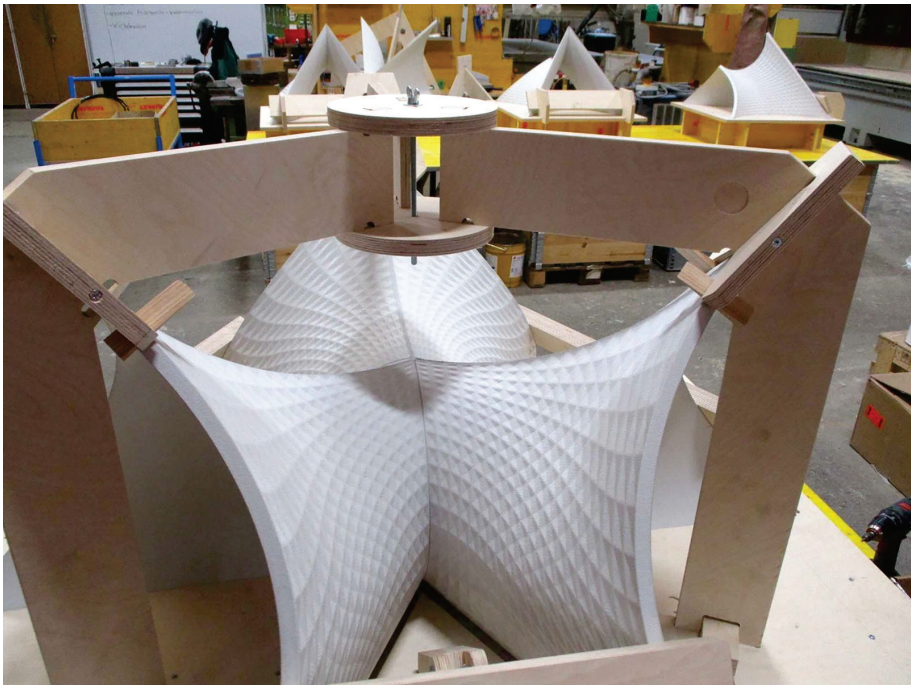

Figure 5. Assembly of the cast elements by gluing of the interfacing surface. The achieved precision of the edges plays a significant role in the construction of the entire structure.

3. 3 Results and Discussion

The result is a minimal surface structure assembled from 32 GFRC elements, cast with 4 individual formwork elements, each mold was reused 8 times. The accurate rendering of the cast elements allowed for the seamless assembly of the 32 parts with less than a millimeter precision at their interfacing surfaces (Figure 6).

Only minor post-processing steps were necessary. In comparison to 5-axis CNC milling with high-density foam, the manufacturing time can be reduced, and both the production of waste and the costs are considerably lower. The high precision of the printed parts resulted in cast components with remarkably smooth surfaces and sharp, sub-millimeter details (Figure 7 and 8), and allowed for the effortless assembly of the different elements.

The presented Minimal Surface Structure showcases a cast GFRC element based on binderjet formwork, where the freeform geometry, surface finishing, high resolution detailing, and high precision in assembly could be tested.

The surface quality achieved with this method is comparable to the results obtained in traditional concrete casting with milled formwork and silicon negatives. The intricate surface detailing could be fabricated with the same speed and cost of the smooth one, allowing us to rethink the role of detailing in architecture and its potential function as a passive means to control, i.e, the acoustic - or the energy-performance of the building envelope.

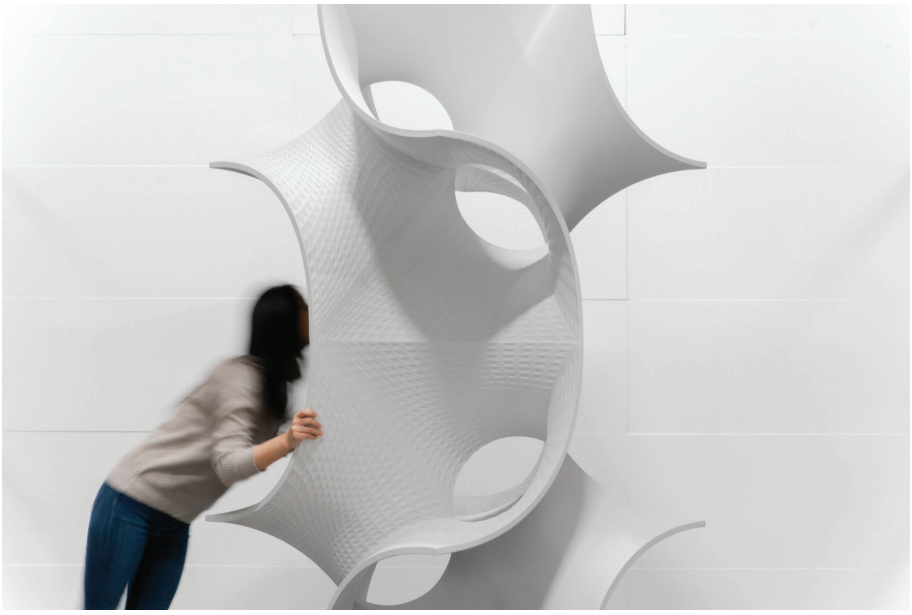

Figure 6. Min Max Structure as exhibited in Swissbau. An 18mm thin shell structure standing 2 meters high with minimal use of material (overall only 80 liters (40 per unit) of GFRC was used).

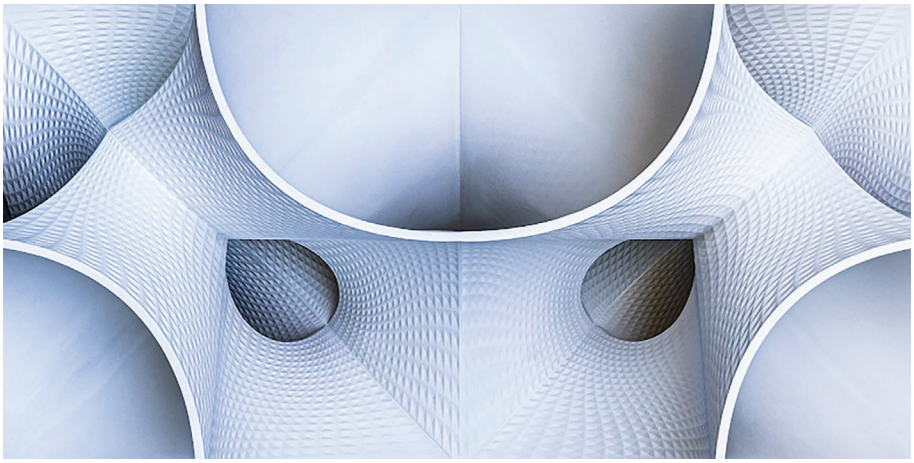

Figure 7. Min Max Structure close up details.

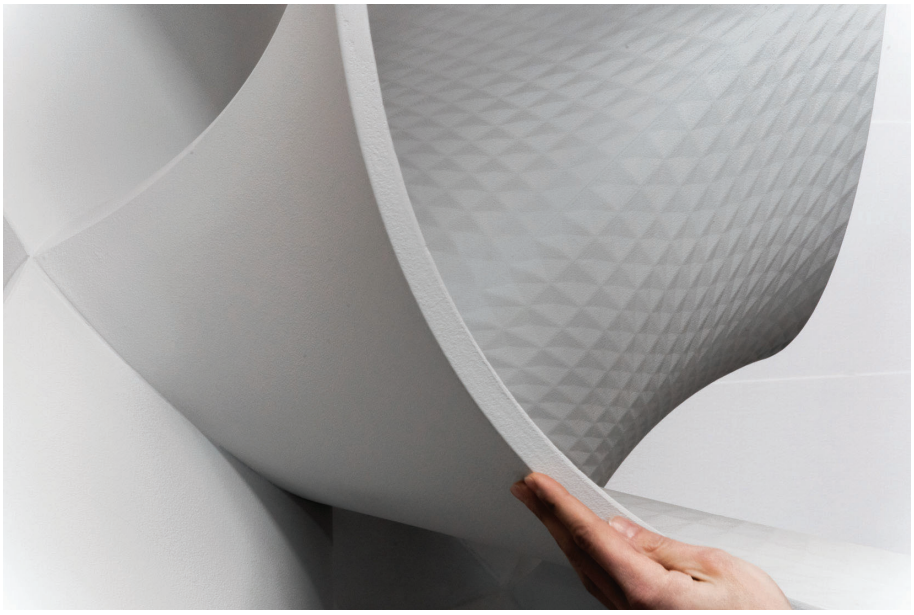

Figure 8. Close up of the surface showing fine surface details on one side and a smooth finish on the other side with an almost seamless connection of elements.

Finally, the use of 3d printed formwork renders the overall process considerably more efficient, minimizing the number of required production steps and decoupling surface detailing from production time.

4. Conclusion

The project demonstrates the production of repetitive parts from only a minimal amount of formwork. The two-sided, composite 3d printed formwork system in this project can be deployed for the production of any thin concrete element that requires high surface quality on all sides, such as free form facade elements.

The reusability of the printed formwork makes it attractive for small series of repetitive parts, which is often the case in architecture. However, in this case, the formwork parts need to be demoldable, which poses some geometric limitations on the GFRC elements.

The presented formwork method can contribute to lowering the entry-level for bespoke and freeform architecture. Hence, it could for example allow to individually adapt building facades better to a specific context, create spatially articulated facades with rich details, ultimately avoiding the monotony of standardized buildings. The presented double-sided form also allows creating lighter, thinner concrete elements, which can integrate details on both sides. It also expands the geometric freedom for building envelopes and enables more environmentally informed building envelopes.

The presented fabrication method of formwork based on additive manufacturing, opens the door to more individualized, freeform architecture using GFRC.combining this fabrication method with the minimal surface can enable the production of freeform lightweight facade elements with high-resolution surface detailing, which can be activated for a function such as saving energy or collecting CO2 emission in the air.

Acknowledgment

We would like to thank Stahlton Bauteile AG for their contribution to this project.

References

Dillenburger, B.: 2016, Maschinelle Übersetzungen, *TEC21,*, **no. 23**, 24–28.

Gardiner, J. B., Janssen, S. and Kirchner, N.: 2016, A Realisation of a Construction Scale Robotic System for 3D Printing of Complex Formwork, *33rd International Symposium on Automation and Robotics in Construction*.

Henriksen, T.: 2017, Advancing the manufacture of complex geometry GFRC for today, *Architecture and the Built Environment*, **5**, 1-194.

Leschok, M. and Dillenburger, B.: 2019, Dissolvable 3DP Formwork, *ACADIA 2019: Ubiquity and Autonomy*, Austin, TX.

Aghaei Meibodi, M., Kladeftira, M., Kyttas, T. and Dillenburger, B.: 2019, Bespoke Cast Facade. Design and Additive Manufacturing for Aluminum Facade Elements, *ACADIA 2019*.

Aghaei Meibodi, M., Volt, C. and Craney, R.: 2020, Additive Thermoplastic Formwork for Freeform Concrete Columns, *ACADIA 2020*.

Morel, P.: 2014, Sand Molds for Ultra-High Performance Concrete, *Architecture trade fair in FRAC Centre*.

Peters, B.: 2014, Additive Formwork: 3d printed Flexible Formwork, *In ACADIA 2014 Design Agency*.

Turcotte, C.: 2010, “GFRC for re-cladding Applications” . Available from <http://www.gfrcconstruction.com/category/green-building-2/> (accessed 10th september 2019).

DIGITAL FABRICATION OF GROWTH

Combining digital manufacturing of clay with natural growth of mycelium

JULIAN JAUK[1], HANA VAŠATKO[2], LUKAS GOSCH[3], INGOLF CHRISTIAN[4], ANITA KLAUS[5] and MILENA STAVRIC[6]
[1,2,3,6]*Graz University of Technology, Institute of Architecture and Media, Graz, Austria*
[1,2,3,6]*{julian.jauk|vasatko|lukas.gosch|mstavric}@tugraz.at*
[4]*Ortwein Master School for Art and Design, Graz, Austria*
[4]*ingolf.christian@progdev.at*
[5]*Faculty of Agriculture, Department for Industrial Microbiology, Belgrade, Serbia*
[5]*aklaus@agrif.bg.ac.rs*

Abstract. In this paper we will demonstrate that a digital workflow and a living material such as mycelium, make the creation of smart structural designs possible. Ceramics industries are not as technically advanced in terms of digital fabrication, as the concrete or steel industries are. At the same time, bio-based materials that use growth as a manufacturing method, are often lacking in basic research. Our interdisciplinary research combines digital manufacturing - allowing a controlled material distribution, with the use of mycelial growth - enabling fibre connections on a microscopic scale. We developed a structure that uses material informed toolpaths for paste-based extrusion, which are built on the foundation of experiments that compare material properties and observations of growth. In this manner the tensile strength of 3D printed unfired clay elements was increased by using mycelium as an intelligently oriented fibre reinforcement. Assembling clay-mycelium composites in a living state allows force-transmitting connections within the structure. The composite named "MyCera" has exhibited structural properties that open up the possibility of its implementation in the building industry. In this context it allows the design and efficient manufacturing of lightweight ceramic constructions customized to this composite, which would not have been possible using conventional ceramics fabrication methods.

Keywords. Mycelium; Clay; 3D Printing; Growth; Bio-welding.

1. Introduction

The interdisciplinary subject of this paper is primarily embedded in the field of architecture, but is also influenced by the latest developments in mycology, bio-based materials, clay and 3D printing. Generally speaking, the overall research

PROJECTIONS, Proceedings of the 26th International Conference of the Association for Computer-Aided Architectural Design Research in Asia (CAADRIA) 2021, Volume 1, 753-762.

goal focuses on finding a viable, long-term solution to the global problem of waste management and CO2 emissions, which also affect the building industry and construction waste management. This research focuses on extraction and utilization of highly accessible and widespread materials, clay and mycelium.

Mycelium is the vegetative part of mushrooms, which consists of a system of filamentous hyphae. It grows on lignocellulosic substrates and can be moulded into lightweight composites. This has been applied in the past decade by several artists and designers in the production of furniture and structures for short-term exhibitions, as well as companies (Ecovative, MOGU, MycoWorks) that launched commercially available products, such as leather, foam, packaging material and acoustic panels. Further to these developments, universities such as IAAC Barcelona (Claycelium 2019), ETH Zürich (MycoTree 2017), CITA (Fungar 2019) and Vrije Universiteit Brussel (Elsacker 2017) have organized workshops, courses and research programs exploring the usage of mycelium composites. One of the important questions to be answered is whether the structural properties of these existing materials, which primarily use mycelial growth as a manufacturing process, can now be improved. Although mycelium composites have a great potential for substituting some building components, the viability of their actual application and manufacturing processes on a large scale is still open.

The utilization of clay in architecture, in terms of digital fabrication, is not as technically advanced as concrete or steel industries are. The production and application of bricks has not fundamentally changed since the introduction of dies in piston extruders in 1855 (Händle 2009). In masonry brick production, firing and drying are the most energy consuming phases. The use of mortar results from correcting production tolerances and ensuring the stability of the single elements within a wall component, while posing an issue of leading to high fossil CO2 emissions during cement production (World greenhouse gas emissions 2005) and resource procurement. As for recycling, fired clay could be used as a chamotte for new products, but since the separation of clay and mortar remains challenging, the two materials are usually discarded as one compound after a building has fulfilled its life expectancy of approximately 60 years (Kleiber and Simon 2006). Until now, only the concrete industry has demonstrated commercial potential in 3D printing of single elements (Hansemann et al. 2020), as well as whole buildings (Khoshnevis and Hwang 2006). 3D printing of clay is currently limited to small size elements (Ugarte et al. 2020) and requires further investigation.

The research presented in this paper is based on references that have already developed techniques for the extrusion of mycelium composites (Soh et al. 2020), material mixtures of mycelium and clay (Digital seismograph 2017), development of bio-hybrid architectural systems (Como and Ayres 2020) and 3D printed material assemblies from cellulose and mycelium (Goidea et al. 2020). The work in this paper extends beyond the existing research by evaluating structural properties of a bio-based and digitally fabricated material, as well as observing material distribution on a microscopic scale. This enables the use of natural growth as an additional parameter in architectural design by assembling the clay-mycelium composites in a living state.

2. Methodology

The method of this research was carried out through material experiments and a design study. A series of material mixtures was created, as well as samples with different geometries that have the aim of elaborating different properties based on the respective material and fabrication process. The research was conducted in four phases: 1) material experimentation, 2) setting up hardware and software, 3) testing and measurement, 4) case study - combined structure.

2.1. EXPERIMENTATION WITH MATERIAL MIXTURE

The composite ”MyCera” consists of inorganic parts - clay and water, and organic parts - mycelium and substrate. The main challenge in this phase was finding an optimal substrate type and optimum ratio of organic and inorganic parts, which have following properties: 1) using a high proportion of organic material ensures enough nutrition for homogeneous mycelial growth that influence the effective porosity left by the organic components after the firing process, 2) using a high proportion of clay ensures the specific viscosity and elasticity required for a 3D printing fabrication process.

To restrict the number of samples with various material combinations, common modelling clay, type Nigra 2002 of company Sibelca was used. The material is composed of 65.50% SiO_2, 1.10% TiO_2, 21.50% Al_2O_3, 8.9% Fe_2O_3, 0.30% CaO, 0.80% MgO, 1.80% K_2O, 0.10% Na_2O, 0.4% Mn. Black clay enables the visual differentiation between clay and mycelium and is highly obtainable. Finally, the very fine chamotte increased the plasticity without causing too much abrasion inside the 3D printer, which would be the case with a rougher chamotte.

The goal of the first set of experiments was mixing clay and different substrate types in order to choose the one optimal for mycelial growth (Figure 1). Those substrates were sawdust, bleached and unbleached cellulose, which were obtained from the Austrian paper producer Mayr-Melnhof Karton. The used sawdust consists of mixed wood types with a majority of hardwood that has less resin. It is therefore a suitable additive for mixing with clay and also feasible as a substrate for mycelium.

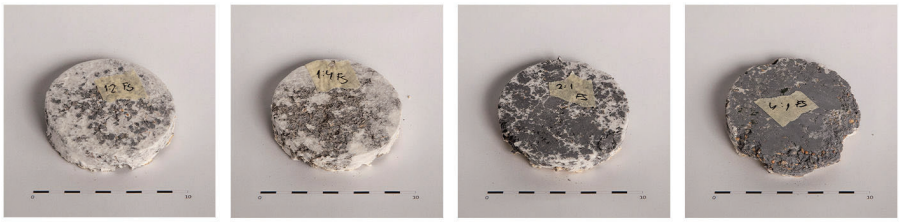

Figure 1. Samples with a different clay:substrate rate: a) 1:2, b) 1:4, c) 2:1, d) 4:1.

Two types of mycelium strains were used, *Ganoderma lucidum* and *Pleurotus ostreatus*. After several experiments, *Ganoderma lucidum* was abandoned because of frequent contamination problems. *Pleurotus ostreatus* was used, because it has the ability to digest a great variety of lignocellulosic substrates (Elsacker

et al. 2020), has a fast growth rate and becomes denser in its second growth phase (Ghazvinian et al. 2019). A series of samples with clay and the three substrate types were blended into seven different ratios of organic and inorganic components. The rate of *Pleurotus ostreatus* was 10% of the material mixtures' weight for all samples. Distributing more spawn would have accelerated the growth, but would not have influenced the quality of the final outcome.

After a series of experiments and evaluation of mycelial growth, sawdust was chosen as a substrate. Compared to cellulose, wood has a better local availability and a higher control of the grain size is possible. To prepare the material for printing, a series of different experiments was performed to find optimal material viscosity for the 3D printer. The quantity of water added to the mixture does not affect the dried geometry but rather the printing workflow. It was necessary to keep it as low as possible while retaining required viscosity for printing. A high water percentage decreases the possibility for an overhanging geometry, while also increasing drying time and problems related to shrinkage. The sawdust was sieved to ensure a particle size <2 mm not to block the nozzle of the 3D printer. Both components were mixed in a dried and pulverized state to achieve a homogeneous distribution and were then blended with water by a mixing machine. The weight ratio of the final mixture from clay to sawdust was 7:1. 35% water was added for printing, measured from the weight of the mixture. In a final step of material preparation, the wet mixture was filled into material tanks, each containing a material volume of up to 4600 cm^3 and closed airtight to prevent moisture loss. Once the material was printed and then sterilized, inoculation was carried out differently, depending on the geometry. The mycelium spawn was dispersed on the surface of the solid objects, whereas the hollow ones were filled. The mycelium spawn quantity added to the mixture was higher than that usually added to purely organic composites, since the material mixture mainly consisted of inorganic components. Inoculating the printing mixture before extrusion was tested out as well, but due to elaborate preparation of maintaining sterility during printing, this method was discarded. The approach of printing the elements firstly, then sterilizing and inoculating them was considered to be a more efficient method.

2.2. SETTING UP HARDWARE AND SOFTWARE

Customizing the standard hardware and developing new software for direct transmission of Rhino 3D Geometry into G-Code was necessary in order to 3D print the composite mixture. New material tanks of hard anodized aluminium and a rastered printing bed were added to the 3D Clay printer Delta WASP 40100.

2.2.1. Hardware

A 4 mm nozzle was chosen for extruding the mixture. Nozzles with a smaller diameter (1-2 mm) caused an occasional blockage, whereas bigger sizes presented a less precise option. A constant pressure of 6 bar on the material tank was necessary for printing. Another influence on the physical design was the available printing area, which is defined by the printer model. The maximum area was 40 cm in diameter and 100 cm in height.

2.2.2. Software

A custom Grasshopper script for Rhino 3D was developed for using the 3D printer in the most flexible manner. By this means the designing and providing of machine data is directly connected in a single software allowing a highly efficient workflow. The printing paths were created through curves that are discretized and divided in parts where the control points are transferred into a G-Code with specific printing speeds and material flow values. A single-lined spiralized printing path was introduced for the cylindrical objects. Solid elements were printed along alternating directions of the printing paths for each layer in order to have a crossed structure and more stability. The spiralized toolpaths reduce printing time by not having to start and stop the extrusion for each layer, while also creating the smoothest possible surface. A method of having a variable speed and factor of extrusion - extrusion flow - was developed in order to allow a variable wall thickness within a single printed line. A simulation of extruded volume and the movement of the printer head was included to predict potential geometrical collision.

2.3. TESTING AND MEASUREMENT

The following experiments refer to the paste-based extruded material mixture described in the previous chapter. All tests in the context of tensile strength were conducted at the Institute of Technology and Testing of Building Materials at Graz University of Technology. Two kinds of tests were carried out: 1) tensile strength along the extrusion axis, 2) binding force between the printed layers. Additionally, an experiment was carried out to observe the growth depth of mycelium through clay. The hypothesis was that printed layers with mycelium have better binding connection than the 3D printed layers without mycelium. This assumption was based on the examination of mycelium acting as an additional binding agent that connects two adjacent layers.

2.3.1. Tensile strength along extrusion axis

Samples for testing tensile strength along the extrusion axis were printed from the material mixture described in the previous chapter in dimensions 60x170x15 mm, whereby all printing paths were created in parallel to the stress axis. These were then dried and sterilized and one half were inoculated. The incubation was terminated after 14 days and the samples were dried once again. Finally, all samples were sanded down to have identical dimensions before testing.

The test results show (Figure 2) an increase of the average of maximum tensile strength values of 66.62% for the samples with mycelial growth. Samples without mycelial growth showed an average value of maximum tension of 122.60 N with a top value of 178.37 N, while samples after 14 days of mycelial growth showed an average value of maximum tension of 204.28 N with a top sample of 278.30 N. There is no notable change of elongation behaviour in these samples. Some of the samples were damaged during the fixture in the testing machine due to internal bending behaviour of clay while drying. The test objects showed no recognizable crack pattern after reaching maximum tensile force.

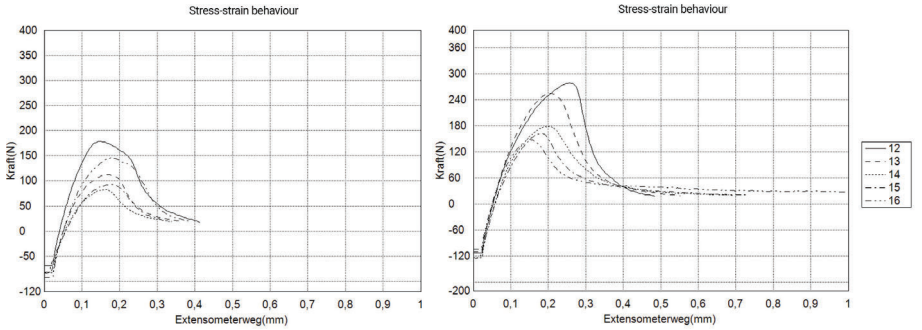

Figure 2. Comparing the load curves regarding tensile strength along the extrusion axis of the individual samples without (left) and with (right) mycelial growth.

2.3.2. Binding force between printed layers

To evaluate the increased strength of the consolidated layers, the samples were prepared in a cylindrical form. The printing path consisted of three concentric circles per layer, each with alternating starting points. Subsequently, these were randomly shifted per layer to avoid a weak seam along the object. The samples had a height of 40 mm, a diameter of 45 mm and a void with a diameter of 20 mm, thus a wall thickness of 12.5 mm. The samples were prepared by filling the central void with a wooden cylinder and the total volume was capped with a piece of acrylic glass, which was glued only to the ceramic surface. An anchor was drilled into the wooden piece to transmit the force to the acrylic glass once it had been pulled. The samples were tested using a Shimadzu AG-X plus testing machine.

The test results confirmed the hypothesis by showing an increase of average of maximum tensile strength values of 32.34% in favor of specimens with mycelium. Samples without mycelial growth showed an average value of maximum tension of 83.80 N with a top value of 93.14 N, while samples after 14 days of mycelial growth showed an average value of maximum tension of 110.90 N with a top sample of 174.82 N. The fracture at maximum tensile force occurred between the top two layers at all samples. There was no notable change of elongation behaviour in these samples.

2.3.3. Observation of growth depth

Samples with wall thicknesses ranging from 2.5 mm to 9.5 mm have been produced to evaluate the maximum extent of mycelial growth through clay. Pieces of 10 mm width were broken out from different positions within the samples. To observe the superficial growth of mycelium on clay, an Eschenbach stereo light microscope, with a maximum magnification of 90, was used to examine the surface of fracture.

Successful mycelial growth through a 3D printed clay wall of 9.5 mm is evident (Figure 3, left). The 9.5 mm wall is seen on the left side of the picture and mycelium reaching for nutrients. Displaying hyphae within the area of fracture was not possible using a light microscope. The expected effective porosity is

assumed to take place on a much smaller scale. Further investigation of the inner porosity caused by hyphal growth is required by scanning through an electron microscope.

Figure 3. Mycelial advancement through the 3D printed clay wall (9.5 mm) at 20x magnification (left). Surface growth on a 3D printed clay wall (2.5 mm) at 20x magnification (middle). Hyphae connection between two elements at 30x magnification (right).

2.4. CASE STUDY - COMBINED STRUCTURE

The main goal of the design study was incorporating material design in the structural properties of an architectural element. Two types of elements were designed to fulfill different static requirements: 1) bar elements which consist of fired clay and primarily bear pressure loads (Figure 4, right), 2) node elements that consist of unfired clay and a large amount of mycelium, which have more capacity of bearing tensile and torsion loads (Figure 4, left, middle). Both of these element types were 3D printed from the same material mixture consisting of 87.5% clay and 22.5% sawdust. The following step was preparing the elements for inoculation, which was achieved by wrapping them in a tear resistant aluminum foil and autoclaving at 117-120°C at 0.8-1 bar for 120 minutes. After the elements cooled down to room temperature, inoculation commenced.

Figure 4. Inoculated node (left, middle) and bar (right) elements after 14 days of growth.

Cylindrical objects were filled with mycelium spawn. For the node elements, the spawn was evenly dispersed on the surface. The objects were then moistened with sterilized water. The inoculated elements were incubated in microfilter bags (PP75/BEH6/V37-53, SacO2) at 24°C and 80% relative humidity in a

dark environment. After two weeks, the bars were removed from the growing environment, dried at room temperature and then fired at 600°C for 6 hours, followed by 960°C for 2.5 hours. During that process, all organic elements burned up leaving an effective porosity through a branching inner structure in the ceramic. The node elements were kept in the same growing conditions, without firing, with the aim of establishing enhanced mycelial growth.

In order to design a structure that reflects the possibilities which result from material qualities and digital fabrication, a "combined structure" was developed. The geometry was defined by a topological optimization algorithm (via Topos plugin for Grasshopper). Exemplary support and load conditions were applied within a 380x380x380 mm boxed space. The result was then abstracted to an axis diagram, in which the axes were rebuilt with cylindrical objects and nodes as streamlined meshes (via Kangaroo plugin for Grasshopper).

The structure was assembled by putting the two types of elements together in a state where mycelium continues its growth. Mycelium fibres of the still growing node elements formed connections through expansion of the hyphal network and bio-welded adjacent elements together. The mycelial connections were able to structurally connect bar and node elements. After a minimum growth duration of 14 days, the structure was dried under atmospheric conditions and the assembly was finished. The material showed two important aspects after the assemblage: 1) it is able to fill out the gaps that occur while assembling and it tolerates an uneven contact between two surfaces - the same way as mortar, 2) it developed a connection within multiple elements by expansion of the hyphal network.

The combined structure (Figure 5, right) was designed and built to be a showcase for the exhibition *Steiermark Schau 2021 (Styrian Show)* starting in April 2021 at Kunsthaus Graz. The exhibition objective is to present research to the public, to connect art and science and to make all of this work accessible to a non-academic audience.

To visualize mycelial growth in the design phase, the Metaballs algorithm was used. It creates n-dimensional isosurfaces that are characterised by their ability to meld together when in close proximity, to form contiguous objects (Figure 5, left). This algorithm is often used for digital modelling of organic objects (Martinez 2017). Threshold of this melding is set according to previous observations of how far the hyphae reach out in mid-air. For the current stage of the research, this algorithm is a useful tool to visually propose a grown structure.

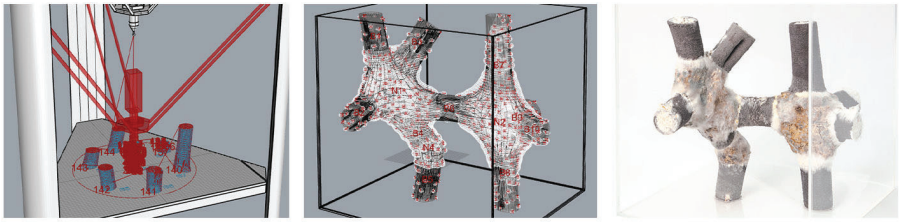

Figure 5. Software setup showing the simulation of printing (left) simulation of mycelial growth (middle) and realization of the combined structure (right).

3. Conclusion

We developed a composite material and produced two different 3D printed types: 1) bar elements based on fired clay to deal with pressure forces; 2) node elements based on mycelium to deal with tension and shear forces. Both types consist of a mixture of clay and sawdust inoculated with mycelium. After a sufficient growing process, the bar elements were fired, whereby the organic elements burn up leaving an effective porosity through a branching inner structure. The growth process of the node elements was terminated where mycelium remained as a fibre reinforcement. The two element types were assembled in a state during which mycelium was still growing, until it fully dried out under atmospheric conditions. In this manner, we built a combined structure in which mycelium fibres formed connections, which are able to transmit forces between adjacent elements by penetrating the tube-like inner structures of the fired elements.

The composite "MyCera" shows notable structural properties when compared to the same material mixture without mycelium. This has been proven on a set of samples tested for tensile strength along the extrusion axis, as well as within connections between the single 3D printed layers. Mycelium enhances tensile strength along the extrusion axis by 66.62% and the connection between the single layers by 32.34%. It is assumed that the high increase of tensile strength is caused by the growth process which takes place after printing. This kind of intelligent fibre distribution could not have been achieved with a non-growing material. Currently, the main limitation is preserving a sterile fabrication process.

4. Perspectives

After accomplishing sufficient research, the proposed material composition could replace cement based binders. Furthermore, utilizing this new material and fabrication method, which increases tensile strength, ceramic elements in architecture can be assembled in less solid configurations. To verify the assumption of an advantageous structural effect of grown fibre connections, a comparison of mycelial fibre reinforcement and other fibres that are commonly used to increase tensile strength, such as basalt and glass fibres (Naughton and Grennan 2017), is planned. The question of the actual application and durability of the material after a long-term exposure to atmospheric conditions still remains open. Another open topic is the possibility of introducing coatings such as Xyhlo Biofinish (van der Berg and Konings 2019) (made from the *Aureobasidium pullulans* fungus) and sodium silicate (Stark and Wicht 2000) to extend its lifespan until it matches the one of a standard ceramic brick.

Future work is planned based on the results of this research: 1) creating a multi nozzle system to distribute different material properties within one element, 2) scanning samples with an electronic microscope, 3) implementing growth as a design parameter in 3D modelling software.

Acknowledgements

This work was (partially) funded by the Austrian Science Fund (FWF), project no. F77.

References

"World greenhouse gas emissions" : 2005. Available from <https://www.wri.org/resources/charts-graphs/world-greenhouse-gas-emissions-2005> (accessed 22nd October 2020).
"Digital seismograph" : 2017. Available from <https://designbydata.org/project/digital-seismograph-adrien-rigobello> (accessed 09th December 2020).
"Mycotree - Block Research Group" : 2017. Available from <https://block.arch.ethz.ch/brg/project/mycotree-seoul-architecture-biennale-2017> (accessed 27th November 2020).
"Elsacker, E. - Architectural Engineering Lab of the Vrije Universiteit Brussel" : 2019. Available from <https://www.vub.be/arch/people/elise-elsacker> (accessed 27th November 2020).
"Fungar - Royal Danish Academy" : 2019. Available from <https://royaldanishacademy.com/news/forskere-skal-skabe-levende-svampearkitektur> (accessed 27th November 2020).
"Claycelium - Institute for Advanced Architecture of Catalonia" : 2019. Available from <http://www.iaacblog.com/programs/claycelium/> (accessed 22nd October 2020).
J. van den Berg and B. Konings (eds.): 2019, *Material Atlas; Materialen Atlas; The Growing Pavillon*, Company New Heroes, Amsterdam.
Brian, D. and Händle, F.: 2007, *Extrusion in Ceramics*, Springer Berlin Heidelberg, Berlin.
Colmo, C. and Ayres, P.: 2020, 3d Printed Bio-hybrid Structures – Investigating the architectural potentials of mycoremediation, *eCAADe*.
Elsacker, E., Vandelook, S., Van Wylick, A., Ruytinx, J., De Laet, L. and Peeters, E.: 2020, A comprehensive framework for the production of mycelium-based lignocellulosic composites, *Science of The Total Environment*, **725**, 138431.
Ghazvinian, A., Farrokhsiar, P., Vieira, F., Pecchia, J. and Gursoy, B.: 2019, Mycelium-Based Bio-Composites For Architecture: Assessing the Effects of Cultivation Factors on Compressive Strength, *eCAADe*.
Goidea, A., Andreen, D. and Floudas, D.: 2020, Pulp Faction: 3d printed material assemblies through microbial biotransformation, *Fabricate*, London.
Hansemann, G., Schmid, R., Holzinger, C., Tapley, J., Kim, H., Suskovic, V., Freytag, B., Trummer, A. and Peters, S.: 2020, Additive Fabrication of Concrete Elements by Robots, *Fabricate*, **4**, 124-129.
Khoshnevis, B. and Hwang, D.: 2006, Mega-scale fabrication by Contour Crafting, *International Journal of Industrial and Systems Engineering*, **Vol.1**(3), 301-320.
Kleiber, W. and Simon, J.: 2006, *Verkehrswertermittlung von Grundstücken*, Bundesanzeiger Verlag.
Martinez, F., Martinez, F. and Hernández, C.: 2017, Organic-Shaped Structures Design Using Genetic Algorithms and Metaballs, *Contemporary Engineering Sciences*, **Vol.10**(21), 1001-1010.
Naughton, P. J. and Grennan, R. M.: 2015, The strength of fibre reinforced clays; La force de l'argile renforcées par des fibres, *XVI European Conference on Soil Mechanics and Geotechnical Engineering*.
Soh, E., Chew, Z.Y., Saeidi, N., Javadian, A., Hebel, D. and Le Ferrand, H.: 2020, Development of an extrudable paste to build mycelium-bound composites, *Materials and Design*, **195**, in print (Article 109058).
Stark, J. and Wicht, B.: 2000, *Zement und Kalk; Der Baustoff als Werkstoff*, F.A. Finger-Institut für Baustoffkunde der Bauhaus-Universität Weimar.
Ugarte, J. P., Mhatre, S., Norman, S. and Bechthold, M.: 2020, Extruded Tessellations: A novel structural ceramic system at the intersection of industrial ceramic extrusion and CNC fabrication, *SIGraDi 2020: XXIV International Conference of the Iberoamerican Society of Digital Graphic*, Medellín.

Index of Authors

In a time of unprecedented global challenges, the need to reflect on our changing society has rarely been more obvious. As the pandemic highlights the precariousness of our fragile climate, limited resources and unequitable urban areas, there is a new mandate for new technology-enabled processes that positively impact our profession, communities, and planet.

'PROJECTIONS' focuses on recent research around computational methodologies in architecture and urbanism, reflecting upon the different ways innovation will impact the future. A collection of 149 papers, selected through a rigourous double-blind peer reviewing process, highlights the challenges and opportunities around the current status of computer aided research and design.

www.caadria2021.org

ISBN:978-988-78917-5-8

9 789887 891758